WOODS HOLE OCEANOGRAPHIC INSTITUTION

COLLECTED REPRINTS

1957

SEP 1959
LIBRARY
FISH & WILDLIFE SERVICE

JULY, 1958

PERIODICA

Woods Hole
Oceanogr.
Institution

Collected
Reprints

1958

LIBRARY
BUREAU OF COMMERCIAL FISHERIES
U. S. FISH AND WILDLIFE SERVICE
P. O. BOX 3830
HONOLULU 12, HAWAII

LIBRARY
BUREAU OF COMMERCIAL FISHERIES
U. S. FISH AND WILDLIFE SERVICE
P. O. BOX 3830
HONOLULU 12, HAWAII

Digitized by the Internet Archive
in 2025

https://archive.org/details/collected-reprints-woods-hole-oceanographic-institution_1957

WOODS HOLE OCEANOGRAPHIC INSTITUTION

COLLECTED REPRINTS

1957

2138

JULY, 1958

This volume contains contributions from the Woods Hole Oceanographic Institution which were published in 1957; also the Annual Report of the Director for the year 1957.

TABLE OF CONTENTS

Contribution No.

ATHEARN, WILLIAM D.
Comparisons of Clay from the Continental Shelf off Long Island with the Gardiners Clay 905

AYERS, JOHN C. and ROGER BACHMANN
Simplified Computations for the Dynamic Height Method of Current Determination in Lakes 883

BACKUS, RICHARD H.
Notes on Western North Atlantic Sharks 857

BACKUS, RICHARD H.
Northern Record of the Snake Eel *Ophichthus gomesi* (Castelnau). 854

BACKUS, RICHARD H. and HAROLD BARNES
Television-Echo-Sounder Observations of Midwater Sound Scatterers 894

BARLOW, JOHN P.
Effect of Wind on Salinity Distribution in an Estuary (Dated 1956) 752

BARNES, HAROLD
The Northern Limits of *Balanus balanoides* (L) 897

BLANCHARD, DUNCAN C.
Discussion of Raindrop Distributions made during Project Shower, Hawaii, 1954 812

BLANCHARD, DUNCAN C.
The Supercooling, Freezing and Melting of Giant Waterdrops at Terminal Velocity in Air 809

BLANCHARD, DUNCAN C. and A. H. WOODCOCK
Bubble Formation and Modification in the Sea and its Meteorological Significance 875

BOWEN, VAUGHAN T. and T. T. SUGIHARA
Strontium 90 in North Atlantic Surface Water 907

BUMPUS, DEAN F., JOSEPH CHASE, C. GODFREY DAY, DAVID H. FRANTZ, JR., DAVID D. KETCHUM and ROBERT G. WALDEN
A New Technique for Studying Non-Tidal Drift with Results of Experiments off Gay Head, Mass., and in the Bay of Fundy 926

BUNKER, A. F.
Turbulence Measurements in a Young Cyclone over the Ocean 833

CHASE, JOSEPH
The Bermuda-Azores High Pressure Cell. Its Surface Wind Circulation (Dated 1956) 835

EWING, J. I., C. B. OFFICER, H. R. JOHNSON and R. S. EDWARDS
Geophysical Investigations in the Eastern Caribbean: Trinidad Shelf, Tobago Trough, Barbados Ridge, Atlantic Ocean 861

Contribution No.

FOLSOM, THEODORE R. and ALLYN C. VINE
On the Tagging of Water Masses for the Study of Physical Processes in the Oceans 929

FRIEDMAN, I. and A. H. WOODCOCK
Determination of Deuterium-Hydrogen Ratios in Hawaiian Waters 860

GIBBS, ROBERT H., JR.
Preliminary Analysis of the Distribution of White Marlin, *Makaira albida* (Poey), in the Gulf of Maine 922

GIBBS, ROBERT H., JR.
A Taxonomic Analysis of *Myctophum affine* and *M. nitidulum*, two Lantern-Fishes Previously Synonymized, in the Western North Atlantic 912

GORDON, M. S.
Observations on Osmoregulation in the arctic char (*Salvelinus alpinus* L.) . . 868

GORDON, M. S. and RICHARD H. BACKUS
New Records of Labrador Fishes with Special Reference to those of Hebron Fjord 800

HAHN, JAN
Oceanus Goes to the Bottom of the Sea 909

HULBURT, E. M.
The Taxonomy of Unarmored Dinophyceae of Shallow Embayments on Cape Cod, Massachusetts 838

HULBURT, E. M.
Distribution of Phosphorus in Great Pond, Massachusetts (Dated 1956). . . . 748

KANWISHER, J. W.
Freezing and Drying in Intertidal Algae 887

KANWISHER, J. W. and ALFRED EBELING
Composition of the Swim-Bladder Gas in Bathypelagic Fishes 888

KANWISHER, J. W. and H. LEIVESTAD
Thermal Regulation in Whales 878

KETCHUM, BOSTWICK H.
The Effects of the Ecological System on the Transport of Elements in the Sea . . 871

MALKUS, JOANNE STARR
Trade Cumulus Cloud Groups: Some Observations Suggesting a Mechanism of Their Origin 843

MARKS, WILBUR and JOSEPH CHASE
Observation of the Growth and Decay of a Wave Spectrum 769

MATHER, FRANK J., III, and ROBERT H. GIBBS, JR.
Distributional Records of Fishes from Waters off New England and the Middle Atlantic States 901

Contribution No.

McLEOD, G. C.
The Effect of Circularly Polarized Light on the Photosynthesis and Chlorophyll *a* Synthesis of Certain Marine Algae 911

MILLER, ARTHUR R.
The Effect of Steady Winds on Sea Level at Atlantic City 829

MOULTON, JAMES M.
Sound Production in the Spiny Lobster *Panulirus argus* (Latreille) 914

OFFICER, C. B., J. I. EWING, R. S. EDWARDS and H. R. JOHNSON
Geophysical Investigations in the Eastern Caribbean: Venezuelan Basin, Antilles Island Arc and Puerto Rico Trench 839

PLUNKET, MARY A.
The Qualitative Determination of Some Organic Compounds in Marine Sediments 924

REDFIELD, ALFRED C. and ARTHUR R. MILLER
Water Levels Accompanying Atlantic Coast Hurricanes 828

RICHARDS, FRANCIS A.
Some Current Aspects of Chemical Oceanography 844

RICHARDS, FRANCIS A.
Oxygen in the Ocean 714

RUTSTEIN, M. S.
Flooded Quarries for Experimental Work 866

RYTHER, JOHN H. and CHARLES S. YENTSCH
The Estimation of Phytoplankton Production in the Ocean from Chlorophyll and Light Data 902

SANDERS, H. L.
The Cephalocarida and Crustacean Phylogeny 882

SCHOLANDER, P. F.
Oxygen Dissociation Curves in Fish Blood 921

SCHOLANDER, P. F. and L. VAN DAM
The Concentration of Hemoglobin in Some Cold Water Arctic Fishes 892

SCHOLANDER, P. F., L. VAN DAM, J. W. KANWISHER, H. T. HAMMEL and M. S. GORDON
Supercooling and Osmoregulation in Arctic Fish 891

STOMMEL, HENRY
A Survey of Ocean Current Theory 917

STOMMEL, HENRY
Florida Straits Transports, 1952–1956 845

STOMMEL, HENRY and GEORGE VERONIS
Steady Convective Motion in a Horizontal Layer of Fluid Heated Uniformly from Above and Cooled Non-Uniformly from Below 899

Contribution No.

SUTCLIFFE, W. H., JR.
An Improved Method for the Determination of Preserved Plankton Volumes . . 903

SWALLOW, J. C. and L. V. WORTHINGTON
Measurements of Deep Currents in the Western North Atlantic 910

TORPHY, SHANNON R. and JOHN M. ZEIGLER
Submarine Topography of Eastern Channel, Gulf of Maine 885

TURNER, HARRY J. and DAVID L. BELDING
The Tidal Migrations of *Donax variabilis* Say 886

von ARX, WILLIAM S.
An Experimental Approach to Problems in Physical Oceanography 820

WALDEN, ROBERT G., DAVID D. KETCHUM and DAVID H. FRANTZ, JR.
Buoy Telemeters Ocean Temperature Data 895

WALDEN, von H. and H. G. FARMER
Auswertung von Seegangsregistrierungen des Forschungsschiffes "Atlantis" mit dem "Ship-Borne Wave Recorder" sowie Vergleich mit entsprechenden Seegangsberechnungen aus den Windverhältnissen (Hindcasting) 850

WHITNEY, G. G., JR.
Factors Effecting the Accuracy of Thermometric Depth Determinations . . . 916

WOODCOCK, A. H. and A. T. SPENCER
An Airborne Flame Photometer and its Use in the Scanning of Marine Atmospheres for Sea-Salt Particles 889

WOOSTER, W. S. and BOSTWICK H. KETCHUM
Transport and Disposal of Radioactive Elements in the Sea 870

WORTHINGTON, L. V. and WILLIAM E. SCHEVILL
Underwater Sounds Heard from Sperm Whales 908

YENTSCH, CHARLES S.
A Non-Extractive Method for the Quantitative Estimation of Chlorophyll in Algal Cultures 898

YENTSCH, CHARLES S. and JOHN H. RYTHER
Short-Term Variations in Phytoplankton Chlorophyll and Their Significance . . 893

ZEIGLER, JOHN M., W. D. ATHEARN and H. SMALL
Profiles across the Peru-Chile Trench 919

ZEIGLER, JOHN M. and F. C. RONNE
Time-Lapse Photography - - an Aid to Studies of the Shoreline 884

ZEN, E-AN
Preliminary Report on the Mineralogy and Petrology of Some Marine Bottom Samples off the Coast of Peru and Chile 913

THE WOODS HOLE OCEANOGRAPHIC INSTITUTION

Report for the Year 1957

LIST OF CONTRIBUTIONS

The following contributions are not included in this volume:

	Contribution No.
BACKUS, RICHARD H. The Fishes of Labrador	896
BERGEIJK, WILLEM A. van and EMIL WITSCHI The Basilar Papilla of the Anuran Ear	980
BIGELOW, HENRY B. and WILLIAM C. SCHROEDER A Study of the Sharks of the Suborder Squaloidea	848
BUMPUS, DEAN F. Surface Water Temperatures along Atlantic and Gulf Coasts of the United States	904
BUMPUS, DEAN F. Oceanographic Observations 1956, East Coast of the United States	918
BUMPUS, DEAN F. and C. GODFREY DAY Drift Bottle Records for Gulf of Maine and Georges Bank, 1931–56	941
HOLMES, R. W. The Annual Cycle of Phytoplankton in the Labrador Sea, 1950–51. (Published in 1956.)	813
VINE, ALLYN C. Some Trends in Oceanographic Instrumentation	851

Contribution No. 714

Geol. Soc. America
p. 185–238, 11 figs.

Memoir 67, Vol. 1, 1957
Made in U. S. A

Chapter 9

Oxygen in the Ocean*

FRANCIS A. RICHARDS

Chemical Oceanographer, Woods Hole Oceanographic Institution, Woods Hole, Mass.

> "Circulation is responsible for the aeration of The Deeps, without which all but the uppermost stratum would be a waste more desert than the Sahara" —H. B. Bigelow

INTRODUCTION

In the early investigations of marine biology, many scientists believed that the deeper parts of the ocean must be anaerobic and azoic. However, deeper and deeper probes in the latter half of the nineteenth century showed that life existed and that dissolved oxygen was present to the greatest depths sounded (C. W. Thompson, 1874). As early as 1869, the oxygen content at depths as great as 2090 fathoms had been determined by W. L. Carpenter (1874), the chemist aboard the PORCUPINE; he ventured to predict to the biologists whether their dredge hauls would be "good" or "bad", depending on the proportions of dissolved oxygen and carbon dioxide he found in the water.

Dittmar's analyses of oxygen samples taken on the CHALLENGER expedition in 1873–1876 (Dittmar, 1884) were the first relating to the general distribution in the world oceans. Dittmar was surprised to find surface-oxygen contents showing "negative deficits" from the amounts he computed for saturation, and he noted "very small values for the dissolved oxygen. . . at many places of the ocean bottom [and] . . .occasionally even at moderate depths. . . ." (p. 226). He also observed (p. 225) "Amongst the many deep-sea waters which were analysed for their gas contents, we found none that were quite free from absorbed oxygen, which confirms our conviction that absolute stagnation nowhere exists in the ocean, not even at its greatest depths".

Since the time of the CHALLENGER expedition, investigation of the distribution of dissolved oxygen in the sea has closely attended oceanographic exploration, and at present a body of data exists which is the most extensive for any of the nonconservative, biologically conditioned variables of the marine environment.

Oxygen can be added to the sea only in the upper layers, by absorption of air and, in a layer strictly limited by the depth of light penetration, by photosynthesis. At the surface, oxygen can be lost from the sea by exchanges with the atmosphere, but at all depths it is consumed by the respiration of plants and animals, including the decomposition of organic material by bacteria. Reactions of oxygen with reduced materials such as sulfides, iron^{I}, manganese^{II} and ^{III}, other auto-oxidizable substances, and the consumption of oxygen actuated by enzymes are of limited extent and largely confined to the surface and bottom layers (Thompson, *et al.*, 1934; ZoBell, 1939). The respiratory processes of practically all organisms require the oxidation of organic compounds which are formed only in the upper layers, and so consumption of oxygen at all depths is limited by processes which have occurred in the upper, photic zone. Since the rate of molecular diffusion through water is too small to be effective in carrying dissolved matter great distances, replenishment of oxygen to the deeper parts of the ocean can take place only by the circulation of waters oxygenated in the surface layers, which themselves insulate the deeper waters from atmospheric exchanges.

---

* Contribution No. 714 from the Woods Hole Oceanographic Institution.

The distribution of oxygen in the oceans of the world is, therefore, the manifestation of processes which (1) add oxygen to the surface layers, (2) consume oxygen by respiratory, chemical, and enzymatic oxidation, and (3) distribute it to all depths (Gaarder, 1927; Wattenberg, 1927; Sverdrup, 1929; Bigelow, 1931; Vaughan, 1940). Its distribution differs from that of the conservative properties of sea water because it is intrinsically involved in the biological processes, which are invariably accompanied by corresponding changes in oxygen, carbon, phosphorus, nitrogen, and the other elements of which protoplasm is composed.

SOLUBILITY OF OCEAN GAS IN SEA WATER

When in equilibrium with 1 normal atmosphere of dry air containing 20.90 per cent oxygen, the solubility of oxygen in sea water decreases with increased temperature and salt content according to the equation

$$1000a = 10.291 - 0.2809t + 0.006009t^2 - 0.0000632t^3 - \mathrm{Cl}(0.1161 - 0.003922t + 0.0000631t^2)$$

$1000a$ is the solubility of oxygen in ml at NTP in 1 liter of water
t is the Centigrade temperature
Cl is the chlorinity in parts per mille

This relationship was definitively determined by C. J. J. Fox (1909)[1]. Dittmar (1884) investigated the solubility of oxygen in sea water, but his data did not fully show the effect of the salt content (Whipple and Whipple, 1911). In the range of salinity found in most sea water, a temperature change of 1°C corresponds to a solubility change of 0.1 to 0.2 ml/liter.

Whipple and Whipple (1911) were in the process of determining these constants when Fox's data came to them. They abandoned further experiments, since their results at that point agreed with Fox's, and used his data to compute the amount of oxygen dissolved in sea water when in equilibrium with a normal atmosphere saturated with water vapor, expressing the solubilities in parts per million. The amounts of oxygen soluble in sea water in equilibrium with 1 atmosphere (760 mm) of pure oxygen gas have been computed by Sverdrup *et al.* (1942) and by Redfield (1948b) from Fox's (1909) data.[1] The basic data of Fox and the Whipples have been used to construct expanded tables, graphs, and nomograms (Table 1).

"Percentage saturation" is frequently computed using the formula

$$O_2/O_2' \times 100 = O_2\%$$

where O_2 is the observed oxygen content, O_2' is "100% saturation". The term "100% saturation" has no physical meaning in subsurface waters, where there is a hydrostatic head directly proportional to the height of the water column (Rakestraw and Emmel, 1938). Subsurface concentrations corresponding to greater than "100% saturation" are frequently referred to as "supersaturated" but do not necessarily represent a metastable system, as this term ordinarily does in physical chemistry.

The difference between the actual oxygen content and the concentration at "100% saturation"

---

[1] P. F. Scholander has pointed out to the author that neither 20.90 nor 20.99 per cent oxygen is acceptable for the composition of the atmosphere. The latter figure is quoted by Humphreys (1926), Sverdrup *et al.*, (1942), and other writers. Glueckauf (1951) recommends 20.946 ± 0.002 per cent as the most likely figure for the O_2 content of uncontaminated air, but Scholander states that it is somewhere between 20.93 and 20.95, depending on the method of analysis and on possible real fluctuations in the composition of air. *See also* Hock *et al.* (1952).

Since the writing of the present paper, new oxygen solubility data have been published (Truesdale, G. A., Downing, A. L., and Lowden, G. F., The solubility of oxygen in pure water and sea-water, Jour. Appl. Chem., vol. 5, no. 2, pp. 53–62, 1955) which indicate that the solubility is appreciably lower than Fox reported.

TABLE 1.—*Representations of oxygen solubility in sea water*

Nature	Expression of salt content	Expression of temperature	Expression of oxygen solubility	Dry air	Saturated air	Reference
Equation and Table	‰ Cl	°C	ml/liter	X		Fox (1909)
Table	ppm Cl	°C	ppm		X	Whipple and Whipple (1911)
Nomogram	‰ Cl	°C	ml/liter	X		Kalle (1939)
Nomogram	‰ Cl	°C	mg-atoms/liter		X	Tully (1949)
Table	‰ S or ‰ Cl	°C	ppm		X	Redfield (1948b)

$(O_2' - O_2)$ was referred to by Dittmar (1884), Brennecke (1909), and others as the "oxygen deficit", and by Redfield (1942) as the "apparent oxygen utilization". Buch (1929) used the term "biologically uninfluenced" oxygen, O_2^N, and computed it from the observed nitrogen content of the water and its salinity, because he felt these were less subject to *in situ* changes than was temperature. The salinity and the temperature at which this amount of nitrogen just saturated the water, found from Fox's tables, were used to compute what the oxygen content of the water was when it became saturated with both oxygen and nitrogen—*i.e.*, when the oxygen content was still "biologically uninfluenced". Rakestraw and Emmel (1938) redetermined nitrogen-solubility data, accounting for the presence of the small amounts of other inert atmospheric gases, chiefly argon, by improved methods, thus improving the precision of determining the "biologically uninfluenced" oxygen content.

The assumption that all the waters of the oceans have at one time been at the surface and at that time became approximately saturated with the atmospheric gases was made by Dittmar (1884) and has been confirmed by observations that all ocean waters are approximately saturated with nitrogen.[2] Oxygen and nitrogen are subject to the same physical and hydrographic influences, but nitrogen is essentially uninfluenced by biological and chemical changes and thus affords a measure of what the oxygen content would be if unchanged by the latter (Buch, 1929; Rakestraw and Emmel, 1938; Hamm and Thompson, 1941, and others).

Oxygen-solubility relationships are such that, on mixing two masses of water of different temperature, each just saturated with oxygen, the resulting mixture will be "supersaturated" with respect to the equilibrium solubility of oxygen (Rakestraw and Emmel, 1938).

PROCESSES AFFECTING THE DISTRIBUTION OF OXYGEN IN THE OCEANS

EXCHANGES ACROSS THE SEA SURFACE

The difference between the partial pressures of oxygen in sea water and in air will determine the direction of exchange with the atmosphere. Near the surface, local nonequilibrium concentrations may exist in the sea because of biological activity and upwelling, but contact of the surface layers with the atmosphere and vertical mixing tend to eliminate these deficits and excesses. In regions where there is extensive photosynthetic production of oxygen, excess gas will tend to escape into the atmosphere, and, in regions where upwelling brings unsaturated water to the surface, oxygen will tend to be absorbed by the water (Fleming and Revelle, 1939), and a homogeneous surface layer, in equilibrium with the atmosphere, will result. The thickness of this layer will vary with geography, season, climate, and weather (Fig.

---

[2] D. E. Carritt, in a paper read before the American Society of Limnology and Oceanography Meeting at Gainsville, Florida, September 1954, pointed out that changes in barometric pressure can account for appreciabe fluctuations in the amounts of atmospheric gases that will be in solution when equilibrium is established with the natural atmosphere.

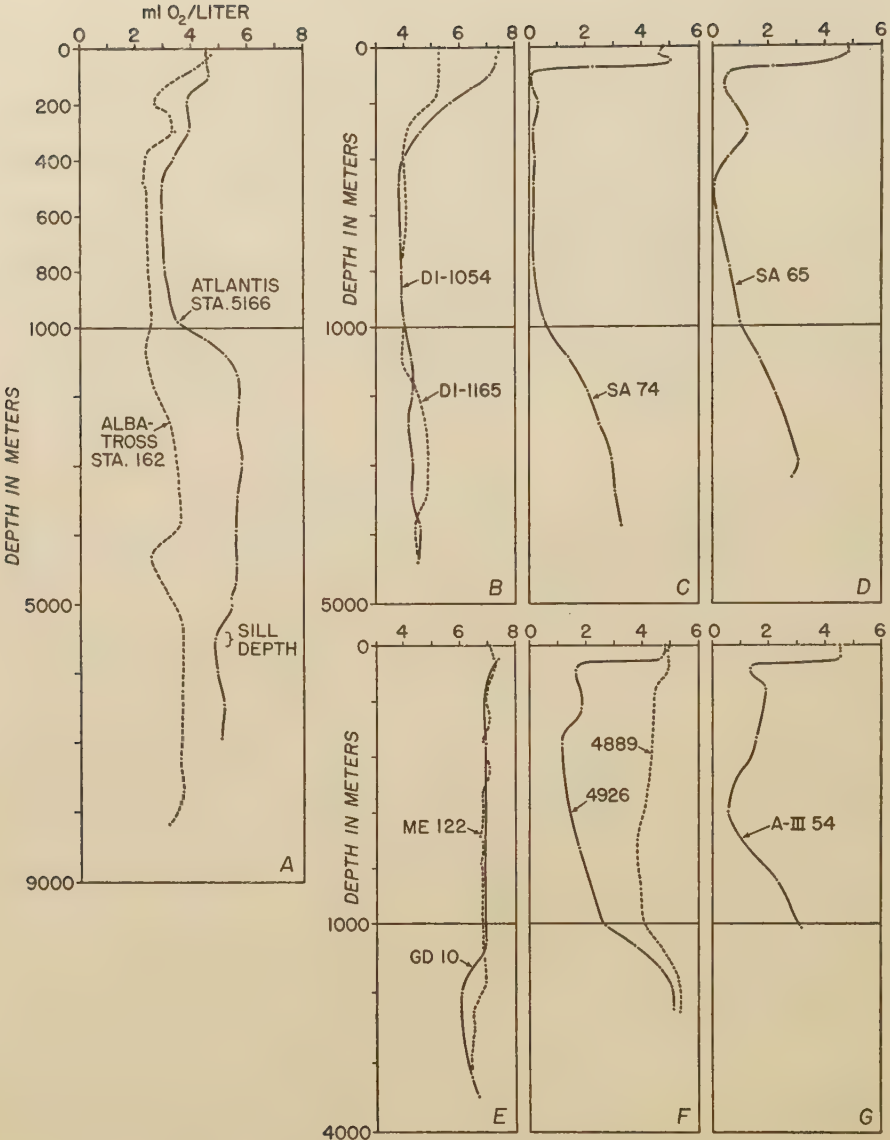

FIGURE 1.—*Representative vertical distributions of oxygen*

A. Albatross station 162 in Mindinao deep. 23 January, 1948. 5°23′N.,127°48′E., data from Bruneau *et al.* (1953), and Atlantis station 5166 in the Brownson Deep, 24 February, 1954. 19°55′N., 64°51′W. B. Discovery Station 1054 in Antarctic Convergence. 3 December, 1932. 50°07.8′S, 35° 48.6′N. Discovery station 1165 in Subantarctic Convergence, 24 February, 1932. 41°00′S., 09°30′E. Data from Discovery Committee (1949). C. Albatross Station 74, in eastern tropical Pacific. 22 September, 1947. 11°39′N., 114°15′W. Data from Bruneau, *et al.* (1953). D. Albatross station 65 in eastern tropical Pacific, showing two minima. 16 September, 1947, 6°21′N., 103°42′W., data from Bruneau *et al.*, (1953). E. Godthaab station 10, 3 June, 1928, 56°56′N., 51°17′W., and Meteor station 122, 55°03′N., 44°46′W., 9 March, 1935, in North Polar Front. Data from Bulletin Hydrographique for 1929 and 1936. F. Atlantis stations 4926 in tropical eastern Atlantic 28 February, 1952, 12°53′N., 22°59′W., and 4889 in southeastern North Atlantic, 4 February, 1952, 29°52′N., 30°12′W. G. Albatross III station 54 showing two minima and lowest concentrations observed in tropical eastern Atlantic. 16 February, 1952, 17°00.5′N., 30°03′W.

1 *A*, *B*, *F*, and *G*). In most parts of the oceans, the processes of photosynthesis, respiration, upwelling, and vertical mixing are such that very few subsurface concentrations of just 100 per cent saturation are found. Large near-surface oxygen deficits are found in regions of upwelling; these areas in the south Atlantic are shown in Wattenberg's (1939a, Beilage L to LVIII) charts of the percentage of saturation found at several depths. The depth to which equilibrium with the atmosphere is achieved is largely determined by the stability of the water, which in turn determines the ease of vertical mixing, is related to the depth of the seasonal thermocline, and is markedly affected by winds. Seiwell (1934) found that in the western North Atlantic the oxygen content generally begins to decrease at about the same depth as does the temperature. In the latitude of Bermuda the uniform oxygen layer was about 350 m thick, but it was less than 35 m thick off Chesapeake Bay (36°12′N., 73°32′W.). The thickness of the layer corresponded to the depth of the thermocline in both places. Rakestraw and Carritt (1948) found a seasonally fluctuating correspondence between the depth of the oxygen minimum and of the thermocline at stations in the western Atlantic slope water and in the Sargasso Sea. According to Wattenberg (1939a, Beilage LI), the layer of uniform oxygen content is about 50 m deep in the Atlantic south of 50°S., and at 100 m the water in these latitudes is still 90–95 per cent saturated. In many places in the equatorial regions, the surface waters are less than 92.5 per cent saturated, and at 100 m large areas of low-oxygen concentrations occur.

Redfield (1948a) studied the annual cycle of oxygen exchanges across the sea surface in the Gulf of Maine. He assumed that *biological* changes in the oxygen content in ml/liter, ΔQ_x, could be estimated from the equation

$$\Delta Q_x = 28.3\,\Delta PO_4^{\equiv},$$

where ΔPO_4 is the change taking place in the inorganic phosphate in milligram atoms/M^3. Assuming that in the area studied exchanges of oxygen across the sides and lower surface of the water column were negligible, the total change in oxygen content, ΔQ_o, is given by

$$\Delta Q_o = \Delta Q_x + \Delta Q_E,$$

where ΔQ_E is the exchange of oxygen across the sea surface, and can be computed from changes in the dissolved oxygen and phosphate in the water column. If ΔQ_E is negative, it represents the escape of oxygen to the atmosphere; if positive, oxygen has been taken up by the water. Redfield estimated that about 30×10^4 ml of oxygen leaves a square meter of surface of the Gulf of Maine during the spring and summer, and a similar amount re-enters from the atmosphere during the winter months. About two-fifths of the partial-pressure differences bringing about this exchange was attributable to biological activity, the remainder to the effects of temperature on the solubility of oxygen. Redfield computed that pressure-head differences ranged from -0.021 atmospheres in May to 0.103 atmospheres in January. The values given are for $P - p$, in which p is the partial pressure of oxygen in sea water and P the partial pressure of oxygen in a water-saturated atmosphere. Positive values of $P - p$ favor the movement of oxygen from the atmosphere into the water. They were computed from the equation

$$P - p = P(C_o - C_x)/C_o$$

in which C_x is the oxygen content of the water and C_o the solubility of oxygen in sea water in equilibrium with air saturated with water vapor at the temperature in question. Using these pressure-head differences, he computed that the coefficient of oxygen exchange was about 13×10^6 cc/m^2 per atmosphere per month in winter and 2.8×10^6 in summer. The range in the coefficients reported by Redfield can be attributed to conditions at the sea surface (sea state, stability, etc.), which make the actual amount of surface on a water column of 1 square meter cross section highly variable. Redfield's estimates, based on observations of phosphate and oxygen concentrations in the Gulf of Maine, are of the same order of magnitude as those of Krogh (1910) and Adeney and Becker (Dorsey, 1940; p. 552–555) based on laboratory experiments in which the absorption of oxygen from bubbles was observed. The coefficient reported by Krogh equals 33.5×10^6 cc per month per square meter per atmosphere; that estimated by Dorsey from Adeney and Becker's data is 7.3×10^6.

The general ideas presented by Redfield must apply to the sea as a whole, with oxygen entering the sea surface for most of the year in polar regions and in regions where upwelling brings oxygen-deficient water to the surface, and leaving the sea surface most of the year in the tropics, where photosynthesis and high temperatures favor excesses of oxygen. Seasonally alternating periods of oxygen exchanges in opposite directions would be expected in the temperate zones.

PHOTOSYNTHETIC PRODUCTION OF OXYGEN

In the photic zone the oxygen content may increase appreciably above that found at the surface and in many places reaches values greater than 100 per cent of equilibrium-saturation concentrations (Fig. 2). Rakestraw (1933) found the upper 20–40 meters of the Gulf of Maine were invariably "supersaturated" in August 1932, and values up to 120 per cent of saturation were regularly observed in the spring. At depths down to the *compensation depth* photosynthetic production of oxygen exceeds its respiratory consumption, by definition, and at all greater depths the net change is a loss of oxygen, even though photosynthetic production continues. The penetration of light is probably the most important factor in determining the compensation depth, but temperature, differences in the species of plankton, and nutrient supply are also important. In regions of intense photosynthetic activity the compensation depth will be nearer the surface because of decreased transparency corresponding to the large phytoplankton populations.

Rates of photosynthetic production and respiratory consumption of oxygen and the compensation depth can be determined by suspending transparent and opaque bottles containing sea water and its organisms at various depths in the ocean, and noting changes in the oxygen concentration. Only respiration can occur in the opaque bottles, but both processes can proceed in the transparent bottles; the differences in the changes in oxygen content are a measure of the photosynthetic production.

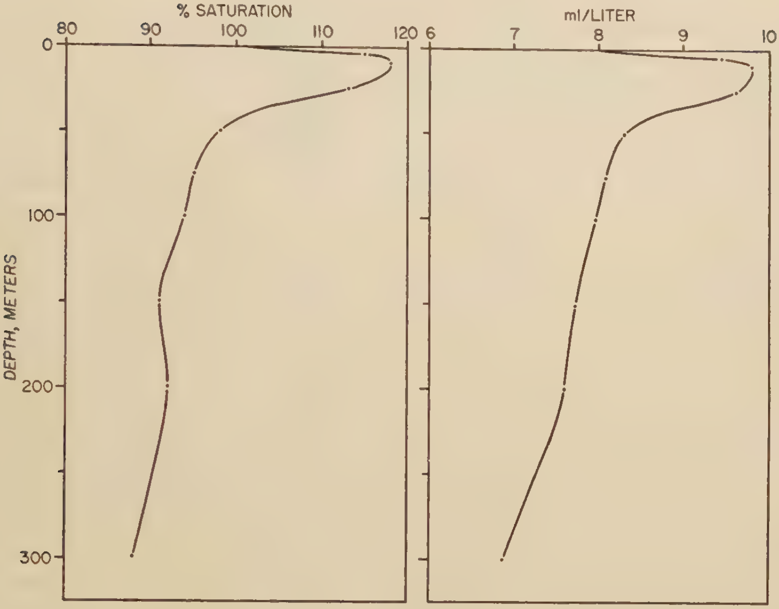

FIGURE 2.—*Representative vertical distribution of oxygen showing greater than 100 per cent saturation* POLARBJØRN Station 20, 14 August, 1932, off East Greenland Coast. Data from Jakhelln (1936).

If

ΔO_l = change in oxygen content in transparent bottle,

ΔO_d = change in oxygen content in dark bottle,

ΔO_p = photosynthetic change in oxygen content,

ΔO_r = respiratory change in oxygen content,

$\Delta O_p = \Delta O_l - \Delta O_r$

and at the compensation depth

$$\Delta O_p = \Delta O_d.$$

Ketchum (1951) has reviewed the depths at which the compensation depth has been found in various parts of the world (Table 2). They range from 0.8 to 2.1 meters in Great South Bay to more than 100 meters in the Sargasso Sea. The latter probably represents an extreme value for the compensation depth but may be typical of those parts of the ocean which correspond to the Sargasso—*i.e.*, the gyrals of the South Atlantic, North Pacific, and South Pacific.

Ketchum (1951) has also reviewed the rates of total organic production estimated by various workers. These can be converted to rates of oxygen production by using Redfield's (1934) or Fleming's (1940) equivalents, from which most of the rates of organic production were originally computed (Table 3).

If natural, mixed plankton is used in these experiments, the respiration of the

TABLE 2.—*Depths at which the photosynthetic and respiratory rates are equal (compensation depth) at various locations*

Location	Date	Compensation depth (Meters)	Reference
Sargasso Sea	August	100*	Clarke (1936)
Georges Bank	June max.	59**	Clarke (1946)
English Channel	July	45†	Jenkin (1937)
Gulf of Maine	June	24–30*	Clarke and Oster (1934)
Loch Striven	Summer	20–30†	Marshall and Orr (1928)
Passamaquoddy Bay	Summer	17*	Gran and Braarud (1935)
Puget Sound	Summer	10–18*	Gran and Thompson (1930)
Oslo Fjord	March	10*	Gaarder and Gran (1927)
Georges Bank	April min.	9**	Clarke (1946)
Woods Hole Harbor	August	7*	Clarke and Oster (1934)
Loch Striven	March	5†	Marshall and Orr (1928)
Helsingør Sound	Annual range	4.5–7†	Steeman Nielsen (1937)
Great South Bay Long Island	July-August	0.8–2.1†	Unpublished observations

* Exposed for short periods during daylight only

† Exposed for 24-hour period

** Calculated from incident light and transparency

TABLE 3.—*Total oxygen production from various estimates*

Computed from estimates of total organic production from Ketchum (1951).

Location	Production	Reference
English Channel	72.5–188 × 10^3 ml. O/m^2/6 mos.	Harvey (1945)
Long Island Sound	177–1861 × 10^3 ml. O/m^2/ year	Riley (1941)
Western Atlantic		
28°–38°N.	986 × 10^3 ml. O/m^2/ year	Riley (1941)
38°–41°N.	595 × 10^3 ml. O/m^2/ year	Riley (1941)
28°–41°N.	260–986 × 10^3 ml. O/m^2/ year	Riley (1941)
3°–12°N.	517 × 10^3 ml. O/m^2/ year	Seiwell (1935)
Pacific, off S. Cal.	400 × 10^3 ml. O/m^2/ year	Sverdrup and Fleming (1941)
Gulf of Maine	223 × 10^3 ml. O/m^2/ year	Redfield *et al.* (1937)*
Barents Sea	316 × 10^3 ml. O/m^2/ year	Kreps and Verjbinskaya (1932)
Helsingør Sound	82 × 10^3 ml. O/m^2/ year	Steemann Nielsen (1937)

* Calculated for this table using the C:P ratio of 100:2.5

animals is added to that of the plants, so some investigators have used phytoplankton cultures, in order to find the depth at which photosynthesis just balances plant respiration (Jenkin, 1937; and others). In either case, it is assumed that the respiratory rates of both the plants and animals are unaffected by light. Steemann Nielsen (1952) holds that this assumption is not valid and that errors in the light- and dark-bottle method are so great that, where the numbers of organisms and oxygen changes are small, the results are invalidated. However, Ryther and Vaccaro (1954) have compared rates of biological activity as measured by oxygen changes and as measured by radioactive carbon (C^{14}) uptake by plankton organisms (as advocated by Steemann Nielsen); in actively growing cultures of phytoplankton they found only small differences in the results of the two methods. In regions where phytoplankton populations and productivity are small, there are consistently large differences in the results of the two methods. Ryther (unpublished results) has made observations of productivity in bacteria-free cultures that lead him to conclude that a portion of the photosynthetically bound C^{14} is quickly expelled by the respiration; when photosynthesis is small, this may amount to a large fraction of the total radiocarbon involved. He concludes that the C^{14} method measures *net* photosynthesis, and the oxygen method measures *gross* photosynthesis.

Rates of oxygen changes have been determined directly in very few parts of the world, and such wide variations have been found that it is impossible to estimate the oceanic production or to draw any accurate general conclusions concerning the consumption of oxygen (or total organic production). Riley (1939) found that the mean oxygen production in the northern waters between Cuba and Woods Hole, Massachusetts, was about 0.18 mg per liter per day, about twice that found in the tropical waters. However, he suggests that, because of the greater transparency of the southern waters, the maximum depth of photosynthesis is about three times as great as in the north, and that the total oxygen production in southern waters may equal or exceed that of northern waters.

BIOLOGICAL CONSUMPTION OF OXYGEN

At all depths of the ocean, oxygen is consumed by the respiration of plants and animals, including bacteria. The consumption is limited by the amount of organic matter (except for small amounts reacting with Fe^{II}, Mn^{II}, Mn^{III}, etc.) which can be produced in the water, and in the open ocean is so balanced by ventilating processes that the oxygen supply is never completely exhausted. However, in the Black Sea, threshold fjords, and other arms of the sea, hydrographic conditions are such that the oxygen is completely consumed, and anaerobic metabolism of bacteria produces sulfides. These regions are invariably characterized by hydrographic traps into which disproportionately large amounts of organic material, with its attendant reducing capacity, collect. Nikitin (1931) found that in the Black Sea, at depths greater than about 200 meters, oxygen was absent; hydrogen sulfide was present and increased from 1.48 ml/liter at 300 meters to 6.17 ml/liter at 1500 meters. There is no free circulation of the deep water of the Black Sea; its only connection with the Mediterranean is the shallow Bosporus. Fresh-water tributaries enter the sea, and their waters flow out as a shallow surface layer. During their stay in the region, their inorganic nutrients are consumed by growing plankton organisms. These settle through to the stagnant underlying layers, continually adding organic matter to the deeper parts of the basin. Oxygen consumption far exceeds its supply, and in the absence of oxygen anaerobic bacteria continue to decompose the organic matter with the formation of sulfides. (*See* Chapter 25.)

The direct measurement of rates of oxygen consumption is difficult or impossible in the deep sea. Laboratory experiments, in which the oxygen consumption is observed over a period of time, represent static conditions, rather than the dynamic systems of the seas, and more nearly measure the oxygen-consuming potential of a parcel of water than the rate at which oxygen consumption proceeds in nature. Seiwell (1937c) incubated samples of sea water from various depths for 11 days and found that the average daily oxygen consumption was 0.122 cc per liter at 24°C. and 0.0487 cc/liter at 11°C. He realized that these rates were probably much higher than those in nature, and Rakestraw (1947) found that the rates of consumption are higher in the earlier stages of incubation than they are later on. Bacterial growth is accelerated when a surface is presented (Waksmann and Renn, 1936; ZoBell and Anderson, 1936), accounting for the rapid consumption of oxygen in the first few days. Seiwell's work indicated that the amount of oxygen consumed was roughly proportional to the oxygen concentration found at the depth from which the samples were taken.

Rakestraw incubated water samples from the surface, the oxygen minimum layer, and from deep water, at temperatures near those found at the depths from which they were taken. Rates of consumption decreased rapidly with time, and in all cases stopped after 50 days. The highest rates of consumption in waters of subsurface origin, 0.025 ml/liter per day at 8–9°C. for water from the oxygen minimum layer, and 0.035 ml/liter per day at 4–5°C. for deep water, were observed during the first 2 days. Increased temperatures resulted in increased oxygen consumption. The total amounts of oxygen consumed were about 0.5 to 1.0 ml/liter (8–25 per cent of the original oxygen) in the surface samples and 0.15 to 0.4 ml/liter (1–4 per cent of the original) in the subsurface samples. The rapid changer in rates of consumption observed in the early stages of *in vitro* captivity would not be expected in nature, because, to maintain a steady state, such changes have to be balanced by corresponding changes in rates of replenishment, which, in the depths of the ocean, would require improbably large changes in the velocity of water movements.

A quasi-direct estimation of the rate of oxygen consumption was made by Redfield (Rossby, 1936), who observed the changes in oxygen content below 200 meters in a stagnant pool of water below sill depth in the Gulf of Maine. He estimated that the annual oxygen consumption there was 0.36 ml/liter. E. F. Thompson (1939) estimated that the annual consumption of oxygen was 2 ml/liter in the Red Sea.

Rates of biological consumption of oxygen can also be estimated indirectly. One can calculate the oxygen content which will result from physical and hydrographic forces acting on water masses. The difference between this quantity and the amount of oxygen actually present is assumed to be the result of biological activity. If the rate at which the physical and hydrographic changes have taken place can be evaluated, then the rate of biological changes in the oxygen content can be estimated. Physical and hydrographic changes, including mixing and velocities, can be evaluated from the salinity, temperature, and density distribution. In the superficial layers of the sea, current velocities can be estimated with considerable accuracy, either directly or by the application of the theorems of physical oceanography, but, at great depths, reliable estimates of the velocities of water movements cannot now be made with precision.

Sverdrup and Fleming (1941) estimated rates of biological consumption (and production) off the coast of California by an application of the above principles. In the region studied, two water masses, one of northern, one of southern origin and each having characteristic temperature-oxygen and temperature-salinity correlations, enter a region between 32 and 35°N., and mix. The *T-S* and *T-O* correlations were used to compute the proportions of the parent water masses in the mixtures and the oxygen content which should be present if it were unaltered by continuing biological activity. The oxygen concentrations actually observed varied in a systematic way from those expected on the basis of simple mixing along isopycnals; the anomalies were attributed to photosynthesis and biological consumption. The velocities of the water masses were computed; they indicated that, in a water column of 1 sq. cm cross section reaching from a depth of 50 to 700 meters, oxygen was consumed at the rate of 0.11 to 0.22 ml per day, or 0.000169 to 0.000338 ml per liter per day. Other results are summarized in Table 4.

Rates of oxygen consumption in the Atlantic Ocean have been estimated by Riley (1951). He analyzed, statistically, the physical oceanographic observations available from the Atlantic Ocean, and from them computed current velocities and lateral and vertical coefficients of eddy diffusivity. These values were then used to compute the effects of physical processes on the distribution of oxygen, phosphate, and nitrate. Knowing the observed oxygen content, and the effect which physical proc-

TABLE 4.—*Rates of oxygen consumption off the California Coast*
From Sverdrup and Fleming (1941)

Depth, meters	O_2 consumption
200	1.8 ml/liter/year
400	0.6 ml/liter/year
700	0.05 ml/liter/year
50–700 (range)	3580 milligram atoms O_2/M^2/year

TABLE 5.—*Rates of oxygen consumption in the Atlantic Ocean*
From Riley (1951)

Sigma$_t$	Mean depth (Meters)	O_2 consumption ml/liter/year	Depth range (Meters)	O_2 consumption mg-at/M^t/year
26.5	200	.21	200–1250	3780
26.7	280	.08	1250–4250	145
26.9	370	.050	>4250	33
27.1	510	.055		
27.3	700	.035		
27.5	1000	.013		
27.7	1250	.005		
	1500	.0016		
	2000	.0013		
	2500–4000	.00013		

esses had had on it, he could compute rates of biological changes which had to act to maintain a steady state distribution. These rates were estimated for a series of sigma$_t$ (potential density) surfaces at mid-depths and in a north-south profile in the deep waters. Table 5 presents a summary of these rates of change.

Riley's estimates of rates of consumption are somewhat lower than those of Sverdrup and Fleming (Table 4), but they are of the same order of magnitude. On the other hand, they are much smaller than those made earlier by Seiwell (1934), who computed that the consumption within the oxygen-poor sratum of the western North Atlantic was 0.34 to 0.63 cc per liter per year—*i.e.*, 10–18 per cent of the oxygen present in the minimum layer appeared to be consumed each year. Seiwell's estimates were based on the assumption that maxima and minima observed in the average oxygen content of the layer between the 5° and 10° isotherms were annual. Riley (1951) pointed out that this assumption may not be valid, that Seiwell ignored possible effects of diffusion and transport normal to the profile analyzed, and that it is probably not valid to average the entire layer between the 5° and 10° isotherms. The rates Seiwell computed are about 10 times those computed by Riley (1951) and by Sverdrup and Fleming (1941) at comparable levels.

The apparent oxygen consumption in the oxygen-minimum layer indicates that it is the result of about 100 years' oxidation at the rates Riley calculated. His estimates of minimum rates in the deep water (2500–4000 m) indicate that oxidation has been continuing there for as much as 10,000 years. These estimates can be compared with Kulp's (1953) estimates of the age of ocean waters, made by carbon-14 age dating of the carbonate released from large water samples. Kulp's estimates range from 450 ± 150 years to 1950 ± 200 years (Table 6). There are uncertainties in the carbon-14 method, but it promises to be very useful in deducing the speed of deep-ocean circulation. Kulp's estimates and Riley's are not contradictory, but it can only be concluded that, between the oxygen-minimum layer and the bottom, oxygen consumption has continued for between 100 and 10,000 years. Kulp's

TABLE 6.—*Apparent ages of sea-water samples dated by carbon-14 content*
From Kulp (1953)

Location	Depth (Meters)	Apparent age (Years)
13°35′N.66°35′W.	Surface	Recent
19°24′N.78°33′W.	Surface	Recent
41°00′N.54°35′W.	Surface	Recent
38°42′N.67°54′W.	4,115	450 ± 150
63°46′N.00°26′W.	3,182	500 ± 200
34°56′N.68°14′W.	5,047	1,550 ± 300
35°46′N.69°05′W.	4,641	1,950 ± 200
58°19′N.32°57′W.	1,829	1,600 ± 130
53°53′N.21°06′W.	2,774	1,900 ± 150

figures indicate that the 10,000-year figure (which Riley designates as a maximum age) may be about five times too large.

It is interesting to compare Kulp's first, third, and fourth subsurface samples (Table 6); their locations are not too far apart, and neither are their depths, yet the first is dated at 450 ± 150 years, the latter two at 1550 ± 300 and 1950 ± 200 years, respectively. Salinity, temperature, and oxygen data are not available for these samples; they could be internally consistent if the younger sample represents lower North Atlantic deep water and the older sample the subantarctic bottom water of Wüst (1935, Beilage XXIII).

If Riley's estimates of rates of oxygen consumption are applied to Seiwell's data, an apparent age of the water in the oxygen-minimum layer can be derived. Riley estimated maximal rates (0.055 ml/liter/year) at the σ_t surface 27.1. Seiwell found the oxygen minimum at $\sigma_t = 27.23$, where the apparent oxygen consumption was 2.87 ml/liter (ATLANTIS station 2639, 35°07′N., 66°25′W., Seiwell, 1937b). Combination of these data indicates an apparent age of 52 years. This isentropic surface rises to a depth of 100 meters at about 50°N.—*i.e.*, the water in the minimum zone had traveled at least 15° of latitude (900 nautical miles), and the minimum average drift of the water was 17 nautical miles per year. Seiwell's assumptions led him to estimate that the southerly component of drift was 180 to 360 nautical miles per year.

Riley estimates that 90 per cent of the organic matter produced in the photic zone is consumed in a layer approximately 200 meters thick, and only the remaining 10 per cent is oxidized in the deeper waters. In the deep water, oxygen consumption doubtlessly proceeds very slowly indeed, which would be expected from the low temperatures and the paucity of both living organisms and dead organic matter. Probably wherever excess organic matter is present, biological consumption of oxygen can proceed more rapidly than mixing processes can replenish it. The fact that the deep waters are not anaerobic is further evidence that rates of consumption must be very slow because, to maintain a steady state, these must exactly equal the rate of oxygen replenishment, which can be brought about only by the slow circulation of deep waters. It is probable that rates of consumption depend, in final analysis, on the rates at which organic matter enters the system.

CIRCULATORY AND MIXING PROCESSES

Since the processes by which oxygen can be added to the ocean are confined to the surface layers, it is necessary to examine the processes of advection and diffusion, by which surface waters become distributed into and throughout the deeper layers.

The coefficients of molecular diffusion of oxygen in 1 per cent and 20 per cent sodium chloride are $1{,}98 \times 10^{-5}$ and 1.7×10^{-5} cm^2/sec respectively (Bruins, 1929).

Rates of this magnitude are negligible in accounting for transport of oxygen throughout the ocean, which must therefore depend upon the transport of water. This transport can be accomplished by advection, the mass movement of a body of water, or by eddy diffusion, in which transport of solutes is accomplished by mixing across concentration gradients. When mixing occurs across a concentration gradient, dS/dz, the same mixing coefficient, A, applies to all solutes, and the transport, T_s, is the product of this coefficient and the gradient:

$$T_S = A \frac{dS}{dz}$$

Replacement of oxygen to the deeper parts of the oceans (below the main thermocline) is probably brought about by advection, in which cold highly oxygenated water is formed and sinks in the high latitudes and is carried to greater depths and lower latitudes by subsequent lateral and vertical movements. Eddy diffusion along isentropic surfaces may also be important in this transport and is probably predominant above the main thermocline, but it is at present impossible to evaluate the relative importance of advection and diffusion on transport of oxygen. Both oxygen and surface-formed organic material will sink at the high latitudes, and the decomposition of this organic matter, accompanied by oxygen consumption, will proceed within the water mass.

Mixing can take place with the least change in potential energy and entropy along surfaces of equal potential density (isentropic surfaces), and it is generally accepted that, in the absence of vertical mixing, water flows along these surfaces (Montgomery, 1938). Analyses of the distribution of oxygen along isentropic surfaces have been made by Montgomery (1938) and Riley (1951). The former analysis was made as an aid in deducing the circulation in the upper layers of the Atlantic between the equator and 30°N. Riley's analysis enabled him to estimate the rates of biological changes in nonconservative properties. An isentropic analysis of the apparent oxygen utilization in a longitudinal section through the Atlantic from 60°N. to 60°S. was made by Redfield (1942).

These analyses show tongues of characteristic oxygen content extending along isentropic surfaces, with the oxygen content gradually changing in the direction of flow. Redfield's diagrams show a region of maximum oxygen utilization between 50°N. and about 15°S. Between the equator and about 25°N., it is deeper than the main thermocline and nearly concurrent with the salinity minimum which marks the Antarctic Intermediate water, but, south of the equator, the maximum in oxygen utilization lies somewhat above this salinity minimum. In all latitudes, oxygen utilization is maximal between the surfaces $\sigma_t = 27.0$ and 27.25. Montgomery's figures extend no deeper than the surface $\sigma_t = 27.0$, but they clearly show how the lowest oxygen concentrations in the upper layers arise in the eastern tropical Atlantic, extend westward, and are eroded horizontally by mixing along isentropic surfaces.

The distribution of oxygen in a detailed section across the Gulf Stream (Fig. 3) shows that, in the upper layers, the waters of the Stream contain up to 2.5 ml/liter less oxygen than do adjacent waters of the same density, but this oxygen-poor water

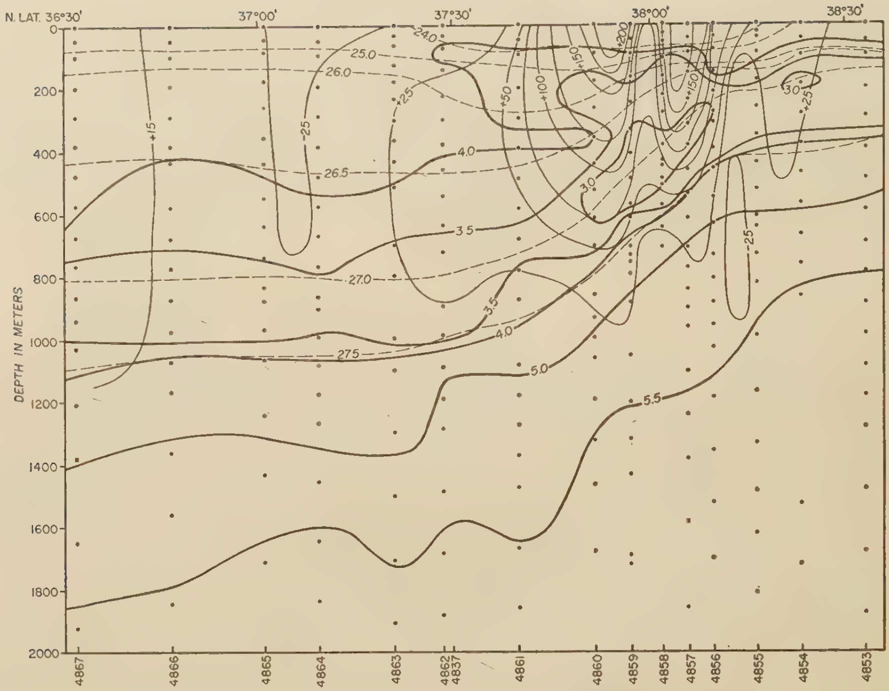

FIGURE 3.—*Oxygen, ml/liter, σ_t, and velocity in cm/sec., in a detailed section across the Gulf Stream*

Oxygen range, <3.5 to >5.5 ml/liter, σ_t range <24.0 to >27.5, velocity range −25 to +200 cm/sec. The figure shows oxygen concentrations of less than 4.0 ml/l at densities less than 26.5 in the region of high current velocities, but not in regions outside the main body of the Gulf Stream—*i.e.*, where velocities are less than about 25 cm/sec. Current velocity data from Worthington (1953).

is in the process of spreading out and mixing, along σ_t surfaces, with the waters on either side. An unpublished section extending south from the tail of the Grand Banks across the Gulf Stream system indicates that oxygen-poor waters are still present, but in smaller amounts, having been reoxygenated by mixing both quasi-horizontally along σ_t surfaces and vertically.

The ease of vertical mixing is inversely related to the stability of the water column, which is nearly proportional to the vertical rate of change in density. The depth to which vertical mixing is effective in the surface layers is reflected in the thickness of the surface layer of homogeneous oxygen content and the depth of the seasonal thermocline. Evaluation of the magnitude of vertical-mixing processes in deeper waters is a difficult problem, but according to Riley (1951) vertical transport is more important than lateral transport in the replenishment of oxygen to the deep parts of the ocean.

The importance of stability to the distribution of oxygen has been shown by Wattenberg (1938, Beilage I). In the southern Atlantic, the oxygen content in the core of the minimum layer decreases as the stability increases—*i.e.*, it tends to retain its low-oxygen concentration best when the stability is great and vertical mixing requires more energy. Wattenberg has also shown (1938, Beilage II) that the depth at which the oxygen minimum occurs is great where the stability is small. This is most apparent in the southern convergences.

In this connection, Montgomery (1939) states that the potential-density layers reaching the sea surface in regions of strong convergence may be expected to be thicker (less stable) than those reaching the surface in regions of weak or negative convergence. He concluded, from studying METEOR data, that in certain cases layers of relatively low stability can be attributed to strong convergence at their intersection with the surface, and that these layers have high-oxygen content.

Horizontal and vertical mixing effects are reflected in the shape of the low-oxygen zones extending westward from the west coast of Africa and the Gulf of Panama. Formed near the coasts in dynamic systems flowing generally westward, vertical mixing tends to decrease their thickness, while mixing along isentropic surfaces tends to decrease their latitudinal extent. The zones become thinner, more oxygenated, and cover less and less latitude as they extend westward. Figure 4 shows the shape of the oxygen minimum zone, at whatever depth it occurred, as observed in the Atlantic by ATLANTIS and ALBATROSS III during January to April and in December 1952, and demonstrates the effect of mixing along the westward course of these

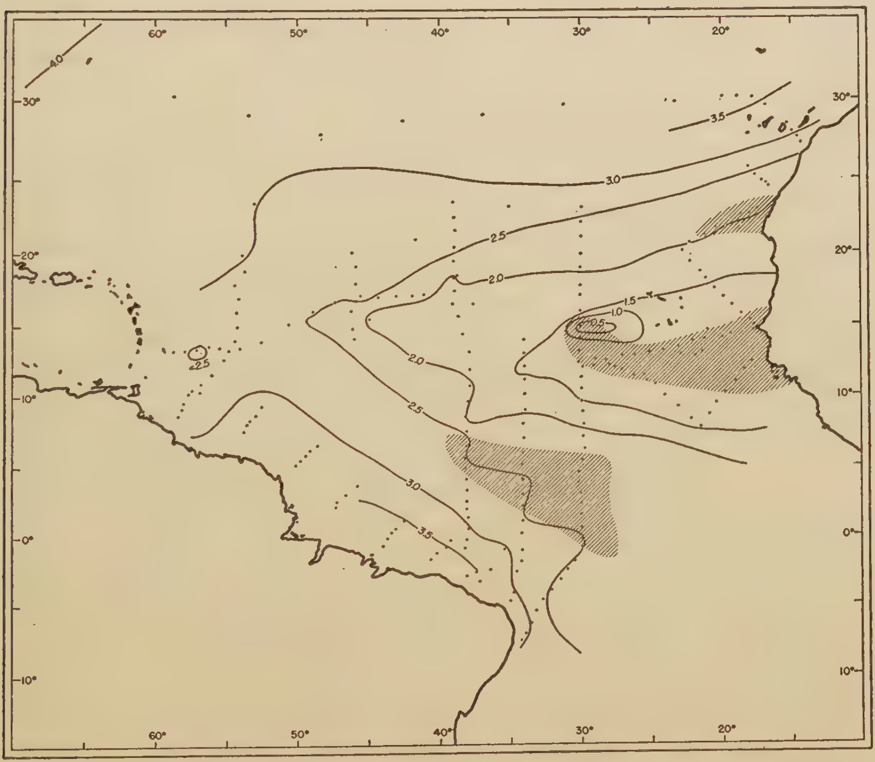

FIGURE 4.—*Minimum oxygen content (ml/liter) at whatever depth it occurred, in the Atlantic Ocean*

As observed by the ATLANTIS and ALBATROSS III January–April and December 1952. Double minima were found in the shaded areas.

waters. These effects are also shown in Montgomery's (1938) charts of the distribution of oxygen along isentropic surfaces. Along the surface $\sigma_t = 27.0$, oxygen concentrations of less than 2 ml/liter are found in a region covering about 20° of latitude at 20°W., but at 40°W. they extend over only 2° or 3° of latitude, and at about 48°W. they disappear. The zone becomes thinner and covers less latitude with increasing distance westward. Examination of data from the oxygen-poor zone in the tropical Pacific shows a similar erosion of the minimum zone by lateral and vertical mixing processes.

Riley (1951) has attempted to assess transport and mixing rates and the rates of biological change in oxygen content necessary to balance them and maintain a steady state distribution. In the steady state

$$AX + K'Z - V + R = 0$$

where AX and $K'Z$ are the net rates of increase caused by lateral and vertical diffusion, respectively, V is the net rate of increase caused by both lateral and vertical advection, and R is the net rate of increase caused by biological change. Riley's statistical values of these rates of change of oxygen in the upper layers are shown in Table 7.

Negative values for the effect of vertical sheer and a maximum (negative) value of advection are found at $\sigma_t = 27.3$—*i.e.*, near the statistical value of the density at the oxygen minimum (Seiwell, 1937b) and show the tendency of vertical mixing and advection to erode the oxygen-minimum zone.

Riley's analysis of the deep and bottom waters was simplified to consideration of a north-south vertical profile, so that only one component of horizontal velocity was involved. With the exception of one value (0.25×10^{-4} cm/sec at the 3500–4000 meter depth at 45°–54°S.) vertical velocity ranges from .15 (downward) through zero to $-.15$ (upward) $\times 10^{-4}$ cm/sec at depths greater than 1000–1500 meters (Riley, 1951, Table XIV). Coefficients of vertical eddy diffusivity were approximated by Riley (1951, Table XVII), and represent results of an important attempt to establish the order of magnitude of the effects of the various physical and biological processes on oxygen in the ocean. The scarcity of data makes it difficult to determine the reli-

TABLE 7.—*Statistical values of net rates of diffusive, advective, and biological change in oxygen in the upper layers of the Atlantic Ocean*

From Riley (1951)

σ_t	AX	K'Z	V	R
26.5	9.4	13.5	−44.4	−67.3
26.7	2.7	9.9	−12.6	−25.2
26.9	2.0	10.9	−3.5	−16.4
27.1	1.7	6.1	−9.3	−17.1
27.3	.3	−8.1	−19.2	−11.4
27.5	.3	−.4	−4.3	−4.2
27.7	.2	.1	−1.0	−1.3

Values are ml/liter $\times 10^{-10}$ per second.

ability of the estimates, but no direct methods are available for measuring these quantities in the deep oceans, and Riley has attempted to estimate them indirectly from the spatial distributions of salinity, temperature, and the concentrations of oxygen and other nonconservative elements, which have been observed.

It should be emphasized that the assumption of a steady state may not be valid, especially in deep waters. Worthington (1954) has presented preliminary evidence of possible secular changes in the oxygen concentration of the North Atlantic Deep water which supports the hypothesis that deep-water formation is catastrophic in nature—the very opposite to a steady-state model. Worthington's studies indicate that there has been a decline of about 0.3 ml/liter in the over-all oxygen content of the North Atlantic Deep water in the past 2–3 decades. That this is a real decline and not attributable to systematic errors in the oxygen determinations is attested by the fact that comparative data for the Mediterranean show no comparable decrease in the oxygen content there. This decline represents an annual loss of 0.015 ml/liter and, upon extrapolation to fully saturated water, leads to the date 1810 for the formation of this water mass. The decade 1810–1820 was one of catastrophically low temperatures in the high latitudes, and Worthington proposes that a vast mass of North Atlantic Deep water was formed at that time. This implies that a large mass of the deep water is essentially stagnant, and it could be assumed that it will become anaerobic, unless replaced by a future catastrophe or mixed away by slow convective processes. This also introduces the corollary possibility that large areas of deep-ocean waters may have been anaerobic in the past, but we know of no evidence to support or refute this possibility.

RELATIONSHIPS BETWEEN OXYGEN CONTENT AND PHYSICAL PROPERTIES OF SEA WATER

In the study of the oceans it is useful to identify or characterize water masses by correlations between their conservative properties. The temperature-salinity correlation (Helland-Hansen, 1916) is one of the most useful and most uniform characteristics. However, nonconservative properties change, *in situ*, by biochemical processes, altering correlations between non-conservative and conservative properties without mixing. On the other hand, a non-conservative property may distinguish one water mass from another in which the conservative properties are quite similar, or may help in the study of dynamic relationships within a single water mass.

Rossby (1936) used the oxygen-salinity correlation as a quasi-conservative property of the Gulf Stream; he found it more useful than the salinity-temperature correlation in studying exchanges between the stream and the surrounding waters (Fig. 5). The salinity-temperature correlation was too conservative to distinguish between the waters of the Gulf Stream on one hand and of the Sargasso Sea and Western Atlantic Slope water on the other. Although the oxygen-salinity correlation changed along the course of the stream, it was characteristic and distinctive in sections normal to the stream.

A study of the oxygen-density (σ_t) correlation in the waters of the western North Atlantic, particularly in the Gulf Stream system, has been made by Redfield and the author (Figs. 3, 6). In a near-surface layer, the oxygen content of the Gulf Stream

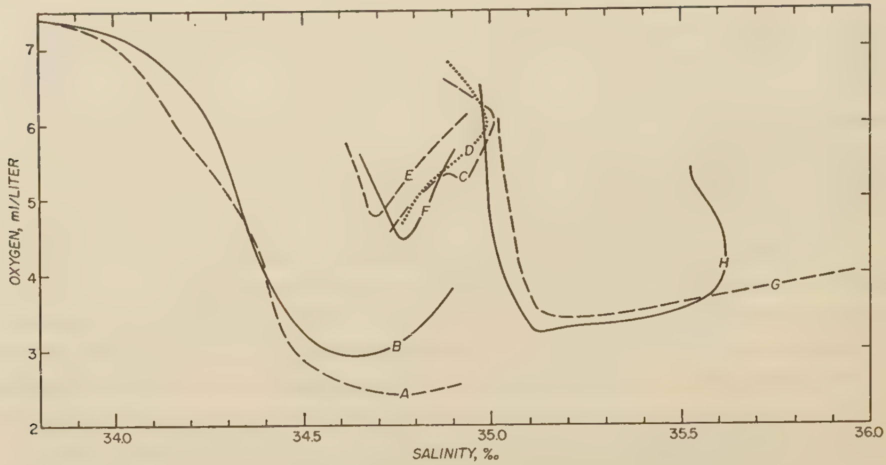

FIGURE 5.—*Characteristic oxygen-salinity correlations*, S = f(O_2)
A. Core of Subantarctic Intermediate Water, Eastern Atlantic
B. Core of Subantarctic Intermediate Water, Western Atlantic
C. Core of Intermediate Deep Water, Eastern Atlantic
D. Core of Intermediate Deep Water, Western Atlantic
E. Antarctic Bottom Water, Eastern Atlantic Basin
F. Antarctic Bottom Water, Western Atlantic Basin
A, B, C, D, E and F redrawn from Wüst (1935)
G. North Atlantic Slope Water
H. Western Sargasso Sea
G and H redrawn from Rossby (1936)

is as much as 2.5 ml/liter lower than that of adjacent Sargasso Sea waters of the same density, in the σ_t range 24.0 to 26.5 (Fig. 6 c). At greater densities, the waters are indistinguishable from those of the Sargasso Sea. Three detailed cross sections of the Gulf Stream have been made and analyzed; these show oxygen-low waters centered at about the maximum current velocities in the stream (Fig. 3). It is indicated that the waters of the Gulf Stream left their origins in the Caribbean and equatorial Atlantic regions with a characteristically low-oxygen content, which is persistent at least as far as the tail of the Grand Banks. This correlation with density seems particularly useful because horizontal mixing can take place most readily along isopycnals.

Other workers have used correlations between the oxygen content and other conservative properties. Jacobsen (1929) plotted percentage saturation against salinity, but, since percentage saturation depends on salinity as well as temperature, it does not appear to be suitable as a characteristic diagram (Montgomery, 1938). Oxygen content was plotted against salinity by Wüst (Fig. 5) to show the correlation between these properties in several water masses of the Atlantic. Seiwell (1937a, Fig. 8) found that at one station which was occupied for 60 hours, the oxygen-salinity correlation behaved essentially as if oxygen were a conservative property at all depths greater than 100 meters. Dietrich (1937) plotted oxygen against temperature (Fig. 7) and showed that the oxygen content varied as much as 2.4 ml/liter at about 13°C. in 12

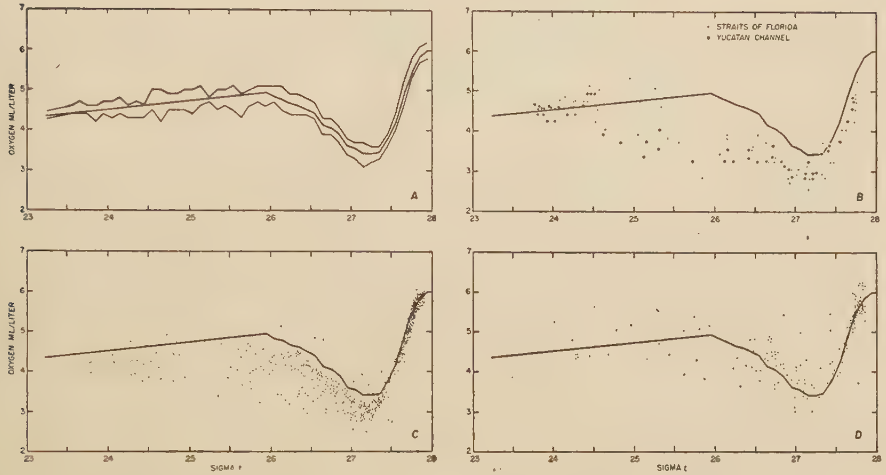

FIGURE 6.—*Oxygen-*σ_t *correlations,* $\sigma_t = f(O_2)$, *in A, the Western Sargasso Sea; B, the Yucatan Channe and Straits of Florida; C the Gulf Stream system between 36° and 39° N., and D southeast of the Grand Banks, between 39° and 45° N., and 45° to 50°W.*

The correlation in A is from all observations in the Sargasso Sea between 30 and 40°N latitude. The envelope contains half of all observations made in this area. Between σ_t values of 23.1 and 25.95 the correlation (heavy line) is the least-squares regression; at greater values, the arithmetic mean of all observations. In B, C, and D, the correlation shown in A is repeated. The lower oxygen content of the samples having σ_t values between about 24 and 26.5 is characteristic of the southern waters, but water of these same characteristics was observed in the Gulf Stream system southeast of the Grand Banks.

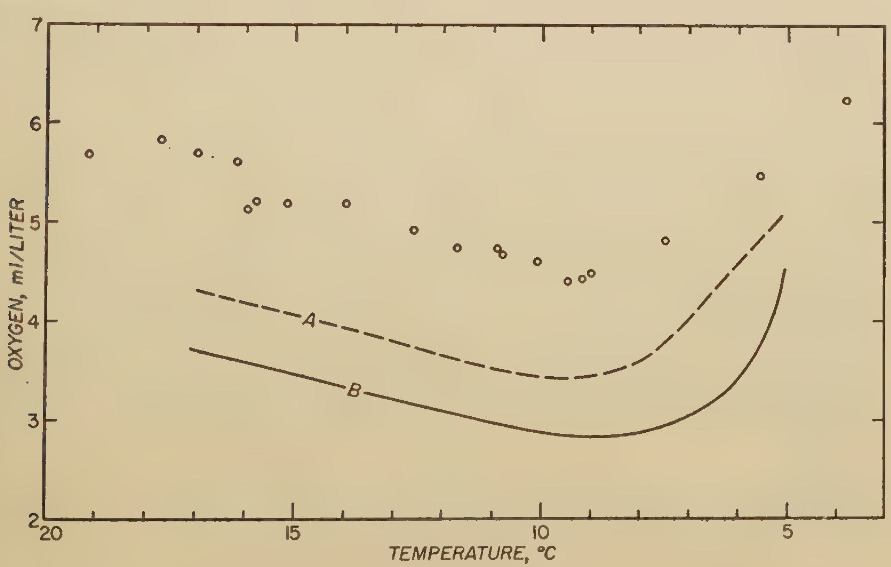

FIGURE 7.—*Characteristic oxygen-temperature correlations,* $T = f(O_2)$

A, Western North Atlantic and B, Western Caribbean Sea and Florida Strait, redrawn from Dietrich (1937). Circles are values observed at DANA station 1369, 12 June, 1922, near the Azores, 35° 44′N., 29°33′W., data from Schmidt (1929).

stations between Chesapeake Bay and Bermuda, but at the oxygen minimum, which uniformly occurred very close to 10°C., it varied only about 0.6 ml/liter. Between Bermuda and the Azores, the minimum was found at about the same temperature, but at all temperatures the water contained less oxygen than in the Chesapeake Bay-Bermuda section. In stations through the Caribbean to the Straits of Florida, the oxygen at any one temperature decreased as much as 0.4 ml/liter along this course. Other diagrams by Dietrich show the lowest oxygen at a given temperature in the waters south and east of Bermuda and in the Caribbean and Gulf Stream, with the Sargasso waters immediately adjacent to the latter containing considerably more oxygen. Oxygen was plotted against density by Riley (1951) to enable him to determine the characteristic oxygen content of the Atlantic at discrete σ_t surfaces of areas bounded by parallels and meridians with their centers 1000 kilometers apart (Riley 1951, Fig. 11). Miyake (1948) used oxygen-chlorinity correlations to evaluate the effect of the mixing of two water masses on the diurnal variation in the oxygen content of shallow waters.

In addition to these characteristic correlations, Seiwell (1937b) established statistically that in the western North Atlantic the oxygen minimum occurred at that depth where σ_t was 27.23. Sverdrup and Fleming (1941) noted that this was near the density at which the minimum was found, on the average, off the California coast but declined to comment on any possible significance in this relatively close agreement. The main oxygen minimum is also found near this density in most of the central Indian Ocean (data of Bruneau *et al.*, 1953).

Seiwell (1937b) also studied the value of the salinity anomaly at the depth of the oxygen minimum in the western North Atlantic. According to Helland-Hansen (1930) the normal temperature-salinity relationship for the northern North Atlantic is

$$S_t‰ = 34.737 + 0.038t + 0.0029t^2$$

and the salinity anomaly is

$$SA = 100(S‰ - S_t‰).$$

Seiwell used these equations to compute the mean salinity anomaly at the depth of the oxygen minimum; he found a systematic distribution of these values in the western North Atlantic. He attributed high negative anomalies (*i.e.*, salinities lower than normal) to waters of subantarctic origin; these were associated with low minimum oxygen contents. A tongue of high positive anomalies was attributed to waters of Mediteranean origin, and these had relatively high oxygen contents in the minimum layer.

RELATIONSHIPS BETWEEN BIOLOGICAL CHANGES IN DISSOLVED OXYGEN AND OTHER CHEMICAL CONSTITUENTS

The rates at which biological changes in the oxygen content of sea water take place were discussed in an earlier section. Physiologically, these changes are accompanied by concurrent changes in the other elements which constitute living matter. Oxygen is involved in the photosynthetic formation and respiratory decomposition of carbohydrate, as represented by the simple reversible equation

$$CO_2 + H_2O \underset{respiration}{\overset{photosynthesis}{\rightleftarrows}} CH_2O + O_2.$$

However, the bodies of plants and animals do not consist exclusively of carbohydrate. Nitrogen, phosphorus, sodium, calcium, potassium, iron, chlorine, sulfur, and other elements (especially silicon in the marine environment) are also involved in the processes of formation and decomposition of living tissue. It follows that the above equation should be accompanied by a series of equations showing the fixation and release of nitrogen, phosphorus, and the other elements in definite proportions to the amount of oxygen released and consumed. These proportions will depend upon the composition of the living matter.

Redfield's (1934) study of the proportions in which phosphate and nitrate occur in sea water revealed that these two elements are found in statistically definite proportions one to another, suggesting that the deep water contains the products of the complete oxidation of varying amounts of organic matter of similar composition. Further studies showed a close correspondence between the ratios in which changes in the concentrations of nitrogen and phosphorus take place in sea water and the ratios in which they occur in plankton organisms. Redfield was also able to show statistically significant correlations between changes in total carbon dioxide, the amount of oxygen consumed, and the concentrations of phosphate and nitrate. He concluded that carbon dioxide, phosphate, nitrate, and oxygen are bound and released in statistically definite proportions during the formation and decomposition of organic matter in the sea.

The ratios reported by Redfield were O:C:N:P = 239:140:20:1 by atoms. This O:C ratio is smaller than the theoretical 2:1 ratio involved in the formation of carbohydrate, which Gilson (1937) suggested should be increased by about 20 per cent to allow for the oxidation and reduction of nitrogen. On the other hand, investigations by Sargent and Hindman (1943) indicated that, during the active photosynthetic period, the correspondence between moles of CO_2 absorbed and O_2 evolved was not significantly different from 1. Redfield pointed out that the available estimates of changes in the total carbon-dioxide content of sea water were not very precise.

Cooper (1938) showed that the phosphate figures used by Redfield should be corrected for the analytical error known as the salt effect. Sverdrup *et al.* (1942, p. 236) applied the salt-effect correction and, using the ratio O:C = 2:1, settled on the ratios O:C:N:P = 212:106:16:1 by atoms or 109:41:7.2:1 by weight. These relationships are shown schematically in Figure 8.

Deviations (other than statistical) from these ratios would be expected and are found. In surface waters, particularly near shore, land drainage and other features can appreciably affect the composition. Variations in the composition of plankton populations will affect the ratios of the elements in their decomposition products, and nitrogen and phosphorus compounds are not necessarily released in the same ratio in which they are found in the whole organism. Phosphate is released by living zooplankton (Gardiner, 1937), and nitrogen is excreted rapidly by copepods fed on

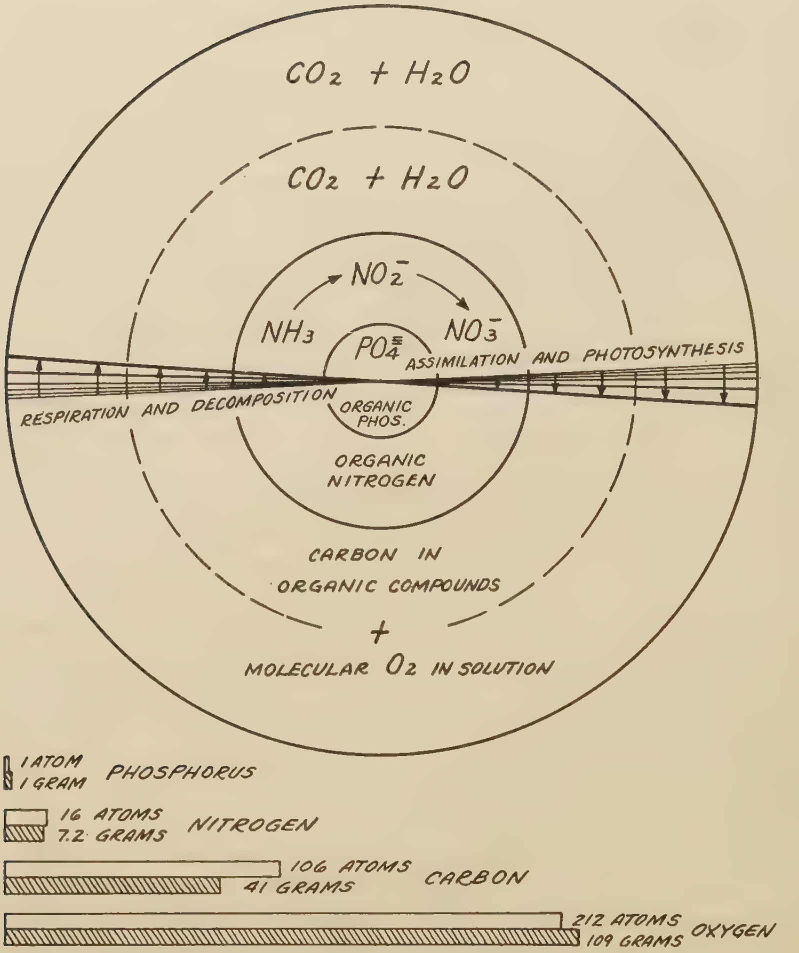
$CO_2 + H_2O$
$CO_2 + H_2O$
NO_2^-
NH_3
NO_3^-
$PO_4^{\equiv}$
ASSIMILATION AND PHOTOSYNTHESIS
RESPIRATION AND DECOMPOSITION
ORGANIC PHOS.
ORGANIC NITROGEN
CARBON IN ORGANIC COMPOUNDS
+
MOLECULAR O_2 IN SOLUTION
1 ATOM
1 GRAM
PHOSPHORUS
16 ATOMS
7.2 GRAMS
NITROGEN
106 ATOMS
41 GRAMS
CARBON
212 ATOMS
109 GRAMS
OXYGEN

FIGURE 8.—*Representation of the average proportions in which oxygen, carbon, nitrogen, and phosphorus are bound and released by biological processes in the sea*

diatoms (Fuller, 1937). There are doubtlessly other mechanisms by which nitrate or phosphate are released to the water without involving oxygen and carbon dioxide in the statistically normal ratios; refractory compounds may retain one or the other of these elements in bound form, and local concentrations of phosphate may be out of proportion to the concentration of nitrate or the accompanying oxygen consumption. It is probable that in the deeper parts of the ocean, however, oxidation goes essentially to completion and only minute quantities of relatively stable organic compounds are present in the water at any one time. It is here that the ratios hold most reliably.

Even in deep waters, major deviations between the phosphate or nitrate concentrations and the apparent oxygen consumption are found. Redfield (1934) found this true of deep waters having their origins in the convergences in high latitudes. These deviations are the result of the fact that these waters are fully oxygenated when they sink from the surface of the sea, but contain appreciable quantities of inorganic nitrate and phosphate, contrary to the situation in most saturated surface waters, in which virtually all the phosphorus and nitrogen are bound in organic compounds. The former circumstance leads to subsurface water containing larger amounts of nitrate and phosphate than would be computed from the apparent oxygen consumption. Redfield (1942) referred to these excesses as "preformed" and computed that the surface waters from 20° to 60°N. contained over 1 milligram atom per cubic meter of preformed phosphate, assuming the relationship

$$O_2(ml/liter) = 0.373\ mga\ P/M^3.$$

This relationship yields negative values in the upper layers from 48°N to 33°S., however, and Riley (1951) pointed out that this can only mean that Redfield over-rated the phosphate regeneration ratio.

Riley (1951) computed a series of nitrogen and phosphorus oxidative ratios for different levels in the Atlantic Ocean. These ratios are highly variable, but they indicate that the O:P ratio is large in the neighborhood of the oxygen-minimum layer. However, the average ratio he computed for the water column between σ_t 26.5 and the bottom is O:P = 255:1 compared with the ratio O:P = 239:1 which Redfield used and the ratio 212:1 which Sverdrup *et al.* (1942) settled on. The numbers empirically arrived at by Riley and Redfield both tend to substantiate Gilson's (1937) factor of 20 per cent additional oxygen needed to oxidize nitrogen compounds, which would require a ratio of O:P = 264:1 by atoms.

The ratios in which oxygen, carbon dioxide, phosphate, and nitrogen are bound and released correspond, statistically and approximately, to the chemical law of combining proportions and enable one to make quasi-stoichiometric computations relating these variables. Oxygen and carbon dioxide are radically changed by exchanges with the atmosphere, but this is not the case with phosphate and nitrate. Thus it is possible, by observing changes in phosphate and nitrate, to assess the extent of biological changes in the oxygen and carbon-dioxide content; and to distinguish them from changes attributable to exchanges with the atmosphere; these principles were used by Redfield (1942) to estimate the exchanges of oxygen across the sea surface, as discussed in a previous section.

Ecologically, these biochemical relationships between dissolved oxygen and the nutrient salts should be more useful, in describing changes in the environment, than a consideration of dissolved oxygen alone. The world-wide distribution of dissolved oxygen is better known than is the distribution of the other nonconservative properties, and, although in most parts of the world ocean the concentration of dissolved oxygen is not important as a factor in limiting the growth of populations, it is functionally linked to the concentrations of nitrate and phosphate, which may become limiting factors.

ORIGIN OF THE OXYGEN-MINIMUM ZONE

The widespread occurrence of minimum concentrations of oxygen at intermediate depths is probably the most striking feature of the distribution of oxygen. Although these minima have counterparts in maximum concentrations of phosphate and nitrate at intermediate (usually somewhat greater) depths, the oxygen feature has received much attention in attempts to explain its *raisons d'etre*. Many oceanographers, beginning with J. P. Jacobsen (1916) and including Wattenberg (1929; 1938; 1939b), Le Danois (1934), Wüst (1935), and Seiwell (1937b; 1937d; 1937e) have offered explanations. These were examined on theoretical bases by Sverdrup (1938), who, with Seiwell, distinguished two basic explanatory concepts. The first, proposed by Jacobsen and held to by Wüst and Dietrich (1936) and supported by Parr (1939), was that the minima (and maxima) are dynamically conditioned by circulatory processes; the intermediate oxygen minima characterize nearly resting boundary layers between different branches of the deep-sea circulation (Wüst), and at the oxygen minimum the replenishment of oxygen by mixing and circulatory processes is at a minimum. Le Danois referred to the very poorly oxygenated zones of the Atlantic and Pacific as fossil waters, implying essentially no circulation. The second concept, held mainly by Seiwell, proposed that the oxygen minimum zone is conditioned chiefly biochemically and represents the depth at which the specific gravity relationships between sea water and sinking detritus are such that the detritus accumulates at intermediate depths, resulting in excessive oxygen consumption at these levels.

Seiwell (1937b) and Sverdrup (1938) point out that in the Gulf Stream System the oxygen-minimum zone does not coincide with a minimum in the mixing and horizontal replenishment processes, and Sverdrup shows that the dynamic explanation requires that (1) the consumption of oxygen must be independent of the amount of oxygen-consuming organic matter, or (2) the amount of oxygen-consuming matter must be at a minimum at the depth of the minimum. The first condition appears to be ruled out on general grounds, and the second seems inconsistent with observations on the distribution of organic matter in the sea, including the recently reported extensive observations of the particle distribution in the ocean made by Jerlov (1953). Sverdrup states other conditions under which the dynamic explanation may be valid: (1) if the amount of oxygen-consuming matter is independent of depth while the oxygen consumption decreases with decreasing oxygen content, or (2) if the consumption is independent of the amount of organic matter but decreases with decreasing oxygen content. The latter condition of both these alternatives is at least tentatively ruled out by ZoBell's (1940) observations that the oxygen tension (in the range 0.31 to 12.74 ml/liter) had little effect on the rate of oxidation of organic matter in sea water by bacteria, and it appears fairly general that within wide limits the oxygen tension has little direct bearing on rates of oxygen consumption by most aquatic organisms.

Another serious discrepancy in the dynamic explanation of the oxygen minimum is its failure to include an explanation of the related phosphate and nitrate maxima. In most parts of the world, these lie somewhat deeper than the oxygen minimum, although this depth difference diminishes if one considers not the minimum-oxygen concentration but the maximum in apparent oxygen consumption (Redfield, 1942) and accounts for the "preformed" phosphate. The phosphate and nitrate maxima are clearly of biochemical origin, since they are not related to the resupply of oxygen by processes of aeration, nor can their concentration be independent of the amounts of organic, oxygen-consuming material originally present.

Rakestraw, Rudd, and Dole (1951) have observed that, at one station in the Pacific, the ratio of the two oxygen isotopes, O^{18}/O^{16}, reached a maximum value coincident with the minimum in the oxygen content, and that at all depths to 2870 meters there was a close correspondence between the rise in the isotope ratio and the decline in oxygen percentage. They conclude that O^{16} must be metabolically consumed preferentially over O^{18}. It is difficult to conceive that physical or hydrographic processes—*i.e.*, mixing and flow—could alter this ratio, but it is well known that isotope ratios can be altered by biological processes.

Seiwell and Seiwell (1938) conducted laboratory experiments on the sinking rates of plankton organisms, but their emphasis on the specific-gravity relationships between sinking detritus and sea water appears to have been misplaced. For one thing, it emphasizes relationships between the oxygen minimum and conditions in the surface layers directly above, and for another Parr (1939) seriously criticized their conclusion that sinking particles will asymptotically approach a depth at which differences between their density and the density of the surrounding medium disappear, and sinking stops. Parr's criticism is largely based on the Seiwells' failure to recognize that the density of sinking particles must increase as the particles sink, so that sinking must continue to the bottom.

On the other hand, Sverdrup (1938) showed that Seiwell's theory fails if the oxygen consumption is intrinsically independent of the oxygen content. It is difficult to assume that the oxygen consumption is not independent of the oxygen content, at least within wide ranges of the latter, which forces the conclusion that neither explanation discussed by Sverdrup and Seiwell is wholly satisfactory.

Thompson, Thomas, and Barnes (1934) proposed that the minimum zone in the northeastern Pacific could arise from excessive consumption in the bottom waters in the Gulf of Alaska, which then move southward and are floated on the cold abyssal waters of the Pacific. They postulated that contact with the bottom itself should result in decreased oxygen concentrations, as is demonstrable in many parts of the ocean, and that water thus depleted can move outward and find an equilibrium, intermediate depth. This type of movement appears to have been occurring in the Labrador Sea when sampled by the U. S. C. G. C. GENERAL GREEN (Fig. 9; Soule, 1940, Fig. 55), and Thompson and Barkey (1938) found evidence that waters deoxygenated by the bottom are found at intermediate levels in certain fjords on the western Canadian Coast.

The analysis by Redfield (1942) is enlightening and introduces a new concept: within the depths of the Atlantic Ocean, the oxygen minimum occurs in that layer of water which bore maximal amounts of organic, oxygen-consuming material at the time of its sinking in high latitudes. The density of this water is such that it moves at intermediate depths, and, upon the oxidation of its organic burden, its oxygen content drops well below that of waters above or below it. This explanation does not require that the oxygen minima coincide either with minimum rates of oxygen replenishment or with maximum rates of oxygen consumption, and it is free of assump-

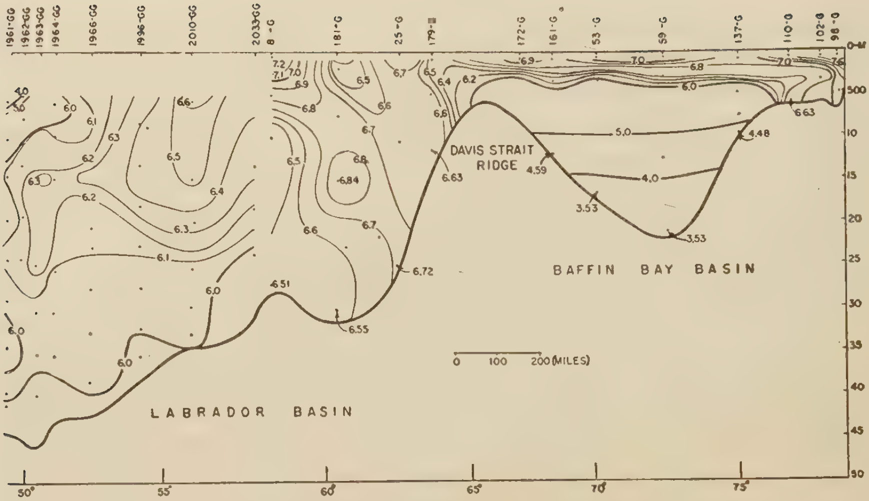

FIGURE 9.—*Oxygen profile*, (ml/liter), *Labrador Sea to Baffin Bay* After Smith, Soule, and Mosby (1937, Fig. 148).

tions concerning the vertical distribution of current velocities. However, Riley (1951) showed that the rates of oxygen consumption do pass through maxima along isentropic surfaces nearly coincident with the average density at which Seiwell found the oxygen minimum in the western North Atlantic. To maintain a steady-state distribution, this requires that the rate of supply of oxygen-consuming organic matter must also pass through maxima at these levels.

Redfield's analysis involves the zone of maximum apparent oxygen utilization, which lies deeper than the zone of minimum-oxygen content because the lighter, warmer water originally contained less oxygen, and a given oxygen utilization reduces its oxygen content to a lower value. The remaining discrepancy between the depth of maximum-oxygen utilization and maximum phosphate can be attributed to preformed phosphate.

It might be argued that if Parr's (1939) criticism of the Seiwells' views on specific-gravity relationships is correct, then there is no reason to believe that the intermediate layers would retain their organic burden. However, it is reasonable to assume that a large fraction of the oxygen consumption occurs rather rapidly, and also that an early step in the decomposition of particulate matter is the formation of soluble organic compounds not subject to sinking. Redfield, Smith, and Ketchum (1937) found that not more than 6 per cent of the total phosphorus in the Gulf of Maine was bound in particulate matter, although up to 22 per cent of it was present in soluble organic compounds.

On the basis of Redfield's analysis, one can distinguish between the oxygen-minimum zone attributable to waters sunk in high latitudes and the oxygen consumed in the shallower layers of the tropical Atlantic. The latter appears as another minimum zone superimposed on the deeper minimum zone. In large parts of the Atlantic, Indian, and Pacific oceans, the superimposed, lenticulate zones show up as two minima or as inflections in the oxygen-depth curves (Fig. 3). The overlying zones apparently owe their origin to more or less local introduction of large amounts of organic matter into the upper layers, which in the Atlantic and Pacific is consequent to upwelling along the West African and American coasts. Redfield's analysis clearly relates the oxygen-minimum layer to areas where organic productivity is known to be high and also clearly explains the great differences in the depths at which the oxygen minimum is found in various parts of the oceans.

Comparisons of the Atlantic and Pacific make it obvious that the Pacific is more deficient in oxygen than is the Atlantic. This is true not only of the oxygen-minimum zone but of all the subsurface waters of the Pacific. Many authors, including Schmidt (1925), H. Thomsen (1931), Moberg (1930), and Sverdrup *et al.* (1942), have attributed the very low concentrations of oxygen in the oxygen-minimum zone of the Pacific to its "greater staleness" or to the deflection of aerated polar waters westward at intermediate latitudes, leaving the tropical eastern Pacific a region of very slow and ineffective ventilation. Sverdrup *et al.* (1942, p. 240–241, 754–755) also attribute the higher nitrate and phosphate and lower oxygen content of the Pacific to its slow circulation, which permits the further decomposition of its organic matter.

These explanations do not seem adequate to account for the generally greater oxygen deficit of the Pacific, although it partially explains the location and shape of the minimum zone. Oxidative processes probably go essentially to completion in deep-ocean waters, and, although rates of replenishment of oxygen are important in the equilibrium, steady-state distribution which exists, the amount of oxygen consumed in a body of water is stoichiometrically limited by the amount of reducing compounds introduced into it. Rakestraw's (1947) experiments prove this point fairly conclusively; oxygen consumption stopped after 50 days, but excesses of dissolved oxygen were still present after 2 years, although his bottled samples represented a perfectly static, nonventilated system. It is accepted that phosphate and nitrate concentrations are usually the limiting factors in phytoplankton productivity, and the Pacific is richer in these nutrients than is the Atlantic, making the potential for organic productivity of the Pacific greater. There are no integrated averages for the phosphate concentration or for the apparent oxygen utilization in the oceans, but the highest phosphate concentrations in the Atlantic are about 2 microgram atoms per liter, while in the Pacific up to 3.5 microgram atoms per liter are found (Sverdrup *et al.*, 1942, p. 240). The oxygen consumption corresponding to 0.5 microgram atoms per liter of phosphate is close to 1 ml/liter, so one might expect the Pacific to contain up to 3 ml/liter less oxygen than the Atlantic. This conclusion is based on the biochemical relationships between oxygen consumption and phosphate release alone and is free of any comparisons of circulatory rates.

OXYGEN CONCENTRATION AND POPULATIONS OF THE SEA

The oxygen content of the aqueous environment contrasts markedly with that of the atmosphere. In the lower layers of the atmosphere, oxygen constitutes about 200 ml/liter, with great uniformity, but the maximum in sea water is about 9 ml/liter and ranges between this concentration and nil. It might seem that such extreme variations in an environmental factor would have an important effect on the distribution of species and population densities, but most marine organisms are physiologically better adapted to wide variations in oxygen tension than are many land organisms. Although there are wide variations in the respiratory requirements of marine organisms, the literature reveals no simple relationships between these requirements, the distribution of organisms, and population densities.

In general, the literature indicates that, in most aquatic organisms, respiratory consumption of oxygen is essentially independent of the oxygen tension down to some lower limit of the latter. Below this limit, the respiratory consumption may decrease with decreasing oxygen tension, until the tension becomes so low that the organism can no longer survive. Thus, most organisms can withstand large variations in oxygen tension, and only at some low level are the variations reflected in the respiratory rate or survival (Von Ledebuhr, 1939).

ZoBell (1940) found that the *in vitro* rate of respiration by bacteria in sea water was not influenced by varying the oxygen tension between 0.34 and 12.74 ml/liter, but below 0.3 ml/liter the respiratory rate decreased. However, if oxidizable organic matter were present, the bacteria could remove the last detectable trace of dissolved oxygen. A wide variety of observations concerning the oxygen requirements of higher aquatic organisms has been made (reviewed by Bishop, 1950), from which the conclusions in the above paragraph can be drawn.

Under completely anaerobic conditions, only obligate and facultative anaerobic bacteria can live, and their respiration is marked by the production of hydrogen sulfide. In the oxygen-minimum zone of the eastern tropical Pacific, the oxygen content becomes so low that it is scarcely detectable by the Winkler method, but hydrogen sulfide is not present, and oxygen is probably present in minute traces. The region appears to be in a state of delicate balance between oxygen-consuming and replenishing processes. Vaughan (1934) suggested that this region might be of interest in studying the effect of oxygen depletion on the distribution of organisms. Unfortunately, very little study of the vertical distribution of organisms in this region has been published. Graham (1941) sampled the plankton and oxygen content of the upper 100 meters during the CARNEGIE cruise from San Francisco to Samoa, and his data indicate that an abundance of organisms is associated with low-oxygen concentrations in this region. However, this reflects the high oxygen-consuming organic content of the water, and the data show nothing concerning the occurrence of living organisms in the oxygen-poor layer itself. Thompson, Thomas, and Barnes (1934) report that Guberlet and Miller found a scarcity of plankton between 500 and 1000 meters, although very rich hauls were made between 400 and 500 meters, these facts cannot be clearly related to the distribution of oxygen, however. Wooster (1952) reports large catches of lantern and hatchet fish, euphausiids, and squid from waters containing from 0.5 to less than 0.1 ml/liter of oxygen, suggesting that these animals can and do live for at least part of the time in waters containing only a few per cent of the saturation value of oxygen. It would be of great interest to ascertain whether these animals are respiring aerobically while in this low-oxygen zone, since respiration by such large populations as indicated would conceivably affect the oxygen concentration in the zone.

Vertical migrations of copepod populations are well known (Russell, 1925, and subsequent papers; Clarke, 1934a, 1934b; Nicholls, 1933; and others), and many observations of the vertical diurnal migration of the scattering layer have been made in recent years (Hersey and Moore, 1948; Moore, 1950; and others). The oxygen gradients through which these migrations take organisms do not appear to deter their movements. Clarke (1934a) observed copepod migrations and oxygen at a station in the Gulf of Maine where the animals must have passed through oxygen gradients of up to 1.7 ml/liter. Hersey and Moore observed euphausiid movements between 20 and 400 meters off Bermuda, corresponding to oxygen changes of about 0.5 ml/liter. At a station occupied in the Mediterranean in May 1948, the scattering layer migrated from about 183 meters and 4.6 ml/liter of oxygen to some 400 meters (Moore, 1950), where the oxygen content was 4.2 ml/liter. Moore also reports a vertical migration of the scattering layer from 150 to 400 fathoms on entering the Gulf Stream from colder water. At this location, the depth difference involved an oxygen difference of at least 2.0–2.5 ml/liter. Moore concluded that the same species was involved in the layer at the different depths.

It appears that in most parts of the ocean the oxygen content is not a primary factor in limiting life and growth, except where sulfides develop under completely anaerobic conditions. When this occurs, bacterial metabolism continues, but combined oxygen, in the form of sulfate, nitrate, and other oxidized substances, or oxidized forms of metal ions, especially ferric iron, constitute the sources of energy.

The abundance of plants and animals decreases with depth, but not in the same way as the oxygen content, and there is no evidence that the abundance increases with depth below the oxygen minimum. On the contrary, the decreased populations can more readily be accounted for in terms of decreased temperature, light, food, and other environmental necessities than in terms of oxygen supply and demand.

OXYGEN CONTENT OF BOTTOM WATERS

The bottom water-sea floor interface forms a zone of particular interest to zoologists, bacteriologists, and especially geologists. The effect of the oxygen content of the bottom waters on this environment is of considerable interest to all three groups. Detritus settles into the region and there serves as food for bottom fauna or is incorporated into the bottom sediments. Oxidative processes leading to the decomposition of organic material will in large degree depend on the oxygen content of the water and in turn will consume the dissolved oxygen. Thus, changes in the amount and composition of organic materials entering this area will be related to the amount of oxygen present. Organic compounds arriving at the ocean floor can be assumed to be those relatively resistant to oxidation, but this will depend on many factors, among which their composition, the rate of sedimentation, the oxygen content, and the temperature of the water will be important.

Within the interstitial waters of bottom sediments, the oxygen may soon be consumed (ZoBell, 1939), leading to reducing conditions, limiting life to anaerobic bacteria, and greatly reducing rates of further decomposition of organic materials. In the overlying water, the amount of oxygen will depend upon the state of balance between the rates at which organic materials arrive and are oxidized and the rate of resupply of oxygen. Where the latter is slow and the former rapid, the anaerobic conditions established in the sediments may extend well upward into the overlying water as they do in the Black Sea and other stagnating areas. However, in most parts of the open ocean, the bottom waters are not anaerobic, although they may contain less oxygen than waters directly above. This conclusion is based on the widespread occurrence of benthic animals and on some observations of the oxygen content of near-bottom waters. Wattenberg (1927; 1938) observed depletion of oxygen in near-bottom waters in the Atlantic during the METEOR (1925–1927) Atlantic Expedition, and it was observed by the 1947–1948 Swedish Deep-Sea Expedition (Bruneau *et al.*,

TABLE 8.—*Temperature, salinity, oxygen, and phosphate of near-bottom deep waters in the Indian Ocean*
Data from Bruneau *et al.* (1953)

Station	Position	Depth (Meters)	Distance From Bottom (Meters)	T°C	S‰	O_2ml/L	$PO_4^{\equiv}$, μga/L
205	4°47′S88°18′E	4999	43	1.37	34.73	4.29	2.55
			14	—	34.73	3.52	2.55
207	0°01′S88°18′E	4486	40	1.40	34.73	4.08	2.65
			11	1.40	34.74	3.69	2.55
211	4°36′N82°36′E	4133	41	1.34	34.71	3.89	2.49
			12	—	34.76	3.38	2.49
213	4°12′N77°78′E	3120	49	1.48	34.75	3.64	3.23
			24	1.86	—	—	—
			13	—	—	—	—
			7	—	34.95	0.87	2.13
216	0°04′N74°53′E	4268–4286	4215*	1.37	34.73	4.12	3.39
			4241*	1.33	—	4.09	3.59
			4258*	—	34.75	3.59	3.42
220	1°22′S70°28′E	3885	50	—	34.73	3.97	3.30
			25	1.58	"	4.01	3.20
			19	1.67	34.75	4.03	3.13
			14	1.66	34.75	3.99	3.10
			8	—	"	3.68	3.04
223	1°19′S66°16′E	4344	50	1.51	34.73	4.09	3.13
			25	—	"	"	3.23
			19	1.53	"	4.07	3.04
			13	—	34.74	4.07	3.04
			7	1.55	34.73	3.66	2.65
225	1°22′S62°38′E	4658	50	—	34.71	—	—
			23	1.35	34.71	4.22	3.46
			17	—	34.69	4.26	3.46
			12	1.32	—	4.16	3.46
235	7°14′N52°49′E	5073	97	1.30	34.71	4.28	3.23
			23	—	"	4.25	3.20
			18	1.36	34.69	4.27	3.17
			12	—	"	4.22	3.07
			7	1.38	34.83	3.40	3.07
240	10°23′N52°22′E	3703	50	1.52	34.76	3.91	3.33
			25	—	—	3.86	3.33
			19	1.54	34.75	3.89	3.17
			14	—	34.74	3.88	3.00
			8	1.55	34.74	3.68	3.13

* Sample depths.

1953) in the Indian Ocean. Van Riel (1943) found rapid declines in the oxygen content at 30 meters from the bottom in several of the basins of the Dutch East Indies; he further noted that there were systematic patterns in the magnitude of these near-bottom decreases.

Table 8 shows the temperature, salinity, oxygen, and phosphate contents of near-bottom deep waters observed in the Indian Ocean, during the 1947–1948 Swedish-Deep-Sea Expedition (Bruneau *et al.*, 1953). Special techniques were used to extend their sampling to within 7 meters of the bottom. At all these stations, there were appreciable decreases in the oxygen content in the bottom 50 meters, which in most cases amounted to about 0.5 ml/liter. In several cases, this decrease in oxygen was accompanied by an increase in temperature of a few hundredths of a degree C. and a decrease in inorganic phosphate. These low-oxygen concentrations in a very thin bottom layer must result from the accumulation of detritus sinking to the bottom layer, an effect which shows itself in a more exaggerated way in the accumulation of relatively stable organic materials in bottom sediments. Brouardel and Fage (1954) report sampling oxygen at different levels near the bottom, using a special device which captures samples at five successive levels adjacent to the bottom; the authors are uncertain as to the exact strata from which their samples are taken, but they appear to come from the bottom 10 meters of water. In this layer the oxygen content decreased an average of 0.1 mg/liter (0.07 ml/liter) between the second and third stage from the bottom, and 0.3 mg/liter (0.27 ml/liter) between the water adjacent to the bottom and the next stage above. These observations were made off Morocco in less than 500 meters of water.

There is considerable opinion and some evidence that the oxygen content of the waters above the sediments is important in determining their organic content (Fleming and Revelle, 1939). Correns (1939) states that the relatively high oxygen content of the deep water of the Atlantic is not favorable to the preservation of organic substances, and Trask (1939) states that the decomposition of organic matter depends mainly on the supply of oxygen. Although Kuenen (1942) found no correlation between the organic nitrogen content of sediments in the Dutch East Indies and the oxygen content of the bottom waters, a good correlation between these functions is demonstrable in the northwestern Gulf of Mexico (Richards and Redfield, 1954). Figures 10 and 11 show the location of the maximum organic content of these sediments, redrawn from Trask (1953), and the minimum oxygen content of the bottom waters drawn from observations made by the ATLANTIS in 1935 (Conseil Permanent Internat., 1936). The zones of maximum organic content and minimum oxygen content coincide, and both roughly parallel the 100-fathom isobath. This zone represents the area where the oxygen-minimum layer impinges on the bottom (sides) of the basin of the Gulf of Mexico, and is consequently the zone of the lowest oxidation diffusion gradient.

The extreme case, in which the bottom waters are anaerobic, is again represented by the Black Sea, threshold fjords, and other stagnant regions in which the organic content of the bottom sediments is unusually high.

The oxygen content of the water has another, although indirect, bearing on the composition of bottom sediments. Because of the inverse relationship between oxygen

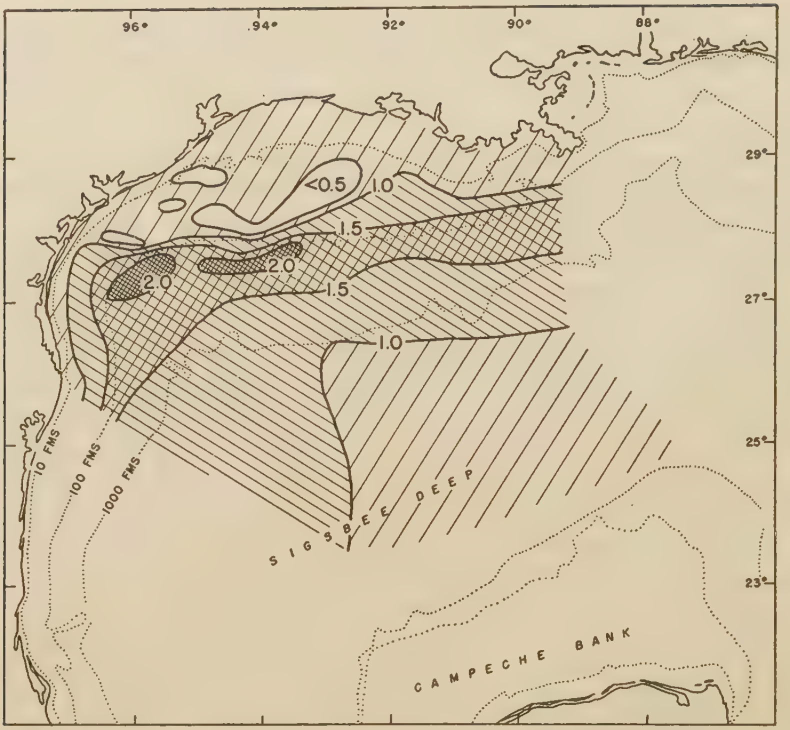

FIGURE 10.—*Organic content of sediments of Northwestern Gulf of Mexico*

From Trask (1953). Numbers represent per cent of organic matter, estimated as 1.8 times the carbon content.

consumption and carbon-dioxide release, low-oxygen values are associated with high total carbon dioxide and low pH values. This in turn increases the solubility of calcium carbonate. The oxygen content of the bottom waters of the Pacific decreases northward, and so does the calcium-carbonate content of the bottom sediments (Trask, 1937). In general, the calcium-carbonate content of Atlantic marine sediments is greater than that of Pacific marine sediments, in agreement with the generally higher oxygen content of Atlantic than of Pacific deep waters.

DISTRIBUTION OF OXYGEN IN THE OCEANS

ANTARCTIC CIRCUMPOLAR OCEAN

The Antarctic Circumpolar Ocean is an important area in which oxygenated surface waters sink and spread northward. Two areas of convergence exist: the Subtropical Convergence, found at about 40°S., and the Antarctic Convergence, between 50 and 60°S. The area between these convergences is the Subantarctic region. Between the Antarctic Convergence and the Antarctic Continent is the Antarctic region, where winter cooling and freezing yield highly oxygenated, cold, saline water. In the Weddell Sea, the Antarctic region south of the western Atlantic, the oxygen content is more than 7 ml/liter in the surface water, but upon sinking it mixes with water entering the area from the northwest through the Drake Passage. The latter

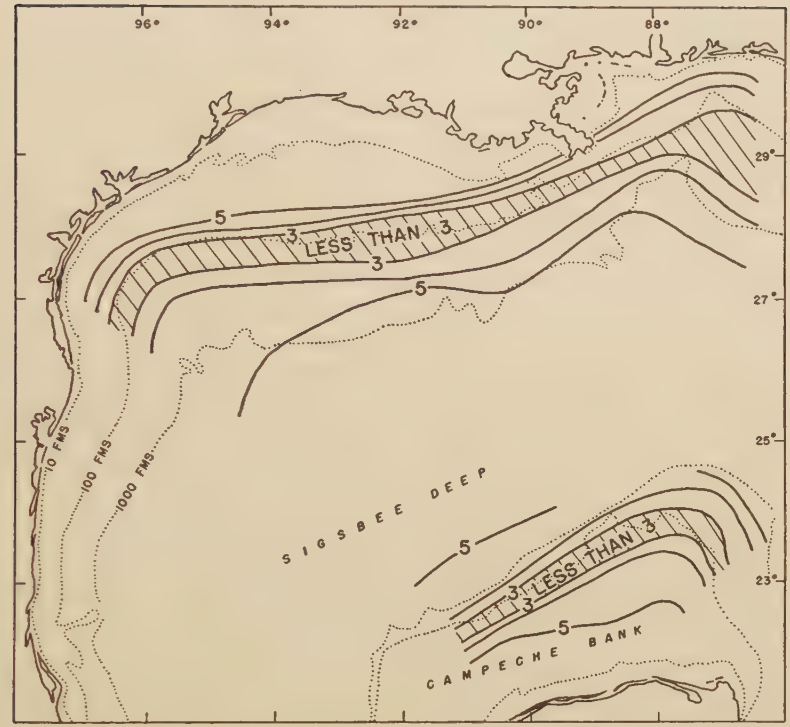

FIGURE 11.—*Oxygen content,* ml/liter, *of waters overlying the bottom, northwestern Gulf of Mexico*
Data from Bulletin Hydrographique for 1936

water contains at most 4.2 ml/liter (in the subsurface layers), and the mixture at the bottom of the Weddell Sea contains about 5.5 ml/liter (Mosby, 1935; Deacon, 1937). This mixture contributes to the Antarctic Bottom water, which fills the bottom layers of the Atlantic to 20°N. The minimum-oxygen content of the Weddell Sea, approximately 5.0 ml/liter, is found at an intermediate depth of about 1000 meters. The circumpolar circulation carries this water eastward around the Antarctic continent, and in general the oxygen content gradually diminishes along its course. Deacon's section from Cape Leeuwin, Australia, to the Antarctic Continent (Deacon, 1937, Pl. XXI) shows this water at about half its circumpolar distance from its source in the Weddell Sea. At this longitude the oxygen minimum, less than 4.0 ml/liter, is found at about 600 meters in the Antarctic region, but at 41°S. it is less than 3.4 ml/liter at 2000 meters.

The water sinking at the Antarctic Convergence forms the low-salinity Antarctic Intermediate water, which flows[3] northward into all the oceans at depths between 800 and 1200 meters. Upon sinking, this water is relatively highly oxygenated and is apparent in the Western Atlantic as an oxygen maximum nearly to the equator; however, consumption within the water mass decreases its content from about 7 ml/liter at 60°S. to less than 4 ml/liter near the equator. On the other hand, the

---

[3] This "flow" may occur either as a mass movement of a body of water or by the transfer of solutes by eddy diffusion along isentropic surfaces.

TABLE 9.—*Features of the oxygen distribution in the Atlantic Ocean*

After Wattenberg (1938)

Geographical latitude	60° S	50° S	40° S	30° S	20° S	10° S	0°	10° N	20° N	30° N	40° N	50°
WESTERN SECTION												
Upper layer, O_2CC/liter	7.5	7.1	5.9	5.2	4.6	4.6	4.3	4.4	4.9	5.0	4.8	5.6
Depth of boundary:												
Upper layer/intermediate layer (60%O_2 line) (Meters)	400	700	1100	1300	900	200	250	150	550	700	850	350
Intermediate layer (O_2 min.)												
O_2CC/liter	5.2	4.1	4.1	4.4	4.3	2.3	2.9	2.7	3.2	3.8	3.4	3.5
O_2%	64	54	54	59	58	37	45	40	48	56	52	53
Depth of boundary:												
Intermediate layer/bottom layer	—*	2600	1900	1550	1300	1250	1250	1400	1100	1000	1050	500
Bottom layer (O_2 max.)												
O_2CC/liter	5.2	5.2	5.7	5.7	5.8	5.7	5.6	5.8	5.9	6.0	6.2	6.6
O_2%	67	67	71	76	78	75	76	79	80	82	84	89
EASTERN SECTION												
Upper layer, O_2CC/liter	7.6	7.2	6.2	5.4	5.4	4.9	4.5	4.4	4.9	5.8	5.8	6.1
Depth of boundary:												
Upper layer/intermediate layer (60%O_2 line) (Meters)	200	400	1200	1120	100	50	50	100	200	1000	—*	—*
Intermediate layer (O_2 min.)												
O_2CC/liter	4.5	4.0	4.1	4.3	3.1	0.7	1.7	1.7	1.5	3.7	4.1	4.7
O_2%	56	53	55	57	44	10	27	25	25	60	65	71
Depth of boundary:												
Intermediate layer/bottom layer (Meters)	950	2100	1900	1700	1450	1400	1500	1500	1500	1100	—*	—*
Bottom layer (O_2 max.)												
O_2CC/liter	5.6	4.9	5.0	5.1	5.3	5.2	5.3	5.4	5.3	?	?	6.4
O_2%	69	61	67	69	70	70	70	71	71	?	?	86

tropical and subtropical oxygen minima are found in the nucleus of the Subantarctic Intermediate layer (Schumacher, 1932).

THE ATLANTIC AND ITS ADJACENT SEAS

The distribution of oxygen in the South Atlantic has been classically described by Wattenberg (1938), and a detailed study of the distribution in the Northeastern Atlantic has been made by Gaarder (1927). The oxygen distribution in the western basin of the North Atlantic and the Caribbean has been reported by Seiwell (1934; 1937b; 1937d; 1937e). Earlier contributions were made by Brennecke (1909), J. P. Jacobsen (1916; 1929), and others, and many other papers touch on the distribution of oxygen in various parts of the Atlantic.

The concentrations of oxygen found in the surface waters of the Atlantic are largely a function of the temperature and latitude; they diminish from about 7 ml/liter in high latitudes to about 4 ml/liter in the tropics. Major anomalies occur where upwelling brings oxygen-poor water into the surface layers. The minimum layer is in the upper 1200 meters, finds its greatest depth about 40°N. and 40°S., and rises to about 500 meters near the equator and at 60°N. and 60°S.; the lowest concentrations in the minimum layer are found near the equator in the eastern part of the ocean. Most of the Atlantic contains more than 5 ml/liter of oxygen at depths greater than 2000 meters, and in general there is more oxygen in the northern deep water than in the southern deep water. The general features of this distribution were summarized by Wattenberg (1938; 1939a) (Table 9).

It is of interest to compare the longitudinal sections in the western, central, and eastern Atlantic reported by Wattenberg (1939a) with the average distribution of oxygen computed by Riley (1951) (Tables 9, 10). Wattenberg's sections are composites of observations by the METEOR, ARMAUER HANSEN, DANA, DISCOVERY, ATLANTIS, and GODTHAAB, and Riley's table shows values averaged by latitude for

TABLE 10.—*Average distribution of oxygen (ml/liter) in the deep water of the Atlantic*
From Riley (1951)

Latitude	1000	1500	2000	2500	3000	3500	4000	4500
54–63°N.	5.96	6.26	6.44	—	—	—	—	—
45–54	5.80	6.32	6.36	6.30	6.24	6.22	—	—
36–45	6.16	6.38	6.34	6.16	6.14	6.16	6.23	—
27–36	4.20	5.80	6.02	6.02	6.07	6.13	6.18	6.20
18–27	3.68	5.18	5.55	5.69	5.70	5.67	5.57	5.48
9–18	3.12	4.83	5.47	5.54	5.54	5.52	5.48	5.42
0–9	3.35	4.88	5.42	5.50	5.48	5.45	5.40	5.37
0–9°S.	3.67	4.94	5.40	5.45	5.42	5.38	5.30	5.07
9–18	3.67	4.80	5.35	5.45	5.42	5.30	5.19	5.07
18–27	4.18	4.60	5.34	5.46	5.48	5.42	5.27	5.07
27–36	4.78	4.42	4.94	5.42	5.50	5.43	5.19	5.08
36–45	5.10	4.38	4.78	4.96	4.95	4.89	4.81	4.70
45–54	4.13	4.40	4.52	4.52	4.56	4.74	4.94	5.08
54–63°S.	4.46	4.62	4.80	4.85	4.88	4.92	5.00	5.12

observations deeper than 1000 meters. The correspondence is best between Riley's averaged section and Wattenberg's central section, as would be expected. Generally, the eastern section contains less oxygen than the average, except in the south. The central section is slightly higher in oxygen toward the south, slightly lower toward the north, than Riley's "average" section. Practically all the western section contains more oxygen than the average (Wattenberg, 1927).

The oxygen-minimum zone in the Atlantic may be considered to be composed of two components. The first is deeper lying, and represents water which sank at high latitudes; this component is therefore oriented north and south. It is thickest at about 4°S. but there it is not so strikingly low in oxygen as it is in the equatorial region. The other component is oriented east to west in the equatorial region and owes its origin to the more local oxidation of organic products which result from the nutrient enrichment brought about by upwelling off the west coast of Africa. These two components cross and merge in the eastern tropical Atlantic, but in much of the region they are distinguishable by "double minima" or inflections in the oxygen-depth curves (Fig. 1, F and G).

The general pattern of oxygen distribution described above is modified by additions of Mediterranean water to the Atlantic and by the circulation through the Caribbean and Cayman seas, Gulf of Mexico, and Gulf Stream system.

THE CARIBBEAN

The Caribbean is characterized by a series of basins and sills which restrict the inflow of water from the North Atlantic below a depth of 1000 meters. Equatorial surface water and some Antarctic Intermediate water enters the Caribbean over this sill.

In the Venezuela Basin in the central Caribbean, the oxygen content is greater than 4.8 ml/liter at all depths below 1500 meters and increases to more than 5 ml/liter at the bottom (3600 to 3800 meters), indicating a relatively rapid renewal of these waters (Seiwell, 1938). The minimum occurs at 400–600 meters, where it is less than 3 ml/liter in the southern part of the section. The oxygen content of the western part of the Caribbean basin is somewhat less than in the eastern section and decreases in the direction of flow. Farther west, in the Cayman Basin, the oxygen content is a little higher than that of the Caribbean Basin because of the entrance of oxygen-rich water through the Windward Passage (Rakestraw and Smith, 1937; Seiwell, 1938; Sverdrup *et al.*, 1942).

The influx of waters relatively rich in oxygen to the Cayman Basin through the Windward Passage is interesting in connection with the oxygen content of the Gulf Stream system and the Sargasso Sea and demonstrates that the Sargasso is a source of subsurface oxygen.

Water moves through the Caribbean and the Cayman seas, Yucatan Channel, Gulf of Mexico, and Straits of Florida into the high-velocity Florida Current-Gulf Stream System. Sill depths in the Yucatan Channel and Straits of Florida limit this circulation to the upper layers. The upper layers of the Florida Current and the Gulf Stream contain less oxygen than adjacent slope or Sargasso Sea water of the same density (σ_t). This effect is confined to an upper layer, above the minimum zone (Fig.

3), and has been detected as far northeast as the tail of the Grand Banks. This oxygen-deficient layer owes its existence to its relatively recent origin in the equatorial region. On progressing downstream from the Straits of Florida, these waters are reoxygenated by vertical turbulence and by lateral mixing into the adjacent areas. The density at which the oxygen minimum is found is essentially the same for both Gulf Stream and Sargasso waters.

MEDITERRANEAN AND BLACK SEAS

In the Mediterranean, evaporation exceeds precipitation and run-off (Sverdrup *et al.*, 1942), and surface waters sink to the bottom (perhaps intermittently, according to Nielsen, 1912) renewing the deep-water oxygen. The oxygen content of the western Mediterranean was relatively high at all depths when observed by the DANA in April and June 1930. The minimum zone was poorly developed, and with one exception concentrations were greater than 4.0 ml/liter at all depths. East of Sicily the minimum zone was more markedly developed than in the western Mediterranean, although farther east the oxygen decreased constantly to the bottom and showed no intermediate minimum. In this region and in the minimum zone in the western part of the eastern section the oxygen content drops below 4.0 but not below 3.5 ml/liter.

The Black Sea is a special case in which the deep waters become anaerobic, and hydrogen sulfide is produced, but, because of the small water exchange through the Bosphorus, the Sea of Marmora, and the Dardanelles, Black Sea water has little or no effect on the Mediterranean.

Mediterranean waters flow into the Atlantic through the deeper parts of the Straits of Gibraltar, forming a characteristic water mass which can be detected over wide areas of the Atlantic by a salinity maximum at intermediate depths. In the straits, warm and saline Mediterranean water mixes with incurrent Atlantic water, yielding a mixture of about 37.00 ‰ salt at 13°C., containing about 4.5 ml/liter oxygen. According to Wüst (1935), Mediterranean water outside the Straits of Gibraltar was observed to have a temperature of 11.9°, a salinity of 36.5 ‰, and a σ_t of 27.78. In the eastern Atlantic, this water is centered at 1000 meters depth at 40°N. latitude, where it has an oxygen content a little less than 4.5 ml/liter, slightly more than the waters immediately north or south of it. Wüst (1935) traces this water in the eastern Atlantic from 20°N. to 51°N. by its salinity, but it is no longer apparent in his central Atlantic section. However, Seiwell (1937b) attributed high positive salinity anomalies at the depth of the oxygen minimum in the region west of 40°W. and between 25° and 35°N. to water of Mediterranean origin.

THE ARCTIC MEDITERRANEAN SEA

This region includes the Norwegian, North, Baltic, Barents, and North Polar seas and is bounded on the south by the Iceland-Greenland ridge, the Faeroe Islands-Iceland Ridge, and the Wyville Thomson Ridge which runs between the Orkney and the Faeroe islands. It is an important source of oxygenated waters, formed by sinking in the Norwegian Sea in the winter time (Knudsen, 1899; Nansen, 1906; 1912; Nielsen, 1907; J. P. Jacobsen, 1916).

In general, the Arctic Mediterranean is oxygen rich at all depths, but low concentrations are found in coastal areas where the circulation is limited, and Sverdrup (1929) observed low values near the bottom on the North Siberian Shelf. Very high oxygen contents, largely attributable to photosynthesis, were observed in surface waters off the East Greenland coast by Jakhelln (1936) and may well contribute to the ventilation of underlying Atlantic and Irminger sea waters (Fig. 2). In seven stations occupied by the submarine NAUTILIS north of Spitzbergen (Sverdrup, 1933, Fig. 43), the water at all but one station contained more than 6.6 ml/liter at all depths less than 100 meters. The minimum zone, containing between 6.4 and 6.6 ml/liter, lay between 1000 and 3000 meters, and values between 6.6 and 6.8 ml/liter were found at greater depths.

LABRADOR SEA

The Labrador Sea is another important region of convergence and sinking. Sections through this sea and Baffin Bay have been made by the GODTHAAB (Fig. 1, E) (Conseil Permanent Internat., Bulletin Hydrographique, 1929) and U. S. C. G. C. GENERAL GREEN (Fig. 9) (Smith, Soule, and Mosby, 1937). The region is the source of much of the North Atlantic Intermediate water, which, like the Antarctic Intermediate water, is characterized by a salinity minimum. Water containing about 7 ml/liter oxygen sinks in the Labrador Sea (Wüst, 1935; Wattenberg, 1938). Soule (1940) has discussed the formation of bottom water in this region, which contains about 6.4 ml/liter. Low-oxygen concentrations develop in the poorly circulating deep water of Baffin Bay (Fig. 9), and water containing about 5 ml/liter can flow across the Davis Strait ridge into the Labrador Sea, where it has been observed as an oxygen-minimum layer (at 2200–2500 meters) separating the intermediate and deep waters. Upon mixing with Labrador Sea water having an oxygen content of 6.9 ml/liter, it forms deep water containing about 6.4 ml/liter (Soule, 1940), which then flows southward. At 30°N. it forms the middle Atlantic deep water, at 2300 meters depth, and its oxygen content has decreased to about 6 ml/liter; at the equator it is at about the same depth and contains about 5.75 ml/liter. At about 30°S., it deepens to 3000 meters and then begins to shoal, and at about 50°S. it contains about 4.5 ml/liter at a depth slightly greater than 2000 meters. This water apparently then rises to join waters which again sink in the southern convergences.

Bottom Arctic water of high-oxygen content is traced by Wüst (1935) as far south as 20°N. in the Western Atlantic, where it has 5.75 ml/liter at 4000 meters. Farther south, it is replaced in the bottom by subantarctic waters. At 20°S., this water of northern origin is found shoaler, containing a little more than 5.5 ml/liter at 3000 meters depth.

SARGASSO SEA

The Sargasso Sea is a source of oxygen for the shallow layers of the North Atlantic. In March, mixing and aeration produce an isothermal surface layer extending to a maximum depth in this season. In the following warm season, a sharp thermocline develops above these waters and isolates them from the atmosphere.[4] The waters thus oxygenated spread out over the area, retaining their oxygen for an undetermined time and distance. Presumably it is water of this genre that enters the Caribbean through the Windward Passage.

---

[4] The author is indebted to Mr. L. Valentine Worthington for this information.

INDIAN OCEAN AND THE RED SEA

The Red Sea is a source of warm, highly saline, oxygen-poor water traceable into the northwestern Indian Ocean, although its exchanges of water through the Suez Canal are too small to be of any significance to the Mediterranean. According to Vercelli (1925) and E. F. Thompson (1939), north-northwest winds prevail in summer, and surface waters flow from the Red Sea to the Gulf of Aden, Indian Ocean waters flow into the Red Sea at intermediate depths, and bottom, highly saline waters flow from the Red Sea to the Gulf of Aden. Opposite winds prevail in winter, so that the deeper Red Sea waters are discharged into the Indian Ocean while surface waters enter the Red Sea from the Gulf of Aden. At the end of winter, the deep oxygen content of the Red Sea is only a little more than 2 ml/liter (E. F. Thompson, 1939), while at the end of summer it is less than 1 ml/liter. Oxygen-poor Red Sea water appears in the Indian Ocean at 8°N. in the section of Clowes and Deacon (1935, Fig. 1), where the layer between 300 and 1000 meters deep contains less than 0.8 ml/liter, but at 11°S. the minimum concentration, 2.0 ml/liter, is at 1200 meters.

Antarctic Intermediate water enters the Indian Ocean from its southern boundary which, oceanographically, is the Subtropical Convergence. Clowes and Deacon (1935) show Antarctic Intermediate water, with about 3.6 ml oxygen/liter, entering the western Indian Ocean from the south at about 1500 meters, extending northward at shoaler depths, and gradually diminishing in oxygen content from south to north. The deep water in the southern part of this section, which parallels the east African Coast, is of Atlantic origin, according to them, but it contains only about 4.4 ml/liter of oxygen, which is 0.5–0.75 ml/liter less than Wattenberg (1938) found at these latitudes and depths in the eastern Atlantic. Clowes and Deacon suggest that the Atlantic water is influenced by Indian deep water from the north. Off the East African coast, the deep-water oxygen decreases northward from about 4.4 ml/liter at 40°S. to about 3.6 ml/liter at 10°N. In the east-west direction, the deep water oxygen content is uniformly around 4 ml/liter between 10°S. and 9°N. (Fig. 193 in Sverdrup, *et al.*, 1942, and ALBATROSS observations), but at about 88°E. it decreases in the northward direction to less than 3.0 ml/liter at 4°36′N. Eastward from 11°S., and 88°E., it decreases slightly, but contains 4.64 ml/liter in 5877 meters at 109°10′E.

The observations of the DANA and the Swedish Deep-Sea Expedition (Bruneau *et al.*, 1953) show that the oxygen-minimum zone of the Indian Ocean is centered at about 5°N. and is most pronounced between 52° and 77°E. This central location (in the east-west direction) is in marked contrast to the location of the minimum zones of the Atlantic and Pacific, probably because relatively highly oxygenated waters enter from the western Pacific, a phenomenon which has no counterpart in the Atlantic and Pacific.

On approaching this minimum core from the south and east, the ALBATROSS observed the minimum concentration of 1.76 ml/liter at 568 meters south of Java. At about the same latitude (11°S.) and at 88°E. the same minimum concentration was found at 768 meters. In their section to the north along 88°E., minimum concentrations gradually decreased, and overlying minima were found at depths ranging from about 150 to about 500 meters. Double minima occurred along the remainder of their westward course to at least 56°E. At the stations where double minima were found, the lower of them occurred at a density close to $\sigma_t = 27.3$ and at depths slightly less than 800 meters. This deeper oxygen-poor layer was observed from 11°S. to 7°N. at 88°E. and extended southwestward to a point south of the equator at 54°49′E. West of the latter point, the zone ends or curves northward, because at DISCOVERY station 1584 at 49°E. and about 1°S. the minimum was 3.6 ml/liter at 1500 meters, but the ALBATROSS found 0.53 ml/liter at 763 meters ($\sigma_t = 27.26$) at 10°23′N. and 52°22′E. The minimum concentration in the lower oxygen-poor layer, 0.45 ml/liter, was found at 7°14′N., 52°49′E., at a depth of 790 meters and a σ_t of 27.29. This deep oxygen-poor layer was not observed in the Gulf of Aden, where the minimum was found at 143 meters ($\sigma_t = 26.11$), contained 0.24 ml/liter, and was presumably of Red Sea or local origin.

The depth and density at which the shallower minimum layer was found ranged from 148 meters ($\sigma_t = 25.75$) at 52°E. to 389 meters ($\sigma_t = 26.9$) at 82°36′E. The lowest concentration in it, 0.48 ml/liter, occurred at 77°28′E.

In contrast to the Atlantic and Pacific, there is no supply of oxygen-rich waters of far northern origin in the Indian Ocean, and water entering the system from the east tends to shift the overlying minimum zone of local origin westward.

THE PACIFIC

The outstanding feature of the Pacific Ocean is the large wedge-shaped area of very low oxygen extending at intermediate depths westward from the Gulf of Panama, where it was first observed by Schmidt (1925) that the minimum-oxygen content was much smaller and much shallower than on the other side of the Isthmus of Panama in the Atlantic. H. Thomsen (1931) showed that this very low minimum zone extended far to the west. Data now available make it apparent that this zone has a counterpart in the southern hemisphere, and that two oxygen-low tongues extend westward from the Americas. Lowest concentrations are found at about 15°N. and 10°S., with somewhat higher concentrations at corresponding depths (down to around 1000 meters) in the intervening zone. A similar feature is apparent in the oxygen distribution in the eastern Atlantic. Not only is the oxygen content of the minimum zone lower, but the whole subsurface water mass of the Pacific is generally lower in oxygen than is the Atlantic. Possible causes of this have been discussed.

The far southern Pacific was investigated by the DISCOVERY (Deacon, 1937, Pls. 33, 36, 39, 42; and others); four DISCOVERY sections cover the area from about 45° to nearly 65°S., from New Zealand to the southern tip of South America and include parts of the circumpolar Antarctic Ocean. In the northern part of the section from New Zealand to the Ross Sea, minimum-oxygen concentrations of about 3.5 ml/liter are found at 1300 to 2000 meters; a deeper maximum, containing a little more than 4.0 ml/liter, is centered at about 3000 meters, and below this the oxygen decreases to slightly less than 4 ml/liter in the deepest waters. At the southern end, the lowest concentrations, less than 4.0 ml/liter, are found at depths of 600–900 meters, and 4.5 to 4.75 ml/liter is found at the bottom. In Deacon's section from the ice edge to 41°03′S., 126°04′W., the oxygen content decreases from south to north, and the depth of the oxygen minimum slopes steeply downward in this same direction; at about 65°S. it is at about 600 meters and contains 3.60 ml/liter, but at 40°S. it is at 3000 meters and contains 3.25 ml/liter. The surface concentrations decrease from about 6.9 ml/liter at about 63°S. to 5.9 ml/liter at 40°S. In the section from 41°03′S., 126°04′W., to the Antarctic Shelf and in the section from the end of the latter section to the western end of the Straits of Magellan, southern surface values reach 7.5 and 7.0 ml/liter, respectively, the depth at which the minimum is found increases sharply to the north, and the northern parts of the sections contain generally less oxygen than do the southern ends.

Few other data are available on the oxygen distribution in the Southern Pacific. Conditions just off the coast of Peru were investigated by the WILLIAM SCORESBY (DISCOVERY Committee, 1949). Schott constructed a longitudinal section (Schott, 1935, Fig. 50) from data of the DISCOVERY, DANA, and CARNEGIE, but only two CARNEGIE stations between the track of the DANA and the areas investigated by the DISCOVERY were available to him. However, this section shows two zones of very low oxygen, centered at about 4°S. and 12°N., lying less than 500 meters deep with somewhat higher oxygen concentrations at equal depths in the intermediate latitudes. A fairly detailed section was constructed from DANA observations by Sverdrup *et al.* (1942, Fig. 206) extending from about 48°S. to 10°S. at about 180° Long., and a new section from 10°N. to 15°S. along 85°W. has been made available to the author by the kindness of Dr. Warren Wooster of the Scripps Institution of Oceanography). There are practically no data available east of the 180th meridian between 20° and 40°S.

The southern end of the section drawn from DANA data (Sverdrup *el al.*, 1942, Fig. 206) is just east of New Zealand. A deep minimum occurs at about 2000 meters and gradually decreases in depth and oxygen content northward to about 1800 meters and 3 ml/liter at 14°S. At about 38°S., a shallower minimum appears, containing between 4.0 and 4.5 ml/liter, centered at about 500 meters. The oxygen of this layer increases to between 4.5 and 5.0 ml/liter in 350 meters at 30°S., and then decreases northward. At about 15°S., an abrupt decrease in the oxygen content of the layer above 1000 meters takes place, and the two minimum layers containing less than 3 ml/liter tend to merge and in the north end of this section at about 10°S. extend from about 350 meters to more than 2000 meters. At 4000 meters the oxygen content decreases from more than 4.0 ml/liter at the south to less than 3.5 ml/liter at the north. According to Sverdrup *el al.*, the intermediate oxygen maximum lies a few hundred meters above the Antarctic Intermediate water, marked by a salinity minimum.

Schott's section (Schott, 1935, Fig. 50) shows, at 30°S., two minima, one at about 400 meters, the other at about 1500 meters. Probably the lower one can be related to Antarctic deep or bottom water, and the other appears to lie slightly above the core of the Antarctic Intermediate water. There is a distinct tendency for the oxygen content of the deep water to decrease northward.

It can be reasoned by analogy that the oxygen distribution off the western coast of South America should be similar to that off the West African Coast, and it is known that active upwelling occurs along the Peruvian coast although it may not involve especially deep-water masses (Sverdrup, 1930; Gunther, 1936; Sears, 1954). Five sections extending 100-200 miles out from the Peruvian coast were occupied by the WILLIAM SCORESBY between about 16° and 4°S. There is essentially no continental shelf in this region, so these sections lie in deep water. At about 16°S. there is a region about 100 miles offshore in which low-oxygen values (less than 1.0 ml/liter) extend to great depths; at 2500 meters the oxygen in this zone was 1.09 ml/liter, but both inshore and farther offshore higher values were observed at this same depth; this low-oxygen mass is still apparent at 12°S., where less than 0.25 ml/liter was observed at 2500 meters, and even at 5°S. there is a suggestion that the deep water 100 miles offshore contains less oxygen than farther offshore or closer inshore. In all the sections, less than 0.25 ml/liter appears at depths of 200-400 meters. The section at 12°S. has the largest zone of these low-oxygen concentrations, which extend from 100 to 400 or 500 meters, but in the three sections farther north, at 7°S., 5°S., and 4°S., concentrations under 0.27 ml/liter probably do not extend over more than 100 meters of depth. The minimum values are not appreciably lower than at the equator (CARNEGIE Station 41, 1°37′S., 86°58′W.) (Fleming *et al.*, 1945), where 0.29 ml/liter was found at about the same depth (323 meters). However, the SCORESBY sections are short and doubtlessly reflect local coastal conditions.

A section from 10°N. to 15°S. along 85°W., occupied by the Scripps Institution of Oceanography, shows a large oxygen-poor area containing less than 0.25 ml/liter extending from about 2°S. to the southern end of the section, and a similar zone extending from about 3°N. to the northern end. The southern zone has its maximum thickness, extending from about 150 to 600 meters, at 8°-9°S. The section does not extend far enough south to permit determination of where the most intensely deoxygenated water lies, but a section published by Sverdrup *et al.* (1942, Fig. 207) indicates that the oxygen-poorest water is centered at about 12° in the northern hemisphere. In the section in the southern hemisphere, the 2.0 ml/liter isoxy line slopes downward to the north from 1400 meters at 15°S., but in the corresponding section in the northern hemisphere this line is found regularly at 2100-2500 meters.

The now-classic observations of the DANA (Thomsen, 1937) and CARNEGIE (Moberg, 1930; Graham and Moberg, 1944; Fleming *et al.*, 1945) have recently been supplemented by the Swedish Deep-Sea Expedition (1947-1948) (Bruneau *et al.*, 1953) and the U. S. Fish and Wildlife Service operating out of Hawaii (Cromwell, 1951). The DANA section from Panama to New Caledonia (Thomsen, 1931) clearly shows the oxygen-minimum zone extending westward from the Gulf of Panama, gradually dissipating with increased westing. Concentrations under 0.10 ml/liter were found at 300-500 meters in the Gulf of Panama, but, at about 144°W., no values less than 2 ml/liter were found in the entire water column. Between 145°W. and 150°W., the oxygen content increases rather abruptly to the west at depths less than 1000 meters, more gradually at greater depths. At DANA Station 3570 (148°W.) minima at 400-500 meters and at 1200-1500 meters were separated by a maximum at 1000 meters. At about 174°E., the upper layers contained more than 5 ml/liter to a depth of 800 meters, below which concentrations decreased to a minimum of about 3.16 ml/liter at 2500 meters. At all depths concentrations increased westward, but only at great depths (4000 meters or more) did the water contain as much as 4 ml/liter.

Sverdrup *et al.* (1942) have constructed a section showing the oxygen content a few hundred miles from the coast of Central America and North America, extending from the equator to about 50°N. (Sverdrup *et al.*, 1942, Fig. 207). This shows the most intensely de-oxygenated zone, in which the oxygen content is practically nil, extending from about 100 to nearly 1000 meters between 10°N. to 22°N. The deep water in this section contains a little more than 3 ml/liter, and at 2000 meters the oxygen content is uniformly less than 2 ml/liter. At about 120°W. in these latitudes and depths, the oxygen content drops to less than 0.25 ml/liter between about 100 and 600–800 meters. At 7°S., 2.0 ml/liter is found at about 1000 meters, but this concentration occurs in 2400 meters at 25°N.

Three sections occupied by the Swedish Deep-Sea Expedition extend in a zig-zag course from Panama to 2°44′S., 92°46′W., thence to 17°46′N., 126°51′W., and then to 03°0′S., 136°20′W. The first section shows concentrations under 0.5 ml/liter between 250 and 500 meters at the south and between 250 and 700 meters at the north. The low-oxygen zone is thicker and contains lower concentrations at the northern part. In the second section, these low values extend to depths of 1000 meters (compare with the section of Sverdrup *et al.*, 1942, Fig. 207) at about 18°N., but only to 500 meters at its southern end. Much of the northern part of this minimum zone contains less than 0.1 ml/liter and is near the core of the low-oxygen zone of the Pacific. Less than 0.1 ml/liter is found only at the northernmost station in the third section (about 15°33′N.), and the minimum zone is again thinner and more oxygenated at the southern end. CARNEGIE's section V extends from San Francisco to Samoa. Concentrations less than 0.1 ml/liter are found centered at about 12°N. and extend north of 16°N and south to about 9°N. The oxygen content of the upper layers increases markedly toward San Francisco, and the layer containing less than 0.5 ml/liter thins and deepens to the northeast, although less than 0.3 ml/liter is found at around 700 meters all the way to the San Francisco end. Southwest of the minimum zone, the oxygen content increases more rapidly than northeast of it; at about 5°S. and 152°W. the whole water column contains at least 1.0 ml/liter. At Station 157 (1°48′S., 152°22′W.), the column showed three minima: one contains less than 1.0 ml/liter at 100–250 meters; a second, at 500 meters, contains less than 1.0 ml/liter in a layer more than 100 meters thick; and a deeper bubble contains less than 2.0 ml/liter centered at about 2250 meters. The oxygen content between 500 and 3500 meters increases rather sharply toward the Southwest. Beyond 6°S. and 155°W., the minimum occurs at about 450 meters and contains slightly less than 2 ml/liter.

Two north-south sections from around 22°N. to 10°S. have been reported by Cromwell of the U. S. Fish and Wildlife Service. These sections (Cromwell, 1951, Figs. 14, 15) extend only to 1000 meters depth but are in great detail. They alternate with two nearly parallel sections occupied by the Swedish Deep-Sea Expedition. The easternmost of these four sections is at about 150°W., the westernmost extends to about 175°W. They show the gradual erosion of the de-oxygenated zone which originated farther eastward. Minimum concentrations occur regularly at about 12°N., and concentrations less than 0.5 ml/liter are found only in the northern parts of the sections.

The oxygen content of two sections in the southwestern North Pacific has been reported by Ito (1930). One section extends from the equator to 34°N. at about 145°E., the other from 127°E. to 161°E. at about 7°N. The first shows the oxygen minimum, with concentrations between 1.0 and 2.0 ml/liter, 800–1000 meters deep at 20°–25°N. This appears to be the residue of the core of the low-oxygen zone of the Pacific. However, along 7°N., a large zone of these low concentrations is found between 250 and 1000 meters as far west as 154°E. West of 140°E., there is a distinct increase in the oxygen content of the water column, which Ito relates to the western limit of the prevailing northeast winds. The oxygen at 250 to 1000 meters increases steadily to about 130°E., west of which it again decreases. The eastern part of this section should be in the North Equatorial Current (Sverdrup *et al.*, 1942, Chart VII), but the currents in the westward part of the section set southward. In the north-south section, the currents north of 20°N. set northeast, east, and southeast and presumably introduce waters of the Kuroshio into the section. These appear as a relatively highly oxygenated zone containing more than 3 ml/liter as far down as 800 meters. Between 10° and 20°N., this section crosses the North Equatorial Current, which contains less oxygen than the more northern part.

THE JAPAN SEA

This adjacent sea of the Pacific has been widely studied by the Japanese, and Uda (1934) has reported on a detailed survey of its oxygen content made in May and June 1932, when it contained more than 5 ml/liter to a depth of 1000 meters. No intermediate oxygen minimum was present, and, below 200 meters in the warm-water area and below 400 meters in the cold-water area, the oxygen content was essentially constant at all depths. Vertical distribution of temperature and salinity has this same uniform characteristic, and there is apparently active vertical mixing in the region.

THE DUTCH EAST INDIES

The oxygen content of the waters of the Dutch East Indies was studied by Van Riel (1943), on the SNELLIUS 1929–1930 expedition. The area covered by this expedition extended from 12°S. to 10°N. and from 112° to 134°E. This region, with its many islands and complicated topography, has an oxygen distribution subject to many local influences. In general, the deep-water oxygen content of the East Indian Archipelago reflects the circulation of the waters. In many cases, heavier waters enter deep basins across threshold sills and carry their characteristic oxygen content to the bottom. The Morotai Basin is a typical case. Pacific waters having an oxygen content of 3.0 to 3.1 ml/liter flow over the Snellius Ridge entrance sill into the basin, where the oxygen content is 3.0–3.1 at all depths between 2600 and 3800 meters. In contrast, concentrations increase to more than 3.4 ml/liter at corresponding depths on the Pacific side of the ridge. A similar situation was found in the Boeroe Basin (Van Riel, 1943, Fig. 11), in which the remarkably uniform oxygen content shows that there must be very little *in situ* consumption—*i.e.*, the oxygen content of the

TABLE 11.—*Oxygen content of deep waters of the East Indian Archipelago*
Compiled from Van Riel (1943)

Regions Where Deep O_2 Content Decreases Appreciably

Region	Content at bottom	Source	Entering water	
			Depth, m.	O_2
Batjan Basin	2.63	Ternate Trough	2600	2.8–3.0
Sawoe Basin	1.8	Wetar Basin	2100	2.0
Aroe Basin	2.25	Ceram Sea	1600	2.4–2.5
Kaoe Bay	O_2 nil 0.3 ml/1 H_2S	Pacific Ocean	50	4.0

Regions Where Deep O_2 Content is Essentially That of Entering Waters

Region	Content at bottom	Source	Entering water	
			Depth, m.	O_2
Celebes Sea	2.14	Sangihe Trough	1400	2.2
Sangihe Trough	2.73	Pacific Ocean	2000	2.7
Morotai Basin	3.06	Pacific Ocean	2400	3.0–3.1
Ternate Trough	3.04	Morotai Basin	3000	3.0
Boeroe Basin	2.5–2.6	Batjan Basin	2000	2.51–2.57
Banda Sea	2.4–2.5	Batjan Basin	3200	2.5
Halmahera Basin	2.9	Pacific Ocean	700–940	2.9
Aroe Basin	2.3	Timor Trough	1400	2.2–2.4

O_2 contents in ml/liter.

water is established before its entry into the basin. Circulatory processes must be sufficiently rapid and oxygen consumption sufficiently slow or sufficiently complete that no appreciable consumption takes place during the stay of these waters in the basin.

Other basins in this region represent regions of reduced oxygen content and stagnation in the bottom waters. In Kaoe Bay, oxygen disappears at around 400 meters, and appreciable concentrations of hydrogen sulfide were found in the bottom 100 meters. Decreases in the oxygen content (below sill depth) were also observed in the Batjan (Van Riel, 1943, Fig. 8), Sawoe, and Aroe basins.

The oxygen distribution in the deep waters of some of the basins of this region is summarized in Table 11, compiled from Van Riel's data.

THE NORTHEAST PACIFIC, BERING STRAIT, AND BERING SEA

The oxygen distribution in the northeast Pacific, Bering Strait, and Bering Sea has been studied by T. G. Thompson and his coworkers. Their data (Barnes and Thompson, 1938) extending from 54°N. in the Aleutians through the eastern part of the Bering Sea and Straits into the Chukchi Sea show that shallow waters of this generally shallow region are highly oxygenated and well mixed from surface to bottom. Between Dutch Harbor and about 56°N., the waters are deeper but still on the eastern shelf area and show no well-developed minimum zone, decreasing rather steadily from 6–7 ml/liter at the surface to 3.5–4.5 ml/liter at 400 meters.

Thompson, Thomas, and Barnes (1934) reported on the oxygen content of the waters off the coast of Washington, Vancouver Island, the North Pacific (south of the Aleutian Ridge), and the Bering Sea. Except in the Bering Sea, there is a well-developed intermediate oxygen minimum zone in this region; its depth tends to increase from north to south. Just south of the Aleutian Ridge it occurred at 800 meters, but off the coast of Washington and Vancouver Island it was found at 1000–1100 meters at several stations. Minimum concentrations increased northward, from about 2.2 ml/liter off the Washington coast to about 6.7 ml/liter in the Bering Sea. In the Gulf of Alaska off Cape Spencer (57°39′N.) the intermediate minimum zone was absent, and concentrations decreased steadily to 4.2 ml/liter in the bottom water at 1900 meters. Hamm and Thompson (1941) found the minimum concentration, 2.46 ml/liter, at 1000 meters, beyond the continental shelf off the coast of Washington (48°24′N., 127°02′W.), but at a station west of the Queen Charlotte Islands (54°10′N., 134°10′W.) the oxygen content decreased steadily with depth to 2.91 ml/liter at 1100 meters.

Vast areas of the Pacific Ocean remain unexplored in so far as the oxygen content is concerned. The evidence leads Sverdrup *et al.* (1942) to assume that the tongue of low oxygen extending westward in the northern equatorial Pacific has a counterpart in the southern equatorial region. The section constructed by Schott (1935, Fig. 50) and the high populations encountered on the drift of the KON TIKI (Heyerdahl, 1950) indicate such a zone is present in these southern latitudes; this view is strengthened by the WILLIAM SCORESBY observations off the Peruvian coasts and is confirmed, for the eastern part of the ocean, by recent observations.

APPENDIX: DETERMINATION OF DISSOLVED OXYGEN

Oxygen determination: The introduction, in 1888, of the Winkler titrimetric method for the determination of dissolved oxygen offered a real stimulus to the observation of this quantity in the oceans. Prior to its first extensive oceanographic use aboard the PLANET (Brennecke, 1909) oxygen was determined gasometrically by a variety of methods. Except for special researches, such as those of Hamm and Thompson (1941), these methods have only historical interest. The Winkler method, in several modified forms, is now used universally in oceanography.

A need for improvement in methodology, in keeping with the high speed and continuously recording methods of oceanography, has developed in recent years. Micro or semimicro methods would be desirable for use in conjunction with the Spilhaus-Miller sea sampler (Spilhaus and Miller, 1948). Semimicro methods based on the Winkler method have been tried with varying degrees of success (Thompson and Miller, 1928; Van Dam, 1934; Harper, 1953). A method in which the concentration of the iodine solution is measured colorimetrically instead of by titration has been described by Austin (1950), but the author has had indifferent success with it at sea, chiefly because of difficulties in achieving the required niceties of technique aboard ship. A microcolorimetric method, in which a solution of reduced indigo carmine is partially oxidized by the oxygen in the test sample, has recently been described by Loomis (1954).

Polarographic and amperometric methods appear to have little advantage for shipboard use, unless they can be made continuously operating, either along a ship's course at a fixed depth or with depth at a fixed location, as the salinity-temperature-depth recorder (Jacobson, 1948) operates. Advances along this line have been made, and Ippen, Yoseph, and Posthill (1951) have described a method for continuously recording the oxygen content in water during aeration processes, using a dropping mercury electrode in water of low turbulence, or a rotating platinum electrode in a system of higher turbulence. It appears that the latter might be useful in a flowing system. Other aspects of this subject have been discussed by Olson, Brackett, and Crickard (1949), by Manning (1940), and by Giguère and Lauzier (1945).

THE WINKLER METHOD: This method employs the oxidation of manganous hydroxide, by dissolved oxygen, to give tetravalent manganese. Upon acidification in the presence of iodide ion, free iodine (or I_3^- ion) is formed equivalent to the amount of dissolved oxygen:

$$Mn^{++} + 2OH^- \rightarrow Mn(OH)_2$$

$$2\ Mn(OH)_2 + O_2 \rightarrow 2\ MnO(OH)_2$$

$$Mn(OH)_2 + 2H^+ \rightarrow Mn^{++} + 2H_2O$$

$$MnO(OH)_2 + 4H^+ + 3I^- \rightarrow Mn^{++} + I_3^- + 3H_2O$$

The complex iodine-iodide ion (I_3^-) thus released is then titrated against thiosulfate solution, using starch as an indicator:

$$I_3^- + 2S_2O_3^= \rightarrow 3I^- + S_4O_6^=.$$

The water samples are drawn from the sampling device, in the absence of air, as soon as they are brought on board. The sample bottles are filled and kept stoppered. With the least practicable delay, solutions of manganous salt and of basic iodide are added, the bottle again stoppered, shaken, and the precipitate allowed to settle. Later, the mixture is acidified, and the liberated iodine is titrated.

The method has been reviewed in more detail by Bjerrum (1904), Jacobsen and Knudsen (1921), Helland-Hansen (1923), Thompson and Robinson (1932; 1939) and others. Thompson and Robinson (1939), Ohle (1953), H. Barnes (1953), and others have discussed sources of error and their prevention. T. G. Thompson (unpublished notes) has estimated that in nearly saturated samples the error in a determined value is about 0.002 mg atom or 0.02 ml/liter of sea water.

A committee of the Association d'Océanographie Physique on Chemical Methods and Units consisting of Bjørn Helland-Hansen, J. P. Jacobsen, and T. G. Thompson (Helland-Hansen *et al.*, 1948) has recommended that the oxygen content be reported as the amount, in milligram atoms, dissolved in an amount of sea water that at 20° has the volume of 1 liter, or in ml at NTP dissolved in a similar amount of water. Because the large majority of data is reported in the latter units, they have been most generally used in this paper. The molecular volume of O_2 is 22.393 liters, its atomic weight is 16.00. Therefore, the atomic volume of oxygen is 11.1965 liters, and the units can be interconverted as follows:

$$11.1965 \times \text{milligram atom/liter} = \text{ml/liter}$$

or

$$\text{ml/liter} \div 11.1965 = \text{milligram atoms/liter.}$$

The factor for the conversion from cubic centimeters to milliliters is 0.999972, and the two units have been used interchangeably in this discussion.

To convert oxygen concentrations to parts per million:

$$11.1965 \text{ mg-a/liter} = 1 \text{ ml/liter} = 0.179144 \text{ grams/liter}$$

$$= 179.144 \text{ grams/1000 liters}$$

If the density of the solution is 1.0, this equals parts per million. If the density is other than 1.0, divide by the density to get parts per million.

ACKNOWLEDGMENT

The author takes this opportunity to thank Drs. A. C. Redfield, B. H. Ketchum, Mary Sears, and D. E. Carritt for their many helpful suggestions and for reading the manuscript. Mr. Henry Stommel's criticism of the section on Circulatory and

Mixing Processes was greatly appreciated, as were data from recent Scripps Institution of Oceanography cruises, which were made available by Dr. Warren Wooster. The help of Mr. G. G. Pasley was indispensable in preparing the illustrations.

REFERENCES

Austin, Lynn H. A spectrophotometric determination of dissolved oxygen in water: Univ. Wash. (Seattle), unpublished thesis (‡), 1950.

Barnes, Clifford A., and Thompson, Thomas G. Physical and chemical investigations in Bering Sea and portions of the North Pacific ocean: Univ. Wash. (Seattle), Publs. in Oceanog., vol. 3, no. 2, p. 35–79 and appendix of tables and figs., 164 pp., 1938.

Barnes, Harold. A double syringe-pipette for dissolved oxygen determinations: Analyst, vol. 78, no. 929, pp. 501–503, 1 fig. 1953.

Bigelow, Henry B. Oceanography, its scope, problems, and economic importance: vi + 263 pp. Houghton Mifflin Co., Boston and New York. 1931.

Bishop, David W. Respiration and metabolism, *in* Comparative Animal Physiology: C. Ladd Prosser, ed. Chap. 8, pp. 209–289, 28 figs. W. B. Saunders & Co., Philadelphia. 1950.

Bjerrum, Niels. On the determination of oxygen in sea water: Komm. Havundersøg., Kbh., Medd., Serie Hydrog., vol. 1, no. 5, pp. 1–13, 1904.

Brennecke, W. Ozeanographie: Forschungsreise S.M.S. Planet 1906/07: vol. 3 and Tafeln. ix + 154 pp., tables, volume of illustrations. Karl Siegismund, Berlin, 1909.

Brouardel, Jean, and Fage, Louis. Variation de la teneur en oxygene de l'eau au proche voisinage des sediments: Deep-Sea Research, vol. 1, no. 2, pp. 86–94, 4 figs., 1954.

Bruins, H. R. Coefficients of diffusion in liquids: *in* International Critical Tables, vol. 5, p. 64. National Research Council. McGraw-Hill, New York, 1929.

Bruneau, L., Jerlov, N. G., and Koczy, F. F. Physical and chemical methods: Reports of the Swedish Deep-Sea Exped. 1947–1948 Rep., vol. 3, fasc. I, Göteberg 1953.

Buch, K. Die Verwendung von Stickstoff-und Sauerstoffanalysen in der Meeresforschung: Jour. du Conseil, vol. 4, no. 2, p. 162–191, 1 fig., tables of data, 1929.

Carpenter, William Lant. Summary of the results of the examination of samples of sea-water taken at the surface and at various depths: pp. 502–511 in "The Depths of the Sea" by C. Wyville Thompson, xx + 520 pp. illus. Macmillan and Co., London, 1874.

Clarke, George L. Further observations on the diurnal migration of copepods in the Gulf of Maine: Biol. Bull. Woods Hole vol. 67, no. 3, pp. 432–455, 6 figs., 4 tables, 1934a.

——. Factors affecting the vertical distribution of copepods: Ecol. Mon., vol. 4, pp. 530–540, 3 figs., 1934b.

——. Light penetration in the western North Atlantic and its application to biological problems: Cons. int. Explor. Mer, Rapp., vol. 101, pt. 2, no. 3, 14 pp., 6 figs., 1936.

——. Dynamics of production in a marine area: Ecol. Mon., vol. 16, pp. 321–337, 9 figs., 1946.

—— and Oster, R. H. The penetration of blue and red components of daylight into Atlantic coastal waters and its relation to phytoplankton metabolism: Biol. Bull. Woods Hole, vol. 67, no. 1, p. 59–75, 6 figs., 4 tables, 1934.

Clowes, A. J., and Deacon, G. E. R. The deep-water circulation of the Indian ocean. Nature, vol. 136, pp. 936–938, 4 figs., 1935.

Conseil Permanent International pour l'Exploration de la Mer. Bulletin Hydrographique pour l'Annee 1928, pp. 108, 1929; pour l'Annee 1935, pp. 86, 101–102, 1936; pour l'Annee 1948, pp. 80–87, 1953.

Cooper, L. H. N. Salt error in determinations of phosphate in sea water. Redefinition of the anomaly of the nitrate-phosphate ratio: Jour. Mar. Biol. Assoc. vol. 23, pp. 171–179, 3 tables, 1938.

Correns, Carl W. Pelagic sediments of the North Atlantic ocean: *in* Parker D. Trask, ed., Recent Marine Sediments, A Symposium, pp. 373–395, 4 figs., Am. Assoc. of Petrol. Geol., Tulsa, Thomas Murby & Co., London, 1939.

Cromwell, Townsend. Mid-Pacific oceanography, January through March, 1950: U. S. Fish & Wildlife Serv. Special Sci. Rpt., no. 54, 9 pp. + figures and tables of data (‡) July, 1951.

Deacon, G. E. R. The hydrology of the southern ocean: Discovery Rep., vol. 15, pp. 1–124, illus., 1937.

Dietrich, Günter. Aufbau und Bewegung von Golfstrom und Agulhasstrom, eine vergleichende Betrachtung: Naturwissenschaften, vol. 15, pp. 225–230, 11 figs., 1936.

——. Über Bewegung und Herkunft des Golfstromwassers: Inst. Merresk. Univ. Berl. Veröff., N. F. Ser. A., vol. 33, Teil 2, pp. 53–91, 25 figs., tables of data, 1937.

Discovery Committee. Station List, William Scoresby 1931–1938: Discovery Rep., vol. 25, pp. 143–280, plates 34–37, 1949.

Dittmar, William. Report on researches into the composition of ocean-water, collected by H. M. S. Challenger, during the years 1873–1876: Sci. Res. Voyage Challenger 1873–76, Sci. Res. Chem. Phys., vol. 1, 251 pp., 3 plates, tables and figures, 1884.

Dorsey, N. Ernest. Properties of ordinary water-substance: Am. Chemical Soc. Monog., no. 81 xxiv + 673 p., New York, Reinhold Publ. Corp., 1940.

Fleming, J. A., Sverdrup, H. U., Ennis, C. C., Seaton, S. L., and Hendrix, W. C. Observations and results in physical oceanography: Carnegie Inst. Washington Pub. 545, iv + 315 pp., 254 figs., Tables of data, remarks, 1945.

Fleming, Richard H. Composition of plankton and units for reporting populations and production: Sixth Pac. Sci. Congr. Proc., vol. 3, pp. 535–540, 2 tables, Univ. of California Press, Berkeley and Los Angeles, 1940.

—— and Revelle, Roger. Physical processes in the ocean: *in* Parker D. Trask, ed., Recent marine sediments, a symposium, pp. 48–141, 24 figs., Am. Assoc. of Petrol. Geol., Tulsa, Thomas Murby & Co., London, 1939.

Fox, C. J. J. On the coefficients of absorption of nitrogen and oxygen in distilled water and sea water, and of atmospheric carbonic acid in sea water: Faraday Soc. Trans., vol. 5, pp. 68–87, 6 tables, 7 figs., 1909.

Fuller, J. L. Feeding rates of *Calanus finmarchicus* in relation to environmental conditions; Biol. Bull., vol. 72, no. 2, pp. 233–246, 3 figs., 1937.

Gaarder, Torbjørn. Die Sauerstoffverhältnisse im östlichen Teil des nordatlantischen Ozeans: Norske Videns. Akad., Geophys. Pub., vol. 4, no. 3. 72 pp., illus. and tables, 1927.

Gaarder, Torbjørn, and Gran, H. H. Investigation of the production of plankton in the Oslofjord: Cons. int. Explor. Mer. Rapp., vol. 42, pp. 1–48, 2 fig., 1927.

Gardiner, A. C. Phosphate production by planktonic animals: Jour. du Conseil. vol. 12, pp. 144–146, 3 tables, 1937.

Giguère, P. A. and Lauzier, L. Analyse polarométric de l'oxygène dissous avec une microélectrode de platine. Canadian Jour. Research. Sect. B, vol. 23, no. 5, pp. 223–233, 9 figs., 1945.

Gilson, H. C. The nitrogen cycle: Murray Exped. 1933–34. Sci. Repts., vol. 2, no. 8, pp. 21–81, 16 figs., 1937.

Glueckauf, E. The composition of atmospheric air: *in* T. F. Malone, ed., Compendium of Meteorology, pp. 3–4, Am. Meteor. Soc., Boston, 1951.

Graham, Herbert W. Plankton production in relation to character of water in the open Pacific: Jour. Marine Research, vol. 4, no. 3, pp. 189–197, 2 figs., 1941.

—— and Moberg, Erik G. Chemical results of the last cruise of the Carnegie. Chemistry I: Carnegie Inst. Washington Pub. 562, vii + 58 pp., 23 figs., 1944.

Gran, H. H. and Thompson, Thomas G. The diatoms and the physical and chemical conditions of the sea water of the San Juan Archipelago: Puget Sd. Mar. (biol.) Sta. Pub., vol. 7, pp. 169–204, 9 figs., 1930.

—— and Braarud, T. A quantitative study of the phytoplankton in the Bay of Fundy and the Gulf of Maine (including observations on hydrography, chemistry, and turbidity): Biol. Bd. Can. Jour., vol. 1, pp. 279–467, 69 figs., 1935.

Gunther, E. R. A report on oceanographical investigations in the Peru Coastal Current: Discovery Rep., vol. 13, pp. 107–276, 71 figs., 1936.

Hamm, Randall E. and Thompson, Thomas G. Dissolved nitrogen in the sea water of the northeast Pacific with notes on the carbon dioxide and the dissolved oxygen: Jour. Marine Research, vol. 4, no. 1, pp. 11–26, 6 tables, 1941.

Harper, E. L. Semimicro determination of dissolved oxygen: Analyt. Chem., vol. 25, no. 1, pp. 187–188, 1 fig., 1953.

Harvey, H. W. Recent advances in the chemistry and biology of sea water: vii + 164 pp., 29 figs., 16 tables, Cambridge Univ. Press, 1945.

Helland-Hansen, Bjørn. Nogen hydrografiske metoder. Skand. Naturforsker möte, Kristiana (Oslo), 1916.

——. The ocean waters, an introduction to physical oceanography, part II: Int. Rev. Hydrobiol., vol. 11, no. 5/6, pp. 393–488, 14 figs., 1923.

——. Physical oceanography and meteorology: Sars N. Atl. Deep Sea Exped. Rep., vol. 1, pt. 1, (text), 115 pp., 47 figs., 1930.

——, Jacobsen, J. P., and Thompson, Thomas G. Chemical methods and units: Assoc. Oceanogr. Phys. Publ. Sci., no. 9, 28 pp., 1948.

Hersey, J. B. and Moore, Hilary B. Progress report on scattering layer observations in the Atlantic Ocean: Am. Geophys. Union Trans., vol. 29, no. 2, pp. 341–354, 16 figs., 1948.

Heyerdahl, Thor. Kon Tiki: Rand McNally & Co., Chicago, 304 pp., illus. 1950.

Hock, R. J., Erikson, Harald, Flagg, Walter, Scholander, P. F., and Irving, Laurence. Composition of the ground-level atmosphere at Point Barrow, Alaska: Jour. Meteor. vol. 9, no. 6, p. 441–2, one fig., 1952.

Humphreys, W. J. Compositions of the atmosphere: *in* International Critical Tables v. I, p. 393, National Research Council, McGraw Hill, New York, 1926.

Ippen, A. T., Yoseph, R. S., and Posthill, B. N. The continuous measurement of oxygen concentration in water during aeration processes: Mass. Inst. Tech. Hydrodyn. Lab. Tech. Rept., no. 3, vol. v, 24 pp., 18 figs. (‡), 1951.

Ito, Koichi. Oxygen-gas content of sea water in the south-western portion of the North Pacific: Rec. Oceanogr. Wks. Jap., vol. 2, no. 2, pp. 82–91, 3 figs., table of data, 1930.

Jacobsen, J. P. Contribution to the hydrography of the Atlantic: Komm. Havundersøg. Kbh. Medd. Ser. Hydrografi., vol. 2, No. 5, 7 figs., 8 diagrams, tables of data, 1916.

——. Contribution to the hydrography of the North Atlantic. The Dana Exped. 1920–1922 Oceanogr. Rep., no. 3, 98 pp., 25 tables, 63 figs., 1929.

—— and Knudsen, Martin. Dosage de l'O_2 dans l'eau de mer par la methode de Winkler: Inst. Oceanogr. Monaco, Bull., No. 390, 19 pp., 3 figs., 1921.

Jacobson, A. W. An instrument for recording continuously the salinity, temperature, and depth of seawater: Am. Inst. Elec. Eng., Trans., vol. v 67, pp. 1–9, 14 figs., 1948.

Jakhelln, Anton. Oceanographic investigations in East Greenland waters in the summers of 1930–32: Skr. Svalb. og Ishavet, no. 67, 79 pp., 28 figs., 2 plates, 1936.

Jenkin, Penelope M. Oxygen production by the diatom *Coscinodiscus excentricus* Ehr. in relation to submarine illumination in the English Channel: Jour. Mar. Biol. Assoc., vol. 22, pp. 301–343, 9 figs., 1937.

Jerlov, N. G. Particle distribution in the ocean. Swedish Deep-Sea Exped. 1947–1948 Rep., vol. 3, Physics and Chem., no. 3, p. 73–97, 25 figs., 1953.

Kalle, Kurt. Einige verbesserungen zur Bestimmung des gelösten Sauerstoffs im Meerwasser: Annal. Hydrogr. Berl., vol. 67, pp. 267–269, 3 figs., 1939.

Ketchum, Bostwick H. Plankton algae and their biological significance: *in* Manual of Phycology—an introduction to algae and their biology. ed. Gilbert M. Smith, Chap. 17, p. 335–346, 2 tables, Waltham, Mass., The Chronica Botanica Co., 1951.

Knudsen, Martin. Hydrography: Danish Ingolf Exped., vol. 1, no. 2, pp. 21–161, 34 plates, 1899.

Kreps, E., and Verjbinskaya, N. The consumption of nutrient salts in the Barents Sea: Jour. du Conseil, vol. 7, no. 1, pp. 25–45, 8 figs., 1932.

Krogh, August. Some experiments on the invasion of oxygen and carbonic-oxide into water: Skand. Arch. Physiol., vol. 23, pp. 224–235, 1 fig., 3 tables, 1910.

Kuenen, Ph. H. Geological results; Bottom samples; Collecting of the samples and some general aspects: Snellius-Exped., vol. 1, pt. 3, Sect. I, pp. 1–48, 6 figs., 2 plates, 1942.

Kulp, J. Laurence. Carbon-14 measurements on geological samples: Atomics, vol. 4, April, 1953.

LOOMIS, W. F. Rapid microcolorimetric determination of dissolved oxygen: Analyt. Chem., vol. 26, no. 2, pp. 402–404, 2 figs., 1954.

LE DANOIS, ED. Les transgressions oceaniques: Off. Pêches Marit. Rev. Trav., vol. 7, Fasc. 4, no. 28, pp. 369–459, 50 figs., 1934.

MANNING, W. M. A method for obtaining continuous records of dissolved oxygen in lake waters. Ecology, vol. 21, pp. 509–512, 3 figs., 1940.

MARSHALL, S. M., AND ORR, A. P. The photosynthesis of diatom cultures in the sea: Jour. Mar. Biol. Assoc., vol. 15, pp. 321–360, 24 figs., 1928.

MIYAKE, Y. The diurnal variation of dissolved oxygen in sea water consisting of different water masses: Geophys. Mag. Tokyo, vol. 16, no. 24, pp. 66–70, 6 figs., 1948.

MOBERG, ERIK. Distribution of oxygen in the Pacific: *in* Contr. to Marine Biology, No. IV, p. 69–78, 1 fig., Stanford Univ. Press, Stanford Univ., Calif., 1930.

MONTGOMERY, RAYMOND B. Circulation in upper layers of southern North Atlantic deduced with use of isentropic analysis: Pap. Phys. Oceanog. Meteor., vol. 6, no. 2, 55 pp., 10 figs., 19 charts, 1938.

——. Some relationships of vertical stability to salinity and oxygen extremes in the Atlantic: Beitr. Geophys., vol. 54, p. 194–202, 2 figs., 1939.

MOORE, HILARY B. The relation between the scattering layer and the Euphausiacea: Biol. Bull. vol. 99, no. 2, pp. 181–212, 28 figs., 1950.

MOSBY, HÅKON. The waters of the Atlantic Antarctic ocean: Norweg. Antarctic Exped., 1927–1928, Sci. Results, vol. 1, no. 11, 131 pp., station list, 50 figs., Norske Vidensk., Akad., Oslo, 1935.

NANSEN, FRIDTJOF. Northern waters: Captain Roald Amundsen's oceanographic observations in the Arctic Seas in 1901. With a discussion of the bottom waters of the northern seas: Vidensk. Selsk. Skr. I. Math.-Naturv. Klasse, no. 3, 145 pp., 4 figs., 11 plates, tables of data, 1906.

——. Das Bodenwasser und die Abkühlung des Meers: Int. Rev. Hydrobiol., vol. 1, no. 1, pp. 1–42, 12 figs., 1912.

NICHOLLS, A. G. On the biology of *Calanus finmarchicus*. III. Vertical distribution and diurnal migration in the Clyde Sea area. Jour. Marine Biol. Assoc., vol. 19, no. 1, pp. 139–164, 4 figs., 1933.

NIELSEN, J. N. Contribution to the hydrography of the north-eastern part of the Atlantic Ocean: Komm. Havundersøg. Medd. Ser. Hydro., vol. 1, no. 9, pp. 1–25, 3 plates, 1907.

——. Hydrography of the Mediterranean and adjacent waters: Danish Oceanogr. Exped. 1908–1910 Rep., vol. 1, pp. 77–191, 19 figs., 10 plates, 1912.

NIKITIN, W. M. Die untere Planktongrenze und deren Verteilung im Schwarzen Meer: Int. Rev. Hydrobiol., vol. 25, pp. 102–130, 4 figs., 1931.

OHLE, WALDEMAR. Die chemische und die elektrochemische Bestimmung des molekular gelösten Sauerstoffs der Binnengewässer: Int. ver Ver. Limnol., Mitt., no. 3, 44 pp., 14 figs., 10 tables, 1953.

OLSON, R. A., BRACKETT, F. S., AND CRICKARD, R. G. Oxygen tension measurement by a method of time selection using the static platinum electrode with alternating potential. Jour. General Physiol., vol. 32, no. 6, pp. 681–703, 18 figs., 1949.

PARR, A. E. On the possibility of a biological mechanism controlling the occurrence of the oxygen minimum layer in the sea: Am. Philos. Soc. Proc., vol. 80, no. 1, pp. 49–56, 1939.

RAKESTRAW, NORRIS W. Studies on the biology and chemistry of the Gulf of Maine. I. Chemistry of the waters of the Gulf of Maine in August, 1932: Biol. Bull., vol. 64, no. 2, p. 149–158, 4 figs., 1933.

——. Oxygen consumption in sea water over long periods: Jour. Marine Research, vol. 6, no. 3, pp. 259–263, 1947.

—— AND CARRITT, D. E. Some seasonal chemical changes in the open ocean: Jour. Marine Research, vol. 7, no. 3, pp. 362–369, 6 figs., 1948.

—— AND EMMEL, VICTOR. The relation of dissolved oxygen to nitrogen in some Atlantic waters: Jour. Marine Research, vol. 1, no. 3, pp. 207–216, 4 figs., 1938.

——, RUDD, DEFOREST P., AND DOLE, MALCOLM. Isotopic composition of oxygen in air dissolved in Pacific ocean water as a function of depth: Amer. Chemical Soc. Jour., vol. 73, p. 2976, 1 fig., 1951.

—— AND SMITH, H. P. A contribution to the chemistry of the Caribbean and Cayman Seas: Bingham Oceanogr. Coll. Bull., vol. 6, art. 1, pp. 1–41, 32 figs., 1937.

REDFIELD, ALFRED C. On the proportions of organic derivatives in sea water and their relation to the composition of plankton: James Johnstone Memorial vol., pp. 179–192, 5 figs., Univ. Press, Liverpool, 1934.

——. The processes determining the concentration of oxygen, phosphate, and other organic derivatives within the depths of the Atlantic Ocean: Pap. Phys. Oceanogr. Meteor., vol. 9, no. 2, 22 pp., 13 figs., 1942.

——. The exchange of oxygen across the sea surface: Jour. Marine Research, vol. 7, no. 3, pp. 347–361, 4 figs., 1948a.

——. Characteristics of sea water: *in* The Corrosion Handbook, H. H. Uhlig, ed., pp. 1111–1122, New York, John Wiley & Sons, Inc., 1948b.

——, SMITH, H. P., AND KETCHUM, B. H. The cycle of phosphorus in the Gulf of Maine: Biol. Bull. vol., 73, pp. 421–443, 4 figs., 1937.

RICHARDS, FRANCIS A., AND REDFIELD, ALFRED C. A correlation between the oxygen content of sea water and the organic content of marine sediments: Deep-Sea Research, vol. 1, no. 4, pp. 279–281, 2 figs., 1954.

RILEY, GORDON A. Plankton studies. II. The western North Atlantic, May–June, 1932: Jour. Marine Research, vol. 2, no. 1, pp. 145–162, 3 figs., 1939.

——. Plankton studies. III. Long Island Sound: Bingham Oceanogr. Coll. Bull., vol. 7, art. 3, pp. 1–93, 14 figs., 1941.

——. Oxygen, phosphate and nitrate in the Atlantic Ocean: *Ibid.*, vol. 13, art. 1, 26 pp., 33 figs., 25 tables, 1951.

ROSSBY, C.-G. Dynamics of steady ocean currents in the light of experimental fluid mechanics: Pap. Phys. Oceanogr. Meteor., vol. 5, no. 1, 43 pp., 16 figs., 2 charts, 1936.

RUSSELL, F. S. The vertical distribution of marine macroplankton. An observation on diurnal changes: Jour. Mar. Biol. Assoc., vol. 13, pp. 769–809, 1 pl., 6 figs., 1925.

RYTHER, JOHN H. AND VACCARO, RALPH F. A comparison of the oxygen and C^{14} methods of measuring photosynthesis: Jour. du Conseil, vol. 20, no. 1, pp. 25–34, 3 figs., 1954.

SARGENT, MARSTON C., AND HINDMAN, J. C. The ratio of carbon dioxide to oxygen evolution in sea water in the light: Jour. Marine Research, vol. 5, no. 2, pp. 131–135, 1943.

SCHMIDT, JOHANNES. On the contents of oxygen in the ocean on both sides of Panama: Science, vol. 61, pp. 592–593, 1 fig., 1925.

——. Introduction to the oceanographical reports including list of the stations and hydrographical observations: DANA Exped., 1920–1922 Oceanogr. Rep., no. 1, 87 pp., 6 plates, 1929.

SCHOTT, GERHARD. Geographie des indischen und stillen Ozeans: xix + 413 pp., 37 charts, 114 figs., Hamburg, C. Boysen, 1935.

SCHUMACHER, ARNOLD. A survey of present knowledge of oceanic circulation based upon modern physical and chemical observations: Natl. Research Council Bull., no. 85, chap. 9, pp. 358–383, 10 figs., 1932.

SEARS, MARY. Notes on the Peruvian coastal current. I. An introduction to the ecology of Pisco Bay: Deep-Sea Research, vol. 1, no. 3, 4 figs., 1954.

SEIWELL, H. R. The distribution of oxygen in the western basin of the North Atlantic, 1934: Pap. Phys. Oceanogr. Meteor., vol. 3, no. 1, 86 pp. illus., 1934.

——. The annual organic production and nutrient phosphorus requirement in the tropical western North Atlantic: Jour. du Conseil, vol. 10, pp. 20–32, 1 fig., 1935.

——. Short period vertical oscillations in the western basin of the North Atlantic: Pap. Phys. Oceanogr. Meteor., vol. 5, no. 2, 44 pp., 9 figs., 21 tables, 1937a.

——. The minimum oxygen concentration in the western basin of the North Atlantic: *Ibid.*, vol. 5, no. 3, 24 pp., 8 figs., 1937b.

——. Consumption of oxygen in sea water under controlled laboratory conditions: Nature, vol. 140, pp. 506–507, 1 fig., 1937c.

——. The oxygen-poor layer in the western North Atlantic: Jour. du Conseil, vol. 12, no. 3, pp. 277–283, 2 figs., 1937d.

——. Relationship of minimum oxygen concentration to density of the water column in the western North Atlantic: Beitr. Geophys., vol. 50, pp. 302–306, 2 tables, 1 fig., 1937e.

——. Application of the distribution of oxygen to the physical oceanography of the Caribbean sea region, 1938: Pap. Phys. Oceanogr. Meteor., vol. 6, no. 1, 60 pp., 42 figs., 1938.

——, AND SEIWELL, GLADYS EDDY. The sinking of decomposing plankton in sea water and its relationship to oxygen consumption and phosphorus liberation: Am. Philos. Soc. Proc., vol. 78, no. 3, pp. 465–481, 5 figs., 2 tables, 1938.

SMITH, ED. H., SOULE, F. M., AND MOSBY, OLAV. The MARION and GENERAL GREEN expeditions to Davis Strait and Laborador Seas under direction of the United States Coast Guard 1928–1931–1933–1934–1935. Scientific results. 2. Physical oceanography: U. S. Coast Guard Bull., vol. 19, vi + 259 p., illus., 1937.

SOULE, FLOYD M. Oceanography, Excerpt from International Ice Observation and Ice Patrol Service in the North Atlantic Ocean. Season of 1938: U. S. Coast Guard Bull., no. 28, pp. 113–173, 12 figs., tables, 1940.

SPILHAUS, ATHELSTAN F., AND MILLER, ARTHUR R. The sea sampler: Jour. Marine Research, vol. 7, no. 3, pp. 370–385, 11 figs., 1948.

STEEMAN NIELSEN, E. The annual amount of organic matter produced by the phytoplankton in the sound of Helsingør: Komm. Havundersøg. Kbh. Medd., Serie: Plankton, vol. 2, nr. 3, 38 pp., 6 figs., 1937.

——. The use of radio-active carbon (C^{14}) for measuring organic production in the sea: Jour. du Conseil, vol. 18, no. 2, pp. 117–140, 7 figs., 1952.

SVERDRUP, H. U. The waters on the North-Siberian Shelf. Norweg. N. Pol. Exped. MAUD 1918–1925 Sci. Rep., vol. 4, no. 2, 131 pp., Tab. of Results, 47 figs., 4 plates, 1929.

——. Some oceanographic results of the CARNEGIE'S work in the Pacific—the Peruvian Current: Am. Geophys. Union Trans., 10th and 11th Annual Meetings, pp. 257–264, 11 figs., 1930.

——. Scientific results of the NAUTILIS expedition, 1931, under the command of Captain Sir Hubert Wilkins. Oceanography: Pap. Phys. Oceanogr. Meteor., vol. 2, no. 1, part 2, pp. 16–63, 41 figs., 1933.

——. On the explanation of the oxygen minima and maxima in the oceans: Jour. du Conseil, vol. 13, no. 2, p. 163–172, 6 figs., 1938.

—— AND FLEMING, R. H. The waters off the coast of southern California. March to July, 1937: Calif. Univ. Scripps Inst. Oceanog. Bull., vol. 4, no. 10, pp. 261–378, 66 figs., 1941.

——, JOHNSON, MARTIN W., AND FLEMING, R. H. The Oceans: x + 1087 pp. illus., tables. New York, Prentice-Hall, Inc., 1942.

THOMPSON, C. WYVILLE. The depths of the sea: xx + 527 pp. illus. London, Macmillan & Co., 1874.

THOMPSON, E. F. The general hydrography of the Red Sea. The exchange of water between the Red Sea and the Gulf of Aden over the "Sill": John Murray Exped. 1933–34 Sci. Rep., vol. 2, no. 3, 4, pp. 83–119, 22 figs., 1939.

THOMPSON, THOMAS G. and BARKEY, KENNETH T. Observations on fjord-waters: Am. Geophys. Union Trans., 19th Annual Meeting, pp. 254-260, 3 figs., 3 tables of data, 1938.

—— AND MILLER, ROBERT C. Apparatus for the micro-determination of dissolved oxygen: Industr. Engng. Chem. (Anal.), vol. 20, no. 7, pp. 774–776, 1 fig., 1928.

—— AND ROBINSON, REX J. Chemistry of the Sea: Natl. Research Council Bull., no. 85, Chap 5, pp. 95–203, 18 figs., 1932.

—— AND ROBINSON, REX J. Notes on the determination of dissolved oxygen in sea water: Jour. Marine Research, vol. 2, no. 1, pp. 1–8, 1939.

——., THOMAS, B. D., AND BARNES, C. A. Distribution of dissolved oxygen in the Northa Pcific Ocean: James Johnstone Memorial Vol., pp. 203–234, 7 figs., 10 tables, Univ. Press, Liverpool, 1934.

THOMSEN, HELGE. Oxygen in the tropical Pacific: Nature, vol. 127, no. 3204, pp. 489–490, 1 fig., 1931.

——. Hydrographical observations made during the DANA Expedition 1928–30: Dana Rep., No. 12, 46 pp., 1937.

TRASK, PARKER D. Relation of salinity to the calcium carbonate content of marine sediments: U. S. Geol. Survey, Prof. Paper No. 186-N, pp. 273–299, 8 figs., 1 plate, 1937.

——. Organic content of recent marine sediments: *in* Recent marine sediments, a symposium. edited by Parker D. Trask, pp. 428–453, Tulsa; Am. Assoc. of Petrol. Geol. London, Thomas Murby and Co., 1939.

——. Chemical studies of sediments of the western Gulf of Mexico: Pap. Phys. Oceanogr. Meteor., vol. 12, no. 4, part 2, pp. 47–120, 21 figs., 16 tables, 1953.

TULLY, JOHN P. Oceanography and prediction of pulp mill pollution in Alberni Inlet: Fish. Res. Bd. Can. Bull., no. 83, 169 pp., 62 figs., tables, appendices, 1949.

UDA, MITITAKA. Hydrographical studies based on simultaneous oceanographical surveys made in the Japan sea and in its adjacent waters during May and June, 1932: Rec. Oceanogr. Works Jap., vol. 6, no. 1, pp. 19–107, 36 figs., 1934.

VAN DAM, L. A method for determining the amount of oxygen dissolved in 1 c.c. of water. Jour. Experimental Biology, vol. 11, pp. 80–85, 3 figs., 1934.

VAN RIEL, P. M. Oceanographic results, the bottom water. Introductory remarks and oxygen content: SNELLIUS-Exped., vol. 2, part 5 chap. 1, 77 pp. 33 figs., 1 plate, tables of data, 1943.

VAUGHAN, T. WAYLAND. Present trends in the investigation of the relation of marine organisms to their environment: Ecol. Monogr., vol. 4, 1 fig., pp. 501–522, 1934.

——. Ecology of modern marine organisms with reference to paleogeography: Geol. Soc. Am. Bull., vol. 51, pp. 433–468, 6 figs., 1940.

VERCELLI, FRANCESCO. Richerche de oceanografia fisica, pt. 1, Correnti e Maree: Ann. idrogr., vol. 11, 188 pp., 33 figs., table of data, 1925.

VON LEDEBUHR, JOACHIM F. Der Sauerstoff als ökologischer Faktor: Ergebn. Biol., vol. 16, pp. 173–261, 7 figs., 1939.

WAKSMAN, SELMAN A. AND RENN, CHARLES E. Decomposition of organic matter in sea water by bacteria. III. Factors influencing the rate of decomposition: Biol. Bull., vol. 70, no. 3, pp. 472–483, 2 figs., 1936.

WATTENBERG, HERMAN. Berichte über die chemischen Arbeiten. Die deutschen atlantischen Expedition, IV. Bericht, Profil XII–XIV: Ges. Erdk. z. Berl. Z., no. 45–6, pp. 307–315, 3 figs., 1927.

——. Die Durchlüfting des atlantischen Ozeans: Jour. du Conseil, vol. 4, no. 1, pp. 68–79, 4 figs., 1929.

——. Die Verteilung des Sauerstoffs und des Phosphats im atlantischen Ozean: Dtsch. Atlant. Exped. METEOR 1925–1927, Wiss. Eregbn., vol. 9, 132 pp., 41 figs., 1938, [Atlas, vii, 72 Beilage], 1939a.

——. Die Entstehung der sauerstoffarmen Zwischenschicht im Ozean: Ann. Hydrogr. Berl., vol. 67, pp. 257–266, 5 figs., 1939b.

WHIPPLE, GEORGE C. AND WHIPPLE, MELVILLE C. Solubility of oxygen in sea water: Am. Chemical Soc. Jour. vol. 33, p. 362–365, 2 tables, 1911.

WINKLER, LUDWIG WILHELM. Die Bestimmung des im Wasser gelösten Sauerstoffes: Dtsche. Chem. Ges. Ber., vol. 21, pp. 2843–2855, 3 figs., 1888.

WORTHINGTON, L. V. Three detailed cross-sections of the Gulf Stream: Woods Hole Oceanogr. Instn. Unpublished manuscript Ref. No. 53–85, 6 pp., 11 figs., (‡), Oct., 1953.

——. A preliminary note on the time scale in North Atlantic circulation. Deep-Sea Research vol. 1, no. 4, pp. 244–251, 5 figs., 1954.

WOOSTER, WARREN S. Shellback expedition, 17 May to 27 August, 1952. Univ. Calif., Scripps Inst'n Oceanogr., Unpublished Manuscript, Ref. 52–63. 14 pp., 8 figs., (‡) 1 Dec., 1952.

WÜST, GEORG. Schichtung und Zirkulation des atlantischen Ozeans. Die Stratosphäre: Dtsch. Atlant. Exped. METEOR 1925–1927, Wiss. Ergebn., vol. 6, pt. 1, 288 pp. 1935.

ZOBELL, CLAUDE E. Occurrence and activity of bacteria in marine sediments: *in* Parker D. Trask, ed., Recent marine sediments, a symposium. pp. 416–427, Tulsa. Am. Assoc. Petrol. Geol., London, Thomas Murby & Co., 1939.

——. The effect of oxygen tension on the rate of oxidation of organic matter in sea water by bacteria: Jour. Marine Research, vol. 3, no. 3, pp. 211–223, 1940.

—— AND ANDERSON, DON QUENTIN. Observations on the multiplication of bacteria in different volumes of stored sea water and the influence of oxygen tension and solid surfaces: Biol. Bull. Woods Hole, vol. 71, no. 2, pp. 324–342, 2 figs., 1936.

MANUSCRIPT COMPLETED NOVEMBER 1, 1954

Contribution No. 748

DISTRIBUTION OF PHOSPHORUS IN GREAT POND, MASSACHUSETTS[1]

By

EDWARD M. HULBURT

ABSTRACT

Inorganic phosphate and total phosphorus were determined during 1950 in Great Pond, Massachusetts. Except in deeper water during summer, the concentration of inorganic phosphate was less in Great Pond than in its sources of fresh and salt waters. In summer the total phosphorus concentration was greater in the Pond than in the Sound or River, this being particularly so in deep water of the Pond. During the remainder of the year concentrations were about the same in Sound, Pond, and River. Up to 92% of the total phosphorus within the Pond was organic phosphorus. The summer accumulation of phosphorus is explained as being the result of increased photosynthesis, the products of which settle from the surface to the deeper waters which return them up-pond in the countercurrent.

INTRODUCTION

Studies of the plankton ecology of coastal bays appear to show a greater productivity within these embayments than in the open ocean. For instance, Riley (1952) described a ten-fold increase in plant pigments in Long Island Sound when compared to the ocean beyond the eastern entrance. Tully (1949) showed greater oxygen saturation in the surface waters of Alberni Inlet than in the river feeding it or in the ocean at its mouth. Hutchinson and Lucas (1931) described much the same sort of situation at the mouth of the Fraser

---

[1] Contribution No. 748 from Woods Hole Oceanographic Institution.

Reprint from SEARS FOUND. JOURN. MAR. RES.

River. In Oslo fjord, phytoplankton appeared to be greater in the inner reaches of the fjord (Braarud and Bursa, 1939). It would be of interest to know on what factors such enhanced productivity depends and how it is related to the hydrography, to the form of the basin, and to the land drainage.

Greater productivity within embayments could be the result of a locally enhanced rate of conversion of inorganic nutrients to organic substance without any increase in the quantity of nutrient elements present. Greater productivity could also result from contributions of nutrient substances by land drainage. Braarud and Bursa (1939) attribute the greater productivity in the surface waters of the inner portion of Oslo fjord to pollution from the city of Oslo. Finally, greater productivity could be produced by a suitable combination of hydrographic and biological factors such that the quantity of the nutrient element would be greater in the embayment than in the source waters, fresh and salt. Characterization of the organic content and of the processes that determine its production should lead to an understanding of features of phytoplankton growth that are indigenous and yet of general importance.

THE EMBAYMENT

Great Pond, a small estuary near Falmouth, Massachusetts, proved to be a convenient embayment in which to study features suggested by the foregoing considerations. Its hydrography has been well studied and reported by Barlow (1956). Fig. 1, which shows the shape and depth of Great Pond, reveals clearly its division into a wide portion, the main pond, and a narrow portion, the arm; it is 1.5 miles long, does not exceed 9 feet in depth at highest tide, and has a localized fresh and salt water inflow. Stations where samples were taken are numbered so that those with lower numbers are seaward, those with higher numbers landward.

METHODS

Measurements of inorganic phosphate and total phosphorus concentrations in the pond water were made along the axis of Great Pond at various times throughout 1950. At the same time phytoplankton cell counts and turbidity determinations were made. Water samples were taken from a rowboat within a space of several hours except during February and March, when they were taken from the shore. Water samples were obtained within several inches of the surface and approximately ten inches above the bottom.

Inorganic phosphate was determined by the Atkins-Deniges method,

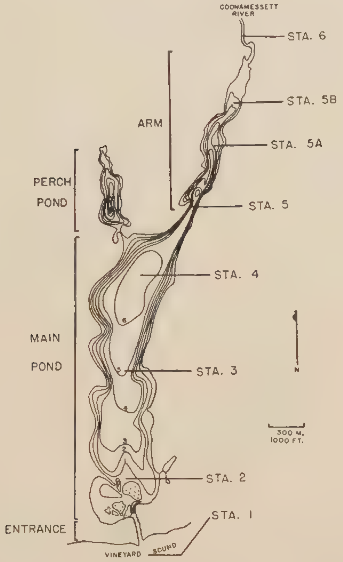

FIGURE 1. The morphometry of Great Pond. Depths are in feet.

total phosphorus by the Harvey method (1948). The difference between total phosphorus and inorganic phosphate was considered to be organic phosphorus. No attempt was made to separate the soluble and particulate fractions of organic phosphorus. The phytoplankton concentration was determined by counting all living cells under high magnification (X440) after filtration through a porcelain filter manufactured by the Selas Corporation. Turbidity determinations were the values of absorption of red light (0.66 μ) in a four centimeter thickness of sampled water. Measurements of the fraction of light removed by representative samples were made with a photoelectric cell that was sensitive to all wave lengths of visible light. Thus, absorption values could be converted to extinction coefficients.

RESULTS

Distribution of Inorganic Phosphate. Table I gives an extract of the basic data. Table I and Fig. 2 show that the concentration of inorganic phosphate in surface waters was least in the midreaches of the Pond and that there was usually an increasing concentration of phosphate from midpond to the Sound and from midpond to the River. At times the gradient was relatively uniform but at other times it increased abruptly at the mouth of the River. In bottom waters the inorganic phosphate concentration was variable; at times it was negligible and at other times it was higher than that in the Sound or River.

The changing concentrations of phosphate follow different seasonal cycles in the Sound, Pond, and River (see Fig. 3). In the Sound, concentrations were consistently high from late summer to the end of winter; during spring they fell to a minimum in May, and during summer they rose to a maximum on August 23. In the surface waters of midpond the values were low throughout the year, February 25, March 6, and July 22 being the only exceptions. Comparison of the concentrations at Sts. 1 and 4 shows large gradients in fall and winter and slight gradients in late spring and early summer (see Fig. 7). In the River, concentrations were higher in winter and lower in summer. The seasonal cycles at Sts. 1 and 6 were roughly similar, except that the maximum and minimum of the River were later by two to four months than those of the Sound. Inorganic phosphate in the bottom water of the Pond, represented by Sts. 4 and 5a, was low in the fall, at the end of May, and during June, resembling the surface concentrations. During July and August it rose to high values. At St. 4, values were higher in July than in August, while farther up-pond at St. 5a the reverse was observed.

TABLE I. Inorganic Phosphate, μg-at P/L

		Surface			*Bottom*	
Sts.	1	4	5a	6	4	5a
January 30	0.37	0.07	—	0.65	—	—
March 26	0.36	0.20	0.15	0.50	—	—
May 25	0.10	0.07	0.20	0.30	0.10	0.10
June 30	0.30	0.00	0.05	—	0.15	0.00
August 23	0.47	0.02	0.05	0.20	0.35	1.07
October 20	0.55	0.07	0.13	0.30	0.05	0.05
December 7	0.30	0.10	0.04	0.63	0.13	0.05

Total Phosphorus, μg-at P/L

Sts.	1	4	5a	6	4	5a
May 25	0.90	0.90	1.05	0.60	1.10	1.50
June 30	0.85	0.90	0.95	—	1.70	1.20
July 22	0.80	1.60	2.70	0.70	2.40	3.20
August 23	1.20	1.55	2.85	1.00	1.75	7.00
October 20	1.20	0.85	0.50	0.35	1.40	1.00
December 7	1.00	0.50	1.25	1.00	0.70	1.40
January 10	1.00	0.60	0.40	0.70	0.50	0.80

Distribution of Total Phosphorus. In summer, total phosphorus concentrations were usually considerably higher within the Pond than in the Sound or River (see Table I, Fig. 4) and were much greater in the bottom water of the Pond than at its surface. Thus, the chief total phosphorus gradients were negative from Pond toward Sound or River. During the remainder of the year, total phosphorus within the Pond was approximately the same as or slightly lower than that in the Sound or River.

The seasonal cycle is shown in Fig. 5. In the Sound a slight increase in total phosphorus during summer was followed by a decrease thereafter. The surface waters of midpond had about the same cycle as the Sound. On several dates during summer, values in midpond were slightly higher than those in the Sound or River, and during the latter part of the year, values were slightly lower than those in the Sound or River. In the River there was little seasonal change.

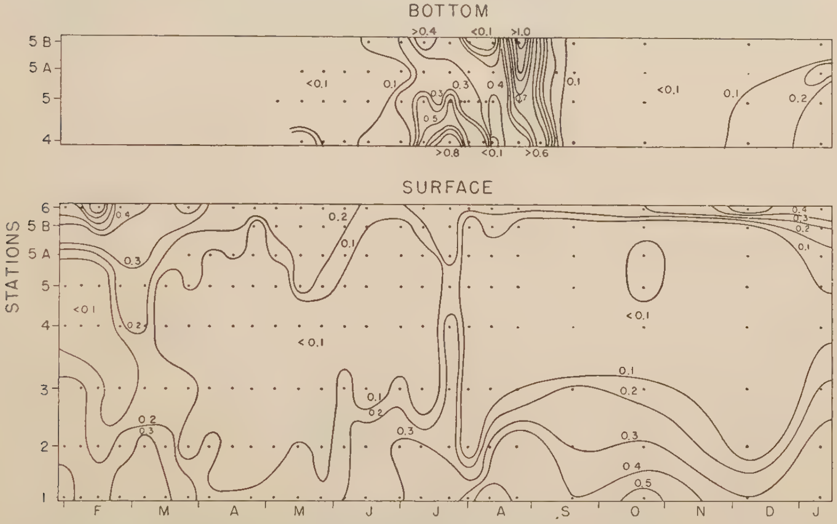

Figure 2. The distribution of inorganic phosphate in time and space. Concentrations are expressed in μg-at P/L.

Bottom samples contrasted sharply with surface samples in that total phosphorus increased to much higher concentrations during summer. Both Figs. 4 and 5 show these conditions. It is clear that the increases were larger and later at up-pond St. 5a than at mid-pond St. 4.

In the Sound, 71% of the total phosphorus was organic, on the annual average; at the surface in the arm, 91.5% was organic phosphorus. These values spanned values at other locations. Therefore, the distribution of organic phosphorus was similar to that of total phosphorus, with the exception that throughout summer there was a distinct negative gradient in the surface water from the arm to the Sound. As for total phosphorus, the concentrations in the bottom water increased during summer to much higher values at up-pond St. 5a than at midpond St. 4 (see Fig. 5). At St. 5a this increase occurred later in the summer than the lesser increase at St. 4.

Relation of Organic Phosphorus to Phytoplankton and Turbidity. Data on phytoplankton and turbidity are summarized in Table II. Phytoplankton showed greater concentrations during summer within the Pond than in the source salt water; these large summer concentrations were greater than any concentrations during the remainder of the year. A similar situation existed for turbidity, amounts within the Pond in summer being greater than those of the source salt and fresh waters and exceeding values anywhere at other seasons. Surface and bottom concentrations of phytoplankton were approximately the same; much greater turbidity was present in deep water than at the surface, particularly in summer. Fig. 6 shows the relation of phytoplankton and turbidity at two bottom stations. During summer, phytoplankton increases were roughly paralleled by increases in turbidity; this is particularly well shown by the correlation of the monthly means of phytoplankton concentration and turbidity. It is noteworthy that at up-pond St. 5a a greater amount of turbidity is associated with phytoplankton concentration than at St. 5. The changes in phytoplankton concentration throughout summer were erratic, whereas turbidity showed somewhat smoother changes.

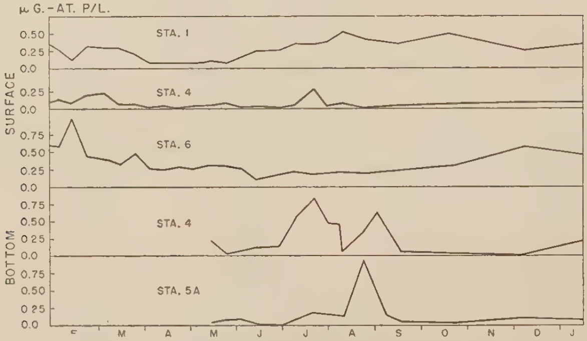

FIGURE 3. The seasonal cycle of inorganic phosphate.

Thus, in water of the same turbidity the quantity of phytoplankton was low on one date but high on another. These features suggest that the large concentrations of organic phosphorus in summer could by attributed, in part, to the large concentrations of phytoplankton and particulate matter that cause turbidity. Since turbidity and phytoplankton were related in a general way by monthly averages, this particulate matter would appear to be derived from phytoplankton. Since, however, the ratio of turbidity to plankton fluctuated greatly from time to time, the turbidity did not appear to be related directly to plankton numbers. One is led to believe that the accumulated remnants of dead phytoplankton cells persisted, thus causing turbidity in the pond water and accentuating its organic content.

TABLE II. Seasonal Averages of Phytoplankton and Turbidity

PHYTOPLANKTON

Summer				*Surface*						*Bottom*	
Sts.	1	2	3	4	5	5a	5b	6	4	5	5a
Cells/1 x 10^6	1.8	5.9	13.6	17.8	25.5	22.9	22.4	—	16.4	26.0	20.9
Fall, Winter, Spring				*Surface*						*Bottom*	
Sts.	1	2	3	4	5	5a	5b	6	4	5	5a
Cells/1 x 10^6	5.7	8.3	7.9	6.5	8.4	9.0	4.0	—	7.1	11.3	12.0

TURBIDITY

Summer				*Surface*						*Bottom*	
Sts.	1	2	3	4	5	5a	5b	6	4	5	5a
k*	0.37	0.44	0.55	0.95	1.15	1.09	1.32	0.69	1.68	2.17	2.51
Fall, Winter, Spring				*Surface*						*Bottom*	
Sts.	1	2	3	4	5	5a	5b	6	4	5	5a
k*	1.91	0.72	0.53	0.67	0.76	0.93	0.67	0.63	1.04	0.90	1.13

* k is the extinction coefficient in the equation, $I_z = I_o e^{-kz}$, where I_o and I_z are respectively light intensities at the sea surface and at depth z (in meters).

It is possible that, during summer, turbidity was accentuated by silt from river water or by stirring of bottom mud. However, this possibility appears to be minimal, since the river water (St. 6) was relatively clear and since winds and tidal action were less in summer than in fall or winter.

THE EFFECT OF UPWELLING ON THE PHOSPHORUS DISTRIBUTIONS

During summer the surface water of the arm usually had a salinity of less than 15‰ while the bottom water there had a salinity greater than 25 ‰. However, on July 22 the surface waters of the arm had salinities in the neighborhood of 25 ‰ as a result of a north wind blowing surface water downpond with consequent upwelling of deep water to the surface. Both inorganic and total phosphorus concentrations in the surface of the arm were much higher on this day than on previous days in the summer and they were rather similar to the concentrations in the bottom water (see Figs. 2 and 4).

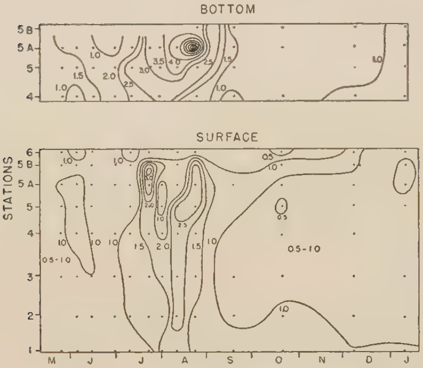

Figure 4. The distribution of total phosphorus in time and space. Concentrations are expressed in µg-at P/L.

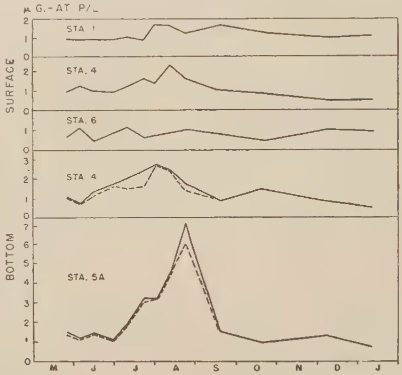

Figure 5. The seasonal cycle of total phosphorus (solid line) and organic phosphorus (dashed line).

When bottom concentrations of total phosphorus were the same as those in the main pond or River, upwelling caused no discernible change in the pattern of distribution, as can be seen by comparing data of December 7, a day of upwelling, with data of May 25, a normal day. When bottom concentrations of inorganic phosphate were negligible (fall and winter), the data for days of upwelling (September 18, October 20) showed that there were negligible concentrations at all surface stations in the arm, an abrupt increase occurring at the mouth of the River. Normal days, such as May 25, showed usually intermediate values between those in the River and those at midpond.

CHARACTERISTICS OF THE PHOSPHORUS GRADIENTS

In general, the concentration of inorganic phosphate decreases from the Sound and from the River toward the midreaches of the Pond. At the surface the gradient is always present (see Fig. 7). Only between waters of the Sound and the bottom water of the Pond or between water of the River and the bottom water of the Pond, during July and August, is this gradient reversed. When the difference between the water of the Sound and the average of surface and bottom water in midpond is plotted for the year, as in Fig. 7, this inward gradient is almost always present. This indicates that inorganic phosphate is being consumed in the synthesis of organic matter to a greater extent within the Pond than in the Sound or River. It also indicates that tidal mixing along the Pond is perpetually transporting inorganic phosphate into the Pond.

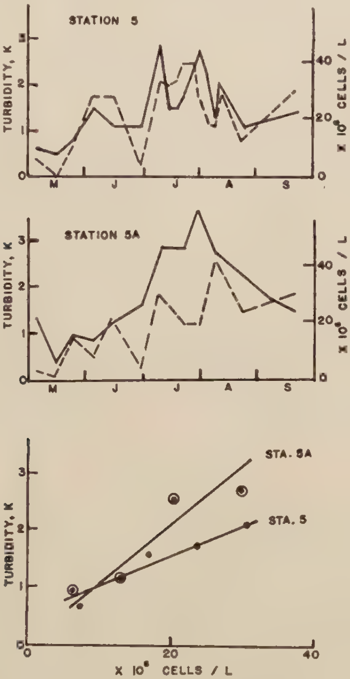

FIGURE 6. The relation of phytoplankton and turbidity in the bottom water. In the upper two graphs the dashed line represents phytoplankton and the solid line turbidity. In the lower graph unencircled points are monthly means for May through August at St. 5; encircled points are those at St. 5a. Turbidity is expressed as the extinction coefficient, *k* (see Table II).

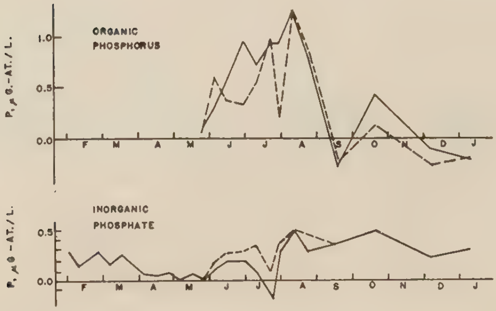

FIGURE 7. The difference in phosphorus throughout the year; upper graph, St. 4 minus St. 1; lower graph, St. 1 minus St. 4. Dashed lines represent the use of the surface value at St. 4 and solid lines represent the use of the average of surface and bottom at St. 4.

The gradient in organic phosphorus between the Pond and the Sound is shown as the difference between its concentrations at Sts. 4 and 1 from May 25 to January 10 (Fig. 7). The gradient is large during summer only. Elaboration of organic phosphorus appears to occur to a greater extent within the Pond than in the Sound or River, where the mean amount is even less than that in the Sound.

DISCUSSION

At the end of May, total phosphorus is essentially uniform. During summer it increases two to six times in various parts of the Pond, this increase being greatest in deep water. During fall and winter, total phosphorus is again uniformly distributed. The gradient of inorganic phosphate is inward at all times and upward in summer. The gradient of organic phosphorus is outward and upward.

The accumulation of organic phosphorus in summer may be explained in the following manner. Inorganic phosphate is transported inward from the Sound and from the River by tidal mixing; evidence for this is found in the gradient. Inorganic phosphate is converted to organic phosphorus by photosynthesis, the high phytoplankton concentration within the Pond being indicative of photosynthetic conversion. Organic phosphorus accumulates in the bottom water due to the sinking of photosynthetic products, evidence for which is found in the vertical stratification of turbidity but not of phytoplankton. Organic phosphorus is transported seaward due to its gradient. Thus, losses of organic phosphorus from surface waters are in two directions, outward and downward. As indicated by the salinity distribution (Barlow, 1956), the deep water has a net drift upstream and carries with it the organic phosphorus lost from the surface by sinking. This feature accounts for the fact that the greatest accumulation is found at St. 5a, well up the arm, and explains why the turbidity-phytoplankton ratio is greater at St. 5a than at St. 5. Surface accumulation of organic phosphorus at Sts. 4 and 5 is due to renewal of surface water by deep water through mixing and upwelling. It is apparent that the accumulation of phosphorus during summer depends on an enhanced photosynthetic activity whereas during fall and winter photosynthesis is lessened and the accumulated phosphorus is removed from the pond water.

Unsolved is the problem as to what extent summer accumulation of organic phosphorus depends on the hypothetical mechanism just described, which involves simple hydrography primarily, and to what extent it depends on exchanges with the bottom sediment. Phosphorus exchange between water and sediment has been well demonstrated in a lake (Mortimer, 1941) and in an estuary (Miller, 1952). Part of the summer accumulation may become entrapped in the bottom mud, to be released again the following summer. During fall and winter organic phosphorus may settle to the bottom, to remain until the enhanced regenerative processes of summer release it again. Evidence for the latter process is found in the slightly lower surface values of total phosphorus within the Pond than in the source fresh and salt waters in fall and winter.

Greater productivity within embayments than in the ocean may result in three ways: by enhanced conversion of inorganic nutrients, by contributions of nutrients from land drainage, and by accumulation of nutrients. It is concluded that the exceptional productivity of Great Pond is an example of the third way, wherein a combination of hydrographic and biological factors cause the nutrients to accumulate in greater concentrations than are present in the sources of fresh and salt water.

ACKNOWLEDGMENTS

The author wishes to express his gratitude to Dr. A. C. Redfield and Dr. W. R. Taylor for their help during this study, to Dr. J. P. Barlow for the pleasantest association during many trips to Great Pond and for use of salinity data prepared by him, to Mr. Harry Turner for use of the chart of Great Pond prepared by him, and to many others on the staff of the Woods Hole Oceanographic Institution who extended aid during the pleasant stay there.

REFERENCES

BARLOW, J. P.

1956. Effect of wind on salinity distribution in an estuary. J. mar. Res., *15* (3): 193–203.

BRAARUD, T. AND A. BURSA

1939. The phytoplankton of the Oslo fjord, 1933–34. Hvalrad. Skr., *19:* 1–63.

HARVEY, H. W.

1948. The estimation of phosphate and of total phosphorus in sea waters. J. Mar. biol. Assoc. U. K., *27* (2): 334–359.

HUTCHINSON, A. H., AND C. C. LUCAS

1931. The epithalassa of the Strait of Georgia; salinity, temperature, pH and phytoplankton. Canad. J. Res., *5* (2): 231–284.

MILLER, S. M.

1952. Phosphorus exchange in a subtropical marine basin. Bull. mar. Sci. Gulf Carib., *1* (4): 257–265.

MORTIMER, C. H.

1941. The exchange of dissolved substances between mud and water in lakes. J. Ecol., *29* (2): 280–329.

RILEY, G. A.

1952. Hydrographic and biological studies of Block Island Sound. Phytoplankton of Block Island Sound, 1949. Bull. Bingham oceanogr. Coll., *13* (3): 40–64.

TULLY, J. P.

1949. Oceanography and prediction of pulp mill pollution in Alberni Inlet. Bull. Fish Res. Bd., Canad., *83:* 3–169.

Contribution No. 752

EFFECT OF WIND ON SALINITY DISTRIBUTION IN AN ESTUARY[1]

By

JOHN P. BARLOW[2]

ABSTRACT

The distribution of salinity in a small tidal estuary, Great Pond, through a period of over a year is described. The numerous important variations in salinity, both seasonal and short-term, cannot be attributed to tides or to day-to-day changes in the supply of fresh water. It is shown that they are related to day-to-day changes in wind force and direction and that the general seasonal change in average salinity is related to a general seasonal change in prevailing winds.

INTRODUCTION

Of the important time and space variations in properties of estuaries, the most striking are those of salinity. Salinity variations are of particular significance since they may represent marked changes in both the accumulation and distribution of fresh and salt water. Some variations in salinity can clearly be attributed to climatic and seasonal changes in the fresh water supply from land drainage; others are of such short duration and irregular occurrence that their causes are not immediately apparent.

These salinity variations appear to be especially marked in the smaller and shallower estuaries, such as those dissecting the southern shore of Cape Cod. Ketchum (1951) has discussed the circulation and tidal exchanges in one of these small estuaries, Great Pond, near Woods Hole, Massachusetts, and the purpose of this paper is to present the results of a year's study of the variations in salinity of this same estuary. The salinity data have been collected during seasonal surveys of biological and chemical properties of this pond (Barlow, 1955; Hulburt, 1956) and during several detailed hydrographic studies. These data give an exceptionally detailed description of the salinity variations in this estuary and provide the basis for an understanding of their causes.

---

[1] Contribution No. 752 from the Woods Hole Oceanographic Institution.

[2] Present address: Department of Conservation, Cornell University, Ithaca, New York.

Reprint from SEARS FOUND. JOURN. MAR. RES.

METHODS AND SOURCES OF DATA

Great Pond (Fig. 1) is the drowned mouth of a small river, the Coonamessett, which now provides the principal source of fresh water for the pond. Great Pond's northern portion, the arm, is shallow and muddy and is surrounded by high banks and trees which shelter it from most winds. The narrows and main pond are deeper, sandier, and more exposed to winds from all directions. The extensive shallows in the southern end were apparently formed by sand drifting into the pond from Vineyard Sound. The narrow entrance from Vineyard Sound is maintained in the barrier beach by a set of stone revetments and jetties.

Twenty-eight regular surveys of the plankton, salinity, phosphate, and temperature were made between March 20, 1950 and July 7, 1951. Surface and bottom salinity samples were usually taken at

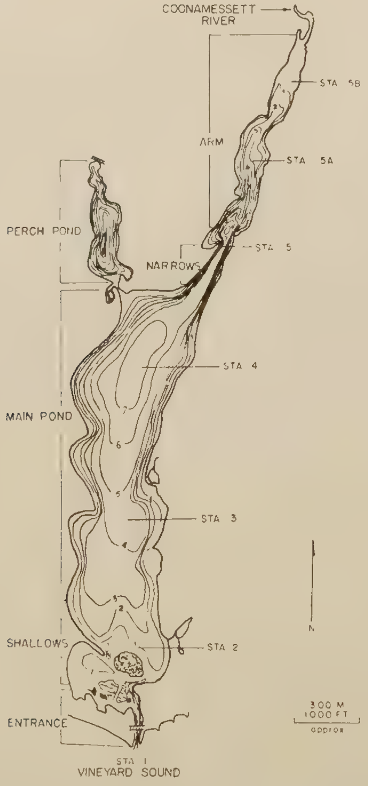
COONAMESSETT RIVER
STA 5B
ARM
STA 5A
PERCH POND
NARROWS
STA 5
STA 4
MAIN POND
STA 3
SHALLOWS
STA 2
ENTRANCE
STA 1
VINEYARD SOUND
N
300 M
1000 FT
approx

Figure 1. Chart of Great Pond. Depths in feet

all of the stations shown in Fig. 1. During spring and summer of 1950, observations were taken at about 10 to 15 day intervals, but during the following winter and spring they were less frequent and less detailed. Intensive surveys during which the salinity distribution was studied in greater detail throughout several stages of the tide were made on June 3 and 26 and August 29, 1950.

Rainfall measurements near the pond were provided by Mr. Wilfred Wheeler of Falmouth, Mass. Wind velocity and direction were recorded on each sampling day; wind measurements recorded at Nantucket Lightship and published by the U. S. Weather Bureau have also been used. River flow just north of Great Pond was measured at irregular intervals.

THE SALINITY DISTRIBUTION AND ITS VARIATIONS

A number of samples taken across the pond have shown only small east-west salinity differences, seldom exceeding 3‰. However, since the river water tends to flow over the mixture which it forms with Vineyard Sound water, there may be large differences at the surface and bottom in parts of the pond. Discussion of the salinity will therefore be limited to the vertical distribution along the land-sea axis of the pond.

Several typical salinity distributions are shown in Fig. 2. The distribution observed on August 29, 1950 is of special interest because the meteorological conditions were then so typical of the most frequent conditions during summer. Vertical and horizontal gradients were strongest in the arm and narrows. In the arm, the surface salinity ranged from zero at the river mouth to over 20‰ at the narrows and was from 10 to 15‰ less than the salinity of the bottom water. The gradients were much less in the main pond.

There were many temporary variations. Sometimes, when the pond was everywhere nearly isohaline from surface to bottom, the salinity gradients were horizontal and were strongest between the pond and the arm, as on June 3. At other times, as on June 26, there were only small and irregular horizontal salinity differences; at such times the gradients were predominantly vertical.

The seasonal distribution at the surface is shown in Fig. 3. It is seen that there were large and abrupt changes in the extent and freshness of the brackish surface layer, which was most pronounced in summer when it usually extended far down the arm into the main pond. In winter, however, the brackish layer seldom extended far from the river. The mean surface salinities in the arm and northern end of the main pond were therefore higher in winter than in summer,

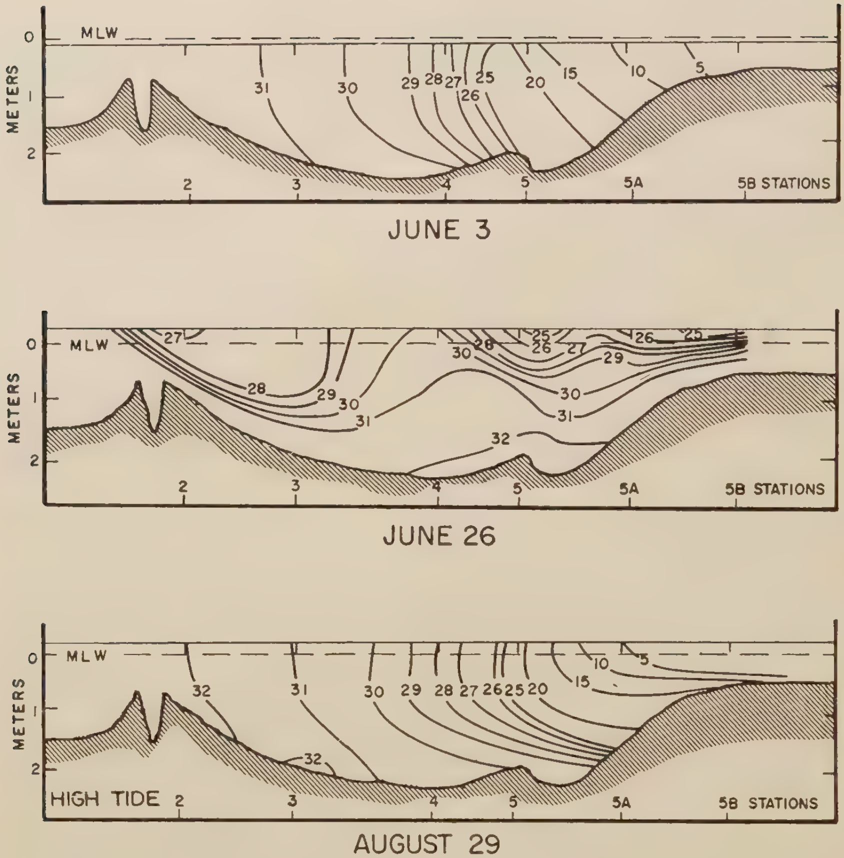

Figure 2. Vertical distribution of salinity (°/₀₀) on June 3, June 26, and August 29 at high tide. Station 1 at left of diagram. Broken line represents mean low water.

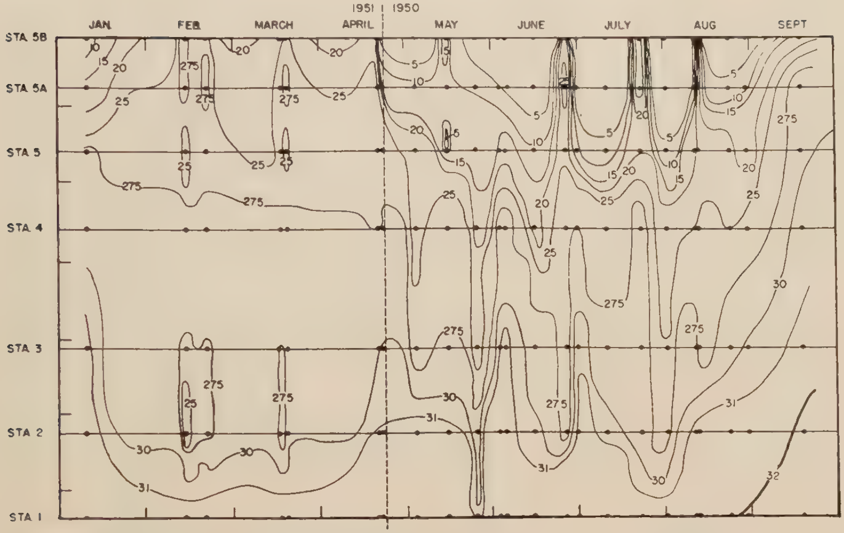

Figure 3. Seasonal distribution of surface salinity (°/₀₀). Closed circles indicate observations.

as shown in Table I. The deeper water in most of the arm and main pond and the surface water in the southern part of the main pond had but small variations seasonally or within seasons.

TABLE I. Mean Salinities (°/₀₀) and Their Ranges in Great Pond
Summer: May 4–August 23, 1950
Winter: Sept. 18, 1950–Apr. 22, 1951

Station	*Summer*			*Winter*		
	Mean	Min.	Max.	Mean	Min.	Max.
1, surface	31.68	31.48	32.09	31.73	31.29	32.32
2, surface	30.56	27.30	31.89	29.11	26.11	32.23
3, surface	27.84	23.08	31.36	29.23	27.18	31.30
4, surface	24.49	14.45	28.83	29.61	27.66	30.01
bottom	30.87	27.99	32.09	30.58	29.22	31.31
5, surface	14.42	3.59	24.47	25.09	11.08	29.85
bottom	29.82	25.99	31.51	29.59	26.87	31.11
5a, surface	10.02	2.35	28.00	25.43	16.00	30.62
bottom	27.92	21.44	30.97	29.02	25.02	30.84
5b, surface	7.21	0.02	25.49	17.60	0.39	29.36
bottom	23.92	1.51	30.77	23.87	3.23	30.37

CAUSES OF VARIATIONS IN SALINITY

Effect of Tides. During the three intensive surveys, horizontal displacement of the salinity was observed at various stages of the tide. These observations showed that some of the differences from survey to survey in the southern part of the pond are probably related to the state of the tide when the surveys were made. However, horizontal movements cannot account for the large changes in the rest of the pond between some of the surveys.

Effect of Variations in the Supply of Fresh Water. During most of the year variations in river flow are caused by variations in precipitation, which in this region changes but little from season to season on an average monthly basis (Table II). Although the river flow may change as much as five-fold in two days when large volumes of water stored in reservoirs are released into the valley in spring and fall for the benefit of local cranberry culture, none of the salinity surveys was made when the river flow was so markedly changed. On the basis of our observations seasonal differences in the salinity distribution are evidently not caused by seasonal changes in the supply of fresh water. In fact, in winter and spring, when surface salinities in the pond are highest, precipitation is greater than the yearly average, and in summer, when surface salinities are lowest, the rainfall is lower than average.

TABLE II. Total Monthly Rainfall (inches) at Falmouth, Massachusetts, 1950 and 1951*

	1950	*1951*
January	3.15	3.39
February	4.39	3.26
March	4.47	4.16
April	3.98	2.54
May	2.67	3.96
June	3.83	1.35
July	1.90	1.47
August	4.13	5.43
September	3.24	1.24
October	1.04	2.95
November	6.25	4.20
December	3.08	4.87

* Recorded by Mr. Wilfred Wheeler, Falmouth, Mass.

Heavy rainstorms, however, may cause immediate but temporary increases of from two to six times in the river flow, and since the surface of the arm is likely to be effected most by these increases, an attempt was made to relate changes in its salinity to changes in rainfall. It appears that salinity of the arm is not effected by rainfall on the day of sampling or by total rainfall during the two, five, or ten days preceding the day of sampling.

Although many of the salinity changes are doubtless caused by changes in total amounts of fresh water in the pond, only the intensive surveys of June 26 and August 29 were detailed enough for satisfactory estimates. Despite a smaller flow in the river on August 29, the fresh water in the pond was twice the amount found on June 26 (see Table III). This increase in fresh water was accompanied by such a decrease in river flow that the flushing time (Ketchum, *et al.*, 1951) on August 29 was more than five times that on June 26. These results differ sharply from those of circulation studies in other estuaries, such as Alberni Inlet (Tully, 1949) and the New York Bight (Ketchum, *et al.*, 1951), where it has been shown that increases in river flow tend to be accompanied by such increases in the accumulation of fresh water that the flushing time remains relatively little changed.

TABLE III. River Flow and Fresh Water in Great Pond

	River flow per hour	*Total fresh water*	*Flushing time*
June 26, 1950	$1.8 \times 10^3 M^3$	$114 \times 10^3 M^3$	2.66 days
August 29, 1950	$0.75 \times 10^3 M^3$	$230 \times 10^3 M^3$	12.7 days

Effect of Variations in Wind. In Great Pond, variations in wind force and direction are the principal cause of variations in the distribution of fresh and salt water, both vertically and horizontally.

When the wind force is 0, the river water flows seaward in a shallow surface layer that is only gradually mixed with salt water. When this condition obtained on May 25 there was a shallow brackish layer extending far down the pond (Fig. 3); only in the shallows and at the southern entrance to the pond was tidal turbulence adequate to produce mixing from surface to bottom. On the other hand, strong winds may increase the vertical mixing so much so that the salinity in the pond is everywhere nearly homogeneous from top to bottom, as on June 3, when the wind was southeast and its force 4.

Though the wind plays an important part in vertical mixing, it has its most marked and probably its most important effect on horizontal distribution, particularly in the arm.

We have examined the relation between the salinity and the wind component parallel to the long axis of the pond, the latter being computed from the mean wind force and direction observed at Nantucket Lightship in the 24 hours preceding sampling. Wind directions at Nantucket Lightship were nearly the same as those at the pond at the time salinities were measured.

In Fig. 4a it is seen that, in the arm, winds directed seaward along its axis are associated with high surface salinities, while winds directed landward are associated with low surface salinities. Hence changes in wind direction are accompanied by abrupt changes in the salinity of the arm. For example, a shift in wind from south on August 11 to north on August 12 caused rapid increases in surface salinity; on August 11 the wind had a component of 0.8 from the south and on August 12, 2.4 from the north (Fig. 3). Inversely, when the wind changed from north on April 21 to south on April 22 there was a rapid decrease in surface salinity; on April 21 the wind had a component of 1.8 from the north and on April 22, 1.8 from the south (Fig. 3).

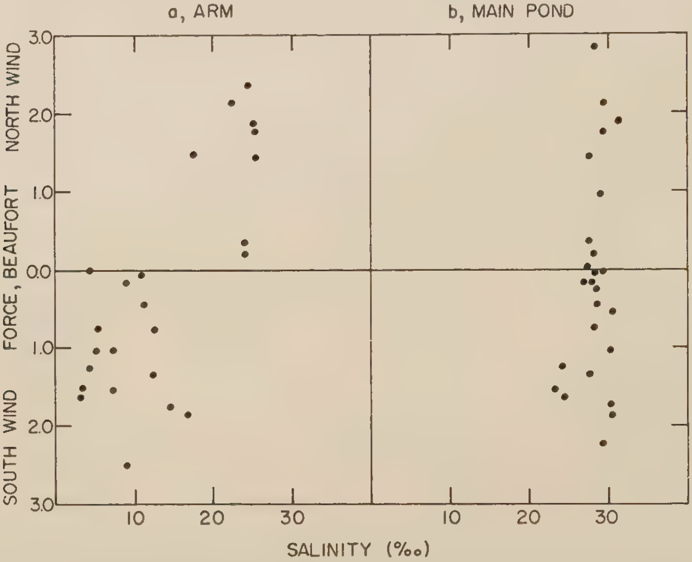

Figure 4. Wind force and direction relative to salinity of the arm and of the main pond. Wind force is north or south component of average Beaufort wind force reported at Nantucket Lightship in 24 hours preceding sampling. Salinities are mean surface salinities.

In the main pond, however, winds seem to have much less effect on the salinity than in the arm (Fig. 4b), probably due in large measure to differences in the topography of the land around the arm and the pond. While the arm is effectively shielded from all winds but those directly landward or seaward, the main pond is exposed about equally to winds from all directions. Nevertheless, on the three occasions when the mean surface salinity in the main pond was below 25‰ there were strong southerly winds.

During the intensive surveys of June 26 and August 29 both current and salinity at the entrance were measured at half-hourly intervals. From these data, volumes of flow and exchanges of fresh water were estimated (see Table IV). Unfortunately the observations did not include a complete tidal cycle, but the periods of ebb and flood observed were about equal. With northerly winds of force 3 and with the flood into the pond greatly exceeding the ebb, the fresh water content of the pond was relatively low; 44 × 10^3m^3 of fresh water escaped from the pond. With southwesterly winds of force 2 only 1.77 × 10^3m^3 of fresh water escaped. Thus, with northerly winds the net loss of fresh water per hour of observation was three times greater than the rate of river flow whereas with southwesterly winds the loss was only 1/5 the river flow. Obviously, then, northerly winds facilitate the loss of fresh water from the pond while southerly winds retard it.

TABLE IV. Exchange of Water Between Great Pond and Vineyard Sound as Affected by Wind Direction

Date	June 26	August 29
Wind direction	Northerly	Southwesterly
Period of Ebb (southerly)	0950–1430 4.7 hours	1148–1300; 1430–1900 5.9 hours
Period of Flood (northerly)	1430–1900 4.5 hours	0745–1148; 1300–1430 5.5 hours
Total Flow, Ebb	438 × 10^3M^3	470 × 10^3M^3
Total Flow, Flood	756 × 10^3M^3	411 × 10^3M^3
Net Loss	−318 × 10^3M^3	59 × 10^3M^3
Fresh Water Loss, Ebb	59 × 10^3M^3	2.91 × 10^3M^3
Fresh Water Gain, Flood	15 × 10^3M^3	1.14 × 10^3M^3
Net Loss	44 × 10^3M^3	1.77 × 10^3M^3
Net Loss per Hour	4.8 × 10^3M^3	0.15 × 10^3M^3
River Flow per Hour	1.8 × 10^3M^3	0.75 × 10^3M^3
Fresh Water Content of Pond	114 × 10^3M^3	230 × 10^3M^3

Seasonal changes in salinity distribution have been summarized in Table I, which shows that all of the average surface salinities in the arm in summer were 10 to 15‰ lower than surface salinities in winter. In the main pond, however, there appear to be no significant seasonal changes in surface salinity.

As would be expected from the foregoing discussion, these seasonal changes in salinity in the arm are also associated with changes in wind direction and force. The northerly or northwesterly winds that prevail in fall, winter and spring allow relatively little fresh water to accumulate in the arm; obviously this results in higher salinities there in winter. Of the seven winter surveys (January through April 1951) which were detailed enough to show the salinity of the entire pond, only two (January 10, April 22) were made on days when the wind had components from the south, and it was only on those days that surface salinities were as low as those which are usual during summer when southwesterly winds prevail.

From May through August in 1950 and 1951 the wind had components from the south on 15 of the 18 days it was observed at the pond. These southerly winds allowed more fresh water to accumulate in the arm, hence surface salinities were generally lower than those found in winter. On the remaining three of those 18 days (June 26, July 22, and August 12, 1950) the wind had components from the north, and on those days the surface salinities in the arm were as high as usual during the winter.

ACKNOWLEDGEMENTS

These studies were suggested by Dr. Alfred C. Redfield, to whom the author is indebted for his continued encouragement and advice. The author has also benefited from discussion of this problem with Dr. Bostwick H. Ketchum.

The observations reported here have been made by a group of investigators from the Woods Hole Oceanographic Institution which included Dr. J. C. Ayers, E. M. Hulburt, D. Norton, F. A. Richards and Messrs. J. A. Posgay, H. J. Turner Jr., and C. Wheeler. Of these, Dr. Hulburt has made a special contribution through his original evaluation of the relation between wind direction and salinity, and Dr. Richards has analyzed fresh water exchange between the Pond and Sound.

REFERENCES

Barlow, J. P.

1955. Physical and biological processes determining the distribution of zooplankton in a tidal estuary. Biol. Bull. Woods Hole, *109* (2): 211–225.

Hulburt, E. M.

1956. Distribution of phosphorus in Great Pond, Massachusetts. J. Mar. Res., *15* (3): 181–192.

1956. The phytoplankton of Great Pond, Massachusetts. Biol. Bull. Woods Hole, *110* (2): 157–168.

Ketchum, B. H.

1951. The exchanges of fresh and salt water in tidal estuaries. J. Mar. Res., *10:* 18–38.

Ketchum, B. H., A. C. Redfield and J. C. Ayers.

1951. The oceanography of the New York Bight. Pap. Phys. Oceanogr. Meteorol., *12* (1): 4–46.

Tully, J. P.

1949. Oceanography and prediction of pulp mill pollution in Alberni Inlet. Bull. Fish. Res. Bd. Can., *83:* 1–169.

Contribution No. 769

INTERACTION OF SEA AND ATMOSPHERE:

a group of contributions

by

A. C. Redfield, A. R. Miller;
G. W. Groves; D. L. Harris;
R. O. Reid;
W. Marks and J. Chase.

OBSERVATION OF THE GROWTH AND DECAY OF A WAVE SPECTRUM[1]

By WILBUR MARKS[2] *and JOSEPH CHASE*[3]

Woods Hole Oceanographic Institution

(Original manuscript received 12 September 1955; revised manuscript received 20 June 1956)

ABSTRACT

In October, 1954, the *R/V Atlantis* of Woods Hole Oceanographic Institution was used for an observation program of wind and waves. This was part of a joint undertaking in wave research designed to obtain the two-dimensional energy spectrum of the sea surface by means of aerial stereophotography techniques. A series of wave records and visual estimates of wave heights were made during two periods of high waves.

The information obtained from the visual observations and from the wave pole records illustrates the way in which the one-dimensional spectrum grows and decays in terms of the distributions of wave height and period. Hindcasts are made to verify the wave forecasting method of Pierson, Neumann and James. Emphasis is made of the fact that prediction of wave statistics is largely subjective when wind parameters are evaluated from meteorological charts.

The results obtained from visual observations, wave records, and the prediction technique are compared. By utilizing the energy spectrum technique, an adequate forecast can be made of the continuance of high seas long after the wind has lessened. Prediction of wave height is in reasonably good agreement with observed heights.

1. Introduction

Our knowledge of the behavior of ocean waves has greatly increased in recent years. The advent of the statistical approach to the characterization of the sea surface as presented by Pierson [8], Longuet-Higgins [3], Neumann [7], and the author [4; 5; 6] has led to new ideas concerning the growth, propagation, and decay of wind generated surface waves.

One of the results of these new ideas was the compilation of a set of wave forecasting rules [9] by which certain parameters of the sea surface could be predicted if the wind field were adequately described from meteorological charts. The procedure is given in such a lucid manner, that it is rapidly taking its place among the established methods already in use. There is clearly a need for verification of its rules so that utilization of the technique may be treated with confidence. One such attempt was made by James [2], who summarized the theory and conducted an excellent verification procedure. Forecasts were made for Long Branch, N. J., during the passage of an east coast storm. The effects of refraction on the lower spectral frequencies were not computed. The decay of the spectrum was not discussed; the first forecast after the most violent portion of the storm was made for a much later time when equilibrium had returned to the system. At the lower wind velocity, the waves due to the decay spectrum had already "passed" Long Branch, and the prediction gave no description of the degeneration of the seaway for this event.

It was desirable, therefore, to make an investigation at a deep water station in order to eliminate refraction effects, and to observe the growth and decay of the wave spectrum. Such an opportunity occurred in October, 1954, when the *R/V Atlantis* was used to make a series of observations that covered the growth and decay of the wave spectrum on two separate occasions.

---

[1] Contribution No. 769 from the Woods Hole Oceanographic Institution.

[2] Research Associate in Mathematics and Oceanography, Woods Hole Oceanographic Institution, Woods Hole, Mass. Present affiliation: David Taylor Model Basin, Washington, D. C.

[3] Research Associate in Oceanography, Woods Hole Oceanographic Institution, Woods Hole, Mass.

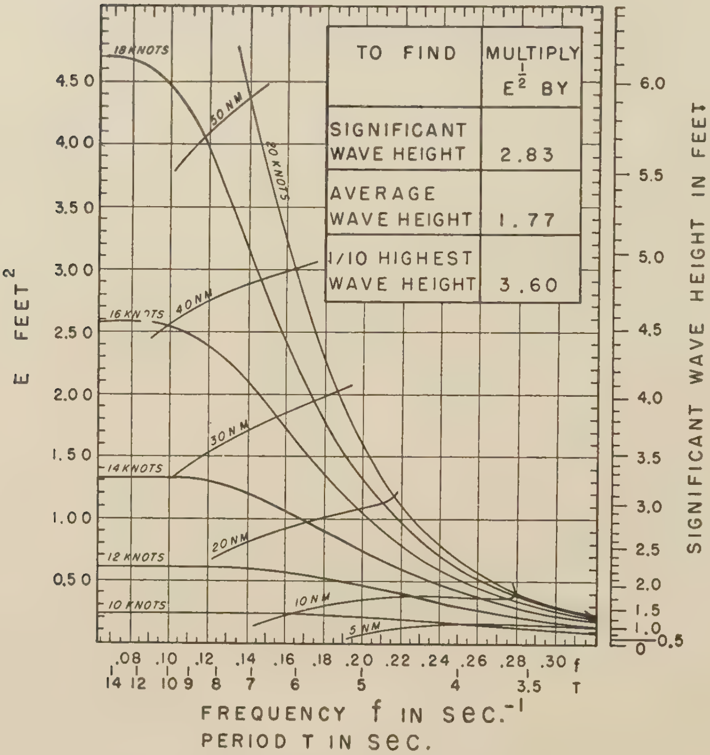

Fig. 1. Fetch graph. Co-cumulative spectra for wind speeds from 10 to 20 kt as function of fetch. (After Pierson, Neumann, and James.)

2. The prediction technique

The intensification and decay of the sea state is predicted by the spectrum theory in terms of change in the wave height and wave period characteristics. A necessary ingredient for the forecast is an adequate description of the wind field. It is subjective at best, because of the relative infrequency of weather maps (one every 6 hr), and because of the scarcity of ship reports. Hence, a statement of the wind parameters is largely dependent on the judgment of the forecaster. Great care must be taken in the interpolation between six-hourly maps, especially when the meteorological situation undergoes a severe change that may effect the wave structure at the point of observation.

The predicted quantities are:

$\bar{H}$—average wave height
$\bar{H}_{1/3}$—average of the one-third highest wave (significant height)
$\bar{H}_{1/10}$—average of the one-tenth highest wave
T_R—period range
$\bar{T}$—average period

Heights are given in feet and periods in seconds.

The forecasting principles in their entirety are described in the manual of Pierson, Neumann and James [9]. The methods will be briefly described with emphasis on the sea state degeneration forecast which is not explained in the manual.

The wave spectrum derived by Neumann [7] gives a description, in the integrated form, of the the height distribution of the waves through the quantity E. This number is related to the sum of the average squares of heights of waves which pass a fixed point; it is therefore a measure of the energy in the wave system. Figure 1 shows a family of co-cumulative spectra (*viz.*, the quantity E in square feet) for wind speeds of 10–20 kt as a function of the fetch length. There are similar curves which are a function of wind duration. For any given wind speed, the sea will be in a fully developed state if certain minimum fetch and duration conditions are fulfilled. For such cases, the E value is read directly at the point where the co-cumulative spectrum for the appropriate wind speed intersects the ordinate axis. Either the fetch or duration graph may be used. Once E is determined, the wave height statistics, as derived by Longuet-

Higgins [3], are given by:

$$\bar{H} = 1.77\, E^{\frac{1}{2}}$$
$$\bar{H}_{\frac{1}{3}} = 2.83\, E^{\frac{1}{2}}$$
$$\bar{H}_{\frac{1}{10}} = 3.60\, E^{\frac{1}{2}}$$

The abscissa of the graph defines the period band in the spectrum which contributes almost all of the energy in the wave system. This band is determined by first taking the intersection of the 0.95E and 0.03E lines with the co-cumulative spectrum for the given wind speed. The intersecting points projected on the period scale determine the high and low period cutoffs of the spectrum, and hence the range of periods. The average period $\bar{T}$ in seconds is given by

$$\bar{T} = 0.285v,$$

where the wind speed v is in knots.

If, for a given wind velocity, the development of the waves is limited by either fetch or duration, the E value is determined by intersection of the particular co-cumulative spectrum with the appropriate fetch or duration line. When both fetch and duration are limiting factors, the lower E value is used. Once the E value is obtained, the procedure is the same as above.

When the sea state degenerates, it is the propagation properties of the individual wave components that are important. There are so many facets to this portion of wave forecasting that only a brief explanation of the method will be attempted.

Consider a fully developed state for a wind speed v_1, followed by a reduction of wind speed to v_2. If the fetch and wind remain constant, then after a certain time t, the seaway will have attained the properties associated with a fully developed sea for the wind

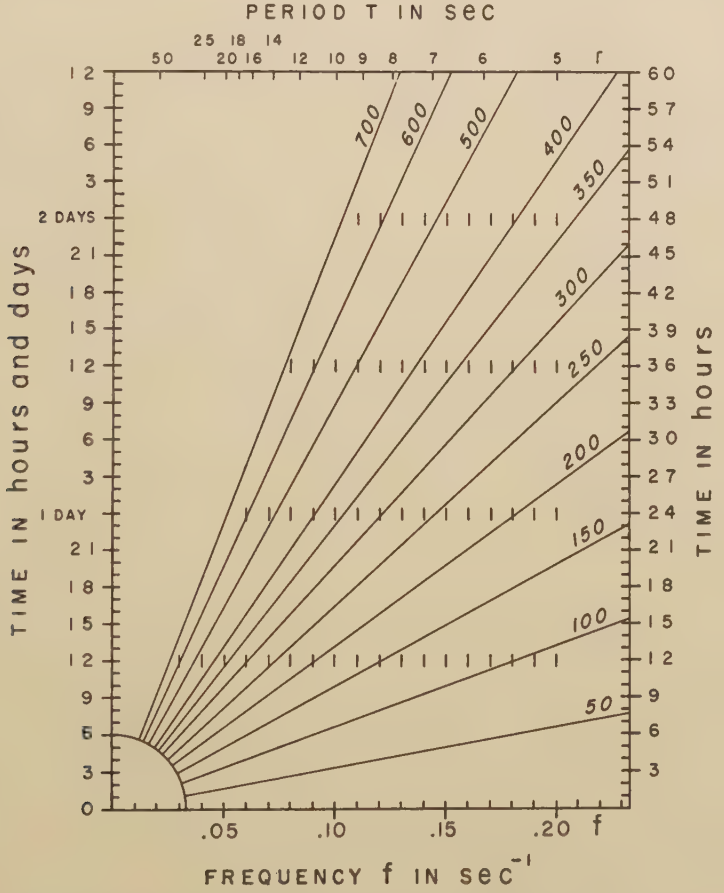

FIG. 2. Dispersion diagram. Frequency (f) from 0 to 0.23 sec^{-1}, Range (R) from 0 to 700 n mi, Time (t) from 0 to 2.5 days, $t = 0.66fR$. (After Pierson, Neumann, and James.)

speed v_2. During the time t, the seaway at any point is undergoing a change from a sea state appropriate to v_1, to a sea state appropriate to v_2. The first indication of a decaying sea is not the reduction in wind speed which may precede decay by hours, but the disappearance of the lowest frequency wave components. The v_2 sea is not capable of generating them and since they are the longest waves, they travel fastest and will disappear first. The disappearance of the low frequency components will depend on the distance of the forecast point from the line which defines the minimum fetch length.

The dispersion diagram (fig. 2) illustrates graphically how long it takes a given wave component to pass a fixed point. Suppose the forecast point, A, is in the generating area, but 100 n mi beyond the minimum fetch length. In addition, let 12 sec be the duration for the highest period wave in the sea state associated with v_1. When v_1 ceases, A will continue to observe the same sea structure for 5.5 hr after which time no more 12-sec waves will appear at A. This result is determined by projecting the intersection of the period line with the distance curve on the ordinate scale. The same procedure is used for 11 sec, 10 sec, *etc.*, until the fully developed state associated with v_2 is reached. In this manner, any state in between v_1 and v_2 can de described.

3. Ship observations

Wave heights were determined on board the *Atlantis* by means of visual observations and on two occasions by a series of wave pole measurements. The visual observations were made by estimating the heights of 30 successive well formed waves that passed an arbitrary point out of range of interference from the ship. The average of these 30 numbers was recorded. The deck level of the *Atlantis* is good for this purpose, since the observer's eye is about 10 ft above the waterline. Height estimations by the different observers showed a difference between observers of less than 1 ft and often as little as 0.2 ft. Hence, the authors contend that this method of height estimation and averaging is reasonably reliable and consistent. The number found by this procedure is called the *significant height* which is the average of the one-third highest waves [11]. These numbers will be compared to the predicted significant heights and to those computed from wave records.

The wave pole was of the capacitance type [1]. The measurements were transmitted from the instrument to the ship by radio where they were recorded automatically on magnetic tape.

The wind at the ship was determined by anemometer and wind vane about 18 ft above the waterline. Instrument exposure was good, except possibly for winds passing within 10° of dead astern. The apparent wind seldom came from this sector because of the forward motion of the ship, but on those few occasions the apparent wind was estimated. The true wind was obtained by graphically subtracting the vector due to the ship velocity from the apparent wind vector given by the wind vane and anemometer. A vector given by this procedure was taken as the surface wind at the point of observation.

Six-hourly synoptic charts for the period 21–25 October 1954 were obtained from the U. S. Navy Hydrographic Office. These were supplemented by daily 1230 GCT charts from the U. S. Weather Bureau.

The parameters of wind velocity and direction, fetch length and duration of wind were determined by two principal means: directly from the observations reported on the weather charts together with those observations taken on board the *Atlantis*, and indirectly from isobaric patterns on surface maps or interpolation between them. No direct geostrophic measurements were made; instead, the isobaric patterns were used to delineate the spatial extent of the fetch and to estimate the duration of the wave-generating areas. Consequently, the determination of the wind parameters is subjective, and the prediction of the wave statistics is heavily dependent on the interpretation of the meteorological data. When the spectrum method is used for forecasting, the services of an experienced synoptic meteorologist are needed to determine the wind distribution in time and space.

4. The weather patterns

i. *Part I.* The first significant wave heights of over 5.5 ft were observed at 1100 GCT 20 October 1954, at which time the *Atlantis* was stationed near 38N 68W. These larger waves were associated with the wind system of an extra-tropical cyclone located near the ship (fig. 3a). The wind at the ship was north, whereas it was northeasterly over the major part of the generating area.

The cyclone subsequently moved northeastward (fig. 3b, 3c) leaving the *Atlantis* in a northwesterly flow with the fetch length limited to the distance to the coast. A cold front developed in eastern Canada by the time of fig. 3b. It moved southward, passing the ship on the morning of 22 October. A small low pressure center developed on this front near the ship at 1230 GCT 22 October (fig. 3d).

ii. *Part II.* Early on 24 October 1954, the area of interest lay under westerly flow in advance of a southward-moving cold front. By 1230 GCT (fig. 4a) the flow became west-northwesterly and at about

1730 GCT it veered to north-northwesterly with the passage of the front (fig. 4b).

The principal cyclonic disturbance near the area at this time was centered east of Newfoundland and was moving eastward. The *Atlantis* moved eastward to 39N 65W during 24–25 October in order to retain moderate to fresh breezes.

On the final day (25 October), the wind was north-northwest 17 kt at 1230 GCT (fig. 4c) diminishing to 13 kt by 1830 GCT (fig. 4d). The duration of wind, up to the time of the wave observations, was from 17.5 to 25 hr making this test period the longest of consistent wind force and direction for the cruise.

For the entire period 20–25 October, there appears to have been little or no possibility of any appreciable contribution to the waves observed by wind fields in other parts of the North Atlantic. Therefore, the ship was effectively in the generating area at all times and probably was never under the influence of swell from distant storms.

5. Interpretation of wave records

Small differences in the forecast of wind velocity, fetch, or duration may cause as much as 1 ft difference in the prediction of the significant heights (or the other height parameters). Therefore, it is required that limits be set on the forecast parameters for the purpose of forecast verification. It is obvious that visual observation is not the most desirable means to provide confidence in a method of wave prediction. The wave records, on the other hand, represent fairly accurate time histories of the height and period of the waves which pass a fixed point in space. The wave pole is sensitive to the high frequency components in the sytem, the result being a generally smooth wave profile with considerable high frequency activity superimposed on it (fig. 5).

The problem of interpretating the wave records resolves itself into two questions: (1) How shall a *wave* be defined? (2) How is the *wave height* measured? The calculation of the statistics that are supposed to characterize the state of the sea depends on the answers to these questions. Consider fig. 5a. The records showed that there were often great differences between the vertical distance from crest to trough on one side of the wave and on the other. It was decided that the wave height would be defined as the average of these two distances. Figure 5b shows the complex nature of the sea surface and the difficulty involved in effectively filtering out the high frequency components. When these components are ignored, it becomes apparent that the results obtained by wave height statistics are higher than when the height of every component is measured. In this study the major components were determined by visual smoothing of the records in a completely arbitrary manner. Therefore, the results obtained here, though quantitative in nature, can be used only as a relative (rather than an absolute) check on the forecasts. However, the consistent manner in which the smoothing was accomplished makes the wave record information a useful tool for observing the growth and decay of the spectrum.

Period measurements were made as follows: the *mean sea level line* was determined by averaging the heights of a series of equally spaced points and plotting them against time; the wavelength of the resulting curve was called the *period*.

Visual estimates of the significant height were made by the scientists aboard the *Atlantis* and are considered to be as reliable indications of the sea state as it is possible to obtain. As previously stated, the heights of 30 successive well defined waves were measured and averaged yielding a figure called the *significant height*. The procedure is open to criticism, since it has been suggested [11] that at least 10 min of waves are necessary for determining significant height.

6. Results

The results of observation, prediction, and wave record analysis are shown in table 1. The meaning of the symbols is given below.

v—mean wind velocity in fetch area (kt)
D_w—mean wind direction in fetch area (° true)
F—length of fetch (n mi)
D—duration of wind in fetch area (hr)
$\bar{H}$—average height of waves (ft)
$\bar{H}_{\frac{1}{3}}$—average height of the one-third highest waves (ft)
$\bar{H}_{\frac{1}{10}}$—average height of the one-tenth highest waves (ft)
T_R—difference between lowest and highest periods (sec)
$\bar{T}$—average period (sec).

The first forecast time was 1030 GCT 21 October 1954. The effects of the previous northeasterly flow (fig. 3a) had disappeared, because of partial destruction by a 90° shift in wind direction, and because of dispersion of the components left in that system. The new system (fig. 3b) achieved a fully developed state for 20 kt by forecast time and the appropriate spectrum forecast was made. The observed and predicted significant heights agreed within 0.5 ft. By 1500 GCT, 4.5 hr later, the wind velocity in the generating area had decreased to 15 kt and by 1700 GCT to 13 kt.

Table 1. Results obtained by visual observation, prediction by spectrum method, and computation from wave records. For explanation of symbols see text.

					Waves										
	Wind				Visual	Predicted					Calculated (wave pole)				
Date/time	v kt	D_w °	F n mi	D hr	$\bar{H}_{1/3}$ ft	$\bar{H}$ ft	$\bar{H}_{1/3}$ ft	$\bar{H}_{1/10}$ ft	T_R sec	$\bar{T}$ sec	$\bar{H}$ ft	$\bar{H}_{1/3}$ ft	$\bar{H}_{1/10}$ ft	T_R sec	$\bar{T}$ sec
10–21/1030	20	312	240	15.5	7.5	5.0	8.0	10.2							
10–21/1500	15	313	240	20	7.2	5.0	8.0	10.2	3.0–11.1	5.7	3.1–3.9	5.1–5.9	6.6–7.3	1.0–9.3	5.1
10–21/1700	13	335	240	22	7.3	5.0	8.0	10.2	3.0–11.5	5.7	2.9–3.7	5.0–6.0	6.4–7.3	1.3–9.1	5.2
10–21/2030						4.3	6.9	8.8	2.5–10.0	5.1					
10–22/0030						2.0	3.3	4.2	1.5– 8.0	4.0					
10–24/1200	20	295	240	9	8.5	5.0	8.0	10.2							
10–24/2200	20	345	340	4.5	6.8	4.6	6.6	8.4							
10–25/1030	17	340	300	17.5	7.9	5.0	8.0	10.2							
10–25/1300	18	330	300	20	9.9	5.0	8.0	10.2							
10–25/1500	16	335	300	22	8.4	4.3	6.9	8.9	2.7–10.5	5.5	2.9–3.5	4.8–5.4	6.1–6.6	1.5–8.9	5.2
10–25/1800	15	335	300	25	7.5	2.9	4.4	5.8	2.0– 9.0	4.6	2.5–3.1	4.4–5.1	5.6–6.4	0.9–8.3	4.6

Even though the wind velocity in the generating area was diminishing, the forecast point was so situated in the fetch area (215 n mi from the minimum fetch boundary) that it continued to receive the effects of the fully developed sea (corresponding to $v = 20$ kt) for 3.5 hr beyond this entire period. Because of these conditions, the predicted values during this time were necessarily constant. During the period of decay the height parameters obtained from the wave records differed at most by 0.2 ft, and the observed heights ($\bar{H}_{\frac{1}{3}}$) varied by only 0.3 ft. The observed and computed values were in pretty good agreement with the predictions since all described the sea state as remaining fairly constant while the wind decreased.

The height and period statistics computed from the wave records were consistently lower than either

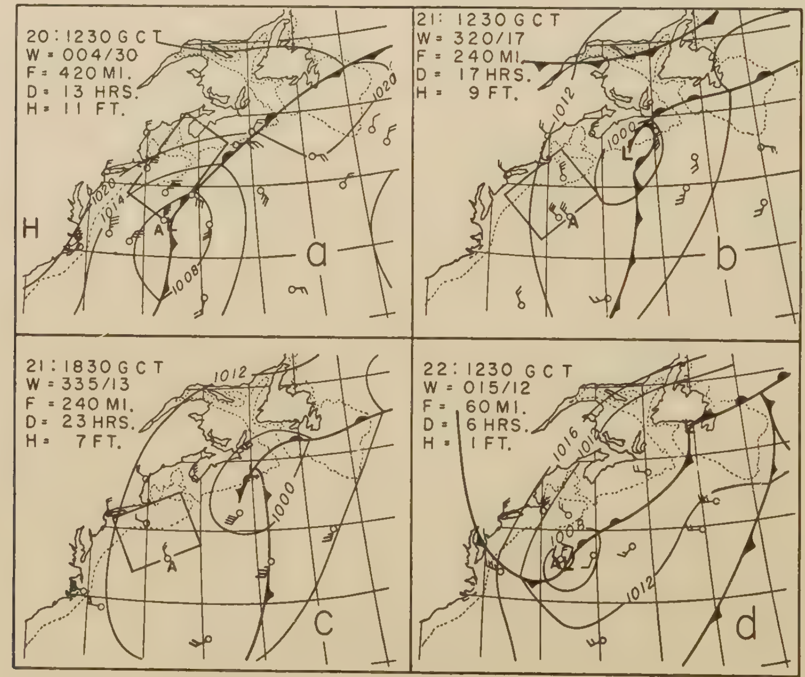
20 : 1230 G C T
W = 004/30
F = 420 MI.
D = 13 HRS.
H = 11 FT.
1020
1020
1014
1008
H
A
a
21 : 1230 G C T
W = 320/17
F = 240 MI.
D = 17 HRS.
H = 9 FT.
1012
1000
L
A
b
21 : 1830 G C T
W = 335/13
F = 240 MI.
D = 23 HRS.
H = 7 FT.
1012
1000
A
c
22 : 1230 G C T
W = 015/12
F = 60 MI.
D = 6 HRS.
H = 1 FT.
1016
1012
1008
1012
A
d

Fig. 3. Surface weather maps, 20–22 October 1954. Rectangle outlines fetch. Letter *A* marks position of *Atlantis*.

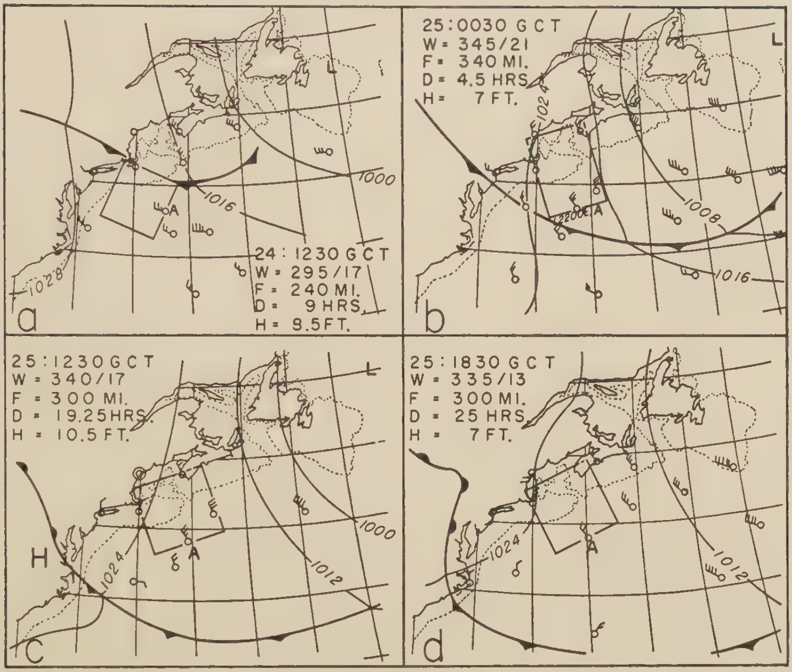

FIG. 4. Surface weather maps, 24–25 October 1954. Rectangle outlines fetch. Letter *A* marks position of *Atlantis*.

the observed or predicted values, even for the case of analysis of major wave components only. The only explanation that can be offered at the moment is the one given above in terms of the filtering technique. From a qualitative viewpoint, the results are encouraging in that they are all consistent; that is, the three methods showed a persistence of the fully developed state during the time when the wind was diminishing.

From the dispersion diagram (fig. 2), it was calculated that by 2030 GCT on the same day the 11-sec waves would no longer exist at the point of forecast, and that 4 hr later the 10- and 9-sec waves would also have passed. Appropriate height statistics were computed, but neither wave records nor visual observations were obtained. The best that can be said is that by 0030 GCT on 22 October, it was generally agreed aboard the *Atlantis* that the waves had considerably decreased in height. This agreed in a qualitative way with the prediction of $\bar{H}_{\frac{1}{3}} = 3.3$ ft.

The situation of 25 October was different in that a west-northwesterly wind field changed abruptly to north-northwesterly with the passage of a cold front at 1730 GCT on 24 October. The effect of the wind shift accompanying the frontal passage was to destroy partially the existing sea while the "new" sea began to develop due to the winds behind the front. Before the cold front passed (fig. 4a), the sea was in a fully developed state for $v = 20$ kt and the predicted $\bar{H}_{\frac{1}{3}}$ agrees quite well with the value observed. Four and one-half hours after the front passed, the new regime was in the process of becoming established. How much of the old regime remained in unknown. A purely intuitive guess that it had retained half of its intensity permitted an estimate of the energy in the sea surface. This was added to the energy of the 20-kt post-frontal sea that was limited to 4.5 hr. The resulting statistics coincided with those which would have existed for a fully developed sea appropriate to $v = 18.5$ kt. The observed value ($\bar{H}_{\frac{1}{3}}$) agreed remarkably well with the predicted value, but no credit is claimed for the technique on this account. The "new" sea continued to increase at $v = 20$ kt until it became fully developed, and all the effects of the "old sea" disappeared. At about 0130 GCT 25 October, the wind began to decrease in intensity and continued to do so during the rest of the observation period (fig. 4c, 4d). The forecasting technique required that the same forecast be made for 1030 GCT and 1300 GCT even though the visual observations indicated that

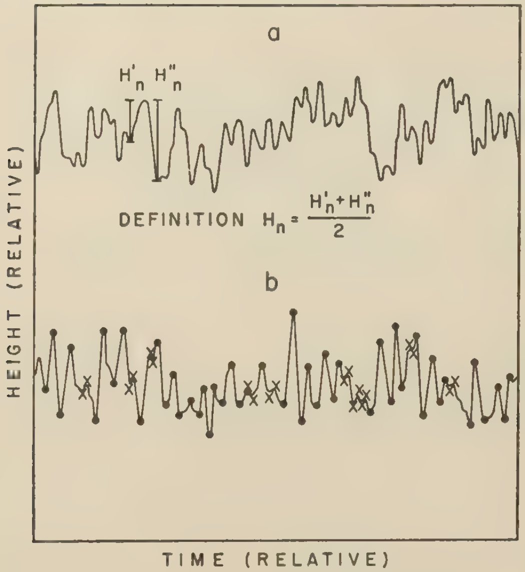

Fig. 5. Analysis of wave pole records. ●—major high components. ×—additional high frequency components.

the significant height increased by 2 ft in that period. By 1500 GCT the wind was down to 16 kt and the dispersion graph had accounted for the disappearance of the 11-sec waves. By 1800 GCT the 10- and 9-sec waves had also passed the forecast point. There is disagreement numerically in the results obtained by the three methods, but they all concur qualitatively in that they specify a decaying condition. For 1800 GCT, the wave record statistics agree very well with the predicted values, and the average periods for that time check exactly with the forecasts.

7. Conclusions

The prediction of the sea state in the decay period was well corroborated by the visual observations and the wave records. Especially gratifying was the confirmation of sustained sea while the winds in the generating area died down. The possible cause of the numerical discrepancies is discussed in section 5. It might be possible to make a more realistic evaluation of the height and period statistics from the wave records if the cutoff at the low period end of the spectrum is determined. Once this is known, the records can be mechanically filtered on the basis of the established cutoff. The heights and periods computed from the filtered record will then provide an absolute check on the forecasts.

An exact numerical check of the predictions can be made by calculating the energy spectrum measured by the wave pole [10]. Integration of the computed spectrum with respect to frequency will yield the number E which will provide a direct comparison with the forecasts. In addition, $0.03E$ taken from a cumulative graph of the spectrum will provide the low period cutoff described above.

In a qualitative sense, the observed, predicted, and computed parameters agreed in their descriptions of the change in the state of the sea. More observations are needed for many more sea conditions before the spectrum theory, with all of its many features, can be quantitatively assessed.

Acknowledgment—This work was sponsored by the Office of Naval Research under contract Nonr 769(00).

The authors wish to thank Messrs. R. G. Walden, G. G. Whitney, Jr., and E. H. Chute for their part in the observational portion of the program. Captain W. Scott Bray and his crew, of the *R/V Atlantis*, were very cooperative. Also, grateful appreciation is extended to Mrs. Eileen Bergstrom and Mrs. Sondra Marshall who aided in the computations and preparation of the figures, to Mrs. Mary C. Thayer who, in addition to the work performed in conjunction with the ladies above, tirelessly typed and retyped the manuscript, to Miss Mildred S. Clark for drafting the figures, and to Mrs. Bettie A. Stephenson for final typing of the manuscript.

REFERENCES

1. Farmer, H. G., W. Marks, R. G. Walden, and G. G. Whitney, Jr., 1955: A technique for ocean wave measurements. *Proc. Conf. Ships and Waves*, Stevens Inst. Tech., Oct. 1955.
2. James, R. W., 1954: An example of a wave forecast based on energy spectrum methods. *Trans. Amer. geophys. Union*, **35**, no. 1, 153–160.
3. Longuet-Higgins, M. S., 1952: On the statistical distribution of the heights of sea waves. *J. mar. Res.*, **11**, no. 3, 245–266.
4. Marks, W., 1955: The two-dimensional wave spectrum. *Allerton Conf. on Sea State and Sea Clutter*, University of Illinois, April, 1955. Unpublished manuscript.
5. ——, 1955: Contouring the sea surface. *Res. Rev.*, March, 1955, pp. 12–16.
6. —— and F. C. Ronne, 1955: Aerial stereo-photography and ocean waves. *Photogr. Engng.*, **21**, no. 1, 107–110.
7. Neumann, G., 1953: On ocean wave spectra and a new method of forecasting wind-generated sea. *Tech. Memo. no. 43, Beach Erosion Board, U. S. Army Corps of Engnrs.*
8. Pierson, W. J., Jr., 1952: A unified mathematical theory for the analysis, propagation and refraction of storm generated ocean surface waves, Parts I and II. *Res. Div., Coll. Engng.*, New York University.
9. ——, G. Neumann, and R. W. James, 1953: Practical methods for observing and forecasting ocean waves by means of wave spectra and statistics. *Tech. Rep. no. 1, BuAer. Proj. AROWA*, U. S. Naval Air Station, Norfolk, Va.
10. —— and W. Marks, 1952: The power spectrum analysis of ocean wave records. *Trans. Amer. geophys. Union*, **33**, no. 6, 834–844.
11. Scripps Institute of Oceanography, 1944: Proposed uniform procedure for observing waves and interpreting instrument records. *Wave Proj. Rep. no. 26.*

Contribution No. 800

Reprinted from COPEIA, 1957, No. 1, pp. 17-20, April 5
Printed in U.S.A.

New Records of Labrador Fishes with Special Reference to those of Hebron Fjord[1]

Malcolm S. Gordon and Richard H. Backus

THE Labrador cruises of the R/V Blue Dolphin during the summers of 1952 and 1954 resulted in fish collections containing new distributional data for a number of species. These collections also provide new information on morphology and relative abundances of several forms, especially those from Hebron Fjord (58°10′N). The fishes of Labrador, including those collected by previous Blue Dolphin expeditions, are discussed by Backus (1951 and MS[2]).

The 1952 and 1954 operations were supported in part by the Office of Naval Research through the Arctic Institute of North America and in part by the U. S. Navy Hydrographic Office. In addition the senior author was supported in part by National Science Foundation Predoctoral Fellowships for 1954–56. The authors' thanks for aid in making the present collections are due Mr. William Z. Lidicker, Jr. of the University of Illinois, biologist on the 1952 expedition; Commander David C. Nutt of Dartmouth College, master; Dr. Per F. Scholander of the University of Oslo, Norway, leader of the shore party on the 1954 expedition; Dr. Levie van Dam of the Philadelphia Academy of Arts and Sciences, physiological chemist on the 1954 expedition, and the members of the crew of the Blue Dolphin during both summers. Peter Hay, a native of Nain, Labrador, gave invaluable aid as guide to the 1954 expedition.

Areas Studied

Between 28 June and 25 August 1952 forty-three collections of fishes were preserved by Mr. Lidicker at numerous points along the Labrador coast between Pigeon Cove, on the west side of Newfoundland Island (53°51′ N, 57°00′W) and Jerusalem Bight, just north of Hebron (58°14′N, 62°38′W). The fishes from these collections discussed in the following account are those providing noteworthy new information.

The senior author's fish collections in 1954 were concentrated in central Hebron Fjord just off the expedition's base camp on the south shore (58°06′N, 62°59′W). Nine collections of bottom fishes were made with a fifteen foot otter trawl between 9 and 31 July. Water depths were in the range 110–125 meters. Temperatures below 100 meters were very near −1.7°C throughout. Salinity below 100 meters was very near 32.6 0/00. A single additional collection in the fjord was made in 220–250 meters about seven miles east of the camp (approximately 58°10′N, 62°50′W), off Winnie Bay, on 18 July. Temperature and salinity conditions in the bottom waters in the latter area were the same as for the camp area. The bottom in both areas was gray to brown mud, with scattered small rocks also present off Winnie Bay.

Commander Nutt and the crew of the Blue Dolphin made additional collections of fishes mostly with a ten foot beam trawl, in the vicinity of Hebron settlement, near the entrance to Hebron Fjord, and at Eastern Harbor, Palliser Island, Saglek Bay (58°33′N, 62°42′W) between 1 and 3 August, 1954.

Fishes preserved during both summers are deposited in the collections of the U. S. National Museum, Washington, D. C., and the Museum of Comparative Zoology, Cambridge, Massachusetts.

Distributional and Systematic Notes

Salvelinus fontinalis (Mitchill). Brook trout. —50 specimens, 104–188 mm. in standard length, were caught by hook and line in and off the mouth of the brook flowing into Nutak Harbor north of Nutak village (57°28 N, 61°50′W) on 29 July and 6 and 7 August 1952. Heretofore this species had been collected north only to Nain (56°35 N). Although it is largely replaced in coastal streams north of Nain by the arctic charr (*S. alpinus*), it is probable that small populations such as the one reported here are more or less continuously distributed around Cape Chidley into Ungava Bay, where Dunbar and Hildebrand (1952) report it common in the George River.

---

[1] Contribution No. 800 from the Woods Hole Oceanographic Institution.

[2] This and subsequent citations of Backus (ms) refer to an unpublished Ph.D. thesis submitted to Cornell University in 1953.

Pholis fasciatus (Bloch and Schneider).—1 specimen, 171 mm., beam trawl, 4–15 fm., channel E of Semekutak I. (57°33 N, 61°44′W), on 29 July 1952; 2 specimens, 170 and 211 mm., beam trawl, 3–4 fm., Nutak Hbr., 4 August 1952; 3 specimens, 121–135 mm., 10 foot seine, surface to 2.5 feet, Nutak Hbr., 6 August 1952; and 1 specimen, 215 mm., beam trawl, 6–10 fm. rocky bottom, Eastern Hbr., Palliser I., Saglek Bay, 2 August 1954. Heretofore only 2 Labrador specimens had been collected. This species is not found in tide pools where its congener, *P. gunnellus*, is so abundant but occurs below low tide level. Dorsal fin spines vary as follows (in same order as listing above): 87; 89, 89; 88, 88, 88; 89.

Pholis gunnellus (Linnaeus). Gunnel.—10 specimens, 70–240 mm., 10 foot seine, surface to 2.5 feet, Nutak Harbor, 6 August 1952. Heretofore the gunnel had been found north to West Turnavik Island (55°15′N). This species is unknown from Hudson and Ungava Bays, so the Nutak record is the northernmost on the American shore. The dorsal fin ray count was as high as 85 in this collection. Since we have counted as few as 84 rays in Labrador *P. fasciatus*, the clean separation between the two species found by Jensen (1942) in Greenland does not exist here.

Two males, 227 mm. and 226 mm., with swollen testes have an extension of the margin of the dorsal fin membrane which extends posteriorly for about 40 fin rays in the larger specimen and about 20 fin rays in the smaller. This extension is scalloped, the indentations between the thickened membranous tabs corresponding to the position of the fin rays. The extension is orange with a dusky margin. Six males 186 to 240 mm. with unswollen testes lack this extension.

Lumpenus lumpretaeformis (Walbaum). Snake blenny.—1 specimen, 121 mm., from codfish stomach, channel E of Semekutak I., 29 July 1952. Fin ray counts are D74, A49. Excepting Dunbar's (1947) report of two planktonic post-larvae from Hebron this is the most northerly record from our coast. We follow Bigelow and Schroeder (1953) in the spelling of the trivial name.

Lumpenus fabricii Reinhardt.—1 specimen, 230 mm., beam trawl on rocky bottom, 6–10 fathoms, Eastern Harbor, Palliser Island, Saglek Bay, 2 August 1954. Fin ray counts are D62, A43; no palatine teeth. This is the first record for this species from Labrador. Vladykov (1933) and Dunbar and Hildebrand (1952) have shown this species to be quite widely distributed in Hudson and Ungava bays, respectively. It is also of regular occurrence in west Greenland (Jensen 1944).

The closely related form, *Lumpenus medius* Reinhardt, is widely distributed in Labrador (Backus 1951 and MS) and east and west Greenland (Jensen 1944). It has not been recorded, however, from Hudson or Ungava Bays.

Lycodes pallidus Collett—5 specimens, 115 to 222 mm., Hebron Fjord: 2 from area off camp, 3 from deeper water off Winnie Bay, 11–18 July 1954. This is the second collection of this form from Labrador, bringing to 8 the total of specimens known from this area—all from Hebron Fjord (see Backus MS).

Myoxocephalus quadricornis (Linnaeus)—6 specimens: 5, 17–22 mm., 1, 82 mm., seine head of Jerusalem Bight, 19 July 1952. The second collection from Labrador. Previously known only from Nain (Backus MS). This species is also scarce in Ungava Bay (Dunbar and Hildebrand 1952), where *M. scorpius*, again as in Labrador, is common. Vladykov (1933) records both *M. quadricornis* and *M. scorpius* as being widespread and common in Hudson Bay.

Myoxocephalus scorpioides (Fabricius)—1 specimen, 46 mm., seined at the head of Jerusalem Bight, 19 July 1952. Only 7 Labrador specimens are known of this species which is common in Ungava and Hudson Bays.

Triglops nybelini Jensen—1 specimen, a male, 105 mm., area off Hebron Fjord camp, 24 July 1954. The second record from Labrador.

Cyclopterus lumpus Linnaeus—18 specimens, 18 to 31 mm., in shallows in Nutak Harbor, many found clinging to kelp, 6 to 9 August 1952. This is the most northerly locality for Labrador, though as pointed out by Backus (MS), the species probably occurs all along the coast.

Liparis atlanticus (Jordan and Evermann)—2 specimens, 35 and 36 mm., beam trawl in 4–8 fathoms, on hard sandy mud bottom, Hebron Harbor, 18 July 1952; 1 specimen, 52 mm., seined along shore at low tide, sand bottom, Nutak Harbor, 6 August 1952. These are the third and fourth collections of this fish from Labrador. Dunbar and Hildebrand (1952) record 1 specimen from Ungava Bay taken in

1949, that fish having been the first of the species taken north of the Gulf of St. Lawrence.

Liparis tunicatus (Reinhardt)—1 specimen, 61 mm., beam trawl in 4–5 ½ fathoms on mud bottom, Indian Harbor, Hamilton Inlet (54° 27′N, 57°12′W), 16 August 1952; 1 specimen, 46 mm., beam trawl in 6–10 fathoms on rocky bottom, Eastern Harbor, Palliser Island, Saglek Bay, 2 August 1954. The former locality is the most southerly station for the species on this coast. According to Dunbar and Hildebrand (1952) this form is very abundant in Ungava Bay. It is apparently unrecorded from Hudson Bay.

Liparis cyclostigma Gilbert—31 specimens, 55–192 mm., 15 foot otter trawl, 65 ± fm., mud bottom, Hebron Fjord off 1954 expedition camp, 9–31 July, 1954; 1 specimen, 128 mm. 15 foot otter trawl, 120–135 fm., mud bottom with some rock, Hebron Fjord off Winnie Bay, 18 July 1954.

The inclusion of several large individuals in the present collections enables us to determine that the specimens reported by Backus (ms.) as *Liparis sp.* belong here. In the new material the distance from the posterior margin of the disc to the origin of the anal fin varies from 14 to 21 per cent of the standard length. In the single large Labrador specimen heretofore known this distance constituted 12 per cent. According to Gilbert and Burke (1912) this distance constitutes 20 per cent in *L. cyclostigma.*

Color notes on large, fresh specimens in the present collections describe the species as having a background of pale reddish-pink with brassy-yellow overtones; the chin and disc white; upper parts of head and sides vermiculated with greenish brown, melanophores fairly dense on upper head; edges of pectorals dark with green tone; vertical fins alternately banded with light and blackish areas. This agrees well with the description of *L. cyclostigma* given by Gilbert (1895).

Fin ray counts for fifteen specimens are as follows: Dorsal fin: 40 rays—2 specimens; 41–1; 42–4; 43–5; 44–3. Anal fin: 32 rays—2 specimens; 33–2; 34–5; 35–4; 36–2.

This species, described from the Bering Sea by Gilbert (1895) and reported by Vladykov (1933) from Hudson Bay, thus appears to have an arctic American distribution. The fact that it lives in the very cold water suggests that it may prove to be circumpolar when the systematics of this genus are better known.

Reinhardtius hippoglossoides (Walbaum)—2 specimens, 83 and 107 mm., 15 foot otter trawl in 110–125 meters on mud bottom, off 1954 expedition camp, Hebron Fjord, 11 July 1954. This is the first record of this species for Labrador. Dunbar and Hildebrand (1952) record the first captures of this form from Ungava Bay, in the vicinity of Port Burwell. The species is known in the western North Atlantic from northwest Greenland to a point on the slope off Georges Bank in about longitude 68°W (Schroeder, 1955).

RELATIVE ABUNDANCES OF FISHES IN HEBRON FJORD

As described above, nine collections of bottom fishes were made between 9 and 31 July 1954 in the 110–125 meters in the portion of Hebron Fjord adjacent to the expedition base camp. For five of these collections, involving seven 20–30 minute hauls with the 15 foot otter trawl between 9 and 15 July, careful notes were kept on the exact numbers of each species of fish captured; hence we can estimate their relative abundances. That larger and more active individuals of some of the species may have eluded our small net, though it was towed fairly rapidly, is recognized as a source of error. The majority of the forms, however, are small and fairly sluggish.

The following table lists the species in these five collections, with the numbers of each captured:

Species	No. captured
1. *Icelus spatula*	69
2. *Boreogadus saida*	45
3. *Lycodes turneri turneri*	42
4. *Liparis cyclostigma*	17
5. *Liparis koefoedi*	10
6. *Gymnacanthus tricuspis*	5
7. *Lumpenus medius*	2
8. *Lycodes reticulatus*	2
9. *Lycodes pallidus*	2
10. *Reinhardtius hippoglossoides*	2
11. *Leptoclinus maculatus*	1
12. *Triglops pingeli*	1
13. *Eumicrotremus spinosus*	1

One or two individuals of three additional species were captured during the course of later operations in the same area: *Triglops nybelini, Agonus decagonus, Aspidophoroides olriki*. None of the otter trawl collections made in the deep waters of the interior of Hebron Fjord by earlier BLUE DOLPHIN expeditions contain any additional species. The relative abundances of the various species are very similar in these other collections to those listed here.

LITERATURE CITED

BACKUS, R. H. 1951. New and rare records of fishes from Labrador. COPEIA: *288–94*.

BIGELOW, H. B., AND W. C. SCHROEDER. 1953. Fishes of the Gulf of Maine. *U. S. Fish and Wildlife Service, Fishery Bull. 74: 1–577*.

DUNBAR, M. J. 1947. Marine young fish from the Canadian eastern Arctic. *Bull. Fish. Res. Bd. Canada, 73: 1–11*

DUNBAR, M. J., AND H. H. HILDEBRAND. 1952. Contribution to the study of the fishes of Ungava Bay. *Jour. Fish. Res. Bd. Canada, 9: 83–128*.

GILBERT, C. H. 1895. The ichthyological collections of the steamer ALBATROSS during the years 1890 and 1891. *Rept. U. S. Comm. Fish and Fisheries, 1893, App. 6: 393–476*.

GILBERT, C. H., AND C. V. BURKE. 1912. Fishes from the Bering Sea and Kamchatka. *Bull. U. S. Bur. Fish., 30: 31–96*.

JENSEN, A. S. 1942. Contributions to the ichthyofauna of Greenland 1–3. *Spolia Zool. Mus. Hauniensis, Copenhagen, 2: 1–44*.

———. 1944. Contributions to the ichthyofauna of Greenland 4–7. *Spolia Zool. Mus. Hauniensis, Copenhagen, 4: 1–60*.

SCHROEDER, W. C. 1955. Report on the results of exploratory otter-trawling along the continental shelf and slope between Nova Scotia and Virginia during the summers 1952 and 1953. *Deep Sea Research, Pap. Mar. Biol. and Oceanogr., Suppl. to 3: 358–372*.

VLADYKOV, V. D. 1933. Biological and oceanographic conditions in Hudson Bay. 9. Fishes from the Hudson Bay region (except the Coregonidae). *Contrib. Canadian Biol. Fish, 8: 15–61*.

OSBORN ZOOLOGICAL LABORATORY, YALE UNIVERSITY, NEW HAVEN, CONNECTICUT, AND WOODS HOLE OCEANOGRAPHIC INSTITUTION, WOODS HOLE, MASSACHUSETTS.

Contribution No. 809

THE SUPERCOOLING, FREEZING AND MELTING OF GIANT WATERDROPS AT TERMINAL VELOCITY IN AIR

DUNCAN C. BLANCHARD

Woods Hole Oceanographic Institution, Woods Hole, Mass.

Abstract—Giant water drops have been freely suspended in a vertical wind tunnel at temperatures below 0°C. The manner of freezing of these supercooled waterdrops is a function of the wet bulb temperature. At temperatures above T_w −4 or −5°C, a shell of ice, first forming on the bottom of the drop, will envelope the drop and then freeze inward. This is thought to be analagous to the formation of sleet since many of the phenomena associated with sleet have been observed in this study. At wet bulb temperatures below −4 or −5°C the freezing appears to occur nearly simultaneously over the entire surface of the drop causing the drop to turn to an opaque white. An explanation for the clear and the opaque freezing is partially attributed to the scattering of light by minute air bubbles that form as air comes out of solution as the water freezes.

At temperatures above T_w −5°C drops will often remain supercooled for ten minutes or longer while at about T_w −8°C supercooling does not generally extend beyond a minute. The initiation of freezing in drops in this temperature range is explained by freezing nuclei that might be expected to be active at these temperatures.

The melting of a frozen drop of less than about 10 mm diameter will proceed with no shedding of liquid water. However, if the frozen drop exceeds this diameter water will be shed from a liquid ring that forms around the horizontal midsection of the ice pellet. Melting is such that a spherical ice pellet will transform into a disc.

Introduction—The literature on the supercooling of water presents a complex and confusing picture [Bigg, 1953a]. Recent investigations have stressed the importance of using doubly distilled water and scrupulously clean containers, and Wylie [1953] has shown that the very nature of the glass containers that hold a water sample precludes the maximum degree of supercooling. By suspending water drops at the interface between two liquids and thus out of contact with glass or contaminated air, Mossop [1955] obtained the inverse relationship between freezing point and drop diameter that had been previously found by others with the exception that his freezing points were considerably lower. For example, he found that giant water drops (about eight mm diameter) would supercool to −32°C and smaller drops even lower. Measurements such as these, while possibly approaching the extremes in supercooling, cannot be interpreted as representing the freezing temperatures of raindrops at terminal velocity, at least not in the case of the giant drops. Raindrops are contaminated by collisions with particles within their fall path which, in turn, can bring about freezing at temperatures far higher than −32°C. It seems certain that the freezing of large raindrops is brought about by these collisions and the temperature at which freezing occurs can be best determined by observing the freezing during free fall through the air. The very manner in which the freezing occurs should shed light on the mechanism of the formation of sleet and hail.

The experiments to be discussed were started at the Pennsylvania State University in 1950 and continued during succeeding winters at Woods Hole, Massachusetts. The giant waterdrops were freely suspended at the top of a vertical wind tunnel [Blanchard,

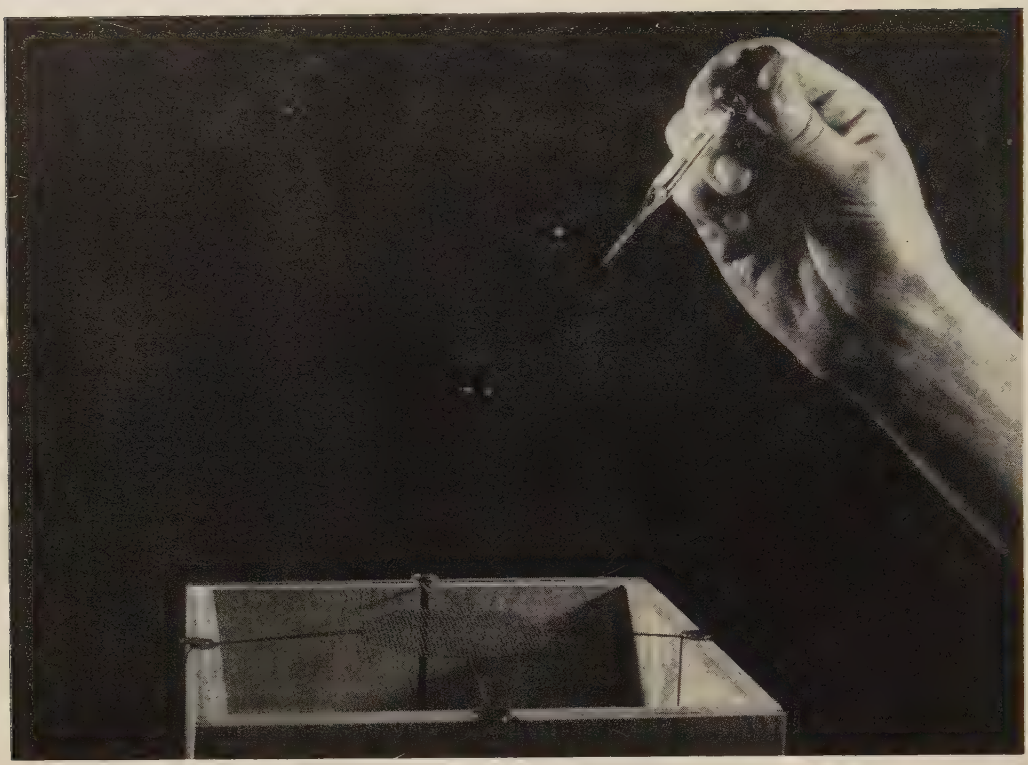

FIG. 1—The manner in which a giant water drop is freely suspended in the air stream at the exit of the vertical wind tunnel

1950] that was housed in an unheated shelter with free access to the outside air (see Fig. 1). This insured that the air temperature and nuclei content of the air through which the drop was falling was similar to that of the outside air. The wet- and dry-bulb temperatures were obtained in the air stream at the point where the drop was freely suspended. Readings were usually made before and after an observation of the freezing of a drop. Inasmuch as the waterdrop will closely attain the wet-bulb temperature of the ambient air [KINZER and GUNN, 1951] it is this temperature that governs the maximum amount of supercooling. The waterdrops, all about eight mm diameter, were injected into the air stream with an eye dropper. Water of various temperatures (+60 to −1°C) and from several sources (distilled, tap and water contaminated with dirt and dust) was used. As no obvious differences in the freezing of distilled and contaminated water were noted very little mention will be made of it in this paper. BIGG [1953a] found that water grey with room dust froze at almost exactly the same average temperature as distilled water. In order to eliminate one of the variables (the temperature of the waterdrop at the time of injection into the tunnel) the only experiments discussed here will be those in which the initial drop temperature was between 0 and +5°C.

Types of freezing—It soon became evident in the course of the experiments that two basic types of freezing occurred. In Fig. 2 an attempt has been made to summarize the results of over a hundred observations. These two types of freezing depend, in general on the degree of supercooling attained by the waterdrop at the moment at which freezing begins. The first type is characterized by the formation of a clear ice shell around the drop. This ice shell, which originates at the bottom of the drop, is remarkably clear in the initial stages of formation and often the only evidence of its existence is the cessation of the drop oscillation that occurs when the ice proceeds to grow up around the edges of the drop. It will be noted from Fig. 2 that clear freezing (represented by dots) will always occur if the T_w is higher than −4 or −5°C. If the T_w is below this temperature clear freezing may still occur if freezing commences within about 20 sec from the time the drop is injected into the air stream. Within this time, presumably, the drop has not had time to cool below a T_w of −4 or −5°C.

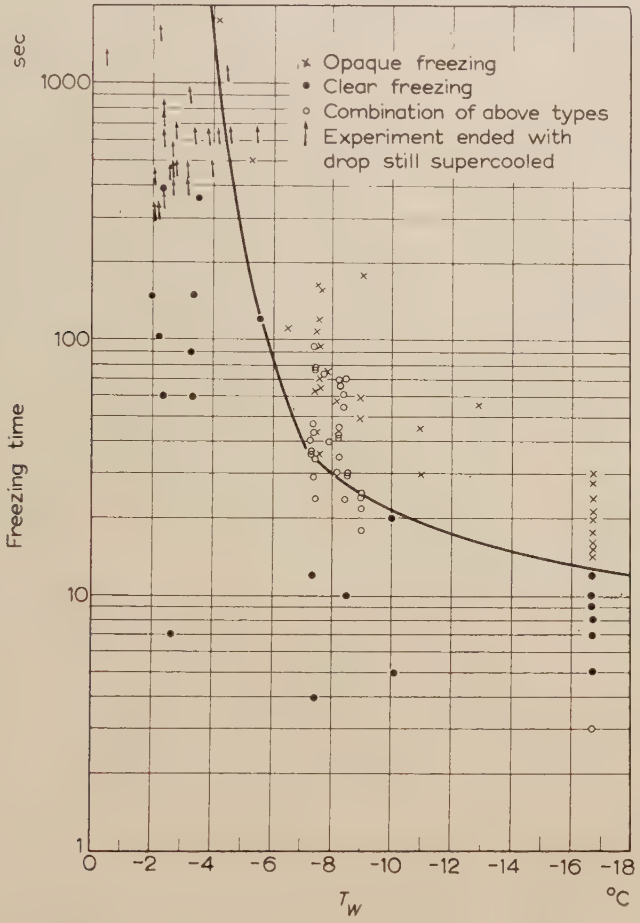

FIG. 2—The type of freezing of a giant drop as a function of time and the wet bulb temperature

If, on the other hand, the drop remains for more than about 20 sec in an air stream below a T_w of −4 or −5°C an opaque form of freezing will occur. This freezing is characterized by what appears to be a near instantaneous formation of opaque or 'milky-colored' ice over the entire surface of the drop. The ice forms with such rapidity that it is impossible to visually determine at what point freezing began. Similar observations on water freezing in containers have been reported by DORSEY [1948] and JOHANNSEN [1948]. Close examination of these partially frozen drops reveals that the periphery is a mixture of ice, water and minute air bubbles. It is undoubtedly the scattering of light from the numerous air bubbles and ice planes that gives the characteristic opaque appearance. The curve on Fig. 2 is a rough boundary, above which only opaque or near opaque freezing usually occurs.

Discussion of two types of freezing—The formation of clear or opaque ice is probably familiar to all who have examined sleet pellets and hailstones. It has been observed by many investigators who have studied the riming of rods exposed to supercooled clouds. CLARK [1948], who carried out such studies on Mount Washington, New Hampshire, found that the temperature of about —5°C could be considered a rough dividing point such that above this temperature the ice formation was mainly clear with virtually no entrapped air. At temperatures below —5°C the ice was predominantly opaque or milky with considerable numbers of entrapped bubbles. Similar results have been obtained by WEICKMANN [1953]. It is interesting that these riming studies indicate a transition in ice type at about —5°C but the results must be interpreted with caution. It is not clear as to what proportion of the numerous air bubbles found in the opaque ice are formed by air being forced out of solution when the water freezes or formed by trapping of the air in small 'pockets' in the spaces between the presumably frozen cloud droplets which form the rime.

The explanation of the clear and opaque ice in the present study is based on the fact that the solubility of air in water is an inverse function of temperature and that the solubility of air in ice is less than a thousandth that in water [SCHOLANDER and others, 1953]. The writer has found no data on air solubility in water at temperatures below 0°C but an extrapolation has been made from data obtained for temperatures above 0°C [DORSEY, 1940]. This indicates that a drop of eight mm diameter at air saturation at —8°C might well contain 10·5 mm^3 dissolved air as compared to only 7·9 mm^3 at 0°C. When freezing is initiated in an eight mm drop at —8°C the release of the latent heat of fusion (80 calories g^{-1} of water) will rapidly raise the drop temperature to 0°C and allow only 0·1 of the available water to freeze. Subsequent freezing will occur at a rate dependent upon the latent heat transfer away from the drop. In the very short time that the first 0·1 of the drop changes into ice the same relative amount of air $(0{\cdot}1 \times 10{\cdot}5)$ or 1·05 mm^3 must come out of solution. This has to occur for, as pointed out above, the air solubility in ice is relatively insignificant. Inasmuch as the opaque structure is not observed on drops freezing at temperatures at —4°C where about 0·5 mm^3 of air must initially come out of solution it appears that a trapping or retaining of the air must occur at freezing at T_w —8°C while not at T_w —4°C. It was mentioned earlier that opaque freezing was characterized by an apparently instantaneous formation of ice over the entire surface of the drop. At T_w —8°C the initial ice undoubtedly must start from a single point but rapidly envelopes the entire drop with the interior still liquid. It is probable that an intertwining maze of ice crystals exists with liquid water and the minute air bubbles that form from the air forced out of solution. At temperatures above T_w —4°C, on the other hand, the freezing can be seen to start in one region and progress slowly around the drop. The freezing is sufficiently slow to allow most of the air to escape and consequently produce clear ice.

Forms of clear ice—The manner in which the clear ice grows on a freely falling drop is indeed interesting to observe. With the proper lighting and background and by positioning himself at the edge of the tunnel an observer is able to be within four inches of the drop and observe the various phenomena that accompany the freezing. One of the most interesting of these is the formation of spicules [BLANCHARD, 1951]. Spicules have been observed when clear ice forms around the drop and then, due to expansion of the ice as it freezes inward, builds up a pressure on the interior water. This, in turn, will cause a fracture in the ice shell through which the remaining water will emerge. This water will form a spicule that freezes from the outside in. As the remaining water freezes along the central core of the spicule numerous air bubbles can be seen. This undoubtedly represents the air that is forced out of solution as the ice progresses inward. The writer has observed similar spicules on natural sleet pellets.

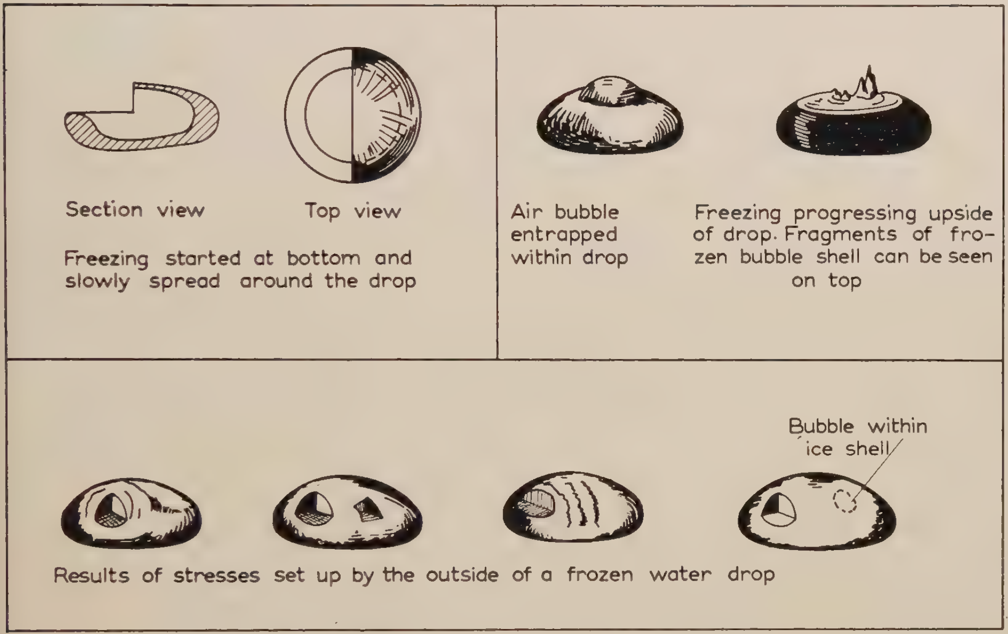
Section view
Top view
Freezing started at bottom and slowly spread around the drop
Air bubble entrapped within drop
Freezing progressing upside of drop. Fragments of frozen bubble shell can be seen on top
Bubble within ice shell
Results of stresses set up by the outside of a frozen water drop

FIG. 3—Sketches of phenomena observed with the clear type of freezing of freely suspended water drops

The slow clear freezing of an ice shell around a falling waterdrop results in high internal pressures with concomitant stresses within the ice shell. As ice is most easily fractured along its main crystallographic axis (which in the case of freezing waterdrops is usually radially inward) these stresses undoubtedly aid in producing radial fracture. The writer has never observed this fracture on freezing drops suspended in the air stream. However, the fracture was often noted on semi-frozen drops which had been removed from the air stream. This was definitely the case for the drop shown in the upper left of Fig. 3. The drop, injected into an air strem, of T_d −9·5°C, began to freeze from the bottom in a clear manner. Within a minute the ice had advanced upward and completely enveloped the drop. At that time the semi-frozen drop was removed from the air stream and examined. Nearly an exact quarter of the ice shell was missing revealing the liquid interior. It seems quite apparent that the stresses in the ice shell caused the fracture to occur when the drop was disturbed upon 'capture'.

The lower section of Fig. 3 illustrates smaller triangular-shaped sectors which were missing when the frozen drops were examined outside of the air stream. Here again it appears that this separation occurred as the drop was disturbed on removal from the air stream. On several occasions in natural sleet storms the writer has noticed sleet pellets with similar missing portions. In the light of the present work it appears that much of this separation occurs as the sleet pellet strikes the ground.

In an earlier study [BLANCHARD, 1950] the writer has described how the usual oscillations of the large waterdrops at terminal velocity are effectively eliminated when the drop contains an air bubble constituting upwards of about ten per cent of the drop volume. Not only is drop breakup in turbulent air eliminated but breakup by drop collision is diminished. One of these 'air-bubble' drops was observed to freeze in an air stream of about T_w −0·5°C. After three minutes, a surface layer of ice had advanced from the bottom to about half way up the drop. At this time the water film of the bubble, that had been protruding at the top of the drop, froze, broke, and left only a few jagged ice fragments. A sketch showing the drop before and after freezing is included in Fig. 3. It is not at all improbable that under some conditions raindrops would contain large air bubbles. Air bubbles have been observed by the writer both in natural sleet and in sleet artificially produced in the wind tunnel (see Fig. 3). If, in the case of natural sleet, the pellets were to fall through a layer of warm air and melt to raindrops the air bubble might stay intact. If so, the very presence of the bubbles would insure extreme stability of the large drops.

The initial freezing of a falling drop is occasionally accompanied by the growth of thin planes of ice up through the interior of the drop. An interesting observation of this was obtained with a drop in an air stream of T_w −3·3°C. When the drop oscillations ceased, close observation showed that a thin film of ice had formed on the comparatively flat bottom of the drop, and two extremely thin planes of ice had risen from the bottom ice layer. One appeared to rise perpendicular to the bottom plane, the other at an angle of about 45°. At this time neither the top surface nor the main bulk of the drop was frozen. The slow rotation of these ice planes about the drops vertical axis indicated a rotation of the entire drop. These rotary motions of about one quarter revolution per second would often stop and proceed in the other direction.

Photographs of partially frozen drops—Figures 4–6 are photographs of partially frozen drops and illustrate some of the types of freezing discussed in the last section. As it was somewhat difficult to focus the camera on the drops in the air stream or to insure proper lighting the partially frozen drops were removed and photographed outside the tunnel. The scale shown to the right of each photograph is one mm per square. The air temperature was T_a+0·3°C T_w−3°C.

The frozen drop shown in Fig. 4 was allowed to freeze for about two minutes before

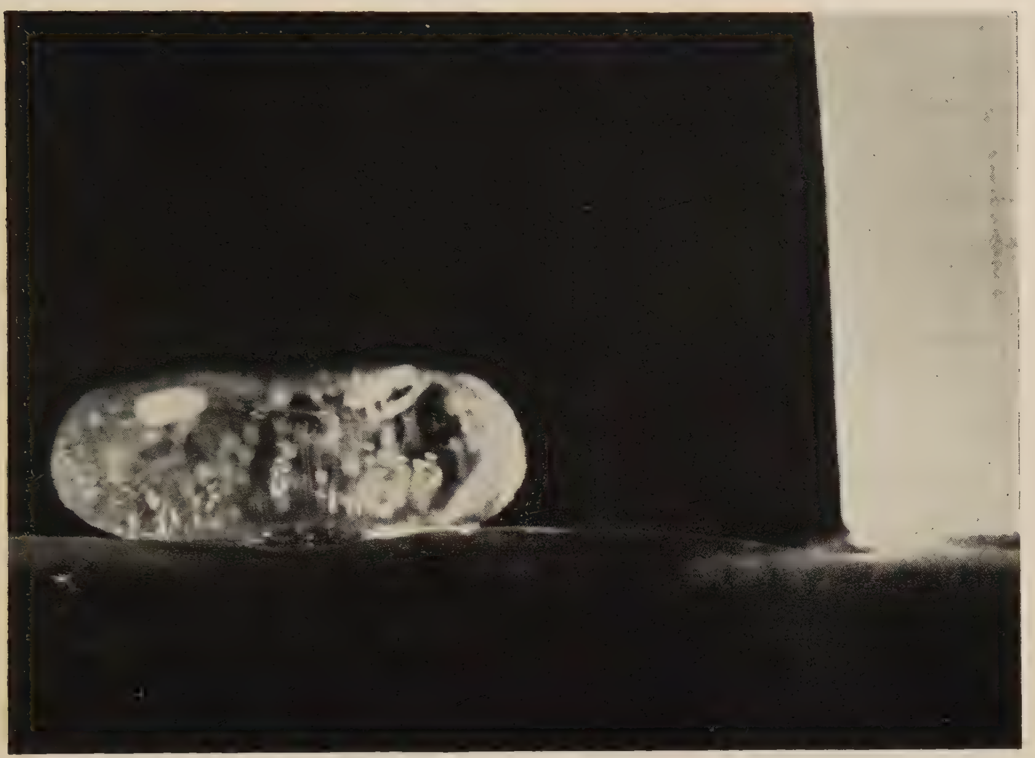

Fig. 4—Photograph of the side view of a drop that was removed from the wind tunnel after ice had formed completely around the drop; the concave appearance at the bottom is due to water melted by the flood light

removal from the tunnel. At this time the entire surface was frozen but the inside was still liquid. The stresses in the ice shell resulted in ridges that may be seen on the photograph extending from the upper left to the lower right section of the drop. Fig. 5 illustrates a drop that was removed from the tunnel when most of the upper part was still liquid. It is interesting to note that a three mm wide band of ice extended over the top of the drop at the mid section. This band was not observed when the drop was in the air stream. It was revealed only when the drop was removed and the water on either side allowed to drain away. Presumably this upward ice growth started with thin planes of ice growing up from the bottom.

Fig. 6 illustrates a drop that had been removed from the air stream with the top part entirely liquid. Much of the interior was still liquid giving the frozen part a bowl-like appearance. Over a hundred bubbles of approximately 200μ diameter were observed within the ice. Some of these can be seen in the photograph.

Stability of frozen drops—In a very thorough study of the equilibrium shape of a large water drop falling at terminal velocity McDonald [1954] has found that the aerodynamic plus the surface tension pressures combine to produce internal drop pressures that satisfy the hydrostatic equation. He has pointed out to the writer that the center of gravity of the drop is above the upward acting center of pressure for these aerodynamic

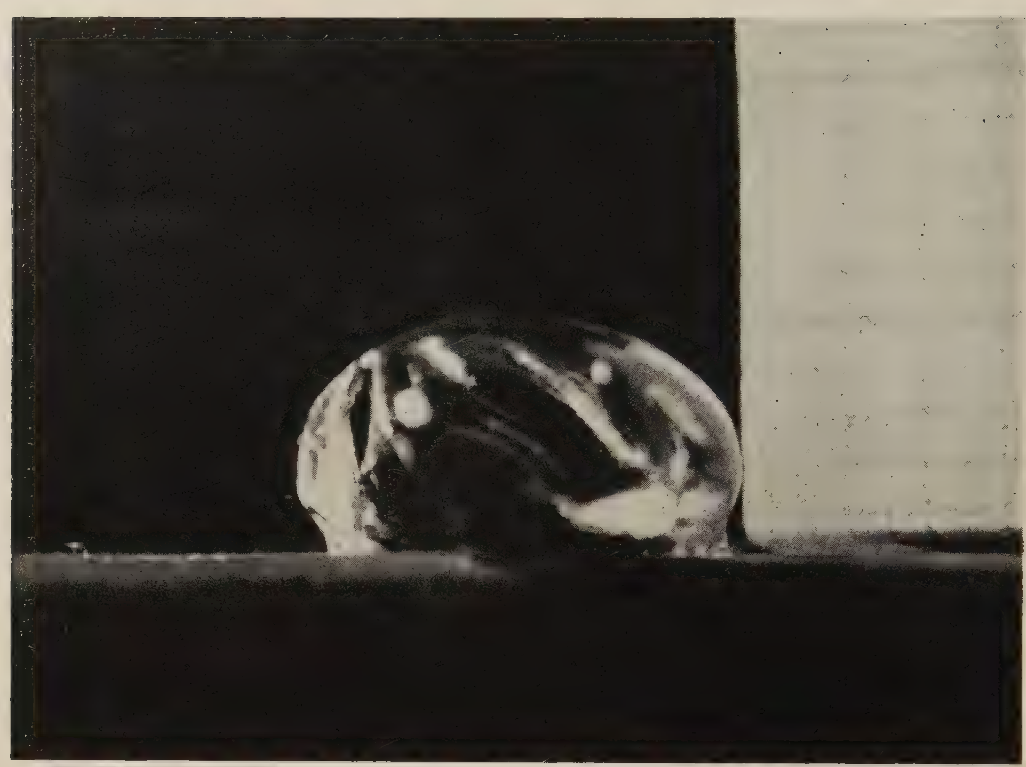

FIG. 5—Photograph of side view of a drop that was removed from the wind tunnel when a portion of the upper part was still liquid. The concave section is caused by liquid water

forces. This would, at first appear to be a case of unstable equilibrium but as the drop is liquid it can always adjust its shape to prevent the above couple force from acting. When the equilibrium shape is not subject to adjustment, as is the case when a shell of clear ice forms around the drop, it might be expected that the afore-mentioned couple would cause the frozen drop to turn upside down where it would fall in stable equilibrium Observation shows, however, that frozen drops will often remain stable for many minutes. On occasions their stability has been interrupted by rapid oscillations about a horizontal axis which sometimes are damped out but often end in the frozen drop falling out of the air stream. Could these oscillations be a result of the couple force in which the aerodynamic center of pressure is continually changing in a direction to bring the drop back to the equilibrium position?

If the drops freeze opaque the stability is noticeably changed. Almost immediately upon freezing oscillations will begin and only rarely will the drop remain in the wind tunnel for more than a few seconds. The drop has often been observed to be carried up and out of the air stream at the instant of freezing. This suggests that a slight increase in cross section has occurred or that the drag has been increased.

An explanation for the freezing of the giant drops—In literature on the supercooling of water [BIGG, 1953a] there is general agreement that freezing temperatures of

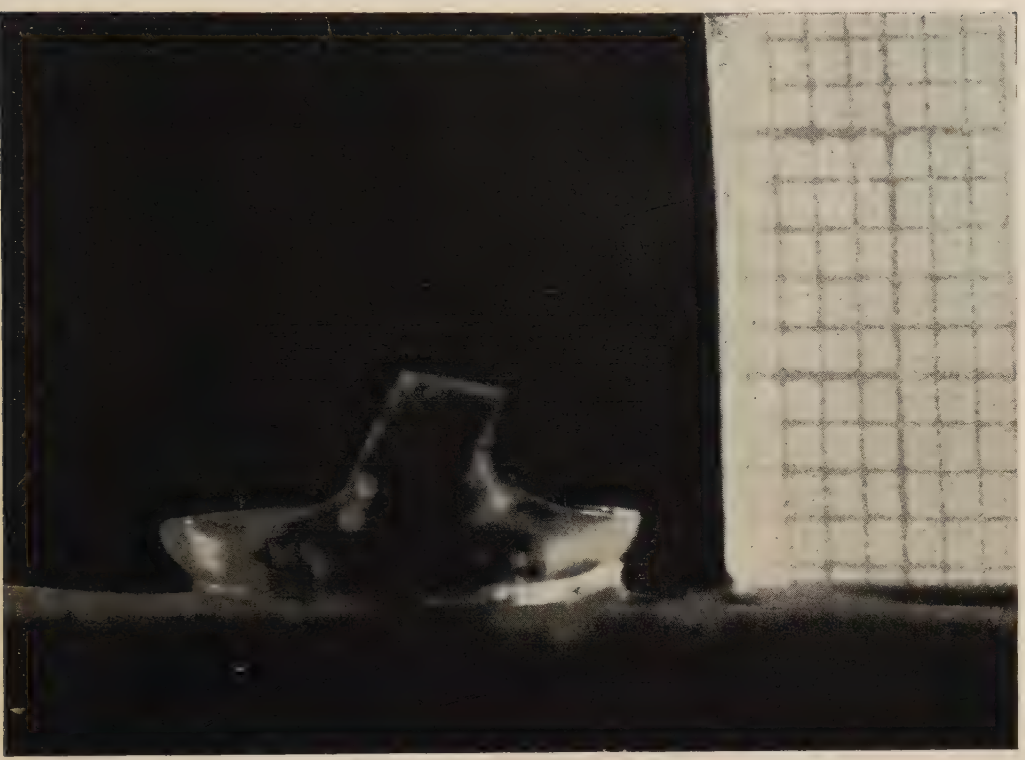

FIG. 6—Photograph of the side view of a drop that was removed from the wind tunnel when the top was still liquid; only the ice portion is shown here

the order reported here are considerably higher than those that would be obtained in the absence of freezing nuclei. As was mentioned earlier in this paper MOSSOP [1955] found that drops of the size used here supercooled to about —32°C. With the present results indicating freezing of drops as high as —3°C it appears that freezing nuclei carried by the air stream and impinging on the supercooled drop could be responsible for the freezing.

Investigations by FINDEISEN and SCHULZ [1944] on ice crystal formation as a function of temperature have been studied by BIGG [1953b] who has explained the results, at temperatures below about —20°C, on the basis of homogeneous nucleation which does not necessitate the existance of any external freezing or sublimation nuclei. However, he cannot explain observations of ice at higher temperatures, an example of which are those reported by BOWEN [1952] where, on three separate water-seeding flights through clouds whose tops were —6, —6, and —7°C, both rain and hail was found. With the cloud tops at these temperatures the freezing of the drops probably occurred at even higher temperatures and suggests the existence of freezing nuclei that are active at these temperatures.

If, then, we assume that freezing nuclei, and not homogeneous nucleation, are responsible for freezing at temperatures above about —10°C, then it must be shown that such freezing nuclei do exist in the atmosphere and that they might be expected to impinge on falling supercooled raindrops. There is little doubt that great numbers of minute fragmentation crystals exist during and shortly after a fall of snow. What is believed to be an example of the effect of fragmentation crystals in seeding supercooled drops is illustrated in Fig. 7. The symbols have the same interpretation as those in Fig. 2. The numbers beside the points represent the initial temperature of the water. The observations on the five drops which froze in a clear manner in a minute or less were made at a time when a moderate snowfall was going on outside the small wooden structure that housed the wind tunnel. Although fragmentation crystals were not evident to the eye they presumably were entering the shelter through the many cracks and open louvers and were being carried by the air stream to the drops. With such a continual supply of ice crystals long periods of supercooling were impossible. Several hours later and sometime after the snow fall had stopped the observations were repeated with the result that out of nine drops all but two remained unfrozen for at least seven minutes. One drop remained supercooled for 29 minutes, at which time opaque freezing occurred. It appears that the fragmentation crystals associated with the earlier snow fall had diminished in number and thus increased the probability of prolonged supercooling.

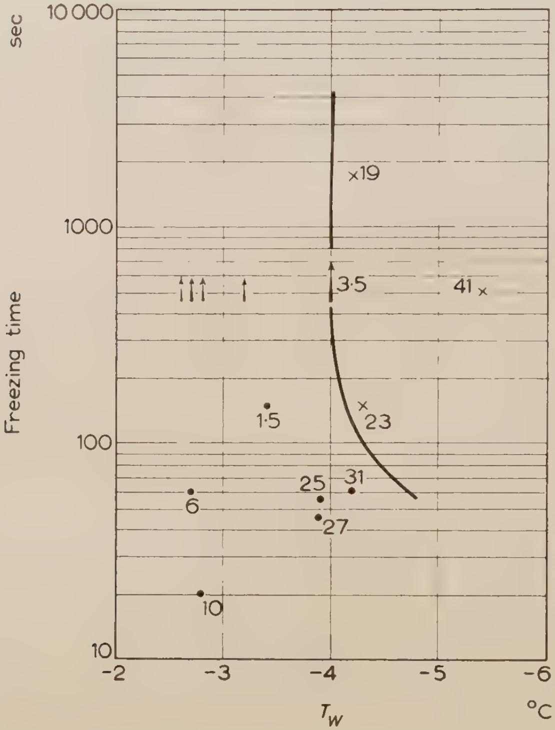

FIG. 7—The effects of seeding supercooled drops with natural ice crystals

Freezing has been successfully initiated in supercooled drops by burning strips of AgI impregnated paper at the intake of the wind tunnel. It was found that at temperatures near 0°C the AgI nuclei were inactive but became active as ice crystal nuclei somewhere between —3 and —5°C. VONNEGUT [1947] and HEVERLY [1949] found that large grains of AgI placed in bulk water or suspended in drops, respectively, made it difficult to supercool the water below about —4°C. In this case the AgI was acting, not as a sublimation nucleus but as a freezing nucleus and, as SCHAEFER [1952] has shown, AgI is quite effective in either role.

The main bulk of the observations of Fig. 2 cannot be accounted for on the basis of fragmentation nuclei as much of the data were obtained at times when the ground and atmosphere were free from snow. The only recourse in these cases is to look for other natural aerosols that may be acting as freezing nuclei. Our knowledge of freezing nuclei active at temperatures above —10°C is very incomplete. The small volumes of air which have been used by most investigators are quite sufficient for the determination of natural freezing nuclei at temperatures below —10°C, but are much too small to determine the concentrations of nuclei of the order of one every 10 or 100 liters. It is just this range which may be of importance to the supercooling of the large drops. AUFM KAMPE and WEICKMANN [1951] have carried out investigations on the occurrence of freezing nuclei in natural aersols as a function of temperature. Although their results indicate higher concentrations of nuclei for a given temperature than other investigators [PALMER, 1949, FINDEISEN and SCHULTZ, 1944], only their results will be considered. In the first place the aerosols they tested were from a variety of air masses all of which were probably simultaneously common to the present experiments. (Asbury Park, N. J., the place where their work was carried out is only about 200 miles WSW of Woods Hole, Mass., the site of most of the present work.) Secondly, SCHAEFER [1954] has reported on more than 15,000 observations of natural ice nuclei made atop Mt. Washington, New Hampshire

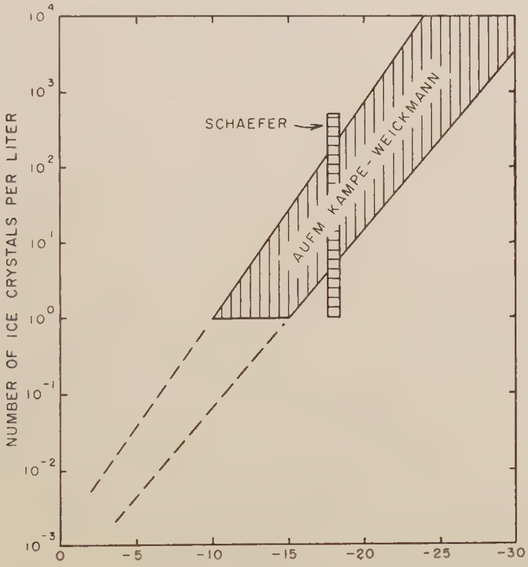

FIG. 8—The concentration of freezing nuclei in the northeastern U.S. as a function of temperature; see text for the interpretation of the data, especially those of Schaefer

(about 200 miles NNW of Woods Hole) over the past few years. Though he finds seasonal fluctuations, and fluctuations from day to day, the great majority of observations which were made during the winter months and concurrent with the work reported here, indicated from one to 500 ice nuclei per liter at a cold box temperature of —18°C. It can be seen that Schaefer's values are centered very well (see Fig. 8) around those found by aufm Kampe and Weickmann at the same temperature. The good agreement between these investigators, whose work was carried out in locations that are reasonably near the site of the present work, leads the writer to believe that the relation of freezing nuclei to temperature at Woods Hole might be most nearly approximated by the aufm Kampe and Weickmann data. One must realize that great fluctuations probably occur around the values which they have found. Schaefer reports that over the years the count has varied from none to a maximum of 10^4 per liter.

Considerable disagreement with the aufm Kampe-Weickmann and Schaefers freezing nuclei values have been found in recent measurements of freezing nuclei over Arizona, Australia, and Hawaii [KASSANDER and others, 1956]. It was found that, in general, the number of freezing nuclei activated at about —29°C was of the order of one per liter, far less than would be expected from the data of aufm Kampe-Weickmann and Schaefer. It must be realized however that the above locations are probably not subjected to such a high degree of contamination from industrial smokes as is the northeastern United States where the aufm Kampe-Weickmann and Schaefer work was done. These industrial smokes may well be responsible for the higher level of freezing nuclei.

An estimate of the order of magnitude of the freezing nuclei that might be expected at temperatures above —10°C has been arrived at by extrapolating aufm Kampe and Weickmann's data. From Fig. 8 it can be seen that one might expect about one freezing nucleus per 100 liters at —4°C and one every ten liters at —8°C. (As the freezing nuclei are determined by examination of a water cloud the T_d is assumed to equal T_w.) Now a simple calculation shows that a drop of eight mm diameter (flattening during fall gives a cross section of about nine mm diameter) falling at a terminal velocity of nine m sec^{-1} would have to fall for five minutes to sweep out 100 liters and, at a temperature of —4°C to overtake one freezing nucleus. At a temperature of —8°C where one freezing nucleus every ten liters is expected, the drop would have to fall only 0·1 as long or 30 seconds. Reference to Fig. 2 indicates that at T_w —4°C the freezing times were centered at about five minutes or 300 sec. Wide deviations occur but this is to be expected and may only reflect the great variation that can exist in freezing nuclei. At T_w —8°C it is seen that the freezing times are indeed of the order of 0·1 those at —4°C or 30 sec.

It is realized that the explanation for the observed freezing of drops as advanced above is far from being conclusive. We know almost nothing about the collection efficiency of freezing nuclei for large water drops. The value of unity as assumed here is probably too high. Secondly, there is doubt about the validity of the extrapolation of aufm Kampe and Weickmann's data. SCHAEFER [1949] has examined a considerable number of naturally occurring dusts to determine their temperature range of activity for producing sublimation nuclei. He reports that none of these has shown any activity at temperatures above —12°C. However, it is believed that Schaefer was not too much concerned with low nuclei concentrations such as one per 100 liters that might exist at —4°C. The volume of air that was illuminated in his cold chamber and examined for ice crystals was probably not more than one liter and, even allowing for air motion through the illuminated volume, it is probable that nuclei of concentrations of less than 0·1 per liter would be undetected. A conclusive answer to the whole problem will not be obtained until freezing nucleus counts are made concurrent with observations of the freezing of large drops. The writer is hopeful that he will be able to carry out such experiments in the near future.

The melting of a frozen drop—The manner in which a frozen drop melts and sheds water has always been an interesting one to the cloud physicist. Besides the changes in raindrop size distribution that may be brought about, the radar meteorologists must be concerned with any basic change in the shape of the particles which produce the radar return.

In order to find out the nature of the melting process, experiments were carried out with giant drops in the following way. A water drop in an air stream of T_d +0·5°C, T_w −2·7°C was allowed to freeze for about 2·5 minutes. At this time the outside of the drop was covered with clear ice and stresses were beginning to cause surface irregularities to appear. A 2000 watt heater was then placed near the tunnel intake. Within 40 sec, the ice shell on the drop, which had appeared greyish-white, became covered with a film of liquid water that reflected the light of a flood light as if it were a mirror. As the ice shell melted, a few entrapped air bubbles were released and rose to the top of the drop. Finally the characteristic rigidity of the ice pellet was gone and the drop was entirely liquid. During this freezing and melting process, the drop was stable and showed no tendency to change in shape or to shed water. This behavior is just what would be expected, since the equilibrium shape of the drop does not change as freezing occurs and, consequently, no change should occur upon melting. At the completion of the melting process the air temperature at the tunnel exit was T_d 11·4°C, T_w 3°C.

Water drops at terminal velocity are not stable at sizes much above 10 mm diameter [Blanchard, 1950], so it would appear that shedding of water must occur with the melting of ice spheres above this size. As the literature appears to have no information on this subject it may be of interest to briefly describe some simple experiments carried out at about 25°C. Crude ice spheres of about 20 mm diameter were fashioned from ice cubes obtained from a refrigerator. These spheres were mounted at the exit of the wind tunnel in several ways. One procedure was to drill a small hole through the sphere and thread it upon a thin string mounted along the vertical axis of the tunnel. Proper adjustment of the air speed will allow the sphere to 'fall' at terminal velocity and remain suspended on the string. With this same air velocity the sphere was sometimes supported from a horizontal string. Another technique of holding the ice sphere was to mount it at the end of a stiff thin rod and support it in the air stream from above. Regardless of the manner in which it was held, the following melting phenomena were noted. As shown in the sketch of Fig. 9 the water from the melting sphere would collect in a ring around the horizontal midsection, a region where the air pressure is probably lowest [McDonald, 1954]. As the melt water builds up in this water ring instability sets in and drops up to perhaps five mm will break away. With rapid motions they often will be carried over the top of the sphere and coalesce with the ring on the opposite side from whence they came. (This recapturing effect has been observed in earlier studies [Blanchard, 1949] and is believed to be important in raindrop growth.) Sometimes these drops do not coalesce with the liquid ring, but travel out beyond the edge of it, receive the full impact of the air flow there, and break into many fragments. On other occasions the drops will break away from the ring and continue upwards being but little influenced by the large ice sphere. In any event all shedding of water is confined to the liquid ring around the mid-section.

The ring of water tends to insulate part of the ice sphere, causing most of the melting to occur on the top and bottom. This differential melting results in the sphere of ice becoming a horizontally oriented disc of ice. As the transition is going on, the ice pellet often begins to spin about the vertical axis with such rapidity that the water is centrifuged off in small drops. The spin appears to be upwards of five revolutions sec^{-1} and not always in the same direction thus it does not appear to be due to a rotary nature of the air stream.

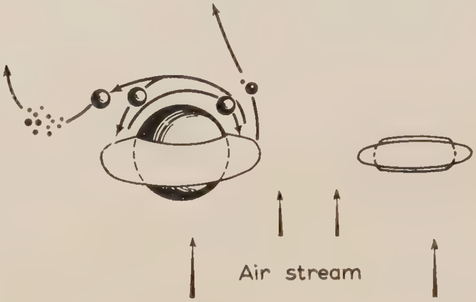

FIG. 9—A proposed melting process for large freely falling ice pellets; the sketch at left shows the shedding of drops from the ring of water that develops around the mid-section of the pellet; the insulating effect of this water causes the pellet to transform into a disc, as seen edgewise in the sketch at the right

The observations described above were made on spheres suspended with threads. Some preliminary attempts to freely suspend the large spheres have been successful for only a few seconds, but it appears from this that the behavior is still as described. It is possible that a large ice pellet in nature will rotate and tumble as it falls but as melting occurs the water will tend to remain oriented around the horizontal mid-section and thus provide a drag force that will tend to oppose the tumbling motion of the pellet. If any rotation about the vertical axis sets in, the resultant centrifugal forces should further stabilize the ice pellet. Further experiments on this interesting and potentially important phenomenon are badly needed before one can fully understand the melting process of these large ice pellets in nature.

Conclusions—It seems likely that the time a supercooled drop in free fall can exist before freezing is a function of the freezing nuclei content of the atmosphere. Certainly the occurrence of clear or opaque freezing is a function of temperature. Further work must be done to determine the behavior of the drops as the opaque freezing process proceeds to completion. This work to date has been difficult as the drops become unstable very shortly after freezing. It may be necessary to remove the drops from the air stream after the initial freezing has occurred and observe the final freezing process while they are artificially supported.

The melting of an ice pellet less than ten mm diameter can occur with no shedding of water. On the other hand, the fascinating behavior of an ice sphere greater than ten mm diameter, as it undergoes melting, indicates that water is shed from the liquid ring that forms around the horizontal periphery of the drop. It is probable that this ring, and the spinning motion of the ice pellet around the vertical axis, are responsible not only for the stability of the drop but for its final evolution into a circular disc.

Acknowledgments—The writer would like to thank Hans Neuberger, head of the Division of Meteorology at the Pennsylvania State University for his guidance in the initial phases of the work. Thanks are also due to A. H. Woodcock of the Woods Hole Oceanographic Institution for critical discussions as the experimental work evolved.

This is Contribution No. 809 from the Woods Hole Oceanographic Institution. A part of this work was drawn from a thesis submitted to the Pennsylvania State University in June 1951 for the partial fulfillment of the degree of Master of Science. The rest of the work was done under the Office of Naval Research, Contract Nonr 798(00) (NR-082-124).

REFERENCES

aufm Kampe, H. J. and H. K. Weickmann, The effectiveness of natural and artificial aerosols as freezing nuclei, *J. Met.*, v.8, pp.283–288, 1951.

Bigg, E. K., The ‘freezing point’ of water, *Scientific J. R. College Science*, v.23, pp.107–114, 1953a.

Bigg, E. K., The formation of atmospheric ice crystals by the freezing of droplets, *Q.J.R. Met. Soc.*, v.79, pp.510–519, 1953b.

Blanchard, D. C., Experiments with water drops and the interaction between them at terminal velocity in air, *Occ. Rep.* 17, Proj. Cirrus, Gen. Elec. Co., 1949.

Blanchard, D. C., The behavior of water drops at terminal velocity in air, *Trans., Amer. Geophys. Union*, v.31, pp.836–842, 1950.

Blanchard, D. C., A verification of the Bally-Dorsey theory of spicule formation on sleet pellets, *J. Met.*, v.8, pp.268–269, 1951.

Bowen, E. G., A new method of stimulating convective clouds to produce rain and hail, *Q.J.R. Met. Soc.*, v.78, pp.37–45, 1952.

Clark, V., Icing nomenclature, in Harvard-Mt. Washington Res. Report 1946–1947, Air Force Tech. Rep. 5676, pp.415–481, 1948.

Dorsey, N. E., *Properties of Ordinary Water-Substance*, Amer. Chem. Soc., Monograph ser., Reinhold Pub. Corp., New York, 673 pp., 1940.

Dorsey, N. E., The freezing of supercooled water, *Trans. Amer. Philosoph. Soc.*, v.38(3), pp.247–328, 1948.

Findeisen, W. and G. Schulz, Experimentelle Untersuchungen über atmosphärische Eisteilchenbildung, 1, *Forschungs-und Erfahrungsberichte Reichswetterd.*, A, no.27, 1944.

Heverly, J. R., Supercooling and crystallization, *Trans., Amer. Geophys. Union*, v.30, pp.205–210, 1949.

Johannsen, R. S., Some experiments on the freezing of water, *Science*, v.108, pp.652–654, 1948.

Kassander, A. R., L. L. Sims, and J. E. McDonald, Observations of freezing nuclei over the southwestern U.S., paper in this publication, pp.392–401, 1956.

Kinzer, G. D. and R. Gunn, The evaporation, temperature and thermal relaxation-time of freely falling water drops, *J. Met.*, v.8, pp.71–83, 1951.

McDonald, J. E., The shape and aerodynamics of large raindrops, *J. Met.*, v.11, pp.478–494, 1954.

Mossop, S. C., The freezing of supercooled water, *Proc. Phys. Soc.*, v.68, pp.193–208, 1955.

Palmer, H. P., Natural ice particle nuclei, *Q.J.R. Met. Soc.*, v.75, pp.15–22, 1949.

Schaefer, V. J., The formation of ice crystals in the laboratory and the atmosphere, *Chem. Reviews*, v.44, pp.291–320, 1949.

Schaefer, V. J., Formation of ice crystals in ordinary and nuclei-free air, *Ind. and Engr. Chem.*, v.44, pp.1300–1304, 1952.

Schaefer, V. J., The concentration of ice nuclei in air passing the summit of Mt. Washington, *Bul. Amer. Met. Soc.*, v.35, pp.310–314, 1944.

Scholander, P. F., W. Flagg, R. J. Hock, and L. Irving, Studies on the physiology of frozen plants and animals in the arctic, *J. Cellular and Comparative Physiology*, V.42, sup.1, pp.1–56, 1953.

VONNEGUT, B., The nucleation of ice formation by silver iodide, *J. App. Phys.*, v.18, pp.593–595, 1947.

WEICKMANN, H., Observational data on the formation of precipitation in cumulonimbus clouds, in *Thunderstorm Electricity*, Univ. Chicago Press, pp.66–138, 1953.

WYLIE, R. G., The freezing of supercooled water in glass, *Proc. Phys. Soc.*, v.66, pt.3, pp.241–254, 1953.

DISCUSSION

Dr. L. J. Battan—Have you tried any experiments where you permitted small drops to collide with the bigger drop in any of these stages of freezing or melting? When it occurred did it accelerate freezing or did it have no effect; or did it accelerate break up of the drop when it started melting? Furthermore, how often did bounceoff occur?

Mr. D. C. Blanchard—I'm afraid I can't answer either. I did not make that kind of experiment; my main concern has been trying to see at what temperature a drop would freeze.

Dr. Battan—It would be interesting to do some work with a one-mm drop bouncing off a six-mm drop, for example.

Mr. Blanchard—I haven't done that, either. I admit it's something that should be tried.

Dr. Battan—We took some photographs in Chicago taken with a Fastex camera where water was injected through a jet and one could follow the drops at this high speed and see the bounceoff. When the drops collided, the smaller one would sink into the larger one and come right out again. What effect would this have on the drop size distribution?

Mr. Blanchard—I couldn't say; however I have also observed what you just mentioned.

Dr. Richard M. Schotland—I have two comments. One concerns the appearance of the murky type of ice which you describe. I obtained similar results except when I changed the rate of freezing. By varying the cooling rate I could vary the line of separation between clear and murky ice. If the rate of cooling was high, I obtained this murky type of ice at a relatively high temperature and conversely, at a low rate of cooling the murky ice appeared at a lower temperature.

The second comment is on the case where a large water droplet is hit by a smaller droplet. I have used a Fastex camera, and the results indicate that with freshly formed water drops sometimes one can get coalescence and sometimes not. This apparently depends strongly upon the nature of the collision.

Dr. E. J. Workman—I should like to mention an idea of Reynolds in connection with the question raised about collisions and bouncing and the effect upon freezing. If one could form the union of two drops which are so structurally organized as to be unable to freeze by themselves, then the disorder which would be introduced by bringing these two drops into coalescence might account for or favor the freezing of supercooled droplets in thunderstorms, even when they are quite small.

Dr. James E. McDonald—There was one thing I want to ask. Did you say that after the drops froze they still stayed in the air stream?

Mr. Blanchard—If they freeze clear, they will. If they freeze in the opaque manner, they will fall out. They become unstable almost immediately.

Mr. McDonald—Well, the freezing does proceed from the bottom.

Mr. Blanchard—In the clear ice.

Dr. McDonald—The difficult thing to understand about the frozen raindrops falling in the way they do is that the center of pressure of an object of raindrop shape is below the center of mass, which is an aerodynamically unstable situation. Once, then, the drops lose their fluidity by virtue of freezing, it is not clear how they can avoid tumbling out of the airstream. Fluidity and the attendant ability for dynamic balance between shape and aerodynamic factors are essential to the stable (non-tumbling) movement of a raindrop shaped object through the air.

Dr. Horace R. Byers—Mr. Blanchard's method appears to have a very good application to the problem of hailstones. I wonder, if you would care to express any ideas on that subject in amplifying the paper that you have given.

Mr. Blanchard—Well, if you mean growing hailstones by suspending frozen pellets in the wind tunnel, I think a lot more work would have to be done actually to do that. I haven't been able to suspend an ice pellet for more than five or ten seconds. It is something that might be worth trying although I do not plan to try it, at least not this winter. I think I shall continue on the problem of the shedding of water from a melting ice pellet. This can be easily done by the methods outlined in my paper.

Dr. Vincent J. Schaefer—I wonder if this is not being done by Prof. R. Sänger and his group at the Polytechnic Institute at Zurich, Switzerland, because when I was there last year, they had a working vertical wind tunnel in which they were suspending large spheres of clay, much heavier than any of the hailstones we have to worry about. And, at that time, the plan was to install this at an observatory for research on this problem. So my guess is that this is already being done.

Dr. Byers—There is no published material however.

Dr. Schaefer—No.

Contribution No. 812

DISCUSSION OF RAINDROP DISTRIBUTIONS MADE DURING PROJECT SHOWER, HAWAII, 1954

D. C. BLANCHARD

Woods Hole Oceanographic Institution, Woods Hole, Mass.

Abstract—Concurrent with other Project Shower measurements in Hawaii, raindrop size distribution samples were obtained within the clouds with a portable mechanical device. At two-minute intervals these devices, called drop recorders, automatically collected a sample of rain on a section of a water-soluble dye-impregnated paper. The time rate of change of the drop size distribution was obtained from the exposed paper tapes. At the end of a shower the time rate of decrease of drop size has been found to be from 0·07–0·01 mm min^{-1}. It is felt that this fact is in some way a reflection of the basic mechanism of the rain formation, but as yet no explanation has been forthcoming.

Introduction—During the fall months of 1954, Project Shower [SQUIRES, 1955], a cooperative cloud-physics study, was carried out on the Island of Hawaii. This project was an attempt to make simultaneous measurements of the wind field, cloud liquid-water

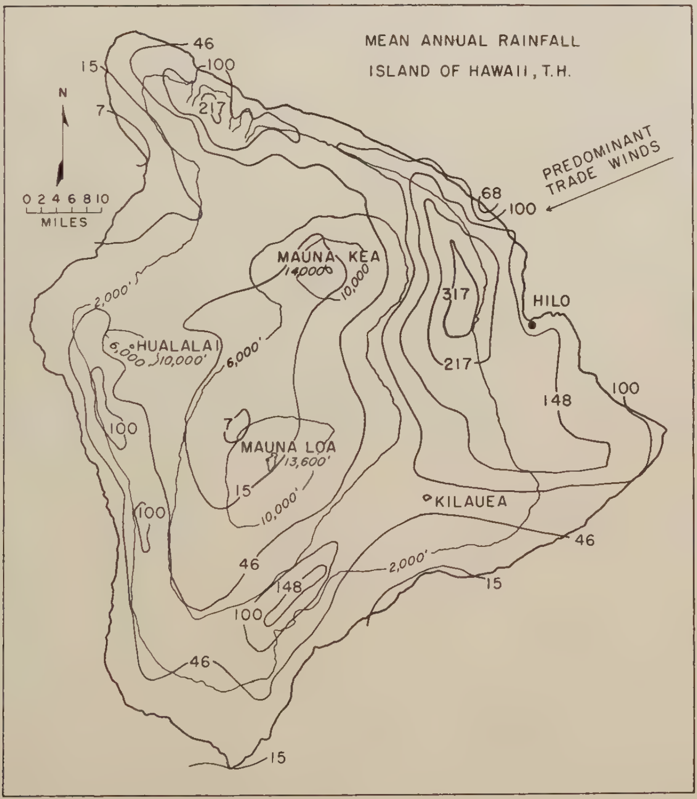
MEAN ANNUAL RAINFALL
ISLAND OF HAWAII, T.H.
N
0 2 4 6 8 10
MILES
PREDOMINANT TRADE WINDS
46
100
15
7
217
68
100
MAUNA KEA
14,000'
10,000'
2,000'
HUALALAI
6,000
10,000'
6,000'
317
HILO
217
148
100
100
7
MAUNA LOA
13,600'
15
10,000'
KILAUEA
100
46
46
2,000'
148
15
100
46
15

FIG. 1—The island of Hawaii, T. H.; the heavy lines represent the mean annual rainfall in inches; the light lines are elevation contours

content and drop size distribution, chemical constitution of the rainwater, salt-nuclei distribution in the free air in and below the cloud layer and the raindrop size distribution. Mr. Woodcock, Mr. Spencer, and the writer, all from the Woods Hole Oceanographic Institution, were concerned with the latter two measurements, the last of which will be discussed in this paper.

These measurements were made on the east slopes of the volcanoes of Mauna Kea and Mauna Loa on the Island of Hawaii, the largest and southernmost of the Hawaiian Island chain. This Island is located entirely within the Pacific northeast trades. These trades are characterized by a temperature inversion with a modal elevation of 6000 ft. Below the inversion the air is moist and turbulent with an average lapse rate of 8·3°C/1000 m. The usual orographic clouds that form on the volcano slopes are affected by this inversion and do not penetrate it to any great extent. Nevertheless a high annual rainfall prevails on the east slopes and is illustrated on the map of Fig. 1. Further information on Hawaiian weather can be found in a paper by LEOPOLD [1949].

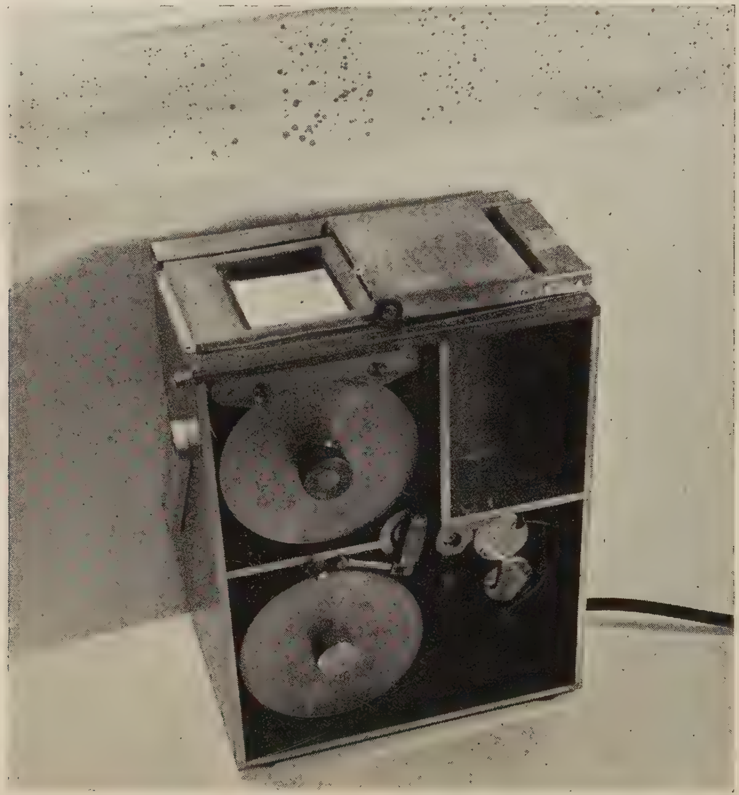

FIG. 2—A drop recorder with the front cover removed and the sliding door open in the exposure position; a sample record is shown at the top

Although some of the drop size distributions were obtained with the filter-paper method, as used in an earlier field trip to Hawaii [BLANCHARD, 1953a], a majority of the measurements were obtained with the aid of portable mechanical devices called drop recorders (see Fig. 2). These drop recorders, powered by a 12-volt automobile battery, had the following sequence of operation. At approximately two-minute intervals a sliding door at the top opened for a 2·7-sec period. The raindrops that fell through the 33 cm^2 opening impinged on a methylene blue dye-treated paper tape. A fine mesh wire screen around the opening prevented splash from the drops that struck in the immediate vicinity. During the 2-minute interval between exposures a resistance-wire heater dried the paper tape and the tape was advanced to a new exposure position. In this manner a drop recorder was run continuously for 15 hours collecting some 450 drop distribution samples.

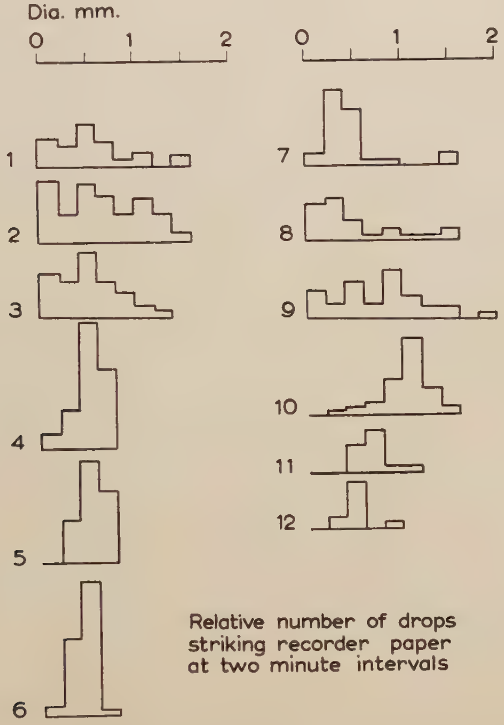

FIG. 3—Twelve consecutive drop recorder samples obtained at the 2000-ft level

Although the area exposed in each sample was only 33 cm^2, the raindrops are sufficiently small and numerous (usually less than two mm diameter and many thousands m^{-3}) such that 60–200 can usually be collected. The laborious work involved in reducing the more than 4000 raindrops samples makes such a task somewhat unfeasible and thus, to date at least, only a few selected samples have been evaluated in respect to the rain intensity R and liquid water W. The results merely confirm the conclusion reached in an earlier paper [BLANCHARD, 1953a] in which relationships between R, W, and the radar reflectivity Z were given.

The three drop recorders were usually run simultaneously at three different elevations on the slopes of the saddle region between the Volcanoes Mauna Kea and Mauna Loa. They were positioned beside the saddle road which runs nearly due west from Hilo. The first recorder was placed at the 2000-ft elevation near the cloud base. The other recorders were placed at higher levels with the last recorder never above the 5500-ft level (about 14 km from the lowest recorder).

Raindrop distributions—The raindrop size distribution has been determined from a number of the drop recorder samples. It has become increasingly evident from examination of these records that any conclusions based on a single drop size sample can be very misleading. The rains are of a showery type and show great variations in drop size and number. Comparison of adjacent samples on the recorder records will often bring out the transient nature of any single sample. This is illustrated by Fig. 3 which shows the relative number of drops, in 0·2 mm size ranges, that were obtained with twelve consecutive drop recorder samples. The transient nature of the rain over a period of 22 minutes is clearly evident. In samples 1–6 a diminishing of the drops above one mm is occurring concurrent with an increase in the drops in the range 0·4–0·6 mm. In sample 7 the appearance of a relatively small number of drops of about 1·5 mm is followed by an increase in the number of larger drops in samples 8–10 and, finally, in samples 11 and 12 a decrease in drop size followed by the end of the rain. In studying the 12 samples as a whole one might conclude that sample 7 illustrates the beginning of the superposition of a second rain shower upon the end of the first shower of samples 1–6. It is probable that the drops smaller than 0·5 mm associated with samples 7 and 8 are the remains of the first shower while the larger drops are the initial drops of the second shower. Had only one or two samples been obtained at the time of samples 7 and 8 an interpretation of the drop distribution would have been difficult to make.

It should be kept in mind that the samples of Fig. 3 have been especially selected to illustrate the changes in drop size that may occur. On other occasions the rain has been steady over a sufficiently long period of time such that adjacent samples showed no significant change. In agreement with earlier work [BLANCHARD, 1953a] samples obtained high up on the mountain slope showed very small drops present in numbers of tens of thousands m^{-3}. It is probable that these small drops are the winnowed remains of the heavier rain that fell further down the mountainside. Table 1 gives, in tabular form, the results of five consecutive samples taken at an altitude of 5500 ft and about 14 km downwind from the 2000-ft elevation, the site where the samples of Fig. 3 were obtained. It is to be noted that these five samples, each obtained two minutes apart, indicates from about 250,000 to 430,000 drops m^{-3} less than 300 microns diameter. The diameters of the spots on the rain recorder tapes were measured with the aid of a low power microscope. Although the methylene blue dye had been thoroughly buffed into the paper, the dye particles often approached 20 microns diameter. This fact, plus the 'grain' of the paper, made it difficult to detect the spots left by drops smaller than 20 microns diameter. It is the writer's opinion that they were present in very low numbers, if at all, and this seems to be borne out by the fact that the 20–40 microns drops were, in general, less plentiful than those in the 40–60-micron size range. The sum total of the drops represents less than 0·5 drop cm^{-3}. With the usual methods of sampling cloud drops, which sample about one cm^3, these drops would be missed entirely.

Although only the five samples of Table 1 have been evaluated to date, there is no reason to believe that these are unique. Visual examination of other sections of the rain recorder record indicated a similar distribution. With filter paper techniques in the same

Table 1. *Drop recorder samples, Hawaii,* 1954

Sample	Date	Time (Hawaiian Standard)	Position	R	W	Number of drops m^{-3} within 20-micron size interval centered about indicated size (microns)				
						30	50	70	90	110
	1954	h m	ft	mm/hr	mg/m^3					
1	Oct. 26	17 07	5500	0·129	99	38,800	77,000	34,000	33,000	27,500
2	Oct. 26	17 09	5500	0·374	197	101,360	120,000	78,000	44,000	26,000
3	Oct. 26	17 11	5500	0·171	118	91,650	95,000	76,000	40,000	26,500
4	Oct. 26	17 13	5500	0·361	177	71,640	60,000	62,000	37,000	22,500
5	Oct. 26	17 15	5500	0·177	118	52,220	56,000	34,000	39,000	30,000

Sample	Number of drops m^{-3} within 20-micron size interval centered about indicated size (microns)										
	130	150	170	190	210	230	250	270	290	310	330
1	25,200	9,400	2550	985	365	...	...	...	...	...	...
2	21,500	16,000	8100	4400	2300	1850	1940	380	195	100	235
3	16,500	8,800	3250	1600	870	880	473	127	...	...	...
4	17,000	13,000	8000	5500	2740	1620	1570	400	320	350	...
5	19,500	11,500	6400	2350	875	145	230	...	...	...	...

region [BLANCHARD, 1953a] drop concentrations approaching 100,000 m^{-3} were often found. Due to limitations of the filter-paper technique in the detection of drops less than 100 microns diameter, it is felt that these earlier measurements gave an underestimate of the actual number of drops.

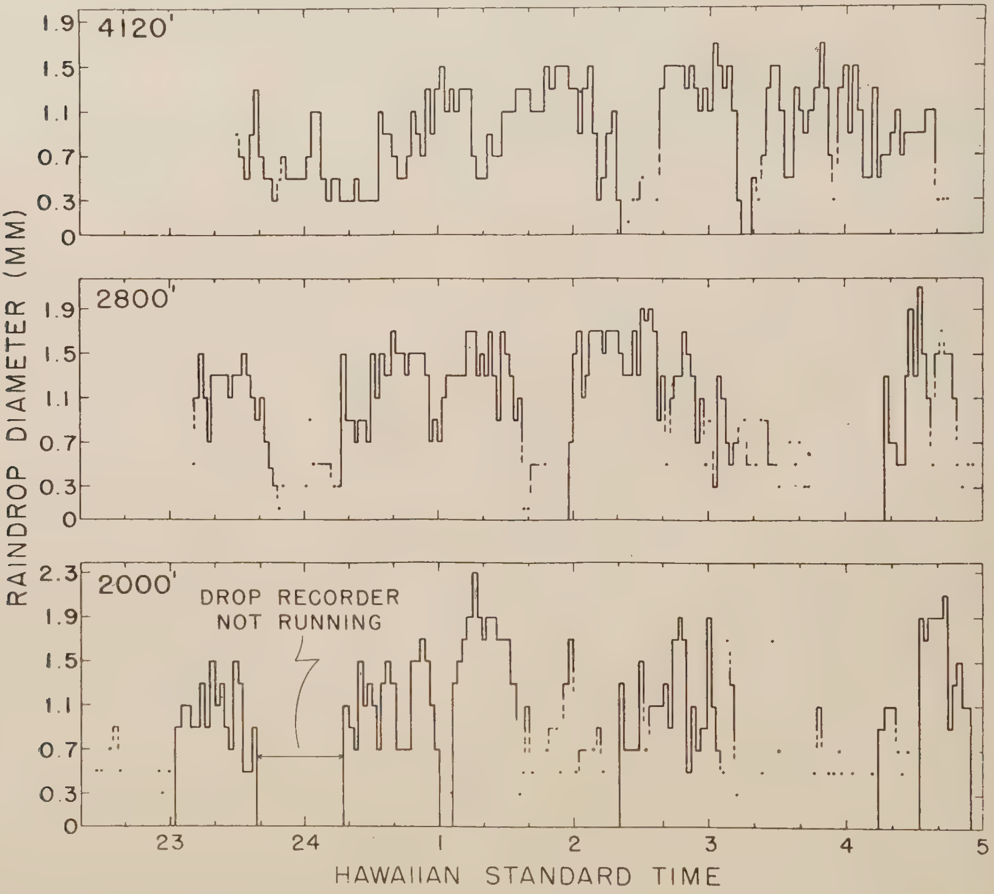

FIG. 4—The maximum drop size versus time for successive rain recorder samples, Dec. 1–2, 1954

Relation of maximum drop size to time—Although a determination of the raindrop distribution for each of the several thousand drop recorder samples has not been made, it was felt that much may be learned of the rain mechanism from the rate of change of the maximum drop size with time. Figures 4 and 5 illustrate this rate of change for an eleven hour period during 1–2 December 1954.

These block diagrams were made by drawing lines through points that were obtained at two minute intervals for the maximum drop size versus time. The points on Figures 4 and 5 through which lines have not been drawn represent samples on which ten or less drops were counted. All three recorders were started prior to 22h 00m but no rain fell until about 22h 28m when a few drops were picked up by the recorder at the 2000-ft level. Note how the rain progressed up the mountain slope as indicated by successively later times of arrival at 2800- and 4120-ft elevations. The downward directed arrows indicate the times that the recorders were stopped.

The three recorders, placed along the volcano road at altitudes of 2000, 2800, and 4120 ft were not in a straight line. If the winds from the Hilo radiosonde can be taken as representative of the winds over the drop recorder area, and this is doubtful, then the rain showers can be considered as coming in from a bearing of N 70° E. Rain showers passing over the 2000-ft station would miss the upper stations by from three to four km, while the rain drifting over the 2800-ft station should pass within a km of the 4120-ft station. Hence one would not necessarily expect to find any correlation between the occurrence of rain showers at the lower two stations but might find it between the upper two. There is a suggestion on Fig. 4 that the showers at the 2800-ft station that began at about 00h 17m, 01h 00m and 02h 00m also passed over the 4120-ft station. If these are

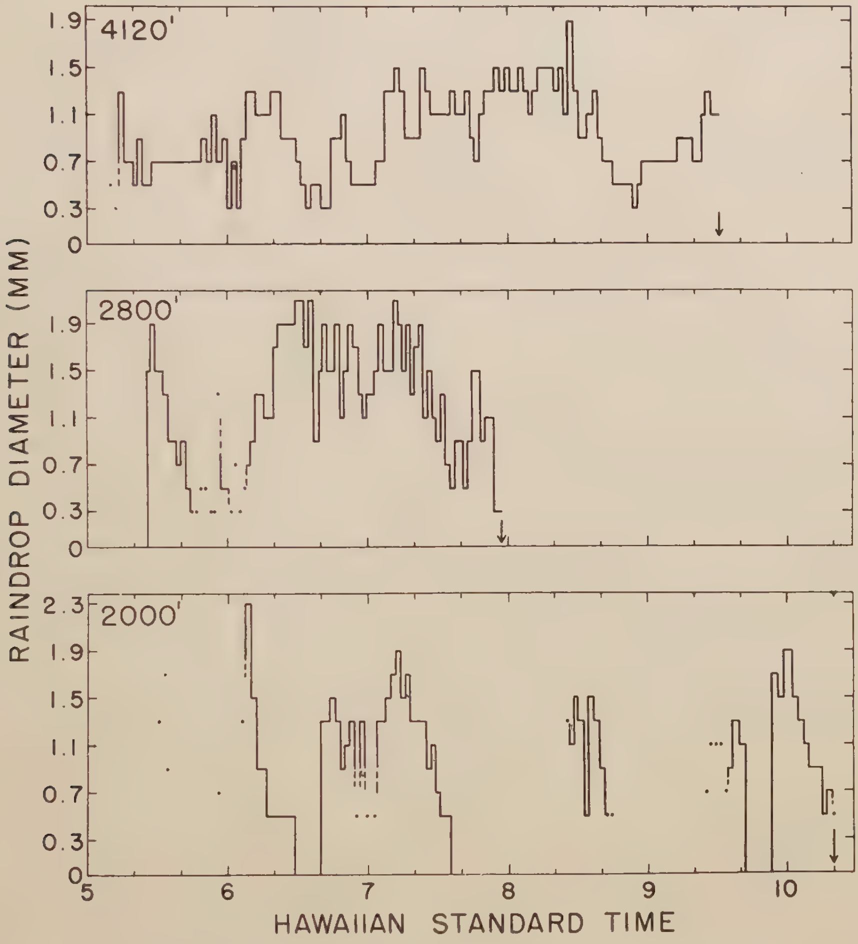

Fig. 5—A continuation of Fig. 5, Dec. 2, 1954

in fact the same showers, a decrease of maximum drop size of about 0·2 mm diameter occurred between stations. With the distance between the stations of 6·5 km and the time of passage of the showers, as obtained from Fig. 4, one computes transit speeds for the three showers mentioned above as 13, 10·5, and 5·2 knots, respectively. The Hilo radiosonde winds between 2000 and 10,000 ft at 23h 00m on December 1 and 05h 00m on December 2 were from seven to 21 knots.

One of the useful facts to come out of the drop recorder study is that the rain is far from a steady, uniform nature. A glance at Figures 4 and 5 shows that showers of one-half to one hour's duration closely follow one another and appear to be superimposed on a background of light, nearly continuous rain. Some of the fluctuations in the rain are extremely light and probably would not be picked up by a standard recording rain gauge [BLANCHARD, 1953b].

A characteristic common to many of the showers, and one that may be useful in the study of the mechanism of raindrop formation, is the rate of decrease of maximum drop size at the end of the shower. Examples of this may be found on Figures 4 and 5 at the 2000-ft station at 07h 20m and 10h 00m and at the 2800-ft station at 23h 40m and 05h 40m. The maximum drop size undergoes a steady decrease at a rate of 0·07—0·1 mm min^{-1} for a period of about 20 minutes. Two explanations for this have already been considered, and neither of them is, in all respects, satisfactory. When all of the data from the other investigators on Project Shower are available, including information on cloud tops and structure, an explanation may be forthcoming.

The simplest model that was considered was that of a stationary steady-state rain source producing a complete spectrum of raindrops at a height h above the observing station. At time t_0 the rain source stops, leaving only the rain in a column of height h to provide the end of the shower. The largest drops D_1, will continue to be observed at the ground for a time t_1, measured from t_0, which is merely h/V_1 where V_1 is the terminal velocity of the drops D_1. From time t_1 onward a steady decrease of maximum drop size will be observed. Drops of diameter D_2 $(D_2 < D_1)$ will be the largest observed at a time $t_2 = h/V_2$. In this manner the rate of decrease of maximum drop size can be obtained. In Fig. 6 the results of calculations with $h = 1000$, 2000 and 4000 m are shown with the observed rates of decrease of drop size as found on the drop recorders. Only the calculation for $h = 4000$ m can compare with the observations and this cannot be accepted, as the rain source region does not extend 4000 m above the drop recorder stations and probably seldom reaches 2000 m.

A second model, a bit more involved than the first but perhaps more realistic, assumes that a wind exists that increases linearly with altitude. It can be shown that the rain, in falling from a steady-state source moving with the wind, will fall in parabolic trajectories with the smaller drops striking the ground at great distances from the cloud. The side view (neglect the top view and assume one-dimensional shear for the present) of the schematic sketch of Fig. 7 shows trajectories, with respect to the moving cloud, of the large and small drops. It is evident that any drop recorder placed in the path of such a rain system will record the end of the shower as a steady decrease in the maximum drop size. Calculations made with this model, assuming a rain source height of 1500 m and a wind of 10 m sec^{-1} at 1500 m uniformly decreasing to 2 m sec^{-1} at the ground, gave the result shown in the lowest curve on Fig. 6. It is apparent that this second model gives results that are even more widely at variance with the observations.

It thus appears that the above two models cannot account for the observed rate of decrease of maximum drop size. It is hardly worthwhile to consider more complicated models in the absence of the other observations that were made on these rain systems. When all the data has been tabulated it is hoped that the present picture will become clearer.

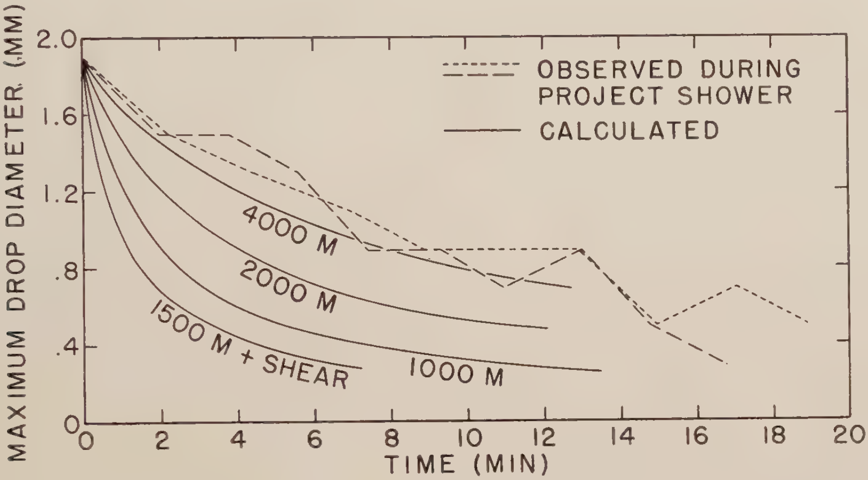

FIG. 6—The decrease of the maximum raindrop diameter with time

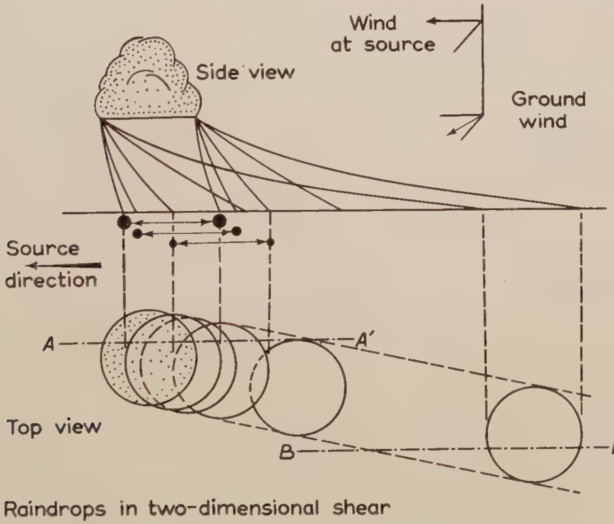
Wind at source
Side view
Ground wind
Source direction
A
A′
Top view
B
B′
Raindrops in two-dimensional shear

FIG. 7—The trajectories of raindrops subjected to wind shear

Two-dimensional shear—It is possible that the wind not only varies in speed with height but with direction as well. When this occurs the various drops in the spectrum will not only be spread out in the direction of motion of the source but also at right angles to it. The smallest drops, subjected to the wind shear for the longest period of time, would be deflected to the greatest degree. The schematic drawing of Fig. 7 illustrates how the drop size distribution on the ground is spread out at an angle to the direction of motion of the source. This angle will depend on the nature of the wind shear. A complete discussion of the effects of wind shear on rain has been given by GUNN and MARSHALL [1955].

It is evident that any observer on the ground in the path of an oncoming shower will receive only a certain range of the total raindrop distribution, this range varying with the orientation of the observer and the wind shear. For example, an observer at A in Fig. 7 would see the shower pass over him along the line AA' and an observer at B along the line BB'. The first observer would observe large drops only and the second observer only small drops. At intermediate points one may find only the middle of the raindrop spectrum with the largest and smallest drops missing entirely.

Although nothing can be said at the present as to whether any significant two dimensional shear existed in the region where Project Shower was carried out, some of the drop recorder samples suggest that this may have occurred. When the wind data are available the samples will be analyzed with this in mind.

Acknowledgments—I should like to thank sincerely my colleague, A. T. Spencer, who not only designed and built the drop recorders but assisted in obtaining the observations in Hawaii. This study was supported by the Office of Naval Research, Contract Nonr 798(00) (NR–082–124). Contribution No. 812 from the Woods Hole Oceanographic Institution.

REFERENCES

BLANCHARD, D. C., Raindrop size distribution in Hawaiian rains, *J. Met.*, v.10, pp.457–473, 1953a.

BLANCHARD, D. C., A simple recording technique for determining raindrop size and time of occurrence of rain showers, *Trans. Amer. Geophys. Union*, v.34, pp.534–538, 1953b.

GUNN, K. L. S. and J. S. MARSHALL, The effect of wind shear on falling precipitation, *J. Met.*, v.12, pp.339–349, 1955.

LEOPOLD, L., The interaction of trade wind and sea breeze, Hawaii, *J. Met.*, v.6, pp.312–320, 1949.

SQUIRES, P., Project Shower. An investigation on warm rain in the Hawaiian islands, *Nature*, v.175, pp.748–750, 1955.

DISCUSSION

Dr. Horace R. Byers—I think that in considering the effect of wind shear on drop size distribution in the shower, you must take into account the possibility of the existence of an outflow or first-gust type of flow, such as occurs in a well-developed thunderstorm and often in other types of showers. In this case the shear would be negative, with strongest winds at about two or three hundred feet and a sharp dropping off around two thousand or so.

Dr. David Atlas—As I remember a description of some of your work, trade-wind cumulus clouds move inland and seem to create pulsations on the orographic cloud. The pulsations in rain intensity that occur are in general attributed to this effect. The interaction between the cumulus impulse and the orographic cloud would vary with distance inland and that perhaps is why you always get your broadest distributions toward the shore.

Mr. Duncan C. Blanchard—These high-level distributions we find fit in rather well with the idea that they are nothing more than the remains of showers which have fallen further down. In the distributions at low levels, we find few small drops; at high levels we find the missing drops.

Dr. Helmut Weickmann—I would like to suggest the possibility of these differences in drop size occurring simply because the water gets swept from the cloud.

I will describe a model which I have considered. Underneath the melting level, there is a cloud, maybe several thousand feet thick, with one gram per cubic meter water content. We have a snow crystal falling from above, which seeds the cloud. If you want to have steady precipitation you need a continuous updraft in order to supply the water. If you don't have an updraft and you just let the particles fall through and sweep it out, then in the beginning you have large particles, but as the time goes on, in ten or twenty minutes, the size decreases. Simultaneously the water content of the lower layers decreases more rapidly than the water content of the upper layers.

One way to check up on this would be to observe the cloud base. If the cloud base lifts it would indicate that such a process takes place. But, it doesn't necessarily have to lift, because the water content may be appreciably reduced without visible lifting of the cloud base.

Dr. Roscoe R. Braham, Jr.—If the precipitation is of such nature that it is showery, having periodical bursts of rainfall to the ground, that is characteristic of what we get from cumulus clouds, and we usually ascribe it to a non-steady state condition with vertical motions but presumably the cloud under discussion is an orographic cloud, the trade wind being rather steady in its character; this means that the nature of the precipitation itself, not the motion, must have to provide some non-continuing or periodic showery aspect of the precipitation.

Mr. Alfred H. Woodcock—Although the usual picture of an orographic cloud is one which is exclusively over the mountain, actually the trade winds are continually flowing inland and, in many areas, individual cumulus clouds can be seen drifting in on the trades from the open sea and merging with the orographic cloud. Therefore, built into the orographic cloud are parcels with quite different cloud histories. This is a possible explanation of the irregular nature of the rain.

Dr. Braham—This then is an interesting example of nature's way of seeding with water drops. There must be rather large drops in the cumulus cloud to start with.

Contribution No. 820

3

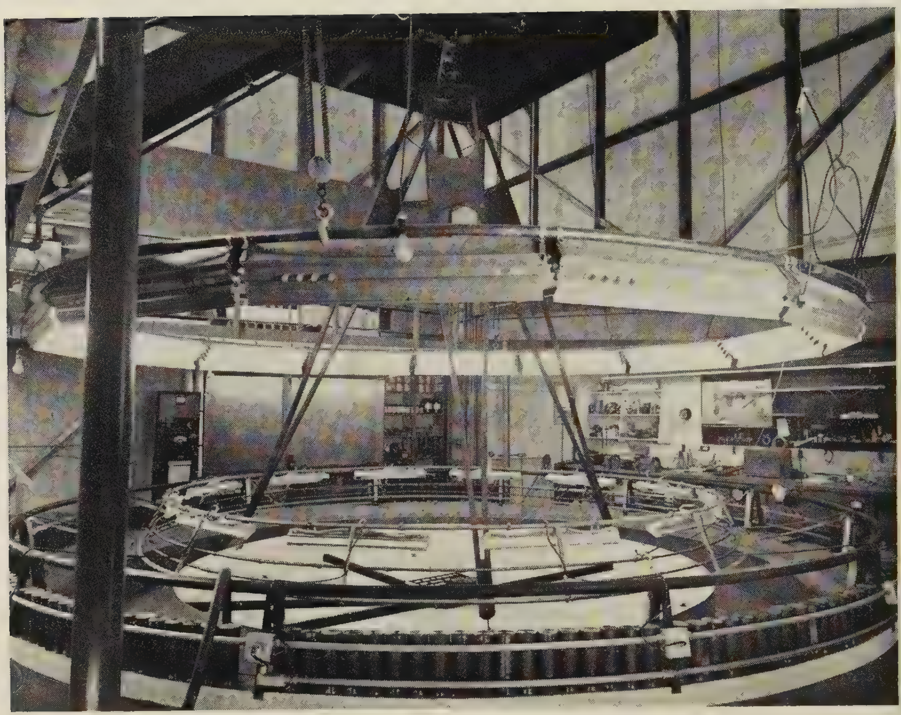

The 4-metre rotating tank apparatus recently constructed at Woods Hole for study of the primary ocean circulations.

The central white area is the 4-metre (13·12-ft) working surface. This is surrounded by a dry annulus 1·5 ft wide which provides buoyancy and stability as the rotor floats in the water-filled concrete stator tank some 2 ft deep by 20 ft in diameter. The cylinders in the foreground are 10-kg (22·2-lb) weights which are placed in the dry annulus to increase the draft of the rotor and permit a suitable volume of water to flood the working surface. Since the weight of water on the working area is equal to the total dead weight added to the dry annulus of the rotor the volume of water on the working surface is known for each experiment. The working surface drains dry when these weights are removed. A ring of fluorescent lights provides shadowless illumination without appreciable heat so that the progress of experiments can be recorded continuously by cameras mounted on top of the tripod which straddles the working surface. Infra-red heaters are mounted over the perimeter of the working surface on a circular frame which also carries the compressed air manifolds and auxiliary blowers for reproducing the planetary wind fields.

Reprinted from "Progress in Physics and Chemistry of the Earth" Vol. 2
(1957) Pergamon Press; London, New York, Paris

1

AN EXPERIMENTAL APPROACH TO PROBLEMS IN PHYSICAL OCEANOGRAPHY*

By William S. von Arx

INTRODUCTION

Study of marine circulations with the aid of laboratory models is a relatively new part of physical oceanography that has come into use with the growth of interest in synoptic problems. This interest has arisen partly through the development of rapid measuring devices for use on moving ships and aircraft, and partly through the success of some mathematical theories. The observed motion of the sea is so complicated and the mathematical descriptions so bare of details that firm connections between the two are hard to find. In some ways experimental laboratory models seem capable of providing a useful middle ground. Two quite different experimental approaches are possible: one favours mathematical conceptions and deals with the behaviour of fluids under the influence of isolated forces, and the other (with which this article is concerned) favours observational syntheses and deals with fundamental forces combined so as to produce simplified analogues of nature. The study of analogues has an element of subjectivity, for with each important change of scale there is a different set of fundamental forces at work. Three size categories are discussed, but with emphasis on the planetary scale.

These three categories can be distinguished by the predominant manner in which the pressure gradient forces, common to all, are opposed, namely: (1) by friction, (2) by a combination of friction and inertial effects due to the earth's rotation—Coriolis force, and (3) by the Coriolis force alone. In a broad way the first applies to small-scale flow in rivers, narrow estuaries and some lakes; the second to marginal and mediterranean seas and some large lakes; and the third to oceans and ocean systems. The three cases can be characterized more or less as shown in Table 1.

The small-scale circulations in shallow water near land are influenced mainly by the forces due to tides, local wind stress, river flow, stratification, and bottom and internal friction. In most instances flow is accelerated down the resultant of one or more temporary or fluctuating pressure gradients and is retarded by nearly opposed frictional forces. The characteristic complexity of inshore flow patterns arises from the manner in which these pressure patterns are combined, and the inertial lag in the response of the water motion to them. Such areas are ordinarily studied by means of Froude models if the flow is predominantly influenced by gravitational forces, Reynolds models if internal friction predominates, and much less often in models based on a combination of the two. Oceanographic modelling procedures appropriate to this scale are based on hydraulic engineering conventions but are extended to include the effects of wind stress and permanent currents as required. These matters are discussed in the first section of this article.

---

* Contribution No. 820 of the Woods Hole Oceanographic Institution.

Table 1

Local circulations	Regional circulations	Planetary circulations
Lakes, bays, rivers, atolls and narrow estuaries	Large lakes, bays, marginal and mediterranean seas	Oceans and ocean systems
Pressure gradient force opposed by friction	Pressure gradient force opposed by friction and Coriolis force	Pressure gradient force opposed by Coriolis force
Pressure gradients due to: river flow, runoff, evaporation, seepage, local wind, tides, salt water intrusion	Pressure gradients due to: synoptic winds, synoptic pressure gradients (air), balance of runoff, evaporation, precipitation and tides	Pressure gradients due to: planetary winds, climatic distribution of seasonal winds, insolation, evaporation and precipitation
Motion directly across isobars predominates. Seiching is rectilinear	Motion has a cross-isobar component. Seiching tends to follow inertia circles	Motion predominantly geostrophic. Inertia circles negligibly small
System approximated on a flat stationary reference frame using ordinary Froude (and Reynolds) models	System approximated on a flat rotating reference frame using rotating Froude (and Reynolds) models	System approximated on a curved rotating reference frame using vorticity models

The intermediate scale relates to the marginal and smaller mediterranean seas of the earth in which the forces due to tides, local wind stress, river flow, stratification, and bottom friction are all significant, but where in addition the effects of earth rotation become apparent. To the writer's knowledge, no experimental studies of areas in this intermediate size category have been made with rotation.* It seems probable that the effects of earth rotation can be added to otherwise straightforward Froude modelling procedures by the means indicated in the middle section of this article.

Finally there is the oceanic model of planetary scale in which the character of the circulation is practically independent of the influence of waves, tides, and river flow, but is driven primarily by the stress of the planetary wind field and influenced by both the rotation and curvature of the earth. The effects of heating, evaporation, and precipitation on stratification may also be important. The flow in planetary models is predominantly geostrophic, but in detail both inertial and frictional effects are present which may serve in a model to represent nature more faithfully than would be the case otherwise. The scaling procedures applicable to planetary models relate the rotation of the earth and the meridional variation of the Coriolis parameter to laboratory conditions. The effects of earth rotation can be produced directly but those due to earth curvature cannot, because of our present inability to provide or simulate a radial gravitational field in the laboratory. This technical limitation makes it impossible to produce geometrically similar planetary models (which can be achieved only when it becomes possible to model the earth on a spherical working surface), hence the variation of the Coriolis parameter with latitude must be reproduced by other physical means which are described in the latter section of this article.

---

* (Footnote added in proof.) Preparations for such work are being made at the Laboratoire National d'Hydraulique in Chatou, France, and at l'Universite de Grenoble employing turntables of 3- and 15-metres diameter respectively. Experiments are already in progress at Chatou which concern the effects of rotation on the flow in the English Channel, and at the Hydrodynamics Laboratory of the University of Chicago on generalized channel flow with rotation.

Similarity and Characteristic Numbers

The problem in modelling is to construct a system which is like its prototype in all physically significant respects. In the fluid mechanics of the earth's hydrosphere the vector equation of motion contains the following terms:

$$\frac{\mathrm{d}\boldsymbol{C}}{\mathrm{d}t} + 2\boldsymbol{\Omega} \times \boldsymbol{C} = -\frac{1}{\rho}\nabla p + \boldsymbol{g} + \boldsymbol{F}$$

where $\boldsymbol{C}$ is the vector velocity, t the time, $\boldsymbol{\Omega}$ the angular velocity vector of the earth's rotation, ρ the fluid density, ∇p the gradient of pressure, $\boldsymbol{g}$ the acceleration vector due to gravity, and $\boldsymbol{F}$ the friction vector. The terms may be identified in the following verbal statement: that the

$$\begin{array}{c}\text{inertial}\\ \text{term}\end{array} + \begin{array}{c}\text{Coriolis}\\ \text{term}\end{array} = -\begin{array}{c}\text{pressure}\\ \text{gradient}\\ \text{term}\end{array} + \begin{array}{c}\text{gravitational}\\ \text{term}\end{array} + \begin{array}{c}\text{frictional}\\ \text{term}\end{array}$$

Ratios of these terms (shown in simplified parametric form) have been used to define several dimensionless numbers

$$\text{Euler Number} \equiv \frac{\text{inertial force}}{\text{pressure gradient force}} \equiv \frac{\rho V^2}{\nabla p}$$

$$\text{Froude Number} \equiv \frac{\text{inertial force}}{\text{gravitational force}} \equiv \frac{V^2}{Lg}$$

$$\text{Rossby Number} \equiv \frac{\text{inertial force}}{\text{Coriolis force}} \equiv \frac{V}{fL}$$

$$\text{Reynolds Number} \equiv \frac{\text{inertial force}}{\text{frictional force}} \equiv \frac{VL}{\mu/\rho}$$

$$\text{Ekman Number} \equiv \frac{\text{Coriolis force}}{\text{frictional force}} \equiv L\sqrt{\frac{f}{2\mu/\rho}}$$

where L is a characteristic length, V is a characteristic velocity, ρ is the fluid density, g is gravity, f is the Coriolis parameter, p is pressure, and μ is the dynamic viscosity. These ratios are characteristic of flow conditions in which the forces defined are predominant. The modelling problem may be analysed by means of these ratios, and laboratory conditions arranged so that the numerical value of each significant ratio is the same in the model as it is in the full-scale prototype. A model based primarily on one or another of these dimensionless numbers is usually referred to by name; e.g. Froude model, Reynolds model, or other according to the case.

This list of dimensionless numbers is incomplete, being sufficient only for the present stage of oceanographic experimentation. Nothing has been said concerning, for example, the effects of heat exchange, buoyancy, or short period effects involving fluid compressibility, all of which exist in the oceans. These and other phenomena must be reckoned with as time goes on.

In practice one may construct a ratio which is by convention

$$J_r = \frac{J_m}{J_p}$$

where J_m is the value of a physical property of the model, J_p is the value of the corresponding property in the prototype, and J_r is their ratio. If J is one of the dimensionless numbers, J_r should be unity, but the ratios of the individual parameters defining a dimensionless number may have other values. These are the scaling ratios which permit the model to be smaller or larger than its prototype, and for time to pass correspondingly faster or slower and still behave in the same physical manner.

In the case of the Froude model, for example, we may write in general

$$(Fr)_r = \frac{(Fr)_m}{(Fr)_p} = \frac{(V^2/Lg)_m}{(V^2/Lg)_p} = 1,$$

and for each physical parameter

$$V_r^2 = \frac{V_m^2}{V_p^2}; \quad L_r = \frac{L_m}{L_p}; \quad g_r = \frac{g_m}{g_p}.$$

Since the model will be operated under the same gravitational field as its prototype, $g_r = 1$. This leaves L, and the velocity of the gravity wave $V = \sqrt{gz}$, as adjustable parameters. Again g is the same in both model and prototype so that z the vertical length and L the horizontal length determine V the wave velocity which is itself L/T where T is time. Thus

$$V_r = \frac{L_r}{T_r} = \sqrt{z_r}.$$

The Froude model may be geometrically similar to its prototype, in which case $z_r = L_r$, or distorted such that $z_r > L_r$. In this manner the scaling ratios for this and other physical properties of the distorted and undistorted open-channel Froude model have been derived. Table 2 gives a partial list of scale ratios in terms of length. Others may be derived quite simply.

*Table 2**

Property	Undistorted Froude model	Distorted Froude model
Length, horizontal	L_r	L_r
Length, vertical	L_r	z_r
Time	$(L_r)^{\frac{1}{2}}$	$L_r(z_r)^{-\frac{1}{2}}$
Velocity	$(L_r)^{\frac{1}{2}}$	$(z_r)^{\frac{1}{2}}$
Total discharge	$(L_r)^{\frac{5}{2}}$	$L_r(z_r)^{\frac{3}{2}}$

* Assuming that the model and prototype are operating under the same gravitational acceleration, and that the fluid filling both is identical.

The problems of dimensional analysis and model laws have been studied since the rise of classical physics. Recent discussions of the subject by Bridgeman (1931), the heat transfer problem by Fishenden and Saunders (1950), and the relations of logic and fact by Birkhoff (1950), state the modern viewpoint. The modelling problem in relation to engineering fluid mechanics is discussed academically by Rouse (1938, 1946) and with laboratory practice foremost in mind by Stevens *et al.* (1942) and Allen (1947).

ON MODELS OF SMALL INSHORE AREAS

The small-scale oceanographic model such as that in Fig. 1 may be defined as one in which gravity and friction are dominant forces, and the direction of flow is primarily down the gradient of pressure. This is the case in most bays, rivers, and narrow estuaries. The treatment of these small-scale oceanographic problems follows engineering precedent closely except for the introduction of forces due to the local wind stress and external flow fields which have been applied most successfully to models based on the Froude law and which involve a single layer of liquid.

In general the oceans are about a thousand times broader than they are deep, and estuaries perhaps an order of magnitude less so. In order to reduce the effects of surface tension in relation to inertial forces it is often necessary to exaggerate the vertical dimensions of the model estuary in nearly this proportion. Table 2 contains some of the dimensionless ratios that must be maintained for the undistorted and distorted open-channel Froude models.

Length and Time Scales

The choice of a horizontal scale for a Froude model depends primarily on fitting the geographic area into the dimensions of the laboratory. In the absence of density contrasts in oceanographic models, L_r may range from 1/5000 to as little as 1/200,000. To cite characteristic examples; the salinity distribution and current system of Puget Sound have been studied in a model with a horizontal scale 1/40,000 (Rattray and Lincoln, 1955) while Bikini and Rongelap Atolls were represented for other purposes on horizontal scales of 1/100,000 and 1/150,000 respectively (von Arx, 1954).

The vertical scale must generally be chosen so that the least depth of water in which the flow is to be studied is approximately 1 cm to prevent capillary effects from being important. Because of the complexity of some water-land boundaries it is usually imprudent to attempt to build a model of an estuary on a horizontal scale smaller than $L_r = 1/20,000$. In general the vertical exaggeration may be larger than that usually regarded as acceptable for engineering purposes.

In simplest terms the Froude law concerns the rate of motion of a long gravity wave in shoal water. The celerity of such a wave is $\sqrt{gz}$ where g is the acceleration of gravity and z is the depth of water. The acceleration of gravity is the same in both the model and the prototype, hence the velocity ratio V_r is entirely controlled by the square root of the vertical scale, $\sqrt{z_r}$, thus

$$V_r = \sqrt{z_r} = \frac{L_r}{T_r}.$$

One can see from this that the time scale shortens with increasing depth and lengthens with the increase of horizontal scale of the model. One is led to a choice of scales by a path which touches first the minimum depth requirement and then an adjustment of the length L_r and time T_r scales such that either

$$\frac{L_r}{T_r} = \text{const} = \sqrt{z_r}$$

or

$$\frac{L_r}{\sqrt{z_r}} = \text{const} = T_r$$

where L_r is adjusted to the dimensions of the laboratory. The time ratio is usually the most flexible parameter available.

Density Scale

The circulation in estuaries may involve the interaction of two or more water masses of different density. When water is used in the Froude model these density differences should be maintained one to one, that is, $\rho_r = 1$ and $\Delta\rho_r = 1$. This leads to satisfactory results when the problem being studied involves only the kinematics of flow. For example, in the intrusion of a large mass of salt water flowing in from the sea under fresh water in an estuary, the velocities, volumes, and times of arrival of the main water masses may be correctly represented by following the Froude law, but the mixing and mutual dilution of the two water masses will be usually quite dissimilar and unrealistic, particularly if the model is distorted vertically. In such situations one must either satisfy Reynolds and Froude criteria simultaneously or depart from strict scaling procedures.

It is possible through a choice of fluids other than water and suitable linear dimensions to satisfy the requirements of both the Froude and Reynolds laws simultaneously. As fortunate as this possibility seems, it is rarely utilized because few fluids have the necessary properties when the model is small compared with its prototype. Specifically: the Froude law requires that the time ratio $T_r = L_r^{\frac{1}{2}}(\rho/\gamma)_r^{\frac{1}{2}}$, while the Reynolds law requires that $T_r = (L^2\rho/\mu)_r$ where L is the length scale, ρ the fluid density, γ the specific weight, μ the dynamic viscosity. Equating these two requirements leads to the following relationship

$$T_r = L_r^{\frac{1}{2}}\left(\frac{\rho}{\gamma}\right)_r^{\frac{1}{2}} = \left(\frac{L^2\rho}{\mu}\right)_r.$$

If the model and prototype operate under the same gravitational acceleration the ratio $(\gamma/\rho)_r = g_r = 1$; and a length scale satisfying both criteria at the same time scale will be

$$L_r = \left(\frac{\mu}{\rho}\right)_r^{\frac{2}{3}} = (\nu_r)^{\frac{2}{3}}.$$

Unless L_r is nearly 1 or chosen such that a real fluid other than water satisfies the above criterion of similarity, it is difficult to meet its requirements.

As a less satisfactory alternative one may reduce the density contrast between the fresh and salt layers and thus reduce the gravitational forces tending to cause the two layers to stratify. This permits the vertical component of the existing level of turbulence to cause the layers to mix more realistically. As a guide to the reduction of vertical density contrast one may equalize the force per unit area acting in the horizontal and vertical directions on the vertically distorted unit volume

$$\Delta\rho_m = \Delta\rho_p\left(\frac{L_r^3}{L_r^2 z_r}\right) = \Delta\rho_p\left(\frac{L_r}{z_r}\right)$$

which amounts to a reduction of density contrast by the reciprocal of the vertical exaggeration. For practical reasons this cannot be carried to extremes. In oceanographic models a vertical exaggeration of 100 is often necessary; hence the normal difference in density between ocean and river water, 0·025 g/cm^3, would thereby be reduced to 0·00025 g/cm^3, which is beyond experimental control. Differences in density amounting to 0·001 g/cm^3 can be maintained experimentally, and if it is sufficient to represent approximately the mixing of a salt wedge intrusion and its rate of motion it is possible to choose a horizontal length scale, and/or a suitably adjusted vertical exaggeration z_r/L_r, such that the corresponding difference in density in the fluids is greater than 0·001 g/cm^3.

Verification

Because the natural situation is not ever a pure case to which any special modelling law chosen applies exactly, and because of "scale effects" (emergent properties of unavoidably different combinations of forces than those in nature), a model cannot be relied on to represent nature faithfully at first. A new model must be compared with field data from its prototype. These field observations must be of fundamentally consistent and recurrent phenomena so that the model will not be forced to produce an atypical flow pattern under the influence of the normally predominant forces. To begin with, observations may be made repeatedly at a number of points believed to be representative of the general character of the fluid motions. The model is verified against these as a first approximation. Following this the truly critical points usually reveal themselves in the model, and with further field observations at these new points verification can proceed. When this cycle of comparisons has been carried forward to a practical conclusion, it is assumed that the behaviour of the model at all intermediate points is also essentially correct. Verification in its simplest form consists of roughening and smoothing the courses of flow. In a distorted open-channel model it is usually difficult to make the bottom rough enough, and in the undistorted model it is equally difficult to make the bottom smooth enough. The optimum distortion can be determined from the Manning formula, which is discussed in some detail by ROUSE (1938, 1946) and applied to specific problems by STEVENS (1942).

In oceanographic models the minimum depth restriction (1 cm) may preclude application of the Manning formula. Vertical exaggeration must then be increased, in which case the bottom roughness usually becomes too slight. Roughness elements may be placed in a suitable pattern on the bottom, or if the horizontal scale is very small and connecting channels narrow it may be more convenient to interpose wire screens of suitable meshes in the channels to retard the flow.

Wind Stress

The effects of wind stress on the circulation in estuaries and bays are often important and sometimes predominant. To scale the wind-driven circulation in a model requires knowledge of the dynamics of momentum transfer across the air-sea interface, which in the present state of affairs is simply not available. The transfer of momentum from the wind to the ocean must involve consideration of the wind stress coefficient which is usually part of an equation of the form

$$\tau = \tfrac{1}{2}\rho C_d V^n$$

where τ is the wind stress, ρ the density of air, C_d the wind stress coefficient, V the wind velocity at some arbitrary level, and n the exponent to which this wind speed is raised. According to most authors n has the value 2 above the "critical" wind speed, other values below, and indeed C_d is also a function of V. Because of the lack of firm knowledge of these processes, empirical procedures must suffice and be used only where the utmost precision is not required.*

These procedures involve the calibration of a set of blowers arranged to move air across the model at rates which will produce circulations in the surface layer of the model which are to scale and in accordance with field observations under given wind conditions. It is desirable that the field data represent conditions where one can be reasonably sure that wind is the only important influence. When this requirement cannot be met one may assume that, where the fetch is greater than an equivalent of 5 to 10 thousand metres and a steady state exists, a layer of surface water will be moved downwind at a speed between 2 and 3 per cent of the steady wind speed measured at some level between 3 and 10 metres above the water surface. In practice the actual speed of the wind on the model is disregarded, and only the velocity of the wind-driven motion of the surface layer is scaled. This is, to be sure, a very crude approach, but it results in a closer approximation to the natural situation than the practice often seriously followed of ignoring the effects of wind. The calibration of blowers supplying the wind-drift effects should be referred to a clean water surface having some standard surface tension.

Wind waves on an oceanographic model are generally slight, and those present are usually dominated by capillary rather than gravitational forces. Capillary, in contrast with gravity waves move faster as their lengths diminish. To be in scale a modelled wave would have a height z_r and a length L_r in a distorted open-channel model. Such dimensions soon become physically impossible as the vertical exaggeration is increased. In cases where the roughness of the sea surface has been accounted for through direct scaling of the wind-drift current it is unnecessary to be concerned with waves. But if waves contribute to mixing a small model with vertical distortion cannot be used.

Tides

An estuary is by definition under the influence of the tides. The reproduction of tides in oceanographic models of estuaries may be simplified if taken from broader considerations than those relating to the tidal waves in the estuary itself. When the tide generator is located offshore and arranged to act along a cotidal line in a modelled portion of the ocean, the tidal wave will advance into shoal water with the proper phase differences and heights determined by the

---

* (*Footnote added in proof.*) This problem has been examined very recently at Woods Hole. There are serious experimental difficulties still to be overcome, but results thus far indicate that when air is moving over a smooth water surface at rates between 30 and 100 cm/sec., measured at an "anemometer height" of 1 cm, the skin friction coefficient C_d is approximately 0·0014. This is in general agreement with the value 0·002 cited by JEFFREYS (1925: *Proc. Roy. Soc. Lond.* **A107**; 189–205) for somewhat higher wind speeds. The value of n remains to be determined but has been assumed to be 2.

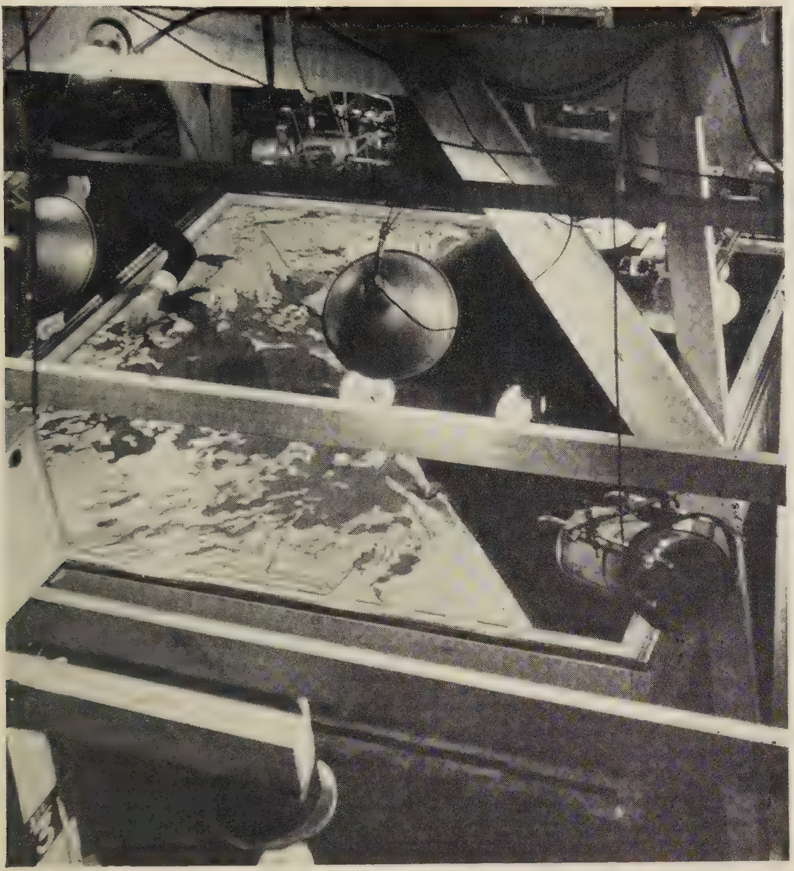

Fig. 1 (a). A representative oceanographic (Froude) model built and operated at the Woods Hole Oceanographic Institution to study the circulation of waters in and around Barataria Bay, Louisiana, under varying conditions of wind, tide, and river discharge. This study was sponsored by the Freeport Sulphur Company.

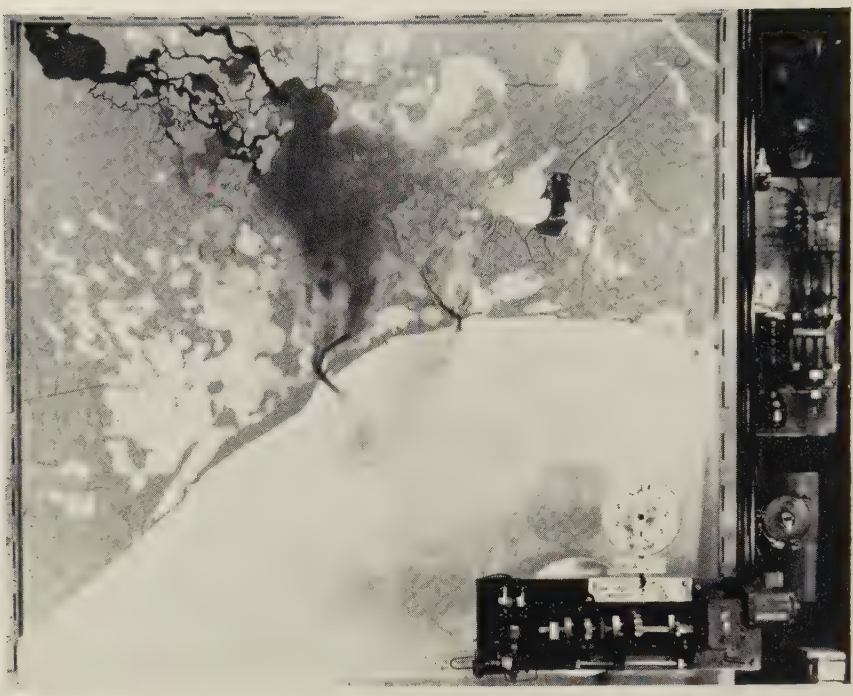

Fig. 1 (b). In the modelled area, roughly 25 miles square, the characteristic depth of water is about 3 feet. This necessitated either a very large model or a highly distorted smaller one. The surface shown is eight feet square and the topography is carved in plaster on a horizontal scale 1/20,000 and vertical scale 1/192; that is, the vertical exaggeration is 104. The time to the scale 1/1440 is indicated by the clock at the lower right attached to the tide machine. The darkened area is river flow from principal discharge sources in the upper left-hand corner of the area.

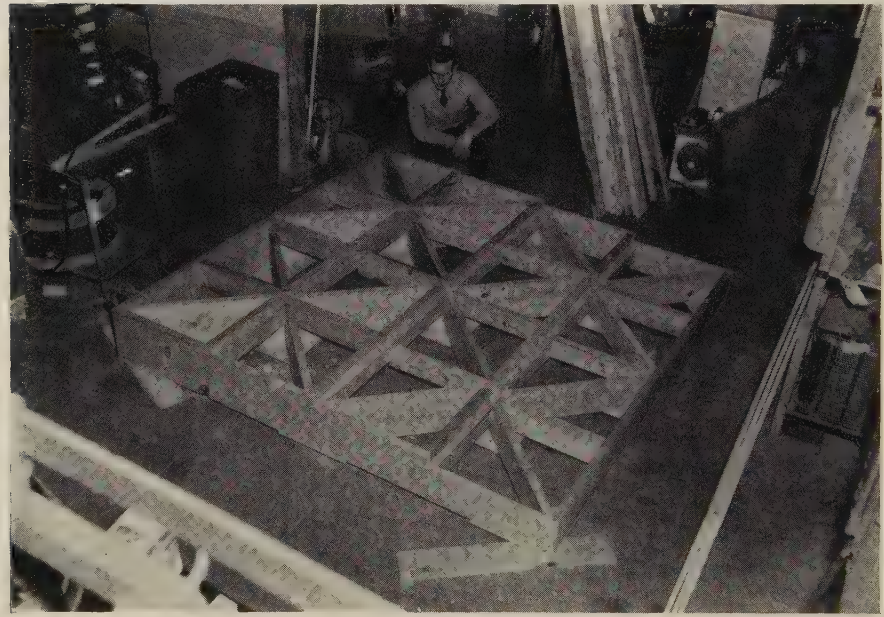

Fig. 1 (*c*). The cellular sub-framework of 2-inch thick timbers. Successive stages in the construction of the Barataria Bay model

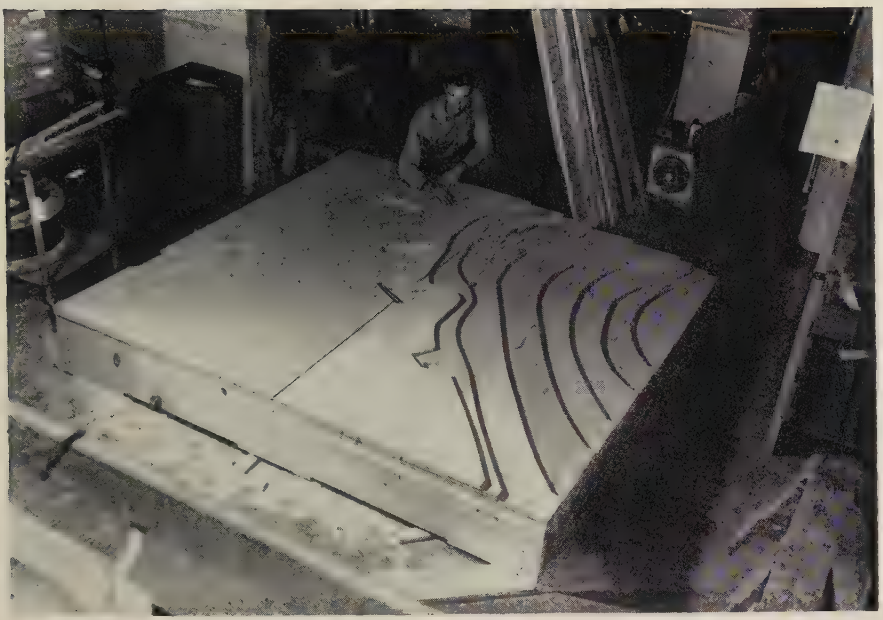

Fig. 1 (*d*). Plywood lifts cut to coarse pattern of contours.

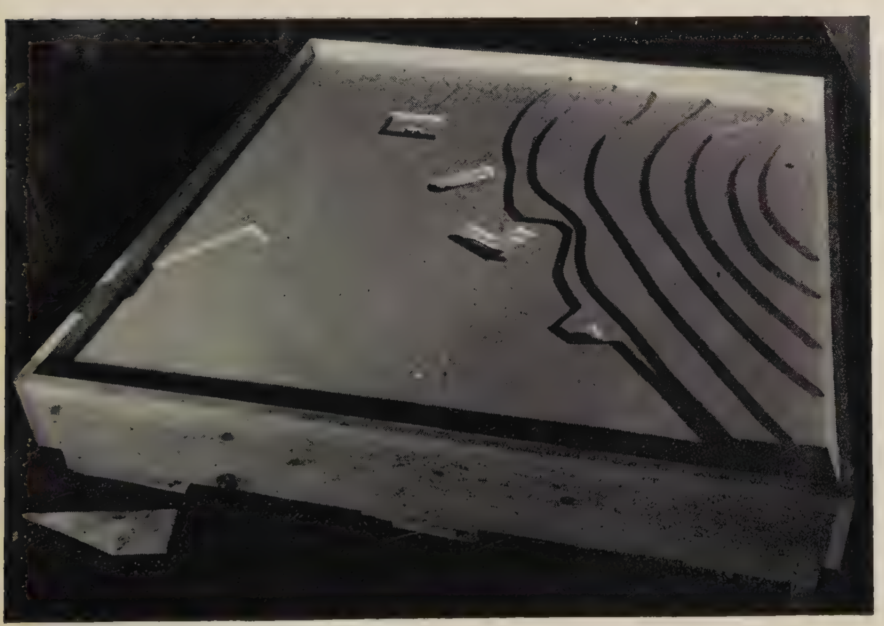

Fig. 1 (*e*). The finished waterproof box for the model.

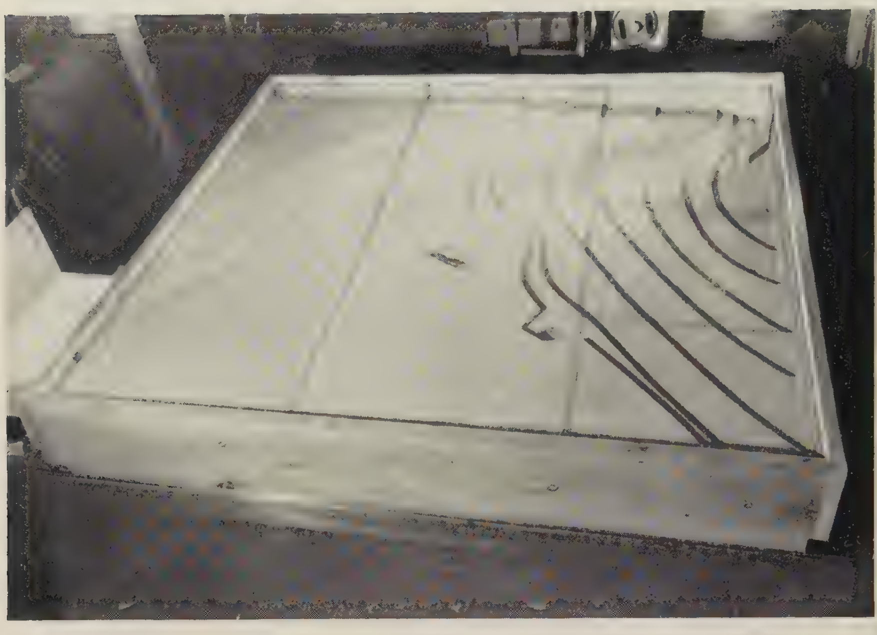

Fig. 1 (f). Wire lathe in place to bond and reinforce the plaster monolithe.

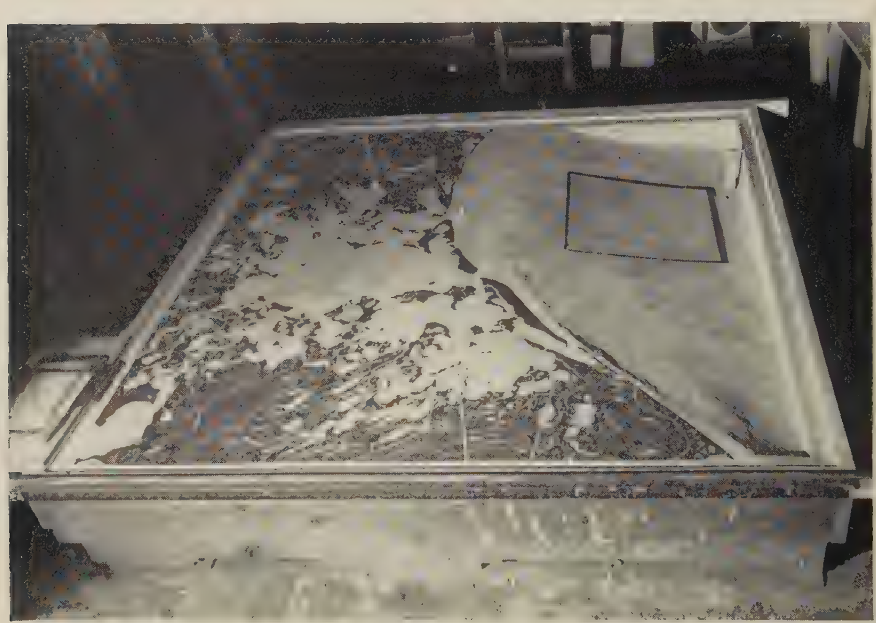

Fig. 1 (g). The monolithe of pattern-maker's plaster in place. The land areas and submarine contours were transferred to the plaster by optical projection.

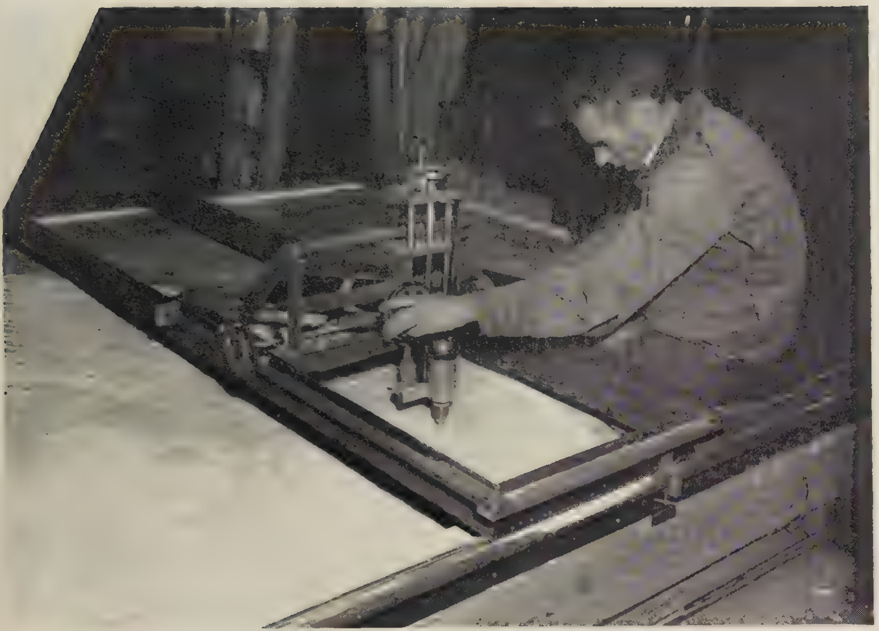

Fig. 1 (*h*). Routing submarine contours in "2-foot" stops.

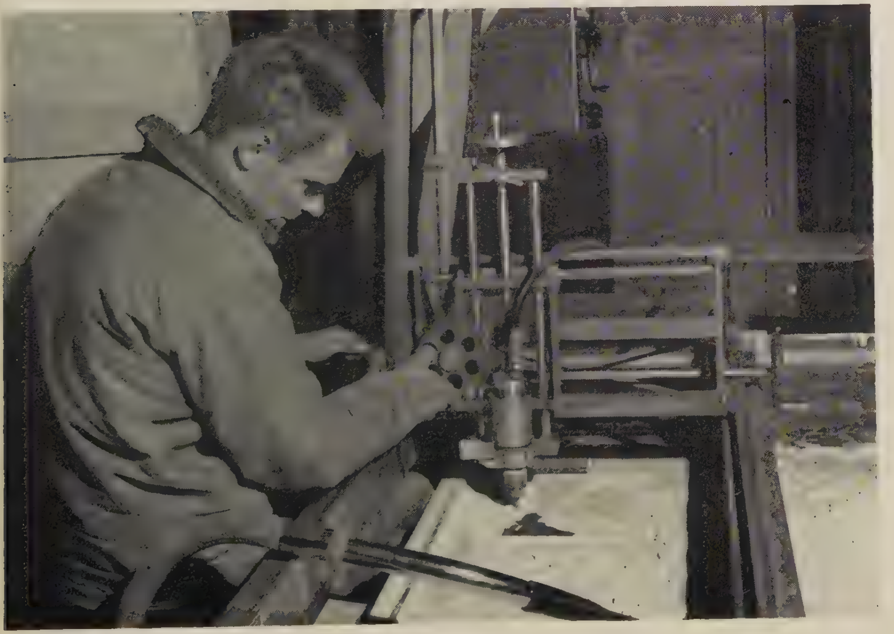

Fig. 1 (i). Planing the land surfaces to a uniform height above mean sea level to avoid differential sheltering effects in the wind-drift experiments.

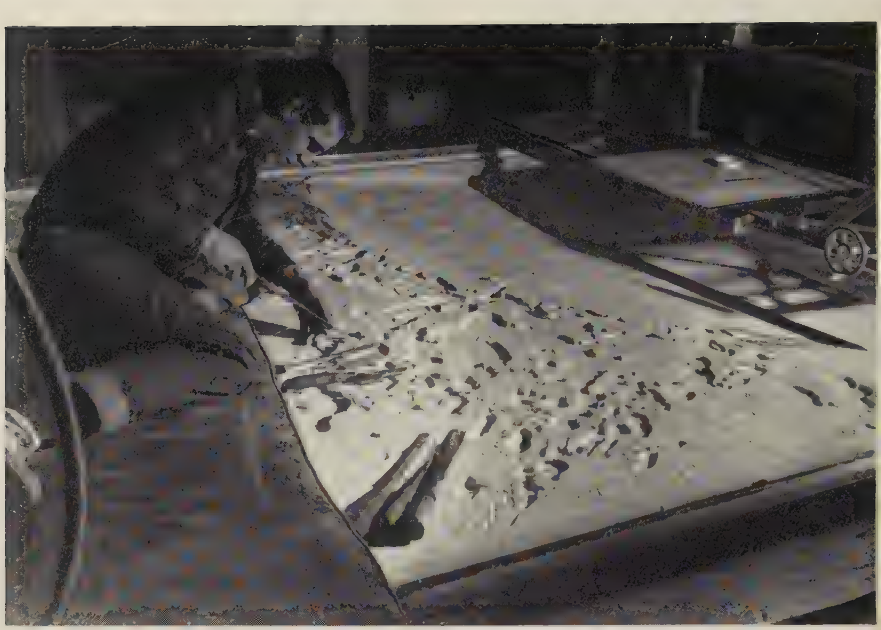

Fig. 1 (j). Blending the contoured submarine slopes.

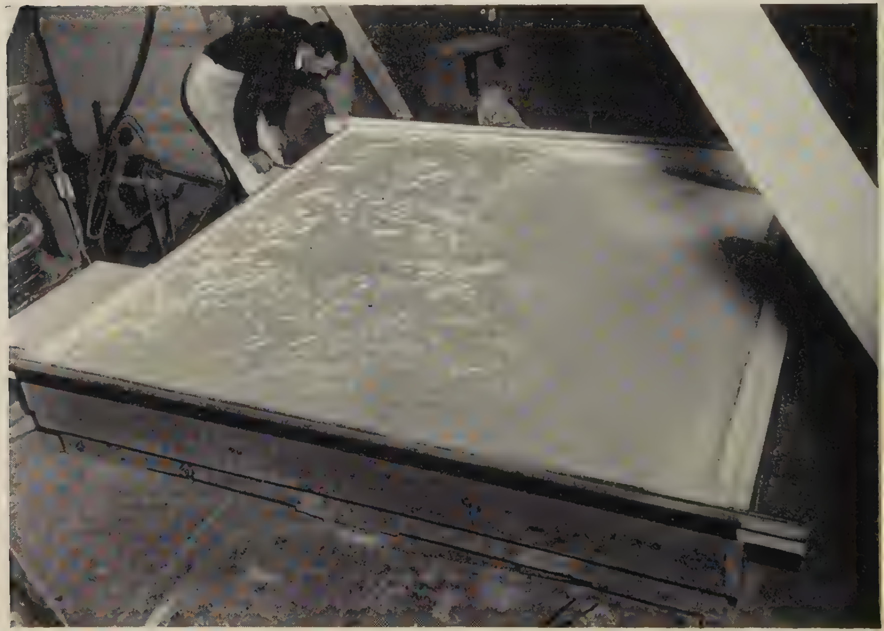

Fig. 1 (k). The finished model surface ready for painting.

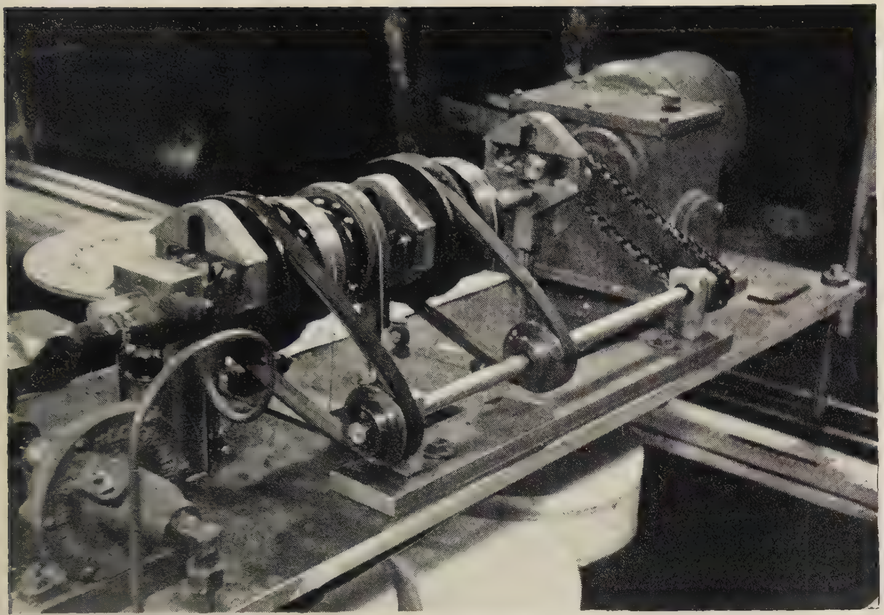

Fig. 2 (a). A tide machine composed of three displacement elements driven by one motor. The shaft in the foreground is connected to Scotch yokes by way of variable diameter pulleys which are set to drive the yokes at their appropriate speed numbers.

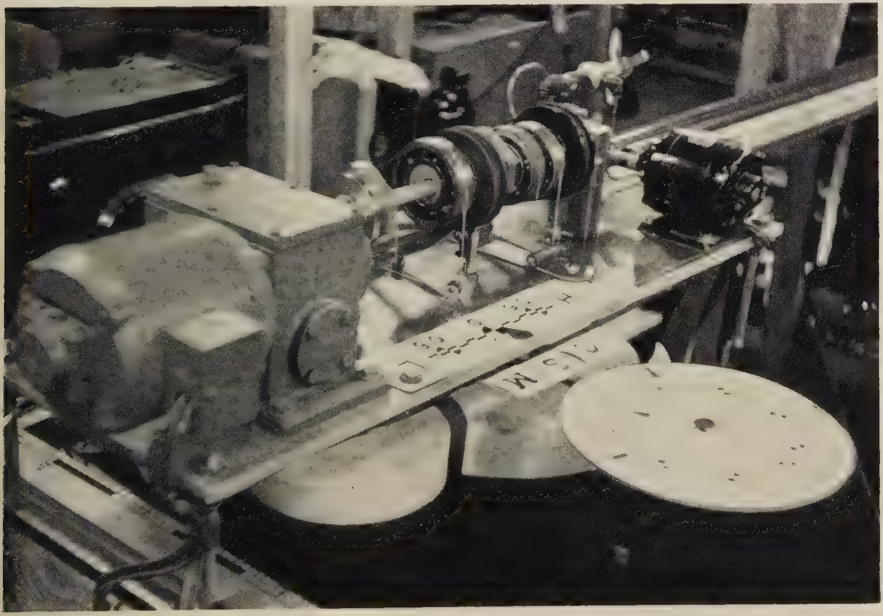

Fig. 2 (b). Opposite view of the three-component tide machine showing the string integrator which moves an index across the tidal height scale. The clock in the foreground indicates the lapse of hours, days, weeks, and months in scaled time units.

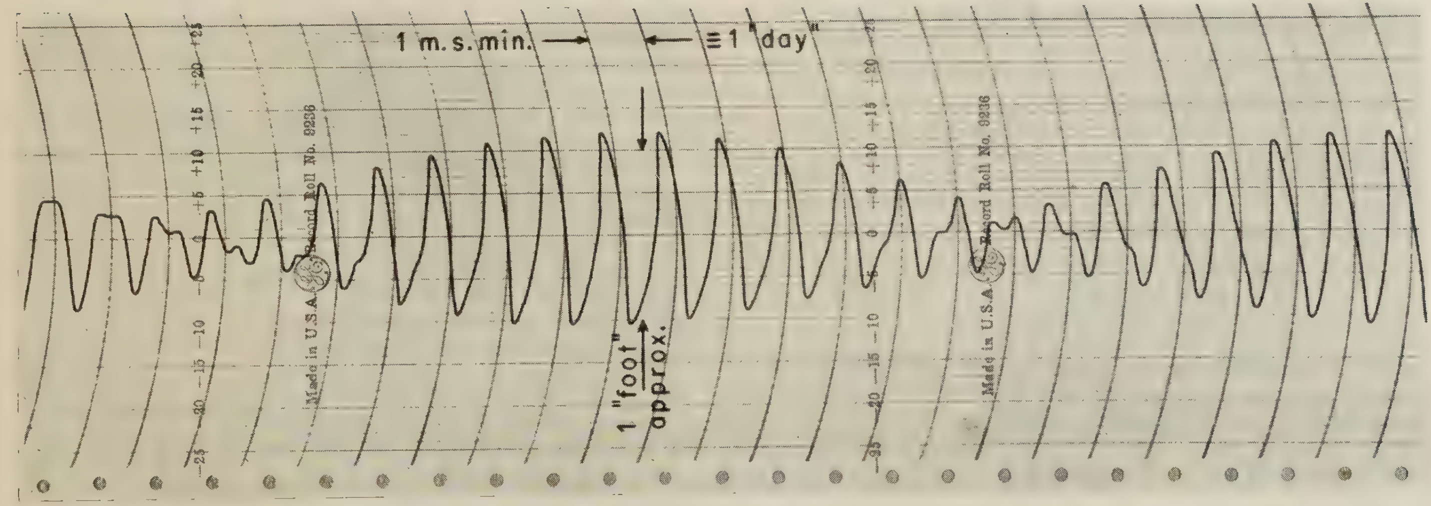

Fig. 2 (c). A representative specimen of the output of the three-component tide machine. The signature is characteristic of the Gulf of Mexico where the diurnal tide predominates, but waxes and wanes each fortnight. At the time of minimum diurnal tides the weaker semidiurnal species emerges.

depth sequence along each route. However, the tidal coefficients are less well known offshore than at coastal stations. As a first approximation, the offshore tidal components can be estimated from a weighted average of the tidal coefficients at the most seaward of a number of shore stations some distance away in both directions along the coast. Further empirical adjustments are then to be made as comparison of the tide records from the model and area under study may require.

The complexity of a tide generator depends on the fidelity with which the tidal trace at any point is to be reproduced. The number of components to be considered is determined from the relative importance of each of the several tidal coefficients compared with their sum. Coefficients regarded as unimportant can be collected and introduced as a single component driven at their mean rate. The important tidal species having speed numbers sufficiently close together can be collected to simplify the mechanism. Separate tidal components must be set apart if their amplitudes and speed numbers are such that they largely determine the characteristic sequence of tides.

In middle latitudes near open sea coasts the tides are predominantly semidiurnal with more or less diurnal inequality and a small semimonthly sequence of ranges. If neither the diurnal inequality nor the semimonthly range sequence is of importance to the experiment, the tide can be approximated by a single element driven at the weighted mean rate for all the significant semidiurnal species. If the diurnal inequality is too great to be neglected but the diurnal species are still unimportant, two elements will suffice. If the diurnal species and semimonthly species are both significant, three elements will be required as in Fig. 2. Only rarely will four or more elements be necessary unless extraordinary fidelity is required.

The volume of water to be displaced in the model to effect the rise and fall of tides is the volume ratio ($L_r^2 z_r$) times the volume change (tidal prism) in the corresponding areas of the prototype. To calculate the volume contribution of each of the tide-generating elements in the model, it is convenient to scale the mean volume of the tidal prism and then to prorate this among the important harmonic constituents in proportion to the ratio of their amplitudes to the sum of all terms. By this means the contributions of the neglected constituents are distributed impartially among other terms to effect the necessary total rise and fall.

The mechanical means by which tides have been introduced range in complexity from adjustable weirs in river models or simple cylindrical drums driven by Scotch yokes at appropriate speed numbers, such as shown in Figs. 2 (a), 2 (b), and 2 (c) for a system of bays, to electromechanical servomechanisms controlling either a single plunger or a pump, in turn controlled by a cam representing a day's or fortnight's sequence of tides actuating a cam follower. The effects of evaporation in the model can be compensated automatically if the cam follower is coupled to a point or capacitance gauge or other device (sometimes optical) for detecting the rise and fall of the free surface with respect to an arbitrary datum. Such servo apparatus has become common in hydraulic laboratories during the past decade.

ON MODELS OF INTERMEDIATE-SIZE AREAS

The circulation in marginal seas and the smaller mediterranean seas of the earth may be influenced by the same forces considered above and yet be large enough for the effects of the earth's rotation to appear. This would be manifested in shallow seas by a tendency for a tidal flow or impulsively generated wind currents to follow inertial paths closing a circuit once each half-pendulum day and for some other kinds of motion to be developed at an angle *cum sole* from the direction of the pressure gradient. This angle should increase as the frictional influence of the bottom grows smaller in comparison with the Coriolis force. Ideally, the angle increases to 90° when frictional influences are negligible and the state of motion is steady. While no experiments have been undertaken involving the effect of earth rotation on the flow in areas of this size, it is of interest to consider how this might be done.

If the area to be modelled is a very large estuary, a marginal or a small mediterranean sea having dimensions in the order of 1000 km on a side, and if in nature, the frictional influence of the bottom on the flow is small compared with the Coriolis force, then it becomes desirable to rotate the Froude model in order to provide the effects of the Coriolis force. The Coriolis force $fv = 2\Omega \sin \phi v$, where f is the Coriolis parameter, v the fluid velocity, Ω the angular velocity of the rotating earth, and ϕ the latitude. When the latitude change between the meridional limits of the area is small compared with a right angle it is sufficient to rotate the model around its centre of gravity at a certain rate.

To determine this rate it is simplest to consider motion in an inertia circle. When a parcel is subjected to an impulse and then moves freely without the action of other forces, the earth's rotation will cause it to trace a nearly circular path over the earth such that

$$\frac{v^2}{r} = 2\Omega \sin \phi v \qquad \ldots.(1)$$

where v is the velocity of the parcel with respect to the earth and r is the radius of curvature of the path. Consideration must be given to this inertial motion in order to produce phenomena such as the Kelvin wave in tidal estuaries, the amphidromic seiching of lakes such as that described by Mortimer (1955), and of marginal seas, some rotary tides, and geostrophic flow.

The rate of rotation required can be determined from the following considerations in which we will assume that $\Delta\phi$ is small, hence the variation of Coriolis parameter with latitude can be neglected, and that the model therefore can be centred on a turntable. We will also assume that the model is being operated under the same gravitational acceleration as that acting on the prototype, and that water will be used to fill it. To provide the effects of earth rotation, then, it is required that

$$\left(\frac{v^2}{r} = 2\Omega \sin \phi v\right)_m = \left(\frac{v^2}{r} = 2\Omega \sin \phi v\right)_p \qquad \ldots.(2)$$

where the subscripts m and p refer to the model and the prototype, respectively. If the Coriolis force ratio be defined $f_r V_r = \frac{f_m v_m}{f_p v_p}$ we can write the balance of inertial accelerations as follows:

$$\frac{\left(\frac{v^2}{r}\right)_m}{\left(\frac{v^2}{r}\right)_p} = f_r V_r = \frac{2\Omega_m \sin \phi_m v_m}{2\Omega_p \sin \phi_p v_p}. \qquad \ldots.(3)$$

Now since the axis of rotation of the model is vertical $\sin \phi_m = 1$, hence

$$f_r = \frac{\Omega_m}{\Omega_p \sin \phi_p}. \qquad \ldots.(4)$$

To express these statements in terms of the dimensional ratios of Table 2, it can be said that

$$\frac{v_m r_p}{v_p r_m} = \frac{V_r}{L_r} = f_r = \frac{\Omega_m}{\Omega_p \sin \phi_p}, \qquad \ldots.(5)$$

and we know from Table 2 that $V_r = (z_r)^{\frac{1}{2}}$ and $T_r = L_r(z_r)^{-\frac{1}{2}}$, therefore

$$\frac{1}{T_r} = \frac{(z_r)^{\frac{1}{2}}}{L_r} = \frac{\Omega_m}{(\Omega \sin \phi)_p} \qquad \ldots.(6)$$

and finally

$$\Omega_m = \frac{(\Omega \sin \phi)_p}{T_r}. \qquad \ldots.(7)$$

Such rotation will result in the mean sea level of the model being paraboloidal with the vertex centred over the axis of rotation. It is necessary to refer all vertical dimensions in the model to this surface.

If, toward the margins of the model, the slope of the paraboloid reference surface is so great that the sine of this slope cannot be considered essentially equal to the slope itself, the assumption made earlier that $\sin \phi_m = 1$ is no longer valid nor is the assumption that the gravitational acceleration in the prototype is substantially the same as that in the model. In such a case it would be desirable to reduce the vertical scale or increase the horizontal scale to lengthen the time scale and diminish the rate of rotation required.

The foregoing can only be applied to models filled with a single homogeneous fluid. Long gravity waves move on a rotating model with a velocity

$$c = \sqrt{g'D + \frac{\Omega^2 \lambda^2}{4\pi^2}}$$

where Ω is the angular velocity of the tank, λ is the wavelength, D is the depth and $g' = (\Delta\rho/\rho)g_0$ the effective gravitational acceleration. In the case of surface waves $\Delta\rho/\rho = 1$ essentially and the rotational term can be neglected, but for internal waves g' may be quite small in comparison with g_0, and the effects of the rotational term become dominant.

ON PLANETARY MODELS

The term "planetary model" is intended to embrace laboratory experiments representing large-scale fluid motions in which effects analogous to both the *rotation* and the *curvature* of the earth are present. Planetary phenomena have come within the scope of laboratory study more recently than the smaller scale processes, and the literature has not been digested. Therefore it seems appropriate to attempt to trace the origins of basic concepts as well as to describe some of the technical procedures and results of recent experiments.

History of Planetary Models

Models of planetary fluid motions were first conceived in connection with the atmospheric circulation. These attempts antedate oceanic studies by many years. VETTIN (1857, 1884) was probably the first to study the motions in a rotating fluid heated zonally from below. Since then EXNER (1923, 1925), ROSSBY (1926) and more recently FULTZ (1951), and LONG (1951) and their associates have made intensive studies of laboratory models in which the regime of motion is analogous to that in the upper levels of the atmosphere. FALLER (1956) has succeeded in simulating low-level frontal structures of the atmosphere using similar methods. Studies by HIDE (1953) made with reference to the fluid motions of the earth's mantle have been of interest to meteorologists as well as to geomagneticians. These methods are essentially independent realizations of a suggestion by J. J. THOMSON (1892) who, with remarkable insight, foresaw both the experimental scheme and the results that might be obtained.

The first attempt to simulate the ocean circulation was probably that by LASAREFF (1929) in which the trade winds were simulated over a plaster model at rest. SPILHAUS (1937) studied the motion of a jet entering a fluid in solid rotation. Since then the writer has made some attempts to represent the oceanic circulation in the laboratory (1952, 1955) taking account of the rotation of the earth, certain effects due to the curvature of the earth, aspects of the geometry of the ocean basins, and the stress of the mean zonal wind field. Thus far nearly all experimental efforts have been concerned with homogeneous water.

Vorticity as a Basis for Planetary Modelling

The Froude law will not serve as a fundamental basis for scaling planetary fluid motions unless long free gravity waves are dominant as they might be, for example, in a study of global tides, where the effects of rotation on wave velocities have to be taken into account. Ordinary wind waves and swell are too small to influence the circulation directly. The Reynolds law also falls short of planetary requirements because the fluid motion in this case is not predomintly controlled by forces due to internal friction. For these and other reasons, ordinary modelling techniques seem inadequate to deal directly with planetary problems, but appropriate alternatives exist.

One of the most promising points of view is that originally opened by SVERDRUP (1947) and broadened by STOMMEL (1948) and MUNK (1950) which relates the curl of the zonal wind stress over the oceans, the planetary vorticity, and lateral friction to account for the zonal asymmetry of the primary ocean circulation. It can be shown (see SVERDRUP, 1954) that if $\beta = \partial f/\partial y$ and left-handed Cartesian co-ordinates are used

$$\frac{\partial}{\partial t}\left(\frac{\partial M_x}{\partial y} - \frac{\partial M_y}{\partial x}\right) = \beta M_y + \left(\frac{\partial \tau_x}{\partial y} - \frac{\partial \tau_y}{\partial x}\right) + \left(\frac{\partial H_x}{\partial y} - \frac{\partial H_y}{\partial x}\right)$$

where M is the mass transport, τ is the stress on the sea surface exerted by the wind, and H is the integrated lateral stress due to friction. With an absence of change in transport the three right-hand terms remain, and when reassembled as follows—

$$\left(\frac{\partial \tau_x}{\partial y} - \frac{\partial \tau_y}{\partial x}\right) + \beta M_y = -\left(\frac{\partial H_x}{\partial y} - \frac{\partial H_y}{\partial x}\right)$$

—state that the sum of the change of vorticity due to wind stress on the ocean surface and that due to meridional motion (planetary vorticity) is balanced by the vorticity change due to friction. The change in planetary vorticity, which can be thought of as arising from conservation of angular momentum in parcels moving over the meridional curve of the earth, reverses sign with the sense of meridional motion. In the case of poleward transport, changes in the vorticity due to the wind stress and the planetary vorticity tendency have the same sign. In order for frictional stresses to balance this summation the ocean currents crowd against western shores, becoming narrow and swift. In the case of equatorward transport the change in planetary vorticity (it turns out) nearly balances that due to wind stress; hence little or no lateral friction is required and the flow equatorward is broad and consequently slow. This condition is most clearly exemplified in the northern hemisphere where there are no zonal connections of any consequence between adjacent oceans.*

The simplicity of the vorticity theory of westward intensification of the primary ocean circulation makes it attractive as a basis for preliminary experimental studies of the oceans. Since the desired effects arise without regard for heating or density contrast, a homogenous fluid can be used in the model. Earth rotation and the stress of the zonal winds can be provided by straightforward methods. But the meridional variation of the Coriolis parameter over a quadrant cannot be supplied through geometric similarity, since there is at present no means by which a radial gravitational field of uniform strength can be produced or simulated in the laboratory. Even if a suitable gravitational field could be provided, there is some doubt that it would be satisfactory in combination with a homogeneous fluid because of the "Taylor effect" (Taylor, 1921) which calls attention to the fact that in a rotating fluid the component velocities are independent of distance in the direction of the axis of rotation.

The Taylor effect and some further properties of this kind of flow have been discussed by Görtler (1944), Fultz (1951), Long (1954), and others. Faller and von Arx (1955) conclude that because of the Taylor effect the only apparent means for simulating the meridional variation of the Coriolis parameter in a uniform fluid is by means of horizontal divergence accompanying meridional motion in the presence of rotation. Physically this can be accomplished most simply by building a model of the earth in a flat-bottomed rotating tank in which the free surface of the water is necessarily paraboloidal. As vertical columns of water (parallel with the axis of rotation) move toward the centre of the tank (poleward) they are squeezed vertically, extended horizontally and thereby acquire anticyclonic vorticity relative to the tank. Vertical columns moving toward the rim (equatorward) will be stretched vertically, and in shrinking horizontally will acquire cyclonic vorticity relative to the tank. Were the relative vorticity so produced to be in proper proportion to that theoretically produced in transferring a column in either direction between the equator and the pole over the corresponding curve of the earth, the planetary vorticity tendency of the earth would be simulated in the model. (The odd thing about this arrangement is that, while the variation of the Coriolis parameter can be simulated in a flat-bottomed tank, the local value of the Coriolis parameter is everywhere the same. Fortunately the local value of the Coriolis parameter has no direct consequences in the vorticity theory or in experiments based upon it.)

---

* It is sometimes helpful to regard the oceans as being distributed radially around the Antarctic; extending northward as three spokes of unequal length, rooted in the hub-like Southern Ocean. This point of view tends to place perhaps more proper emphasis on the role of the Southern Ocean in the primary circulation of the world ocean system than the equatorial view that has become traditional.

The problem of simulating the planetary vorticity of the earth through the effects of horizontal divergence and curvature of the tank bottom, as when paraboloids are employed (VON ARX, 1952), has been examined analytically by FALLER and VON ARX (1955) in the following way:

It is required that the ratio of the partial change of the vertical component of relative vorticity with latitude to the planetary vorticity be the same in the prototype and in the model; symbolically that

$$\frac{\left(\frac{\partial \zeta}{\partial \phi}\right)_p}{2\Omega_p} = \frac{\left(\frac{\partial \zeta}{\partial \phi}\right)_m}{2\Omega_m} \qquad \ldots.(1)$$

where ζ is the vertical component of relative vorticity, ϕ the latitude, Ω_p the angular velocity of the prototype, and Ω_m the angular velocity of the model.

In the prototype the left-hand term is taken to be due solely to the change in the value of the Coriolis parameter with meridional curvature, and the right-hand term is the equivalent effect in the model produced by the sum of a change in the Coriolis parameter due to curvature and a divergence effect. Equation (1) may therefore be written

$$\left(\frac{\frac{df}{d\phi}}{2\Omega}\right)_p = \left(\frac{\frac{df}{d\phi} + \frac{(\zeta + f)\,\mathrm{div}_2 V}{d\phi/dt}}{2\Omega}\right)_m \qquad \ldots.(2)$$

where $df/d\phi$ is the change of Coriolis parameter with latitude for a column of fluid moving meridionally, $f = 2\Omega \sin \phi$, $(\zeta + f)$ is the total absolute vorticity of a column of fluid in the model, $\mathrm{div}_2\, V = \partial u/\partial x + \partial v/\partial y$, namely the two-dimensional divergence due to stretching and shrinking of a column as it moves meridionally, and $d\phi/dt$ is the meridional velocity in terms of latitude.

If the fluid is uniform it follows that $\mathrm{div}_2\, V = \frac{\partial w}{\partial z}$ where $\frac{\partial w}{\partial z}$ is the change with height of the vertical velocity in the column (due to stretching and shrinking). But $\frac{\partial w}{\partial z} = \frac{1}{D}\frac{dD}{dt} = \frac{1}{D}\frac{dD}{d\phi}\frac{d\phi}{dt}$, hence equation (2) reduces to

$$\frac{d \sin \phi}{d\phi} = \frac{d \cos \alpha}{d\phi} + \left(\frac{\zeta + f}{2\Omega}\right)\left(-\frac{1}{D}\frac{dD}{d\phi}\right) \qquad \ldots.(3)$$

where $f = 2\Omega \cos \alpha$, and α is the angle between the axis of rotation and the tangent plane. (In the case of the prototype α would be the colatitude.) If $\zeta \ll f$, as is the case everywhere but in the zone of westward intensification, we may write

$$d(\sin \phi) = d(\cos \alpha) - \cos \alpha \frac{dD}{D}. \qquad \ldots.(4)$$

The above relation should apply to any shape model in which the depth increases or decreases monotonically along the meridians.

The simplest shape to consider is that of the plane model where $\alpha = 0$. Equation (4) then reduces to

$$d(\sin \phi) = -\frac{dD}{D}. \qquad \ldots.(5)$$

Equation (5) states the requirement for the distribution of latitude circles on a plane model. The depth at any latitude may be determined in terms of the central depth by integrating equation (5).

$$\int_{\pi/2}^{\phi} d(\sin\phi) = -\int_{D_0}^{D} d(\ln D) \qquad \ldots.(6)$$

$$\sin\phi = 1 - \ln\frac{D_0}{D} \qquad \ldots.(7)$$

$$D = D_0 e^{1-\sin\phi}. \qquad \ldots.(8)$$

Thus, for any given variation of depth, the locations of the latitude circles may be determined from (7), or if the positions of the latitude circles are dictated by other considerations (such as an arched or dished tank bottom) the proper variation of depth is determined by (8). In particular, if in a flat-bottomed tank D_0 is the depth of fluid at the centre of rotation, considered to be a pole, and the latitude $\phi = 0$ is taken to be at the rim of the model the depth at the rim must be eD_0. The rotation rate necessary to produce the proper depth at the rim is a function of the size of the model and of the central depth as given by the equation for the free surface of a rotating fluid

$$D_r - D_0 = \frac{\Omega^2 r^2}{2g} \qquad \ldots.(9)$$

$$\Omega^2 = \frac{2gD_0(e-1)}{R^2} \qquad \ldots.(10)$$

where R is the radius at the equator.

It should be noted that the spacings of the latitude circles relative to the radius of the model are (for a plane model) independent of all other parameters, and are given by

$$\left(\frac{r_\phi}{R}\right) = \sqrt{\frac{e^{1-\sin\phi} - 1}{e - 1}}. \qquad \ldots.(11)$$

The following table gives the relative positions of the latitude circles for a plane model.

Table 3

ϕ	0°	10°	20°	30°	40°	50°	60°	70°	80°	90°
r_ϕ/R	1·000	0·864	0·735	0·615	0·498	0·392	0·288	0·190	0·095	0·000

This result has been applied successfully in two recent experiments by the present writer (1955) which concerned the primary ocean circulation of both the northern and southern hemispheres. Models of oceanic circulations on a planetary scale and based on these modelling criteria have been called vorticity models.

EXPERIMENTAL PROCEDURE WITH PLANETARY MODELS

Rotation

The most essential feature of a vorticity model is that the supporting tank rotate in a manner that is smooth and steady to an extraordinary degree. The rotation provided by simply mounting a tank on a vertical spindle is fundamentally unsatisfactory because the spindle must be precisely plumb (within

3×10^{-5} radian) in addition to rotating smoothly. It is better in many ways to adapt the simple method originally used by TAYLOR (1921) in which the model is floated in a stationary tank and driven by water jets, or by a fluid clutch.

In the latter case the apparatus may consist of a stationary tank partly filled with water and fitted with a 3- or 6-bladed impeller just above the bottom. Floating in this water with a clearance above the bottom of at least twice the vertical dimension of the impeller blades is the rotating tank. This rotating tank should have the same radius as the impeller, both being less than the radius of the fixed tank by about the depth of water to be used. The rotating tank may be divided into two concentric compartments, an outer dry annulus and an inner free-flooding model area. The annulus provides for both the positive buoyancy and stability of the floating tank, and the area inside can be flooded freely through valves in the bottom. While in vorticity models it is necessary to work with reference to a rigid bottom surface, it is sufficient to provide the tank floor with only enough stiffness to maintain its plane or other predetermined figure in the absence of gravitational or other forces. Such is the case when the tank is built of a stiff buoyant material such as plywood and loaded to a state of neutral buoyancy by means of metal fittings required to hold it together.

In an apparatus such as this the tank will turn under the action of the impeller at a very steady rate, maintain itself in a level attitude, and at the same time remain centred in the outer tank (if the outer tank is precisely level) by virtue of the secondary circulations excited by the impeller acting as a centrifugal pump, perhaps aided by the tip vortices produced by the impeller blades. When necessary the centring action can be emphasized by increasing the shear in the fluid coupling. Shear may be increased sufficiently to stabilize the largest tanks used so far (about 5 metres diameter) if braking action is produced as by three rubber tubes attached to the rotor which barely touch the stator. Stable equilibrium can be achieved at all speeds up to that at which the tip speed of the impeller blades equals or exceeds the speed of a free gravity wave in the outer tank.

Horizontal Length and Time Scales

In order for planetary models to be housed, the horizontal scale must necessarily be in the order 1/10,000,000. Mixing in these extremely small-scale models is usually excessive. The coefficient of eddy diffusivity in the oceans is said to reach values ranging from 10^4 to 10^8 cm²/sec for large-scale phenomena. In a planetary model the diffusivity ratio is

$$A_r = \frac{A_m}{A_p} = \frac{L_r^2}{T_r} = \frac{(10^{-7})^2}{10^{-4}} = 10^{-10}.$$

But since $A_m = 2 \times 10^{-5}$ cm²/sec at the least, due to molecular diffusion, the turbulence in a planetary model must be undetectable if diffusion is to be kept in scale. Toward this end a decrease in time scale or an increase in the length scale is desirable, but T_r is effectively limited to the range 10^{-4} to 10^{-5} and L_r cannot be carried farther than 10^{-6} in even the most formidable installations.

Vertical Scale

The theory of the vorticity model indicates nothing directly with regard to vertical scale. Experimentally a model of the surface-layer circulation of the oceans (above the main thermocline) can be satisfactorily produced in homogeneous water when the bottom topography of the oceans is represented only to the depth of the 200-metre isobath. This depth reaches the shoulder of most continental shelves, and suggests the subsurface bulk of ocean islands and island chains, but excludes the deeper features such as swells and ridges on the ocean floor. It is found that when the Mid-Atlantic Ridge, for example, is modelled in the North Atlantic, the wind-driven flow across it is strongly affected. This is undoubtedly due to the fact that between the upper Ekman friction layer (about 1 mm thick) and the bottom Ekman friction layer (also about 1 mm thick) the flow is essentially two-dimensional. Therefore in the presence of rotation, any obstacle that protrudes above the bottom friction layer will act as though it extended through the full depth of the fluid even though it may not actually do so.

With these facts in mind one may consider, as significant to the vertical scale, preservation of the ratio of the thickness of the friction layer to the total depth in the oceans and in the model. The Ekman layer in the oceans is in the order of 100 metres thick, and the average total depth perhaps 4000 metres, so that their ratio is 1:40 approximately. The mean depth of water in the model should therefore be in the neighbourhood of 4 cm. This has proved to be a convenient and apparently suitable depth.

The materials useful in constructing shapes of this thickness to represent the continental masses and submerged shelves are numerous, but may be selected so that the weight of the volume of water they displace is equal to their weight in air. In this manner they contribute no inequality of load on the floor of the tank, which otherwise would cause flexure and an unwanted gradient of depth. It is also desirable that the upper surface of the continental modelling be curved, preferably as a paraboloid, so that the elevation of the land mass above the free surface of the water is everywhere the same and the obstruction offered by the land masses to the free flow of air over the oceans is the same at all latitudes.

The layout of continents and continental shelves fitting the grid of meridians and latitude circles defined by Table 3 is of course different from any of the standard cartographic projections and most easily transferred to the model by optical projection. Fig. 3 shows the earth's geography replotted in the manner appropriate for a flat-bottomed vorticity model.

Soundings

To simulate certain effects of earth curvature in the vorticity model it is necessary to establish an appropriate ratio of water depths over the pole and equatorial regions. The depths D_0/D_{90} can be considered in satisfactory adjustment when their ratio is equal to the value of e to the second decimal place. In southern hemisphere experiments the pole is inaccessible, being covered by the Antarctic continent. The depth ratio is therefore set from soundings at the equator and at 70° south latitude, the proper ratio at these points being $D_0/D_{70} = 2{\cdot}64$.

A technique found useful for measuring these depths consists of sounding the tank bottom with glass rods coated with a thin mixture of bentonite and cobalt chloride. Cobalt chloride has the property of changing colour from blue to red in the presence of moisture. Bentonite has the property of being very readily wetted. Therefore a coating of bentonite and cobalt chloride on the rod permits a clear line to be established by the water level with merely an instant's wetting.

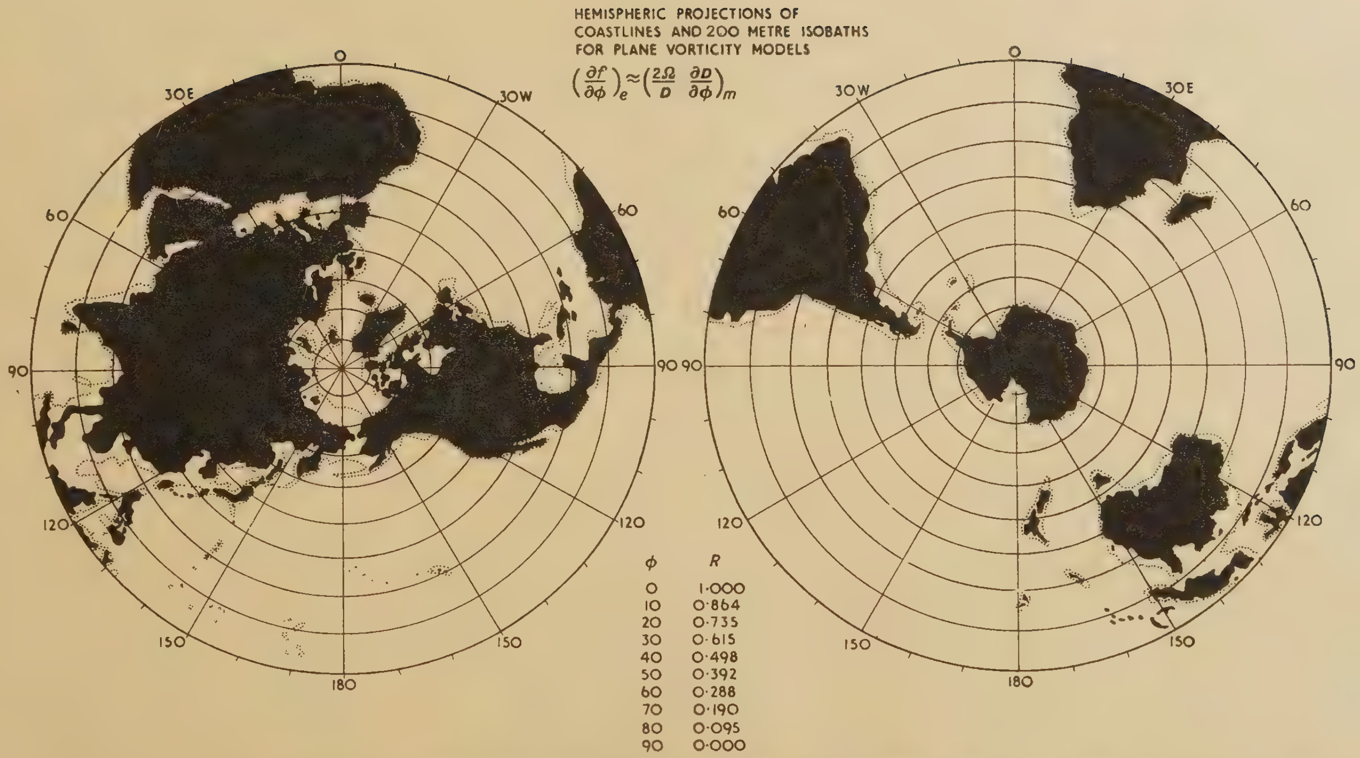
HEMISPHERIC PROJECTIONS OF
COASTLINES AND 200 METRE ISOBATHS
FOR PLANE VORTICITY MODELS
$\left(\frac{\partial f}{\partial \phi}\right)_e \approx \left(\frac{2\Omega}{D}\frac{\partial D}{\partial \phi}\right)_m$
0
30E
30W
60
60
90
90 90
90
120
120
120
120
150
150
150
150
180
180
30W
30E
60
60
0

ϕ	R
0	1·000
10	0·864
20	0·735
30	0·615
40	0·498
50	0·392
60	0·288
70	0·190
80	0·095
90	0·000

Fig. 3. Charts of the northern and southern hemispheres of the earth replotted in accordance with the spacing of latitude circles given in Table 3 for the plane vorticity model. The dotted line represents the 200-metre isobath which together with the shoreline has been somewhat simplified for convenience in carving.

Tracers

Tracers are required in all models for the detection and measurement of water motion, but in planetary models the motion is both slow and nearly laminar so that the materials must be quite close to neutrally buoyant. In past experiments two tracers have been used, namely: fountain-pen ink diluted 5:1 and potassium permanganate solution or crystals. In an acidified (15 cm^3 of 6N HCl per 50 litres of water) diluted ink will not flocculate and remains nearly neutrally buoyant. The oxidizing effect of potassium permanganate mixing with the ink in neighbouring parts of the model may cause a colour change in the dyestuff of the ink. Such admixtures can produce singularly beautiful colour combinations that change with time and thus serve to identify water parcels that have passed through successive revolutions of the ocean circulation.

Permanganate tends to sink and to stain the water at the bottom friction layer, while the surface film of the ink tends to stain the water of the surface friction layer. Thus in an ocean gyre there is a strong tendency for the central water mass to become blue while the coastal water masses become red. The swiftly moving currents in the region of westward intensification are regions of mixing which become coloured in a variety of ways intermediate between these two, and are thus clearly distinguished from them in colour photographs. But the value of these substances is limited in that they do not lend themselves to tracing the motions of individual parcels of water.

Particulate tracers are of two kinds—surface and internal. Where wind stresses are employed, surface tracers must be awash so that the usual substances (lycopodium powder, aluminium flakes, talc, crushed cork, and so on) must be replaced by wetted particles or oil droplets having very slight positive buoyancy as with an *n*-butyl phthalate and xylene mixture. The task with surface tracers is to avoid coalescence. Small discs of polyethylene having a larger diameter below water than above have been used in this connection, but paper discs do almost as well. Internal tracers present a more difficult problem. Neutrally buoyant droplets of *n*-butyl phthalate and xylene, or condensed milk and alcohol mixtures, serve in some cases. Degreased aluminium tristearate flocculate, bits of seaweed, the larger species of phytoplankton, colonies of myxomycetae, have served in others. Cleaner materials can be produced by electrolytic decomposition of potassium iodide solution, or of water itself to produce a stream of fine slowly rising bubbles over platinum points, or of tellerium electrodes. The ideal material, still to be found, might be described as follows: A substance having a high albido, definite particulate shape, and integrity of shape, which is insoluble in water but enormously permeable and porous, and itself of nearly the same density as water. It would be convenient if the material could be stored dry and yet be readily wetted, and desirable if it were inexpensive or recoverable.

Planetary Wind Tongues

The vorticity model responds to the curl of the wind stress over its water surface. The direction of zonal air flow is of no consequence but it is of great importance that the inflection points in the mean zonal wind field are properly placed in latitude and that the ratio of tongues between the trades and waterlies, and between the westerlies and polar easterlies, are reproduced in accordance with nature. In order for the ratio of zonal wind tongues to be preserved one has

Erratum: PLANETARY WIND TORQUES
Please substitute torques for "tongues" in this context.

either to know the value of the wind-stress coefficient and compute the required wind speed or adjust these values in some empirical fashion.

As mentioned earlier, the level of turbulence in vorticity models is generally too high; hence it is desirable to keep the wind speed as low as possible everywhere, preferably well below that which will produce ripples. The lowest wind speeds of suitable strength are obtained when the directions of air flow are as they are in nature; from east to west in the trades and polar easterlies and from west to east in the westerlies. The rotation of the model through the air at rest in the laboratory provides a ready-made easterly wind which need only be shaped to the proper profile to serve. Westerly winds must be produced by an air blast of sufficient strength to overtake the model.

Experience has shown that, through careful adjustment of the west-wind nozzles, a core of air will remain at rest over the polar regions of the model and provide a suitable anticyclonic torque as the model rotates. Trade winds must be augmented by air streams from a system of nozzles so directed as to produce a maximum trade at latitude 15°. The resulting decrease of wind stress equatorward seems to be required to produce the equatorial countercurrents in the ocean circulation. The westerlies nozzles are then adjusted to produce a maximum wind speed near latitude 45° in the northern hemisphere and near − 50° in the southern with inflection points at 30° and 60°, and − 30° and − 68° respectively.

STARR (1954) has shown that the balance of angular momentum of east and west winds over the world is always maintained; that is, when the easterly and westerly winds of the northern hemisphere are out of balance, they are also out of balance in the southern hemisphere, and when in balance in the northern hemisphere they are also in balance in the southern hemisphere. But the strength of westerlies and trades is different in the two hemispheres. In terms of annual means, the trades are approximately twice as strong as the westerlies in the northern hemisphere, while in the southern hemisphere the two are nearly equal as shown in Fig. 4. The world mean surface-pressure maps by SHAW (1931) and recent studies of the annual mean surface wind field by MINTZ and DEAN (1952), and unpublished data on world mean monthly surface pressure profiles made available to the writer through the kindness of Professor H. C. WILLETT of the Massachusetts Institute of Technology, all reflect this condition. These findings have been used as a basis for the winds applied to both the northern and southern hemisphere models.

Rossby Number

While the zonal wind-speed ratios mentioned above are to be preserved, the actual wind speeds employed in the model experiments are adjusted through their effect on the ocean circulation. To be in scale, the velocities of the ocean currents should bear the same ratio to the tangential velocity of the model at its equator as do the velocities of the actual ocean currents to the tangential velocity of the earth at its equator. This is a definition of the kinematic Rossby number which for the swift western currents has values in the vicinity of $0{\cdot}3 \times 10^{-2}$. When the Rossby number is small, all accelerations may be considered small in comparison with the Coriolis acceleration, and the flow will be nearly geostrophic. While flow in the oceans is essentially geostrophic in high latitudes, there can be no geostrophic balance at the equator where the Coriolis parameter vanishes. In the plane model the Coriolis parameter is the same everywhere, so that the model cannot be considered to be representative of conditions in low latitudes. For this reason it is desirable to adjust the Rossby number in the model to high middle-latitude occurrences, which are fortunately the site of strongly intensified currents for which velocities are best known.

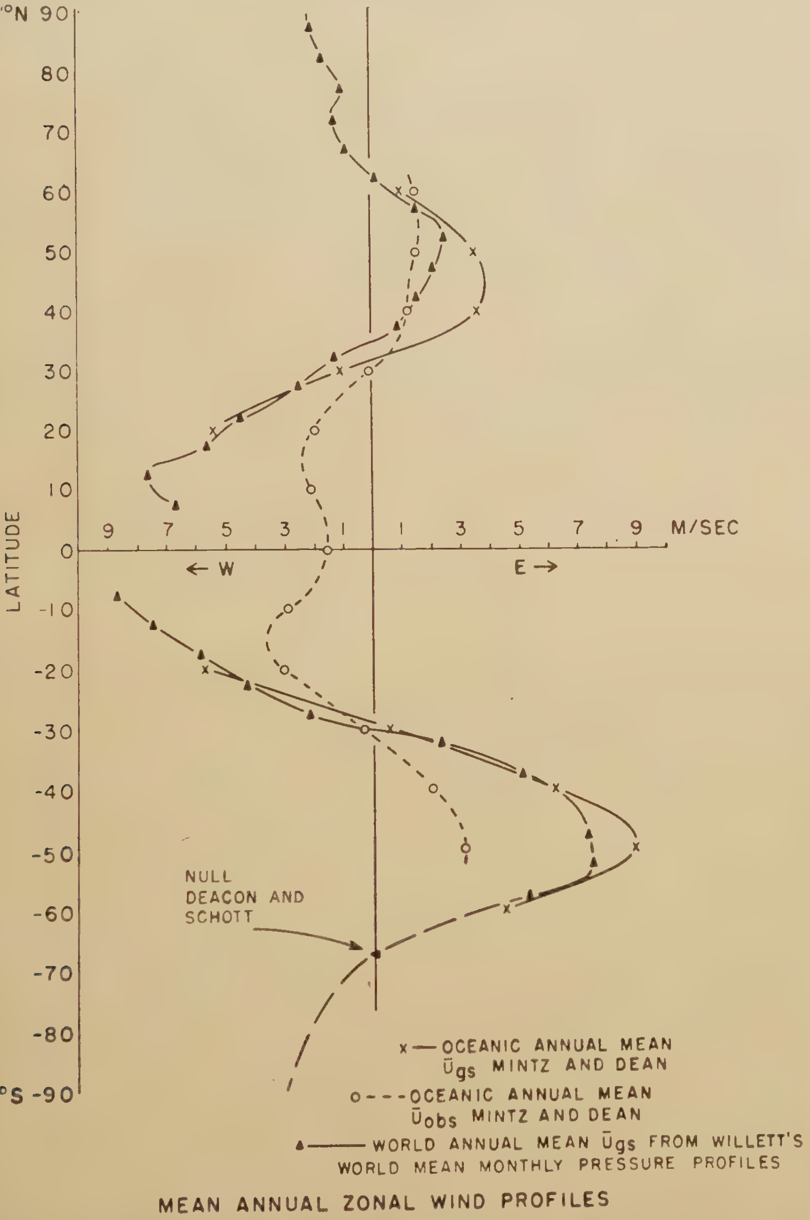

Fig. 4. Mean annual zonal wind profiles of the whole world plotted from data supplied by Y. MINTZ and G. DEAN (1952) and by H. C. WILLETT (personal communication). The observed and geostrophic zonal winds over the oceans alone are shown in comparison with the geostrophic winds for both land and sea areas.

Wind Force and Direction

Measurement of the force and direction of the winds over the model has been accomplished by two separate means. The wind speed at and near the free surface has been measured by means of the drift of ping-pong balls floating in the water. The quasi-instantaneous direction of air motion has been detected by photographing a set of shuttlecocks suspended on fine threads at 10° latitude intervals along midocean meridians. The drift of the ping-pong balls is representative of the mean motion of the air at a small "anemometer height", while the shuttlecocks indicate the mean direction statistically and the turbulent fluctuations on a quasi-instantaneous basis.

It is convenient to photograph the headings of the shuttlecocks at random intervals of time and to plot wind roses which indicate both the variability and the direction of mean stress. Periodic photographs of the drift of ping-pong balls initially laid out in meridional lines yield data on the wind speed. But ping-pong balls do not yield convenient data on wind direction because they are deflected *cum sole* from the wind direction by the transport in the upper friction layer. Due to this they change latitude rapidly and tend to collect near the locus of the inflection point of the wind field. The zonal component of motion of the balls is measured as an index of the zonal wind force. The rate of motion of a standard ping-pong ball floating in fresh water in a rotating tank is very nearly 20 per cent of the wind speed in the range 10 to 150 cm/sec measured at a level 1 cm above the free surface. The speed of the water motion below the friction layer in the "midocean" portions of a vorticity model is sufficiently small to be neglected (well under 5 per cent of the ball speed) in wind-field calibration by the ping-pong-ball method.

By these methods, the flow of air in the trades has been shown to be quite smooth owing to the use made of the relative motion of the tank through the undisturbed air in the laboratory. The westerlies, on the other hand, are highly unsteady since they are produced by the zonal blast from a finite number of nozzles (ten have been used), each of which produces a turbulent air stream diverging at an angle of some 14°. The character of this turbulent flow is thought to be in keeping with that of the westerlies in nature, as is the smoother flow of the trades.

EXPERIMENTAL RESULTS

The Northern-Hemisphere Model

The apparatus built for the northern and southern hemisphere experiments is shown partly assembled in Fig. 5 (a), together with a closeup of the observer's position and controls in Fig. 5 (b), and the eight-foot tank with northern-hemisphere modelling and the wind-field nozzles in place in Fig. 5 (c). This apparatus was mounted on a vertical shaft, driven by an electric motor through a variable-speed transmission. The difficulties mentioned in the section on rotation were encountered here. Nevertheless, the apparatus gave interesting results once the wind fields were properly set up.

The data compiled in Fig. 4 show Mintz and Dean's observed mean zonal winds for the whole year over the oceans alone, and the geostrophic wind computed from an annual mean-pressure profile for land and sea obtained from Willett's monthly mean-pressure profiles for the years 1949 through 1950.

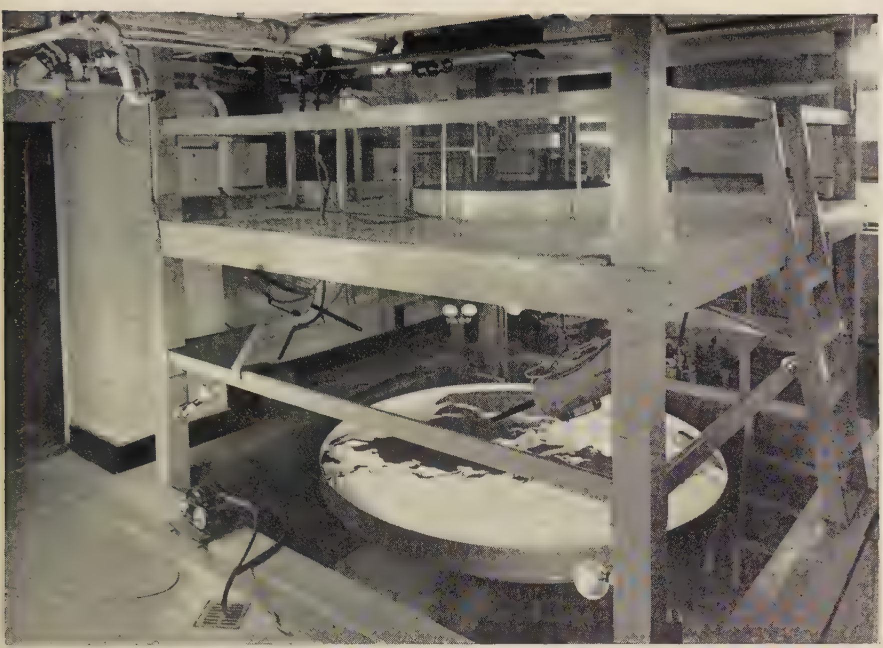

Fig. 5 (a). General view of the northern-hemisphere model apparatus showing the eight-foot cylindrical tank mounted below a platform from which the observer could control the apparatus and watch the progress of the circulation through a wide-field rotoscope bolted to the ceiling of the laboratory. Funds for the construction and operation of this model were provided by the US Navy, Office of Naval Research.

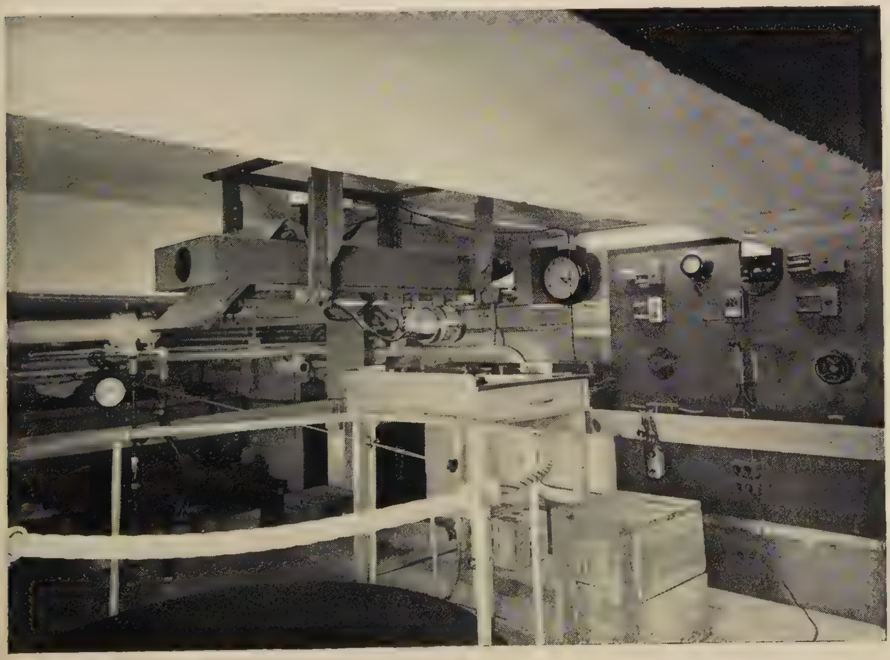

Fig. 5 (b). The observer's position on the platform over the rotating model showing the wide-field rotoscope in the foreground, and the control panel in the background of the desk where the observer could be seated.

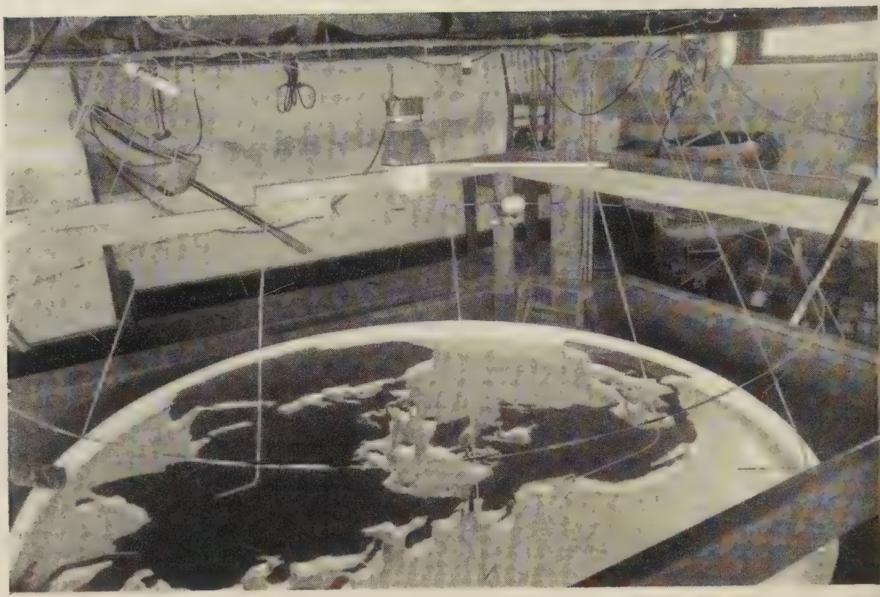

Fig. 5 (c). View of the tank with northern-hemisphere modelling in place showing the small-bore pipes through which air could be forced at some 15 to 25 pounds pressure to simulate the trade winds and westerlies.

These formed the observational basis for the wind fields shown in Fig. 6 which were applied to the northern-hemisphere model.

It was necessary to preserve the profile of the zonal wind field and still drive the ocean currents at the appropriate Rossby number. The degree of refinement of detail obtained with the model seems to depend on the choice of Rossby number to the extent that approximately double or half the values thought to obtain for the earth lead to different characteristic details in regions where shearing instability plays a part in forming the character of the circulation. This is especially noticeable in the landward margin of the Gulf Stream in the North Atlantic Ocean and the Kuroshio in the North Pacific Ocean.

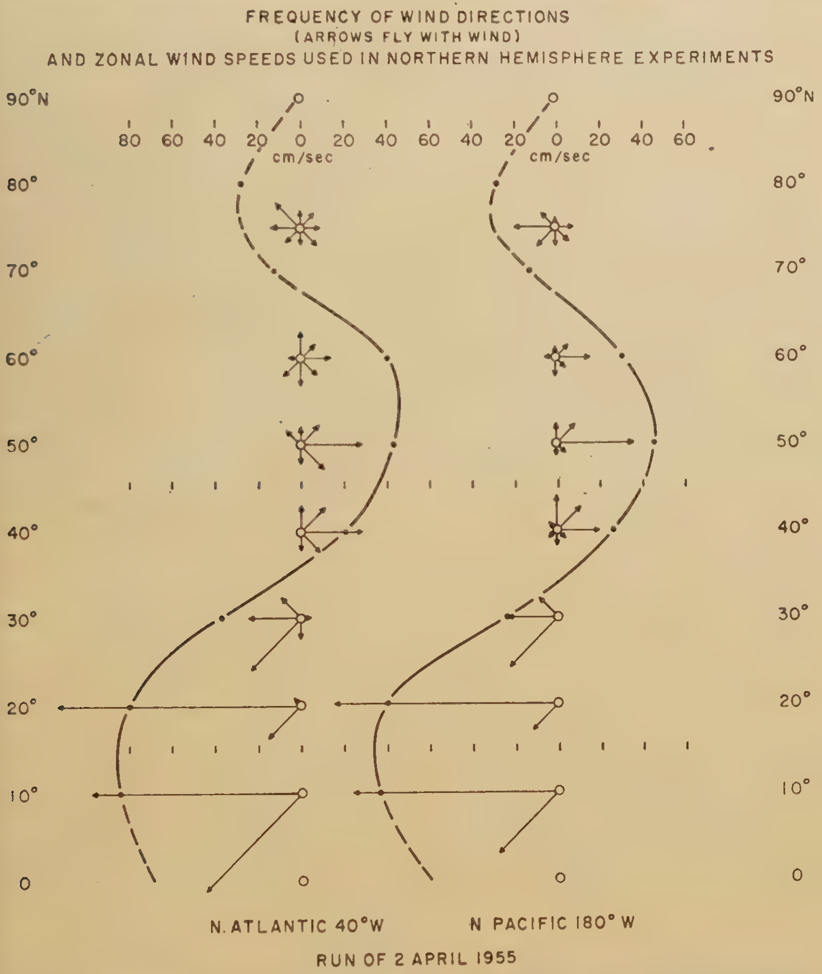

Fig. 6. Frequency of wind direction and zonal wind speeds used in experimental studies of the ocean circulation of the northern hemisphere. The values shown were determined by the methods described in the text.

In general the model results agree fairly well with older climatological charts of the ocean circulation, but differ from the more recent field measurements in that the prototype Gulf Stream is observed to cross the North Atlantic Ocean at somewhat higher latitudes, while the Kuroshio actually crosses the North Pacific somewhat south of its course in the model. This may be due to the facts that the average vorticity of the wind field over the North Atlantic is twice that over the North Pacific in nature (see MINTZ and DEAN, 1952) while in the model the values must be nearly the same, and that the latitude of the inflection points of the mean zonal wind profiles differ from ocean to ocean in nature but are identical in the model.*

The positions of the halostases and principal convergences in the North Atlantic and North Pacific Oceans were found to differ by a degree or two from those given, for example, in the current chart prepared by SCHOTT (1942) for the Deutschen Seewarte, but it was found that adjustments of the positions of these features through alterations of the mean zonal wind field produced undesirable changes in the geometry of the intensified currents of the western parts of the oceans. Part of the difficulty may lie in the fact that the mean zonal wind field measured on the model along the central meridian of each ocean was not entirely representative of that which actually occurred in the continental extremities of the oceans due to the sheltering effects of the continents.

Despite these shortcomings it is felt that these most recent experiments on the circulation of the northern hemisphere shown in Fig. 7 (VON ARX, 1955) represent an improvement over those which were possible previously (VON ARX, 1952), especially in the way that they represent the circulation at high latitudes.

The Southern-Hemisphere Model

The wind fields applied to the southern hemisphere model and shown in Fig. 8 were selected through measurement of the Rossby numbers applicable to the Agulhas Current (see MERZ, 1925) and the Brazil Current (DEFANT, 1932) for which velocities are best known. It was found very early in the adjustments of the southern-hemisphere model that the balance of forces due to westerlies and trades was of critical importance to the pattern of circulation in the vicinity of the Cape of Good Hope where the Agulhas and Benguela Currents interact, and near the La Plata River estuary where the Brazil Current and Falkland Current meet to form the western extension of the subtropical convergence in the South Atlantic. When the force of trades and westerlies was adjusted to produce an acceptable regime of motion around the southern tip of Africa the position of the subtropical convergence across the South Atlantic was also in acceptable adjustment. At the same time the continuation of the subtropical convergence around the world was properly related to Tasmania and New Zealand and disappeared in the eastern South Pacific, as it does in nature. A prominent feature in this part of the world turned out to be the divergence west of South America following the 50th parallel south. The Antarctic convergence was harder to discern. This may be due to the manner in which the model ocean water masses were dyed, but no really suitable method was found which would reveal the Antarctic convergence clearly or as a single continuous feature. Instead it invariably took the form of a spiral shown in Fig. 9 with eastward and northward-reaching arms rooted in the offing of Sabrina Land and the Palmer Peninsula, respectively.

---

* Recent work on the effects of ocean width (fetch) on the speed of the flow in the zone of westward intensification has shown that the latitude at which these strong currents break away from the coast tends to increase with fetch, other wind conditions being the same.

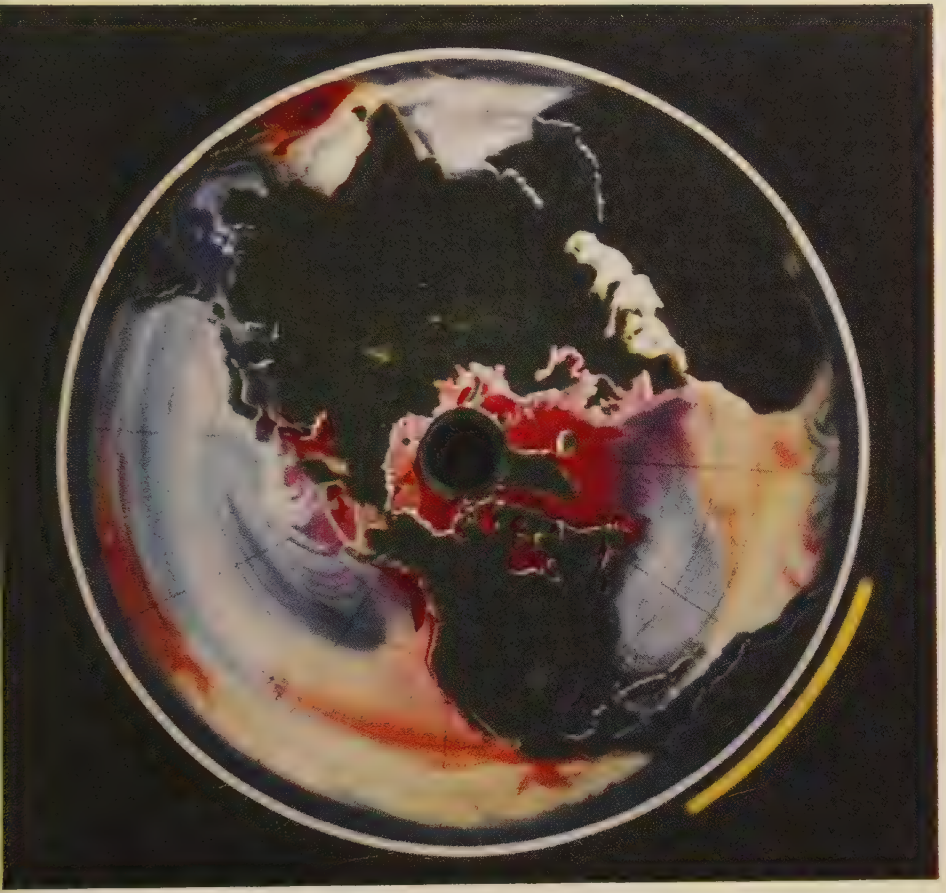

Fig. 7. A representative photograph of the circulation patterns produced in the experiments with the northern-hemisphere model. The "cold" water masses are coloured red, the "warm" water masses are blue, and mixtures show intermediate tints. The narrowness of the Gulf Stream and Kuroshio is shown together with the manner in which both broaden by meandering after leaving the east coasts of North America and Asia respectively.

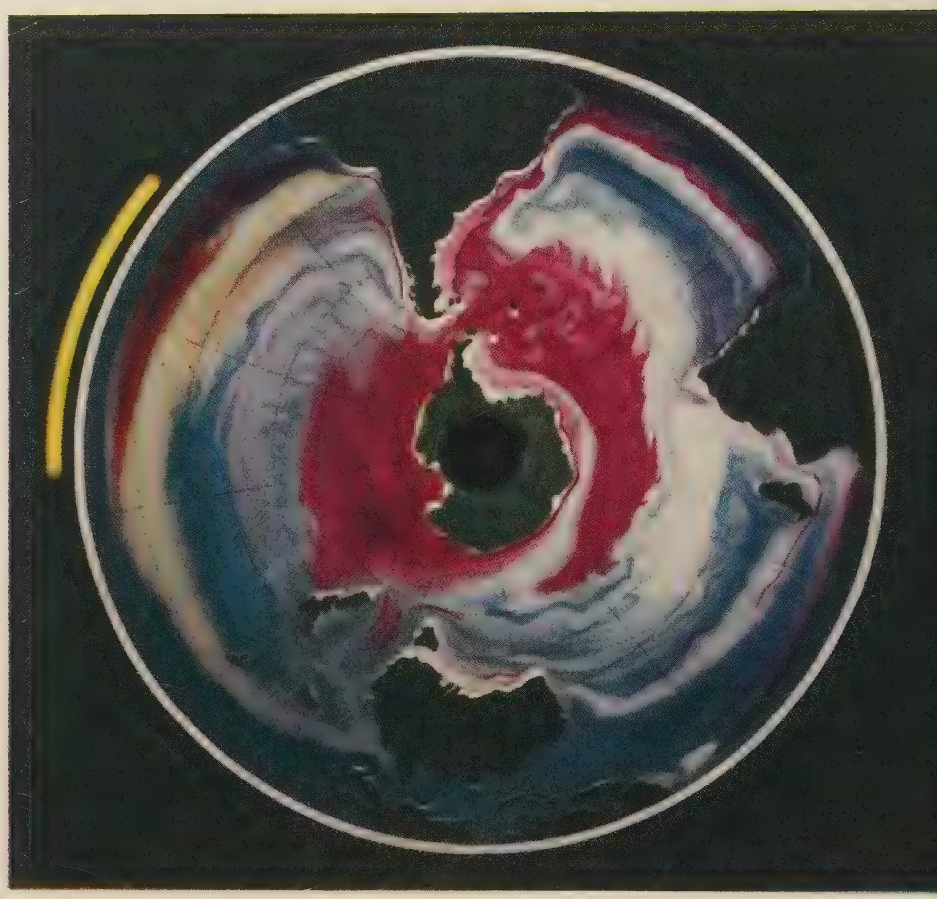

Fig. 9. A representative photograph of the circulation patterns produced in the experiments with the southern-hemisphere model. With the exception of the equatorial current, which was stained both red and blue, the "cold" currents and water masses are coloured red, the "warm" water masses and currents are blue, and mixtures show intermediate tints. The northern edge of the red coloration in the Southern Ocean corresponds fairly closely to the observed position of the subtropical convergence. North of this line each ocean compartment contains its own nearly isolated gyre. Flow in the Southern Ocean is circumpolar except for stagnation in the small area midway between New Zealand and South Victoria Land.

The southern-hemisphere experiments were made primarily to see if a model would conform easily to the picture of the ocean circulation given by the Deutschen Seewarte chart (1942), by Deacon (1933, 1937) and Schott (1935, 1942). In most respects the representation of the general circulation of the southern-hemisphere oceans seemed satisfactory, except for three general features: namely, the spiralling of the Antarctic convergence, the structures of currents flowing northward along the west coast of continents, specifically the Peru or Humboldt Current, the Benguela Current, and the West Australian Current, which were poorly defined in the model and, in latitude 60° south, 180° west, a virtually motionless water mass which may or may not have a counterpart in nature.

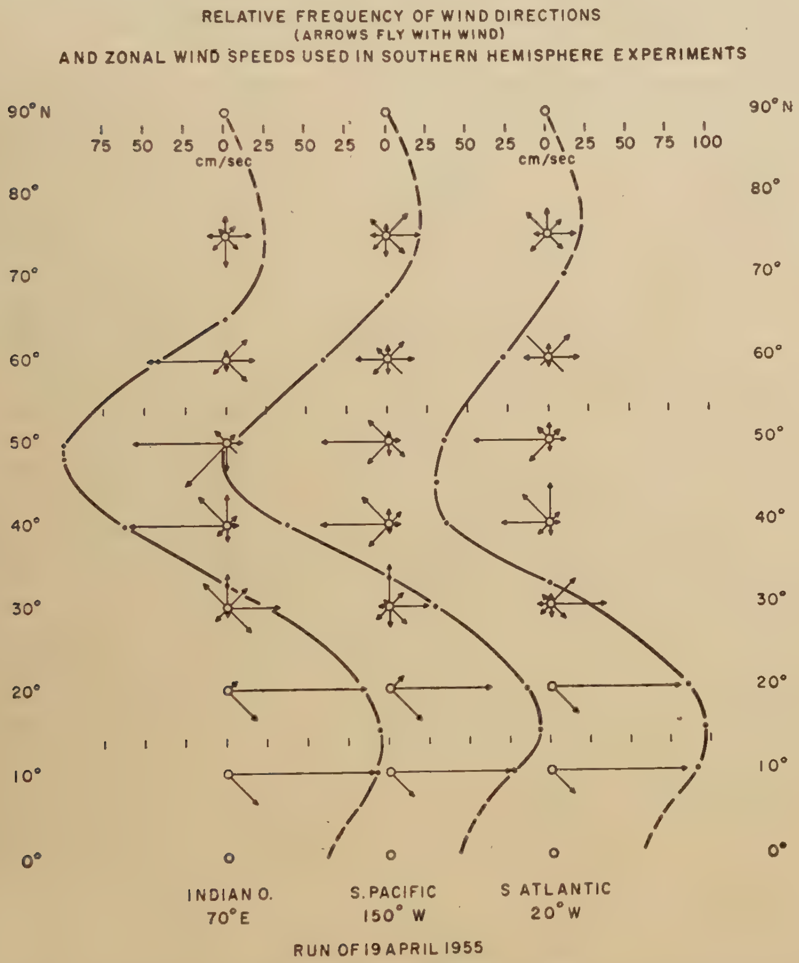

Fig. 8. Frequency of wind direction and zonal wind speeds used in experimental studies of the ocean circulation of the southern hemisphere. The values shown were determined by the methods described in the text.

Factors Still to be Considered

Work with planetary models to date has been concerned with the circulation of homogeneous water under climatological mean wind conditions. Problems obviously requiring attention are the effects on the oceans of seasonal variations in the wind field, studies of shearing instability in the zones of westward intensification, and of the effects of heating and stability on each of these.

In both of the homogeneous fluid models it has been observed that the wind-driven circulation responds rapidly, within a matter of a "week" or two, to changes of seasonal amount in the applied wind field. It is believed that the response of the natural oceans to seasonal change in the atmospheric circulation is both smaller and much slower. It may be that baroclinicity acts in nature as a stabilizing influence or that there are compensating effects between hemispheres in the oceans as well as in the atmosphere. It is a matter of some interest, therefore, to observe experimentally how density fields play their role in the general circulation of the oceans.

The model experiments with homogeneous water demonstrate that barotropic conditions are quite sufficient to maintain a realistic steady state circulation, but by their failure to produce the proper time of response to changing wind fields of seasonal character they suggest that the baroclinic structure of the oceans is required to store potential energy in a less accessible way than by simple lifting against gravity. In the barotropic model potential energy is accumulated as a slight rise of water level in the interior of each ocean gyre. This rise is produced and maintained by the lateral mass transport in the Ekman layer of frictional influence accompanying the wind stress. Beneath the surface layer of frictional influence there is a uniform horizontal gradient of pressure at every level which supports the geostrophic motion of the interior fluid. At the bottom, friction prevents geostrophic motion and there is some transport down the pressure gradient, but this loss is amply compensated by the more vigorous frictional transport up the pressure gradient at the surface. Dyes injected into the surface and bottom friction layers are selectively distributed on the sides of geostrophic currents, and with further dispersion and mixing by the interior circulations they eventually tint the ocean model in a manner which resembles the areal pattern of water masses observed in the layer above the main thermocline of the natural oceans. It seems probable that one need only substitute a difference in specific volume for the dyes to produce baroclinic structures in the pathways of geostrophic motion in middle depths.

In an attempt to study this effect, a rotating tank 4 metres in diameter has been constructed and equipped with infra-red heaters to warm the surface layer of the model in low latitudes. The radiation of the heaters is of such a wavelength that the energy is almost completely absorbed within the thickness of the surface friction layer, as is the case in nature. Early results with this apparatus show that in addition to being applied to only a thin layer the heating must be very slow for the transport of the friction layer to carry a large fraction of the warmed water to the interior of each ocean compartment without appreciable conduction or diffusion vertically downward in the zone of surface heating.

There may be meaning in these results to the extent that the influence of climate on the natural oceans is similarly weak and shallow, permitting the friction layer to transport warm surface water from the tropics to the interior of the wind-driven gyre in each ocean and with the result that the main thermocline lies deeper there than in the zone of maximum surface heating. Furthermore, if it is essential that the heating and deepening of the central water masses of the natural oceans take place very slowly to occur where they do, and the

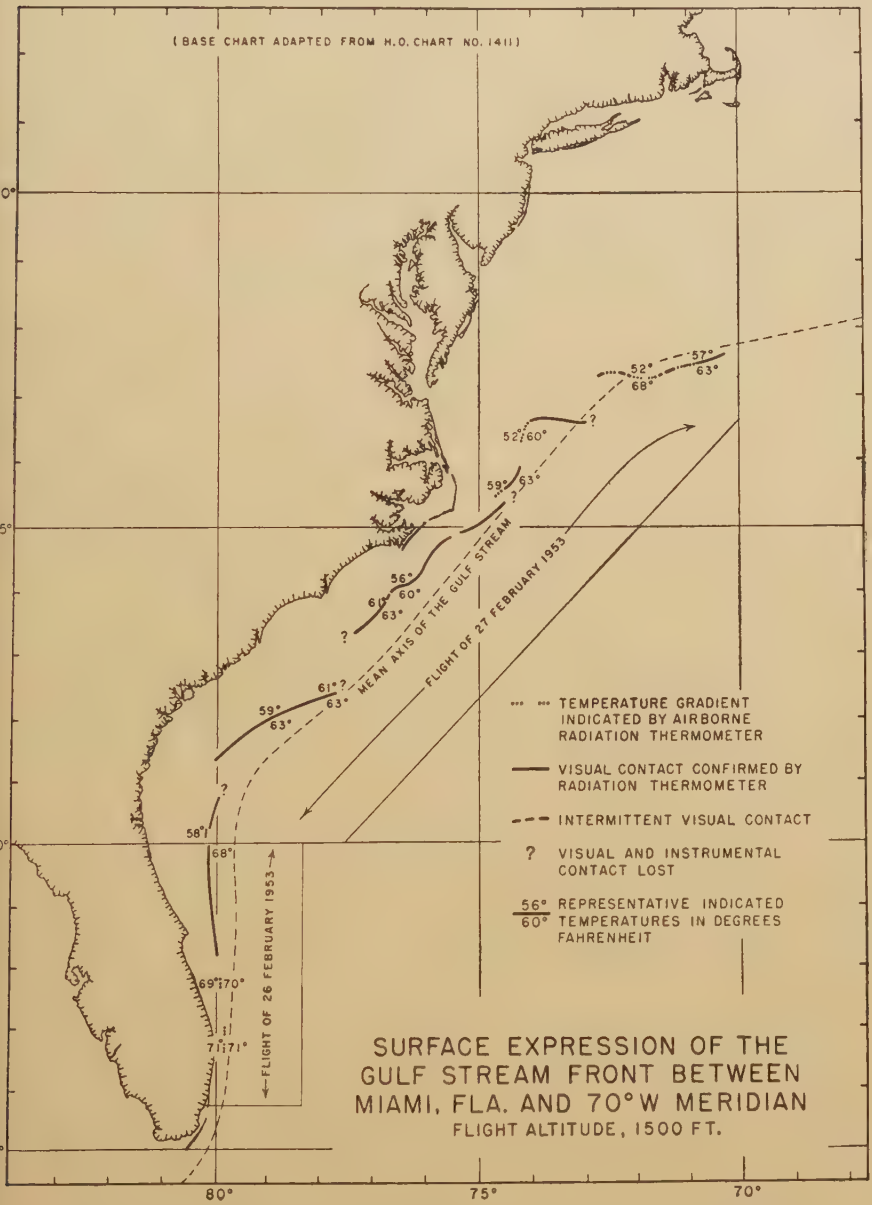
(BASE CHART ADAPTED FROM H.O. CHART NO. 1411)
40°
35°
30°
25°
80°
75°
70°
52°
57°
63°
68°
52°
60°
59°
63°
56°
60°
61°
63°
61°
63°
59°
63°
58°
68°
69°
70°
71°
71°
?
MEAN AXIS OF THE GULF STREAM
FLIGHT OF 27 FEBRUARY 1953
FLIGHT OF 26 FEBRUARY 1953
TEMPERATURE GRADIENT INDICATED BY AIRBORNE RADIATION THERMOMETER
VISUAL CONTACT CONFIRMED BY RADIATION THERMOMETER
INTERMITTENT VISUAL CONTACT
? VISUAL AND INSTRUMENTAL CONTACT LOST
56° / 60° REPRESENTATIVE INDICATED TEMPERATURES IN DEGREES FAHRENHEIT
SURFACE EXPRESSION OF THE GULF STREAM FRONT BETWEEN MIAMI, FLA. AND 70°W MERIDIAN
FLIGHT ALTITUDE, 1500 FT.

Fig. 10. The surface expression of the Gulf Stream Front observed from the air during 26–27 February, 1953. Structures of a similar nature have been observed in the northern-hemisphere models.

barotropic mode of the wind-driven circulation is capable of being excited within a matter of a few weeks or months, then it seems probable that the shape of the main thermocline and the geographic distribution of baroclinicity in the upper layer of the oceans is both consequent and subsequent to the pattern of the wind-driven circulation. A comparison of experimental results obtained by heating without wind stress, with those involving wind stress without heating should clarify this matter.

In the course of recent work it has been found that the swift western currents are very unsteady features in the models as well as in nature. There is no assurance that the character of the unsteadiness bears any resemblance to that in nature, but the coincidence of instability at these vastly different scales does prompt curiosity. The peculiar frontal structure of the Gulf Stream and short-term fluctuations in velocity which appeared in the northern-hemisphere models has been given preliminary study in the field (von Arx, Bumpus, and Richardson, 1955). Some of these results are shown in Fig. 10.

As a matter of further verification it would be interesting to examine the behaviour of the Agulhas Current in response to seasonal changes in the trade/westerly wind-stress ratio suggested by both the southern-hemisphere model and Merz's work (1925), and to see if the stagnation area in the Southern Ocean at latitude 60°S on the 180° meridian really exists.

CONCLUSION

Considering the relative simplicity of the ocean model experiments, it is a pleasant surprise that the circulation is reproduced in recognizable form. Moreover, the few ingredients employed thus far seem sufficient to account for some of the features of the ocean surface motion that have been interpreted only with reference to a much greater variety of forces. It is to be hoped that with continued effort along these lines the order of importance of the major physical factors involved in the ocean-atmosphere system may be discerned and their relationships identified clearly enough to aid in the interpretation of field data as well as to suggest problems for theoretical study.

REFERENCES

Allen J. (1947) *Scale Models in Hydraulic Engineering.* Longmans Green & Co., London. 407 pp.

Birkhoff G. (1950) *Hydrodynamics—A Study of Logic, Fact, and Similitude.* Princeton Univ. Press. 186 pp.

Bridgeman P. W. (1931) *Dimensional Analysis.* Yale Univ. Press, New Haven (2nd Ed.), 113 pp.

Deacon G. E. R. (1933) A general account of the hydrology of the South Atlantic Ocean. "*Discovery*" *Reports* 7, 171–238.

Deacon G. E. R. (1937) The hydrology of the Southern Ocean. "*Discovery*" *Reports* 15, 1–124.

Defant A. (1932) *Die Wissenschaftliche Ergebnisse der Deutschen Atlantische Expedition* "*Meteor*", Bd. VII, Teil (1), Berlin-Leipzig. 318 pp.

Schott (1942) *Weltkarte sur übersicht Meereströmungen.* Deutschen Seewarte, Hamburg.

Exner F. M. (1923) Über die Bildung von Windhosen und Zyklonen. *Z.B. Akad. Wiss. Wein, Abt.* IIa, 132, 1–16.

Exner F. M. (1925) *Dynamische Meteorologie.* Julius Springer, Wien. 421 pp. (see p. 341).

Faller A. J. (1956) A demonstration of fronts and frontal waves in atmospheric models. *J. Meteor* **13** (1), 1–4.

Faller A. J. and von Arx W. S. (1955) On the variation of the Coriolis parameter and its simulation in models of the ocean circulation. *Woods Hole Oceanogr. Inst. Tech. Rept., Ref. No.* 55–13 (unpublished manuscript).

Fishenden M. and Saunders O. A. (1950) *An Introduction to Heat Transfer.* Oxford Univ. Press, London. 205 pp.

Fultz D. (1951) Experimental analogies to atmospheric motions. In *Compendium of Meteorology.* Amer. Meteor. Soc., Boston. 1235–1248.

Görtler H. (1944) Einige Bemerkungen über Strömungen in rotierenden flüssigkeiten. *Z. angew. Math. Mech.*, 24, 210–214.

Hide R. (1953) Fluid motions in the earth's core; and some experiments on thermal convection in a rotating fluid. *Symposium on Model Experiments, Dept. Civil Eng., Johns Hopkins Univ.*

Lasareff P. (1929) Sur une méthode permettant de démontrer la dependence des courants océaniques des vents alizes et sur le rôle des courants océaniques dans le changement du climat aux époques géologiques. *Gerlands Beitr. Geophys.*, 21, 215–233.

Long R. R. (1951) A theoretical and experimental study of the motion and stability of certain atmospheric vortices. *J. Meteor.*, **8**, 207–221.

Long R. R. (1954) Note on Taylor's "Ink Walls" in a rotating fluid. *J. Meteor.* **11** (3), 247–249.

Merz A. (1925) Die Deutsche Atlantische Expedition auf dem Vermessungs und Forschungsschiff *Meteor. I Bericht. XXXI Sitz. Preuss. Akad. Wiss.*, 562–586.

Mintz Y. and Dean G. (1952) The observed mean field of motion of the atmosphere. *Geophys. Res. Pap. No.* 17, *Geophys. Res. Dir., U.S. Air Force.* 65 pp.

Mortimer C. H. (1955) Some effects of the earth's rotation on water movements in stratified lakes. *Proc. Int. Assoc. Theoret. & Appl. Limnology*, XII, 66–77.

Munk W. H. (1950) On the wind-driven ocean circulation. *J. Meteor.* **7** (2), 79–93.

Rattray M. Jr. and Lincoln J. H. (1955) Operating characteristics of an oceanographic model of Puget Sound. *Trans. Amer. Geophys. Un.* **36** (2), 251–261.

Rossby C.-G. (1926) On the solution of problems of atmospheric motion by means of model experiments. *Mon. Wea. Rev. Wash.* **54**, 237–240.

Rouse H. (1938) *Fluid Mechanics for Hydraulic Engineers.* McGraw-Hill, New York. 422 pp.

Rouse H. (1946) *Elementary Mechanics of Fluids.* John Wiley & Sons, New York. 376 pp.

Schott G. (1935) *Geographie des Indischen und Stillen Ozeans.* C. Boysen, Hamburg. 413 pp.

Schott G. (1942) *Geographie des Atlantischen Ozeans.* C. Boysen, Hamburg. 438 pp.

Shaw Sir N. (1931) The surface wind and geostrophic wind at sea level. *Manual of Meteorology*, Vol. 4 (revised), Cambridge Univ. Press. 95–112.

Spilhaus A. F. (1937) Note on the flow of streams in a rotating system. *J. Mar. Res.* **1**, 29–33.

Starr V. P. (1954) Studies of the atmospheric general circulation. *Final Report I, General Circulation Project, Geophys. Res. Dir., U.S. Air Force.* 534 pp.

Stevens J. C. *et al.* (1942) Hydraulic models. *Manuals of Engineering Practice No.* 25, *Amer. Soc. Civil Eng.* 110 pp.

Stommel H. (1948) The westward intensification of wind-driven ocean currents. *Trans. Amer. Geophys. Un.* **29**, 202–206.

Sverdrup H. U. (1947) Wind-driven currents in a baroclinic ocean; with applications to the equatorial currents of the Eastern Pacific. *Proc. Nat. Acad. Sci.* **33**, 318–326.

Sverdrup H. U. (1954) Oceanography. In *The Earth as a Planet.* G. P. Kuiper (Ed.), Univ. Chicago Press. 215–256.

Taylor G. I. (1921) Experiments with rotating fluids. *Proc. Roy. Soc., Lond. A*, 100, 114–121.

Thomson J. J. (1892) On the grand currents of atmospheric circulation. *Phil. Trans. Roy. Soc., Lond. A*, 183, 653–684.

Vettin F. (1857) Meteorologische Untersuchungen. *Ann. Phys. Leipzig*, Vol. 2 (100), 99–110.

Vettin F. (1884) Experimentelle Darstellung von Luftwegungen unter dem Einfluss von Temperatur-Unterschieden und Rotations-Impulsen. *Meteor. Zeit.* 1, 227–230, 271–276.

von Arx W. S. (1952) A laboratory study of the wind-driven ocean circulation. *Tellus* **4**, 311–318.

von Arx W. S. (1954) Circulation systems of Bikini and Rongelap Lagoons. In *Bikini and Nearby Atolls, Part* 2, *Oceanography.* U.S. Geol. Survey Prof. Pap. 260-B-I, 265–273.

von Arx W. S. (1955) An experimental study of the dependence of the primary ocean circulation on the mean zonal wind field. Doctoral dissertation, Mass. Inst. Tech., Dept. of Meteor.

von Arx W. S., Bumpus D. F., and Richardson W. S. (1955) On the fine structure of the Gulf Stream Front. *Deep-Sea Research* **3**, 46–65.

Contribution No. 828

INTERACTION OF SEA AND ATMOSPHERE:

a group of contributions

by

A. C. Redfield, A. R. Miller;
G. W. Groves; D. L. Harris;
R. O. Reid;
W. Marks and J. Chase.

WATER LEVELS ACCOMPANYING ATLANTIC COAST HURRICANES[1]

By ALFRED C. REDFIELD[2] and A. R. MILLER[3]

Woods Hole Oceanographic Institution

(Manuscript received 13 February 1956)

ABSTRACT

The water levels that occurred along the Atlantic coast during five recent hurricanes are described and compared. The forerunner, a rise in water level which may precede the passage of the storm by many hours, is found to depend upon the force and direction of the general wind field into which the storm advances. The surge that accompanies the violence of the storm depends in duration on the speed of progression of the storm center. Maximum water levels of 8 to 9 ft above the predicted tide developed at positions between 40 and 100 n mi to the right of the storm center; elevations in excess of 5 ft occurred from 50 n mi to the left to 150 n mi to the right of the center.

Although the elevation of the surge appears to depend primarily on the distance and direction from the storm center, local topography and the structure of the wind field may influence the effects of individual storms. The wind fields of the storms which have crossed the latitude of southern New England are characterized by convergence zones at which the wind direction shifts abruptly. The distribution of these convergence zones relative to the storm center is variable. It appears to account for the degree to which the surge extends into the left semicircle of the storm, and for the time at which maximum water levels occur.

Following the passage of the storm center, resurgences occur which are attributed to the motion of the disturbed water in returning to normal elevations. Examples include: (1) a surging of water, impounded by the wind on one side of Buzzards Bay, to the opposite shore when the wind shifts; (2) a solitary wave which traverses Long Island Sound producing a surge which arrives at its western end approximately 4 hr after the storm's passage; and (3) undulations of the sea surface on the open coast having periods of 5.5 to 7.2 hr depending on the location.

The nature of the surge, its character on oceanic islands, its relation to tidal phenomena, and the value of past experience as a guide to future hazard are discussed.

1. Introduction

More than three-fourths of all loss of human lives in tropical cyclones has been due to inundations [31], and similar proportions must apply to property damage. Yet, until recently, very little systematic information has been compiled on the disturbances of the sea surface that accompany these marine storms; a fact which contrasts with the attention their meteorological characteristics have received [2]. There exist, of course, records of the extreme heights of water experienced during many of the more disastrous hurricanes and typhoons. The generalizations which emerge from a study of the historical record are, that the development of extreme water levels depends on the slope of the ocean bed and the contour of the coast line, that the elevations are greatest to the right of the storm center,* that water levels are exaggerated in embayments, and that the principal inundation usually occurs on the left bay shore [31]. More recently, detailed studies have been made of the water levels produced by hurricanes on the coast of the Gulf of Mexico [5; 6; 7; 13], and by typhoons in the embayments of the coast of Japan [35]. The description of what actually happens when tropical cyclones cross the coast of the North Atlantic states is entirely inadequate.

---

[1] Contribution No. 828 from the Woods Hole Oceanographic Institution. Supported in part under contracts with the U. S. Weather Bureau and the Office of Naval Research.

[2] Associate Director, Woods Hole Oceanographic Institution, Woods Hole, Mass.

[3] Research Associate in Physical Oceanography, Woods Hole Oceanographic Institution, Woods Hole, Mass.

* EDITOR'S NOTE: Every mention of right and left "handedness" in this monograph refers to conditions in the Northern Hemisphere. Interchanging *right* for *left*, and vice versa, will make sentences in the text containing these terms read correctly for conditions in the Southern Hemisphere.

Prior to 1938, New Englanders considered their coast to be immune from severe hurricane damage. However, Tannehill [31] lists nine severe tropical storms in New England since 1635, a total brought to 12 by the recent hurricanes. A recent review lists 40 tropical cyclones which have passed within 200 n mi of Providence, R. I., since 1874. This fact shows that these disturbances not infrequently follow paths potentially dangerous to New England [23]. An analysis of the paths of tropical cyclones, by five-degree squares, indicates that the area most frequently traversed during the past 20 yr lies in the offing of the Gulf of Maine at about 40N, 65W [21]. The probable recurrence of such storms, with the attendant inundations, must be considered along the coast of the northeastern states.

The passage of four severe hurricanes across the coast of southern New England in recent years has provided a substantial quantity of data. Not only is this coast densely populated, but many sheltered bays and harbors exist where extreme elevation of the water could be ascertained. Tide gauges are maintained by the U. S. Coast and Geodetic Survey and the U. S. Army Corps of Engineers. The latter agency surveys the damage and records the water levels after each disaster. The purpose of this paper is to describe and compare the effects of these recent storms on the water levels along the affected coast line, and to call attention to some theoretical problems suggested by the observations.

i. *Data*. This study is based on data for the hurricanes of 21 September 1938, 14–15 September 1944, 31 August 1954 (Carol), 11 September 1954 (Edna), 15–16 October 1954 (Hazel). Fragmentary records of the water levels developed during three earlier severe New England hurricanes are referred to; *viz.*, those of 1636 [3], 1815 [8; 12], and 1821 [27]. The available data consist of tide gauge records supplied by the U. S. Coast and Geodetic Survey and the New York District, U. S. Army Corps of Engineers, and field observations made by the Boston, New York, Norfolk, Wilmington, and Charleston Districts of the Engineer Corps, by the Massachusetts Geodetic Survey, by the Rhode Island Development Council, by the authors, and by other sources listed in the references [16; 22; 23; 32; 33]. Data on hurricanes at Bermuda were supplied by Colonel W. Elliot Stevens of the Bermuda Biological Station for Research. Meteorological data were supplied by the U. S. Weather Bureau.

Departures from mean sea level are due to three principal effects: (1) the stage of the astronomical tide; (2) short-period waves; and (3) changes in the general elevation of the sea surface due to the storm. The latter effect appears to be the principal basis for damage and disaster, and to it we apply the term *water level*.

Although the stage of the astronomical tide may be crucial in determining whether a given storm produces disastrous effects in a given location, it is desirable to eliminate this factor in order to discover the relation of the storm field to general water levels. In a similar way, it is desirable to eliminate wave action from the examination of general water levels. Although wave action may frequently be the final agent in destruction, its effect is determined very largely by the local conditions of exposure.

The water levels reported are estimated as the difference between the observed and predicted elevation of the tide. Wave action is eliminated satisfactorily by the tide gauge, but where there are uncertainties in the local tidal constants, or where the tide curve is distorted by shallow water and other effects, errors in the estimated water level may be present. This is particularly true for values at the times when the tidal elevation is changing rapidly. Interpretations of field observations are subject to large error, because the reported elevations are due to wave action as well as to the general level about which the waves oscillate. Additional error is introduced by the uncertainty of the time at which maximum levels occurred.

The water levels estimated from the tide gauge records available for the period of the several storms are shown in fig. 2–6.

ii. *Phenomena to be discussed*. The recent storms have followed the diverse paths across the New England coast shown in fig. 1. The effects produced on water levels at any one place have differed from storm to storm. Certain regularities in the water level changes are apparent when the course of the storms relative to the geography of the coast are examined. Because these phenomena are discussed from a comparative viewpoint, a treatment which obscures the picture of each storm as a whole, the storms are reviewed individually in section 6.

The disturbed water levels associated with the passage of hurricanes are discussed under three categories: *forerunners*, the *hurricane surge*, and *resurgences*.

1. A *forerunner* is the gradual rise in sea level along the coast which precedes the arrival of the cyclone, and which may occur while the storm center is at a

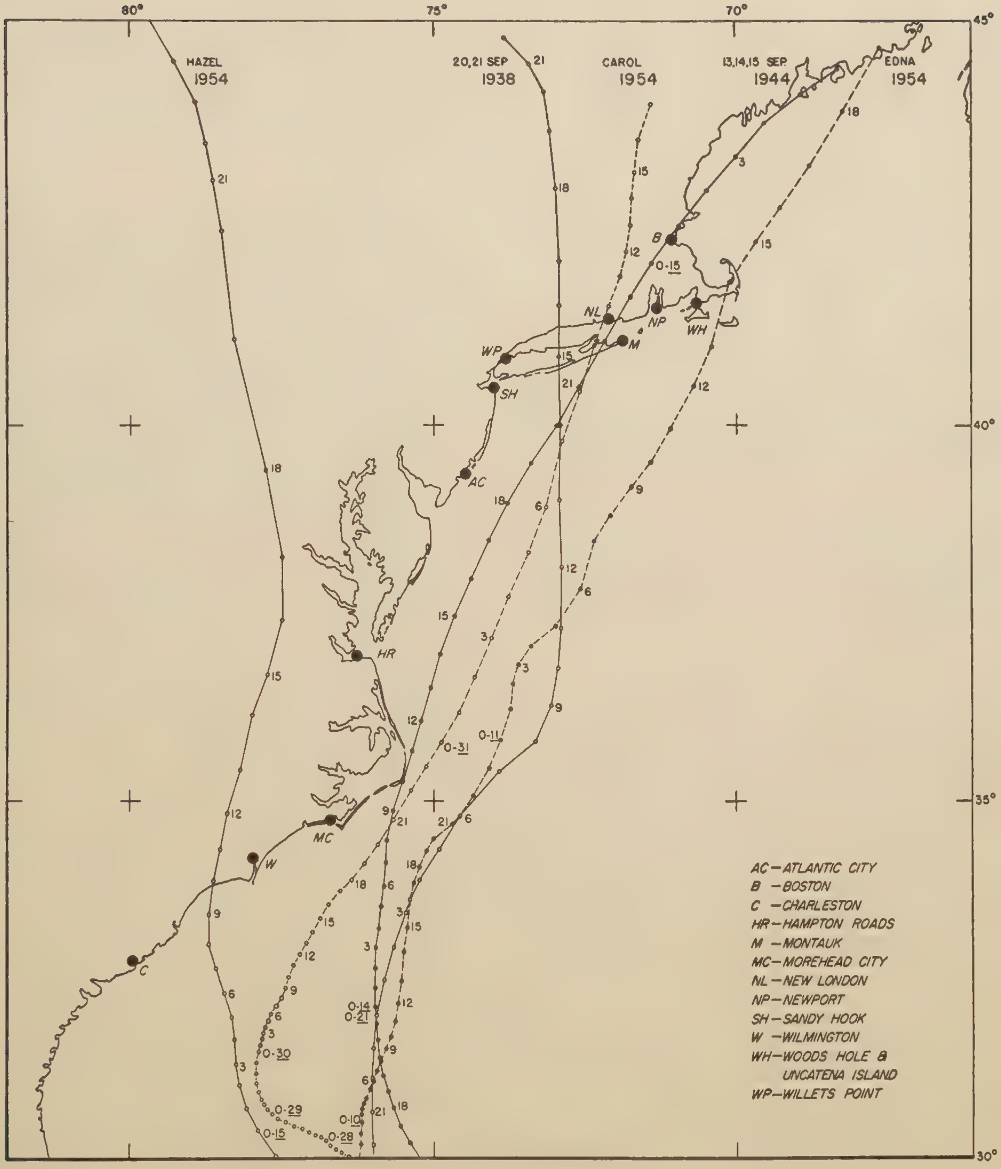
80°
75°
70°
45°
40°
35°
30°
HAZEL 1954
20,21 SEP 1938
CAROL 1954
13,14,15 SEP 1944
EDNA 1954
B
NL
NP
WH
M
WP
SH
AC
HR
MC
W
C
AC—ATLANTIC CITY
B —BOSTON
C —CHARLESTON
HR—HAMPTON ROADS
M —MONTAUK
MC—MOREHEAD CITY
NL—NEW LONDON
NP—NEWPORT
SH—SANDY HOOK
W —WILMINGTON
WH—WOODS HOLE & UNCATENA ISLAND
WP—WILLETS POINT

Fig. 1. Tracks of the recent New England hurricanes. *Solid circles:* Position of tide gauges. *Points on curves:* Hourly position of storm center.

great distance from the coast irrespective of whether it reaches the point of observation.

2. The *hurricane surge* is the sudden and substantial rise in water level which accompanies the violent winds of the storm. It is the primary basis for damage by high water levels.

3. *Resurgences* include a number of phenomena which occur after the passage of the storm center. They may be attributed in general to the free motion of the water in returning to the normal level, but are augmented in some cases by wind blowing in a changed direction.

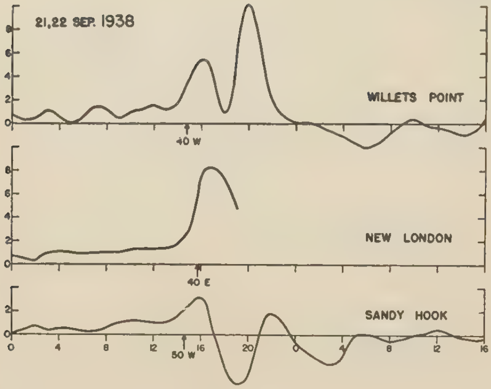

FIG. 2. Water levels recorded by tide gauges during hurricane of 21–22 September 1938. *Ordinate:* Elevation above predicted tide (ft). *Abscissa:* Time EST. *Arrows:* Time of nearest approach of center, distance (n mi) and direction of tide gauge from storm track.

In interpreting these disturbances, it is recognized that changes in water level may arise from local changes in barometric pressure, and from the transport of water due to wind stress, acting singly or in combination. The separation of the causes is not simple when transient moving disturbances, which may involve resonance, are considered. Consequently, no attempt is made to correct the reported water levels for the effects of barometric pressure, except in a few special situations.

2. Forerunners

i. *Characteristics.* Cline called attention to a gradual rise in sea level which preceded the arrival of hurricanes on the coast of the Gulf of Mexico, and suggested that such forerunners might be of value in predicting the arrival of the storms [5; 6; 7]. He observed that sea level commenced to rise above the predicted tidal level one or two days prior to the arrival of the storm. In one case this occurred while the center was as much as 800 n mi distant. Extra elevations of several feet developed before the more rapid rise characteristic of the surge proper. Cline attributed these forerunners to the transport of water by swells which have been long recognized to run out in advance of tropical cyclones.

The data for the recent storms show that the water levels tended to rise gradually many hours in

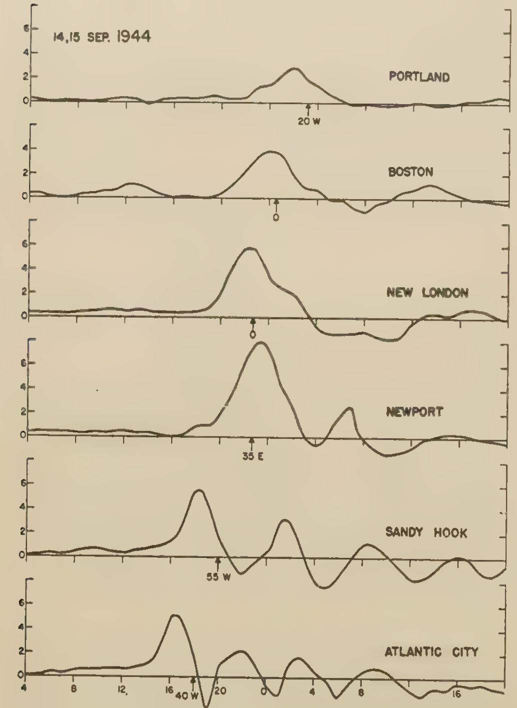

FIG. 3. Water levels recorded by tide gauges during hurricane of 14–15 September 1944. See legend fig. 2 for explanation.

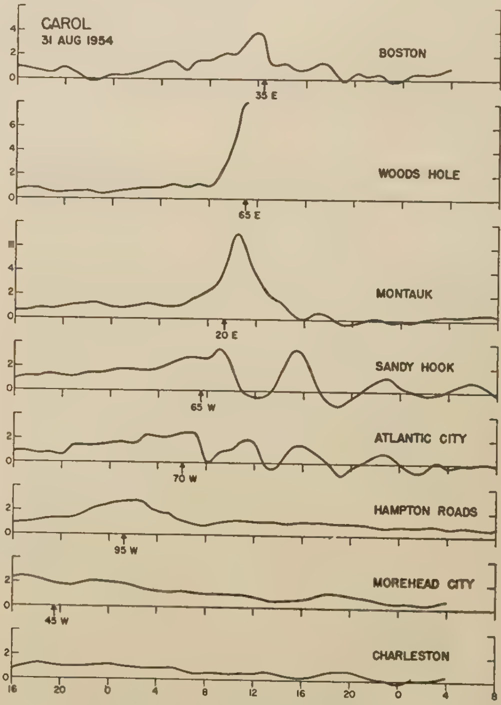

FIG. 4. Water levels recorded by tide gauges during hurricane Carol, 31 August 1954. See legend fig. 2 for explanation.

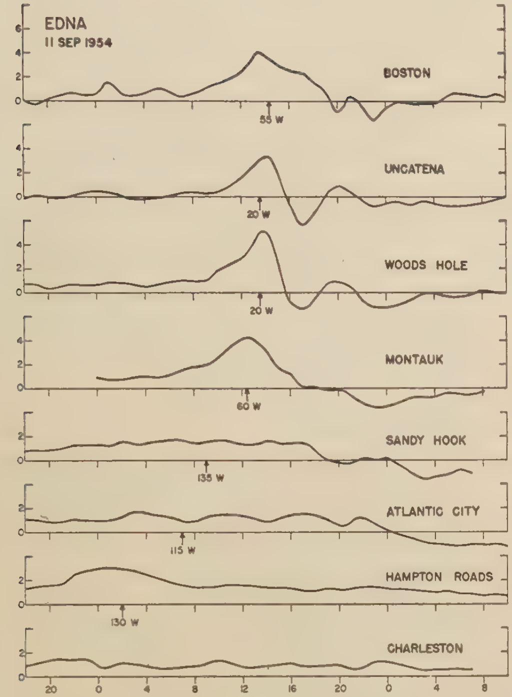

Fig. 5. Water levels recorded by tide gauges during hurricane Edna, 11 September 1954. See legend fig. 2 for explanation.

advance of the passage of the storm center. If the tide gauge lay within 50 n mi to the left of the storm track, or 100 n mi to the right of it, the rate of rise of the water level increased to more than 1 ft per hr beginning 3 or 4 hr before the passage of the center. This rapid rise is called the *hurricane surge*, and the more gradual rise which precedes it is the *forerunner*. In fig. 2–6, an arrow indicates the time when the storm center was closest to the station in question; the associated notation gives the distance in nautical miles and the position of the tide gauge, east or west, relative to the storm track.

The development of forerunners is quite variable. Excellent examples developed at Atlantic City and Sandy Hook during the storm of 1938, and during hurricanes Carol and Hazel (fig. 2, 4, 6). At Atlantic City during hurricane Carol, the rise in sea level began before the storm center passed Cape Hatteras, 260 n mi to the south. It continued for 8 to 12 hr when, following the passage of the center and the attendant wind shift, it dropped abruptly. The fall in level was followed by a remarkable series of oscillations which are discussed under the heading *resurgences*.

In the case of the storm of 1944 (fig. 3), which passed close to the coast, the forerunner was weaker, the principal rise in water level at Atlantic City and Sandy Hook being attributable to a surge. Hurricane Edna (fig. 5), which passed more than 100 n mi from the coast, was not attended by any significant forerunner. In contrast to those from the New Jersey coast, the tide gauge records from Montauk and from southern New England show only trivial increases in water levels in advance of the surge.

ii. *Factors associated with the development of forerunners.* Possible causes of the forerunners are the transport of water by swells running out in advance of the storm [7], compensations of sea level for barometric pressure, and the effect of the wind field in advance of the storm.

The water levels developed at Atlantic City during four storms are assembled in fig. 7, together with the wind force and direction at that station and the effects attributable to barometric pressure. The forerunners appeared long in advance of any significant fall in barometric pressure, as noted by Cline for the Gulf coast hurricanes. The rise in water level that would compensate for the reduced barometric pressure

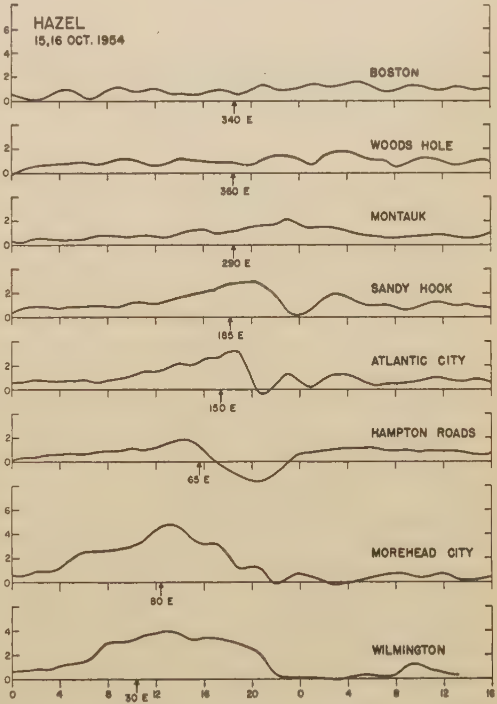

Fig. 6. Water levels recorded by tide gauges during hurricane Hazel, 15–16 October 1954. See legend fig. 2 for explanation.

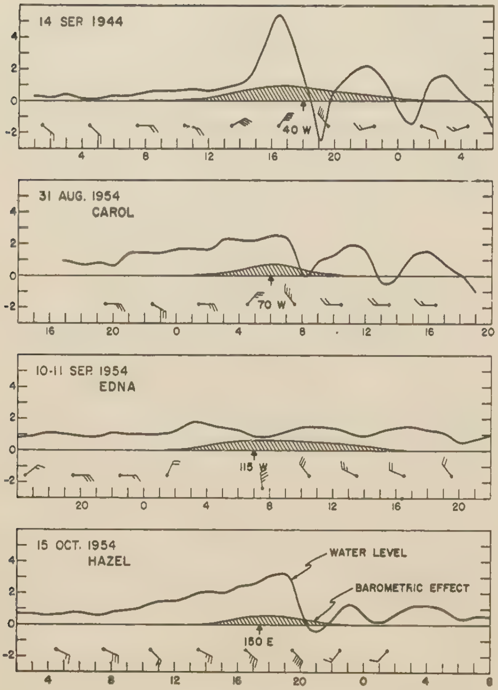

Fig. 7. Comparison of water levels at Atlantic City during four storms. *Solid line:* Water level. *Shaded area:* Estimated equilibrium effect of barometric pressure on sea level. *Barbed shafts:* Wind vector (Beaufort scale) at Atlantic City. Other specifications same as fig. 2.

was inadequate to account for the observed rise in water level.

Wind appears to be the major factor responsible for the development of forerunners at Atlantic City. The best developed forerunners accompanied hurricanes Carol and Hazel when easterly or southeasterly winds in excess of force 4 (16 kt) prevailed for 10 hr in advance of the storm passages. The fact that the water levels dropped abruptly, when the wind shifted to a westerly direction at the storm passages, is additional evidence that the wind was responsible for the forerunners.

In the hurricane of 1944, the forerunner was less pronounced and the wind speed at Atlantic City did not exceed 16 kt until the arrival of the surge shortly before the storm passage. Hurricane Edna did not produce any definite forerunner. Easterly winds of variable strength backed to the north about seven hours before the passage of the center 115 n mi offshore, and blew parallel to the coast with increasing intensity as the storm approached. It is reasonable to assume that winds from this quarter would not greatly increase the water level at Atlantic City [17]. A similar explanation will account for the limited development of forerunners at Montauk and along the coast of southern New England, since the trend of the coast at these locations is easterly and thus parallel to the winds that preceded the storms.

The data do not preclude the possibility that swell may be responsible in part for increasing water levels ahead of the storms. Atmospheric pressure certainly contributes something to the effect. Even though there may be other causes in operation, it is evident that the magnitude of the forerunners of Atlantic coast hurricanes is dominantly controlled by the strength and direction of the general wind field over adjacent coastal waters.

3. The hurricane surge

i. *Maximum water levels recorded.* At positions along the outer coast, the maximum water levels recorded by tide gauges during hurricanes have been 8 to 9 ft above the predicted tide. The destruction of tide gauges under extreme conditions, or their absence from critical positions, may have prevented the recording of greater elevations. The recorded observations from Japanese typhoons [35] suggest that 10 ft is about the maximum "still water" level to be expected along the Japanese coast.

Many field observations from exposed positions on the Long Island, Rhode Island, and Massachusetts coasts report elevations of 15 to 18 ft, but these probably include wave action effects.

In confined embayments, such as Buzzards Bay, Narragansett Bay, and Long Island Sound, there is unquestionable evidence that greater levels (up to 15 ft above the normal tide) have occurred repeatedly. Such water levels have occurred also in the case of hurricanes which have crossed the coast of the Gulf of Mexico [13].

ii. *The time course of the surge.* Records of the surges observed during the present storms are illustrated in fig. 8. The sharpness of the peak appears to be a characteristic of the storm, being greatest in the

Table 1. Relation of duration of surge to size and speed of storm

Storm	Time half-level preceded maximum level (hr)	Speed at coast (kt)	Diameter of 980 mb isobar (n mi)	Time pressure <980 mb (hr)
1938	1.0–1.5	52	168	3.2
1954 Carol	1.1–1.3	40	114	2.9
1944	2.1–2.2	36	150	4.2
1954 Edna	2.0–3.0	34	162	4.8
1954 Hazel	3.0–5.0	25	162	6.5

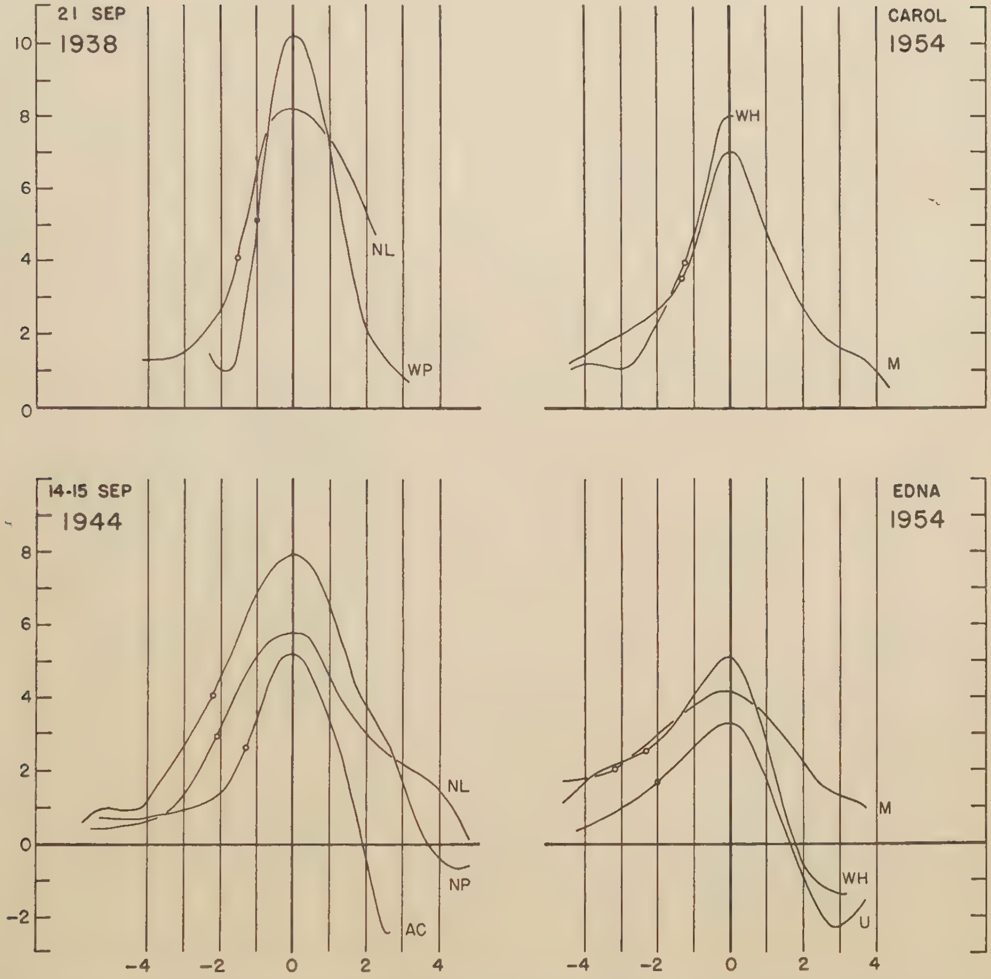

FIG. 8. Comparison of the surges recorded by tide gauges during four storms. *Ordinate:* Elevation of water level above predicted tide (ft). *Abscissa:* Time relative to occurrence of maximum elevation (hr). *Circles:* Time when elevation was half maximum. *Location code:* AC—Atlantic City; M—Montauk; NL—New London; NP—Newport; WP—Willets Point; WH—Woods Hole; and U—Uncatena Island.

hurricane of 1938 and in hurricane Carol. Broader peaks were recorded during the storm of 1944 and hurricane Edna. However, during the 1944 storm, the peaks recorded at Atlantic City and Sandy Hook were of short duration. During hurricane Hazel, the increased elevation of the water developed slowly at Morehead City and Wilmington, N. C., and persisted for many hours after the passage of the storm center without showing any clear separation of forerunner and surge.

The rapidity with which the surges developed is indicated quantitatively by the *half-level time, i.e.,* the time required to develop from one-half the maximum to the maximum water level achieved. For the storms crossing the New England coast, the half-level time varied from about 1.25 hr to more than 2 hr (table 1). In these storms, the rate at which the water level fell after reaching the maximum was more variable than that of the rise. In general, however, the peak is nearly symmetrical. Water levels of one-half the maximum have been maintained for 2.5 to 4.5 hr depending on the sharpness of the surge.

The sharpness of the surge, as expressed by the half-level time, appears to vary directly with the

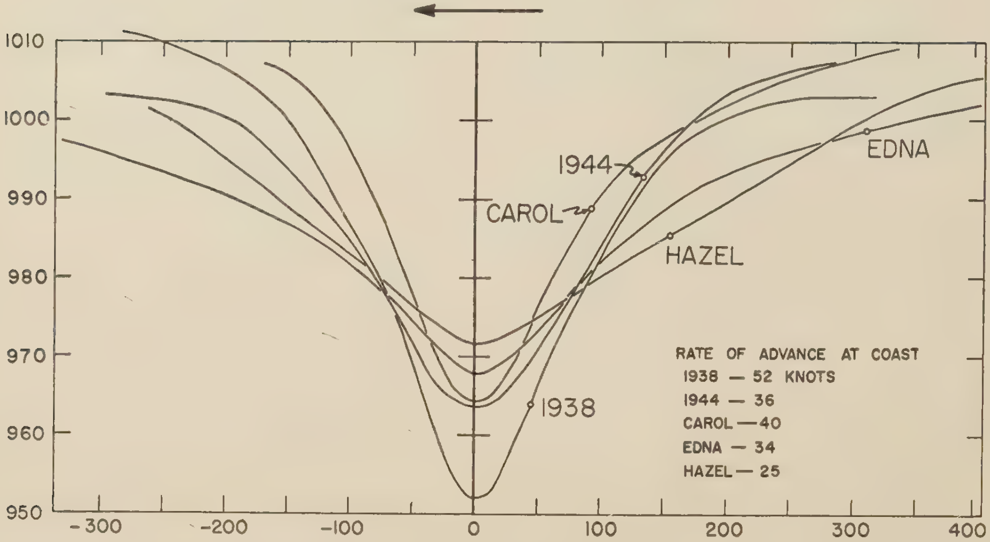

Fig. 9. Barometric pressure along path of storms at time of crossing coast. *Ordinate:* Pressure (mb). *Abscissa:* Distance from center (n mi). *Arrow:* Direction of storm movement.

speed of the storms at the time they crossed the coast (see table 1). The sizes of the depressions associated with these storms did not differ greatly, as shown in fig. 9. If the diameter of the 980 mb isobar is taken as an arbitrary measure of the size of the depression, and is divided by the speed, the time during which the pressure was less than 980 mb is obtained. The result, shown in the right-hand column

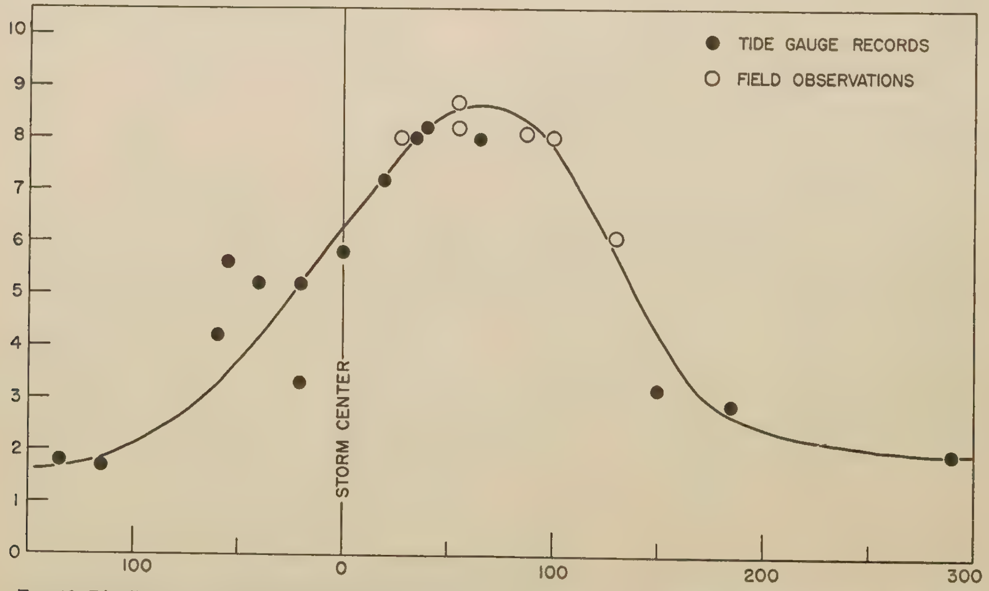

Fig. 10. Distribution of maximum water levels, recorded by tide gauges or reliable field observations along outer coast, relative to distance from path of storm center. *Ordinate:* Elevation above predicted tide (ft). *Abscissa:* Shortest distance between station and storm center track (n mi).

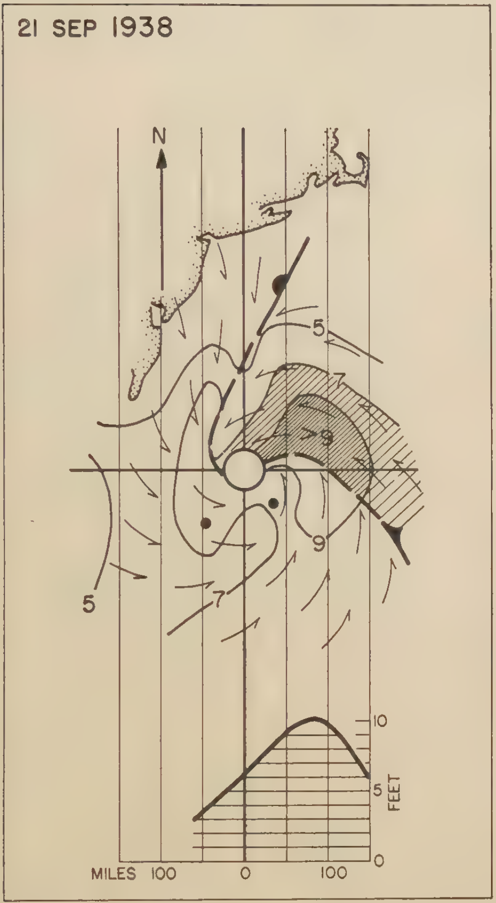

FIG. 11. Diagram of wind field of hurricane, 21 September 1938, as it crossed coast moving at 52 kt. *Contours:* Isotachs (Beaufort scale). *Curved arrows:* Streamlines. *Dashed lines:* Directional convergence area dividers. *Shaded areas:* Distribution of winds of greatest flood-producing potential. *Vertical lines:* Parallels to storm center trajectory. *Heavy arrow:* True north; coast outline shown relative to storm trajectory. *Solid circles:* Position in wind field at which maximum levels were attained. *Below:* Graph of maximum water levels reported on coast along storm trajectory.

of table 1, is about twice the half-level time of the surge. This is a reasonable relationship if the duration of the surge depends on the time of passage of the violent part of the storm.

iii. *Relation of the surge to the path of the storm.* The distribution of maximum water levels along the coast to the right and left of the path of the storm centers is shown in fig. 10. This figure is based on existing tide gauge records from the five storms. It is supplemented by field observations, between 75 and 125 n mi to the right of the storm paths, which are believed to be reliable indications of the water levels. Maximum elevations of 8 to 9 ft occurred between 40 and 100 n mi to the right of the storm center; elevations in excess of 5 ft are distributed from 50 n mi to the left, to 150 n mi to the right of the center. Beyond these limits, elevations of a few feet extend for many miles. These elevations are comparable to those brought about by severe gales.

The general impression that disastrous floods tend to occur to the right of the storm path is confirmed by these data. However, field observations along the Carolina coast indicate that the highest water levels, following hurricane Hazel, occurred very close to the point at which the storm center crossed, and that the levels decreased sharply east of Cape Fear, only 40 n mi to the right of the track of the storm center

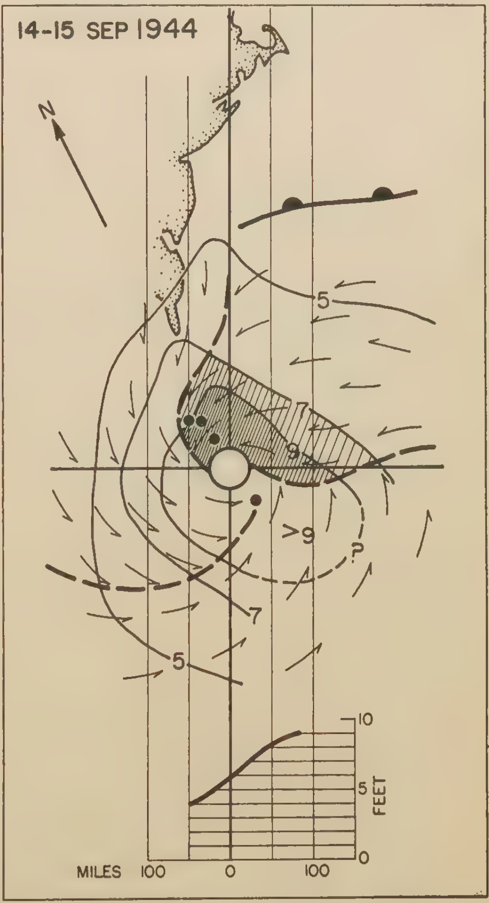

FIG. 12. Diagram of wind field of hurricane of 14–15 September 1944 as it crossed coast moving at 36 kt. For explanation see legend fig. 11.

(fig. 16). The data for Gulf coast hurricanes [13] also indicate that maximum water levels occur close to the center, or only slightly to the right of it. This difference in behavior of the northern and southern storms suggests that important differences may occur, due either to the individual structure of the different storms, or to the topography of the coasts on which they impinge.

iv. *The time of maximum water level.* The time at which maximum water levels occurred, in relation to the passage of the storm center, also differed from storm to storm and from place to place. If the storm center passed close to the tide gauge, maximum levels were attained within one hour before or after the storm passage. Differences in time of highest level can be explained reasonably well by local differences in the exposure of the gauges and by the fact that the wind center and pressure center of a hurricane may not coincide [20]. At positions more remote from the center's path, the time of highest level was much more variable. In the storm of 1944 maximum levels were achieved and the water levels began to fall nearly 2 hr before the passage of the storm center (fig. 3). During hurricane Hazel the high water levels persisted for an equal period after its passage (fig. 6).

These observations also suggest that differences in the structure of storms may acccount for differences in behavior of the water levels that they produce.

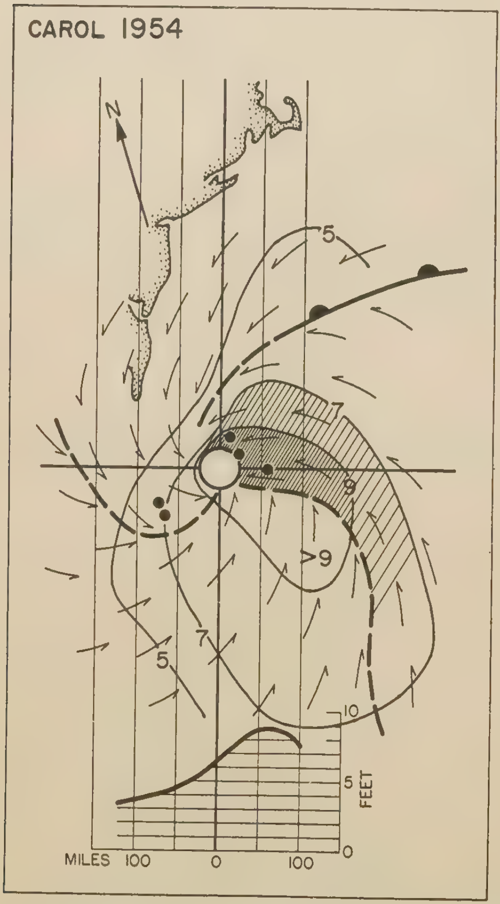

Fig. 13. Diagram of wind field of hurricane Carol, 31 August 1954, as it crossed coast moving at 40 kt. For explanation see legend fig. 11.

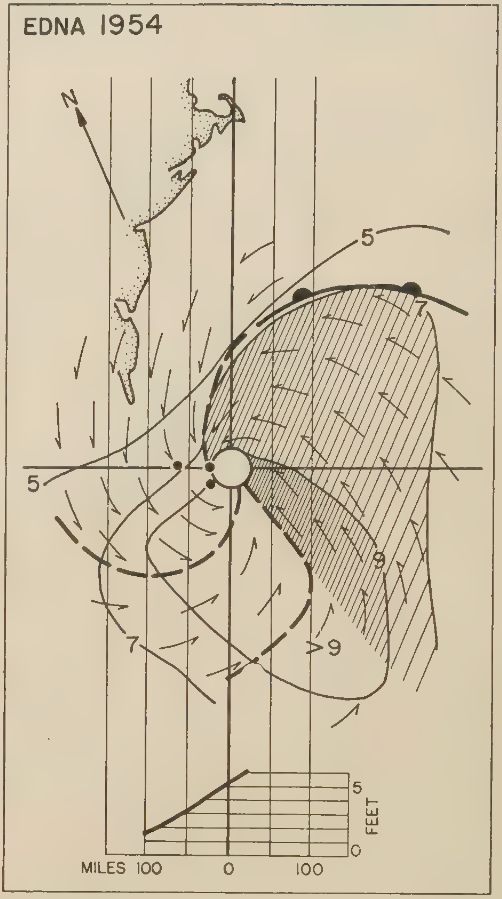

Fig. 14. Diagram of wind field of hurricane Edna, 11 September 1954, as it crossed coast moving at 34 kt. For explanation see legend fig. 11.

v. *The wind fields of New England hurricanes.* In describing the New England hurricane of 1938, Pierce [24] noted that this storm had developed fronts characteristic of extratropical storms before it

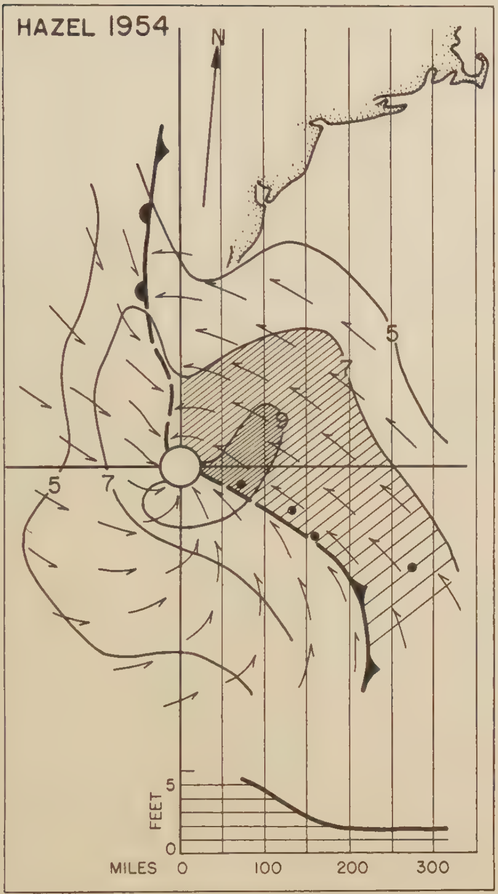

FIG. 15. Diagram of wind field of hurricane Hazel, 15–16 October 1954, as it crossed the North Atlantic states moving at 50–75 kt. For explanation see legend fig. 11.

reached the coast. He also discussed the tendency of tropical cyclones to acquire the properties of extra-tropical storms when they move into a region where there is a definite cold front. In order to examine the structure of the subsequent storms that have crossed the New England coast, the diagrams shown in fig. 11–16 were prepared. In addition to the direction and force of the winds surrounding the storm center, these diagrams indicate the position and angle of the coast relative to the storm movement and the maximum water levels recorded across its path.

The wind fields were obtained by superposing the plotted winds shown on three or four successive three-hourly weather maps as the storm crossed the coast. This procedure served to fill in the seaward quadrants where ship data were meager. From the plotted winds, smoothed streamlines were constructed. The direction of these streamlines are shown by arrows in the diagrams, whereas the contours are isotachs in the Beaufort wind scale. The trajectories of various parts of the moving wind field, as they crossed the coast, are represented by the vertical lines. The solid circles represent the position, within the wind field, of the several tide gauges when maximum water levels occurred, as judged by the trajectory and speed of the storm. The small graph at the bottom of each figure indicates the approximate maximum water levels reached along the coast, as indicated by tide gauge records and field observations.

It is not claimed that these diagrams are exact, but it is believed that they indicate the principal variables acting on each part of the coast during the

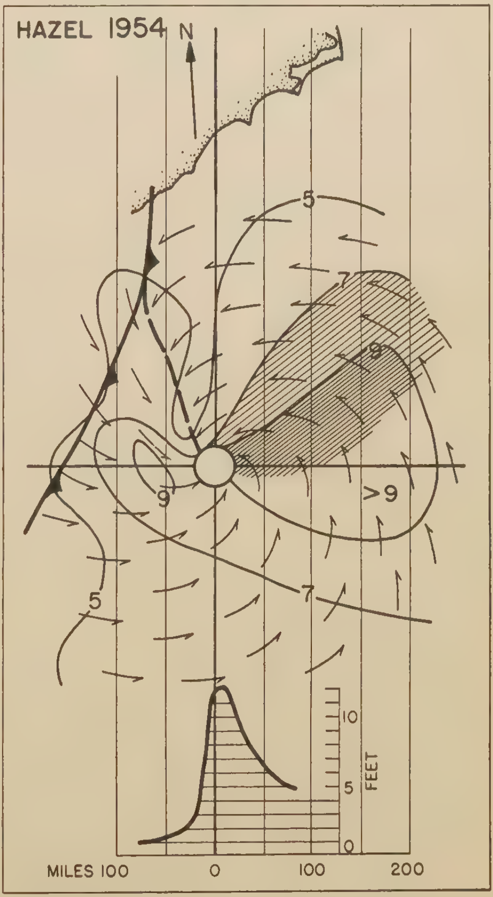

FIG. 16. Diagram of wind field of hurricane Hazel, 15–16 October 1954, as it crossed coast of S. C. moving at 25 kt. For explanation see fig. 11.

passage of the storms; thus, they provide a useful basis for a comparison of the storm effects.

The most striking feature of the diagrams is the presence of as many as three zones of convergent winds, which vary in their position relative to the trajectory of the storm center. These zones are delineated by the heavy dashed lines in the figures.

One area of convergence lies in the right rear quadrant, is marked by a shift of wind from SE toward SW, and traverses the area of maximum wind force. In the case of hurricane Hazel, this convergence zone was associated with peak wind gusts as the storm moved northward across the eastern United States [18]. Arakawa attributed the mountainous seas in the right rear quadrant of a typhoon off Japan to convergence in this position [1].

A second convergence zone usually lies in the forward quadrant of the storm. It enters the center of the storm from the left front quadrant, but extends forward in some cases to cross to the right of the storm track. This convergence zone separates easterly winds from northeasterly or northerly winds. In those storms that follow a trough in their northward movement (1938, Hazel), the convergence areas are continuous with the front.

A third convergence zone may be present in the left rear quadrant, indicated by a shift of wind from a northwesterly to a southwesterly direction (1944, Carol, Edna).

If it is assumed that the exceptional water levels developed during the storms were the direct effect of transport by the wind, and allowance is made for the trend of the coast and the fact that transport is somewhat to the right of the wind direction, it is evident that the winds most likely to have produced the floods lay between the first and second of the convergence zones described above. The area between these zones, in which the wind exceeded 33 kt (Beaufort force 7), has been shaded in the diagrams to indicate that part of the wind field most likely to produce high water levels. These winds, in turn, will be called *effective winds*.

The relative positions of the areas of convergence has varied in different storms. In 1938 and 1944 their positions were such that the area of effective winds was almost entirely in the front semicircle and sometimes projected into the left front quadrant. This appears to account for the presence of a definite surge well to the left of the storm center at Sandy Hook and Atlantic City. Hurricane Edna shows the opposite extreme, with the maximum effective winds confined to the right rear quadrant and only a limited intrusion of effective winds into the left semicircle.

The detailed structure of the wind field in each storm appears to account rather well for the time at which maximum water levels occurred at positions remote from the storm center. In the storm of 1944, when maximum levels at Atlantic City and Sandy Hook occurred well in advance of the passage of the center, the water levels began to fall shortly before the convergence area passed by, causing the wind shift to the north. In the case of hurricane Hazel the water level at these stations was maintained long after the passage of the center, and until just before the arrival of the convergence area in the right rear quadrant.

It is not clear why the maximum water levels were maintained so long at positions to the left of the storm path in the case of the 1938 storm, and of hurricane Carol. Possibly, these levels were maintained by water accumulated along the Long Island coast to the eastward, which moved onto the Jersey coast across the locally prevailing winds as a resurgence similar to that described below for Long Island Sound.

It appears that the wind field, accompanying those hurricanes that have crossed the New England coast, has a complex structure that determines the details of the distribution of water levels across the storm track. The concept of the tropical cyclone as a symmetrical circular wind field, is a simplification that cannot be applied rigorously to account for the detailed effects observed on water levels.

vi. *Local coastal phenomena.* The preceding discussion has been concerned with the general relation of water levels along the outer coast to the wind field of the moving storm. It is based primarily on records from tide gauges. The effects that the local topography of the coast may have in modifying the elevations of the surge will now be examined. For this purpose one must depend upon field observations that are deficient with respect to the time of the maximum inundation.

The maximum water levels recorded along the coast of southern New England for the hurricanes of 21 September 1938 and of 31 August 1954 (Carol), and the time of their occurrence, are shown in fig. 17–20. The other storms, because of the stage of the tide or the positon of the track, did not produce sufficient effects to be recorded by observers in the field; consequently, analyses of water levels are not shown.

Embayments are recognized to be the site of the most extreme water levels developed during hurricanes [31]. It is noteworthy that the disastrous floods which accompany typhoons in Japan [35] are reported to occur in bays or inland seas rather than on the outer coast. This fact is perhaps related to the bold character of the outer coast of Japan, and the

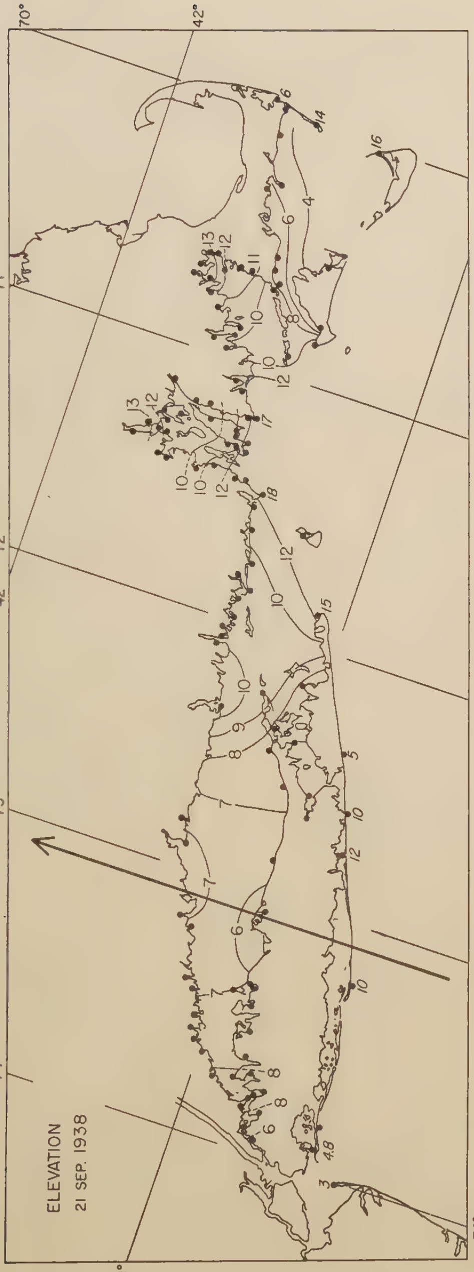
ELEVATION
21 SEP. 1938
70°
42°
71°
72°
73°
74°
41°
3
4.8
6
8
7
9
10
12
5
15
18
17
13
11
4
14
16

Fig. 17. Distribution of maximum water levels reported from shores of southern New England and Long Island during the hurricane of 21 September 1938. *Contours:* Elevation above predicted tide (ft). *Solid circles:* Points of observation. *Arrow:* Storm center trajectory.

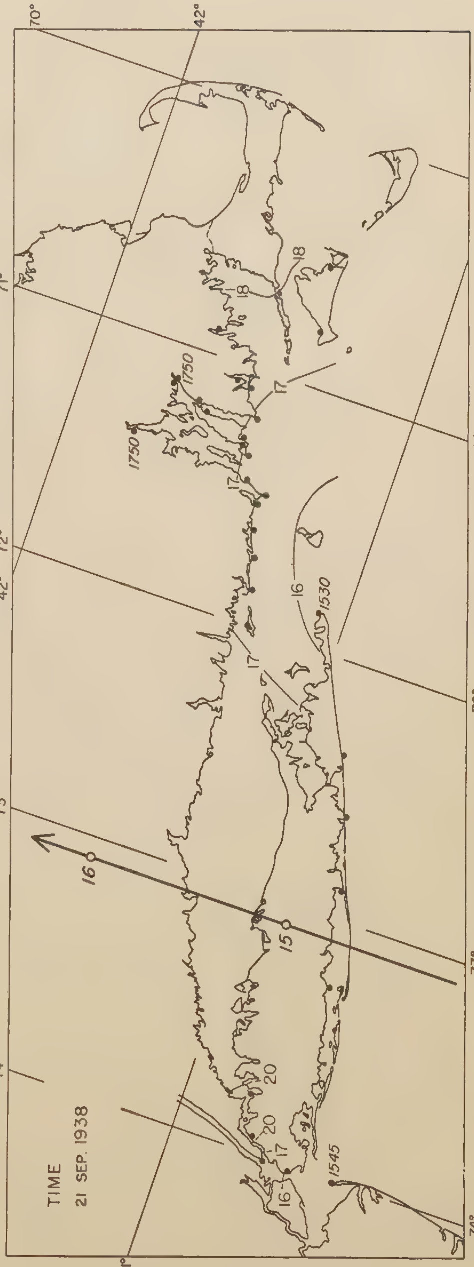
TIME
21 SEP. 1938
70°
42°
71°
72°
73°
74°
41°
1545
16
17
20
15
16
1530
17
1750
1750
18

Fig. 18. Time of maximum water level reported from shores of southern New England and Long Island during hurricane of 21 September 1938. *Contours:* Isochrones, EST. *Solid circles:* Points of observation. *Arrow:* Storm center trajectory.

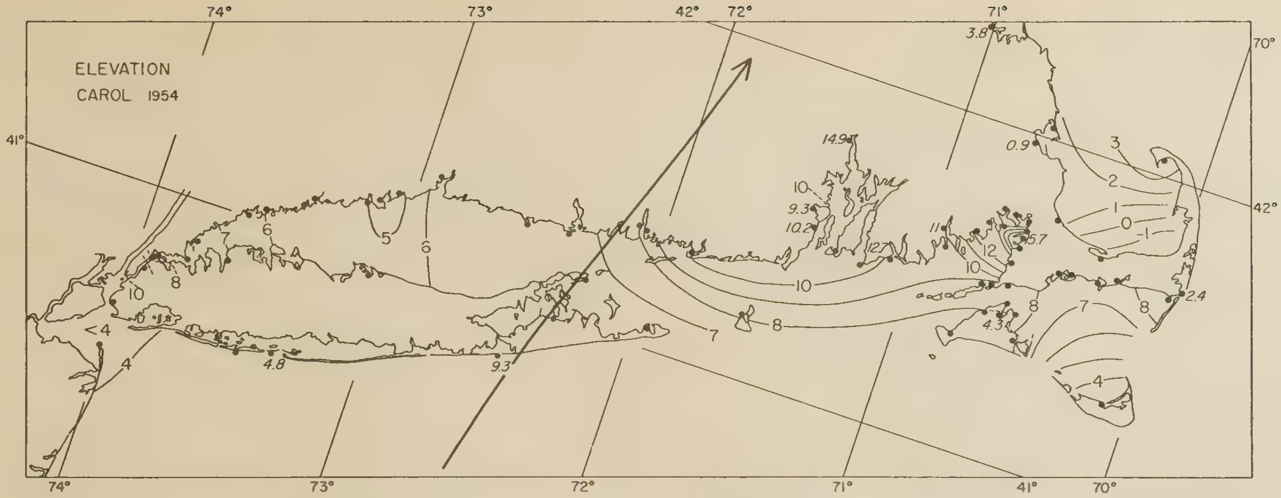
ELEVATION
CAROL 1954
74°
73°
42°
72°
71°
70°
41°
3.8
0.9
14.9
10
9.3
10.2
11
12
12.7
5.7
3
2
1
0
-1
2.4
8
7
4.3
4
10
8
7
6
5
6
10
8
<4
4
4.8
9.3

Fig. 19. Distribution of maximum water levels reported from shores of southern New England and Long Island during hurricane Carol, 31 August 1954. *Contours:* Elevation above predicted tide (ft). *Solid circles:* Points of observation. *Arrow:* Storm center trajectory.

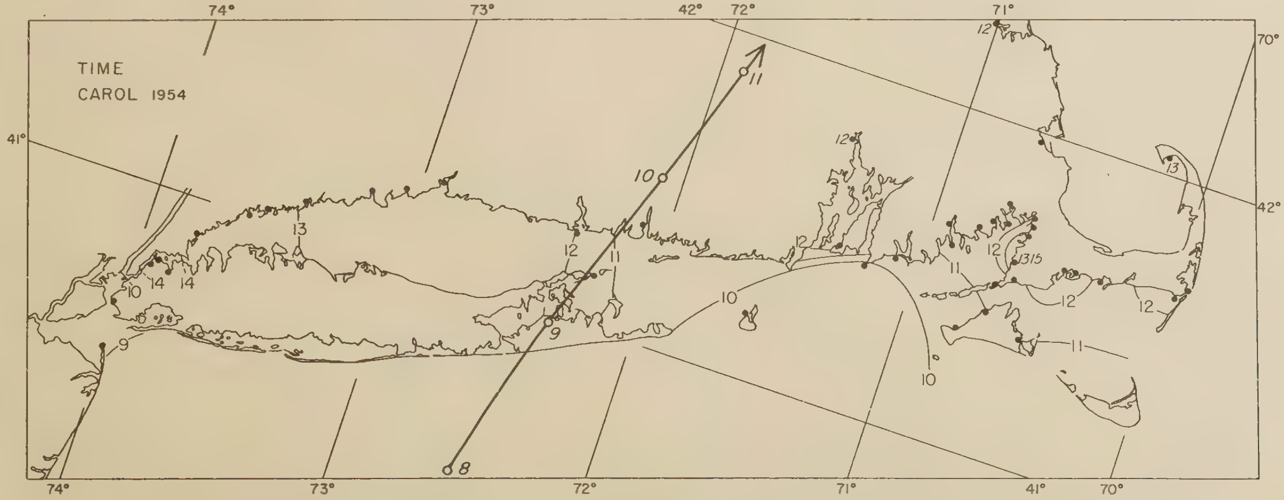
TIME
CAROL 1954
74°
73°
42°
72°
71°
70°
41°
12
13
11
10
12
13
12
11
13
15
12
12
11
10
10
9
8
10
14
14
9

Fig. 20. Time of maximum water level reported from shores of southern New England and Long Island during hurricane Carol, 31 August 1954. *Contours:* Isochrones, EST. *Arrow:* Storm center trajectory.

depth of the offlying water, in contrast to the shallower water of the embayments.

The coast of southern New England is bordered by a relatively wide and shallow shelf which may favor the development of high water levels along the outer coast. Between Montauk Point, at the eastern extremity of Long Island, and Martha's Vineyard, the coast is broken by a broad bight. This is itself something of an embayment. In this region the most extreme inundations have been experienced. The question arises, consequently, whether the topography of this area may not be responsible for the particular relation of the height of the surge to the position of the storm tracks that have been described. The fact that the records, made during storms whose tracks vary greatly in position, fall together consistently (fig. 10–15) is evidence against a topographic effect. Nevertheless, it remains a possibility that the topography of the coast may have influenced the observed distribution of water levels.

Narragansett Bay was the site of the greatest concentration of property damage and extreme water levels caused by these storms. The water levels are especially well documented for the hurricane of 1938. The bay opens on the bight between Montauk Point and Martha's Vineyard. In 1938 the extra elevation of the sea there is judged to have been about 12 ft. The mouth of the bay within which maximum levels of less than 10 ft were reported, is obstructed by islands. Within the bay, the levels increased to a maximum of 13 ft at Providence, R. I. The approach to Providence is from the southeast, with a wind fetch of about 10 n mi across water less than 20 ft in depth.

The hurricane of 1944 developed water levels at Providence of about 11 ft, but came at a low stage of tide and was less damaging. On 31 August 1954, however, the levels developed in the city were 15 ft above the predicted tide. It is also recorded that during the hurricane of 1815 "the tide rose 12–14 feet above the usual mark of high water" [12]. These records place Providence among the most frequently flooded cities in this country.

Buzzards Bay also illustrates the effect of embayment in augmenting the water level. The extreme levels reported were about the same as those experienced at Providence; namely, 13 ft in 1938 and over 15 ft during hurricane Carol in 1954.

The earliest recorded hurricane of New England also produced floods at the head of Buzzards Bay. This storm appears to have been a close analogue to those of 21 September 1938 and 31 August 1954. It doubtless also inundated the area where the city of Providence now stands. Governor Bradford recorded in his diary [3]:

> "This year (1635) the 14th or 15th of August was such a mighty storm of wind and rain as none living in these parts, either English or Indians, ever saw. Being like, for the time it continued, to those hurricanes and typhoons that writers make mention of in the West Indies. . . . It caused the sea to swell to the southward of this place above 20 foot right up and down, and made many of the Indians to climb into trees for their safety. It took off the boarded roof of a house which belongs to this Plantation at Manomet[4] and floated it to another place, the posts still standing in the ground. . . . It began in the south east and parted toward the south and east, but the greater force of it here was from the former quarters. It continued not (in the extremity) above five or six hours but the violence began to abate."

As the surge moves across the bight south of Rhode Island and ascends into Narragansett and Buzzards Bays, the time of maximum water levels occurs progressively later. In September, 1938, the crest arrived at the mouth of Narragansett Bay 1.5 hr after reaching Montauk Point and it occurred at Providence and the head of Buzzards Bay about an hour later than that. In August 1955 (Carol), there was a similar delay, 2.5 hr intervening between the time reported from Block Island and Providence. An analysis of the times reported for this storm suggests that: (1) the principal delay to the crest of water entering Narragansett Bay occurred in the narrow passages between the islands at the entrance; and (2) maximum levels were reached almost simultaneously within the bay. This situation did not occur in Buzzards Bay where the time of maximum level reported became progressively later toward the head, and where the conditions were modified by a resurgence to be described below.

In Cape Cod Bay and Nantucket Sound, the water levels reported along the shore appear to depend on the direction of the wind relative to the shore line. In Cape Cod Bay, the level reported from Barnstable, from a position in the lee of the land, was actually 1 ft below the predicted tide level at the time of the storm of 31 August 1954, although extra levels of 2 and 3 ft were reported at Plymouth and Provincetown which were not similarly protected. In Nantucket Sound, the reported levels at Nantucket Harbor, in the lee of the island, were several feet lower than those along the south side of Cape Cod which was exposed to an onshore wind.

Long Island Sound was protected from the attack of these storms from the sea. The subsequent effects of the resurgence there obscured whatever local effects may have developed during the immediate passage of the storms. This was not the case, however, at Willets Point where the tide gauge record shows two distinct peaks of high water during the storm of 1938 (fig. 2).

---

[4] Manomet was the name of a trading post located near the present entrance to the Cape Cod Canal from the head of Buzzards Bay.

North of Cape Cod the inundations produced by the hurricanes appear to have been relatively small. Surges of less than 4 ft developed at Boston and Portland during several storms which passed close to the coast (fig. 4–6). The storm of 11 September 1954 (Edna) crossed the Maine coast to the west of Eastport which was in a position that might be expected to experience flooding; however, extra elevations of only 1 ft were recorded by the Eastport tide gauge. The authors have found no record of floods during hurricanes along this part of the coast more serious than those accompanying severe autumnal gales. The bold character of the shores and the great depth of the offlying water in the Gulf of Maine are suggested as reasons for the difference in water level behavior between the regions to the north and south of Cape Cod.

4. Resurgences

The most novel feature revealed by these storms is the occurrence of resurgences which take place after the passage of the storm center. The resurgences appear to be due primarily to the free motion of the water as it returns to its normal level. Undoubtedly they are modified, at least initially, by winds blowing from changing directions. Resurgences are a particular hazard, because coming as they do after the storm appears to be subsiding, they are usually unexpected.

i. *Buzzards Bay.* During the storm of 31 August 1954 (Carol), water that was impounded against the northwest shore of Buzzards Bay was apparently released as the southeasterly wind veered to the southwest. The water surged across the bay to the opposite shore where it rose to the highest levels and caused the most severe damage reported from the Cape Cod region. Its effect was undoubtedly augmented by the strong southwesterly winds.

Figures 19 and 20 show that maximum water levels of some 12 ft were reported along the western shore of Buzzards Bay shortly before 1200E, coinciding with the nearest approach of the storm center. On the eastern side, maximum levels of more than 15 ft developed, but not until more than one hour later.

In 1938 a similar resurgence appears to have occurred in Buzzards Bay. Although the time of events was not recorded, much of the material damage and loss of life at Woods Hole was due to flooding from Buzzards Bay after the wind had shifted. It was proposed at that time that the loss was caused by a resurgence of the kind revealed subsequently by the data for hurricane Carol [25]. This type of resurgence is an exception to the generalization that the most severe inundations occur on the left-hand side of embayments.

ii. *Long Island Sound.* A striking resurgence occurred in Long Island Sound following the passage of the hurricanes of 21 September 1938 and of 31 August 1954 (fig. 17–20; table 2). These storms produced high water levels along the Rhode Island coast approximately at the time of storm center passage. From that point the peak of high water moved westward along the sound arriving at the western end 3–4 hr later. This event occurred after the wind had shifted to a westerly quarter. During the 1938 storm, the wind at New Haven shifted to southwest at 1600E, which was 1 hr before maximum water levels were reported at the eastern entrance of the sound, and 4 hr before their occurrence at Willets Point at the western extremity of the sound. The water evidently moved as a free solitary wave under its own momentum and against the prevailing wind.

During both storms, as the resurgent wave progressed westward, its amplitude diminished in the wider parts of the sound, only to increase again in the narrower parts at its western end. The effects were essentially similar on both sides of the sound, except that there is some indication that the water levels were slightly lower on the southern side during the storm of 1938.

In the waters surrounding New York City, two peaks of high level occurred. At Willets Point, at the junction of the sound with the East River, a peak of 5 ft elevation above the predicted tide occurred about 1 hr after the passage of the center of the 1938 hurricane. This peak coincided in time with the small

TABLE 2. Time and elevation of maximum water level above predicted tide in Long Island Sound and approaches during hurricane Carol, 31 August 1954

Station	Time (EST)	Maximum water level (ft)
Sandy Hook	0900	3.4
Fort Hamilton (1st peak)	0915	2.8
Block Island	0930	8.0
Sakonnet Point	1000	12.7
New London	1015	7.7
Orient Point	1130	6.8
Saybrook	1200	6.8
New Haven	1240	6.8
Bridgeport	1250	4.9
New Rochelle	1320	7.9
Willets Point	1330	7.4
Hell Gate	1445	10.9
Fort Hamilton (2nd peak)	1515	3.5
Sandy Hook (1st resurgence)	1500	3.3

surge recorded from Sandy Hook and may be attributed either to water entering Long Island Sound from New York Harbor, or more probably, to the direct action of the winds on the water of the sound. Four hours later, a second peak of twice the amplitude resulted from the arrival of the Long Island resurgence (fig. 2). The record from New London shows the time of passage of this wave at the eastern end of the sound. During hurricane Carol, the first peak was not discernable at Willets Point, but the resurgent wave produced a water level of 7.4 ft 4 hr after maximum levels were reported at Block Island off the eastern end of the sound. Two peaks that occurred during hurricane Carol at Fort Hamilton (the entrance to New York Harbor), are recorded in table 2. The first corresponds in time with the surge at Sandy Hook. The second coincides in time with the first wave of the coastal resurgence recorded from Sandy Hook (fig. 4) and is attributed to that event.

The western extremity of Long Island Sound is densely populated, is the scene of intense yachting activity, and is the site of the LaGuardia Airport, built on low ground. It is most important that those concerned be aware of the possibility that hurricanes crossing Long Island can produce disastrous inundations several hours after the passage of the storm center.

iii. *Coastal resurgence.* A third type of resurgence is shown by tide gauge records from points along the coast between Atlantic City, N. J. and Cape Cod, Mass. After water levels have reached a maximum, the elevation of the sea surface drops abruptly to values below that of the predicted tide and then rises again in a series of undulations having periods of several hours. The phenomenon is most fully developed at Atlantic City and Sandy Hook, N. J. where three or four successive waves were recorded during each of several storms (fig. 2–6). It occurred also at Newport, R. I. (fig. 3) and at Woods Hole and Uncatena Island, Mass. (fig. 5), but at these places only one well-developed resurgent wave followed the initial surge. It was virtually absent at Montauk, N. Y. (fig. 4–5).

Smaller undulations of shorter period are quite generally present in the tide gauge records during the storms, and these distort the form of the greater resurgent waves. However, the latter recur with sufficient regularity to show that the period of resurgence is a characteristic of the locality. In fig. 21, the recorded water levels for several storms at Atlantic City and Sandy Hook are grouped so that the times of the first resurgences correspond. It may be seen that the times of the subsequent wave crests also coincide approximately. At Atlantic City the periods are about 5.5 hr, whereas at Sandy Hook they are about 7.2 hr. The period of resurgence appears to be independent of the rate of progression of the storms which has varied from about 35 to 50 kt.

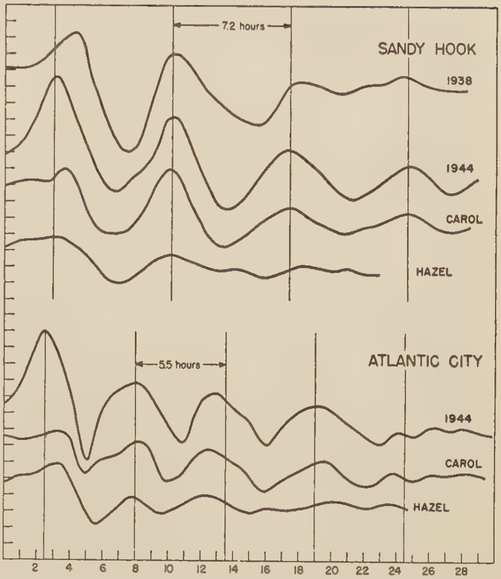

FIG. 21. Comparison of resurgences following passage of several storms at Sandy Hook and Atlantic City. *Curves:* Elevations relative to predicted tide adjusted timewise to make first resurgent waves coincide. *Vertical lines:* Time separation, 7.2 hr for Sandy Hook; 5.5 hr for Atlantic City. *Ordinate:* Elevation (ft). *Abscissa:* Duration (hr).

The rate of damping of the successive waves at Sandy Hook has been estimated for the storm of 1944 which produced the largest and most regular series of resurgences recorded. The attenuation coefficient is about 0.5 per period or 0.07 per hr.

Munk, Snodgrass and Carrier [19] propose that the coastal resurgences observed at Atlantic City and Sandy Hook are edge waves generated by a disturbance traveling along the coast. The theory of edge waves leads to satisfactory values for the period of the waves at the two places. An alternate possibility which merits investigation is that the resurgences are due to seiche-like oscillations of the water on the continental shelf in a direction normal to the coast line.

Although the elevations attained during the resurgences on the New Jersey coast were not great, it is possible that a future storm, passing close to the coast, may lead to the development of a substantial surge. In that event, the resurgences might become destructive. The period of these oscillations is about half that of the semidiurnal tide. Should a storm pass along the coast at low tide the accompanying rise in water level might be inconsequential, but the resurgence occurring some 6 hr later would arrive at high tide, and might thus prove more destructive than the original rise in water level.

5. Discussion

i. *The nature of the surge.* The surge has been considered to be due primarily to *setup* caused by the onshore component of wind stress [28], or to a wave generated by resonant phenomena offshore and approaching the coast from the open sea [10]. Both hypotheses account for the development of maximum water levels on the coast to the right of the path of the storm center and for the increased elevations associated with shallow water off the shore.

Present observations do not provide critical evidence to discriminate between these alternatives. In general, high water levels have developed at those places and times when the wind blows strongest in an appropriate direction relative to the coast, thus conforming to the requirements of the first hypothesis. The progressive advance of the crest of high water across the shallow water south of the Rhode Island coast and into the tributary bays and sounds indicates that wave motion plays a part in determining the distribution and time of high levels along the shore (fig. 17–20).

The supposition that the surge is developed as a wave accompanying a storm that advances across the open sea depends upon the existence of resonance effects. They will be expected when the depth of water is such that a free gravity wave will be propagated at a speed equal to the rate of progression of the storm. It is certain that every storm entering the coast will traverse a contour of this critical depth. In the case of the New England storms, moving at rates of 35–50 kt, the critical depths are 20–40 fm. For storms moving at 10 kt, a speed typical of many of those crossing the Gulf coast, the critical depth is less than 2 fm. It is uncertain whether the storms blow across the critical depths long enough to develop substantial waves by resonance, but the question may be raised whether rapidly moving storms, in which resonant effects could come into play at a greater distance from the coast, may not develop greater surges than those which approach more slowly.

Because of the speed with which gravity waves are propagated in deep water, it is unlikely that any substantial elevation of the sea surface is produced over oceanic depths other than that due to compensation for the reduced barometric pressure. That this inference is correct is supported by analysis of data from tide gauge records made at Bermuda during the passage of severe tropical cyclones.

ii. *Water levels during Bermuda hurricanes.* The water levels in excess of the predicted tide developed at Bermuda during a hurricane are shown in fig. 22. The center of this storm passed 10 n mi to the north of the island on 7 October 1948. The rise in level with the approach of this storm coincided closely with the effect to be expected from the fall in barometric pressure. After the passage of the center, the water level continued to rise and remained above the level attributed to the current barometric pressure. At no time, however, did the extra elevation attributable to the wind exceed 0.6 ft. Similar effects were produced by hurricanes which passed near Bermuda on 13 September 1948 and 17 September 1953. In these storms the water levels were less than 1 ft in excess of the predicted tide, and less than 0.1 ft in excess of the level due to the maximum atmospheric pressure recorded.

The Bermuda tide gauge is located on the south side of a lagoon, in a reach connecting the lagoon with the ocean. In the storm of 7 October 1948, the wind effect was lacking while the winds blew from the south across the shear slope of the island; it appeared only as the wind shifted to blow across the shallow water of the lagoon.

The records from these Bermuda storms indicate that the water levels were developed in response to the lowered barometric pressure, and that wind effects were minor. However, by no means should it

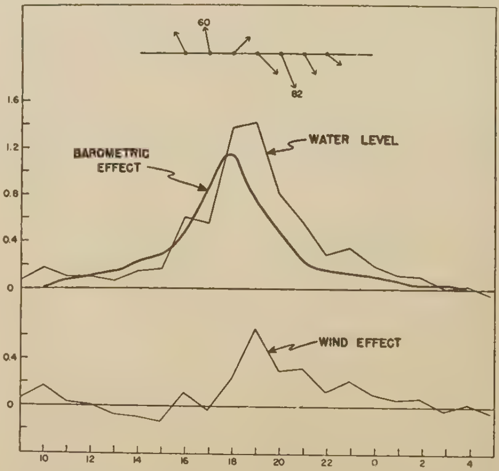

FIG. 22. Water level recorded by tide gauge at Ferry Reach, Bermuda, and barometric effect estimated as equilibrium elevation from barometer at Hamilton. *Above:* Coincident wind direction and speed (mph). *Below:* Estimated wind effect (difference between water level and barometric equilibrium elevation). *Ordinate:* Elevation above predicted tide (ft). *Abscissa:* Time AST.

be concluded that oceanic islands are immune from damaging inundation by hurricanes or typhoons.

A number of authentic reports of disastrous floods are recorded from oceanic islands [29; 31; 34]. At St. George's Bermuda, the market square was flooded during hurricanes on 12–13 September 1899; 21 September 1922; and 22 October 1926. During the storm in 1899 the water rose more than 6 ft above the predicted tide. During a typhoon which swept the island of Mille in the Marianas in 1905 the sea is reported to have reached places 12–15 m above ordinary sea level [11]. Mille lay 55 n mi to the right of the center of this storm which moved toward the west-northwest. It was thus exposed to easterly winds as the storm passed, and these winds swept across 25 n mi of lagoon before reaching the island. It may be assumed that the storm surge developed in the shallow water of the lagoon.

iii. *Geographical differences.* From the foregoing discussion, it may be concluded that shallow water is required for the development of water levels greatly in excess of the barometric equilibrium level. The recent storms of the Atlantic coast, and the many Gulf coast hurricanes which were accompanied by destructive floods, have approached the shore across broad, shallow continental shelves. On the bold coast of the Gulf of Maine, hurricane Carol which passed about 60 n mi inland, and hurricane Edna, which crossed the coast near Machias, produced only trivial increases in water level.

The distribution of maximum water levels relative to the storm path appears to have been consistent for the New England hurricanes, in which maximum elevations occurred between 40 and 100 n mi to the right of the center. Records from the coast of the Carolinas and from the Gulf of Mexico indicate that maximum effects may occur much closer to the path of the storm center. It is possible that this difference may reflect the tendency of tropical cyclones to acquire extratropical characteristics as they move northward into New England. This has been discussed by Pierce [24]. This tendency would modify the general distribution of the winds in different parts of the storm trajectory. The New England storms all moved with much greater speed than is usual for those striking the southern coasts of the United States. It is suggested that hurricanes moving slowly over the tropical oceans maintain a structure approaching that of the idealized circular storm, whereas those that have turned to approach the New England coast, having become involved in more complex pressure fields, move more rapidly and develop systems of convergence which distort and control the relative distribution of water levels about their paths. A comparison of the wind field attending hurricane Hazel, as it approached the Carolina coast (fig. 16) and as it traversed the northeastern States (fig. 15), is instructive in this respect.

iv. *Relation to tidal phenomena.* Whatever may be the nature of the hurricane surge as it appears on the outer coast, there is no doubt that in tributary embayments the effects are due in part to purely hydrodynamic factors. A sudden rise in water level at the mouth of an embayment obviously leads to hydraulic adjustments within, and these may be large relative to the effects of winds with limited fetch. A comparison of hurricane water levels with the astronomical tide in embayments is of interest, since the latter is of purely hydrodynamic origin.

In Long Island Sound the resurgent wave is doubtless hydrodynamic, since its progress is against the prevailing direction of the wind. The time required for the crest of high water to traverse Long Island Sound (3–4 hr) agrees well with the time taken by the primary wave of the astronomical tide in covering the same distance [26]. Moreover, its velocity is close to the theoretical value estimated for the mean depth of the sound [15]. The distribution of maximum levels of the resurgent wave and the time of their occurrence along the sound is quite different from that of tidal high waters. The dimensions of the sound are such that, relative to the length of the tidal wave, the tide behaves approximately as a standing wave with high water occurring almost simultaneously along the length of the sound, and only slightly later at its western end. The hurricane surge is of much shorter length than the tidal wave. Consequently, the distance over which reflection can augment the elevation is much more limited and is confined to the western part of the sound. The progressive character is evident in the case of the resurgence, but it is concealed in the tidal wave by the effects of reflection.

In Narragansett Bay and Buzzards Bay, the tide also approximates a standing wave, being slightly delayed and definitely augmented as the heads of the bays are approached. The behavior of the water levels during hurricanes is similar, but the differences in time and elevation along the bay appear to be somewhat greater. The times of highest level are not accurately enough reported to warrant discussion; the differences in elevation, on the other hand, are more reliable. In Narragansett Bay, the mean range in tide is 30 per cent greater at Providence than at Newport. At these two locations during the hurricanes of 1938, 1944, and 1954 (Carol), the extra elevation of the sea surface differed by 45 to 50 per cent. If 30 per cent of the augmentation of the surge at

Providence is assigned to hydrodynamic effects similar to those which influence the tide, a residue of 20 per cent, or about 2 ft, remains to be attributed to the local action of the wind.

It is evident that the local topography, as well as the position and strength of the storm, is important in determining the water levels developed along coasts. In attempting to anticipate such effects in embayments, an understanding of local tidal behavior may be helpful, but allowance should also be made for the difference in character of the wave responsible for the tide and that engendered by the hurricane surge.

v. *Evaluation of experience.* With the present state of understanding, past experience is the best indication of future hazard. The four hurricanes that have crossed the southern New England coast since 1938 were all full-scale tropical cyclones. It is not evident from the records whether they differed much in the severity or pattern of their effects on water levels, when differences in their course and the stage of the tide are allowed for. From consideration of the kinetic energy of the cyclostrophic wind within a radius of 100 n mi of their centers, the storms of 1938 and 1944 have been estimated to have been among the six most powerful of a total of 73 storms that crossed the Atlantic or Gulf coasts during the period 1901–1949 [20]. Although it is possible that a more destructive storm might occur, it seems probable that the recent storms have been about as severe as those likely to occur in the future.

The recent storms have been sufficiently well distributed to provide a useful indication of the inundations to be expected by major storms crossing the coast east of central Long Island. The region west of Cape Cod has been in a position to experience the maximum effects of three great storms. Should a storm follow a path more to the eastward, crossing the coast between Narragansett and Buzzards Bays, the south shore of Cape Cod might suffer inundation somewhat greater than experienced previously.

The assurance is not so good for the area west of central Long Island, since it has not been located beneath the dangerous semicircle of any of the recent storms. Residents of this area should take warning from a hurricane which, in 1821, swept along the Atlantic coast crossing Long Island close to New York. It is reported that at New York "... more damage was sustained in two hours than was ever before witnessed in the city. . . . At the time of low water the wharves were overflowed, the water having risen thirteen feet in one hour" [27]. This record should serve as a warning that the New York area may be subject to water levels much greater than those experienced during the recent hurricanes, in the event that a storm center passes nearer to the city at the time of high water. In discussing this possibility, Brooks [4] wrote, "If such a storm tide should coincide with high spring tide and the Hudson in flood, lower Manhattan and its subway entrances might be inundated suddenly."

6. Summary of individual storms

The various phenomena which have affected water levels along the Atlantic coast during five hurricanes have been considered from a comparative point of view. The characteristics of the individual storms have been necessarily obscured by this treatment. In this section the major effects of each of these storms is reviewed.

i. *The hurricane of 21 September 1938.* The New England Hurricane of 1938 was probably the most violent of the five storms studied, being marked by the lowest barometric pressure, greatest pressure gradient, and most rapid forward movement (52 kt) as it crossed the Atlantic coast (fig. 1, 2, 11, 17, 18); [4; 22; 24; 32; 33]. It was also the most destructive not only for the reasons mentioned, but because the coastal population was unprepared; no such storm as that had ever been experienced within the memory of persons then living. The path of the storm was due north, crossing Long Island almost at right angles 50 n mi east of New York City at about 1500E.

Prior to crossing the coast, the storm changed from a tropical to an extratropical disturbance with definite frontal characteristics [24] maintaining, however, its hurricane intensity. Associated with the angle of approach and the disposition of the leading convergence zone, the winds along the New Jersey shore were northerly, paralleling the coast as the storm advanced. This led to a forerunner at Sandy Hook of only about 1 ft elevation. Strong northeasterly winds, however, blew across the path of the storm in advance of the center, extending westward to within 20 n mi of New York City. At Mineola, Long Island, the wind veered from north to northeast at about 1300E and blew strongly from this quarter for about 2 hr. Although these winds did not reach Sandy Hook, they appear to explain a small surge which was recorded at Sandy Hook and within New York Harbor. The tide gauge at Atlantic City was destroyed by this storm, although the winds were evidentally offshore during its passage. This may have been the result of a surge engendered by the easterly winds on the right side of the leading convergence zone that passed approximately 30 n mi offshore.

The major effect on water levels was evident between Montauk Point and Martha's Vineyard where all tide gauges were destroyed. Field observations indicate water levels of 8 to 10 ft in this area which was the zone of strongest southeasterly winds. At exposed positions along the coast of eastern Long Island, at Point Judith, Sakonnet, and the south side of Martha's Vineyard and Nantucket, water levels of 14 to 18 ft above the predicted tide were reported. These probably include the added effect of wave action. Reliable still water levels of 13 ft were reported from the heads of Narragansett and Buzzards Bays. East of Woods Hole, the maximum elevations decreased along the south shore of Cape Cod to about 6 ft at Chatham. At the eastern end of Long Island Sound, a surge of 5 ft elevation developed as the storm center passed, followed 4 hr later by a resurgence which produced an elevation of 10 ft above the predicted tide at Willets Point.

ii. *The hurricane of 14–15 September 1944.* The Great Atlantic Hurricane was one of the most powerful hurricanes of record as it passed Cape Hatteras, but it declined in strength before crossing the New England coast (fig. 1, 3, 12); [20; 30]. The center passed closer to the New Jersey coast than the others, and it is remembered by residents along that shore as the most damaging. Light northeasterly winds paralleling the shore preceded the storm and led to little forerunner. Because of the westward displacement of the leading convergence area, northeasterly winds in excess of 40 kt blew onto the New Jersey coast for 2 hr and produced a sharp surge well in advance of the storm center passage. When the wind shifted to the northwest as the convergence zone passed, the water level dropped quickly; it was followed thereafter by a well-developed series of resurgences.

The storm center crossed Long Island well to the east of the path that was followed by the storm of 1938. Accordingly, the zone of maximum water levels lay more to the eastward, along the south shore of Cape Cod. Water levels of 6 to 8 ft were reported between Montauk Point and Woods Hole, increasing to 9 ft at the eastern end of Nantucket Sound.

At the head of Narragansett Bay the water level reached 11 ft, and in Long Island Sound a resurgent wave occurred producing an elevation of about 5 ft at New Haven and destroying the gauge at Willets Point. At Mill Rock in the East River, two peaks of high water level were recorded, one of 5 ft at about the time of the nearest approach of the center, followed 5 hr later by a smaller surge attributed to the Long Island resurgence. At Boston, which lay in the path of the center, the extra elevation of the sea surface was only 4 ft.

West of Cape Cod relatively little damage was done by high water levels, because the storm arrived after the tide had fallen. Along the south shore of Cape Cod, high water occurred later and coincided with the arrival of the surge. This storm was the most destructive of the series in this region.

iii. *The hurricane of 31 August 1954.* This storm (hurricane Carol) paralleled the New Jersey coast at a distance of some 70 n mi, and crossed Long Island near its eastern extremity, slightly west of the path followed by the storm of 1944 (fig. 1, 4, 13, 19, 20); [9; 23]. The coasts of Rhode Island and southern Massachusetts were thus exposed to the right-hand semicircle of the storm.

The wind field differed from that in the preceding storms by showing a less distinct convergence zone in advance of the center. The major area of convergence in the right semicircle lay south of the storm center. The winds in advance of this convergence zone were northeasterly and, although they did not attain exceptional intensity until after they had shifted to the west following the passage of the center, they appear to have produced a substantial forerunner at Atlantic City and Sandy Hook. This forerunner dropped abruptly, without the development of a surge, at about the time of arrival of the convergence area in the left rear quadrant, when a sudden backing of the wind from north to west took place.

Maximum water levels were produced along the coast between Montauk Point and Martha's Vineyard. In general, they were very similar to those experienced in 1938, reaching 8 to 10 ft. Along the south shore of Cape Cod slightly lower levels were reported, ranging from 8 to 6 ft. At the head of Narragansett and Buzzards Bays maximum levels of approximately 15 ft were reported. These are the highest values reliably reported for any of the storms at any place along this coast. A resurgence traversed Long Island Sound producing elevations of about 8 ft at its western end about 4 hr after the surge at Montauk Point. At Boston the water level was 4 ft above the predicted tide.

Like the hurricane of 1938, the surge of this storm coincided with high water along the portion of the coast principally effected.

iv. *The hurricane of 11 September 1954.* Hurricane Edna was the largest of the storms to cross the New England coast, but it did not develop such low pressures or steep pressure gradients as some others (fig. 1, 5, 14); [9; 14]. The course of the center lay 115 n mi or more off the New Jersey coast and crossed the eastern part of Cape Cod. It was thus the easternmost of the storms considered.

Because of its course, the region of potential inundation lay offshore to the east of Cape Cod and substantial water levels did not develop along the southern New England coast, except at the eastern end of Nantucket Sound where elevations of 6 ft were reported. The Nantucket lightship, moored some 40 n mi east of the storm track, encountered mountainous seas and went adrift. A small surge (4 ft) was recorded as far west as Montauk Point, but came during a low stage of the tide and did not result in damaging inundation.

The interesting feature of the wind field of this storm was the well-developed convergence area that lay in advance of the center. West of this line, northeasterly winds paralleled the shore and produced no well-developed forerunner.

This storm recrossed the coast in eastern Maine. Water levels of nearly 4 ft above the predicted tide occurred at Boston, but at Portsmouth, New Hampshire, Portland and Eastport, Maine, the extra elevation associated with the storm was only about 1 ft.

v. *The hurricane of 15–16 October 1954.* The center of this storm (Hazel) crossed the coast of South Carolina at Long Bay, about midway between Cape Fear and Cape Romain, traveling nearly due north (fig. 1, 6, 15, 16); [9; 18]. The pressure profile near the center was shallower than those of the storm crossing the New England coast (fig. 9). The direction of the easterly winds in advance of the center changed abruptly to west of north at a convergence area in the left front quadrant. Other convergence zones were not evident from the wind data available at the coast, but developed in the right rear quadrant as the storm moved inland [18].

The water levels developed along the Carolina coast by this storm were very different in distribution from those of the New England storms. Maximum elevations occurred within 40 n mi east of the storm center. The sharp cutoff in water levels to the left of the storm track were related to the position of the leading convergence area, for beyond this line strong offshore winds prevailed. It is not clear why the levels dropped so rapidly east of Cape Fear. Possibly the slope of the sea bottom was a decisive factor, since the water deepens more abruptly east of Cape Fear than it does in Long Bay.

This storm was very destructive to beach property along the entire area where water levels in excess of 5 ft were observed. Much of the damage was augmented by the effect of waves.

After passing inland, hurricane Hazel moved northward along a cold front. As it did so, the configuration of the storm changed and a broad band of strong southeast winds developed in its right semicircle. A well-marked convergence area developed in the rear of this band, behind which the winds veered to the south and west (fig. 15). The effect of the southeast winds on water levels was evident along the Atlantic coast as far east as Montauk which was nearly 300 n mi from the track of the storm center. At Hampton Roads a 2 ft forerunner that had developed slowly, suddenly gave way to a drop of 2 ft below predicted tide level. This event occurred when the wind shifted to the southwest at the time of passage of the convergence zone in the right rear quadrant. At Atlantic City and Sandy Hook, 3 ft forerunners gave way with the passing of the convergence zone and were followed by resurgences. Even at Woods Hole and Boston, some 350 n mi away, gentle oscillation of the sea surface was recorded during the passage of this storm.

REFERENCES

1. Arakawa, H., 1954: On the pyramidal, mountainous, and confused sea in the right or dangerous semi-circle of typhoons. *Pap. Meteor. Geophys.*, Tokyo, **5**, 114–123.
2. Bergeron, T., 1954: The problem of tropical hurricanes. *Quart. J. roy. Meteor. Soc.*, **80**, 131–164.
3. Bradford, W., 1952: *Of Plymouth Plantation 1620–1647.* Ed. by S. E. Morison, New York, Knopf, 448 pp.
4. Brooks, C. F., 1939: Hurricanes into New England, meteorology of the storm of September 21, 1938. *Geogr. Rev.*, **29**, 119–127. (Reprinted with changes in *Rep. Smithson. Instn.*, 1939.)
5. Cline, I. M., 1920: Relation of changes in storm tides on the coast of the Gulf of Mexico to the center and movement of hurricanes. *Mon. Wea. Rev.*, **48**, 127–146.
6. ——, 1926: *Tropical cyclones.* New York, Macmillan, 301 pp.
7. ——, 1933: Tides and coastal currents developed by tropical cyclones. *Mon. Wea. Rev.*, **61**, 36–38.
8. Darling, N., 1842: Notice of a hurricane that passed over New England in September 1815. *Amer. J. Sci.*, **42**, 243–252.
9. Davis, W. R., 1954: Hurricanes of 1954. *Mon. Wea. Rev.*, **82**, 370 pp.
10. Doodson, A. T. and H. D. Warburg, 1941: *Admiralty manual of tides.* London, His Majesty's Stationery Office, 270 pp.
11. E. K., 1907: Orkan in den Marschall-Inseln am 30 Juni 1905. *Ann. Hydrogr. mar. Meteor.*, **35**, 183–184.
12. Farrar, J., 1818: An account of the violent and destructive storm of 1815. *Mem. Amer. Acad. Arts Sci.*, **4**, 92–97.
13. Hubert, L. F. and G. B. Clark, 1955: *The hurricane surge.* Interim Report, U. S. Dept. Commerce, Weather Bureau, June 1955, 34 pp. (Unpublished manuscript.)
14. Malkin, W. and G. C. Holzworth, 1954: Hurricane Edna, 1954. *Mon. Wea. Rev.*, **82**, 267.
15. Marmer, H. A., 1926: *The tide.* New York and London, Appleton, 270 pp.
16. Massachusetts Geodetic Survey, 1939: *Storm tide, hurricane of September 1938 in Massachusetts.* Sponsored by Mass. Dept. Public Works. (Unpublished Manuscript.)
17. Miller, A. R., 1957: The effect of steady winds on sea level at Atlantic City. *Meteor. Monogr.*, **2**, no. 10, 24–31.

18. Mook, C. P., 1955: The distribution of peak gusts in hurricane Hazel 1954. *Weatherwise*, **8**, 92–96.
19. Munk, W., F. Snodgrass, and G. Carrier, 1956: Edge waves on the continental shelf. *Science*, **123**, 127–132.
20. Myers, V. A., 1954: Characteristics of United States hurricanes pertinent to levee design for Lake Okeechobee, Florida. *Hydromet. Rep. no. 32*, U. S. Weather Bureau, Washington, 106 pp.
21. Namias, J., 1955: Secular fluctuations in vulnerability to tropical cyclones in and off New England. *Mon. Wea. Rev.*, **83**, 155–162.
22. Neumann, F., 1939: Storm wave data for the New England hurricane of September 21, 1938. *Bull. Amer. Meteor. Soc.*, **20**, 357–358.
23. New England-New York Interagency Committee, 1954: *Long Island, New York and vicinity hurricanes, their effects and measures against them.* (Unpublished manuscript 29 November 1954.)
24. Pierce, C. H., 1939: The meteorological history of the New England hurricane of September 21, 1938. *Mon. Wea. Rev.*, **67**, 237–285.
25. Redfield, A. C., 1939: This hurricane and others. *Collect. Net*, March 1939, pp. 10–14.
26. ——, 1950: The analysis of tidal phenomena in narrow embayments. *Pap. phys. Oceanogr.*, **9**, no. 3, 36 pp.
27. Redfield, W. C., 1831: Remarks on the prevailing storms of the Atlantic coast of the North American States. *Am. J. Sci. and Arts*, **20**, 1–36.
28. Reid, R. O., 1957: On the classification of hurricanes by storm tide and wave energy indices. *Meteor. Monogr.*, **2**, no. 10, 58–66.
29. Reid, W., 1849: *The progress of the development of the laws of storms and of the variable winds.* London, John Weale, 424 pp.
30. Sumner, H. C., 1944: The North Atlantic hurricane of September 8–16, 1944. *Mon. Wea. Rev.*, **72**, 187–189.
31. Tannehill, I. R., 1950: *Hurricanes.* Princeton University Press, 304 pp.
32. U. S. Army Corps of Engineers, 1938: *Data on storm conditions.* U. S. Engineer Office, New York. (Unpublished manuscript dated 17 October 1938.)
33. ——, 1939: *Supplemental report on hurricane of September 21, 1938 and its effect on the coastal region.* U. S. Engineer Office, Providence, R. I. (Unpublished manuscript.)
34. Visher, S. S., 1925: Tropical cyclones of the Pacific. *Bull. Bishop Mus.*, Honolulu, **20**, 163 pp.
35. Wadati, K. and T. Hirono, 1955: Storm tides caused by typhoons. *Proc. UNESCO Symp. on Typhoons*, Japanese Nat. Comm. for UNESCO, Tokyo, pp. 31–48.

Contribution No. 829

INTERACTION OF SEA AND ATMOSPHERE:

a group of contributions

by

A. C. Redfield, A. R. Miller;
G. W. Groves; D. L. Harris;
R. O. Reid;
W. Marks and J. Chase.

THE EFFECT OF STEADY WINDS ON SEA LEVEL AT ATLANTIC CITY[1]

By ARTHUR R. MILLER[2]

Woods Hole Oceanographic Institution

(Original manuscript received 9 April 1956; revised manuscript received 15 August 1956)

ABSTRACT

From a study of tidal records for Atlantic City, New Jersey, and daily weather maps over a period of six months, the elevation of the sea surface associated with the geostrophic wind field has been evaluated as a function of the geostrophic wind velocity. The relationships are expressed in a nomogram.

Assuming the angle of deviation between surface and geostrophic winds to be 20°, and allowing for the static effects of atmospheric pressure, maximum elevation above the predicted tide level is observed when the surface wind blows 40° from the right of normal to the coastline. In general, there appears to be a 12 hr lag between the winds and the associated state of sea level.

1. Introduction

Along a coast tide gauge records show that varying perturbations of sea level are superimposed upon the regular tidal oscillations. In addition to the transient and often dramatic changes in sea level due to tsunamis, hurricanes and other violent storms, variations in the predicted sea level frequently occur in association with the regular passage of cyclonic disturbances across the coastal waters. These changes in sea level may be attributed in part to adjustments to the varying atmospheric pressure, and in part to the accumulation or depletion of water at the coast due to the tangential stress of wind over the water surface.

Atlantic City is a favorable place to examine the effects of steady winds on sea level, because the tide gauge is situated at an exposed location on a long open coastline, without significant prominences or embayments to influence the general level of the water. Fluctuations of sea level from the predictions for the astronomical tide were determined for the period 1 November 1952 to 30 April 1953. The part played by atmospheric pressure in producing these fluctuations was estimated from the mean atmospheric pressure over a large area off Atlantic City. For the same period the geostrophic wind field over the adjoining sea surface was determined from the daily weather maps. A comparison of these data with those for the nontidal changes in sea level, after correction for barometric effect, has permitted the effect of the geostrophic wind to be evaluated as a function of the velocity relative to the coastline.

The daily changes in the geostrophic winds were usually sufficiently slow to approach steady wind conditions. It was assumed that associated sea levels were in equilibrium with the forces of wind stress when reasonably steady winds prevailed. It is not to be expected that the relationships that were developed apply to fast moving storms.

The term *meteorological effect* generally includes all departures of sea level from the level of the predicted tide. It includes the effects of (1) atmospheric pressure, (2) transient winds that accompany rapidly moving storms, and (3) the steadier winds that are the object of study. The analytical procedure employed is believed to minimize the effects of the more transient disturbances. Accordingly, when meteorological effects are used, they will refer to the combined effect of wind stress and atmospheric pressure associated with slow moving meteorological disturbances.

---

[1] Contribution No. 829, Woods Hole Oceanographic Institution.

[2] Research Associate in Physical Oceanography, Woods Hole Oceanographic Institution, Woods Hole, Mass.

The term *barometric effect* is applied to the direct effect of atmospheric pressure on the local sea level.

The term *setup* is restricted to the changes in elevation of the sea surface along the coast, brought about by tangential wind stresses normal to the coastline. Use of the term *setup*, in the above sense, follows the practice of the Beach Erosion Board, U. S. Corps of Engineers [7], and is selected over such terms as *wind tide* or *Windstau* to eliminate any connotation of periodicity or atmospheric pressure interference.

The term *nontidal sea level* is used to designate the elevation of the sea surface after the effects of the astronomical components of the tide have been eliminated.

2. Meteorological effect

The most direct means for separating the meteorological effect from the observed tide is to subtract the predicted astronomical tide from the observed elevations. The difference will include secondary phenomena, such as, seiches or surges. This is not objectionable, provided these oscillations are small relative to the meteorological effect.

This method has limited application since it depends on adequate predictability. If the location is in a region of complex tides or unknown tides, and if shallow water effects alter the constituents of the tide, the results may not be useful. Furthermore, setup and barometric effect are difficult to identify if transient irregularities are comparable in magnitude.

Systems of averaging may be used to minimize the transient phenomena and cancel out the regular motion of the astronomical tide. The simplest of these methods consists of averaging 24 successive hourly heights of tide [2] centering about the time in question. A residue is left, made up of mean sea level with superimposed irregularities. The 24 hr average filters out the solar short-period constituents but only partially eliminates the lunar constituents.

Doodson and Warburg [1] have developed a method which eliminates both the lunar and solar constituents from the tide. The system makes use of an average of multiple combinations of hourly heights spanning a period of 39 hr. This method not only removes the astronomical tide from the data, but considerably minimizes irregularities of short duration. Consequently, it was adopted for the purpose at hand. The result is designated as the *nontidal sea level.*

Results from applying the Doodson method were compared with the differences between tidal observations and published predictions at Delaware Break-

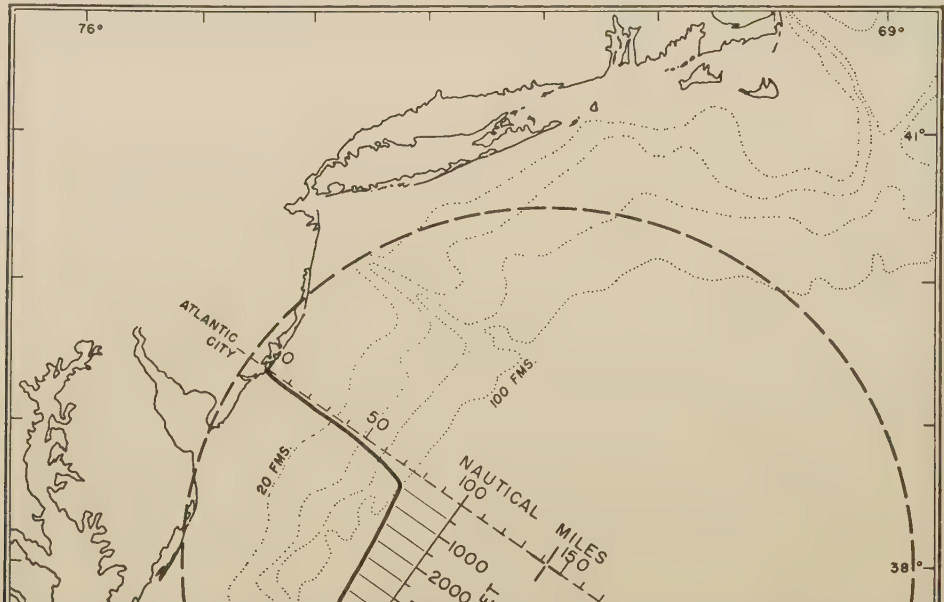

Fig. 1. Chart showing bathymetry of region off Atlantic City and size of assumed effective wind field.

water, a primary tidal station. A standard deviation of 0.16 ft was obtained from the comparison of 235 successive observations of high and low water levels with a correlation coefficient of 0.985 ± 0.0034. Apparently, transient irregularities were not significant during this period, and either method was applicable. The Doodson filter was preferable for this research, since Atlantic City is not a primary tidal station.

3. The barometric pressure correction

The change of sea level, in response to atmospheric pressure variations in time, equals a column of water having the same weight per unit area as the change in atmospheric pressure [4]. In other words, it varies in the ratio of the densities of air and water which is about 1 cm per mb. Barometric data showed that it was possible for sea level to rise or fall as much as 0.5 to 0.75 ft to compensate for the observed variation of atmospheric pressure. Dynamic effects, however, may be important if the rate of change in pressure is rapid. Furthermore, these fluctuations of sea level are also dependent on the mean distribution of pressure over distance. For example, pressure changes in time have no effect over a small lake.

It was uncertain whether the atmospheric pressure observed at Atlantic City was representative of the adjoining pressure over the sea surface. For this reason, mean pressure over a large area of the sea surface has been estimated and compared with sea level to obtain the barometric relation. The daily mean pressure field over a large oceanic area was determined from weather maps. Pressure was read off at eight points about a circle 300 n mi in diameter centering about 38N, 72W (fig. 1), its circumference including Atlantic City. The average of these pressures was assumed to apply to the ocean surface affecting sea level at that station.

It was assumed that the meteorological effect was primarily induced by atmospheric pressure when the wind was light and variable for sufficient duration [6]. To select intervals of little surface wind, weather maps for the period of observation were examined for slow-moving cells and small pressure gradients. Also, the meteorological effect at Atlantic City was examined for intervals of apparent equilibrium when it remained more or less constant, During the six month period, there were eighteen instances in which intervals of little wind coincided with periods of constant meteorological effect. From the data during these periods, the barometric effect applicable to the sea level at Atlantic City was found to be 1 cm per mb. This value corresponds to the theoretical equilibrium value.

4. Winds, time lag, and setup

Geostrophic winds from daily weather maps have been used to infer the strength and direction of wind stress on the sea surface. This procedure is not completely satisfactory, since the relationship between surface and geostrophic winds is not always consistent; but within reasonable limits, it is useful to assume that surface wind varies linearly with the geostrophic wind [3]. The geostrophic wind was estimated from the maximum surface pressure difference across the 300 n mi circle (fig. 1).

The time required to develop a condition of equilibrium between the height of water and the wind stress on the sea surface is dependent, among other factors, upon the fetch of wind. For individual storms both fetch and time lag may vary, but the scale of the geostrophic parameter permits the assumption that constancy holds in a statistical sense.

An approximate time lag was obtained through a series of harmonic analyses of tidal heights (from which the astronomical components had been eliminated by the Doodson-Warburg method) against wind directions prevailing at various intervals prior to the tidal observations. If increasing time intervals are taken between wind observations and tidal heights, the derived amplitude varies inversely as the degree of randomness between direction of wind and the associated water level. The time interval showing the greatest amplitude among successive analyses is interpreted as giving the statistical time lag between the maximum effect of wind and the height of water at the tide gauge.

Nontidal heights, or to be more specific, nontidal sea levels with barometric variations eliminated, were sorted according to wind directions. By denoting t as the time of weather observations, nontidal heights at times $t + 0, t + 6, \ldots, t + 24$ hr were successively grouped with wind directions at time t. Analyses showed that the derived amplitude for the primary sine wave of each series converged to a maximum with the $t + 12$ series. Consequently, it was concluded that there is a 12-hr time lag between the wind and the maximum setup at the tide gauge. This time lag was applied in subsequent treatment of the data.

Since the observations of sea level were made at a long open coastline where selective entrapment of water would not likely occur, it was assumed that sea level varied symmetrically with wind directions of a given speed. Harmonic analysis was used to determine the relation between setup and wind speed. The daily geostrophic winds were classified in five groups according to speed, the range of speed in each class being broad enough to give good statistical

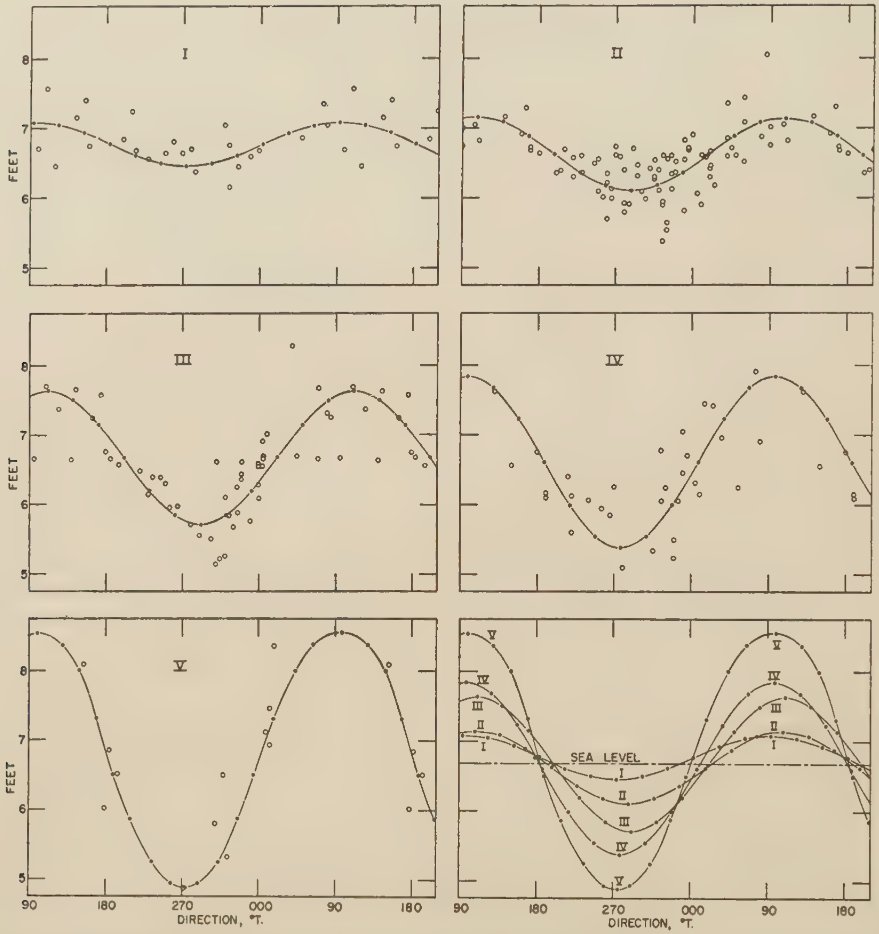

Fig. 2. Harmonic analyses of non-tidal sea levels for various classes (4 mb intervals) of geostrophic wind speeds. *Ordinate:* Non-tidal sea levels shown as tide staff heights and corrected for direct pressure effect. *Abscissa:* Direction of geostrophic wind.

distribution in direction as well as in numbers of observations. Nontidal heights taken 12 hr after the wind observations, and corrected for pressure, were plotted against wind direction. Five separate analyses were carried out and compared. The results of these analyses showed increasing amplitudes of nontidal sea level with increasing wind classes and the same maxima with respect to direction of wind (fig. 2).

5. General relations

In order to present the general relations between the atmospheric pressure field off the coast (with its associated geostrophic wind) and the setup at Atlantic City, a nomogram (fig. 3) was constructed from the curves shown in fig. 2. In this nomogram the direction of the geostrophic wind is represented by a polar coordinate system. The strength of the geostrophic wind, expressed as the maximum pressure difference (in millibars) across the 300 n mi pressure field off the coast, is represented by a series of concentric isotachs surrounding the center. The elevation of the sea surface due to wind setup is indicated by a scale along the horizontal axis of the diagram.

For reference the dashed line passing through the center of the nomogram shows the orientation of the coast line at Atlantic City. The inset shows wind speed corresponding to the designated pressure differences.

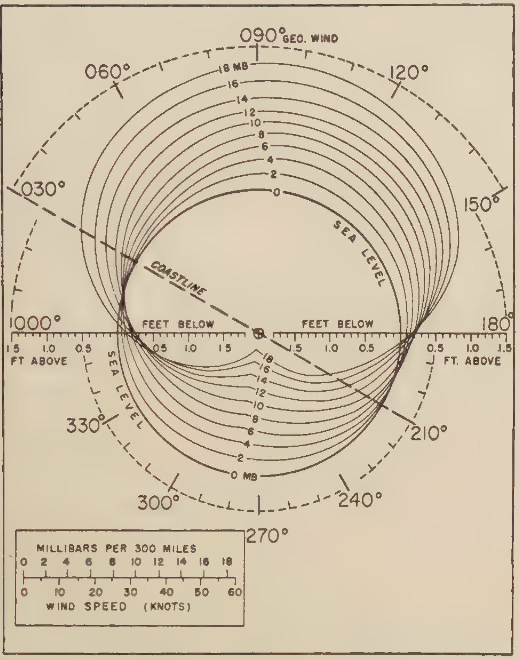

Fig. 3. Nomogram for wind setup at Atlantic City. For explanation see text.

To use this nomogram, place a straight edge to intercept the center at the angle of the geostrophic wind determined from the weather map. Measure from the center to the isotach representing the maximum pressure difference across the pressure field off the coast. This distance, when laid out along the scale on the horizontal axis, will give the estimated setup at the coast 12 hr after the time represented by the weather map. The setup is added to the predicted tidal elevation and the barometric correction in order to obtain the total elevation of the sea surface.

The *Sea Level* circle in the nomogram was established by plotting values of speed for each pair of opposing directions of wind. One direction was taken arbitrarily as positive (with its opposite as negative), and plotted against corresponding values for sea level in terms of tide staff heights. At the same time, it was noted where these lines intersected zero speed. This intersection, 6.68 ft on the Atlantic City tide staff, was interpreted to constitute mean sea level for the period, in the absence of wind and departures from mean atmospheric pressure. The circle marked *Sea Level* in fig. 3 represents this elevation of the sea surface when no wind is present and atmospheric pressure differences are neglected.

Table 1. Examples of setup at Atlantic City for various wind forces and directions as determined from fig. 3

Pressure Gradient		16 mb	10 mb	6 mb
Geostrophic Wind		51 kt	32 kt	18 kt
	Calculated Surface Wind	34 kt	21 kt	12 kt
Wind Direction	Wind Direction	Height	Height	Height
010°	350°	0.1 ft	0.0 ft	−0.1 ft
100	050	1.5	1.0	0.6
190	170	−0.2	0.0	0.1
280	260	−1.6	−1.0	−0.6

The curve representing least wind force was altered somewhat in the construction since the small setup in this class is easily affected by inequalities in directional distribution of wind and residual pressure effects.

Some examples from the nomogram, tabulated in table 1, give the deviation of sea level from its mean value, after a 12-hr lag, for given geostrophic winds and associated surface winds.

The surface wind in table 1 was obtained by assuming a 2:3 ratio between surface and geostrophic winds [3]. An approximate relation of 20° deviation of surface wind to the left of the geostrophic wind was used for the latitude of Atlantic City. This relation was based on calculations according to a method by Rossby and Montgomery [5].

"Hindcasts" of setup, compared with observed effects, gave correlation coefficients greater than 0.80 with the exception of observations made in January and February. Figure 4 shows the comparison for January where open circles mark the calculated setup. It was possible to improve the correlations by eliminating the data involving local pressure cells. Measurements of these local cells were complicated by several factors and were not well suited to the statistical treatment.

Independent application of the nomogram was made for the month of October 1952, a period not included in its empirical derivation. Cape Henlopen, at the entrance to Delaware Bay, was selected for comparison because its coastline is oriented similarly

Table 2. Correlation coefficients between elevations of observed and predicted tides at Cape Henlopen, October 1952

	High water	Low water
Astronomical predictions (60 cases)	0.665 ± 0.048	0.794 ± 0.032
Astronomical predictions, corrected for wind and pressure (60 cases)	0.872 ± 0.021	0.947 ± 0.009

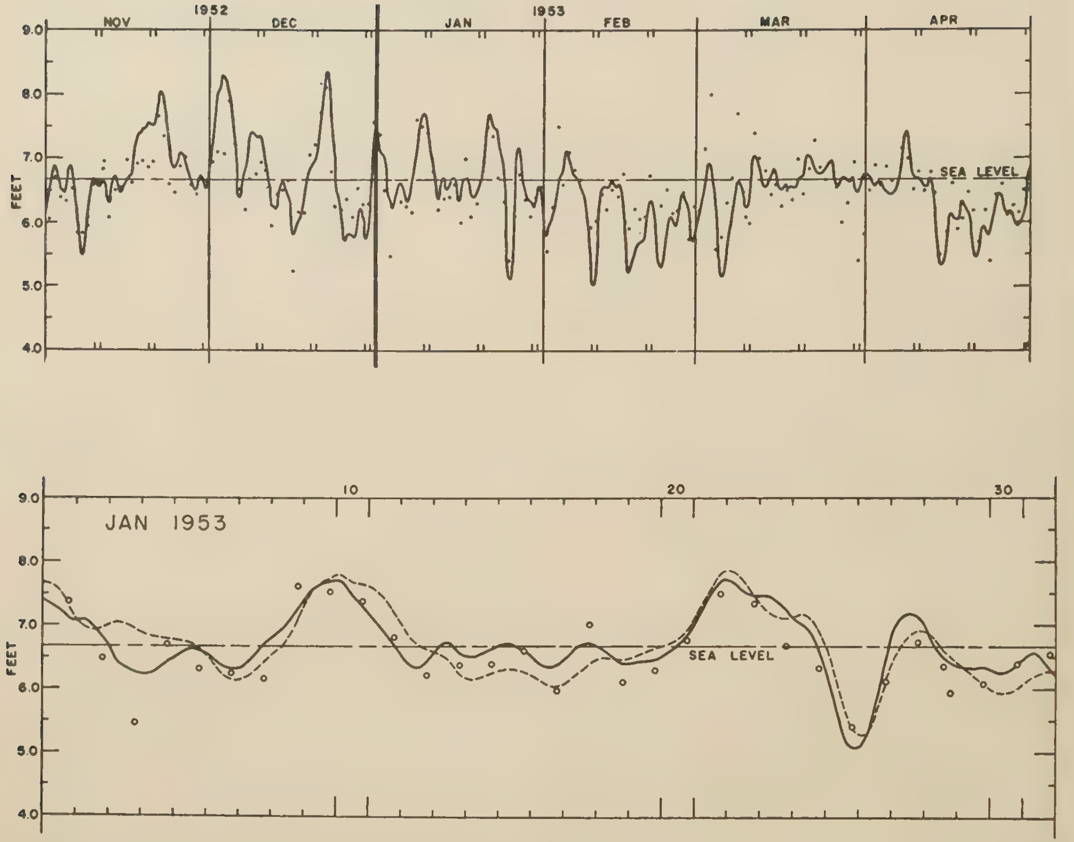

Fig. 4. Above: *Solid line:* Observed tidal elevations, from which astronomical components have been eliminated, observed at Atlantic City from 1 November 1952 to 30 April 1953. *Points:* Non-tidal elevations calculated from weather maps using fig. 3. *Ordinate:* Elevations on tide staff at Atlantic City. The setup is given by the departure of the data from the horizontal line marked *Sea Level.* Below: The data for January 1953 expanded. *Broken line:* Observed non-tidal sea level. *Solid line:* Same, corrected for barometric effect. *Circles:* Setup determined from weather maps using fig. 3.

to that at Atlantic City. The predictability of the tides was considerably improved after taking into account the effects of atmospheric pressure and of setup (see table 2).

6. Discussion

The maximum deviations of sea level may be expected to result from that component of net wind drift that is normal to the coast, if the small deviations of height, which may result from changes in the longshore gradient current, are neglected. Assuming symmetrical response of sea level to wind direction, elevation may be expressed as a cosine function of the geostrophic wind. In this treatment, the following relationships are considered constant: (1) the angles of coastline orientation, (2) the component of wind drift normal to the coast, and (3) the angular relation between wind drift and geostrophic wind. Thus, the setup at any time t, is given approximately by the relation

$$\zeta_t = K(\Delta p_a)_{\max} \cos\,(\psi + 90 - G - \phi)_{t-12\ \mathrm{hr}} - (kp_a)_t,$$

where

ζ_t is the amount of departure from predicted sea level at time t,

K is a dimensional constant,

Δp_a is the geostrophic wind expressed as a pressure difference measured at $t - 12$ hr,

$(kp_a)_t$ is the barometric correction at the time t.

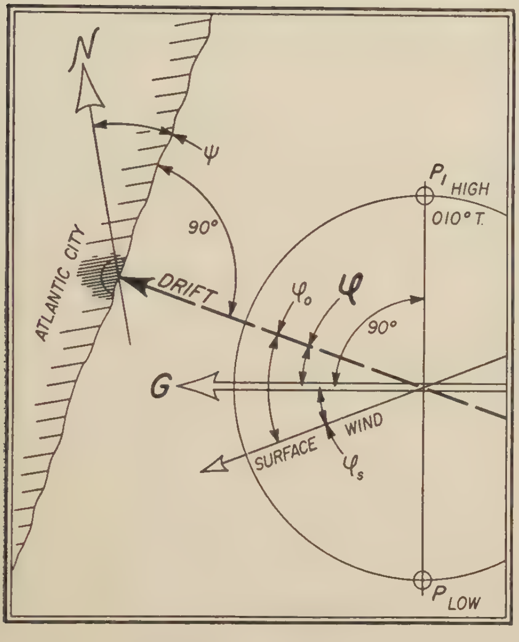

Fig. 5. Schematic diagram showing conditions for maximum setup at Atlantic City.

For the angular notation,

ψ is the angle of coastline from the north (30° at Atlantic City),

G is the direction of geostrophic wind,

ϕ is the angle between wind drift and geostrophic wind.

The schematic diagram of fig. 5 shows the derived relations for the maximum positive deviation of sea level.

According to Rossby and Montgomery [5], the angle of deviation between surface wind and gradient wind ϕ_s, for the latitude of Atlantic City, should be about +20°. This condition is for the case of an ideal friction layer where air currents are initially slightly stable and the air is stirred up to a height corresponding to some theoretical limit. The same authors have dealt with the angle between surface drift and wind stress ϕ_0 and have computed it for various latitudes and wind speeds, assuming a constant stress factor. For the latitude of Atlantic City, the angle ϕ_0 will vary between 39° and 48°, the latter value being for high wind velocities. It follows that the angle between surface drift and gradient wind $\phi_0 - \phi_s$ will vary from 19° to 28°.

If it is assumed that greatest departures from sea level occur when net transport is normal to the coastline, the nomogram shows greatest departure when the geostrophic winds blow 20° from the right of normal to the coastline (100° True or 280° True). If the net transport represents surface drift and the gradient wind is replaced by geostrophic wind, the empirical angle of 20° is comparable to the computed angles ($\phi_0 - \phi_s = 19°$ to 28°) between surface drift and gradient wind.

When the net transport of water due to wind stress is parallel to the coastline, sea level at Atlantic City may be assumed to be unaffected by the wind, if dynamic adjustments for coastwise currents are neglected. This condition is fulfilled where the isotachs in fig. 3 intercept the reference circle marked *Sea Level*. The angle of geostrophic wind under this condition varies from 13° to 25° to the right of the coastal orientation, which again agrees reasonably well with the theoretical values.

It is important to note that results of this study, as indicated in the nomogram, show a nearly linear relationship between setup and speed of geostrophic winds, except for winds parallel to the coastline.

7. Summary

This study has used an empirical approach to the problem of wind setup. To summarize, the limitations of the problem should be reviewed.

In the first place, the wind force is determined geostrophically from sea level pressures. The use of the geostrophic wind in place of actual surface wind is convenient and practical as long as the relationship between them remains constant. Local intense storms are eliminated by this restriction.

Second, the 12-hr lag between equilibrium of sea level and state of wind is a statistical relationship; it may be variable, depending on the size, position and movement of the effective wind field. Intense storms, such as hurricanes, are not effectively treated by this approach.

In the third place, no allowances have been made for stability of the air, or of the water. The study is concerned with the winter months when either medium is relatively homogeneous. This fact possibly excludes its application to summer months when stability may become a significant factor.

Finally, the correction for atmospheric pressure is indecisive since it depends upon an arbitrary pressure field.

Acknowledgments—Copies of processed tidal data were obtained from the U. S. Coast and Geodetic Survey. Weather maps were issued from the New York Office of the U. S. Weather Bureau.

REFERENCES

1. Doodson, A. T. and H. D. Warburg, 1941: *Admiralty manual of tides*. Hydrographic Dept., Admiralty, London, pp. 110–112.
2. Marmer, H. A., 1951: Tidal datum planes. *Spec. Pub. No. 135, U. S. Dept. Commerce, Coast and Geodetic Survey*, 142 pp.
3. Petterssen, S., 1940: *Weather analysis and forecasting*. McGraw-Hill, New York, 505 pp.
4. Proudman, J., 1953: *Dynamical oceanography*. John Wiley & Sons, New York, 409 pp.
5. Rossby, C.-G. and R. B. Montgomery, 1935: The layer of frictional influence in wind and ocean currents. *Pap. phys. Oceangr. Meteor.*, **3**, no. 3, 101 pp.
6. Schalkwijk, W. F., 1947: A contribution to the study of storm surges on the Dutch coast. *Koninklijk Nedelandsch Meteorologisch Instituut de Bilt, No. 125, Med. e. Ver.*, Ser. B, 1, no. 7, 111 pp.
7. Saville, T., Jr., 1952: Wind setup and waves in shallow water. *Tech. Memo. no. 27, Beach Erosion Board, U. S. Army Corps of Engnrs.*, 36 pp.

Contribution No. 833

Turbulence Measurements in a Young Cyclone Over the Ocean[1]

Andrew F. Bunker

Woods Hole Oceanographic Institution

Abstract

A flight was made through a young coastal storm with a PBY-6A aircraft equipped to measure both mean temperatures and rapid variations of the temperature and turbulent gust velocities. Low level observations were obtained which show the thermal structure of the cyclone and the magnitude of the turbulence, the shearing stresses and the heat flows. Particularly strong turbulence was noted in the transition zone between the cool air of the anticyclone and the faster moving air of the warm sector. Stable air and downward heat flow was observed in the cold air mass.

Introduction

On January 22, 1955 a PBY-6A amphibian aircraft fitted out with instruments designed to measure the vertical and horizontal turbulent components of the wind, shearing stresses, vertical heat flows, and the mean air temperatures, flew from Bermuda to Quonset Point, Rhode Island. The path of the airplane cut through a cyclone that had generated on a cold front in the Cape Hatteras region and was accelerating over the ocean in a northeasterly direction. Upon take-off the airplane sounded the relatively cool air that had arrived earlier from the continent and was drifting eastward under the influence of the Bermuda anticyclone. About 400 km out of Bermuda increased turbulence was encountered in a zone that marked a rapid transition from the sluggish anticyclonic circulation to the jet of warm air that constituted the warm sector of the cyclone. The warm sector was so narrow that the airplane passed from this transition zone to air with prefrontal characteristics in just a few minutes. Here a large wafer of cold air underlay the warm air ahead of the main cold front, creating an irregular temperature pattern which increased the stability of the air. As the airplane approached the cold front, the air became rougher, reaching a maximum in the cold front. The nose of cold air behind the front was exceedingly stable as it left the land and remained so even after flowing over 300 km of warmer water. As a result of this, turbulence was slight and the heat flow was directed downward even at 100 m above the sea surface.

The airplane, its equipment, the turbulence observing program and procedures have been explained in references [1] and [2]. The basic quantities recorded are: (1) the vertical accelerations, (2) the attitude, (3) the air-speed of the airplane, and (4) the temperature variations of the air. From these measurements time series of (1) w', the vertical turbulent component of the wind, (2) u', the horizontal tubulent component in the direction of the airplane's flight, and (3) T', the temperature deviation, are computed. From the time series root-mean-square deviations, shearing stresses ($-\bar{\rho}\,\overline{w'u'}$) and heat flow ($c_p\bar{\rho}\,\overline{w'T'}$) are computed. An observational program is being carried out for the measurement of these quantities in air masses with differing stabilities in various regions of the ocean. The present set of observations is a by-product of this work.

Isentropic Cross-Section

All of the values of the quantities computed from the data collected during the flight have been plotted on a single cross-section, Figure 1, representing the lower regions of the atmosphere between Bermuda and Rhode Island. A map of the pressure field and frontal system has been inserted in a corner of the cross-section. The ordinate of the section is height in meters, while the abscissa has the double scale of Greenwich Civil Time of a given airplane observation, and the approximate distance from Bermuda in kilometers. The distance scale in the center of the section may be in error by nearly 50 km due to reception difficulties of LORAN signals and the frequent changes in the wind field. The heavy lines depict the isentropes computed from the readings of the airplane psychrograph. The small dots on the diagram give the location of a given temperature observa-

---

[1] Contribution No. 833 from the Woods Hole Oceanographic Institution. Work supported by the Office of Naval Research, U. S. Navy, under contract number Nonr-1721(00) (NR-082-021).

tion. Along the top of the section a few notes have been drafted concerning the cloud type and amount and occurrence of rain. The results of seventeen series of turbulence measurements have been entered at the appropriate time and height on the diagram according to the legend given in the center of the section. The units of the root-mean-square values are cm sec^{-1} and °C. Heat flows are expressed in mcal cm^{-2} sec^{-1}, while the stresses are expressed in dynes cm^{-2}. Here mcal is defined as 10^{-3} calorie. FIGURE 2 has been drafted to show more clearly the heat flux pattern through the cyclone. Lastly, sea temperatures are given in the ovals at the bottom of the diagram. The values are actually the potential temperatures of air in thermal equilibrium with the sea. The water temperatures were obtained from records of *R/V ATLANTIS* which was working from the east coast to Bermuda on this and previous days.

TURBULENCE AND TRANSPORT IN THE BERMUDA ANTICYCLONE

Homogeneity is the most outstanding feature of the air mass occupying the area around Bermuda and extending 300 km along the course of the aircraft. Throughout all of this region and up to 1000 m the potential temperatures were all within one degree of one another. The air mass which was continental in origin was warming slowly as it was then only one degree cooler than the water. The heat flow measurements indicate a transport of about 1 mcal cm^{-2} sec^{-1} near the surface throughout the region. This heat flow is to be contrasted with flows found to be five times greater in air masses fresh from the cold continent. The turbulence was likewise quite moderate and uniform, receiving most of its energy from the decreasing convective activity. These observations coupled with the stratocumulus overcast give a good description of the final stages of air mass modification over the ocean.

The negative shearing stresses arise from the direction of flight and the shifting of the winds from 300° near the surface to 250° at 850 mb. Thus the component of the wind along the airplane's path decreases with height, and since with the present equipment only the component of the stress along the path can be measured, only a negative component of the total stress is recorded. As no detailed wind profiles are available for this or other stresses rather little of value can be gleaned from them.

TURBULENT ZONE BETWEEN ANTICYCLONIC AND WARM SECTOR FLOWS

The existence of a turbulent zone between the air of the Bermuda anticyclone and the warm sector was noted 400 km out of Bermuda during the third series of observations. From the sparce data at hand, it appears that this region constitutes

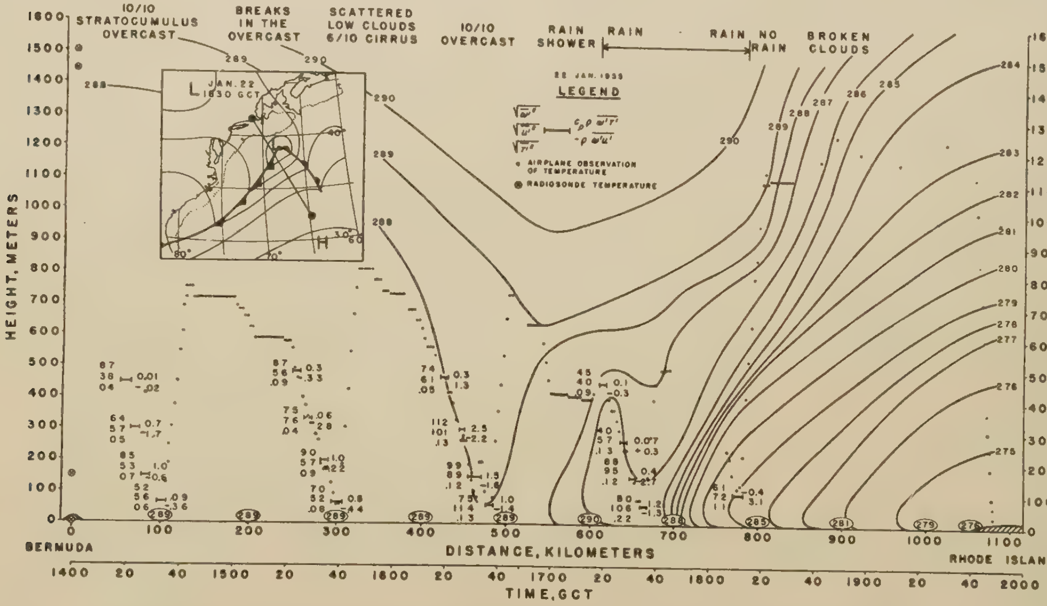

FIG. 1. Isentropic cross-section from Bermuda to Rhode Island. Turbulence and flux measurements expressed in cm sec^{-1}, °C, mcal cm^{-2} sec^{-1}, and dynes cm^{-2} are entered at the proper height and distance.

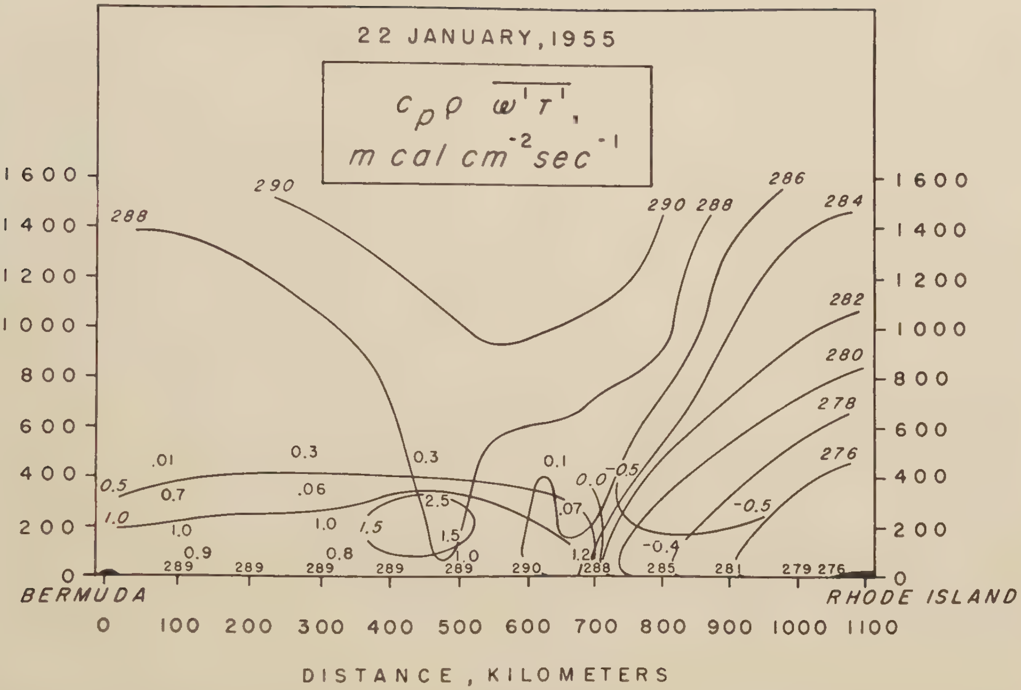

Fig. 2. Heat flux cross-section. Values of the heat flux, water temperatures, and even-valued isentropes have been replotted for Figure 1 to show the heat flux pattern.

a shearing zone between the two air circulations rather than a trailing section of warm front. Ship observations are too few to settle this point by accurately locating the warm front at the time of the airplane's nearest approach. From the cloud observations made at the time and the absence of any rain in this area it seems certain that no front existed which conforms to the definition of a front which requires organized lifting or replacement of cool air by warmer air. Here then, is a turbulence field generated primarily by the shearing of one air stream past another. Convection is not a likely source of the increased energy since the horizontal component of the turbulent wind increases to nearly the value of the vertical component. In other cases studied by the author where it is known that active convection is occurring, the vertical component may be two or more times the horizontal component. Irregular acceleration of the air by the rapidly changing pressure field undoubtedly contributed some energy to the turbulence. No references are known to the author of previous reports of turbulence in this boundary region. However, the turbulence noted here may be related to the turbulence reported in and near jet streams. The parallel between the two cases is far from exact but many features are present in both circumstances.

The heat flows and stresses obtained in this region are puzzlingly large. The large heat flows are most likely a result of the greater turbulence. Without wind data no useful interpretation of the stress values can be given.

Warm Sector Turbulence

In the warm sector all turbulence quantities dropped off to minimum values for the flight. This decrease is the result of the increased stability of the air moving in from the southwest. It is noteworthy that the stability overcame both the tendency for increased turbulence that accompanies greater wind speeds and the lateral diffusion of turbulent energy from the previously discussed shearing zone. The sub-normal values of the turbulence lasted for only two of the four observations made in the warm air. The third and fourth observations were made in a cool mass of air that presumably had forerun the main cold front and squeezed under the warm air. In this cool air the turbulence increases again as do the stresses, heat flows and temperature deviations. The origin of the cool air is open to question since rain was falling at the time of observation. Consequently the air may have been cooled by the rain and thus merely appears as a fore-runner of the front.

STABILITY AND DIRECTION OF HEAT FLOW IN THE COLD AIR SECTOR

No turbulence measurements were made during the frontal crossing as the front's position was not recognized until after the penetration and navigational requirements prohibited a recrossing. The air was rougher in the frontal zone, but not violently turbulent. The author estimates the root-mean-square vertical velocity to be 150 ± 50 cm sec^{-1} at 300 m within the zone.

The most unusual feature of the cold air mass was its great stability which was found to be 25×10^{-8} cm^{-1} in the 100 m to 400 m region. Such stability, rarely found in a cold air mass that has traveled over 300 km of warmer water, is maintained by strong subsidence behind the cold front. Beneath the level of the airplane observation great instability must have existed because the water was 6°C warmer than the air. The only turbulence observation taken in the cold air showed decreased turbulence and a downward flow of heat at 100 m about 80 km behind the front. The shearing stress value was large and positive as would be expected since the airplane was flying directly upwind and hence the total shearing stress was recorded.

The downward flux of heat at 100 m in an air mass blowing over warmer water both demands careful consideration and offers an opportunity of testing diffusion theory and the theory developed by Priestley [3] concerning the upward heat transport by impressed temperature fluctuations. Previous measurements [4] of heat flows in slightly stable air have shown that upward heat flows do exist and with a magnitude that confirms Priestley's theory. The question to be answered now is whether the present observation of a downward flow is consistent with Priestley's expressions. It can be shown that the computed heat flow is not the result of too small a sampling of the atmosphere.

To demonstrate that Priestley's theory is consistent with the observations, let us compute the maximum possible upward heat flow due to buoyant parcels, estimate the downward flow due to diffusion and compare the resulting net flow with the measured value. Assuming the mixing rates for momentum and heat to be equal, and using the observed root-mean-square temperature deviations, one finds the maximum flow to be 0.4 mcal cm^{-2} sec^{-1}. At the same time a downward flow of heat by eddy diffusion of 1 mcal cm^{-2} sec^{-1} is found if the conservative value of 50 gm cm^{-1} sec^{-1} for the coefficient of turbulent mass exchange is placed in the heat diffusion equation. As the airplane gives the net heat flow in the atmosphere, it is apparent that a downward flow should be indicated by the airplane measurements. This demonstration is insufficient to prove the correctness of Priestley's theory under conditions of great stability, but it does show the theory gives results consistent with the observations. The process operating in this region of the cold air may be described as follows. Strong subsidence, the magnitude of which cannot be measured, is occurring behind the frontal zone. This sinking of the air preserves the great stability and results in a large downward flow of heat by advection and diffusion even under conditions of slight turbulence. The air at the lower level is heated by the ocean, becomes unstable and rises in small parcels into the stable air. The heat transport by this convection process is small in comparison with the downward flows. Thus the cold air mass is heated more by the warm stable air aloft than by the warm water.

ACKNOWLEDGMENTS

All of the turbulence and flow data presented in this paper were computed from the raw data by Miss Marilyn Sorum. Mr. John G. Fraser was responsible for the maintenance of the instruments and aided in the observing.

REFERENCES

[1] Bunker, A. F., and K. McCasland, 1954: "Description and Installation of Meteorological Equipment Aboard Navy PBY-6A, 46683." Technical Report to Office of Naval Research. W.H.O.I. Ref. No. 54–82, 14 pp. plus figures. Unpublished manuscript.

[2] Bunker, A. F., 1955: "Turbulence and Shearing Stresses Measured Over the North Atlantic Ocean by an Airplane Acceleration Technique." *J. Meteor.*, Vol. 12, No. 5, pp. 445–455.

[3] Priestley, C. H. B., 1954: "Vertical Heat Transfer from Impressed Temperature Fluctuations." *Aus. Journ. Phys.*, Vol. 7, No. 1, pp. 202–209.

[4] Bunker, A. F., 1956: "Measurements of Counter-Gradient Heat Flows in the Atmosphere." *Aus. Journ. Phys.*, Vol. 9, No. 1, pp. 133–143.

Contribution No. 835

J. CHASE

THE BERMUDA-AZORES HIGH PRESSURE CELL. ITS SURFACE WIND CIRCULATION

SEPARATA DE

MISCELÂNEA GEOFÍSICA

PUBLICADA PELO SERVIÇO METEOROLÓGICO
DE ANGOLA EM COMEMORAÇÃO DO X ANIVERSÁRIO DO
SERVIÇO METEOROLÓGICO NACIONAL

LUANDA
1956

THE BERMUDA-AZORES HIGH PRESSURE CELL
ITS SURFACE WIND CIRCULATION(1)

by
Joseph Chase
Woods Hole Oceanographic Institution, U. S. A.

ABSTRACT: The Bermuda-Azores High is associated with a clockwise wind circulation over the surface of the North Atlantic Ocean. This circulation is oval shaped with the long axis running east-west. From the standpoint of averages over several years it is a very regular circulation. When considered for shorter periods, however, its regularity vanishes at times during the presence of other meteorological phenomena. These phenomena make convenient handles to denote the various types of irregularities, which frequently persist for periods of from one to six weeks.

Introduction

The title, "The Bermuda-Azores High Pressure Cell" refers to that cell of high atmospheric pressure usually located in the North Atlantic Ocean between the 20th and 50th parallels. This "high" is known by several other names among which are "The Azores High", "The Bermuda High", "The Mid--Atlantic High", and "The Semi-permanent North Atlantic High". The words Bermuda-Azores were chosen as being somwhat more descriptive of the high's average position and domain.

It is the purpose of this paper to describe briefly, for oceanographers, the habits of this high, discussing its average location and shape, and the clockwise circulation of surface winds associated with it, as well as some anomalies of location, shape, and circulation.

It is assumed that any changes in average pressure which may have occurred in the last half century, can be ignored in the discussion.

The maps used for the study are the:

1. Historical Weather Maps, Northern Hemisphere, Sea Level (Weather Bureau, 1943).

---

(1) Contribution No. 835 from the Woods Hole Oceanographic Institution. This work was performed under the auspices of the Office of Naval Research Contract N6onr-27701.

2. Normal Weather Maps, Northern Hemisphere, Sea Level Pressure (Weather Bureau, 1946).

These maps cover the period beginning January 1, 1899 and ending June 30, 1939. The former are daily maps and the latter are averages for the 40-1/2 years.

Annual Pressure Distribution

The average pressure distribution for the entire period of the maps shows two main features in the North Atlantic, viz: the so-called Icelandic Low and the Bermuda-Azores High. These features may be seen in Figure 1.

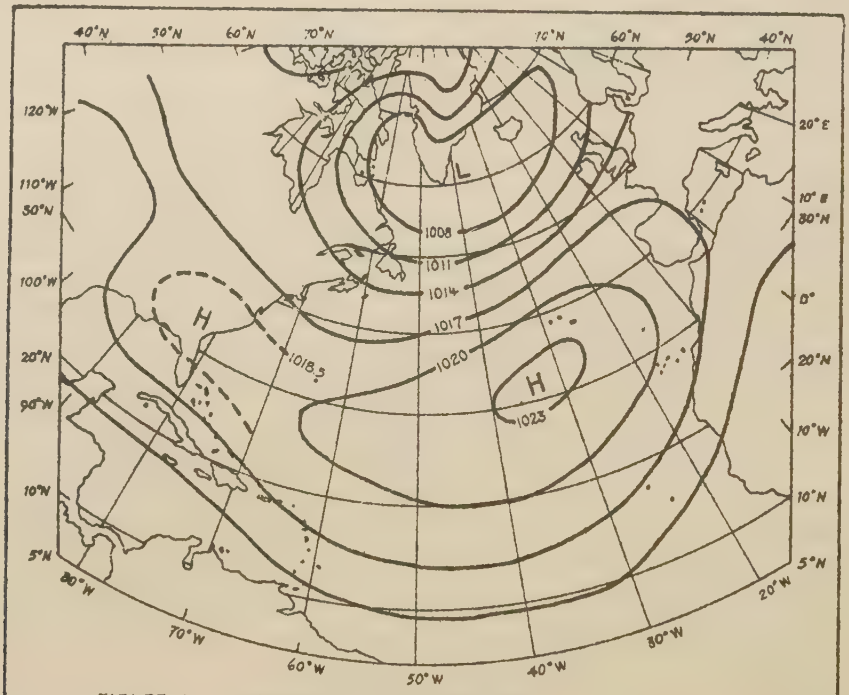
40°N
50°N
60°N
70°N
70°N
60°N
50°N
40°N
120°W
110°W
30°N
100°W
20°N
90°W
10°N
5°N
80°W
70°W
60°W
50°W
40°W
30°W
20°W
5°N
10°N
10°W
20°N
0°
10°E
30°N
20°E
L
H
H
1008
1011
1014
1017
1020
1023
1018.5

FIGURE 1 NORMAL SEA LEVEL PRESSURE ANNUAL

WHOI APRIL 1951

The "Icelandic Low" is centered just east of the southern tip of Greenland at about 62°N., 38°W., and is elongated in a curve from Davis Strait to Novaya Zemlya. The Bermuda-Azores High is centered some 600 miles southwest of the Azores at 32°N., 33°W., which is about twice as far from Charleston,

S. C. as from Casablanca, and is elongated east-west in a curve from the Georgia-Carolina area to Spain. It is part of a belt of high pressure encircling the earth near the 30th parallel (i.e., the Horse Latitudes).

In summer, thermal conditions are un favorable for the formation of high pressure over the land and the Horse Latitude high pressure belt is continuous only over the cooler oceans. In winter, the belt can readily be traced around the globe, but weak troughs, one over the Gulf Stream and the other over the Mediterranean, partially separate the Bermuda-Azores High from the rest of the belt. In the annual picture, therefore, we see the Bermuda-Azores High as a separate cell, bounded on the north by the prevailing westerlies, on the south by the Trade Winds, on the east by northerlies and on the west by weak southerlies. The strongest of these winds are the westerlies. The average wind force in the area of the westerlies is much stronger than indicated by the average pressure gradient. The difference is due to the great variability of wind direction in that area especially in winter. Changing wind directions greatly lower the average gradient at the east end of the high and leave a very gentle net southerly flow at the west end. While wind strengths are generally lower in the trades than in other sectors, the directions there are much more constant and this gives an average gradient which is nearly equivalent to that in the westerlies.

The winds flow clockwise around the high at an angle of about 20° to the left of the isobars (toward lower pressure) but deviate by as much of an angle as 70° in some instances in tropical regions. The deviation is largest in the Cape Verde Island region, but diminishes rapidly to 20° to 30° in the rest of the Trades and is 10° to 20° in the westerlies and at the east and west ends of the high.

Average Pressure Distribution by Months

The positions of the centers of the Bermuda -Azores High on the monthly Normal Weather Maps make a rather orderly path about the annual position of the center, (32°N., 33°W.). The easterly positions of the centers for November through February are the result of a greater incidence of high pressure over Europe and North Africa in those months and the linkage of this high pressure with the Bermuda-Azores High. The centers for the remaining months are closely grouped near 38°W. All of the centers are plotted in Figure 2.

The general appearance of the mean monthly pressure distributions is similar to that of the annual average. Although the westerlies are normally stronger in winter than in summer, the circulation around the Bermuda -Azores High, when taken as a whole, is greater in summer. The mean maps for

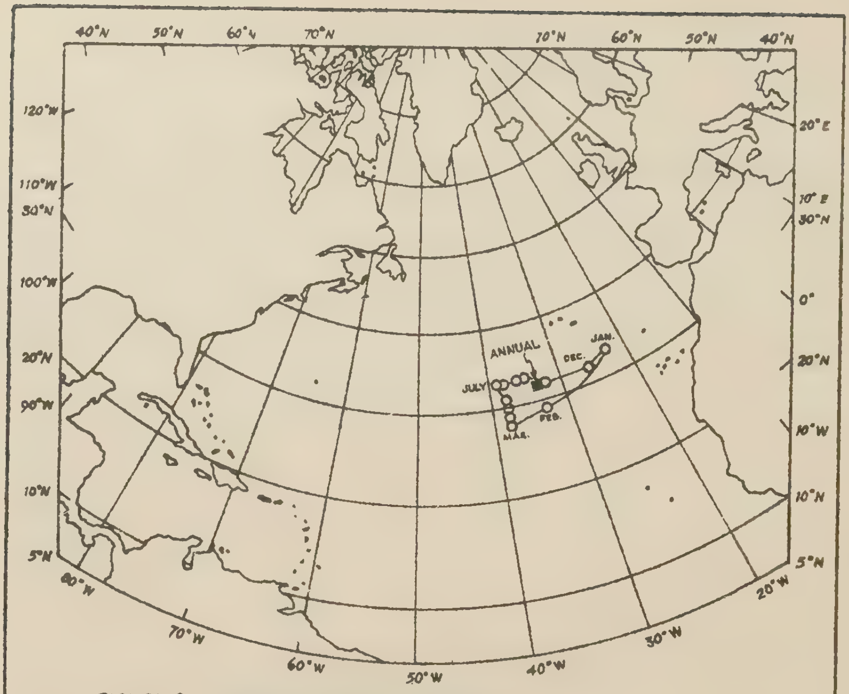
40°N
50°N
60°N
70°N
70°N
60°N
50°N
40°N
120°W
110°W
30°N
100°W
20°N
90°W
10°N
5°N
20°E
10°E
30°N
0°
20°N
10°W
10°N
5°N
80°W
70°W
60°W
50°W
40°W
30°W
20°W
ANNUAL
JAN.
DEC.
JULY
FEB.
MAR.

FIGURE 2 NORMAL SEA LEVEL PRESSURE
MONTHLY POSITIONS OF CENTER OF B-A HIGH.

WHOI APRIL 1951

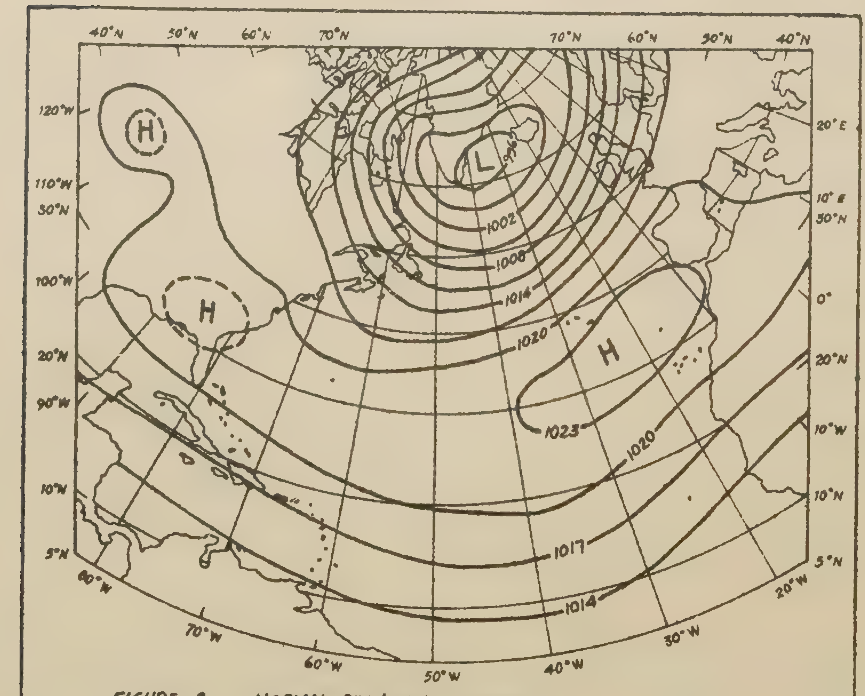
40°N
50°N
60°N
70°N
70°N
60°N
50°N
40°N
120°W
110°W
30°N
100°W
20°N
90°W
10°N
5°N
20°E
10°E
30°N
0°
20°N
10°W
10°N
5°N
80°W
70°W
60°W
50°W
40°W
30°W
20°W
H
H
L
996
1002
1008
1014
1020
H
1023
1020
1017
1014

FIGURE 3 NORMAL SEA LEVEL PRESSURE
JANUARY

WHOI APRIL 1951

January and July (Figs. 3 and 4) illustrate this fact. In July the trades are stronger in proportion to the increased pressure gradient and the east and west ends of the high are much better developed. The westerlies show a decrease in width of band and in pressure gradient. The decrease is greatest in the area north of 50°N. South of that parallel, the average westerlies are nearly as strong as in winter. This is the result of more steadiness of direction in summer rather than of high velocities. The other months represent parts of the gradual spring and fall transitions between January and July. Figures 5 and 6 are for April and October, the mid-points in the transitions. Note the weak northerly flow off Hatteras in October and in January which is associated with a small average high over the land. This high and this reversal of normal flow are also present in November and December, and are strongest in November.

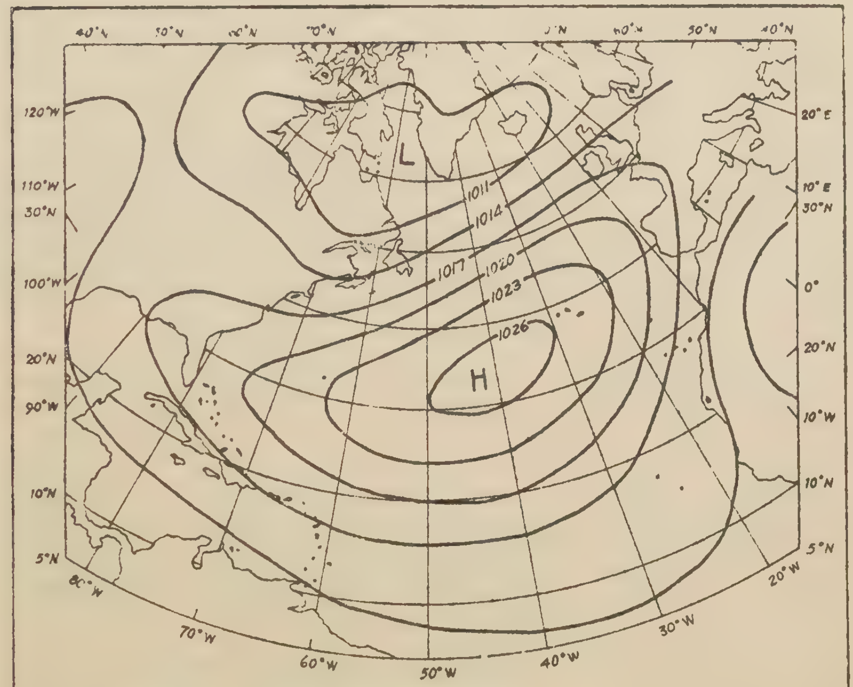
40°N
50°N
60°N
70°N
60°N
50°N
40°N
120°W
110°W
30°N
100°W
20°N
90°W
10°N
5°N
80°W
70°W
60°W
50°W
40°W
30°W
20°W
20°E
10°E
30°N
0°
20°N
10°W
10°N
5°N
L
1011
1014
1017
1020
1023
1026
H

FIGURE 4 NORMAL SEA LEVEL PRESSURE
JULY

WHOI APRIL 1951

The highest pressure in the Bermuda-Azores High for the monthly mean charts varies between 1023 mb. (April, October, November)

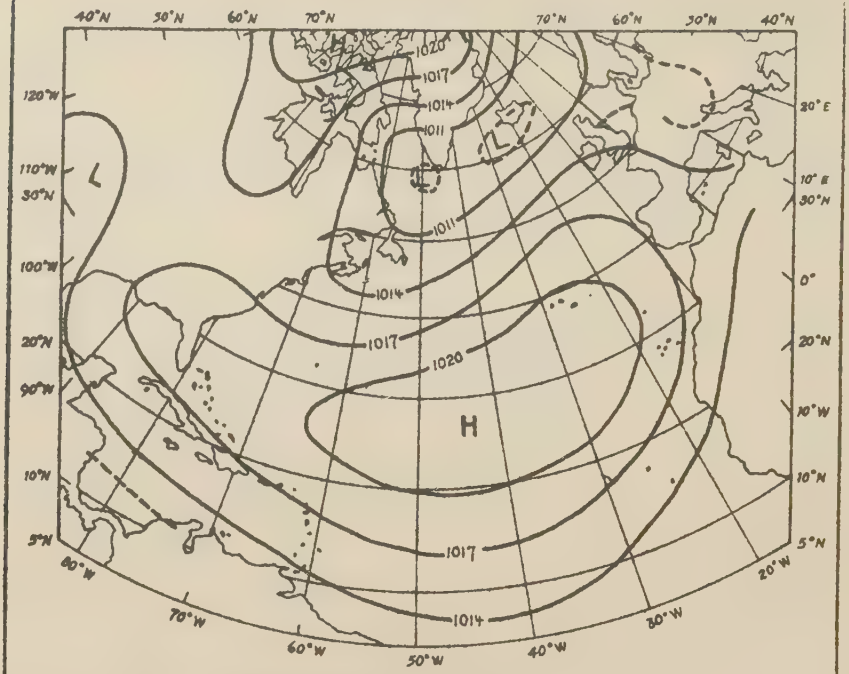
40°N
50°N
60°N
70°N
70°N
60°N
50°N
40°N
120°W
110°W
30°N
100°W
20°N
90°W
10°N
5°N
80°W
70°W
60°W
50°W
40°W
30°W
20°W
5°N
10°N
10°W
20°N
0°
30°N
10° E
20° E
1020
1017
1014
1011
1011
1014
1017
1020
1017
1014
L
L
L
H

FIGURE 5 NORMAL SEA LEVEL PRESSURE
APRIL

WHOI APRIL 1951

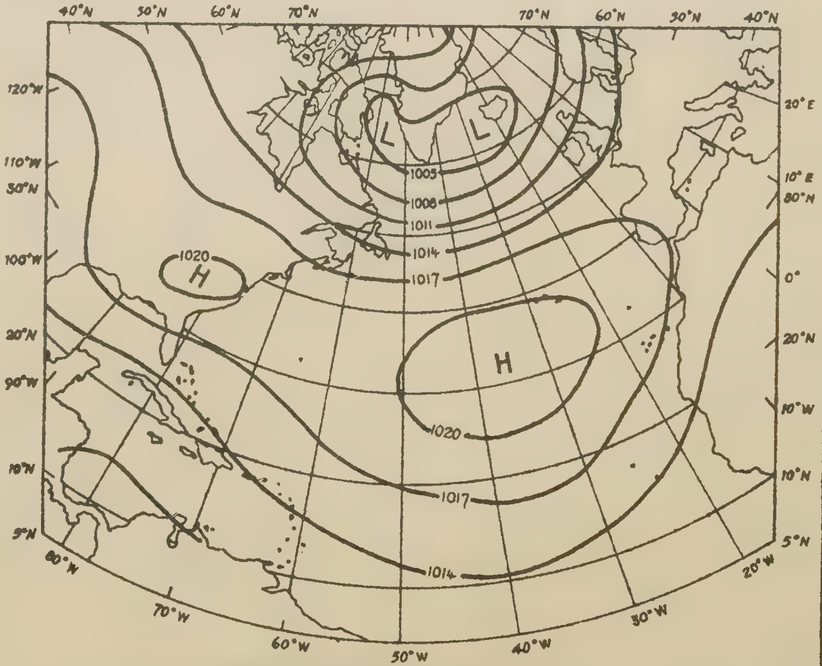
40°N
50°N
60°N
70°N
70°N
60°N
50°N
40°N
120°W
110°W
30°N
100°W
20°N
90°W
10°N
5°N
80°W
70°W
60°W
50°W
40°W
30°W
20°W
5°N
10°N
10°W
20°N
0°
30°N
10° E
20° E
L
L
1005
1008
1011
1014
1017
1020
H
H
1020
1017
1014

FIGURE 6 NORMAL SEA LEVEL PRESSURE
OCTOBER

WHOI APRIL 1951

and 1027.5 mb. (July). Figure 7A is a graph of these highest pressures. While it is not the purpose of this paper to discuss ocean currents it is interesting to note that this graph with its maxima in January and July and minima in April and October-November is remarkably close in date and amplitude to the graphs for ocean current strength in a test rectangle off the Guianas (Fuglister, 1951) (Figure 7B).

The center pressure is in some degree a measure of the relative pressure gradient and surface wind over this test rectangle, if the following conditions obtain: (1) average maps with smoothed isobars, (2) small (2 mb.) variation in mean monthly pressure along the Guiana coast, (3) monthly positions of the center of the Bermuda-Azores High confined to a relatively small area. Since these three conditions are satisfied in the Normal Weather Maps the correlation suggests that variations in the surface wind are directly and within a short time reflected in the variations of velocity of ocean currents in the area of the test rectangle at least.

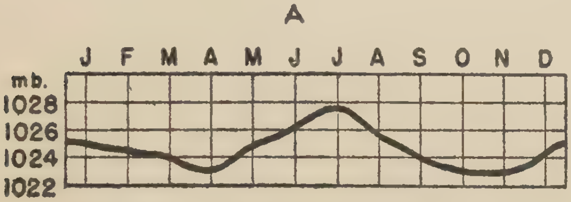

CENTER PRESSURE B-A HIGH
——— AVERAGE 1899-1939

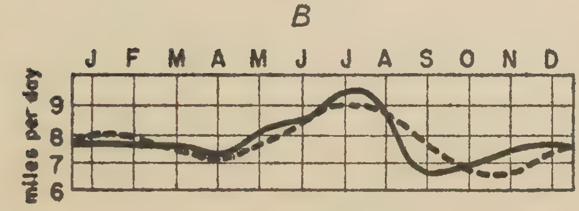

CURRENT SPEEDS - FUGLISTER
——— OBSERVED
- - - - CALCULATED COMBINATION ANNUAL & SEMI-ANNUAL PERIODS. (HARMONIC ANALYSIS)

FIGURE 7

Daily Weather Maps

A large proportion of the daily maps resemble the average maps in position and orientation of the Bermuda-Azores High and in the circulation about it. These situations are most common in the summer (frequentcy estimated at some 60% of the time) and least common in winter (about 30%). The frequency for fall is slightly higher than that for spring.

The situation in Figure 8 is a typical summer "good" circulation;

i.e., "good" in respect to speed and direction of wind clockwise about a normally centered high. (Note that the isobars are drawn for 5 mb. intervals on the daily maps while 3 mb. spacing is used on the average maps). The gradient in the trades and at the east and west ends of the Bermuda-Azores High is well developed. The westerlies are broken up north of 50°N. with the overthrow of the reign of the Icelandic Low. South of 50° however, there is a respectable gradient in the westerlies along the northern edge of the Bermuda-Azores High.

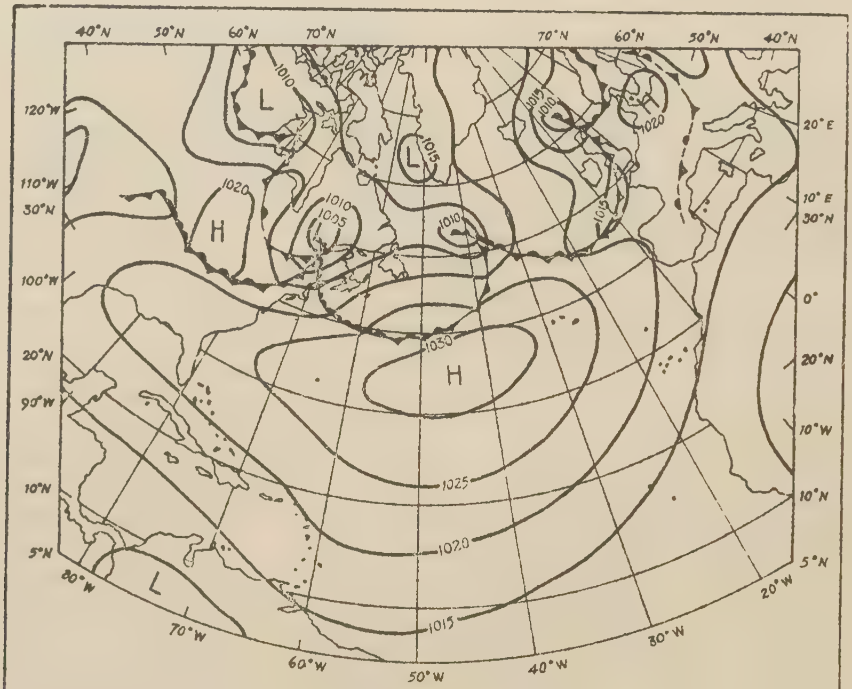
40°N
50°N
60°N
70°N
70°N
60°N
50°N
40°N
120°W
110°W
30°N
100°W
20°N
90°W
10°N
5°N
80°W
70°W
60°W
50°W
40°W
30°W
20°W
20°E
10°E
30°N
0°
20°N
10°W
10°N
5°N
L
1010
L
1015
1015
1010
H
1020
1020
H
1010
1005
1010
1030
H
1025
1020
1015
L

FIGURE 8 SURFACE SYNOPTIC CHART 1300 GMT
JUNE 27, 1917

WHOI APRIL 1951

In January of 1918, wind circulation about the Bermuda-Azores High was far below average. In the next month, however, the circulation became far better than average. The map of February 13, 1918 (Fig. 9) is typical of that month. The Bermuda-Azores High is close to its normal position southwest of the Azores, and has the very high value for center pressure of 1037 mb. The resultant strong gradient flow starts at the African coast, runs to the Caribbean in a wide band then turns north in a good "west end" flow.

North of Bermuda it is joined by strong westerlies associated with a frontal wave in the Maritimes and heads eastward to Europe. The one weak sector in this circulation is at the "east end" in the area of an old occlusion. The Icelandic Low is in normal position and the westerlies extend to higher latitudes than in the previous example.

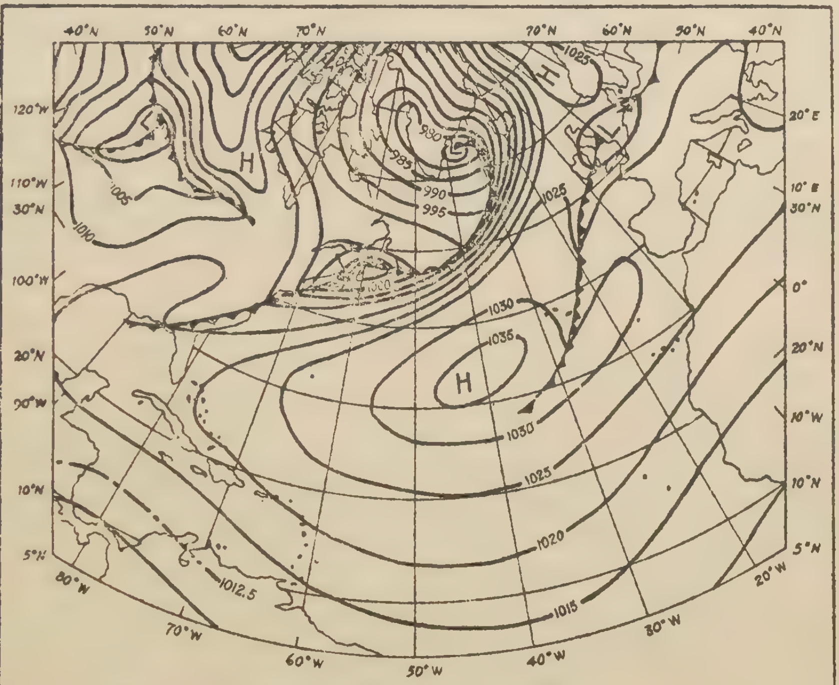
40°N
50°N
60°N
70°N
70°N
60°N
50°N
40°N
1025
H
L
20°E
120°W
H
980
985
990
995
1005
1010
110°W
30°N
10°E
30°N
1025
100°W
0°
1030
1035
20°N
20°N
H
90°W
1030
10°W
1025
10°N
10°N
1020
5°N
5°N
1012.5
1015
20°W
80°W
30°W
70°W
60°W
40°W
50°W

FIGURE 9 SURFACE SYNOPTIC CHART 1300 GMT
FEBRUARY 13, 1918

WHOI APRIL 1951

Interruptions to Normal Circulation

While about half of the daily maps show a "normal" circulation, the remainder contain some interruptions in that circulation. Such interruptions occur whenever the wind direction turns from the normal or when its velocity is below normal. A study of interruptions reveals that they are not a collection of freak situations but rather are situations associated with normal meteorological phenomena and may be classified according to these phenomena.

The types of interruptions to normal circulation delineated here are associated with the following:

1. Fronts
2. Stagnant Lows
3. Linkage of the Bermuda-Azores High to Continental Highs
    a. uniting
    b. replacement
4. Hurricanes

The percentages of frequency quoted in the paper for the various types are estimates based on perusal of the 40-1/2 year daily series.

Fronts

Some fronts move along the northern side of the Bermuda-Azores High without interrupting the westerlies much. In many cases they serve to increase the pressure gradient and consequently the speed of the westerlies. Other fronts, however, move into the general area of the Bermuda-Azores High accompanied by winds from directions other than those indicated by the normal maps.

Two frontal systems and a weakened Bermuda-Azores High which is well south of its normal position are seen in Figure 10. There are northerly winds from Newfoundland to the Bahamas, variable wind directions off Portugal and winds from the northeast and southeast between Newfoundland and Europe. The trades are about average except for a break near Puerto Rico. A similar description fits Figure 11, but here the circulation about the frontal systems is stronger and the Bermuda-Azores High is weaker and its position farther away from normal. The trades are strong only off the Guiana coast and west winds are found just north of Puerto Rico. The frequency figures for frontal interruptions are 50% of the time in winter; i.e., half of all winter maps, 40% in spring, 25% in summer, and 30% in fall. While any one front will normally cross the ocean from the Carolinas to Portugal in about a week, a series of fronts can extend a period of frontal interruptions to three to four weeks. When the interruptions associated with one front persist longer than one week the situation can often be classified under "Stagnant Lows".

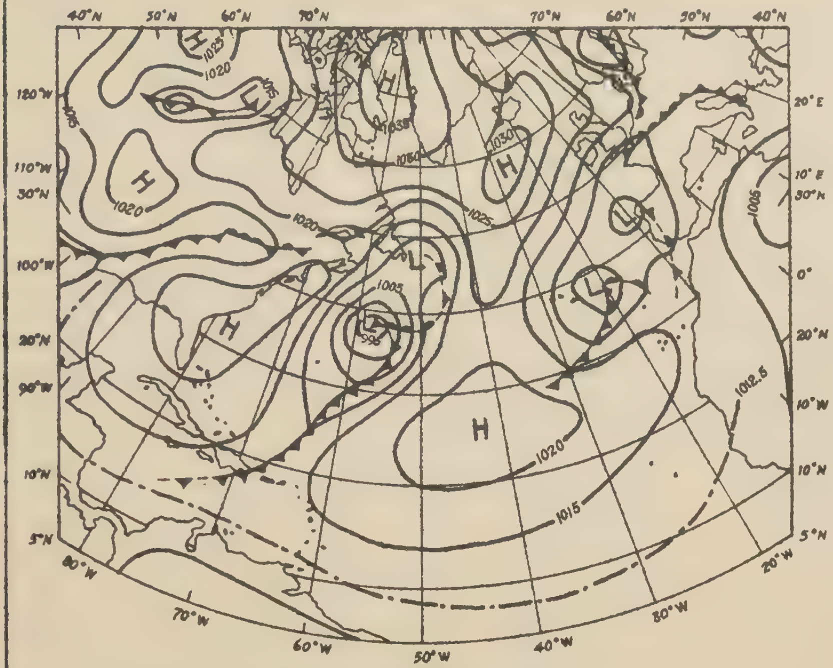
40°N
50°N
60°N
70°N
70°N
60°N
50°N
40°N
120°W
110°W
30°N
100°W
20°N
90°W
10°N
5°N
80°W
70°W
60°W
50°W
40°W
30°W
20°W
20°E
10°E
30°N
0°
20°N
10°W
10°N
5°N
H
H
H
H
H
H
L
L
L
L
L
1025
1020
1020
1020
1035
1030
1030
1025
1020
1005
995
1020
1015
1005
1012.5

FIGURE 10 SURFACE SYNOPTIC CHART 1300 GMT.
MAY 1, 1916

WHOI APRIL 1951

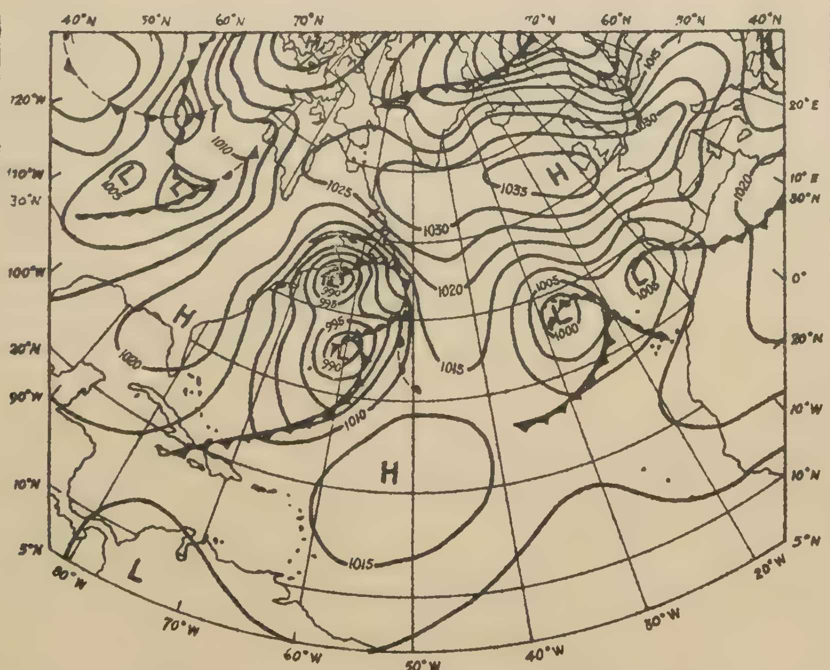
40°N
50°N
60°N
70°N
70°N
60°N
50°N
40°N
120°W
110°W
30°N
100°W
20°N
90°W
10°N
5°N
80°W
70°W
60°W
50°W
40°W
30°W
20°W
20°E
10°E
30°N
0°
20°N
10°W
10°N
5°N
H
H
H
L
L
L
L
L
L
L
1010
1005
1025
1030
1035
1030
1015
1020
1020
990
995
990
1020
1015
1010
1005
1000
1005
1020
1015

FIGURE 11 SURFACE SYNOPTIC CHART 1300 GMT
JANUARY 4, 1918

WHOI APRIL 1951

Stagnant Lows

The stagnant low in the Atlantic not to be confused with the semi-permanent Icelandic Low, usually wanders about in some Atlantic area for 1 to 2 weeks before moving away from the area. After a 2 to 5 day break, another stagnant low often appears somewhere in the Atlantic so that the duration of this type of interruption may be 4 to 6 weeks if we except the short breaks. Perhaps the most frequent Atlantic areas for stagnant lows to be found in are:

a. Southeast of Newfoundland

b. The Azores

c. West of Ireland

d. Between Bermuda and the Azores

Figure 12 shows a stagnant low which wandered about in the area southeast of Newfoundland for about 10 days before escaping eastward. It was preceded by a stagnant low of short duration in the Bay of Biscay and followed by one between Bermuda and the Azores. Figure 13 shows a stagnant low near the Azores which persisted for 16 days after which it weakened and split, one part escaping northeastward and the other southwestward. The low in Figure 12 has a mean diameter of about 2,500 nautical miles, while that of Figure 13 is about 800 miles across. The extend of the interruptions to normal circulationconcurrent with these 2 lows is best described by the figures themselves. The winter frequency for stagnant lows runs around 30% and the summer frequency is about 15%, but the yearly deviation from the mean frequency is large.

Linkage

When a cold continental high nears the North Atlantic, its circulation often links in some measure with that of the Bermuda-Azores High, thereby interrupting normal circulation. Such linkage can take place along the North American east coast, in the Greenland-Iceland region(1), along the west coast of Europe, and along the northwest coast of Africa. Considerable interruption by linkage is seen on some 30% of maps in summer and 50% in winter.

---

(1) Here the polar ice cap and Greenland are considered as continental in contrast to the open ocean.

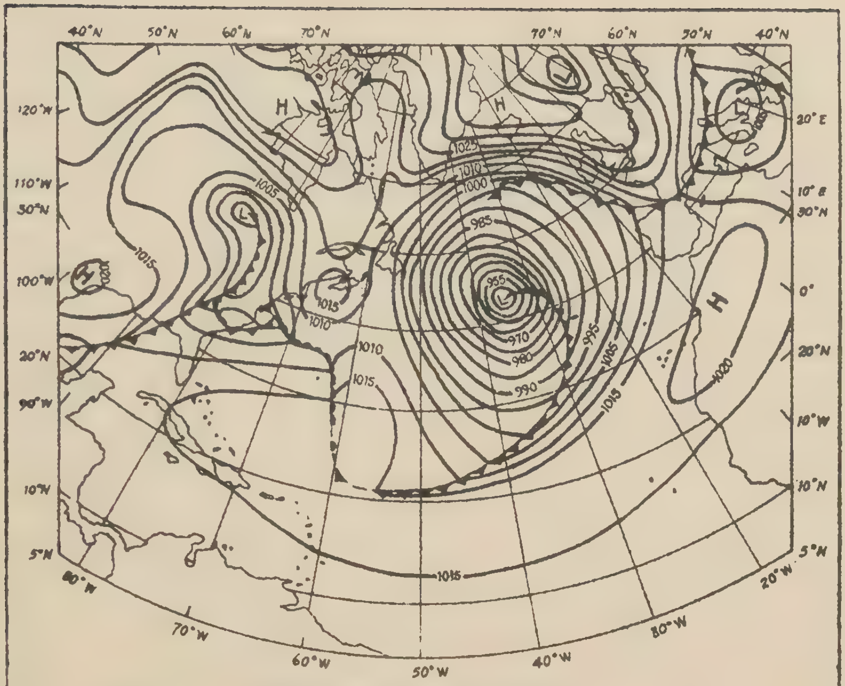
40°N
50°N
60°N
70°N
70°N
60°N
50°N
40°N
120°W
110°W
30°N
100°W
20°N
90°W
10°N
5°N
80°W
70°W
60°W
50°W
40°W
30°W
20°W
20°E
10°E
30°N
0°
20°N
10°W
10°N
5°N
H
H
H
L
L
L
1025
1010
1000
985
955
970
980
990
995
1005
1015
1020
1015
1010
1005
1015
1010
1015
1015
1015

FIGURE 12 SURFACE SYNOPTIC CHART 1300 GMT
DECEMBER 16, 1927

WHOI APRIL 1951

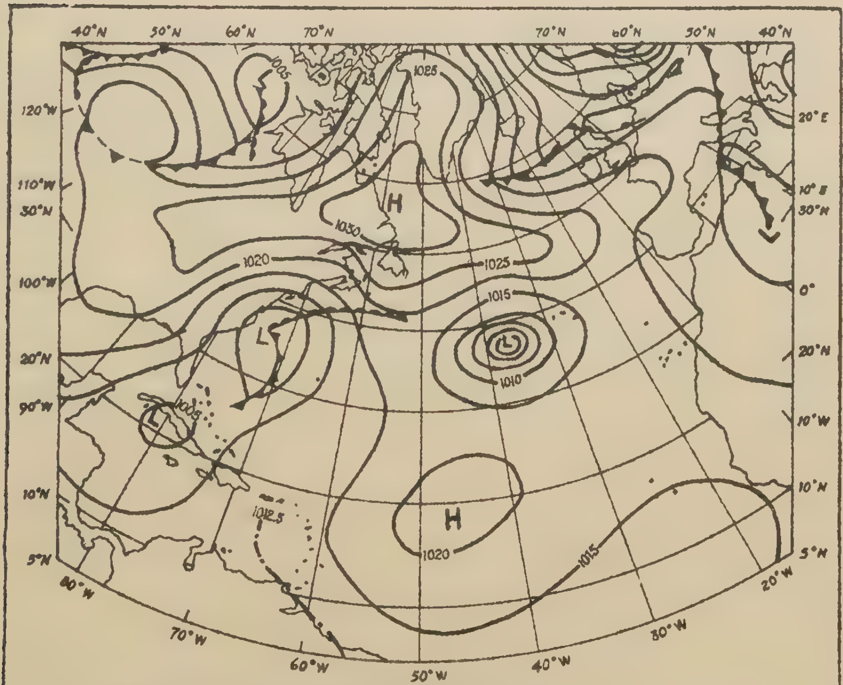
40°N
50°N
60°N
70°N
70°N
60°N
50°N
40°N
120°W
110°W
30°N
100°W
20°N
90°W
10°N
5°N
80°W
70°W
60°W
50°W
40°W
30°W
20°W
20°E
10°E
30°N
0°
20°N
10°W
10°N
5°N
1005
1025
H
1030
1020
1025
1015
L
L
L
L
1005
1010
1012.5
H
1020
1015

FIGURE 13 SURFACE SYNOPTIC CHART 1300 GMT
OCTOBER 18, 1927

WHOI APRIL 1951

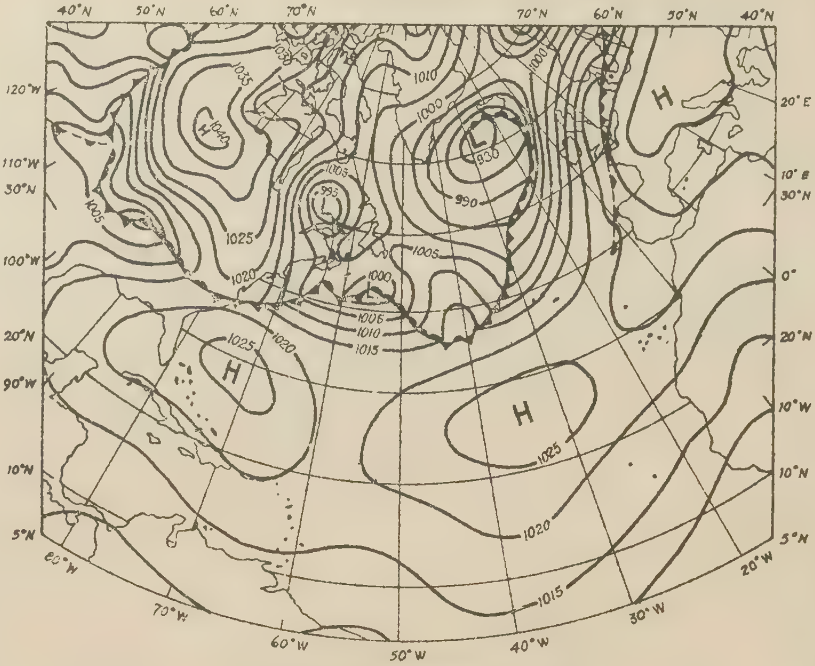
40°N
50°N
60°N
70°N
70°N
60°N
50°N
40°N
120°W
110°W
30°N
100°W
20°N
90°W
10°N
5°N
80°W
70°W
60°W
50°W
40°W
30°W
20°W
20°E
10°E
30°N
0°
20°N
10°W
10°N
5°N
H
H
H
H
L
L
L
1040
1035
1030
1025
1020
1005
1010
1000
995
1005
1005
1000
1005
1010
1015
1025
1020
990
980
1000
1025
1020
1015

FIGURE 14 SURFACE SYNOPTIC CHART 1300 GMT
JANUARY 26, 1918

WHOI APRIL 1951

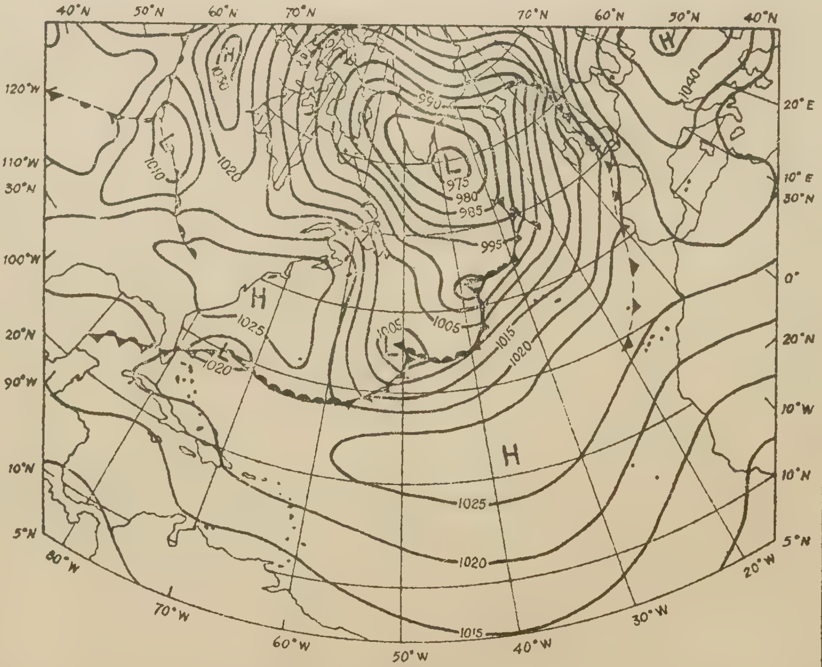
40°N
50°N
60°N
70°N
70°N
60°N
50°N
40°N
120°W
110°W
30°N
100°W
20°N
90°W
10°N
5°N
80°W
70°W
60°W
50°W
40°W
30°W
20°W
20°E
10°E
30°N
0°
20°N
10°W
10°N
5°N
H
H
H
H
L
L
L
L
1030
1040
1010
1020
990
975
980
985
995
1005
1005
1015
1020
1025
1020
1025
1020
1015

FIGURE 15 SURFACE SYNOPTIC CHART 1300 GMT
FEBRUARY 2, 1918

WHOI APRIL 1951

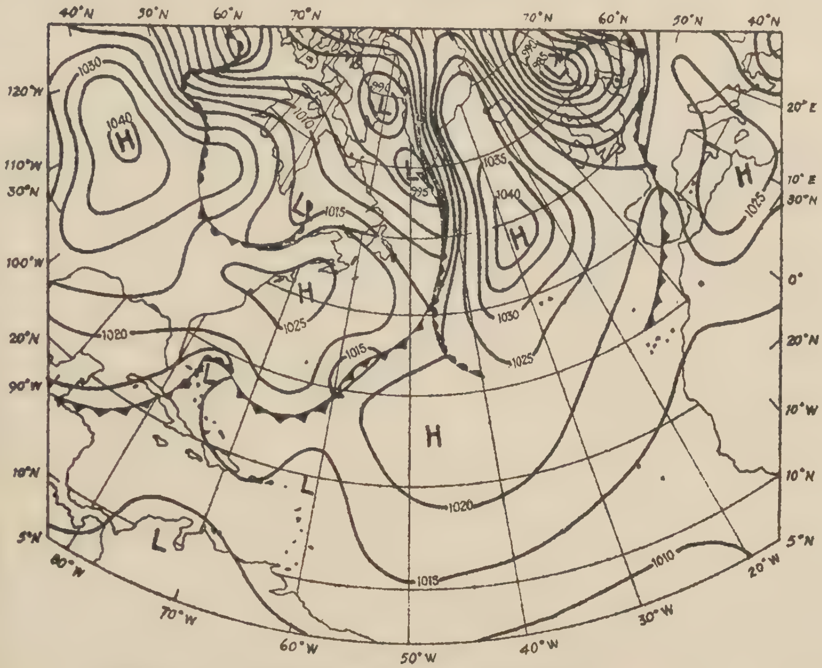
40°N
50°N
60°N
70°N
70°N
60°N
50°N
40°N
120°W
110°W
30°N
100°W
20°N
90°W
10°N
5°N
80°W
70°W
60°W
50°W
40°W
30°W
20°W
20°E
10°E
30°N
0°
20°N
10°W
10°N
5°N
1030
1040
H
L
990
995
1010
1015
1025
1020
L
L
L
H
H
985
990
1035
1040
1030
1025
H
H
1025
1020
1015
1010

FIGURE 16 SURFACE SYNOPTIC CHART 1300 GMT
DECEMBER 7, 1918

WHOI APRIL 1951

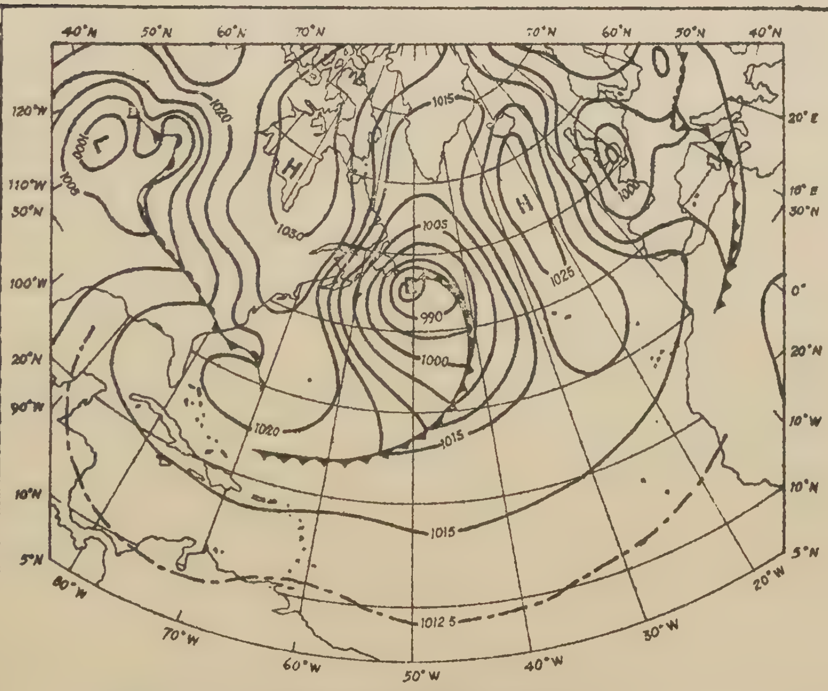
40°N
50°N
60°N
70°N
70°N
60°N
50°N
40°N
120°W
110°W
30°N
100°W
20°N
90°W
10°N
5°N
80°W
70°W
60°W
50°W
40°W
30°W
20°W
20°E
10°E
30°N
0°
20°N
10°W
10°N
5°N
L
1000
1005
1020
H
1030
1015
1005
990
1000
1020
1015
H
1025
1000
1015
1012.5

FIGURE 17 SURFACE SYNOPTIC CHART 1300 GMT
APRIL 9, 1927

WHOI APRIL 1951

Though these figures are higher than those for stagnant lows, linkage is ranked 3rd because in many of its cases the sector affected is comparatively small.

Figures 14, 15, 16, and 17 illustrate cases of linkage showing first a small area, then gradually larger areas affected.

Two series of maps with linkage sequences are next shown. In the first of these there is a uniting of a cold continental high with the Bermuda-Azores High and in the second a replacement of the Bermuda-Azores High by a cold continental high.

Uniting

The first sequence begins on April 26, 1928. In the course of 5 days a cold continental high (C) situated over Winnipeg travels southeast and joins the Bermuda-Azores High. While enroute, it is split into two parts, C_1, and C_2, which unite with the Bermuda-Azores High at different locations and times. On the 26th, the Bermuda-Azores High is centered at 31°W., 36°W., about 130 miles from its normal April position (29°N., 38°W.). After uniting with C_1, southeast of Nova Scotia it is centered at 40°N., 44°W., some 700 miles from the normal center. It then moves south and after uniting with C_2 east of Bermuda it heads east toward its normal position. The interruptions are of two categories: (1) deflection of isobars (winds) to include the approaching C_1, and C_2, and (2) eccentric displacement of the whole network. These may be seen in Figures 18, a through f. Note the weakened gradient in the trades in Figure 18d.

Replacement

A replacement sequence beginning on May 27, 1926 is illustrated in maps 19, a through e. In this sequence a cold continental high (C) migrates southeast across the Great Lakes behind a cold front. In bulldozer fashion it appears to push the Bermuda-Azores High (B) eastward into Europe and the Mediterranean and by June 4th, it is centered at 35°N., 40°W., having completely replaced B. (Note the small section C_1 which after squeezing out to the eastward unites with part of B north of the Azores.)

Hurricanes

The fourth type of interruption is associated with hurricanes. Although the diameter of a typical hurricane can cover only a small part of

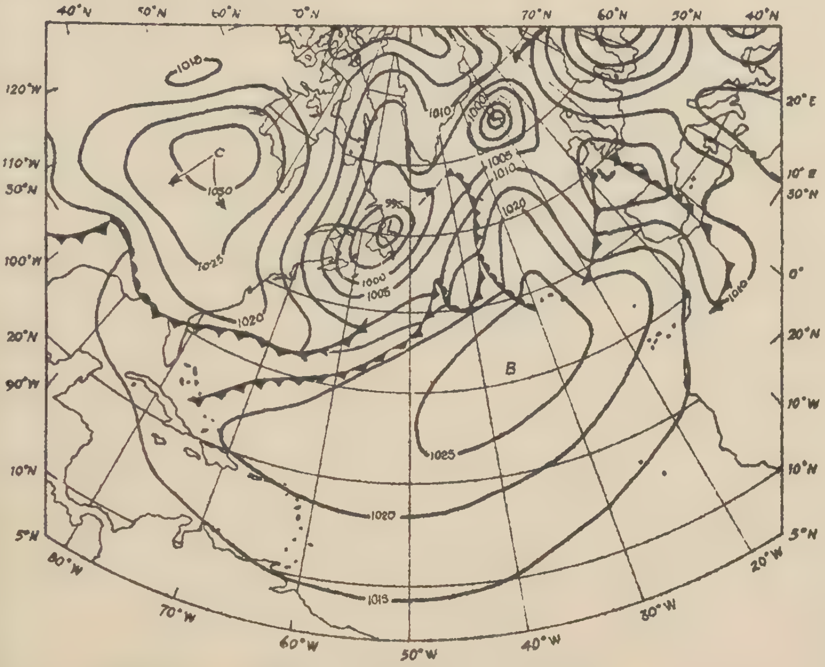
40°N
50°N
60°N
70°N
70°N
60°N
50°N
40°N
120°W
110°W
30°N
100°W
20°N
90°W
10°N
5°N
80°W
70°W
60°W
50°W
40°W
30°W
20°W
20°E
10°E
30°N
0°
20°N
10°W
10°N
5°N
1010
1010
1000
1005
1010
1020
C
1030
1025
995
1000
1005
1020
1010
B
1025
1020
1015

FIGURE 18a. SURFACE SYNOPTIC CHART 1300 GMT
APRIL 26, 1928

WHOI APRIL 1951

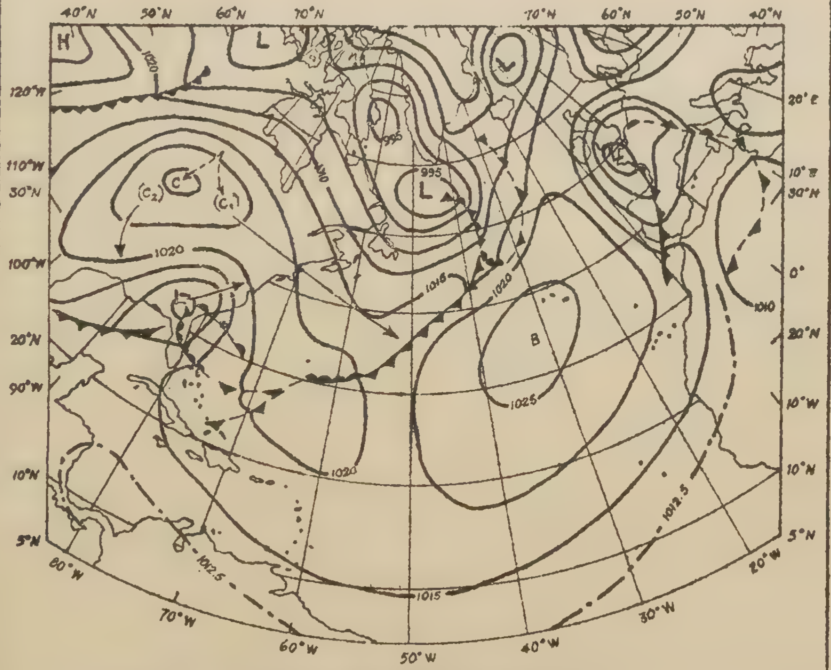
40°N
50°N
60°N
70°N
70°N
60°N
50°N
40°N
H
L
1020
120°W
110°W
30°N
100°W
20°N
90°W
10°N
5°N
80°W
70°W
60°W
50°W
40°W
30°W
20°W
20°E
10°E
30°N
0°
20°N
10°W
10°N
5°N
995
995
L
C
(C2)
(C1)
1020
1015
1020
B
1025
1010
1020
1012.5
1012.5
1015

FIGURE 18b. SURFACE SYNOPTIC CHART 1300 GMT
APRIL 27, 1928

WHOI APRIL 1951

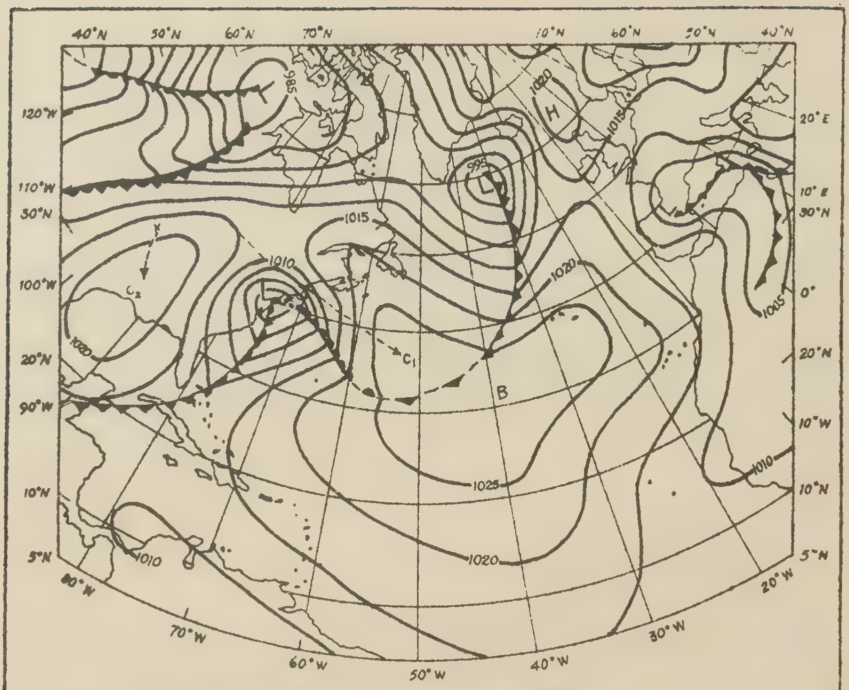
40°N
50°N
60°N
70°N
70°N
60°N
50°N
40°N
120°W
110°W
30°N
100°W
20°N
90°W
10°N
5°N
80°W
70°W
60°W
50°W
40°W
30°W
20°W
20°E
10°E
30°N
0°
20°N
10°W
10°N
5°N
985
1020
H
1015
995
L
1015
1010
1020
C₂
1000
C₁
B
1025
1020
1010
1010
1005

FIGURE 18c SURFACE SYNOPTIC CHART 1300 GMT
APRIL 28, 1928

WHOI APRIL 1951

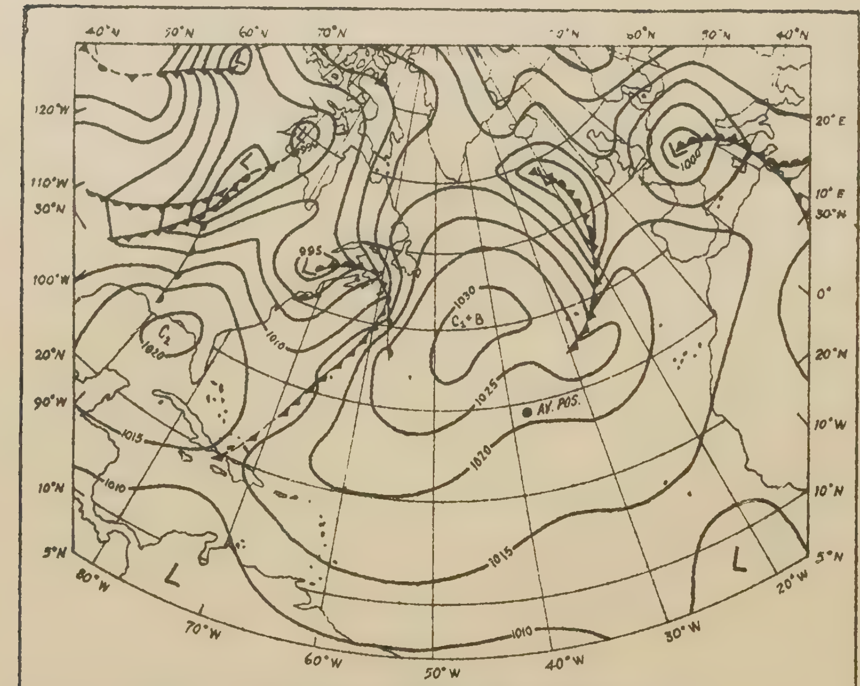
40°N
50°N
60°N
70°N
70°N
60°N
50°N
40°N
120°W
110°W
30°N
100°W
20°N
90°W
10°N
5°N
80°W
70°W
60°W
50°W
40°W
30°W
20°W
20°E
10°E
30°N
0°
20°N
10°W
10°N
5°N
L
L
990
1000
L
995
L
1030
C₁+B
C₂
1020
1010
1025
AV. POS.
1020
1015
1010
1015
1010
L
L

FIGURE 18d. SURFACE SYNOPTIC CHART 1300 GMT
APRIL 29, 1928

WHOI APRIL 1951

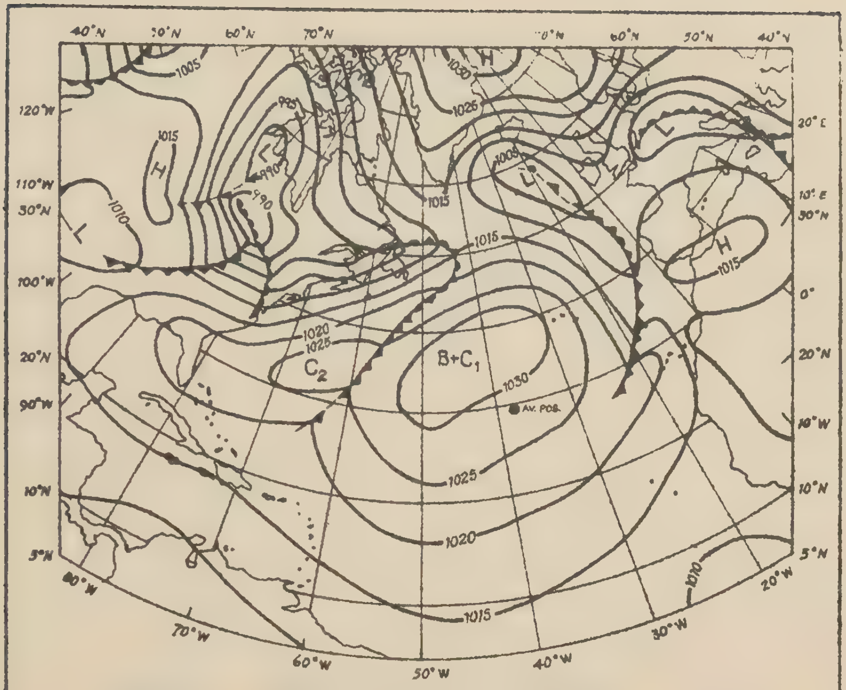
40°N
50°N
60°N
70°N
70°N
60°N
50°N
40°N
120°W
110°W
30°N
100°W
20°N
90°W
10°N
5°N
80°W
70°W
60°W
50°W
40°W
30°W
20°W
20° E
10° E
30°N
0°
20°N
10°W
10°N
5°N
H
L
L
H
L
H
1005
995
1015
990
990
1010
1030
1025
1015
1008
1015
1015
1020
1025
C₂
B+C₁
1030
AV. POS.
1025
1020
1015
1010

FIGURE 18e. SURFACE SYNOPTIC CHART 1300 GMT
APRIL 30, 1928

WHOI APRIL 1951

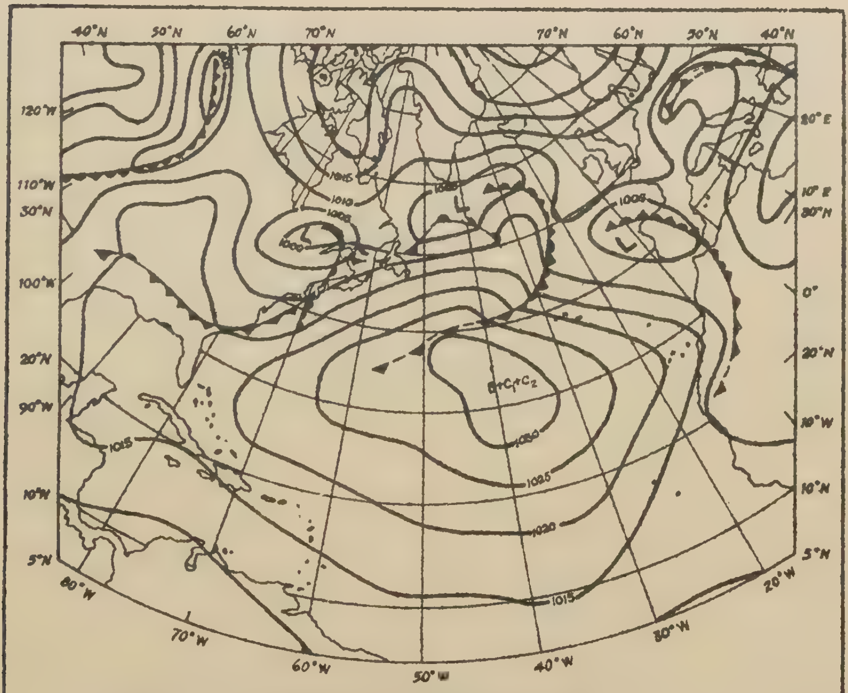
40°N
50°N
60°N
70°N
70°N
60°N
50°N
40°N
120°W
110°W
30°N
100°W
20°N
90°W
10°N
5°N
80°W
70°W
60°W
50°W
40°W
30°W
20°W
20° E
10° E
30°N
0°
20°N
10°W
10°N
5°N
1015
1010
1005
1000
L
L
L
1000
1005
B+C₁+C₂
1030
1025
1020
1015
1015

FIGURE 18f. SURFACE SYNOPTIC CHART 1300 GMT
MAY 1, 1928

WHOI APRIL 1951

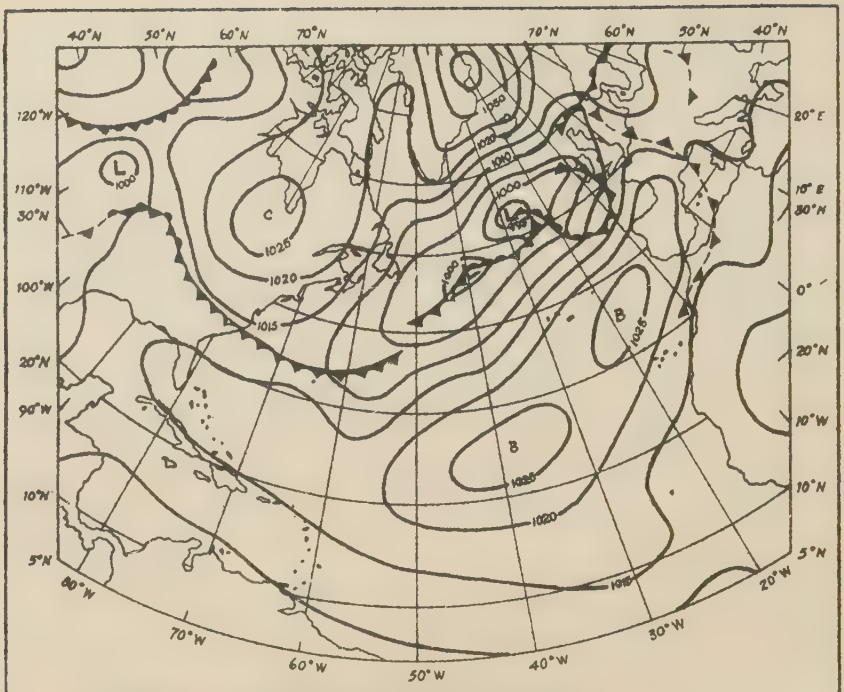
40°N
50°N
60°N
70°N
70°N
60°N
50°N
40°N
120°W
110°W
30°N
100°W
20°N
90°W
10°N
5°N
80°W
70°W
60°W
50°W
40°W
30°W
20°W
20° E
10° E
30°N
0°
20°N
10°W
10°N
5°N
L
1000
C
1025
1020
1015
1030
1020
1010
1000
L
995
1000
B
1025
B
1025
1020
1015

FIGURE 19a SURFACE SYNOPTIC CHART 1300 GMT
MAY 27, 1926

WHOI APRIL 1951

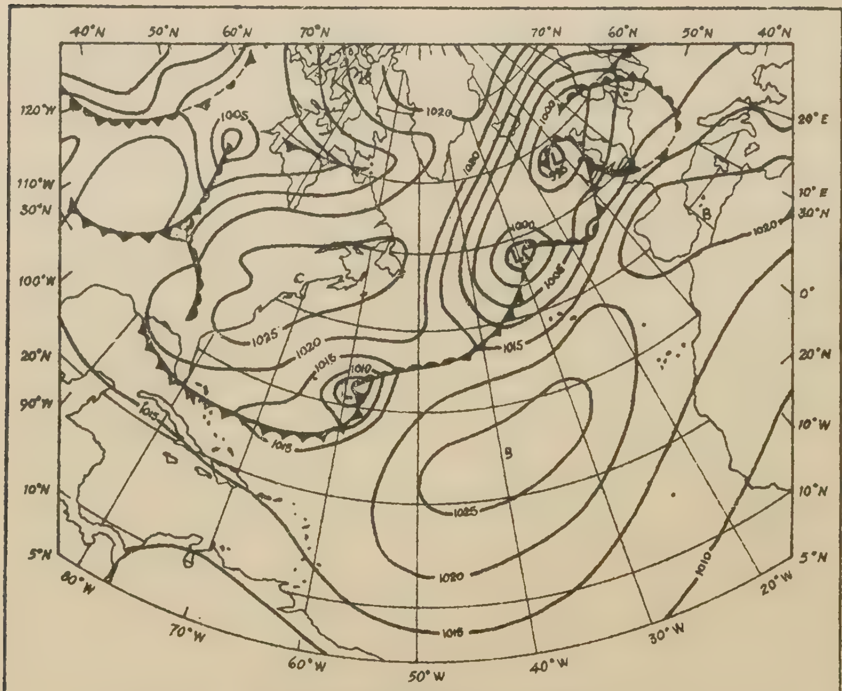
40°N
50°N
60°N
70°N
70°N
60°N
50°N
40°N
120°W
110°W
30°N
100°W
20°N
90°W
10°N
5°N
80°W
70°W
60°W
50°W
40°W
30°W
20°W
20° E
10° E
30°N
0°
20°N
10°W
10°N
5°N
1005
L
1020
1030
1000
L
995
B
1020
C
1000
L
1005
1025
1020
1015
1010
L
1015
1015
1015
B
1025
1020
1015
1010

FIGURE 19b. SURFACE SYNOPTIC CHART 1300 GMT
MAY 29, 1926

WHOI APRIL 1951

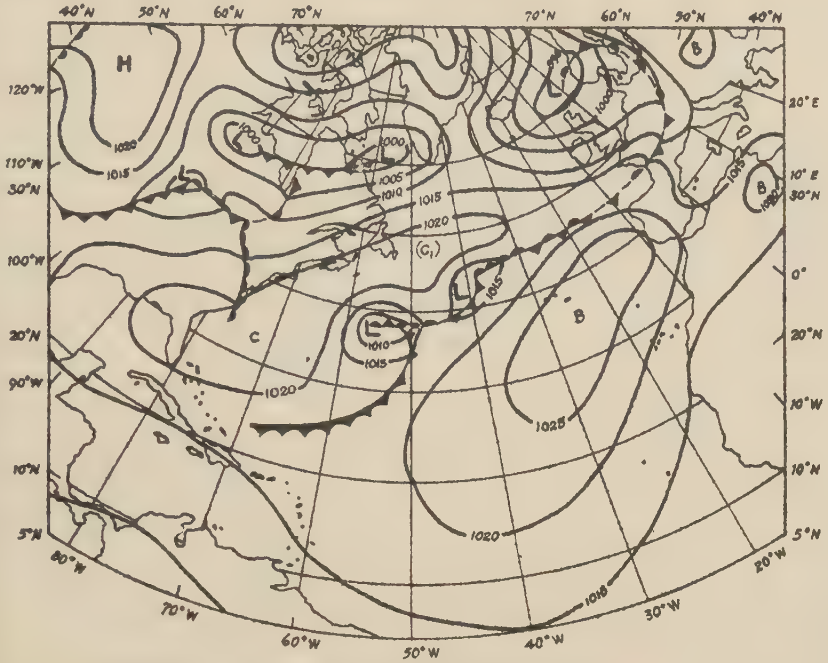
40°N
50°N
60°N
70°N
70°N
60°N
50°N
40°N
120°W
110°W
30°N
100°W
20°N
90°W
10°N
5°N
80°W
70°W
60°W
50°W
40°W
30°W
20°W
20°E
10°E
30°N
0°
20°N
10°W
10°N
5°N
H
L
L
L
L
B
B
B
C
(C1)
1020
1015
1000
1000
1005
1010
1015
1020
1010
1015
1020
1015
1025
1020
1018
1015
1000

FIGURE 19c SURFACE SYNOPTIC CHART 1300 GMT
MAY 31, 1926

WHOI APRIL 1951

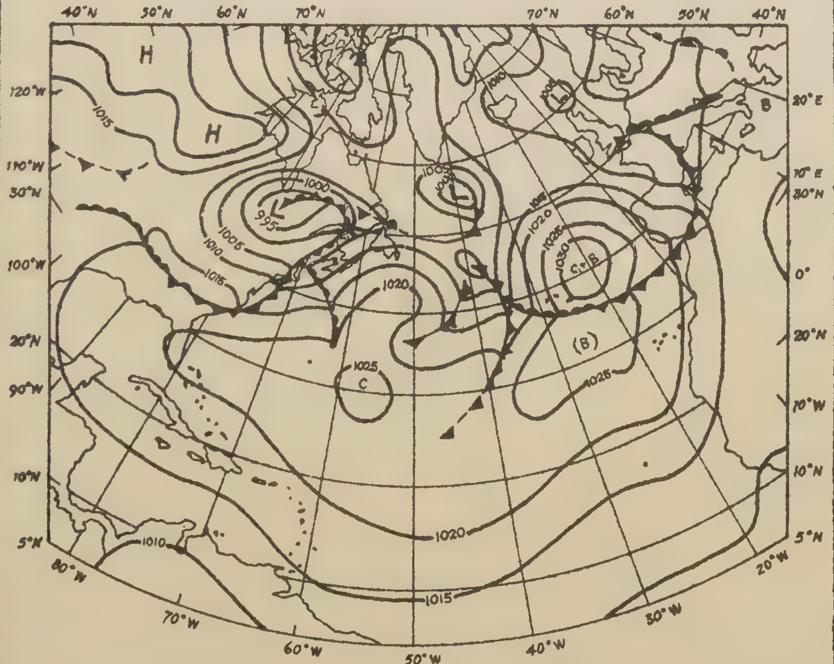
40°N
50°N
60°N
70°N
70°N
60°N
50°N
40°N
120°W
110°W
30°N
100°W
20°N
90°W
10°N
5°N
80°W
70°W
60°W
50°W
40°W
30°W
20°W
20°E
10°E
30°N
0°
20°N
10°W
10°N
5°N
H
H
L
L
L
B
C1 B
(B)
C
1015
1000
995
1005
1010
1015
1020
1005
1000
1010
1005
1015
1020
1025
1030
1025
1025
1020
1015
1010

FIGURE 19d. SURFACE SYNOPTIC CHART 1300 GMT
JUNE 2, 1926

WHOI APRIL 1951

the periphery of the Bermuda-Azores High, a hurricane is often surrounded by a much larger area of slack gradient, so that it is common for the normal circulation to be interrupted over a larger part of its arc. In addition, linkage of the Bermuda-Azores High to a continental high in the direction of England or France often begins a few days before the appearance of a hurricane and sometimes continues while the hurricane moves north off the U. S. east coast. The influence of hurricanes is generally confined to the months from May through November with a maximum frequency in September. The number of hurricanes per year varies so much that it is difficult to estimate a percentage of frequency for this type of interruption. Perhaps 10% is a fair figure for the active period. The duration of interruption by one hurricane varies from about five days to two weeks depending on path and speed. In the situation of September 15, 1921 (Fig. 20), the hurricane near Bermuda is about 800 miles in diameter. Beyond its edge is an area of slack gradient from Nova Scotia to the Caribbean. A weak ridge extends northeastward from the Bermuda-Azores High to England, but the circulation in the eastern

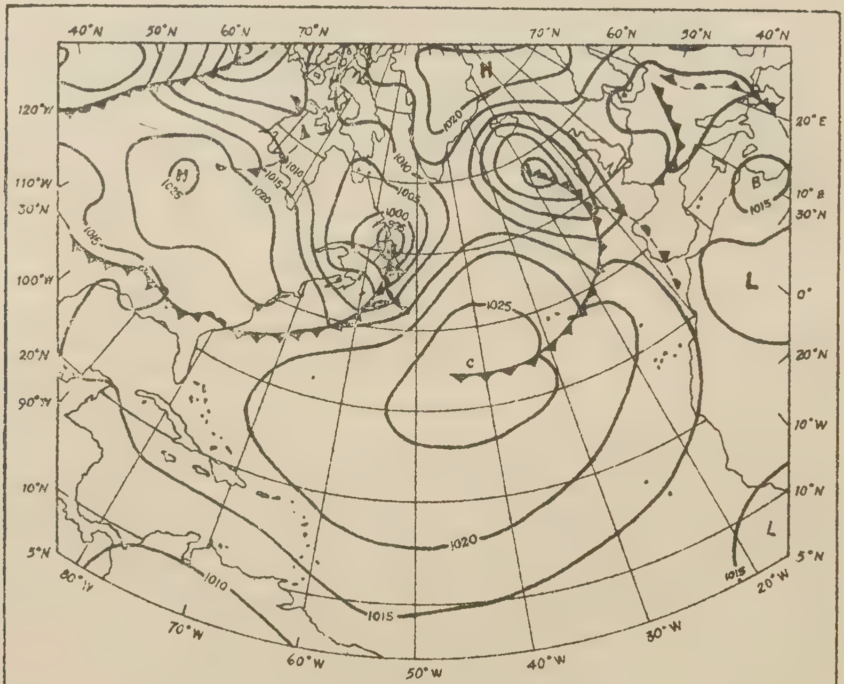
40°N
50°N
60°N
70°N
70°N
60°N
50°N
40°N
120°W
110°W
30°N
100°W
20°N
90°W
10°N
5°N
80°W
70°W
60°W
50°W
40°W
30°W
20°W
20°E
10°E
30°N
0°
20°N
10°W
10°N
5°N
H
H
B
L
L
C
1035
1030
1025
1020
1015
1010
1005
1000
995

FIGURE 19e SURFACE SYNOPTIC CHART 1300 GMT JUNE 4, 1926

WHOI APRIL 1951

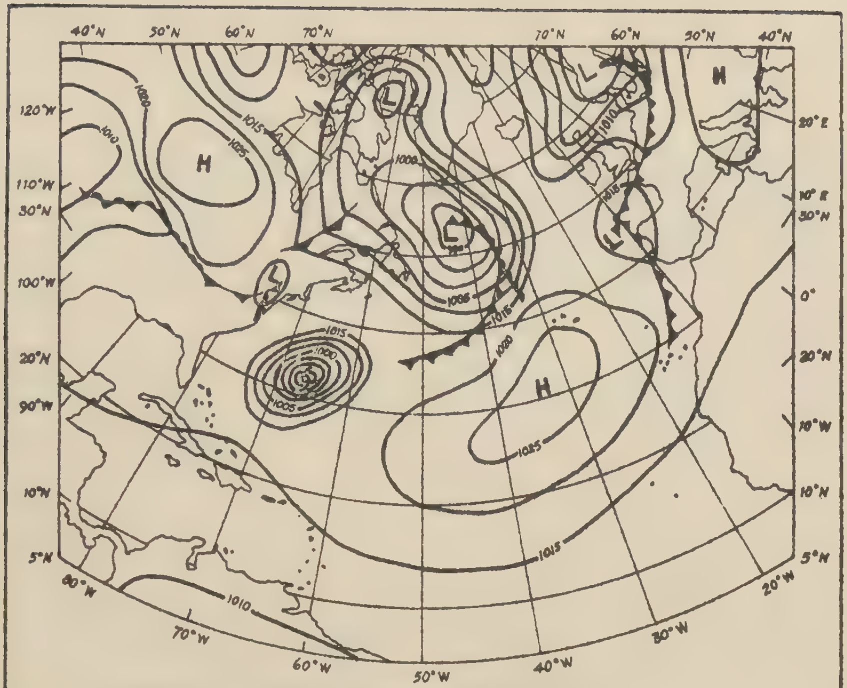
40°N
50°N
60°N
70°N
70°N
60°N
50°N
40°N
120°W
110°W
30°N
100°W
20°N
90°W
10°N
5°N
80°W
70°W
60°W
50°W
40°W
30°W
20°W
20°E
10°E
30°N
0°
20°N
10°W
10°N
5°N
H
L
H
H
1020
1010
1015
1025
1000
1005
1010
1015
1020
1025
1015
1010
1005
1015
1018

FIGURE 20 SURFACE SYNOPTIC CHART 1300 GMT
SEPTEMBER 15, 1921

WHOI APRIL 1951

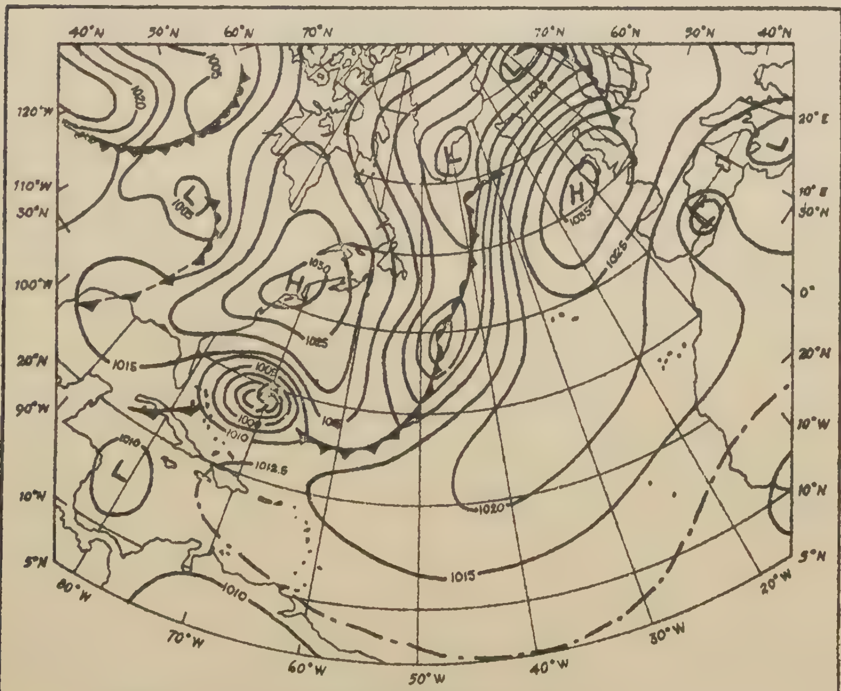
40°N
50°N
60°N
70°N
70°N
60°N
50°N
40°N
120°W
110°W
30°N
100°W
20°N
90°W
10°N
5°N
80°W
70°W
60°W
50°W
40°W
30°W
20°W
20°E
10°E
30°N
0°
20°N
10°W
10°N
5°N
H
L
H
1020
1005
1005
1030
1025
1015
1005
1010
1000
1012.5
1010
1010
1035
1025
1020
1015

FIGURE 21 SURFACE SYNOPTIC CHART 1300 GMT
OCTOBER 27, 1921

WHOI APRIL 1951

Atlantic and trade belt is good. In Figure 21 the slack area is confined to the Caribbean. The Bermuda-Azores High is linked with a high pressure circulation extending across the British Isles into Russia. There is a fairly normal flow from Portugal along the African coast which continues in normal trades westward to about 50°W. But here it is deflected northeastward instead of carrying on across the Caribbean.

Though on any one map the number of hurricanes is rarely in excess of two, as many as five on one map can be seen in the Historical Series. Figure 22 is one of these rare cases of more than two simultaneous hurricanes, having four.

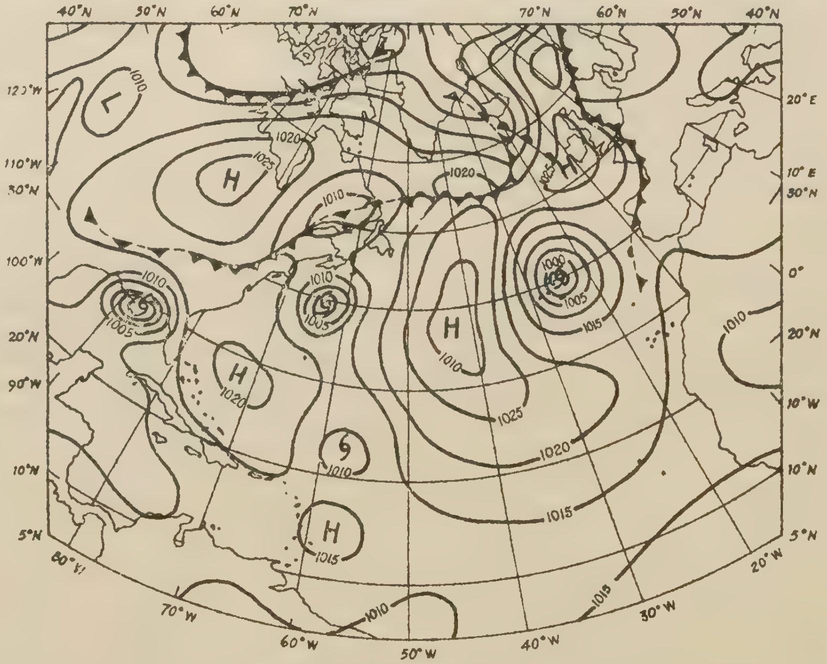
40°N
50°N
60°N
70°N
70°N
60°N
50°N
40°N
120°W
110°W
30°N
100°W
20°N
90°W
10°N
5°N
80°W
70°W
60°W
50°W
40°W
30°W
20°W
20°E
10°E
30°N
0°
20°N
10°W
10°N
5°N
L
H
H
H
H
H
H
1010
1020
1025
1020
1025
1010
1010
1005
1010
1005
1000
1005
1015
1010
1025
1020
1015
1010
1015
1010
1015
1010
1020

FIGURE 22 SURFACE SYNOPTIC CHART 1300 GMT
SEPTEMBER 20, 1926

WHOI APRIL 1951

Three of the four hurricanes of Figure 22 have interrupted the normal circulation to the extent that only short segments remain, viz: Trades from Africa to 50°W. and from Puerto Rico to Florida, a weak west end circulation and westerlies for a short stretch off Newfoundland.

To show that more than one type of interruption can be present on any given map, Figure 23 is included. It contains two hurricanes, one stagnant low, linkage to a cold high and a frontal interruption.

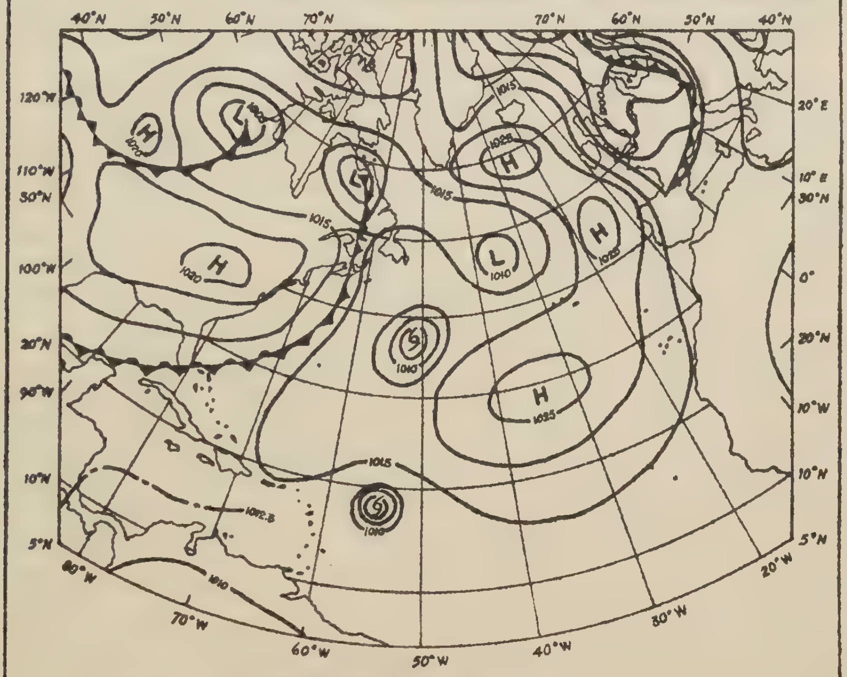
40°N
50°N
60°N
70°N
70°N
60°N
50°N
40°N
120°W
110°W
30°N
100°W
20°N
90°W
10°N
5°N
80°W
70°W
60°W
50°W
40°W
30°W
20°W
20°E
10°E
30°N
0°
20°N
10°W
10°N
5°N
H
L
H
L
H
L
H
H
1015
1020
1025
1010
1012.5
1010

FIGURE 23 SURFACE SYNOPTIC CHART 1300 GMT SEPTEMBER 19, 1916

WHOI APRIL 1951

Summary

The Bermuda-Azores High is associated with a clockwise wind circulation over the surface of the North Atlantic Ocean. This circulation is oval-shaped with the long axis running east-west on the average. The annual average position of the center is about 600 miles southwest of the Azores, and the average positions by months are all within about 700 miles of the annual average center. The average wind flow runs northward from the Antilles to north of Bermuda, thence eastward and southeastward to between the Azores and Portugal, southward along the African coast to the Cape Verde Islands, then westward to the Antilles. The winds are steadiest from

Africa to the Caribbean (the trade winds). The strongest wind forces are normally found in the westerlies, but variability of direction in this area reduces the average gradient to an amount about equivalent to that in the trades. Variable directions reduce the gradient in the west end of the high to a very weak average, but do not affect the east end as much. Air diverges from the high, cross-isobar at an average angle of some 20°. The angle is larger near the Cape Verde Islands and smaller in the westerlies.

Daily situations can be divided into two nearly equal categories containing: (1) those which show a circulation resembling the average and (2) those in which the circulation has been interrupted by normal meteorological phenomena. The interrupting phenomena are by order of importance: fronts, stagnant lows, linkage of cold continental high cells to the Bermuda-Azores High, and hurricanes.

Interruptions due to hurricanes are most frequent in September, but can occur anytime in the period from May through November. Interruptions associated with fronts, stagnant lows, and linkage are more frequent in the winter. This latter is especially true with respect to the trades.

Due to fewer interruptions and to higher center pressure, the circulation about the Bermuda-Azores High is stronger in summer than in winter.

Acknowledgments

The writer wishes to extend his thanks and appreciation to Mr. F. C. Fuglister for his time, interest, and assistance in the preparation of this paper and to Dr. C. O'D. Iselin, Dr. Bernhard Haurwitz, Mr. Henry Stommel, and Mr. Andrew F. Bunker for their many helpful suggestions.

References

Fuglister, F. C.
1951. Annual variations in current speeds in the Gulf Stream system, Jour. Mar. Res.., Vol. X, No. 1. pp 119-127

U.S. Weather Bureau
1943. Historical Weather Maps, Northern Hemisphere Sea Level, Washington, D. C.

U.S. Weather Bureau
1946. Normal Weather Maps, Northern Hemisphere Sea Level Pressure, Washington, D. C.

Contribution No. 838

Reprinted from Biological Bulletin, Vol. 112, No. 2, 196–219, April, 1957
Printed in U. S. A.

THE TAXONOMY OF UNARMORED DINOPHYCEAE OF SHALLOW EMBAYMENTS ON CAPE COD, MASSACHUSETTS

EDWARD M. HULBURT

Woods Hole Oceanographic Institution, Woods Hole, Mass.

THE TAXONOMY OF UNARMORED DINOPHYCEAE OF SHALLOW EMBAYMENTS ON CAPE COD, MASSACHUSETTS[1]

EDWARD M. HULBURT

Woods Hole Oceanographic Institution, Woods Hole, Mass.

Several papers give brief accounts of unarmored Dinophyceae found along the eastern coast of the United States. Calkins (1902) described from Woods Hole three European species, with one as a new variety. Herdman (1924a) listed five European, sand-living species from Woods Hole. Lackey (1936) listed thirteen species, all European, in his account of Woods Hole protozoa. Martin (1929) described thirteen species, four of which were new, from Barnegat Bay. It would be expected that further study would show many more extensions of range from the east to the west side of the Atlantic. One wonders, though, whether new species would be few, as suggested by these figures, or on the contrary would be many, since studies hitherto have not been very detailed. Further, the Barnegat Bay list suggests that the shallow, estuarine type of habitat has as many species as coastal waters, since Martin's number is matched only by that of Lackey.

The following study covers twenty-six species, of which twelve are completely

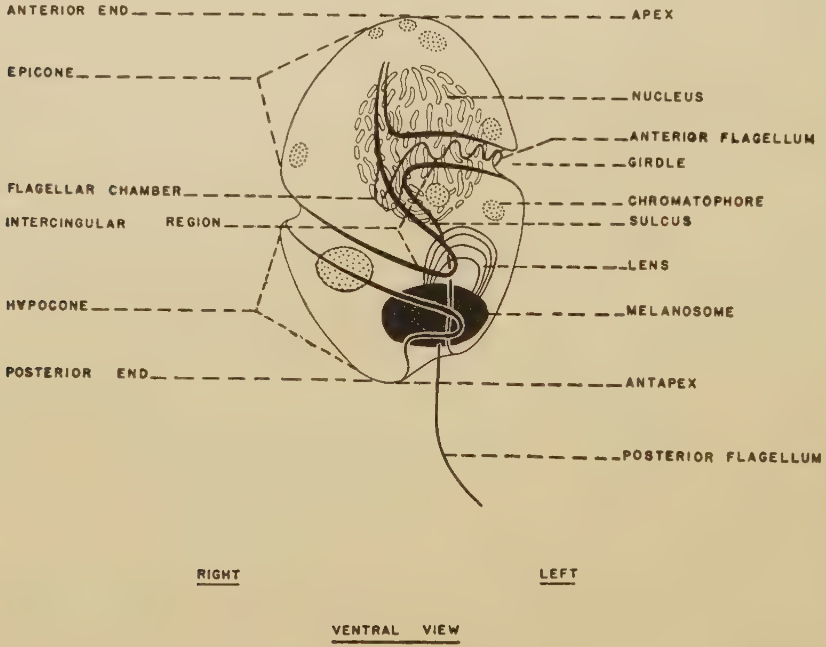
ANTERIOR END
APEX
EPICONE
NUCLEUS
ANTERIOR FLAGELLUM
GIRDLE
FLAGELLAR CHAMBER
CHROMATOPHORE
INTERCINGULAR REGION
SULCUS
LENS
HYPOCONE
MELANOSOME
POSTERIOR END
ANTAPEX
POSTERIOR FLAGELLUM
RIGHT
LEFT
VENTRAL VIEW

FIGURE 1. Structure of a dinophycean.

---

[1] Contribution No. 838 from the Woods Hole Oceanographic Institution.

new and nine show extensions of range from Europe. The collections which furnished the great majority of the material were from Great Pond, Falmouth Harbor, Salt Pond, and Uncatena Island Pond, all very shoal embayments on the southern shore of Cape Cod. The expectations, consequently, seem to be fulfilled.

Water samples were concentrated by centrifuging and the Dinophyceae were studied alive in water mounts. At magnifications of × 440 and × 980 drawings were made of specimens which had ceased to swim but showed no deformity due to approaching disintegration. Outline, girdle, and sulcus were drawn with camera lucida; the rest of the structures were drawn free-hand.

For those unacquainted with the morphology of unarmored Dinophyceae and its special nomenclature, Figure 1 illustrates the typical structure of such a dinophycean.

The species studied fall into eight genera, which may be characterized as in the following key:

Key to Genera

Girdle and sulcus rudimentary	*Oxyrrhis*
Girdle and sulcus well-developed:	
Solitary:	
Without ocellus and nematocysts:	
Girdle not markedly displaced:	
a) Girdle in anterior third of body	*Amphidinium*
b) Girdle in central portion of body	*Gymnodinium*
c) Girdle in posterior third of body	*Massartia*
Girdle markedly displaced	*Gyrodinium*
With ocellus but without nematocysts	*Warnowia*
With ocellus and nematocysts	*Nematodinium*
Colonial	*Polykrikos*

OXYRRHIS Dujardin

Oxyrrhis marina Dujardin

Oxyrrhis marina Dujardin in Kofoid and Swezy, 1921, p. 117, text fig. R, 3.
Oxyrrhis marina Dujardin in Lebour, 1925, p. 19, pl. 1, figs. 6a–6e.

Woods Hole area: Uncatena Island, Salt Pond; March, August, October. New Jersey; White Sea; England; brackish estuary near Nieuport, Belgium; Marseilles harbor; Genoa harbor.

This species is distinguished by the posterior position of its flagella, by the broad excavation of the posterior sulcus, divided midway by a tentacle-like lobe, and by the partial encirclement of the girdle. Other characters are its elongate ellipsoidal form and absence of chromatophores.

AMPHIDINIUM Claparède and Lachmann

Key to Species

Chromatophores present:	
Chromatophore single	*A. carteri*
Chromatophores many	*A. wislouchi*
Chromatophores absent:	
Body stout, with rounded ends	*A. crassum*
Body very slender, with pointed ends	*A. sphenoides*

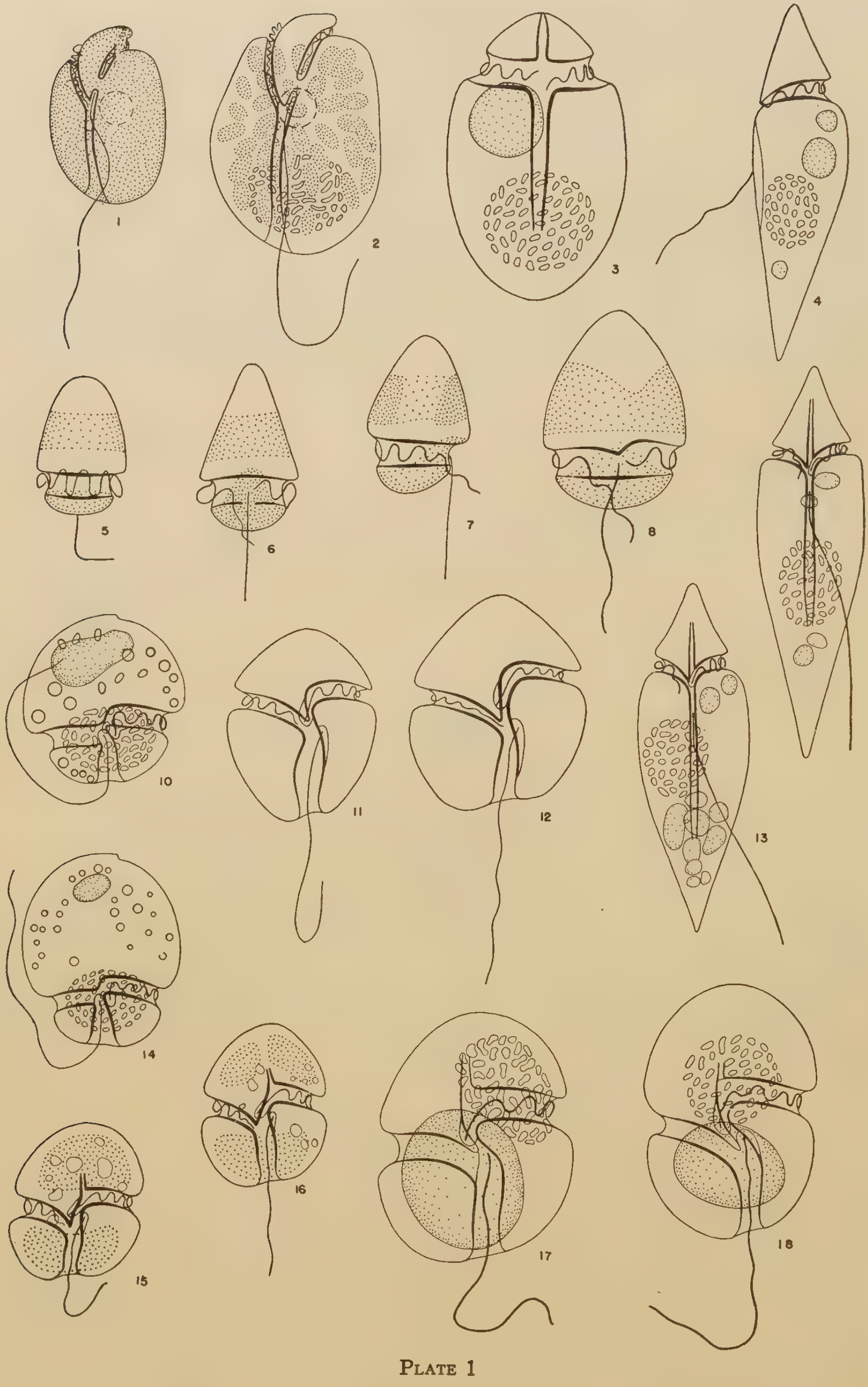
1
2
3
4
5
6
7
8
9
10
11
12
13
14
15
16
17
18

Plate 1

Amphidinium **carteri** nom. nov.

(Plate 1, Figure 1)

Amphidinium klebsi Carter, 1937, p. 58, pl. 8, figs. 12, 13, 14, 15. (*non* Kofoid & Swezy, 1921).

Body dorsi-ventrally flattened, oval in outline in ventral view, elongate-elliptical in lateral view. Length 12–15 μ, width 8–9 μ. Epicone small, asymmetric, crescent-shaped in ventral view, somewhat flattened at apex; in dorsal view beak-like, rising near right margin and projecting toward left margin. Hypocone truncate-elliptical in ventral or dorsal view, asymmetric, with its right margin convex and left straight or very slightly convex, the antapex broadly rounded. Left limb of girdle starting some distance above posterior end of epicone, running in an arching course anteriorly and laterally, then extending transversely around dorsal surface of epicone, finally leading posteriorly near right margin to round posterior end of epicone, failing, however, to meet the end of the left limb. Sulcus nearer right margin, extending from posterior end of epicone in curving course to antapex. Anterior flagellum inserted at the end of the left limb of girdle; posterior flagellum inserted just below the anterior, separated from it by a "bridge" that separates girdle ends, extending 1.5 body lengths.

Chromatophore single, covering whole inner surface, often perforate, golden brown. Nucleus at posterior end of hypocone, containing short chromatin corpuscles. Pyrenoid present, in center of hypocone. Assimilate granules present or absent.

Woods Hole area: Uncatena Island; October, July. Isle of Wight, England, in brackish pool.

The species described here as *Amphidinium carteri* is identical with Carter's *A. klebsi*. It is considered an independent species since it is much smaller than the forms described as *A. klebsi* by Kofoid and Swezy (1921), Herdman (1924a), and Lebour (1925), and since it has only a single chromatophore.

Amphidinium **wislouchi** n. sp.

(Plate 2, Figure 2)

Amphidinium sp. Wislouch, 1924, p. 121, pl. 3, fig. 11.

Body dorsi-ventrally flattened, oval in outline in ventral view. Length 20–25 μ, width 14–16.5 μ. Epicone small, asymmetric, crescent-shaped in ventral view,

---

Plate 1

Figure 1. *Amphidinium carteri* nom. nov.
Figure 2. *Amphidinium wislouchi* n. sp.
Figure 3. *Amphidinium crassum* Lohmann
Figures 4, 9, 13. *Amphidinium sphenoides* Wulff
Figures 5, 6, 7, 8. *Massartia rotundata* (Lohmann) Schiller
Figures 10, 14. *Massartia asymmetrica* (Massart) Schiller
Figures 11, 12. *Gyrodinium metum* n. sp.
Figures 15, 16. *Gyrodinium estuariale* n. sp.
Figures 17, 18. *Gyrodinium glaebum* n. sp.

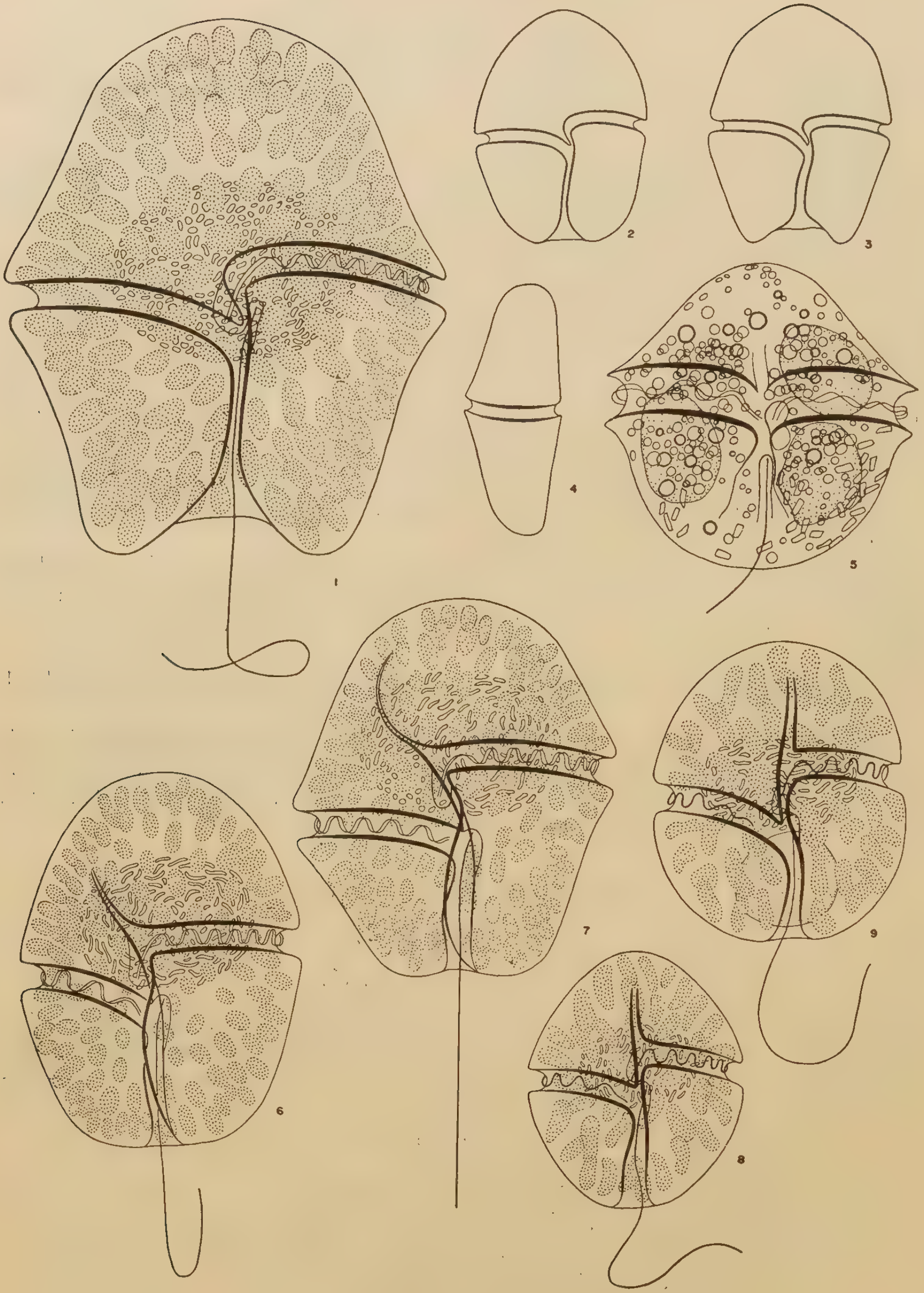

PLATE 2

somewhat flattened at apex; in dorsal view beak-like, rising near right margin and projecting toward left margin. Hypocone truncate-elliptical in ventral or dorsal view, asymmetric, with its right margin convex and left almost straight, the antapex broadly rounded. Left limb of girdle starting some distance above posterior end of epicone, running in an arching course anteriorly and laterally, then extending transversely around dorsal surface of epicone, finally leading posteriorly near right margin to round posterior end of epicone, failing, however, to meet the end of the left limb. Sulcus nearer right margin, extending from posterior end of epicone in curving course to antapex. Anterior flagellum inserted at the end of the left limb of girdle; posterior flagellum inserted just below the anterior, separated from it by a "bridge" that separates girdle ends, extending 1.5 body lengths.

Chromatophores many, elliptical, often arranged in a somewhat radiating manner, with pyrenoid as center.

Woods Hole area: Uncatena Island, Great Pond; October, March. Poland.

This species is about the same as Wislouch's *Amphidinium* sp. and is quite similar to *A. carteri* except for having many chromatophores.

Amphidinium crassum Lohmann

(Plate 1, Figure 3)

Amphidinium crassum Lohmann, 1908, p. 261, pl. 17, fig. 16.
Amphidinium crassum Lohmann in Lebour, 1917, p. 188, fig. 2; 1925, p. 31, pl. 3, figs. 2a–2c.

Body elongate elliptical, circular in cross-section. Length 23–30 μ, width 11–17 μ. Epicone very small, 0.20–0.25 the body length, broadly conical with a pointed apex; hypocone with its sides parallel in the anterior half, rounding into a broad antapex. Girdle not displaced, wide, shallow, its posterior margin wider than the anterior. Sulcus very narrow and shallow, straight, reaching from the apex to 0.66 of the length of hypocone. Flagellar chambers not seen. Anterior flagellum completely encircling body, posterior flagellum not seen.

Chromatophores absent. Nucleus close to antapex, spherical, containing short chromatin corpuscles. Brown ingested bodies and assimilate bodies common.

Woods Hole area: Great Pond, Falmouth Harbor; April, May. Baltic Sea off Kiel; English Channel; Plymouth Sound; Adriatic Sea.

Lohmann (1908) described two similar amphidiniums, *A. crassum* and *A. longum,* the second more slender and with a smaller, more pointed epicone than the first. Lebour (1917, 1925) described as *A. crassum* a type intermediate between these two in proportion of length to width, but with the "fuller" epicone of Lohmann's *A. crassum.* Lebour's type is identical with that described here.

PLATE 2

FIGURES 1, 2, 3, 4. *Gymnodinium nelsoni* Martin
FIGURE 5. *Gymnodinium lazulum* n. sp.
FIGURES 6, 7. *Gyrodinium resplendens* n. sp.
FIGURES 8, 9. *Gyrodinium aureolum* n. sp.

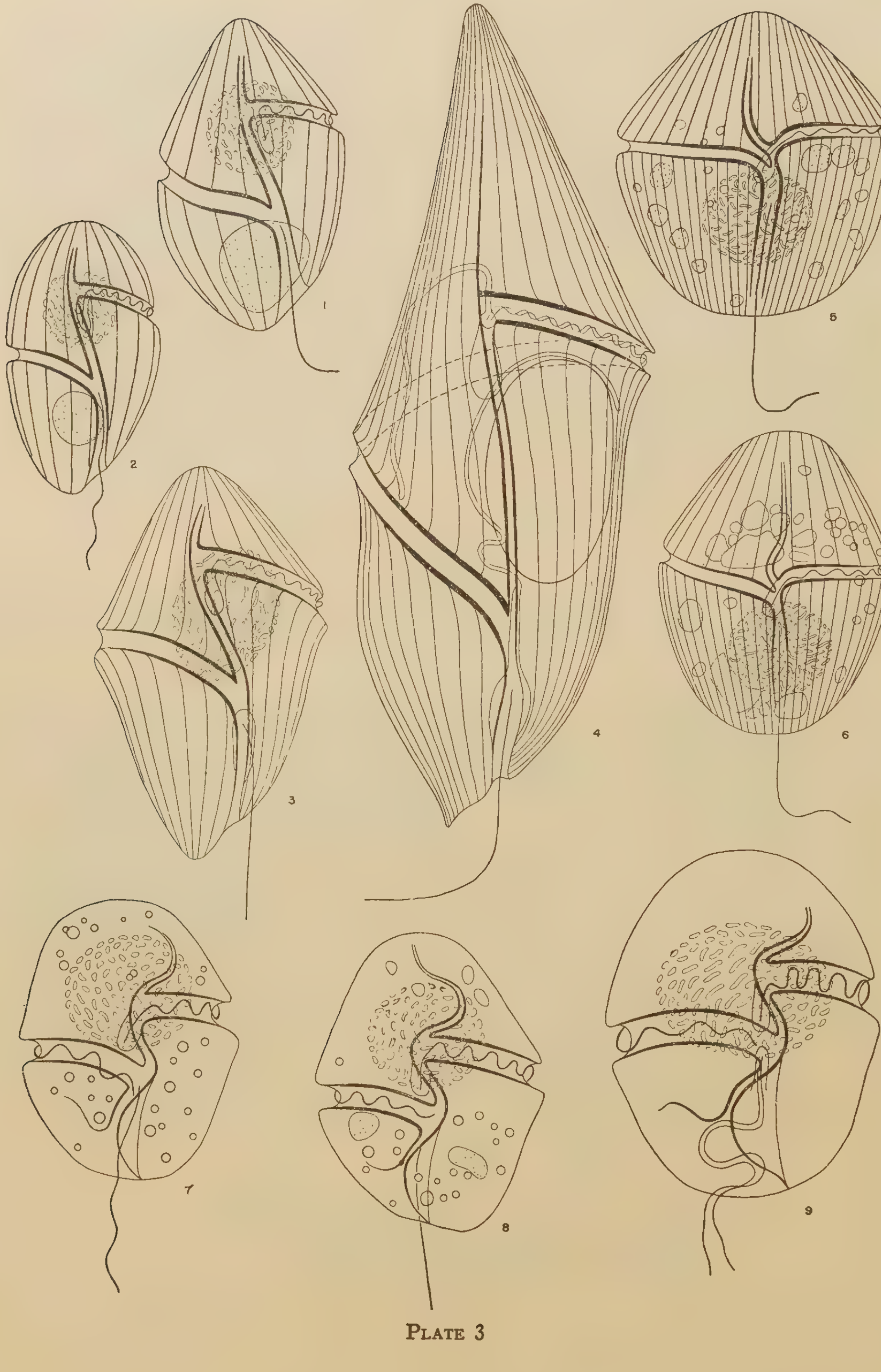

Plate 3

Amphidinium sphenoides Wulff

(Plate 1, Figures 4, 9, 13)

Amphidinium sphenoides Wulff, 1916, p. 105, pl. 1, figs. 9a–9b.

Body cylindrical, of slender proportions, tapered posteriorly to a sharp point, tapered anteriorly more abruptly to an equally sharp point. Length 35–42 μ, width 12–13 μ. Epicone 0.20–0.25 the total length, symmetrically diamond-shaped or triangular, respectively, in ventral or dorsal view, but asymmetrically triangular in side view, with the dorsal margin more sloping than the ventral; outline contours concave. Hypocone similar but more elongate, triangular in dorsal and ventral view and more sloping along the dorsal than the ventral margin. Girdle deep, broad dorsally but narrowed ventrally, so that in side view the margins appear to converge. Sulcus narrow, running from near the apex to 0.66 the length of the hypocone. Anterior flagellar chamber a mere deepening of the left girdle end (posterior chamber not seen). Anterior flagellum encircling body; posterior flagellum somewhat shorter than the body.

No chromatophores. Nucleus midway the length of hypocone. Assimilate spherules of various sizes present or absent.

Woods Hole area: Great Pond; January. Barents Sea.

GYMNODINIUM Stein (emended by Kofoid and Swezy)

KEY TO SPECIES

Without striations:	
Chromatophores present	*G. nelsoni*
Chromatophores absent:	
Body globular	*G. lazulum*
Body laterally flattened	*G. stellatum*
With striations	*G. striatissimum*

Gymnodinium nelsoni Martin

(Plate 2, Figures 1, 2, 3, 4)

Gymnodinium nelsoni Martin, 1929, p. 14, pl. 3, figs. 25–26.

Body broadly fusoid, with truncate antapex, very much flattened dorsi-ventrally. Length 50–70 μ, width 38–53 μ. Epicone in ventral view sub-hemispherical to somewhat angled, its sides then straight or concave, and its apex broadly pointed. Hypocone trapezoidal, its sides convex, straight, or concave; its apex wide, emarginate to broadly indented. In lateral view dorsal contour somewhat convex, ventral contour somewhat concave; end-on view with a similar dorsal convexity and ventral concavity. Girdle narrow, deep, displaced one-two girdle widths. Sulcus not present on epicone, narrow and sigmoid in intercingular region, straight and

---

PLATE 3

FIGURES 1, 2, 3. *Gyrodinium dominans* n. sp.
FIGURE 4. *Gyrodinium spirale* (Bergh) Kofoid and Swezy
FIGURES 5, 6. *Gymnodinium striatissimum* n. sp.
FIGURES 7, 8, 9. *Gyrodinium undulans* n. sp.

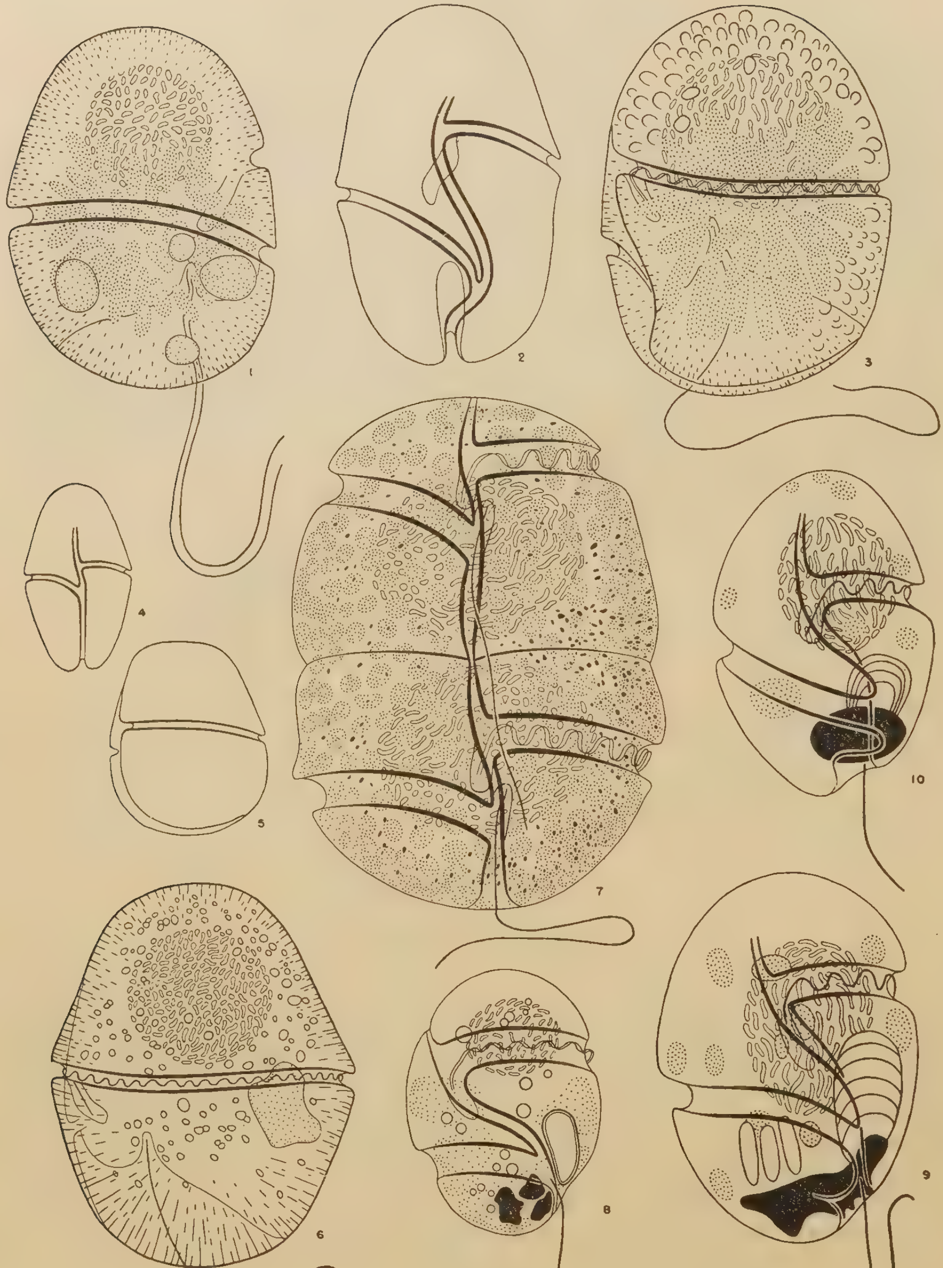
1
2
3
4
5
7
10
6
8
9

Plate 4

somewhat wider on hypocone, widening abruptly and showing a large excavation at antapex. Anterior and posterior flagellar chambers overlapping. Anterior flagellum not completely encircling cell; posterior flagellum equal to the body length.

Chromatophores many, rich brown, elliptical, radiating from center of cell. Nucleus central, wider than long, with numberless, elongate chromatin corpuscles. Cells usually free from assimilate and ingested bodies.

Woods Hole area: Great Pond; September. Barnegat Bay, United States east coast.

G. nelsoni is distinguished from its close relative, *G. splendens* (Lebour, 1925), by having short, elliptical chromatophores instead of elongate slender ones.

Gymnodinium **lazulum** n. sp.

(Plate 2, Figure 5)

Body globular, circular in cross-section, epicone and hypocone subequal. Length 28–30 μ, width 30–32 μ. Epicone conical bell-shaped, with marked concavity of outline near girdle; hypocone hemispherical bell-shaped, with concavity of contours less extensive but closer to girdle than in epicone. Girdle wide, deep, without displacement. Sulcus short, narrow, and faintly defined on epicone; on hypocone abruptly widening, more so on the right than the left, its margins fading out about halfway to antapex. Girdle ends dipping in markedly to the bottom of the sulcus, deeply excavating sulcus in girdle region. Anterior flagellum inserted at opening of a pore; pore extending as small pustule from left girdle end posteriorly. Posterior flagellum inserted in trough-like depression of posterior sulcal floor. Anterior flagellum a delicate band completely encircling body; posterior flagellum short, 0.5 body length.

Chromatophores absent. Nucleus not visible. Cytoplasm clear, quite transparent, smoke blue in color. Colored spherules, grading from copper-red through orange and brown to lemon-yellow, abundant, scattered throughout cytoplasm, often clustered near girdle. Angular, crystal-like, slate-gray bodies scattered at random through hypocone. Large, brown ingested bodies common.

Woods Hole area: Great Pond; December, May.

This species was the only one studied with a clear, blue, instead of a granular, gray, cytoplasm. The array of hues of the numberless small spherules, as well as the blue of the cytoplasm, are matched by similar structures in *G. violescens* (Kofoid and Swezy, 1921).

Gymnodinium **stellatum** n. sp.

(Plate 4, Figures 4, 5, 6)

Body laterally flattened, elliptical in side view with sub-truncate anterior end. Length 25–47 μ, thickness 22–39 μ, width 17–25 μ. Epicone in dorsi-ventral view taller than wide, with slightly sloping sides; in lateral view as wide as tall, trape-

---

PLATE 4

FIGURES 1, 2, 3. *Gyrodinium uncatenum* n. sp.
FIGURES 4, 5, 6. *Gymnodinium stellatum* n. sp.
FIGURE 7. *Polykrikos hartmanni* Zimmermann
FIGURE 8. *Warnowia parva* (Lohmann) Lindemann
FIGURES 9, 10. *Nematodinium armatum* (Dogiel) Lebour

zoidal, more sloping dorsally than ventrally. Hypocone similar to epicone in shape in dorsi-ventral view, with antapical notch dorsally; in lateral view sub-hemispherical, wider than tall. Girdle narrow, displaced 0.16–0.20 body length. Sulcus narrow, straight except for slight leftward divergence in girdle region, forming a deep hypoconal excavation with anterior limit marked laterally by a vague line running diagonally from posterior dorsal corner toward girdle region on ventral surface. Anterior flagellar chamber a long finger-like pocket extending posteriorly and somewhat dorsally; posterior flagellar chamber a narrow prolongation of hypoconal excavation, reaching almost to anterior chamber. Anterior flagellum encircling less than half the circumference, wide, band-shaped; posterior flagellum body length, sometimes double.

Chromatophores absent. Nucleus within epicone, containing elongate chromatin corpuscles. Peripheral cytoplasm with distinct radial structure. Assimilate occasionally abundant.

Woods Hole area: Salt Pond; October, December, January.

This species is very much like *Gyrodinium uncatenum* in this paper, differing principally in lacking chromatophores, in having a less displaced girdle, and a straighter sulcus. Among hitherto described species, it is similar only to *Gymnodinium bifurcatum* (Kofoid and Swezy, 1921) in its lateral flattening and deep hypoconal excavation.

Gymnodinium **striatissimum** n. sp.

(Plate 3, Figures 5, 6)

Body globular to elliptical, not flattened, its hypocone slightly larger than epicone. Length 29–43 μ, width 23–31 μ. Epicone conical, pointed, or somewhat truncate. Hypocone similar but more truncate, varying from tapered type with moderately sloping sides and rounded antapex to type with slightly sloping sides and broad antapex. Surface with striations, fewer on epicone (15) than on hypocone (25). Girdle narrow, rather deep, slightly displaced, with distinctive posterior flexure to end of left limb. Sulcus shallow, narrow on epicone, somewhat wider on hypocone, from near apex almost to antapex, distinguished by sharp leftward bend just anterior to girdle. Anterior flagellar chamber prolonged posteriorly. Anterior flagellum completely encircling body; posterior flagellum one body length, sometimes double.

No chromatophores. Nucleus posterior, wholly within hypocone, with elongate chromatin corpuscles. Assimilate bodies of various sizes often abundant.

Woods Hole area: Great Pond; May.

Gymnodinium striatissimum is similar in different number of striations on epicone and hypocone to the much larger *G. multistriatum, G. rubrum,* and *G. translucens* (Kofoid and Swezy, 1921).

MASSARTIA Conrad

KEY TO SPECIES

Without striations:
  Chromatophores present .... *M. rotundata*
  Chromatophores absent .... *M. asymmetrica*
With striations .... *M. glauca*

Massartia rotundata (Lohmann) Schiller

(Plate 1, Figures 5, 6, 7, 8)

Amphidinium rotundatum Lohmann, 1908, p. 261, pl. 17, fig. 9.
Amphidinium rotundatum Lohmann in Wulff, 1916, p. 103, pl. 2, fig. 11.
Amphidinium rotundatum Lohmann in Van Goor, 1925, p. 285, fig. 4.
Gymnodinium minutum Lebour, 1925, p. 45, pl. 5, fig. 4.
Massartia rotundata (Lohmann) Schiller in Conrad, 1939, p. 11, figs. 17–22.

Body top-shaped, circular in cross-section. Length 8–17 μ, width 6–12 μ. Epicone 2.5 times as long as hypocone, conical, with straight to gently convex sides, its apex pointed or somewhat rounded. Hypocone half as long as wide, broadly rounded, in lateral view asymmetric so that the dorsal portion is larger than the ventral one. Girdle very wide, very slightly displaced, its anterior margin overhanging and of greater diameter than the posterior margin. Sulcus not discernible. Flagellar chambers absent. Anterior flagellum up to twice the girdle circumference in length; posterior flagellum equal in length to the cell body.

Chromatophores two, yellow-brown; one band-shaped, partially encircling periphery of epicone; the other filling bottom of hypocone, extending on ventral surface to epicone. Nucleus not seen. Assimilate bodies present or absent. Pellicle occasionally present.

Woods Hole area: Great Pond, Falmouth Harbor; January to April, August, September. Barents Sea; White Sea; Baltic off Kiel; brackish estuaries near Nieuport (Belgium) and along the coast of Holland; Plymouth Sound; Adriatic Sea.

Several different populations were studied. One had straight sides to the epicone and a pointed apex. Another had convex sides to the epicone and a pointed apex. A third was rather variable, rotund in appearance, often almost colorless, with apex rounded or pointed. In a similar way this distinctive species shows considerable variation as it receives treatment from various investigators. Lohmann describes it with relatively very small hypocone, whereas Wulff describes it with relatively very much larger one. In contrast to these, which have pointed apices, Conrad's has a rounded apex. Van Goor shows a very slender form. Lohmann's and Wulff's figures show a lobed epiconal chromatophore, whereas Lebour's shows a band-shaped chromatophore.

Massartia asymmetrica (Massart) Schiller

(Plate 1, Figures 10, 14)

Gymnodinium asymmetricum Massart, 1920, p. 132, figs. 22A–D.
Massartia asymmetrica (Massart) Schiller in Carter, 1937, p. 59, pl. 8, figs. 17–18.

Body globular, oval in outline, compressed dorsi-ventrally. Length 14–22 μ, width 13–20 μ. Epicone 0.66 body length, hemispherical, with small apical notch. Hypocone small, 0.33 body length, twice as wide as long, broadly rounded, often with slight oblique flattening in antapical region. Girdle very wide, shallow, displaced one girdle width, its anterior margin wider than posterior. Sulcus extending from girdle to antapex, widening abruptly during its course. Anterior flagellum incompletely encircling body; posterior flagellum 1.0–1.5 body lengths.

Chromatophores absent. Nucleus almost wholly within hypocone, wider than long, containing relatively few, short, unoriented chromatin corpuscles. Large, brown ingested body and smaller assimilate bodies frequent.

Woods Hole area: Great Pond; October, January, February. Isle of Wight, England; estuary near Nieuport, Belgium.

Massartia asymmetrica is similar to *M. vorticella* (Stein) Schiller and *M. stigmaticum* (Lindemann) Schiller, which, however, contain stigmas, and to *M. glandula* Herdman, which differs, however, in its larger size (20–35 μ long) and helmet-shaped instead of hemispherical epicone. Massart's and Carter's figures of *M. asymmetrica* show somewhat greater displacement of girdle than in the specimens described here.

Massartia glauca (Lebour) Schiller

Spirodinium glaucum Lebour, 1917, p. 196, fig. 13.
Gyrodinium glaucum (Lebour) Kofoid and Swezy, 1921, p. 308, pl. 9, fig. 94, text fig. DD, 16.
Gyrodinium glaucum (Lebour) Kofoid and Swezy in Lebour, 1925, p. 54, pl. 7, fig. 4, text fig. 15.

Woods Hole area: Great Pond; October, May. Plymouth Sound; Adriatic Sea; La Jolla, California.

The specimens studied agreed closely in shape with those of Lebour and were not like Kofoid and Swezy's somewhat different form. They were, however, considerably smaller than Lebour's, 28–32 μ instead of 40–56 μ in length. This form is different from other species of *Massartia* in its striations; it is distinguished by its slender form, the slight twist to the apex, and its absence of chromatophores.

GYRODINIUM Kofoid and Swezy

Key to Species

- Without striations:
  - Chromatophores present:
    - Chromatophores 2 to 4 .... *G. estuariale*
    - Chromatophores many:
      - Body dorsi-ventrally flattened:
        - Sulcus not deflected on epicone .... *G. aureolum*
        - Sulcus deflected to right on epicone .... *G. resplendens*
      - Body laterally flattened .... *G. uncatenum*
  - Chromatophores absent:
    - Sulcus sigmoid:
      - Epicone rounded-conical .... *G. metum*
      - Epicone hemispherical .... *G. glaebum*
    - Sulcus bisigmoid .... *G. undulans*
- With striations:
  - Length 18–43 μ .... *G. dominans*
  - Length 66–96 μ .... *G. spirale*

Gyrodinium **estuariale** n. sp.

(Plate 1, Figures 15, 16)

Body ellipsoid; apex often somewhat pointed compared to broadly rounded antapex; often with slight asymmetry, the right side more convex than the left; slightly flattened dorsi-ventrally; with equal epicone and hypocone. Length 11–16 μ, width 9–12 μ. Epicone broadly conical to sub-hemispherical, the right margin often a bit more sloping than the left; hypocone hemispherical to somewhat trapezoidal, with rounded to flattened, oblique, sometimes indented antapex. Girdle deep, moderately wide, displaced 0.25–0.33 body length, strongly posteriorly bending in right limb. Sulcus slight on epicone, markedly deflected to right in intercingular area, widening, and proceeding straight to antapex on hypocone. Anterior flagellar chamber an elongate pocket diverging to right and running beneath posterior flagellar chamber which is a leftward underhollowing of sulcus between girdle ends. Anterior flagellum encircling body completely; posterior flagellum body length.

Chromatophores yellow-brown, one or two in epicone, one or two in hypocone, distinctively inset from periphery. Nucleus not seen. Assimilate bodies usually sparse.

Woods Hole area: Great Pond, Salt Pond, Uncatena Island; July, August, October to January.

Gyrodinium estuariale is very similar to *Gymnodinium vitiligo* and *Gymnodinium veneficum* (Ballantine, 1956), differing in greater displacement of girdle ends, in wider, deeper girdle and sulcus, and in an oblique, instead of symmetrically rounded, antapex. In the intercingular region the sulcus is deflected to the right (passing from anterior to posterior end) in these species, contrary to most gyrodinia. *Gyrodinium estuariale* is similar to *Gymnodinium marylandicum* (Thompson, 1947); but the latter's sulcus follows the longitudinal axis or is deflected slightly to the left.

Gyrodinium **aureolum** n. sp.

(Plate 2, Figures 8, 9)

Body essentially globular, its dorsi-ventral outline either somewhat ellipsoidal or somewhat fusiform, slightly dorsi-ventrally flattened, with subequal epicone and hypocone. Length 27–34 μ, width 17–32 μ. Epicone hemispherical to broadly conical, sometimes slightly truncate. Hypocone similar, but usually distinctly truncate, with antapex faintly indented at times. Girdle wide, moderately deep, displaced 0.20 body length. Sulcus reaching from just behind apex all the way to antapex, with slight, left deflection in girdle region, rather narrow on epicone, wide on hypocone. Anterior flagellar chamber a posteriorly pointed, finger-shaped cavity; posterior flagellar chamber an underhollowing of left sulcal margin opposite right girdle limb. Anterior flagellum completely encircling body; posterior flagellum very long, up to two body lengths.

Numerous yellow-brown chromatophores present, elliptical in shape, usually arranged in a somewhat radiating manner. Nucleus spherical or wider than long, with elongate chromatin corpuscles.

Woods Hole area: Great Pond, Uncatena Island, Falmouth Harbor; December to April.

This species is rather similar to *Gyrodinium aureum* (Conrad, 1926). It is, however, different in its less elongate chromatophores, wider grooves, greater width for the same length, more conical outline of epicone and hypocone, and somewhat less displacement of girdle ends.

Gyrodinium **resplendens** n. sp.

(Plate 2, Figures 6, 7)

Body broadly fusoid, with truncate apex and antapex, moderately flattened dorsi-ventrally. Length 36–62 μ, width 32–48 μ. Epicone and hypocone similar, equal, trapezoidal in outline, their sides convex, straight, or concave; the apex somewhat rounded, the antapex with sulcal indentation. Girdle deep, moderately wide, displaced 0.20–0.25 body length. Sulcus extending onto epicone as very narrow superficial groove, diverging to right; in intercingular region narrow, vertical or left deflected; on hypocone running straight to antapex, superficially narrow but broad beneath projecting lappet of left margin. Anterior and posterior flagellar chambers elongate pockets projecting toward but not reaching each other. Anterior flagellum completely encircling body; posterior flagellum one body length.

Chromatophores oval, rich brown, radiating, many-tiered. Nucleus somewhat anterior of center, wider than long, with numerous, elongate chromatin corpuscles. Ingested bodies occasional; assimilate absent.

Woods Hole area: Great Pond; July, August.

This species is close to *Gyrodinium aureolum.* It is also quite like *Gymnodinium nelsoni,* differing in greater girdle displacement (so that it falls into the genus *Gyrodinium*), less dorsi-ventral flattening with no ventral concavity, and truncate rather than hemispherical epicone.

Gyrodinium **uncatenum** n. sp.

(Plate 4, Figures 1, 2, 3)

Body laterally flattened, elliptical to quadrangular in side view, elongate elliptical in ventral or dorsal view, with epicone and hypocone subequal. Length 40–54 μ, width 28–33 μ. Epicone in ventral and dorsal views helmet-shaped, taller than wide, broadly rounded at apex, its sides sloping gently, with slight concavities at girdle; in lateral view, sub-hemispherical to trapezoidal, wider than tall. Hypocone very similar but often slightly more truncate at antapex and more distinctly trapezoidal in side view. Girdle narrow, deep, displaced 0.33 body length, the right limb bending steeply posteriorly. Sulcus projecting slightly on epicone, curving to left in intercingular area, then sharply to right between right girdle end and antapex; carried across antapex all the way to dorsal side; deeply excavating hypocone, the anterior extent of excavation seen laterally as an oblique line running from dorsal end of sulcus toward ventral surface. Anterior flagellar chamber long, finger-like, projecting posteriorly and somewhat dorsally and rightward; posterior flagellar chamber a long extension of sulcal excavation, reaching nearly to anterior chamber. Anterior flagellum wide and strap-shaped, completely encircling body; posterior flagellum occasionally double, twice the body length; both flagella reaching all the way to the end of the chambers.

Chromatophores elongate, yellow-brown, radiating from center, leaving marginal area clear (lateral view). Nucleus spherical, in the epicone, with slightly elongate chromatin corpuscles. Crytoplasm showing vague radiating structure in peripheral region. Countless, dark assimilate bodies often present.

Woods Hole area: Great Pond, Uncatena Island; July, August, October.

This species is rendered distinctive by its lateral flattening, a rarity among gyrodinia. Very striking is the deep excavation in the hypocone, identical to that in *Gymnodinium stellatum* and *G. bifurcatum* (Kofoid and Swezy, 1921).

Gyrodinium metum n. sp.

(Plate 1, Figures 11, 12)

Body somewhat asymmetric, the right side more convex than the left, circular in cross-section, with hypocone slightly larger than epicone. Length 14.5–22 μ, width 11–16 μ. Epicone rounded-conical in outline; hypocone truncate with straight to convex sides. Girdle deeply excavated, displaced about 0.20–0.25 body length, its right limb curving steeply posteriorly. Sulcus sigmoid, not extending onto epicone, narrow in intercingular region, and wide and deep on hypocone, flattening or indenting the antapex. Anterior flagellar chamber produced inward and posteriorly; posterior flageller chamber a mere excavation in the sulcal floor. Anterior flagellum completely encircling the body; posterior flagellum 1.5 times body length.

Chromatophores absent. Cytoplasm gray, foamy in texture. Nucleus not seen.

Woods Hole area: Great Pond; May, June, July, December, February.

This species is distinguished by the Chinaman-hat shape of the epicone. A smaller-size variant was often seen. Its features are identical except respecting size—9.5–12 μ × 9–7 μ.

Gyrodinium glaebum n. sp.

(Plate 1, Figures 17, 18)

Body elliptical, very slightly compressed dorsi-ventrally, with equal epicone and hypocone. Length 17–25 μ, width 12–19 μ. Epicone hemispherical but slightly asymmetric, with right contour more sloping or less fully curved than left. Hypocone similar, but broader, the asymmetry more marked, the left contour more sloping or less fully curved than right, often with oblique flattening in region of sulcus end. Girdle wide, rather deep, displaced two-three times its own width. Sulcus extending slightly onto epicone, narrow and leftward diverging in intercingular region, wide and deep in a straight course on hypocone. The two flagellar chambers overlapping each other, the anterior one a pronounced, posteriorly directed excavation, the posterior one an underhollowing of left girdle margin. Anterior flagellum only partially encircling body, posterior flagellum as long as body.

Chromatophores absent. Nucleus somewhat anterior of girdle, with large and relatively few chromatin corpuscles. Large, brown ingested bodies often present, as well as small, refractive assimilate bodies.

Woods Hole area: Great Pond; July, October.

Gymnodinium variabile (Herdman, 1924a) is close in shape but lacks any marked girdle displacement.

Gyrodinium **undulans** n. sp.

(Plate 3, Figures 7, 8, 9)

Body elliptical, somewhat dorsi-ventrally flattened with equal epicone and hypocone. Length 27–38 μ, width 21–31 μ. Epicone varying from sub-hemispherical to truncate-pyramidal, with rounded apex and straight but sloping sides. Hypocone asymmetric, truncate-pyramidal with rounded to flattened, oblique antapex, and sloping sides. Girdle wide, deep, displaced 0.20 body length, its right limb curving strongly posteriorly. Sulcus distinctive, forming a bi-sigmoid curve; very narrow on epicone, swerving leftward and then rightward to meet left girdle end, curving again to left in intercingular area and widening, then bending to right on hypocone to form large overlapping lobe, finally returning leftward to antapex. Floor of sulcus on hypocone extending straight to antapex; and right margin of sulcus "bearing away" laterally to form a swelling. Anterior and posterior flagellar chambers projecting toward, but not reaching, each other. Anterior flagellum completely encircling body; posterior flagellum one body length, occasionally double.

Chromatophores absent. Nucleus large, principally within epicone, of elongate chromatin corpuscles. Assimilate bodies sometimes in form of large blocks.

Woods Hole area: Great Pond; February, January.

Few Dinophyceae have either bi-sigmoid sulci or overlapping sulcal lobes.

Gyrodinium **dominans** n. sp.

(Plate 3, Figures 1, 2, 3)

Body broadly fusiform, circular in cross-section, epicone and hypocone subequal. Length 18.5–43 μ, width 10–22 μ. Epicone and hypocone conical to rotund-conical, their sides varying from convex to straight. Both epicone and hypocone occasionally with slight concavities near girdle. Surface with continuous striations, the number the same on epicone and hypocone, between 7 and 10 across ventral face. Girdle of moderate depth and width, displaced 0.25–0.33 body length. Sulcus sigmoid, deflected to left 0.25 transdiameter in intercingular region, reaching halfway up epicone, extending to posterior margin of hypocone on left side of antapex. Anterior flagellar chamber a posteriorly directed, finger-like projection from left end of girdle. Posterior flagellum inserted at posterior end of girdle (flagellar chamber not seen). Anterior flagellum not completely encircling body; posterior flagellum short, 0.50 body length.

Chromatophores absent. Nucleus anterior, in epicone, containing elongate, oriented chromatin corpuscles.

Woods Hole area: Great Pond, Falmouth Harbor, Salt Pond; April, July, August, October to December.

Gyrodinium dominans is an ally to three very similar species of *Gyrodinium*: *G. pingue* (Schütt, 1895, as *Gymnodinium spirale* var. *pinguis;* Wulff, 1916, as

Spirodinium varians; Kofoid and Swezy, 1921; Lebour, 1925), *G. obtusum* (Schütt, 1895, as *Gymnodinium spirale* var. *obtusa;* Kofoid and Swezy, 1921; Lebour, 1925), and *G. fissum* (Kofoid and Swezy, 1921). The chief distinction is the flexure of the sulcus in *G. dominans,* contrasting with the comparative straightness of the sulcus in the other three.

Gyrodinium spirale (Bergh) Kofoid and Swezy

(Plate 3, Figure 4)

Gyrodinium spirale (Bergh) Kofoid and Swezy, 1921, p. 332, pl. 4, fig. 43, text fig. DD, 14.
Gyrodinium spirale (Bergh) Kofoid and Swezy in Lebour, 1925, p. 56, pl. 8, fig. 1.

Body slender fusiform; circular in cross-section; somewhat twisted on its longitudinal axis; with epicone longer but narrower than hypocone. Length 66–96 μ, width 30–38 μ. Epicone narrowly conical, convex or straight along left and dorsal contours. Hypocone with sides parallel anteriorly, convex posteriorly; its antapex pointed, excentric, to right of ventral, longitudinal axis; with sulcal notch to left of antapex. Surface with continuous striations, 8–13 on epicone, 15–20 on hypocone. Girdle narrow, rather shallow, displaced more than 0.33 the body length, its right limb curving strongly posteriorly. Sulcus very narrow, from somewhat behind apex to left girdle end as a heavy line, a very narrow but distinct groove between girdle ends, widening and deepening from right girdle end to antapical notch. Anterior flagellum inserted at opening of a pustule, which is composed of a short, sac-shaped portion, extending posteriorly, and of a long, thread-like portion, extending somewhat anteriorly, then laterally, finally posteriorly along right contour to region of right girdle limb. Posterior flagellum likewise inserted at opening of a pustule having a long, thread-like extension anteriorly and leftward to region of left girdle limb. Anterior flagellum following girdle 0.33 or less of girdle length. Posterior flagellum short, about 0.25 of body length.

Chromatophores absent. Nucleus elongate-ellipsoidal on left side (ventral view), in intercingular area, without apparent structure.

Woods Hole area: Great Pond, Falmouth Harbor; December, April, May, August. Baltic Sea; Norway; Port Erin, Ireland; Plymouth Sound; Adriatic Sea; La Jolla, California; Indian Ocean; coast of Australia.

The organism defined here agrees closely with those described by Kofoid and Swezy and by Lebour. Distinctive characteristics are the slender form, twist of body, greater dorsal than ventral curvature, and a longer epicone than hypocone.

WARNOWIA Lindemann

Warnowia parva (Lohmann) Lindemann

(Plate 4, Figure 8)

Pouchetia parva Lohmann, 1908, p. 264, pl. 17, fig. 23.

Body elliptical, circular in cross-section, slightly tapered posteriorly, epicone somewhat larger than hypocone. Length 22.5–30 μ, width 15–18 μ. Epicone hemispherical, hypocone similar but narrowed toward antapex and with sulcal indentation along left contour. Girdle shallow but very wide, displaced 0.50 the body length, with strongly descending right limb. Sulcus narrower than girdle, extending in sigmoid path from apex to antapex, bending from right margin toward center anterior to girdle, diagonal across ventral face between girdle ends, recurving from left margin toward center posterior to girdle. Anterior flagellar chamber an elongate pocket from left end of girdle limb, the posterior flagellar chamber not seen. Anterior flagellum not encircling body completely; posterior flagellum short, 0.33 body length.

Yellow bodies, resembling chromatophores in color and peripheral position but unlike in large size and irregular shape, sparse anteriorly but abundant posteriorly. Nucleus anterior, with elongate, oriented corpuscles. Melanosome near antapex, black, diffuse and spreading, or ellipsoidal and globular. Lens simple without evident laminations, projecting anteriorly on left side from melanosome. Nematocysts absent. Cell often within a pellice. Assimilate bodies frequent.

Woods Hole area: Great Pond; July. Baltic off Kiel.

The organism studied here is probably a close match to Lohmann's *Pouchetia parva,* but Lohmann showed no girdle and sulcus. It is close to *Nematodinium armatum,* but the tapered hypocone, large irregular chromatophores, absence of nematocysts, and cyst differentiate it, as well as the characteristics mentioned under *N. armatum.*

NEMATODINIUM Kofoid and Swezy

Nematodinium armatum (Dogiel) Lebour

(Plate 4, Figures 9, 10)

Pouchetia armata Dogiel, 1906, p. 36, pl. 2, figs. 48–49.
Nematodinium armatum (Dogiel) Lebour, 1925, p. 71, pl. 10, figs. 5a–5b
Nematodinium armatum (Dogiel) Lebour in Martin, 1929, p. 19, pl. 2, figs. 5–7.

Body elliptical, with equal epicone and hypocone. Length 33–53 μ, width 20–33 μ. Epicone evenly rounded, slightly asymmetric in ventral view, its right margin more sloping than the left; hypocone also slightly asymmetric with more sloping left than right side, the antapex either somewhat pointed and off-center, or, usually, obliquely truncate. Girdle deep, moderately wide, displaced 0.33 the body length, with strongly descending right limb. Sulcus extending from near apex in a sigmoid path to antapex, widening on the oblique margin of antapex, a portion of it curving sharply to the right, delimiting a knob-like protuberance on ventral face of the hypocone. Anterior flagellar chamber an elongate pocket from left end of girdle limb (posterior chamber not seen). Posterior flagellum one body length (anterior flagellum not fully studied).

Chromatophores yellow, circular or subcircular, few, and scattered. Nucleus large, anterior, of elongate chromatin corpuscles. Melanosome near antapex, black, diffuse and spreading, or ellipsoidal and globular. Lens single with concentric laminations, projecting anteriorly on left side from melanosome. Nematocysts present or absent, in region of right girdle limb.

Woods Hole area: Great Pond; August. Barnegat Bay, New Jersey; Plymouth Sound; Naples.

Some of the specimens were of full, ellipsoidal proportions, as in Dogiel's figure. Some were more slender, though not quite so slender as in Lebour's Figure 5a. Some had a slight tapering of hypocone and pointed antapex as in Martin's figures. They are all intermediate between the smaller *Warnowia parva* (Lohmann, 1908) without rightward curvature of sulcus on hypocone and with comparatively wider, shallower furrows, and the larger *Nematodinium lebourae* (Schiller, 1933; Kofoid and Swezy, 1921, as *N. armatum*), with rightward curvature of sulcus on hypocone and with comparatively greater transverse displacement of the sulcus.

POLYKRIKOS Bütschli

Key to Species

Chromatophores present:
  Body cylindrical .... *P. hartmanni*
  Body laterally flattened .... *P. lebourae*
Chromatophores absent .... *P. schwartzi*

Polykrikos hartmanni Zimmermann

(Plate 4, Figure 7)

Polykrikos hartmanni Zimmermann, 1930, p. 436, figs. 8–9.

Colony cylindrical in form with rounded ends, consisting of two zooids, delimited by a slight constriction. Length 60–68 μ, width 42–47 μ. Epicone often smaller than hypocone in anterior zooid but equal to hypocone in posterior zooid. Girdles wide, rather shallow, displaced twice their width. Sulcus continuous from apex to antapex, roughly straight, narrowed at the constriction between zooids and in intercingular regions. Sulcus produced inward as anterior and posterior flagellar chambers, which extend posteriorly and anteriorly, respectively, their diverging ends overlapping. Anterior flagella incompletely encircling zooids; posterior flagella about 0.66 as long as the colony.

Chromatophores circular, small, numerous, yellow-brown in color. Nuclei always two, with elongate chromatin corpuscles. Several long nematocysts often, but not always, present in region just below anterior girdle. Innumerable black granules may fill peripheral cytoplasm of whole colony or may be restricted to posterior end.

Woods Hole area: Great Pond; August. Adriatic.

Slight differences between our specimens and Zimmermann's are the smaller size of ours (Zimmermann's 80–120 μ × 55–75 μ) and the yellow-brown instead of yellow-green chromatophores. *Polykrikos barnegatensis* (Martin, 1929), also composed of two cells, is close to *P. hartmanni* but has a single nucleus and a more elliptical outline.

Polykrikos schwartzi Bütschli

Polykrikos schwartzi Bütschli in Kofoid and Swezy, 1921, p. 400, text fig. F, 4.
Polykrikos schwartzi Bütschli in Lebour, 1925, p. 67, pl. 10, figs. 2a–2b, text fig. 16c.

Woods Hole area: Great Pond; August. Arctic near Iceland; off coast of Norway; Skagerack; Baltic off coast of Denmark; Baltic off Kiel; North Sea off

Helgoland; Plymouth Sound; Atlantic off Concarneau, France; Mediterranean off French coast.

This species is distinguished by its many cells (zooids), averaging about eight, with four nuclei; by its cylindrical form; and by the absence of chromatophores.

Polykrikos lebourae E. C. Herdman

Polykrikos lebourae E. C. Herdman, 1924b, p. 60, fig. 6.
Polykrikos lebourae E. C. Herdman in Lebour, 1925, p. 68, pl. 10, fig. 3.

Woods Hole area: Salt Pond, beach sand; November. Port Erin, Ireland, in sand.

This species is quite distinctive in its lateral flattening. It has eight cells, two nuclei, and yellow-brown chromatophores. It is recorded from beach sand at Woods Hole by E. C. Herdman.

Diagnoses of New Species

Amphidinium **carteri** n. sp.

Corpus dorsali-ventraliter compressum, a fronte visum ovale; epicono minuto, asymmetrico et rostroformi; hypocono truncato-elliptico; sulco prope marginem dextrum, leniter curvato; chromatophoro uno, parietali, perforato, fulvo. Longitudo 12–15 μ, latitudo 8–9 μ. United States, in loco dicto Great Pond, Barnstable County, Massachusetts.

Amphidinium **wislouchi** n. sp.

Corpus simile *Amphidinio carteri* sed paullo majus; chromatophoris multis, ellipticis, paululum radiatim ordinatis. Longitudo 20–25 μ, latitudo 14–16.3 μ. United States, in loco dicto Great Pond, Barnstable County, Massachusetts.

Gymnodinium **lazulum** n. sp.

Corpus globosum; epicono conico vel campaniformi; hypocono hemispherico vel campaniformi; sulco tenui; corpore sine striis; chromatophoris absentibus; cytoplasmate pellucido, subcaeruleo, saepe cum multis corporibus multi-coloratis. Longitudo 28–34 μ, latitudo 30–32 μ. United States, in loco dicto Great Pond, Barnstable County, Massachusetts.

Gymnodinium **stellatum** n. sp.

Corpus lateraliter compressum; epicono quadrangulato et hypocono hemispherico; extremis cinguli 0.17 longitudinis corporis transpositis; sulco a vicinitate apicis ad cavernam profundam hypoconi extendente; corpore sine striis; chromatophoris absentibus; structura cytoplasmatis exterioris perspicue radiata. Longitudo 25–47 μ, latitudo 22–39 μ, crassitudo 13–25 μ. United States, in loco dicto Salt Pond, Barnstable County, Massachusetts.

Gymnodinium **striatissimum** n. sp.

Corpus globosum vel ellipticum; epicono et hypocono conico, aculeato, vel truncato; cingulo angusto, flexuram posterioram extremi sinistri habente; sulco a vicinitate apicis ad antapicem extendente; corpore cum striis, in hypocono pluribus quam in epicono ornato; chromatophoris absentibus. Longitudo 29–43 μ, latitudo 23–41 μ. United States, in loco dicto Great Pond, Barnstable County, Massachusetts.

Gyrodinium **estuariale** n. sp.

Corpus ellipticum, paululum asymmetricum, margine dextro convexiore quam margine sinistro; epicono late conico vel sub-hemispherico; hypocono hemispherico; extremis cinguli 0.25–0.33 longitudinis corporis transpositis; sulco ad latus dextrum inter extrema cinguli multum deflecto; corpore sine striis; chromatophoris fulvis, 2–4, paulum intra peripheriam positis. Longitudo 11–16 μ, latitudo 9–12 μ. United States, in loco dicto Great Pond, Barnstable County, Massachusetts.

Gyrodinium **aureolum** n. sp.

Corpus globosum; epicono et hypocono hemispherico vel conico; extremis cinguli 0.33 longitudinis corporis transpositis; sulco a vicinitate apicis ad antapicem extendente; corpore sine striis; chromatophoris multis, fulvis, plerumque omnibus plus minusve radiatim ordinatis. Longitudo 27–34 μ, latitudo 17–32 μ. United States, in loco dicto Great Pond, Barnstable County, Massachusetts.

Gyrodinium **resplendens** n. sp.

Corpus late fusiforme, apice et antapice truncato, dorsaliventraliter compressum; extremis cinguli 0.20–0.25 longitudinis corporis transpositis; sulco in epicono augusto, tenui; ad latus dextrum curvato, in hypocono profundo et recto; corpore sine striis; chromatophoris multis, fulvis, radiatim ordinatis. Longitudo 36–62 μ, latitudo 32–48 μ. United States, in loco dicto Great Pond, Barnstable County, Massachusetts.

Gyrodinium **uncatenum** n. sp.

Corpus lateraliter compressum, a late visum ellipticum vel quadrangulum; extremis cinguli 0.33 longitudinis corporis transpositis, parte dextra ad antapicem multum curvata; sulco in epicono tenui, ad sinistram prope extremitatem posteriorem cinguli deflecto; hypocono excavationem profundam antapicis praehente; corpore sine striis; chromatophoris luteo-fuscis, elongatis, radiatim ordinatis; cytoplasmate circa peripheriam structuram radiatam habente. Longitudo 40–54 μ, latitudo 28–33 μ. United States, in loco dicto Uncatena Island, Barnstable County, Massachusetts.

Gyrodinium **metum** n. sp.

Corpus paulum asymmetricum, latere dextro convexiore quam latere sinistro; epicono conico, multo latiore quam hypocono; hypocono truncato, multo longiore quam epicono; cingulo profundo, extremis cinguli 0.20–0.25 longitudinis corporis

transpositis; sulco S-curvato, in epicono absente, in hypocono lato; corpore sine striae; chromatophoris absentibus. Longitudo 14.5–2 μ, latitudo 11–16 μ. United States, in loco dicto Great Pond, Barnstable County, Massachusetts.

Gyrodinium **glaebum** n. sp.

Corpus ellipticum, paulum asymmetricum; epicono hemispherico, hypocono late hemispherico; cingulo lato, extremis cinguli 2–3 latitudinibus cinguli transpositis; sulco in epiconum vix extendente, in hypocono lato et profundo; corpore sine striis; chromatophoris absentibus. Longitudo 17–25 μ, latitudo 12–19 μ. United States, in loco dicto Great Pond, Barnstable County, Massachusetts.

Gyrodinium **undulans** n. sp.

Corpus ellipticum; epicono subhemispherico vel truncato-pyramidali; hypocono truncato-pyramidali; extremis cinguli 0.20 longitudinis corporis; sulco in duo S-formata curvamina facto, margine sinistro in hypocono marginem dextrum superposito; corpore sine striis; chromatophoris absentibus. Longitudo 27–38 μ, latitudo 21–31 μ. United States, in loco dicto Great Pond, Barnstable County, Massachusetts.

Gyrodinium **dominans** n. sp.

Corpus fusiforme; epicono et hypocono conico; extremis cinguli 0.25–0.33 longitudinis corporis transpositis; sulco S-curvato, in epiconum extendente, in hypocono ad marginem sinistrum prope antapicem extendente; corpore cum striis, 7–10 a ventrale viso in epicono et hypocono; chromatophoris absentibus. Longitudo 18.5–43 μ, latitudo 10–22 μ. United States, in loco dicto Great Pond, Barnstable County, Massachusetts.

The author wishes to express the greatest gratitude to Dr. William Randolph Taylor for his guidance in this study. He is also greatly obligated to Dr. Alfred C. Redfield and Dr. Trygve Braarud for their kindness in reading the manuscript.

SUMMARY

1. Unarmored Dinophyceae were collected from very shallow embayments on the south shore of Cape Cod, Massachusetts.

2. Twenty-six species, distributed in eight genera, were studied. Twelve were considered as new species and nine showed extensions of range from Europe.

LITERATURE CITED

BALLANTYNE, D., 1956. Two new marine species of *Gymnodinium* isolated from the Plymouth area. *J. Mar. Biol. Ass. U. K.*, **35** (3): 467–474.

CALKINS, G., 1902. Marine protozoa from Woods Hole. *Bull. U. S. Fish Comm.*, **21**: 413–468.

CARTER, N., 1937. New or interesting algae from brackish water. *Archiv. f. Protist.*, **90**: 1–68.

CONRAD, W., 1926. Recherches sur les Flagellates de nos eaux saumâtres. Ie Partie, Dinoflagellates. *Archiv. f. Protist.*, **55**: 63–100.

CONRAD, W., 1939. Notes Protistologiques. X. Sur le schorre de Lilloo. *Bull. Mus. Roy. Hist. Nat. Belg.*, **15** (41): 1–18.

DOGIEL, V., 1906. Beiträge zur Kenntnis Peridineen. *Mitt. Zool. Stat. Neapel,* **18**: 1–45, pls. 1–2.

HERDMAN, E. C., 1924a. Notes on dinoflagellates and other organisms causing discoloration of the sand at Port Erin. IV. *Proc. Trans. Liverpool Biol. Soc.,* **38**: 75–84.

HERDMAN, E. C., 1924b. Notes on dinoflagellates and other organisms causing discoloration of the sand at Port Erin. III. *Proc. Trans. Liverpool Biol. Soc.,* **38**: 58–63.

KOFOID, C. A., AND O. SWEZY, 1921. The free-living unarmored Dinoflagellata. *Mem. Univ. Calif.,* **5**: 1–562.

LACKEY, J. B., 1936. Occurrence and distribution of the marine protozoan species in the Woods Hole area. *Biol. Bull.,* **70**: 264–278.

LEBOUR, M. V., 1917. The Peridiniales of Plymouth Sound from the region beyond the breakwater. *J. Mar. Biol. Assoc. U. K.,* **11** (2) : 183–200.

LEBOUR, M. V., 1925. The dinoflagellates of Northern Seas. Pps. I–VIII, 1–250, Mayflower Press, Plymouth, England.

LOHMANN, H., 1908. Untersuchungen zur Feststellung des völlstandigen Gehaltes des Meeres an Plankton. *Wiss. Meeresunters., Abt. Kiel., N. F.,* **10**: 129–370.

MARTIN, G. W., 1929. Dinoflagellates from marine and brackish waters of New Jersey. *Univ. Iowa Stud., Stud. Nat. Hist.,* **12** (9) : 1–32.

MASSART, J., 1920. Recherches sur les organismes inférieurs. VIII. Sur la motilité des Flagellates. *Bull. Acad. Roy. Belgique, Cl. de Sc.,* 5me, Sér. VI (4–5) : 116–141.

SCHILLER, J., 1933. Dinoflagellatae. *In* L. Rabenhorst's "Kryptogamen-Flora von Deutschland, Österreich und der Schweiz." **10** (3) (1) : 1–167.

SCHÜTT, F., 1895. Peridineen der Plankton-Expedition. *Ergebn. Plankton-Expedition der Humboldt-Stiftung,* **4** (M,a,A) : 1–170.

THOMPSON, R. H., 1947. Fresh-water dinoflagellates of Maryland. *State of Maryland Board of Natural Resources,* pub. no. **67**: 1–24.

VAN GOOR, A. C. J., 1925. Einige bemerkenswerte Peridineen des holländischen Brackwassers. *Rec. Trav. Bot. Néerl.,* **22**: 275–291.

WISLOUCH, S., 1924. Beiträge zur Biologie und Entstehung von Heilschlamm der Salinem der Krim. *Act. Soc. Bot. Polon.,* **2** (2) : 99–129.

WULFF, A., 1916. Über das Kleinplankton der Barentssee. *Wiss. Merresunters.,* Kiel, N.F., Abt. Helgoland, **13** (1) : 97–117.

ZIMMERMANN, W., 1930. Neue und wenig bekannte Kleinalgen von Neapel. I–V. *Zeitschr. Botanik,* **23**: 419–442.

Contribution No. 839

INTRODUCTION

During the past few years crustal structure beneath oceanic areas has been examined extensively by seismic-refraction techniques. The results have increased knowledge of the crust under the ocean basins and in the vicinity of oceanic islands and knowledge of the changes that occur from ocean basins to continents. A next logical step was an intensive examination of an interior-basin, island-arc, deep-sea trench, exterior-basin sequence, because of its importance in large-scale geologic processes. The area studied includes the interior Venezuelan basin, island arc of the Lesser Antilles and Puerto Rico, Puerto Rico trench, Barbados ridge, and Atlantic basin. This paper covers the Venezuelan basin, the more northerly portion of the arc, and the Puerto Rico trench; a paper by Ewing *et al.* (in press) covers the more southerly portions including the Barbados ridge and the Trinidad shelf. There have been three

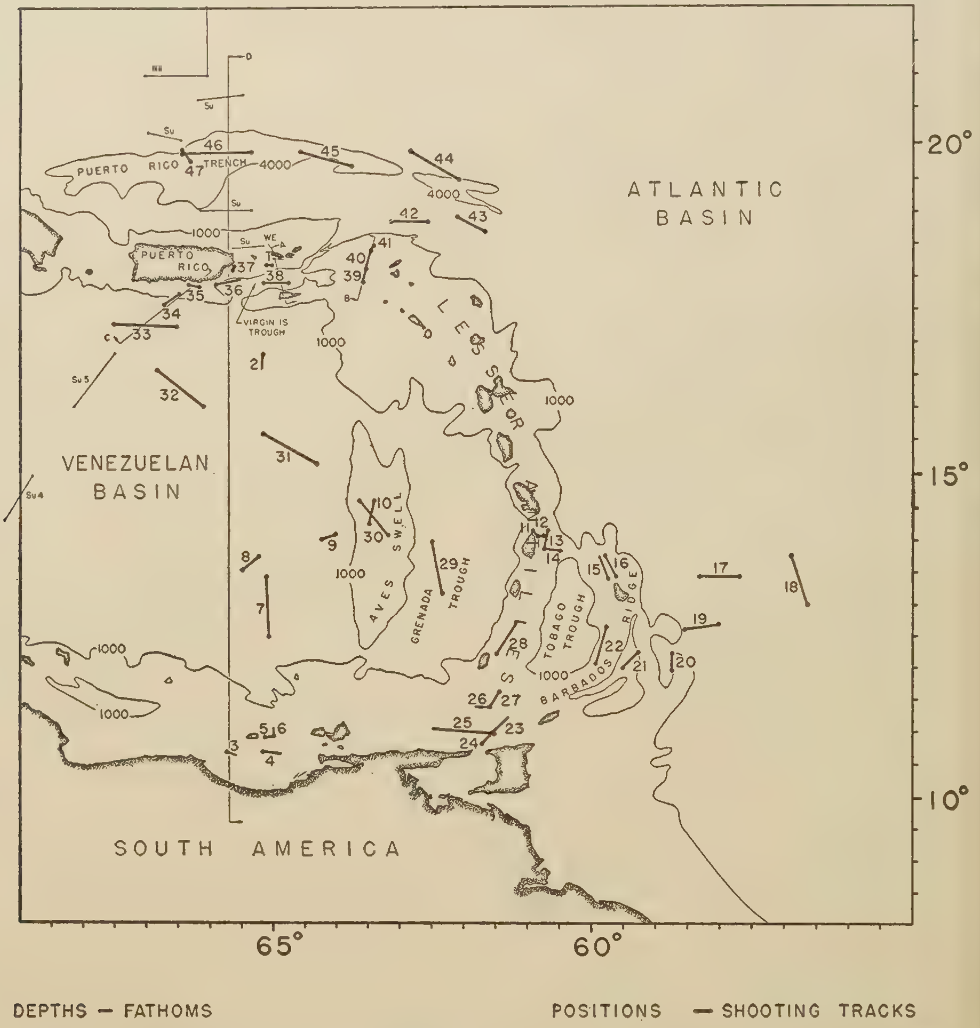
ATLANTIC BASIN
VENEZUELAN BASIN
SOUTH AMERICA
PUERTO RICO TRENCH
PUERTO RICO
VIRGIN IS TROUGH
LESSER ANTILLES
AVES SWELL
GRENADA TROUGH
TOBAGO TROUGH
BARBADOS RIDGE
4000
1000
Su
WE
He
20°
15°
10°
65°
60°
1 2 3 4 5 6 7 8 9 10 11 12 13 14 15 16 17 18 19 20 21 22 23 24 25 26 27 28 29 30 31 32 33 34 35 36 37 38 39 40 41 42 43 44 45 46 47
DEPTHS — FATHOMS
POSITIONS — SHOOTING TRACKS

FIGURE 1.—GEOGRAPHIC LOCATION OF SEISMIC-REFRACTION STATIONS IN THE EASTERN CARIBBEAN

The 1000- and 4000-fathom depth contours taken from H. O. Chart 5487 have been included for reference. Profiles from this investigation are shown by heavy lines. Profiles from other investigations referred to in the text are shown by thin lines: those from G. H. Sutton (*in* Ewing and Worzel, 1954) are labelled Su, those from Hersey *et al.* (1952) by He, those from Worzel and Ewing (1948) by WE.

ATLANTIC SECTIONS

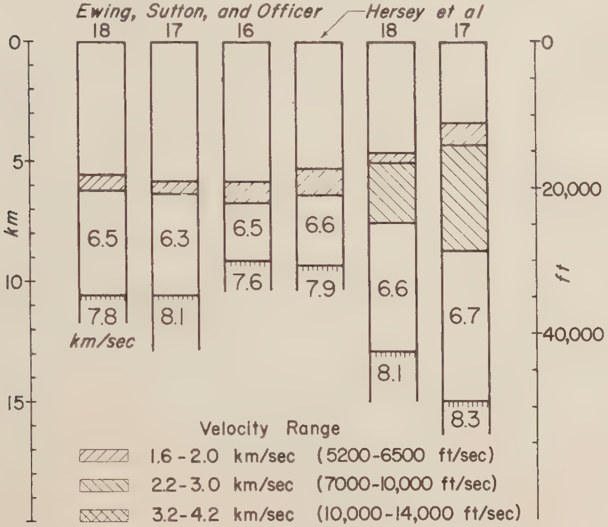

PUERTO RICO TRENCH AND ADJACENT SECTIONS

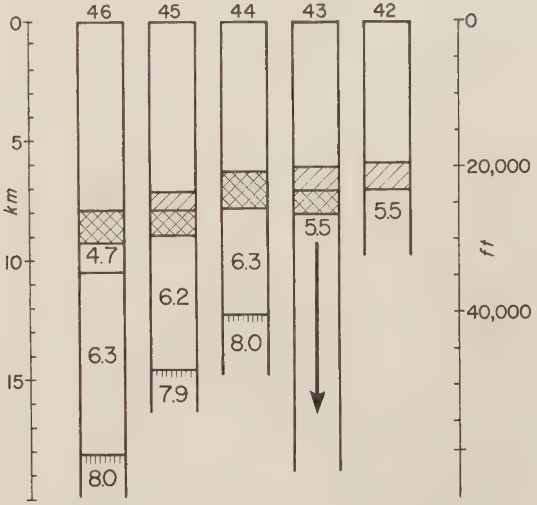

CARIBBEAN SECTIONS

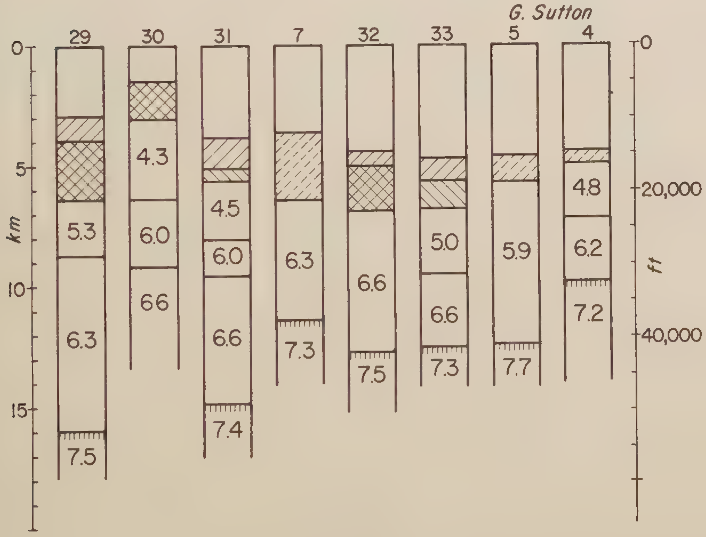

ISLAND ARC SECTIONS

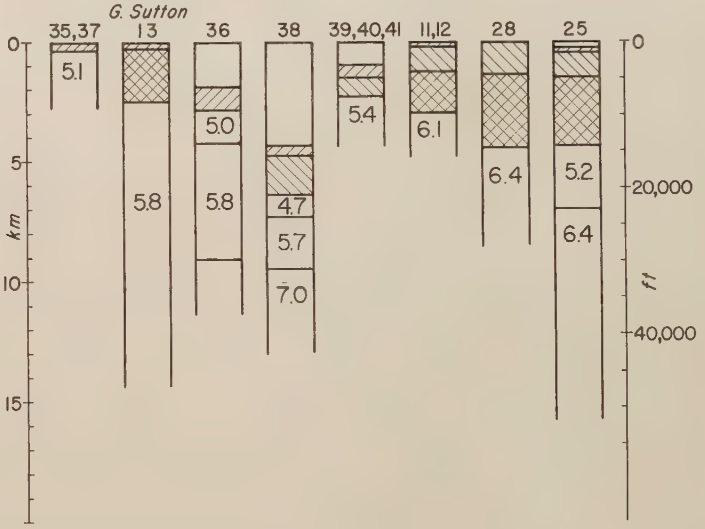

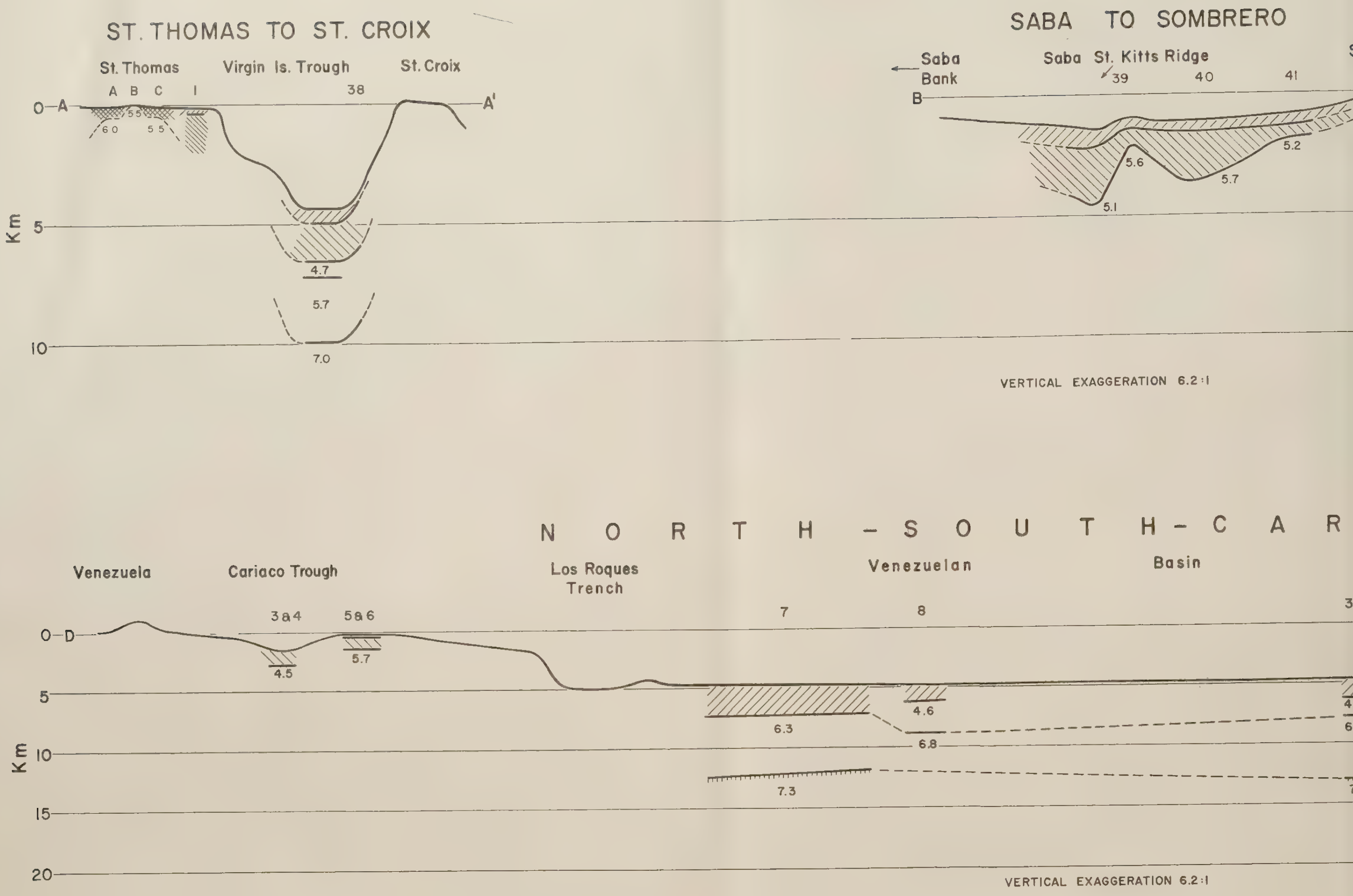
ST. THOMAS TO ST. CROIX
St. Thomas
Virgin Is. Trough
St. Croix
A B C I
38
0—A
A'
60
55
55
Km
5
4.7
5.7
10
7.0
SABA TO SOMBRERO
Saba Bank
Saba
St. Kitts Ridge
39
40
41
B
5.6
5.2
5.7
5.1
VERTICAL EXAGGERATION 6.2:1
NORTH–SOUTH–CAR
Venezuela
Cariaco Trough
Los Roques Trench
Venezuelan
Basin
3a4
5a6
7
8
0—D
4.5
5.7
5
4.6
6.3
6.8
Km
10
7.3
15
20
VERTICAL EXAGGERATION 6.2:1

SEISMIC SECTIONS AND STRUCTURE CROSS SECTIONS

Summary of seismic sections for Atlantic, Caribbean, Puerto Rico trench and adjacent area, and island-arc areas. On the structure cross sections profiles A, B, and C are from Worzel and Ewing (1948); profiles D, E, F, G, and H are from G. H. Sutton (*in* Ewing and Worzel, 1954); and profile I is from Hersey *et a* (1952). The locations of the cross sections are shown in Figure Unreversed velocities are in parentheses; they are not considere true seismic velocities.

PUERTO RICO SLOPE SOUTH

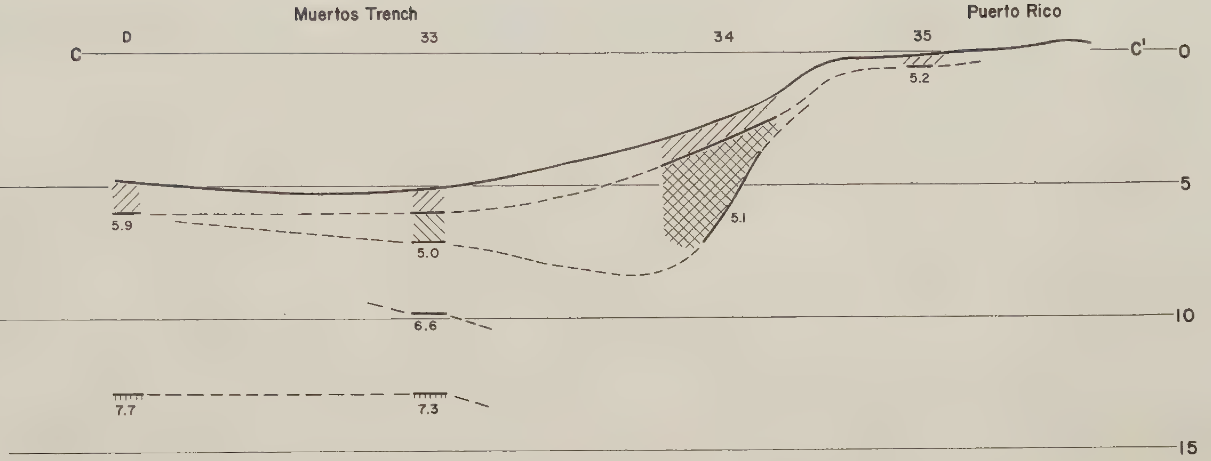
Muertos Trench
Puerto Rico
D
33
34
35
C
C'
0
5.2
5
5.9
5.0
5.1
10
6.6
7.7
7.3
15

BBEAN TO ATLANTIC

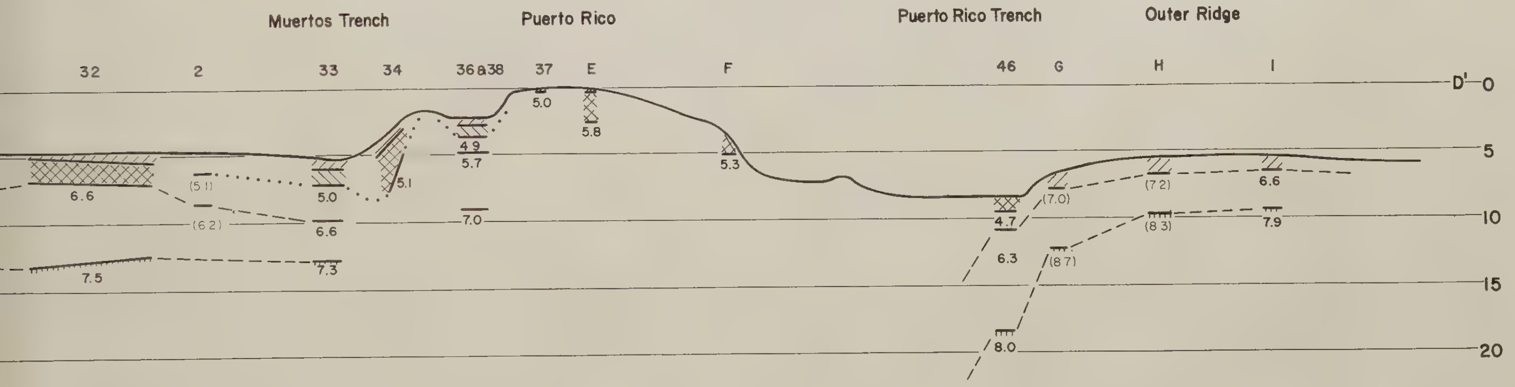
Muertos Trench
Puerto Rico
Puerto Rico Trench
Outer Ridge
32
2
33
34
36 a 38
37
E
F
46
G
H
I
D'
0
5.0
5.8
4.9
5.7
5
5.3
6.6
(5.1)
5.0
5.1
(7.0)
(7.2)
6.6
4.7
(6.2)
6.6
7.0
(8.3)
7.9
10
6.3
(8.7)
7.5
7.3
15
8.0
20

TABLE 1.—VENEZUELAN BASIN AND VICINITY

Layer \ Profile	2		7				8				9				10		29			
	T	V	Ts	Vs	Vn	Tn	Tw	Vw	Ve	Te	Tw	Vw	Ve	Te	T	V	Ts	Vs	Vn	Tn
Ocean	4.21		4.22			3.50	3.67			3.98	3.21			3.06	1.28		2.93			2.93
A	1.69	(2.14)	2.74	1.97		2.48	1.76	1.75		1.44	.46	1.78		.32	1.02		1.37	2.00		.66
B											.96	2.81		1.82						
C											2.67	3.71		2.40			2.88	3.82		2.05
D	2.56	(5.08)					2.39	4.57		2.74					1.37	(5.17)	2.69	5.29		1.94
E1		(6.16)	5.49	6.27		4.45		6.82				6.28				(6.32)	8.70	6.34		5.64
E2																				
F				7.27														7.47		
			12.45			10.43											18.57			13.33

Layer \ Profile	30				31				32				33				34			
	Ts	Vs	Vn	Tn	Ts	Vs	Vn	Tn	Ts	Vs	Vn	Tn	Tw	Vw	Ve	Te	Tw	Vw	Ve	Te
Ocean	1.30			1.68	3.44			4.28	4.45			4.45	4.50			5.01	3.28			1.59
A	.60			.36	.86	1.86		1.72	.45			.83	.38	2.03		1.52	.94	2.00		.80
B					1.08	(2.81)							2.31	(3.04)						
C	1.45	3.76		1.49					1.90	3.64		1.80					5.56	3.80		.67
D	2.78	4.33		3.89	3.22		4.47	1.57					2.41	5.00		2.98		5.11		
E1	4.07	6.02		1.50	3.05	(5.96)			6.73	6.60		4.94	4.83	6.62		1.23				
E2		6.63			7.83	6.58		2.79												
F						7.36				7.54				7.26						
					19.48			10.36	13.53			12.02	14.43			10.74				

A—unconsolidated sediment, velocity range 1.6–2.0 km/sec.
B—partially lithified to lithified sediment, velocity range 2.2–3.0 km/sec.
C—sedimentary or volcanic rock, velocity range 3.2–4.2 km/sec.
D—Sedimentary, igneous, or metamorphic rock.
E—crustal velocities, E1 and E2 where two are measured on same profile.
F—velocity beneath major discontinuity.

Numbers are given in km and km/sec. To convert to ft. and ft./sec. multiply by 3280. T and V columns are thickness and velocity respectively. n, s, e, w refer to the relative position of one receiving station on a given profile with respect to the other. Unreversed velocities are in parentheses. On some of the reversed profiles a layer measured at one end of the profile was not measured at the other, as shown by values for the thicknesses and velocities. Where a thickness for layers A through E with no associated velocity is given for a particular layer, the velocity has been assumed from a near-by profile. The number below row F in the thickness columns where given is the total depth from sea level to the major discontinuity. Each seismic layer in a refraction profile is measured over a limited range interval from the receiving station; thicknesses quoted above have been extrapolated back from the range interval of measurement by straight lines to beneath the receiving station.

TABLE 2.—PUERTO RICO TRENCH AND VICINITY

<table>
<tr><th rowspan="2">Layer \ Profile</th><th colspan="4">42</th><th colspan="4">43</th><th colspan="4">44</th></tr>
<tr><th>Tw</th><th>Vw</th><th>Ve</th><th>Te</th><th>Tw</th><th>Vw</th><th>Ve</th><th>Te</th><th>Tw</th><th>Vw</th><th>Ve</th><th>Te</th></tr>
<tr><td>Ocean</td><td>5.94</td><td></td><td></td><td>5.94</td><td>6.31</td><td></td><td></td><td>5.94</td><td>6.30</td><td></td><td></td><td>6.34</td></tr>
<tr><td>A</td><td>1.13</td><td></td><td></td><td>1.24</td><td>.89</td><td></td><td></td><td>1.08</td><td>.13</td><td colspan="2">1.70</td><td>.13</td></tr>
<tr><td>B</td><td></td><td></td><td></td><td></td><td></td><td></td><td></td><td></td><td></td><td></td><td></td><td></td></tr>
<tr><td>C</td><td></td><td></td><td></td><td></td><td>.20</td><td colspan="2">4.10</td><td>1.76</td><td>1.62</td><td colspan="2">3.78</td><td>.70</td></tr>
<tr><td>D</td><td></td><td colspan="2">5.49</td><td></td><td></td><td colspan="2">5.47</td><td></td><td></td><td></td><td></td><td></td></tr>
<tr><td>E</td><td></td><td></td><td></td><td></td><td></td><td></td><td></td><td></td><td>3.41</td><td colspan="2">6.33</td><td>5.42</td></tr>
<tr><td>F</td><td></td><td></td><td></td><td></td><td></td><td></td><td></td><td></td><td></td><td colspan="2">8.00</td><td></td></tr>
<tr><td></td><td></td><td></td><td></td><td></td><td></td><td></td><td></td><td></td><td>11.46</td><td></td><td></td><td>13.09</td></tr>
</table>

<table>
<tr><th rowspan="2">Layer \ Profile</th><th colspan="4">45</th><th colspan="4">46</th><th colspan="4">47</th></tr>
<tr><th>Tw</th><th>Vw</th><th>Ve</th><th>Te</th><th>Tw</th><th>Vw</th><th>Ve</th><th>Te</th><th>Ts</th><th>Vs</th><th>Vn</th><th>Tn</th></tr>
<tr><td>Ocean</td><td>7.51</td><td></td><td></td><td>6.72</td><td>7.92</td><td></td><td></td><td>7.89</td><td>8.28</td><td></td><td></td><td>8.28</td></tr>
<tr><td>A</td><td>.17</td><td></td><td></td><td>1.60</td><td></td><td></td><td></td><td></td><td></td><td></td><td></td><td>1.13</td></tr>
<tr><td>B</td><td></td><td></td><td></td><td></td><td></td><td></td><td></td><td></td><td></td><td></td><td></td><td></td></tr>
<tr><td>C</td><td></td><td></td><td>(4.33)</td><td>1.93</td><td>2.11</td><td colspan="2">3.23</td><td>.63</td><td></td><td colspan="2">4.14</td><td>3.78</td></tr>
<tr><td>D</td><td></td><td></td><td></td><td></td><td></td><td></td><td>(4.71)</td><td>1.23</td><td></td><td></td><td></td><td></td></tr>
<tr><td>E</td><td>2.19</td><td colspan="2">6.24</td><td>10.25</td><td>6.76</td><td colspan="2">6.32</td><td>8.45</td><td></td><td colspan="2">5.95</td><td></td></tr>
<tr><td>F</td><td></td><td colspan="2">7.90</td><td></td><td></td><td colspan="2">7.95</td><td></td><td></td><td></td><td></td><td></td></tr>
<tr><td></td><td>9.87</td><td></td><td></td><td>18.26</td><td>16.79</td><td></td><td></td><td>19.43</td><td></td><td></td><td></td><td></td></tr>
</table>

See Table 1 for identities of A, B, C, D, E.

F—velocity beneath major discontinuity, in this case identified by its velocity with the Mohorovicic discontinuity beneath continental areas.

TABLE 3.—ISLAND ARC

Profile	Puerto Rico and Vicinity																																	
	1				35				36		37				38				39				40				41			
Layer	Tw	Vw	Ve	Te	Tw	Vw	Ve	Te	T	V	Tw	Vw	Ve	Te	Tw	Vw	Ve	Te	Ts	Vs	Vn	Tn	Ts	Vs	Vn	Tn	Ts	Vs	Vn	Tn
Ocean	.03			.03	.02			.02	1.88		.01			.01	4.34				1.35			1.04	1.09			.82	.82			.71
A	.04	1.97		.41	.75	1.95		.37	.96	(2.01)	.25	1.96		.09	.62				.91	1.92		.48	.34			.46	.46			.52
B		2.56													1.47	3.14			1.86	2.95		.97	1.37	2.92		.60	.60	2.34		.63
C																														
D						5.23			1.41	(4.98)		5.00			.92	4.72				5.37				5.70				5.24		
E										(5.83)					2.12	5.67														
																7.01														

Profile	Lesser Antilles										South American Shelf									
	11				12				28		3		4		5				6	
Layer	Ts	Vs	Vn	Tn	Tw	Vw	Ve	Te	T	V	T	V	T	V	Tw	Vw	Ve	Te	T	V
Ocean	.08			.08	.09			.95	.04		1.36		.95		.08			.08	.08	
A	.13	1.76		.05	.11	1.71		.61	.06						.07	1.67		.36	.46	(1.84)
B	1.66	2.68		1.37	1.52	2.39		1.43	1.34	(2.33)	1.37	(2.32)	3.13	(2.32)	1.03	2.17		1.52	1.09	(2.19)
C	2.49	3.44 + 4.41		.62	2.56	3.25 + 4.29		1.51	3.05	(4.00)		(4.48)		(5.27)		5.72				(5.96)
D		6.31				5.97				(6.40)										
E																				

See Table 1 for identities of A, B, C, D.

E—higher-velocity layers, in some cases grading to crustal velocities of Tables 1 and 2.

previous crustal seismic investigations over island-arc structures: a single profile by J. B. Hersey in 1949 in the Puerto Rico trench and a series of eight profiles in 1951 across the Eastern Caribbean, interpreted by G. H. Sutton, both reported in Ewing and Worzel (1954) and Ewing and Heezen (1955); a series of three profiles by Raitt *et al.* (1955) across the Tonga island arc. Excellent discussions of the correlation of the geologic sequences and history of the Caribbean islands have been given by Schuchert (1935), Trechman (1935), Maxwell (1948), and Woodring (1954).

The present investigation consisted of taking 47 seismic-refraction profiles during a cruise of the research vessels ATLANTIS and CARYN of the Woods Hole Oceanographic Institution from January to March 1955. The seismic equipment and procedures were similar to those used on other cruises (Officer *et al.*, 1952), with some improvements. A large number of shots was fired to determine the refraction lines on each profile, so that possible vagaries in the interpretations of the geophysical data would be reduced to a minimum. Nearly 2000 seismic shots, using about 23 tons of TNT, were fired during the cruise. The longer profiles, such as 29, 30, 31, had about 80 shots per profile. The profiles were shot to give a seismic-reflection profile, not reported here, at the shorter ranges and a seismic-refraction profile at the longer ranges. Profile locations are given in Figure 1. A receiving station at each end of a profile indicates a reversed profile; a receiving station at only one end indicates an unreversed profile.

The data taken from the seismic-refraction records and the travel-time curves are not included here. They will be given in a data report from the Woods Hole Oceanographic Institution. For those profiles where resultant velocities or thicknesses are questionable, as on many unreversed profiles, the various possibilities are discussed. The resultant seismic velocities and thicknesses are given in Tables 1, 2, and 3 and presented in Plate 1.

The presentation and discussion of the geophysical results are divided into four parts: the exterior Atlantic basin; the interior Venezuelan basin including the Aves swell and the Grenada trough; the Puerto Rico trench and the area adjacent to it; the island arc of the Lesser Antilles and Puerto Rico. The latter two are the border region between the first two.

In Plate 1, the lower velocity layers have been grouped into three velocity ranges. The groupings were sensible from the distribution of measured velocities and layering in the tables. The first group from 1.6–2.0 km/sec. are unconsolidated sediments. The second group from 2.2–3.0 km/sec. are more consolidated sediments, which grade to lithified sedimentary rock. The third group from 3.2–4.2 km/sec. are more difficult to identify; the velocities are valid for either sedimentary or volcanic rock. Higher-velocity layers are labelled with their measured seismic velocities.

ACKNOWLEDGMENTS

This investigation was supported through contact NObsr 43270 with the Bureau of Ships, U. S. Navy, contract Nonr-1367(00) with the Office of Navel Research, U. S. Navy, and the Associates fund of the Woods Hole Oceanographic Institution. The explosives were supplied through the U. S. Navy. The assistance in many ways of the U. S. Naval stations at Hamilton, Bermuda, Port of Spain, Trinidad, and Roosevelt Roads, Puerto Rico, were important to the success of the expedition.

Mr. G. R. Hamilton and the staff of the Columbia University Geophysical Field Station at St. Davids, Bermuda, provided their usual excellent co-operation in making the facilities of the station available.

It is a pleasure to acknowledge the support and co-operation of the captains, S. Bray and A. Karlson, and the crews of the research vessels, ATLANTIS and CARYN. The other scientists involved in one or more phases of the geophysical program were Messrs. A. Bradshaw, W. Dunkle, G. Duys, J. Hahn, W. Moss, D. Owen, M. Rutstein, and R. Vaccaro, Drs. F. Richards and J. Ryther of the Woods Hole Oceanographic Institution, Mr. W. Hudson of the Western Electric Company, and Mr. S. Wardani of the Scripps Institution of Oceanography. The geophysical equipment for the ATLANTIS and the echo-sounding equipment for both ships were supplied by the Woods Hole Oceanographic Institution; the geophysical equipment for the CARYN was supplied by the Lamont Geological Observatory, Columbia University. Drs. J. B. Hersey and C. O'D. Iselin of the Woods Hole Oceanographic Institution and Prof. M. Ewing of Lamont Geological Observatory were helpful in making this expedition possible. In addition the authors wish to acknowledge the helpful criticisms and suggestions given by Prof. D. T. Griggs, H. H. Hess, and J. C. Maxwell who reviewed the paper before publication.

All four authors took part in the expedition and the preliminary analysis of the data. The final analysis, interpretations, and conclusions are those of the first two authors.

Geophysical Results

Atlantic Basin

The Atlantic basin profiles are presented in Plate 1. Profiles 16, 17, and 18 from Ewing *et al.* (1954) are north of the Puerto Rico trench on a line toward Bermuda; the profile from Hersey *et al.* (1952) is also north of the Puerto Rico trench at latitude 21°N.; the final two profiles, 17 and 18, are from this cruise and are discussed by Ewing *et al.* (in press). The first four profiles are in the Atlantic basin proper; the last two are in the border region from the Barbados ridge to the Atlantic. The last two show a shoaler depth of water and a greater thickness of sedimentary material; but the deeper crustal structure is the same for all the profiles.

The uniformity of crustal structure of the Atlantic sections in regions which have not been disturbed is one of their outstanding features. The depth to the major seismic discontinuity is about 10 km under the basin and deepens with approach to the continents. The velocity beneath this discontinuity is 8.0 km/sec. with small variation. The material above has an average thickness of 4–5 km and velocity 6.5 km/sec. Above this, under the basins, is a kilometer or less of primarily sedimentary material.

This major discontinuity beneath the ocean basins is identified as the *Mohorovicic discontinuity*, found 30–40 km beneath the continents, because (1) it is the major discontinuity, and (2) it is a velocity contrast to a value of 8.0 km/sec. The velocity beneath the Mohorovicic discontinuity is surprisingly similar under the ocean basin and continental areas; the average value under the continents is about 8.1 km/sec., but the average deviation from a value of 8.0–8.1 km/sec. for the earth is certainly not greater than .1 km/sec. Corresponding with the terminology used for the continents the material above the Mohorovicic discontinuity is called the *crust*. For the ocean basins this is the 4–5 km of 6.5 km/sec. material. The material above the crust of sedimentary or volcanic origin is identified where possible from its velocity, stratigraphy, and correlation with known geology.

Caribbean Basin—Venezuelan Basin, Aves Swell, Grenada Trough

The profiles from the interior basin are presented in Plate 1. Profile 29 is over the Grenada trough, profile 30 over the Aves swell, and profiles 31, 7, 32, and 33 over the Venezuelan basin. The locations are indicated in Figure 1. Only the longer profiles have been included; the data from the shorter profiles, 2, 8, 9, and 10, are given in Table 1 and are in agreement with the results presented in Plate 1 but do not measure the entire crustal section. Profiles 5 and 4 from G. H. Sutton's investigation (*in* Ewing and Worzel, 1954) have been included. They were also in the Venezuelan basin on a line from Aruba Island to Mona Island, near the left border of Figure 1. None of these profiles covers the central portion of the basin.

The similarities and differences of these sections compared with those in the Atlantic are immediately apparent. In general, the Caribbean sections resemble the Atlantic; the Caribbean is not a drowned continental area, but there are striking differences of crustal structure. (1) There is a major seismic discontinuity in the Caribbean, but the velocity beneath the discontinuity is significantly less than that in the Atlantic. This difference is apparent from a comparison of the Atlantic and Caribbean sections (Pl. 1); the Caribbean has an average value of 7.4 km/sec. beneath the discontinuity. Its depth is also somewhat greater—13 km, compared with 10 km. Because the velocity change is not to a value of 8.0–

8.1 km/sec., it shall not be referred to as the Mohorovicic discontinuity; that term is reserved for the universal velocity change beneath the continents and the ocean basins. It is the authors' opinion that the Caribbean is an altered oceanic section in the process of becoming an addition to the continent and that the Caribbean structure is temporary; it may be considered permanent only in the sense of permanency of an orogenic region. (2) The crustal velocities have a wider range in values on the low side than is found in the Atlantic. The velocities vary from about 6.0 km/sec. up to 6.6 km/sec. There is more variability in crustal structure and thickness than in the Atlantic; the average thickness of 5½ km is greater. Some profiles show a single velocity crust with variations from 7 km of 5.9 km/sec. on profile 5, 3 of 6.2 on 4, 5 of 6.3 on 7, 7 of 6.3 on 29, 3 of 6.6 on 33, to 6 of 6.6 on 31; others show two velocities such as 30 and 31 having 6.0 and 6.6 km/sec. (3) Above the crust and intimately associated with it in some cases is a greater thickness of material, averaging 4 km. The increase is due primarily to the addition of higher-velocity material, which is indicative of lithified sediments or igneous rocks or both.

The Caribbean, and presumably other interior basins associated with other orogenic regions of island arcs and deep-sea trenches, is not continental; nor is it oceanic, although it is more like the ocean-basin structure. One might expect that there should be a difference between the structure of the Atlantic and Caribbean; otherwise it would be difficult to understand how an island arc and deep-sea trench might develop between them. Also, from a consideration of the strength and thickness of material down to the depth of compensation it is difficult to imagine how an area as large as the Caribbean could be a drowned continent. With an understanding of this difference in structure lies one of the clues for the origin of such orogenic regions and the mechanisms involved in the formation of island arcs and deep-sea trenches.

Puerto Rico Trench and Adjacent Area

The island arc of the Lesser Antilles and Puerto Rico, with the associated Puerto Rico trench in the northern portion and Barbados ridge in the southern, form the border region between the Atlantic and Caribbean. The Puerto Rico trench and the Barbados ridge are not continuous features; the topographic extension of the axis of the ridge is inside that of the trench, *i.e.*, between the axis of the trench and the axis of the Lesser Antilles. The Puerto Rico trench has a maximum depth of about 4400 fathoms north of Puerto Rico, follows the trend of the island arc to the southeast at diminishing depth, and gradually disappears. The results of the profiles in the trench and adjacent to it are given in Plate 1. Profile 46 is in the deeper portion of the trench near its northern boundary. Profiles 45 and 44 are also in the trench, farther east. Profiles 42 and 43 are in the region south of the trench but still in deep water north of the submarine slope from the island arc.

The crustal structure of the trench profiles is similar to that for the Atlantic. The major seismic discontinuity shows a change to a velocity of 8.0 km/sec. The crustal velocity is 6.3 km/sec., a little lower than the average of 6.5 km/sec. for the Atlantic, but from this sample not significantly lower. There is a thickening of the crust, proceeding into the deeper part of the trench, from 4 km to 7 km.

The thickness of sedimentary and igneous rocks is about 2 km, and on profiles 44 and 46 there is no measurable thickness of unconsolidated sediment. However, profile 47 across the deeper portion of the trench shows the higher-velocity horizons dropping down from the north toward the center of the trench by what appear to be, from the seismic results, a series of normal faults. The ocean bottom remains nearly flat along this profile. The sediment thickens to 1 km, and the sedimentary and igneous rock layers thicken to 3½ km at the southern end of profile 47.

The adjacent profiles to the south, 43 and 42, show a different structure. Profile 42 unfortunately was shot over a ridge with observed structural complications; a lower horizon of 5.5 km/sec. was observed. Profile 43 was a long profile and showed no break from the 5.5 km/sec. line on either leg of the reversed profile. A minimum thickness calculation gives 8 km of 5.5 km/sec. material, as indicated in the Puerto Rico trench section (Pl. 1). Such minimum thickness calculations should always be held in doubt; for although the size of explosives and receiving techniques used measured seismic discontinuities at this depth in adjacent deep-water locations, there may be complications beneath this section which do not allow a detectable signal to be returned.

Island Arc

All the island-arc profiles are included in Plate 1. Many are too short to measure a complete crustal section, and of the five longer profiles four are not reversed, and three have possible structural complications. The resultant picture is not complete, but several features stand out. Profiles 35 and 37 are south and east of Puerto Rico. Profile 36 is in an extension of the Virgin Islands trough at a depth of 1000 fathoms, and profile 38 is in the deeper central portion of the trough at about 2000 fathoms. Profiles 39, 40, and 41 are short profiles, because of the structural changes between Saba and Sombrero islands. Profiles 11 and 12 are short profiles off the island of St. Lucia. Profile 28 is a long unreversed profile along the trend of the Grenadine Islands. Also included are profile 25 from Ewing *et al.* (in press), a long unreversed profile on the Trinidad shelf, and profile 13, from G. H. Sutton (*in* Ewing and Worzel, 1954) a long unreversed profile in shallow water northeast of Puerto Rico.

Consider these seismic sections from the top of the column to the bottom. First, there is a variable amount of unconsolidated to consolidated sediments, velocities 1.6 to 3.0 km/sec. For those profiles in the vicinity of the Virgin Islands trough the thickness increases regularly with depth from profiles 35 and 37 to 39, 40, 41 and 36 to 38; the deeper profiles have the thicker sediments, as might be expected for transportation eventually toward the deeper basins. The source area is the near-by islands. On profile Su 13 an additional thickness of 1.8 km of 3.8 km/sec. material, shown by double crosshatching on Plate 1, is measured. This entire sequence is correlated from the land geology on Puerto Rico (Meyerhoff, 1933) with the Tertiary to recent coastal-plain development of limestones and shales with interspersed bioherms built out north and south from the Cretaceous platform of Puerto Rico. The development of this coastal plain out from Puerto Rico, which is indicated by the results of Su 13, is better seen on the profiles off the south coast and slope of Puerto Rico shown in Plate 1. For the profiles along the Lesser Antilles arc—39, 40, 41, 11, 12, and 28—the upper layers of 1.6 to 3.0 km/sec. are considered a combination of volcanic debris, material eroded from the near-by volcanoes and perhaps some recent pyroclastics, and reef material built out from the volcanic platform.

Below this is a large thickness of higher-velocity material. The velocities have been divided into two groups, one shown by crosshatching with velocities from 3.2 to 4.2 km/sec. and the other of higher velocities from 4.7 to 5.8 km/sec. These velocities are characteristic of many types of rocks; the only general statement that can be made is that they are too high for loose sediments and too low for the material generally associated with an oceanic crust. Velocities from 3.2 to 4.2 km/sec. would be appropriate for extrusive igneous or sedimentary rocks, and velocities from 4.7 to 5.8 km/sec. for hard limestones, intrusive igneous, or metamorphosed rocks. For the profiles along the Lesser Antilles the writers interpret this material as the igneous platform there. For those profiles off St. Lucia, 11 and 12, and the Grenadine Islands, 28, along the southern portion of the Lesser Antilles, the material, with velocities of 3.9, 4.1, and 4.0 km/sec., indicates primarily extrusive igneous rock. For those profiles along the northern and older portion of the Lesser Antilles, 39, 40, and 41, the velocity of material immediately beneath the sediments has an appreciably higher value —5.1, 5.6, 5.7, and 5.2 km/sec.—and indicates that the igneous platform there has been appreciably intruded during a later stage of development following the initial eruptive stage.

For the profiles near Puerto Rico and the Virgin Islands—35, 37, Su 13, 36, and 38—the material beneath the sediments has a range of velocity from 4.7 to 5.8 km/sec. From the land geology of Puerto Rico (Meyerhoff, 1933), this material is interpreted as the Cretaceous basement of folded shales, tuffs, and agglomerates, all of which have been severely intruded. The higher velocities in this area approach that associated with crustal material, and the distinction between the crust and the overlying material is not as pronounced here as it is in the rest of the Eastern Caribbean. The writers interpret this as the eastward development of the Greater Antilles orogenic belt and believe that through the processes associated with that development, particularly metamorphism and extensive igneous intrusion, the clear-cut distinction between crustal and overlying material observed elsewhere in the Eastern Caribbean has been diminished. Although a distinction can be made from land geology between the Puerto Rico-Virgin Islands area of the Greater Antilles and the volcanic islands of the Lesser Antilles, this distinction is not evident in the deeper structure of the northwestern portion of the Lesser Antilles, as evidenced by the results of profiles 39, 40, and 41.

Crustal velocities are measured only on profile 38 in the deeper portion of the Virgin Islands trough, profile 25 north of Trinidad, and profiles 11, 12, and 28 of the Lesser Antilles. Crustal velocities are reached at a moderately shallow depth of about 4 km on profiles 11, 12, and 28, compared with 6½ km for the Atlantic basin, 7½ km for the Venezuelan basin, and 9 km for the Puerto Rico trench. The volcanics rest on material of crustal velocity which is above the depth at which it is normally found in an oceanic section. This material has been raised at least partially by the activity associated with the vulcanism and perhaps also by deformation contemporaneous with or prior to the vulcanism.

Under the Aves swell the seismic structure is similar to that described here for the Lesser Antilles, although the development has been less vertical and more horizontal. Material of crustal velocity has been raised above its normal depth and is overlain by material whose velocity is characteristic of extrusive igneous rocks; the topographic ridge is formed by a combination of the volcanics and raised crust. A structure cross section over the Aves swell is shown by Ewing *et al.* (in press).

This set of island-arc and trench profiles shows that the crust is raised under the island arc and depressed beneath the trench. The crust tends to follow the topography. This conclusion is strictly true only for those features in the first stage of development, such as the Lesser Antilles and the Puerto Rico trench. The Lesser Antilles development has been affected appreciably by igneous activity and probably by deformation producing uplift of the arc and depression of the trench. The Puerto Rico area of the Greater Antilles arc has been through one period of orogenesis and is in what might be called a second stage of development; the resultant structure is more complicated and in general thicker. The distinction between the crust and overlying material here is not as pronounced as it is in the younger islands of the Lesser Antilles.

INTERPRETATION OF GRAVITY MEASUREMENTS IN TERMS OF SEISMIC RESULTS

As is well known from the measurements of Vening Meinesz (1948), there is a large negative gravity anomaly associated with the deep-sea trenches and a positive anomaly associated with the adjacent island arcs. The axis of the negative anomaly is offset from the axis of the trench toward the island arc. Gravity measurements from various submarine cruises over the Caribbean are summarized by Vening Meinesz (1948), Hess (1938), and Ewing and Worzel (1954). Two simple structures have been hypothesized to explain these anomalies. One hypothesis, advanced by Vening Meinesz (1930; 1948), and Vening Meinesz *et al.* (1934), involves a plastic buckling of the crust which forms a large downbulge of lighter more sialic material into a heavier more simatic substratum. A presumed aftereffect is the generation of a convective overturn in the adjacent substratum caused by the higher radioactive heat generation of the downbuckled material; this overturn has such structural effects as the formation of deep interior basins. This hypothesis has been extended and ramified by Hess (1938) and Griggs (1939). The other hypothesis, advanced by Gunn (1936; 1937; 1947; 1949), involves through over-all compression a bending of the crust with movement along a major fracture zone, so that the lighter continental side moves up and the heavier oceanic side down. This sequence is presumed to be altered in time through continued erosion of the raised portion to fill the lowered portion.

The seismic results do not agree in detail with either hypothesis, but in general they agree with the geometry of Gunn's hypothesis and logical ramifications of it. The crust is raised above its normal level under the volcanic island arc and lowered beneath its normal level under the trench. There is a slight increase in crustal thickness under the trench to a value of 7 to 8 km, compared with 3 to 4 km under the ridge north of the trench. It is important to state here, to avoid possible confusion, that the seismic results measure only a relatively thin section of the earth of the order of 10 to 20 km beneath the ocean bottom; they show that no large downbuckle is measured in the oceanic crust, which itself is relatively thin under the normal ocean basin. They do not preclude the Vening Meinesz hypothesis of convection cells at greater depths.

The writers conclude that Gunn's hypothesis is the primary explanation of gravity anomalies over the trenches and island arcs. Before these seismic investigations Ewing and Worzel (1954) had come to much the same conclusion from an interpretation of gravity data. They demonstrated that the gravity anomalies could be as well explained by a smaller thickness of lighter sedimentary material near the ocean bottom as by a large downbuckle of crustal material at greater depth. On profile 46, the deepest trench profile, near the northern edge of the trench, no unconsolidated sediment was measured. A small thickness of material whose velocity is characteristic of sedimentary and igneous rock was observed, but from profile 47 across the trench this material and an overlying sediment thicken appreciably toward the central and southern portion of the trench. The effect of the large thickness of 5.5 km/sec. material measured on profiles 42 and 43 between the trench and the arc is unknown but may contribute appreciably to the negative anomaly.

Geological and Geophysical Identification of Atlantic and Caribbean Crust

Certain conclusions can be reached concerning the composition of the crust under the exterior (Atlantic) and the interior (Caribbean) regions from an identification of the measured seismic velocities with types of crustal material. An average for the Atlantic and Caribbean seismic columns is given in Figure 2. The Atlantic has a small thickness of sediment, probably not entirely unconsolidated sediment as shown. This is underlain by a 4–5 km crust with a velocity of 6.5 km/sec. and the Mohorovicic discontinuity below which is a velocity of 8.0 km/sec. The 6.5 km/sec. velocity is characteristic of basaltic material and the 8.0 km/sec. of peridotitic material. This is in agreement with the conclusions drawn from the igneous petrology of oceanic islands (Hess, 1954; Turner and Verhoogen, 1951); there the evidence also points to a crust of basaltic material underlain by peridotitic material.

The Caribbean has a somewhat different seismic structure. It has an increased, 4 km, section of sediment and sedimentary and igneous rocks. It is underlain by a thicker crust with velocities varying from about 6.1 to 6.5 km/sec. and a major discontinuity below which is found a velocity of 7.4 km/sec. The 6.1 km/sec. velocity is intermediate between that for the more basic and the more acidic rocks and would be characteristic of andesitic material. This again is in agreement with the petrographic evidence. The igneous rocks of the island arcs are andesites and diorites (Turner and Verhoogen, 1951), not olivine basalts. This petrographic difference between the island arcs and the oceanic islands led to the concept of the andesite line (Marshall, 1912), which circumscribes the Pacific and divides areas characteristically of andesites on the interior from areas of olivine basalts on the exterior. The same difference is found for the Atlantic; the igneous rocks of the Lesser Antilles where exposed are generally diorites and andesites (Schuchert, 1935; Christman, 1953). The andesite line is still considered by some to be the dividing line between continents and oceans, but this is not the case. It is a dividing line between an exterior region of oceanic structure and an interior orogenic region of Caribbean structure; the Caribbean structure is neither continental nor oceanic but resembles more the oceanic type. This conclusion could be expected from a consideration of gravitational equilibrium. Many of these interior regions, such as the Caribbean, are broad basins with depths of water only slightly less than that of the exterior ocean basins. Such broad areas must be in gravitational equilibrium; they cannot be supported by the strength of the crust. Therefore, they cannot be drowned continental areas and must resemble oceanic areas at least to the degree that the total mass to the depth of compensation—*i.e.*, to the depth of superposition of equal density and pressure surfaces—is the same as that beneath an ocean basin.

The identification of the 7.4 km/sec. material is difficult. It is an uncommon velocity to observe in crustal refraction profiles, probably because of the petrologic fact that rocks between olivine basalts and peridotites are uncommon. Four possibilities are suggested: (1) It is a material whose chemical composition is intermediate between an olivine basalt and a peridotite. (2) It is a physical intermixture of 6.5 and 8.0 km/sec. material; each retains its individual identity more or less, but the whole has an average velocity. (3) It is a peridotitic material in a different phase or crystalline state, which results in a lowered seismic velocity. (4) It is a partially serpentinized peridotitic material, which also results in a lowered velocity. There is a suggestion of a pattern for this lower-velocity media over the Caribbean which, if true, should help in its identification. Profiles toward the margins of the Venezuelan basin—7, 31, 33, and Su 4—have lower velocities (7.3, 7.4, 7.2, and 7.2 km/sec.) than the profiles toward the central portion (32 and Su 5 with 7.5 and 7.7 km/sec.).

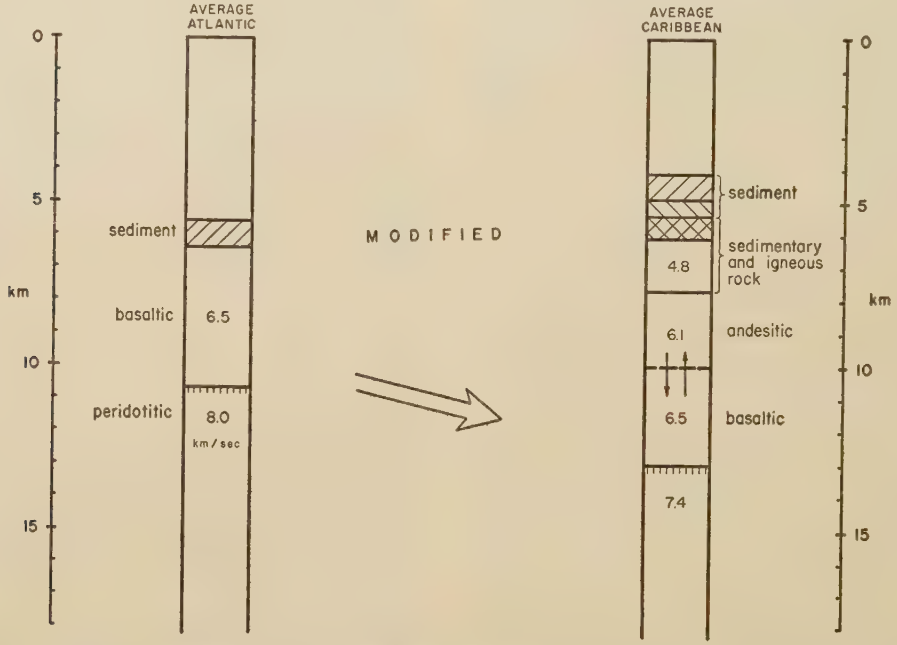

FIGURE 2.—AVERAGE SEISMIC SECTIONS FOR THE ATLANTIC AND VENEZUELAN BASINS WITH INFERRED GEOLOGIC IDENTIFICATIONS

Other more or less isolated instances of measurements of velocities around 7.4 km/sec. have occurred. J. I. Ewing (unpublished) obtained velocities like this for his deepest seismic layer in the Norwegian basin between Norway and Greenland. Bentley and Worzel (1956) found the same under the continental rise south of the Grand Banks off Newfoundland. Officer *et al.* (1952) reported a velocity of 7.2 km/sec. under the Bermuda rise south and southeast of Bermuda. Under the Bermuda rise, there seems to have been mixing of the crustal and subcrustal material, probably through intrusive activity associated with the Bermuda volcanoes. Out from Bermuda 400–500 km, on the two lines of profiles made, the normal layering of a crust of 6.6 km/sec. overlying 8.0 km/sec. is obtained, but closer in on the Bermuda rise there is the single velocity of 7.2 km/sec.

More pertinent to this examination are the results that Raitt *et al.* (1955) obtained in the vicinity of the Tonga trench. On the Pacific side of the Tonga trench they measured a normal oceanic crust with a thickness of 4½ km and a velocity of 6.5 km/sec., underlain by the Mohorovicic discontinuity at a depth of 12 km with a subcrustal velocity of 8.2 km/sec. Under the trench the crust was 8 km thick with a velocity of 6.5 km/sec., underlian by the Mohorovicic discontinuity with a subcrustal velocity of 8.1 km/sec. Under the Tofua trough on the Tonga Islands side of the trench a crustal layer of 5 km thickness with a velocity of 7.0 km/sec., underlain by a major discontinuity at a depth of 12 km to a velocity of 7.6 km/sec., was measured. These results are remarkably similar to those presented here for the corresponding areas of the Atlantic basin, Puerto Rico trench, and Antilles arc and Venezuelan basin.

The boundary between the Atlantic and Caribbean types is drawn between the island arc and the trench. The seismic results for the Puerto Rico trench identify it with the exterior Atlantic basin; those for the island arc identify it with the interior Caribbean basin.

STRUCTURE CROSS SECTIONS

Plate 1 also shows a series of structure cross sections derived from the seismic-refraction profiles. The first three are across local features, and the fourth is a long north-south section from South America across the Venezuelan basin, Puerto Rico area, and Puerto Rico trench out to the Atlantic. The vertical exaggeration on all four is the same; the scale of the first three is double that of the fourth.

Section A is across the Virgin Islands trough separating St. Croix to the south from the Virgin Islands to the north. Profiles A, B, and C from Worzel and Ewing (1948) measured a moderately high-velocity basement at a moderate depth off the north and south shores of St. Thomas. This correlates with the intruded agglomerates and tuffs of the island. Farther seaward this horizon drops off in depth. Under profile 1 is an undetermined thickness of sediment. Profile 38 is in the Virgin Islands trough and gave a good determination of the trough structure. The higher-velocity horizons dip upward steeply on the slope up to St. Croix. From this data alone it is not possible to discern whether the Virgin Islands trough is a graben or simply a gap in the island-arc chain.

Section B is across the northern end of the Lesser Antilles. To the south of the section is Saba bank. Directly to the north-west of the northern end of the section is the island of Sombrero, which is part of the outer and older line of limestone-capped volcanoes. This line extends down from Sombrero to Anguilla, St. Martin, Barbuda, Antigua, Grande Terre, and Marie Galente (Schuchert, 1935; Davis, 1926). To the southeast of the central portion of the section are Saba and St. Kitts, part of the inner and younger line of volcanoes. This line extends down from Saba and St. Kitts to Montserrat, Basse Terre, Dominica, Martinique, St. Lucia, St. Vincent, the Grenadine Islands, and Grenada. The structure cross section shows the subsurface extension of the Saba-St. Kitts ridge. This extension is indicated in the surface topography but is more pronounced across the buried ridge itself.

Section C is along the line of profiles 33, 34, and 35 from the Muertos trench up the south slope of Puerto Rico. A rather large thickness of sedimentary rock above the high-velocity (5.1 km/sec.) basement is measured under the slope to deep water off Puerto Rico. This thick sediment correlates with the Miocene and Oligocene sediments of the south coast of Puerto Rico, and the 5.1 km/sec. basement correlates with the folded Cretaceous shales and igneous rocks of Puerto Rico (Meyerhoff, 1933). From this correlation and the known geologic history of Puerto Rico the writers conclude that this entire sequence of sediment is primarily Tertiary in age. Off the east coast of the United States a larger thickness of sediments of Atlantic Coastal Plain age is found beneath the corresponding geographic location of the continental slope and continental rise (Officer and Ewing, 1954). This type of development probably exists for many other localities where the adjacent land mass has remained high for a sufficiently long time; it seems likely that this process is one of the more important ones in the continued outward growth of the continental land-mass areas.

Section D is a long north-south section across the Venezuelan basin and the border region of Puerto Rico and the Puerto Rico trench to the Atlantic. The differences between the Atlantic and Venezuelan structures are apparent. The crust and overlying sediments and volcanics in the Venezuelan basin are thicker, and their velocities are more variable than in the Atlantic; the velocity beneath the lowest horizon has an average value of 7.4 km/sec., compared with 8.0 km/sec. Both the upper and lower boundaries of the Atlantic basin crust can be observed at progressively lower depths from the Outer ridge into the Puerto Rico trench; the greatest decrease occurs under the slope on the northern side of the trench. Off the south of Puerto Rico is the Tertiary sedimentary development, and off the north a similar development is indicated, although it is not so well defined from the existing seismic profiles. Under Puerto Rico and the area north of it down to the trench, the deeper structure is not as well defined as elsewhere; only material of velocity between 5.3 and 5.8 km/sec. was observed.

Origin of the Venezuelan Basin

Up to this point this paper has been concerned primarily with the presentation of the geophysical data on the Venezuelan basin, the island arc, the Puerto Rico trench, and the Atlantic basin; the correlation of this data with other seismic and gravimetric information; and the geologic identification of the seismic results where possible. The remainder of this paper is speculative; it is a guess, primarily from this recent data, as to the possible origin and development of the island-arc, deep-sea trench, and interior basin areas of the Eastern Caribbean. It is realized that geologic speculations can often be a pitfall and ultimately of dubious value; however, the writers believe that the data point to some interesting deductions which are consistent within themselves and in accord with some of the ideas held by others on the origin and development of an area such as this.

From the several geophysical investigations of crustal structure two general types have been recognized: (1) the continental areas, which have a thickness of 30 to 40 km to the Mohorovicic discontinuity, generally thicker under mountain ranges, and a variable seismic-velocity structure to the Mohorovicic discontinuity; (2) the ocean-basin areas which have a crustal thickness of 5 km of rather uniform seismic-velocity composition and a depth to the Mohorovicic discontinuity of 10 km below sea level. The Venezuelan basin has a composition different from either of these. The crustal structure of the Venezuelan basin should not be considered as a general type in the sense of the first two. The Venezuelan basin is part of the active region of the Eastern Caribbean, and the writers believe that its present crustal structure was originally developed from one of the first two and is perhaps in the process of being altered from one to the other.

The Venezuelan basin probably did not develop from a continental area. For a former continental mass to be stable gravitationally at the depths of the Venezuelan basin, about 2600 fathoms, as such a large block would be, there must have been a large change in the mass-per-unit column down to the depth of compensation. This might have occurred through horizontal flow of material at depth or volume changes from chemical processes or through some other mechanism, but it does not seem possible for such a large change to take place without the occurrence of resultant observable subsidiary effects. This deduction is supported by the observation that throughout geologic time the trend has been toward growth of the continents, not diminution (Lawson, 1932; Wilson, 1949).

The alteration from an oceanic crust would not require an appreciable change in mass. Several mechanisms seem possible, each related for verification to the identification of the 7.4 km/sec. material. (1) There may be a rise in the isotherms under the Venezuelan basin. This basin has a thick cover, 4 km, of sediment and sedimentary and igneous material which acts as a blanket over the crust and could produce a rise in the isotherms; in addition, the material of 4 km thickness may be more radioactive than the crust and give a further rise in the isotherms. This change in the isotherms might cause a shift in the equilibrium of the basaltic and peridotitic materials and create a continued alteration of these materials with perhaps some contamination from above. The result would be a crust of composition variable from the differentiate of andesitic material to the original basaltic material and of variable thickness; the Mohorovicic discontinuity would represent a different contrast in velocity and probably be shifted in depth. All these features are observed. However, it does not seem likely that the rise in isotherms, if it occurs at all, would be sufficient to cause the changes discussed above.

(2) There may have been mixing or intermixture of the 6.5 and 8.0 km/sec. material through igneous activity or physical forces. This would explain the development of a 7.4 km/sec. material, but such a process by itself could only reduce the thickness of the crust and would not explain the observed variability of crustal velocity and thickness.

(3) There may have been some sort of phase change of the submohorovicic material, as suggested by F. Press (personal communication). He mentioned the probable existence of a low-velocity section in the upper part of the mantle under the continents (Gutenberg, 1955) and stated that a comparison of the seismic-refraction results under the ocean basins with the earthquake surface wave results—the former measuring the material immediately below the Mohorovicic discontinuity and the latter a larger thickness of the mantle—shows slightly higher velocities for the refraction measurements; thus a similar low-velocity section may exist there. If there were a change in the conditions for existence of this low-velocity section, for example through a rise in the isotherms, the low velocity might occur immediately below the Mohorovicic discontinuity. This mechanism does not explain the variability within the crust, and it implies that the combination of increase of pressure and temperature with depth in the mantle beneath the continents, capable of causing a low-velocity section there, is such that a similar decrease under the ocean basins at different pressures and temperatures will produce a decrease there.

(4) Partial serpentinization of the submohorovicic and crustal material may have occurred. This suggestion has been advanced by Hess (1954; 1955) as a possible epeirogenic mechanism under the oceanic areas. Serpentinization would decrease the seismic velocity in agreement with the observations. The question is raised how this process by itself can explain all the apparent alterations observed for the crustal sections of the Venezuelan basin.

(5) The entire Caribbean area may have been extensively intruded by large bodies of primary basalt magma which differentiated deep in the mantle and migrated upward because of a density differential. This suggestion has been advanced by Ewing *et al.* (in press). This process may have contaminated the upper portion of the mantle with intrusives of material with crustal velocities and produced the observed decrease in velocity. It may also have caused crustal thickening and contamination of the upper portion of the crust with the more siliceous differentiates of the primary magma; this process explains the decrease of crustal velocities observed there. The continued ascent of the more volatile constituents of the magma could produce the extensive volcanic activity which has resulted in the widespread occurrence of material whose velocity is characteristic of extrusive igneous rocks.

Of the five possibilities the last seems to explain more of the features observed on the seismic-refraction profiles than the others. The emphasis here, however, has been on attempting to find a possible physical process which would explain the observed seismic results and not necessarily on discussing the probability of occurrence of the various possible processes.

An interesting demonstration can be given to show that the mass-per-unit column for the Atlantic, including the ocean, is approximately equal to that for the Venezuelan basin. This must be the case, for such broad areas as these can only have a small amount of their support from the strength of the crust and must be effectively in isostatic balance.

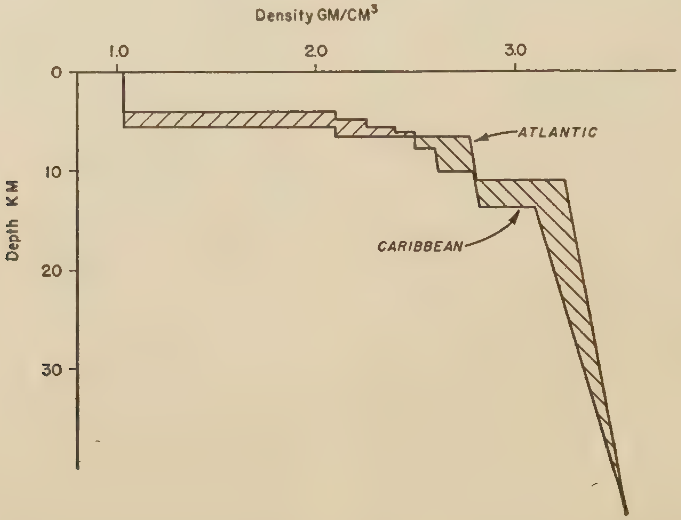

Figure 3.—Density Distribution for the Atlantic and Caribbean Basins Inferred from the Seismic Velocities

The density distributions for the two basins are derived empirically from the seismic velocities and the rock identifications. Usually the density increases with velocity, particularly through an orderly suite of related rocks (*see* Birch *et al.*, 1942); this is true because, although in the formula for velocity

$$v = \left(\frac{k + \frac{4}{3}\mu}{\rho}\right)^{1/2}$$

the density, ρ, is inversely proportional to velocity, the bulk modulus, k, and rigidity, μ, increase more rapidly than density, so that the resultant effect is an increase in velocity with increase in density. This relation holds in general, but exceptions can exist. In the present case if the difference between the 8.0 and 7.4 km/sec. material represented a phase change, the decrease in velocity would not necessarily imply a decrease in density.

The derived density distribution for the Venezuelan and Atlantic basins are sketched in Figure 3. The average depth of the Atlantic profiles is about 1½ km deeper than that of the Caribbean profiles. The Atlantic has 1 km of sediment whose density is taken to be around 2.1 gm/cm³ and is underlain by 4 km of basaltic material, density 2.8 to 2.9, which in turn is bounded by the Mohorovicic discontinuity and peridotitic material, density 3.2 to 3.3. The Caribbean has a thicker accumulation, 4 km, of sediment and sedimentary and igneous rocks. This is underlain by about 6 km of andesitic material, density 2.7 to 2.8, and basaltic material. The major discontinuity occurs at a lower depth and is a contrast to a lower velocity. A density of 3.1 to 3.2 is chosen for the 7.4 km/sec. material; gradually with depth this material is considered to approach the density of the submohorovicic material. The mass-per-unit column is the integral of density with respect to depth; thus, the difference in mass between the two is simply the difference between the two shaded areas and is approximately zero.

Origin and Development of an Island-Arc–Deep-Sea-Trench Sequence

The primary objective of this cruise was to determine the crustal structure of the Eastern Caribbean for the evidence it might give of the origin and development of such an orogenic region. The writers consider that there is a complementary relation between the origin of an island arc and deep-sea trench and the origin of the altered interior basin. An interior basin can be in various stages of development depending on its own past history and that of its associated island arcs and trenches. Similarly, along any orogenic belt the various portions are not in the same stage of development or necessarily strictly continuous one with the other. The Caribbean is a good example. The Greater Antilles forms two orogenic belts, one from Yucatan through Cuba, northern Hispaniola, Puerto Rico, and the Virgin Islands, and the other from Nicaragua through Jamaica and southern Hispaniola (Hess, 1938). The age along this belt becomes progressively younger to the east, and all of it has been through at least one stage of development. Farther east is the volcanic island arc of the Lesser Antilles, consisting essentially of an older and a younger line of volcanoes emerging from a raised crust. A distinction is made between the orogenic island arc and the volcanic island arc. Outside the arc is the Puerto Rico trench facing on both the older orogenic arc from Puerto Rico to Hispaniola and the younger volcanic arc of the Lesser Antilles. Along the middle portion of the Lesser Antilles, the Puerto Rico trench diminishes in depth toward the southeast and disappears; the Barbados ridge emerges with its axis between that of the trench and the island arc. Along the southern portion, the Lesser Antilles are fronted by the Barbados ridge with total thicknesses of deposited material of geosynclinal proportions extending out from South America. All along this sequence different stages of development are seen.

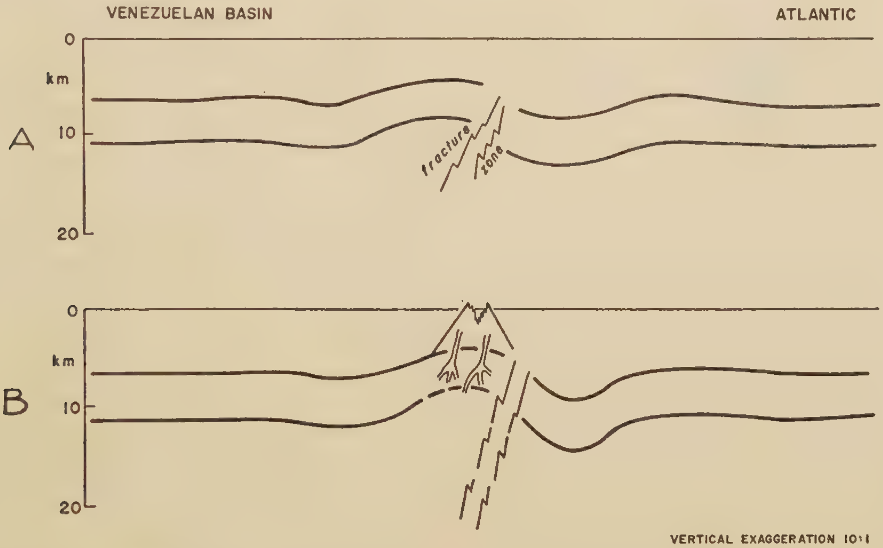

Figure 4.—Resultant Island-Arc–Trench Structure

A, Origin of an island arc and deep-sea trench through compression. B, Additional developments contemporaneous with the deformation.

Starting with adjoining Venezuelan and Atlantic basin structures, it is possible to deduce what border effects might develop. The seismic results have indicated that the crustal material is raised above its normal level beneath the island arc and depressed beneath the trench. As discussed above, the writers believe that a portion of this elevation has been the direct result of the ascent of a differentiate of lighter material from deep in the mantle. It also seems likely that in this border region there has been strictly structural deformation related directly to the changes that have occurred within the Venezuelan basin and creating a border effect between the altered Venezuelan basin and the undisturbed adjacent Atlantic basin.

Associated with the increased volume of crustal and related material in the Venezuelan basin there may be outward horizontal compression on its borders. As the compression increases, fracturing may occur along zones where rather abrupt changes in crustal properties occur. Along the boundary between the Atlantic and Venezuelan basins the fracturing would occur in such a manner that the lighter Caribbean crust would override the heavier Atlantic crust. The resultant configuration, resembling Figure 4*A*, would depend upon the proportions of deformation and movement along the fracture zone. This supposition is in agreement with observed seismic and topographic evidence; both infer that the structure is a raised island arc bordered on the Atlantic side by the depressed Puerto Rico trench. It can be argued further that the effect of compression of the Venezuelan basin against the South American continent would be the reverse of that for the Atlantic; the lighter South American continent would tend to override the heavier Venezuelan basin. This provides an explanation for the Los Rocques trench bordering the Venezuelan basin to the south.

During deformation and as a consequence of the deformational stresses an additional effect may take place, as indicated in Figure 4*B*. Along the raised island arc a relaxation of compression will develop in its upper portion. This relaxation of compression will encourage the upward movement of magma from depth. With the supposed alteration of the Venezuelan basin that has occurred it might be expected that the release of the more volatile constituents would be concentrated in such a zone and form a line of volcanoes; as observed, the Lesser Antilles is a chain of volcanic islands.

There is substantial evidence from earthquake seismology for the existence of the fracture zone between the island arc and deep-sea trench. It is the zone of major earthquakes and is well defined for the numerous Pacific island arcs, as well as for the Antilles island arc (Gutenberg and Richter, 1949). The earthquakes describe a zone which starts at the surface between the island arc and the trench and dips down under the island arc at approximately 45°.

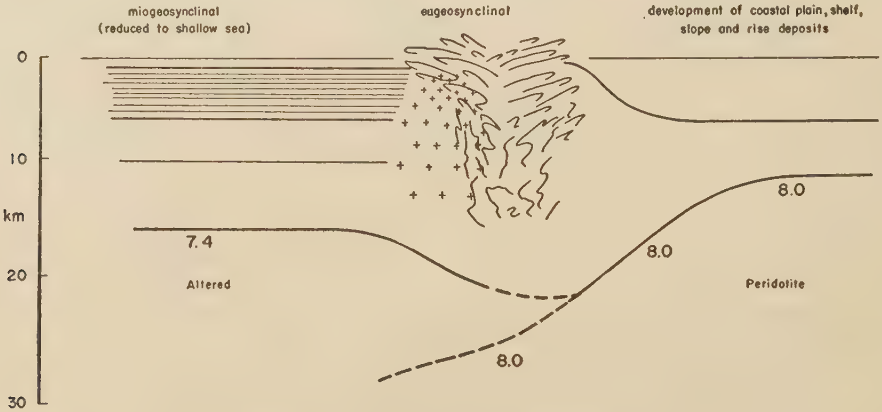

Figure 5.—Later Developments of Island-Arc–Trench Structure into an Addition to the Continents

The eugeosynclinal belt may include more than one period of trench–island arc and subsequent mountain building developments.

Later Developments

At present there is extensive igneous activity along the island arc gradually changing from a more extrusive stage in the younger parts to a more intrusive stage in the older. The volcanic islands have been severely eroded, and subsidence of the islands is evident (Davis, 1926). On the subsiding volcanoes lagoon limestones and reefs have been built up, as is well shown by the tilted bevelled-off island of Antigua, where a section of 8000–10,000 feet of Tertiary carbonate deposits overlying the volcanics can be seen (Schuchert, 1935). In addition there has been appreciable offshore deposition into deeper water with thicknesses up to 12,000–14,000 feet, as is shown by the results of the seismic profiles south of Puerto Rico (Pl. 1). The enclosed basin of the Virgin Islands trough appears to be a permanent resting place for sediments from the near-by islands with a present thickness of 7000 feet. For the Puerto Rico trench the sediments are very thin along the northern boundary but thicken up to about 10,000 feet toward the southern portion of the trench. Along this border region of the island-arc–deep-sea trench area there is ample evidence of extensive igneous activity and intense sedimentation. In the authors' opinion it is one of the more active geologic areas of today.

The island-arc–deep-sea trench area is at present out of isostatic equilibrium. There is a large negative anomaly across the trench and a smaller positive anomaly across the island arc. In time a period of readjustment might begin and lead to an orogeny and formation of a folded and thrust-faulted mountain system.

Complementary to this and probably extending over a longer period of time there would be continued alteration of the crust under the interior (Venezuelan) basin and continued sedimentation from the surrounding land masses through turbidity currents and other depositional mechanisms into the enclosed basin. Essentially flat-lying, structurally undisturbed beds would develop. The total thickness should be less than that for the border regions, and true eolian deposits should be found only at the top of the stratigraphic column. The continued alteration of the crust under the interior basin would produce epeirogenic movements through volume changes.

The suggestion is advanced that through such processes as this additions to the continents are made. The island arc and deep-sea trench with their subsequent orogenies form the eugeosynclinal belts (Kay, 1951), and the interior basin with its continued alteration and sedimentation forms the miogeosynclinal basin. The result might resemble what is illustrated in Figure 5; the final step is presumed to be the development of a coastal plain and continental-shelf, continental-slope, and continental-rise deposits as are found off the east coast of North America (Officer and Ewing, 1954), and off the Gulf coast (Weaver, 1955). The change between the addition to the continent and the ocean is now gradual and gradational.

References Cited

Bentley, C. R., and Worzel, J. L., 1956, Geophysical investigations in the emerged and submerged Atlantic coastal plain. Part X: Continental slope and continental rise south of the Grand Banks: Geol. Soc. America Bull., v. 67, p. 1–18

Birch, F., Schairer, J. F., and Spicer, H. C., 1942, Handbook of physical constants: Geol. Soc. America Special Paper 36, 325 p.

Christman, R. A., 1953, Geology of St. Bartholomew, St. Martin, and Anguilla, Lesser Antilles: Geol. Soc. America Bull., v. 64, p. 65–96

Davis, W. M., 1926, The Lesser Antilles: Am. Geog. Soc. Pub. no. 2, 200 p.

Ewing, J. I., Officer, C. B., Johnson, H. R., and Edwards, R. S., in press, Geophysical investigations in the Eastern Caribbean-Trinidad shelf, Tobago trough, Barbados ridge, Atlantic Ocean: Geol. Soc. America Bull.

Ewing, M., and Heezen, B. C., 1955, Puerto Rico trench topographic and geophysical data, p. 255–267, *in* Poldevaart, A., *Editor*, Crust of the earth: Geol. Soc. America Special Paper 62, 762 p.

Ewing, M., and Worzel, J. L., 1954, Gravity anomalies and structure of the West Indies. Part I: Geol. Soc. America Bull., v. 65, p. 165–173

Ewing, M., Sutton, G. H., and Officer, C. B., 1954, Seismic refraction measurements in the Atlantic ocean, Part VI, Typical deep stations, North America basin: Seismol. Soc. America Bull., v. 44, p. 21–38

Griggs, D. T., 1939, Theory of mountain building: Am. Jour. Sci., v. 237, p. 611–650

Gunn, R., 1936, On the origin of the continents and their motion: Jour. Franklin Inst., v. 222, p. 475–492

—— 1937, A quantitative study of mountain building on an unsymmetrical earth: Jour. Franklin Inst., v. 224, p. 19–53

—— 1947, Quantitative aspects of juxtaposed ocean deeps, mountain chains, and volcanic ranges: Geophysics, v. 12, p. 238–255

—— 1949, Isostasy extended: Jour. Geology, v. 57, p. 263–279

Gutenberg, B., 1955, Channel waves in the earth's crust: Geophysics, v. 20, p. 283–294

Gutenberg, B., and Richter, C. F., 1949, Seismicity of the earth: Princeton, N. J., Princeton Univ. Press, 273 p.

Hersey, J. B., Officer, C. B., Johnson, H. R., and Bergstrom, S., 1952, Seismic refraction observations north of the Brownson deep: Seismol. Soc. America Bull., v. 42, p. 291–306

Hess, H. H., 1938, Gravity anomalies and island arc structure with particular reference to the West Indies: Am. Philos. Soc. Proc., v. 79, p. 71–96

—— 1954, Geological hypotheses and the earth's crust under the oceans: Royal Soc. London Proc., A, v. 222, p. 341–348

—— 1955, Serpentines, orogeny, and epeirogeny, p. 391–407, *in* Poldervaart, A., *Editor*, Crust of the earth: Geol. Soc. America Special Paper 62, 762 p.

Kay, M., 1951, North American geosynclines: Geol. Soc. America Mem. 48, 143 p.

Lawson, A. C., 1932, Insular arcs, foredeeps, and geosynclinal seas of the Asiatic coast: Geol. Soc. America Bull., v. 43, p. 353–381

Marshall, P., 1912, Oceania, *in* Handbook of Regional Geology, v. 7, no. 2, 36 p.

Maxwell, J. C., 1948, Geology of Tobago: Geol. Soc. America Bull., v. 59, p. 801–854

Meyerhoff, H. A., 1933, Geology of Puerto Rico: Univ. Puerto Rico Mon. B, 306 p.

Officer, C. B., and Ewing, M., 1954, Geophysical investigations in the emerged and submerged Atlantic coastal plain. Part VII: Continental shelf, continental slope, and continental rise south of Nova Scotia: Geol. Soc. America Bull., v. 65, p. 653–670

Officer, C. B., Ewing, M., and Wuenschel, P. C., 1952, Seismic refraction measurements in the Atlantic ocean. Part IV: Bermuda, Bermuda rise, and Nares basin: Geol. Soc. America Bull., v. 63, p. 777–808

Raitt, R. W., Fisher, R. I., and Mason, R. G., 1955 Tonga trench, p. 237–254, *in* Poldewaart, A., *Editor*, Crust of the earth: Geol. Soc. America Special Paper 62, 762 p.

Schuchert, C., 1935, Historical geology of the Antillean-Caribbean region: N. Y., John Wiley & Sons, Inc., 767 p.

Trechman, C. T., 1935, Geology and fossils of Carriacou, West Indies: Geol. Mag., v. 72, p. 529–555

Turner, F. J., and Verhoogen, J., 1951, Igneous and metamorphic petrology: N. Y., McGraw-Hill Book Co., 602 p.

U. S. Hydrographic Office, 1939, Bathymetric chart of the Caribbean sea: H. O. Chart 5487

Vening Meinesz, F. A., 1930, Maritime gravity surveys in the Netherlands East Indies, tentative interpretation of the results: Kon. Med. Akad. v. Wetens Proc., v. 33, p. 566–577

—— 1948, Gravity expeditions at sea, 1923–1938, v. 4: Delft, Netherlands Geod. Comm., 233 p.

Vening Meinesz, F. A., Umbgrove, J. H. F., and Kuenen, Ph. H., 1934, Gravity expeditions at sea, 1923–1932, v. 2: Delft, Netherlands Geod. Comm., 208 p.

Weaver, P., 1955, Gulf of Mexico, p. 269–278, *in* Poldervaart, A., *Editor*, Crust of the earth: Geol. Soc. America Special Paper 62, 762 p.

Wilson, J. T., 1949, Origin of continents and Precambrian history: Royal Soc. Canada Trans., v. 43, p. 157–184

Woodring, W. P., 1954, Caribbean land and sea through the ages: Geol. Soc. America Bull., v. 65, p. 719–732

Worzel, J. L., and Ewing, M., 1948, Explosion sounds in shallow water, p. 1–53 *in* Ewing, M., Worzel, J. L., and Pekeris, C. L. Propagation of sound in the ocean: Geol. Soc. America Memoir 27, 205 p.

RICE INSTITUTE, HOUSTON, TEXAS, AND WOODS HOLE OCEANOGRAPHIC INSTITUTION, WOODS HOLE, MASSACHUSETTS; LAMONT GEOLOGICAL OBSERVATORY, PALISADES, NEW YORK; WOODS HOLE OCEANOGRAPHIC INSTITUTION, WOODS HOLE, MASSACHUSETTS; WOODS HOLE OCEANOGRAPHIC INSTITUTION, WOODS HOLE, MASSACHUSETTS

MANUSCRIPT RECEIVED BY THE SECRETARY OF THE SOCIETY, APRIL 16, 1956

WOODS HOLE OCEANOGRAPHIC INSTITUTION CONTRIBUTION NO. 839

LAMONT GEOLOGICAL OBSERVATORY CONTRIBUTION NO. 233

Contribution No. 843

Särtryck ur Tellus nr 1, 1957

Trade Cumulus Cloud Groups: Some Observations Suggesting a Mechanism of Their Origin[1]

By JOANNE STARR MALKUS. Woods Hole Oceanographic Institution

(Manuscript received June 18, 1956)

Abstract

On a recent field trip to the western Caribbean, temperature gradients in the surface layers of the trade-wind oceans were found and related to the presence of cumulus cloud groups. The cloud groups generally formed over and slightly downwind of warm spots which were several kilometers in extent along the wind and 0.1—0.3° C in amplitude. Clouds were not found in the absence of warm spots although warm spots were occasionally encountered without clouds.

Air circulations, similar to but weaker than those produced by heated land masses, are hypothesized to exist over oceanic warm spots and their magnitude is estimated from previous work on heated islands. Observed differences in low-level moisture structure between clear and cloudy areas may be interpreted in terms of such circulations and their evolution with time. Some suggestions are made concerning the life cycles of trade cumuli.

I. Introduction

Oceanic trade cumulus commonly appear in irregular groups about 10—50 km across separated by somewhat wider clear spaces. Cloud grouping and structure do not seem to vary from day to night. Early observations showed that individual trade cumuli do not have "roots" in thermals extending up from the sea surface, nor are they observed in regular patterns suggesting polygonal convection cells. In fact, these two possibilities of their origin are excluded because the air layer below cloud is actually slightly stable at all elevations above the first few meters.

Time-lapse motion pictures suggest that trade-wind clouds almost always form in groups, and that the groups themselves go through a life cycle, beginning their existence as a large number of small cloudlets, a considerable fraction of which may later attain the precipitation stage together. Isolated swelling cumulus or shower clouds are exceptional. In view of the probable importance of large precipitating cloud areas in the initiation of tropical storms and of the interaction of cloud elements with one another to form larger clouds, we have become concerned with the original formation of these groups. We wish to ask what processes are at work below cloud to permit large numbers of moist air parcels simultaneously to reach the condensation level in particular localities.

The base of trade-wind clouds averages about 650 meters, with extreme variations ranging between 300 and 1,000 m. The lowest four-fifths of this subcloud layer is well mixed, with a temperature lapse rate about 0.9 adiabatic and a very slow vertical decay of mixing ratio (about 10^{-8} cm^{-1} or less). The upper 100—200 m is usually more stable, with a mean potential temperature increase of 1° C and an order of magnitude increase in moisture lapse rate. The stable layer is more pronounced in the clear regions than in those topped by clouds, where it is often absent altogether. On the average in clear areas the top of the mixed layer is at about 85 % of the height of the lifting condensation level of the air composing it, while in cloudy areas the mixed region reaches to 95—100 % of the L.C.L. or 75 m higher. These figures suggest that the origin of trade cumulus groups is to be sought in factors producing weak convergences on the 10—50 km horizontal scale in the subcloud layer. Small variations in one or more sea surface properties such as roughness, radiative character, temperature, or evaporation might suffice to set up such circulations; in particular it seemed desirable to determine whether or not slight differences in sea surface temperature (below the sensitivity of standard oceanographic instruments) might not be common and perhaps associated with cloud groups.

---

[1] Contribution No. 843 from the Woods Hole Oceanographic Institution.

The latter suggestion arose from theoretical and observational studies of air flow over small heated islands, both in the tropics and in middle latitudes. In the sunny hours, islands in the trades are vigorous sources of cumulus, and in fact the cloud towers have often been used by pilots and mariners to locate an island when too far away to discern the land mass itself. The theory of flow over a heat source (Stern and Malkus, 1953) shows why these islands are such excellent producers of cumulus. Corresponding to each heated island may be derived an "equivalent mountain", its height depending directly upon the land temperature excess and inversely upon the stability of the undisturbed air, with a shape corresponding closely to that of the island temperature profile. This "mountain" builds up and decays diurnally. For islands in the trade stream, every degree (Centigrade) temperature excess adds about 500 m to the mountain's magnitude. The mountain itself, rather than being a solid obstacle, consists of a deeper turbulent mixed layer which has been thickened due to the added heat flux and the convergent circulation, so that the low-level streamlines crossing it are deformed upward corresponding to its amplitude and shape.

Thus over the oceans themselves, very slight surface temperature patchiness might be responsible for the initial formation of cloud groups. Since the top of the mixed layer falls short of the condensation level by 50—100 meters or less, island-sized warm spots exceeding the temperature of their surroundings by just a few tenths of a degree could give rise to "equivalent hills" high enough to permit the air in the subcloud layer to reach the height of its average condensation level, so that the moister eddies near its top attain saturation and appear as small cloudlets. The surrounding areas would be clear spaces in which compensatory subsidence occurs, similar to the clear subsidence rings observed around the islands (Malkus, 1955). Randomly distributed low hills of 10—50 km scale, giving rise to clouds clustered over and slightly downwind of them, would present a picture of cloud patterns similar to those photographed and mapped by the Wyman-Woodcock expedition to the trades (Fig. 1). It remained to determine whether adequate temperature gradients are present in the surface layers of the tropical oceans.

Recently an airborne instrument has been developed at the Woods Hole Oceanographic Institution which detects slight sea surface temperature differences. In April 1956, a short field trip to the western Caribbean was made, flying this instrument in the Institution's PBY airplane. The observations were made in such a manner that it was possible to relate sea surface thermal structure to cloud formations. In the few flights made to date, a remarkably clear relation between these patterns was observed. The first part of this paper describes the methods and results of the field work. Then some deductions are made concerning the convective air motions associated with surface thermal gradients of the sizes and magnitudes observed. These are used to interpret previously obtained data on the structure of clear and cloudy areas and to discuss the life cycles of trade cumulus clouds and cloud groups.

II. Observations of surface temperature anomalies and their relation to cloud groups

The airborne radiation thermometer is a device which measures the long wave-length radiation from the surface over which it is being flown. The detector looks through an optical system alternately at the surface and at a reference black body and compares the temperature of the two. The black body is main-

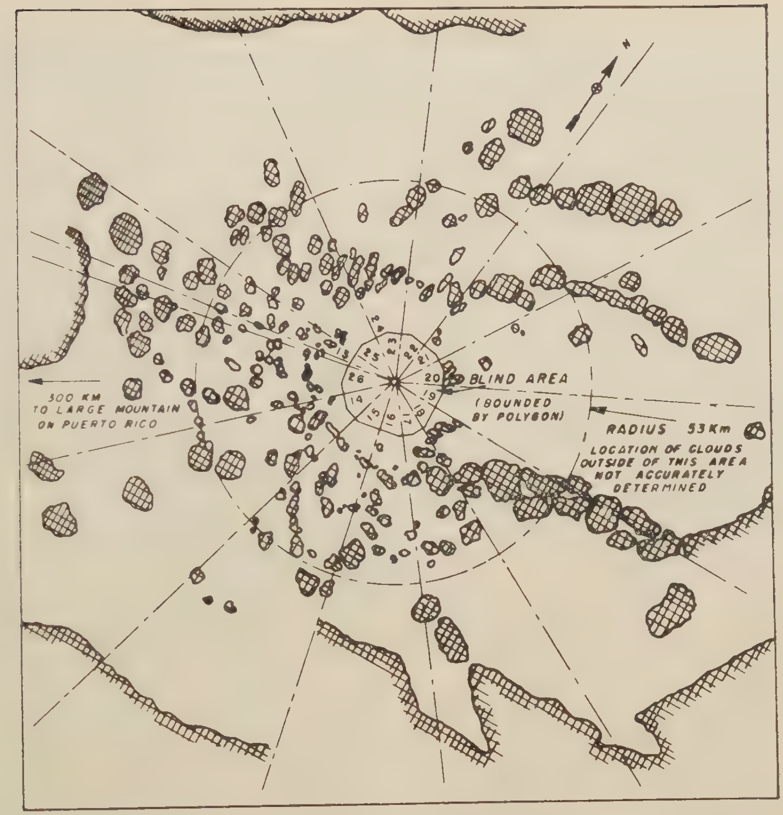

Fig. 1. Map made from cloud photographs showing a typical distribution of oceanic trade cumuli. Calculated from high altitude photographs Nos. 13—26 made by the Wyman-Woodcock Caribbean expedition. The radius of the dashed circle is 53 km; location of its center at 20°00′ N, 64°25′ W. The wind was east-southeast decreasing slightly with elevation. Note the rather irregular spacing of clear and cloudy areas. Only the medium and large clouds within the 53-km circle have been accurately located. The shaded areas are distant cloud banks.

tained at a temperature about five degrees higher than ambient in the aircraft. The instrument is calibrated so that the recorded signal is linearly proportional to the difference between the temperature of the surface and the constant temperature of the black body; at maximum sensitivity it resolves gradients of hundredths of a degree occurring over horizontal distances down to 50—100 m (when carried at the speed of the PBY). On the recent field trip, it was flown at 1,000 ft across the coastline of Jamaica (18° N, 77°30′ W) and neighboring small islands, and up- and downwind over the surrounding oceans. A small source of error arises from water vapor variations in the air column between the instrument and sea level; however, the column would have to possess sudden humidity gradients greater than five times the observed maxima to make this error larger than a few hundredths of a degree. It may be shown further that this error slightly minimizes the oceanic gradients detected. The best corroboration of the records presented here, however, lies in similar measurements obtained in the same area on the same days by the Research Vessel ATLANTIS, which was equipped with sensitive recording thermometers mounted near the surface and at several depths down to 80 ft.

On the aircraft flights, the locations of cloud formations were marked on the surface temperature records by hand punching a key from the blister as each cloud passed overhead and by a motion picture camera aimed vertically upward. Examination of the results shows that sea surface temperature differences from about 0.1—0.3° C were common on days with active cumulus convection. On days of light winds the gradients were often extremely sharp, a "step" up or down occupying less than 50 m in the horizontal, while with strong winds the edges appeared more diffuse, the same temperature change taking about 1 km. Both "warm spots" and "cold spots" were found, the sizes of which could often be determined from the records. Over the open sea these ranged from 4—20 km in extent along the direction of the wind. Larger scales probably also occurred, since frequently the aircraft crossed a gradient up or down without crossing any noticeable one in the opposite sense before the run had to be ended. Insufficient cross-wind flying was done to determine scales in that direction.

The association of thermal and cloud patterns was surprisingly good and may be summarized as follows: For four flights near Jamaica (10—60 miles offshore)

1) Clouds when present were always associated with warm spots (not cold spots) although they frequently were best developed at the downwind boundary of a warm spot where the temperature gradient was steepest.

2) Cloud groups were generally displaced slightly downwind relative to warm spots, as would be the case over a hill or island.

3) Groups of clouds were generally associated with warm spots, individual clouds being of a much smaller scale. Some individual clouds could be detected on the temperature records since their shadows occasionally produced cloud-sized cool spots as much as a few hundredths of a degree in amplitude.

4) Warm spots were sometimes found without any clouds. In the majority of those cases over the open sea, however, the temperature anomalies did not exceed about one-half the amplitude of those with which clouds were associated on a given day. Warm spots without clouds were also occasionally encountered within the subsidence zone surrounding Jamaica.

5) Oceanic cloud groups were not found in the absence of temperature anomalies.

The temperature records were quite reproducible: on return flights across the "step" zone the same gradients in the opposite sense were invariably found although on one occasion successive crossings made it appear that both the step and associated cloud group were

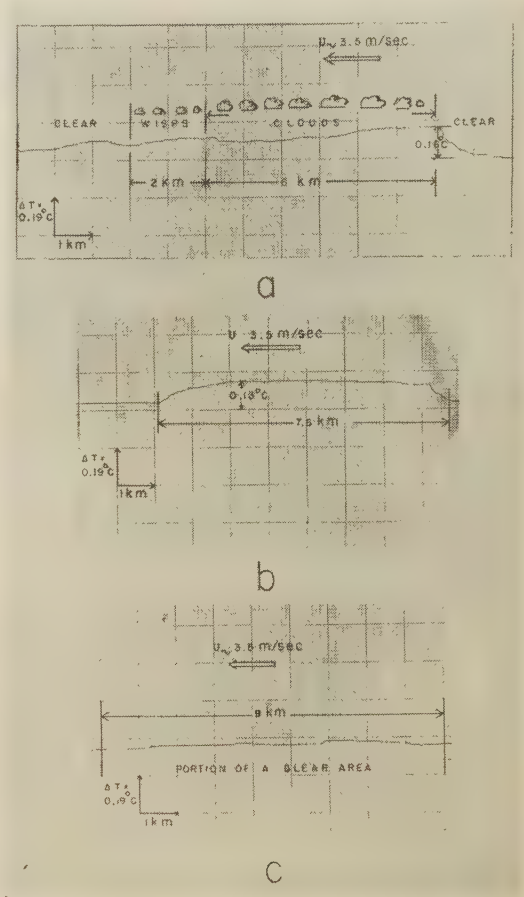

Fig. 2. Sea surface temperature records from radiation thermometer on day of light wind ($U \sim 3.5$ m/sec) and fair trade cumulus. All flights made into wind. Temperature increases upward.

a. Warm spot with cumulus. Clouds drawn somewhat larger than actual widths. Only beginning and end of group marked accurately.

b. Warm spot without cumulus. Found within subsidence ring off island of Jamaica (about 15 miles north). This warm spot has typical temperature profile for light wind day, steeper on upwind edge and more gradual on lee edge.

c. Typical record from clear zone on same day. On this occasion the clear zones were much wider than the cloudy ones and the warm spots were few and far between. No temperature anomalies greater than about 0.04° C were found in clear zones except near the island (see b.).

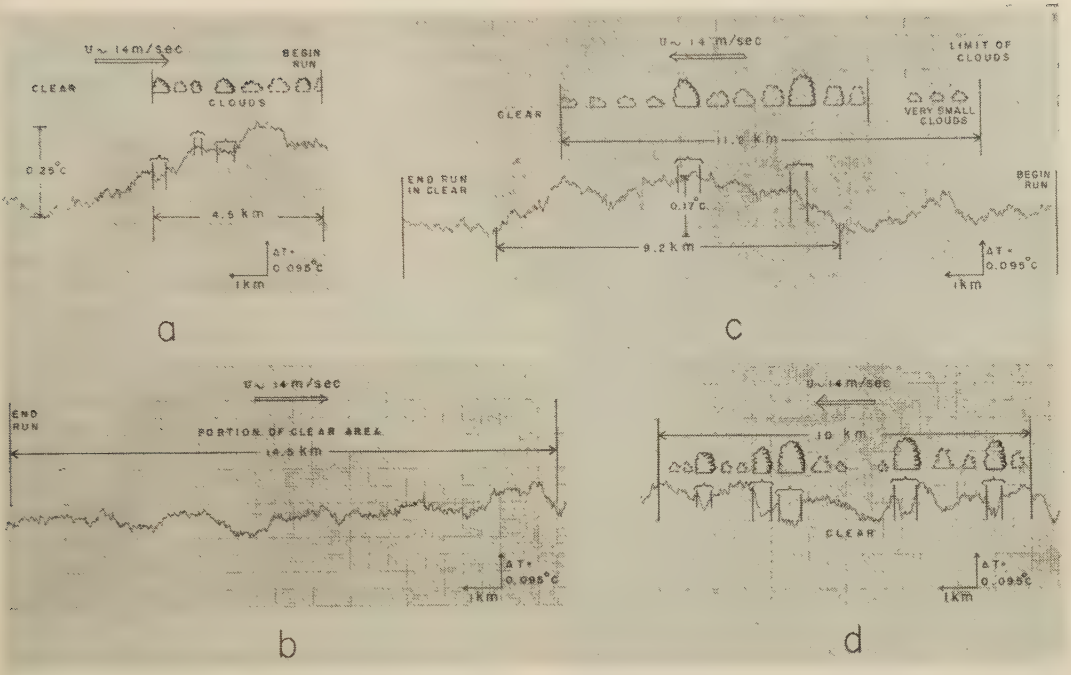

Fig. 3. Sea surface temperature records from radiation thermometer on day of strong wind ($U \sim 14$ m/sec) Some of the increased small-scale fluctuations on these records are real (some small dips are cloud shadows; a few are marked) and some are undoubtedly instrumental. The instrument was operated on this occasion in a manner bound to give more noise than on the occasions of Fig. 1 and 4. Temperatures increase upward.

a. Warm spot 0.25° C in amplitude associated with clouds. Run was made upwind and begins at right edge of figure (within cloudy area) and continued past its downwind edge far into clear area to left. Some of the cloud shadows were marked on the record and are denoted by small brackets with solid-line clouds above. The remaining (dotted) clouds are located approximately.

b. Typical clear area record for the same day. Direct continuation of upwind run begun in Fig. 3 a. Some of the small-scale noise may be instrumental in origin.

c. Upwind run completely traversing 9-km warm spot 0.17° C in amplitude. This warm spot was located on repeated traverses up- and downwind across it and showed little change in amplitude in the time studied. The solid-line clouds were coded accurately on the record as was the beginning and end of the cloud group. The remaining (dotted) clouds are located approximately.

d. Portion of a downwind run made within a warm spot at least 20 km across. Reproduced to show cloud shadows which had the most pronounced effect on the temperature record of any observed over water, due probably to clouds of greater vertical thickness and blacker appearance from below. The bracketed shadows with solid-line clouds drawn above were coded accurately on the record. The remaining (dotted) clouds are sketched approximately.

gradually dying out. No good idea of the duration of the warm spots could be obtained from the flights, although time-lapse photographs from the Jamaica beach (which were directed to following the life histories of cloud groups as a whole) suggest that often they persisted in nearly the same locality for at least 3—4 hours.

The Atlantis records confirmed the aircraft temperature data, and on certain rather calm days showed even sharper steps than the gradients reported above; on occasions a 0.1—0.2° C temperature rise or fall occupied only about 10—20 ft in the horizontal. Steps of the same amplitude were recorded on all the lower-level thermometers, with only very slight changes in shape with increasing depth. It appears that this temperature patchiness of the sea surface layers is not a peculiarity of the waters around Jamaica, for the Atlantis obtained similar anomalies on the homeward voyage to Charleston, South Carolina.

Several typical records from the airborne instrument are reproduced in Figures 2—4.

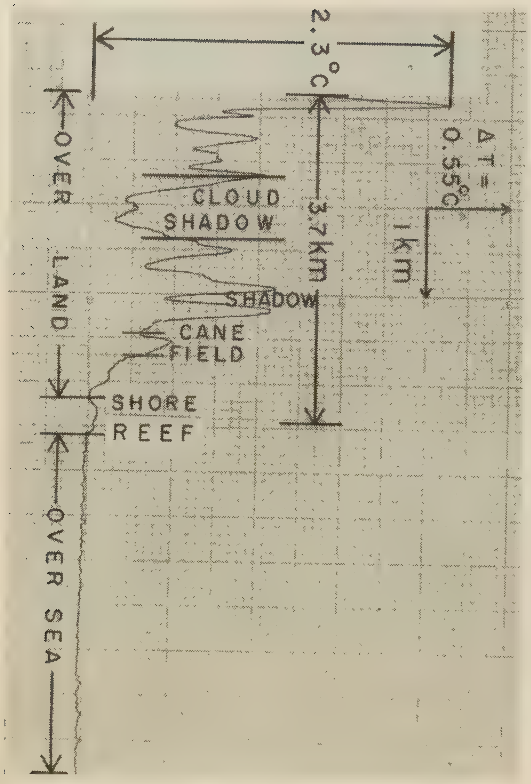

Fig. 4. Island run made at 10.00 a.m. local time on the same strong wind day as the records of Fig. 3. Run made from land to sea across Jamaica north coastline, which lies east-west or nearly parallel to the wind. All fluctuations shown over land are real. Some could be associated with terrain features and several marked dips occurred under cloud shadows; two of these were coded on the record. Instrument is operated on much lower sensitivity than preceding records so that maximum land temperature excess was 2.3° C.

One trace obtained from flying across the Jamaica coastline on a sunny day is shown for comparison. Even though the island record was not made at the maximum of diurnal heating (when the island thermal excess might be expected to be about 25 % greater), the land warming may at first appear small. To understand this it should be pointed out that the radiation instrument operates in the infra-red wave length range 8—13 microns, in order to minimize absorption by the water vapor intervening between the surface and the detector.

While a water surface is a nearly perfect black body in this part of the spectrum, a beach and soil surface undoubtedly has significant albedo. Thus what was measured here might be called the "equivalent black body temperature" of the island. The actual ground temperature, if measured, probably would have been much higher. However, the island temperature rise of Figure 4 is quite in keeping with the land thermal profiles deduced elsewhere as consistent with observed convective and sea-breeze circulations (see MALKUS and STERN, 1953; MALKUS, 1955). This agreement between "equivalent black body temperature" of the land surface and the temperature excess necessary to drive convective motions is probably more than coincidence—if the emission of infra-red radiation is one of the major processes controlling the heat flux from the boundary to the lowest air. Thus we may hypothesize that the radiation thermometer gives approximately the "effective" (for convective motions) boundary temperature of a land as well as a water surface. The contrast between the observed sea and land thermal profiles of Figures 2—4 is striking, the land showing enormously larger fluctuations, due both to differences in soil character and to cloud shadows.

III. Air circulations produced by differential heating

A mechanism for the initiation of cumulus groups over sea surface warm spots was suggested by the "equivalent mountain" analogy which, in fact, provided the incentive for the observations reported above. The "equivalent mountain" effect is associated with a horizontally convergent circulation across the warmed region and concomitant weak updrafts above it, superimposed upon the mean wind flow. If we may continue applying the island model of differential heating to the tradewind oceans, the approximate magnitude and structure of similar convergent circulations over the warm spots is readily deduced. This permits derivation of a quantitative relation between the observed temperature excess and the expected differences in air structure across a warm spot. While this picture undoubtedly oversimplifies the complex interactions between ocean and atmosphere, circulations of the deduced strength and scale account for several features of the subcloud air which were inexplicable in terms of turbulent fluxes alone, and in so doing provide a plausible connection between the evolution of cloud groups and processes occurring below cloud.

The maximum height of the "equivalent mountain" corresponding to a heated island has been shown to be

$$M = \frac{\tau}{\Gamma - \gamma} \tag{1}$$

where M is in cm; τ is the effective island temperature excess in °C; Γ is the adiabatic lapse rate, and γ is the lapse rate of the undisturbed air upwind. This maximum is reached at a distance sufficiently inshore from the upwind beach to allow for the establishment by turbulence of a well-mixed ground layer. Thus the equivalent mountain slope may be more gradual than that of the temperature profile and in mid-latitudes on days of poor mixing the maximum height may not be attained in passage across the island. In the trades, the lower air is nearly adiabatic to begin with and the amplitude prescribed by the temperature profile is normally reached within 3—5 km downwind of the island boundary. The greatest "mountain" elevation and streamline deformation are thus commonly encountered at the lee shore where τ is largest. Since the average lapse rate of the trade-region moist layer (surface to inversion height at 2—3 km) varies little from about 0.8 adiabatic, the height of the equivalent mountain in kilometers is usually close to one-half the temperature excess in degrees.

The main features of the heat-produced circulation may now be deduced if we know the height at which the "sea breeze" reverses direction, because this is also the height of maximum vertical velocity: that is to say, it is the height at which the streamline deformation reaches the full amplitude prescribed by equation (1). This height has been derived as

$$h = \frac{\pi}{2} \frac{U}{\sqrt{gs}} \tag{2}$$

where h is in cm; U is the undisturbed wind in cm/sec; s is the upwind static stability, $\Gamma - \gamma / \overline{T}$, where $\overline{T}$ is the mean absolute temperature of the air layer and g is the acceleration of gravity. Since in the trades gs varies little from about 7×10^{-5} sec^{-2}, this relation may be written approximately

$$h \text{ (km)} \cong 0.2\, U \text{ m/sec} \tag{3}$$

Thus for a normal wind speed of 5 m/sec the height of the sea-breeze reversal is about 1 km, being proportionally higher or lower for a stronger or weaker trade.

It is now possible to estimate the average vertical motion at level h, since the air must ascend the height of the equivalent mountain in the time it requires to cross the island, namely U/d where d is the island width. Thus

$$\overline{w} = \frac{\tau}{\Gamma - \gamma} \frac{U}{d} \tag{4}$$

Clearly this is only the average upward motion, for the vertical ascent rate depends on the slope of the equivalent mountain and thus on the features of the temperature profile; it no doubt varies across the island. Larger islands will show weaker mean ascent rates than smaller ones since τ does not rise linearly with island width. The prediction of equation (4) was borne out in comparing the vertical motions over Anegada (2 by 10 km) with those over Puerto Rico (50 by 160 km).

Thus up to maximum $\overline{w}$, its average rate of increase with height is $\overline{w}/h$ and if the island is larger in its cross-stream than down-stream extent, the average horizontal wind difference across it is approximately

$$\frac{\overline{\Delta u}}{\tau} \cong \frac{U}{(\Gamma - \gamma)\, h} \tag{5}$$

and when h is substituted from (2)

$$\frac{\overline{\Delta u}}{\tau} \cong \frac{2}{\pi \overline{T}} \sqrt{\frac{g}{s}} \tag{6}$$

or

$$\frac{\overline{\Delta u} \text{ (m/sec)}}{\tau} \cong 2.5 \tag{7}$$

for normal trade-region stabilities. Equation (7) gives the wind difference across an island averaged from the surface up to the height where it vanishes. Observations indicate that the tropical sea breeze is about constant up to 300 m or so, from which it decreases roughly linearly to zero at h. Thus we deduce that the low-level wind difference across a heated region should be approximately 3.6 m/sec per °C mean effective surface temperature excess or that the sea-breeze component at each boundary should be about 1.8 m/sec per degree. Therefore for islands and oceanic warm spots in the trades, the "sea-breeze" strength and equivalent mountain height should depend primarily on the effective temperature excess. The height of sea-breeze reversal (maximum updraft) should vary directly as the wind speed.

These relations have been tested satisfactorily for three islands in the Atlantic trade-wind region, two large (about 50 by 150 km) and one small (about 2 by 10 km). The methods, observations used, and results are reported elsewhere (Malkus, 1955; 1956). If they may now be applied to the oceanic warm spots, the expected circulations are inferred as follows: For a typical warm region 0.2° C in amplitude and 10 km horizontal extent in the direction of the wind, the equivalent mountain is 100 m high; Δu at the surface is 0.7 m/sec, and if the trade is blowing at 6.7 m/sec (15 miles per hour) the height of "sea-breeze" reversal is 1,350 m. The air would take about 25 minutes to cross the warm spot and the upward motions at 650 m (average level of cloud base) will be 4.3 cm/sec so that the streamline starting at that height at the upwind edge will have risen 65 m by the downwind boundary. The wind profiles expected at the two edges of the warm region are shown in Figure 5. These have been obtained by adding the heat-produced motions to an average oceanic trade-wind profile.

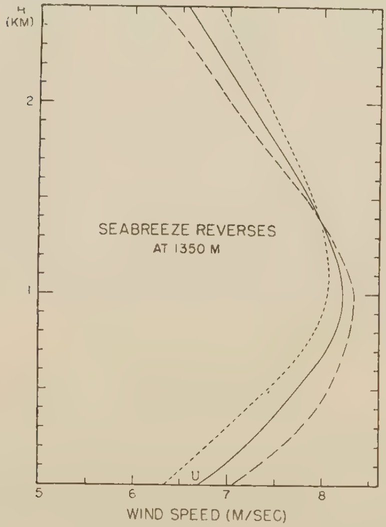

Fig. 5. Calculated wind anomalies associated with typical warm spot. An average oceanic trade-wind distribution with height is given by the solid curve *U*. The long dashed curve shows the modified profile expected at the upwind edge of a 0.2° C warm spot 10 km across, and the short dashed curve is the expected profile at the downwind edge. The surface value of the "sea breeze", its elevation of reversal, and its height distribution are obtained as outlined in text and equations. These profiles are believed to prevail after the warm spot has been in existence long enough for a quasi-steady circulation to develop.

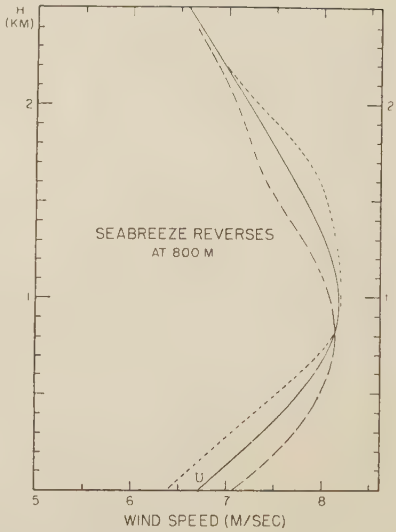

Fig. 6. Calculated wind anomalies associated with an oceanic warm spot in an intermediate stage of development. The solid curve *U* is the same as the solid curve of Fig. 5. In this case the expected profiles at the upwind (long dashed curve) and downwind short dashed curve) edges of the warm spot have been obtained assuming that the sea breeze changes sign at 800 m, instead of 1,350 m as in Fig. 5. The surface wind anomalies are the same in the two figures.

This situation is envisaged after the warm spot has been in existence long enough for the establishment of a quasi-steady flow pattern. The time dependence of the motion field should not be ignored. Island observations suggest that although the offshore subsidence ring is formed and the sea breeze sets in at the coast within an hour after the land becomes warmer than the water, the growth in size of the cell is slower, the maximum depth and inshore penetration requiring several hours. Thus it is probable that the main feature of the aging of the circulation is its deepening with time up to the maximum-depth configuration of Figure 5. A likely intermediate flow condition might be the one of Figure 6 in which the surface $\triangle u$ is the same but the "sea breeze" reverses at 800 m. The corresponding $\overline{w}$ at cloud-base level is 3.3 cm/sec. The effects of such circulations and their changes with time upon the air flowing through them is considered in the next section.

IV. Effects upon the air structure

During the Wyman-Woodcock expedition to the trades in 1946, numerous vertical soundings of air temperature and humidity were made over the open ocean. On many of the observing days, soundings were taken both in clear and cloudy areas. These have been segregated and the features of the lower air compared. Marked differences in moisture structure below cloud-base level were apparent. The top of the mixed layer averaged 550 m, or less than 100 m below cloud base. In this layer, the air in cloudy regions contained 2 % more moisture than that in the clear, with a 0.3—0.4 gm/kgm higher mixing ratio at the top. This means that the moisture lapse rate in the cloudy-zone mixed layer was on the average 22 % less than in the clear-zone mixed layer. In the 100-m "stable" layer just below cloud base, the differences were even more striking. The moisture lapse rate in cloudy zones fell short of that in clear zones by 33 %, and at cloud-base level (but generally away from clouds) the mixing ratio in cloudy zones exceeded that in clear zones by an average of about 1 gm/kgm. On three occasions in cloudy areas, the upward moisture lapse rate was actually zero or negative in this last 100 m below cloud base and the mixing ratio at cloud-base level exceeded that in nearby clear zones by 1.5—2.0 gm/kgm. The mean surface wind varied little throughout the observation period.

Turbulent fluxes do not account for these distributions. Furthermore, the effects upon turbulent transports of the small surface temperature excesses are unlikely to alter the air structure appreciably above the lowest 100 m or so in the time the air spends crossing the warm spot. Evaporation from the sea surface is increased by 4 % at most. On the other hand, weak circulations caused by the heating can account for the differences. The effectiveness of these scales of motion in transporting water vapor is illustrated when we calculate that the moisture flux produced by a 4 cm/sec vertical velocity exceeds locally the observed evaporation rate and turbulent flux by an order of magnitude. This does not imply that the net integrated upward flux due to these motions exceeds the turbulent transports, as will be seen later, but it does suggest local variations depending upon position relative to the flow pattern.

A typical trade-wind air stream flowing across a warm spot and through its circulation is now considered. The air starts at the upwind edge with the moisture structure typical of a clear area and the laws of mass and water vapor conservation are applied assuming that the air passes through the region in a time small compared to that needed for the motion field to change. Fluxes into and out of the mixed and stable layers are balanced successively using the circulations shown in Figures 5 and 6. The tacit assumption has been made that the evaporation and the upward turbulent flux through cloud-base level are about equal to each other and vary little with position. The results may be discussed using Figure 7. If we consider the mixed layer and apply first the circulation of Figure 6 and then the more mature flow of Figure 5, we get the results in Figures 7a and 7b respectively. Although the motion field differs slightly between a and b the resulting differences in moisture structure are negligible. If the air crosses the upwind boundary of the warm spot with the water vapor distribution typical of a clear area, then it may cross the downwind boundary with a distribution typical of a cloudy area. The depicted average mixing ratio increase of about 2 % is required by the superposition of the motion field upon an air stream which dries out with height in the manner of the trades: To satisfy continuity in a steady, horizontally convergent flow, the air column with the smaller wind must be more moist than the column with the stronger wind, in direct proportion that the mixing ratio at the top boundary is less than the average value at the inflow end. It is not a unique solution from these diagrams, which deal with the mixed layer as a single box, that the greatest

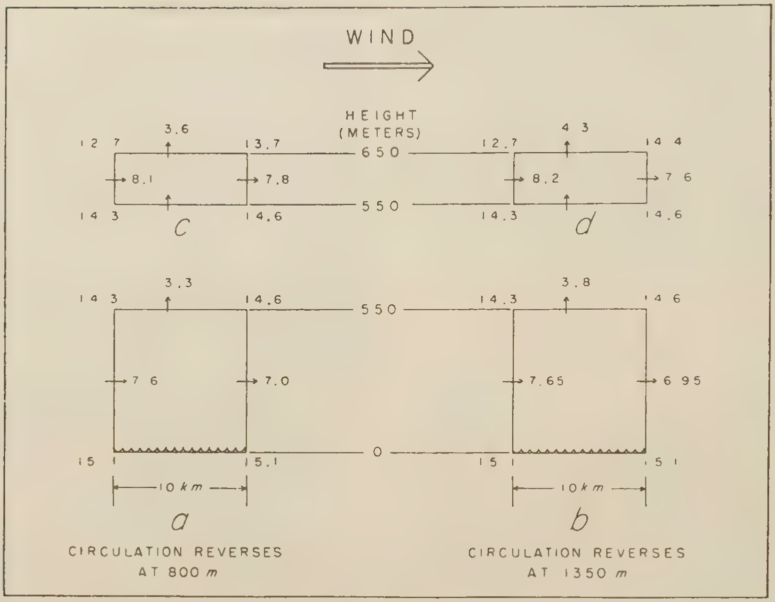

Fig. 7. Diagrams showing mixing ratio and velocity structures obeying mass and moisture conservation laws when typical trade-wind air flows across a 10-km warm spot. The horizontal arrows are wind speeds in m/sec; vertical arrows are mean vertical motions in cm/sec; and the numbers at the corner of each box are mixing ratios in gm/kgm. All figures are rounded off. Boxes a and c use the velocities of the shallower circulation of Fig. 6; boxes b and d use those of the deeper circulation of Fig. 5. In a and b the 550-m deep mixed layer is dealt with as a section 10 km across and unit width into the page. The air and water vapor entering per sec at the upwind (left-hand) side must equal the outflow per sec through the top and downwind (right-hand) side. In c and d the next higher stable layer is treated as a similar section 100 m deep. In each case the inflow air has the moisture distribution of a clear area. The moisture distribution at the outflow end is adjusted to satisfy continuity.

vapor accumulation occurs at the top. This must be so, however, if the moisture lapse rate increases upward as it does in the trade. The greatest moisture addition has thus been made at 550 m, which gives a diminution of mixing ratio lapse rate of 38 % between the extreme ends of the warm spot. This is consistent with the average difference of 22 % between clear and cloudy areas and gives a downwind-end sounding identical to many actually made in cloudy zones.

The required downstream accumulation of moisture becomes greater in the next higher layer through which the vertical decay of mixing ratio is much stronger. Applying the circulation of Figure 6 ("sea breeze" changing sign at 800 m) to the 100-m thick stable layer, we get the results of Figure 7 c. The upwind (left-hand) air column has the moisture structure of a clear area. Continuity is satisfied when the air leaving (right-hand column) has the structure of a cloudy area, with a 1 gm/kgm greater mixing ratio at cloud-base height and a moisture lapse rate smaller by 50 %. The deeper circulation of Figure 5 has a more striking effect, which is shown in Figure 7 d. The mixing ratio at cloud base must now be 1.7 gm/kgm greater at the downwind edge of the warm spot and the moisture lapse rate there practically disappears. This corresponds closely to the observed cases of vanishing or negative mixing ratio gradient just below cloud base. These distributions cannot be produced by turbulent fluxes alone, which on the contrary would shortly destroy such accumulations were not other scales of motion operating to maintain them. The observations and calculations presented here suggest a plausible origin of circulations of approximately the required amplitude and size.

Although the upward flux of water vapor is large above these warm regions due to the gradual ascent of air, mass continuity requires that it be large in the opposite sense in the surrounding regions of subsidence. Whether or not flows of the sort hypothesized lead to any net upward transport of moisture through cloud-base level depends upon the correlation between vertical motions and mixing ratio, which is unknown. If the correlation were perfect and if the clear areas were twice as wide as the cloudy ones, these circulations could produce a net upward flux through cloud-base level of about 1.3×10^{-6} gm cm^{-2} sec^{-1}. This is 33 % of the evaporation rate or about 43 % of the total moisture flux at that height. While this maximum figure is undoubtedly too large, there is evidence that motions of this scale contribute to the net upward pumping of moisture in the lower trade. If small-scale turbulence alone were to be responsible, it has been found that overly large eddy exchange coefficients are required (see BUNKER, HAURWITZ, MALKUS, STOMMEL, 1949, p. 70).

V. The life cycles of trade-wind clouds and cloud groups

If the velocity profiles of Figures 6 and 5 represent successive time stages in the development of the flow over an oceanic warm spot, it appears likely that the air below cloud will accumulate moisture as the circulation ages, particularly at the downwind edge. For a typical trade-wind sounding, an increase of mixing ratio of 1 gm/kgm would lower the condensation level by about 260 m or 850 ft. Between Figures 7 c and 7 d, the mean mixing ratio of the 100-m layer just below cloud base has risen by 0.35 gm/kgm. Therefore, as a typical circulation reached maximum growth, we might expect cloud base to descend by about 90 m or 300 ft. Some corroborative observational evidence has been gathered by Woodcock[1] near Hawaii. On successive flights below cloud in a fixed locality, he frequently found the cumulus bases lowering from 100—500 ft in one or two hours.

Some of the factors controlling the lifetimes of individual clouds within a group may also be understood in terms of these temperature anomalies and associated circulations. For the observed horizontal dimensions of the warm spots, the time required for normal trade-wind air to pass across them ranges from about five minutes to two hours. This coincides with the range of lifetimes of individual tropical cumuli. While the warm spot circulation remains relatively steady, it can be envisaged that individual clouds will form at some interval after the air crosses the temperature up-step and will dissipate shortly after passing the down-step, many kilometers further downwind. During passage across the warm spot, each cumulus may put up several towers, depending upon the time available. This picture has received support from a series of time-lapse films of some small oceanic clouds north of Jamaica. The group as a whole remained in nearly the same location for more than four hours, despite a 5—6 m/sec wind. The lifetime of a single cumulus measured about 30 minutes, or just the time required to cross the group. Each cloud first appeared at the upwind edge of the population, travelled across the region at approximately the wind speed, and perished as it became the last cloud on the downwind edge. This behavior of the group could not be accounted for in terms of the wind shear, which was strongly negative. Each cloud leaned upwind, put up new towers ahead (downwind) of itself, and evaporated on its rear (upwind) edge, consistent with the predicted asymmetry of a single cumulus in a windfield decreasing upward. None of these small clouds produced showers, which upon occurrence could give rise to different mechanisms of cloud propagation and production.

VI. Concluding remarks

Further observations with the airborne radiation thermometer are planned in other parts of the Atlantic trade and at other seasons. It is hoped to learn whether or not sea surface temperature patchiness of the sort described here is a common phenomenon and how generally it is related to cloud formations. More detailed measurements of the lowest air temperature, moisture, wind and turbulent structure directly over the warm regions are desired to shed light on the mechanisms of interaction between sea and air and to check the predictions concerning the circulations presented here.

---

[1] Reported in conversation with the writer.

It is hoped that such meteorological observations may be combined with measurements from a surface vessel in an attempt to elucidate the oceanographic factors controlling the origin, scale, and duration of these thermal anomalies, about which little or nothing is known at the present time.

Acknowledgments

An essential contribution to this work was made by Dr. William S. Richardson, who designed and developed the radiation thermometer, and who generously took part in the field program described here, and by Mr. Charles Wilkins who operated the instrument on many of the flights. Much gratitude is also due to Mr. Claude Ronne who participated in every phase of the effort.

This study has been supported by the United States Office of Naval Research.

REFERENCES

Bunker, A. F., Haurwitz, B., Malkus, J. S., and Stommel, H., 1949: Vertical distribution of temperature and humidity over the Caribbean Sea. *Pap. Phys. Oceanogr. Meteorol., Mass. Inst. of Tech. and Woods Hole Oceanogr. Inst.*, **11**, 82 pp.

Malkus, J. S., 1955: The effects of a large island upon the trade-wind air stream. *Quart. J. Roy. Meteor. Soc.*, **81**, pp. 538—550.

Malkus, J. S., 1956: Differential heating in the trades and its relation to cloud formations. Unpublished manuscript on file at the Woods Hole Oceanogr. Inst.

Stern, M. E., and Malkus, J. S., 1953: The flow of a stable atmosphere over a heated island, Part II. *J. Meteor.*, **10**, pp. 105—120.

PRINTED IN SWEDEN ESSELTE, STHLM 57

Contribution No. 844

Reprinted from "Progress in Physics and Chemistry of the Earth" Vol. 2
(1957) Pergamon Press; London, New York, Paris

5

4

SOME CURRENT ASPECTS OF CHEMICAL OCEANOGRAPHY*

By Francis A. Richards

Chemical oceanographers are concerned with the composition of sea water, the distribution of the variable chemical constituents of sea water, and the biochemical and hydrochemical cycles in the sea which bring about the observed distributions. These aspects are considered in a dynamically circulating system, across the boundaries of which chemical and energetic exchanges are constantly proceeding. The boundaries may be phase boundaries at the surface and bottom, or they may be water-mass boundaries established by density gradients, kinematics, or chemical properties; they may be largely determined or described chemically, because of the effect of the salt content on the density of sea water, and because specific water masses often have characteristic chemical properties.

The sea must also be considered as an ecological environment; its chemical and energetic makeup will largely determine its populations, which in turn will leave their mark on the chemistry of the water, in cyclic successions. The bases of modern oceanography were established in large part by marine biologists, and it is natural that studies of biochemical cycles should have sprung from these beginnings. The interest of fishery biologists in practical matters of organic productivity and the effects of the chemical system on fish populations have stimulated investigations in chemical oceanography.

Geochemical interest in the distribution of elements on land, in the sea, and in the sea floor requires detailed knowledge of the constituents of sea water, and a large part of our knowledge concerning the minor elements in the sea is owed to geochemical researches, notably those of V. M. Goldschmidt and his co-workers.

Historically, the analysis of sea water has received much emphasis and continues to do so. This is not only because knowledge of the composition of sea water is necessary for progress in all branches of oceanography, but also because sea water presents rather specialized and challenging analytical problems. Barnes (1955) has reviewed this general subject, and points out some of the difficulties arising from the complex chemical nature of sea water and the conditions under which the analyst must work when at sea. Superimposed on these difficulties are those of obtaining uncontaminated representative samples from many depths over immense areas.

Prior to the *Challenger's* circumnavigation of the globe in 1873 to 1876, no valid generalizations concerning the chemistry of the seas were possible. Since that time, there has been a gradual accumulation of observations so that to-day the distributions of some of the constituents of sea water are more or less well known on a world-wide basis. Other constituents have been observed less frequently or in limited regions, and still others have been detected or determined only once or a few times. Some constituents are known to be present in sea water only because they have been found in the bodies of marine organisms, where they must have been concentrated from the sea water itself. The variations in the concentration of many constituents from place to place and time to time cannot be described, and it is obvious that chemical, biological, and physical reactions of these constituents in the sea cannot be fully recounted. We have a reasonably good general picture of the total salt content, the distribution of dissolved oxygen, and of some of the nutrient salts, especially phosphate, but the distributions of most of the materials present in very small concentrations in sea water are almost wholly unknown. Progress has been more rapid in describing the distributions of properties of demonstrable interest for which good analytical methods are available. For example, knowledge of dissolved oxygen in the oceans was scanty and of poor accuracy until the Winkler titrimetric analysis, easily and accurately workable aboard ship, replaced older gasometric methods. Since the first use of this method on an extensive cruise, aboard the *Planet* during her round-the-world cruise in 1906 and 1907, there has been built up a large body of data on the distribution of dissolved oxygen which has led to interesting interpretations of physical and biological processes in the ocean. Similarly, the salt content, one of the parameters determining the density of sea water, and in turn, the circulation of the sea, is fairly well known because good methods are available for its determination and the subject is of general interest to oceanographers.

---

* Contribution No. 844 from the Woods Hole Oceanographic Institution.

Since the descriptive phase of chemical oceanography must await the development of adequate analytical methods, comments on the present status of the analysis of sea water will be included in this review.

THE MAJOR CONSTITUENTS

One of the most important findings in DITTMAR's (1884) analyses of seventy-seven samples of sea water collected by the *Challenger* was that the *major*

Table 1. The Major Constituents of Sea Water, and their Ratios, by Weight (from SVERDRUP *et al.*, 1942) *to Chlorinity*

Ion	Chlorinity ratio, g per unit Cl	Grams per kg of water of 19‰ chlorinity
Chloride, Cl^-	0·99894	18·9799
Sulphate, $SO_4^=$	0·1394	2·6486
Bicarbonate, HCO_3^-	0·00735	0·1397
Bromide, Br^-	0·00340	0·0646
Fluoride, F^-	0·00007	0·0013
Boric Acid, H_3BO_3	0·00137	0·0260
Sodium, Na^+	0·5556	10·5561
Magnesium, Mg^{++}	0·06695	1·2720
Calcium, Ca^{++}	0·02106	0·4001
Potassium, K^+	0·02000	0·3800
Strontium, Sr^{++}	0·00070	0·0133

Fluoride is included in this list with some misgivings; it is considerably more concentrated in sea water than the so-called minor or trace elements, but there appear to be relatively large variations in the fluoride/chlorinity ratio. For this reason, it is also included in the table of minor elements, which is given later (p. 90).

constituents of sea water occur in constant ratios to one another. These major constituents, the ions of sodium, magnesium, calcium (with strontium), potassium, halides, sulphate, carbonate, and undissociated boric acid, make up 99·8 to 99·9 per cent of the total material dissolved in sea water, and it follows that the determination of any one of them suffices to give a measure of the total salt content of the water. Classically, the halides have been determined by titration with silver nitrate, and the *chlorinity* thus determined is related to the salinity by Knudsen's (1901) formula,

$$S = 0{\cdot}03 + 1{\cdot}805 \times \text{chlorinity}.$$

From what has been said of the constant ratios in which the major constituents of sea water occur, it follows that the concentrations of the other major constituents can be computed from the chlorinity and the proper chlorinity ratio (Table 1).

More recent determinations of chlorinity ratios have been made, and are summarized in Table 2. In some instances, variations in them may reflect small real differences in the different water masses analysed.

Anomalies in Chlorinity Ratios

From the investigations that have been made to date, it can be concluded that variations in the chlorinity ratios of the major constituents in the ocean are small, generally so near the accuracy of the available methods that most careful analyses must be made to detect them. The major differences that may be found are in places where rivers enter the ocean, where the ratio is altered by freezing out of sea ice, or by *in situ* biological activity. The latter appears to apply almost exclusively to the sulphate-chlorinity ratio, which may be affected in stagnant areas which become anaerobic; under these conditions, sulphate ions are reduced to sulphide, and the ratio changes. Calcium and strontium may be depleted by deposition as animal shells. Obara (1951) has used anomalies in the sulphate-chlorinity ratio as an indicator of stagnation of sea water in a bay. However, approximate calculations indicate that the sulphate-chlorinity ratio should be changed by only about 0·0005 in the depths of the Black Sea, where concentrations of about 10 mg of sulphide sulphur per litre are found.

Lewis and Thompson (1950) have reported on the effect of freezing on the sulphate chlorinity ratio in sea water; the ratio in the brine left behind was smaller than in the salts retained by the ice, and was found to be a nonlinear function of the rate of freezing and of the temperature at which the freezing takes place.

Properties of Sea Water Dependent on the Constant Ratios in which the Major Constituents Occur

Because the major constituents of sea water occur in essentially constant proportion to one another, leaving the amount of water as the chief variable (Redfield, 1948), there are several properties of sea water which vary with the total concentration of the major elements. It is apparent that the precise determination of one of the major constituents suffices to fix the concentration of the others. Density, the colligative properties, and other physicochemical properties of sea water, are thus all interrelated.

Table 2. Recent Determinations of Chlorinity Ratios

Chlorinity ratios (from Table 1)	Recent values	Source of samples	Reference
Na^+/Cl^- (0·5556)	0·5549		Webb (1939)
	0·5549	Three Pacific Sta.	Robinson & Knapman (1941)
	0·5562	Straits of Juan de Fuca and Puget Sd.	Robinson & Knapman (1941)
	0·555(a)		Nisikawa *et al.* (1939)
	0·5554, 0·5517	Tokyo Bay	Matida (1951)
Mg^{++}/Cl^- (0·6695)	0·0669	Northeast Pacific	Miyake (1939c)
	0·0676	Northwest Pacific	Miyake (1939c)
	0·067(a)		Nisikawa *et al.* (1939)
	0·06697	Tokyo Bay	Matida (1951)
Ca^{++}/Cl^- (b) (0·02106)	0·022(a)		Nisikawa *et al.* (1939)
	0·02136	Tokyo Bay	Matida (1951)
	0·02188 ± 0·00008	Gulf of Alaska	Chow & Thompson (1955a)
K^+/Cl^- (0·02000)	0·018(a)		Nisikawa *et al.* (1939)
	0·02009 ± 0·0002		Webb (1939)
	0·0191	Pacific Waters	Miyake (1939c)
	0·02021	Tokyo Bay	Matida (1951)
Sr^{+++}/Cl^- (0·00070)	0·00075		Miyake (1939b)
	0·0005		Smales (1951)
	0·00042		Odum (1951)
	0·00042 ± 0·00002		Chow & Thompson (1955b)
$SO_4^=/Cl^-$ (0·1394)	0·142(a)		Nisikawa *et al.* (1939)
	0·13991 ± 0·00019	Irish Sea	Bather & Riley (1954)(c)
	0·1394	Tokyo Bay	Matida (1951)
Boric Acid/Cl^- (0·00137)	0·00136	Increasing w/depth	Miyake (1939d)
	0·00162		Miyake & Matui (1939)
Br^-/Cl^- (0·00340)	0·00340		Thompson & Korpi (1942)
	0·00343	Coasts of Gt. Britain	Haslam & Gibson (1950)
	0·00347 ± 0·000034	Coasts of Japan and Tokyo Bay	Matida & Yamauchi (1951)
HCO_3^- (0·00735)	0·00741	Tokyo Bay	Matida (1951)

(a) The values from Nisikawa *et al.* (1939) are mean values from 125 analyses of water taken between Yokohama and London and 104 taken between Yokohama and San Francisco.

(b) Calcium exclusive of strontium.

(c) Bather and Riley (1954) also noted that the $SO_4^=/Cl^-$ ratio increased to 0·1640 in going upstream in the river Mersey in March 1954.

The colligative properties of solutions are those which depend on the activities of the ions in solution. The activities are the products of the concentrations of the ions and their respective activity coefficients. Since these properties, the vapour-pressure lowering, freezing-point depression, boiling-point elevation, and osmotic pressure, depend on the activities of the ions, if any one of them is empirically determined the others can be computed. Until recently, empirical determinations of only the freezing point (Sverdrup *et al.*, 1942, p. 65) and of vapour pressures between 25° and 175°C (Higashi *et al.*, 1931) had been made.

Robinson (1954) has now made measurements of the vapour-pressure lowering, $\Delta p/p^0 = (p^0 - p)/p^0$, in which p is the vapour pressure of the sea water and p^0 is the vapour pressure of pure water (23·756 mm Hg at 25°C). His measurements were made by equilibrating sodium-chloride solutions of known concentration with sea water in a vacuum desiccator. At 25°C, the vapour-pressure lowering and the osmotic pressure (which was calculated from the vapour-pressure lowering) were determined as follows:

‰ Cl	Vapour-pressure lowering	Osmotic pressure (atmospheres)
10	0·00946	12·87
11	0·01042	14·19
12	0·01139	15·51
13	0·01237	16·85
14	0·01334	18·19
15	0·01433	19·55
16	0·01532	20·91
17	0·01632	22·29
18	0·01732	23·66
19	0·01833	25·06
20	0·01936	26·47
21	0·02039	27·89
22	0·02142	29·33

New determinations of the vapour pressures of sea-salt solutions have also been made by Arons and Kientzler (1954). These determinations were made at temperatures between freezing and 25°C, covering salinity values between 5 and 160 ‰. Arons and Kientzler combined their data with those of Higashi *et al.* (1931), which covered temperatures from 25 to 175°C.

Miyake (1939e) had previously computed the depression of the vapour pressure (in mm of Hg) for sea waters of different salinities at their boiling points from (1) the pressure of saturated water vapour near 100°C under a pressure of 760 mm Hg and (2) from boiling points at pressures slightly lower than 760 mm Hg. The two methods gave results which never differed more than 0·02 mm Hg; the averages from the two calculations are shown below in mm Hg:

Salinity ‰	5	10	15	20	25	30	35	40
Av. Vapour-Pressure Depression	2·17	$4{\cdot}33_5$	$6{\cdot}76_5$	8·92	11·07	$13{\cdot}20_5$	15·61	17·75

MIYAKE (1939e) reported that the freezing-point depression of sea water could be represented by the simple formula $\Delta T = 0{\cdot}102710\ Cl$, where Cl is the chlorinity in parts per mille. This can be related to the osmotic pressure at 0°C by the equation $P_0 = 12{\cdot}05 \times \Delta T$ or at other temperatures $P_T = 1{\cdot}240 Cl + 0{\cdot}00454 Cl \cdot T$. The boiling-point elevation was also calculated by MIYAKE to be $\Delta T = 0{\cdot}01645 S$, where S is the salinity in parts per mille.

WILSON and ARONS (1955) have also computed the osmotic pressure of sea water from the vapour-pressure-lowering data of ARONS and KIENTZLER, over the temperature range 0 to 35° and the chlorinity range 5 to 100‰ *Cl*. They estimate that the errors in their osmotic pressure computations range from ± 2·8 atmospheres at 0°C to 0·4 atmospheres at 35°C. At a temperature of 20°C, their results were about 1 to 2 atmospheres lower than those calculated from ideal-solution theory.

Direct observations of the boiling points of sea water and sea water concentrates have been made by HAMPEL (1950) for engineering purposes. The concentrates were prepared by evaporating sea water under an infra-red lamp while passing a stream of carbon dioxide free air over its surface. HAMPEL reports the following boiling points:

Boiling Points of Sea Water of Various Chlorinities

(*from* HAMPEL, 1950)

(Barometer, 747 mm Hg)

Chlorinity, ‰	Boiling point, °C
18·0	100·3 ± 0·1
20·4	100·7 ± 0·1
29·4	100·9 ± 0·1
48·3	101·3 ± 0·1
61·2	101·9 ± 0·1

Other Physicochemical Properties of Sea Water

The ionic strength of sea water is important not only in physical measurements, but is of biological interest, especially where relationships between the composition of sea water and the body fluids of marine organisms are concerned. BARNES (1954a) has published a series of tables in which he has computed the concentration of chloride, bromide, sulphate, bicarbonate, calcium, magnesium, potassium, strontium, and sodium ions and of boric acid in sea water, using the following concentration units:

1. Grams per kilogram of sea water.
2. Grams per litre (20°C) of sea water.
3. Millimoles (milligram-ions) per kilogram of sea water.
4. Millimoles (milligram-ions) per litre (20°C) of sea water (molarity).
5. Grams per kilogram of water.
6. Millimoles (milligram-ions) per kilogram of water (molality).

In another table, he has computed the vapour pressure and osmotic equivalence of sea water at 25°C.

The ionic strength and temperature are parameters determining the electrical conductivity of solutions, and it is apparent that measurements of electrical conductivity could be used for the determination of salinity and density. Fundamental data relating the specific conductance, temperature, and the chlorinity were empirically determined and reported by Thomas, Thompson, and Utterback (1934). Pollack (1954) has discussed possible errors in the values of Thomas *et al.*, which include errors in the specific conductance values of their standard reference solutions and in the design of the conductivity cell they used. He points out that there may be errors related to the absolute constancy of relationships between chlorinity and specific conductance, which would vary with departures from the constancy of the ratio of the total ionic strength to the chlorinity value; there may be variations in differing water masses and variations arising from differences in the total carbon dioxide-bicarbonate-carbonate equilibrium system. For the most practical purposes, these errors are small enough for the method to be used satisfactorily for salinity and density determinations for oceanographic purposes. Practical necessities are provision for making the measurements at accurately thermostated temperatures, scrupulous cleanliness of the cells and water samples, and provisions for degassing the samples, since any bubble formation in the cells arising from the evolution of dissolved atmospheric gases cannot be tolerated. Nonetheless, the conductivity method has been in use by the International Ice Patrol for many years, using an apparatus described by Wenner, Smith, and Soule (1930). An improved conductivity bridge has recently been constructed and described by Schleicher and Bradshaw (1956). This instrument has been used on several cruises from the Woods Hole Oceanographic Institution, and promises to be not only more rapid and convenient than titrations, but also of being capable of a higher order of precision, even when used on a routine basis aboard ship. This instrument should permit considerably more critical analyses of salinity data, affording surer distinctions between salinities and densities than have formerly been possible.

In addition to using the conductivity of sea water for the determination of salinity in discrete samples, a continuously recording salinity, temperature, and depth analyser has been built (Jacobson, 1948). This instrument employs a head containing a sensitive zylol thermometer, a sylphon bellows which activates a variable resistance in response to pressure changes, and a conductivity cell. The signals from the thermometer and conductivity cell are fed into a computing mechanism (based on data of Thomas *et al.*, 1934) which converts them into salinity. Salinity, temperature, and depth are simultaneously recorded by servomotor driven pens. In practice, the "head" can be mounted on a ship under way to give a continuous record of salinity and temperature, or may be lowered into the water while hove to, to give these same variables recorded against depth. Neither the salinity nor the temperature-records are highly precise, but the instrument has the great advantage of giving a continuous record which can be spot-checked against more precise measurements. The instrument has been put to good use in inshore waters where there may be frequent and large variations in the water, and high precision may be less important than is a knowledge of the details of the changes taking place. The instrument described by Jacobson is limited to a depth of about 1200 ft; Hamon (1955) has published preliminary notes on a temperature-salinity-depth recorder being built in Australia which compares with Jacobson's instrument as follows:

	Hamon	Jacobson
Temperature	0° to 30°C ± 0·1°C (32 to 86°F)	29° to 90°F ± 0·2° (− 1·67 to 32·22°C)
Chlorinity	18·3 to 20·5‰ ± 0·03‰	(11·07 to 22·15‰ ± 0·16‰)
Salinity	(33 to 37‰ ± 0·05‰)	20 to 40‰ ± 0·3‰
Depth	0 to 1000 m ± 20 m (0 to 3281 ft ± 65·5 ft)	(0 to 366 m ± 3·7 m) (0 to 1200 ft ± up to 12 ft)

(Parentheses indicate quantities equivalent to those the authors report.)

The thermal coefficient of conductivity of sea water is relatively high. Gheorghiu and Calinicenco (1940) pointed out that it is much larger than would be expected from the thermal coefficient of conductivity of sodium chloride, and attribute this augmentation to the hydrolysis of sea water, which has an excess of strongly basic cations, and to the marked effect of temperature on hydrolysis. Their measurements indicated that the conductivity varies linearly with temperature, and report the following equations relating conductivity and temperature:

$$10^3 k_T = 14{\cdot}30 + 0{\cdot}512T, \text{ for salinities of } 17{\cdot}5‰$$
$$10^3 k_T = 11{\cdot}46 + 0{\cdot}452T, \text{ for salinities of } 14{\cdot}0‰$$
and
$$10^3 k_T = 8{\cdot}92 + 0{\cdot}290T, \text{ for salinities of } 10{\cdot}0‰$$

In these equations, k_T is the specific conductivity in $\text{ohm}^{-1} \times \text{cm}^{-1}$ at the centigrade temperature T. (These findings are not in agreement with those of Thomas *et al.* (1934) who found a small but appreciable departure from linearity in the variation of specific conductance with temperature.) Gheorghiu and Calinicenco propose that this large temperature coefficient of conductivity be taken advantage of in constructing a thermometer. They reported the following thermal coefficients, α,

α	S‰
0·0358	17·5
0·0371	14·0
0·0325	10·0

The refractive index of sea water can be represented as a function of the chlorinity by the equations

n_D, $25° = 1{\cdot}33250 + 0{\cdot}000328 Cl$ (Utterback, Thompson, and Thomas, 1934)

n_D, $25° = 1{\cdot}332497 + 0{\cdot}000334 Cl$ (Miyake, 1939f).

According to Tarnøe (1900), it is related to the salinity by the equation

$$\log n_D,\ 17{\cdot}5°/S = 6{\cdot}14340 - 0{\cdot}00006S.$$

In these equations, n_D is the refractive index for the sodium D line at the temperature, 17·5 or 25°C, specified, Cl and S are the chlorinity and salinity, respectively, in parts per mille. Miyake has shown that the refractive index of sea water is the summation of the refractions of pure water and the dissolved salts.

Gamez (1942) and others have discussed the possibility of using measurements of the refractive index for the determination of the density of sea water. Saint-Guily (1954) has published tables, based on the data Bein, Hirsckorn and Möller (1935) of the refractive index as a function of the temperature, between 0° and 30°C, and of the density at 17·5°C for the range 1·02 to 1·032 g/cm^3.

The viscosity of sea water decreases with increasing temperature and increases with the chlorinity. Coefficients of viscosity can be calculated from the formula

$$\eta = \eta_w \frac{\rho t}{\rho_w t_w}$$

in which η is the coefficient of viscosity of sea water at a given temperature, η_w is the coefficient for pure water at the same temperature, ρ and ρ_w are the density of sea water and pure water, respectively, at a given temperature, and t and t_w are the time in seconds of flow of sea and pure water through the capillary of a viscometer (Miyake and Koizumi, 1948).

The relationship between the viscosity of sea water and the temperature is

$$\eta = \frac{\eta_0}{1 + \alpha T + \beta T^2};$$

η_0 is the viscosity at 0°C, T is the temperature, and α and β vary with the chlorinity. Miyake and Koizumi have reported experimental values of α and β for chlorinities from 1 to 20‰, and have computed viscosity coefficients for each part per mille of chlorinity up to 20‰ and for each degree from 0° to 30°C.

R. and J. Darmois (1947) investigated the viscosity of Mediterranean waters and found that the specific viscosity divided by the salinity (η_s/S) varied only slightly about the average value of $2{\cdot}117 \times 10^{-3}$ at 20°C. They postulated that the value of this ratio constituted a characterization of the "purity" of sea water. However, later measurements of the ratio (R. and J. Darmois, 1950) in the North Sea averaged $2{\cdot}134 \times 10^{-3}$ at 20°C and $2{\cdot}197 \times 10^{-3}$ at 28°C, and they did not find especially high values in regions of good fisheries, where they suspected the viscosity might be high owing to large amounts of impurities in the water. Thus, the specific viscosity does not seem to be a sensitive measure of the purity of sea water.

The surface-tension of sea water is important in studies of phenomena such as the generation of waves and the occurrence of slicks. The property is especially sensitive to impurities in the sea surface, and Fox *et al.* (1952) have shown that relatively large quantities of marine leptopel are found in the water in regions of slicks. Lumby and Folkard (1954) have adopted a method described by Adam (1937) for determining the lowering of the surface tension at sea. It depends on the fact that certain fatty substances will just spread against a contaminating film, which lowers the surface tension. Drops of successive solutions of gradually increasing concentration of *n*-dodecyl alcohol in medicinal paraffin are placed on the sea surface until a pair is found, one of which just spreads, the other does not, thus bracketing the spreading force of the surface, which is given by the expression

$$\gamma_{aw} - (\gamma_{ao} + \gamma_{wo}).$$

The terms stand for the surface tensions at the air-water, air-oil, and water-oil interfaces, respectively. Observations could be made at sea in winds up to force 3.

LUMBY and FOLKARD have observed that in ruffled areas, the depression of the surface tension was between 2 and 3 dynes/cm, but much higher values were obtained in slicks, up to 22½ dynes/cm. They suggest that the surface contamination may have come from land in those areas where the highest values were found.

The foaming of sea water is a commonly observed phenomenon, of importance in the studies of ships' wakes and in the formation of whitecaps, on which part of the Beaufort scale of wind force is based. The phenomenon has been studied by MIYAKE and MIYAKE and ABE (1943, 1948) and their work has been summarized by ABE (1954). By shaking sea water in an ampoule under standardized conditions, they have observed relationships between the temperature and chlorinity and the height of the foam layer; the foaming ability of sea water increases with chlorinity and decreases with temperature (as does viscosity) and the mean diameter of the bubbles decreases exponentially with increasing chlorinity according to the equation

$$\bar{d} = 5{\cdot}4 \times 8{\cdot}5^{-Cl}$$

in which $\bar{d}$ is the radius in millimetres and Cl is the chlorinity in parts per mille.

Bubble-size frequencies and mean bubble radii as functions of time, decay rates, mean lives of bubbles, their activation energies and the "equivalent radius of foam" have also been described for sea waters. It has also been observed that the height of the foam layer in organic acids is small (i.e. they are almost non-foaming) but in solutions of salts and alkalis, the foaminess goes through a maximum as the concentration is increased. Field observations have been made on the stability of foam on white crested waves at sea.

Determination of Chlorinity, Salinity, and Density

The chloride content of sea water is the major constituent most readily determined by precise chemical methods. Oceanographers have adopted standardized variations in the classical Mohr titration of halides against silver nitrate, referring their results to samples of sea water furnished and carefully analysed by the Laboratoire Hydrographique in Copenhagen. More recently there has been established a new standard based on the mass of silver required completely to precipitate the halogens from a kilogram of sea water.

The original Mohr titration used potassium chromate as an indicator; this had the disadvantage of not showing the stoichiometric end point of the titration, thus requiring considerable subjective judgment on the part of the analyst. Recent researches in the chlorinity titration have been aimed at improving the detection of the endpoint with indicators and by potentiometric methods, in decreasing the size of the sample titrated to take advantage of the speed and convenience of semimicro analytical methods, and in devising more nearly automatic methods of titration. Fluorescene has been used as an indicator, and MIYAKE (1939a) introduced the use of a starch-uranin indicator, which shows the endpoint more clearly than does potassium chromate. SARUHASHI (1953a) has described a semimicro determination, using MIYAKE'S indicator, which requires only one tenth of the volume of sea water used in the original Mohr titration. It should be pointed out that, in general, absolute errors assume greater proportionate values in semimicro procedures. Van Landingham of the Pacific Oceanic Fisheries Investigations Laboratory in Honolulu, uses a mixed starch-phenosafranine indicator, which also gives a stoichiometric endpoint, in preference to the fractionally precipitated chromate (personal communication). Attempts to make a completely automatic titrator, in which the addition of the titrant is controlled electronically by potentiometric signals from the solution, have met with indifferent success, requiring, as they do, complicated servo-operated mechanisms and the use of electrode systems which are subject to instabilities. Potentiometric determination of the endpoint of a manually controlled titration is more successful; this method has been adopted and described by Bather and Riley (1953). The potentiometric determination of the endpoint has been made the subject of a critical study by Proctor (1956), who has analysed the errors introduced by day-to-day variations in the electrode potential at the endpoint. Christie and Newman (1955) have reported on a statistical study comparing the effectiveness of hand stirring compared with magnetic stirring, concluding that there are no significant differences in the results of the two methods. Electrically powered propeller-type glass stirrers were introduced with satisfactory results at the Woods Hole Oceanographic Institution several years ago. These are important matters of technique, since precipitated silver halides occlude unprecipitated halide ions, introducing errors which are significant in terms of the density of sea water and the identification of water masses by temperature-salinity correlations.

The flame photometric determination of sodium is a common analytical technique, but appears to lack the degree of accuracy required for the determination of the salinity of sea water. Homna (1955) has described a flame photometric determination of chloride in sea water, which depends on adding copper nitrate to the water, and photometry of the CuCl band peak at 435·4 mμ. No great sensitivity is claimed for the method.

Many attempts have been made at the more direct determination of the density of sea water by means of hydrometers, pycnometers, and such. Simple hydrometers usually lack the precision required and are very sensitive to the surface tension effects of contaminants. Cox (1954a) has recently described a total immersion hydrometer, which he reports to be comparable with titration for accuracy and about twice as fast. However, it has the disadvantage of not being useful at sea because it is sensitive to the vertical oscillations of the ship. Rochford (1954) has described a chainomatic pycnometer, now commercially available, for the direct determination of chlorinity, which he reports to be useful at sea.

THE MINOR CONSTITUENTS OF SEA WATER

The constituents making up the two or three tenths of a per cent of the dissolved solids in sea water not included in the "major constituents" are far from minor in their biochemical and geochemical importance; the use of the term minor refers solely to relative concentrations. For convenience, they can be divided into the principal nutrient elements, phosphorus, nitrogen, and silicon, into the micronutrients such as iron, copper and manganese, which are known to be necessary for the nutrition of at least some marine organisms, and into the remainder, which might be referred to as trace elements. It is apparent that elements may be moved from the trace element class into the micronutrient class with increased information regarding the nutritional requirements of marine organisms. It might be possible to add arsenic, iodine, and cobalt (as vitamin B_{12}) to the list of micronutrients on the basis of current information. Although some major constituents are also nutrients, the fraction of their total amount which is incorporated into the organic cycle in the sea is negligible, not appreciably affecting the constancy of their ratios to each other, and their concentrations never fall so low as to limit the further growth of plants or animals. The nutrient elements and biochemical cycles will be discussed in a later section.

It may be said, conservatively, that very little is known about the distribution of the nonnutrient minor elements in sea water. HABER'S (1927, 1928, JAENICKE, 1935) many determinations of gold in sea water are probably the most extensive observations made on any one element, but it is now fairly well established that his analyses were not valid, because of the adsorption of the gold on the storage containers, so this body of information must be discarded, unless subsequent investigations should confirm his results.

At least some of the minor constituents are of importance biologically; for example, it has been shown that the cobalt-containing vitamin B_{12} is necessary for the growth of some marine forms; marine organisms concentrate minor elements within their bodies (for examples, see BLACK and MITCHELL, 1952, and WEBB, 1937), although in most cases it is not certain whether this is because they are necessary for life processes or incidental to their environment.

Harvey (1955) lists three mechanisms by which minor elements are concentrated by marine organisms: (a) by adsorption of ions at cell-water or intercellular interfaces; (b) by the combination of ions in solution into organic matter within plant or animal cells; and (c) the attachment of colloidal nicelles to the mucus of plants and animals.

With the advent of nuclear fission, the concentration of radioactive isotopes by marine organisms assumes a new importance, making exact information on the distribution of certain of the minor elements a matter of some urgency.

Geochemically, information on the distribution of minor elements is of considerable interest, and it is to geochemists that we owe much of our limited knowledge of the abundance of many of the elements. The classical works of GOLDSCHMIDT and his group are particularly important contributions. In matters concerning the dating of marine sediments with radioactive elements and their decay products, more precise information on the concentration and distribution of radium, thorium, ionium, and uranium is certainly wanting. (See, for example, the contradictory papers by HOLLAND and KULP, 1954a, b, and by KOCZY, 1956.)

Although few details are known of the distribution of these elements, BULJAN (1949) has noted an inverse relationship between their abundance and their increasing atomic weights, in general accordance with the periodic table of the elements. ISHIBASHI (1953) has also noted a tendency for the amount of the elements in the same group in the periodic table to decrease with increasing atomic weight.

An attempt has been made, in Table 3, to summarize current information on the quantities of the micronutrients and other minor elements. Reference is made to THOMPSON and ROBINSON (1932) for a discussion of older investigations, since many of these have been omitted from the table, as they appear to have been superseded by more reliable determinations. In some cases, there are large discrepancies between the results of various workers. Some of these are no doubt due to faulty analytical methods, others to real variations in the concentration of the elements in different parts of the oceans. One might expect that surface waters could be depleted of elements in solution by biological consumption and by adsorption on particulate matter. Many of the analyses have been made on shallow and surface waters where these mechanisms might be expected to operate. Where possible, very brief descriptions of the analytical methods used are included to help in making more critical evaluations of the determinations.

Analyses of trace elements in sea water have long been hampered by contamination from the metallic sampling devices which have been necessary for subsurface sampling. Nonmetallic samplers have now been devised (THOMPSON and CHOW, 1955; DEVEREUX, 1955) which should alleviate this problem, providing samples free of metallic contamination, suitable for the determination of trace metals.

Isotopic Composition of Sea Water

In recent years, new techniques have made possible the determination of the distribution of several of the isotopes of some of the elements found in sea water. Some of these isotopes are radioactive and of transient existence; these are useful in dating procedures. Others, such as isotopes of hydrogen, oxygen, and sulphur, are preferentially favoured in physicochemical and biophysical processes, such as evaporation, precipitation, dialysis and osmosis, and have become separated by the many repetitions of these processes in hydrochemical and biochemical cycles; isotopic ratios can therefore be used to elucidate something of the past history of a water sample.

The abundance of the radioactive isotope of carbon, C^{14}, in sea water is of considerable interest because of the possibility of using it to determine the time that a parcel of water has been isolated from exchanges with the atmosphere. The assumptions which have to be made so to use carbon-14 concentrations are complicated, and their validity cannot yet be assessed. Among other assumptions are that atmospheric and aqueous carbon-14 reach equilibrium at the surface of the sea. RAFTER (1955) has shown that surface sea waters from New Zealand were not in equilibrium with the C^{14} of the atmosphere unless it takes several hundred years for the establishment of equilibrium between atmospheric CO_2 and HCO_3^- ions in the ocean. Two other assumptions are that the contribution of modern carbon from the decomposition of organic matter settling from the surface layers to the depths is negligible or can be corrected for, and that exchanges between the sea water and sedimentary carbonate are negligible. Such changes would give the sea water fictitiously great ages, while decomposition of organic carbon compounds settling from the surface waters would lead to unrealistically short age estimates. KULP (1953) and his co-workers have published determinations of the age of sea waters from carbon-14 determination of surface and bottom waters which do not appear to take these possible errors into consideration. As yet, the data seem insufficient to be converted into "ages" of sea water, but the carbon-14 dating technique is a potentially powerful tool for investigating the past history of water masses.

Carbon^{13} is a nonradioactive isotope which MURPHY and NIER (1941) have found in the ratio $C^{12}/C^{13} = 89{\cdot}3$ in sea water, marine shells and limestone. They

Table 3. *Some Determinations of the Minor Constituents of Sea Water*

Notes:

1. All concentrations given in milligrams per cubic metre unless otherwise noted.
2. Goldschmidt (1937) and Wattenberg (1938, 1943) are review articles in which all sources of information are not specifically set forth.
3. The analyses by Noddack and Noddack (1940) were on water from Gullmarfjord; the elements were first subjected to chemical separations and then determined by optical spectrography, and checked by X-ray spectrography.
4. The analyses of Black and Mitchell were of samples of sea water taken off Plymouth, England, and the west coast of Scotland; they are all spectrographic.
5. The determinations of Webb (1937) were made spectrographically. He reported the concentrations as percentages of the total cations. The concentrations shown in the table were computed assuming that the sea water had a chlorinity of 19·00‰.
6. This is apparently an inadequate method, giving results much too high.
7. See page 78 on inclusion of fluorine in this table.

Element	Concentrations	Source of samples	Reference	Analytical method
Aluminium	600 mg/1000 kg		Goldschmidt (1937)	See Note 2
	ca. 1200		Webb (1937)	See Note 5
	162–1512 max. found at 900–1000 m	N.E. Pacific San Juan Archipelago	Haendler and Thompson (1939)	Precipitated w/oxine; oxine then diazotized and coupled with sulphanilic acid; determined colorimetrically
	295–3250	Near Aksahi City	Ishibashi and Kawai (1952)	Colorimetric comparison of aluminon lake
	315–360 ± 5%	100 samples from Japan Sea	Ishibashi and Kawai (1952)	Colorimetric comparison of aluminon lake
	0–10	Atlantic Coast, Fla. to Nova Scotia and Gulf of Mexico	Simons, Monaghan, and Taggart (1953)	Fluorimetric determination with Pentachrome Blue Black R
Antimony	< 0·5	Gullmarfjord shallow water	Noddack and Noddack (1940)	See Note 3
Arsenic	7–24	Western North Atlantic	Rakestraw and Lutz (1933)	Gutzeit method
	20 mg/1000 kg		Goldschmidt (1937)	See Note 2
	15		Wattenberg (1938, 1943)	See Note 2
	3	Gullmarfjord shallow water	Noddack and Noddack (1940)	See Note 3
	1–15 avge. 5·7	Azov Sea	Fedosov (1940)	
	5–15 avge. 10	Black Sea	Fedosov (1940)	

	5–15 avge. 6	Kerch Strait	Fedosov (1940)	
	3–12 avge. 6	Caspian Sea	Fedosov (1940)	
	15–35	Pacific	Gorgy, Rakestraw, and Fox (1948)	Gutzeit method; 50–60% found as arsenite
	2·5–6·6	Off Shirahama, Japan	Ishibashi (1953)	Concentrated from 1–2 litres by coprecipitations with $Fe(OH)_3$
	3·3–4·0	32·5° N, 135° E	Ishibashi (1953)	Concentrated from 1–2 litres by coprecipitations with $Fe(OH)_3$
	1·6–5 avge. 2·6	Waters less than 100 m off Cornwall	Smales and Pate (1952)	Radioactivation methods, directly on water samples
	2·4–3·1	English Channel	Harvey (1955)	Arsenomolybdate colorimetry
Barium	30–90		Von Engelhardt (1936)	Spectrographic
	50 mg/1000 kg		Goldschmidt (1937)	See Note 2
	< 120 mg/1000 kg		Webb (1937)	See Note 5
Bismuth	0·2	Gullmarfjord shallow water	Noddack and Noddack (1940)	See Note 3
Cadmium	0·032–0·057 mg/metric ton	Surface of Irish Sea	Mullin and Riley (1954)	Extraction with dithizone and CCl_4 followed by spectrophotometric determination. Results checked spectrographically.
	< 0·5	Gullmarfjord shallow water	Noddack and Noddack (1940)	See Note 3
Cæsium	2 mg/1000 kg		Goldschmidt (1937)	See Note 2
	2–10		Harada (1943)	Chemical concentration followed by spectrographic determination
	0·42–0·57	Eastern North Atlantic	Smales and Salmon (1955)	Concentration by ion-exchange, cobaltinitrite and bismuth iodide precipitation followed by neutron radioactivation and counting of chloroplatinates
	3·3–4·3	Japanese waters	Ishibashi and Hara (1955)	Coprecipitation with Rb and K as cobaltinitrite followed by chemical separation and colorimetric determination
Cerium	0·4 mg/1000 kg		Goldschmidt (1937)	See Note 2
Chromium	< 0·2	Gullmarfjord shallow water	Noddack and Noddack (1940)	See Note 3
	0·04, 0·05, 0·07	3 samples from Japan Sea	Ishibashi and Shigematsu (1950); Ishibashi (1953)	Concentrated with $Al(OH)_3$ and determined colorimetrically with diphenylcarbazide
	1–2·5		Black and Mitchell (1940)	See Note 4

Table 3 (contd.)—

Element	Concentrations	Source of sample	Reference	Analytical methods
Cobalt	0·1	Gullmarfjord shallow water	Noddack and Noddack (1940)	See Note 3
	< 0·3		Black and Mitchell (1952)	See Note 4
	0·38–0·67	Off Shirahama, Japan	Ishibashi (1953)	Coprecipitated with $Fe(OH)_3$; extracted with dithizone-chloroform; determined colorimetrically with thiocyanate and stannous chloride
Copper	5–11	Northern Gulf of Mexico	Riley (1937)	Copper diethyldithiocarbamate extracted w/ amyl alcohol and determined colorimetrically
	ca. 12		Webb (1937)	See Note 5
	90		Bardet, Tchakirian, and LaGrange (1938) -	Colorimetric
	10–30	Central North Atlantic; increased with depth	Kalle and Wattenberg (1938)	Method of Meyer (1938)
	< 3–12	Upper layers of Sargasso Sea		
	5		Wattenberg (1938)	See Note 2
	4	Gullmarfjord shallow water	Noddack and Noddack (1940)	See Note 3
	0·2		Wattenberg (1943)	See Note 2
	1–93	Long Island Sound	Galtsoff (1943)	Electrolytic concentration followed by colorimetric determination of copper diethyldithiocarbamate
	1·0–5·7 avge. 2·4	Japanese waters	Morita (1950)	
	0·7–1·9	Friday Harbour and Seattle, Washington surface waters	Chow and Thompson (1952)	Spectrophotometric determination of copper diethyldithiocarbamate
	1·5–24·8	Annual variation in surface water at 50° 02′ N, 04° 22′ W	Atkins (1953)	Electrolytic concentration followed by copper diethyldithiocarbamate colorimetry, or colorimetry of copper diethyldithiocarbamate concentrated in CCl_4
	0·5–0·7	Offshore surface waters	Morita (1953)	Colorimetric titration with dithizone
	0·3–1·5	Sagami and Suruga Bays	Morita (1953)	Colorimetric titration with dithizone

Fluorine See Note 7	1400	Inland and coastal waters off Washington and British Columbia	Thompson and Taylor (1933)	Colorimetric determination of bleaching by fluoride of zirconium-alizarin lake
	1416–1547	Off British Columbia; max. at 1500–2000 m		
	1000 mg/1000 kg		Goldschmidt (1937)	See Note 2
	ca. 960		Webb (1937)	See Note 5
	1400		Wattenberg (1938, 1943)	
	1300		Miyake (1939g)	
	Analytical Method	Only	Anselm and Robinson (1951)	Spectrophotometric determination of bleaching by fluoride of zirconium-alizarin lake
	1400 mg/ton	In clear sea water	Borchert (1952)	
	1305 mg/ton	At great depths	Borchert (1952)	
	770–1330 mg/1000 kg	Surface and shallow waters, Tokyo Bay	Matida (1954)	Method of Anselm and Robinson (1951)
Gallium	0·5	Gullmarfjord shallow water	Noddack and Noddack (1940)	See Note 3
Germanium	Identified		Bardet, Tchakirian, and La Grange (1938)	
Gold	< 0·1	Gullmarfjord shallow water	Noddack and Noddack (1940)	See Note 3
	0·004		Haber (1927, 1928), Wattenberg (1938, 1943)	
	0·1–0·2 mg/metric ton	Puget Sound and other Pacific inshore waters	Caldwell (1938)	Concentration w/colloidal Hg–HgCl followed by fire assay
	0·008	Gullmarfjord shallow water	Noddack and Noddack (1940)	See Note 3
	0·02	Adriatic Sea	Stark (1943)	Gold concentrated on charcoal and then determined by a combination of fire assay and micrographic methods
	0·4	Mediterranean	Stark (1943)	
	2	Iberian Atlantic Coast	Stark (1943)	
	0–46	Friday Harbour, Copalis Beach and Mutiny Bay, Washington	Putnam (1953)	Detected in sea water on amalgamated silver-zinc couple
Iodine	43		Reith (1930)	Winkler's method (Iodate reduced with arsenous and hydrochloric acids, iodine then liberated w/nitrate, extracted w/CCl_4 and determined colorimetrically)

Table 3 (contd.)—

Element	Concentrations	Source of sample	Reference	Analytical methods
Iodine (*contd.*)	26–56	Surface waters, White Sea	Skopintzev and Mikhailovskaya (1933)	
	50 mg/1000 kg		Goldschmidt (1937), Wattenberg (1938, 1943)	See Note 2
	61	Croatian Adriatic Coast	Dubravčic (1955a,b)	Colorimetric determination of the ceric ions remaining after the reduction of ceric ions by iodide, catalyzed by chloride ions
Ionium	$< 2 \times 10^{-7}$		F. F. Koczy (1956)	
Iron	60		Goldschmidt (1937)	See Note 2
	ca. 1·2		Webb (1937)	See Note 5
	2		Wattenberg (1938, 1943)	See Note 2
	Avg. 13·2 ± 5·8 0–50 m; avg. 24·4 ± 9·0 60–75 m; avg. 27·0 ± 20·1 Bottom layer	Western English Channel	Cooper (1948)	Total iron reported. Determined by 2 : 2′ dipyridyl colorimetry
	8	Gullmarfjord shallow water	Noddack and Noddack (1949)	See Note 3
	0–7	Atlantic coast, Florida to Nova Scotia and Gulf of Mexico	Simons, Monaghan, and Taggert (1953)	Colorimetric determination with ortho phenanthroline
	Particulate 0–50 Soluble 0·7–5·5	North Pacific	Lewis and Goldberg (1954)	2 : 2′ bipyridyl and bathophenanthroline spectrophotometry. Soluble iron (no particles $> 0{\cdot}5\ \mu$) and particulate iron separated by membrane filtration
Lanthanum	0·3		Goldschmidt (1937)	See Note 2
Lead	2		Wattenberg (1938)	
	3·5, 4, 8	French coastal waters, surface	Boury (1938)	Concentrated by evaporation and coprecipitation with copper sulphide; determined with dithizone
	5	Gullmarfjord shallow water	Noddack and Noddack (1940)	See Note 3
	< 8, < 5		Black and Mitchell (1952)	See Note 4

Lithium	100		Thomas and Thompson (1933)	
	70 mg/1000 kg	North Sea	Goldschmidt, Berman, Hauptmann, and Peters (1933)	Spectrographic
	70		Wattenberg (1938)	See Note 2
	100	Yamaguchi Prefecture	Ishibashi and Kurata (1939)	
	170	Brittany Coast	Bardet, Tchakirian, and Lagrange (1937)	Concentrated by evaporation, and chemical removal of major constituents. Purity confirmed spectrographically
	ca. 284–318	Heligoland	Strock (1936)	Spectrographic. Per cent of total salt reported. The figure shown assumes sea water of 35‰ salinity
	101		Webb (1937)	See Note 5
Manganese	1·1–9·9	Northeast Pacific	Thompson and Wilson (1935)	Chlorides replaced by sulphate; permanganate formed by treatment with paraperiodate and determined colorimetrically
	4 mg/1000 kg		Goldschmidt (1937)	See Note 2
	ca. 3		Webb (1937)	See Note 5
	3		Noddack and Noddack (1940)	See Note 3
	1·5–16	Baltic surface, low salinity waters	Koroleff (1947)	Adaptation of Thompson and Wilson's (1935) method
	0·7–1·0	English Channel	Harvey (1949, 1955)	Catalysis of oxidation of tetramethyldiaminodiphenylmethane
Mercury	0·03 mg/1000 kg		Stock and Cucuel (1934)	
Molybdenum	0·3–0·7	Heligoland and North Atlantic	Ernst and Hoermann (1936)	Spectroscopic
	0·7 mg/1000 kg		Goldschmidt (1937)	See Note 2
	0·5		Wattenberg (1938)	See Note 2
	2		Bardet, Tchakirian, and Lagrange (1938)	
	0·5	Gullmarfjord shallow water	Noddack and Noddack (1940)	See Note 3
	12–16		Black and Mitchell (1952)	See Note 4
	10–11	Off Maiko and Shirahama, Japan and at 33° N, 135° E	Ishibashi (1953)	Mo from 1 to 3 litres concentrated with ferric hydroxide and hexamin; separated and determined photometrically as thiocyanate in butyl acetate
	9–10	Off Shirahama, Japan	Ishibashi (1953)	Concentrated as above, separated and determined photometrically as dithiol complex in butyl acetate

Table 3 (contd.)—

Element	Concentrations	Source of samples	Reference	Analytical method
Nickel	0·07–0·17	Around Heligoland	Ernst and Hoermann (1936)	Spectroscopic
	0·07 mg/1000 kg		Goldschmidt (1937)	See Note 2
	0·1		Wattenberg (1938)	See Note 2
	0·5	Gullmarfjord shallow water	Noddack and Noddack (1940)	See Note 3
	1·5–6		Black and Mitchell (1952)	See Note 4
	0·7–0·8	Off Shirahama, Japan	Ishibashi (1953)	Coprecipitated with $Fe(OH)_3$; extracted with dimethyl glyoxime-chloroform; determined photometrically with dimethylglyoxime in alcohol
Radon	0–22 × 10^{-10} curie/M^3	Off La Jolla, California	Evans, Kip, and Moberg (1938)	Method of Evans (1935)
Radium	3·3–6·9 × 10^{-6}	Pacific	Devaputra, Thompson, and Utterback (1932)	
	38–47 × 10^{-6}	Atlantic and Hudson Bay		
	ca. 10^{-7}		Wattenberg (1938)	See Note 2
	0·0–0·32 × 10^{-6}	Pacific and Atlantic	Evans, Kip, and Moberg (1938)	Method of Evans (1935). Data of Devaputra *et al.*, believed too high
	0·28–2·9 × 10^{-7} mg/1000 kg	Eastern North Atlantic waters	Føyn, Karlick, Petterson, and Rona (1939)	Coprecipitated with $BaSO_4$, fused with sodium-potassium carbonate, leached with water, dissolved in HCl; emanated radon measured
	0·07–0·58 × 10^{-7}	Off Georges Bank, Western North Atlantic	Rona (1943) Rona and Urry (1952)	Concentrated by method of Føyn, *et al.* (1939); Radon determined by method of Urry and Piggot (1941)
	0·035–0·17 × 10^{-6}	Atlantic, Pacific, and Indian Oceans, 0–8200 m	Petterson (1955)	Method of Føyn *et al.* (1939)
Rubidium	200 mg/1000 kg	North Sea waters	Goldschmidt, Berman, Hauptmann, and Peters (1933)	Spectroscopic
	450	Black Sea	Kovaleva and Bukser (1941)	Rb and K precipitated from concentrated sea water with sodium cobaltinitrite, followed by separation and gravimetric determination

	240	English Channel	Kovaleva and Bukser (1941)	
	340	Mediterranean	Kovaleva and Bukser (1941)	
	35	Japanese Coastal waters	Ishibashi and Harada (1942)	Spectroscopic
	90–220 mg/1000 kg	Barents, Okhotsk, Black, Japan, and Karskii Seas, Greek Archipelago	Borovik-Romanova (1944)	Spectrographic. Reported probably accurate to ± 10–25 per cent
	102–136	Eastern North Atlantic	Smales and Salmon (1955)	See under Cæsium for methods
	250–400	Japanese waters	Ishibashi and Hara (1955)	Coprecipitated w/Cs and K as cobaltinitrite followed by chemical separation and gravimetric determination
Scandium	0·04 mg/1000 kg		Goldschmidt (1937)	See Note 2
Selenium	3·3–4·4	Heligoland	Goldschmidt and Strock (1935)	Concentrated by evaporation, separated by distillation; also coprecipitated with $Fe(OH)_3$
	4 mg/1000 kg		Wattenberg (1938, 1943)	See Note 2
	4–6	Japanese Coastal waters	Ishibashi, Shigematsu, and Nakagawa (1953); Ishibashi (1953)	Se from 20 litres concentrated by coprecipitations with (a) $Fe(OH)_3$ and (b) As_2S_3; Se distilled off, determined colorimetrically
Silver	0·3		Haber (1927)	
	0·5		Wattenberg (1938)	See Note 2
	0·15	Gullmarfjord shallow water	Noddack and Noddack (1940)	See Note 3
	< 0·4–2·9		Black and Mitchell (1952)	See Note 4
Thallium	< 0·01	Gullmarfjord shallow water	Noddack and Noddack (1940)	See Note 3
Thorium	< 2		Wattenberg (1938)	See Note 2
	< 0·5–< 2·0 mg/1000 kg	Scandinavian waters	Føyn, Karlick, Petterson, and Rona (1939)	Coprecipitated w/$Fe(OH)_3$; emanated thoron measured in electrometer. Upper concentration limits reported
	0·01–0·001		Koczy (1949)	By calculation
Tin	3	Gullmarfjord shallow water	Noddack and Noddack (1940)	See Note 3
	< 5		Black and Mitchell (1952)	See Note 4
Titanium	< 0·5	Gullmarfjord shallow water	Noddack and Noddack (1940)	See Note 3
	6–9		Black and Mitchell (1952)	See Note 4
	traces to 1·9		Griel and Robinson (1951, 1952)	Concentrated by coprecipitation w/$Al(OH)_3$; determined spectrophotometrically using a thymol reagent

Table 3 (contd.)—

Element	Concentrations	Source of sample	Reference	Analytical methods
Titanium (*contd.*)	3370–33,700 mg/ 1000 kg	In red tide waters off Florida	Collier (1953)	Spectrographic analyses giving range within which concentration fell
	< 337	Waters outside red tide	Collier (1953)	
Tungsten	0·09–0·10	Off Shirahama, Japan	Ishibashi (1953)	Concentrated from 60 litres by coprecipitation with $Fe(OH)_3$ by hexamethylenetetramine; Mo separated as sulphide; and Mo plus tungsten determined photometrically, tungsten determined by difference
Uranium	0·36–3·37	Scandinavian waters	Hernegger and Karlick (1935)	Concentrated by evaporation and coprecipitation w/$Fe(OH)_3$. Fe removed as carbonate, U determined by fluorescence spectrography of a uranium-sodium fluoride bead
	2		Wattenberg (1938)	See Note 2
	0·15–1·8 mg/ 1000 kg	Atlantic, Pacific, Baltic, and Adriatic water	Føyn, Karlick, Petterson, and Rona (1939)	Concentrated by coprecipitation w/$Fe(OH)_3$; chemically separated. Determined by fluorescence spectrography in NaF bead
	1·1–1·6	North Atlantic	Føyn, Karlick, Petterson, and Rona (1939)	
	1·1–1·8	North Pacific	Føyn, Karlick, Petterson, and Rona (1939)	
	0·012–0·120		F. Koczy (1949)	Calculated
	1·1, surface 1·4 at 1000 m		G. Koczy (1949)	Fluorescence methods of Hernegger and Karlick (1935)
	0·3–1·00	Off George's Bank, western North Atlantic	Rona (1943)	Method used by Føyn *et al.* (1939)
			Rona and Urry (1952)	
	2·49	Pacific	Stewart and Bentley (1954)	By fission fragment counting after dibutyl phosphate concentration
	2·8, average	31° N, 135° W	Nakanishi (1951)	Fluorimetric determination in NaF bead, concentrated with $Fe(OH)_3$
	0–1·96, surface. Up to 3·37 at depth		Nakanishi (1951)	

	1·1–1·4 × 10^{-6}	Atlantic, Pacific, and Indian Oceans, 0–7500 m	PETTERSON (1955)	Method of FØYN *et al.* (1939)
Vanadium	0·2–0·4	Heligoland and Atlantic	ERNST and HOERMANN (1936)	Spectroscopic
	0·3 mg/1000 kg		GOLDSCHMIDT (1937); WATTENBERG (1938, 1943)	See Note 2
	< 0·5	Gullmarfjord shallow water	NODDACK and NODDACK (1940)	See Note 3
	3·4–4·6	Wakayama Prefecture, Japan	ISHIBASHI, SHIGEMATSU, NAKAGAWA and ISHIBASHI (1951)	Coprecipitated w/iron by cupferron, determined colorimetrically as phosphotungstate
	2·4–7		BLACK and MITCHELL (1952)	See Note 4
	2·6–3·1	31° N, 135° E	ISHIBASHI (1953)	Coprecipitated with iron by cupferron. Separated and determined photometrically as phosphotungstate
	3·4–3·5	31·5° N, 135° E	ISHIBASHI (1953)	
Yttrium	0·3 mg/1000 kg		GOLDSCHMIDT (1937)	See Note 2
Zinc	< 8		ATKINS (1936)	Turbidimetric estimation using sodium diethyldithiocarbamate
	7 mg/1000 kg		GOLDSCHMIDT (1937)	See Note 2
	ca. 6·3		WEBB (1937)	See Note 5
	ca. 5		WATTENBERG (1938, 1943)	See Note 2
	3100 (See Note 6)	North Sea	BERTRAND (1938)	Concentrated by evaporation; sulphate removed as $BaSO_4$, Zn precipitated as calcium zincate; weighed as zinc sulphate. See Note 6
	3800 (See Note 6)	Mediterranean	BERTRAND (1938)	
	4400 (See Note 6)	Dead Sea	BERTRAND (1938)	
	14	Gullmarfjord shallow water	NODDACK and NODDACK (1940)	See Note 3
	2·8–11·7	Tokyo and Ise Bays	MORITA (1950)	
	Avge. 5·6	Misaki Channel, Japan		
	9–21		BLACK and MITCHELL (1952)	See Note 4
	1·3–1·5	Offshore surface waters	MORITA (1953)	Dithizone colorimetry
	1·8–4·4	Sagumi and Suruga Bays	MORITA (1953)	
Zirconium	337–3370 mg/1000 kg	In red tide waters off Florida	COLLIER (1953)	Spectrographic analyses giving range within which concentrations fell
	< 337	Water away from red tide		

suggest that it would be of interest to determine the C^{13} content of CO_2 collected above the surface of the sea, since the sea is considered a regulator of the atmospheric carbon dioxide.

Rakestraw, Rudd, and Dole (1951) found that the O^{18}/O^{16} ratio in oxygen dissolved in sea water varied with depth, being at a maximum at the same depth as the minimum concentrations of total dissolved oxygen. They postulated that this coincidence arises because the vertical variation in dissolved oxygen is the result of differing amounts of biological consumption of dissolved oxygen, and that the isotopes are fractionated by this same biological activity, with O^{16} being metabolized preferentially at a higher rate than O^{18}.

Oxygen and hydrogen isotopes bound as water have been investigated by a number of workers (Table 4), who have reported excesses in the density of water due to the presence of H^2, O^{18}, or both.

Table 4. Excesses in Density of Water from Various Sources due to H^2, O^{18}, *or both*

	Δd_x	Δd_y	Δd	Investigator
Polar glaciers and waters from E. Siberian Sea and Alaska	− 1·7	+ 4·3		Brodskiĭ, *et al.* (1939, 1940)
Novaya Zemlya, Franz Joseph, and Chukhot Seas	+ 2·4	0·0		Brodskiĭ, *et al.* (1939, 1940)
Kara Sea, Ob River, Greenland waters	+ 0·38	+ 2·08		Brodskiĭ, *et al.* (1939, 1940)
Pacific Ocean			+ 1·00 to + 1·67	Wirth, *et al.* (1935)
Atlantic			+ 2·3	Gilfillan (1934)
Atlantic			+ 2·28 to + 2·95	Greene & Voskuyl (1939)
Indian			+ 1·30 to + 1·67	Wirth, *et al.* (1935)
Antarctic			+ 1·01, + 1·22	Wirth, *et al.* (1935)
Bering Sea			+ 1·00 to + 1·42	Wirth, *et al.* (1935)
Baltic Sea			+ 0·21 to + 0·53	Wirth, *et al.* (1935)
Red Sea			+ 1·36 to + 1·38	Wirth, *et al.* (1935)
Mediterranean			+ 1·32 to + 1·36	Wirth, *et al.* (1935)
Pacific, Yoshihama, Kanagawa Pref.			+ 5·9	Oana (1953)
Pacific, Ajiro, Shizuoka Pref.			+ 5·2	Oana (1953)
Pacific, 25° 00′ N, 143° 40′ E			+ 4·3	Oana (1953)
Japan Sea, Hamada, Shimane Pref.			+ 3·3	Oana (1953)

Δd values are excesses in density, in parts per million, due to the heavy isotopes. Δd_x and Δd_y are the same, due to H^2 and O^{18} respectively.

Brodskiĭ *et al.*, conclude that the isotopic composition of sea water cannot be explained simply by differences in the rates of evaporation of the isotopes; clearly the origin of the water masses is also an important part of the history of the isotope ratios. Baertschi (1950) found that Hawaiian sea water contained about 0·7 per cent less O^{18} than the silicates in granite, basalt, lava, and sandstone. He assumes this effect to arise from the exchange equilibria between the total oxygen content of sedimentary silicates and the oxygen of the hydrosphere. The difference might equally well be explained on the basis of differences in isotopic separations brought about by different biogenic histories, which would be consistent with the postulate of Rakestraw, Rudd, and Dole that O^{16} is metabolized more rapidly than O^{18}.

It has been found that the partition between O^{16} and O^{18} in the reaction $\frac{1}{3}(CO_3{}^{16})^{=} + H_2O^{18} = \frac{1}{3}(CO_3{}^{18})^{=} + H_2O^{16}$ is a function of the temperature, and that $\Delta K/\Delta T = 0{\cdot}0002$ (Epstein, 1953). Using this relationship, various investigators have attempted to establish a geological thermometer, by determining the ratio of oxygen isotopes found in shellfish carbonate, and from that computing the temperature of the water in which the animal lived when forming its shell.

Deuterium is a stable isotope of hydrogen which is subjected to biological activity. Swartout and Dole (1939) found that the protium to deuterium ratio (H/D or H^1/H^2) in Atlantic Ocean water was 6880. Friedman (1953) found that the ratio in waters from the Atlantic, Pacific and Indian Oceans varied between 6536 and 6410, compared with a range of from 7519 to 6493 for fresh waters of the United States. Friedman reports that his methods of analyses are accurate to better than one part of deuterium in 6700 parts hydrogen, i.e. 1·000 ± 0·0005 parts D in 6700 parts H. According to him, the surface waters of the oceans have widely different isotopic compositions, and equatorial waters are "heavy", owing to their preferential loss of light hydrogen during evaporation. Redfield and Friedman are currently carrying on extensive investigations of the deuterium content of the oceans; their results are as yet unpublished, but a generally good direct correlation is found between the salinity and the deuterium content (Redfield, personal communication).

Tritium is a radioactive isotope of hydrogen of mass 3, a product of cosmic ray collisions in the atmosphere of 12·5 years half life and 18 years average life. It has been made the subject of extensive studies by Libby and his co-workers which have been reviewed by Libby (1955). Sea water samples contained between 0·19 ± 0·05 and 1·6 ± 0·1 tritium atoms per 10^{18} hydrogen atoms. The coastal samples were higher in tritium presumably because of run-off of recent (in terms of the half-life of tritium) rainfall. The concentrations in the open ocean led Libby to conclude that the amounts of tritium observed corresponded to complete mixing to a depth of about 100 metres. It is evident from other oceanographic results that there is a surface layer of the ocean in which vertical mixing takes place freely, but that mixing of this layer and the deeper layers is markedly hindered by density stratification. The depth of this layer depends on the stability of the water column, i.e. the change in the density of the water column with depth, and its thickness varies geographically and seasonally. Libby's conclusions appear to be of the right order for the area and time his samples were taken, and it would be interesting to see his investigations extended to include areas of considerable variation in the thickness of the mixed surface layer (which can be fairly well determined by other methods) in an attempt to assess the time that water has been in the layer.

Sulphur isotopes have been made the subject of extensive studies by Thode and his co-workers (Szabo, Tudge, Macnamara, and Thode, 1950; Thode, Kleerekoper and McElcheran, 1951; Macnamara and Thode, 1951; Thode, MACNAMARA and FLEMING, 1953, and other papers). They found that the S^{32}/S^{34} ratio in the sulphates in sea water from the Atlantic, Pacific, and Arctic oceans varied between 21·70 ± 0·02 and 21·80 ± 0·01, averaging 21·75 ± 0·02; this ratio is lower than that found in meteorites and in most terrestial sulphur, and in general is lower than that found in sulphide sulphur. It is indicated that S^{32} is enriched in sulphides produced by bacterial activity, and the values found in sea water sulphur indicate that it has been fractionated by bacterial action in the biological sulphur cycle. From the isotopic ratios in samples of known geologic chronology, THODE, MACNAMARA and FLEMING conclude that life of the sort involved in sulphur metabolism probably originated 700–800 × 10^6 years ago.

TRAFIMOV (1949) found a ratio of S^{32}/S^{34} of 21·74 for sea water, slightly lower than the average value 21·88 he found in terrestrial objects. He also reports finding the S^{32}/S^{33} ratio to be 123·4 in sea waters.

DISSOLVED ATMOSPHERIC GASES: CONSERVATIVE PROPERTIES

All the atmospheric gases are found in solution in sea water. At the interface between ocean and atmosphere, the laws of gas solubility determine the amounts of these gases which pass into solution. In solution, the fate of the dissolved gases depends on the circulation and mixing of the water containing them, and on chemical and biochemical reactions into which they may enter. Oxygen and carbon dioxide concentrations are altered within the water mass by biological action, and are said to be nonconservative. On the other hand, the other gases may be said to be conservative. Although nitrogen may be produced *in situ* by nitrogen-fixing bacteria, and is probably produced in anaerobic parts of the ocean, these are special cases which appear to have little effect on its general distribution.

The roles which dissolved oxygen and carbon dioxide play in biochemical cycles will be discussed in a later section.

Solubility of Atmospheric Gases

The solubilities of oxygen, nitrogen, carbon dioxide, argon, and helium-neon in sea water at various temperatures and chlorinities have been determined empirically by several workers. Recent new determinations of the solubility of oxygen reported by TRUESDALE, DOWNING, and LOWDEN (1955), indicate that the older results of FOX (1909), which have long been considered definitive, are too large by up to 4 per cent at the lower temperatures and by smaller amounts at higher temperatures. The new results are expressed by the following equation (TRUESDALE, *et al.*, 1955):

$$C_s' = 14{\cdot}161 - 0{\cdot}3943T + 0{\cdot}007714T^2 - 0{\cdot}0000646T^3 - S(0{\cdot}0841 - 0{\cdot}00256T + 0{\cdot}0000374T^2),$$

in which C_s' is the solubility of oxygen in parts per million, T is the centigrade temperature, and S the salinity, in parts per thousand. TRUESDALE *et al.*, suspect that equilibration methods used by FOX resulted in slightly supersaturated solution.

The solubility of nitrogen, corrected for the amount of argon plus the other rare gases, was reported by RAKESTRAW and EMMEL (1938a), and the solubility of helium plus neon was determined by Urry (1935). These nitrogen solubilities are also somewhat lower than the solubilities reported by Fox. Rakestraw and Emmel also determined the solubility of argon plus the other inert gases remaining after the removal of carbon dioxide, oxygen, and nitrogen.

If one assumes (a) constant composition of the atmosphere, (b) a total atmospheric pressure of 760 mm Hg, and (c) that in the surface layers equilibrium is established between the fugacities of the several gases in the water and air phases, one can compute the amounts of the various gases in solution. If it is then further assumed that the heat and salt content of sea water can be altered only near the surface by exchanges of energy, water and salt across the sea surface, the gaseous content which a subsurface water sample had when it left the surface of the sea can also be computed from the observed salinity and temperature. These so-called 100 per cent saturation values (O_2', N_2', etc.) are useful in estimating the quantity of oxygen which has been consumed (or produced) in subsurface waters by biological activity.

Several recent papers bear on the validity of these assumptions. Callendar (1938, 1940, 1949) has suggested that there has been a substantial increase in the carbon dioxide content of the atmosphere since the turn of the century, due to the burning of enormous quantities of fossil fuels. However, Slocum (1955) has shown that Callendar's conclusions cannot be accepted as conclusive, rather, that the question is still unanswered, since there are factors other than the burning of fuels which would alter the carbon dioxide content of the atmosphere, and Slocum's statistical analysis of the data which he selected somewhat differently than Callendar selected his, shows no appreciable change. A committee under the auspices of the Meteorological Institute of Stockholm University (Fonselius, Koroleff, and Buch, 1955), has recently been formed to examine this matter, emphasizing the collection of accurate and representative data for assessing the carbon dioxide content of the atmosphere to-day. The effect of this possible change on the sea is as yet unassessed; its effect on the amount of the other atmospheric gases in solution at equilibrium is certainly too small to measure either as an indirect secular change in the dissolved oxygen or nitrogen, or in the carbon dioxide content, particularly in view of the limited data on the CO_2 content of the sea at the end of the nineteenth century.

P. F. Scholander has pointed out that 20·9 per cent oxygen, used by Fox and commonly accepted for the composition of air, is imprecise; actually the figure is somewhere between 20·93 and 20·95 per cent, depending on the air mass sampled and the method of analysis.

Carritt (1954) has suggested that variations from a total atmospheric pressure of 760 mm Hg may bring about measurable variations in the amounts of oxygen and nitrogen dissolved in sea water at equilibrium. In high latitudes, seasonal variations of 19 to 22 mm of Hg may occur, corresponding to variations in solubility of 0·34 and 0·65 ml/litre of oxygen and nitrogen, respectively, in sea water of 20‰ chlorinity at 0°C. These variations can be measured within the accuracy of analytical methods, and in the case of nitrogen, might provide a means of detecting annual cycles in the formation of subsurface water masses.

There is considerable doubt that carbon dioxide in the air and in sea water reaches equilibrium (see Callendar, 1938, 1940, 1949, Rafter, 1955, Slocum, 1955). However, the oceans appear to be almost fully saturated with nitrogen and the noble gases, argon, helium, and neon (Rakestraw and Emmel, 1938a, 1938b, RAKESTRAW, HERRICK, and URRY, 1939), and it is probable that the assumption of equilibrium saturation at the surface with oxygen is reasonably valid. It is of interest to note that the paper by RAKESTRAW, HERRICK, and URRY supersedes the earlier, puzzling results of URRY (1935) which indicated that the helium-neon concentration varied with depth as did the oxygen concentration, a dubiously tenable proposition when one considers the chemical inactivity of the rare gases and that the characteristic vertical distribution of oxygen is clearly a function of its entering into biochemical reactions. However, URRY'S work was shown to be in error in his paper with RAKESTRAW and HERRICK, who found that the sea water was essentially saturated with neon and helium at all depths, quite contrary to the situation in the case of oxygen.

Oxygen as a Water Mass Characteristic

Although the concentration of oxygen is subject to change by biological activity, RILEY (1951) indicates that in parts of the ocean, the rates of changes are sufficiently slow that the oxygen content may be sometimes used as a quasi-conservative property, characteristic of a water mass.

ROSSBY (1936) used oxygen-salinity relationships to characterize Gulf Stream water, and more recently, ICHIYE (1954) has used oxygen concentrations to characterize waters in the Kuroshio region. RICHARDS and REDFIELD (1935) have used oxygen and its correlated density to identify and trace waters of Caribbean (and possibly other southern) origins in the Gulf Stream. The advantages of oxygen correlations is that there frequently are marked differences in the oxygen concentration of two water masses which have the same or similar temperature-salinity characteristics.

Determination of Dissolved Oxygen

Great dependence has been placed, in chemical oceanography, on the validity of the Winkler Titrimetric Method for the determination of dissolved oxygen. Comparisons of the titrimetric and gasometric methods have frequently been made in the past, and the comparable results of the two methods have recently been reconfirmed by WHEATLAND and SMITH (1955), using modern and reliable gasometric techniques. No differences greater than the errors in the methods were found. In regard to the reliability of Winkler determinations, replicate titrations of the same sample invariably give good checks in the hands of a reliable analyst. However, COOPER (1956) has discussed the considerable variability which arises, depth for depth, when one attempts to occupy replicate oceanographic stations. These appear to result from real variations in the oxygen concentration within relatively short horizontal and vertical distances. On the other hand, WORTHINGTON'S (1954) analysis shows that the oxygen concentration in the upper layers of the western North Atlantic and at all depths in the Mediterranean can be contoured as if observed synoptically although observations taken over a span of about twenty-five years are included.

There are certain dissatisfactions with the Winkler titrimetric method. Satisfactory adaptations exist for coping with small amounts of organic matter in the sample, but highly contaminated samples give poor results. SCHOLANDER, VAN DAM, CLAFF, and KANWISHER (1955) have described a microgasometric method of determining both oxygen and nitrogen which is unaffected by even large amounts of organic matter; it has the further advantage of requiring only one millilitre of sample, making it useful for the analysis of body fluids, swim-bladder gases, etc. The method appears to have an accuracy of ± 1 or 2 per cent.

Føyn (1955) has described a simple submersible dropping mercury electrode polarograph for the continuous recording of the dissolved oxygen content as a function of depth. Such an instrument should be very useful in shallower waters where the microstructure is of interest.

Other improvements over the Winkler method might be sought to permit more rapid determinations, continuous recording, or greater sensitivity. Greater sensitivity is of particular concern where near-anaerobic waters are concerned; a new colorimetric method, useful in the 2 to 25 parts per billion concentration range, has been described by Buchoff *et al.* (1955), which might find some application in chemical oceanography. However, for most oceanographic purposes, the Winkler method still very successfully combines adequate sensitivity and accuracy, simplicity, and rugged reliability.

Carbon Dioxide

Carbon dioxide enters into the equilibria

$$H_2O + CO_2 \rightleftharpoons H_2CO_3 \rightleftharpoons H^+ + HCO_3^- \rightleftharpoons 2H^+ + CO_3^=,$$

reacting as a weak acid with the excess base of sea water. The distribution of the equilibria is a function of the salinity, temperature, pressure, alkalinity and pH. At the pH of sea water, the bicarbonate (HCO_3^-) ion is the most abundant species. The carbon dioxide equilibria are described fully by Harvey (1955), who gives methods and extensive tables for calculating the components of the equilibria as functions of the above variables. Saruhashi (1955) has published new tables for computing the amounts of H_2CO_3, HCO_3^-, and $CO_3^=$ when the pH and total carbonic acid are known. Her method is implemented by a new, simple microdetermination of the total carbon dioxide, based on a Conway diffusion method, which she has described (Saruhashi, 1953b). These methods should somewhat simplify the description of the carbon dioxide system. The titration alkalinity of sea water is almost directly proportional to the salinity, but the pH and total carbon dioxide vary considerably; the total carbon dioxide content is altered by photosynthesis and respiration, in the opposite sense to the variation in dissolved oxygen.

The determination of the variables fixing the equilibrium distribution of the components of the carbon dioxide system is somewhat more difficult and frequently less precise than one might desire. Improvements in the determination of pH and alkalinity have resulted from the introduction of the glass electrode pH meter, and Anderson and Robinson (1946) have discussed the practical details of the method and factors which affect the accuracy of the determination.

BIOCHEMICAL RELATIONSHIPS IN THE OCEAN

Protoplasm is formed in the ocean by photosynthesis, from the chemicals found in sea water, sunlight supplying the required energy. Carbon dioxide, water and a variety of inorganic nutrient materials are thus taken up from the water, oxygen is liberated, and organic matter is formed. Ultimately, most of these organic compounds decompose, with the consumption of oxygen and the release of carbon dioxide and the nutrient elements to the water. Some small percentage of organic matter is lost, part temporarily, part permanently, by deposition in the sediment on the ocean floor, another small part is removed by man and animals as fish and vegetable products useful to their economy. These processes are cyclic in time and space; nutrient cycles, the food chain and the cycles of organic matter, carbon dioxide, and oxygen are aspects of them. All are interrelated; all are more or less at the mercy of the horizontal and vertical circulation of the waters.

If one imagines an initial state of the sea in which inorganic compounds of nitrogen and phosphorous are present in uniform concentration, and then introduces typical marine communities, the growth of photosynthetic organisms will proceed in the photic zone, with the consumption of the inorganic nutrients. These processes start a sequence of events in which the organic matter originally produced by the plants becomes food for herbivores, the herbivores are eaten by carnivores, which are in turn preyed upon by other carnivores through a varying number of steps until the largest animals emerge. Any of the steps may be short-circuited, but all along the chain there is a recycling of inorganic and organic excrement and remains, which, if particulate, tend to rain downward until they eventually reach the bottom where they may become incorporated into the sediment. The sequence of events is everywhere accompanied by the metabolism of bacteria, which are instrumental in the breakdown of both particulate and soluble organic matter; soluble inorganic materials formed along the chain are returned to the photic zone, and these inorganic nutrients can again enter the cycle. Even those deposited as sediment on the ocean floor can be released to the water again; this aspect of the regeneration of nutrients has recently been studied in some marine basins off the California coast by RITTENBERG, EMERY, and ORR (1955). They report that (a) nitrogeneous organic matter is partially regenerated as ammonia, and subsequently oxidized to nitrate, a process which apparently proceeds throughout the water column, (b) phosphate is regenerated most intensively in anaerobic sediment, (c) net phosphate deposition occurs in aerobic sediments of low *p*H, and (d) dissolved silicate increases with depth in the sediments.

Photosynthetic and respiratory cycles are functions of the chemical and energetic environments. Photosynthesis can proceed only when both nutrient salts and light energy from the sun are available, and respiration depends on energy chemically bound in the photic zone. In this zone, the availability of phosphate and/or nitrogen compounds will most frequently limit photosynthesis. These nutrients are present in such small concentrations that they may be completely consumed, preventing further growth until fresh supplies are brought to hand, either by recycling or by the arrival of new supplies of nutrient rich sea water into the photic zone. Recycling of nutrients and the advection of nutrient rich waters are both difficult to estimate quantitatively.

In the sea, processes of consumption and regeneration are separated in time and in horizontal and vertical space. Dead organisms and organic particulate matter tend to sink, regeneration accompanying the sinking. The return of inorganic nutrients, thus released in the deeper layers of the ocean, to the upper photic layers, where they can re-enter the cycle, and the replenishment of oxygen to the deeper layers depend on vertical water movements.

Vertical water movements may dominate the circulation, returning regenerated nutrients to the surface layers close to where they sank as particulate matter.

This type of circulation may prevail in more or less confined bodies of water vhere exchanges in and out of the area are secondary, and was assumed to xist in the Gulf of Maine by Redfield, Smith, and Ketchum (1937) who studied he cycle of phosphorous in that area. They found a net transfer downward of hosphorus during the summer months, as particulate matter sank, decomposed, nd built up concentrations of inorganic phosphate in the deep layers at the xpense of surface waters. With the advent of winter, vertical mixing was rought about by increased density of the surface waters and increased winds; he effect was to restore phosphorus to the surface layers, ready to re-ener the ycle. Seasonal cycles of nutrients in English waters have also been investigated y Harvey, Atkins, Cooper, Armstrong, and others (Harvey, 1955).

On the other hand, nutrients may sink in their organic forms in regions remote rom the areas where they return to the surface layers. This return to the surface ccurs most actively in areas of upwelling, predominantly along the west coasts f continents. In these regions, prevailing offshore winds remove the surface vater, and water from deeper layers rise to replace them. Such locations are ich in plant and animal life, in consequence of the continuing good supply of norganic nutrients.

It has been shown by Redfield (1934) that in the open ocean the fixation and egeneration of carbon dioxide, oxygen, nitrogen and phosphorus compounds ake place in statistically definite and fixed ratios one to the other. The same atios were shown to relate the amounts of these elements in inorganic solution n sea water and combined in the bodies of plankton organisms (Redfield, 1938, Fleming, 1940). Richards and Vaccaro (1956) have shown that in two naerobic environments, the Cariaco Trench and the upper layers of the Black Sea, the release of phosphorus accompanies oxygen consumption in the same atio that it does in aerobic waters, but in addition to dissolved gaseous oxygen, xygen atoms combined in the sulphate ion are reduced, with the formation of ulphides. In the deeper parts of the Black Sea there is less phosphate than vould be predicted from the combined amount of oxygen and sulphate con-umed, but it is probable that this deficit of phosphate is the result of direct naerobic fixation of phosphate by bacteria. A deficit from the predicted uantity of inorganic nitrogen compounds was observed in the Cariaco Trench. However, only the ammonia fraction was determined in the anaerobic layers, nd although nitrite and nitrate were absent, it is probable that the balance of he nitrogen is present as dissolved, free, molecular N_2, which was not measured, nd is probably present in too small quantities to be observed in the presence of he nitrogen dissolved from the atmosphere.

Thus, statistically, the populations of the oceans have, in general, a fixed omposition, which is reflected both synthetically, in the composition of plankton rganisms, and analytically in the composition of sea water. These ratios, ummarized in Table 5 from Richards and Vaccaro (1956), represent quasi-toichiometric relationships in which these elements are involved in biochemical hanges in the sea, and are in a sense a less exact counterpart of the chemical law f combining proportions. Wide variations in the ratios would be expected, and re found, especially in inshore waters and in isolated areas. Presumably the niformity in them which is found throughout the oceans reflects the general niformity of the composition of sea water when in a hypothetical base state in vhich only inorganic forms of matter might be present.

Table 5. Ratios of Carbon, Nitrogen, and Phosphorus Bound in Organic Matter and of Oxygen Consumption to Phosphate and Inorganic Nitrogen Compounds formed upon its Decomposition, by Atoms

Derivation	O	C	N	P	Reference
1. Changes in sea water and analysis of plankton organisms. Phosphate analyses corrected for salt effect according to Cooper, 1938	—	105	15	1	Redfield, 1934
2. Ratios in line 1, assuming two atoms of oxygen consumed on oxidizing one atom of carbon	210	105	15	1	
3. Ratios in line 2, further assuming the oxidation of nitrogen compounds requires four atoms of oxygen for each atom of nitrogen	270	105	15	1	Gilson, 1937
4. Average composition of plankton organisms	—	106	16	1	Fleming, 1940
5. Ratios in line 4, and the assumptions in lines 2 and 3 regarding consumption of oxygen and nitrogen	276	106	16	1	
6. Analyses of sea water, phosphate analyses corrected as in line 1	180	—	15	1	Redfield, 1934 Cooper, 1938b
7. Cariaco Trench, 50 m	235	—	15	1	
8. Cariaco Trench, 50 m to top of anærobic layer	235	—	15–3	1	
9. Cariaco Trench, anærobic layer	235*	—	2–4	1	

* Total redox reactants, AOU + $4S^{=}$, to account for oxidation by sulphate ions.

Variations in these ratios are found which are neither local and isolated nor mere statistical deviations from the mean. If one computes the amount of oxygen consumed and observes the phosphate or nitrate concentration in a sample of sea water, it is found in certain parts of the ocean that the phosphate and nitrate concentrations are greater than would be expected from the amounts of oxygen consumed (Redfield, 1942). This arises from the fact that in the major convergences, areas in high latitudes where water sinks below the sea surface, the water is fully saturated with oxygen and presumably has an appreciable burden of organic matter, but still contains fairly large concentrations of phosphate and nitrate. This is in contrast to the surface layers of the Atlantic in low and middle latitudes which are saturated with oxygen, but in which the growth of plants and animals has depleted the phosphate and nitrate to very low levels. (This is not true of equatorial Pacific waters, which contain such high concentrations of phosphate that phosphate depletion does not appear to be the limiting factor in the growth of plants.) These residual quantities of nutrients, in excess of the concentrations which would be computed from the oxygen consumption, have been called "preformed" by Redfield (1942), and can be useful tracers of water masses.

The cycles of phosphorus and nitrogen are of fundamental importance economically and practically, because they represent steps in the food chain. It may be said that all the organic matter in the sea, from the phytoplankton to the fishes and whales, is made from the sea water itself. The amount of organic matter which can be produced in the sea depends fundamentally on the amounts of nutrients present and on the circulatory processes which bring them into the photic zone, where the energy of the system can be acquired. The quantities of nutrients in the ocean are vast, but only small fractions of them are available to the food chain at any one time; below 200 to 400 metres, all but a small portion of the phosphorus is present in the inorganic form, and remains essentially isolated from the food chain. The most productive areas of the oceans are those where the circulation constantly brings renewed supplies of the nutrients into the upper layers, where they can start recycling in the food chain.

It is of interest to attempt to assess the amount of organic production taking place in the ocean. The methods involve evaluating the equation:

$$CO_2 + H_2O \xrightleftharpoons[\text{respiration}]{\text{photosynthesis in the presence of light}} CH_2O + O_2.$$

This can be done in several ways. Older methods involve measuring the changes in the carbon dioxide or oxygen content of the water. Methods for the analysis of oxygen are simpler than those for the analysis of carbon dioxide, and so changes in the oxygen content have frequently been followed. In practice, samples of the sea water are placed in bottles, some transparent, others opaque. The bottles are then exposed to as nearly natural conditions as the experiment will permit, e.g. they are frequently suspended at various depths in the sea. After a passage of time the oxygen contents of both opaque and transparent bottles are determined. Photosynthesis and respiration can both take place in the transparent bottle, but only respiration proceeds in the opaque bottle. If one assumes that the rate of respiration is the same in *both* bottles, then the difference in the amount of change in the oxygen content represents the amount of photosynthesis which has taken place. The method is open to question for several reasons which all centre about the fact that the conditions in the captive water sample do not reproduce those of the natural ocean. Some controversy has arisen lately concerning the evaluation of the method (see Steemann Nielsen, 1954; Riley, 1953; Ryther and Vaccaro, 1954; Vaccaro and Ryther, 1954), and Steemann Nielsen (1952), proposed that most of the difficulties could be circumvented by measuring the carbon fixation directly, using radiocarbon-14 to trace the amount of photosynthetic productivity. Using this method, it soon appeared that in much of the ocean, particularly areas where the organic productivity was low, the measured photosynthesis was much lower than had formerly been estimated by the oxygen method. This problem awaits a final solution, but it seems unlikely that experiments conducted in an isolated parcel of water can fully represent the dynamic system of the seas, although they may be able to give an approximation of the productive potential of a parcel of sea water and its contained plankton.

Other methods have been employed to estimate the organic productivity of the sea. One is based on relationships between the amounts of carbon, oxygen, nitrogen, and phosphorus involved in the growth and decomposition of marine organisms. Redfield, Smith, and Ketchum (1937) measured the changes in the inorganic phosphate content of the Gulf of Maine and from them computed the amount of organic production represented by the seasonal decrease in the phosphate content. Odum and Odum (1955) have measured the increase in oxygen concentration as water passed over a coral reef, and computed the amount of organic production from it. Cooper (1933) estimated the productivity in the

English Channel by measuring changes in the oxygen, carbon dioxide, phosphate, nitrate, and silica contents of the water. A balance could not be struck between the amount of silica consumed and other estimates of the productivity, and it was proposed that the silica was recycled several times. ATKINS (1945) proposed that the surplus production was to be found in the standing crop of autotrophic flagellates, because laboratory observations indicated that silica from diatom tests was redissolved too slowly to permit its rapid regeneration and recycling. More recent observations are in disagreement with this conclusion, and the amount of regeneration and recycling of silica in the upper layers has not been accurately estimated (COOPER, 1952). The extensive diatomaceous oozes on the ocean floor make it clear, however, that quantities of silica are removed from the ocean by the sinking of diatoms. SVERDRUP and FLEMING (1941) estimated the amount of organic productivity off the coast of southern California by observing the production of oxygen in the upper layers. It should be pointed out that in this method, it is difficult to eliminate the effects of the exchange of oxygen across the sea surface. These latter methods are free of experimental artifacts, but they involve estimates of the effects of a large number of other variables, none of which can be very precise.

Organic Matter in the Oceans: Quantitative and Qualitative Aspects

The organic matter in the sea may be divided among living and dead particulate matter and soluble organic compounds. Supposedly a whole spectrum of intermediate colloids exists. FOX *et al.* (1952), have described the recovery, measurement and distribution of *marine leptopel*, a term used to include all forms of particulate organic and inorganic matter suspended in the water.

Very few direct analyses of the dissolved organic carbon in sea water have been made. These have been reviewed recently in a paper by PLUNKETT and RAKESTRAW (1955), who report new analyses from three stations off Lower and Southern California and two from the northwest Pacific. They used methods described by KROGH (1934), who found little variation in the dissolved organic carbon, 2·36 mg/litre, in six samples from one Atlantic station. PLUNKETT and RAKESTRAW, however, found that at the three stations off California, organic carbon content varied between 2 and 3 mg/litre. Usually the smaller concentrations were found at intermediate depths. At the northwest Pacific stations, the concentrations ranged from 0·59 to 2·72 mg/litre, and the zone of lower carbon concentrations seemed to lie somewhat above the steep oxygen gradient.

FOX, ISAACS, and CORCORAN (1952) found widely variable amounts of organic carbon in marine leptopel; surface and near-surface water was found in and near slicks which contained from 4·16 to 19·64 mg organic carbon per litre; water taken from various ocean depths off San Diego (100 to 600 metres) contained from 0·14 to 0·47 mg/litre of organic carbon; they report a limited number of data which indicate that the organic carbon in leptopel may vary over much greater ranges than dissolved organic carbon. These data also include three analyses of organic (KJELDAHL) nitrogen in samples of leptopel from a slick area, which contained 0·71, 0·45, and 0·63 mg/litre of nitrogen. In a later paper, FOX, OPPENHEIMER, and KITTREDGE (1953) showed that the leptopel content of two random samples exhibited a threefold variation, and the organic content of the leptopel showed more than a twofold difference.

Older analyses by ROBINSON and WIRTH (1934a, 1934b) of the organic nitrogen concentration in Puget Sound waters indicated that the amounts varied widely up to 0·32 mgN/litre, with the higher values generally in the upper layers. The organic nirtogen content of Pacific waters at one station off Vancouver Island was found to vary little (0·07 to 0·09 mgN/litre) between the surface and 2000 metres. However, at another station 200 miles offshore, the values varied between 0·05 and 0·12.

Analyses of both organic carbon and nitrogen in waters from the Greenland, White, Azov, Black, and Caspian Seas have been reported by DATZKO (1939). Concentrations of 5·2 to 5·9 mgC/litre and 0·48 to 0·50 mgN/litre were found in the Caspian Sea, 2·0 to 2·6 mgC/litre and 0·21 to 0·32 mgN/litre in the Greenland and White Sea. The C/N ratio was a little over 11 in the Caspian Sea, and 8·3 and 9·5 in the White and Greenland Seas, respectively. These ratios include both particulate and dissolved organic nitrogen but only dissolved organic carbon. However, the ratios were not greatly changed by a prior precipitation with silver sulphate, which was used to remove particulate matter. In all but the Black Sea, DATZKO found the organic matter rather uniformly distributed with depth, but the organic nitrogen content of the Black Sea increased with depth. In more recent studies, DATZKO (1951) has reported that there is a gradual increase in the dissolved organic matter in the Black Sea up to 2000 metres, and a gradual decrease in the colloidal and suspended organic matter. He suggests the possibility that the processes of reduction of sulphates in the deep, anaerobic layers of the Black Sea are accompanied by the utilization of organic carbon compounds. DATZKO and DATZKO (1950) have described improvements over the KROGH and KEYS (1934) method for the determination of organic carbon in sea water.

SKOPINZEV (1939) has reported on the "oxidizability" of waters in the Barents, Polar, and Kara Seas. The quantities were determined by reduction of permanganate in neutral medium, and are reported in terms of oxygen equivalents. However, the results from these far northern waters are interesting, especially in that the northern and eastern Barents Sea, which is ice covered much of the year, contained markedly less organic matter than the west and northwestern Barents Sea. The latter contained admixtures of Atlantic water, which had not been ice-covered. It should be noted that the permanganate oxidation method is open to criticisms; among others, all the organic compounds may not be completely oxidized, and some may not be oxidized at all by this procedure. LÓPEZ-BENITO (1955) has recently made a critical study of both the alkaline and acidic permanganate oxidation in sea water, and has concluded that it cannot be satisfactorily related to the quantity of organic matter present.

Specific Organic Compounds in the Ocean

Even less is known of the occurrence of specific organic compounds in sea water than is known of the gross concentration of organic carbon. Some general classes and a few specific compounds have been detected and determined, either by chemical or biological assays.

COLLIER, RAY, and MAGNITZKY (1950), and COLLIER, RAY, MAGNITZKY, and BELL (1953) have described the occurrence of organic substances in sea water which affected the feeding and pumping of oysters. Although they did not identify the material, they showed that it passed through bacteriological filters and was not thrown down by the ordinary centrifuge. They referred to it as carbohydrate, and measured it photometrically with an N-ethyl-carbozole reagent which can be used for the quantitative estimation of small amounts of carbohydrates. The material, reported as equivalents of arabinose (which was used to standardize the photometric determination), was found in widely varying quantities (2 to 25 mg/litre).

WANGERSKY (1952) reports concentrating the material described by COLLIER *et al.*, and separating from it two fractions, one of which gave some indications of being a rhamnoside, while the other was tentatively identified as dehydroascorbic acid.

Since the papers of COLLIER *et al.*, and WANGERSKY, other workers, using their techniques, have met with varying degrees of success in determining this "carbohydrate" component in sea water. It is apparently absent (or present in very low concentration) in offshore waters, and is most usually found associated with relatively dense plankton populations.

DROOP (1955) has reported on the use of the marine organism *Monochrysis lutheri* in a bioassay for vitamin B_{12}. He reports that all assays of surface water taken on incoming tides at Millport, Scotland, between February and March 1954, gave results of between 5 and 10 mμg of vitamin B_{12} per litre. LEWIN (1954) deduced, from the growth of a marine *Stichococcus* species, that the sea water of the Northwest Arm (Halifax, Nova Scotia) contained on the order of 10 mμg of free, soluble vitamin B_{12} in the winter of 1952–53, and that this may be higher than would be found in water from the open sea. PROVASOLI and PINTNER (1953) had earlier reported 20 to 30 mμg of vitamin B_{12} in freshly collected sea water.

There has been considerable evidence in recent years to indicate that organic compounds in the sea, originating from the metabolism of marine organisms, may act either as growth promoters or inhibitors. The evidence has recently been reviewed by JOHNSTON (1955); it is largely based on observations that marine organisms may or may not grow in sea waters which are indistinguishable by their gross chemistry, including the concentration of nutrient elements. In a few cases, the effects have been more specifically demonstrated, such as in the work of COLLIER *et al.* (1950), discussed above, and by the work of PROVASOLI, HUTNER, and others (PROVASOLI and PINTER, 1953; HAMILTON, HUTNER, and PROVASOLI, 1952), who demonstrated the requirement of thiamin and cobalamine (vitamin B_{12}) in culture media, and the sensitivity of organisms to certain metabolites. JOHNSTON (1955) has reported on the effects on growth of a group of organic fractions separated from material adsorbed from sea water by activated carbon. JOHNSTON'S work does not include the specific identification of any compounds, but is an indication of a line of research likely to yield results of importance to marine biology perhaps more quickly than would rigorous qualitative organic analyses.

Oxygen Consumption in the Ocean

One of the fundamental problems in chemical oceanography involves assessing the rates at which oxygen is consumed in the ocean; knowledge of these rates would be of value in estimating rates of circulation, overturn and replacement of ocean waters and other biochemical processes. To date, estimates of the time which subsurface waters have been out of contact with the surface vary widely, and there are no direct measurements on which to base estimates of the rates of deep-water circulation. Estimates based on considerations of the oxygen content of the ocean have been made by Seiwell (1934), Sverdrup and Fleming (1941), Riley (1951), and others, but there is considerable lack of agreement among them. Although Kulp and his co-workers (Kulp, 1953) have published a few analyses of the radioactive carbon content of sea water, these do not offer convincing evidence of the "age" of the water masses sampled.

Another approach has been made by Worthington (1954), who has observed that throughout the deeper water (2000 metres) of the western North Atlantic, there has been a general decrease in the concentration of dissolved oxygen. He suggests that these waters are not in a steady state; i.e. a gradual overall change is taking place in the oxygen content of this part of the ocean, and that the water itself is not being replaced at the same rate that its oxygen content is being consumed. His observations of the rate at which oxygen appears to be disappearing lead him to believe that the deep water of the western North Atlantic was formed around the beginning of the eighteenth century. He points out that this was a period of extreme cold, and postulates that at that time surface water in high latitudes became denser than at any time since; that this water sank into the depths of the ocean, flowed southward, and has not been renewed.

Worthington's (1954, 1955) postulates concerning the "age" of the North Atlantic and Caribbean deep water are controversial, but the decrease in the oxygen content of both the deep Atlantic and deep Caribbean water in the past twenty to twenty-five years is well established, and is good evidence that appreciable changes do take place in the chemistry of deep ocean waters; this is perhaps the first of such evidence and should lead eventually to a clearer understanding of processes of ocean circulation.

In essentially all parts of the oceans, the oxygen content is at a minimum at an intermediate depth. In the Atlantic, this depth is usually between 200 and 800 metres, and minimum concentrations of between 0·5 and 1·0 ml/litre occur at about 15° north and south latitudes off the African coast. A corresponding oxygen minimum layer exists in the Pacific, but the zone is much larger and lower oxygen concentrations are found in it. In a personal communication, Dr. Norris Rakestraw has stated that he has recently observed stations in the eastern tropical Pacific where no trace of dissolved oxygen could be detected in part of the water column. It is remarkable, however, that even in these waters, living fishes were taken, in spite of the fact that very low oxygen concentrations prevail through a great depth of the water column.

The greater extremity of the oxygen deficit in the Pacific compared with the Atlantic can be explained in different ways. It has been proposed by some writers that it is the result of the greater sluggishness of the circulation of the Pacific, permitting a longer period of stagnation and concurrent oxygen consumption. However, the consumption of oxygen cannot proceed except in the presence of living or dead organic matter (ignoring the small oxygen demand of ferrous, manganous, and other reduced ions and of enzymatic metabolites); in turn, the organic matter must be formed from the sea itself, and the amount formed is limited by the amounts of phosphate and/or nitrate available in the photic depths. The Pacific is richer in phosphate and nitrate than the Atlantic, which gives it a greater potential for the formation of organic matter, so it may be that the greater consumption of oxygen there is merely the reflection of the greater supply of nutrients in the Pacific.

Present evidence indicates that anaerobic conditions can arise in the ocean only in regions where circulation is cut off or greatly impeded by the geomorphology of the region. RICHARDS and VACCARO (1956) have described the Cariaco Trench, a basin in the continental shelf off the north coast of Venezuela, which is anaerobic from about 400 metres to the bottom at about 1400 metres. This trench differs from other known anaerobic parts of the ocean, which are generally landlocked and receive larger influxes of fresh water run-off. However, the Cariaco Trench is filled with typical sea water and yet has become anaerobic.

These recent observations of the consumption of oxygen in the ocean lead one to ask if extensive portions of the Pacific can be expected to become contaminated with sulphides in the future. The evidence is that sulphides and nitrates cannot coexist in sea water, and that all nitrates would have to be reduced before sulphides could appear. Although this state of reduction has been achieved in the Cariaco Trench, it may be that a continuing supply of oxygen and nitrate to the oxygen-poor regions of the Pacific would postpone or prevent the formation of sulphides there; if a steady state exists, the oxygen and nitrates are being replaced at just the rate they are being consumed, by definition, and anaerobic conditions will not come about.

Silicon

Silicon is included as a nutrient because it is a constituent of diatoms and other phytoplankton organisms, in which it forms the tests, or outer coating. It has been shown that limiting the amount of silica available to diatoms can result in smaller tests containing less silica; it is not clear how long the growth of diatoms can continue in an environment devoid of silica but otherwise nutritionally complete.

It was formerly reported that the lowest concentrations of silica were found at the surface, and that the concentrations increased with depth to the bottom. In many parts of the oceans this is true, particularly in the Antarctic and sub-Antarctic region where the distribution of silicate was investigated by the *Discovery* expeditions and reported by CLOWES (1938). The deep waters of these regions contain concentrations of silica around ten times as high as those observed in the deep waters of the northern Atlantic (COOPER, personal communication). COOPER has suggested that the silica content of sea water may be useful in identifying the sources of certain deep water masses which are difficult to distinguish by their salinity and temperature characteristics.

Observations by the *Discovery* and by the Woods Hole Oceanographic Institution show clearly that there is a zone in the equatorial North Atlantic, between 800 and 1200 metres, in which the silicate concentrations are somewhat greater than those at shallower and at slightly greater depths. It is not clear whether this can be attributed to local regeneration of biologically fixed silicon, or is characteristic of a water mass lying at intermediate depths.

Silicate is found in sea water in true solution and in colloidal and particulate suspensions; the forms which are included in its colorimetric estimation have been investigated by ARMSTRONG (1951), COOPER (1952), and CHOW and ROBINSON (1953a). The older method of determination, due originally to DIÉNERT and WANDENBULCKE (1923) has recently been critically studied by FUKAI (1954b) and improved upon by ARMSTRONG (1951). In ARMSTRONG'S method, the yellow silicomolybic acid, which was formerly estimated colorimetrically, is reduced to molybdenum blue. MULLIN and RILEY (1955a) have further improved on Armstrong's method, by using a different reducing agent which results in a simpler procedure and more stable colour. Both have the advantage of employing a soluble silicate for an internal standard, in contrast to the artificial colour standards which were formerly used. Mullin and Riley (1955b) have also discussed the storage of sea water samples for subsequent silicate analyses.

Micronutrients

The analytical chemistry of the micronutrients, iron, manganese, and copper, has recently been reviewed by Barnes (1955), and the biological importance of these elements has been discussed by Harvey. Reasonably good analytical methods are now available for these constituents.

Iron exists in sea water generally in colloidal suspension. Lewis and Goldberg (1954) found little variation in the concentration of soluble iron in the North Pacific (around 3·4 μg/litre), but there was a wide variability in the "particulate" iron. They define soluble and particulate iron as those fractions which pass through or are retained by, respectively, a membrane filter; this appears to place particles greater than 5 microns in the "particulate" class. Cooper (1948) has listed ten different forms in which iron may be encountered in sea water, dividing them between uniformly dispersed and aggregated or particulate forms. However, these forms would be very difficult to distinguish analytically.

Determination of Nutrient Salts in Sea Water

The determination of phosphorus, nitrogen, and silicon compounds, and other minor constituents of sea water are mainly dependent on colorimetric procedures which are highly sensitive and in general have been modified to account for interferences likely to be encountered in sea water. Several of these procedures have recently been reviewed by Barnes (1955) and by Harvey (1955). Harvey has confined his review mainly to procedures employed at the Marine Biological Association laboratory at Plymouth, England.

Most of the minor constituents of sea water change rapidly upon removal from the sea and during storage, because of biological activity and adsorption on particulate matter and on the container. So the chemical oceanographer is faced with completing his analyses aboard ship as soon as possible after taking the water from the sea. Several methods have been proposed for properly preserving sea water samples for subsequent analysis, by the addition of chemical poisons or by freezing, but the methods present problems of uncertainty as to arresting biological activity, of adsorption, and of storing the accumulated samples. Collier and Marvin (1953) have described freezing techniques, and Mullin and Riley (1955b) have described the storage of silicate samples poisoned with mercuric chloride.

Modern developments in colorimetry have included photoelectric comparisons of colour intensities aimed at removing subjective errors in colour matching. Most standard photoelectric colorimeters and filter photometers are unsuited for use at sea because they are sensitive to ship motions, but satisfactory instruments have now been developed specifically for use at sea. These include the photometer invented by Harvey (1948), the instrument known as the ASOP, described by Snodgrass, Carritt, and Wooster (1954), the photometer (known as the EEP—electric eye photometer) described by FORD (1950), and that reported by COX (1954b). In the ASOP, colour imbalances are self-corrected by a servomotor-driven mechanism which indicates a measure of the optical density when the instrument is in photoelectric balance. In the EEP, the light transmitted by the sample is balanced by manually manipulating a logarithmic slit over a reference light source; the point of balance is indicated by a magic-eye electron-ray indicator tube, and the amount of the slit exposed is read either from a counter wheel or a micrometer screw. These instruments materially improve the accuracy of colorimetric determinations at sea by making colour comparisons objective and more easily standardized.

Phosphorus Compounds

The partition of phosphorus compounds among those in solution as inorganic ions (generally considered orthophosphates), those in solution as organic matter, and those present in particulate matter is of importance because of the role of phosphorus as a nutrient necessary for the growth of plants and animals. Inorganic phosphate is generally determined by the classical phosphomolybdate blue method of DENIGÈS (1920). Adaptations of the method for oceanographic use have been described in critical studies and reviews by ATKINS (1923), SEIWELL (1935), WATTENBERG (1937), ROBINSON and THOMPSON (1948a), FUKAI (1954a), HARVEY (1955), BARNES (1955), and others. In the past, uncertainties in the results have arisen because of the so-called salt-effect error, which comes about because the amount of colour developed by equal concentrations of phosphate differs in sea water and in distilled water in which standards have been made up. COOPER (1938a, b) has studied this problem, and reported various correction factors. This error is to-day largely overcome by (a) making up standards in sodium chloride or phosphate-free sea water, and (b) using photoelectric filter colorimeters. ROBINSON (1941) has described a method for preparing phosphate-free sea water, in which plankton organisms are permitted to assimilate practically all the inorganic phosphate and are then filtered off. SAEKI (1952) reports that a diminution of colour, similar to the salt effect, is brought about by nitrite. However, nitrite is almost always present in sea water in very low concentrations, and this interference may not be generally important.

Increased precision in the phosphate method can be achieved by employing strictly prepared reagents and precision methods for their addition. Such refinements have been described by WOOSTER and RAKESTRAW (1951).

In surface and tropical waters, the inorganic phosphate is usually so low that the above methods are insufficiently sensitive. Improvements in the sensitivity have been reported by GREENFIELD and KALBER (1955), who use an ascorbic acid reducing agent, and report the method sensitive to 0·016 μg atoms of phosphorus per litre. PROCTOR and HOOD (1954) extract the blue compound with isobutanol and claim an increase by an order of magnitude in the sensitivity.

"Organic" phosphate is determined as the difference between the total phosphorus and the inorganic phosphate. Methods for determining total phosphate have been described by HARVEY (1948), REDFIELD, SMITH, and KETCHUM (1937), and HANSEN and ROBINSON (1953). The latter two methods employ oxidation, using hydrogen peroxide and perchloric acid, respectively. Organic compounds are decomposed by high pressure, high-temperature acid hydrolysis in HARVEY'S method. This method and that of Redfield *et al.*, give comparable results, but the blanks are somewhat smaller in the Harvey method; Hansen and Robinson's method is reported to give somewhat higher results and smaller blanks than does the method of Redfield *et al.*

The amount of phosphorus in particulate matter can be determined by filtering off the particulate matter and determining it separately. A peroxide oxidation method has been described by Redfield *et al.* (1937), a perchloric acid method by Hansen and Robinson (1953). Unfortunately, the required manipulations of the samples lead to their contamination, and, since very small absolute quantities of phosphate are usually involved, the errors may be relatively large (Ketchum, private communication).

Some ambiguity arises in referring to particulate phosphorus, because a distinction should be made between that phosphorus which is sorbed* in and on particulate matter and that which is a more nearly integral component of the particles. Sorption reactions between inorganic ions and particles have been studied by Carritt and Goodgal (1954). Important quantities of phosphate (and other ions) may thus be associated with particulate matter; under changing conditions of temperature, salinity, *p*H, the environmental concentration of the ion, etc., materials may be thus bound or released, and possibly the particulate matter constitutes important reservoirs of nutrient materials.

The relative significance of total and inorganic phosphorus analyses from the Atlantic has been studied by Ketchum, Corwin, and Keen (1955), who conclude that the cumulative errors in the methods are such that unless the derived amount of organic phosphorus is greater than 10 per cent of the measured inorganic phosphate, it cannot be considered to represent a significant determination. In the southern North Atlantic, they found no amounts of organic phosphorus which could be considered significant at depths greater than about 1000 metres.

Harvey's determination of total phosphorus is a laboratory method requiring an autoclave, and samples must be stored after removal from the sea until they can be returned to the laboratory and analysed. Phosphorus compounds are strongly adsorbed on glass containers, and must be recovered for analysis. At the Woods Hole Oceanographic Institution, the sample bottles are thoroughly scrubbed with dilute hydrochloric acid before filling, and again prior to removing the sample for analysis. Harvey (1948) adds a quantity of thorium carbonate, which presents a large surface on which the phosphorus compounds are adsorbed to the exclusion of the glass. The carbonate is dissolved at the time of the analysis, which is then carried out on the resulting solution.

Difficulties in the analysis of the various compounds in which nitrogen is found in the ocean have interposed obstacles before the study of the nitrogen cycle in the sea. Nitrogen occurs not only in particulate and soluble organic compounds, but it is released from these to the water as ammonia; it is there subjected to bacterial nitrification processes which yield nitrite and nitrate; in some instances, where anaerobic water or sediments are involved, free gaseous nitrogen may be formed (KRISS, 1949; RITTENBERG, EMERY, and ORR, 1955; RICHARDS and VACCARO, 1956).

---

* Carritt and Goodgal (1954) use the term *sorption* to denote any reaction between a solid and a dissolved substance, whereas *adsorption* results in an accumulation on the solid surface of some environmental constituent at a greater concentration than exists at a distance from the surface, and in *absorption* solids take up a portion of the solution much as a sponge takes up water.

The satisfactory determination of nitrite ions is readily accomplished by diazotization and the formation of a diazo dye in proportion to the amount of nitrite. Recent studies of this method, and suggested improvements in respect to the compounds coupled in the diazotization reaction have been made by ROBINSON and THOMPSON (1948b), BARNES and FOLKARD (1951), BENDSCHNEIDER and ROBINSON (1952) and BARNES (1954b).

The determination of nitrate has caused considerable difficulty in the past, in spite of the fact that it is generally the most abundant nitrogen compound in the sea. Until recently, the most satisfactory reagents have been strychnidine, which is formed when strychnine is reduced either electrolytically or with nascent hydrogen (HARVEY, 1926, ZWICKER and ROBINSON, 1944, ROCHFORD, 1947, and others) and diphenylbenzidine (Atkins, 1954). MARVIN (1955) has reported a careful study of the optimum conditions for the determination of nitrate with strychnidine, coming to conclusions arrived at by WATTENBERG (1937) regarding the importance to the method of adding the reagent and the necessity of diluting the more concentrated samples. MARVIN claims satisfactory results with the method; good results can be achieved by highly experienced analysts, but we incline to agree with HARVEY (1955, p. 198) who states "This method of estimation has played a useful part [in providing a general picture of the nitrate distribution in the ocean] and now needs to be replaced by one which is more precise and certain".

Attempts to provide a "more precise and certain" method for the determination of nitrate have followed three lines (a) the use of other reagents to react with nitrate; ATKINS (1954) used diphenylbenzidine, which has some advantages over strychnidine, but many of the same drawbacks; (b) polarographic methods, one of which has been reported by CHOW and ROBINSON (1953b) and (c) the reduction of the nitrate to nitrite and determination of the latter by the generally satisfactory diazotization method. The reduction method has been investigated by FØYN (1951), who used zinc for the reduction, by MULLIN and RILEY (1955c), and by others. MULLIN and RILEY use hydrazine sulphate reducing agent in a buffered solution; this method has been subjected to some investigation at the Woods Hole Oceanographic Institution and appears to be reproducible, sensitive, and suitable for shipboard use.

A new colorimetric method for the determination of ammonia has now been described by RILEY (1953); it appears to be more satisfactory than the older titrimetric method of KROGH and KEYES (1934), which combined a vacuum distillation of the ammonia from the sea water, the *p*H of which had been carefully adjusted (to avoid the decomposition of organic amino compounds under severely alkaline conditions), and subsequent titration of the distillate by the method of TEORELL. In RILEY's method the vacuum distillation proceeds from a buffered solution; the colorimetric determination of the ammonia in the distillate is sensitive and accurate. For shipboard use, it would be advantageous to remove the ammonia from the sea water by some modification of the Conway diffusion procedure; H. ZEITLIN, of the University of Hawaii, has developed a diffusion cell for this purpose; it is large enough to contain an adequate sample of sea water, and should be convenient to use aboard ship (personal communication).

Classical methods for the determination of total (Kjeldahl) and albuminoid nitrogen were applied to sea water by Robinson and Wirth (1934a, b); Krogh and Keyes (1934) described a micro-method using an alkaline digestion, which has the advantage of not requiring the large quantities of sulphuric acid (which Krogh and Keyes reported always contained ammonia as an impurity) needed in the Kjeldahl method. No marked improvements in these methods have come to the writer's attention; a more elegant method for the determination of organically combined nitrogen is needed.

REFERENCES

Abe T. (1954) A study of the foaming of sea water. *Proc.-Verb. Assoc. d'Océan. Phys. Rome* **6,** 260–261.

Adam N. K. (1937) A rapid method for determining the lowering of tension of exposed water surfaces, with some observations on the surface tension of the sea and inland waters. *Proc. Roy. Soc. London* **B122,** 134–139.

Anderson D. H. and Robinson R. J. (1946) Rapid electrometric determination of the alkalinity of sea water using a glass electrode. *Ind. Eng. Chem. Anal. Edit.* **18,** 767.

Anselm C. D. and Robinson R. J. (1951) The spectrophotometric determination of fluorine in sea water. *J. Mar. Res.* **10** (2), 203–214.

Armstrong F. A. J. (1951) The determination of silicate in sea water. *J. Mar. Biol. Assoc. U.K.* **30,** 149–160.

Arons A. B. and Kientzler C. F. (1954) Vapor pressure of sea salt solutions. *Trans. Amer. Geophys. Union* **35,** 722–728.

Atkins W. R. G. (1923) The phosphate content of fresh and salt waters in its relationship to the growth of the algal plankton. *J. Mar. Biol. Assoc. U.K.* **13,** 119–150.

Atkins W. R. G. (1936) The estimation of zinc in sea water using sodium diethyldithiocarbamate. *Ibid.* **20,** 625.

Atkins W. R. G. (1945) Autotrophic flagellates as the major constituent of the oceanic phytoplankton. *Nature* **156,** 446–447.

Atkins W. R. G. (1953) The seasonal variation in the copper content of sea water. *J. Mar. Biol. Assoc. U.K.* **31,** 493–494.

Atkins W. R. G. (1954) Note on the use of diphenylbenzidene for the estimation of nitrate in sea water. *J. du Cons.* **20,** (2), 153–155.

Baertschi P. (1950) Über die Verteilung der Sauerstoffisotopen in der Lithosphäre. *Helv. Phys. Acta.* **23,** 536–537.

Bardet T., Tchakirian A., and LaGrange R. (1937) Dosage du lithium dans l'eau de mer. *Compt. Rend. Acad. Sci. Paris* **204,** 443–445.

Bardet T., Tchakirian A., and LaGrange R. (1938) Recherche spectrographique des éléments existant à l'état de traces dans l'eau de mer. *Ibid.* **206,** 450–452.

Barnes H. (1954a) Some tables for the ionic composition of sea water. *J. Exp. Biol.* **31** (4), 482–588.

Barnes H. (1954b) The estimation of nitrates. *Mém. Inst. Ital. Idrobiol. de Marchi* **8,** 73–80.

Barnes H. (1955) The analysis of sea water. A review. *Analyst* **80** (953), 573–594.

Barnes H. and Folkard A. R. (1951) The determination of nitrites. *Analyst* **76** (907), 599–603.

Bather J. M. and Riley J. P. (1953) The precise and routine potentiometric determination of the chlorinity of sea water. *J. du Cons.* **18** (3), 277–286.

Bather J. M. and Riley J. P. (1954) The chemistry of the Irish Sea. 1. Sulfate-chlorinity ratio. *Ibid.* **20** (2), 145–152.

Bein W., Hirsckorn H. G. and Möller L. (1935) Konstantenbestimmungen des Meerwassers und Ergebnisse über Wasserkörper. *Veroff. Inst. Meeresk., N.F., A. Geogr. Naturwiss. Reihe* **28,** 240 pp. + 14 Tafeln.

Bendschneider K. and Robinson R. J. (1952) A new spectrophotometric method for the determination of nitrite in sea water. *J. Mar. Res.* **11** (1), 87–96.

Bertrand G. (1938) Sur la quantité de zinc contenue dans l'eau de mer. *Ann. Inst. Pasteur* **62,** 571–575. Also in *Mem. Bul. Soc. Chim.* **6,** 697–700.

Black W. A. P. and Mitchell R. L. (1952) Trace elements in the common brown algæ and in sea water. *J. Mar. Biol. Assoc. U.K.* **30,** 575–584.

Borchert H. (1952) [Geochemistry of fluorine.] *Heidelberger Beitr. Mineral. Petrog.* **3** (1) 36–43. *Chem. Abstr.* (1952) **46,** 11058.

Borovik-Romanova T. F. (1944) On the rubidium content of sea water. *Dok. Akad. Nauk, U.S.S.R.* **42,** 216–218.

Boury M. (1938) Le plomb dans le milieu marin. *Rev. Trav. Off. Pêches Marit.* **11,** 157–165.

Brodskiĭ A. I., Radchenko N. P., and Smolenskaya B. L. (1939) [Isotopic composition of Arctic waters, ices, and glaciers.] *J. Phys. Chem. U.S.S.R.* **13,** 1494–1501. *Chem. Abstr.* (1941) **35,** 353.

Brodskiĭ A. I. and Radchenko N. P. (1940) Die Isotopenzusammensetzung der arktischen Meere and Eise. *Acta. Physicochim. U.R.S.S.* **13** (1), 145–56.

Buchoff L. S., Ingber N. M., and Brady J. H. (1955) Colorimetric determination of low concentrations of dissolved oxygen in water. *Anal. Chem.* **27** (9), 1401–1404.

Buljan M. (1949) The occurrence of elements in the sea water and in the earth's crust in relation to the periodic system of elements. *Acta. Adriatica* **4** (6), 171–253.

Caldwell W. E. (1938) Gold content of sea water. *J. Chem. Education* **15,** 507–10.

Callendar G. S. (1938) The artificial production of carbon dioxide and its influence on temperature. *Quart. J. Roy. Meteorol. Soc.* **64,** 223–240.

Callendar G. S. (1940) Variations of the amount of carbon dioxide in different air masses. *Ibid.* **66,** 395–400.

Callendar G. S. (1949) Can carbon dioxide influence climate? *Weather* **4,** 310–314.

Carritt D. E. (1954) Atmospheric pressure changes and gas solubility. *Deep-Sea Res.* **2** (1), 59–62.

Carritt D. E. and Goodgal S. (1954) Sorption reactions and some ecological implications. *Deep-Sea Res.* **1** (4), 224–243.

Chow D. T. W. and Robinson R. J. (1953a) Forms of silicate available for colorimetric determination. *Analyt. Chem.* **25,** 646–648.

Chow D. T. W. and Robinson R. J. (1953b) Polarographic determination of nitrate in sea water. *J. Mar. Res.* **12** (1), 1–12.

Chow T. J. and Thompson T. G. (1952) The determination and distribution of copper in sea water. I. The spectrophotometric determination of copper in sea water. *J. Mar. Res.* **11** (2), 124–138.

Chow T. J. and Thompson T. G. (1955a) Flame photometric determination of calcium in sea water and marine organisms. *Analyt. Chem.* **27** (6), 910–913.

Chow T. J. and Thompson T. G. (1955b) Flame photometric determination of strontium in sea water. *Ibid.*, 18–21.

Christie A. A. and Newman O. F. (1955) The use of a magnetic stirrer in the determination of the salinity of sea water. *J. du Cons.* **21** (1), 3–5.

Clowes A. J. (1938) Phosphate and silicate in the Southern Ocean. *Discovery Repts.* **19,** 120 pp., 25 plates.

Collier A. (1953) Titanium and zirconium in bloom of *Gymnodinium brevis*. *Science* **188,** 329.

Collier A. and Marvin K. T. (1953) Stabilization of the phosphate ratio of sea water by freezing. *Fish. Bull. U.S.* **79,** 71–76.

Collier A., Ray S. M., and Magnitzky A. W. (1950) A preliminary note on naturally occurring organic substances in sea water affecting the feeding of oysters. *Science* **111,** 151–152.

Collier A., Ray S. M., Magnitzky A. W., and Bell I. O. (1953) Effect of dissolved organic substances on oysters. *Fish. Bull. U.S.* **84,** 167–185.

Cooper L. H. N. (1933) Chemical constituents of biological importance in the English Channel, November 1930, to January 1932. Part II. Hydrogen ion concentration, excess base, carbon dioxide, and oxygen. *J. Mar. Biol. Assoc. U.K.* **18,** 729–753.

Cooper L. H. N. (1938a) Salt error in determination of phosphate in sea water. *J. Mar. Biol. Assoc. U.K.* **23,** 171–178.

Cooper L. H. N. (1938b) Redefinition of the anomaly of the nitrate-phosphate ratio. *Ibid.* **23,** 179.

Cooper L. H. N. (1948) The distribution of iron in the waters of the western English Channel. *J. Mar. Biol. Assoc. U.K.* **27,** 279–313.

Cooper L. H. N. (1952) Factors affecting the distribution of silicate in the North Atlantic Ocean and the formation of North Atlantic deep water. *J. Mar. Biol. Assoc. U.K.* **30,** 511–526.

Cooper, L. H. N. (1956) *Ibid. In Ed.*

Cox R. A. (1954a) An apparatus for determining the salinity of sea water. *J. du Cons.* **20** (1), 9–17.

Cox R. A. (1954b) A filter photometer for use at sea. *J. Sci. Instr.* **31**, 374–376.

Darmois R. and J. (1947) Mesures viscosimétriques en Méditerranée et définition d'une nouvelle constante océanographique. *Compt. Rend. Acad. Sci. Paris* **225**, 1167–1169.

Darmois R. and J. (1950) Déterminations physicochimiques en Mer du Nord. *Ibid.* **230**, 316–317.

Datzko V. G. (1939) Organic matter in water of certain seas. *Compt. Rend. Acad. Sci. U.R.S.S.* **24** (3), 294–297.

Datzko V. G. (1951) [Vertical distribution of organic matter in the Black Sea.] (*In Russian.*) *Dokl. Akad. Nauk U.S.S.R.* **77**, 1059–1062.

Datzko V. G. and Datzko V. E. (1950) [Method of determination of organic carbon in natural waters.] (*In Russian.*) *Dokl. Akad. Nauk U.S.S.R.* **73**, 337–339.

Denigès G. (1920) Réaction de coloration extrêmement sensible des phosphates et des arseniates. *Compt. Rend. Acad. Sci. Paris* **171**, 802–804.

Devaputra D., Thompson T. G., and Utterback C. L. (1932) The radioactivity of sea water. *J. du Cons.* **7**, 358–366.

Devereux R. F. (1955) Progress report on oceanographic instrumentation. *Univ. Calif., Scripps Inst. Oceanogr. Ref.* 55–19, iv + 11 pp. (Unpub. mms.)

Diénert F. and Wandenbulcke F. (1923) Sur le dosage de la silice dans les eaux. *Compt. Rend. Acad. Sci. Paris* **176**, 1478–1480.

Dittmar W. (1884) Report on researches into the composition of ocean-water, collected by H.M.S. *Challenger*, 1873–1876; *Sci. Res. Voyage Challenger* 1873–76, *Chem. Phys.* **1**, 251 pp.

Droop M. R. (1955) A suggested method for the assay of vitamin B_{12} in sea water. *J. Mar. Biol. Assoc. U.K.* **34** (3), 435–440.

Dubravčic M. (1955a) Determination of iodine in common salt by the catalytic reduction of ceric ions. *Analyst.* **80**, 146–153.

Dubravčic M. (1955b) Determination of iodine in natural waters. *Ibid.* **80**, 295–300.

Epstein S. (1953) Mass spectrometer for the measurement of small differences in isotope abundance ratios. *U.S. Natl. Bur. Stand. Circ.* **522**, 133–139.

Ernst T. and Hoermann H. (1936) Bestimmung von Vanadium, Nickel und Molybdän im Meerwassers. *Nach. Ges. Wiss. Göttingen, Math.-Phys. Kl., Fach. IV N.F.* **1** (16), 205–208.

Evans R. D. (1935) Apparatus for the determination of minute quantities of radium, radon and thoron in solids, liquids and gases. *Rev. Sci. Instr.* (*N.S.*) **6**, 99–112.

Evans R. D., Kip A., and Moberg E. (1938) The radium and radon content of Pacific Ocean water, life and sediments. *Amer. J. Sci.* (5), **36**, 241–259.

Fedosov M. V. (1940) Arsenic in waters of the Azov, Black and Caspian Seas. *Compt. Rend. Acad. Sci. U.R.S.S.* **27**, 236–9.

Fleming R. H. (1940) The composition of plankton and units for reporting populations and reproduction. *Proc. Sixth Pacific Sci. Congr. Calif.* 1939 **3**, 535–540.

Fonselius S., Koroleff F., and Buch K. (1955) Microdetermination of CO_2 in the air, with current data for Scandinavia. *Tellus* **7** (2), 258–265.

Ford W. L. (1950) Seagoing photoelectric colorimeter. *Anal. Chem.* **22** (11), 1431–1435.

Fox C. J. J. (1909) On the coefficients of absorption of nitrogen and oxygen in distilled water and sea water, and of atmospheric carbonic acid in sea water. *Trans. Faraday Soc.* **5**, 68–87.

Fox D. L., Isaacs J. D., and Corcoran E. F. (1952) Marine leptopel, its recovery, measurement and distribution. *J. Mar. Res.* **11** (1), 29–46.

Fox D. L., Oppenheimer C. H., and Kittredge J. S. (1953) Microfiltration in oceanographic research. 2. Retention of colloidal micelles by adsorptive filters and by filter-feeding invertebrates; proportions of dispersed organic to dispersed inorganic matter and to organic solutes. *J. Mar. Res.* **12** (2), 233–243.

Føyn E. (1951) Nitrogen determinations in sea-water. *Rep. Norwegian Fish. Mar. Invest.* **9** (14), 7 pp.

Føyn E. (1955) Continuous oxygen recording in sea water. *Rep. Norwegian Fish. Mar. Invest.* **11** (3), 8 pp.

Føyn E., Karlick B., Petterson H., and Rona E. (1939) Radioactivity in sea water. *Göteborgs Kungl. Vetenskaps-och Vitterhets Sämh. Handl., Femte Føljden* (B) **6** (12), 44 pp.

Friedman I. (1953) Deuterium content of natural waters. *Geochim. Cosmochim. Acta* **4**, 89–103.

FUKAI R. (1954a) Critical studies on the analytical methods for minor chemical constituents in sea water. 1. On the estimation of phosphate-phosphorus. *J. Oceanogr. Soc. Japan* **10** (3), 112–120.

FUKAI R. (1954b) Critical studies on the analytical methods for minor chemical constituents in sea water. 2. Some notes on the determination of silicate. *Ibid.* **10** (4), 201–208.

GALTSOFF P. S. (1943) Copper content of sea water. *Ecology* **24,** 263–265.

GÁMEZ J. C. (1942) El indice de refracción en el estudio de la densidad del agua del mar. *Anales fís. y quím (Madrid)* **38,** 148–174 (Revista).

GHEORGHIU V. G. and CALINICENCO N. (1940) Étude sur la variation de la conductibilité électrique de l'eau de la Mer Noire avec la température et son emploi à la mesure de la température de l'eau marine. *Ann. Sci. Univ. Jassy* **26,** Sect. II (1), 3–18.

GILFILLAN E. S., Jr. (1934) The isotopic composition of sea water. *J. Amer. Chem. Soc.* **56,** 406–408.

GILSON H. C. (1937) The nitrogen cycle. *John Murray Exped.*, 1933–34. *Sci. Rept.* **2** (8), 21–81.

GOLDSCHMIDT V. M. (1937) The principles and distribution of chemical elements in minerals and rocks. *J. Chem. Soc.* **1937,** 655–673.

GOLDSCHMIDT V. M., BERMAN H., HAUPTMANN H., and PETERS O. (1933) Zur Geochemie der Alkalimetalle. *Nach. Ges. Wiss. Göttingen, Math. Phys. Kl.* **2,** 235–244.

GOLDSCHMIDT V. M. and STROCK L. W. (1935) Zur Geochemie des Selens II. *Ibid., Fach. IV, N.F.* **1** (11), 123–142.

GORGY S., RAKESTRAW N. W., and FOX D. L. (1948) Arsenic in the sea. *J. Mar. Res.* **7,** 22–32.

GREENE C. H. and VOSKUYL R. J. (1939) The deuterium-protium ratio. 1. The densities of natural waters from various sources. *J. Amer. Chem. Soc.* **61,** 1342–1349.

GREENFIELD L. J. and KALBER F. A. (1955) Inorganic phosphate measurement in sea water. *Bull. Mar. Sci., Gulf and Carib.* **4** (4), 323–335.

GRIEL J. V. and ROBINSON R. J. (1951) The spectrophotometric determination of titanium with thymol. *Anal. Chem.* **23,** 1871–1873.

GRIEL J. V. (1952) Titanium in sea water. *J. Mar. Res.* **11** (2), 173–9.

HABER F. (1927) Das Gold im Meerwasser. *Zeits. Angew. Chem.* **40,** 303–314.

HABER F. (1928) Das Gold im Meer. *Zeits. Ges. Erdk., Berl. Ergänzungsheft* **3,** 3–12.

HAENDLER H. M. and THOMPSON T. G. (1939) Determination and occurrence of aluminium in sea water. *J. Mar. Res.* **2,** 12–16.

HAMILTON L. D., HUTNER S. H., and PROVASOLI L. (1952) The use of protozoa in analysis. *Analyst,* **77,** 618–625.

HAMON B. V. (1955) A temperature-salinity-depth recorder. *J. du Cons.* **21** (1), 72–73.

HAMPEL C. A. (1950) Densities and boiling points of sea water concentrates. *Ind. Eng. Chem.* **42,** 383–386.

HANSEN A. L. and ROBINSON R. J. (1953) The determination of organic phosphorus in sea water with perchloric acid oxidation. *J. Mar. Res.* **12** (1), 31–42.

HARADA Y. (1943) Chemical studies on the ocean. (XVII). [On the determination of cesium in sea water and in bittern.] (In Japanese.) *J. Chem. Soc. Japan* **64,** 1049–1053; *Chem. Abstr.* (1947) **41,** 3394.

HARVEY H. W. (1926) Nitrate in the sea. *J. Mar. Biol. Assoc. U.K.* **14,** 71–88.

HARVEY H. W. (1948) The estimation of phosphate and of total phosphate in sea waters. *Ibid.* **27,** 337–359.

HARVEY H. W. (1949) On manganese in sea and fresh waters. *Ibid.* **28,** 155–164.

HARVEY H. W. (1955) The chemistry and fertility of sea waters. The University Press, Cambridge, v + 224 pp.

HASLAM J. and GIBSON R. O. (1950) The analytical chemistry of bromine manufacture. III. Survey of the in-shore waters round the coasts of Great Britain. *Analyst* **75,** 357–370.

HERNEGGER F. and KARLICK B. (1935) Uranium in sea-water. *Göteborgs Kungl. Vetenskaps-och Vitterhets-Sämh. Handl., Femte Føljden* **4** (12), 15 pp.

HIGASHI K., NAKAMURA K., and HARA R. (1931) [The specific gravity and the vapor pressure of concentrated sea water from 0° to 175°.] *J. Soc. Chem. Ind. Japan,* 34, *Suppl. Bind.* **72.** *Chem. Abstr.* (1931) **25,** 2606.

HOLLAND H. D. and KULP J. L. (1954a) The transport and deposition of uranium, ionium, and radium in rivers, oceans and ocean sediments. *Geochim. Cosmochim. Acta* **5** (5), 197–213.

HOLLAND H. D. and KULP J. L. (1954b) The mechanism of removal of ionium and radium from the oceans. *Ibid.* **5** (5), 214–224.

Honma M. (1955) Flame photometric determination of chloride in sea water. *Analyt. Chem.* **27** (10), 1656–1659.

Ichiye T. (1954) On the distributions of oxygen and their seasonal variations in the adjacent seas of Japan, (I) and (II). *Oceanogr. Mag. Japan* **6** (2), 41–66; 67–100.

Ishibashi M. (1953) Studies on minute elements in sea water. *Rec. Oceanogr. Wks. Japan. N.S.* **1** (1), 88–92.

Ishibashi M. and Hara T. (1955) On the content of rubidium and cesium in sea water. *Rec. Oceanogr. Wks. Japan* **2** (1), 45–48.

Ishibashi M. and Harada T. (1942) [Chemical studies of the ocean. XI. Quantitative determination of rubidium in sea water and in bittern.] (In Japanese.) *J. Chem. Soc. Japan* **63** (3), 211–216. *Chem. Abstr.* (1947) **41**, 2945.

Ishibashi M. and Kawai T. (1952) Chemical studies on the ocean. XXIV. Determination of aluminium in sea water. XXV. Aluminium content of sea water. *J. Chem. Soc. Japan, Pure Chem. Sect.*, 280–2; 491–3.

Ishibashi M. and Kurata K. (1939) [Determination of lithium in sea water and bittern.] (In Japanese.) *J. Chem. Soc. Japan* **60**, 1109–11. *Chem. Abstr.* (1940) **34**, 4314.

Ishibashi M. and Shigematsu T. (1950) Determination of chromium in sea water. *Bull. Inst. Chem. Res., Kyoto Univ.* **23**, 59–60.

Ishibashi M., Shigematsu T., and Nakagawa Y. (1953) Determination of selenium in sea water. *Rec. Oceanogr. Wks. Japan* **1**, 44–48.

Ishibashi M., Shigematsu T., Nakagawa Y., and Ishibashi Y. (1951) The determination of vanadium in sea water. *Bull. Inst. Chem. Res., Kyoto Univ.* **24**, 68–69.

Jacobson A. W. (1948) An instrument for recording continuously the salinity, temperature, and depth of sea water. *Trans. Amer. Inst. Elec. Eng.* **67**, 1–9.

Jaenicke J. (1935) Habers Forschungen über das Goldvorkommen im Meerwasser. *Naturwiss.* **23**, 57–63.

Johnston R. (1955) Biologically active compounds in the sea. *J. Mar. Biol. Assoc. U.K.* **34**, 185–195.

Kalle K. and Wattenberg H. (1938) Über Kupfergehalt des Ozeanwassers. *Naturwiss.* **26**, 630–631.

Ketchum B. H., Corwin N., and Keen D. J. (1955) The significance of organic phosphorous determinations in ocean waters. *Deep-Sea Res.* **2** (3), 172–181.

Knudsen M. (1901) Hydrographical tables. C.E.C. Gad, Copenhagen, v + 63 pp.

Koczy F. F. (1949) Thorium in sea water and marine sediments. *Geol. Fören. Förhandl., Stockholm* **71**, 238–242.

Koczy F. F. (1956) Geochemistry of the radioactive elements in the ocean. *Deep-Sea Res.* **3** (2), 93–103.

Koczy G. (1950) [Further uranium determinations in samples of sea water.] *Sitzb. d. Österr. Akad. Wiss. Math. Naturw. Kl., Sitzber, Abt. IIa* **158**, 113–121.

Koroleff F. (1947) Determination of manganese in natural waters. *Acta Chem. Scand.* **1**, 503–506.

Kovaleva K. N. and Bukser E. S. (1941) Determination of rubidium in sea water. (In English.) *Dopovidi Akad. Nauk, U.R.S.R.* **1940** (5), 35–36.

Kriss A. E. (1949) [The role of micro-organisms in the accumulation of hydrogen sulfide, ammonia, and nitrogen in the depths of the Black Sea.] (In Russian.) *Priroda*, 1949 (6), 35–46.

Krogh A. (1934) Conditions of life in the ocean. *Ecol. Monogr.* **4**, 421–429.

Krogh A. and Keys A. (1934) Methods for the determination of dissolved organic carbon and nitrogen in sea water. *Biol. Bull.* **67** (1) 132–144.

Kulp J. L. (1953) Carbon-14 measurements on geological samples. *Atomics* **4**, 96–98.

Lewin R. A. (1954) A marine *Stichnococcus* sp. which requires vitamin B_{12} (Cobalmin). *J. Gen. Microbiol.* **10**, 93–96.

Lewis G. J., Jr. and Goldberg E. D. (1954) Iron in marine water. *J. Mar. Res.* **13** (2), 183–197.

Lewis G. J., Jr. and Thompson T. G. (1950) Effect of freezing on the sulphate chlorinity ratio in sea water. *J. Mar. Res.* **9** (3), 211–217.

Libby W. F. (1955) Tritium in nature. *J. Wash. Acad. Sci.* **45** (10), 301–314.

López-Benito M. (1955) Sobre determinación de materia organica en el agua del mar con permanganato potásico. *Invest. Pesq.* **1**, 67–71.

Lumby J. R. and Folkard A. R. (1954) Variations in the surface tension of sea water *in situ*. *Proc.-Verb. Assoc. d'Océanogr. Phys. Rome* **6**, 284–285.

MACNAMARA J. and THODE H. G. (1951) The distribution of sulfur^{34} in nature and the origin of native sulfur deposits. *Research, London* **4,** 582–583.

MARVIN K. T. (1955) Notes on the precision of a modified routine nitrate-nitrite analysis. *J. Mar. Res.* **14** (1), 79–87.

MATIDA Y. (1951) [On the chemical composition of the sea water in the Tokyo Bay.] (In Japanese, English summary.) *Contrib. Cent. Fish. Stat. Japan,* 1948–1949, No. 138, 6 pp.

MATIDA Y. (1954) On the source and fate of fluorine in water in Tokyo Bay. *J. Oceanogr. Soc. Japan* **10** (2), 71–76.

MATIDA Y. and YAMAUCHI N. (1951) On the distribution of bromine in the ocean. (In Japanese, English summary.) *Cent. Fish. Stat. Japan, Contrib.,* 1948–1949, No. 139, 5 pp.

MEYER H. (1938) Die photometrische Bestimmung des Kupfers im Seewasser. *Ann. Hydrog. u. Marit. Meteorol.* **66,** 325.

MIYAKE Y. (1939a) A new indicator for the determination of chlorinity in sea water. *Geophys. Mag. Japan* **12,** 299–300.

MIYAKE Y. (1939b) Strontium in sea water. *Geophys. Mag. Japan* **12,** 305–306.

MIYAKE Y. (1939c) Chemical studies of the western Pacific ocean. 1. The chemical composition of the oceanic salt. Part 1. *Bull. Chem. Soc. Japan* **14** (2), 29–34.

MIYAKE Y. (1939d) *Ibid.* II. Part 2. *Ibid.* 55–58.

MIYAKE Y. (1939e) *Ibid.* III. Freezing point, osmotic pressure, boiling point and vapour pressure of sea water. *Ibid.* 58–62.

MIYAKE Y. (1939f) *Ibid.* IV. The refractive index of sea water. *Ibid.* **14** (6), 239–242.

MIKAKE Y. (1939g) *Ibid.* VI. The vertical variation of minor constituents of the "Kurosio" region. Part 2. *Ibid.* **14** (10), 467–471.

MIYAKE Y. (1943) [Foaming properties of sea water.] *Science, Japan* **13,** 358–359. *Chem. Abstr.* (1951) **45,** 9935.

MIYAKE Y. and ABE T. (1948) A study of the foaming of sea water. Part 1. *J. Mar. Res.* **1** (1). 67–73.

MIYAKE Y. and KOIZUMI M. (1948) Measurement of the viscosity coefficient of sea water. *Ibid.* **7** (1), 63–66.

MIYAKE Y. and MATUI H. (1939) Boric acid content in sea water. *Geophys. Mag. Japan* **12,** 301–303.

MORITA Y. (1950) [Distribution of copper and zinc. IV. Copper and zinc contents of sea water.] (In Japanese.) *J. Chem. Soc. Japan, Pure. Chem. Sect.* **71,** 246–248. *Chem. Abstr.* (1951) **45,** 4856.

MORITA Y. (1953) Copper and zinc in Pacific waters. I. *Rec. Oceanogr. Wks. Japan* **1** (2), 49–51.

MULLIN J. B. and RILEY J. P. (1954) Cadmium in sea water. *Nature* **174,** 42.

MULLIN J. B. and RILEY J. P. (1955a) The colorimetric determination of silicate with special reference to sea and natural waters. *Analyt. Chim. Acta* **12** (2), 162–176.

MULLIN J. B. and RILEY J. P. (1955b) Storage of sea water samples for the determination of silicate. *Analyst.* **80** (946), 73–74.

MULLIN J. B. and RILEY J. P. (1955c) The spectrophotometric determination of nitrate in natural waters, with particular reference to sea water. *Analyt. Chim. Acta* **12** (5), 464–480.

MURPHY B. F. and NIER A. O. (1941) Variations in the relative abundance of the carbon isotopes. *Phys. Rev.* (2) **59,** 771–772.

NAKANISHI M. (1951) Fluorometric microdetermination of uranium. V. The uranium content of sea water. *Bull. Chem. Soc. Japan* **24,** 36–38.

NISIKAWA T., OKUNO T., MAEDA M., and OGATA Y. (1939) [Ocean water taken in various parts of the world.] *J. Soc. Chem. Ind. Japan* **42,** Suppl. Bind. 71–72. *Chem. Abstr.* (1939) **33,** 5714.

NODDACK I. and NODDACK W. (1940) Die Haufigkeiten der Schwermetalle in Meerestieren. *Ark. Zool.* **32A** (4), 35 pp.

OANA S. (1953) Distribution of heavy water in natural waters. *J. Earth Sci., Nagoya Univ.* **1,** 42–61.

OBARA N. (1951) Sulfate anomaly as indicator of stagnation. *J. Geogr. Tokyo* **60,** 173–175.

ODUM H. T. (1951) Notes on the strontium content of sea water, celestite radiolaria, and strontianite snail shells. *Science* **114,** 211–213.

ODUM H. T. and ODUM E. P. (1955) Trophic structure and productivity of a windward coral reef community on Eniwetok Atoll. *Ecol. Monogr.* **25,** 291–320.

Petterson H. (1955) Manganese nodules and oceanic radium. *Pap. Mar. Biol. Oceanogr. Deep-Sea Res., Suppl. to* v. 3, 335–345.

Plunkett M. A. and Rakestraw N. W. (1955) Dissolved organic matter in the sea. *Pap. Mar. Biol. Oceanogr. Deep-Sea Res., Suppl. to* v. 3, 12–14.

Pollack M. J. (1954) The use of electrical conductivity measurements for chlorinity determinations. *J. Mar. Res.* **13** (2), 228–231.

Proctor C. M. (1956) Chlorinity titration. I. Evaluation of potentiometric errors. *Trans. Amer. Geophys. Union* **37** (1), 31–37.

Proctor C. M. and Hood D. W. (1954) Determination of inorganic phosphate in sea water by an iso-butanol extraction procedure. *J. Mar. Res.* **13** (1), 122–132.

Provasoli L. and Pintner I. J. (1953) Assay of vitamin B_{12} in sea water. *Proc. Soc. Protozool.* **4,** 10.

Putnam C. L. (1953) The gold content of sea water. *J. Chem. Educ.* **30,** 576–579.

Rafter T. A. (1955) ^{14}C variations in nature and the effect on radiocarbon dating. *New Zealand J. Sci. Tech., Gen. Res. Sect.* **37** (1), 20–38.

Rakestraw N. W. and Emmel V. M. (1938a) The solubility of nitrogen and argon in sea water. *J. Phys. Chem.* **42** (9), 1211–1215.

Rakestraw N. W. and Emmel V. M. (1938b) The relation of dissolved oxygen to nitrogen in some Atlantic waters. *J. Mar. Res.* **1** (3), 207–216.

Rakestraw N. W., Herrick C. E. Jr., and Urry W. D. (1939) The helium-neon content of sea water and its relation to the oxygen content. *J. Amer. Chem. Soc.* **61,** 2806–2807.

Rakestraw N. W. and Lutz F. B. (1933) Arsenic in sea water. *Biol. Bull.* **65,** 397.

Rakestraw N. W., Rudd DeF. P., and Dole M. (1951) Isotopic composition of oxygen in air dissolved in Pacific Ocean water as a function of depth. *J. Amer. Chem. Soc.* **73,** 2976.

Redfield A. C. (1934) On the proportions of organic derivatives in sea water and their relation to the composition of plankton. In James Johnstone Mem. Vol., Univ. Press of Liverpool, pp. 176–192.

Redfield A. C. (1942) The processes determining the concentrations of oxygen, phosphate, and other organic derivatives within the depths of the Atlantic Ocean. *Pap. Phys. Oceanogr. Meteorol.* **9** (2), 22 pp.

Redfield A. C. (1948) Characteristics of sea water. In The Corrosion Handbook, H. H. Uhlig, Ed., John Wiley & Sons, Inc. N.Y., pp. 1111–1122.

Redfield A. C., Smith H. P., and Ketchum B. H. (1937) The cycle of organic phosphorus in the Gulf of Maine. *Biol. Bull.* **73** (3), 421–443.

Reith J. F. (1930) Der Jodgehalt von Meerwasser. *Res. Trav. Chim. Pays-Bas* **49,** 142–150.

Richards F. A. and Redfield A. C. (1955) Oxygen-density relationships in the western North Atlantic. *Deep-Sea Res.* **2,** 182–199.

Richards F. A. and Vaccaro R. F. (1956) The Cariaco Trench, an anærobic basin in the Caribbean Sea. *Deep-Sea Res.* **3** (3), 214–228.

Riley G. A. (1937) The significance of the Mississippi River drainage for biological conditions in the northern Gulf of Mexico. *J. Mar. Res.* **1** (1), 60–74.

Riley G. A. (1951) Oxygen, phosphate, and nitrate in the Atlantic Ocean. *Bull. Bingham Oceanogr. Coll.* **13** (1), 126 pp.

Riley G. A. (1953) Measuring organic production in the sea. *J. du Cons.* **19** (1), 85–89.

Riley J. P. (1953) The spectrophotometric determination of ammonia in natural waters with particular reference to sea water. *Analyt. Chim. Acta* **9** (6), 575–589.

Rittenberg S. C., Emery K. O., and Orr W. L. (1955) Regeneration of nutrients in sediments of marine basins. *Deep-Sea Res.* **3,** 23–45.

Robinson R. A. (1954) The vapour pressure and osmotic equivalence of sea water. *J. Mar. Biol. Assoc. U.K.* **33** (2) 448–455.

Robinson R. J. (1941) A method of freeing sea water of phosphate. *Science* **93** (2405), 117–118.

Robinson R. J. and Knapman F. W. (1941) The sodium-chlorinity ratio of ocean waters from the northeast Pacific. *J. Mar. Res.* **4** (2), 142–152.

Robinson R. J. and Thompson T. G. (1948a) The determination of phosphates in sea water. *Ibid.* **7** (1), 33–41.

Robinson R. J. and Thompson T. G. (1948b) The determination of nitrites in sea water. *Ibid.* **7** (1), 42–48.

Robinson R. J. and Wirth H. E. (1934a) Report on the free ammonia, albuminoid nitrogen and organic nitrogen in the waters of the Puget Sound area during the summers of 1931 and 1932. *J. du Cons.* **9** (1), 15–27.

ROBINSON R. J. and WIRTH H. E. (1934b) Free ammonia, albuminoid nitrogen and organic nitrogen in the waters of the Pacific Ocean off the coasts of Washington and Vancouver Island. *Ibid.* **9** (2), 187–195.

ROCHFORD D. J. (1947) The preparation and use of Harvey's reduced strychnine reagent in oceanographical chemistry. *Conc. Sci. Ind. Res. Australia, Bull.* **220** (*Div. Fish Rept. No.* 13), 32 pp.

ROCHFORD D. J. (1954) A chainomatic pyconometer for the determination of chlorine in sea water. *Nature* **174** (4431), 641–642.

RONA E. (1943) Radioactivity of sea water. *Amer. Phil. Soc. Yearbook*, 1943, 136–138.

RONA E. and URRY W. D. (1952) Radioactivity of ocean sediments. VIII. Radium and uranium contents of ocean and river waters. *Amer. J. Sci.* **250**, 241–262.

ROSSBY C.-G. (1936) Dynamics of steady ocean currents in the light of experimental fluid mechanics. *Pap. Phys. Oceanogr. Meteorol.* **5** (1), 43 pp.

RYTHER J. H. and VACCARO R. F. (1954) A comparison of the oxygen and 14c methods of measuring marine photosynthesis. *J. du Cons.* **20** (1), 25–34.

SAEKI A. (1952) Some substances in sea water which disturb the colorimetric determination of phosphate. *J. Oceanogr. Soc. Japan* **8** (2), 73–78.

SAINT-GUILY B. (1954) Sur la détermination de l'indice de réfraction et de la densité de l'eau de mer par interférométrie, avec une table donnant l'indice de réfraction de l'eau de mer en fonction de la température et de la densité. *Bull. Inst. Océanogr. Monaco*, 1954 (1041), 16 pp.

SARUHASHI K. (1953a) The chlorinity determination of sea water by microanalytical method. *Rec. Oceanogr. Wks. Japan, n.s.* **1** (2), 52–54.

SARUHASHI K. (1953b) On the total carbonaceous matter and hydrogen ion concentration. *Pap. Meteorol. Geophys. Japan* **3**, 202–206.

SARUHASHI K. (1955) On the equilibrium concentration ratio of carbonic acid substances dissolved in natural water. A study on metabolism in natural waters. *Pap. Meteorol. Geophys. Japan* **6** (1), 38–55.

SCHLEICHER K. E. and BRADSHAW A. (1956) A conductivity bridge for the measurement of the salinity of sea water. *J. du Cons.* **22** (1), 9–20.

SCHOLANDER P. F., VAN DAM L., CLAFF C. L., and KANWISHER J. W. (1955) Micro gasometric determination of dissolved oxygen and nitrogen. *Biol. Bull.* **109** (2), 328–334.

SEIWELL H. R. (1934) The distribution of oxygen in the western basin of the North Atlantic. *Pap. Phys. Oceanogr. Meteorol.* **3** (1), 86 pp.

SEIWELL H. R. (1935) The cycle of phosphorous in the western basin of the North Atlantic. *Ibid.* **3** (4), 56 pp.

SEIWELL H. R. (1937) The minimum oxygen concentration in the western basin of the North Atlantic. *Ibid.* **5** (3), 24 pp.

SIMONS L. H., MONAGHAN P. H., and TAGGERT M. S. (1953) Aluminium and iron in Atlantic and Gulf of Mexico waters. *Analyt. Chem.* **25**, 989–990.

SKOPINTZEV A. and MIKHAILOVSKAYA L. (1933) The iodine content of White Sea water. (In Russian, English summary.) *Trans. Oceanogr. Inst. Moscow* **3**, 79–86.

SKOPINZEV B. A. (1939) Organic matter in the waters of the Barentz, Polar, and Kara seas. (In English.) *Compt. Rend. Acad. Sci. U.R.S.S.* **22**, 448–451.

SLOCUM G. (1955) Has the amount of carbon dioxide changed significantly since the beginning of the twentieth century? *Monthly Weather Rev.* **83** (10), 225–231.

SMALES A. A. (1951) Determination of strontium in sea water by a combination of flame photometry and radio-chemistry. *Analyst* **76**, 348–355.

SMALES A. A. and PATE B. D. (1952) The determination of arsenic in sea water. *Analyst* **77**, 188–195.

SMALES A. A. and SALMON L. (1955) Determination of small amounts of rubidium and cæsium in sea water and related materials of geochemical interest. *Analyst* **80** (946), 37–50.

SNODGRASS J. M., CARRITT D. E., and WOOSTER W. S. (1954) Automatic servo-operated filter photometer. *Anal. Chem.* **26**, 249–250.

STARK W. (1943) Über die Goldführung der Meere. *Helv. Chem. Acta* **26**, 424–441.

STEEMANN NIELSEN E. (1952) The use of radio-active carbon (C^{14}) for measuring organic production in the sea. *J. du Cons.* **18** (2), 117–140.

STEEMANN NIELSEN E. (1954) On organic production in the oceans. *Ibid.* **19** (3), 309–328.

STEWART D. C. and BENTLEY W. C. (1954) Analysis of uranium in sea water. *Science* **120**, 50–51.

Stock A. and Cucuel F. (1934) Die Verbreitung des Quecksilbers. *Naturwiss.* **22,** 390–393.

Strock L. W. (1936) Zur Geochemie des Lithiums. *Nach. Ges. Wiss. Göttingen Math.-Phys. Kl. Fach. IV, N.F.* **1** (15), 171–201.

Sverdrup H. U. and Fleming R. H. (1941) The waters off the coast of Southern California, March to July 1937. *Bull. Univ. Calif., Scripps Inst. Oceanogr.* **4** (10), 261–378.

Sverdrup H. U., Johnson M. W., and Fleming R. H. (1942) *The Oceans.* Prentice-Hall, Inc., N.Y., x + 1087 pp.

Swartout J. A. and Dole M. (1939) The protium-deuterium ratio and the atomic weight of hydrogen. *J. Amer. Chem. Soc.* **61,** 2025–2029.

Szabo A., Tudge A., Macnamara J., and Thode H. G. (1950) Distribution of sulphur^{34} in nature and the sulphur cycle. *Science* **111,** 464–465.

Tarnøe H. (1900) On the determination of the salinity of sea water by its powers of refraction. *Rept. Norweg. Fish. Mar. Invest.* **1** (6), 1–13.

Thode H. G., Kleerekoper H., and McElcheran D. (1951) Isotope fractionation in the bacterial reduction of sulphate. *Research, London* **4,** 581–582.

Thode H. G., Macnamara J., and Fleming W. H. (1953) Sulphur isotope fractionation in nature and geological and biological time scales. *Geochim. Cosmochim. Acta* **3,** 235–243.

Thomas B. D. and Thompson T. G. (1933) Lithium in sea water. *Science* **77,** 547–548.

Thomas B. D., Thompson T. G., and Utterback C. L. (1934) The electrical conductivity of sea water. *J. du Cons.* **9,** 28–35.

Thompson T. G. and Chow T. J. (1955) A non-metallic water sampler. *Deep-Sea Res.* **2** (3). 200–203.

Thompson T. G. and Korpi E. (1942) The bromine-chlorinity ratio of sea water. *J. Mar. Res.* **5** (1), 28–36.

Thompson T. G. and Robinson R. J. (1932) Chemistry of the sea. *Nat. Res. Couns. Bull.,* No. 85, Chap. 5, 95–203.

Thompson T. G. and Taylor H. J. (1933) Determination and occurrence of fluorides in sea water. *Ind. Eng. Chem., Anal. Edit.* **5,** 87–89.

Thompson T. G. and Wilson T. L. (1935) The occurrence and determination of manganese in sea water. *J. Amer. Chem. Soc.* **57,** 233–236.

Trafimov A. (1949) [Isotopic composition of sulphur in meteorites and terrestrial objects.] (In Russian.) *Dokl. Akad. Nauk S.S.S.R.* **66,** 181–184. *Chem. Abstr.* (1949) **43,** 6078c.

Truesdale G. A., Downing A. L., and Lowden G. F. (1955) The solubility of oxygen in pure water and sea-water. *J. Appl. Chem.* **5** (2), 53–62.

Urry W. D. (1935) Further studies in the rare gases. III. The helium-neon content of ocean waters. *J. Amer. Chem. Soc.* **57,** 657–659.

Urry W. D. and Piggot C. S. (1941) Apparatus for determination of small quantities of radium. *Amer. J. Sci.* **239,** 633–657.

Utterback C. L., Thompson T. G., and Thomas B. D. (1934) Refractivity-chlorinity-temperature relationships of ocean water. *J. du Cons.* **9,** 35–38.

Vaccaro R. F. and Ryther J. H. (1954) The bactericidal effects of sunlight in relation to "light" and "dark" bottle photosynthesis experiments. *J. du Cons.* **20** (1), 18–24.

Von Engelhardt W. (1936) [Die Geochemie des Bariums.] *Chem. Erde* **10,** 187–246. *Chem. Abstr.* (1936) **30,** 3371^6.

Wangersky P. J. (1952) Isolation of ascorbic acid and rhamnosides from sea water. *Science* **115,** 685.

Wattenberg H. (1937) Critical review of the methods used for determining nutrient salts and related constituents in salt water. I Methoden zur Bestimmung von Phosphat, Silikat, Nitrit, Nitrat, und Ammoniak im Seewasser. *Rapp. Proc. Verb. Cons. Perm. Int. Explor. Mer.* **103,** 1–26.

Wattenberg H. (1938) Zur Chemie des Meerwassers. *Zeits. Anorg. Chem.* **236,** 339–360.

Wattenberg H. (1943) Zur Chemie des Meerwassers. Über die in Spuren vorkommenden Elemente. *Ibid.* **251,** 86–91.

Webb D. A. (1937) Studies on the ultimate composition of biological material. II. Spectrographic analyses of marine invertebrates, with special reference to the chemical composition of their environment. *Sci. Proc. Roy. Dublin Soc., N.S.* **21** (47), 505–539.

Webb D. A. (1938) Strontium in sea water and its effect on calcium determinations. *Nature* **142** (3599), 751–752.

Webb D. A. (1939) The sodium and potassium content of sea water. *J. Exp. Biol.* **16,** 178–183.

Wenner F., Smith E. H., and Soule F. M. (1930) Apparatus for the determination aboard ship of the salinity of sea water by the electrical conductivity method. *J. Res. U.S. Bur. Stand.* **5**, 711–732.

Wheatland A. B. and Smith L. J. (1955) Gasometric determination of dissolved oxygen in pure and saline water as a check of titrimetric methods. *J. Appl. Chem.* **5** (3), 144–148.

Wilson K. G. and Arons A. B. (1955) Osmotic pressures of sea water solutions computed from experimental vapour pressure lowering. *J. Mar. Res.* **14** (2), 195–198.

Wirth H. E., Thompson T. G., and Utterback C. L. (1935) Distribution of isotopic water in the sea. *J. Amer. Chem. Soc.* **57**, 400–404.

Wooster W. S. and Rakestraw N. W. (1951) The estimation of dissolved phosphate in sea water. *J. Mar. Res.* **10** (1), 91–100.

Worthington L. V. (1954) A preliminary note on the time scale in North Atlantic circulation. *Deep-Sea Res.* **1** (4), 244–250.

Worthington L. V. (1955) A new theory of Caribbean bottom-water formation. *Ibid.* **3**, 82–87.

Zwicker B. M. G. and Robinson R. J. (1944) The photometric determination of nitrate in sea water with a strychnidine reagent. *J. Mar. Res.* **5** (3), 214–232.

Contribution No. 845

Reprinted from
BULLETIN OF MARINE SCIENCE
OF THE GULF AND CARIBBEAN
Vol. 7, No. 3, pp. 252-254
SEPTEMBER, 1957

FLORIDA STRAITS TRANSPORTS, 1952-1956[1]

HENRY STOMMEL
Woods Hole Oceanographic Institution
Woods Hole, Massachusetts

Through the generosity of the Western Union Telegraph Company it has been possible to make continuous measurements over weekends of the potential difference between Key West and Havana, across the Florida Straits, since August 1952. The records are obtained at the Key West end of the cable by the Western Union cable engineer, Mr. P. J. Moore, to whom we are very much indebted for volunteering to look after the recording equipment for these years. A preliminary discussion, in detail, of the first year's data (1952-1953) has been published by Wertheim (1954). There are now available nearly four years' data, none of which has been published in tabular form. In order to make these data readily available to oceanographers at large, it has been prepared in summary form in the accompanying table (Table 1).

TABLE 1
24-Hour Averages of Florida Straits Transports
in Millions of Cubic Meters Per Second.

1952			1952			1953			1953		
Aug.	3	30.3	Nov.	1	19.9		11	34.3		29	23.5
	9	26.8		2	22.3		17	30.4			
	10	27.4		4	23.1		18	29.7	Apr.	3	25.3
	16	28.9		8	21.9					4	26.9
	17	26.3		9	21.9	Feb.	1	28.7		5	24.8
	23	19.6		11	26.5		7	32.7		11	26.0
	24	18.3					8	34.6		12	28.8
	31	21.9	Dec.	6	15.8		12	36.6		18	35.0
				7	14.6		14	36.3		19	37.2
Sept.	7	19.1		13	20.5		15	37.5		25	39.0
	13	19.1		14	23.3		21	33.1		26	38.3
	14	18.6		20	27.6		22	31.8			
	27	21.2		21	27.9		23	33.4	May	2	36.9
	28	20.0		25	31.0		28	31.1		3	36.6
				27	30.3					9	36.4
Oct.	4	21.9		28	30.9	Mar.	1	28.4		10	35.6
	5	20.1					7	24.1		16	32.8
	11	23.3	1953				8	21.6		17	34.1
	12	23.7					14	23.0		23	33.4
	18	24.7	Jan.	1	38.0		15	22.0		24	34.1
	19	24.5		3	36.8		21	24.7	May	30	31.2
	25	17.4	Jan.	4	34.7		22	23.1		31	32.1
	26	20.2		10	35.6		28	21.9			

---

[1] Contribution No. 845 of the Woods Hole Oceanographic Institution; this work was done under contract with the Office of Naval Research: N6onr-27701.

TABLE 1—Continued
24-HOUR AVERAGES OF FLORIDA STRAITS TRANSPORTS
IN MILLIONS OF CUBIC METERS PER SECOND.

1953		
June	6	32.9
	7	34.0
	13	27.5
	14	26.8
	20	26.3
	21	26.4
	27	21.5
	28	22.3
July	4	24.7
	5	24.5
	11	27.3
	12	26.8
	25	24.8
	26	25.3
Aug.	1	22.8
	2	23.8
	8	23.3
	9	24.1
	16	23.8
	30	23.8
Sept.	5	25.9
	6	23.0
	7	23.0
	12	16.6
	13	18.2
	19	22.5
	20	23.6
	26	19.7
	27	22.0
Oct.	4	17.7
	10	17.7
	11	16.9
	12	16.4
	17	16.6
	18	15.6
	24	16.6
	31	20.5
Nov.	1	22.0
	7	19.7
	8	20.0
	14	17.7
	15	15.9
	21	25.6
	28	23.6
	29	24.1
1953		
Dec.	5	23.8
	6	23.3
	12	26.1
	13	27.4
	19	22.0
	20	23.0
	25	24.8
	26	24.3
	27	23.3
1954		
Jan.	2	21.8
	3	24.8
	9	20.5
	10	22.5
	16	22.3
	17	24.1
Feb.	6	26.6
	7	27.1
	13	24.1
	20	21.2
	21	20.7
Mar.	7	22.0
	14	26.6
Apr.	3	24.3
	4	24.6
	10	27.6
	11	23.5
	18	24.3
	24	20.7
	25	20.7
May	1	20.0
	2	21.2
	8	21.5
	9	23.8
	15	31.2
	16	30.7
	22	27.6
	23	25.3
	30	27.9
June	5	26.1
	6	25.1
	12	19.7
	13	21.0
	20	26.4
	26	27.4
	27	27.6
1954		
July	17	23.8
	18	23.2
	24	27.1
	25	27.1
	31	29.4
Aug.	1	30.7
Nov.	28	24.8
	29	24.8
Dec.	4	24.3
	5	23.8
	11	24.6
	12	24.8
	18	29.7
	19	31.0
	25	27.4
	26	27.9
1955		
Jan.	1	26.9
	2	27.1
	8	21.4
	9	21.7
	15	18.7
Jan.	16	19.6
	22	16.1
	23	17.4
	29	15.3
	30	15.4
Feb.	5	17.8
	6	20.5
	12	22.5
	13	20.0
Mar.	5	26.1
	6	27.2
	12	27.9
	13	29.2
	19	30.7
	20	30.4
	26	33.5
	27	33.8
Apr.	2	29.9
	9	30.7
	10	29.2
	16	31.1
	17	29.2
	23	27.2
1955		
	24	25.5
	30	23.3
May	1	20.2
CABLE BREAK		
Nov.	12	22.5
	19	24.1
	26	33.4
Dec.	3	32.4
	10	29.2
	17	30.6
	24	29.7
1956		
Jan.	8*	25.7
Jan.	14*	22.8
	21	24.0
	28	27.8
	29	32.3
Feb.	4	25.8
	5	23.8
	11	22.7
	12	25.8
	18	22.4
	26	28.9
Mar.	10	23.0
	11	27.0
	17	23.7
	18	21.7
	24	15.3
	25	16.5
	31	18.6
Apr.	1	18.7
	7	24.1
	8	22.6
	14	21.8
	15	22.5
	22	26.9
	29	30.7
May	5	32.7
	6	32.2
	13	26.4
	19	24.8
	26	24.0
	27	23.0

The figures presented in the table are the 24-hour averages of water transport (in millions of cubic meters per second) through the Florida Straits between Key West and Havana. The averages are always taken from midnight to midnight, local time (75°W meridian), except in two cases marked with an asterisk, where the average is taken from noon to noon of the following day. These figures are computed by multiplying the 24-hour average voltage (in volts) by the factor 25.6, to obtain the transport in millions of cubic meters per second. Wertheim (1954) has emphasized the ambiguities which enter in passing from measured voltage to computed transport; if, in the future, there is reason to doubt the validity of the parameters chosen to obtain the factor 25.6, the tabulated values can always be divided by this factor to recover the original average measured potential difference in volts (for example, the actual average potential difference measured on November 21, 1953 was 1.00 volts).

REFERENCE

WERTHEIM, G. K.
1954. Studies of the electrical potential between Key West, Florida, and Havana, Cuba. Trans. Amer. Geophys. Un., *35* (6): 872-882.

Contribution No. 850

Sonderdruck aus der Deutschen Hydrographischen Zeitschrift. Band 10, Heft 4. 1957

Auswertung von Seegangsregistrierungen des Forschungsschiffes „Atlantis“ mit dem „ship-borne wave recorder“ sowie Vergleich mit entsprechenden Seegangsberechnungen aus den Windverhältnissen (hindcasting)[1]

Von H. Walden* und H. G. Farmer**

(Hierzu Tafel 4 mit Tabelle 3)

Zusammenfassung. Im November und Dezember 1956 wurden auf dem Forschungsschiff „Atlantis“ im Atlantischen Ozean mit dem „ship-borne wave recorder“ nach M. J. Tucker Registrierungen des Seegangs gewonnen. Diese Messungen wurden auf zweierlei Weise statistisch ausgewertet, nämlich 1. durch Berechnung von Mittelwerten aus Einzelwerten, die der Registrierkurve unmittelbar entnommen wurden und 2. durch Bestimmung der entsprechenden Mittelwerte aus einem Wellenspektrum, das vorher mittels spezieller Analyse ermittelt worden war. Die sich ergebenden Größen werden miteinander verglichen. Der Einfluß, den die Bandbreite des Spektrums nach Cartwright und Longuet-Higgins auf bestimmte statistische Seegangsgrößen ausübt, wird berechnet. Die aus den Registrierungen ermittelten Werte für die Wellenhöhe und die Wellenperiode werden mit den entsprechenden Größen verglichen, die sich beim „hindcasting“ unter Benutzung von Wetterkarten nach verschiedenen Methoden ergeben. Die auf Grund der Diagramme von Pierson, Jr.-Neumann-James, von Bretschneider-Wilson und von H. Walden bestimmten kennzeichnenden Wellenhöhen sind höher, die nach dem Verfahren von J. Darbyshire berechneten niedriger als die entsprechenden beobachteten Größen. Bei den Perioden sind die in den behandelten Fällen nach den Methoden von Bretschneider-Wilson und von Darbyshire berechneten Werte durchschnittlich größer, die nach dem Diagramm von Walden bestimmten Größen kleiner als die Perioden, die man aus den Registrierungen mit dem ship-borne wave recorder ermittelt.

Evaluation of sea records obtained from the “ship-borne wave recorder” on board the research vessel “Atlantis” and comparison with corresponding wave computations from wind conditions (“hindcasting”) (Summary). On a cruise with the research vessel “Atlantis” in the North Atlantic, in November and December 1956, sea records were obtained from the “ship-borne wave recorder” after M. J. Tucker. Two different statistical methods were used in evaluating these records, viz. 1. mean values were computed from the records and 2. the respective mean values were derived from a wave spectrum that beforehand had been obtained by special analysis. The resulting values are compared with one another. From the analysis it is found that the relative width of the wave spectrum is significant in determining the wave heights, whether treating recorded wave data or determining the wave height from a forecast or hindcast wave spectrum. The effect is computed according to Cartwright and Longuet-Higgins. The values of wave height and wave period obtained from the records are compared to the corresponding values derived by different methods from weather maps (“hindcasting”). The significant wave heights hindcast with the aid of diagrams by Pierson, Jr.-Neumann-James, by Bretschneider-Wilson and by H. Walden, are higher, those computed by means of J. Darbyshire’s procedure are lower than the appropriate observed values. The values of periods hindcast according to the methods by Bretschneider-Wilson and by Darbyshire are, on an average, greater, those determined from the diagrams by Walden are smaller than the values of periods obtained from the shipborne wave recorder.

Des enregistrements élaborés de la mer agitée obtenus à l’aide d’un instrument enregistreur («ship-borne wave recorder») installé à bord du navire de recherche «Atlantis», sont comparés à des calculs correspondants de la mer agitée déterminée à partir des conditions des vents («hindcasting») (Résumé). En novembre et en décembre 1956, des enregistrements de la mer agitée ont été effectués en Atlantique Nord à l’aide d’un instrument enregistreur des vagues d’après M. J. Tucker, dit le «ship-borne wave recorder», installé à bord du navire de recherche «Atlantis». On

---

[1] Contribution number 850 from the Woods Hole Oceanographic Institution.
* Deutscher Wetterdienst, Seewetteramt.
** Woods Hole Oceanographic Institution.

s'est servi de deux méthodes différentes en exploitant ces enregistrements, à savoir: 1^0 des valeurs moyennes ont été dérivées des valeurs, prises immédiatement des courbes d'enregistrement et 2^0 des valeurs moyennes correspondantes ont été dérivées du spectre des vagues que l'on avait auparavant obtenu au moyen d'une analyse spéciale. Dans le travail actuel, les valeurs résultant de ces processus sont comparées entre elles. L'effet que, d'après Cartwright et Longuet-Higgins, la largeur de bande du spectre a sur des quantités statistiques de la mer agitée est calculé. Les valeurs de la hauteur des vagues et de la période des vagues résultant des enregistrements sont mises en parallèle avec des valeurs correspondantes calculées au moyen des méthodes différentes à partir des cartes météorologiques («hindcasting»). Il se montre que les hauteurs significatives des vagues, résultant de l'application des diagrammes de Pierson, Jr.-Neumann-James et de ceux de Bretschneider-Wilson et de H. Walden sont plus élevées, au revanche, les hauteurs significatives qui résultent de l'application de la méthode de J. Darbyshire sont plus faibles que les valeurs observées. Les valeurs des périodes de vagues calculées dans ce travail d'après les méthodes de Bretschneider-Wilson et de Darbyshire sont, en moyene, plus élevées, celles qui ont été déterminées à l'aide du diagramme de Walden sont plus faibles que les valeurs des périodes prises des enregistrements de l'instrument enregistreur d'après Tucker.

Das Forschungsschiff ,,Atlantis" der Woods Hole Oceanographic Institution ist mit einem an Bord fest eingebauten Wellenmeßgerät (,,ship-borne wave recorder") ausgerüstet. Das Instrument wurde vom National Institute of Oceanography, Wormley, England, entwickelt und ist von M. J. Tucker [1956a] beschrieben worden. Im wesentlichen registriert es den hydraulischen Wasserdruck und die vertikalen Schiffsbeschleunigungen. Beide Größen werden an einem Punkt an der Außenhaut des Schiffes gemessen.

Auch den Versuch, das auf ,,Atlantis" eingesetzte Gerät mit Hilfe einer vom Ozeanographischen Institut Woods Hole entwickelten schwimmenden Meßstange (WHOI wave pole) zu eichen, hat M. J. Tucker [1956b] behandelt. Der Zweck dieser Experimente war es, nach Möglichkeit die Änderungen der Eichung festzustellen, die sich im Vergleich zu der im Versuchsstand an Land durchgeführten Eichung ergeben können, wenn das Gerät auf dem Schiff eingebaut wird. Hierbei mag insbesondere die Form der Schiffswand in der Nähe der Meßelemente von Einfluß sein. Es muß jedoch angenommen werden, daß Tuckers Ergebnisse nicht endgültig sind. Aus diesem Grunde wurde bei der Bearbeitung der hier benutzten Beobachtungen die an Land gewonnene Eichung zum Ansatz gebracht.

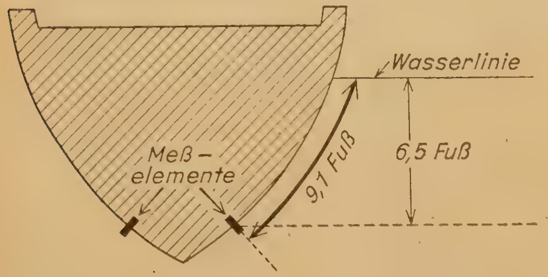

Abb. 1. Querschnitt durch den Schiffsrumpf des F.S. ,,Atlantis"

Auf der ,,Atlantis" liegen die Meßelemente 6,5 Fuß tief unter der Meeresoberfläche. Mißt man ihre Entfernung von der Wasserlinie längs der (rund geformten) Schiffswand, so erhält man 9,1 Fuß (vgl. Abb. 1). Tucker hat für die Meßelemente und für die elektrischen Meßvorgänge eine Genauigkeit von ± 10% angegeben. Für die Gesamtheit der Meßeinrichtung auf dem Schiff wollen wir eine Genauigkeit von 15% annehmen.

Hauptaufgabe auf der Reise Nr. 229 der ,,Atlantis" von Anfang November bis Anfang Dezember 1956 war es, hydrographische Messungen auf Stationen in einem Abschnitt von den Neufundlandbänken bis zum Südamerikanischen Schelf entlang dem Meridian 50,5° W durchzuführen. Die Wellenregistrierungen wurden während des Aufenthaltes auf den hydrographischen Stationen gewonnen. Im allgemeinen lag das Schiff dabei ohne Fahrt dwars zum Wind. In wenigen Einzelfällen fuhr das Schiff gegen die See, jedoch mit sehr geringer Geschwindigkeit. Die Windstärke wurde mit einem Dreischalenkreuz-Anemometer gemessen, das am Besanmast in 30 Fuß Höhe angebracht war. Für seitlich einkommende Winde war der durch die Nähe des Mastes hervorgerufene Fehler wahrscheinlich sehr gering. Bei anderen (scheinbaren) Windrichtungen wurde eine merkliche Abweichung von der wahren Windgeschwindigkeit beobachtet. Die Windrichtung ist visuell mit Hilfe des Schiffs-Kreiselkompasses bestimmt worden. Insgesamt wurden 47 Messungen angestellt, von denen allerdings einige

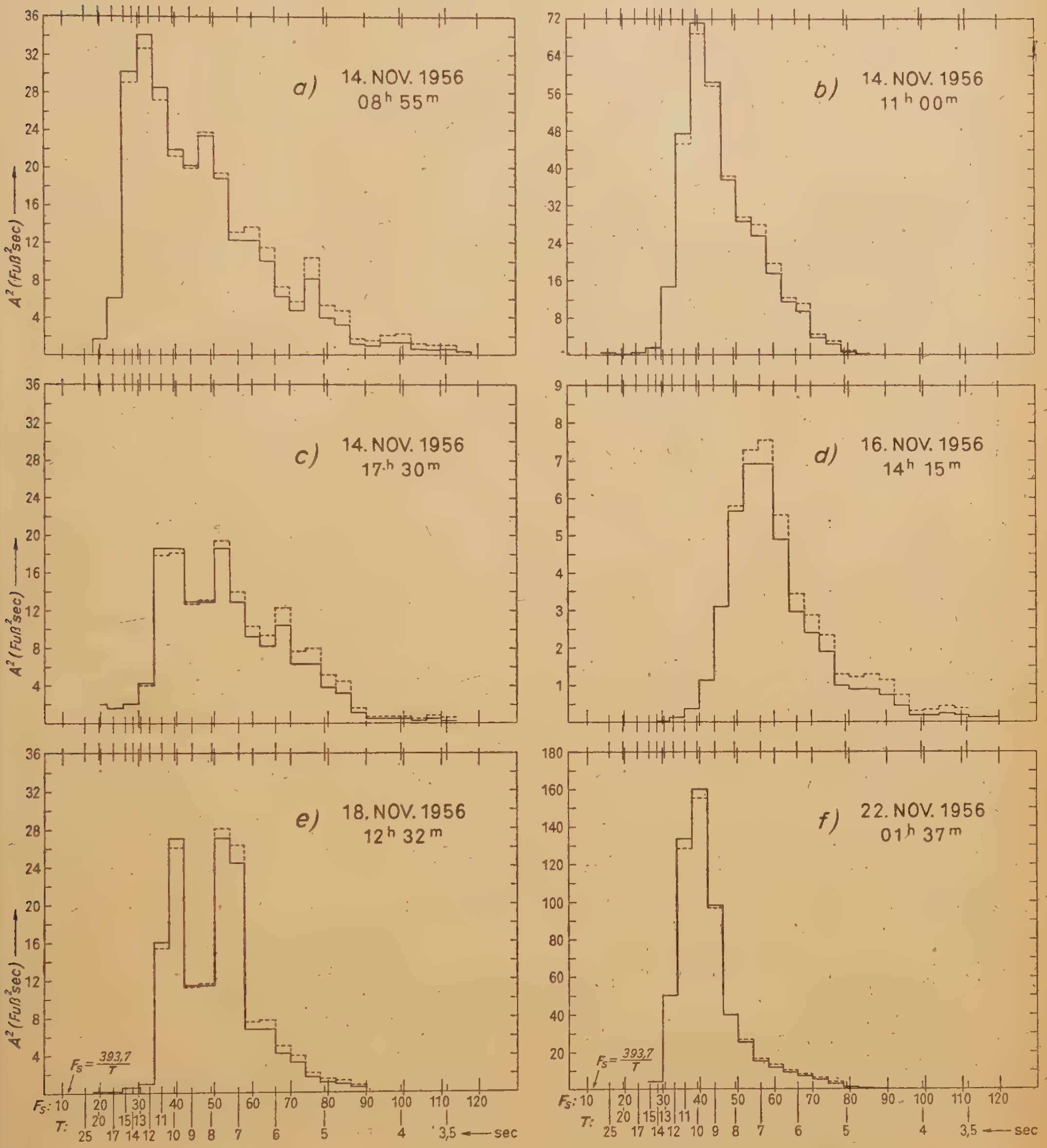

Abb. 2a—f. Spektren nach der Analyse des U.S. Navy Hydrographic Office, Washington

wenige für eine Auswertung unbrauchbar waren. Nach eingehender Prüfung der Wetterlage wurde eine Anzahl von Registrierungen genau ausgewertet; für fast alle vorliegenden Messungen wurde außerdem zu Vergleichszwecken der Seegang nach den Windverhältnissen auf Grund von Wetterkarten berechnet (hindcast).

Statistische Auswertung der Beobachtungen. Die Auswertung erfolgte auf zweierlei Weise: Einmal wurden die Registrierkurven in Woods Hole unmittelbar ausgewertet. Parallel dazu führte das Hydrographic Office in Washington eine Analyse der Registrierungen mit seinem Wellen-Analysator durch.

In Woods Hole wurden unmittelbar aus achtzehn Wellenregistrierungen, von denen sich jede über 20 Minuten erstreckte, die Größe $\sqrt{\frac{\sum z^2}{n}}$ („rms elevation"), die kennzeichnende Wellenhöhe $H_{1/3}$, die mittlere Höhe der dem oberen Zehntel angehörenden Wellen, $H_{1/10}$, und die mittlere Periode $\tilde{T}'_m$ ermittelt. Dabei ist z die an äquidistanten Punkten genommene Abweichung der Registrierkurve von der Mittellinie und n die Anzahl dieser Punkte. Als Wellenhöhe wurde das Mittel der beiden Vertikalabstände zwischen dem Niveau des Wellenherges und dem vorangehenden sowie dem nachfolgenden Wellental definiert. Die Periode $\tilde{T}'_m$ ist definiert als das mittlere Zeitintervall zwischen je zwei aufeinanderfolgenden Wellentälern. $\tilde{T}'_{1/3}$ ist der Durchschnitt jener Perioden, die dem höchsten Drittel aller gemessenen Wellen angehören.

Fünfzehn Registrierungen wurden vom Hydrographic Office, Washington, mit Hilfe eines Spezialgerätes analysiert, um die Verteilung der Wellenenergie in Abhängigkeit von den Perioden festzustellen. Aus diesen „Spektren" (einige Beispiele in Abb. 2a bis f) können durch Ausplanimetrieren die Größe $\sqrt{\frac{\sum z^2}{n}}$ und die Wellenhöhen ebenfalls bestimmt werden, weil $\sqrt{\frac{\sum z^2}{n}}$ proportional zur Fläche unter dem Spektrum ist. Der Vertrauensbereich für 90% ergibt sich bei 58 Freiheitsgraden durch Multiplikation jeder Ordinate mit 0,78 (untere Grenze) bzw. 1,41 (obere Grenze). Die Wellenhöhen oder ihre Maxima lassen sich aus $\sqrt{\frac{\sum z^2}{n}}$ unter Benutzung der Ergebnisse von M. S. Longuet-Higgins [1952] oder von D. E. Cartwright und M. S. Longuet-Higgins [1956] berechnen. Die Wellenhöhen wurden mit einer Genauigkeit von 0,1 Fuß ausgedrückt. M. J. Tucker hat angeregt, an das aus den Registrierungen berechnete Wellenspektrum eine Korrektion anzubringen, die von der Frequenz abhängt, d. h., die für verschiedene Teile des Spektrums eine unterschiedliche Größe besitzt (Abb. 3). Diese Art der Korrektion ist erforderlich, weil die Beschleunigungsregistrierung durch die doppelte Integration bestimmte Verschiebungen erfährt und weil außerdem der durch die Einzelwelle hervorgerufene Druck mit der Wassertiefe unter der Welle abnimmt. In den Abb. 2a bis f entspricht die ausgezogene Linie dem Original-Spektrum, die gestrichelte Linie dem Spektrum nach Berücksichtigung des Korrektions-Faktors von Tucker. Die folgende Tabelle gibt einen Vergleich zwischen der unmittelbaren Auswertung der Registrierkurve und der über das Spektrum durchgeführten Berechnung. Die Zahlen geben an, um wieviel Prozent der Wert, den man mit der spektralen Auswertungsweise erhält, größer (positives Zeichen) bzw. kleiner (negatives Zeichen) ist als bei der unmittelbaren Auswertung. Die zweite Zeile der Tabelle enthält die Streuung der Abweichungen.

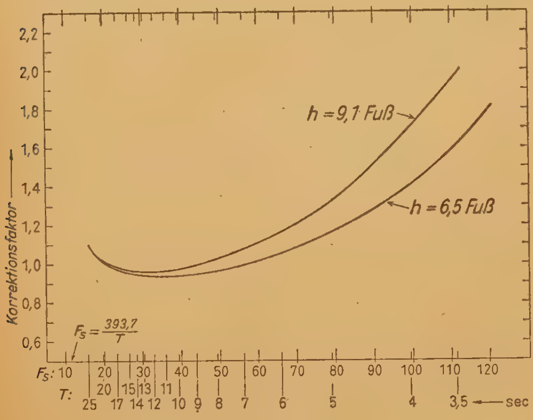

Abb. 3. Korrektionsfaktor nach M. J. Tucker

F_s (Abszisse) $= \frac{393.7}{T}$

Tabelle 1

	Schmales Spektrum		Breites Spektrum	
$\sqrt{\frac{\sum z^2}{n}}$	$H_{1/3}$	$H_{1/10}$	$H_{1/3}$	$H_{1/10}$
− 1,5	+ 5,1	+ 9,2	+ 1,6	+ 6,9
± 3,5	± 4,3	± 4,9	± 3,7	± 1,5

In der ersten Gruppe wurde angesetzt, daß die Wellenspektren schmal sind, also den von Longuet-Higgins [1952] angenommenen Bedingungen entsprechen. Demgemäß dienten die Ergebnisse von Longuet-Higgins als Rechengrundlage. In der zweiten Gruppe wurde die Breite des Spektrums gemäß Cartwright und Longuet-Higgins [1956] in Betracht gezogen. Ihre Ergebnisse beziehen sich jedoch auf die Höhen der Maxima über dem Mittel der Registrierung. Für den obigen Vergleich wurden diese Höhen als Amplituden betrachtet und einfach verdoppelt, um eine angenäherte Gesamtwellenhöhe vom Wellenkamm zum Tal zu erhalten. Die Größen $\sqrt{\frac{\sum z^2}{n}}$ sind in der Tabelle in guter Übereinstimmung; der auf dem Wege über das Spektrum berechnete Wert ist nur wenig niedriger als das unmittelbar aus den Registrierungen ermittelte Ergebnis. Bei den Wellenhöhen ist die Übereinstimmung augenscheinlich bedeutend besser, wenn man die Breite des Spektrums in Betracht zieht (rechts in der Tabelle). Überdies zeigt sich, daß die mit Hilfe des Spektrums bestimmten Höhen durchschnittlich größer sind als die unmittelbar aus der Registrierkurve berechneten.

Mit dem Vergleich ist nicht beabsichtigt zu zeigen, daß die aus den Originaldaten abgeleiteten Höhen die richtigen sind; der Zweck der Gegenüberstellung ist es vielmehr, die Unterschiedlichkeit der Rechenergebnisse herauszustellen, die man bei Benutzung verschiedener Auswerteverfahren erhält.

Bei den Vorhersage-Vorschriften, zum Beispiel nach W. J. Pierson, G. Neumann und R. W. James [1953, 1955], kann die Breite des Spektrums von entscheidender Bedeutung sein. Als Grundlage dienen ihnen das Spektrum nach G. Neumann [1953] und die auf der Annahme eines schmalen Wellenspektrums beruhende statistische Arbeit von M. S. Longuet-Higgins [1952]. Nach Cartwright und Longuet-Higgins [1956] erweist sich das Spektrum von Neumann aber als verhältnismäßig breit.

Die folgende Tabelle stellt die Ergebnisse gegenüber, die Pierson-Neumann-James [1953, 1955] bei Ansatz des schmalen Spektrums erhielten (I) und die man nach Berücksichtigung der Bandbreite des Spektrums von Neumann (II) ermittelt. $h_{1/3}$ und $h_{1/10}$ stellen die Durchschnittshöhe des höchsten Drittels bzw. des höchsten Zehntels aller Wellen über dem Mittelwert dar, während $H_{1/3}$ und $H_{1/10}$ die entsprechenden Größen, gerechnet vom Wellenkamm zum Wellental, bedeuten.

Tabelle 2

I	II	Differenz
$1/2\, H_{1/3} = h_{1/3} = 1{,}41 \sqrt{E}$	$h_{1/3} = 1{,}21 \sqrt{E}$	14,2%
$1/2\, H_{1/10} = h_{1/10} = 1{,}80 \sqrt{E}$	$h_{1/10} = 1{,}64 \sqrt{E}$	8,9%

Dabei ist $E = 2 \frac{\sum z^2}{n}$. Sieht man die Verdoppelung der beim breiten Spektrum behandelten Höhen $h_{1/3}$ und $h_{1/10}$ als brauchbare Näherungsannahme für die vollen Wellenhöhen vom Kamm zum Tal an, so müßten die von Pierson-Neumann-James [1953, 1955] für die ausgereifte Windsee angegebenen Wellenhöhen um die oben genannten Prozentzahlen vermindert werden. Möglicherweise ergibt sich hieraus wenigstens teilweise eine Erklärung dafür, daß andere Autoren niedrigere Werte für die Wellenhöhe erhalten haben.

Die Tabelle 3 (s. Anhangtafel) enthält eine Zusammenstellung von Angaben und Ergebnissen für diejenigen Registrierungen, die ausgewertet worden sind. Rechts sind die in den nächsten Abschnitten behandelten hindcast-Ergebnisse angefügt. Die Beobachtungstermine sind in Eastern Time angegeben; wünscht man Greenwich-Zeit zu erhalten, so sind vier Stunden zu addieren. Die Temperaturdifferenz Luft/Wasser ($T_L - T_W$) ist in Fahrenheit-Graden notiert. Als Maß für die Wellenhöhen dient der Fuß. Die mittlere scheinbare Periode $\tilde{T}$ wurde unter Berücksichtigung der zu erwartenden Zahl von „zero-up crossings“ (Wellen, deren Wellenberg nicht unter der Mittellinie oder deren Wellental nicht über der Mittellinie liegt) bestimmt.

Die Berechnung von T erfolgte unter Benutzung der Fläche unter dem Spektrum gemäß einer von W. J. Pierson, Jr. [1954] mitgeteilten Formel. ε ist der bei Cartwright und Longuet-Higgins [1956] besprochene Faktor für die relative Breite des Spektralbandes. Bei den Berechnungen aus dem Spektrum (Spalte: ,,Aus dem Spektrum bestimmt") beinhaltet die erste Zeile für jeden Termin Ergebnisse ohne die Korrektion nach Tucker, die zweite Zeile die Werte nach Anbringung dieser Korrektion. In dem Abschnitt: ,,Hindcast-Ergebnisse" stehen die Wellenhöhen in der ersten, die Perioden in der zweiten Zeile. Die Buchstaben sind Abkürzungen und bedeuten: P: Pierson-Neumann-James, B-W: Bretschneider bzw. Wilson, W: Walden und D: Darbyshire.

Hindcasting nach verschiedenen Verfahren. Für den größten Teil der Registrierungen wurden Berechnungen des Seegangs auf Grund von Wetterkarten (,,hindcasting") für den betreffenden Zeitpunkt und für den jeweiligen Schiffsort angestellt. Dabei wurden die von H. Walden [1953/54, 1954, 1955, 1955/56a, 1955/56b] veröffentlichten Diagramme und Hilfsmittel benutzt. Soweit es möglich war, ist der Seegang außerdem nach den Original-Vorschriften von W. J. Pierson, Jr., G. Neumann und R. W. James [1953, 1955] bestimmt worden. Darüber hinaus sind in allen geeigneten Fällen auch die Methoden von J. Darbyshire [1952] und von C. L. Bretschneider [1952] bzw. B. W. Wilson [1955] zur Anwendung gekommen.

Die rechnerisch-graphische Bestimmung des Seegangs aus den Wind- und Temperaturverhältnissen wurde ohne Kenntnis der Meßergebnisse durchgeführt; denn es war von vornherein beabsichtigt, die nach den verschiedenen Methoden ermittelten Ergebnisse nicht nur einander gegenüberzustellen, sondern auch mit den von der ,,Atlantis" durchgeführten Messungen zu vergleichen.

Zu den genannten hindcasting-Methoden sei folgendes bemerkt: Für die Anwendung der Gleichungen von J. Darbyshire stand eine Veröffentlichung von R. Silvester [1955] zur Verfügung; leider lassen sich den Diagrammen nicht die Seegangseigenschaften bei Windgeschwindigkeiten unter 12 kn entnehmen. Außerdem werden die Abhängigkeiten von der Windwirkungsdauer t_e nicht gegeben. Es blieb keine andere Möglichkeit, als t_e wie folgt zu bestimmen: Nach B. W. Wilson [1955] wurde diejenige Länge F eines Fetches ermittelt, an dessen Ende bei gleicher Windstärke die gleiche Wellenhöhe erzeugt wird wie bei der Windwirkungsdauer t_e. Mit diesem Wert für F wurde in die Diagramme von Darbyshire eingegangen. – Das von Bretschneider gegebene Verfahren beruht auf der grundlegenden Arbeit von H. U. Sverdrup und W. H. Munk [1947]; es bringt jedoch eine Änderung bzw. Verbesserung bei der Bestimmung der Wellenperiode. Bretschneiders Diagramme für die Ermittlung der Dünungseigenschaften enthalten keine Angaben über die Laufzeit. Da die Ausbreitungsgeschwindigkeit der Energie nach Bretschneider [1952] während der Verlagerung als Dünung zunimmt, ist die Berechnung des Eintreffens der Dünung am Beobachtungsort größtenteils sehr umständlich. Wilsons [1955] Ansatz fußt auf Bretschneiders [1952] Angaben, gibt jedoch die Möglichkeit, die Windsee in wandernden Windfeldern zu ermitteln. Bei Pierson-Neumann-James [1953] wird die spektrale Struktur des Seegangs nach G. Neumann [1953] in den Vordergrund gestellt. Walden übernahm die Grundkonzeption von Neumann, änderte jedoch insbesondere die Beziehungen zwischen der Länge der Windbahn bzw. der Dauer der Windwirkung und der Wellenhöhe.

Zur praktischen Durchführung der Seegangsberechnungen aus den Wetterverhältnissen (hindcasts). In Woods Hole, Massachusetts (USA), wo der größte Teil der Ausarbeitungen durchgeführt worden ist, standen Pausdrucke der Originalwetterkarten des Hydrographic Office, Washington, für die Haupttermine 00, 06, 12 und 18 MGT zur Verfügung. Bei der Entnahme der Windverhältnisse aus Wetterkarten sind bestimmte Ungenauigkeiten unumgänglich; beispielsweise erfolgt die Eintragung der Windstärke in die Wetterkarte von 5 zu 5 Knoten, während die Beobachtung an Bord in den meisten Fällen vermutlich nach der Beaufort-Skala durchgeführt wird. Dadurch können erhebliche Verschiebungen auftreten.

Die Berechnungen waren zum großen Teil sehr zeitraubend, da neben der Bestimmung der Windsee in jedem Falle geprüft werden mußte, ob ,,Fremdsee", also Dünung, aus benachbarten oder auch entfernt gelegenen Seegebieten anwesend sein konnte. Es stellte sich heraus, daß bei den Messungen nicht ein einziges Mal eine voll ausgereifte, durch Fremdsee ungestörte Windsee getroffen worden war. Dies liegt zum Teil daran, daß in dem Seegebiet, in dem stetiger Passat erwartet werden konnte, ein kleines, zeitweise aber sehr kräftiges Tief (vgl. Abb. 4) zunächst langsam westwärts wanderte und später stationär wurde. In einigen Fällen war die Windsee zwar „rein“, aber nicht ausgereift.

Leider tritt auch die in der Wellenliteratur als eine Art „Normallage“ betrachtete Situation, nämlich daß der Wind in einem festliegenden Fetch schlagartig aufkommt und dann seine Stärke nicht mehr wesentlich ändert, im freien Ozean so gut wie überhaupt nicht ein. Es ist also beim praktischen „hindcasting“ der Windsee notwendig, die regionale Verteilung der Windstärke sowie ihre zeitliche Entwicklung innerhalb des eigentlichen Windfeldes (Fetch) zu berücksichtigen. Hierfür standen Diagramme nur von H. Walden [1955, 1955/56 b] und für bestimmte Fälle von B. W. Wilson [1955] zur Verfügung. Wandernde Windfelder wurden nach den Angaben von B. W. Wilson [1955] sowie nach einem Diagramm behandelt, das die „propagation lines“ von B. W. Wilson [1955] zur Grundlage hat, aber für die Wellenhöhe und -periode die von H. Walden [1955/56 a] gegebenen Abhängigkeiten benutzt. Der Unterschied zwischen der Lufttemperatur und der Temperatur des Wassers an der Meeresoberfläche wurde gemäß H. U. Roll [1952] berücksichtigt. Nimmt die Windstärke zeitlich oder innerhalb des Fetches in der Richtung des Luftstromes ab, so ist eine Berechnung des Spektrums in der Windsee nicht möglich; man muß sich dann mit einer rohen Schätzung der Welleneigenschaften begnügen, indem man die von P. Bracelin [1952] oder von B. W. Wilson [1955] für solche Fälle genannten Vorschriften anwendet. Auch das Diagramm von B. W. Wilson [1955] ist bei abnehmender Windstärke in vielen Fällen nicht anwendbar, weil es unmöglich ist, eine bei einer relativ großen Windstärke weit entwickelte oder nahezu ausgereifte Windsee auf eine kleinere Windstärke zu beziehen.

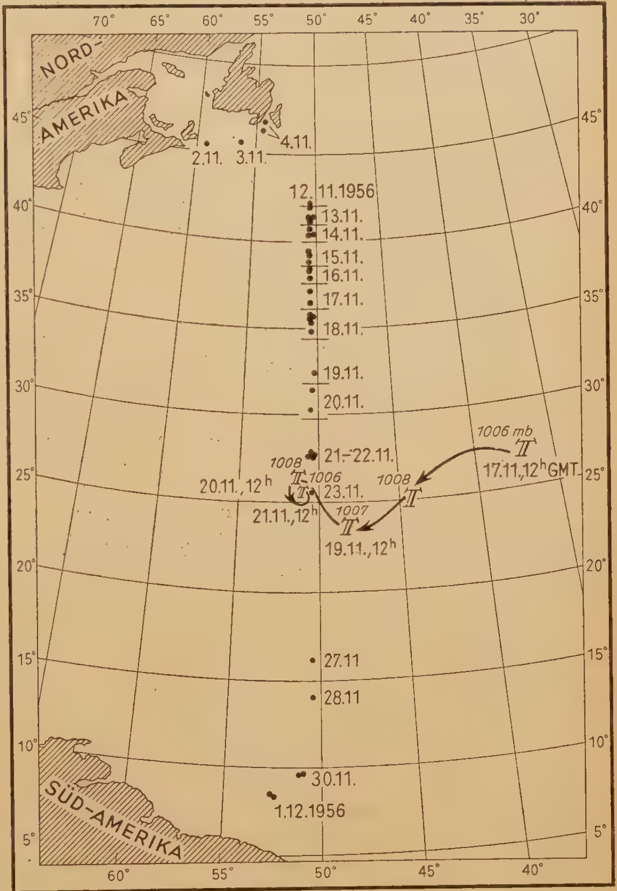

Abb. 4. Meßpositionen des F.S. „Atlantis“ und Bahn eines Tiefs vom 17. bis 21. November 1956

Bei der Berechnung der Dünung treten noch größere Schwierigkeiten auf. Zunächst gilt für die Bestimmung der Windsee, aus der die Dünung hervorgeht, das soeben Gesagte. Häufig aber trifft die Dünung auf ihrer Verlagerungs- oder Ausbreitungsstrecke (decay distance) Quer- oder Gegenwinde an, deren Wirkung auf die Wellenzüge noch nicht genau bekannt ist. In anderen Fällen geht das dünungserzeugende Windfeld unmittelbar in den für die Windsee maßgebenden Fetch langsam über, wenn am Beobachtungsort wesentlich schwächere Winde (der gleichen Richtung) herrschen als in einigem Abstand davon. Während die meisten Autoren annehmen, daß sich die Energie, welche eine Wellenkomponente bestimmter Periode besitzt, mit gleichbleibender Geschwindigkeit verlagert, rechnet Bretschneider [1952] mit einer Zunahme dieser Periode während der Verlagerung und entsprechend mit einer Zunahme der Verlagerungsgeschwindigkeit. Dieser Unterschied in der Grundauffassung hat zur Folge, daß nach den verschiedenen Rechenmethoden u. U. nicht die gleichen Windgebiete als Dünungserzeuger zu betrachten sind; d. h.: Die Dünung, die ein bestimmtes Windgebiet in größerer Entfernung vom Beobachtungsort entsendet, trifft nach der einen Methode den Beobachtungsort zum Beobachtungszeitpunkt, nach der anderen jedoch nicht. Schwierigkeiten treten auch auf, wenn das am Orte der Messung zu erwartende Periodenband der Dünung sehr schmal ist.

Faßt man die Dünung als Überlagerungserscheinung von Wellenkomponenten innerhalb eines Spektralbandes auf, so hat man bei breiten Dünungsspektren zu bedenken, daß die Anlauf- und somit auch die Dämpfungsstrecke für die einzelnen Wellenkomponenten verschieden lang sein können. Dieser Umstand ist bei der Dünungsbestimmung hier in einigen Fällen berücksichtigt worden.

Zur Bestimmung der Kreuzsee aus der berechneten Windsee und aus der berechneten Dünung bzw. aus mehreren Dünungen müssen die ermittelten Wellenenergien addiert werden; dabei wurde die Größe des „Kreuzungswinkels" „α" berücksichtigt. Die einfache Addition der Wellenenergien ist berechtigt, wenn Windsee und Dünung in entgegengesetzter Richtung oder unter etwa 90° zueinander laufen und solange die Dünung durch den Einfluß des die Windsee erzeugenden Windes keine Schwächung erfahren hat. Haben Windsee und Dünung die gleiche Richtung oder sind die beiden Wellenzüge schräg mitlaufend zueinander gerichtet, so treten andere Gesichtspunkte in den Vordergrund.

Betrachten wir zunächst den Fall, daß Windsee und Dünung in genau gleicher Richtung laufen: Die beiden Periodenspektren überlagern einander. Im allgemeinen ist die längste Periode in der Windsee, T_{LW}, kürzer als die längste Periode im Dünungsspektrum, T_{LD}. Angenommen, es seien auch sehr kurze Wellenkomponenten in der Dünung vorhanden. Daß sich dann die Energien beider Wellenzüge im Intervall ~ 0 bis T_{LW} einfach addieren, indem die Steilheit der Wellen zunimmt, ist schlecht vorstellbar; vielmehr wird vermutlich ein Teil der Energie in diesem Periodenbereich durch Überbrechen der Wellen vernichtet, womit möglicherweise eine Verlagerung der Energie auf längere Perioden verbunden ist. Man kann daher den Standpunkt vertreten, daß im Periodenintervall 0 bis T_{LW} in der Regel die der Windsee zukommende Energie allein übrig bleiben wird. Im Intervall T_{LW} bis T_{LD} ist dagegen der volle langwellige, aber auf der Laufstrecke gedämpfte Dünungsanteil vorhanden.

Treffen sich Windsee und Dünung schräg mitlaufend zueinander, so macht sich auch bei den kurzen Perioden ein bestimmter Anteil der Dünung als Kreuzsee-Effekt bemerkbar, der nicht in der Windsee „aufgeht". Für diesen Periodenbereich (0 bis T_{LW}) wurden die anlaufenden Dünungsenergien mit $\sin^2 \alpha$ multipliziert und dann der Windsee-Energie durch einfache Addition zugeschlagen. Dieser vorläufige Ansatz, der einer Arbeitshypothese gleichkommt, beruht auf der Vorstellung der Winkelausbreitung (angular spreading) der Wellenenergie nach dem $\cos^2$-Gesetz (vgl. Pierson-Neumann-James [1953]).

Vergleich der Höhenberechnungen (hindcasts) mit den Messungen. Für den Vergleich der hindcasting-Resultate mit den entsprechenden Meßergebnissen ist die Wellenhöhe besser geeignet als die Periode, weil der auf dem Forschungsschiff „Atlantis" benutzte „ship-borne wave recorder" die kurzen Wellen unter 7 sec Periode nicht voll erfaßt. Die von diesem Wellenschreiber gemessenen Werte der mittleren Periode müssen daher zu hoch liegen.

Zum Vergleich bietet sich die kennzeichnende Wellenhöhe $H_{1/3}$[2] an, die beim hindcasting üblicherweise berechnet wird. Da der Wellenmesser stets den Gesamt-Seegang, gegebenenfalls also das Überlagerungsergebnis von Windsee und Dünung mißt, ist nur der Vergleich mit dem Rechenresultat für den Gesamtseegang sinnvoll.

---

[2] Man denkt sich alle im Seegang auftretenden Wellen der Größe nach geordnet und dann in drei zahlenmäßig gleich starke Gruppen eingeteilt. Den Durchschnittswert der dem oberen Drittel angehörenden Wellen bezeichnet man als „kennzeichnende Wellenhöhe" („significant height").

In Abb. 5 sind die Abweichungen der hindcasts für die kennzeichnende Wellenhöhe des Gesamt-Seegangs von der unmittelbaren Auswertung der entsprechenden Registrierung eingetragen. Die Abweichungen (Ordinate) sind in Prozenten, bezogen auf das Meßergebnis, in Abhängigkeit von der am Orte herrschenden Windgeschwindigkeit (Abszisse) dargestellt. Zur Aufzeichnung konnten nur solche Fälle kommen, für die eine Auswertung der Registrierung vorlag; außerdem hatte in vielen Fällen nur ein Teil der hindcasting-Methoden angewendet werden können.

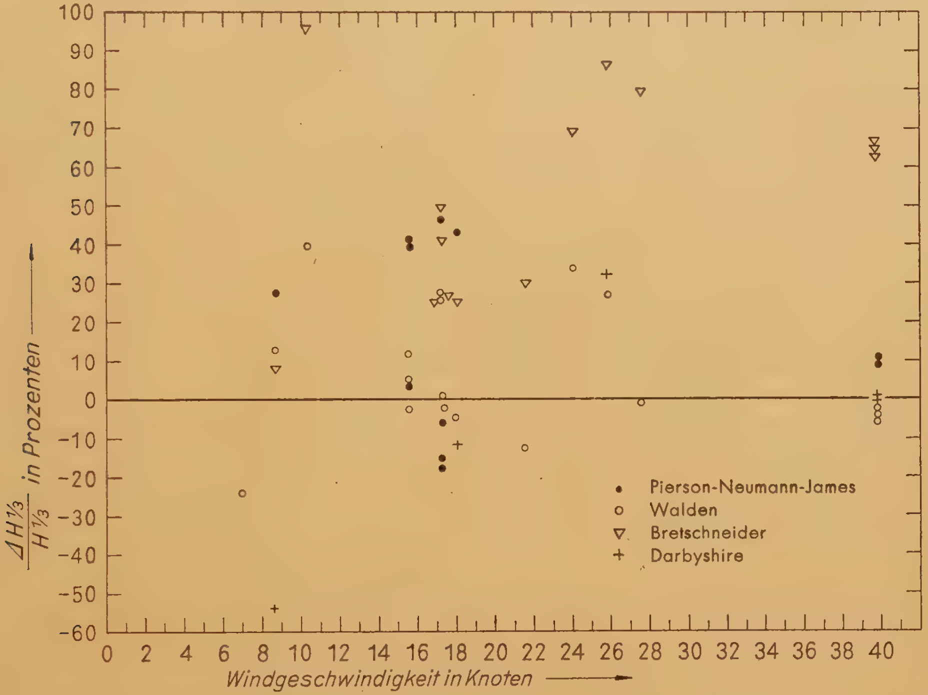

Abb. 5. Abweichungen der „hindcasts" für die Wellenhöhen vor der Beobachtungsauswertung (in Prozenten)

Man erkennt, daß sich bei der Bestimmung der Wellenhöhe aus den Wetterkarten durchschnittlich ein höherer Seegang ergab als beobachtet. Es kann dies an den Verfahren selbst liegen; möglicherweise war auch die Anwendung fehlerhaft; schließlich ist es nicht ausgeschlossen, daß die Messung mit dem „ship-borne wave recorder" unrichtig ist. Eine Abhängigkeit der Abweichungen von der Windgeschwindigkeit ist nicht festzustellen; sie ist auch kaum zu erwarten, weil in den meisten Fällen die Fremdsee, also die Dünung, eine für die Eigenschaften des Gesamt-Seegangs wichtige, zum Teil ausschlaggebende Rolle spielt.

Bildet man für die vier hindcasting-Verfahren getrennt die Mittelwerte der Abweichungen, so ergibt sich folgende Gegenüberstellung (die Zahl der benutzten Fälle ist in Klammern angegeben):

Tabelle 4

Pierson Neumann James	Bretschneider bzw. Wilson	Walden	Darbyshire
+ 19,6% (10)	+ 52,0% (14)	+ 7,1% (17)	− 7,0% (5)

Die Arbeitsanweisung von Pierson-Neumann-James [1953, 1955] liefert in den zehn auswertbaren Fällen also eine kennzeichnende Wellenhöhe, deren Mittel um 19,6% über dem beobachteten Wert liegt. Berücksichtigt man, daß sich $H_{1/3}$ von Pierson-Neumann-James [1953, 1955] bei Ansatz der relativen Spektralbreite nach Cartwright und Longuet-Higgins [1956] um einen gewissen Prozentsatz ermäßigt (bei ausgereifter Windsee um 14,2%), so erhält man in dieser sowie in der folgenden Tabelle kleinere mittlere Abweichungen, also günstigere Ergebnisse. Bretschneiders [1952] bzw. Wilsons [1955] Diagramme ergaben auffällig große positive Abweichungen; dies hängt zum Teil damit zusammen, daß diese Methoden kein Wellenspektrum, sondern nur eine kennzeichnende Periode liefern. Es war daher in bestimmten Fällen nicht möglich, die Wellenenergien von Windsee und Dünung in der auf S. 128 beschriebenen Weise zu addieren.

Will man die Brauchbarkeit eines Rechenverfahrens für die Praxis beurteilen, so ist es nötig, die Absolutwerte der Abweichungen zu berücksichtigen. Mittelt man die Abweichungen auf diese Weise, so ergibt sich:

Tabelle 5

Pierson Neumann James	Bretschneider bzw. Wilson	Walden	Darbyshire
24,3% (10)	52,0% (14)	14,2% (17)	18,2% (5)

Danach muß bei hindcasts der Wellenhöhe im Gesamt-Seegang auf dem freien Ozean zur Zeit eine durchschnittliche Abweichung von (mindestens) 15% in Kauf genommen werden.

Vergleich der Periodenberechnungen (hindcasts) mit den Meßresultaten. Der ship-borne wave recorder nach Tucker ist für die Messung von kurzen Wellen wenig geeignet. Die Spektren, die sich aus den Registrierungen nach der Analyse des Hydrographic Office in Washington ergeben haben, lassen erkennen, daß die Komponenten mit einer Periode $< 3{,}0$ sec praktisch nicht erfaßt werden und daß Komponenten zwischen 3 und 7 sec Periode mehr oder weniger abgeschwächt mitgezeichnet werden. In einzelnen Fällen hat der Seegang, in dem die Wissenschaftler bei der Augenbeobachtung an Bord keine Dünung feststellen konnten, ein Spektrum ergeben, bei dem die mittellangen Perioden die meiste Energie besitzen, die aber keinesfalls der Windsee zugeschrieben werden kann. Ein Beispiel dafür ist das Spektrum vom 14. November, $08^{h}\,55^{min}$ Uhr (Abb. 1a). Nach der Messung der „Atlantis“ herrschte zu diesem Zeitpunkt ein Wind von 18,9 kn aus 190°. Für die dabei angefachte Windsee ist eine mittlere Periode von etwa 6 sec und eine $T_{\max}$ von etwa 8 sec anzunehmen. Eine Dünung im 13 sec-Band hätte den Beobachtern auffallen müssen.

Aus diesem Grunde ist es wenig erfolgversprechend, die für die Windseeanteile mit den hindcast-Verfahren ermittelten Perioden $\tilde{T}_m$ bzw. $\tilde{T}_{1/3}$ in den Spektren wiederfinden zu wollen und etwaige Abweichungen zu berechnen. Es ist trotzdem versucht worden, die Einflüsse von Windsee und Dünung in den Spektren zu trennen, und ein roher Überschlag hat für die Windsee ergeben, daß die in den Diagrammen von Bretschneider [1952] bzw. Wilson [1955] gegebenen kennzeichnenden Perioden $\tilde{T}_{1/3}$ um durchschnittlich 22% höher, die Perioden nach Darbyshire [1952] um durchschnittlich 16% höher, dagegen die von H. Walden [1955/56a] angegebenen Größen für $\tilde{T}_m$ im Mittel um 35,6% kleiner waren als die auf dieser Fahrt mit dem ship-borne wave recorder beobachteten Perioden maximaler Energie (Maximum im Spektrum). Nach Pierson-Neumann-James hatten so wenige Windsee-Perioden berechnet werden können, daß ein Vergleich mit den Beobachtungen unangebracht ist. Für ausgereifte Windsee soll das Verhältnis von $T_{\max}$ zu $\tilde{T}_m$ nach Pierson-Neumann-James wie 1:1,417 sein; das bedeutet, daß $\tilde{T}_m$ um 29,5% kleiner sein soll als $T_{\max}$ und daß das Diagramm von Walden im vorliegenden Falle Periodenwerte lieferte, die durchschnittlich etwa 6% zu niedrig sind. – Bei sieben unserer Registrierungen war $\tilde{T}_{1/3}$ im Mittel rund

1,25 mal so groß wie $\tilde{T}_m$. Die nach Bretschneider, Wilson und nach Darbyshire ermittelten Perioden $\tilde{T}_{1/3}$ müßten also um rund 20% verkleinert werden, um mit der Periode $\tilde{T}_m$ nach Pierson-Neumann-James und nach Walden vergleichbar zu werden. Auch bei Berücksichtigung dieses Unterschiedes kann jedoch mit einiger Sicherheit geschlossen werden, daß die von Bretschneider, Wilson und Darbyshire gegebenen Perioden – wenigstens bei den Windgeschwindigkeiten bis zu etwa 25 kn – zu hoch liegen.

Außerdem sind unmittelbar aus den Wellenregistrierungen die „mittleren“ Scheinperioden $\tilde{T}'_m$ und aus den Spektren eine mittlere Periode $\tilde{T}$ berechnet worden. Diese Größen sind für Vergleichszwecke nur dann geeignet, wenn ein kontinuierliches Spektrum mit einem bestimmenden Maximum sowohl beobachtet als auch aus den Windverhältnissen berechnet (hindcast) wurde. Dieser Fall ist bei unseren Registrierungen nicht aufgetreten.

Die energiereichen Wellenkomponenten der Dünung liegen in den meisten Fällen im Bereich der längeren Perioden, so daß die Verfälschung durch die Eigenart des benutzten Wellenschreibers weniger in Erscheinung tritt. In einer Anzahl von Fällen war es auch möglich, die im Spektrum stark heraustretenden Periodenbänder einer berechneten Dünung zuzuordnen und Vergleiche mit den durch „hindcasting“ ermittelten Perioden zu ziehen. Es ergab sich, daß die nach Bretschneider, Wilson und nach Darbyshire berechneten Perioden auch hier wieder wesentlich zu hoch lagen; die Abweichung betrug durchschnittlich + 34,5% bzw. + 24,5%. Dagegen war die vorausberechnete Periode nach Pierson-Neumann-James nur 9,9% größer und nach Walden 1,8% kleiner als die beobachtete.

Vergleich der hindcasting-Ergebnisse untereinander. Für die Gegenüberstellung der mit den verschiedenen hindcast-Verfahren erzielten Ergebnisse standen mehr Werte zur Verfü-

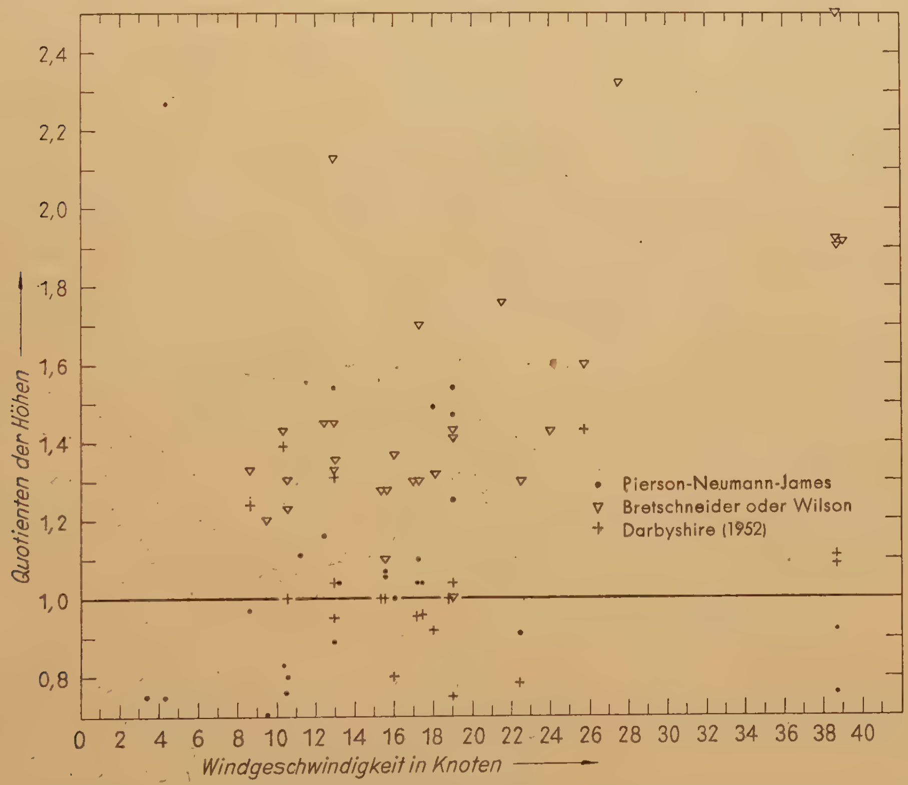

Abb. 6. Für Wellenhöhen in der Windsee: Quotienten $H_{1/3}$ nach W. J. Pierson, Jr., G. Neumann and R. W. James [1953], C. L. Bretschneider [1952] oder B. W. Wilson [1955] und J. Darbyshire [1952] durch $H_{1/3}$ nach H. Walden [1955/56]

gung als für den Vergleich mit den Messungen; denn nur ein Teil der Registrierungen ist ausgewertet worden. Da nach den Diagrammen von Walden der Seegang in nahezu allen Fällen hatte berechnet werden können, wurden die mit den übrigen Arbeitsverfahren erzielten hindcasts auf die entsprechenden Resultate von Walden bezogen. Dies geschah durch Bildung der Quotienten. Diese Zahlen sind für die Windsee in Abhängigkeit von der Windgeschwindigkeit, die während der Messung herrschte, in Abb. 6 dargestellt. Es zeigt sich, daß die nach Bretschneider bzw. nach Wilson berechneten Wellenhöhen sämtlich größer als nach dem Diagramm von Walden sind. Pierson-Neumann-James' [1953, 1955] Co-cumulative liefern bei schwachen Winden mit einer Ausnahme kleinere und bei Winden über 12 kn überwiegend größere Wellenhöhen als nach Walden. In Tab. 6 sind die Mittelwerte der Quotienten, für Wellenhöhe und -periode sowohl für die Dünungs- als auch die Windsee-hindcasts zusammengestellt. Bei der Windsee erfolgte aus den eben angeführten Gründen eine Unterteilung nach der zur Zeit der Messung herrschenden Windgeschwindigkeit v, nämlich nach $v < 12$ kn und $v \geq 12$ kn.

Tabelle 6

	$\frac{\text{Pierson-N.-J.}}{\text{Walden}}$	$\frac{\text{Bretschneider}}{\text{Walden}}$	$\frac{\text{Darbyshire}}{\text{Walden}}$
Windsee			
Wellenhöhe, $v < 12$ kn	0,88 (9)	1,30 (5)	1,19 (3)
$v \geq 12$ kn	1,14 (17)	1,49 (25)	0,98 (16)
alle v	1,03 (26)	1,45 (30)	1,01 (19)
Periode	1,19 (26)	1,76 (30)	1,51 (19)
Dünung			
Wellenhöhe	1,31 (15)	1,14 (22)	0,42 (16)
Periode	1,03 (14)	1,25 (22)	1,20 (15)

Die in Klammern gesetzten Zahlen bezeichnen die Anzahl der Fälle.

Bei der Dünung ergibt sich nach Pierson-Neumann-James in den behandelten fünfzehn Lagen durchschnittlich eine bedeutend größere Wellenhöhe als nach Waldens Diagramm. Bretschneiders Wellenhöhen sind sowohl für Windsee als auch für Dünung sehr wesentlich höher als nach Walden. Dagegen ist die Übereinstimmung zwischen Darbyshire [1952] und Walden [1955/56a] bei der Windsee verhältnismäßig gut. Andererseits erhält man nach Darbyshire [1952] eine sehr viel niedrigere Dünung als nach Walden.

Bei der Wellenperiode liefert das von Walden [1955/56a] gegebene Diagramm niedrigere Werte als alle übrigen hindcast-Verfahren (Abb. 7).

Es sei bemerkt, daß zwischen der von Bretschneider und von Darbyshire benutzten kennzeichnenden bzw. ,,charakteristischen" Wellenperiode $\tilde{T}_{1/3}$ und der bei der Auswertung der Registrierungen hier ermittelten Periode $\tilde{T}'_{1/3}$ kein wesentlicher Unterschied besteht. Es erscheint aber fraglich, ob die in den Diagrammen von Pierson-Neumann-James und von Walden auftretende ,,mittlere Periode" $\tilde{T}_m$ der Periode $\tilde{T}'_m$ bzw. $\tilde{T}$ entspricht, die sich bei der Auswertung der Registrierungen ergibt. Die Größe $\tilde{T}_m$ in den Diagrammen beruht – wenigstens teilweise – gleichfalls auf Beobachtungen einer Art ,,charakteristischer" oder signifikanter Periode im Seegang.

Leider kann hier nicht entschieden werden, welche hindcasting-Ergebnisse die richtigen sind, weil der ,,ship-borne wave recorder" nicht das volle Wellenspektrum erfaßt und daher – wenigstens bei den kürzeren Perioden – keine zuverlässigen Messungen liefert. Es besteht aber der Eindruck, daß die Perioden in dem Diagramm von Walden [1955/56a] etwas zu klein sind.

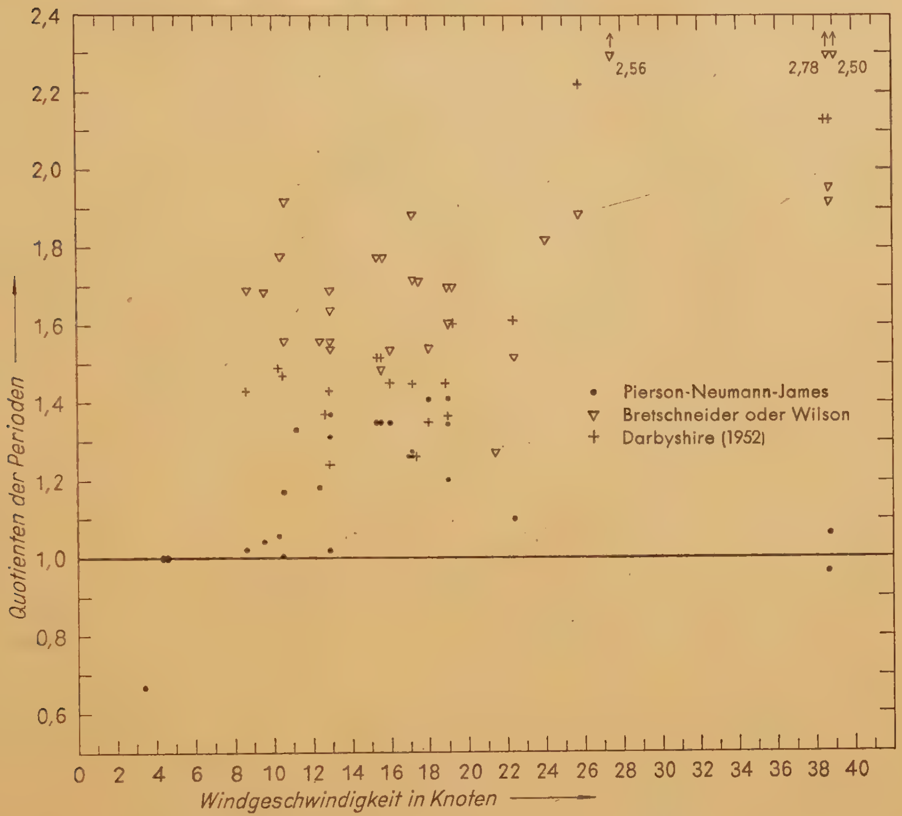

Abb. 7. Für Windseeperioden: Quotienten $\tilde{T}$ bzw. $T^{1/3}$ nach W. J. Pierson, Jr., G. Neumann and R. W. James [1953], C. L. Bretschneider [1952] oder B. W. Wilson [1955] und J. Darbyshire [1952] durch T nach H. Walden [1955/56]

Ausblick. Ein großer Teil der in der letzten Zeit durchgeführten Seegangsmessungen bzw. -registrierungen hatte zum Ziel, die Eigenschaften des Periodenspektrums und die Energie im Seegang zu ermitteln oder wenigstens ermitteln zu helfen. Es ist sehr ratsam, sich dabei zunächst auf die Untersuchung der ausgereiften Windsee zu konzentrieren. Wie die Erfahrung lehrt, ist es schwierig, eine voll ausgereifte, durch „Fremdsee“ (Dünung) ungestörte Windsee am Beobachtungsorte zu treffen. Oftmals wird die anwesende Fremdsee der Beobachtung sogar entgehen. Man sollte bei der Festlegung der Meßtermine daher keinesfalls auf die Mitarbeit eines in der Synoptik erfahrenen Meteorologen verzichten, der an Hand von großräumigen, fortlaufend gezeichneten Wetterkarten ein Urteil über das Heranlaufen von Dünung aus den Nachbargebieten oder aus ferngelegenen Seeräumen geben kann. Er ist auch in der Lage, die Grenzen des die Windsee erzeugenden Windfeldes und die Schwankungen der Windstärke im Fetch zu ermitteln.

Daß das Meßinstrument frei von Fehlern und Ungenauigkeiten arbeiten muß und daß der kurzperiodische Teil des Spektrums nach Möglichkeit in gleicher Weise erfaßt werden sollte wie der langperiodische, ist eine weitere selbstverständliche Forderung. Sobald diese Bedingungen erfüllt sind, wird es möglich sein, die Eigenschaften des Seegangsspektrums mit einiger Genauigkeit zu ermitteln. Bei den Auswertungen ist die Breite des Spektrums nach Cartwright und Longuet-Higgins [1956] zu berücksichtigen. Insbesondere wird sich dann auch herausstellen, von welcher Potenz der Windgeschwindigkeit v die Energie im Seegang abhängt (vgl. H. Walden und J. Piest [1957]) und welchen Einfluß der Temperaturunterschied Luft–Wasser bei den verschiedenen Windstärken ausübt. Sobald endgültige Werte darüber vorliegen werden, in welcher Weise das Windseespektrum und die Energie im Seegang vom Wind und von der Temperaturdifferenz sowie schließlich auch von der Winddauer und vom Fetch abhängen, kann mit einer wesentlichen Verbesserung der hindcasts und ebenso der Seegangsvoraussagen gerechnet werden.

Acknowledgements. The senior author wishes to express his appreciation to the Woods Hole Oceanographic Institution for making possible his visit to Woods Hole in February and March, 1957. The authors also wish to thank the U. S. Hydrographic Office for their assistance in providing the necessary weather charts and power spectra of fifteen wave records. This research was sponsored in part by the U. S. Navy Office of Naval Research under contract with the Woods Hole Oceanographic Institution.

Schrifttum

Bracelin, P., 1952: Observing, forecasting and reporting ocean waves and surf. Naval Weather Service. Mem. No. 147/52.

Bretschneider, C. L., 1952: The generation and decay of wind waves in deep water. Transact. Amer. Geophys. Un. **33**, 381–389.

Cartwright, D. E., and Longuet-Higgins, M. S., 1956: The statistical distribution of the maxima of a random function. Proc. Roy. Soc. A, Vol. **237**, 212–232.

Darbyshire, J., 1952: The generation of waves by wind. Proc. Roy. Soc. A, **215**, 299.

Longuet-Higgins, M. S., 1952: On the statistical distribution of the heights of sea waves. J. Mar. Res., Vol. **11**, No. 3.

Neumann, G., 1953: On ocean wave spectra and a new method of forecasting wind-generated sea. Beach Eros. Bd., Techn. Mem. No. **43**, Dec.

Pierson, Jr., W. J., 1954: An interpretation of the observable properties of sea waves in terms of the energy spectrum of the Gaussian record. Trans. Amer. Geophys. Un. **35**, 747–757.

Pierson, Jr., W. J., G. Neumann, and R. W. James, 1953, 1955: Practical methods for observing and forecasting ocean waves. New York Univ., Coll. Eng., Dept. Meteorol. & Oceanogr., Techn. Rep. No. 1; U. S. Navy Dept., Hydrogr. Office Publ. No. 603, Wash.

Roll, H. U., 1952: Über Größenunterschiede der Meereswellen bei Warm- und Kaltluft. Dtsch. Hydrogr. Z. **5**, 111–114.

Silvester, R., 1955: Practical application of Darbyshire's method of hindcasting ocean waves. Appl. Science **6**, 261–266.

Sverdrup, H. U., and Munk, W. H., 1947: Wind, sea and swell. Theory of relation for forecasting. U. S. Navy Dept., Hydrogr. Off. Publ. No. 601.

Tucker, M. J., 1956 a: A shipborne wave recorder. Transactions of the Institute of Naval Architects, Vol. **98**, 236–250.

Tucker, M. J., 1956 b: Comparison of wave spectra. Nat. Inst. Oceanogr. (England), Int. Report No. A 6.

Walden, H., 1953/54: Die Wellenhöhe neu angefachter Windsee nach Beobachtungen atlantischer Wetterschiffe und des Fischereischutzbootes „Meerkatze". Ann. Meteorol. **6**, 296–304.

Walden, H., 1954: Über die Dünung aus einem Windfeld, welches am Beobachtungsort in einiger Entfernung vorbeizieht. Dt. Hydrogr. Z. **7**, 190.

Walden, H., 1955: Die Höhe der Windsee bei gleichmäßig zunehmendem Wind. Dt. Hydrogr. Z. **8**, 236–241.

Walden, H., 1955/56a: Ein neues Diagramm zur Berechnung des Seegangs aus den Windverhältnissen. Ann. Meteorol. **7**, 213–218.

Walden, H., 1955/56b: Die Höhe der Windsee bei regionaler Zunahme der Windstärke in der Richtung mit dem Winde. Ann. Meteorol. **7**, 337–341.

Walden, H., und J. Piest, 1957: Beitrag zur Frage des Wellenspektrums in der Windsee. Dt. Hydrogr. Z. **10**, 93.

Wilson, B. W., 1955: Graphical approach to the forecasting of waves in moving fetches. Beach Eros. Bd., Corps of Eng., Techn. Mem. No. 73.

Eingegangen im September 1957

Nr.	Datum, Uhrzeit (Eastern time)	Position	Wind		$T_L - T_W$	Unmittelbar von der Registrierung			
			Richtung	Geschw. (Kn.)	°F	$\sqrt{\frac{\Sigma z^2}{n}}$	$H_{1/3}$	$\tilde{T}'_m$	$\sqrt{\frac{\Sigma z^2}{n}}$
1.	13. Nov., 11^{40}–12^{00}	41,6° N 50,5° W	150°	17,2	–2,5°				1,10 1,12
2.	13. Nov., 18^{05-21}	41,3° N 50,5° W	170°	18,0	–1,2°	1,03	4,0	6,1	1,09 1,14
3.	14. Nov., 08^{55}–09^{16}	40,9° N 50,5° W	190°	18,9	–7,0°				2,85 2,91
4.	14. Nov., 11^{00-20}	40,8° N 50,5° W	315°	24,0	–7,4°	3,20	11,7	7,3	3,26 3,30
5.	14. Nov., 17^{30-50}	40,5° N 50,5° W	340°	~16	–7,0°				2,26 2,33
6.	15. Nov., 17^{42-58}	39,3° N 50,5° W	315°	6,9	–6,7°	2,23	8,5	8,5	
7.	16. Nov., 14^{15-38}	38,6° N 50,3° W	270°	10,3	–2,0°	1,17	4,6	7,3	1,15 1,22
8.	18. Nov., 08^{21-41}	35,8° N 50,5° W	080°	15,5	–1,0°	1,90	7,1	7,8	
9.	18. Nov., 10^{13-35}	35,8° N 50,5° W	085°	15,5	+4,8°	1,91	7,2	8,4	1,95 2,01
10.	18. Nov., 11^{13-33}	35,8° N 50,5° W	095°	15,5	+5,0°	1,88	7,0	8,6	[1,85] [1,95]
11.	18. Nov., 12^{32-53}	35,6° N 50,5° W	095°	15,5	+5,0°				2,18 2,20
12.	18. Nov., 19^{15-41}	34,8° N 50,5° W	090°	8,6	+3,0°	3,28	12,8	9,4	3,08 3,05
13.	20. Nov., 07^{02-22}	31,6° N 50,5° W	045°	17,2	+0,6°	2,11	7,7		1,97 2,00
14.	20. Nov., 17^{37-57}	30,2° N 50,5° W	070°	17,2	–0,8°	1,62	5,9		
15.	20. Nov., 20^{43}–21^{09}	30,2° N 50,5° W	070°	17,2	–0,8°	1,78	6,5		1,74 1,81
16.	20. Nov., 21^{34}–22^{03}	30,2° N 50,5° W	070°	17,2	–0,8°	1,78	6,6		
17.	21. Nov., 17^{00-23}	27,9° N 50,5° W	080°	25,8	~0°	2,05	7,5	6,7	2,00 2,08
18.	21. Nov., 21^{02-24}	27,9° N 50,5° W	075°	27,5	~0°	2,69	9,9	7,5	
19.	21. Nov., 22^{25-47}	27,9° N 50,5° W	085°	38,7	~0°	3,58	13,6	8,1	3,47 3,49
20.	21. Nov., 23^{40} bis 22. Nov., 00^{10}	27,9° N 50,5° W	085°	38,7	~0°	3,94	14,8	8,4	
21.	22. Nov., 01^{37}–02^{00}	27,9° N 50,5° W	090°	38,7	~0°	4,30	16,0	8,5	4,25 4,24
22.	22. Nov., 08^{10-30}	27,9° N 50,5° W	110°	21,5	~0°	3,34	12,8	8,2	

ng der Seegangsregistrierungen des Forschungsschiffes „Atlantis“ mit
mit entsprechenden Seegangsberechnungen aus den Windverhältnissen

Tabelle 3

Aus dem Spektrum bestimmt							H			
		Schmales Spektrum		Breites Spektrum			Windsee			
$\Delta\sqrt{\frac{\Sigma z^2}{n}}$	$\tilde{T}$	$H_{1/3}$	$\Delta H_{1/3}$	$H_{1/3}$	$\Delta H_{1/3}$	ε	P	B/W	W	D
%	7,2 7,1	4,4	%	4,2	%	0,61			2,4 2,3	
+5,5	6,7 6,6	4,4 4,6	+10,0	4,1 4,3	+2,5	0,57	5,7 4,9	5,0 5,4	3,8 3,5	3,5 4,7
	7,9 7,5	11,5 11,7		10,5 10,8		0,63	7,6 5,3	8,7 7,5	6,1 4,4	6,1 6,4
+1,8	8,3 8,1	13,0 13,2	+11,1	12,7 12,9	+8,5	0,41		18,1 11,9	12,6 6,6	
	7,1 6,9	9,0 9,3		8,5 8,8		0,57	3,5 3,9	4,8 4,5	3,5 2,9	2,8 4,2
									5,0 4,3	
−1,7	6,3 6,1	4,6 4,9	0,0	4,4 4,6	−4,3	0,45			1,4 1,5	
							5,4 5,8	6,4 7,7	5,0 4,3	5,0 6,5
+2,0	7,3 7,3	7,8 8,0	+8,3	7,7 7,9	7,0	0,33	5,1 5,8	6,3 7,7	4,8 4,3	4,8 6,5
							5,1 5,8	6,3 7,7	4,8 4,3	4,8 6,5
	7,7 7,5	8,7 8,8		8,5 8,6		0,41	5,1 5,8	6,3 7,7	4,8 4,3	4,8 6,5
−6,0	9,5 9,5	12,3 12,2	− 3,9	12,1 12,0	−5,5	0,37	2,3 3,4	3,4 5,6	2,6 3,3	3,0 4,7
−7,1	7,9 7 6	7,9 8,0	+ 2,6	7,5 7,6	−2,6	0,55	5,2 5,7	8,5 8,5	5,0 4,5	
							5,3 5,7	6,6 7,8	5,1 4,5	4,9 6,5
−2,3	7,2 6,9	7,0 7,2	+ 7,7	6,7 7,0	+3,1	0,54	5,3 5,7	6,6 7,8	5,1 4,5	4,9 6,5
							5,3 5,7	6,6 7,8	5,1 4,5	4,9 6,5
−2,5	6,9 6,7	8,0 8,3	+ 6,7	7,8 8,0	+4,0	0,41		10,0 ∼ 7,5	6,2 4,0	8,8 9,1
								15,0 10,0	6,5 3,9	
−3,2	8,0 7,9	13,9 14,0	+ 2,2	13,6 13,7	0,0	0,39	8,7 5,0	20,0 ∼10,3	10,2 4,7	
							11,5 5,9	22,0 ∼10,5	11,4 5,2	12,3 11,0
−1,2	9,1 8,9	17,0 17,0	+ 6,2	16,6 16,5	+3,7	0,42		24,0 ∼11,0	12,5 5,6	13,7 12,0
								14,0 11,0	7,3 4,8	

„ship-borne wave recorder“ casting)

Tafel 4

C A S T - Ergebnisse							Bemerkungen
Dünung			Gesamtseegang				
B/W	*W*	*D*	*P*	*B/W*	*W*	*D*	obere Zeile einer Querreihe jeweils in ft, untere Zeile in sec
	0				2,4 2,3		Windstärke nahm in den letzten Stunden zu
0	0	0	5,7 4,9	5,0 5,4	3,8 3,5	3,5 4,7	
0	0	0	7,6 5,3	8,7 7,5	6,1 4,4	6,1 6,4	Kurz vor Frontdurchgang
8,0 7,7	8,4 5,3			19,8 ×	15,6 ×		Wanderndes Windfeld
11,6 11,7	12,3 ∼6			13,8	12,3*		Ältere See aus NW, junge See aus NNW. *α = 22,5°
0	5,4 ∼7				6,4* ×		Stetige Windabnahme *α = 45°
9,0 15,5	6,2 7,5	4,0 14,0		∼9,0 ×	6,4 × *		Winde im Auffrischen, *Spektrum nicht kontinuierlich
	4,8 ∼10		7,3 ∼10		6,9 ∼7,5		Wind war gleichbleibend
	5,8 ∼11		9,1 ∼11		7,5 ∼9		Innerhalb des Windfeldes Windstärke regional abnehmend in Windrichtung
	6,2 ∼11,3		9,8 ∼11		7,8 ∼9		
	6,5 ∼11,5		10,6 ∼11		8,1 ∼9		
13,1 10,6	13,8 ∼10,5	∼5,0 11,5	16,3 ∼9	13,8 ×	14,4 ∼8	5,8*	Zwei Dünungen: 090° und 105° *Energien von Windsee und Dünung voll addiert
6,7 11,4	7,2 ∼8,5	2,2 9,8	11,3 ∼7	10,8 ∼10	9,8 ∼7		Regionale Windabnahme
5,9 12,0	6,0 ∼8	2,3 9,9	5,5* ∼5,0	8,8 ∼10	6,6* ∼6,5	5,3 ∼8,5	Windsee und Dünung aus nahezu gleicher Richtung. *Da Windsee und Dünung aus etwa gleicher Richtung, bei Addition spektrale Energieverteilung berücksichtigt.
5,1 10,7	5,4 ∼7	2,0 8,8	5,5* ∼5	8,3 ∼9,5	6,5* ∼6,5	5,2 ∼7,5	
5,1 10,7	5,4 ∼7	2,0 8,8	5,5 ∼5	8,3 ∼9,5	6,5 ∼6,5	5,2 ∼7,5	
9,6 10,7	8,2 ∼8	4,5 8,8		13,9 ∼9	9,5 ×	9,9 ∼9,0	Wind hat zeitlich und regional zugenommen
9,6 10,7	8,2 ∼8	7,0 8,8		17,8 ×	9,8 ×		
10,3 11,4	9,8 ∼8	8,0 9,3		22,5 ×	13,2 ×		
10,3 11,4	9,8 ∼8	8,0 9,3	16,3 ×	24,3 ×	14,1 ×	14,6 ∼10,0	
10,3* 11,4	9,8 ∼8	8,0 9,3	17,5 ×	26,1* ×	15,1 ×	15,9 ∼10,5	* Unsicher, Dünung möglicherweise schon duchgelaufen
9,0 ∼8,0	9,2 ∼8	5,6 8,1		16,6 ×	11,2 ×		Wind abnehmend

Contribution No. 854

Reprinted from COPEIA, 1957, No. 1, p. 61, April 5
Printed in U.S.A.

NORTHERN RECORD OF THE SNAKE EEL *OPHICHTHUS GOMESI* (CASTELNAU).—Shortly after sunset on July 16, 1954 the R/V Atlantis was hove to in 40 fathoms at 40°32′N, 70°54′W (50 miles S of Gay Head, Mass.) when 3 eels were seen swimming at the surface close by the vessel's hull. They were separated from one another by distances less than their length. Two of the eels had disappeared when the writer returned with a dipnet but the remaining one was caught. About one-half hour later, a blue shark (*Prionace glauca*), which had been in the vicinity of the vessel for several hours was caught and a second eel was removed from its stomach. It was obvious from the latter eel's condition that it had been very recently swallowed and may have been one of the uncaught two earlier seen. The eels prove to be specimens of *Ophichthus gomesi* (Castelnau), 472 mm. and 374 mm. in total length respectively. Both are females and appear to have recently spawned. A few ripe eggs about 1 mm. in diameter and pale yellow in color had been retained.

This eel is easily separated from its congeners by the long tail (61 and 60 hundredths of the total length in the present specimens) and by the characteristic dentition and coloration (see Ginsburg, 1951, Tex. Jour. Sci., 3(3) : 466–67 and 478). According to Ginsburg there is not much good information on the habitat of this species, but it appears to be known mainly from shallow coastal waters. It occurs most commonly from Florida to Brazil, although there is a record for Charleston, S. C., the northernmost heretofore. Thus this species should be added to the lengthy list of weak-swimming tropical and subtropical animals which appear during the summer in Atlantic shelf and coastal waters off northern United States and southern Canada. The means by which these animals are transported thither is as yet little understood since the popular supposition that they are carried north by the Gulf Stream, although perhaps correct, is insufficient to explain their presence in waters many miles inshore of the Stream's direct effect.—Richard H. Backus, *Woods Hole Oceanographic Institution, Woods Hole, Massachusetts.*

Contribution No. 854 of the Woods Hole Oceanographic Institution.

Contribution No. 857

Reprinted from COPEIA, 1957, No. 3, pp. 246–248, August 26
Printed in U.S.A.

NOTES ON WESTERN NORTH ATLANTIC SHARKS.—Systematic records of shark captures have been kept by the Research Vessel ATLANTIS of the Woods Hole Oceanographic Institution for about the last three years. The data for *Prionace glauca*, *Eulamia falciformis*, *Eulamia obscura*, and *Scoliodon terrae-novae* in this paper come from that source and the author is indebted to the officers and crew of ATLANTIS, particularly Capt. W. Scott Bray. The writer is further indebted to Mr. George Berglund and Mr. Anthony E. Silva of Provincetown, Mass. and to Capt. Stanley E. Poole of Menemsha, Mass. for specimens of *Squatina dumeriil*. Capt. Arthur C. Nelson of Woods Hole, Mass. collected the specimen of *Hexanchus griseus*. A/1c Gene A. McMahon of Lowell, Massachusetts captured the basking shark and Dr. Robert H. Gibbs, Jr. of WHOI provided the data from the white shark. The specimens of *Squatina* and *Hexanchus* have been deposited in the Museum of Comparative Zoology. This paper is Contribution No. 857 from the Woods Hole Oceanographic Institution.

Hexanchus griseus (Bonnaterre), the six-gilled shark. A female 236 cm. in total length and weighing 81 kg. was taken in an otter trawl near 41°55′N, 68°05′W on February 11, 1956. The depth was about 102 fathoms.

This species is common in the deep water north of Cuba but the only other western Atlantic records heretofore are one from near Currituck Lighthouse, North Carolina, and one from northern Argentina (Bigelow and Schroeder, 1948, Fishes of the western North Atlantic, 1: 84). The northernmost records in the eastern Atlantic are for Iceland (two, see Saemundsson, 1949, The Zoology of Iceland, 4 (72): 117), the population center being in the Mediterranean.

The stomach of the present specimen contained three cephalopod beaks; one pollock (*Pollachius virens*) about 60 cm. long; two skates, probably *Raja laevis*, both about 50 cm. long; and other fish remains including a flatfish.

The right ovary appeared to be the functional one and bore four or five prominent "scars", perhaps corpora lutea.

Carcharodon carcharias (Linnaeus), the white shark. A juvenile female of this uncommon shark 298 cm. in total length was taken in a fish trap in Cape Cod Bay two miles off the beach at Dennis, Mass., on August 16, 1956.

Cetorhinus maximus (Gunnerus), the basking shark. An immature female 396 cm. in total length was harpooned at the surface two miles off the beach at Sandwich, Mass. on October 18, 1956. This specimen had the produced, subcylindrical snout typical of juveniles. The gill rakers were lacking. Van Deinse and Adriani (1953, Zool. Mededel. Rijks. Natuur. Hist. Leiden, 31 (27): 307–310) first pointed out that gill rakers are sometimes absent in this species. Recently Parker and Boeseman (1954, Proc. Zool. Soc. Lond., 124: 185–194) have shown that in north European waters the gill rakers are shed about October and replaced by about February. Parker and Boeseman suggest that the fish "undergoes a resting, non-feeding, demersal stage" at this time. Van Deinse and Adriani (*op. cit.*) report partly digested plankton in the stomach of a specimen without gill rakers and suggest that the rakers are thus not essential to feeding. Parker and Boeseman (*op. cit.*) also report such a specimen but argue that the stomach contents were in a somewhat advanced stage of digestion and may have been ingested before the rakers were lost. The stomach of the present specimen contained several gallons of a smooth, homogeneous, somewhat stiff, reddish-brown, greasy paste. This appears to be the normal contents of the pyloric limb of the stomach (Matthews and Parker, 1950, Proc. Zool. Soc. Lond., 120: 548). In animals that have recently fed, the cardiac stomach contains material in which the whole or parts of individual plankters are discernible (Matthews and Parker, *op. cit.*). Thus while the stomach contents of our specimen perhaps supports the reasonable contention that individuals without gill rakers do not feed, the fact that the animal was actively swimming at the surface when captured (as it had been for two days previously) does not fit the notion of a demersal, inactive stage when gill rakers are absent.

Prionace glauca (Linnaeus), the great blue shark. The little that is known about development and reproduction in this presumably common and widespread animal comes mainly from Lo Bianco (1909, Mitt. Zool. Sta. Neapel, 19: 666). Data from four litters of pups taken from females caught at the surface by hook and line are summarized in Table I.

Our data together with those of Lo Bianco(1909, *op. cit.*) suggest that the seasons of mating and pupping are not restricted as they seem to be in the white-tip (*Pterolamiops longimanus*), another common high-seas shark (Backus, Springer, and Arnold, 1956, Deep-Sea Res., 3: 185–186). Lo Bianco reports embryos from 16 cm. in length to those "apparently completely developed" (this would be about 50 cm.) taken in the Mediterranean during May and June.

Scoliodon terrae-novae (Richardson). A male about 75 cm. in total length was taken at the surface on July 13, 1956 in 18°49′N, 61°57′W (about 65 miles N of Barbuda) where the water depth is about 3300 fathoms. The specimen is of interest because Bigelow and Schroeder (1948 Fishes of the western North Atlantic, 1: 300) say "so far as we are aware it has never been reported more than a mile or two out from the land or from water more than a few fathoms deep." Springer (1950, Amer. Mus. Novit., 1451: 7) reports specimens from the surface over more than 200 fathoms at Bimini but only several miles off the shelf.

TABLE I

DATA ON EMBRYOS, BLUE SHARK (*Prionace glauca*)

Position	Date	Length of mother	No. of embryos			Total length of embryos
			Male	Female	Total	
37°06′N 65°00′W	23 Sept. 1954	277 cm.	17	17	34	294–335 mm.
35°00′N 65°00′W	25 Sept. 1954	302 cm.	26	37	63	90–118 mm.
32°00′N 59°25′W	13 Nov. 1954	256 cm.	—	—	14	—
33°00′N 64°00′W	10 Oct. 1955	251 cm.	18	17	35	130–153 mm.*

* One embryo, about 100 mm. in length, was dead in the mother.

TABLE II

RECORDS OF *Eulamia falciformis*

Position	Date	Sex	Total length
19°33′N, 75°09′W	20 March 1953	M	c. 90 cm.
19°15′N, 75°10′W	21 March 1953	F	103 cm.
19°05′N, 75°05′W	22 March 1953	F	110 cm.
19°05′N, 75°06′W	29 March 1953	F	97 cm.
38°00′N, 68°00′W	19 October 1954	F	c. 115 cm.
37°44′N, 68°14′W	20 October 1954	F	152 cm.
11°30′N, 60°45′W	27 February 1955	F(2)	61, 201 cm.
11°30′N, 60°45′W	27 February 1955	M(5)	122, 145, 149, 150, 173 cm.

For the time being I follow Springer (*op. cit.*) in regarding the sharpsnouted *S. lalandi* (Müller and Henle) as a distinct species. The present specimen has a short, broad snout and the critical head measurements fall within the limits given by Bigelow and Schroeder (*op. cit.*) for *S. terrae-novae* (*s. strict.*). I can add little about the presence or absence of a mid-dorsal ridge in this species, not having seen the present specimen in a fresh condition. Springer (*op. cit.*) has observed the ridge in *S. lalandi* but did not find it in fresh Mississippi specimens of *S. terrae-novae*. The present specimen has a faint suggestion of this structure (which often disappears after preservation). However, if it were no more evident in a fresh specimen it would probably be regarded as absent.

Eulamia falciformis (Müller and Henle), the scythe-fin shark. Our records (Table II) are from hook and line captures at the surface and add little to the concept of the geographical distribution of this little-known shark as delineated by Bigelow and Schroeder (1948, Fishes of the western North Atlantic, 1: 332–333). All are from tropical waters save two near latitude 38°N taken in October when the water there is at about its maximum temperature. The depth of water where our captures were made varies from about 250 fathoms to 3000 fathoms and the distance offshore from about 12 to 240 miles.

In deep water in the eastern Cayman Sea between March 18, 1953 and April 2, 1953 four specimens of this species and 15 specimens of the white-tip shark (*Pterolamiops longimanus*) were taken, these being the only sharks observed there. In 11°30′N, 60°45′W (north of Tobago I., about 12 miles offshore in a water depth of 250 to 300 fm.) seven specimens were taken within a half-hour and many more were seen about the vessel.

The color of *E. falciformis* has been described as "dark gray above, grayish white below" or "after preservation . . . mouse gray above and a paler shade of the same tint below" (Bigelow and Schroeder, 1948, Fishes of the western North Atlantic, 1: 332). Fresh-caught specimens are a grayish-brown above with a peculiar brassy overtone. The undersides are of the purest, most gleaming white. As soon as the shark is handled on deck a bit, it becomes a uniform gray beneath because of its placoid scales which cause a very even soiling. The upper parts become grayer and darker as soon as the shark dies. When the shark is viewed at large, swimming in clear water a few feet beneath the surface, the upper parts appear a handsome golden-brown.

We have examined seven stomachs of which two were empty. In the remaining, cephalopods occurred in four (one cephalopod had many photophores); fish in three; garbage in one; and one had some red roe probably from a fish.

All of our captures have been of juveniles or perhaps, in one or two cases, young adults. *E. falciformis* is active by both day and night.

Eulamia obscura (Lesueur), the dusky shark. This species is known from Cape Cod to Brazil in the western North Atlantic. However, "information in its occurrence south of Florida is scanty", (Bigelow and Schroeder, 1948, Fishes of the western North Atlantic, 1: 388) so we report the following specimen: a male, 271 cm. in total length taken in the night at 18°40′N, 65°45′W (about 15 miles offshore north of San Juan, P. R.) on March 8, 1954 by hook and line at the surface in about 800 fathoms of water.

Squatina dumerili (Lesueur), the angel shark. A female 117 cm. in total length was found dead in the intertidal zone of Nashaquitsa Pond (41°19′.8N, 70°49′.7W), at Menemsha, Martha's Vineyard, about December 6, 1955. This specimen weighed 15.4 kg. Fish remains, including a portion of vertebral column about 18 cm. long, were found in the stomach. Ten eggs, 35 to 50 mm. in diameter, were found in the left ovary. This specimen bore no indication as to why it died. Surface water temperature at Woods Hole at the time that this specimen was found was between 41° and 42°F.

On December 4, 1956 a male 107 cm. in total length was taken in an otter trawl in Provincetown Harbor where the water depth was 15 fathoms. This specimen weighed 10.7 kg. The stomach was empty.

This species has been reported from Martha's Vineyard, Mass., south to Jamaica (Bigelow and Schroeder, 1948, Fishes of the western North Atlantic, 1: 542). It is most common off the Central Atlantic States. The two previous Massachusetts records come from Menemsha, the northeasternmost locality from which the species had been reported. In addition to the present Menemsha specimen, one was taken in a fish trap there on September 1, 1873 (Baird, 1873, Rept. Comm. Fish and Fisheries, 1871–1872: 827; Smith, 1898, Bull. U. S. Fish. Comm., 1897: 89) and another on September 23, 1921 (Smith, 1922, Copeia, 106: 33). All Massachusetts specimens have been between 90 and 120 cm. long. The nearest localities from which other records come are Newport and West Passage, Rhode Island.—RICHARD H. BACKUS, *Woods Hole Oceanographic Institution, Woods Hole, Massachusetts.*

Contribution No. 860

Särtryck ur Tellus nr 4, 1957

Determination of Deuterium-Hydrogen Ratios in Hawaiian Waters

By I. FRIEDMAN, U. S. Geological Survey, Washington, D. C.[1] and A. H. WOODCOCK, Woods Hole Oceanographic Institution, Woods Hole, Massachusetts[2]

(Manuscript received December 27, 1956)

Abstract

Previous determinations of the deuterium-hydrogen ratios in natural waters revealed the fractionation of deuterium; a fractionation resulting from differences in the vapor pressure of H_2O and HDO. Measurements of the deuterium in sea, rain, and condensate waters of Hawaii, are reported here. These results show a concentration of deuterium in sea-surface waters, and an inverse relationship of D with altitude in rain and condensate taken on a mountain side. The possible significance of these measurements for cloud physics studies is briefly discussed.

The technique of the D/H determination is essentially as follows (FRIEDMAN, 1953): 0.01 ml of water is converted to hydrogen gas by reaction with hot uranium metal. The hydrogen gas is then introduced into a mass spectrometer especially constructed for the purpose and the deuterium/hydrogen ratio in the sample gas is compared to the D/H ratio in a standard hydrogen. The standard gas was prepared from Lake Michigan water, and our D/H results are expressed as per cent enrichment or depletion of deuterium relative to our standard water:

$$\frac{(D/H)_{\text{sample}} - (D/H)_{\text{Standard}}}{D/H \text{ Standard}} \times 100$$

The precision of the method is ±0.1 per cent. Figure 1 shows the results of previous D/H analysis of natural waters from various localities. During the course of "Project Shower", water samples were taken at the positions marked D_1 to D_7 on the location map (see Figure 3).

The major source of fractionation of deuterium in nature is the difference in the vapor pressure of H_2O and HDO as shown by EPSTEIN et al. (in press). Figure 2 shows the fractionation that occurs during the change from liquid to vapor. Note that at 10°C the vapor phase is depleted by 8.8 per cent in deuterium compared to the liquid in equilibrium with it, while at 50°C the fractionation is only 5 per cent. During freezing (at 0° C) ice is enriched by about 2 per cent in deuterium relative to the water from which it is freezing.

The fractionations that take place during change of state are the ones that are important in changing the hydrogen isotopic composition of water. In the case of atmospheric water the source of the water vapor, plus the fractionation processes it has undergone, will determine its final isotopic composition. The

---

[1] Publication authorized by the Director, U.S. Geological Survey.

[2] Contribution No. 860 from the Woods Hole Oceanographic Institution.

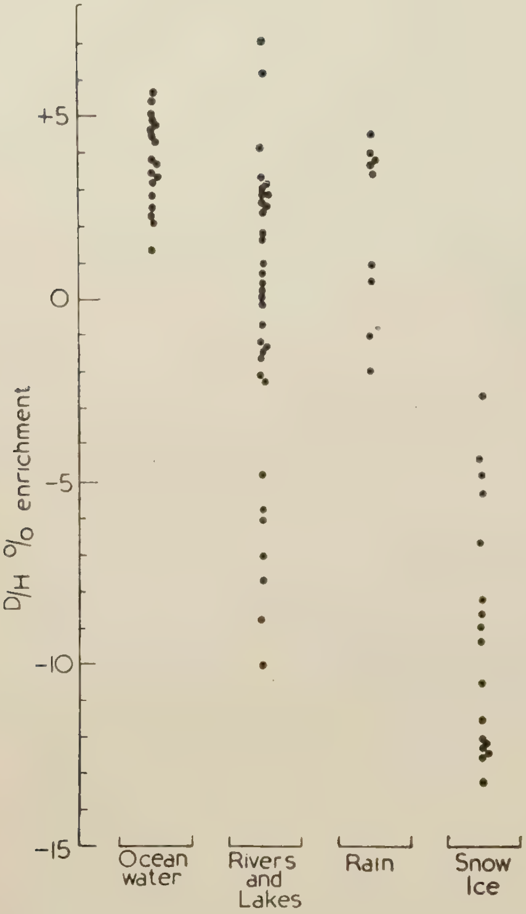

Fig. 1. Deuterium/Hydrogen ratios which have been observed in various natural waters. These results have not been previously published.

trade wind clouds that we are concerned with in Hawaii are composed of water which has evaporated from the open ocean.

The surface composition of the ocean in this latitude varies between about +4.0 and +5.0 per cent relative to our Lake Michigan standard. If we assume that evaporation occurs at about 20°C, and that the sea represents an infinite reservoir of essentially unchanging composition, the water vapor will be about 8.0 per cent "lighter" (depleted in deuterium) than the ocean, or approximately −3.5 per cent on our scale. This compares to the −3.9 per cent that we found for condensate (water from ice formed on exterior of vessel containing solidified carbon dioxide) at the windward shore of the island (see location map Figure 3 and Table 2).

Table 1 shows the D/H ratios in rain water sampled at various altitudes on the mountain side, and in lake water (station D6). Lake Waiau water is thought to come largely from melted snow near the mountain top. It is subject to excessive evaporation, due to the low water content of the air at high levels, and the D/H ratio is not therefore considered to represent that of the original precipitation

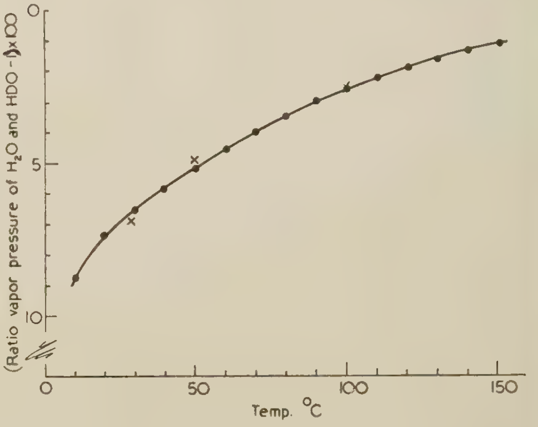

Fig. 2. Ratio of the vapor pressures of H_2O and HDO taken from experimental data derived by measuring the isotopic composition of liquid and vapor secured during a single-stage distillation. (Epstein et al., in press.)

Table 1. Deuterium in rain and lake waters.

Time	Date (1954)	Elevation (feet)	Position (see map)	Source of Water	Number of Samples	D/H per cent
0930	Nov. 6	50	D1	Rain	2	+3.5 and +4.3
1030—1350	Nov. 7	2,000	D2	Rain	5	+3.5 to +4.0
—	Nov. 2	2,700	D3	Rain	1	+2.5
1500	Oct. 26	5,500	D4	Rain	2	+2.0 and +2.3
1400	Nov. 21	13,000	D6	Lake Waiau	1	+1.9

Table 2. Deuterium in sea surface and condensate waters.

Time	Date (1954)	Elevation (feet)	Position (see map)	Source of Water	Number of Samples	D/H per cent
—	—	0	D7	Sea surface	2	+4.1 and +4.5
—	Nov. 18	50	D1	Condensate	1	— 3.9
0900—1100	Nov. 21	9,500	D5	Condensate	1	— 12.1

falling at that height. The rain samples were obtained in a few seconds, using a 0.5 m² stainless steel funnel, and were not subject to a significant amount of evaporation after arrival at ground level. Rain samples coming from stations D2, D3, and D4 were taken within the clouds on the mountain slope. (See location map Figure 3.)

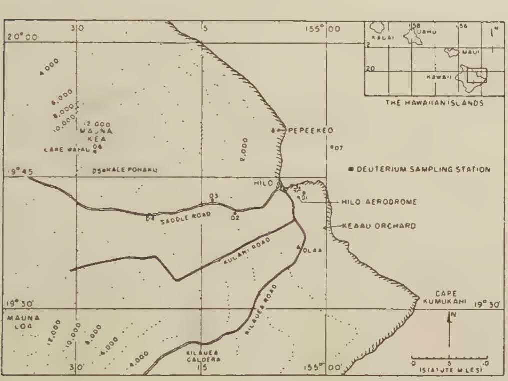

Fig. 3. Map of Hawaii showing location of the stations where rain water, sea water, and water vapor were sampled for deuterium analysis.

It should be mentioned that cloud motion was, in general, from east to west; hence from position D1 up the mountain slope and through the "Saddle" which lies westward of position D4. It is interesting that the rains sampled at progressively higher elevations show a trend toward depletion of deuterium (see Table 1). A comparison of the D/H values for condensate (Table 2) obtained near sea level and at 9,500 feet altitude also shows markedly the reduction of deuterium with height.

The number of rain and condensate samples analyzed is low. It seemed pertinent, however, to point out that the trend toward decreased D/H values in rains falling at successively greater distances from the windward coast has been previously noted. (Kirschenbaum, 1951.) This decrease may be explained as follows:

At the start of precipitation (assuming a wet bulb temperature of about 10° C) the first fraction precipitating will have a composition of about +4.5 per cent and the rain will get progressively lighter as the cloud becomes depleted in deuterium. Our rain samples from the 50 ft. level analyzed +4.3 and +3.5. At higher elevations we were sampling later periods in the precipitation and therefore the rain should become lighter as we proceed up the mountain and in the direction of motion of the clouds. Note that at 2,000 ft. rain varies from +3.6 to +4.0, at 2,700 ft. +2.5, and at 5,000 ft. +2.0 and +2.3.

An alternate explanation for these observed effects is that a cloud system represents a large distilling column with reflux. In this case the cool top (high altitude) will be enriched in the component of higher vapor pressure (H_2O) and the warmer bottom will be enriched in the component of lower vapor pressure (HDO). Rains formed near the bases of the orographic clouds are more likely to fall on the lower slopes of the mountain, while the rain formed near the cloud tops will be carried by the winds to the upper slopes before they fall to the ground.

In all probability the two processes (i.e. depletion of deuterium as the cloud loses water, and the distilling column effect) are both operative in the clouds. The relative importance of each process can only be decided by more

Table 3. Deuterium, salinity, and intensity in rains sampled on Nov. 7 at position D2 (see Table 1 and Figure 3).

D/H per cent	Salinity mg l^{-1}	Intensity mm hr^{-1}
+ 3.5	1.5	21.2
+ 3.8	3.4	4.8
+ 3.6	4.2	3.8
+ 3.8	4.5	9.0
+ 4.0	8.1	3.0

measurements continuing to use samples taken under known conditions.

On November 7, five rain samples were taken for deuterium measurements at position D2 at a time when rain samples were also taken for intensity and salinity determinations. Table 3 shows these results. It is interesting that there is a suggestion of a relationship between salinity and D/H. The number of samples is inadequate, however, to indicate a definite relationship.

At the present time it is not clear to what extent the D/H ratios may be useful in studying rain-forming mechanisms. The results given here clearly suggest that deuterium should be added to the list of properties of cloud, rain and condensate waters which may be useful in cloud physics studies.

This work was conducted in part by the U.S. Geological Survey on behalf of the U.S. Atomic Energy Commission.

REFERENCES

EPSTEIN, S., FRIEDMAN, I., and UREY, H. C.: In press. *Isotopic fractionation during vaporization and freezing of water.* Journal of Chemical Physics.

FRIEDMAN, IRVING, 1953: *Deuterium content of water and other substances.* Geochimica et Cosmochimica Acta Vol. 4, 89—103.

KIRSCHENBAUM, ISIDOR, 1951: *Physical properties and analysis of heavy water.* McGraw-Hill Book Co., p. 398.

PRINTED IN SWEDEN
ESSELTE, STHLM 58

Contribution No. 861

BULLETIN OF THE GEOLOGICAL SOCIETY OF AMERICA
VOL. 68, PP. 897-912, 6 FIGS., 1 PL. JULY 1957

GEOPHYSICAL INVESTIGATIONS IN THE EASTERN CARIBBEAN: TRINIDAD SHELF, TOBAGO TROUGH, BARBADOS RIDGE, ATLANTIC OCEAN

By J. I. Ewing, C. B. Officer, H. R. Johnson, and R. S. Edwards

Abstract

A number of seismic-refraction stations were occupied in the eastern Caribbean area, and the results are correlated with other geophysical measurements and with land geology. The purpose of the investigation was to measure the crustal and subcrustal structure in the Caribbean, along the island arc, and in the Atlantic to determine the structural relationship of the interior-basin—island-arc—deep-sea-trench sequence.

The measurements indicate that the Caribbean was formerly an oceanic area which in a large part has been altered to produce a thickened crust and a lowered seismic velocity in the subcrustal material. Along the island arc the crust has been considerably thickened, and its upper surface approximately parallels the topography. On the Atlantic side of the islands the crustal and subcrustal layers are downwarped or downthrust to parallel approximately the topography across the Puerto Rico trench and its extension.

CONTENTS

TEXT

	Page
Introduction	897
Acknowledgments	898
Seismic-refraction results	898
Section A-A′	898
Section B-B′	903
Section C-C′	904
Section D-D′	904
Caribbean—Lesser Antilles—Atlantic section	905
Results not included in structure sections	906
Discussion of results	906
Island arc	906
Puerto Rico trench and Barbados ridge	907
Grenada Trough, Aves Swell, Venezuelan Basin	908
The 3.2–4.5 km/sec. layer	908
Possible southern extension of the island-arc structure	909
Origin and development of the Eastern Caribbean	909
References cited	911

ILLUSTRATIONS

Figure	Page
1. Chart showing seismic-station locations and traverses along which structure sections were drawn	899
2. Structure section from Grenada eastward to deep water in the Atlantic (section A-A′)	902
3. Structure section from Trinidad to Grenada (section B-B′)	903
4. North-south structure section along the Barbados ridge (section C-C′)	904
5. Structure section from St. Lucia to the Barbados ridge (section D-D′)	904
6. Generalized structure section from the Aves swell to deep water east of the Barbados ridge	905

Plate	Facing page
1. Travel-time graphs	912

TABLE

Table	Page
1. Layer velocities and thicknesses	900

Introduction

During the winter and spring of 1955, 47 seismic-refraction stations were occupied in the eastern Caribbean area to study the crustal structure in and around the Antillean orogenic belt. Measurements were made in the Puerto Rico trench, in the Venezuelan basin of the Caribbean, along the island arc, on the Barbados ridge, and on the Trinidad shelf. Previous refraction work has been done by Worzel and Ewing (1948) in the Barbados-Trinidad area, by Tolstoy *et al.* (1953) near Martinique, by Hersey *et al.* (1952) in the Puerto Rico trench, by Sutton and Ewing (In preparation) in the Venezuelan basin, around Puerto Rico, and in the Puerto Rico trench, and by J. Ewing (Unpublished) around Barbados. This paper is primarily concerned with the stations in the southeastern part of the area; a companion paper by C. B. Officer *et al.* (1957) deals primarily with the northern part. Some overlapping of data and discussion occurs in the two papers.

ACKNOWLEDGMENTS

This work was supported by the Bureau of Ships of the U.S. Navy under Contracts NObsr 43270, NObsr 43355, and NObsr 64547 and by the Associate Fund of the Woods Hole Oceanographic Institution. The explosives were supplied by the United States Navy Bureau of Ordnance. In making the explosives and other essentials available the assistance of the U.S. Naval establishments at Hamilton, Bermuda, Port of Spain, Trinidad, and Roosevelt Roads, Puerto Rico, was important to the success of the expedition.

Mr. G. R. Hamilton and the staff of the Columbia University Geophysical Field Station at St. David's, Bermuda, provided their usual excellent co-operation in making the facilities of the station available. The co-operation and assistance received from the officers and crew of the ATLANTIS and CARYN are gratefully acknowledged. The authors are particularly indebted to the following members of the scientific parties, without whose help the work would not have been successful: A. Bradshaw, W. Dunkle, G. Duys, J. Hahn, W. Moss, D. Owen, F. Richards, M. Rutstein, J. Ryther, and R. Vaccaro of the Woods Hole Oceanographic Institution; W. Hudson of the Western Electric Corporation; and S. Wardani of the Scripps Institution of Oceanography. Drs. J. B. Hersey and C. O'D. Iselin of the Woods Hole Oceanographic Institution and Prof. M. Ewing of the Lamont Geological Observatory were helpful in making this expedition possible. The illustrations were prepared by Grace E. Quest.

All four authors took part in the expedition and the preliminary analysis of the data. The final analysis, interpretations, and conclusions presented here are those of the first two authors.

SEISMIC-REFRACTION RESULTS

Measurements and Interpretation

The results reported here were obtained using the standard methods of measurement and interpretation described by Ewing *et al.* (1937; 1939; 1950), Officer *et al.* (1952), Officer and Wuenschel (1951), and Sutton and Bentley (1953). The station locations and section lines are shown in Figure 1. Reversed stations are indicated by circles or crosses at both ends of the line showing the shooting track; other stations shown are unreversed. The bathymetry, showing the 500-fathom contour intervals, was taken from the U.S. Navy Hydrographic Office Chart No. 5487.

The travel-time graphs of stations 11–28 from this cruise and of stations G-5, G-6, G-7, and G-8 from J. Ewing (Unpublished) are shown in Plate I. The graphs for stations 29, 30, 31, and others discussed in the companion paper by Officer *et al.* (1957) will be published in a later report. Most of the seismic results discussed here are presented in the form of structure sections (Figs. 2–6). and all results are listed in Table 1. Section A - A′ is made up from the stations lying near a line running east from Grenada. Section B - B′ runs north from Trinidad to Grenada, C - C′ runs north from station 22 past the western side of Barbados, and D - D′ runs southeast from St. Lucia. The last is a generalized section from the Aves Swell to deep water east of Barbados.

Section A - A′

From Grenada out to about 2700 fathoms water depth east of Barbados (Fig. 2), seismic velocities in km/sec. are shown at the points of measurement. Throughout most of the section two low-velocity sediment layers are found. The average velocities are about 1.7 km/sec. for the upper layer (stippling) and about 2.4 km/sec. for the second layer (narrow crosshatching). Underneath these, along most of the section, is a layer whose average velocity is about 4 km/sec., shown by the wide crosshatching; from its velocity it could be identified as lithified sediments, volcanic rocks, or possibly metamorphosed sediments. The next higher velocity layer is found only in the middle portion of the section. Its average velocity is about 5.1 km/sec. and could indicate intrusive or metamorphic rocks. The layer is not found at either end of this section, and apparently does not extend under the island arc here. At other places around the arc a similar velocity is found under or near the islands.

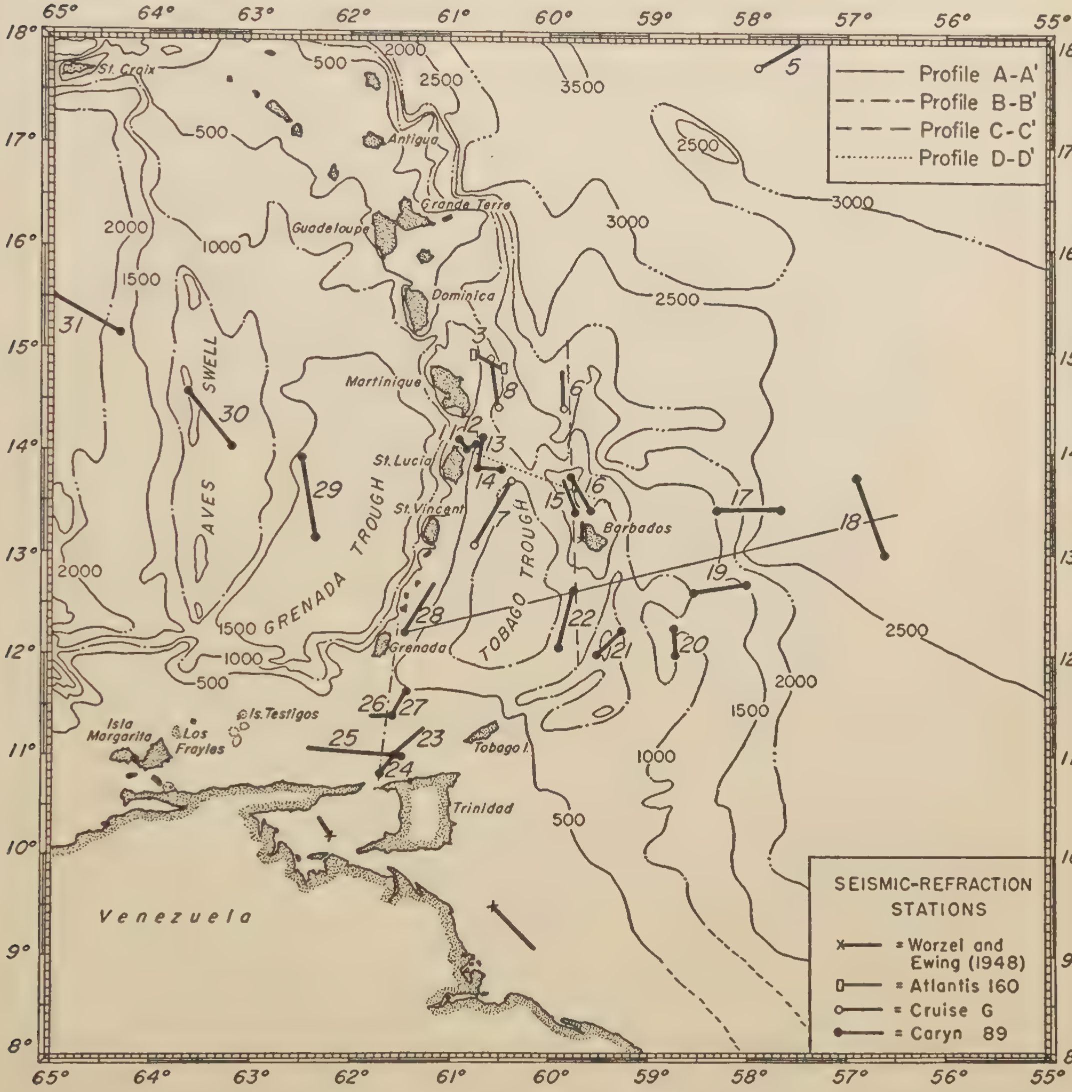
65° 64° 63° 62° 61° 60° 59° 58° 57° 56° 55°
18° 17° 16° 15° 14° 13° 12° 11° 10° 9° 8°
Profile A-A'
Profile B-B'
Profile C-C'
Profile D-D'
St. Croix
Antigua
Grande Terre
Guadeloupe
Dominica
Martinique
St. Lucia
St. Vincent
Barbados
Grenada
Tobago I.
Trinidad
Isla Margarita
Los Frayles
Is. Testigos
Venezuela
AVES SWELL
GRENADA TROUGH
TOBAGO TROUGH
500
1000
1500
2000
2500
3000
3500
1 2 3 5 6 7 8 13 14 15 16 17 18 19 20 21 22 23 24 25 26 27 28 29 30 31
SEISMIC-REFRACTION STATIONS
= Worzel and Ewing (1948)
= Atlantis 160
= Cruise G
= Caryn 89

Figure 1.—Chart Showing Seismic-Station Locations and Traverses along Which Structure Sections Were Drawn

The next deeper layer has an average velocity of 6.7 km/sec. and is identified as the high-velocity crustal layer commonly found at oceanic stations. The seaward end of the section shows a thickness of 5–6 km, which is normal for oceanic crust, and although the layer cannot be followed across the middle portion of the section, it appears again at the Grenada end considerably thickened. The measurement near Grenada is unreversed but was made with the shot line running parallel to the bottom contours and should give a reasonably accurate velocity. The second station from the left (G-7) is reversed and shows almost the same velocity

TABLE 1.—LAYER VELOCITIES AND THICKNESSES

(In km and km/sec.)

		Layer Velocity								Layer Thickness						
Station	Ocean	A	B	C	D	E	F	G		Ocean	A	B	C	D	E	F
G- 5	1.51	(1.73)					6.82	8.23	E.	5.49	0.74					5.92
									W.	5.49	0.76					7.44
17	1.50	(1.70)	2.58				6.74	8.32	E.	4.07	1.20	2.62				5.79
									W.	2.85	0.54	6.21				6.79
18	1.51	(1.70)	2.23				6.64	8.09	N.	5.05	0.25	1.99				7.07
									S.	4.73	0.11	2.99				3.62
19	1.50	(1.70) + 1.91	2.41		4.31		6.77*		E.	2.37	2.38	2.87		3.10*		
									W.	2.01	0.67	5.37		3.92*		
G- 6	1.51	(1.74)	2.73*	3.35*			6.17 to 6.88*		N.				3.80* to 5.09*			
									S.	3.14*	0.86*	2.67*				
15	1.50	1.81*	2.50*	3.38*					N.							
									S.	0.73*	0.78*	2.18*				
16	1.50	(1.72)	2.22	3.21	4.27				N.	0.37	0.38	2.00	5.20			
									S.	1.09	0.27	0.51	3.32			
Barbados†	1.50	1.71*	2.75*	3.38*					N.							
									S.	0.05*	0.75*	0.95*				
20	1.50	(1.70)	2.95*		[3.70]				N.	1.27	[5.63]	[2.23]				
									S.	2.10	0.87	2.23*				
21	1.50	(1.70) + 1.93			3.81	5.31			N.	2.19	3.48			4.70		
									S.	2.19	2.17			3.39		
22	1.50	(1.70)			3.97	4.91	(6.74)		N.	1.10	1.07			2.56		
									S.	1.23	0.32			2.82		
Orinoco (Shoal)†	1.50	1.76*	2.43*			5.15*			N.							
									S.	0.02*	0.55*	3.12*				
Orinoco (Deep)†	1.50	1.67*	2.00* + 2.37*	3.43*			6.62*		N.	0.04*	0.48*	1.53*	4.85*			
									S.							

23	1.52	(1.66) + 2.01*	2.71*	3.68*		5.10*	6.83*		N.							
									S.	0.19	1.03	2.51	0.34		2.19	
24	1.52	(1.66) + 1.93	2.75	3.43		4.80	6.38		N.	0.19	1.03	2.51	0.34		2.19	
									S.	0.19	0.81	0.37	1.74		3.03	
25	1.52	(1.70) + 2.01	2.93*			5.20*	6.47*		E.	0.26*	1.24*	2.95*			2.18*	
									W.							
26	1.51	1.64*	2.57*		4.33*				E.	0.18	1.29	2.35				
		2.03*							W.							
27	1.51	1.64 + 2.03	2.57		4.33				N.	0.68	1.66	1.93				
									S.	0.18	1.29	2.35				
A-160-3††	1.5	(1.7)	2.6	3.9							?	?	?			
G- 7	1.50	(1.72)	2.86		4.01		6.84		N.	1.72	1.24	1.57		4.80		
									S.	2.09	0.95	1.98		2.72		
8	1.50	1.68	2.64		4.07		6.62		N.	2.12	1.06	2.12		3.12		
									S.	1.58	0.27	1.70		1.96		
11	1.54	1.76	2.68	3.44	4.40		6.31		N.	0.08	0.05	0.96	0.41	0.62		
									S.	0.08	0.13	0.77	0.88	2.49		
12	1.52	1.71	2.39	3.25	4.29		5.97		E.	0.95	0.61	0.18	1.25	1.51		
									W.	0.09	0.11	0.67	0.85	2.56		
13	1.50	(1.70)			4.33	5.30			N.	1.10	1.30			3.48		
									S.	0.82	1.30			2.96		
14	1.50	(1.70)			4.19	5.35			E.	1.54	1.48			3.20		
									W.	0.82	1.31			2.63		
28	1.51	(1.70)	2.33*		4.00*		6.40*		N.							
									S.	0.04*	0.06*	1.34*		3.05*		
29	1.51	2.00		3.82		5.29	6.34	7.47	N.	2.93	0.66		2.05		1.94	5.64
									S.	2.93	1.37		2.88		2.69	8.70
30	1.51	(1.80)		3.76	4.33	6.02	6.63		N.	1.68	0.36		1.49	3.89	1.50	
									S.	1.30	0.60		1.45	2.78	4.07	
31	1.51	1.86	2.81*		4.47	5.96*	6.58	7.36	N.	4.28	1.72			1.57		2.79
									S.	3.44	0.86	1.08*		3.22	3.05*	7.83

A—Unconsolidated sediment: velocity range 1.6–2.0 km/sec.
B—Partially lithified to lithified sediment: velocity range 2.0–3.0 km/sec.
C—Lithified sediments, volcanic rocks, metamorphic rocks: velocity range 3.2–3.8 km/sec.
D—Volcanic or metamorphic
E—Metamorphic or igneous
F—Crustal velocities
G—Velocity beneath major discontinuity
N., S., E., W.—Locations of receiving positions relative to each other
†—From Worzel and Ewing (1948)
††—From Tolstoy *et al.* (1953)

Velocities with asterisks are unreversed. Thicknesses with asterisks have been computed with unreversed measurements. Assumed velocities are enclosed in parentheses and in most cases are governed by measured values near by. Numbers in brackets indicate uncertain velocities or thicknesses obtained from a complex interpretation.

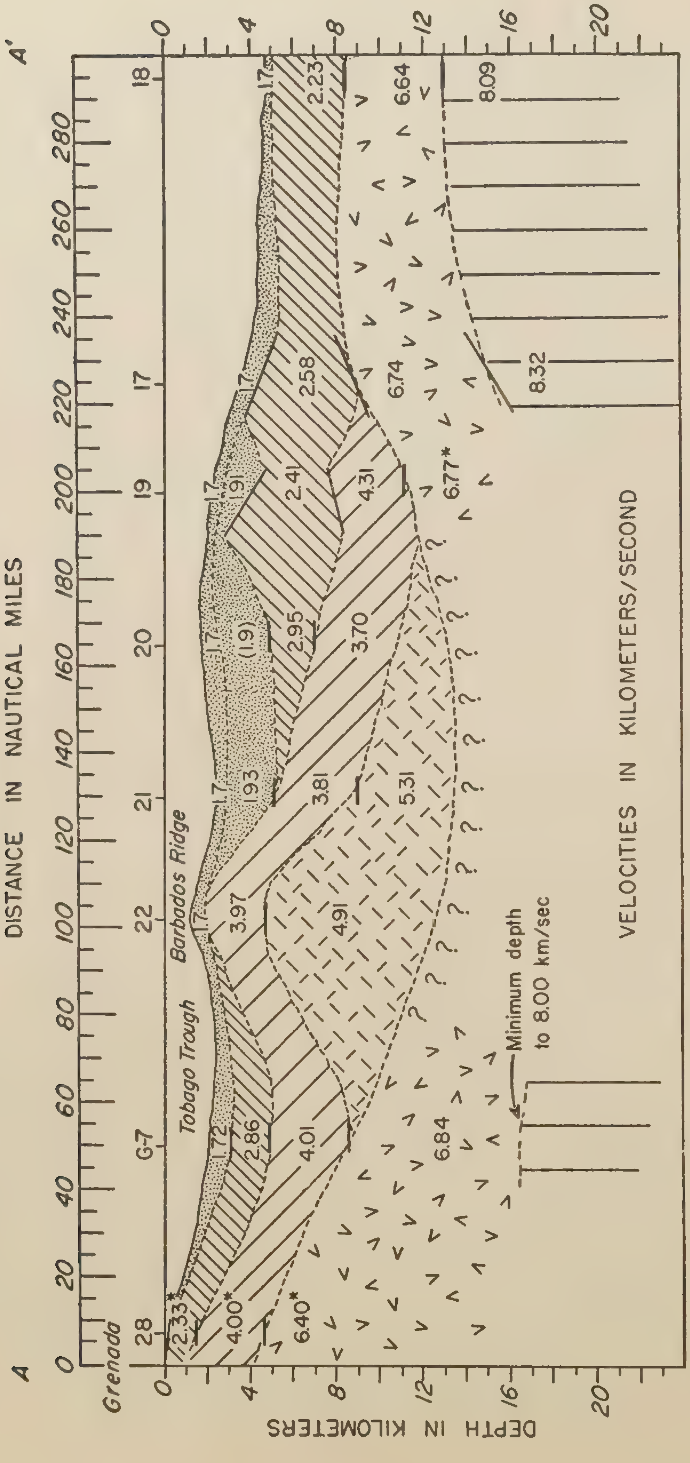
A
A'
Grenada
DISTANCE IN NAUTICAL MILES
0
20
40
60
80
100
120
140
160
180
200
220
240
260
280
28
G-7
22
21
20
19
17
18
Tobago Trough
Barbados Ridge
DEPTH IN KILOMETERS
0
4
8
12
16
20
2.33*
4.00*
6.40*
1.72
2.86
4.01
6.84
3.97
4.91
1.7
1.93
3.81
5.31
(1.9)
2.95
3.70
1.91
2.41
4.31
6.77*
2.58
6.74
8.32
2.23
6.64
8.09
Minimum depth to 8.00 km/sec
VELOCITIES IN KILOMETERS/SECOND

VERTICAL EXAGGERATION = 9:1

Figure 2.—Structure Section from Grenada Eastward to Deep Water in the Atlantic
(Section A–A')

* Unreversed velocity

as at the seaward end. Thus oceanic crust is found at both ends of this section dipping down toward the center; it was not found in the central part, probably because it is too deep there to be detected without larger shots and longer profiles.

The mantle was reached at the two seaward stations only. At station 18 it is found at about 13 km depth and at station 17 it is approximately 2 km deeper and has a 1.5° westward dip.

The structure in the middle portion of the section is probably oversimplified. Most of the stations around the Barbados ridge are complicated; they show fairly large dips and in some cases horizontal discontinuities which indicate severe folding and faulting. A striking example is station 20, where the G_3 line is offset by about 2.5 sec. near the north end. It is not possible to give more than an approximate structural interpretation here. Travel times indicate that the highest-velocity layer slopes upward from south to north and has been faulted or folded down (north relative to south) by several kilometers in the region of the offset. Because of complications like this, the results given for some Barbados ridge stations may have errors in velocity determinations as high as 15 per cent and even larger errors in depth determinations. The reader can estimate the possible error at individual stations by examining the travel-time graphs (Pl. 1) for complexity and scatter of points.

This section shows the high-velocity crustal layer and the subcrustal material to be downfolded or down dropped in the Barbados ridge area and overlain by a considerable amount of low-velocity sediments and a large thickness of material in which the velocity of sound is 4–5 km/sec. The upwarping of the deeper layers under Grenada shows in cross section a raised crustal platform under the island arc.

Section B - B′

Figure 3 shows a north-south section between Trinidad and Grenada. In the middle of the section a large syncline is indicated but not positively determined. Station 27, located about midway between B and B′, was heavily shot, but no velocity higher than 4.3 km/sec. was determined by first arrivals, even by the longest shots which were at a range of about 30 miles. Second arrivals give some indication of a 6.4 km/sec. layer at a depth of about 12 km, but the evidence is not good enough to warrant drawing lines on the travel-time graph. However, the failure of the travel-time graph to show a break from the 4.3 km/sec. layer means that the depth to a high-velocity basement must be on the order of that shown.

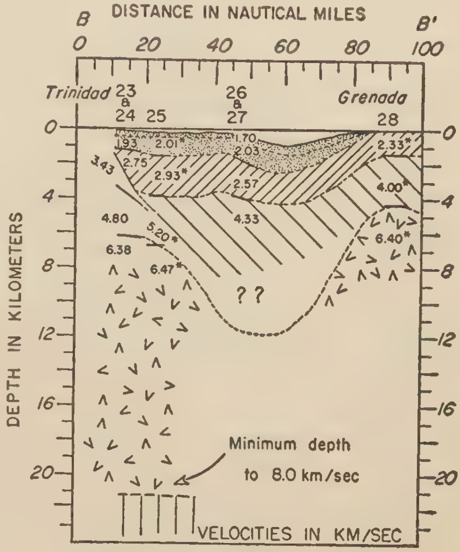

VERTICAL EXAGGERATION = 9:1

FIGURE 3.—STRUCTURE SECTION FROM TRINIDAD TO GRENADA (SECTION B-B′)
* Unreversed velocity

To the right (north) in this section the higher-velocity layers rise under the Lesser Antilles arc. To the left (south) they rise similarly under northern Trinidad. The synclinal or downdropped area between is possibly a southwestward-trending branch of the main downbuckle under the Barbados ridge. Near Trinidad the structure becomes more complex. The preferred interpretation of the travel-time data of stations 23, 24, and 25 is shown in Figure 3. This shows the 2.3–2.9 km/sec. sedimentary layer almost pinching out in station 24, as both the 3.4 km/sec. layer and 4.8–5.2 km/sec. layers slope up rather sharply southward. These upward-sloping layers probably represent the northern flank of the Northern Coast Range of Trinidad and Venezuela.

The alternate interpretation of the data results in approximately the same structure, except that the 3.4 km/sec. layer and the 2.7 km/sec. layer would be included in a single layer with a velocity of about 2.9 km/sec. In either case the 6.4 km/sec. crustal layer is at about the depth shown.

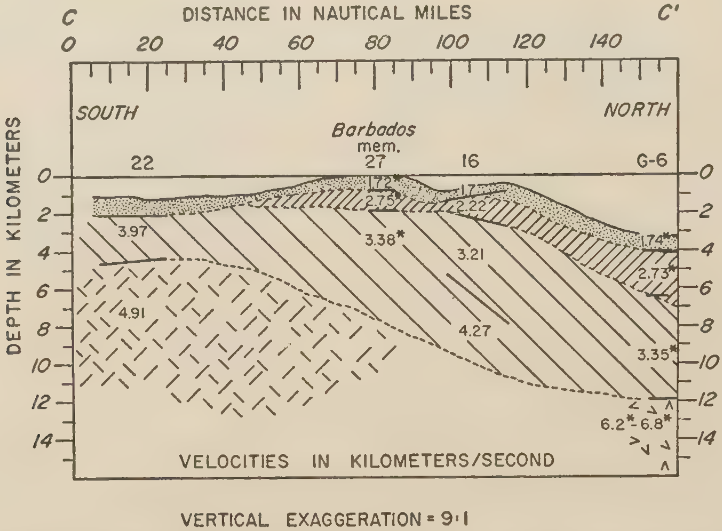
C
DISTANCE IN NAUTICAL MILES
C'
0
20
40
60
80
100
120
140
SOUTH
NORTH
Barbados
mem.
22
27
16
G-6
DEPTH IN KILOMETERS
0
2
4
6
8
10
12
14
1.72*
2.75*
1.7
2.22
1.74*
3.97
3.38*
3.21
2.73*
4.91
4.27
3.35*
6.2*-6.8*
VELOCITIES IN KILOMETERS/SECOND
VERTICAL EXAGGERATION = 9:1

Figure 4.—North-South Structure Section along the Barbados Ridge (Section C-C′)
* Unreversed velocity

Station 25 was long and heavily shot, and minimum depth to the mantle was determined as 21 km, a reasonable figure for a station near the edge of a continent.

Section C - C′

Figure 4 shows a north-south section passing just off the west shore of Barbados. The high-velocity crustal layer was not reached at any of the stations on the shallow part of the ridge. The northernmost station, G-6, shows it to be at a depth of 10–12 km. Possibly it is even deeper, since the shots at the station were fairly widely spaced at the longer ranges because of misfires, and a thickness of up to 2 km of the 4.5 to 4.9 km/sec. layer could have been missed between the 3.35 km/sec. layer and the crust. Although the velocity in the deep crustal layer is not well determined, the two lines, $G_4^{(a)}$ and $G_4^{(b)}$, on the travel-time graph show reasonable limits. Interpretation of the data at the Barbados ridge stations is not straightforward, as can be seen in the travel-time graphs. Complexity of travel-time data indicates complexity of layering.

Section D - D′

Figure 5 shows a section running southeast from St. Lucia along the ridge which bounds the Tobago trough on the north. Correlation of the deeper layers along this traverse is uncertain, and the interpretation shown may be incorrect in detail. As in section A - A′, the highest velocity measured was the 6.0 – 6.3 km/sec. at stations 11 and 12 just offshore from the island arc. Although the shot lines at these stations were relatively short and therefore may not give an accurate determination of the

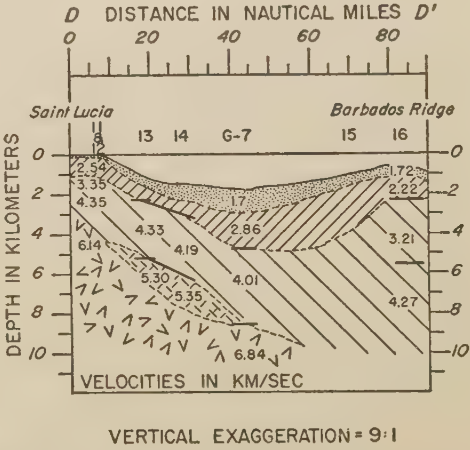
D
DISTANCE IN NAUTICAL MILES
D′
0
20
40
60
80
Saint Lucia
Barbados Ridge
11
12
13
14
G-7
15
16
DEPTH IN KILOMETERS
0
2
4
6
8
10
2.54
3.35
4.35
1.7
1.72
2.22
2.86
4.33
4.19
3.21
6.14
5.30
5.35
4.01
4.27
6.84
VELOCITIES IN KM/SEC
VERTICAL EXAGGERATION = 9:1

Figure 5.—Structure Section from St. Lucia to the Barbados Ridge (Section D-D′)

velocity in the deepest layer, the measured velocity probably corresponds to the 6.5 km/sec. oceanic crustal layer, perhaps somewhat altered to account for the subnormal velocity. There is no control on the interface between the 5.3 km/sec. and the 6.1 km/sec. layers east of station 12, but there are indications that the 5.3 km/sec. layer is relatively thin under stations 13 and 14.

The crust and subcrust under the Barbados ridge are believed to be deformed into a large northward-trending syncline. This was indicated first by section A - A′ and further by the other stations on the ridge that fail to show a velocity higher than about 5 km/sec. for the deepest layer detected.

Caribbean-Lesser Antilles-Atlantic Section

Figure 6 shows a generalized section running from the Aves swell in the Caribbean across the Lesser Antilles and the Barbados ridge and out to deep water in the Atlantic. This does not represent a particular traverse and is primarily intended to show the general structural relationship of the island arc to the oceanic and the Caribbean areas. Details of the structure under the islands are not known but may be more complicated than this drawing shows. The same is probably true of the Barbados ridge and some parts of the Aves swell.

The upper two layers, one the unconsolidated sediment with velocities around 1.7 km/sec. and the other the partially lithified sediments with velocities from 2.0 to 2.9 km/sec., have been combined into the stippled layer. Sediments from the Orinoco river transported by turbidity currents may have contributed appreciably to the accumulation of the great thickness of low-velocity deposits in the Tobago trough and particularly on the deep-sea floor east of the Barbados ridge.

The 3.5–4.5 km/sec. layer, shown by cross-hatching, is probably less uniform than the drawing indicates; it is probably not a continuous geologic sequence across the area, but the presence throughout the area of material with this velocity range is significant. These velocities are characteristic of a wide variety of materials from lithified sediments and volcanic rocks to some metamorphic rocks. Along the Lesser Antilles and the Aves swell this layer is

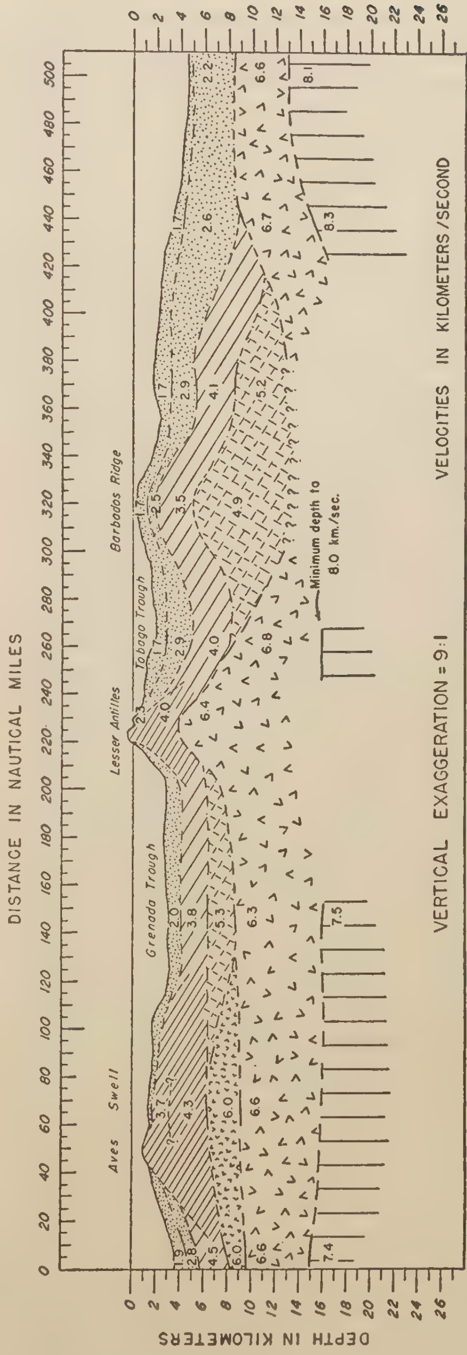
DISTANCE IN NAUTICAL MILES
0 20 40 60 80 100 120 140 160 180 200 220 240 260 280 300 320 340 360 380 400 420 440 460 480 500
DEPTH IN KILOMETERS
0 2 4 6 8 10 12 14 16 18 20 22 24 26
VELOCITIES IN KILOMETERS/SECOND
VERTICAL EXAGGERATION = 9:1
Aves Swell
Grenada Trough
Lesser Antilles
Tobago Trough
Barbados Ridge
Minimum depth to 8.0 km./sec.
1.9 2.8 4.5 6.0 6.6 7.4
3.7 4.3 6.0 6.6
2.0 3.8 5.3 6.3 7.5
2.3 4.0 6.4
1.7 2.9 4.0 6.8
1.7 2.5 3.5 4.9
1.7 2.9 4.1 5.2
1.7 2.6 6.7 8.3
2.2 6.6 8.1

FIGURE 6.—GENERALIZED STRUCTURE SECTION FROM THE AVES SWELL TO DEEP WATER EAST OF THE BARBADOS RIDGE

probably primarily composed of extrusive volcanic material; under the Grenada trough, Tobago trough, and Barbados ridge it is more likely to be a combination of lithified pyroclastics and other sediments. The 4.9–5.3 km/sec. material is found only in the Grenada trough and under the Barbados ridge in this section, but at other locations around the arc a similar velocity is found on and near the islands. This velocity range is characteristic of metamorphic or intrusive igneous rocks.

The high-velocity crustal layer was traced across the entire area, with the exception of the Barbados ridge. Although a tendency is noticed toward a lower velocity and some differentiation or contamination in the Caribbean, the widespread occurrence of this layer, with a velocity characteristic of oceanic crust, indicates that the Lesser Antilles island-arc structure resulted from tectonic forces in a formerly oceanic, rather than continental, area. Ewing and Worzel (1954) and Ewing and Press (1955), reporting the preliminary results from earlier seismic work in the Caribbean, point out that the crustal structure is of oceanic rather than continental type. Subcrustal material on the Atlantic side of the arc has a velocity normally associated with the mantle, but an appreciably lower velocity is found for the subcrust[1] under the Caribbean. This contrast and its structural implications are discussed below and also by Officer *et al.* (1957).

Results Not Included in Structure Sections

Although stations G-5 and G-8, station A-160-3, and the two Orinoco delta stations of Worzel and Ewing (1948) were not included in the preceding structure cross sections, the results (Table 1) are not contradictory to those included.

Discussion of Results

Island Arc

From Puerto Rico to Grenada, and possibly to Margarita, the islands of the eastern Caribbean lie along an extensive arcuate belt of positive free-air gravity anomalies (Hess, 1938). Prominent gaps in the island chain are the Anegada passage, which separates the Greater Antilles from St. Croix and the Lesser Antilles, and the Dominica passage. The Lesser Antilles in the north have been divided into two groups: the outer or limestone Caribbees and the inner volcanic islands. South of Dominica there is only the volcanic group of islands. The Greater Antilles are older and more severely folded, metamorphosed, and intruded than the Lesser Antilles. The oldest dated rocks of the Greater Antilles appear to be progressively older toward the west—Jurassic in Cuba and Cretaceous or possibly Jurassic in Hispaniola and Puerto Rico (Schuchert, 1935, p. 455, 471, 495). In the Lesser Antilles the limestone Caribbees are believed to be older than the inner group. On St. Bartholomew and St. Martins tuffs and breccias of Eocene age are reported (Christman, 1953); Oligocene on Martinique (Senn, 1940) and Oligocene or early Miocene or Carriacou (Trechman, 1935) are the oldest reported for the inner volcanic islands. Volcanic activity apparently ceased in the outer group in Oligocene and was followed by erosion, submersion, and deposition of the Oligocene-Miocene limestones, whereas activity has continued in most of the inner group up to the present.

The volcanic and intrusive rocks throughout the Greater and Lesser Antilles are predominantly andesites and diorites, although basalts and ultramafic rocks are found in varying amounts. All the islands of the arc show strong short-period magnetic anomalies (Davidson and Miller, unpublished) in sharp contrast to the relatively smooth field in the surrounding area. High anomalies are also associated with the Dutch Leeward Islands, the Northern Coast Range of Trinidad, Tobago, and the Aves swell. Measurements show that no anomaly is associated with the north wall of the Puerto Rico Trench or its extension to the southeast, and none is associated with Barbados (E. T. Miller and M. Ewing, in preparation).

The seismic results (Fig. 2, 5, 6) show that the topographic ridge, along which the southern end of the Antillean island arc is located, is the surface expression of a prominent ridge in the underlying crust (6.3–6.8 km/sec. velocity). Associated with the elevation of the crust is an apparent decrease in the seismic velocity.

---

[1] As used throughout this paper, subcrust refers to the material directly beneath the 6.5 km/sec. layer.

The writers believe that the uplift and the associated volcanism come primarily from crustal thickening resulting from extensive intrusion from below by material with crustal velocity and density. The islands are believed to be composed dominantly of the volcanic rocks and the lighter, more siliceous components of the intruding material.

Puerto Rico Trench and Barbados Ridge

Previous seismic work in and around the Puerto Rico trench consisted of three stations by Hersey *et al.* (1952), and seven stations interpreted by G. H. Sutton which have been reported in brief (Ewing and Worzel, 1954). The results of the early work, as well as of recent work (Officer *et al.*, 1957), can be summarized as follows: The structure just north of the trench (½–1 km of sediment and 3 km of 6.6 km/sec. oceanic crust overlying the M discontinuity at a depth of 9–10 km below sea level) is approximately standard oceanic structure. It deviates from the standard in that the crust is only a little more than half normal thickness, and the M discontinuity is higher by about 2 or 3 km. In the trench the crust is 2–3 km thicker than normal and is underlain by the M discontinuity at a depth of 18 km. Above the crust is a thickness of material whose velocity is characteristic of lithified sediments, volcanic rocks, or metamorphic rocks. Between the trench and the slope to the islands the highest velocity measured was around 5.5 km/sec.

Southeastward around the Lesser Antilles, the Puerto Rico trench gradually decreases in depth and disappears. In its place the northern extension of the Barbados ridge begins to emerge and continues to the south as a prominent topographic feature. According to the bathymetry in the area, the axis of the Barbados ridge is not a direct continuation of that of the Puerto Rico trench extended but lies between the axis of the trench and the Lesser Antilles. In this area two stations have been occupied before those reported here: one near the west coast of Barbados (Worzel and Ewing, 1948) and the other in 1000 fathoms northeast of Martinique (Tolstoy, Edwards, and Ewing, 1953). Although neither of these stations was long enough to detect deep layering, the results are in good agreement with more recent work. Results reported here show the main features of this part of the orogenic belt. In the Barbados ridge area, which is near the axis of the negative gravity belt, the structure consists primarily of a great thickness of severely folded and faulted rocks with velocities between 3.2 and 5.2 km/sec.; this is believed to be a sequence of lithified sediments and volcanic rocks, possibly metamorphosed and probably intruded in the deeper parts. In the Tobago trough and east of the Barbados ridge the higher-velocity materials are appreciably deeper than along the crest of the ridge and are overlain by 3–5 km of unconsolidated and lithified sediments. Oceanic crustal velocities were found near Grenada and St. Lucia and offshore about 100 miles east of the ridge. Near the islands stations 28 and G-7 show this layer dipping east, and the offshore stations 17 and 18 show it dipping west. These results, coupled with the inability to detect this layer under the Barbados ridge, are evidence that the crust and presumably the upper mantle are deformed into a large syncline 200 miles wide with its axis centered about on the Barbados ridge (Figs. 2, 6). The structure is not known in detail under the Barbados ridge or under the Lesser Antilles, but the gross features must be approximately as shown.

Although the Barbados ridge and the Lesser Antilles are similar topographically, they are different in composition. The Lesser Antilles are formed by a rise in the underlying high-velocity crustal material; the Barbados ridge is formed by a rise in the overlying lithified sediments, volcanic and intrusive rocks, which lie within a broad crustal syncline. The Lesser Antilles are actively volcanic and highly magnetic; the Barbados ridge is not.

Complementary to the results discussed above is the observation from earthquake studies that, although no deep-focus shocks and only four intermediate ones are plotted, the seismicity of the Antillean area appears to conform to the type of the Pacific arcs (Gutenberg and Richter, 1954, p. 38). The epicenters of most shallow quakes are within the negative gravity zone, whereas three of the deeper earthquake epicenters are along the island arc, and the fourth is slightly inside the axis of the negative gravity zone.

Grenada Trough, Aves Swell, Venezuelan Basin

One station in the Grenada trough, one on the Aves swell, and one in the Venezuelan basin are shown in the section of Figure 6. Other Venezuelan basin stations are described by Officer *et al.* (1957) and by G. H. Sutton and M. Ewing (In preparation).

The Aves swell is a volcanic ridge and owes its elevation to a thickening of the 3.7–4.3 km/sec. material and to a rise and probable thickening of the crust. The crust is thinner in the Grenada trough and still thinner in the Venezuelan basin, which probably accounts for the deeper water in these areas. The layer above the crust in the Grenada trough has a velocity of 5.3 km/sec. much like the deep material under the Barbados ridge. No velocity higher than 6.6 km/sec. was found at the Aves swell station, and the subcrustal velocities found at the others are 7.4 km/sec. in the Venezuelan basin and 7.5 km/sec. in the Grenada trough. These velocities are appreciably lower than the velocity usually associated with the upper mantle that is found at approximately this depth in the ocean basins. Thus the Caribbean, at least part of it, is not typically oceanic in structure. This should not be interpreted to mean that the Caribbean structure is continental. It is approximately like the oceanic structure in crustal velocity and thickness but differs in the velocity below the deep discontinuity.

Other areas where measurements have shown a velocity similar to that found for the subcrust in the Caribbean are: along the continental margin of eastern North America (Officer and Ewing, 1954; Bentley and Worzel, 1956; J. Ewing and M. Ewing, unpublished; the Tonga ridge (Raitt *et al.*, 1955); Bermuda rise (Officer *et al.*, 1952); Mid-Atlantic Ridge and Norwegian Sea (J. Ewing and M. Ewing, unpublished); northeast of Eleuthera in the Bahamas (Katz and Ewing, 1956). In these areas, with the possible exception of the Tonga ridge, the normal oceanic crustal layer (6.5 km/sec.) is absent. In most places the 7.1–7.7 km/sec. material is overlain by a 5.0–5.5 km/sec. layer, except on the deep parts of the Mid-Atlantic ridge, where the overburden appears to consist largely of unconsolidated sediments. In the Venezuelan basin a section with normal oceanic crustal velocity (6.0–6.6 km/sec.) overlies the 7.2–7.7 km/sec. material.

The 3.2–4.5 km/sec. Layer

Throughout most of the area covered by these measurements a layer was found in which the velocity determinations ranged from 3.2 to 4.5 km/sec. (the layer shown by the wide cross-hatching). Identification of the layer from velocity considerations only is difficult, since the layer falls within the range of many lithified sediments, volcanic rocks, and some metamorphic rocks. Figure 6 shows it pinching out east of Barbados, but in deep water, a layer 1–2 km thick with this velocity would be masked by the water-wave arrivals and might not be seen as second arrivals. Recent sub-bottom reflection data and data on transformed shear waves from several deep-water stations have indicated that such a layer, lying just above the crustal layer, may be present in many parts of the Atlantic Ocean (J. Ewing and M. Ewing, unpublished.[2]) The presence of the layer in many parts of the Caribbean but not throughout the Atlantic might be accounted for by the fact that where the water is shallower it is not masked.

The writers believe that the 3.2–4.5 km/sec. layer is the result of widespread volcanism and intrusion. Since the layer apparently has no correlation with magnetic anomalies (M. Davidson and E. T. Miller, unpublished), it probably is not a massive flow but a mixture of lithified volcanic ash, tuff, breccia, sediments, and possibly thin flows. A layer with approximately this velocity is found underneath the low-velocity sediments near Bermuda (Officer *et al.*, 1952) and has been accounted for in the same way.

---

[2] In these measurements the horizon from which the strongest sub-bottom reflections are received and the horizon at which the transformation from compression to shear occurs are consistently shallower than the top of the crustal layer, as determined by the refracted compressional arrivals. Thus, either there is an additional intermediate layer between the low-velocity sediments and the crust, which is not seen as a refractor, or the upper 1–2 km of the crust has a velocity gradient.

Possible Southern Extension of the Island-Arc Structure

The seismic section B-B′ indicates that the Lesser Antilles volcanic ridge does not continue southward from Grenada to Trinidad. From this and from topographic considerations, it therefore appears that the Lesser Antillean ridge extends south and west from Grenada through Testigos and Los Frayles and probably on to Margarita. From observations of southward thrusting and overfolding in the Venezuelan Coast Range and in the metamorphic rocks south of Caracas and observations of northward overturning on Margarita and along the coast north of Caracas, Maxwell and Dengo (1951) postulate a northeastward-trending orogen whose axis passes south of Caracas, through the Cariaco trough, and between Margarita and the mainland. Thus this is excellent agreement of conclusions derived from field geology and from geophysical methods.

There are insufficient measurements to determine what relationship the broad synclinal development east of the Lesser Antilles has to the Venezuelan geosyncline. Possibly this broad feature, on approaching South America, is split into two smaller branches; one passes between Grenada and Trinidad, and the other bends around Tobago and joins the Venezuelan geosyncline. If this synclinal development and the negative gravity belt associated with it continue into South America, a comparison may be drawn between this and the apparent continuation of the negative strip of the East Indies into Burma (Evans and Crompton, 1946).

ORIGIN AND DEVELOPMENT OF THE EASTERN CARIBBEAN

The remainder of this paper is speculation on the physical and chemical processes which might have produced the structural features described above. For other theories on the origin of the Caribbean structure, the reader is referred to Eardley (1954).

In the development of the Caribbean area from oceanic structure to the existing structure, volcanism and intrusion have obviously been of major importance. This is evident from widespread occurrence of volcanic and intrusive rocks throughout the exposed land portions of the area and from the presence in most places of seismic layers whose velocities are characteristic of volcanic and intrusive material. Although the volcanism and intrusion may be secondary processes in the tectonic development of the area, the writers believe that they are the primary processes and that they occur on such a scale that a large area of the earth's crust may be altered in a manner that results in the creation of island-arc structure. The seismic results show that large areas of the Caribbean crust are thickened and have lower than normal velocity in the upper portion; the velocity in the crust is appreciably lower than is normal for the upper mantle. These features of the seismic results strongly suggest that the crust and upper mantle have been contaminated by the introduction of a lower-velocity material. This probably occurred from widespread intrusion by a primary differentiate which migrated upward from deep in the mantle in a manner like that referred to by Poldervaart (1955, p. 138) as degassing of the mantle.

A most significant feature of the results is the presence of material with crustal velocities, 6.1 to 6.4 km/sec., high in the seismic sections under the Lesser Antilles. Since these islands are mainly built of material of andesitic composition, the seismic sections (Figs. 2, 6) should provide clues to the processes involved in the formation of such material. One possibility is that the andesitic material is the result of fractional crystallization from an olivine basalt magma. According to Turner and Verhoogen (1951, p. 126) the possibility of such an origin is generally accepted. This might be a plausible process here, since the crustal material, presumed to be olivine basalt, underlies the Lesser Antilles ridge and is at an elevated position there. However, the source of heat necessary to raise the temperature in the layer sufficiently to allow differentiation is not in evidence. Furthermore, although laboratory experiments have shown that it is possible to derive the full range of igneous rocks from a basalt melt, field evidence (Tilley, 1950; Waters, 1955) indicates that where thick sills of basalt have differentiated, they form feldspathic gabbros and end-stage granophyres but not intermediate andesites. In addition, it is difficult to imagine how the total volume of extrusive and intrusive material along the Lesser Antilles ridge and the Aves swell and in the Venezuelan basin could have been derived solely from the thin 5 km oceanic crust, particularly since observations show that where the largest amounts of andesitic material are found, the remaining crust is thicker than normal.

A second possible process of deriving andesites might be by contamination of an upward-migrating basalt magma as it passed through the sediments. Andesites may have been produced in this way here early in the volcanic cycle when perhaps the entire area was overlain by a thick sedimentary cover, but recent volcanism is occurring in the zone of thinnest sedimentary cover, where contamination would be at a minimum.

A third possible process, the one preferred here, involves differentiation and separation of the lighter components deep in the mantle. This could lead to upward migration of volatiles and lighter, more siliceous components which, during the passage through the upper mantle and crust, could acquire by inclusion and partial melting the more basic constituents of andesitic rocks or could lead to the upward migration of a differentiate of andesitic composition.

On the assumption that upward migration of material from deep in the mantle is the primary process involved in the alteration of an area such as this, a possible sequence of developments is suggested. After further differentiation, some process of convective circulation or overturn might cause a large body or many smaller bodies of primary basaltic magma to be collected and to begin migrating upward through the mantle. In addition to an initial density differential, the heat generated during the crystallization of such minerals as olivines and pyroxenes from the primary magma and possible volume increases associated with changes of state may be major driving forces in the migratory process. The rising magma might thus permeate a large area of the upper mantle and crust. Except in the upper regions of the mantle and in the crust, passage of the magma would probably cause little or no permanent change in the penetrated materials, since the rising magma would presumably be differentiating during the ascent, leaving behind the more basic constituents. In the upper regions, however, where cooling would eventually halt the migration, the end product could be a contaminated mantle and crust, which would perhaps have the accumulation of varying amounts of the lighter, more siliceous materials on the surface. In addition, broad areas of sediments might be metamorphosed or cemented by the volatiles that reach the surface. Where vast amounts of the migrating magma rose, such as along the Antilles arc and the Aves swell, the portion with crustal density would have no tendency from buoyant forces to rise above the existing crust, and the result would be a thickening of that layer, as is observed. Isostatic forces acting on such a thickened crustal section would produce the observed elevation of that material. The lighter, more siliceous constituents would constitute most of the upper part of the section, including the islands.

The earliest-rising materials, accompanied by larger amounts of water vapor and other volatiles than those succeeding, may provide the mechanism for the implacement of ultramafic rocks, particularly serpentines, as suggested by Hess (1955, p. 402). This is believed to occur at an early stage in the intrusive process.

Depression in the form of deep-sea trenches probably results from compressional forces. For orogenic belts along continental margins, the compression could be supplied by the tendency of continents to spread into the oceans (Stille, 1955). For an island-arc orogenic belt, the compressional forces may originate from extensive intrusion, as postulated, which contaminates and expands a large area of the upper mantle and crust. As a result of this expansion, laterally and vertically, the tendency at the borders will be for the altered interior basin to move out over the exterior oceanic basin. Such a stress distribution could account for the down-buckled deep-sea trench and for the major fracture zone of earthquakes dipping down under the island arc, as suggested by Gunn (1947). Along the raised ridge of the island arc local relaxation of compression in the upper portion of the mantle and crust will provide a zone of weakness along which volcanic activity would be concentrated.

Visualization of island-arc orogenesis resulting from differentiation and upward migration of volatiles and the more siliceous materials from the deep mantle must be concerned with the problem of concentration or focusing of energy. Why does this process occur in the neighborhood of continents only and never in the middle of an ocean? Any hypothesis of accretion and growth of the continents in place must imply localization or focusing, throughout geologic time, of the processes involved in collecting the more siliceous, lower-density materials. Thus a recent migration might follow the pattern of the past and occur under a continent or near a continental boundary. Further intrusion under a continent would produce continental growth by thickening, uplift, and subsequent spreading. Extensive intrusion under the ocean might produce a result similar to that observed in the Caribbean, *i.e.*, alteration and expansion of a broad region of the crust and upper mantle; the expansion would supply the tectonic forces which produce the island-arc—deep-sea-trench structure.

References Cited

Bentley, C. R., and Worzel, J. L., 1956, Geophysical investigations in the emerged and submerged Atlantic Coastal Plain. Part X: Continental Slope and Continental Rise south of the Grand Banks: Geol. Soc. America Bull., v. 67, p. 1–18

Christman, R. A., 1953, Geology of St. Bartholomew, St. Martin, and Anguilla, Lesser Antilles: Geol. Soc. America Bull., v. 64, p. 65–96

Eardley, A. J., 1954, Tetonic relations of North and South America: Am. Assoc. Petroleum Geologists Bull., v. 38, no. 5, p. 707–773

Evans, P., and Crompton, W., 1946, Geological factors in gravity interpretation: Geol. Soc. London Quart. Jour., v. 102, p. 211–244

Ewing, M., and Press, F., 1955, Geophysical contrasts between continents and ocean basins, p. 1–6 *in* Poldervaart, Arie, *Editor*, Crust of the Earth: Geol. Soc. America Special Paper 62, 762 p.

Ewing, M., and Worzel, J. L., 1954, Gravity anomalies and structure of the West Indies. Part I: Geol. Soc. America Bull., v. 65, p. 165–173

Ewing, M., Crary, A. P., and Rutherford, H. M., 1937, Geophysical investigations in the emerged and submerged Atlantic Coastal Plain. Part I: Methods and results: Geol. Soc. America Bull., v. 48, p. 753–802

Ewing, M., Woolard, G. P., and Vine, A. C., 1939, Geophysical investigations in the emerged and submerged Atlantic Coastal Plain. Part III: Barnegat Bay, N. J., section: Geol. Soc. America Bull., v. 50, p. 257–296

Ewing, M., Worzel, J. L., Steenland, N. C., and Press, F., 1950, Geophysical investigations in the emerged and submerged Atlantic Coastal Plain. Part V: Woods Hole, New York, and Cape May section: Geol. Soc. America Bull., v. 61, p. 877–892

Gunn, R., 1947, Quantitative aspects of juxtaposed ocean deeps, mountain chains, and volcanic ranges: Geophysics, v. 12, p. 238–255

Gutenberg, B., and Richter, C. F., 1954, Seismicity of the earth: Princeton, N. J., Princeton Univ. Press, 310 p.

Hersey, J. B., Officer, C. B., Johnson, H. R., and Bergstrom, S., 1952, Seismic refraction observations north of the Brownson Deep: Seismol. Soc. America Bull., v. 42, p. 291–306

Hess, H. H., 1938, Gravity anomalies and island arc structures with particular reference to the West Indies: Am. Philos. Soc. Proc., v. 79, p. 71–96

— 1955, Serpentines, orogeny, and epeirogeny, p. 291–407 *in* Crust of the Earth: Geol. Soc. America Special Paper 62, 762 p.

Katz, S., and Ewing, M., 1956, Seismic-refraction measurements in the Atlantic Ocean. Part VII: Atlantic Ocean basin west of Bermuda: Geol. Soc. America Bull., v. 67, p. 475–510

Maxwell, J. C., and Dengo, G., 1951, The Carupano area and its relation to the tectonics of northeastern Venezuela: Am. Geophys. Union Trans., v. 32, p. 259–266

Officer, C. B., and Ewing, M., 1954, Geophysical investigations in the emerged and submerged Atlantic Coastal Plain. Part VII: Continenta shelf, continental slope, and continental rise south of Nova Scotia: Geol. Soc. America Bull., v. 65, p. 653–670

Officer, C. B., and Wuenschel, P. C., 1951, Reduction of deep-sea refraction data: Palisades, N. Y., Lamont Geol. Observatory Tech. Rep. 1, 12 p.

Officer, C. B., Ewing, M., and Wuenschel, P. C., 1952, Seismic refraction measurements in the Atlantic Ocean. Part IV: Bermuda, Bermuda Rise, and Nares Basin: Geol. Soc. America Bull., v. 63 p. 777–808

Officer, C. B., Ewing, J. I., Edwards, R. S., and Johnson, H. R., 1957, Geophysical investigations in the eastern Caribbean: Venezuelan basin, Antilles island arc, and Puerto Rico trench: Geol. Soc. America Bull., v. 68, p. 359–378

Poldervaart, A., 1955, Chemistry of the earth's crust, p. 119–144 *in* Poldervaart, Arie, *Editor*, Crust of the Earth: Geol. Soc. America Special Paper 62, 762 p.

Raitt, R. W., Fisher, R. I., and Mason, R. G., 1955, Tonga Trench, p. 237–254 *in* Poldervaart, Arie, *Editor*, Crust of the Earth: Geol. Soc. America Special Paper 62, 762 p.

Schuchert, C., 1935, Historical geology of the Antillean-Caribbean region: N. Y., John Wiley & Sons, 811 p.

Senn, A., 1940, Paleogene of Barbados and its bearing on history and structure of Antillean-Caribbean region: Am. Assoc. Petroleum Geologists Bull., v. 24, p. 1548–1610

Stille, H., 1955, Recent deformations of the earth's crust in the light of those of earlier epochs, p. 171–191 *in* Poldervaart, Arie, *Editor*, Crust of the Earth: Geol. Soc. America Special Paper 62, 792 p.

Sutton, G. H., and Bentley, C. R., 1953, Topographic correction curves: Palisades, N. Y., Lamont Geol. Observatory Tech. Rep. 3, 5 p.

Tilley, C. E., 1950, Some aspects of magmatic evolution: Geol. Soc. London, Quart. Jour., v. 106, p. 37–61

Tolstoy, I., Edwards, R. S., and Ewing, M., 1953, Seismic refraction measurements in the Atlantic Ocean. Part III: Seismol. Soc. America Bull., v. 43, p. 35–48

Trechman, C. T., 1935, Geology and fossils of Carriacou, West Indies: Geol. Mag., v. 72, p. 529–555

Turner, F. J., and Verhoogen, J., 1951, Igneous and metamorphic petrology: N. Y., McGraw-Hill Book Co., 602 p.

U. S. Hydrographic Office, 1939, Bathymetric chart of the Caribbean Sea: H. O. Chart 5487

Waters, A. C., 1955, Volcanic rocks and the tetonic cycle, p. 703–722 *in* Poldervaart, Arie, *Editor*, Crust of the Earth: Geol. Soc. America Special Paper 62, 762 p.

Worzel, J. L., and Ewing, M., 1948, Explosion sounds in shallow water, p. 1–53 *in* Ewing, M., Worzel, J. L., and Pekeris, C. L., Propagation of sound in the ocean: Geol. Soc. America Memoir 27, 205 p.

LAMONT GEOLOGICAL OBSERVATORY (COLUMBIA UNIVERSITY), PALISADES, N. Y.; THE RICE INSTITUTE, HOUSTON, TEXAS, AND WOODS HOLE OCEANOGRAPHIC INSTITUTION, WOODS HOLE, MASS.; WOODS HOLE OCEANOGRAPHIC INSTITUTION, WOODS HOLE, MASS.; WOODS HOLE OCEANOGRAPHIC INSTITUTION, WOODS HOLE, MASS.

MANUSCRIPT RECEIVED BY THE SECRETARY OF THE SOCIETY, DECEMBER 13, 1956.

LAMONT GEOLOGICAL OBSERVATORY CONTRIBUTION NO. 250 WOODS HOLE OCEANOGRAPHIC INSTITUTION CONTRIBUTION NO. 861

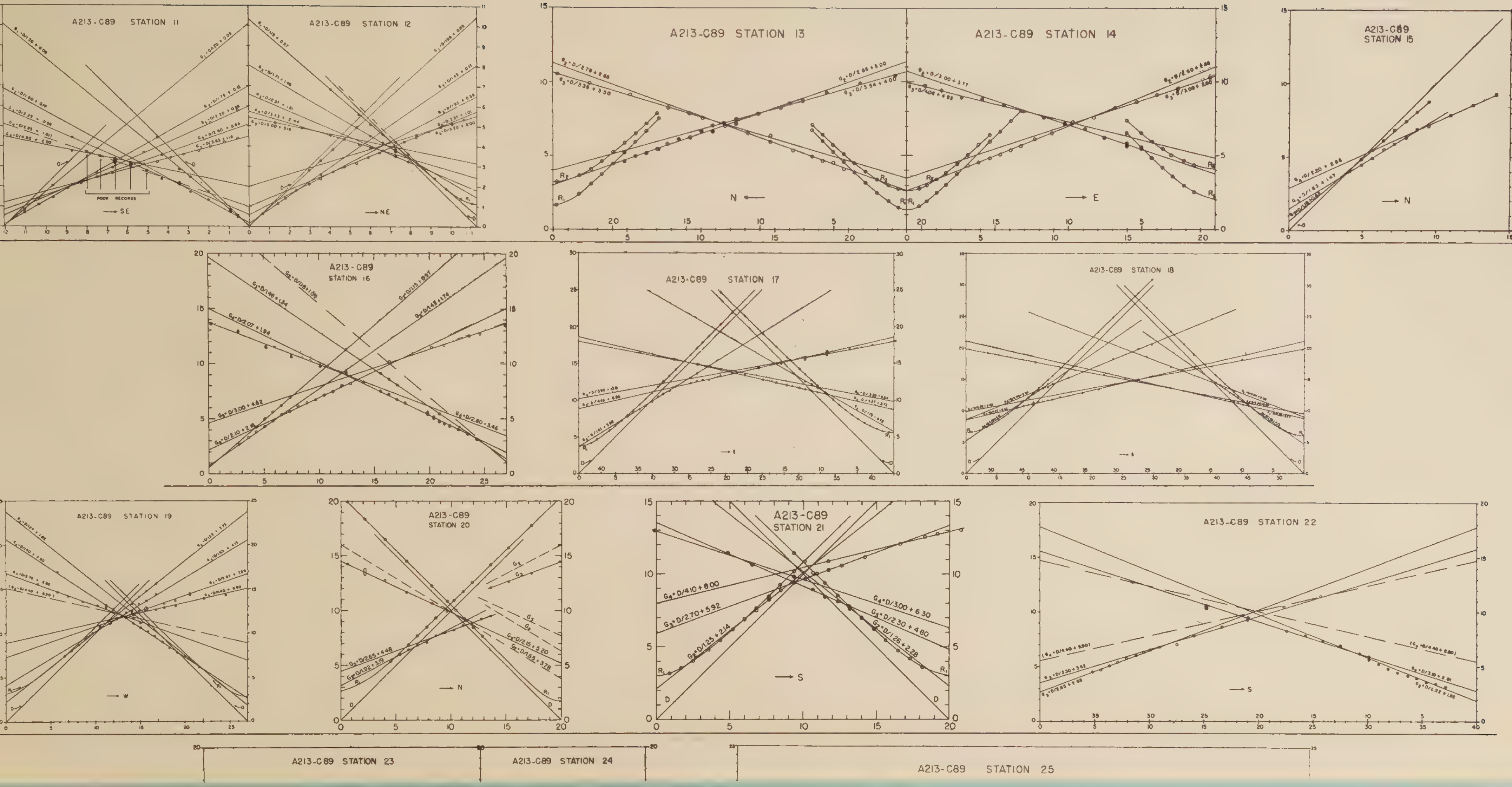
A213-C89 STATION 11
POOR RECORDS
→ SE
A213-C89 STATION 12
→ NE
A213-C89 STATION 13
N ←
A213-C89 STATION 14
→ E
A213-C89 STATION 15
→ N
A213-C89 STATION 16
G₃=D/2.07+1.94
G₃=D/3.00+4.62
G₄=D/2.60+3.46
A213-C89 STATION 17
A213-C89 STATION 18
A213-C89 STATION 19
→ W
A213-C89 STATION 20
→ N
A213-C89 STATION 21
G₄=D/4.10+8.00
G₃=D/2.70+5.92
G₂=D/1.25+2.14
G₄=D/3.00+6.30
G₃=D/2.30+4.80
G₂=D/1.26+2.28
R₁
D
→ S
A213-C89 STATION 22
→ S
A213-C89 STATION 23
A213-C89 STATION 24
A213-C89 STATION 25

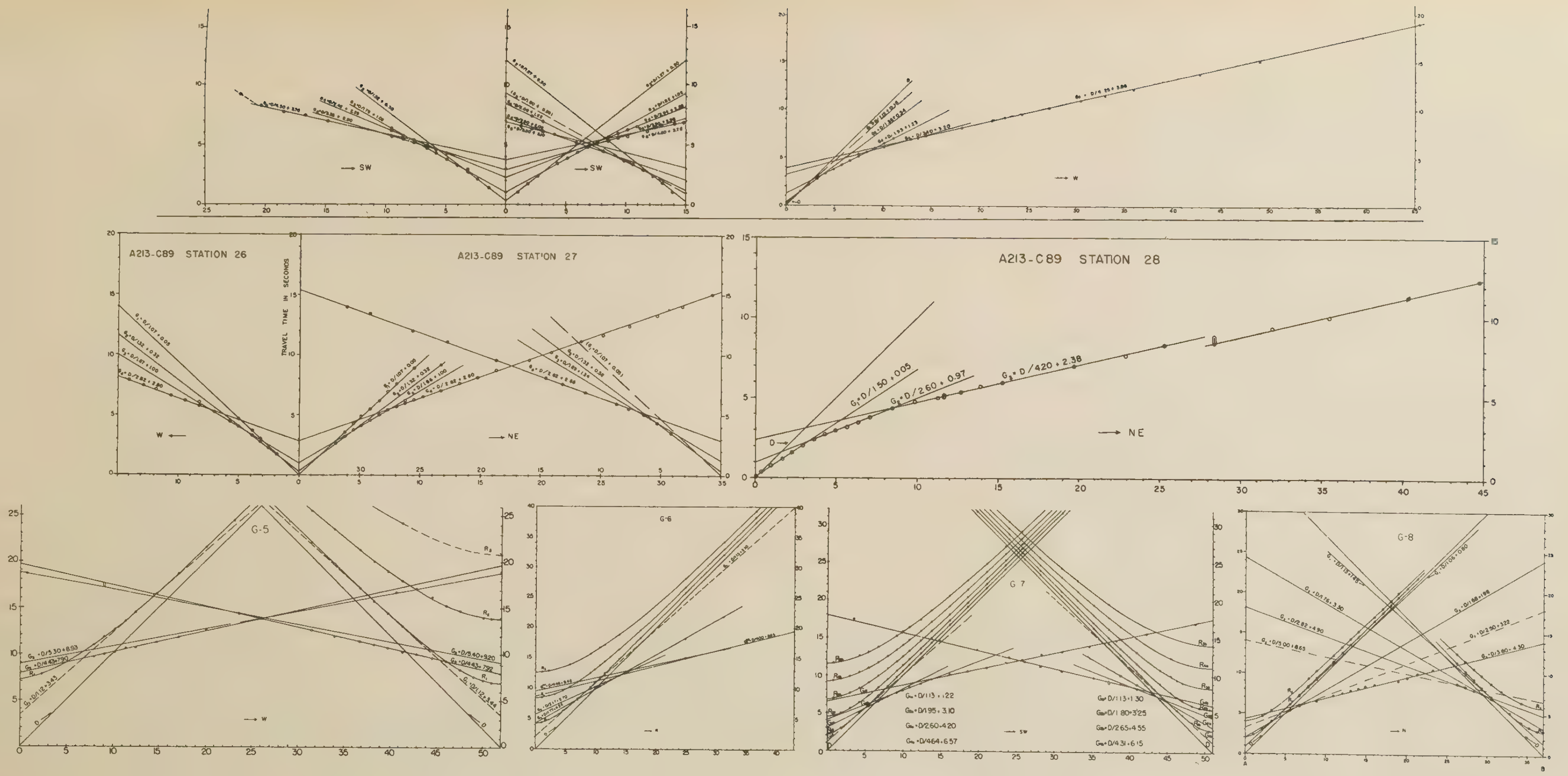

TRAVEL-TIME GRAPHS

Stations A213 to C89 (nos. 11-28) and stations G-5 to G-8. Distance on the abscissa is plotted in increments of direct water-wave (d) travel time, *i. e.*, 1 second is approximately equal to 5030 feet. The lines G_1, G_2, and G_3 are determined by refracted arrivals traveling in the first, second, and third layers beneath the ocean floor. At stations where no G_1 line appears, velocity in the top layer was assumed.

Contribution No. 866

Vol. 38, No. 5 Transactions, American Geophysical Union October 1957

Flooded Quarries for Experimental Work*

Milton S. Rutstein

Abstract—Flooded quarries have some technical and economic advantages for underwater experimental work and for testing oceanographic equipment, particularly where explosions are involved or where wave action must be minimized. The quarries visited in and near New England are described.

Introduction—In the course of underwater-sound work at the Woods Hole Oceanographic Institution, there developed a need for a body of water for short-range experiments using explosives. Ponds, lakes, and rivers were not suitable because of size, depth, or the impracticality of using explosives even though the damaging effects of explosives on fish are over-rated. This particular experiment required that the body of water should be at least 300 ft long, 100 ft wide, and 75 ft deep; by far the most difficult requirement was that the quarry be sufficiently removed from houses so that the explosives would not cause any annoyance or physical damage to the local community.

An abandoned flooded quarry satisfying these requirements was selected and used during the summers of 1954 and 1955. This quarry was the Blackington Farm quarry owned by the Rockland-Rockport Lime Company of Rockland, Maine. During the course of several months of testing, there was ample opportunity to appreciate the convenience of a land base and the relative stability of water conditions. The sides of the quarry were so steep that there was 90 ft of water under the end of a small cantilever platform ten feet from the edge.

A quarry is, of course, no substitute for the ocean, but certain aspects of some problems or of instrument development can be studied or tried out without the use of a ship. A land base provides an economic and convenient means for repeating experiments without the hindering influence of high seas or bad weather.

SCIENTIFIC AND ENGINEERING USES OF QUARRIES

In considering uses for quarries, points to keep in mind are the accessibility, the calm water surface, and the ease of handling equipment. Abandoned quarries will seldom have electrical power convenient. Suggested uses for quarries are listed as follows:

Explosive research—Some experiments in high explosive research can be handled nicely in quarries. The walls or banks of the flooded holes are usually high enough so that a grid of wires may be stretched across the quarries. This will allow explosives to be lowered to various depths at specific ranges from receiving instruments, and measurements of underwater sound and explosive intensities may be made.

For this type of work quarries that are privately owned have many advantages over those that are not. This involves dealing with fewer people and reduces the amount of negotiations necessary to shoot explosives near a community. Moderate remoteness is essential. For example, at one mile 10 pounds of TNT should do no damage, but it might bother some people.

Underwater sound—There are good opportunities for experimental work in this direction. During the summer months, sharp thermal gradients exist, and the quarries are often large enough to provide 30 milliseconds before any echos return.

Mixing problems—Wind exposure is usually less than with large lakes or ponds, resulting in relatively quiet surface water and nearly motionless bottom water. High quarry walls reduce the effects of wind on the water [*Stommel*, 1952].

Pressure testing—Large apparatus can be tested. At Tilley Foster Mine in Brewster, N. Y., there is a water-filled hole believed to be somewhat deeper than 600 ft. If so, it is possible to test equipment within 40 miles of New York City at a steady pressure equivalent to that along the continental shelf at the 100 fathom line.

Figure 1 is a map of New England showing the locations of the various quarries that were inspected. The principal quarries visited are listed in Table 1. A good many of these quarries are remote enough to allow the use of small explosive charges.

A useful guide for anyone beginning a search for

---

* Contribution No. 866 from the Woods Hole Oceanographic Institution.

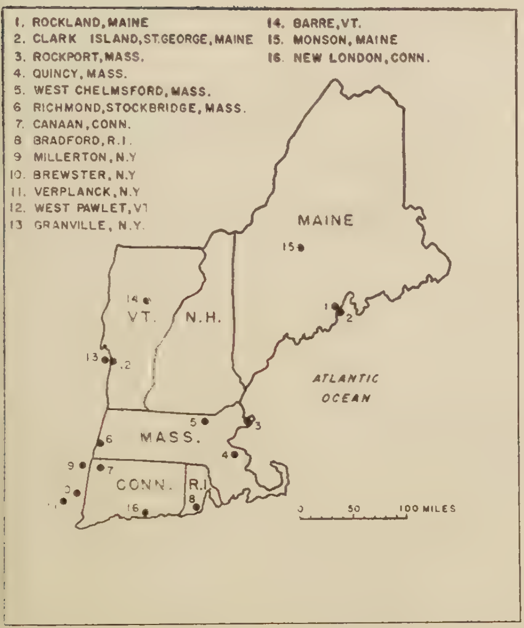
1. ROCKLAND, MAINE
2. CLARK ISLAND, ST. GEORGE, MAINE
3. ROCKPORT, MASS.
4. QUINCY, MASS.
5. WEST CHELMSFORD, MASS.
6 RICHMOND, STOCKBRIDGE, MASS.
7. CANAAN, CONN.
8 BRADFORD, R.I.
9 MILLERTON, N.Y
10. BREWSTER, N.Y
11. VERPLANCK, N.Y
12. WEST PAWLET, VT
13 GRANVILLE, N.Y.
14. BARRE, VT.
15. MONSON, MAINE
16. NEW LONDON, CONN.
MAINE
VT.
N.H.
MASS.
CONN.
R.I.
ATLANTIC OCEAN
0
50
100 MILES

FIG. 1 — Map showing quarries investigated

flooded quarries is a list of kinds of quarries where operations are being or have been carried out, such as those in *Dale* [1923a, b], *Chute* [unpublished], and *Trefethen* [1953].

For those who are elsewhere and have different requirements, it is recommended that they contact the U. S. Geological Survey, the State Geologist, or the geological department of a nearby university.

Acknowledgments—This investigation was conducted by the Woods Hole Oceanographic Institution under the auspices of Contract Nord-12621 with the U. S. Navy Bureau of Ordnance during the winter and spring of 1954.

The author wishes to express his thanks to H. Wenden of Tufts College Geology Department, K. E. Lowe of the City College of New York, J. W. Peoples of the Geology Department of Wesleyan University, Charles Doll, State Geologist of Vermont, Freeman Burr, former State Geologist of Maine, and L. W. Currier of the U. S. Geological Survey, Boston office, for their kind help and advice in beginning the search for quarries. Many thanks to Allyn C. Vine of Woods Hole for his counsel and aid on the problem.

The author and his co-workers are particularly indebted to the Rockland-Rockport Lime Co. and to their officers for the use of their property and for their enthusiastic cooperation to make our quarry work a success.

TABLE 1 — *Principal quarries visited*

Map key	Name of quarry	Length[a] & Breadth[a]	Depth[a]	Remoteness from houses[a]	Accessibility by roads	Purpose
8	Crumb	300 × 150	50–140	500	Good	Granite
8	Klondike 1	200 × 125	100?	one house 500	Good	Granite
8	Klondike 2	300–500 × 200	100?	one house 500	Good	Granite
7	Lawrence	300 × 200	60	2600	Good	Limestone
10	Tilley Foster	600 × 300	600?	700	Good	Iron Ore
11	Verplanck	1000 × 400	70	800	Good	Limestone
9	Mulby's Ore Body	300 × 250	100?	650	Good	Iron Ore
12	Rising-Nelson Slate	Several various dimensions	75?	2600	Good	Slate
13	Briar Hill	Several various dimensions	same	2600	Good	Slate
14	Canton	350 × 250	90	800	Good	Granite
15	Hebron Pit	250 × 75	400?	500	Good	Slate
1	Blackington Farm	600 × 120	180	800	Good	Lime
16	Bottinelli	300 × 200	50	. . .	Good	Granite
4	Quincy (five)	300 × 100–200	100?	650	Good	Granite
3	Rockport 1	500 × 350	90	2600	Good	Granite
	Rockport 2	300 × 200	50	500	Good	Granite
2	Clark Island	300 × 125	75?	5100	Poor; road is brushed in	Granite

[a] Dimensions in feet (approximate).

References

Chute, N. E., *Iron ore deposits of western Massachusetts*, U.S. Geol. Surv., Boston, 1–39, 1945 (unpublished manuscript).

Dale, T. N., Commercial granites of New England, *U.S. Geol. Surv. Bull. 738*, 1–448, 1923a.

Dale, T. N., The lime belt of Massachusetts, *U.S. Geol. Surv. Bull. 744*, 1–70, 1923b.

Trefethen, J. H., Report of the State Geologist, Maine Development Commission, Augusta, Maine, 1953.

Stommel, H., Streaks of natural water surfaces, Mass. Inst. Tech., Geophysics Research Directorate, *Geophys. Res. Pap. 19*, 145–154, 1952.

Woods Hole Oceanographic Institution, Woods Hole, Massachusetts

(Communicated Manuscript received November 21, 1956; open for formal discussion until March 1, 1958.)

Contribution No. 868

Reprinted from Biological Bulletin, Vol. 112, No. 1, 28-33, February, 1957
Printed in U. S. A.

OBSERVATIONS ON OSMOREGULATION IN THE ARCTIC CHAR (SALVELINUS ALPINUS L.)

MALCOLM S. GORDON

Osborn Zoological Laboratory, Yale University and Woods Hole Oceanographic Institution, Woods Hole, Mass.

OBSERVATIONS ON OSMOREGULATION IN THE ARCTIC CHAR (SALVELINUS ALPINUS L.)[1]

MALCOLM S. GORDON[2]

Osborn Zoological Laboratory, Yale University and Woods Hole Oceanographic Institution, Woods Hole, Mass.

The different groups of euryhaline fishes have developed somewhat different mechanisms for maintaining the relative constancy of the concentration of their "milieu interieur" in the face of large changes in the external osmotic pressure. Following such an external change, many change their internal concentrations only transitorily, in the same direction as the external variation. A return to essentially the original conditions usually follows shortly (in adult female eels (*Anguilla*): Boucher-Firly, 1935; Duval, 1925; in sticklebacks (*Gasterosteus*); Gueylard, 1924; Koch and Heuts, 1943; in killifish (*Fundulus*): Burden, 1956). Anadromous salmonid fishes, however, have long been known to regulate their blood concentrations on two distinct levels (probably the end-points of an acclimation curve). In almost all such salmonids studied so far, the transition from salt to fresh water (or the reverse) is accompanied by a fall (or rise) in total blood concentration of about 25% (the Atlantic salmon, *Salmo salar,* and the Chinook salmon, *Oncorhynchus tshawytscha,* however, change by only 12% (Fontaine and Koch, 1950; Greene, 1926)). Plasma freezing point depressions vary from species to species, being 0.67–0.90° C. in salt water, 0.55–0.72° C. in fresh water (Benditt *et al.*, 1941; Fontaine, 1943, 1948; Fontaine, Callamand and Vibert, 1950; Fontaine and Koch, 1950; Greene, 1904; Kubo, 1953).

The Arctic char (*Salvelinus alpinus* L.) is an anadromous salmonid fish common in fresh and coastal salt waters throughout most of the Arctic. As in other sea-going char, its migrations from fresh to salt water and back again are somewhat different from those of other salmonids in that its winter periods in fresh water lakes and rivers are long compared to its summer periods in the ocean, rather than vice versa (Andrews and Lear, in press; Backus, 1952; Sprules, 1953). Osmoregulation in this form has not been studied, probably due to its inaccessibility. The present paper describes some observations made on the osmoregulatory abilities of adult Arctic char on their return (spawning) migration to fresh water after a summer in the ocean.

---

[1] These studies were aided by contracts between the Office of Naval Research, Department of the Navy, and the Arctic Institute of North America. Reproduction of this paper in whole or in part is permitted for any purpose of the United States Government. The author's activities were also supported in part by National Science Foundation Predoctoral Fellowships. Contribution Number 868 from the Woods Hole Oceanographic Institution.

[2] The author's thanks for aid and cooperation are due the following people: In Labrador (1954 "Blue Dolphin" Expedition), Cmdr. D. C. Nutt, Drs. P. F. Scholander and L. van Dam, and P. Hay. At Churchill, Manitoba, Mr. P. Bussadore, Mr. and Mrs. A. MacIver, Mr. and Mrs. I. Smith, and Dr. D. E. Sergeant. Mr. C. L. Claff kindly permitted the use of his flame photometer. Dr. van Dam performed the plasma chloride determinations at Hebron.

The material is of a preliminary nature in many ways, but serves to show that the Arctic char is similar to other salmonid fishes in regulating its blood concentration on two levels. Agreement between experimental results and data obtained from fish living in fresh and salt waters provides a basis for further experimental study of osmotic phenomena during the migrations of these fish. Some data on regulation of muscle concentrations are also presented. Differences in results obtained from char in northern Labrador and Hudson Bay indicate the possibility of physiologically different populations in this species.

MATERIALS AND METHODS

Regulation of total plasma concentration, chloride and potassium, and of total muscle solids, chloride, and potassium was studied in mature adult char of both sexes by means of observations on fish living in salt or fresh water, and by time series of observations immediately following direct transfers of fish from salt to fresh water. Conditions of temperature, stage in life cycle, etc., were kept fairly constant in these experiments. Char were taken by means of gill nets from Hebron Fjord, Labrador, and Hudson Bay near Churchill, Manitoba, during late July and early August of 1954 and 1955, respectively.

Seven char were used to establish the normal salt water ranges for plasma freezing point and chloride concentration in fish in Hebron Fjord (water of 28.6 ‰ salinity, 9° C. temperature). Five Churchill char were used similarly, observations on these consisting of plasma chloride and potassium concentrations, and total muscle solids, chloride, and potassium concentrations (Hudson Bay water was of approximately 26 ‰ salinity, 10–12° C. temperature).

Fresh water ranges for plasma freezing point and chloride concentration were determined at Hebron in several small land-locked char from a small lake, in some pre-sea-run parr from a river, and in an adult char that had returned to fresh water by itself. No fresh water char were obtainable at Churchill.

The osmotic stresses these fish undergo during the course of their migrations from the sea were approximated by transferring four Hebron fish and seven Churchill fish directly from salt to fresh water. Temperatures at Hebron were: salt water, 9°, fresh water, 5–10°; at Churchill: salt water, 10–12°, fresh water 14–16°. Changes in plasma freezing point with time were followed in three of the Hebron fish via serial blood samples taken at intervals up to 77 hours following transfer. The fourth fish was sampled initially and after 77½ hours. Two of the Hebron char were then returned to the Fjord and sampled again following death (after some fifteen hours in salt water).

Only two of the Churchill char survived for more than one hour after transfer from salt to fresh water—these for two and six hours, respectively. Blood and muscle concentrations were determined in these, after the periods mentioned, as in the salt water fish. The approximately 5° C. thermal shock to which these fish were subjected, combined with a lack of running fresh water, hence a need for aeration by hand dipping, probably explains in great part the lowered survival as compared with the Hebron fish. The speed with which death followed transfer makes it seem unlikely that this is the complete explanation, however.

Blood samples were taken via heart puncture from all fish. The samples were heparinized, centrifuged, and the plasma pipetted off. Plasma freezing points were determined at Hebron using the method of Pounder and Masson (1934) modified for field use (Scholander *et al.*, in press). Plasma chloride determinations were made using the method of Schnohr (1934). Plasma potassium concentration was determined on the Churchill samples following dilution with Pyrex-distilled water on a Baird Associates internal standard flame photometer. Probably due to coagulation of the proteins in these samples, which may have interfered with activation of the ions by the flame, only three of these analyses gave what appear to be reasonable values.

Four samples of tissue from the dorsal muscle mass, averaging about 100 mg. wet weight, were also taken from each of the Churchill fish. Total solids were determined by weighing these before and after complete drying in an oven at 105° C. Following digestion with concentrated nitric acid and 30% hydrogen peroxide, duplicate chloride and potassium analyses were carried out. Methods were as above.

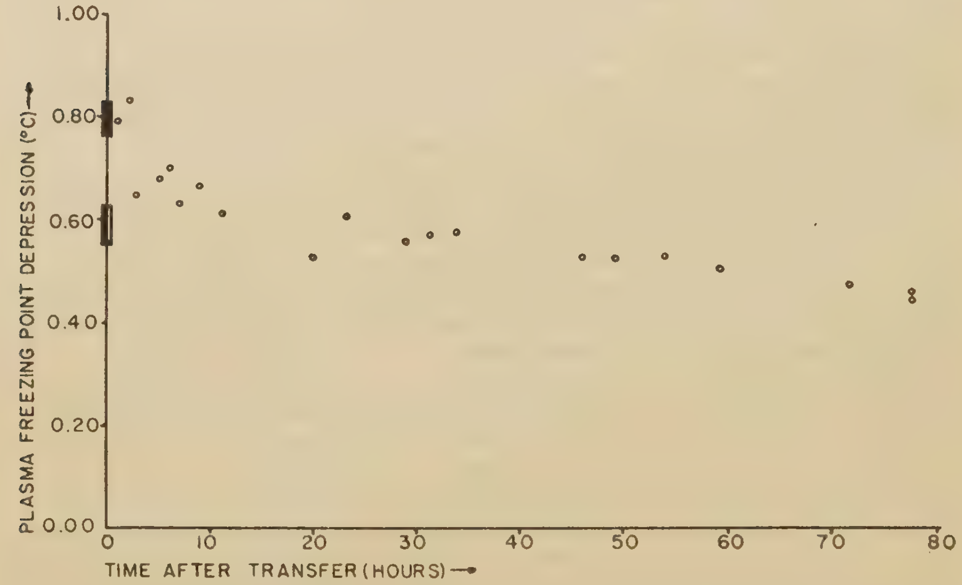

FIGURE 1. Changes of plasma freezing point depression with time following direct transfer from salt to fresh water of Arctic char (*Salvelinus alpinus* L.) from Hebron Fjord, Labrador. Ranges for fish naturally acclimated to salt water (black bar) and fresh water (black and white bar) indicated on ordinate. Temperature 5–10° C.

Precision of the freezing point determinations is ± 0.05° C. Plasma chloride analyses agreed within 1%, as did total muscle solids. Muscle chloride and potassium duplicates agreed within 5%.

RESULTS AND DISCUSSION

Figure 1 shows the behavior of total blood concentration in control and experimental char from Hebron Fjord. The total plasma concentration in Hebron char living in fresh water is about 25% lower than the salt water concentration. The char is thus like most other anadromous salmonids in this regard. Beginning two hours after transfer from salt to fresh water, the experimental fish also decreased their plasma concentrations by about 25% over a period of approximately twenty hours. They then became fairly stable. It therefore seems that sudden transfer experiments duplicate at least some of the physiological events occurring during the migrations of these fish. This last might have been expected, since individual salmonids frequently make the transition from salt to fresh water and back again as rapidly as they can swim through the estuaries involved (Benditt *et al* 1941; Greene, 1910; Killick, 1955).

The continuing decrease in plasma concentration below the normal fresh water level which occurred in the experimental fish after about 35 hours in fresh water could have been the result of several influences. First, the fish were not fed; second, they may well have lost salt via their urine as a result of having been handled (laboratory diuresis of Grafflin, 1931, 1935, and Forster, 1953); and third, their skin permeability, hence rate of water uptake in a hypotonic medium, may well have been increased as a result of loss of slime during handling.

TABLE I

Blood concentrations in arctic char

Source of fish	Plasma Δ_F (° C.)	Plasma $[\mathrm{Cl}^-]$ (meq./l.)	Equivalent Cl^- Δ_F (° C.)*	Plasma $[\mathrm{K}^+]$ (meq./l.)
Hebron Fjord, salt water	0.80	148	0.28	
	0.80	191	0.36	
	0.81	191	0.36	
	0.82	213	0.40	
	0.82	214	0.40	
	0.83			
	0.76			
Hebron Fjord, fresh water	0.59	144	0.27	
(land-locked)	0.61	144	0.27	
	0.63	161	0.30	
Churchill, salt water		177	0.33	5
		153	0.28	8
		156	0.29	1
		130	0.24	1
		132	0.25	2
Churchill				
2-hr. transfer		134	0.25	1
6-hr. transfer		124	0.23	8

* Equivalent $\mathrm{Cl}^-\Delta_F$ calculated from: $\Delta_F = 1.86\ [\mathrm{Cl}^-]$

The two Hebron char transferred back to the Fjord after the experiment, after fifteen hours in salt water, had plasma freezing points of − 0.75° C. This is essentially the original salt water value.

Table I summarizes the data on blood concentrations obtained from both Hebron and Churchill control fish and Churchill transfers. With the exception of the first salt water char from Hebron, the calculated equivalent Cl freezing point is essentially a constant fraction of the total freezing point (45–50%). More exact regulation of the concentrations of other plasma components is thus indicated. Similar behavior of chloride and total concentrations has been noted in brook and brown trout (unpublished data of the writer and van Dam). Fontaine, Callamand and

Vibert (1950), however, found a decrease of only 4% in plasma chloride in Atlantic salmon (*Salmo salar*) when total concentration dropped 13%.

The Churchill material generally supports the Hebron results. Plasma chloride concentration in the Churchill fish in fresh water for six hours is approximately 18% lower than the mean plasma chloride concentration for Churchill char in salt water. Plasma freezing point behaves similarly in the Hebron char. Note, however, that plasma chloride concentrations in the Churchill fish are generally much lower than in the Hebron fish. The mean difference of 20% seems too large to be the result of acclimation to differing salinities (the salinities differing only by 10%.). The marked differences between Hebron and Churchill char with respect to survival following transfer were noted earlier. Even allowing for the poor conditions encountered at Churchill it seems likely that real physiological differences exist between these populations. Marked differences in growth characteristics differentiating these two groups (Andrews and Lear, in press; Backus, 1952; Sprules, 1953; unpublished data of the author) also make this seem likely (though differences in food supply might well account for this last).

TABLE II

Muscle concentrations in Churchill arctic char

Source of fish	Total muscle solids (gm./kg. wet weight)	Muscle [Cl^-] (meq./kg. wet weight)	Muscle [K^+] (meq./kg. wet weight)
Salt water	276	22	123
	224	20	130
	266	8	120
	226	8	120
	260	6	125
2-hr. transfer	242	4	127
6-hr. transfer	244	3	150

Table II indicates that the one Churchill fish surviving transfer for six hours regulated total muscle concentration very well. Muscle potassium, however, seemingly increased markedly. The concentrations of the same muscle components in brook and brown trout under similar conditions behave very differently, however (data of the author and van Dam). In these other forms there is a close parallelism between changes in muscle concentrations and changes in the blood. Further work on the char is obviously needed.

In closing it should be noted that the blood and muscle potassium concentrations reported by Jones (1956) for fresh water brown trout agree very well with the figures given in Tables I and II for the Churchill salt water char (low plasma potassiums excepted).

SUMMARY

1. Adult Arctic char (*Salvelinus alpinus*), taken in summer from Hebron Fjord, Labrador, and Hudson Bay near Churchill, Manitoba, were transferred directly from salt to fresh water under fairly constant conditions.

2. Decreases in blood freezing point and chloride concentration of the order of 25% were found, the char thus being like most other anadromous salmonids in this

respect. The possibility of much better regulation of muscle concentrations is indicated.

3. Data are presented on plasma freezing point, chloride, and potassium, muscle solids, chloride, and potassium.

4. Physiological differences between populations of char are indicated.

LITERATURE CITED

ANDREWS, C. W., AND E. LEAR. The biology of Arctic Char (*Salvelinus alpinus* L.) in northern Labrador. *J. Fish. Res. Bd. Canada* (in press).

BACKUS, R. H., 1952. Growth in the Arctic Char (*Salvelinus alpinus* L.) in the Nain region of Labrador. Unpublished thesis, Cornell University.

BENDITT, E., P. MORRISON AND L. IRVING, 1941. The blood of the Atlantic salmon during migration. *Biol. Bull.*, **80**: 429–440.

BOUCHER-FIRLY, S., 1935. Recherches biochimiques sur les teleostéens apodes (Anguille, Congre, Murène). *Ann. Inst. Oceanogr. (Monaco)*, **15**: 217–327.

BURDEN, C. E., 1956. The failure of hypophysectomized *Fundulus heteroclitus* to survive in fresh water. *Biol. Bull.*, **110**: 8–28.

DUVAL, M., 1925. Recherches sur le milieu interieur des animaux aquatiques. Modifications sous l'influence du milieu exterieur. *Ann. Inst. Oceanogr. (Monaco)*, **2**: 233–407.

FONTAINE, M., 1943. Des facteurs physiologiques déterminant les migrations reproductrices des Cyclostomes et Poissons potamotoques. *Bull. Inst. Oceanogr. (Monaco), No. 848: 1–8.*

FONTAINE, M., 1948. Physiologie du saumon. *Ann. Sta. Cent. Hydrobiol. Appliq.*, **2**: 153–183.

FONTAINE, M., O. CALLAMAND AND R. VIBERT, 1950. La physiologie du saumon. *Ann. Sta. Cent. Hydrobiol. Appliq.*, **3**: 15–26.

FONTAINE, M., AND H. J. KOCH, 1950. Les variations d'euryhalinite et d'osmoregulation chez les poissons. *J. de Physiol.*, **42**: 287–318.

FORSTER, R. P., 1953. A comparative study of renal function in marine teleosts. *J. Cell. Comp. Physiol.*, **42**: 487–509.

GRAFFLIN, A. L., 1931. Urine flow and diuresis in marine teleosts. *Amer. J. Physiol.*, **97**: 602–610.

GRAFFLIN, A. L., 1935. Renal function in marine teleosts. I. Urine flow and urinary chloride. *Biol. Bull.*, **69**: 391–402.

GREENE, C. W., 1904. Physiological studies of the chinook salmon. *Bull. U. S. Bur. Fish.*, **24**: 429–456.

GREENE, C. W., 1910. An experimental determination of the speed of migration of salmon in the Columbia River. *J. Exp. Zool.*, **9**: 579–592.

GREENE, C. W., 1926. The physiology of the spawning migration. *Physiol. Rev.*, **6**: 201–241.

GUEYLARD, F., 1924. De l'adaptation aux changements de salinité. Recherches biologiques et physico-chimiques sur l'Épinoche (*Gasterosteus leiurus* C. et V.). *Arch. Phys. Biol.*, **3**: 79–197.

JONES, I. C., 1956. The role of the adrenal cortex in the control of water and salt-electrolyte metabolism in vertebrates. *Mem. Endocrin., No. 5: 102–120.*

KILLICK, S. R., 1955. The chronological order of Fraser River Sockeye Salmon during migration, spawning, and death. *Intl. Pacific Salmon Fish. Comm. Bull., No. 7: 1–95.*

KOCH, H. J., AND M. J. HEUTS, 1943. Regulation osmotique, cycle sexuel et migration de reproduction chez les épinoches. *Arch. Intern. Physiol.*, **53**: 253–266.

KUBO, T., 1953. On the blood of salmonid fishes of Japan during migration. I. Freezing point of blood. *Bull. Fac. Fish. Hokkaido Univ.*, **4**: 138–148 (English summary).

POUNDER, F. E., AND I. MASSON, 1934. Thermal analysis and its application to the dinitrobenzenes. *J. Chem. Soc.*, 1357–1360.

SCHNOHR, E., 1934. A study of the cause of death in high intestinal obstruction. *Coll. Pap. Univ. Zoofys. Lab. Kjobenhavn, 12A (No. 185): 1–176.*

SCHOLANDER, P. F., L. VAN DAM, J. W. KANWISHER, H. T. HAMMEL AND M. S. GORDON. Supercooling and osmoregulation in Arctic fish. *J. Cell. Comp. Physiol.* (in press).

SPRULES, W. M., 1953. Arctic Char of the west coast of Hudson Bay. *J. Fish. Res. Bd. Canada*, **9**: 1–15.

Contribution No. 870

Reprinted from
THE EFFECTS OF ATOMIC RADIATION ON OCEANOGRAPHY AND FISHERIES
Publication No. 551, National Academy of Sciences—National Research Council, 1957

Chapter 4

TRANSPORT AND DISPERSAL OF RADIOACTIVE ELEMENTS IN THE SEA [1]

Warren S. Wooster, *Scripps Institution of Oceanography,* La Jolla, California

and

Bostwick H. Ketchum, *Woods Hole Oceanographic Institution,* Woods Hole, Massachusetts

The fate of radioactive elements in the sea differs from that of non-radioactive elements since they are subject to radioactive decay. Otherwise, concentrations of radioactive elements are changed by the same physical and biological processes as are those of other isotopes in the same physical state. Thus the fate of radioactive material introduced into the sea depends on:

1. What is introduced — the nuclide, its radioactive properties (half-life, nuclear reaction, kind and energy of radiation), its physical state in sea water (whether particulate, colloidal or ionic) and its chemical properties (including its role in biological processes).
2. Where it is introduced — position and depth with respect to the density and velocity structure of the sea.

This paper describes the physical processes whereby radioactive elements in true solution are diluted by mixing and are carried from one part of the ocean to another. Although all parts of the open ocean appear to be in continuous motion and in communication with each other, the rates of this motion and exchange cover such a wide range that it is convenient to consider separately the questions of near-surface vertical and horizontal exchange, intermediate and deep circulation, and the exchange between the deep sea, coastal areas and enclosed basins.

Near-surface circulation

In middle and low latitudes the surface layer of the ocean, from 10 to 200 meters thick, is separated from the colder deep waters by a layer of rapid density change and great stability, the pycnocline or thermocline. This intermediate layer varies in depth and stability from time to time and from place to place. At times there are two such layers, the seasonal thermocline and a deeper main thermocline. The surface layer is often called the "stirred" or "mixed" layer [2] because of its relative uniformity in temperature and in concentrations of dissolved substances.

It is believed that radioactive material introduced into this surface layer will be rapidly distributed vertically throughout the layer. The general uniformity of concentrations within this layer suggests that forces are present which tend to bring it about. Because density increases only slightly with depth through the layer, little energy is required for vertical stirring.

Some evidence of the rapidity of vertical mixing in the upper layer is given by Folsom (Revelle, Folsom, Goldberg and Isaacs, 1955), who observed that when fission products were introduced at the surface in an area where the surface layer was about 100 meters thick, the lower boundary of the radioactive water reached the bottom of this layer in about 28 hours. Within this period of time radioactivity had become uniformly distributed vertically throughout the layer.

Rapid vertical mixing in the upper layer is brought about primarily by the following two processes:

1. Convection: When the density of surface water is sufficiently increased, owing to either

---

[1] Contribution from the Scripps Institution of Oceanography, New Series, no. 903. Contribution no. 870 from the Woods Hole Oceanographic Institution. This paper, in part, represents results of research carried out by the University of California under contract with the Office of Naval Research. Reproduction in whole or in part is permitted for any purpose of the United States Government.

[2] A distinction is made here between stirring and mixing. In stirring, one causes relative motion of different parts of the liquid, and the average value of the gradient is increased. Mixing then takes place, the gradients disappearing and the liquid becoming homogeneous (Eckart, 1948).

a decrease in temperature or an increase in salinity, the surface water sinks and mixes with deeper water. Convection is maintained by (a) surface cooling due to long wave radiation and heat conduction to the atmosphere, (b) the loss of latent heat and water vapor in evaporation, or (c) the increase of surface salinity from freezing of surface water.

2. Wind stirring: Vertical turbulence in the upper layer results from wind action on the sea surface. The extent of wind stirring depends both on the magnitude and uniformity of wind stress and on the vertical density gradient. Stirring is effective only to a depth where there is sufficient energy to overcome the effect of stability. Both the homogeneity and the depth of the upper layer are affected by wind. Single gales have been observed to deepen the surface layer on the average by about 20–30 feet, (Francis and Stommel, 1953).

Rapid vertical mixing may be brought about by other processes. Thus in shallow coastal areas stirring by strong tidal currents is important. Stirring may also be accomplished by the vertical component of currents, particularly in regions of upwelling and sinking.

It should be noted that even above a well-developed pycnocline there is not complete homogeneity within the so called "mixed" layer. Concentrations of those elements affected by biological activity (such as oxygen and phosphorus) may show significant variation within the euphotic zone. Even so-called "conservative" concentrations (temperature and salinity) may not be uniform within the surface layer. Such heterogeneity may be attributed to incomplete vertical mixing or to vertical shear in the surface layer.

When radioactive materials are introduced into the near-surface layer, they are transported away from the area of introduction by surface currents. These currents extend, in general, through the entire depth of the upper layer and seem to be driven, directly or indirectly, by the wind.

The average locations and velocities of the important surface currents of the world ocean have been studied for many years and are well known (see, for example, Deutsche Seewarte, 1942; U. S. Navy Hydrographic Office, 1947 a and b, 1950; Sverdrup, Johnson, and Fleming, 1942, ch. 15). This knowledge comes primarily from averages of countless ship-drif observations, and from computations based o the observed subsurface distribution of density

These calculations give mean speeds as hig as 193 cm/sec (90 miles per day) in th Florida Current (Montgomery, 1938a) and 8 cm/sec (41 miles per day) in the Kuroshi (Koenuma, 1939). The volume of water flowing through the Florida Straits in 15 years i about equal to that of the upper 500 meters o the whole North Atlantic. Similarly, betwee the northern Ryukyus and Kyushu, the Kuroshio transports a volume equivalent to that o the upper 500 meters of the North Pacific i about 50 years. It seems likely that there i no area of surface water in the ocean that ca be considered as isolated from the remainin surface waters.

Recent intensive studies of the Gulf Strea and other surface currents, using such moder instruments as the bathythermograph, electroni navigational aids, and geomagnetic electro-kinetograph (GEK), have revealed complicated fin structures, with filamentous jets and countercurrents not apparent in the average pictur (Fuglister, 1951). Characteristic maximum surface velocities measured by GEK and Lora dead reckoning in the Gulf Stream were foun to fluctuate between 150 and 300 cm/sec o 70 to 140 miles per day (von Arx, Bumpu and Richardson, 1955). Thus, in estimatin the time at which radioactive materials will b found at various distances from the area o introduction, one must be cautious in the us of average surface current speeds.

Direct evidence of the transport of radioactive materials by surface currents in th western Pacific is given by "Shunkotsu-Maru" survey (Miyake, Sugiura and Kameda, 1955) and the "Taney" survey (U. S. Atomic Energ Commission, 1956) four months and thirtee months respectively after nuclear weapons test in the Marshall Islands in March, 1954. Th earlier survey found significant levels of radioactivity at a distance of 2000 kilometers fro Bikini, suggesting a westward drift of mor than 9 miles per day (about 20 cm/sec). Th later survey found significant levels of radioactivity at least 7000 kilometers downstrea from Bikini; this gives about the same minimu westward drift.

In addition to being drifted away from th area of introduction, radio-active materials ar dispersed by diffusion. Diffusion in the ocean is caused by turbulence or eddies, and the coefficient of eddy diffusivity is usually more than a million times the corresponding molecular coefficient. The rate of eddy diffusion depends on wind speed, current shear, density gradient, gradient of the diffusing concentration, direction of diffusion, and the dimensions of the phenomenon. The calculated rates depend upon the magnitudes of eddy diffusivity coefficients used, and they have been estimated by a number of methods (Sverdrup et al., 1942, p. 484–485; Munk, Ewing and Revelle, 1949).

Because of both the large number of variables concerned and the present unsatisfactory state of our quantitative knowledge of turbulence in the ocean, it is difficult to predict the diffusion of radioactive materials under any given circumstances. The most satisfactory approach at present is to conduct diffusion studies and experiments at the place and under the conditions of contemplated release. The results are only applicable to the particular areas.

During the 1946 preliminary survey in Bikini Lagoon, the state of turbulence was determined by a variety of measurements, and the subsequent observed distribution of radioactivity was in close agreement with the predicted values (Munk, Ewing and Revelle, 1949). A mean value for the radius of the contaminated area was 3 km., which approximately doubled between the first and second days after the burst. The initial distribution of radioactivity as deposited by the atomic bomb was patchy, and the turbulent eddies, which spread the contamination over a larger area, did not appreciably reduce this patchiness during the first three days.

Another pertinent study was made by Ketchum and Ford (1952) who examined the rate of dispersion of acid-iron wastes in the wake of a barge at sea. Computed mixing coefficients showed a tendency to increase with increasing time, and thus with the dimensions of the mixing field, and the radius of the contaminated area was observed to double in time periods ranging from 0.5 minutes to 35 minutes. It should be noted that the scale of this phenomenon was about 10^{-2} that of Munk, Ewing and Revelle (1949); they show that the ratio of lateral eddy diffusivity coefficient to the radius of the area considered is relatively constant over a range of radius between 10^3 and 10^8 cm.

A large scale tracer experiment was carried out in the Irish Sea prior to the discharge of radioactive effluent (Seligman, 1955). During each experiment, 10 tons of 6.7 percent fluorescein solution were introduced near the surface during a 20-minute period, and the sensitivity of subsequent detection was believed to be of the order of 1 part in 10^9. Maximum concentrations detected directly after release were 10^{-4} of the original concentration; 12 hours after release, they were down to 5×10^{-7} of the original concentration. The trial area was probably part of an eddy and was subject to tidal mixing, so the results may not be generally applicable.

Exchange between near-surface and intermediate waters

Since the surface layer is separated from deeper waters by a layer of rapid density increase, and hence of great stability, vertical transfer of materials across this layer by eddy diffusion must be much less rapid than is vertical diffusion in the upper layer. Thus radioactivity introduced at the surface by fallout may remain in the upper layer for a long time and be diluted by only a small part of the total volume of the sea. Conversely, radioactive materials introduced below the pycnocline should only slowly contaminate the upper layer where they are most likely to endanger human activities. However, organisms and particles of sufficient density may readily cross the pycnocline, due both to gravity and to vertical migrations.

There are few observations which show directly the existence of cross-pycnocline exchange on a local scale. In the western Pacific, both the "Shunkotsu-Maru" survey (Japanese Fishery Agency, 1955) and the "Taney" survey (U. S. Atomic Energy Commission, 1956) reported patches with significant concentrations of radioactivity below the thermocline four months and thirteen months, respectively, after mixed fission products were introduced at the surface in the Marshall Island area. It is not known, however, whether this exchange was effected by mixing processes, or by particulate or ecological processes.

Exchange of properties between the near-surface and deeper waters is most likely to take place under the following conditions:

1. In regions where the pycnocline is sufficiently shallow to be eroded at the top by wind stirring. In coastal waters the pycnocline is usually shoaler than in midocean, and shallow pycnoclines may also be found in high latitudes, at the equator, along the north edge of the Equatorial Countercurrent, and at the center of strong cyclonic eddies. This process is not effective to great depths, but could serve to bring radioactive materials into the surface waters from the pycnocline layer.

2. In regions of upwelling, where the pycnocline is relatively weak and where vertical currents not only carry water toward the surface but also stir surface and deeper waters. It is unlikely that water from depths of more than 500 meters is ever brought to the surface by this process. Upwelling is common along western coasts of continents in the trade wind belt, such as the coasts of Peru and Northern Africa. In a simple sense, the persistent trade winds blowing parallel to or offshore develop an offshore component of transport in the surface waters, and deeper waters upwell to maintain the volume continuity. Upwelling may also occur along other coasts when the winds are suitable. The process has been extensively studied along the coast of California where it is not continuous because of the variability of the winds (Sverdrup et al., 1942, p. 725). The speed of coastal upwelling has been variously estimated as 0.6 m/day (McEwen, 1934), 2.25 m/day (Saito, 1951) and 2.7 m/day (Hidaka, 1954). However, since these estimates are theoretical mean values, they may differ significantly from actual instantaneous upwelling rates.

Midocean upwelling, associated with divergence of the surface currents, occurs in a band along the equator in the eastern and central Pacific Ocean (Cromwell, 1953). Observations indicate that the effects of this upwelling extend to 50 meters in the eastern Pacific and to 100–150 meters in the central Pacific (Wooster and Jennings, 1955). Similar but less pronounced upwelling has been observed in the equatorial Atlantic (Bohnecke, 1936).

3. In regions of surface convergence, where sinking waters may fill the depths of the ocean, or may spread at intermediate depths according to their density. In tropical and temperate latitudes such sinking is confined to the surface layer. In such regions mixing in the upper layer may be facilitated but exchange across the pycnocline probably is not, since the sinking water tends to increase the density gradient in the pycnocline.

In high latitudes, on the other hand, sinking waters may reach great depths, and it is in such regions that most of the intermediate and deeper water masses of the ocean are formed. The most extensive and pronounced of these convergences is the Antarctic Convergence which occurs at 50 to 60°S in a band around the entire Antarctic Continent. The cold, low-salinity water which sinks there forms an identifiable water mass, the Antarctic Intermediate Water, which spreads at depths between 800 and 1200 meters in all southern oceans. This water can be identified everywhere in the South Atlantic and extends across the equator as far as 22°N in the North Atlantic (Deacon, 1933; Iselin, 1936).

In the Irminger Sea, between Iceland and Greenland, and in the Labrador Sea, warm high salinity water of the Gulf Stream is partly mixed with cold low-salinity water flowing out of the Arctic Ocean. The resulting mixture may spread in small quantities as Arctic Intermediate Water, or when sufficiently dense may form the deep and bottom water of the North Atlantic (the possibility that the formation of this deep water is not a continuous process is discussed later). Intermediate waters of the North Pacific are probably formed in winter at the convergence between the Kuroshio Extension and the Oyashio (Sverdrup et al, ch. 15). There is apparently no deep or bottom water formed by this process in the Pacific.

4. In regions where the density of surface waters is so increased by evaporation, cooling or freezing, that they sink to intermediate or greater depths. Active formation of Antarctic Bottom Water takes place in the Weddell Sea due to the freezing of high salinity surface waters. In the Mediterranean and Red Seas, bottom water is formed by winter cooling of waters whose salinity has been greatly increased by evaporation. Mediterranean water flows out into the North Atlantic at depths of 1000 to 1500 meters and can readily be identified near Bermuda, 2500 miles from its source.

In summary, exchange between near-surface and deeper waters takes place most commonly (1) in high latitudes, (2) along the equator, and (3) in coastal regions, particularly along the western coasts of continents. Conversely, such exchange is least likely in temperate and tropical latitudes in the vast central regions of the northern and southern oceans.

Exchange between the open sea and coastal areas

In coastal areas or enclosed basins where precipitation exceeds evaporation, there is a seaward surface drift of diluted water and a landward subsurface drift of water derived from the open sea. If radioactive materials were released in such a coastal area, the material which remained in the surface layer would be carried seaward, but the part of the material which mixed or settled to the deeper water would move toward shore and the estuaries of rivers. Conversely, if radioisotopes were liberated in the open sea, some would eventually be carried inshore as a result of the coastal and estuarine circulation.

It is clear that the ultimate distribution in coastal areas of radioactive materials added to the sea would depend on the location of the release, the vertical distribution of radioactivity and density in the area of release, the length of time required for the transport to the coastal area or estuary, and the location of the source sea water which provides for the counter drift. The number of variables involved makes it difficult to discuss the effects in general terms, but it is worthwhile to note that the circulation in coastal areas is rapid, and water bathing the North Atlantic beaches is not uncommonly 90 per cent sea water even off large rivers such as the Hudson and Delaware.

An idea of the lengths of time involved in the coastal circulation can be obtained from the mean age of waters in various parts of the Atlantic seacoast. Such mean ages are computed from the volume of water contained in the region and the estimated transport of water through the region. The waters of the continental shelf from Cape Hatteras to Cape Cod have a mean age of about 2½ years, those of the Bay of Fundy about 3 months, and those of Delaware Bay from the ocean to the height of tide about 3–4 months (Ketchum and Keen, 1953, 1955). The source sea water for all of these circulations is the "slope water" which is formed between the Gulf Stream and the edge of the continental shelf.

A few data are available for confined basins and seas from which estimates of the mean age of the water can be derived. In most cases, however, the sources of water entering into the circulation are uncertain, and it should be emphasized that in all cases some of the waters within the basin will be older or younger than the mean age.

The source waters of the Florida Current are funnelled through the Caribbean Sea. The mass transport is 26 million cubic meters a second (Sverdrup et al., 1942, p. 638), so that this current carries annually a volume of water equivalent to one-sixth of the total volume of the Caribbean. However, there is evidence that the renewal of the deep water of the Caribbean proceeds at a much slower rate than the six year mean age that this ratio implies. Worthington (1955) has calculated, on the basis of loss of oxygen from this deep water during the last 30 years, that the age of the deep water in the various parts of the Caribbean may range from 93–142 years. The mean age of the waters above 2000 meters would be reduced to about 5 years if the deepest ⅕ of the volume of the basin is isolated from the present circulation.

The same current passes through the Yucatan channel into the Gulf of Mexico, before emerging as the Florida Current. No estimate of the mean age of the waters of the Gulf of Mexico is possible, however, since the current data in the Gulf indicate an anticyclonic eddy in the western portion, and suggest that the waters of the Gulf of Mexico are drawn into the Florida Current to only a slight extent (Dietrich, 1939, Sverdrup et al., 1942, p. 642).

The Black Sea probably contains the most isolated and the oldest deep water to be found anywhere in the oceans. Precipitation and runoff exceed evaporation, and the surface waters are dilute (salinities less than 18 per cent) and isolated from the deep water by an intense density gradient. The deep waters are anaerobic; hydrogen sulfide reaches large concentrations below about 200 meters. The sill at the Bosporus is only 90 meters below the surface so that this deeper water is isolated from the more rapid surface circulation. The inflow of sea water is so small that it would take about 2500 years to replace the deep water in the basin (Sverdrup et al., 1942, p. 651). The mean replacement time for the surface layers to a depth of 200 meters is equivalent to about 200 years. Gololobov (1949) has computed the mean age of the deep water on the basis of the annual contribution of phosphorus in the river inflow and the quantity accumulated in the depths. This computation indicates an accumulation time of 5600 years.

The Arctic Basin receives its major inflow north of Scotland and a much smaller inflow through the Bering Strait. Additional sources are from the river runoff and excess of precipitation over evaporation. The outflow is primarily through the Denmark Strait (Sverdrup et al., 1942, p. 655). These flows would provide a volume equal to that of the Arctic Ocean in about 160 years. The Arctic is also stratified because of the addition of fresh water from rivers and melting ice, and it is not known how isolated some of the waters in the deeper basins may be. However, recent analyses have shown that the deeper water in the Arctic Ocean is far from anaerobic, so that it seems unlikely that this water can be considered as isolated from the circulation.

The Mediterranean is a basin in which evaporation exceeds precipitation and runoff. Through the Strait of Gibralter there is an inflow of oceanic surface water and a subsurface outflow of high salinity Mediterranean water. The exchange is sufficiently rapid to replace the entire Mediterranean in about 75 years (Sverdrup et al., 1942, p. 647). The Mediterranean is divided into eastern and western basins by a 500-meter sill between Sicily and Tunisia, and it is not know to what extent the deep waters of these basins are involved in the over-all exchange.

Deep circulation

Most of our present knowledge of the intermediate and deep circulation (see Sverdrup et al., 1942, ch. 15) has been obtained indirectly from the observed distribution of properties. The general uniformity of temperature and dissolved substances in deep water suggests that deep currents are very slow, perhaps at most a few centimeters per second. But deep currents cannot be computed by the geostrophic method because only relative velocities can be thus obtained. Furthermore, small errors in the measurement of salinity or temperature produce uncertainties in velocity of the same magnitude as the currents being computed. The direction of movement in the deep and bottom water has been deduced from the observed distribution of properties such as salinity and potential temperature, but little can be learned about current speeds from such observations.

Existing direct measurements of subsurface currents have been summarized by Bowden (1954). Such measurements have been made since the time of the CHALLENGER Expedition (1873–76), but because of practical difficulties (such as the problem in the open sea of referring observations to a fixed frame of reference) they have taught us little about the deep oceanic circulation. The few successful measurements at depths greater than 1000 meters reported by Bowden showed mean speeds ranging from "negligible" to about 13 cm/sec. At nearly all stations and depths at which current measurements have been made, semidiurnal tidal currents of the order of 10 cm/sec. have been recorded.

Recently measurements of subsurface currents have been made in the North Atlantic by tracking for three days a neutral-buoyant float stabilized at a given depth (Swallow, 1955 and unpublished). These measurements show small resultant speeds (1.7 to 9.1 cm/sec or 0.8 to 4.2 miles/day at depths from 600 to 1900 meters), tidal components of about 10 cm/sec, and in two successive three-day measurements at 1900 meters, a change in direction of 124°. Thus it seems likely that motion below the pycnocline is characterized by more variation, periodic or otherwise, than previously supposed and indeed that the mean drift may represent only a small part of the total motion.

Little is known about the nature and extent of lateral and vertical mixing in the deep sea. It is generally believed, however, that flow and mixing take place along surfaces of constant potential density (isentropic surfaces) and that below the upper layer vertical mixing is very slow except near coastlines and areas where upwelling may occur (Montgomery, 1938). An observation supporting this belief was reported by Revelle, et al. (1955). Introduction of mixed fission products below the pycnocline led to the formation of a lamina of high radioactivity about one meter thick and 100 or more square kilometers in area. The radioactive water apparently spread out along an isentropic surface and resisted destruction by vertical mixing for at least three days.

Age of intermediate and deep waters

It is generally accepted that intermediate and deep waters in most parts of the oceans acquired their characteristics while at or near the surface. Thus the low temperature and relatively high oxygen content of deep water can only be explained by assuming an exchange between deep and surface waters. The problem of the disposal of radioactive wastes in the deep sea has stimulated the oceanographer's natural curiosity as to the rate of this exchange.

The North Atlantic receives surface waters from the South Atlantic and loses deep water to the South Atlantic. Assuming a surface flow from the South to the North Atlantic of 6 million cubic meters per second (Sverdrup et al., 1942, p. 685), and considering only the upper kilometer of the North Atlantic to be affected, the mean replacement time is about 140 years. The gyral in the North Atlantic, which includes the Gulf Stream, carries about ten times the volume of water exchanged between the South and North Atlantic, so that the mean circulation time is only about one-tenth the replacement time.

This surface exchange between the North and South Atlantic is balanced by a deep current from North to South. The mean displacement time for the deep water of the North Atlantic (2000–4000 meters) is calculated as about 250 years. This time is in reasonable agreement with more recent estimates of the age of the deep water discussed below.

Between these surface and deep layers are the intermediate waters which appear to circulate even more rapidly. Deacon (1933) calculated rapid rates of northward flow of the Antarctic intermediate water in the South Atlantic, based upon alternate maxima and minima in the concentrations of oxygen in the oxygen minimum layer. These were interpreted as representing annual cycles when the waters were formed at the surface. He estimated a transit time of about 4½ years between the Antarctic convergence and the equator. Seiwell (1934) has similarly computed rapid flows and a mean transport time of 7–8 years for the drift of the oxygen minimum layer of the North Atlantic Ocean. Deacon's and Seiwell's interpretations have been questioned (see Riley, 1951, p. 77) on various grounds. However, their rates of flow agree with direct current measurements at comparable depths (see earlier) which also indicate rapid rates of circulation.

The deep outflow from the Mediterranean sinks from sill depth to 1000–1500 meters in the North Atlantic Ocean. This water, although much diluted by Atlantic water, is characterized by relatively high salinity and temperature, and spreads out in a sheet which may be identified in most of the temperate North Atlantic, and some spreads into the South Atlantic. It can be readily identified near Bermuda, 2500 miles from its source. Iselin (1936) computed that sufficient excess salt would be produced by the Mediterranean outflow to produce the observed anomaly in 12–15 years. He pointed out that the actual replacement would be more rapid because he neglected admixture of Atlantic water in the immediate vicinity of the Straits of Gibraltar. Defant (1955) has evaluated the mixing processes involved in dissipating the Mediterranean water within the Atlantic Ocean, and has concluded that the total accumulation in the Atlantic Ocean represents the contribution resulting from six years of flow through the Straits of Gibraltar. The rapid dissipation of this large water mass at mid depths suggests a more rapid circulation than had been generally accepted for intermediate waters.

During recent years other lines of investigation have led to the belief that the overturn of water in the ocean basin takes place in less than a thousand years and probably in 200 years or less. Evidence supporting this belief follows. (Carbon-14 and carbon dioxide exchange estimations are discussed in greater detail by Craig elsewhere in this report.)

1. *Heat flow measurements:* Measurements reported by Revelle and Maxwell (1952) have shown a heat flow through the floor of the Pacific Ocean of 1.2×10^{-6} calories per square centimeter per second, or 38 calories per square centimeter per year. If not dissipated by circulation and mixing, this heat flow would lead to warming of the deep and bottom water during its passage from the Antarctic to the equator. From considerations of meridional circulation, observed temperature gradients and mixing in the deep sea, Revelle and Maxwell estimate that the deep water is replenished in less than 1000 years.

2. *Secular change of oxygen:* Worthington (1954) has shown that the North Atlantic Deep Water has suffered a loss of dissolved

oxygen of about 0.3 ml/L over the last twenty years. Assuming a steady rate of attrition he computes that the date at which this water was saturated, presumably while at the surface, was about 1810. A further study (Worthington, 1955) suggests that the Caribbean Deep Water was formed at the same time. Thus it seems possible that formation of the North Atlantic Deep Water, which composes about half of the contents of the Atlantic, is not continuous but sporadic.

3. *Carbon-14 dating:* In recent years the techniques of carbon-14 age determination have been applied to deep sea water samples. The most reliable measurements (Rubin, unpublished), of samples from east of the Lesser Antilles, show the carbon at 1750 meters to be about 200 years older than the surface carbon.

Present estimates of the age of deep waters are based primarily on measurements in the North Atlantic and on geochemical calculations for the entire world ocean. That the deep circulation of the Pacific is significantly slower than that of the Atlantic is suggested by the apparent absence of regions of deep and bottom water formation in the Pacific and the relatively high nutrient salt content and low dissolved oxygen content of deep Pacific waters. In order to determine whether the deep waters of the Pacific would provide a longer period of isolation for radioactive wastes than elsewhere, deep Pacific oceanographic data must be carefully scrutinized.

REFERENCES

BOHNECKE, G. 1936. Atlas: Temperatur, Salzgehalt und Dichte an der Oberflache des Atlantischen Ozeans. Deutsche Atlantische Exped. *Meteor,* 1925–27, Wiss. Erg. **5**: vii+76 pp.

BOWDEN, K. F. 1954. The direct measurement of subsurface currents in the oceans. *Deep-Sea Res.* **2**:33–47.

CROMWELL, T. 1953. Circulation in a meridional plane in the central equatorial Pacific. *J. Marine Res.* **12**:196–213.

DEACON, G. E. R. 1933. A general account of the hydrology of the South Atlantic Ocean. *Discovery Rep.* **7**:171–238.

DEFANT, A. 1955. Die Ausbreitung des Mittelmeerwassers im Nordatlantischen Ozean. Pap. Mar. Biol. and Oceanogr., *Deep-Sea Res.,* suppl. to **3**:465–470.

DEUTSCHEN SEEWARTE. 1942. Weltkarte zur Ubersicht der Meeresstromungen. Deutschen Seewarte No. 2802.

DIETRICH, G. 1939. Das Amerikansiche Mittelmeer. Gesellsch. Erdkunde zu Berlin, Zeitschr., 108–130.

ECKART, C. 1948. An analysis of the stirring and mixing processes in incompressible fluids. *J. Marine Res.* **7**:265–275.

FRANCIS, J. R. D., and H. STOMMEL. 1953. How much does a gale mix the surface layers of the ocean. *Quart. J. Roy. Meteorol. Soc.* **79**:534–536.

FUGLISTER, F. C. 1951. Multiple currents in the Gulf Stream System. *Tellus* **3**(4): 230–233.

GOLOLOBOV, Y. K. 1949. Contribution to the problem of determining the age of the present stage of the Black Sea (in Russian). *Dokl. Akad. Nauk SSSR* **66**:451–454.

HIDAKA, K. 1954. A contribution to the theory of upwelling and coastal currents. *Trans. Am. Geophys. Union* **35**(3):431–444.

ISELIN, C. O'D. 1936. A study of the circulation of the western North Atlantic. *Pap. Phys. Oceanogr. Meteorol.* **4**(4):1–101.

JAPANESE FISHERY AGENCY. 1955. Report on the investigations of the effects of radiation in the Bikini region. Res. Dept., Japanese Fishery Agency, Tokyo, 191 p.

KETCHUM, B. H., and W. L. FORD. 1952. Rate of dispersion in the wake of a barge at sea. *Trans. Am. Geophys. Union* **33** (5):680–684.

KETCHUM, B. H., and D. J. KEEN. 1953. The exchanges of fresh and salt waters in the Bay of Fundy and in Passamaquoddy Bay. *J. Fish. Res. Bd. Can.* **10**:97–124.

1955. The accumulation of river water over the continental shelf between Cape Cod and Chesapeake Bay. Pap. Mar. Biol. and Oceanogr., *Deep-Sea Res.,* suppl. to vol. **3**: 346–357.

KOENUMA, K. 1939. On the hydrography of south-western part of the North Pacific and the Kuroshio. *Kobe Imper. Marine Observ., Memoirs* **7**:41–114.

MCEWEN, G. F. 1934. Rate of upwelling in the region of San Diego computed from serial temperatures. *Fifth Pac. Sci. Congr.*, Toronto **3**:1763.

Miyake, Y., Y. Sugiura, and K. Kameda. 1955. On the distribution of radioactivity in the sea around Bikini Atoll in June, 1954. *Pap. Meteorol. Geophys.*, Tokyo **5**(3, 4):253–362.

Montgomery, R. B. 1938a. Fluctuations in monthly sea level on eastern U. S. coast as related to dynamics of western North Atlantic Ocean. *J. Marine Res.* **1**:165–185.

1938b. Circulation in upper layers of southern North Atlantic deduced with use of isentropic analysis. *Pap. Phys. Oceanogr. Meteorol.* **6**(2):1–55.

Munk, W. H., G. C. Ewing, and R. R. Revelle. 1949. Diffusion in Bikini Lagoon. *Trans. Am. Geophys. Union* **30**(1):59–66.

Revelle, R., and A. E. Maxwell. 1952. Heat flow through the floor on the eastern North Pacific Ocean. *Nature* **170**:199.

Revelle, R., T. R. Folsom, E. D. Goldberg, and J. D. Isaacs. 1955. Nuclear science and oceanography. United Nations International Conference on the Peaceful Uses of Atomic Energy, Geneva, Paper no. 277: 22 pp.

Riley, G. A. 1951. Oxygen, phosphate and nitrate in the Atlantic Ocean. *Bull. Bingham Oceanogr. Coll.* **13**, Art. 1:1–126.

Saito, Y. 1951. On the velocity of the vertical flow in the ocean. *J. Inst. Polytech., Osaka City Univ.* **2**(1) Ser. B.:1–4.

Seiwell, H. R. 1934. The distribution of oxygen in the western basin of the North Atlantic. *Pap. Phys. Oceanogr. Meteorol.* **3**(1):1–86.

Seligman, H. 1955. The discharge of radioactive waste products into the Irish Sea. Part 1. First experiments for the study of movement and dilution of released dye in the sea. Proceedings of the International Conference on the Peaceful Uses of Atomic Energy, Geneva. Paper **9**:701–711.

Sverdrup, H. U., M. W. Johnson, and R. H. Fleming. 1942. The oceans, their physics, chemistry and general biology. Prentice-Hall, N. Y., x+1087 pp.

Swallow, J. C. 1955. A neutral-buoyancy float for measuring deep currents. *Deep-Sea Res.* **3**:74–81.

U. S. Atomic Energy Commission. 1956. Operation Troll. U. S. Atomic Energy Commission, New York Operations Office, NYO 4656, Ed. by J. H. Harley, 37 pp.

U. S. Navy Hydrographic Office. 1947a. Atlas of surface currents, north Atlantic Ocean. H. O. Pub. 571, First Ed., reprinted 1947.

1947b. Atlas of surface currents, northeastern Pacific Ocean. H. O. Pub. 570, First Ed.

1950. Atlas of surface currents, northwestern Pacific Ocean. H. O. Pub. 569, First Ed., reprinted 1950.

Von Arx, W. S., D. F. Bumpus, and W. S. Richardson. 1955. On the fine structure of the Gulf Stream front. *Deep-Sea Res.* **3**:46–65.

Wooster, W. S., and F. Jennings. 1955. Exploratory oceanographic observations in the eastern tropical Pacific, January to March, 1953. *Calif. Fish and Game* **41**:79–90.

Worthington, L. V. 1954. A preliminary note on the time scale in North Atlantic circulation. *Deep-Sea Res.* **1**:244–251.

1955. A new theory of Caribbean bottom-water formation. *Deep-Sea Res.* **3**:82–87.

Contribution No. 871

Reprinted from

THE EFFECTS OF ATOMIC RADIATION ON
OCEANOGRAPHY AND FISHERIES

PUBLICATION NO. 551
NATIONAL ACADEMY OF SCIENCES—
NATIONAL RESEARCH COUNCIL
1957

THE EFFECTS OF THE ECOLOGICAL SYSTEM ON THE TRANSPORT OF ELEMENTS IN THE SEA

CHAPTER 5

THE EFFECTS OF THE ECOLOGICAL SYSTEM ON THE TRANSPORT OF ELEMENTS IN THE SEA[1]

BOSTWICK H. KETCHUM, *Woods Hole Oceanographic Institution,* Woods Hole, Massachusetts

SOME elements may be profoundly influenced by the biological cycle and their resulting distribution in the sea may be quite different from the distribution of elements that are affected only by the circulation of the water. Numerous examples of the modification of distribution by biological activities could be given but it may suffice to review briefly the vertical distribution of phosphorus in the ocean.

The photosynthetic fixation of carbon is limited to the surface hundred meters or less of the sea by the penetration of light, and the plant nutrients, including phosphorus, are assimilated there. The surface concentration of these elements may be reduced to virtually zero. Below the photosynthetic zone, the concentrations of these nutrients increase, reaching maximum values at depths of 200 to 1000 meters, the actual depth depending upon location and the oceanic circulation. These maximum concentrations are produced by two processes. The water at intermediate depths is formed by cooling at high latitudes in the ocean, where it sinks and spreads out. At the time of sinking, it contains some inorganic phosphorus and organic matter which is decomposed, liberating the plant nutrients and decreasing the oxygen content. Additions to the organic matter from the surface waters occur everywhere, increasing the nutrient maximum concentration and decreasing the oxygen minimum. Below the nutrient maximum-oxygen minimum layer the concentration of phosphorus decreases again reaching values which are generally constant and uniform from a depth of about 1500 meters to the bottom (Redfield, 1942).

The general patterns of distribution of the elements important in plankton growth on an ocean-wide scale are thus quite different from the pattern of distribution of the major elements. The processes which must be considered in order to evaluate biological effects on the ultimate distribution of radioisotope wastes or contaminants in the sea include (1) the assimilation or adsorption of the elements by the biological populations, (2) the effects of gravity, (3) vertical migrations, (4) horizontal migrations, and (5) the effects of stationary populations in flowing systems.

It has been shown in another section of this report that biological populations may concentrate by several orders of magnitude various elements and their radioisotopes. To evaluate the possible significance of this in the oceans, it is necessary to determine the quantity of living material present (the biomass) and the rate of production of the populations of the ecological system. The biomass, when combined with the known concentration factor, will indicate how much of an element in the water may be combined in the living organisms. The most active concentration of elements may occur during the rapid growth of populations; consequently it is also essential to know the rate of production of the various populations involved. A few data on both the biomass and the rate of production of various populations in the sea are given in Tables 1 and 2.

The biomass figures indicate that concentration factors of 12,500 or more would be required, *under static conditions,* to incorporate half of an element in a cubic meter of water within the ecological system even in the high concentrations of living material found in red-tide blooms. However, the biological populations are not static; those movements which are independent of the motion of the water can, by repetition, transport larger proportions of elements than is indicated by static equilibrium conditions. The productivity values in Table 2 indicate that several times the standing crop of phytoplankton is produced annually. Both

---

[1] Contribution No. 871 from the Woods Hole Oceanographic Institution.

TABLE 1 ESTIMATES OF BIOMASS OF MARINE POPULATIONS. ALL VALUES HAVE BEEN CONVERTED TO VOLUME (WET WEIGHT) PER CUBIC METER (PARTS PER MILLION)

Population	Location and character	Source	cc/m^3
Phytoplankton	Maximum Atlantic	a	10
	Maximum Pacific	a	25
	Red Tide Blooms	b	41
	Long Island Sound	c	18.2
	Coastal Water	c	1.2
	Sargasso Sea	c	0.3
Zooplankton	Gulf of Maine	d	0.08 — 1.0
	Coastal Water	e	0.08 — 0.8
	Sargasso Sea	f,e	0.006 — 0.09
	N. African Upwelling	f	1.0
	Eastern North Pacific	g	0.042
	Eastern Tropical Pacific	g	0.055
	Peru Current	g	0.124

a. Complete utilization of maximum phosphorus concentrations; conversion $P = 0.5$ per cent of wet weight.
b. Ketchum and Keen, 1948, 17–21, Table 1. Conversion as in a.
c. Riley, Stommel and Bumpus, 1949, Table VI; conversion $C = 10$ per cent wet weight.
d. Redfield, 1941, drained volumes, vertical tows, assumed mean depth 100 meters.
e. Riley, et al., 1949, Table V, displacement weight.
f. Unpublished data, W. H. O. I., surface tows at night, drained volumes.
g. Unpublished data, S. I. O., oblique tows 200–300 meters to surface, wet plankton volumes.

the depth of the photosysthetic zone and the production rate at various depths, are variable, thus the values for production cannot be reduced without excess over-simplification to a volume basis which would permit direct comparison with Table 1. However, Riley's (1941) maximum value for the standing crop of phytoplankton in Long Island Sound, 1.82 gC/m^3, showed a production of 0.187 $gC/m^3/day$ and the annual production was twenty times as great as the maximum standing crop observed at any one time. Estimates of the growth of zooplankton populations have given values ranging up to 5 per cent of the standing crop per day.

TABLE 2 ESTIMATES OF THE PRODUCTIVITY OF MARINE PHYTOPLANKTON POPULATIONS

Location and character	Source	$gC/m^2/$ year	$cc/m^2/$ year[1]
Sargasso Sea (Atlantic)	a	18	180
Coastal Areas (Atlantic)	a	1100	11000
Open Ocean (Pacific)	a	50	500
Equatorial Divergence (Pacific)	a	140	1400
Coastal Areas (Pacific)	a	200	2000
Oceanic Mean	a	55	550
Long Island Sound			
min.	b	95	950
max.		1000	10000
N. Atlantic 3°-13°N.	b	278	2780
Oceanic Mean	c	340 ± 220	1200–5600

a. Steemann Nielsen (1954). Carbon-14 method. This is given as gross production, but Ryther (1954) suggests that it may be net (gross minus respiration) production in nutrient poor areas.
b. Riley (1941). Gross production, oxygen method.
c. Riley (1944).

[1] Conversion assuming one gram of carbon = 10 cc of wet plankton.

It is a truism in ecology that the total quantity of living material which can be produced decreases as the trophic level of the organisms considered increases. In some ecological systems the biomass reflects this progression, i.e., at any one time there will be a larger standing crop of plants than of herbivores and the standing crop becomes progressively smaller as one goes through the various higher steps of the food web. In the oceans, however, this is not necessarily true. It is common to find rather high concentrations of the herbivorous zooplankton when phytoplankton are scarce. Large populations of herbivores will quickly decimate the plants on which they feed. A balance may be maintained as a result of the different lengths of the life cycle of the various parts of the food web. A population of phytoplankton can double in a period of time ranging from hours to days, whereas the life cycles of zooplankton are more commonly measured in terms of weeks or months and the life cycles of the higher elements of the food web, such as fish, are measured in terms of seasons or years. A comparatively small population of phytoplankton doubling rapidly can provide the energy and nutrients of an equivalent or even larger animal population which is increasing more slowly.

The size of various populations and their rate of production in the English Channel has been evaluated by Harvey (1950) and his results are given in Table 3. These illustrate the above conclusions, since the average biomass of animals exceed that of the plants, but the rate of production of the plants exceeds that of the animal populations.

TABLE 3 AVERAGE QUANTITY, THROUGHOUT THE YEAR, OF PLANTS AND ANIMALS BELOW UNIT AREA OF SEA SURFACE IN THE ENGLISH CHANNEL [1]

	Dry wt of organic matter	
Organism	Standing crop g./m^2	Production g./m^2/day
Phytoplankton	4.00	0.4–0.5
Zooplankton	1.50	0.1500
Pelagic Fish	1.80	0.0016 [2]
Bacteria	0.04	—
Demersal Fish	1.25	0.0010
Bottom Fauna	17.00	0.0300 [3]
Bottom Bacteria	0.10	—

[1] From Harvey (1950), depth equals 70 meters.

[2] Based on estimated mortality of 30 per cent per annum.

[3] Based on estimated mortality of 60 per cent per annum.

The plankton organisms in the open sea provide by far the largest quantity of living material and by even more the largest organic absorptive surface. Those radioisotopes which are adsorbed will become bound to the organisms, and they are as subject to the effects of gravitation and migration as if they had been assimilated and utilized.

Gravity affects the organisms in a population and can thus modify the distribution of elements which become incorporated in the biological cycle. Ultimately only two fates await most of the plankton which grows in the surface layers. It may be eaten by the herbivores or it may sink out of the illuminated zone and decompose at greater depths. If the plankton is eaten by a herbivore, a proportion of the organic matter is incorporated into the herbivore body but an even larger proportion is returned to the water as excretion or faecal pellets. The excretions may be present in the water inhabited by the plankton and reused *in situ*. The faecal pellets settle into the deeper water where they decompose. Gravity thus imposes on elements which become incorporated in the biological system a modification of the distribution which would be produced by movements of the water alone, since they tend to accumulate at some intermediate depth in the water column, or on the bottom.

One of the unsolved problems of marine biology is the definition of the proportion of organic matter which is decomposed by the time the particulate material sinks to various depths. This problem must be solved before an evaluation of the biological effects on the distribution of radioisotope contamination of the seas can be made. It may be worthwhile to summarize some of the present thinking on this problem.

In the first place, everywhere that samples have been taken in the deep sea, living organisms have been found. Since we know of no mechanism other than photosynthesis at the surface which can provide the organic material necessary to support these populations, it is clear that some of the surface produced material must reach all depths of the ocean. It may be argued by some that the bacterial chemosynthetic processes are a source of fixed carbon which has not been considered, but the conditions in the deep sea are not suitable for the formation of organic matter by any of these processes.

The presence of the nutrient maximum-oxygen minimum layer at intermediate depths in the sea has led to the conclusion that most of the organic matter formed at the surface must be oxidized by the time it has sunk to a depth of 1000 meters (Redfield, 1942). Analyses of organic phosphorus in the equatorial Atlantic Ocean showed considerable amounts in the waters above 1000 meters, but none at greater depths (Ketchum, Corwin, and Keen, 1955). There is no present evaluation of the quantity of organic carbon which can sink to greater depths, nor is it possible to evaluate whether this quantity would be sufficient to support the known populations of archibenthic organisms. These two extremes thus define the dilemma. Namely that some organic matter must reach the great depths, but, at the same time, most of the decomposition appears to occur above a depth of 1000 meters.

The secular change of oxygen in the deep sea which has been found by Worthington (1954) in the North Atlantic, provides one means of computing the total quantity of organic matter required. Worthington observed a decrease of 0.3 milliliters of oxygen per liter in thirty years at depths between 2500 meters and the bottom. In the Atlantic Ocean this corresponds to an average thickness of 1500 meters and the total quantity of organic matter required to produce this change in oxygen is equivalent to the decomposition of 8 grams of organic carbon per square meter per year in this layer. This quantity of organic matter is nearly 15 per cent of the annual mean production according to Steemann Nielsen (1954) and from 1.4 to 7 per cent of the mean suggested by Riley (1944). Part of the secular change in oxygen may have been produced by eddy diffusion into the oxygen minimum layer, which would reduce the quantity of organic carbon reaching greater depths.

The effects of gravity may be accentuated when the surface currents are opposed to the currents in the deeper layers. This type of circulation pattern is very common in estuaries, on continental shelves, and in those areas where offshore winds produce upwelling of the deeper waters. In all of these cases the nutrient rich deep water is carried inshore in a sub-surface drift, and brought to the surface by upwelling or vertical mixing. The nutrients are assimilated by the plankton in the surface layers and are carried offshore in the surface current. When the organisms sink, they again reach the onshore sub-surface current where they decompose liberating more nutrients into water which is already relatively rich. Thus the elements involved in biological processes follow a different cycle from the circulation of the water and this cycle leads to an accumulation of elements greater than can be found in either of the source waters (Ström, 1936; Hulburt, In press).

Nutrient elements are commonly concentrated by this type of mechanism in fjords. Where the deepest water is relatively stagnant and isolated from the intermediate and surface layers, considerable concentrations of organic derivatives can be developed. In the Norwegian fjords with a relatively shallow sill, for example, anaerobic conditions may be produced in the bottom water and the nutrients are five to ten times as concentrated as in either of the source waters (Ström, 1936). In the Black Sea the deep water is isolated from the surface by a strong density gradient and its average age has been estimated at 2500–5000 years (Sverdrup, Johnson and Fleming, 1942, p. 651). Very large accumulations of organic derivatives are found in this deep water. (Gololobov, 1949.)

Opposed currents can, however, work in the opposite way and lead to a decrease in the concentration of elements involved in the biological cycle. The classic example of this type of circulation is the Mediterranean, where the nutrients available for plant growth are less than half of the concentration available in the adjacent parts of the Atlantic. In the Mediterranean the supply comes from the surface waters of the North Atlantic which are already impoverished by plant growth. Since evaporation exceeds precipitation in the Mediterranean the water becomes more saline, sinks and is lost as a deep outflow over the sill at Gibraltar (Thomsen, 1931). The accumulation of elements in sinking organisms transfers these elements from the inflowing surface water to the outflowing deep water. They are eventually lost from the Mediterranean. A similar process apparently applies to the entire North Atlantic. There is a large inflow of South Atlantic surface water which contains low concentrations of elements involved in the ecological cycle. The outflow from the North Atlantic required to balance the water budget occurs at depths and this water contains considerable quantities of the elements which had been returned to the water (Sverdrup et al., 1942).

In summary the various peculiarities of distribution which can be attributed to gravitational effects on the ecological cycle are therefore (1) the accumulation of elements at intermediate depths as a result of sinking and decomposition, (2) the concentration of elements in areas of opposed flow where the deep water is brought to the surface by upwelling or vertical mixing and (3) the impoverishment of areas where the supply of water is from the surface and the loss from greater depths.

In addition to the passive gravitational effects on organisms, animal plankton forms exhibit vertical migrations. A considerable literature has developed in this field over the last ten years, but the effects of these vertical migrations on the distribution of elements has not been studied directly and must be inferred from our knowledge of the ecological system.

Historically, a few studies of the vertical migration of zooplankton had been made prior to the war. Great impetus was given these studies when a false bottom was repeatedly observed on echo sounding recorders (Dietz, 1948; Hersey and Moore, 1948). This has been called the scattering layer. Although there is still controversy as to which organisms are the principal scatterers in the sea, it has been established that one or more layers are commonly found which migrate vertically over a depth of as much as 800 meters, being at or near the surface at night and at great depths at mid-day.

No observations of the changes of elements involved in the biological cycle which may be associated with vertical migrations have been made. Most of our analytical techniques are too insensitive to detect the day to day changes which might be expected in biologically active elements if our present evaluation of the density of the populations and their respiration and excretion rates is correct. It is known, however, that direct assimilation of some elements is possible by invertebrate forms and vertical transport of radioisotopes might be expected to result. Indeed, the transport of radioisotopes might prove an excellent tool for the study of vertical migrations if a source were provided at one depth within the range of the migration.

Ecologically the following effects might be expected as a result of vertical migration. The zooplankton are certainly in the area of the most dense concentration of their food, the phytoplankton, when they are at the surface at night. During the hours of darkness they may therefore be expected to consume the living material in the water, and some of this, at least, would be excreted or passed as faecal pellets at depth in the day time. This process would thus augment the effects of gravity on those elements incorporated in the biological system. There is also evidence that the zooplankton can assimilate dissolved elements from sea water. If elements were assimilated at depth they might be excreted or exchanged near the surface and thus directly modify the vertical distribution in the sea.

It should not be neglected that larger organisms can certainly migrate vertically over greater distances than we have discussed above. Certainly whales, tuna and sharks, and presumably the smaller forms upon which they feed are known to go to considerable depths in the ocean. Quantitatively, of course, these members high on the food chain are proportionally small compared to the plankton organisms. However, their effects on vertical distribution of materials may not be negligible over periods of several decades.

Horizontal migrations of organisms may also result in the transport of material involved in the biological cycle and are also independent of the currents of the ocean. Here again man does not know enough to assess these quantitatively, but their possible effects should not be ignored.

The migrations of pelagic fishes may be of considerable interest in this regard. The salmon for example reach maturity in the open sea, then migrate in enormous numbers to coastal areas to breed. Such a horizontal migration could transport radioisotopes, since the salmon could accumulate materials from large volumes of the sea and, by their migration, concentrate them many thousand-fold in the rivers and estuaries.

Many other fish also exhibit extensive migrations. Even though some of these do not enter the rivers to breed, they may enter the areas where they are available for commercial capture, thus becoming some of the food supply of the nation. Unfortunately, in many of these species we do not know the complete life history and most of our information concerning their occurrences and migrations is obtained only during the period of year when they are caught. The Atlantic tuna, for example, are caught in the early spring in the Caribbean and off the Bahama Banks. As spring and summer progresses they migrate northward along the coast, and maximum catches occur in New England in late summer and early fall. The winter habitat and breeding area of these large and important food fish is largely unknown, though preliminary data suggest that they practically circumnavigate the North Atlantic Ocean (Mather and Day, 1954). Similarly the mackerel catches are first concentrated in the southern part of the Atlantic coastline in the late spring and early summer. The large catches off New England occur in August and September. This species breeds on the Atlantic continental shelf during its summer northward migration (Sette, 1943, 1950).

Additional examples of mass migrations into the coastal regions are found in the Pacific sardine and the North Atlantic herring. In all of these cases materials assimilated at sea may be concentrated in inshore waters as a result of these migrations, which may cover thousands of miles. Such migrations certainly make it difficult to select any area in the oceans as being sufficiently remote and isolated from human interest to insure that the discharge of radioisotope wastes might not be transported into those areas man is most interested in protecting. It should, however, be pointed out that this is a quantitative problem, and our knowledge is not sufficiently detailed to permit evaluating the quantity of radioisotopes which could be transported in mass migrations of fish.

In addition to the movements of organisms which are independent of the circulation of the water resulting from gravity and vertical and horizontal migrations, many populations remain stationary in a flowing stream of water. The organism is thus able to concentrate remarkably the constituents of the water masses which pass by. Harvey (1950) estimated, for example, that the bottom population was nearly 70 per cent of the total population at a station in the English Channel (see Table 3).

The most apparent of these stationary populations are those which live on or in the bottom. Much of our knowledge concerning such populations is confined to those which occupy shallow waters such as the clams, the oysters, and other economically important species. Stationary populations may be exposed to and feed on populations in many cubic miles of sea water during the course of an active growing season.

Although most of our knowledge is confined to shallow water forms, it is known that such stationary populations are a main source of food for many bottom-feeding commercial fishes. The haddock and cod fisheries of New England and the halibut fishery of the Pacific Coast, for example, are ground fisheries. These important species of fish feed on sedentary or stationary populations. Even in the great depths of the ocean such sedentary populations have been found wherever man has had the opportunity to search for them. Although little is known of their location in the food web and dynamics of the ocean, it seems certain that they play a part.

The importance of such stationary populations is that they can concentrate enormously the density of organic matter in those locations suitable for their survival. In unique situations they may concentrate by several orders of magnitude the available organic matter in the ocean.

Less obvious stationary populations are planktonic and unattached, and one would expect them to be transported away from a given area by the currents. It has been found in some cases, however, that in spite of horizontal currents of considerable velocity, the centers of some planktonic populations can remain relatively stationary. Presumably there is a constant drain from these populations as a result of the currents which carry away some of the organisms, but the rate of production of the population is sufficient to maintain the population in spite of this drain. Examples of such populations are to be found in almost all estuaries which tend to maintain endemic species different from those commonly found in the adjacent sea (Ketchum, 1954; Bousfield, 1955). Even in the open ocean similar stationary populations have been found (Redfield, 1939, 1940, 1941; Johnson and co-workers, unpublished observations). It is necessary to have a rate of reproduction of the population as a whole sufficient to balance the circulatory drain. This rapid rate of reproduction will, of course, lead to the concentration of materials from the water mass moving past.

A special case of biological concentration of materials which probably involves several of the above phenomena is found in the "red tide." It has been shown that the concentration of total phosphorus in the colored water of these dinoflagellate blooms is commonly ten to twenty times as great as the concentration which can be found in any of the adjacent waters (Ketchum and Keen, 1948). Most of this phosphorus is combined in the living cells, and very little is present in the inorganic form. One of the explanations for these high concentrations involves the accumulation of the organisms at the surface because of their buoyancy, and the subsequent further concentration of the surface film by convergence of water masses (Ryther, 1955). In the red tides which have occurred in recent years off the west coast of Florida, the organism involved, *Gymnodinium brevis,* produces a toxin which is lethal to the fish and other organisms in the water, and vast numbers of fish have been killed as a result of these dinoflagellate blooms (Gunter, et al., 1948). Recent evidence indicates that the organisms are almost always present in the water (Collier, A., unpublished), but in such low concentrations that there is no marked fish mortality. It is only after the concentration produced by the biological and hydrographic system that mortalities result.

In evaluating the discharge of radioisotope wastes at sea, the factor of safety must be sufficient so that safe levels of radioactivity can be maintained, even after the various mechanisms of biological accumulation.

REFERENCES

Bousfield, E. L. 1955. Ecological control of the occurrence of barnacles in the Miramichi Estuary. *Nat. Mus. Canada Bull.* No. 137, Biol. Ser. No. 46, pp. 1–69.

Dietz, R. S. 1948. Deep scattering layer in the Pacific and Antarctic oceans. *J. Mar. Res.* **7**:430–442.

Gololobov, Y. K. 1949. (Contribution to the problem of determining the age of the present stage of the Black Sea) in Russian. *Dokl. Akad. Nauk SSSR.* **66**:451–454.

Gunter, G., R. H. Williams, C. C. Davis, and F. G. Walton Smith. 1948. Catastrophic mass mortality of marine animals and coincident phytoplankton bloom on the west coast of Florida, November, 1946 to August, 1947. *Ecol. Monogr.* **18**:309–324.

Harvey, H. W. 1950. On the production of living organic matter in the sea off Plymouth. *J. Mar. Biol. Assoc. U. K.* **29**: 97–137.

Hersey, J. B., and H. B. Moore. 1948. Progress report on scattering layer observations in the Atlantic Ocean. *Trans. Amer. Geophys. Union.* **29**:341–354.

Hulburt, E. M. In press. The distribution of phosphorus in Great Pond, Massachusetts. (Submitted to *J. Mar. Res.*)

Ketchum, B. H. 1954. Relation between circulation and planktonic populations in estuaries. *Ecol.* **35**:191–200.

Ketchum, B. H., N. Corwin, and D. J. Keen. 1955. The significance of organic phosphorus determinations in ocean waters. *Deep-Sea Res.* **2**:172–181.

Ketchum, B. H., and D. J. Keen. 1948. Unusual phosphorus concentrations in the Florida "red tide" sea water. *J. Mar. Res.* **7**:17–21.

Mather, F. J., III, and C. G. Day. 1954. Observations of pelagic fishes of the tropical Atlantic. *Copeia,* 1954, no. 3:179–188.

Redfield, A. C. 1939. The history of a population of *Limacina retroversa* during its drift across the Gulf of Maine. *Biol. Bull.* **76**:26–47.

1941. The effect of the circulation of water on the distribution of the calanoid community in the Gulf of Maine. *Biol. Bull.* **80**:86–110.

1942. The processes determining the concentration of oxygen, phosphate and other organic derivatives within the depths of the Atlantic Ocean. *Pap. Phy. Oceanog. Meteorol.* **9**:1–22.

Redfield, A. C., and A. Beale. 1940. Factors determining the populations of chaetognaths in the Gulf of Maine. *Biol. Bull.* **79**:459–487.

Riley, G. A. 1941. Plankton studies. III. Long Island Sound. *Bingham Oceanog. Coll. Bull.* **7**(3):1–93.

1941a. Plankton studies. V. Regional summary. *J. Mar. Res.* **4**:162–171.

1944. The carbon metabolism and photosynthetic efficiency of the earth as a whole. *Amer. Sci.* **32**:129–134.

Riley, G. A., H. Stommel, and D. F. Bumpus. 1949. Quantitative ecology of the plankton of the western North Atlantic. *Bingham Oceanog. Coll. Bull.* **12**:1–169.

Ryther, J. H. 1954. The ratio of photosynthesis to respiration in marine plankton algae. *Deep-Sea Res.* **2**:134–139.

1955. Ecology of autotrophic marine dinoflagellates with reference to red water conditions. Luminescence of Biological Systems: 387–414.

Sette, O. E. 1943. Biology of the Atlantic mackerel (*Scomber scombrus*) of North America. Part I: Early life history. *Fish. Bull.* **38**:149–237.

Sette, O. E. 1950. Biology of the Atlantic mackerel (*Scomber scombrus*) of North America. Part II. Migrations and habits. *Fish. Bull.* **51**:251–358.

STEEMANN NIELSEN, E. 1954. On organic production in the oceans. *J. Con. Internat. Explor. Mer.* **19**:309–328.

STRÖM, K. M. 1936. Land-locked waters. Hydrography and bottom deposits in badly ventilated Norwegian Fjords with remarks upon sedimentation under anaerobic conditions. *Norske Vidensk. Akad. 1. Mat. Naturv. Klasse No. 7,* 85 pp., Oslo.

SVERDRUP, H. U., M. W. JOHNSON, and R. H. FLEMING. 1942. The Oceans, their physics, chemistry and general biology. x+1087 pp., Prentice-Hall, Inc., New York.

THOMSEN, H. 1931. Nitrate and phosphate contents of Mediterranean water. *Danish Oceanog. Exped. 1908–1910.* **3**:14 pp.

WORTHINGTON, L. V. 1954. A preliminary note on the time scales in North Atlantic circulation. *Deep-Sea Res.* **1**:244–251.

Contribution No. 875

Särtryck ur Tellus nr 2, 1957

SVENSKA GEOFYSISKA FÖRENINGEN

VOLUME 9, NUMBER 2 Tellus MAY 1957

A QUARTERLY JOURNAL OF GEOPHYSICS

Bubble Formation and Modification in the Sea and its Meteorological Significance

By D. C. BLANCHARD and A. H. WOODCOCK[1]

Woods Hole Oceanographic Institution

(Manuscript received November 2, 1956)

Abstract

It is believed that the vast majority of the airborne salt nuclei arise from bursting bubbles at the air—sea water interface. Four natural mechanisms for the production of these bubbles have been studied. These are whitecaps, rain, snow and supersaturation of the surface waters of the sea due to spring warming. The bubble spectra from whitecaps and snowflakes have been measured and semi-quantitative and qualitative observations have been made on the bubble spectrum produced by raindrops. No evidence of bubble production by spring warming has been obtained.

All of the measurements show that a majority of the bubbles are < 200 microns diameter and, in the case of bubbles from snowflakes, < 50 microns. In the vicinity of a breaking wave the bubble production rate is about 30 $\mathrm{cm}^{-2}\ \mathrm{sec}^{-1}$.

Due to the effects of surface tension in increasing the bubble internal pressure all bubbles < 300 microns will go into solution even at sea water air saturations of 102 percent. Bubbles < 20 microns will go into solution at saturations up to 115 percent! The solution time for small bubbles of about 10 microns is about 10 sec and is not markedly affected by the water saturation percentage.

It is concluded that the effects of the rate of solution of bubbles in sea water can, under some conditions, play a significant role in modifying the initial bubble spectrum. This, in turn, should influence the spectrum of airborne nuclei.

1. Introduction

It seemed evident from the work of WRIGHT (1940) and KÖHLER (1941) that large salt particles were playing an active role in visibility changes in the lower atmosphere and perhaps in cloud formation as well. It was not until the work of WOODCOCK (1949 and 1952) however that the existence of these particles throughout the entire subcloud and cloud layers in marine air was shown. CROZIER and SEELY (1950), TWOMEY (1955), and BYERS (1955) have demonstrated that significant concentrations of these aerosols exist in air masses that had traveled many hundreds of miles over land. A consideration of the potential importance of these particles in the mechanism of rainfall production is, therefore, not limited to clouds over oceanic areas. LUDLAM (1951) and BOWEN (1950) have both shown, on a theoretical basis, that hygroscopic particles of the size of the salt nuclei found in the atmosphere are sufficiently large to grow rapidly into raindrops, by the process of coalescence with smaller cloud droplets. Recently WOODCOCK (1952) and WOODCOCK and BLANCHARD (1955) have compared the raindrop spectrum and the rainwater chlorinity with the salt nuclei spectrum in the sub-cloud layer. These results have suggested that each salt nucleus becomes a rain-

---

[1] Contribution Number 875 from the Woods Hole Oceanographic Institution. This paper represents the results of research carried out by the Woods Hole Oceanographic Institution under contract with the Office of Naval Research. Reproduction in whole or in part is permitted for any purpose of the United States Government.

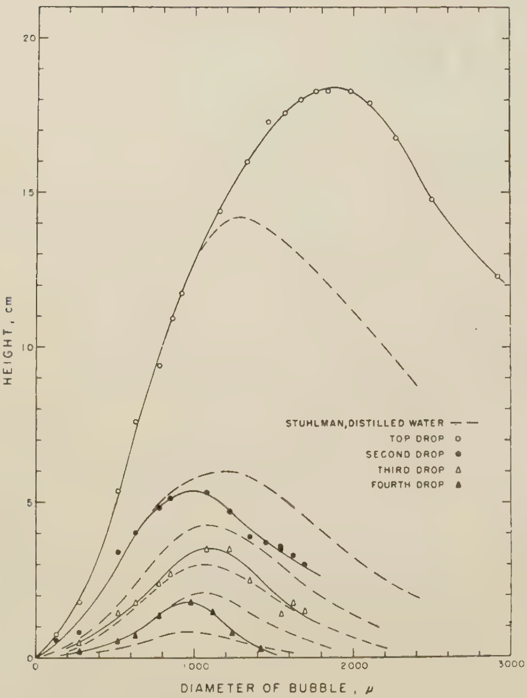

Fig. 1. This illustrates the heights of ejection of the several drops from the jet of a bubble bursting in sea water. STUHLMAN'S (1932) findings are shown for the top drop from bubbles bursting in distilled water.

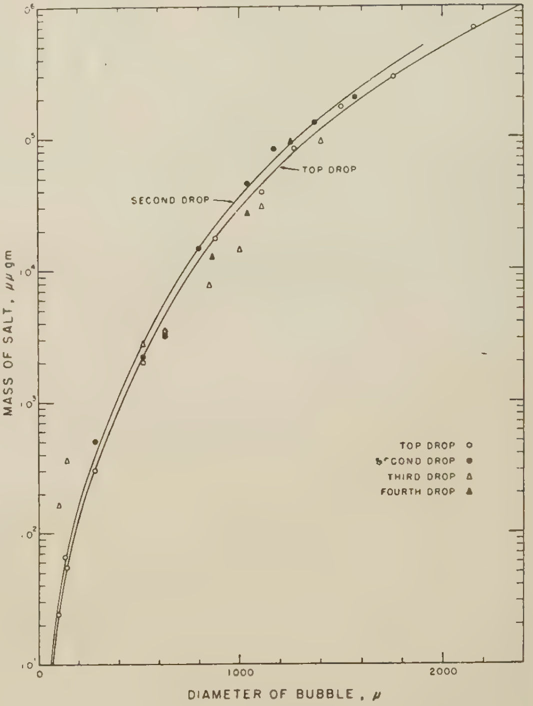

Fig. 2. This indicates the mass of salt contained in the drops that are ejected from bubbles bursting in sea water. This figure combined with Fig. 1 will give the ejection heights and drop size as a function of bubble diameter for the top four of the drops that evolve from the jet of a bursting bubble.

drop and that any modification of the sea salt spectrum will change the raindrop spectrum and possibly the manner of rainfall production. In the present paper we shall discuss the natural methods of production of salt particles at the sea surface and show that these methods should, in fact, be capable of modifying the existing salt nuclei spectrum.

The source of the airborne salt particles is, of course, the sea. Some of the first attempts at measurement of the salt spectrum were made near the sea surface by OWENS (1926). COSTE and WRIGHT (1935) showed that salt nuclei could be produced by spraying sea water and ALIVERTI and LOVERA (1939) produced small particles by bubbling air through sea water. KÖHLER (1941) forced air through sea water and found salt nuclei produced down to a radius of about 0.5 micron. None of these investigators, however, was greatly concerned with the exact mechanism of nuclei production; whether it was by mechanical disruption of the water by breaking bubbles or some other process. In 1948 Woodcock suggested that salt particles were ejected into the air from breaking bubbles by a mechanism first suggested by STUHLMAN (1932). BOYCE (1951) carried out an experiment that suggested that relatively few salt particles were produced by the mere mechanical "tearing" of the water in a breaking wave but that a significantly greater number could be produced a few seconds later when the bubbles resulting from the wave action had burst at the sea surface. A high-speed photographic study (KIENTZLER ET AL., 1954) confirmed the mechanism of the ejection of droplets from a breaking bubble (STUHLMAN 1932). The photographs indicate the manner in which small airborne droplets evolve from the vertical water jet which forms upon collapse of the bubble cavity. As seen in Fig. 1 and Fig. 2 the heights to which these droplets are ejected and their size is a function of the bubble diameter. The heights were obtained with the use of a cathetometer and the bubble size determined from measurements of the buoyant force from a known number of bubbles collected in a small inverted glass hemisphere. The size of the ejected drops was determined by catching them on glass slides and exposing them to an atmosphere of known humidity. The resulting drop size could then be used to compute the sea salt content and thus the original size of the drop.

Mason (1954), Moore and Mason (1954) and Knelman et al. (1954) found that the breaking of the bubble film produces small drops. It appears that the production of droplets by this mechanism is limited to the larger bubbles and any evaluation of their importance in modifying the salt particle spectrum over the sea must await an experimental study on the actual bubble spectrum. This point will be discussed later in the paper.

The foregoing work suggests that it is the breaking bubble at the sea surface that is responsible for the production of the atmospheric salt particles. In the next section the variation in bubble production by wave action and precipitation will be discussed.

2. Bubble Production at the Sea Surface

A. Wave Action

It is well known that increasing winds cause a proportionate increase in the production of "whitecaps" at the sea surface. These whitecaps produce bubbles in the sea which, when they break at the surface, produce airborne salt nuclei. Therefore a direct relation should exist between wind force and the concentration of airborne salt. This in fact has been found at deck levels by Fournier d'Albe (1951), Moore (1952) and at cloud levels by Woodcock (1953). Woodcock found that the weight concentration of sea salt at cloud base levels was increased by a factor of about ten when the wind force changed from three to seven.

It might be well to point out that in strong winds the effective area over which bubbles are breaking is appreciably greater than that covered by the obvious breaking wave. For a minute or more after the wave breaks the water in the immediate vicinity appears cloudy without the presence of a heavy foam patch on the surface. This cloudy appearance is caused by the myriads of bubbles that are formed by the breaking wave. The persistence of the cloudy region signifies that the bubbles are small and thus slow in reaching the surface or that they have been carried far beneath the surface. Presumably the stronger the wind the more bubbles are produced and the deeper they are carried by the turbulent motions of the sea. Observation indicates that little or no coalescence occurs amongst the bubbles when they reach the surface. If this surface is clean the bubbles will break immediately. In the laboratory, experiments have been carried out by bubbling air through fine frits placed a few cm beneath the surface of the water. A rapid coalescence of bubbles occurs on the surface of fresh water but this is not observed in the case of sea water. Even though they are packed tightly at the surface the individual bubble bursts seem unaffected by the adjacent bubbles. It appears safe to assume that bubbles produced in the sea by wave action will in most cases burst individually at the sea surface and not coalesce.

The device that was used to determine the bubble spectrum produced by breaking waves consisted of a small ($9 \times 6 \times 2$ cm) box with one of the 9×6 cm sides transparent. A grid of lines was inscribed on this transparent side of the box, the opposite side being removable. Just prior to making a bubble count the box was completely filled with sea water and the removable side securely attached. The box was then placed, transparent side up, just beneath the sea surface in a region where breaking waves had left the sea cloudy with bubbles. The removable side (now the bottom) was slipped aside for a known time interval during which bubbles were free to rise into the box and become entrapped against the underside of the transparent top. The bottom was then securely attached to prevent leakage and the box removed from the water. Using a scale and a magnifying lens, the bubble spectrum, divided into appropriate size ranges, could be obtained.

A brief consideration of the energies involved showed that there was no danger of a flattening of the bubbles against the underside of the glass. For bubbles < 500 microns diameter the surface free energy is at least 400 times as great as the gravitational energy. Any bubble surface distortion, which must arise from the gravita-

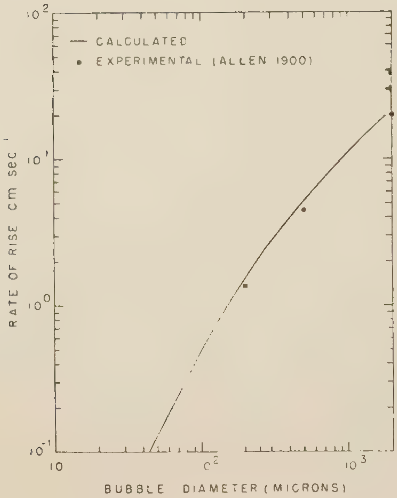

Fig. 3. The rate of rise of air bubbles in water. The calculated values are for sea water while the experimental ones are for fresh water.

tional energy, will be opposed by the surface free energy which, of course, tends to a minimum. It is apparent from the above considerations that the bubble surface distortion could not exceed 1/400 or 1/4 of one percent and thus the diameter will not undergo any significant change.

The bubble density or number per unit volume of water is easily obtained by dividing the number found in each size range by the area that was counted, the time of exposure and the rate of rise of the bubble in water. The size ranges were in 100 microns steps up to 500 microns. The rate of rise of the bubbles in each size range was assumed to be represented by the rising speed of the average sized bubble, with the exception of the first size range, where the representative rise speed was that for a 75 micron diameter bubble.

The rate of rise of bubbles in water may be calculated in the following manner. The general expression for the frictional retarding force is

$$f = 6\pi nrv\left(\frac{C_d \cdot R}{24}\right) \qquad (1)$$

where n is the viscosity of the water; r, the bubble radius; v, the velocity of rise; C_d, the drag coefficient; and R, the Reynolds number. This expression can be derived in a straightforward manner from Stokes' Law and the fundamental relation between actual drag and impact drag. Now the buoyant force on the bubble is

$$f_b = 4/3\,\pi r^3 g\,(\varrho_w - \varrho_a) \qquad (2)$$

where g is the gravitational acceleration and ϱ_w and ϱ_a the density of sea water and air, respectively. At the terminal or steady state velocity of the bubble (2) must equal (1). By equating these expressions and then substituting for v in terms of the Reynolds number

$$v = \frac{nR}{2\varrho_w r} \qquad (3)$$

and letting $\varrho_a << \varrho_w$ we obtain

$$r^3 = \frac{9n^2}{4\varrho_w^2 g}\;\frac{C_d R^2}{24} \qquad (4)$$

C_d has been found to be a function of only the Reynolds number (GOLDSTEIN 1938) so, given any value of R, C_d may be obtained and (4) can be solved for r. With this value of r and R, (3) may be solved for the rate of rise v. In like manner a number of r versus v tabulations can be determined and a graph drawn. Figure 3 shows the calculated values plus some experimentally observed rise velocities (ALLEN, 1900). Allen's values were used for the bubble density calculations in this section while the calculated values outside of Allen's observations were used for the discussions in

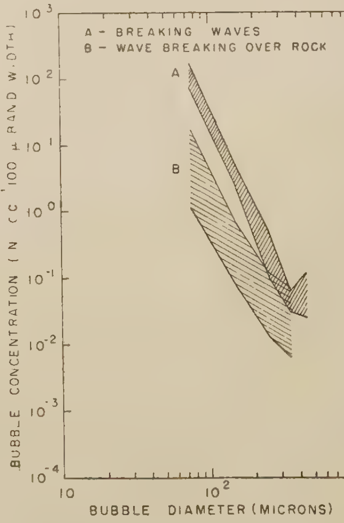

Fig. 4. The bubble concentration (cc^{-1} per 100 μ band width) in sea water produced by breaking waves or whitecaps.

the latter part of the paper. Stokes' law will apply for bubbles below about 110 microns diameter.

Figure 4 summarizes the experiments made on the bubble spectrum from breaking waves. All the experiments were carried out during the summer months on a beach near our laboratory where the water temperature was about 21° C. The hatched region A shows the limits of bubble density for six separate experiments conducted during a 2-hour interval at a time when fresh onshore winds were causing the waves to break about 15 meters from shore. The bubbles were obtained by wading some 5 meters out and exposing the sampling device already described for 2 seconds at a depth of about 10 cm. The measurements were made a few seconds after the breaking wave had passed. It was necessary to wait these few seconds to allow the relatively few bubbles of several mm diameter to rise to the surface. These large bubbles produced undesirable coalescence in the collecting box. It is realized that this method discriminates against the mm sized bubbles but they are present in far fewer numbers then the bubbles $< 500\,\mu$. The bubble spectrum in these experiments was determined out to a diameter of 750—1,500 microns but, as the size interval was 500 microns in this region, the values could not, without approximation, be plotted on Fig. 4. Had this been done the extension of region A and B would have continued with about the same slope as it has at present. Region B, an order of magnitude less than A, represents the spread of six determinations of the bubble spectrum found on the lee side of a rock over which the waves were breaking. The wind was not as strong as it was during the former measurements.

B. Snow

Among the natural sources of small bubbles in surface waters of the sea we have found that snowflake clusters are very significant. These bubbles, which are released as the snowflakes melt, are readily observed by allowing a snowflake to fall into a small beaker which is brimming full of sea water, and then quickly placing a clean glass cover-slip over the water in order to trap the bubbles. From fifty to several hundred bubbles were observed to rise and collect under the cover-slip as single flakes melt. Figure 5 shows the size distribution of some three hundred of these bubbles, which were measured with a low-power microscope using an eyepiece micrometer.

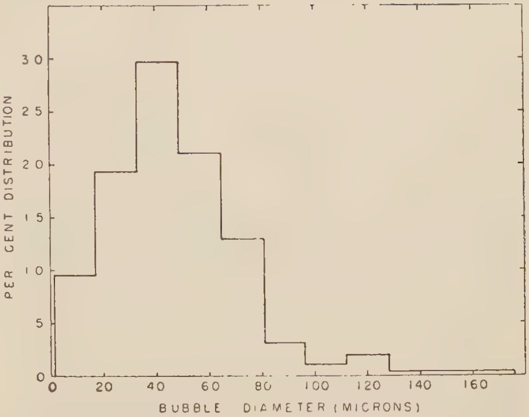

Fig. 5. The size distribution of bubbles, rising from a snowflake cluster melted in sea water.

While making these size measurements, which required perhaps 10 minutes, it was observed that bubbles smaller than about $30\,\mu$ diameter were slowly becoming smaller and that bubbles $50\,\mu$ or larger were growing. Thus the size distribution shown on Fig. 5 is only qualitatively correct, serving here only to emphasize the capabilities of snow in producing (or causing to be produced) a wide range of size among very small bubbles. Since, during the observation period, the small bubbles were becoming smaller and the large bubbles were becoming larger an increase in the size range with time occurred. This means that the initial bubble size distribution, present immediately after the flakes melted, was more limited in range than is shown in Fig. 5. The effects of time of immersion in altering a given initial bubble population depends upon a number of factors, such as depth of water, partial pressure of air in solution, etc. These and other factors are discussed at length in Section 3 of this paper.

C. Raindrops

The production of bubbles and nuclei by the impact of raindrops on the sea surface is a complex problem. It has been found that bubbles, produced directly and indirectly through the impact of raindrops, can produce

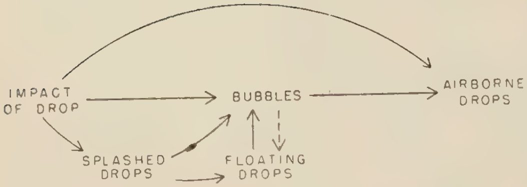

Fig. 6. A diagrammatic sketch of the methods of production of airborne drops by the impact of a freshwater drop on a sea water surface. The dotted arrow indicates that floating drops are associated primarily with the collapse of the larger, less numerous bubbles.

nuclei. Before an attempt is made to describe these bubble-production methods in detail, and to show how they vary over the raindrop spectrum, it might be well to consider them in schematic form as shown in Fig. 6. It can be seen that the nuclei are produced either directly from the impact of the drop, or from bubbles produced as a result of the impact. The bubbles are produced by (1) direct impact of the raindrop on the sea surface, (2) splashed drops resulting from the impact, and (3) drops that momentarily remain floating on the sea surface.

Observations on the splashing of water and production of bubbles by simulated raindrops were made by visually observing, with suitable lighting, the behavior of freshwater drops on impact with a sea water surface. The drops were allowed to fall from a sufficient height to insure terminal velocity. The splashed drops and the smallest bubbles were easily visible in a parallel beam of light from a microscope lamp, using a suitable black velvet background. An estimate of the size of the bubbles and drops was made by applying Stokes' Law to the rate of rise and fall, respectively.

The direct production of bubbles by raindrops is a function of raindrop size. Small drops of the order of 0.4 mm diameter will produce 2 or 3 bubbles of about 50 μ diameter that are carried only 1—3 mm beneath the surface. The production of bubbles increases rapidly with drop size as a 2.2 mm drop was observed to produce from 50—100 bubbles that were often carried down in a vortex ring to depths of 2—4 cm. The vast majority or these bubbles appeared to be under 50 microns diameter. On occasions it appeared that the vortex ring of bubbles formed not at the moment of impact of the drop with the water but at the collapse of the water column that rises from the bottom of the impact cavity. This is quite plausible, for the remarkable photographic work of WORTHINGTON and COLE (1897) shows this water column, and they remark about the vortex ring that it forms upon collapse. They make no mention of bubbles in the vortex ring but they probably passed undetected as only the closest scrutiny will discover them. With increasing drop size an increase in number of bubbles was observed, although the bubble size was predominantly the same. Drops of 3 mm produced 100—200 bubbles while 4.7 mm drops produced an estimated 200—400 bubbles (see Fig. 7). The larger drops also produce several bubbles of about a mm diameter. With increasing drop size the vortex motion of the bubbles plus the depth of penetration decreased. The bubbles from drops of 4.7 mm were carried down less than 2 cm but eddy motions distributed bubble clusters some 3 cm horizontally. These bubbles would go rapidly into solution or grow depending upon whether the sea water was considerably under- or oversaturated, respectively. This, of course, will modify the bubble spectrum which in turn will affect the salt nuclei that are produced when the bubbles burst. This solubility effect of the bubbles is considered in some detail later in the paper.

The indirect production of bubbles by raindrops occurs when the drops produced by the splash of the raindrop fall back into the sea. As this method of bubble production depends

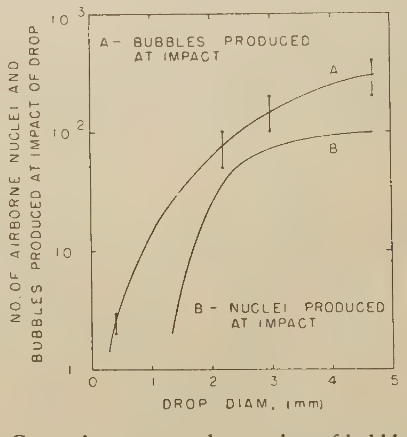

Fig. 7. Curve A represents the number of bubbles produced by the impact of a fresh-water drop on a sea water surface. Curve B represents the direct production of nuclei by the same drop at the moment of impact.

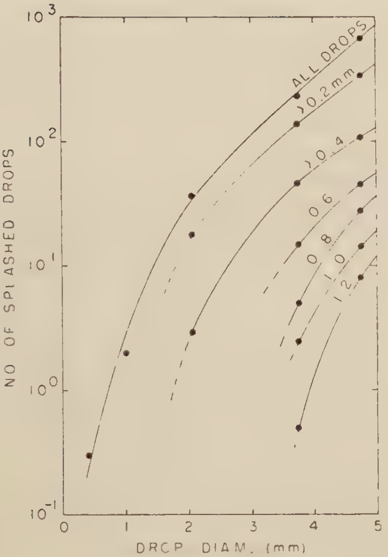

Fig. 8. The number of plashed drops > the indicated size, that are produced by the impact of a fresh-water drop on a sea water surface. As these data were obtained with the aid of filter papers, splashed drops < about 100 microns diameter and those remaining airborne (Curve B, Fig. 7) were not included.

entirely on the size and number of splashed drops it was necessary to determine the "splashed drop spectrum" over the range of raindrop size. This was done by catching the splashed drops on 60 × 90 cm squares of Whatman No. 1 filter paper. The "raindrops" and the sea water contained a sufficient amount of methylene blue dye to enable the splashed drops, at least down to about 100 μ diameter, to be recorded as a blue spot on the filter paper. Tensiometer measurements showed that the blue dye did not significantly change the surface tension, consequently the character of the splash would not be expected to change. The relation of drop size to spot size on the filter paper was determined by letting drops of known size fall on the papers. A semi-disc of 10 cm diameter was cut from the center of the 90 cm edge of the filter paper and the paper then placed about 5 mm above the sea water surface and so positioned that the water drops would splash at the edge of the paper at the center of the semicircular opening. Only half of the splash was recorded so the final count of drops on the filter paper was multiplied by two. The splash from the largest drops extended out to about 50 cm from the point of impact of the drop with the water. The splash from four to six drops in each of three size categories from 2—5 mm was counted. Figure 8 presents the data in the form of a family of curves showing the total number of splashed drops larger than the indicated size. It can be seen that nearly half of the splashed drops are < 0.2 mm. A raindrop of 5 mm might be expected to produce nearly 900 drops of a size that is detected on the filter paper, of which only about 400 exceed 0.2 mm and only 12 exceed 1.2 mm. The splash from raindrops < 2 mm is probably mainly composed of drops < 0.4 mm. Drops < 1 mm produce, on the average, less than one splash drop. These last splash observations were made visually.

It now remains to determine just what this splash means in terms of bubble production. It might be expected that the bubble-producing ability of the splash drops would be a function of their velocity and the angle at which they enter the water. A larger number of combinations may be met with in the splash of a single large drop but fortunately a simplification enables us to make a reasonable estimate of the bubble production. The splash drops are observed to rise up to 40 cm from the water surface, a height sufficient to insure that drops up to 0.5 mm will nearly attain terminal velocity by the time they return to the water surface. Figure 8 indicates that all the splash drops from raindrops < 2 mm and about 80 percent from a 5 mm raindrop are < 0.5 mm. We might reasonably expect then that the splash drops could be considered as raindrops and, as discussed earlier in this section, each produce 2—3 bubbles of about 50 μ diameter. On this basis the splash from a 2 mm raindrop might be expected to produce some 80 bubbles compared to over 2,000 for a 5 mm raindrop.

The third method of bubble production by raindrops falling into the sea is from "floating drops". These drops are similar to those that can be seen skimming across the surface of the water any time the water is violently agitated. As indicated in Fig. 6 the floating drops can be produced by both the splashed drops and the bubbles. Presumably the few that are produced by splashed drops are from drops that were not splashed to any great height while those produced by bubbles are presumably the lower, larger drops in the jet that is produced when the bubble breaks. Observations on floating drops of about 2 mm diameter show that when they finally merge with the main body of water a thin column of bubbles is forced down several mm into the water. When these bubbles, perhaps 40 or more, fan out they are seen to be very small, perhaps $< 25\,\mu$ diameter. Little can be said of the numbers or sizes of these floating drops that are produced by raindrops. It may be that rain produces relatively few compared to those that may be produced by breaking waves.

The airborne salt nuclei produced by direct impact of the raindrops with the water are nothing more than splashed drops that are, for the most part, small enough to remain airborne. Drops of 4.7 mm were observed to produce an estimated several hundred particles of < about 50 microns diameter. At impact these particles seem to appear simultaneously within a region up to 4 cm above the water and some 10 cm from the point of impact. No doubt this is caused by the fact that the production mechanism of the particles gives them sufficient speed to escape detection by the eye until frictional retarding forces decrease their speed to the terminal value. This production mechanism appeared to be associated with the rapid formation and collapse of the large bubble that WORTHINGTON and COLE (1897) observed in their splash studies. In any event the ejection of the particles several cm above the surface increases the probability that they will remain airborne. Some of these particles were so small (< 10 microns) that a collection of them appeared and behaved like a small puff of smoke. There was no doubt that these would remain airborne, especially if the humidity were low over the water surface. The production of these minute splash drops was very much a function of drop size. A 2.4 mm drop produced perhaps 50—80 small particles while a 0.4 mm drop produced none that was visible to the naked eye (see Fig. 7).

D. Air Solubility Change in the Sea

The dissolved air content of the surface layers of the sea is usually at or near saturation and will vary from one season to the next. This seasonal change is presumably explained by the fact that the solubility of air in sea water is a function of temperature and also that the production or utilization of oxygen by marine organisms will vary with the seasons. As the solubility of air is an inverse function of temperature it follows that, at saturation values, a maximum would be found near the end of the winter months when the water is at its lowest temperature and a minimum at the end of summer when the water is warmest. Consequently air should be given off by the sea during the spring and summer and absorbed during the winter. REDFIELD (1948), after an analysis of the seasonal variations of the oxygen distribution in the Gulf of Maine, concluded that about 3×10^5 cc of oxygen leaves the sea through a m^2 of sea surface during March—October and a similar amount re-enters during the winter and spring. It is logical to inquire as to how much of this oxygen might leave the sea in the form of bubbles. If we go to extremes and assume that it all comes out in the form of bubbles of 50 microns diameter we can compute the rather staggering number of 2,500 bubbles sec^{-1} cm^{-2} breaking at the sea surface. This certainly does not occur, as gaseous diffusion across the sea surface probably accounts for the greater part of the oxygen exchange in the normal course of events. However an intriguing question is whether bubble formation occurs in the sea after a short period of intense heating by an overlying warm air mass. If supersaturation by heating can keep ahead of the loss by gaseous diffusion to the air, and if sufficient nuclei for centers of bubble formation exist, there is a possibility that bubbles may form. Inasmuch as little or nothing is known of the interplay between these factors little more can be said.

Precipitation falling into the sea may, under certain conditions, bring about a supersaturation of the rain water—sea water mixture, even though both were only saturated initially. As the inverse relation between air solubility and temperature is not linear but in the form of a curve concave upward, it follows that the mixing of two initially saturated bodies of water at different temperatures will produce a supersaturated mixture. For example, consider raindrops which have essentially the wet bulb temperature (KINZER and GUNN, 1951) and undoubtedly are saturated at that temperature. If raindrops, of a chlorinity essentially zero and saturated with air at 10° C, fall into saturated sea water (Cl = 19 ‰) at 24° C and mix such that the mixture is 90 percent sea water, the resulting supersaturation will be about 102 percent[1]. Such supersaturations are probably not sufficient to cause bubble nucleation, but the rate of solution of the small bubbles produced by wave action and precipitation would be decreased. The important subject of the rates of solution of an air bubble as a function of saturation percentage will be discussed in the next section.

3. The Stability of Air Bubbles in Sea Water

The foregoing experiments have shown that whitecaps and all forms of precipitation particles are effective bubble producers. If these bubbles are produced in subsaturated water there is the possibility that a significant decrease in bubble diameter will be caused by the air within the bubble going into solution. On the other hand, if the water is sufficiently supersaturated many of the bubbles would be expected to grow. It will be clear shortly that for any supersaturation of sea water there exists a bubble size above which all bubbles will grow while those smaller than this size will go into solution. This modification of bubble size is clearly then a function of its initial size, the sea water saturation and the duration of existence of the bubble. Bubbles carried far beneath the surface will be subjected to gas diffusion across the bubble—water interface for considerably longer periods of time and are thus subject to greater change than those near the surface. Consequently it is very important that we obtain some knowledge of the effects of various solution times and rates on the bubble spectrum.

The calculations outlined here are an extension of those given by WYMAN ET AL (1952) and the reader should refer to these authors for a full understanding of the initial formulation. As a first approximation consider that due to the relative motion between the water and the bubble that the only gradient of dissolved gas that exists is across a thin shell with its inner surface at the air—water interface. Further assume that the air within the bubble consists of a single gas with a single diffusion constant and not primarily a mixture of oxygen and nitrogen. The general gas law states:

$$n = \frac{1}{RT}\,\frac{4}{3}\,\pi\, r^3 p \qquad (5)$$

when n is the number of moles of gas in the bubble; R, the gas constant; T, the absolute temperature; r, the radius of the bubble; and p, the pressure within the bubble. The pressure p is the hydrostatic plus the atmospheric pressure. The diffusion of air across the bubble surface can be expressed by Fick's law:

$$dn/dt = -\,\delta\, 4\,\pi\, r^2\,(p - p_0) \qquad (6)$$

where p_0 is the partial pressure of the air in the bulk water and δ is a constant defined by: $\delta = \triangle\,\alpha/d$ where $\triangle$ is the diffusion constant of the air in the water; α, the solubility of the air in the water, and d, the thickness of the thin shell that is assumed to carry the diffusion gradient. It will be seen that this expression is necessary to convert $(p - p_0)$ in (6) into a concentration gradient as called for in Fick's law. If we differentiate (5) with respect to time and combine it with (6) we have:

$$dr/dt = -\,\delta\, RT\, \frac{(p - p_0)}{p} \qquad (7)$$

This is the equation that was derived by WYMAN ET AL. (1952) and found to be in very good agreement with experiment. Experimentally they found that dr/dt at any given pressure was essentially constant, that it approached a limiting value at high pressures and it was essentially independent of temperature over the range 1—27° C. This is just what (7) predicts. As the water was always saturated with respect to air at one atmosphere, pressure p_0 is constant and dr/dt can be seen to approach a limiting value, $\delta\, RT$, at great depths. As the rate of solution is proportional to the absolute temperature dr/dt will change relatively little with the temperature range used in the experiments. With the experimental data one may compute the value of the term $\delta\, RT$ to be 10^{-4} cm sec^{-1} and find that it is approximately constant at all depths. Equation (7) with this substitution combines both theory and experiment to describe the rate of solution of gas bubbles.

It should be noted in (7) that the total pressure p within the bubble is assumed to be only the hydrostatic plus atmospheric pressure

---

[1] This calculation was based on tables of air saturation as a function of temperature and chlorinity as given by MIYAKE (1951).

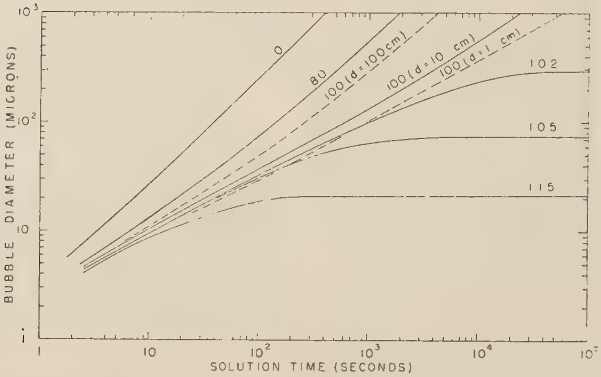

Fig. 9. The time of solution for a bubble in sea water at a depth of 10 cm. The family of curves represents various percentage saturations of air in sea water with respect to atmospheric pressure. The dashed lines show the solution times for bubbles at a depth of 1 and 100 cm in water saturated with air with respect to atmospheric pressure.

and no account is taken of the additional pressure $2\,\gamma/r$ due to surface tension effects (the surface tension of sea water γ is about 74 dynes cm^{-1}). This effect was negligible in the work of Wyman et al. where the bubbles were several mm in diameter but in the present case, where we must be concerned with bubbles < 100 microns, surface tension effects become of prime importance. If then we add the surface tension pressure term $2\,\gamma/r$ to the other pressure term p in (5) and (6) and solve simultaneously we obtain the general expression:

$$\int_0^t dt = -\frac{1}{3\delta RT}\int_{r^1}^{r^2}\frac{3pr+4\gamma\, dr}{r(p-p_0)+2\gamma} \qquad (8)$$

which reduces to (7), as it should, if γ is set equal to zero. The solution of this integral is:

$$t = -\frac{(p-p_0)^{-1}}{3\delta\ RT}\left[3\,pr+\gamma\left\{\frac{4(p-p_0)-6p)}{p-p_0}\right\} ln\ \{(p-p_0)r+2\gamma\}\right]_{r^1}^{r^2} \qquad (9)$$

Figure 9 was constructed from (9) and shows the solution times for bubbles in water of various degrees of saturation at a depth of 10 cm. The dashed lines show the solution times in water saturated at atmospheric pressures at depths of 1 and 100 cm. Note that within these depths there is little significant difference in solution times in saturated water for bubbles < about 40 microns diameter. The significance in Figure 9 would seem to be the equilibrium bubble diameters that are indicated at each value of supersaturation, below which all bubbles will, due to surface tension pressure effects, go into solution. Even at a supersaturation of 115 % all bubbles < 21 microns will be forced into solution. The value of this equilibrium diameter may be very important for if the majority of bubbles in a given bubble spectrum are < this value, the bubbles themselves may be responsible for further increasing the supersaturation. As the supersaturation curves in Fig. 9 were constructed for a depth of 10 cm, it is of interest to determine how the equilibrium bubble diameters vary with depth as a function of supersaturation.

A bubble is at equilibrium with its surroundings when its total internal pressure, which is composed of the atmospheric, the hydrostatic and the surface tension pressures, is equal to the partial pressure of the gas in solution. As we are considering the case where the water is saturated at all depths with respect to atmospheric pressure, the partial pressure of the gas is $x\,A$, where x is the fractional value of the supersaturation and A is the atmospheric pressure. This is equated to the three components of the total internal pressure as given above to obtain

$$xA = A + d + \frac{2\gamma}{r} \qquad (10)$$

where d is the hydrostatic pressure. Solving for r we find

$$r = \frac{2\gamma}{(x-1)A-d} \tag{11}$$

from which it is seen that for any supersaturation x there is a depth d beyond which all bubbles will go into solution. This depth is found by letting the denominator in (11) equal zero and solving for d. For supersaturations < 102 percent this depth is < 10 cm. At supersaturations > 102 percent (11) shows that for depths < 10 cm the critical radius, above which or below which bubbles grow or go into solution, is essentially constant for a given supersaturation and thus similar to the values indicated in Fig. 9. The time required for the bubbles to go into solution will decrease with depth in the range of 0—100 cm but probably not significantly so, judging from the curves for depth of 1 and 100 cm in Fig. 9.

4. Discussion

It will be of interest to examine the experimental data on the effectiveness of bubble production by breaking waves and precipitation in terms of the salt nuclei spectrum found in the atmosphere. The breaking wave is probably the most common method of production of airborne nuclei. With the data from Fig. 3 and Fig. 4 we can derive Table 1 which indicates the rate at which bubbles of various sizes rise to the surface cm^{-2} sec^{-1}. Assuming that only one of the 4 or 5 drops ejected from the breaking bubble remains airborne, column D of Table 1 can also represent the production rate of airborne nuclei from the sea surface shortly after a whitecap has formed. It would be unwise to attempt to compute the total production of nuclei from a breaking wave for we do not know to what depths the bubbles are carried and thus cannot say how long the concentration given in column B will be in existence. If the bubbles are all distributed uniformly to the same depth then the smallest ones will continue to break at the surface for the longest time. The production rate (column D) of about 34 cm^{-2} sec^{-1} is comparable to the value of 40 cm^{-2} sec^{-1} (for nuclei of mass $> 10^{-13}$ g) found by MOORE and MASON (1954) in laboratory tests. It would be well to regard the similarity of these two values as probably fortuitous, and to accept it only as an agreement in order of magnitude. It is not clear as to whether bubbles were breaking over the entire area used in Moore and Mason's laboratory tests or only over a fraction of it. Also, it is not known how the present results will be affected by changes in wind force on the open sea. It is expected that increasing wind force will increase the numbers of bubbles in such a way that the slope of the curve in Fig. 4 will be essentially the same.

Table I. An attempt to estimate the number of bubbles (cm^{-2} sec^{-1}) from a breaking wave. Columns B and C are obtained from Figs. 4 and 3, respectively. Column D is simply the product of B and C. Column E is obtained from D by assuming only 10 percent of the ocean active as a source bubbles.

A	B	C	D	E
Bubble diam. of center of size band (μ)	Bubbles cc^{-1} per 100 μ band width	Rise velocity cm sec^{-1}	Bubbles cm^{-2} sec^{-1}	Bubbles produced cm^{-2} sec^{-1} assuming 10 % of sea active
75	100	0,3	30	3
150	3,6	0,9	3,24	0,32
250	0,25	1,9	0,47	0,047
350	0,05	2,95	0,15	0,015

Probably the most significant aspect of Table 1 is that the great majority of the bubbles are $< 200\,\mu$. From Fig. 2 we see that these bubbles, upon bursting, could produce nuclei of the size found at the small end of the airborne sea-salt spectrum ($<$ about 10^{-10} g) by drops from the jets. MOORE and MASON (1954), with doubts as to the existence of bubbles $<$ about 500 μ from whitecaps, have suggested that airborne salt nuclei $< 10^{-9}$ g originate from the shattering of the film of the large bubbles. Inasmuch as the small bubbles do indeed exist it is likely that the mechanism by which the nuclei are produced is via the jet mechanism and not the bubble film. Observation (BLANCHARD 1954) shows that small bubbles ($< 50\,\mu$) produce no droplets exceeding 1 μ radius, other than those coming from the jet mechanism. MASON (1954) reports that bubbles of 0.5 to 3 mm give 100—200 droplets from the shattered film, with the largest having salt contents of about 2×10^{-14} g. This weight is far less than the minimum of about 10^{-10} g that appears to provide the nuclei for raindrop formation (WOODCOCK and BLANCHARD 1955).

The entire question as to the spectrum of bubbles that produce these large airborne nuclei and the exact method by which it is done may appear to be a trivial one. And it could well be so, if we were to assume that the properties of two drops of equal size, one produced by the jet mechanism and the other by the rupture of the bubble film, were the same. But this may not necessarily be so. It has been found (BLANCHARD 1955) that the droplets arising from the jet mechanism carry an appreciable electric charge that may contribute significantly to electrification processes in the atmosphere. Other considerations indicate that the droplets that are created by the jets may not be representative of the bulk sea water but of the surface film which may be contaminated. If droplets arising from the rupture of bubble films do not have the aforementioned properties they may play a different role in the precipitation process than those arising from the jet mechanism.

The production of bubbles by falling snow was found to be about 25 cm^{-2} sec^{-1} which, again assuming one airborne droplet per bursting bubble, gives a salt nuclei production rate of the same value. This is to be compared to the somewhat similar computed value of about 14 found for the nuclei production from bubbles produced by rain. The nuclei production by rain was estimated by carrying out the following steps, with each of the raindrop size distributions given by BLANCHARD (1953) and BEST (1950) for rain intensities of 20.8 and 25 mm hr^{-1}, respectively. Each distribution was divided into a number of intervals ($\leq 250\,\mu$) and the number of drops striking the sea cm^{-2} sec^{-1} was computed. Then by using Fig. 7 and Fig. 8 one could compute the production rate of airborne nuclei from (a); bubbles produced directly by the drop, (b); impact of the drop and (c); bubbles produced by the drops < 0.4 mm that were splashed by the raindrops. It was found that the bubbles produced at impact were responsible for more than 80 percent of the total airborne nuclei and, even more surprising, Blanchard's rain distribution above (all drops ≤ 2.2 mm) produced about as many bubbles as did Best's (drops as large as 5 mm). It appears that the greater number of drops m^{-3} in the narrow range distribution made up for the fact that larger drops produce more bubbles. These data indicate that a significant increase in the salt nuclei count might be found in atmospheric regions overlying the ocean through which rain or snow had fallen. The build up of airborne nuclei in such regions would be a function of the wind shear between sea level and the precipitation source and the duration of the precipitation.

The question as to the production of bubbles by the warming of the sea in the summer months or by the mixing of two saturated water masses at different temperatures will, as mentioned earlier, have to await more observations on the supersaturations of surface waters of the sea. The existence of supersaturations will depend, in some degree, on the absence of bubble nuclei. In the absence of these nuclei, which are thought to be gas particles surrounded by minute foreign materials in the water, the water may be highly supersaturated without the formation of bubbles (DEAN, 1944). The idea was recently advanced (FOX and HERZFELD, (1954) than minute bubbles in water, which are prevented from going into solution by the stabilizing action of an organic skin, will act as cavitation nuclei. They envisaged that this organic skin, probably produced by the disintegration of living organisms, acted as a mechanical barrier to the diffusion of gases. Upon cavitation the organic skin could be torn and bubble growth would follow. It seems probable that such bubble nuclei could exist in the oceans but their importance in bubble production in natural supersaturated waters is unknown.

From the calculations presented in Section 3 it appears that supersaturations in the surface layers of the sea can be produced by the small bubbles that are forced into solution by the increase in internal bubble pressure due to surface tension. Figure 9 indicates that supersaturation of at least 102 percent could occur if the bubbles are $< 300\,\mu$ diameter. As the results of Section 2 show that a majority of the bubbles produced by natural processes are $< 300\,\mu$, it is to be expected that a slight supersaturation of the surface waters would be produced. In particular, as the majority of the bubbles produced by snowflakes are $< 50\,\mu$ diameter, it is expected that supersaturations of about 105 percent could be obtained. The bubbling process will certainly produce supersaturations, as Rakestraw and Emmel (1938) have measured nitrogen supersaturations of 102 percent in water that had been vigorously shaken with air and let stand until the bubbles were no longer visible.

If we assume that the usual saturation percentage at the sea surface is from 100 to 102, then in either case all bubbles $< 300\ \mu$ will tend to go into solution and at rates, at least for the bubbles < about $100\ \mu$, that are nearly the same. The solution rates for the larger bubbles, though significantly different for 100 and 102 percent saturation, need not be considered, for the rate of rise of these bubbles will bring them to the surface long before any appreciable decrease in diameter has taken place. The small bubbles, with rates of rise of only a few tenths of a cm sec^{-1}, will require several hundred or only a few seconds to reach the surface depending on whether they rise from depths of about a meter or a few cm, respectively. In the former case the bubble may go entirely into solution while in the latter little change in size may be experienced. It appears then that the depth to which a small bubble is carried may be an important factor in controlling the final bubble size. This depth, in turn, will be a function of the stability of the surface layers of the sea and the intensity of the mixing process. For example, we would expect very little downward mixing of bubbles produced by snow falling into a fairly calm sea. On the other hand, a great deal of downward mixing of bubbles from snow is to be expected in strong winds or when the surface waters are convectively unstable.

It is clear that many factors must be considered in order to make broad generalizations on the rate of nuclei production from naturally-produced breaking bubbles. Not only must we consider the various bubble producing mechanisms discussed in this paper, but we also must take into account the stability change of the surface layers of the sea as it varies geographically and with the seasons.

Acknowledgments

The writers would like to thank Mr. A. T. Spencer for his help in carrying out the experiments with simulated raindrops. They gratefully acknowledge the work of Mr. E. Florence on the bubble spectrum from breaking waves. Their former colleague, Dr. C. H. Keith, did all the work relating the bubble size to the mass and height of the ejected drops.

REFERENCES

Aliverti, G., and G. Lovera, 1939: I fenomeni meteorologici sull'Oceano e il campo elettrico terrestre. *Atti della Reale Accademia delle Scienze di Torino* **74**, pp. 573—590.

Allen, H. S., 1900: The motion of a sphere in a viscous fluid. *Phil. Mag.*, **50**, pp. 323—338.

Best, A. C., 1950: The size distribution of raindrops. *Quart. J. Roy. Met. Soc.*, **76**, pp. 16—36.

Blanchard, D. C., 1953: Raindrop size-distribution in Hawaiian rains. *J. Met.*, **10**, pp 457—473.

— 1955: Electrified droplets from the bursting of bubbles at an air—sea water interface. *Nature*, **175**, pp. 334—336.

— 1954: Bursting of bubbles at an air-water interface. *Nature* **173**, p. 1048.

Bowen, E. G., 1950: The formation of rain by coalescense. *Australian J. of Sci. Res.*, **3**, pp. 193—213.

Boyce, S. G., 1951: Source of atmospheric salts. *Science*, **113**, pp. 620—621.

Byers, H. R., 1955: Distribution in the atmosphere of certain particles capable of serving as condensation nuclei. *Proc. Conf. Physics of Cloud and Precip. Particles*, Woods Hole Ocean. Inst., Woods Hole, Mass. To be publ.

Coste, J. H., and H. L. Wright, 1935: The nature of the nucleus in hygroscopic droplets. *Phil. Mag.*, **20**, pp. 209—234.

Crozier, W. D. and B. K. Seely, 1950: Some techniques for sampling and identifying particulate matter in the air, *Proceeding of First National Air Pollution Symposium*, p. 45, Stanford, Calif., Stanford Press.

Dean, R. B., 1944: The formation of bubbles. *J. App. Physics* **15**, pp. 446—451.

Fournier d'Albe, E. M., 1951: Sur les embruns marins. *Bull. Inst. Oceanogr., Monaco*, **48**, No. 995, 7 pp.

Fox, F. E. and K. F. Herzfeld, 1955: Gas bubbles with organic skins as cavitation nuclei. *J. Acoust. Soc. of Amer.* **26**, pp. 984—989.

Goldstein, S., 1938: *Modern developments in fluid dynamics.* Vol. 1, p. 14. Oxford at the Clarendon Press.

Kientzler, C. F., A. B. Arons, D. C. Blanchard, and A. H. Woodcock, 1954: Photographic investigation of the projection of droplets by bubbles bursting at a water surface. *Tellus*, **6**, pp. 1—7.

Kinzer, G. D., and R. Gunn, 1951: The evaporation, temperature and thermal relaxation-time of freely falling waterdrops. *J. Met.*, **8**, pp. 71—83.

Knelman, F., N. Dombrowski, and D. M. Newitt, 1954: Mechanism of the bursting of bubbles. *Nature* **173**, p. 261.

Köhler, H., 1941: An experimental investigation on sea water nuclei. *Nova Acta reg. Soc. Sci. Upsaliensis*, ser. 4, **12**, No. 6, 55 pp.

Ludlam, F. H., 1951: The production of showers by the coalescence of cloud droplets. *Quart. J. Roy. Met. Soc.*, **77**, pp. 402—417.

Mason, B. J., 1954: Bursting of bubbles at the surface of sea water. *Nature*, **174**, pp. 470—471.

Miyake, Y., 1951: The possibility and the allowable limit of formation of air bubbles in the sea. *Papers in Meteorology and Geophysics*, **2**, pp. 95—101.

Moore, D. J., 1952: Measurements of condensation nuclei over the North Atlantic. *Quart. J. Roy Met. Soc.*, **78**, pp. 596—602.

Moore, D. J., and B. J. Mason, 1954: The concentration, size distribution and production rate of large salt nuclei over the oceans. *Quart. J. Roy. Met. Soc.*, **80**, pp. 583—590.

Owens, J. S., 1926: Condensation of water from the air upon hygroscopic crystals. *Proc. Roy. Soc., London*, A, **110**, pp. 738—752.

Rakestraw, N. W., and W. M. Emmel, 1938: The solubility of nitrogen and argon in sea water. *J. Phys. Chem.*, **42**, pp. 1211—1215.

Redfield, A. C., 1948: The exchange of oxygen across the sea surface. *J. Mar. Res.*, **7**, pp. 347—361.

Stuhlman, O., 1932: The mechanics of effervescence. *Physics*, **2**, pp. 457—466.

Twomey, S., 1955: The distribution of sea-salt nuclei in air over land. *J. Met.*, **12**, pp. 81—86.

Woodcock, A. H., 1948: Note concerning human respiratory irritation associated with high concentrations of plankton and mass mortality of marine organisms. *J. Mar. Res.*, **7**, pp. 56—62.

Woodcock, A. H., and Mary M. Gifford, 1949: Sampling atmospheric sea-salt nuclei over the ocean. *J. Mar. Res.*, **8**, pp. 177—197.

Woodcock, A. H., 1952: Atmospheric salt particles and raindrops. *J. Met.*, **9**, pp. 200—212.

— 1953: Salt nuclei in marine air as a function of altitude and wind force. *J. Met.*, **10**, pp. 362—371.

Woodcock, A. H. and D. C. Blanchard, 1955: Tests of the salt-nuclei hypothesis of rain formation. *Tellus*, **8**, pp. 437—448.

Worthington, A. M., and R. S. Cole, 1897: Impact with a liquid surface, studied by the aid of instantaneous photography. *Phil. Trans.*, **189** A, pp. 137—148

Wright, H. L., 1940: Atmospheric opacity at Velentia. *Quart. J. Roy. Met. Soc.*, **66**, pp. 66—77.

Wyman, jr., J., P. F. Scholander, G. A. Edwards, and L. Irving, 1952: On the stability of gas bubbles in sea water. *J. Mar. Res.*, **11**, pp. 47—62.

PRINTED IN SWEDEN
ESSELTE, STHLM 57

Contribution No. 878

*Reprinted from The Norwegian
Whaling Gazette 1957, No. 1,
pages 1 — 5.
In Norwegian and English.*

Thermal Regulation in Whales

J. Kanwisher and H. Leivestad
Woods Hole Oceanographic Institution1) and
Institute of Zoophysiology, University of Oslo

Whales are found in all seas from the Tropics to the edge of the polar ice. They belong, along with man, to that group of animals called homoiothermic which maintain their bodies at a high and nearly uniform temperature. Unlike many mammals which have fur for insulation the whale is bare skinned, another of its similarities to man. One might wonder then how it keeps warm in icy polar waters when it is also at home in the Tropics. Some species like the humpback and grey whales migrate yearly between these extremes. Whales must somehow be able to vary their insulation in a manner analogous to our putting on and taking off clothes.

The rate of internal heat production which keeps the animal warm can also vary greatly. In a whale being chased heat may be produced at 10

---

1) Contribution No. 878 from the Woods Hole Oceanographic Institution.

times the rate in one swimming leisurely. Yet the animal cannot allow itself to become overheated under such conditions. The thermostatic controls in a whale must operate at times to conserve heat and at other times to discard it. The small porpoises are true whales. Because of the great range of size between these and a fin whale one may expect to find some interesting variations in the physics of how the different species handle the problem of thermal regulation.

The layer of blubber that covers most of the body can act as an effective barrier to heat loss, but the flippers and tail are relatively uninsulated. Yet they must be supplied with blood the same as other parts of the body. This blood will become cooled while in these regions and might act as a serious chilling source when it returns to the deep body of the animal. Scholander and Schevill*) found structures in the circulatory system of small whales which they think can prevent this loss of heat. The arteries and veins are arranged in such a way that they form counter-current heat exchangers, much like that in a power plant where the heat of the outgoing flue gases is transferred to the incoming air. In whales the heat of the warm blood from the deep body is used to warm the cool blood returning from the tail and flippers. By this means blood can be supplied to the uninsulated cold areas of the whale without losing large amounts of heat to the surrounding water. The circulatory system also seemed well designed for the discarding of heat, which is probably necessary to prevent overheating in a fast swimming animal. The same authors found vessels which bypass the heat exchangers. The blood flowing by this path is effective in cooling the entire animal. The flippers and tail of these small whales seem to work like the radiator of an automobile to prevent overheating. The whales' temperature may be thermostatically controlled by varying the fractions of the blood flowing through the heat exchanger or the bypass.

---

*) Scholander, P. F., and W. E. Schevill: Counter-current vascular heat exchange in the fins of whales. J. appl. Physiol., 8: 279—282, 1955.

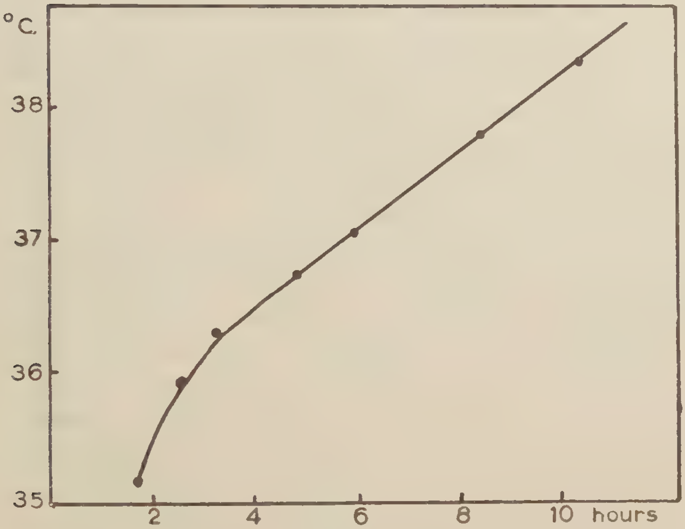

Fig. 1. Temperature in the abdominal cavity of a 54 foot fin whale recorded during towing to the shore station. After 11 hours the belly was split and the measurement had to be stopped.

If this theory is correct, one would find the body uniformly warm and the tail and flippers cold. The change in temperature between the two should occur in the region of the heat exchangers. With this in mind we have attempted to approach the problem by making such temperature measurements. Since large whales are obtained commercially they are the most available. Measurements were to be made on a freshly killed animal. Because of the whale's large size, these temperatures will be very close to those existing before death.

Due to bad weather and a poor season we were only able to make measurements on one animal, a 54 foot fin whale. It was not chased and was apparently killed immediately by the harpoon. The temperature distribution we measured is thus probably close to that of a resting animal.

We were able to make measurements in the abdominal cavity and surrounding body wall, along the peduncle or narrow part of the animal leading to the tail, and also in the tail itself. In addition we followed the temperature in the abdominal cavity and muscle for 20 hours while the whale was towed to the shore station. From these measurements we hoped to get information on the effectiveness of splitting the belly. This is done to cool the animal and thus postpone putrefaction.

The deep muscle and body cavity of the whale had a uniform temperature of 35.6° C. This is within the range of variation found for other mammals and only 1° C below that of man. There was very little temperature drop along the peduncle. At the base of the tail it was still 34.2° C. Half way out the tail fluke the temperature was 25° C 1½ hours after death. The sea water was 12° C. The counter-current system in the fin whale exists through the latter 3 meters of its body. The anatomical arrangement of the blood vessels is much like that described for smaller whales by Scholander and Schevill. Since there was only about 1° temperature drop along this system, it does not seem to function as an efficient heat exchanger in a large whale, and yet a quiet animal such as this should have the most need to conserve heat. There is a surprisingly high temperature well out in the fluke of the tail. Apparently even under such conditions of minimal heat production a large whale can afford the heat to keep its uninsulated tail warm.

The Steinshamn whalers had noted that the tail fluke showed very little bleeding when an animal was killed quietly in the same manner as this one. However, if the whale had been chased for some distance and had struggled after harpooning they found profuse bleeding. This suggests that the whale increased its circulation through the tail, and probably also the flippers, during the periods of greater heat production. This would allow larger amounts of heat to be dissipated from these surfaces. It is unfortunate that measurements could not be made on such an animal to see if one finds the expected warmer body and in particular higher temperatures in the tail and maybe also the flippers.

After death the bacteria in the whale start to multiply rapidly and if allowed to continue will putrefy the flesh, making it inedible. Since this process goes faster at a higher temperature an effort is sometimes made to provide cooling by cutting the belly and allowing the sea water to circulate into the abdominal cavity. Thus it seemed worth while to see what effect this has on the temperature in the rest of the animal. A specially constructed thermometer-spear, with an insulated thermo-sensitive tip, was therefore thrust into the body cavity.

It was left there for 11 hours until the belly was cut. The temperature could conveniently be read at intervals from deck. Heat was produced in the body cavity even after death at a rate which increased the temperature 0.5° C per hour. Since no or very little oxygen was available we can be fairly certain that this heat was due to the growth of bacteria which are always present in large numbers in the digestive system. With the blood no longer circulating in the dead animal the heat cannot be carried away and the temperature rises. The rise in temperature is shown in figure 1.

A thermometer-harpoon left in the muscle 2 meters forward from the tail recorded only a small temperature rise in the first 2 hours. It was then constant for several hours. At the end of 20 hours when the shore station was reached the temperature had fallen less than 1° C. The same thing was observed in the dorsal muscle. The temperature was measured here just before flensing. By this time sea water had been circulating through the abdominal cavity for 7 hours so that the muscle was being cooled from both the inside and the exterior. The temperature was still 34° C in the deep muscle showing that it had cooled only 1.5° C.

It again emphasized how slow a process conduction is for getting rid of heat once circulation has stopped. There may have been some bacterial growth going on in the muscle producing heat. Still the technique of opening the abdominal cavity is only partially effective in cooling the deep muscle of the whale where most of the edible meat lies. The large size of a whale means that the body heat can be discarded quickly only by cutting up the flesh.

We have made measurements on only one animal which was killed immediately, and with the least possible wound. It is possible that bacteria from the gut can spread in large numbers into the muscles if a whale struggles for some time after harpooning. Rotting might then go on much faster in the flesh producing the gas bubbles and «burning» so often noted. In this case, the temperature in the muscle may rise in the manner seen here in the abdominal cavity. There is then a vicious sequence. An increase in temperature causes the bacteria to grow faster which causes a further increase in temperature, and so on.

It is a pleasure to acknowledge the cooperation of the manager and personnel at the Brødrene Sæbjørnsen Whaling Station at Steinshamn, and in particular the crew of the chasers «Berg Bjørn» and «Berg Karl». In another season we hope to continue from this meager start on the problem of how the big whales keep a constant warm temperature under the variety of conditions they find in the sea. In the meantime we may be able to look at the little porpoise, which weighs only 1/1000 as much, and see if there is a different story there.

The investigation was made possible by grants from the State Institute of Whale Research, Oslo, and the Arctic Institute of North America.

A/S HANDELSTRYKKERIET - SANDEFJORD

Contribution No. 882

The Cephalocarida and Crustacean Phylogeny

HOWARD L. SANDERS

Reprinted from Systematic Zoology
Volume 6, Number 3, September 1957

The Cephalocarida and Crustacean Phylogeny

HOWARD L. SANDERS

CRUSTACEAN phylogeny has intrigued zoologists for almost one hundred years. Despite the long sustained interest, this problem still remains largely unclarified due to the fact that each subclass forms a sharp, clearly defined taxonomic unit.

Initial observations (Sanders, 1955) on the newly described crustacean *Hutchinsoniella macracantha* seemed to disclose affinities with the more primitive representatives of the subclasses Branchiopoda, Malacostraca and Copepoda. In an effort to indicate crustacean phylogeny as well as to illustrate the affinities of the Cephalocarida with the extant subclasses of Crustacea, this second paper will compare the Paleozoic arthropods, particularly the Crustacea, with the crustacean subclass Cephalocarida, as exemplified by *Hutchinsoniella.*

Subsequent to the original description, which was based on eight individuals, 320 additional specimens, representing all free-living stages of *Hutchinsoniella macracantha,* have been collected from Long Island Sound, and more recently, Buzzards Bay, Massachusetts by this investigator. On the basis of this material a few observations on the life history of *Hutchinsoniella* and some additional pertinent details on cephalocarid anatomy can now be discussed. These animals are found subtidally in soft mud where the benthic fauna is dominated by the polychaete *Nephthys incisa* and the lamellibranch *Nucula proxima.* A description of development from hatching to maturity will be presented in a subsequent paper.

Recent studies reveal that *Hutchinsoniella* is a hermaphrodite with entirely separate functional ovaries and testes (manuscript in preparation). Individuals are ovigerous from June through September and carry two ovisacs each attached by a short stalk to the limb rudiments of the genital segment. Each ovisac contains a single embryo. Observations in the laboratory indicate that a female can bear only three broods or six embryos during the breeding season. This is a remarkably small recruitment for a marine invertebrate.

Morphological Findings

Additional specimens have made it possible to describe more completely and to reinterpret cephalic and thoracic appendages (Figs. 1, 2 and 3) as well as to observe that ten rather than nine somites comprise the abdomen of the adult. Setae are missing on some of the limb figures and, unless otherwise stated, are considered as being lost in the preparation of the slide. Very fine hairs can be shown on setae and certain limb segments. It is assumed that these very fine structures may be present but not discernable on limbs, limb segments or setae that appear to lack them. The first thoracic appendage in the initial description is now considered to be the second maxilla. The reason for this interpretation is given on page 124, line 3. As a result, there are nine postcephalic appendages rather than ten, and twenty postcephalic segments, including the telson. A thoracic appendage, such as limb three, corresponds to limb four of the original description.

First antennae or antennules (Fig. 1, *A*): with six wide basal points and thin terminal strap-shaped filamentous portion of about 35 joints. Distal surface of second basal segment bearing small single-jointed flagellum with two setae (*B*). Initial joint of filament about equal to length of next four. Clusters of six and five setae on distal edges of third and sixth basal segments.

Second antennae (Fig. 1, *C*): with two-

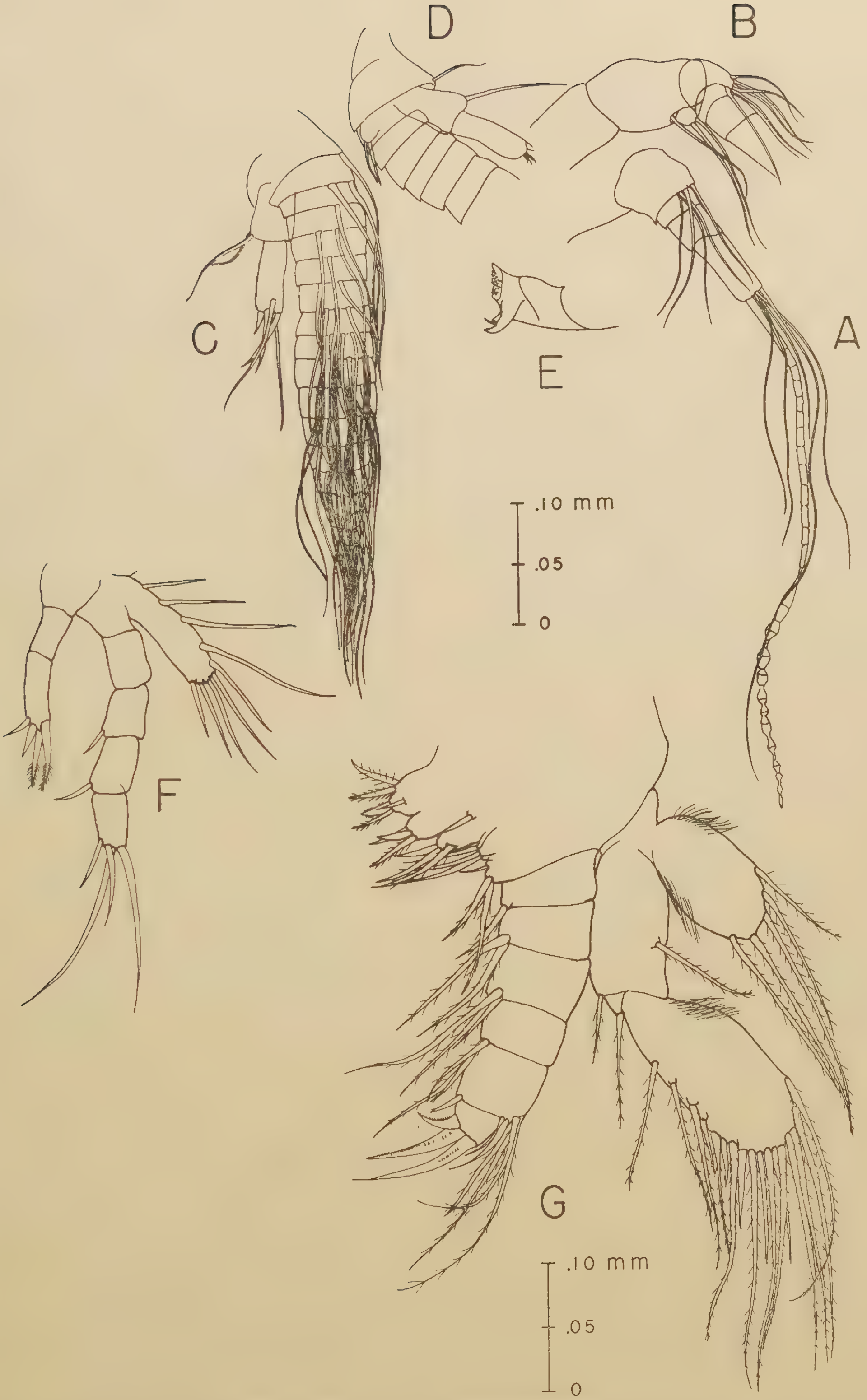

FIG. 1. *A*, first antenna with terminal part of filamentous portion twisted. *B*, basal section of first antenna, showing small articulating knob. *C*, second antenna. *D*, basal section of second antenna, showing knoblike eminence. *E*, mandible. *F*, first maxilla. *G*, second maxilla.

jointed protopodite, bearing knoblike eminence with setae (*D*), and two rami, one a two-jointed endopodite with second segment rectangular with two spines and three setae on distal end, other a large club-shaped exopodite composed of about eighteen joints covered with numerous long setae.

Mandibles (Fig. 1, *E*): without palp, median surface forming grinding molar plate covered with numerous tiny papillae and incisor component of two spines with movable bristle in between.

First pair of maxillae (Fig. 1, *F*): biramous protopodite with elongate two-jointed gnathobase bearing four spines on distal end, two of which have terminal portion covered with fine hairs; five-jointed endopodite with single spine on second and third segments with one long and two shorter spines on fourth segment and terminating with long spine-like dactyl; single-jointed flattened oblong exopodite with nine setae on lateral and distal margins.

Second maxillae and first eight thoracic limbs: all essentially similar. Thoracic appendages six, seven and eight (Fig. 3, *B*, *C* and *D*) successively smaller in size. Thoracic appendage nine has two segments, a small round distal joint on anterior part of larger oblong segment (Fig. 3, *E*). Protopodite apparently unsegmented although there are indications of a possible precoxal suture. Endopodite seven-jointed, distal segment dactyl with shorter medial and longer lateral spine inserting on penultimate segment about half as wide as more proximal joints; segments two, three, four and five similar; segment one wider than others with medial margin longer than lateral. Setae on outer distal edge of first five segments with one or two on first, two or three on second, two or three on third, three on fourth and one on fifth segment, usually haired; cluster of six setae on inner distal margin of fifth segment; terminal spines and dactyl with series of small teeth on inner surface. Endopodite of seventh appendage (Fig. 3, *C*) with fewer setae on each segment, one long spine with teeth rather than cluster of setae on inner margin of fifth segment; long terminal spine fused with dactyl to form elongate conical structure slightly globular at apex which with penultimate segment is markedly flexed toward the midline. Eighth limb with endopodite absent, Fig. 3, *D*). Exopodite four-jointed, flattened; ultimate joint circular in outline, about eighteen setae fringe distal and medial margin with longest on distal edge, setae of two kinds, approximately twelve or thirteen haired setae and four or five shorter bifid setae inserted in slightly different plane, numerous very fine hairs bordering proximal lateral margin; penultimate segment (fused to segment two in appendage eight) small and triangular on medial aspect of ramus and bearing single seta at apex; second segment hexangular, with single seta on distal medial edge, absent on eighth limb and single seta on lateral margin missing on limbs six, seven and eight; first segment somewhat triangular with outer edge giving rise to flattened oar-like pseudepipodite with about seven or eight haired setae on distal third of segment with perhaps less setae on limb eight, both proximal margins bordered by numerous fine hairs.

Medial surface of protopodite with complex six-lobed gnathobase, except five-lobed on second maxilla; gnathic processes reduced on appendage eight. All lobes articulate; proximal four lobes (three in second maxilla) larger; first with two hairy short setae on proximal edge and two short thick spines, one of which is toothed, on medial surface with single short seta inserting below and between spines; second lobe similar to first with two spines and single seta; third lobe with three spines and one seta; fourth with three spines and one or two setae; fifth and sixth lobes each with two setae; somewhat parallel row of about twelve or thirteen setae, oriented at slightly more oblique angle, present along base of lobes. Lines of very fine hairs on the protopodite and endopodite (Fig. 2, *C* and *D*) of some limbs, and combs of hair present on some appendages near proximal medial edge of protopodite (Fig. 2,*D* and Fig. 3,*C*).

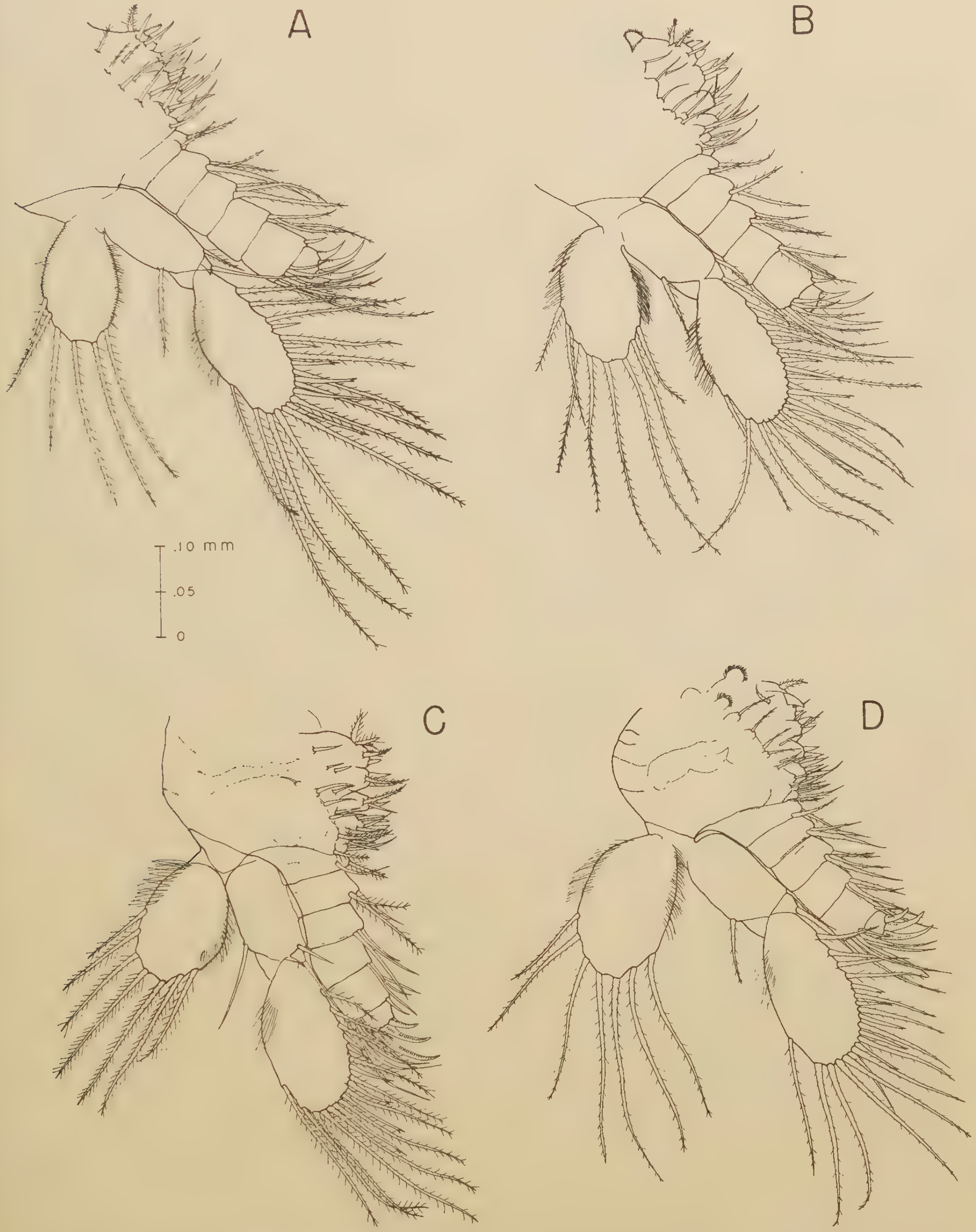

FIG. 2. *A,* first thoracic appendage. *B,* second thoracic appendage. *C,* third thoracic appendage. *D,* fourth thoracic appendage.

Paleozoic Arthropods

It has been assumed by many paleontologists and zoologists that the long extinct arthropods known as trilobites were the ancestors of the Crustacea. Except for the first pair of cephalic limbs which were uniramous, these primitive animals car-

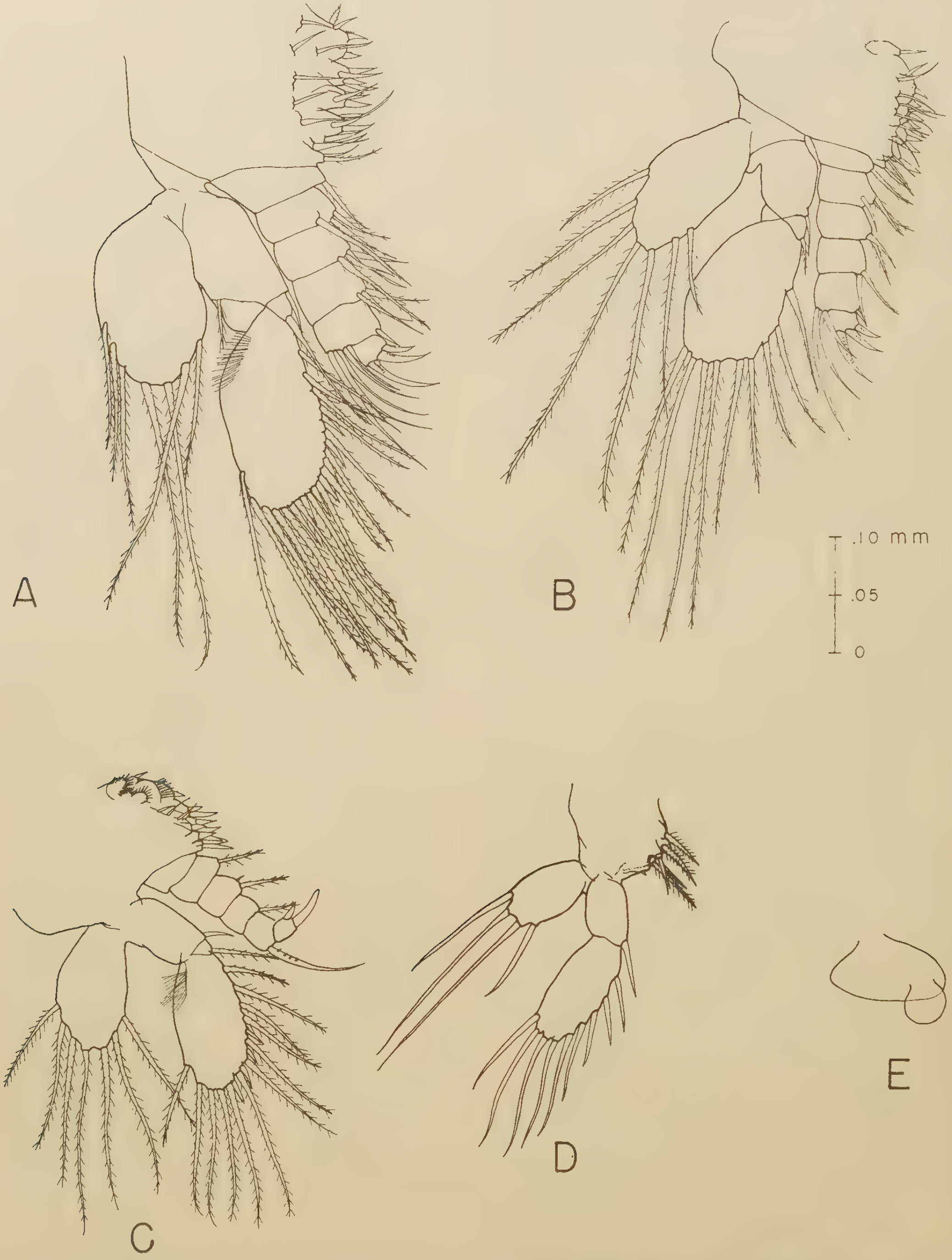

FIG. 3. *A,* fifth thoracic appendage. *B,* sixth thoracic appendage. *C,* seventh thoracic appendage. *D,* eighth thoracic appendage. *E,* ninth thoracic appendage.

ried a series of identical biramous appendages on both the head and the trunk; the first four pair were always restricted to the head. The dorsal shield was divided into three parts, a median axis and lateral pleura.

However, Størmer, in a series of papers (1939, 1942, 1944) dealing with trilobite morphology took sharp issue with this concept. He felt the features that decisively separated the trilobites from the Crustacea were:

1. Trilobation of the dorsal shield and presence of pleura.
2. Tendency towards formation of a styliform telson.
3. Highly ramified intestinal diverticula.
4. Four postoral segments in the larva rather than two.
5. Absence of trilobite appendage in any crustacean.

He carefully documented affinities of the trilobites with the Arachnida, Eurypterida and Xiphosura and placed all these groups in the phylum Arachnomorpha. The phylum, according to Størmer, consists of two subphyla: the Chelicerata, comprising the Eurypterida, Xiphosura and Arachnida; and the Trilobitomorpha, consisting of the Trilobita and a most remarkable assemblage of excellently preserved, mid-Cambrian arthropod fossils from the Burgess Shale deposits of British Columbia.

This latter group presented great diversity in form although they all shared the trilobite limbs; the first head limb was uniramous and all the remaining appendages were biramous and identical, consisting of a seven-jointed endopodite (telopodite) and a flagellar—supposedly respiratory—exopodite (pre-epipodite). In a few forms, however, the second appendage was somewhat modified. Some of these fossils showed affinities with the merostomes while others, at least superficially, indicated crustacean relationships. In certain forms (*Burgessia, Waptia and Hymenocaris*) a carapace was present; the telson was either styliform or possessed caudal rami (*Yohoia, Waptia, Hymenocaris*); the dorsal shield had or lacked pleura; eyes were either sessile or pedunculate and the number of body segments varied widely.

Despite the fact that some of these Cambrian arthropods resembled the crustaceans in the development of a carapace, pedunculate eyes and caudal rami, Størmer (1944) contended that they conformed exactly with the trilobites and the merostomes of the same formation in the structure of the limbs and in the presence of intestinal diverticula. In fact, Størmer postulated that the Crustacea and Arachnomorpha developed independently:

> In spite of the crustacean characters exhibited in certain genera the present author is not inclined to assume an evolution of the Crustacea from groups related to the Trilobita. The chief objection to such a relationship is the complete lack of trilobitan appendages in Crustacea. Calman is obviously right in warning against putting too much weight on more isolated coincidences, or lack of coincidences in structure, but the presence of the characteristic trilobitan limb in many different groups of the Arachnomorpha can hardly be regarded as an isolated coincidence. We have seen how the primitive trilobitan limb is found, more or less modified, in very different groups and traced even in terrestrial forms. It seems therefore difficult to understand why this conservative structure evidently is not preserved in any of the numerous aquatic Crustacea, not even in Devonian representatives. The peculiar development of the intestinal diverticula is, with the exception of a few parasitic copepods, apparently unknown in the Crustacea. Perhaps the most important difference between the Crustacea and Arachnomorpha is the probably different number of larval segments in the two groups.
>
> For these reasons the present author is preliminarily inclined to regard the crustacean-like members of the Trilobitomorpha as not related to the Crustacea. [Størmer, 1944]

Probably the most decisive difference is that the Burgess Shale fossils lacked mouth parts while Crustacea, in common with Insecta and Myriopoda, are mandibulates. Thus by definition these fossils were not crustaceans, although with the modification of the cephalic limbs, the Crustacea, conceivably, could have been derived from such forms.

In the light of the morphology of the Cephalocarida, how valid is Størmer's thesis? Preliminary observations of newly hatched larvae of *Hutchinsoniella* reveal that, unlike other crustaceans, at least three rather than two postoral somites are present. Yet it is questionable how significant this characteristic is, since the four postoral segments found in the trilobite larva may have represented merely a later stage of hatching.

The pronounced ramification of the intestinal diverticula in the Arachnomorpha may be related to the absence of mouth parts. With the elaboration of these latter structures in the crustaceans, need the complexity of the gut persist? Størmer himself pointed out that intestinal diverticulae are found only in certain parasitic copepods among the crustaceans. Interestingly enough, the mouthparts are secondarily lost in these forms, although the ramification of the gut may be merely a response to the parasitic sucking habit.

Hutchinsoniella agrees with the trilobites in having a tripartite dorsal shield with well developed pleura.

Finally, *Hutchinsoniella,* in common with the Trilobitomorpha, is the only known crustacean that has a seven-jointed endopodite with gnathobases on the coxopodite. Thus this animal possesses a limb very much like that of a trilobite.

The justification for assuming that one of the so-called "terminal spines" of the cephalocarid endopodite is a dactyl might be questioned. Sectioned material reveals a muscle band entering the middle "spine" as well as the presence of a well-developed articulating membrane. Furthermore, observations on a living specimen under the microscope show occasional flexures of this same dactyl on the endopodite of the first maxilla as well as on the seven-segmented endopodite posterior to it.

The only serious discrepancy in this comparison is that the exopodite is borne distally on the protopodite rather than proximally as in the trilobites (Fig. 4). Since the protopodite of the Cephalocarida is apparently unsegmented, an increase in growth proximally coupled with a decreased rate of growth distally could displace an initially proximal exopodite to a terminal position. However, if the crustaceans arose from a common ancestor, then the limb as found in *Hutchinsoniella* represents an ideal transitional stage.

Such a view might be criticized on the basis of the trilobite limb having a precoxal segment. Snodgrass (1956), among others, questions the presence of a precoxal segment in the trilobites and sug-

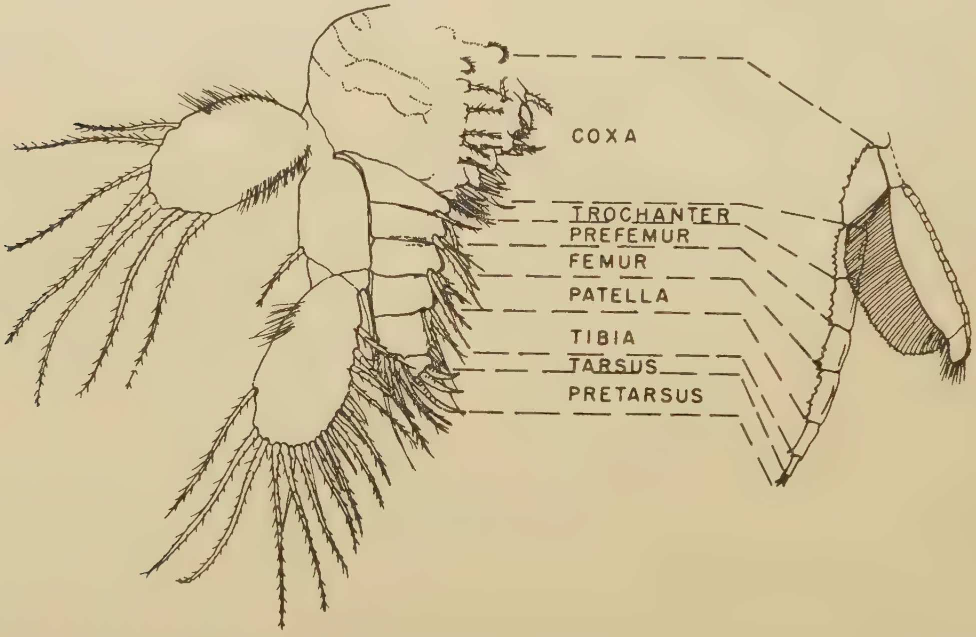

FIG. 4. A comparison of the trilobite (right, *Neolonus serratus,* adapted from Størmer, 1939) and cephalocarid limbs.

gests that the narrow "precoxa" may merely be an internally strengthened ridge for muscle attachment. Concerning the number of segments present in the arthropod limb, he states "If all the podomeres in the legs of the trilobite . . . are true musculated segments, the ancient arthropods had eight limb segments, including a small apical dactylopodite . . . and thus possessed all the segments that are present in any of the legs of modern arthropods. Among the latter, eight segments are present in Pycnogonida and in the legs of the arachnid Solpugidae. . . . The legs of the chilopods and the decapods have seven segments; the insect leg has only six segments. . . ." Therefore *Hutchinsoniella* is the only known mandibulate that retains the primitive arthropod eight-segmented limb pattern.

It is conceivable that the triramous cephalocarid appendage may more closely approximate the limb of the arthropod ancestor than the trilobite appendage does. In such a case the trilobite exopodite would be homologous to either the cephalocarid exopodite or pseudepipodite. Possibly the protocrustacean exoskeleton was only slightly calcified as is the case in modern mysids. In contrast to the trilobites, there is little likelihood that such animals would leave a fossil record. Certainly if one assumes an annelid ancestry for the arthropods, the Crustacea and particularly the Cephalocarida, come closer in approximating such a form than did the trilobites on the basis of a more vermiform shape and the position of the anus. Whatever the true situation may be, the cephalocarid limb does indicate that the Crustacea and the Trilobita were not independently derived.

The evidence obtained from the external anatomy of *Hutchinsoniella macracantha* would seem to indicate that the early crustaceans could have readily been derived from forms similar to the mid-Cambrian pseudocrustaceans.

The evidence of true crustacean remains during the Paleozoic era are few and widely scattered. Triebel (1941) obtained valves with muscle scars from supposed ostracods from the late Silurian. Such information is of little value to this study since none of the anatomy had been preserved.

Brioli (1928) described an obvious malacostracan, *Nahecaris Sturtzi,* with clearly defined first and second antennae, an eight-segmented abdomen and a definite caudal furca from the early Devonian Hunsdruck Shale of Germany. Its relationship to the extant order Leptostraca seems evident, although the abdominal segments are reduced to seven in the latter.

By far the best documented of the early fossil crustaceans is the mid-Devonian *Lepidocaris rhyniensis* described by Scourfield (1926) from the Rhynie Chert deposits of Scotland. The affinities of this animal to the Branchiopoda, particularly the order Anostraca, are striking. It possessed the naupliar first and second antennae of that group, as well as palpless mandibles, reduced first maxillae, a cervical groove, foliaceous limbs with gnathobases on the first three trunk segments, and lacked a dorsal carapace. *Lepidocaris* most probably was related to the forms that gave rise to the modern branchiopodans.

Despite this, the similarities between *Lepidocaris* and *Hutchinsoniella* are conspicuous in the overall length of 3 mm, the general form and the presence of pleura (Fig. 5). Both forms agree in having gnathobases on some (*Lepidocaris*) or all (*Hutchinsoniella*) of their trunk appendages. The first maxilla in *Lepidocaris* is highly reminiscent of the gnathic process of the biramous first maxilla of the adult *Hutchinsoniella.*

The extreme primitiveness of *Lepidocaris* is demonstrated by the fact that it maintained the masticatory process on the second antenna almost to the adult stage, a structure present only in the nauplii of the branchiopods, copepods and cirripedes. The only other known crustacean where such a masticatory process is retained to such a late stage is *Hutchinsoniella* (see Fig. 7, *B*).

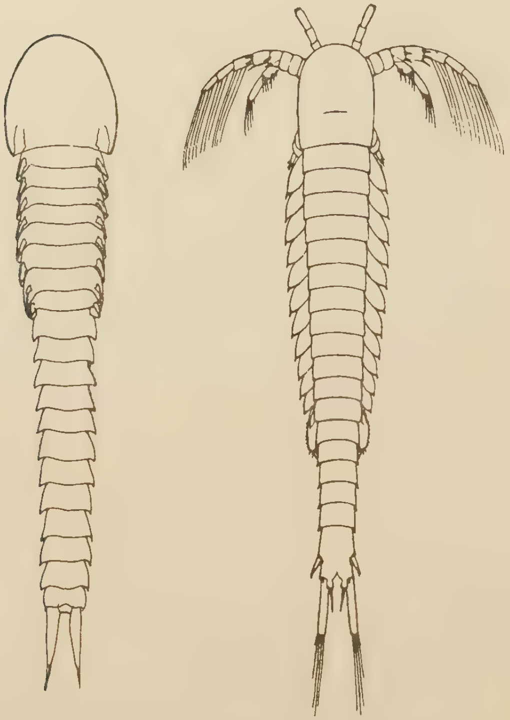

FIG. 5. The extant *Hutchinsoniella macracantha* (left) and the mid-Devonian fossil, *Lepidocaris rhyniensis* (right, after Scourfield, 1926).

Remane, on the basis of the original description of *Hutchinsoniella,* was so impressed by the similarities of these two animals that he suggested in a recent paper (1956)

> Fast könnte man versucht sein, *Lepidocaris* mit *Hutchinsoniella* in die Ordnung der Cephalocarida einzureihen, dann wäre *Hutchinsoniella* ein rezenter Vertreter einer bisher fossil aus dem Paläozoikum bekannten Ordnung, und eine Zeitungsnotiz hätte Recht, nach der dieser Fund ebenso wichtig wäre wie des berühmten Fisches *Latimeria.*

Thus despite the 300 million years that separate these two forms, it is apparent that *Lepidocaris* represents the closest known relative of the extant cephalocarid, *Hutchinsoniella macracantha,* and yet the living species must be considered the more primitive due to its only slightly modified first maxilla, the wholly unmodified second maxilla and its trilobite-like appendages.

Derivation of the Crustacean Trunk Limbs

Because of the large number of distinctive morphological characters common to both these forms, it might prove profitable to compare the thoracic appendages closely. On casual observation they seem widely different; in the Devonian form there is a gradual change from unmistakable foliaceous anterior appendages with gnathobases to copepodan biramous limbs lacking gnathobases on the posterior thorax; while the cephalocarid limb is trilobite-like with a seven-jointed walking endopodite, an exopodite consisting of two large flattened segments separated by a small articulating joint, and an oar-like flattened pseudepipodite.

Yet, if the endopodite in the cephalocarid limb were lost, the resultant appendage would be almost identical with the second and third trunk limbs of *Lepidocaris.* This does actually occur in the eighth postcephalic limb of *Hutchinsoniella* (Fig. 3, *D*).

It is therefore possible to trace by a continuous series of steps the evolution of the trilobite limb as found in the cephalocarid to the foliaceous on one hand (Fig. 6, *1* to *5*), and the biramous copepodan on the other (Fig. 6, *1, 2, 3, 6, 7*). With a reduction of a single segment in the endopodite and a loss of the gnathic processes on the coxa, the cephalocarid appendage can be converted into a limb characteristic of the primitive Malacostraca (*8*). In the primitive Leptostraca we find appendages that are highly reminiscent of the cephalocaridan plan. Again the cephalocarid endopodite together with gnathobases, is reflected in the second maxilla of a larval penaeid shrimp * (*9*).

One might justifiably criticize the derivation of a two-jointed protopodite as exemplified by *Nebalia* from an unjointed cephalocarid protopodite. Therefore it may be necessary to postulate an appendage that is similar in every way to the

---

* In a very recent paper (1957) Heegaard observed that both an exopod and pseudexopod form and later coalesce with part of the basis during the development of the second maxilla in a number of decapods. Such a stage can be interpreted as having the homologous parts of the cephalocarid appendage.

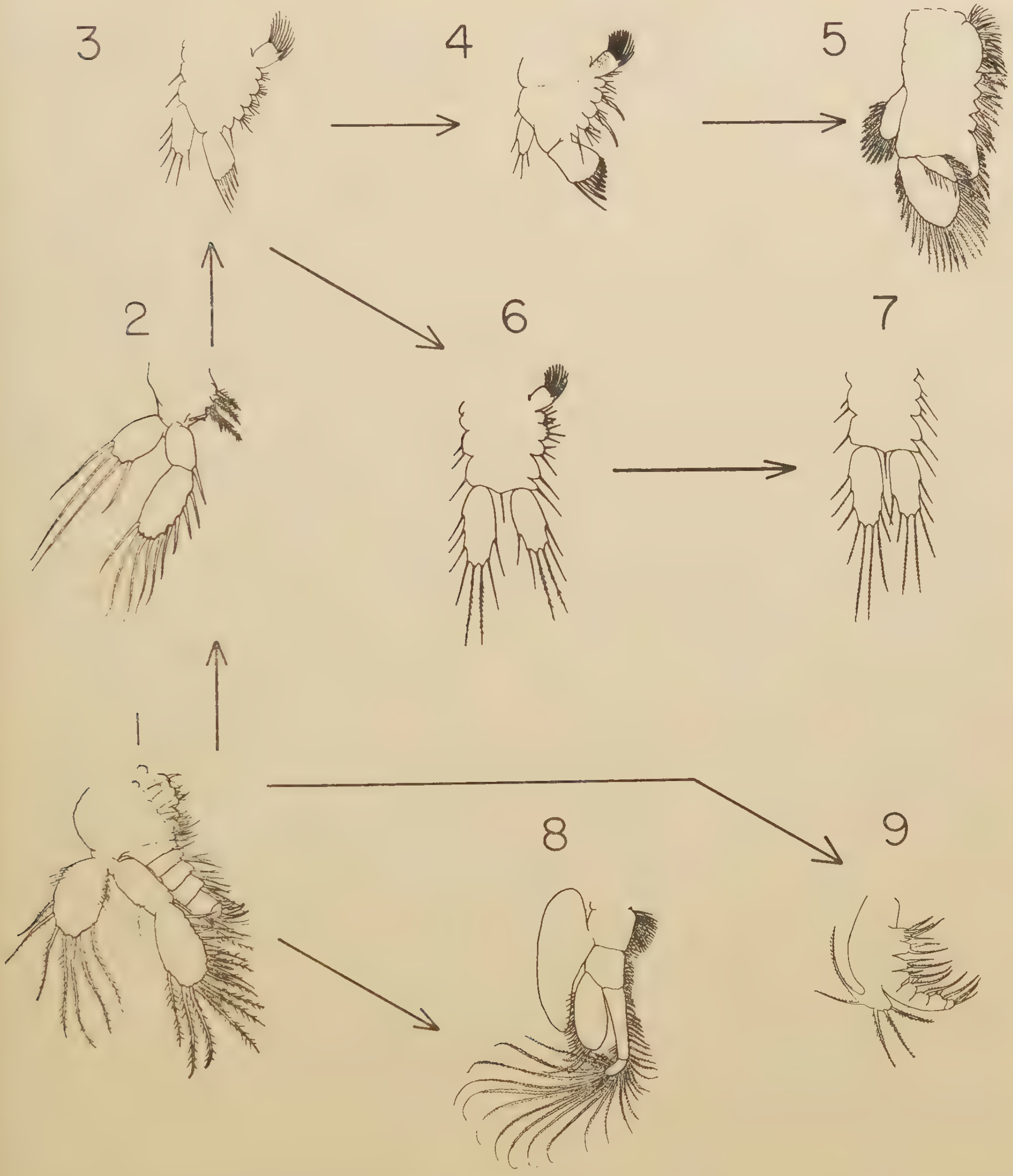

FIG. 6. Scheme showing the possible evolution of the various crustacean appendages from the cephalocarid limb. *1,* fourth thoracic appendage of *Hutchinsoniella. 2,* eighth thoracic appendage of *Hutchinsoniella. 3,* second or third thoracic limb of *Lepidocaris* (Scourfield, 1926). *4,* first thoracic limb of *Lepidocaris* (Scourfield, 1926). *5,* foliaceous thoracic appendage of *Branchionecta paludosa* (redrawn from G. O. Sars, 1896). *6,* fourth to sixth(?) trunk limb of *Lepidocaris* (Scourfield, 1926). *7,* biramous copepodan seventh(?) to eleventh trunk limb of *Lepidocaris* (Scourfield, 1926). *8,* malacostracan thoracic appendage as exemplified by *Nebalia bipes* (redrawn from G. O. Sars, 1896). *9,* second maxilla of a penaeid larva (Claus, 1886). All limbs oriented with endopodite on the right.

cephalocarid limb except that a basipodite is present which separates the exopodite from the pseudepipodite. Such a limb could readily serve as a precursor to the primitive malacostracan appendage. However, this writer can see no objection to the concept of a jointed protopodite evolving from an unjointed one if granted adequate time. For example, the elongation of an unjointed protopodite may make it functionally feasible for an additional segment or two to develop within the protopodite.

This scheme indicates that all known basic types of crustacean limbs could have evolved from an appendage similar to the modern cephalocarid limb which, in itself, is a slightly modified trilobite appendage. Comparing the foliaceous and cephalocarid limbs, (Fig. 6, *5* and *1*), it is apparent that the flabellum is homologous to the pseudepipodite and the apical lobe is derived from the exopodite. Regarding the copepodan type of appendage, the exopodite can be derived from the pseudepipodite and the endopodite from the cephalocarid exopodite (*7* and *1*). Only when contrasting the malacostracan and cephalocarid limbs are the endopodites and exopodites directly homologous (*1* and *8*).

There is one perplexing aspect to this proposed plan of evolution, that is, why should the so-called primitive appendage as exemplified by the Cephalocarida be more complex in structure than the limbs derived from it? In other words, has evolution in regard to the crustacean limb consisted of reduction and simplification? The Arachnomorpha generally have complicated appendages with complex gnathic processes and spines. Among the Trilobitomorpha all appendages except the first antenna had both a trophic and motile function with no limb specialized for any one specific purpose. With the alteration of the mandibles and the first and second maxillae primarily for feeding in the crustaceans, there has been a corresponding modification of the natatory parts as well as a tendency to lose the trophic function of the postcephalic appendages. Trunk limbs that have gnathobases are found today only in the foliaceous appendage of the branchiopods and in the cephalocarids as represented by *Hutchinsoniella.*

Serial Homologies

Observations on living specimens of *Hutchinsoniella* indicate that all limbs have two functions: the first and second antennae, besides the usual sensory function, are utilized in swimming and crawling; each of the remaining limbs is used jointly for locomotion and feeding. The limb movements are metachronal.

All appendages in *Hutchinsoniella,* including the first antenna, are biramous, and if one is inclined to regard as additional rami the pseudepipodite on the thoracic legs, the long gnathic structure on the first maxilla and the masticatory process on the second antenna, then such appendages can be considered triramous. There is one limb, however, that departs widely from this generalized limb pattern and that is the highly reduced, palpless, mandible (Fig. 1, *E*).

Due to the sharp deviation in plan exhibited by the mandible in the adult, it was thought advisable to study a younger stage. Two animals were examined from a juvenile stage with ten postcephalic segments and three postcephalic limbs. The figures of the head appendages are shown in Figure 7. Several things are immediately evident from the illustrations. The mandible at this stage (Fig. 7, *D*) bears a palp made up of a six-jointed exopodite and a bifurcated endopodite; the appearance of the limb is not unlike the same structure in the calanoid copepods. The first antenna (Fig. 7, *A*) is similar to that of the adult, although the flagellum (the articulating knob) is more prominent. This structure somewhat resembles the first antenna of the syncarid malacostracan *Bathynella* (see Siewing, 1956). The exopodite of the second antenna (Fig. 7, *B*) is relatively less massive than in the adult and the setae seem to be restricted to the medial and distal surfaces. A prominent masticatory process is present at the base of the appendage (Fig. 7, *C*). The maxilla (Fig. 7, *E*) appears to lack the large

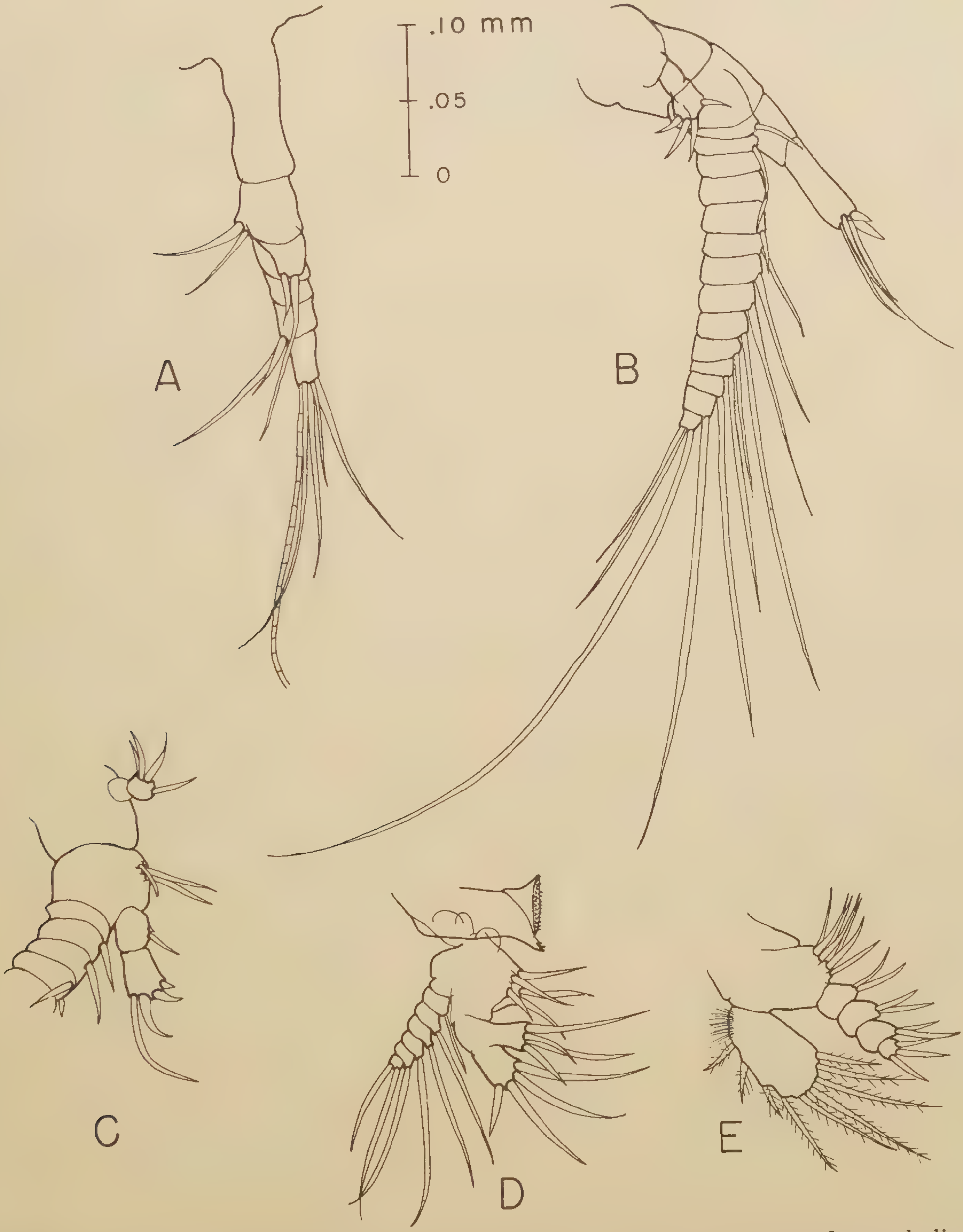

FIG. 7. The juvenile cephalic appendages of *Hutchinsoniella macracantha,* excluding the second maxilla. *A,* first antenna. *B,* second antenna. *C,* base of second antenna, showing gnathic spines between endopodite and masticatory process. *D,* mandible. *E,* first maxilla. Limbs oriented with endopodite on the right.

gnathic process found in the adult, but instead has gnathic spines on the protopodite. Similar spines on the same part of the limb are present on the mandible (Fig. 7, *D*) and the second antenna (Fig. 7, *C*). It is highly probable that these structures, because of their function and location, are homologous to the gnathobases of the thoracic limbs. The second antenna and mandible are remarkably alike; one is inclined to feel that the masticatory processes (which largely makes up the adult mandible) proximally located on the limbs are homologous structures.

It should be mentioned at this point that the second maxilla in both the adult and juvenile is similar in appearance to the trunk limb series. No limb rudiment appears in the ontogeny of *Hutchinsoniella* between this appendage and the first maxilla. In those cases where the second maxilla is secondarily lost in the Crustacea, the first maxilla is appreciably reduced. On the other hand, *Hutchinsoniella* possesses the least modified first maxilla of any known crustacean. It is most probable that *Hutchinsoniella* represents a stage in the evolution of the crustaceans wherein the last cephalic limb represents the as yet unmodified precursor of the second maxilla as found in the other groups.

This study indicates a common basic limb-pattern and implies a strong serial homology among all appendages, excepting, perhaps, the first antenna. Within this limb plan two subseries seem evident: the second antenna and mandible with a many-jointed exopodite, and the first and second maxillae and the trunk limbs with a many-jointed endopodite. It is of some interest that the biramous limb-structure plan with gnathic spines on the coxal segment was precisely the scheme found in the Trilobitomorpha.

Homology of the Cephalic Limbs

How similar are these juvenile cephalic appendages to the same structures in the other crustacean groups? Can a common basic plan be detected in those subclasses where the head appendages have not been markedly modified? The calanoid copepod, *Paracalanus parvus* as described by Sars (1903, Plate VIII) and the cladocopan ostracod, *Polycope punctata* (Sars, 1928, Plate XV) were selected for this comparison. Both of these forms are usually thought of as being representative of the more primitive elements within their subclasses. In addition, the type species of the subclass Mystacocarida, *Derocheilocaris typicus* (Pennak and Zinn, 1943, Plate 2) and the nauplius stage of the barnacle, *Balanus trigonus* (Sandison, 1954, fig. 6) were also included. The second antenna, mandible and first maxilla of these animals, together with the same juvenile head structures of *Hutchinsoniella,* are figured in Figure 8.

The second antennae are remarkably alike in all groups, consisting of an exopodite of numerous segments, each giving rise to a single long seta and the apical joint which bears two or three setae. Except for *Derocheilocaris,* these long setae insert on the inner aspect of the ramus, although Dahl (1952) figures the second antenna in *D. galvarini* with setae on the medial edge. The endopodite always consists of fewer segments than the exopodite. In those forms where the juvenile stages are figured (*Hutchinsoniella, Derocheilocaris* and *Balanus*) the masticatory process is clearly evident.

The mandibles of these widely separated crustaceans show pronounced morphological similarity and, at the same time, bear strong structural resemblance to the second antennae. The exopodite, except in the case of the ostracod representative, consists of numerous segments, with the joints in most cases supporting a single long seta on their inner margins. The endopodite is made up of fewer segments. Gnathic spines are present on the medial aspect of the protopodite although this is less apparent in *Derocheilocaris.*

The first maxilla shows more diversity. The cephalocarid limb seems to be the least modified, having as it does a five-jointed endopodite, a single-jointed flat exopodite, and gnathic processes on the protopodite. This same scheme can be detected in the copepodan and ostracod maxillae, although there is an evident reduction of the endopodite segments and a general fusion of the limb. In the Mystacocarida the exopodite disappears. The first maxilla is not yet formed in the cirripede nauplius.

The comparison reveals remarkable similarity in the cephalic appendages of some of the less specialized representatives of five crustacean subclasses. Among these animals, *Hutchinsoniella* must be

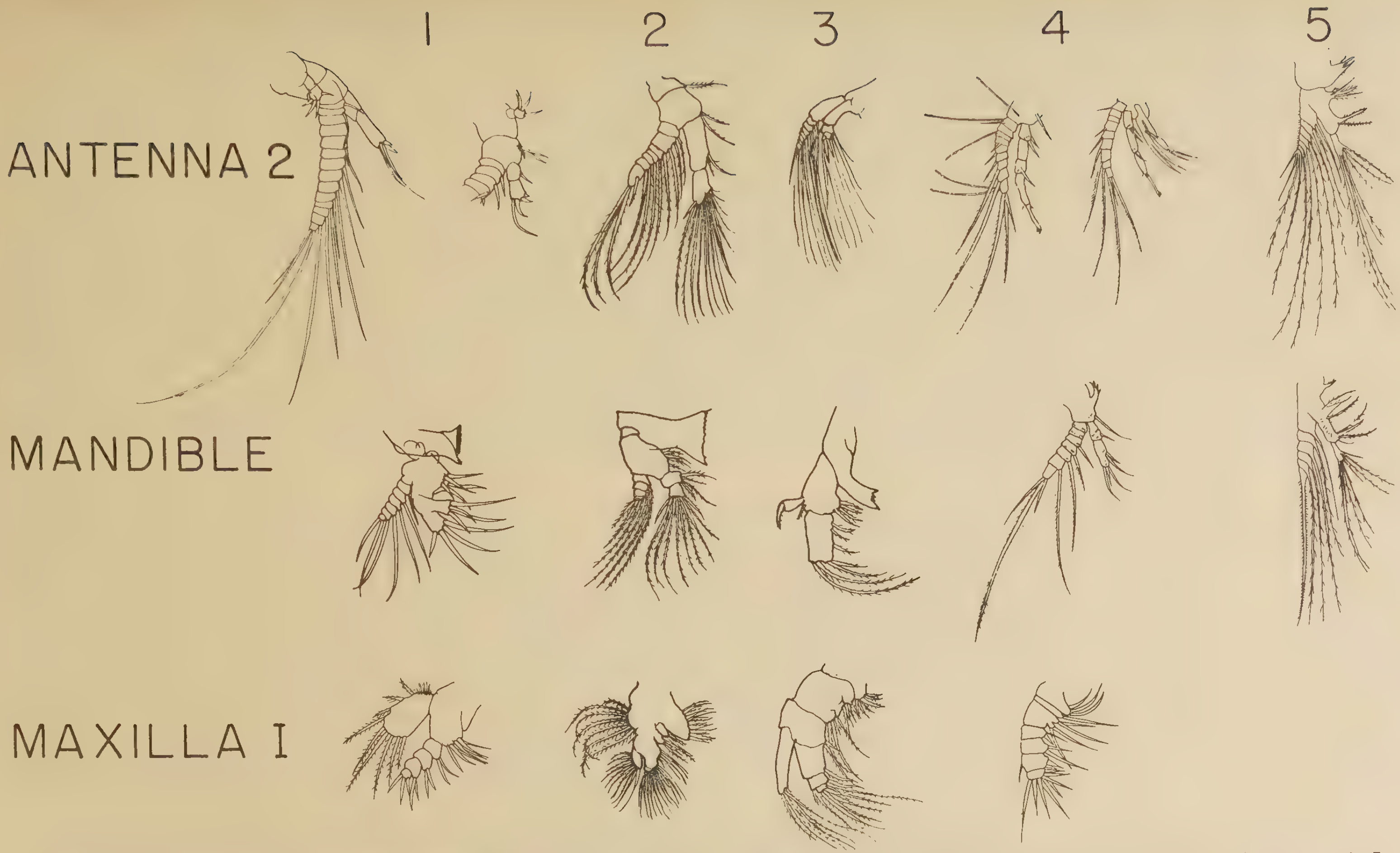

FIG. 8. A comparison of the second antenna, mandible and first maxilla among representatives of five crustacean subclasses. *1.* Juvenile limbs of the cephalocarid, *Hutchinsoniella macracantha.* *2.* Adult appendages of the calanoid copepod, *Paracalanus parvus* (redrawn from Sars, 1903). *3.* Adult limbs of the cladocopan ostracod, *Polycope punctata* (redrawn from Sars, 1928). *4.* Appendages of the mystacocaridan, *Derocheilocaris typicus;* antenna 2 on right is juvenile structure (Pennak and Zinn, 1943). *5.* Naupliar appendages of the cirripedian, *Balanus trigonus* (Sandison, 1954). All limbs oriented with endopodite on the right.

considered as more closely approximating the primitive condition primarily because of the generalized first and second maxillae.

Hutchinsoniella *and the Crustacean Ancestor*

How does *Hutchinsoniella* compare with the hypothetical crustacean ancestor as interpreted by various morphologists? MacBride (1914) stated

> We can now form a picture of the course which evolution followed in transforming the ancestor represented by a Nauplius to a primitive crustacean. The second antenna became gradually shifted forward and lost its masticatory function, while the third appendage became exclusively masticatory and its distal joints shrank to an insignificant palp. At this stage of evolution the animal was assisted in mastication by the modification of the appendage of the next two or three segments, which formed maxillae, but which were never greatly changed from their original parapodia-like condition.

Except for MacBride's belief that the foliaceous trunk limb was the primitive appendage, and the almost unmodified condition of the first and second maxillae in *Hutchinsoniella,* there is no great discrepancy between his prototype and the extant cephalocarid.

The "Urphyllopod" or original crustacean of Claus (1876) was thought to have a mandibular foot and more strongly developed foot-like maxillae. The second antennae were considered to be used in locomotion and feeding and "sie besassen die kräftigen Mundhaken und eine Gestaltung, wie sie in der Larvenzeit des Copepodon, Cirripedien und Phyllopoden so überraschend ähnlich sich wiederhalt." The trunk limbs were considered as being "im Einzelen selbst sehr verschieden gestalteten Phyllopodenfüssen und den Spaltfüssen der Schizopoden standen." The cephalocarid limb, with gnathobases on a mixopodium, has components of both the phyllopod and biramous appendage. *Hutchinsoniella* has, almost to the adult stage, a second antenna and mandible that are utilized both in locomotion and food manipulation. Furthermore, the cephalocarid first maxilla is indeed foot-like, and the second maxilla is almost identical to the trunk limbs.

Calman (1909) wrote

> In order to reconstruct the hypothetical ancestral type, therefore, it is necessary to combine the characters of several existing groups. It may be supposed to have approximated, in general form, to Apus, with an elongated body of numerous similar somites, terminating in a caudal furca; with the postoral appendages all similar, and with a carapace originating as a shell-fold from the maxillary region. The eyes were probably stalked and movable, the antennules uniramous, and the antennae and mandibles biramous and natatory, and both armed with masticatory processes. The trunk limbs were probably biramous but with additional endites and exites, and all provided with gnathobases.

It is questionable whether the stalked eyes are a primitive condition, and neglecting the first antenna, *Hutchinsoniella* readily approximates Calman's hypothetical ancestral type.

After carefully surveying the various major crustacean groups, Dahl (1956) concluded "the evidence brought forward . . . indicates that the Crustacea, and probably other Arthropods as well, had originally a ventral mouth, more or less ventral (antennae and) antennulae and a more or less straight central nervous system. Any other supposed arrangement will be inconsistant with the morphological facts." This description can be applied directly to *Hutchinsoniella.*

It is evident that *Hutchinsoniella macracantha* comes remarkably close to these interpretations of the crustacean ancestor. Can this cephalocarid be regarded as an extremely primitive living fossil?

Crustacean Phylogeny

Some mention must be made of the important contribution by Dahl (1956*a*) to the understanding of crustacean phylogeny based on studies of the Mystacocarida and the Cephalocarida. He designates and characterizes four crustacean subclasses: Ostracoda; Malacostraca; Gnathostraca (including the orders Cephalocarida, Anostraca, and Phyllopoda); and Maxillopoda (containing the orders Mys-

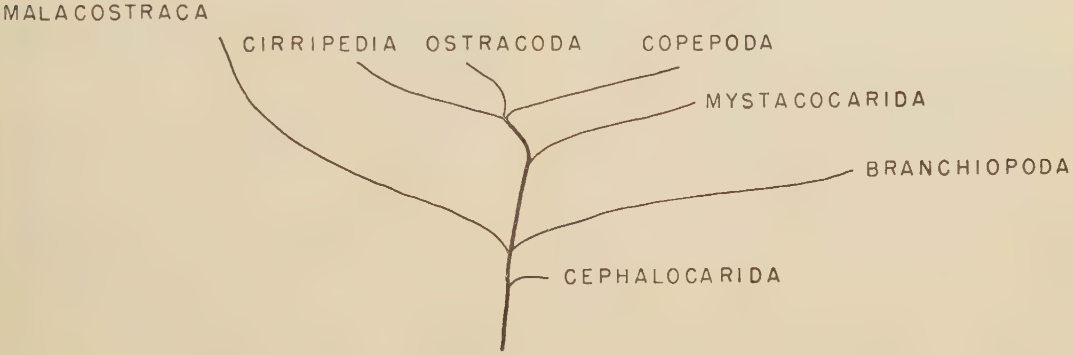

FIG. 9. A proposed scheme showing the evolution of the crustacean subclasses.

tacocarida, Archicopepoda, Copepoda, Branchiura and possibly the Cirripedia). He is quite correct in pointing out that

> Undoubtedly the discovery of the Mystacocarida and the Cephalocarida brought the Anostraca and the Copepoda closer to each other. Within the series Euanostraca–Lipostraca–Cephalocarida the general resemblance to the Copepoda increases step by step. In a similar way it could be said that the Mystacocarida at least in their internal organisation are not as far removed from the Anostraca as are the Copepoda. . . . But although the gap between the Anostraca and the Copepoda is not as wide as it used to be it seems impossible to say that the discovery of the two new crustacean groups obliterated the limits between the two evolutionary lines. It seems probable that they were derived from a common ancestor but it appears certain that they branched off in different directions at an early phylogenetic stage.

The information available to Dahl concerning the Cephalocarida was limited to the original description (Sanders, 1955). According to Dahl's classification, additional morphological details in the present paper indicate that *Hutchinsoniella* has the head of a maxillopodan, the body of a gnathostracan but with thoracic limbs not far removed from those of a trilobite. This writer feels that the two evolutionary lines do converge within the Cephalocarida.

On the basis of the comparative morphology presented in this paper, the author proposes a possible scheme of crustacean affinities (Fig. 9). The Cephalocarida must be placed close to the main stem of crustacean evolution since it uniquely retains the naupliar masticatory process on the second antenna, the only slightly modified trilobite appendage, and a second maxilla that is unaltered from the trunk limb pattern.

The characters that are common to both the Cephalocarida and Branchiopoda are the numerous body segments, the retention of gnathic processes on the trunk limbs and a paired ventral nerve cord. Evolution in a branchiopodan direction would consist of a modification of the cephalocarid trunk limb to the foliaceous limb and a pronounced reduction of all head appendages.

The primitive malacostracan thoracic limb can be directly homologized with the cephalocarid trunk appendage and both groups have a biramous first antenna. A reduction in body segments, the loss of gnathic processes on the trunk limbs and a modification of the mouth appendages were the components of malacostracan evolution.

The generalized head appendages are shared by the Cephalocarida with the Copepoda, Ostracoda, the nauplii of the Cirripedia, and the Mystacocarida. There has been a reduction of trunk segments, a loss of gnathic processes on the trunk limbs and a conversion of the cephalocarid appendage to a biramous copepodan limb or to a mere rudiment as is the case in the Mystacocarida. This latter group, however, has retained the paired ventral nerve cord (Dahl, 1952).

Viewing the morphology of *Hutchinsoniella* on the basis of the entire complex of arthropods, extinct and extant, one is left with the impression that the present day cephalocaridan is not far removed from the ancestral crustacean stock that probably existed during the Silurian or earlier. This impression is based on its apparent affinities to the trilobites, the close relationship between it and the mid-Devonian fossil *Lepidocaris,* and the morphological characters it shares with the more primitive members of the various extant crustacean groups.

Finally, the evidence strongly refutes the polyphyletic origin of the crustaceans suggested by certain investigators such as Garstang and Gurney (1938), and the primitiveness of the foliaceous appendage as advanced by MacBride (1914) and Borradaile (1926). The validity of Størmer's phylum Arachnomorpha as a natural group can be seriously questioned since a concise evolutionary sequence can be traced from certain Trilobitomorpha present in the mid-Cambrian Burgess Shale deposits through a cephalocarid-like intermediary to the other present day crustacean subclasses.

BIBLIOGRAPHY

Borradaile, L. A. 1926. Notes on crustacean limbs. *Ann. Mag. Nat. Hist., London,* Ser. 9, *17*:193–213.

Brioli, F. 1928. Beobachtungen an Nahecaris. *Sitzungsber. M.-N. Abt. Bayerische Akad. Wiss.,* 1–18.

Calman, W. T. 1909. Crustacea, in Sir Ray Lankester (Ed.), *A Treatise on Zoology,* Part VII, fasc. 3.

Claus, C. 1876. Untersuchungen zur Erforschung der genealogischen Grundlage des Crustaceen-Systems. 4 to. Wien.

——— 1886. Neue Beitrage zur Morphologie der Crustacean. *Arb. Zool. Inst. Wien, 6*:1–108.

Dahl, E. 1952. Mystacocarida, con resumen en español. Reports of the Lund University Chile Expedition 1948-49, No. 7. *Lund Univ. Arrsk. N.F. Avd., 2, 48*:1–40.

——— 1956. On the differentiation of the topography of the Crustacean head. *Acta Zoologica, 37*:123–192.

——— 1956*a*. Some crustacean relationships. Bertil Hanström, *Zoological papers in honor of his sixty-fifth birthday November 20, 1956:* 138–147.

Garstang, W., and Gurney, R. 1938. The descent of the Crustacea from trilobites, and their larval relations. In: *Evolution, Essays presented to E. S. Goodrich,* G. R. deBeer, Ed.: 271–286.

Heegaard, P. 1957. The second maxilla in the Decapoda. *Ann. Zool., 2*(3):39–46.

MacBride, E. W. 1914. Text-book of embryology. Vol. 1. Invertebrata. London.

Pennak, R. W., and Zinn, D. J. 1943. Mystacocarida, a new order of Crustacea from intertidal beaches in Massachusetts and Connecticut. *Smithsonian Misc. Coll., 103*(9):1–11.

Remane, A. 1956. Die Cephalocarida, eine weitere neue Ordnung (Unterklasse) der Krebse. *Mikrokosmos, 45*:227–230.

Sanders, H. L. 1955. The Cephalocarida, a new subclass of Crustacea from Long Island Sound. Proc. Nat. Acad. Sci., *41*(1):61–66.

Sandison, E. E. 1954. The identification of the nauplii of some South African barnacles with notes on their life histories. *Trans. Roy. Soc. South Africa, 34*(1):69–101.

Sars, G. O. 1896. Fauna Norvegiae-Phyllocarida and Phyllopoda. Christiania. 140 pp.

——— 1903. A account of the Crustacea of Norway. 4. Copepoda. Bergen Museum. 171 pp.

——— 1928. An account of the Crustacea of Norway. 9. Ostracoda. Bergen Museum, 277 pp.

Scourfield, D. J. 1926. On a new type of crustacean from the Old Red Sandstone (Rhynie Chert bed, Aberdeenshire), *Lepidocaris rhyniensis* gen, et sp. nov. *Phil. Trans. Roy. Soc. London, Ser. B, 214*:153–187.

Siewing, R. 1956. *Thermobathynella amyxi* nov. spec. aus dem Brackwasser der Amazonasmündung. *Kieler Meeresforsch., 12*:114–119.

Snodgrass, R. E. 1956. Crustacean metamorphoses. *Smithsonian Misc. Coll., 131* (10):1–78.

Størmer, L. 1939. Studies on trilobite morphology. I. The thoracic appendages and their phylogenetic significance. *Norsk geol. tidsskr., 19*:143–274.

——— 1942. Studies on trilobite morphology. II. The larval development, the segmentation and the sutures, and their bearing on trilobite classification. *Norsk. geol. tidsskr., 21*:49–163.

——— 1944. On the relationships and phylogeny of fossil and recent Arachnomorpha. *Skr. Vid.-Akad. Oslo 1. M.-N. Kl.,* No. 5:1–158.

Triebel, E. 1941. Zur Morphologie und Ökologie der fossilen Ostracoden. Mit Beschreibung einiger neuen Gattungen und Arten. *Senckenbergiana, 23:*294–400.

HOWARD L. SANDERS is a Research Associate at the Woods Hole Oceanographic Institution, Woods Hole, Massachusetts. This study was made possible by a Grant-in-Aid of Research from the Sigma Xi RESA Research Fund for the summer of 1955 and by subsequent National Science Foundation support for benthic community investigations in Buzzards Bay, Massachusetts where many specimens of *Hutchinsoniella macracantha* were collected. The author would like to thank Dr. Nathan W. Riser (Woods Hole Oceanographic Institution) and Mr. Henry O. Werntz (Osborn Zoological Laboratory, Yale University) for numerous helpful suggestions. This paper is Contribution 882 from the Woods Hole Oceanographic Institution.

Contribution No. 883

Reprinted from LIMNOLOGY AND OCEANOGRAPHY
Vol. II, No. 2, April, 1957
Printed in U.S.A.

Simplified Computations for the Dynamic Height Method of Current Determination in Lakes[1]

INTRODUCTION

A dynamic height method for the determination of current directions and velocities in deep lakes has been developed by Ayers (1956). This method involves very considerable amounts of arithmetical calculation and hence contains numerous possibilities for arithmetical error. Successful reduction of the amount of computation required would achieve both economy of time and reduced chances for error. This paper presents a successful simplified computation routine for the freshwater dynamic height method.

The simplified computation routine consists of a more convenient rearrangement of the original computation method and in no way changes the theoretical considerations upon which that method was based. The reader is referred to Ayers (1956) for the full development of theory and the original method.

Formal thanks are tendered to the University of Michigan Biological Station, where much of this work was carried out.

THE SIMPLIFIED METHOD

The new method differs from the original in two ways: 1) the expansive effects of temperature and the compressive effects of pressure are independently determined and applied, and 2) new tables directly readable to 0.1°C have been prepared. Independent application of the thermal and pressure effects eliminates the laborious double interpolations commonly required in the original method.

The new method first determines the specific volume anomaly at observed temperature and zero hydrostatic pressure ($10^5\ \delta_{t,o}$), then applies a compression correction ($\Delta a_{t,p}$) at observed temperature and *in situ* pressure to obtain the anomaly at temperature and pressure. The new specific volume anomaly table (Table 1) was prepared by graphing the zero-pressure portions of Ayers' (*loc. cit.*, Table 2) original anomaly table and reading anomaly values ($10^5\ \delta_{t,o}$) at each 0.1°C. The new table of coefficients of compression (Table 2) was prepared by graphing and reading at each 0.1°C Ayers' (*loc. cit.*, Table 1) compressibility coefficients. As in the original paper, the coefficient of compressibility (in cm³/cm³/atmosphere) is numerically equal to compression in cm³/atmosphere (C_t) when applied to a volume of one cubic centimeter. The pressure effects are handled, as in the old method, by the decibar system: pressure in atmospheres, p = depth in meters ÷ 10 meters/atmosphere. As before, $10^5 C_t \times p = \Delta a_{t,p}$ and $10^5\ \delta_{t,o} - \Delta a_{t,p} = 10^5\ \delta_{t,p}$, the required anomaly at temperature and pressure.

As in the old method, the resultant anomaly ($10^5\ \delta_{t,p}$) is required for the surface temperature, for each subsurface inflection of the temperature curve, and for the temperature at the reference level.

COMPARISONS OF THE NEW AND OLD METHODS

As indicated above, the required resultant anomaly for any subsurface temperature and pressure can be obtained (in the new method) by two table readings, one division, one multiplication, and one subtraction—a total of five operations. Under the old method obtaining a single resultant anomaly at temperature and pressure involved a total of thirteen operations as follows:

---

[1] Contribution No. 3 from the Great Lakes Research Institute, University of Michigan, and Contribution No. 883 from the Woods Hole Oceanographic Institution.

TABLE 1. *Specific volume anomaly* $(10^5\ \delta_{t,o})$

°C	0	.1	.2	.3	.4	.5	.6	.7	.8	.9
0	13.0	12.4	11.5	10.8	10.2	9.6	9.0	8.4	7.9	7.4
1	7.0	6.6	6.2	5.7	5.3	4.9	4.6	4.2	3.8	3.5
2	3.0	2.8	2.6	2.3	2.0	1.8	1.6	1.4	1.2	1.1
3	1.0	0.9	0.8	0.7	0.6	0.5	0.4	0.3	0.2	0.1
4	0.0	0.1	0.2	0.3	0.4	0.5	0.6	0.7	0.8	0.9
5	1.0	1.1	1.2	1.3	1.5	1.7	1.9	2.1	2.4	2.7
6	3.0	3.3	3.7	4.1	4.5	4.9	5.3	5.7	6.1	6.5
7	7.0	7.5	8.0	8.5	9.0	9.5	10.0	10.5	11.0	11.5
8	12.0	12.6	13.2	13.9	14.6	15.3	16.0	16.7	17.4	18.3
9	19.0	19.7	20.4	21.2	22.0	22.8	23.6	24.4	25.3	26.1
10	27.0	28.0	29.0	30.0	31.0	32.0	33.0	34.0	35.0	36.0
11	37.0	38.0	39.1	40.2	41.3	42.5	43.6	44.7	45.8	46.9
12	48.0	49.1	50.2	51.4	52.6	53.8	55.0	56.2	57.4	58.7
13	60.0	61.3	62.6	63.9	65.2	66.5	67.8	69.1	70.4	71.7
14	73.0	74.4	75.8	77.2	78.6	80.0	81.4	82.8	84.2	85.6
15	87.0	88.6	90.2	91.8	93.4	95.0	96.6	98.2	99.8	101.4
16	103.0	104.7	106.4	108.1	109.8	111.5	113.2	114.9	116.6	118.3
17	120.0	121.8	123.6	125.4	127.2	129.0	130.8	132.6	134.4	136.2
18	138.0	139.9	141.8	143.7	145.6	147.5	149.4	151.3	153.2	155.1
19	157.0	159.0	161.0	163.0	165.0	167.0	169.0	171.0	173.0	175.0
20	177.0	179.1	181.2	183.3	185.4	187.5	189.6	191.7	193.8	195.9
21	198.0	200.3	202.6	204.9	207.2	209.5	211.8	214.1	216.4	218.7
22	221.0	223.3	225.6	227.9	230.2	232.5	234.8	237.1	239.4	241.7
23	244.0	246.4	248.8	251.2	253.6	256.0	258.4	260.8	263.2	265.6
24	268.0	270.6	273.2	275.8	278.4	281.0	283.6	286.2	288.8	291.4

TABLE 2. *Coefficients of compression* $(10^5\ C_t)$

°C	0	.1	.2	.3	.4	.5	.6	.7	.8	.9
0	5.250	5.243	5.236	5.230	5.224	5.219	5.214	5.209	5.204	5.200
1	.195	.191	.187	.183	.179	.176	.173	.170	.167	.163
2	.160	.157	.154	.151	.148	.145	.142	.139	.136	.133
3	.130	.128	.125	.122	.120	.118	.115	.112	.110	.108
4	.105	.103	.100	.098	.095	.092	.089	.087	.085	.082
5	.080	.078	.076	.074	.072	.070	.068	.066	.064	.062
6	.060	.058	.057	.055	.053	.051	.049	.047	.045	.044
7	.043	.041	.039	.038	.036	.034	.033	.031	.029	.028
8	.027	.025	.024	.023	.022	.020	.019	.018	.016	.014
9	.013	.012	.011	.010	.008	.007	.006	.004	.003	.001
10	5.000	4.998	4.997	4.996	4.994	4.993	4.992	4.990	4.989	4.987
11	4.985	.984	.983	.982	.981	.980	.979	.978	.977	.976
12	.975	.974	.973	.971	.970	.969	.968	.967	.966	.965
13	.964	.962	.961	.960	.959	.958	.957	.956	.955	.954
14	.953	.953	.952	.951	.950	.949	.948	.947	.946	.945
15	.944	.943	.942	.941	.941	.940	.939	.938	.938	.937
16	.936	.936	.935	.934	.933	.932	.932	.931	.931	.930
17	.929	.929	.928	.928	.927	.926	.925	.924	.923	.923
18	.922	.921	.921	.920	.919	.919	.918	.918	.917	.916
19	.916	.915	.914	.914	.913	.913	.912	.912	.911	.911
20	.910	.910	.909	.909	.908	.908	.907	.907	.906	.906
21	.905	.905	.904	.904	.903	.903	.903	.903	.902	.902
22	.902	.902	.901	.901	.901	.901	.900	.900	.899	.899
23	.898	.898	.898	.897	.897	.896	.896	.895	.894	.894
24	.893									

a. Reading anomalies at temperatures adjacent to the observed temperature and at pressure less than observed pressure (2 table readings)

b. Interpolating to anomaly at observed temperature and less than observed pressure (1 subtraction, 1 multiplication, and 1 addition)

c. Reading anomalies at temperatures adjacent to observed temperature and at pressure greater than observed pressure
(2 table readings)

d. Interpolating to anomaly at observed temperature and greater than observed pressure (3 operations as in b above)

e. Interpolating between anomalies at observed temperature (items b and d above) for anomaly at observed temperature *and* pressure (3 operations as in b above).

The new computation reduces to less than half the number of operations (and the time, labor, and chance for error) involved in obtaining each individual resultant specific volume anomaly.

Subsequent computations leading to the final dynamic height at each station are carried out as in the original paper and are no less time-consuming and laborious than before. They do benefit, however, by the lesser chance for error inherent in the new method.

As a comparison of the accuracy of the two methods, the dynamic heights of 56 stations taken in Lake Michigan on 28 June 1955 have been worked out by each method. While there were minor variations in the insignificant terminal decimal places, the final dynamic heights rounded off to the same values by either method. There is, then, no loss of accuracy resulting from the simpler new method. The total labor (with calculator) required for the two determinations of this topography was 31 man-hours by the original method and 13.5 man-hours by the new.

REFERENCES

AYERS, J. C. 1956. A dynamic height method for the determination of currents in deep lakes. Limnol. & Oceanogr., **1**: 150–161.

JOHN C. AYERS
Great Lakes Research Institute and Department of Zoology, University of Michigan; and Woods Hole Oceanographic Institution

ROGER BACHMANN
Idaho Cooperative Wildlife Research Unit, University of Idaho,
Moscow, Idaho

Contribution No. 884

Reprinted from

RESEARCH REVIEWS

APRIL 1957

Time-Lapse Photography--An Aid To Studies of the Shoreline

J. M. Zeigler
Research Associate in Geology
Woods Hole Oceanographic Institution

F. C. Ronne
Research Associate in Photography
Woods Hole Oceanographic Institution

CONTRIBUTION NO. 884 FROM THE WOODS HOLE OCEANOGRAPHIC INSTITUTION

OFFICE OF NAVAL RESEARCH
DEPARTMENT OF THE NAVY WASHINGTON, D. C.

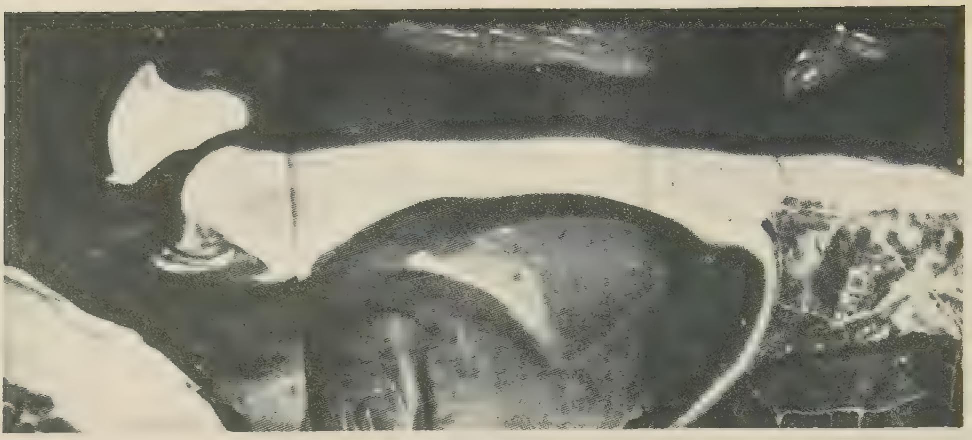

A, June 15, 1955.

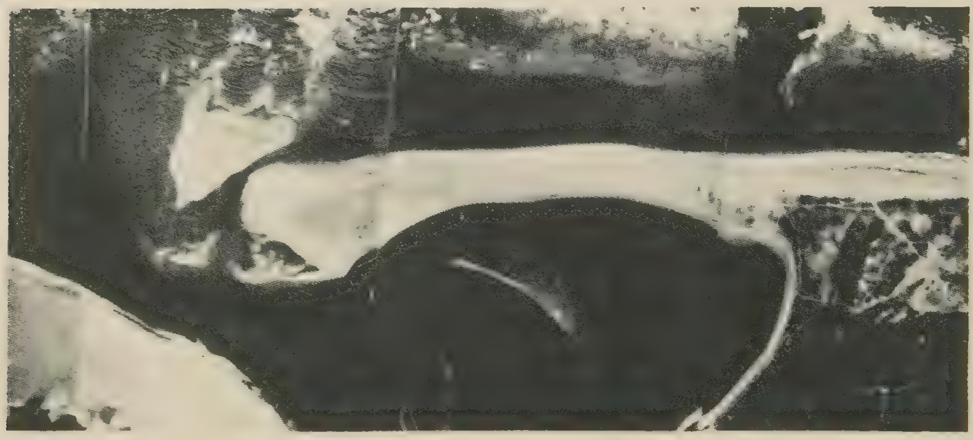

B, July 14, 1955.

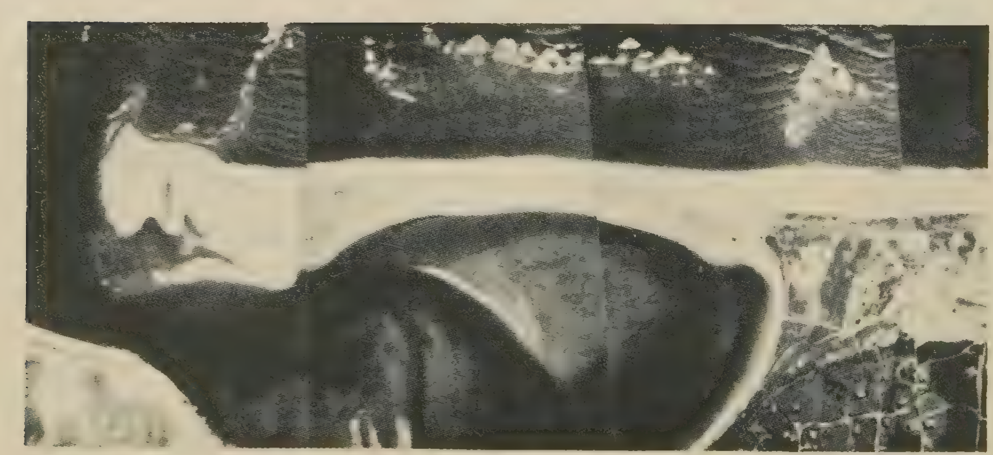

C, August 20, 1955.

Landward movement of a bar off Nauset Inlet, Cape Cod, Massachusetts. All photographs taken at low tide. Scale, 1/2 inch = about 175 yards.

Time-Lapse Photography--An Aid To Studies of the Shoreline

J. M. Zeigler
Research Associate in Geology
Woods Hole Oceanographic Institution

F. C. Ronne
Research Associate in Photography
Woods Hole Oceanographic Institution

What changes do beaches undergo from day to day and from season to season? Do offshore bars come and go, and if so, why? Do inlets migrate back and forth for no reason at all or do they behave systematically? Is it possible to predict the configuration of a specific beach weeks in advance? These are some of the questions which are being studied by a group at the Woods Hole Oceanographic Institution on Cape Cod in Massachusetts. The group has found that beaches change somewhat with every tide and that every aspect of beach research must be studied in terms of changes. Even the forces of change (wind and waves) change, themselves, in complex ways. How, then, can all of these changes be observed and plotted without enormous expenditures of manpower?

Many types of periodic observations of shoreline features are being tried with varying degrees of success or failure. One of these utilizes photography. After all, photography is an inexpensive and fast method of recording changes, considering the amount of information one gets. Of course, the number of pictures to be taken depends on what is being studied. Studies of wave characteristics, for example, require more pictures than those of the movements of sand bars. The beach-studies group, therefore, has experimented with photography as a tool to aid them in describing changes which take place along the shoreline. Essentially four classes of pictures have been obtained:

- Single photographs of specific beach features.
- Aerial photo-mosaics of coastal features (inlets and bars rephotographed every few weeks to record changes). (See frontispiece.)
- Time-lapse pictures (one every two seconds for several hours) of storm waves pounding a beach. The results can be shown as a movie.
- Time-lapse aerial photographs in color (two per second) of the entire coastline of the United States from Eastport, Maine, to Brownsville, Texas. Results shown as a movie. Flights repeated at least once a year.

Of the techniques utilized to obtain these classes of pictures, only the aerial time-lapse method will be discussed here.

The camera used is a 16-millimeter magazine-loading Bell and Howell Model 200. The time-lapse triggering mechanism, which was designed by Dr. William S. von Arx of the Woods Hole Oceanographic Institution, is a simple cam and lever device operated by a 12-volt Magnetorc (Hanson Manufacturing Co.) motor. By changing the gear ratio of the motor, which is driven through a gear train, large changes in cam

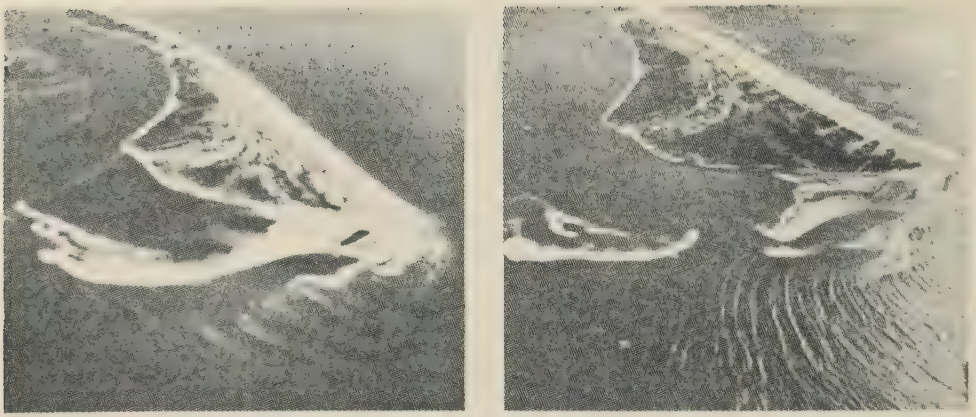

A B

Figure 1 - Changes in the shape of Fire Island Inlet, Long Island, over a period of about 6 months. A, April 28, 1956; low tide. B, October 19, 1956; half tide. Tide range, 4.1 to 5 feet.

speed can be made. Small changes in speed can be made by increasing or decreasing the voltage applied. Power is supplied by standard dry-cell batteries. The motor will operate satisfactorily through a range of from 9 to 15 volts.

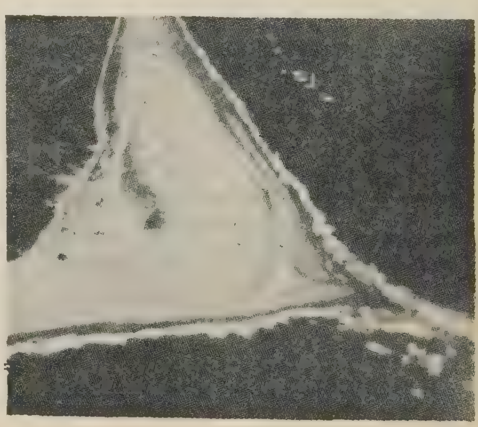

A

Figure 2 - Changes in the shape of Cape Hatteras, North Carolina, over a period of about 6 months. A, April

The camera mount was designed so that the camera can be used from the tail hatch of the aircraft (PBY). Thus the camera looks backward. Although it is ordinarily tilted about 20 degrees downward, the degree of tilt can be changed to suit the needs of the operator or to accommodate the type of lens being used at a particular time. The camera and motor, as a unit, are fastened to a movable plate which can be rotated on a vertical axis through about 75 degrees of arc, making it possible to follow an indented coastline with the camera or compensate for minor errors in the flight course. The axis of rotation is directly under the optical center of the lens. The number of pictures to be taken per second is an important consideration. Enough pictures should be taken to show whatever changes are being studied. However, the number should not be so small as to cause jerking or jumping of the movie, or so large as to make the resulting movie excessively long. These problems have several aspects:

- Projection speed: Some projectors can be slowed down or speeded up through wider ranges than others.
- Speed of aircraft: All aerial work thus far has been done from a Navy PBY flying at a speed of 110 knots.
- Altitude: This is dependent upon weather and the characteristics of the coastline. A broken coast, such as that of Maine, is generally photographed from an altitude of 5,000 feet; a straight coast, such as that of Long Island, from an altitude of 2,500 or 3,500 feet.

The film speed for all aerial photography done by the group thus far has been two frames per second. At this rate, a 50-foot magazine (2,000 frames) is used up in 1,000 seconds (about 17 minutes), a period of time during which the PBY flies about 30 nautical miles along the coast. However, the time taken to view the movie depends on the speed at which the film is projected; at a normal speed of 16 frames per second, one sees the 50-foot reel, or 30 nautical miles of coast, in 125 seconds, or as if one were flying at a speed of about 850 knots. If the projection speed is slowed down to 10 frames per second, the apparent flying speed is about 540 knots. Of course the flying speed appears to increase if the plane flies below the desired altitude, nearby objects moving by much faster than objects farther away. If the plane flies below an altitude of 1,800 feet, as it is often forced to do by clouds and other conditions that reduce visibility, this movement becomes objectionable; individual pictures on the reel are useable, however.

A wide-angle lens (58 degrees) having a focal length of 9.5 millimeters has been used for most of the coastal photography. This lens has an advantage over the conventional 16-millimeter movie camera lens (25-millimeter focal length; 24-degree angle) in that the same ground area can be covered from an altitude only three-eighths of that which would be required by the 25-millimeter lens. Thus it is possible to continue photographing even when clouds or bad weather force the aircraft down to 1,800 feet. This means that the number of days lost on a field trip because of poor flying conditions is greatly reduced. Another advantage of low-altitude wide-angle photography is that ground haze (present to a degree even under the best of circumstances) seldom becomes a serious obstacle.

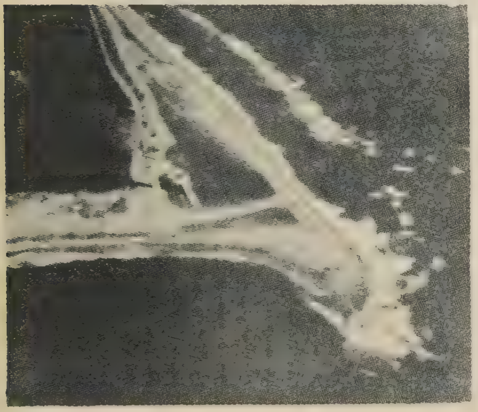

B
29, 1956; 1 hour before low tide. B, October 19, 1956; 2 hours after low tide. Tide range, 3.5 feet.

Figure 3 - Changes in the shape of Cape Fear, North Carolina, over a period of about 6 months. A, April 29, 1956; low tide. B, October 19, 1956; 3 hours after low tide. Tide range, 4.5 feet.

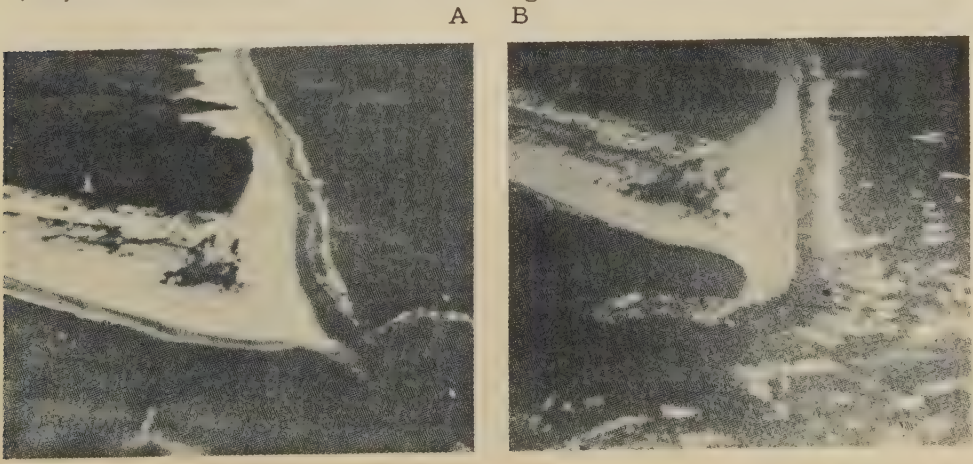

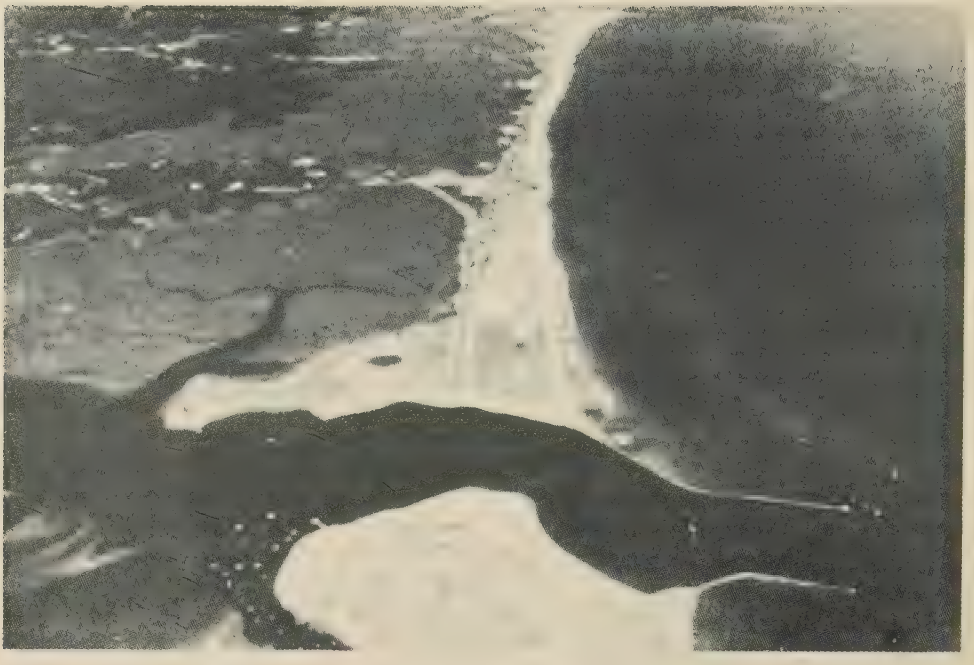

Figure 4 - Near-shore bars, Massachusetts.

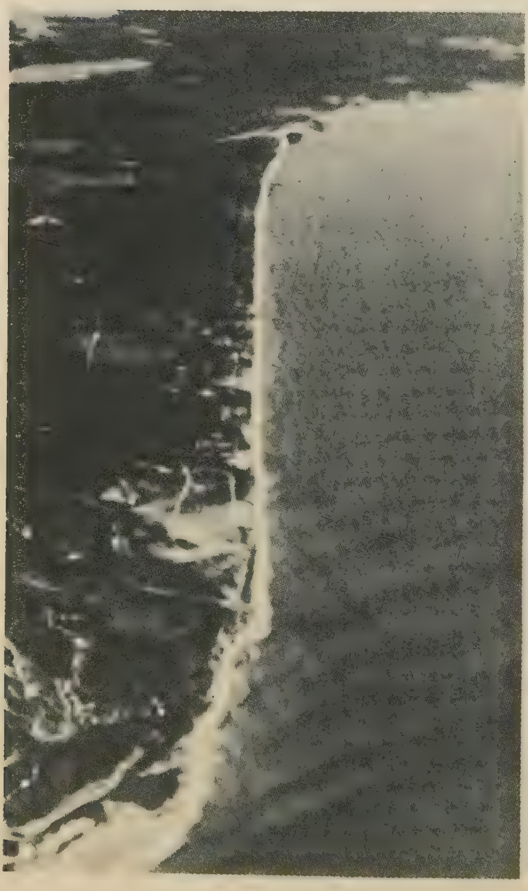

Figure 5 - Ripples diagonal to shore, Eastham, Massachusetts.

Figure 6 - Cuspate shore, Indian River, Florida.

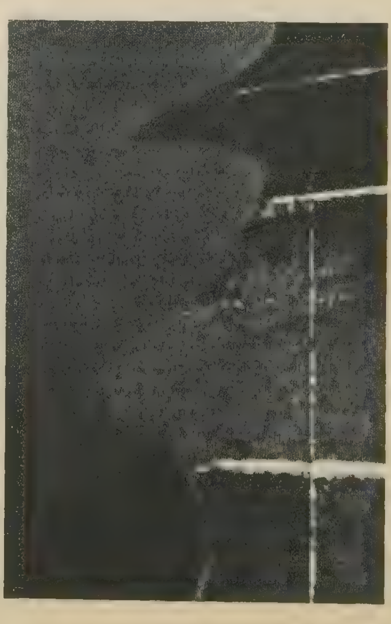

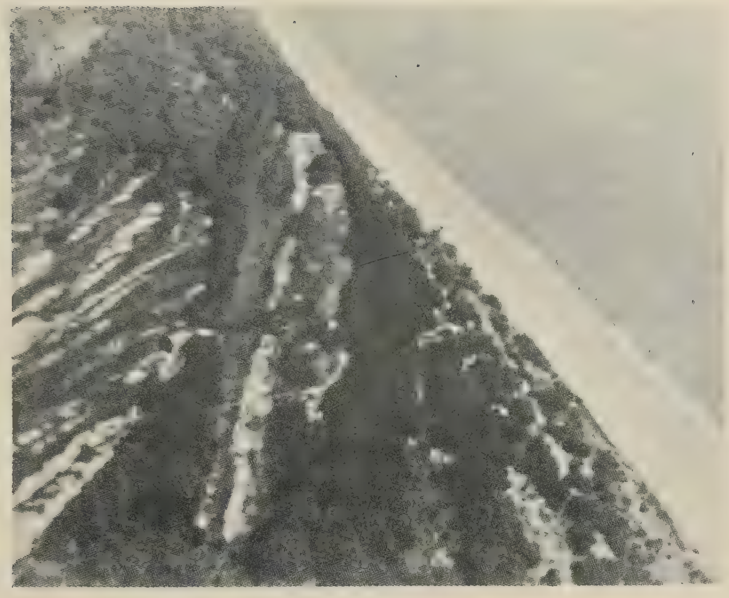

Figure 7 - Beach ridges, Georgia.

Two flights have been made along the Atlantic and Gulf coasts of the United States. On the first flight, made in April 1956, the coast was photographed from the Canadian border to a point on the west side of Florida near Venice. On the second flight, made in October 1956, the coast was photographed from Montauk Point, Long Island, to the Rio Grande in Texas, except for some of the islands off the Georgia coast. Future flights are planned for at least once each year.

Although the reasons for changes that occur along coasts are not always revealed by aerial photographs alone, the photographs do tell us what changes are taking place. Here are a few examples:

Inlets change more often and more spectacularly than any other large features of coasts. The frontispiece shows the landward movement

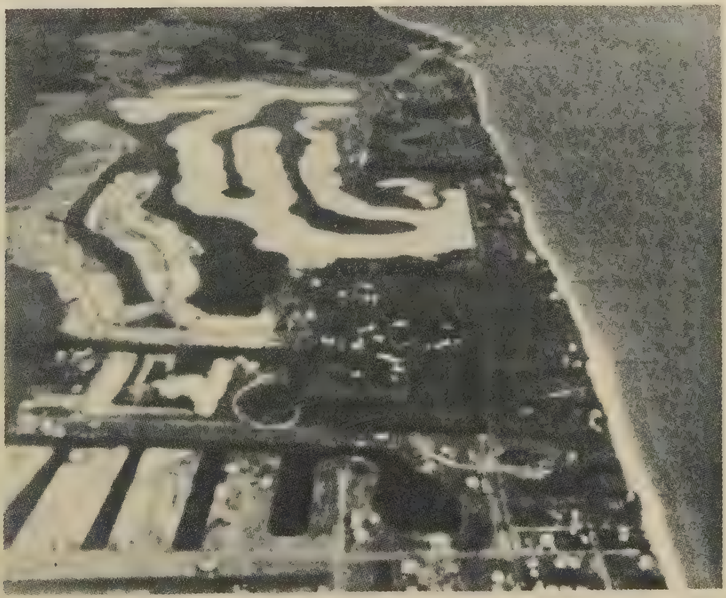

Figure 8 - Land reclamation near Naples, Florida.

of a bar off Nauset Inlet, Cape Cod, Massachusetts (the photographs indicate that within a period of 2 months this bar coalesced with the tip of the spit), and Figure 1 shows how the shape of Fire Island Inlet, on the south shore of Long Island, changed during a period of about 6 months in 1956. Capes and promontories change in many complex ways, too, as indicated by Figures 2 and 3, which show the shapes of Capes Hatteras and Fear in April and October of the same year. Although beaches respond quickly to changing sea conditions, the effects of such changes are not always apparent on small photographs and as yet have not been examined on the films.

Time-lapse aerial photography also provides a means of comparing similar features that occur at different geographic locations. For example, comparisons can be made of near-shore bars (Figure 4), giant ripple patterns (Figure 5), cuspate shores (Figure 6), and beach ridges (Figure 7). Although comparisons of such features merit fuller treatment that can be given them through time-lapse aerial photography, it is entirely possible that fruitful lines of investigation may result directly from what can be seen in the time-lapse movies.

The photography is expected to serve several professions. It hardly needs to be pointed out that the choice of locations and designs for engineering structures in and near inlets or other coastal features depends very much on what changes are known or are believed to have occurred in the past. Therefore, engineers who design such structures can benefit by referring to movies of the coast taken periodically. Economic geographers can benefit from the work, too. By reference to the films, they will be able to observe changes in the pattern of land utilization which take place from year to year and thus gain an insight into future problems. Of particular interest to geologists who have seen the photographs of Florida are the many reclamation projects (Figure 8). As a part of these projects, marsh areas have been filled by material pumped from the bays. Each of these developments will cause changes in water circulation and perhaps, in turn, cause changes outside the developed areas.

Thus far, most of the problems encountered in the aerial time-lapse photography have been operational, such as in maneuvering the aircraft along the coast in such a way that the tail camera can be trained on the shore, and in determining quickly the altitudes at which to fly and the approaches to make over the areas to be photographed. Most of these problems have now been overcome.

Contribution No. 885

Reprinted for private circulation from
THE JOURNAL OF GEOLOGY
Vol. 65, No. 4, July 1957
PRINTED IN U.S.A.

SUBMARINE TOPOGRAPHY OF EASTERN CHANNEL, GULF OF MAINE[1]

SHANNON R. TORPHY AND JOHN M. ZEIGLER
Woods Hole Oceanographic Institution

ABSTRACT

Topography of Eastern Channel between Browns Bank and Georges Bank is similar to submarine glaciated valleys elsewhere, notably Cabot Trough in the Gulf of St. Lawrence. It is possible that glacial ice in these offshore regions was confined to deep embayments such as the Gulf of Maine and that it did not extend out over the continental shelf as a sheet but reached the sea as valley glaciers through older river valleys.

A series of great shoal banks lie off the northeastern coast of North America: Georges Bank off New England; Browns Bank, Sable Island, and Banquereau off the Canadian Maritimes; and St. Pierre Bank and the Grand Banks off Newfoundland (fig. 1). These banks are submerged portions of the continental shelf, but in many places the water separating them from the continent is relatively deep. The Gulf of Maine forms a great bay behind Georges Bank and the New England coast; there is deeper water between Banquereau and Cape Breton Island.

Two prominent troughs cut across the banks: Cabot Strait Trough traverses them from the Gulf of St. Lawrence between St. Pierre Bank and the Grand Banks; Eastern Channel enters the Gulf of Maine between Browns Bank and Georges Bank. A third, smaller trough crosses between Banquereau and Sable Island.

Shepard (1931) discussed the origin of Cabot Strait. He believed the strait to be essentially an ice-cut valley, possibly located along a pre-existing stream valley, which in turn may have been controlled by faulting. Shepard based his conclusions largely on the lack of characteristic features of river valleys and tectonic valleys, such as tributaries entering at grade, an outward-(seaward-)-sloping profile, sinuous trends, and a flat valley floor. He found no tilted floors or precipitous walls or associated grabens and horsts, which would indicate a tectonic valley. On the other hand, the region was unquestionably glaciated, and the valley form is similar to glaciated valleys known in other parts of the world.

---

[1] Woods Hole Oceanographic Institution Contribution No. 885. Manuscript received October 20, 1956.

Press and Beckman (1954, fig. 10, p. 312) provided the structural evidence which Shepard did not have to demonstrate that the present topography of Cabot Strait Trough is not directly related to the underlying structure, unless, as Shepard postulated, a preglacial river cut its valley along the fault zone.

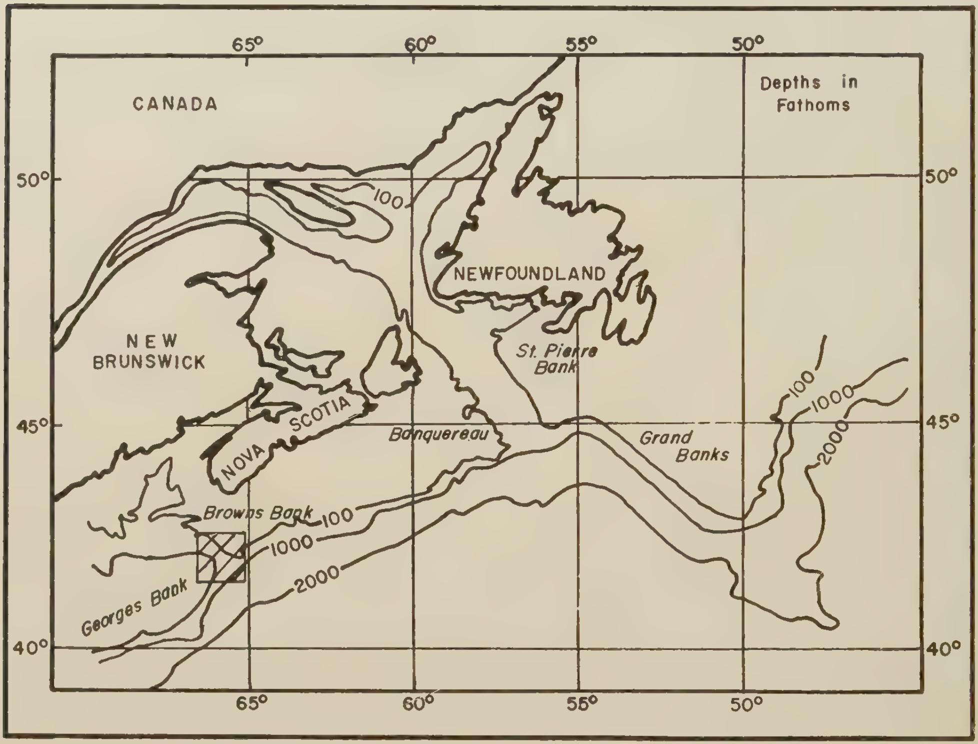

FIG. 1.—Offshore banks of northeastern North America

Information presented in this report concerns the Eastern Channel off New England (fig. 1). Eastern Channel is similar to Cabot Strait Trough, in that both are relatively large troughs across the gross topography. Cabot Trough is the larger feature, being 50–60 nautical miles wide, more than 200 fathoms deep in many places, and longer than 300 miles. Eastern Channel, in contrast, is only 20–30 miles wide, 130–160 fathoms deep, and approximately 100 miles long. Both troughs have undulating longitudinal profiles, and neither has tributaries entering it.

There are also some major dissimilarities. Cabot Trough continues as a trough across the Gulf of St. Lawrence into the St. Lawrence River. It forms a strait between land in two places: between Newfoundland and Cape Breton Island and between the Gaspé Peninsula and Anticosti Island. Eastern Channel is entirely offshore and separates submarine Browns Bank and Georges Bank. Furthermore, Eastern Channel cannot be traced very far into the Gulf of Maine. Where one places the west end of the trough is somewhat arbitrary, because the deep water in the Gulf of Maine spreads out into a crudely Y-shaped basin (U.S.C. & G.S. chart no. 70). There is no evidence for associating Eastern Channel with underlying structure.

The writers believe that Eastern Channel was cut by glacial ice, which probably followed a pre-existing stream valley. Evidence for this is very much the same as that used by Shepard for Cabot Strait Trough. Eastern Channel lacks features characteristic of river valleys but resembles a glacial valley, in showing an undulating valley floor and the absence of a general seaward slope (fig. 2). The region of the Gulf of Maine underwent glaciation, and, if a preglacial stream valley were present, it is logical to expect that glacial ice would follow the stream valley. Johnson's (1925) map of the drainage lines of the preglacial Gulf of Maine region supposes such a preglacial stream. Wells drilled at sites of the offshore radar towers (Texas towers) but failed to penetrate glacial till. Possibly glacial ice did not extend far out on the shelves but was confined to deep embayments such as the Gulf of Maine, and this ice reached the sea as valley glaciers when the sea level was considerably lower than now. Shepard *et al.* (1934) found till on anchor flukes on Georges Bank, but five of these locations were near the inner edge or near channels leading seaward. The writers cannot explain the more seaward till southeast of Texas tower no. 2.

Core samples taken from the "Atlantis" during this study have many of the characteristics of sediment samples from glaciated regions. Pebbles and sand are present in all the cores examined, even in the predominantly clayey portions of the cores. This coarse material could have been transported into the region by glacial ice or by ice-rafting or both.

SOUNDINGS

Soundings presented on the chart (fig. 3) were collected on cruises by various vessels of the Woods Hole Oceanographic Institution. A few soundings from the U.S. Coast and Geodetic Hydrographic Survey field work of 1930 were used (fig. 4). These soundings were adjusted approximately 3 miles to the northwest, to fit the Woods Hole data.

With one exception, the sounding apparatus used by Woods Hole vessels was an AN/UQN-1*b* continuous recording echo-sounder manufactured by the Edo Corporation. The research vessel "Bear" used a new Woods Hole continuous recording system (Knott and Hersey, 1956) on one cruise. All soundings are based on a speed of sound in water of 4,800 feet/sec. If temperature corrections are desired, tables for the velocity of sound in water can be found in Mathews (1939).

In attempting to assay the accuracy of the chart, two basic types of errors were analyzed: errors in navigation and errors in making a sounding. Navigation for all cruises was by Loran. Analysis of the accuracy of the Loran fixes by a graphic method (Zeigler and Von Arx, 1956) was used, and the distribution of navigation errors was graphed (fig. 5). Errors in soundings are summed up in figure 6, which is based on the discrepancy between soundings where the adjusted tracks of vessels cross.

Errors in soundings taken on these cruises arise from a variety of causes. Errors inherent in the AN/UQN-1*b* sounder are caused mainly by fluctuations in electrical frequency, which cause the styli to mark too shallow or too deep and also cause the speed of the paper to vary; slippage of the belt assembly, which affects the styli; and improper adjustment of the styli.

The Woods Hole recording system eliminates these classes of errors. Increased accuracy, however, brings attention to a class of depth uncertainly inherent in all acoustical methods in use. Sound energy induced in the water spreads in all directions, and echoes return first from the closest bottom, whether that bottom be to the side of the ship, in front of it, or beneath it. Furthermore, in regions of rough bottom, many echoes return, and it is virtually impossible to know which response comes from directly beneath the ship on a single run. Figure 7 shows part of a record taken on this survey. Presumably this type of uncertainty exists in all sonic

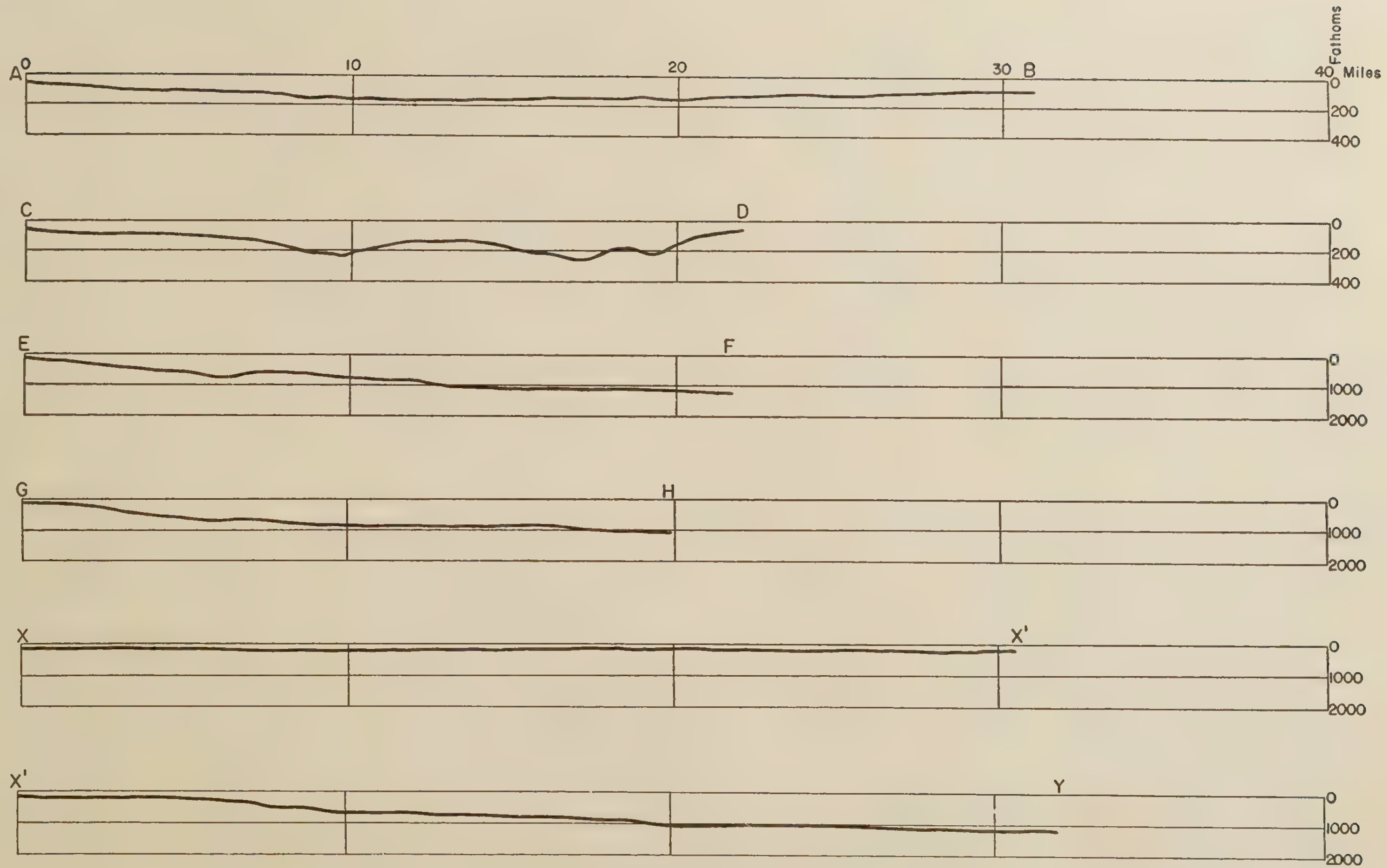

FIG. 2.—Sounding lines in the Eastern Channel

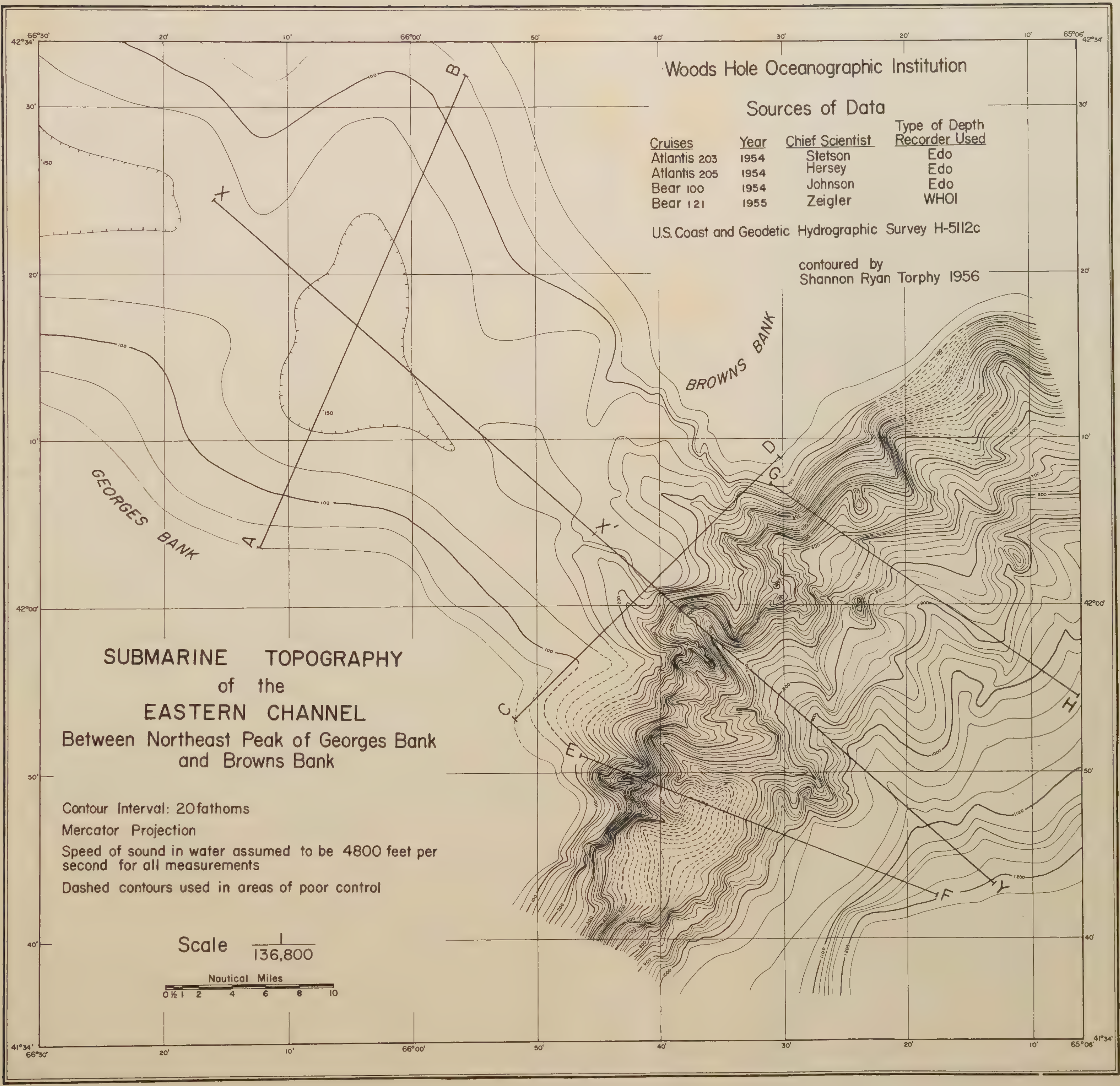
66°30'
20'
10'
66°00'
50'
40'
30'
20'
10'
65°06'
42°34'
30'
20'
10'
42°00'
50'
40'
41°34'
A
B
C
D
E
F
G
H
X
X'
Y
GEORGES BANK
BROWNS BANK
100
150
200
300
400
500
600
700
800
1000
1100
1200
Nautical Miles
0 ½ 1 2 4 6 8 10

Woods Hole Oceanographic Institution

Sources of Data

Cruises	Year	Chief Scientist	Type of Depth Recorder Used
Atlantis 203	1954	Stetson	Edo
Atlantis 205	1954	Hersey	Edo
Bear 100	1954	Johnson	Edo
Bear 121	1955	Zeigler	WHOI

U.S. Coast and Geodetic Hydrographic Survey H-5112c

contoured by
Shannon Ryan Torphy 1956

SUBMARINE TOPOGRAPHY
of the
EASTERN CHANNEL
Between Northeast Peak of Georges Bank
and Browns Bank

Contour Interval: 20 fathoms

Mercator Projection

Speed of sound in water assumed to be 4800 feet per second for all measurements

Dashed contours used in areas of poor control

Scale $\frac{1}{136,800}$

FIG. 3.—Submarine topography of the Eastern Channel between northeast peak of Georges Bank and Browns Bank

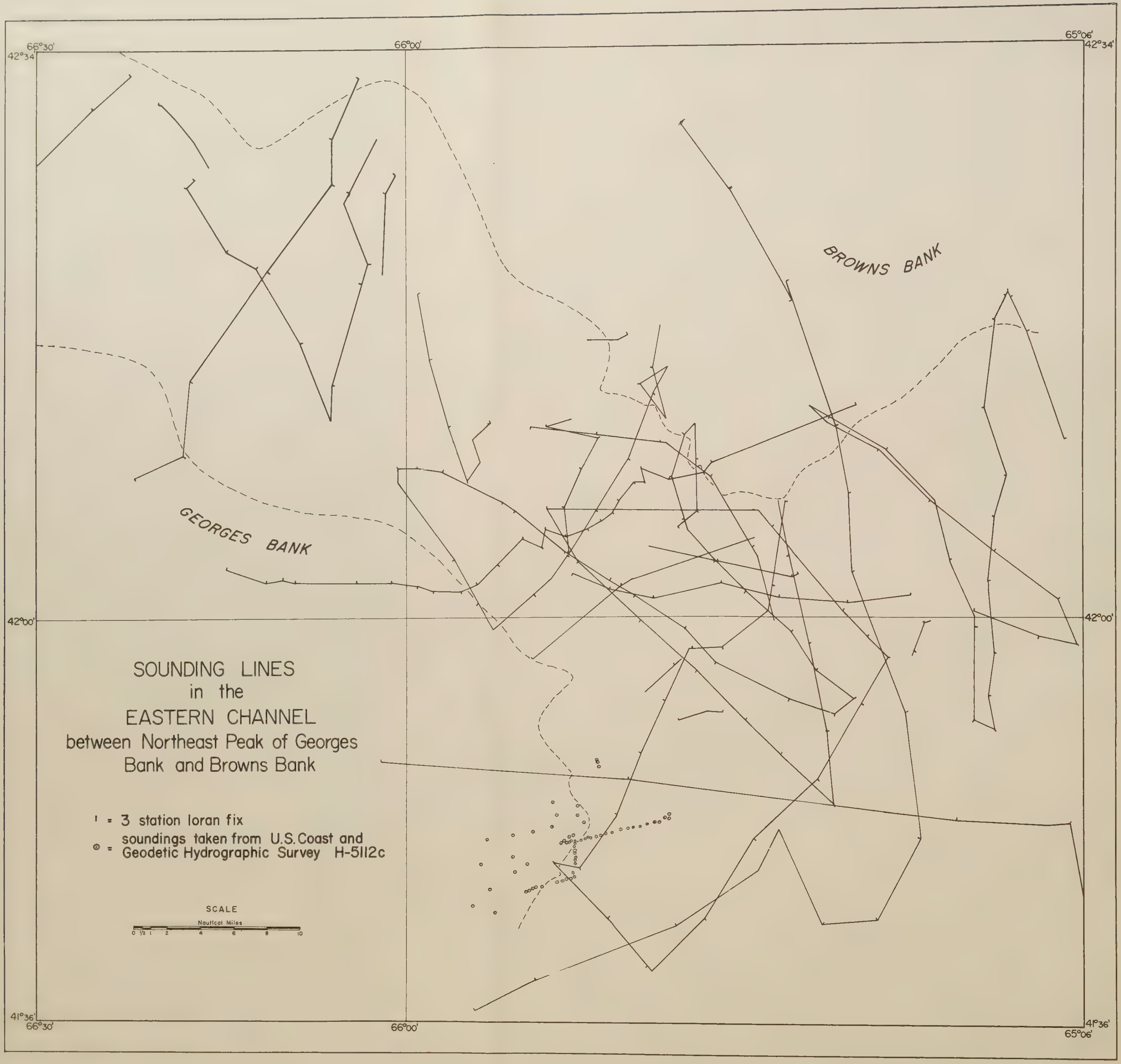
66°30'
66°00'
65°06'
42°34'
42°34'
BROWNS BANK
GEORGES BANK
42°00'
42°00'
SOUNDING LINES
in the
EASTERN CHANNEL
between Northeast Peak of Georges
Bank and Browns Bank
' = 3 station loran fix
⊙ = soundings taken from U.S. Coast and Geodetic Hydrographic Survey H-5112c
SCALE
Nautical Miles
0 1/2 1 2 4 6 8 10
41°36'
66°30'
66°00'
41°36'
65°06'

FIG. 4.—Sounding lines in the Eastern Channel between northeast peak of Georges Bank and Browns Bank

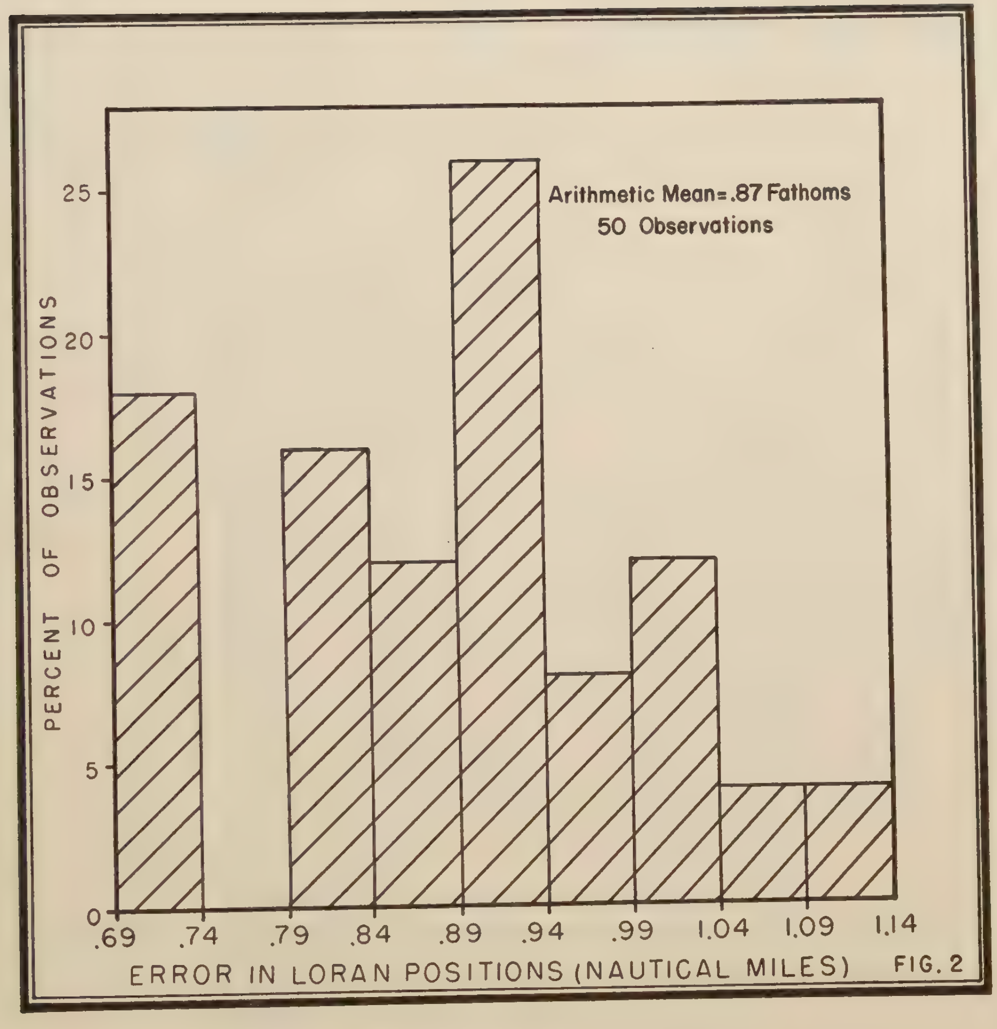

Fig. 5.—Distribution of errors in Loran positions

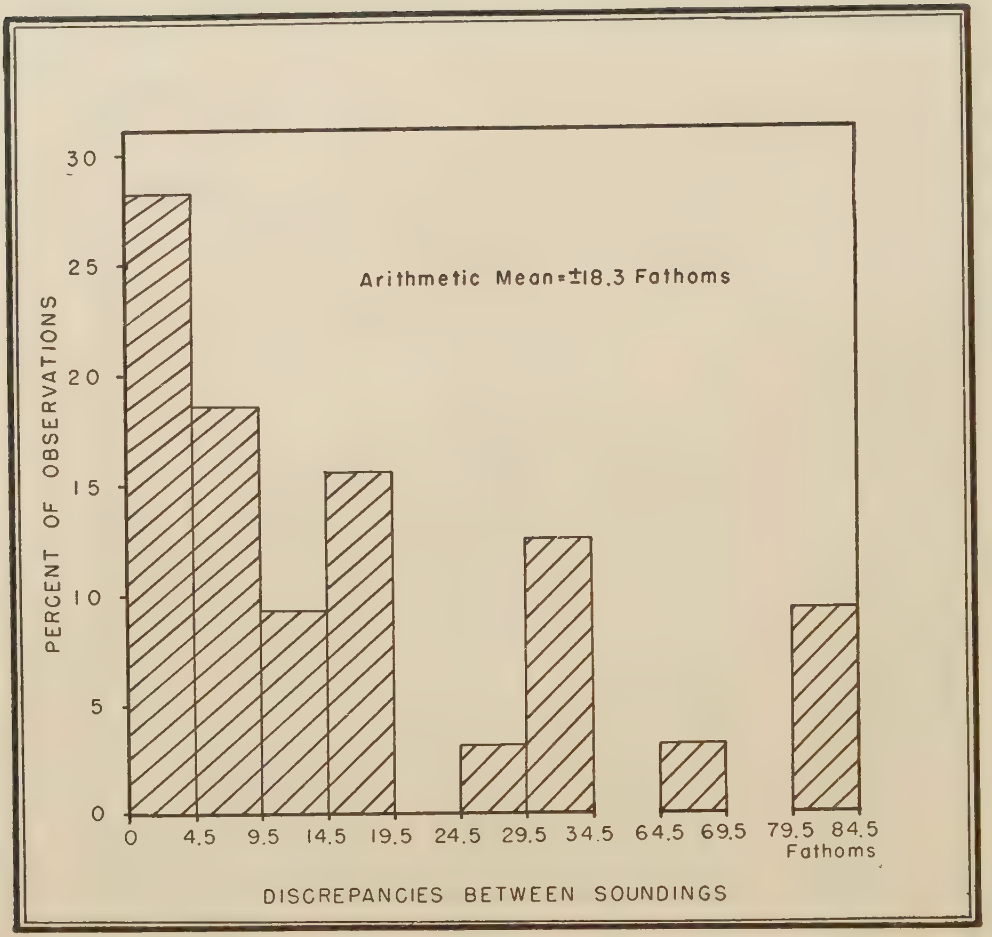

Fig. 6.—Discrepancies between soundings where the tracks of vessels cross

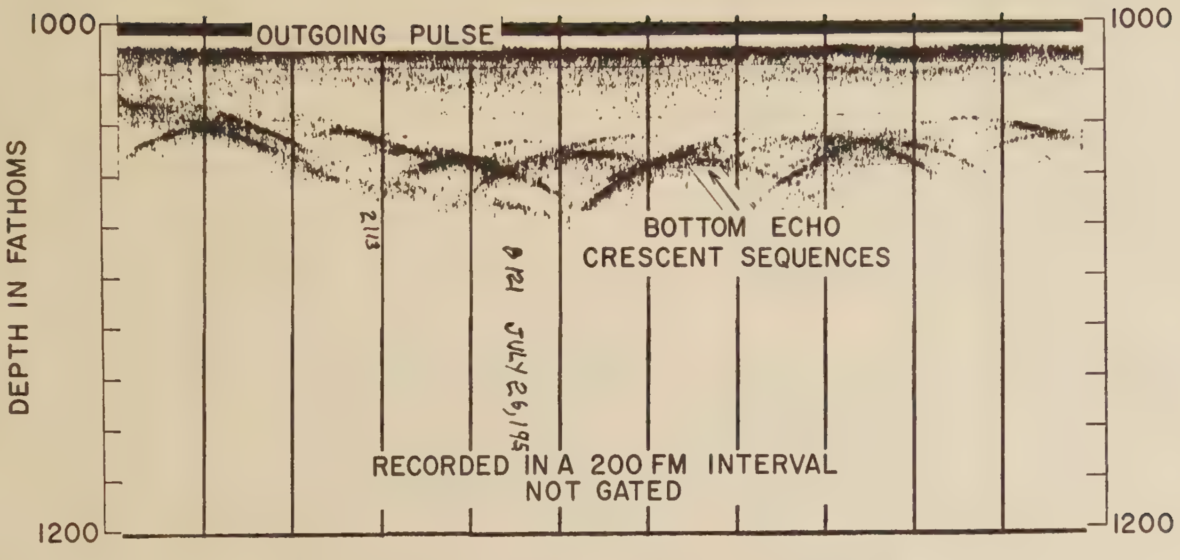

Fig. 7.—Rough bottom topography, Woods Hole recording system

sounders but is not always apparent on the record used.

Examples of this rough-bottom topography can be observed on the seaward face of the slope of the Eastern Channel. Of 677 miles of soundings taken in this area, 84 miles involved the use of the Woods Hole recording device. In analyzing these data, the average maximum difference between multiple echoes proved to be 42.7 fathoms (see fig. 8). This number was determined by measuring the total distance in fathoms from the shoalest echo of a series of multiple echoes to deepest echo and finding the average of the eleven observations found in the sounding track. By taking the midpoint at each observation, possible error was reduced to 21.4 fathoms. It is assumed that such uncertainties would also be present with the Edo recorder, were it sufficiently sensitive.

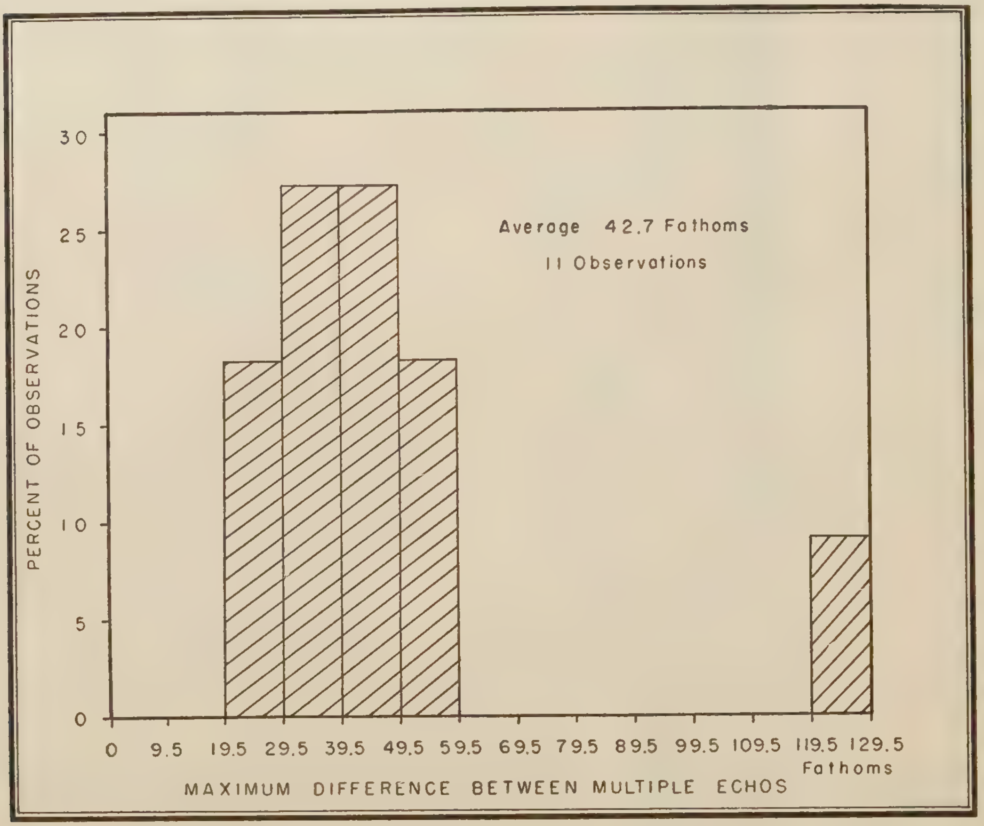

Fig. 8.—Analysis of maximum difference between multiple echoes from fathogram

Acknowledgments.—The writers are particularly indebted to the late Henry C. Stetson, whose suggestion initiated this study and whose thoughtful guidance during the year prior to his death made its completion possible. Dr. H. B. Bigelow freely gave the benefit of his advice and assistance. Dr. J. B. Hersey and Mr. Henry Johnson provided echo-sounding records of the region taken on their cruises. Dr. Wilmot H. Bradley, of the U.S. Geological Survey Office in Washington, D.C., made available the Salzman projector for reduction of the original contour chart. The writers want to thank Mr. F. Claude Ronne and the photographic department of the Woods Hole Oceanographic Institution for their part in the preparation of the illustrations. Finally, the writers would like to express their appreciation to the officers and crews of the research vessels "Atlantis" and "Bear" for their co-operation in the field. This work was carried out under Contract NObsr-43270 and its successor NObsr-72521 with the Bureau of Ships.

REFERENCES CITED

Johnson, Douglas, 1925, The New England–Acadian shoreline: New York, John Wiley & Sons, Inc.

Knott, S. T., and Hersey, J. B., 1956, High resolution echo sounding techniques and their use in bathymetry, marine geophysics, and biology (in preparation).

Mathews, D. G., 1939, Tables of the velocity of sound in pure water and sea water for use in echo sounding and sound ranging: London, Hydrographic Department, Admiralty.

Press, Frank, and Beckman, Walter, 1954, Grand Banks and adjacent shelves. Geophysical investigations in the emerged and submerged Atlantic coastal plain. VIII: Geol. Soc. America Bull., v. 65, p. 299–314.

Shepard, F. P., 1931, St. Lawrence (Cabot Strait) submarine trough: Geol. Soc. America Bull., v. 42, p. 853–864.

———, Trefethen, J. M., and Cohee, G. V., 1934, Origin of Georges Bank: Geol. Soc. America Bull., v. 47, p. 281–302.

U.S. Coast and Geodetic Survey Chart no. 70, West Quoddy Head to New York: 1947 ed.

Zeigler, J. M., and Arx, W. S. von, 1956, "Errors in Loran navigation off the New England coast, with reference to ocean current and precise bathymetric surveys: Woods Hole Oceanographic Institution Reference No. 56-48 (unpublished manuscript).

Contribution No. 886

Reprinted from LIMNOLOGY AND OCEANOGRAPHY
Vol. II, No. 2, April, 1957
Printed in U.S.A.

The Tidal Migrations of *Donax variabilis* Say[1]

HARRY J. TURNER, JR., AND DAVID L. BELDING

Woods Hole Oceanographic Institution, Woods Hole, Mass.

ABSTRACT

The behavior of the beach clam, *Donax variabilis*, resembles that of *Donax semigranosis* in that it migrates up and down the beach with the rise and fall of the tide assisted by the wash of the surf. On the rising tide the acoustic shock of the breaking waves stimulates the bivalve to emerge from the sand in advance of the uprush so that the wash carries it up the beach. On the falling tide it ignores the acoustic stimulus and emerges into the backwash to be carried down the beach. The reactions may be due to an intrinsic rhythm, changes in the water content of the sand, or a trigger-and-memory mechanism.

INTRODUCTION

The beach clam, *Donax*, is a small active pelecypod that lives between the tide lines in the surf-washed zones of sandy beaches exposed to the open ocean. It is one of the few sedentary or semi-sedentary organisms adapted to this precarious environment where there is constant danger of being buried by the shifting sands or of being stranded above the high-trade mark. Other active clams such as *Spissula* and *Mesodesma* live in a similar environment below the low-tide mark, but when storms of exceptional violence force them into the surf zone they either wash up in windrows above the high-tide mark or become buried at a fatal depth. *Donax* on the other hand manages to withstand the action of the surf and sometimes develops incredibly large populations. Coe (1953) described a population of *D. gouldi* on the beach at La Jolla, California, where the average density exceeded 20,000 individuals per square meter in a band 2 to 5 meters wide extending for more than five miles.

The adaptations that permit *Donax* to live in the surf zone do not appear to have been described in detail in the Occidental literature. Pearse *et al.* (1942) reported that *D. variabilis* moved up and down the beach with the rise and fall of the tide at Beaufort, North Carolina, but did not explain how the migrations were accomplished. Hedgpeth (1953) reported information provided by Burkenroad who had observed similar migrations of *Donax* sp. on the sand beaches of the Gulf of Mexico. He indicated that this species accomplished its migrations by popping out of the sand into the surf. On a rising tide the organisms would pop out in front of the uprush to be carried up the beach and on a falling tide they would emerge into the backwash. Hedgpeth also referred to two papers in Japanese by Mori (1938, 1950) which he had not seen. Jacobson (1955) studied *D. fossor* at Rockaway Beach, New York, and came to the conclusion that this species was merely flushed from the sand by the rushing waters to be carried in either direction by the surf. By using the foot and siphons as a drag the organism retarded its motion sufficiently to prevent it from being carried to the full advance of the wash where it would be in danger of being stranded.

In 1953 the present authors made a series of observations on *Donax variabilis* at Wrightsville Beach, North Carolina. The objective of the study was to determine if this species was sorted according to size by wave action in a manner similar to that reported by Turner (1952) for the soft clam, *Mya arenaria*, in Boston Harbor. It soon became apparent that no such sorting took place, but instead specimens of all sizes migrated up and down the beach with the rise and fall of the tide assisted by the wash of the surf. The authors were not aware of the works of Mori or Hedgpeth at that time but later read Hedgpeth's paper. Subsequently,

---

[1] Contribution Number 886 from the Woods Hole Oceanographic Institution.

copies of Mori's papers were obtained and English translations were made of the pertinent portions of the Japanese text. The behavior of *D. semigranosis* as reported by Mori corresponded closely to that of *D. variabilis* observed by the authors. However, in view of the fact that Mori's papers are not readily available and much pertinent material is in Japanese, there seems to be some justification for reviewing his work and describing the behavior of *D. variabilis* for comparison.

Mori (1938) studied the behavior of *Donax semigranosis* on the beach along the coast of Okinosu, Japan. He reported that this species accomplished its flood-tide migration by jumping out of the sand in advance of the uprush of the surf, thereby placing itself in a position to be transported landward. While riding the surf up the beach the foot was extended as a drag so that the organism never reached the upper limit of the wash. As soon as the velocity of the wash subsided, the foot was inserted into the sand and the organism dug in as the backwash began to retreat. Mori reported that 3 to 6 seconds were required for *D. semigranosis* to dig in completely so that the slower individuals were frequently carried back some distance. He also reported that this activity continued as the tide rose, resulting in the entire population moving landward in the upper part of the surf zone, the distance of migration being as much as 30 meters on the spring tide. Mori also noted that the organisms appeared to anticipate only the larger waves which would effect the longest possible transport; when low or moderate waves broke they remained in the sand. He then concluded that the jumping reaction was a response to the acoustic vibrations in the substratum which were generated with sufficient intensity only by the larger waves. Mori demonstrated this experimentally by generating similar shocks with his foot and by dashing water violently on the shore, both of which evoked the jumping reaction.

Mori also studied the movements of *D. semigranosis* on the ebb tide and determined that at this phase the clams remained below the surface of the sand until the surf had begun to retreat down the beach. They then jumped out into the backwash where they were carried seaward. It is not clear from the available translation whether Mori believed there was any difference in the sequence of physical events at the opposite phases of the tide that influenced the timing of emergence with respect to the wash. Later (1950), however, he made further observations and suggested that *D. semigranosis* might be endowed with an intrinsic rhythm synchronized with the tidal cycle, which caused it to anticipate the uprush on the flood and await the backwash on the ebb.

THE BEHAVIOR OF *DONAX VARIABILIS*

Donax variabilis is a common inhabitant of the beaches of the Middle and South Atlantic Coast of the United States. At Wrightsville Beach, North Carolina, where the observations to be reported were made, the shore consists of fine sand which is so compact that footprints made by a person of average stature are scarcely visible. In September, 1953, the beach sloped 2.7 feet per hundred feet so that the 3.8-foot tide produced an intertidal zone approximately 150 feet wide. Some portion of the intertidal zone was always awash with surf which rolled in from a line of breakers plunging on an outer sandbar some distance from shore. There were generally at least three rows of white surf between the breakers and the shore line. Here the turbulence was so great that the bottom sediments were continually agitated, as a result of which finer particles were continually being washed out, leaving an accumulation of shell fragments and other coarse heavy material. As each line of surf reached the slope of the beach, the flow became smoother and the bottom sediments were scarcely disturbed. The few pebbles and shell fragments on the surface of the sand were continually moving back and forth with the advance and retreat of the wash, eventually coming to rest in the usual windrow of debris above the high-tide mark.

The average extent of the wash zone was approximately 45 feet during the study, although irregular wave patterns frequently produced considerable variation. During sequences of regular waves the period averaged seven seconds. The underlying sand in the seaward half of the wash zone was saturated at all stages of the tide, while the sand in the landward half was somewhat undersaturated. Since the sand in the seaward half was incapable of absorbing water, a wet slick remained on the surface as each backwash retreated. The sand in the landward half on the other hand could absorb small quantities remaining on the surface so that no slick remained. Thus at the instant that the backwash had retreated to its fullest extent it was possible to divide the wash zone into a saturated or "wet" portion on the seaward side, and an unsaturated or a "dry" portion on the landward side.

The first collections of *Donax variabilis* were made at dead low tide. The majority of the population was concentrated along the middle of the wash zone with a few scattered specimens occurring up the beach as far as the mid-tide line. All collections produced specimens of mixed sizes indicating that no sorting for size had taken place. Continued collections taken during the first half of the flood tide showed that the population was moving up the beach with the tide, but the rapid sequence of events made it difficult to observe how this was accomplished. Then a fortunate combination of circumstances provided a clue to the mechanism of the migration. During a sequence of high, regular waves the backwash of one wave collided with the uprush of the subsequent one and prevented it from overrunning the wash zone in the usual manner. At the same time an unusually large breaker crashed on the outer bar. Immediately a row of *Donax* emerged from the sand, each specimen lying motionless on its side. The row extended along the beach as far as the eye could see. The next uprush then picked up the specimens and carried them landward, and as the velocity decreased each specimen inserted its foot into the sand, tipped up on its anterior extremity, and dug in in a matter of seconds. Closer observations made during subsequent excursions of the wash showed that similar behavior took place whenever a large wave broke. In general the animals emerged into the uprush just as it passed over them, but there was a number of occasions when they anticipated it by emerging beforehand. It was also determined that the foot was extended as soon as the organisms began to ride the surf to retard their velocity and prevent them from being carried to the limit of the uprush.

The coincidence between the breaking of the waves and the emergence of the animals lead immediately to the idea that the acoustic shock generated by the breakers caused the emergence. To test the theory experimentally, a similar shock was generated during a sequence of low waves by stamping on the sand with the foot. When this was done a number of organisms emerged in a circle several feet in diameter. Such experiments continued whenever circumstances permitted demonstrated that the organisms would emerge only from the "wet" or saturated portion of the wash zone and that one or more washes of surf had to pass over an organism before it would repeat the process. Careful observations revealed the normal pattern of behavior to be as follows: As each large breaker generated an acoustic shock, the organisms would emerge from the saturated sand either in advance of the uprush or immediately into it and be carried up the beach where they would quickly dig in. Specimens failing to reach the unsaturated portion of the wash zone would then wait until one or more washes passed over them before emerging again. In this manner the entire population was carried up the beach, finally arriving at the upper, unsaturated portion of the wash zone at full high tide.

As soon as the tide turned the population began to move seaward. The animals accomplished this by waiting until a large wash of surf had passed over them and had begun to retreat down the beach. They then emerged from the sand into the backwash which carried them down the beach. Again each specimen extended its foot as a drag, and dug in rapidly when the velocity decreased enough to permit the foot to obtain purchase in the sand. During the ebbing phase of the tide the organisms failed to respond to the crash of the breakers or to shocks generated by stamping, but reacted only to water passing over them. The latter reaction was confirmed experimentally by simply splashing a large bucket of water up the beach at an appropriate moment. When this was done the organisms waited for an instant and then emerged from the sand as the water ran back down the beach. This simple experiment performed during periods when the waves were low demonstrated that the organisms reacted to the passage of water over them only if they were in the upper, unsaturated portion of the wash zone. In addition they would react only if a considerable amount of water passed over them, and once transported they would wait until one or more washes passed over before emerging again. In this manner the entire population was carried down the beach with the ebbing tide except for occasional individuals that became stranded.

Observations were continued for a number of tidal cycles and the experiments were repeated whenever the circumstances permitted. The reactions of the organisms to the passage of water over them was tested on the flood tide with negative results. Their reaction to the acoustic shock during the flooding tide was confirmed a number of times. In a like manner the reaction to water and the lack of response to the acoustic shock on the ebbing tide was also confirmed.

DISCUSSION

The results of two independent studies and a third observation leave little doubt that at least two species of *Donax* change their pattern of behavior simultaneously with the change of the tide, resulting in the surf washing them up the beach on the rising tide and down the beach on the ebb. Neither investigation however has revealed the mechanism that caused this change in activity. Mori's suggestion of an intrinsic rhythm synchronized with the tidal cycle is attractive in view of current interest in so-called biological clocks, but it does not seem adequate. Continued survival of the *Donax* populations would depend on nearly perfect synchrony between the activities of the organisms and the cycle of the tide. Slight phase differences might leave the population stranded above the high-tide mark, or transport it into the turbulent surf zone at low tide. Thus it is difficult to see how such perfect synchrony can take place, since the tidal cycle alone is subject to irregularities resulting from meteorological conditions.

Any alternate hypothesis requires that the organisms be capable of sensing some variation between the conditions prevailing during the opposite phases of the tide, or that some stimulus at each extreme of the tide triggers a persistent pattern of behavior. The one obvious difference between the ebb and the flood is the direction of change of the still-water level, which has a maximal rate of less than 0.1 foot per minute. The main effect this slow change has on the organisms is to make their environment become progressively wetter on flood tide and progressively dryer on the ebb. Thus it is possible that the change in moisture content of the sand acts as a controlling mechanism which influences the organism to react to the acoustic shock of the breakers as its environment becomes wetter, and to the rush of the wash as the environment dries out. In order for this mechanism to operate successfully it is necessary for the organism to be able to ignore minor changes in the moisture content produced by sequences of high waves followed by short periods of relatively calm water.

It is also possible that *Donax* may be equipped with a timing mechanism that acts as the controlling stimulus. If this should be the case the acoustic stimulus would affect only those organisms that had been situated in saturated sand for a certain length of time on the rising tide, and on the ebb the stimulus of the wash would affect only those organisms that had been long enough in unsaturated sand. This hypothesis requires that the organism's timing mechanism be accurately tuned to the rate of change of the water level and does not entirely take care of variations resulting from complex wave patterns.

As a final suggestion a trigger-and-memory hypothesis is proposed. This hypothesis also involves a timing mechanism but a less precise one. It is proposed that conditions that occur at each extreme of the tidal cycle trigger the organism to commence the appropriate behavior pattern for the particular phase and that this pattern persists until reversed by the opposite stimulus. Thus as the tide approaches its full height the organism moving from saturated to unsaturated sand finally arrives at a level where the sand never does become saturated. A somewhat prolonged wait in this unsaturated environment might trigger the organism to ignore the acoustic stimulus and react only to the wash. The organism then "remembers" the trigger stimulus and exhibits the appropriate behavior until it finally comes to rest in sand that remains saturated. This then triggers the flood tide behavior. The trigger-and-memory hypothesis thus offers a possibility of explaining the observed abrupt change in the behavior at the tidal extremes and the apparent invariability of the reactions of the organisms during each phase of the tide.

The different behavior of *Donax fossor* described by Jacobson deserves some consideration in view of the suggestion by Abbot (1954) that this species may only be a cold-water variety of *D. variabilis.* It is obvious from Jacobson's account that the character of the beach at Rockaway is quite different from that at Wrightsville. Jacobson states that the wash becomes so completely roiled with sand as to make observations impossible, indicating that the sediments are not nearly so compact as are those at Wrightsville. He also reports that *D. fossor* migrates only twenty feet. If this distance is the full width of the intertidal zone the beach has a slope of nearly 20 feet per hundred feet in contrast to the slope of 2.7 feet per hundred at Wrightsville. The steep profile of the beach provides a situation in which the wash of the surf would run up the beach in a much shorter time after the wave breaks than on beaches of more gentle slope where it could wash the animals out of the loose sand before they could respond to acoustic stimuli. Thus any similarity of the behavior of *D. fossor* and *D. variabilis* may have been obscured by the physical conditions of the environment at Rockaway.

SUMMARY

The observed behavior of *Donax variabilis* agrees with that described independently by Mori for *D. semigranosis.*

On the flood tide *D. variabilis* responds to the acoustic shock of breaking waves by emerging from the sand in advance of the uprush and rides the surf up the beach. It only reacts in this way if it is situated in saturated sand.

On the ebb tide *D. variabilis* responds to the passage of the wash over it and emerges into the backwash, as a result of which it is transported down the beach. It only reacts in this way if it is situated in unsaturated sand.

Three hypotheses are proposed to explain this unique pattern of behavior.

REFERENCES

Abbot, R. T. 1954. *American Sea Shells*, pp. 437–438. D. Van Nostrand Co., New York.

Coe, W. R. 1953. Resurgent populations of littoral marine invertebrates and their dependence on ocean currents and tidal currents. Ecology, **34**: 225–229.

Hedgpeth, J. W. 1953. An introduction to the zoogeography of the northwestern Gulf of Mexico with reference to the invertebrate fauna. *Inst. Mar. Sci.*, **3**: 186.

Jacobson, Morris K. 1955. Observations on *Donax fossor* Say at Rockaway Beach, New York. *The Nautilis*, **68**: 73–77.

Mori, S. 1938. *Donax semigranosis* Dkr. and the experimental analysis of its behavior at the flood tide. Dobutsugaku Zasshi, **50**(1): 1–12.

Mori, S. 1950. Characteristic tidal rhythmic migration of a mussel, *Donax semigranosis* Dkr. and the experimental analysis of its behavior. Dobutsugaku Zasshi, **59**(4): 88–89.

Pearse, A. S., H. J. Humm, and G. W. Wharton 1942. Ecology of sand beaches at Beaufort, North Carolina. Ecol. Monogr., **12**: 135–190.

Turner, H. J., Jr. 1952. The Raccoon Island Set. Fifth report on Investigations of the Shellfisheries of Massachusetts. Commonwealth of Massachusetts, Boston, pp. 30–32.

Contribution No. 887

Reprinted from BIOLOGICAL BULLETIN, Vol. 113, No. 2, 275–285, October, 1957
Printed in U. S. A.

FREEZING AND DRYING IN INTERTIDAL ALGAE[1]

JOHN KANWISHER

Woods Hole Oceanographic Institution, Woods Hole, Mass.

The intertidal region is an environment characterized by widely fluctuating conditions. It will be shown in this paper that in high latitudes the algae in this zone are exposed to extensive freezing and drying. These two aspects of immersion are considered together, since they have the common feature of cellular dehydration. In particular, their separate effects on the metabolism of algae have been investigated.

First will be discussed the effect of low temperatures in freezing a large amount of water in certain algae. Next, the natural dehydration that is caused by evaporation in several of the same species will be described. Finally, measurements will be reported which show a greatly depressed respiration in both the frozen and dried states. Some observations on the winter survival of *Fucus* in the Arctic are also included.

I. FREEZING

In the Woods Hole region in winter there are a number of macroscopic brown, green, and red algae exposed to freezing temperatures by the tide. They frequently feel brittle to a degree which suggests ice in them. Some of them have been observed imbedded in the ice at temperatures as low as − 20° C. Conditions are even more rigorous in the Arctic where *Fucus* is a prominent intertidal alga. It may spend six months or more frozen in the ice at temperatures which go below − 40° C. Since these plants contain 70 to 80 per cent water, it seemed pertinent to determine how much of this water, if any, is frozen at these extreme temperatures. Bieble (1939) reported that several intertidal algae would survive being frozen, but he made no quantitative determinations of the ice.

1. *Method*

Water gives off heat and also expands when it changes to ice. The expansion has been measured directly in a dilatometer by Moran (1935), Gortner (1937), and others to determine the amount of ice. Scholander *et al.* (1955) devised a flotation method to measure specific gravity and found as much as 90 per cent frozen water in the lichen *Cetraria richardsonii.* Volumetric methods were unsuitable here because of the difficulty of the dissolved gases that come out of solution on freezing. This would cause a density change which could not be separated from the same effect due to ice formation. Calorimetric determinations of ice, based on the conveniently large heat of fusion of water, have been used by Greathouse (1935), Ditman *et al.* (1942), and others. Scholander *et al.* (1953) have recently reviewed these two methods.

---

[1] Contribution Number 887 from the Woods Hole Oceanographic Institution.

There has been no previous quantitative work on ice in algae. This author has described a simplified calorimetry for small animals (Kanwisher, 1955) which has been used here on several of the large intertidal algae. The calorimeter vessel is an ordinary Thermos bottle. The temperature of the water inside is read to 0.01° C. by a mercury thermometer through the stopper. The sensitivity is varied by changing the amount of water in the Thermos. Weighed pieces of ice are used for calibration.

A piece of the alga to be frozen, usually a few grams, is sponged free of excess water with filter paper, weighed, and placed in a small vial in a cold chamber set to the desired temperature. At least four hours is allowed for phase equilibrium between the water and ice in the alga. A check weighing at this point usually showed less than 1 per cent loss of water by evaporation.

The Thermos is thermally equilibrated with the desired amount of water and the temperature noted. Then the vial is removed from the cold chamber and alga immediately shaken into the open Thermos. The vial prevents transfer of heat from the hands to the frozen alga. The stopper is replaced quickly and the Thermos is shaken. During the next few minutes the lowest temperature is noted. The measurement is completed by weighing the alga after drying it for two hours in an oven set at 100° C. The amount of water and dry substance in the initially frozen material is then computed.

If no ice is formed the number of calories supplied to the alga is proportional only to its weight and the temperature interval through which it is warmed. In the absence of any change of state the specific heat is nearly constant with temperature. If ice is present the calorimeter must supply 80 additional calories to melt each gram.

The calories supplied to the alga by the calorimeter are equal to the temperature drop observed times the heat capacity which has been determined by calibration with ice. Part of these calories go to warm the dry substance and the water from the cold box temperature T_1 up to the final calorimeter temperature T_2. This is equal to

$$(T_2 - T_1) \times (0.3 \times \text{dry wt.} + \text{wt. of water}),$$

where 0.3 has been separately determined to be the specific heat of the dry substance. That of water is 1.0. The remainder of the calories melt any ice that is present. This is converted to grams of ice. Since the water in the starting sample is known, the fraction of it frozen at the temperature T_1 has been determined. A small correction is necessary because the specific heat of ice is only half that of water (Ditman *et al.*, 1942).

2. *Results*

Figure 1 is typical of the data thus obtained. It is a plot of the per cent of water that is converted to ice at various freezing temperatures in *Fucus vesiculosus*. Similar curves were obtained for *Ascophyllum nodosum, Chondrus crispus,* and *Ulva lactuca*. The following table shows the percentage of water as ice at −15° C., the lowest temperature used.

It is evident that a large fraction of algal water is readily frozen at temperatures which frequently occur in nature. The large surface area of *Ulva* would tend

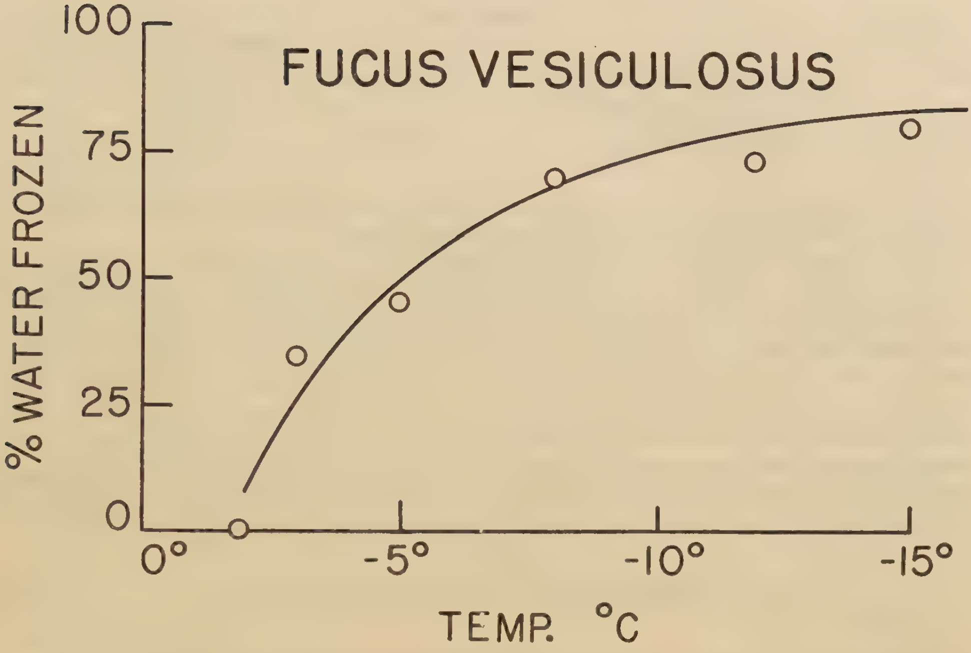

FIGURE 1. Freezing curve of *Fucus*.

to absorb heat during the transfer to the calorimeter. This may account for its having the least ice in Table I.

II. WATER CONTENT IN ALGAE NATURALLY DRIED

Exposed upper intertidal algae become very obviously dried on a windy day when the relative humidity is low. Isaac (1933) measured a 68 per cent loss in weight in *Pelvetia canaliculata* during normal exposure on the short. He did not determine the dry weight. Feldmann (1937) noted that *Bangia fuscopurpurea* can remain out of the water for periods as long as 15 days and still survive. Zaneveld (1937) found only a 30 per cent weight loss in drying conditions. A series of measurements have been made here to determine how much water is normally lost under such conditions.

When the algae looked very dry at low tide on a windy day, samples were taken and weighed immediately. They were then immersed in sea water for several hours and weighed again. Some of them were used to demonstrate photosynthesis by a method described later. Finally, oven drying and weighing gave the necessary

TABLE I

Species	Per cent ice at −15° C.
Fucus vesiculosus	82
Ascophyllum nodosum	76
Chondrus crispus	74
Ulva lactuca	69

TABLE II

Species	Per cent of water lost
Fucus vesiculosus	91
Chondrus crispus	63
Ulva lactuca	77
Enteromorpha linza	84

data to compute the water present when immersed and also in the dried state. Table II gives the maximum dehydration values found.

To measure the rate of loss and reabsorption of water, pieces of *Fucus* were exposed to room air of 22° C. and 40 per cent relative humidity. Such values are not uncommon in nature. They were weighed at intervals and then replaced in sea water and their weight again followed. From Figure 2 it is clear that severe drying can take place during the length of time of tidal exposure. The rate was increased several fold when a breeze was simulated with an electric fan. Less than an hour after re-immersion most of the lost water has been regained. Thin forms such as *Ulva* probably dry even more rapidly. Where the algae grow in many overlapping layers probably only the uppermost are dried very much. The interest here, however, is only in the maximum drying that can be tolerated.

III. RESPIRATION IN FROZEN AND DRIED ALGAE

1. *Method*

Respiration is awkward to measure at freezing temperatures with conventional methods such as the familiar manometric technique. The volume change resulting from water turning to ice cannot readily be separated from that due to oxygen consumption. The Winkler method of following the disappearance of dissolved

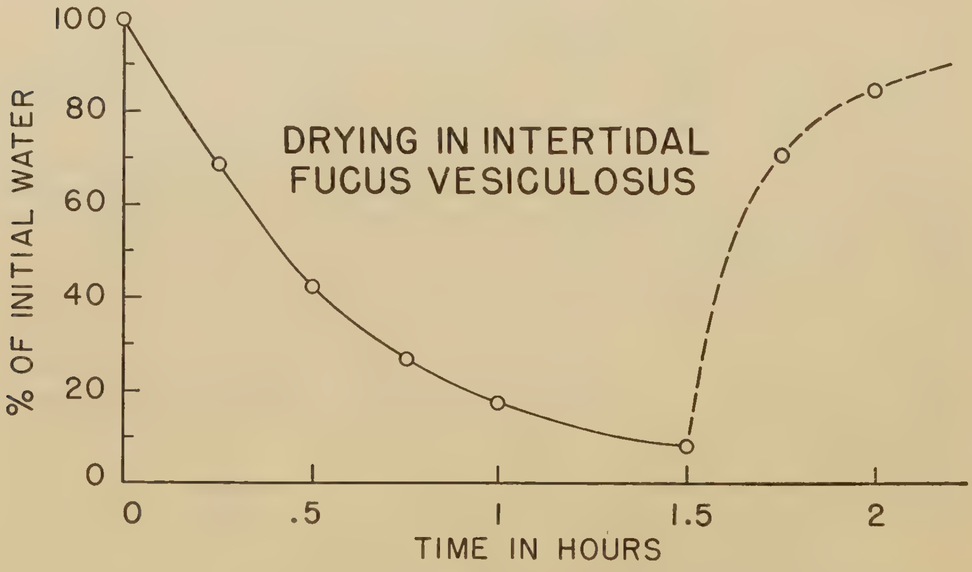

FIGURE 2. Drying curve of *Fucus*.

oxygen cannot, of course, be applied to frozen or dried material. Oxygen consumption in the region of freezing is so sharply temperature-dependent that any method which requires part of the time at higher temperatures is open to gross errors. Scholander *et al.* (1953), in reviewing the literature on respiration in frozen material, concluded that many of the techniques were inadequate for the problem at hand. They used a method of gas analysis which has been applied here with slight modification.

The material is enclosed in a syringe with a known amount of air and kept in the dark. Samples of gas are withdrawn at intervals and analyzed for oxygen. Respiration is computed from the rate of oxygen decrease in the gas phase. Since blanks run in the same way give negligible values, the utilization of oxygen can only be attributed to the frozen or dried algae. The method is specific for oxygen and does not rely on volume decrements which are assumed to result from oxygen being used.

For the low temperature values the algae were placed in darkened hypodermic syringes in a cold bath set at the desired temperature. At least six hours was allowed for the ice-water equilibrium to be reached. The syringes were flushed with chilled outside air and sealed. The tips of the syringes extended above the surface of the coolant. Samples of the gas could be removed without taking the syringes from the bath. The plunger was free to move up as a sample was withdrawn. By thus avoiding any differential pressure when sampling, the danger of leaks is reduced.

The oxygen was measured with the ½-cc. gas analyzer of Scholander (1947) to 0.02 per cent accuracy. Duplicate analyses were made. When a respiratory period was started by flushing in outside air, the initial concentration was assumed to be 20.94 per cent. Repeated measurements varied between 20.93 and 20.96. Because of the possibility of rate of oxygen consumption depending on tension, oxygen was never depleted below 18 per cent. Two readings were usually taken. The time between these varied from 1 to 200 hours. The slope determined by these points was used to compute the rate of oxygen consumption. The figures are in units of mm.^{3} 0_2 per gram of dry weight of alga per hour.

For the dried algae a fresh sample was weighed fully moist and dried by exposing it to air. It was then weighed again and placed in a syringe. The air in the syringe becomes saturated and no additional water is lost. The readings were made by the same method as for the frozen material. The temperature was kept at 15° C.

Fully moist respiration measurements above 0° were made with volumetric respirometers (Scholander *et al.*, 1952). At 0° these checked with the gas analysis method.

2. *Results*

Respiration in *Fucus* above and below 0° is plotted in Figure 3. Similar curves were found for *Chondrus* and *Ulva*. The respiration drops sharply below 0°. In in the interval from 0 to − 10 the apparent Q_{10} is 17. For the same interval above 0° it is 2. The other species had a Q_{10} of 15 and 23 below 0°, respectively, and close to 2 above. At − 15° it was necesary to wait 7 to 8 days for the oxygen in the syringe to decrease by a large enough amount to insure an accurate determination.

When the algae were dried, the oxygen consumption again decreased. Figure 4 shows the respiration of *Fucus* related to the degree of dehydration. When 80 per cent of the normal water was lost, the metabolism was down to one-sixth of its normal value. If a sample was allowed to regain water by soaking, the metabolism increased. The solid points were taken consecutively on the same piece of material and showed the reversible nature of the phenomenon. *Chondrus* and *Ulva* showed the same decreased respiration when dried and also recovered the higher rate when re-immersed.

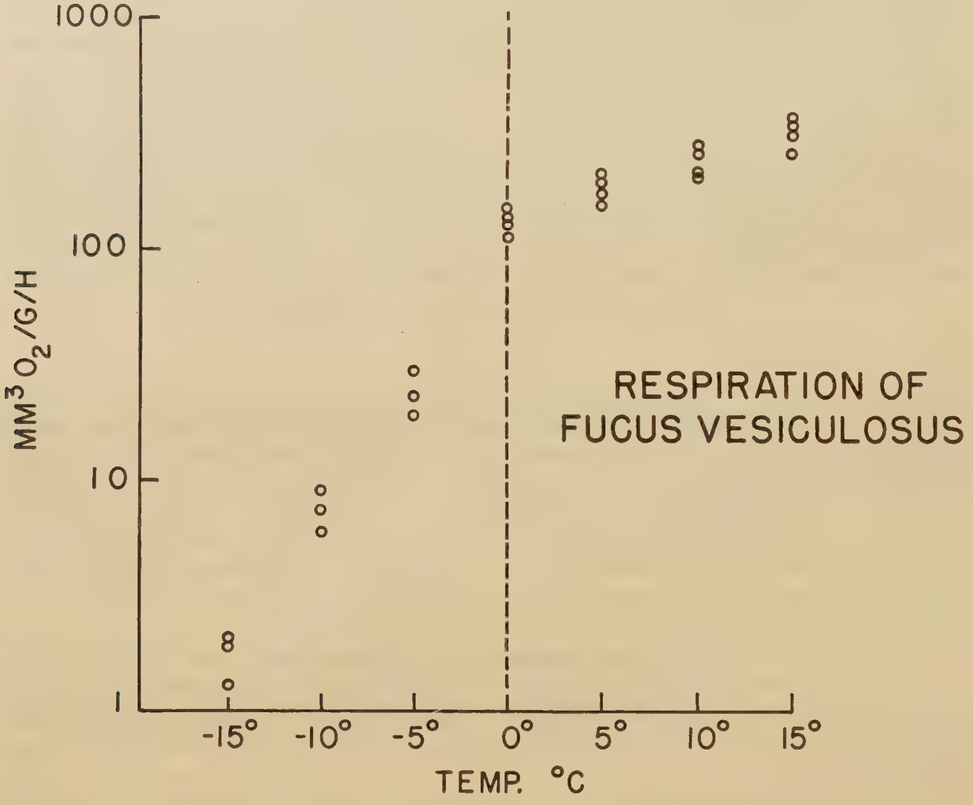

Figure 3. Oxygen consumption vs. temperature of *Fucus*.

Loss of water in freezing or drying must increase the salinity of the remaining fluids. Although part of this fluid is in the inter-cellular space, it is in equilibrium with the interior of the cells. Thus loss of any algal water will raise the salinity inside the cells. To determine whether salinity had a specific effect on metabolic rate, higher salinities were made by draining the brine from frozen sea water. Pieces of *Fucus, Chondrus,* and *Ulva* were immersed in these for 12 hours. The tissue chloride concentration was measured by acid digestion and titration. It was always proportional to that of the external medium. These species show no evidence of regulating chloride. Respiration rates were measured at the various salinities. In all cases oxygen consumption decreased less than 30 per cent when the salinity was increased by three times. This concentration is produced at − 8° C. by freezing out of water. At such a temperature the respiration is decreased 10- to 15-fold below that at 0°. Salinity is clearly not the primary respiratory depressant when water is lost from the cells by either freezing or drying.

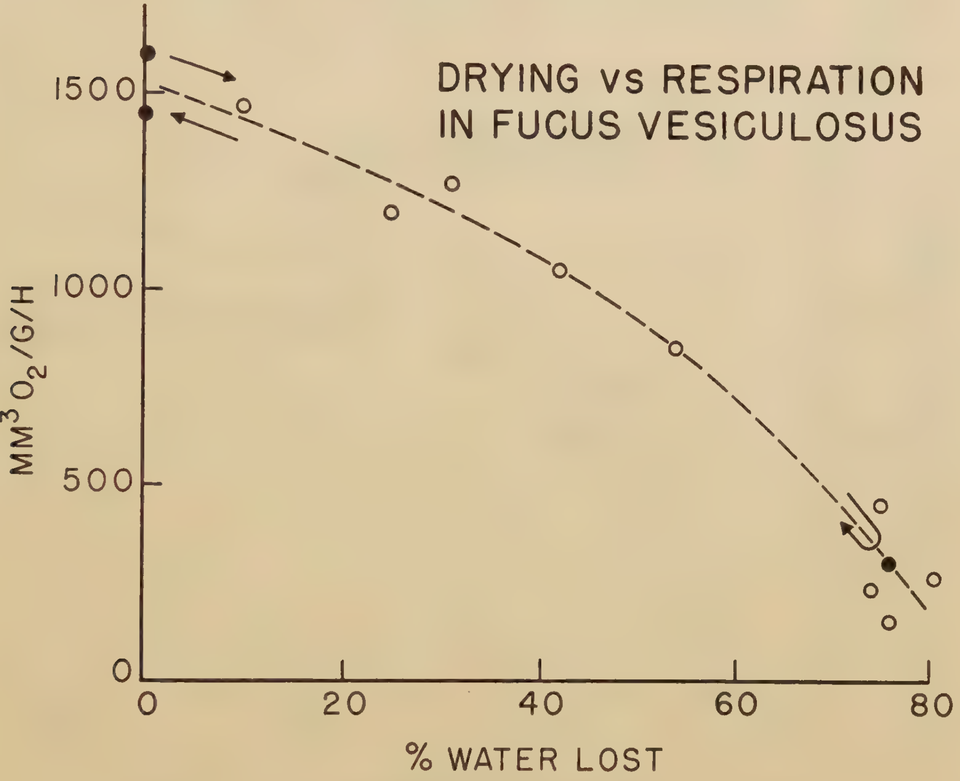

Figure 4. Oxygen consumption at various degrees of dehydration.

IV. Discussion

Previous attempts have been made to determine respiratory gas exchange in frozen plants. Scholander *et al.* (1953) measured a precipitous drop in oxygen consumption of several Arctic phanerograms and lichens below 0° C. Ice determinations by a floatation method showed that at − 20° C., more than 90 per cent of the water in some lichens was frozen. They thought it likely the drop in metabolic rate was due to cellular dehydration. They have reviewed the literature and point out that the techniques used previously to measure low temperature respiration were inadequate for the low rates that occur. At freezing temperatures they found a Q_{10} of 20 to 50, while above 0° the same material showed the usual two- to four-times change in oxygen consumption over a ten-degree interval.

Smyth (1934) found a linear relationship between water content and respiration in lichens. The respiration of air-dried *Acacia* seeds was measured by White (1909) to be only 1/10,000 that of moistened seeds. In dry *Ricinus* seeds he could detect no oxygen consumption. Spores of single-celled forms are dehydrated and are known to show very low oxygen consumption. Respiration in dried algae does not seem to have been previously studied.

The intertidal algae used in these experiments are normally exposed to both freezing and drying. It has been shown here that their respiration under either of these conditions is sharply reduced. In the region of freezing temperatures their Q_{10} is about two times what would be expected from dehydration alone. In going from 0° to − 10°, 75 to 80 per cent of the water is frozen. This water loss alone should cause a decrease of six to ten times in oxygen consumption. When the straight temperature effect of a Q_{10} of two is also included, the total apparent Q_{10} should be in the range of 12 to 20. This is in reasonable agreement with those measured directly in the frozen algae.

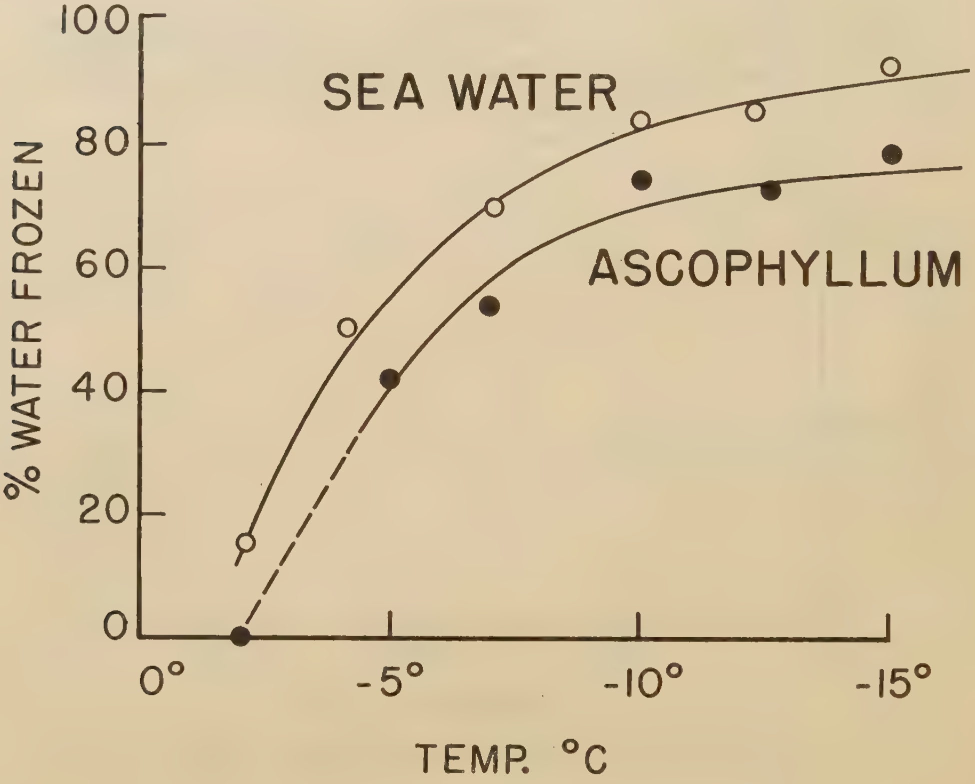

FIGURE 5. Curves showing the freezing of a greater fraction of sea water as compared to algal water.

At progressively lower temperatures calorimetric ice determinations become less accurate. More heat must be supplied to warm the material over the increased temperature range. The calories representing the melting of ice become a smaller fraction of the total measurement and are thus subject to a larger percentage error. It appears from Figure 1, however, that 15 to 20 per cent of the water is resistant to freezing. The same technique of calorimetry has been applied to a vial of sea water to find the amount of ice at various temperatures. It is compared with *Ascophyllum nodosum* in Figure 5. A larger fraction of the water in sea water freezes at all temperatures than in the algae.

It appears that part of the water in algal cells is unavailable for freezing. Many authors have presented evidence for unfreezable water in gels and also in plant and animal material (Moran, 1926; Greathouse, 1935; review of the literature by Scholander *et al.*, 1953). Moran was unable to freeze all of the water in a gelatin, even at − 40° C. The water molecule has a large dipole moment and may well be subject to forces less powerful than conventional bonding but still strong enough to prevent its being frozen. However, Grollman (1931) has rejected the idea of bound water in colloidal systems.

White (1909) found evidence for binding of part of the water in plants at ordinary temperatures. In *Acacia* seeds three per cent remained even after drying over calcium chloride.

Roualt's law expresses a linear relationship between the concentration of a solution and its freezing point depression. If one can assume that the ratio of dry matter to water is equivalent to a concentration, this quantity should increase linearly below freezing. Scholander *et al.* (1953) found this to be so in a *Chironomus* larva. Sea water is nearly linear as would be expected of a solution of crystalloids. The ratio in *Ascophyllum* tends towards a constant value at low temperatures. This could happen if part of the water were bound in such a way that it would not freeze. It would also result from any of the dissolved substances coming out of solution. The concentrations increase as water is frozen out while at the same time the solubility must decrease with temperature. In a frozen alga at − 15° C., the solubility of sodium chloride has been exceeded. The cells can either maintain a supersaturation or must be able to actually cope with internal salt crystals.

Siminovitch and Briggs (1949) measured an increased mobility of water in the frost-hardy cells of the black locust, *Robinia*. They thought this was necessary to allow a more rapid exit of water from the cells when intercellular freezing occurs. Such is likely the case with the algae used here when they undergo rapid freezing and drying. It is generally believed that internal freezing is lethal to cells, probably by the physical disruption of ice crystals in the protoplasm. Direct observation will be necessary, however, to determine the locus of this ice.

The lowered respiration observed in the frozen and dried algae may be of value to them in surviving these periods of stress. There can be little growth at such times since the usual supply of nutrients from the sea water is not available. When the alga is frozen, the light available for photosynthesis is usually limited, such as during the Arctic winter. The slowing-down observed here represents a less serious drain on the food stores. The ability of these algae to survive in the intertidal zone may, however, be merely a case of their not being injured by the freezing and drying that are inevitable in such a location.

Respiration has been called the flame of life. In algae at low temperatures it burns very low but is never entirely out.

V. Observations of Arctic Fucus

The author was a member of an expedition to Hebron in northern Labrador, sponsored by the Arctic Institute of North America in 1954. On arrival early in July, *Fucus* was abundant in the intertidal zone along much of the coast. Large reproducing plants were common although the ice had been gone only a month. It seemed certain they had not grown this much in the brief period of open water. Yet during the winter the ice is several feet thick and is solid to the bottom along the shore. One was led to believe the *Fucus* was frozen solid in the ice during the entire winter.

During this summer visit, pieces of *Fucus* were cooled to − 13° C. in a vial immersed in a salt and ice mixture. Calorimetry showed that ¾ of the water was frozen at this temperature. About two grams wet weight of recently frozen *Fucus* were put in a 20-cc. syringe with sea water. The syringe was placed in the sun and kept close to 0° by a snow and water mixture. One-ml. samples were removed and analyzed for dissolved oxygen by a gasometric method (Scholander *et al.,* 1955). In 30 minutes the oxygen rose from 3.6 to 8.4 mm^3/cc. Soon after this, bubbles formed indicating supersaturation of the dissolved oxygen. Thus the sample of *Fucus* was still able to photosynthesize actively, even directly after being unnaturally frozen during the summer.

Fortunately it was possible to return to the same spot in March and check on the winter condition of the *Fucus.* The ice was many feet thick along the shore. In places tidal stresses had buckled it and the projecting sheets contained some of the algae frozen into the ice when it formed. This *Fucus* was fully exposed to the air temperatures which, during the brief visit, were as low as − 26° C. Earlier in the winter they had dropped to − 40° C. or lower.

Pieces of ice with *Fucus* in them were chipped free and thawed. The melted water contained only about 0.3 per cent salt. The alga was again checked for photosynthesis with the same positive result. The winter respiration rate was found to be close to that in the summer. There was no sign of a large oxygen debt from the long period in the ice. The *Fucus* is apparently ready to start active growth again in the spring where it left off in the fall.

These studies were aided by a contract between the Office of Naval Research, Department of the Navy, and Arctic Institute of North America. Reproduction in whole or in part is permitted for any purpose of the United States Government. I am deeply indebted to Dr. Per Scholander for advice and encouragement. My wife has been of considerable assistance both in the field and laboratory.

Summary

1. As much as 80 per cent of the water in intertidal marine algae is frozen when exposed to the low air temperatures that regularly occur in nature.

2. The same species may lose 90 per cent of their water by ordinary drying during tidal exposure.

3. Metabolism is greatly depressed in both the frozen and dried states.

4. The ability to withstand drying may be related to freezing hardiness.

5. Some extreme conditions in the Arctic are described. *Fucus* spends many months frozen into the sea ice at temperatures down to 40° C., yet it is capable of photosynthesis immediately upon being thawed out.

LITERATURE CITED

Bieble, R., 1939. Über die Temperaturresistenz von Meeresalgen verschiedener Klimazonen und verschieden tiefer Standorte. *Jahrb. Wiss. Bot.,* **88**: 389–420.

Ditman, L. P., G. B. Vogt and D. R. Smith, 1942. The relation of unfreezable water to cold hardiness of insects. *J. Economic Entomology,* **35**: 265–272.

Feldmann, J., 1937. Recherches sur la vegetation marine de la Mediterranée. La côte des Alberes. *Rev. Algologique,* **10**: 1–399.

Gortner, R. A., 1937. Selected topics in colloid chemistry. Cornell Univ. Press, Ithaca, New York.

Greathouse, Ga. A., 1935. Unfreezable and freezable water equilibrium in plant tissues as influenced by sub-zero temperatures. *Plant Physiol.,* **10**: 781–788.

Grollman, A., 1931. The vapour pressure of aqueous solutions with special reference to the problem of state of water in biological fluids. *J. Gen. Physiol.,* **14**: 661–683.

Isaac, W. E., 1933. Some observations and experiments on the drought resistance of *Pelvetia canaliculata. Ann. Bot.,* **47**: 343–348.

Kanwisher, J. W., 1955. Freezing in intertidal animals. *Biol. Bull.,* **109**: 56–63.

Moran, T., 1926. The freezing of gelatin gel. *Proc. Roy. Soc. London, Ser. A,* **112**: 30–46.

Moran, T., 1935. Bound water and phase equilibria in protein systems: egg albumin and muscle. *Proc. Roy. Soc. London, Ser. B,* **118**: 548–559.

Scholander, P. F., 1947. Analyzer for accurate estimation of respiratory gases in one-half cubic centimeter samples. *J. Biol. Chem.,* **167**: 235–250.

Scholander, P. F., C. L. Claff, J. R. Andrews and D. F. Wallach, 1952. Microvolumetric respirometry. *J. Gen. Physiol.,* **35**: 375–395.

Scholander, P. F., L. van Dam, C. L. Claff and J. W. Kanwisher, 1955. Micro-gasometric determination of dissolved oxygen and nitrogen. *Biol. Bull.,* **109**: 328–334.

Scholander, P. F., W. Flagg, R. J. Hock and L. Irving, 1953. Studies on the physiology of frozen plants and animals in the Arctic. *J. Cell. Comp. Physiol.,* **42**: 1–56.

Siminovitch, D., and D. R. Briggs, 1949. The chemistry of the living bark of the black locust tree in relation to frost-hardiness. *Arch. Biochem.,* **23**: 8–17.

Smyth, E. S., 1934. A contribution to the physiology and ecology of *Peltigera canina* and *P. polydactyla. Ann. Bot.,* **48**: 781–818.

White, J., 1909. The ferments and latent life of resting seeds. *Proc. Roy. Soc. London, Ser. B,* **81**: 417–442.

Zaneveld, J. S., 1937. The littoral zonation of some Fucaceae in relation to desiccation. *J. Ecology,* **25**: 431–468.

Contribution No. 888

Deep-Sea Research, 1957, Vol. 4, pp. 211 to 217. Pergamon Press Ltd., London.

Composition of the swim-bladder gas in bathypelagic fishes

JOHN KANWISHER and ALFRED EBELING

(*Received* 7 *February* 1957)

Abstract—Measurements were made of swim-bladder size and gas composition on pelagic fish in the eastern Pacific. The physiological problem of vertical migration with a swim-bladder is discussed. It is concluded that some gas-containing fish migrate vertically but that net-collecting data is too fragmentary to determine if such fish are primarily responsible for scattering layers.

THE gas in the swim-bladder of a fish is at the hydrostatic pressure of its depth. This may be 100 atmospheres or more. In contrast, the dissolved gases in the water itself have been introduced at the surface, and total only one atmosphere of tension. Since the increased pressure of the gases in the swim-bladder indicate active secretion, their composition is of great interest. SCHOLANDER and co-workers (1951, 1953) found that in a series of marine coastal bottom fishes, the oxygen percentage increased with depth. Although the percentage of nitrogen decreased, its partial pressure was larger at greater depths, reaching as much as 15 atmospheres. Similar data are presented here for bathypelagic fishes. The problem of vertical migration with a swim-bladder is also considered since these fishes are thought to be a component of the scattering layer.

Material was collected at various depths with the 10 ft ISAACS-KIDD mid-water trawl towed at 2-3 knots (ISAACS and KIDD, 1953) over much of the eastern tropical Pacific, during the Eastropic Expedition of the University of California Scripps Institution of Oceanography. Surface fishes and vertically migrating species were taken under a light at night with a dip net.

Collections with nets are incomplete, possibly because many of the faster-swimming animals escape. The squid and lantern fishes seen in large numbers on the surface at night were almost never captured during the daytime tows below the surface. There may be many faster fishes at all depths that are not represented in such collections. BEEBE's direct bathysphere observations (1935) led him to conclude that there was a much more abundant fish fauna than he had surmised from years of trawling with the best oceanographic collecting equipment available. This imposes a severe limitation on statements concerning the kinds of animals in the various scattering layers.

The ISAACS-KIDD trawl is also limited in that it cannot be opened and closed at depth. There is always the possibility that specimens have entered the net while it was being lowered or raised. Whenever possible control tows were made, in which the net was brought back up immediately without towing it at depth. By comparing the two tows one is more certain which fishes were caught at which depth. Some species appeared regularly only in the deeper net tows. The hatchet fishes, *Argyropelecus lychnus* and *Sternoptyx obscura*, were commonly caught in nocturnal tows at depths greater than 200 metres, but were rare in collections from lesser depths. Other fishes (adult ceratioids, alepocephalids, certain stomiatoids, melamphaids, etc.) were characteristic of the fishes collected in the still deeper tows.

As soon as the trawl was brought on board, the cod end was removed and the contents emptied into trays. The fishes were immediately separated and placed in a bucket of sea water. Those with swim-bladders which had come from any depth were distended with gas and floated to the surface. Several of the non-floating ones (ceratioids, alepocephalids, bathylagids, some myctophids, etc.) were checked for gas both by needle puncture and in a pressure chamber, with negative results.

The techniques were the same as those of Scholander and van Dam (1953). The fish that floated were held underwater and the gas withdrawn through a hypodermic needle into a syringe lubricated with an acid citrate solution. With the needle capped, such a sample could be stored for several hours without appreciable change in composition. Thus, samples could be taken immediately from all of the desired material and analysed when convenient.

The analyses were performed in a syringe analyser (Scholander *et al.*, 1955) for carbon dioxide, oxygen, and nitrogen to an accuracy of 0·5 per cent of the total volume. Carbon dioxide was always less than 2 per cent, and was not considered significant since it increases on standing and is probably at a very low level in the live fishes. Samples of about 30 mm^3 were transferred from the storage syringe to the analyser. Duplicate analyses were done on all but the smallest fishes which did not contain enough gas.

The volume of gas in some of the fishes was determined before sampling in the apparatus shown in Fig. 1. The fish is placed in the chamber, taking care that no bubbles adhere to it. With the chamber brimming with water, the cap is inserted and clamped down. Thus the only gas in the chamber should be that in the swim-bladder of the fish. Pressure is now applied with the syringe until the manometer indicates that the pressure has doubled. Harden Jones (1951) has shown that fish probably do not resist such a volume change with their musculature. Applying Boyle's law, the excursion of the syringe to produce this pressure change will be $\frac{1}{2}$ the volume of the swim-bladder. A small blank is subtracted for the gas in the manometer. It is essential that such a system be as rigid as possible and that bubbles be scrupulously avoided. Fortunately it is easy to check the system by filling the chamber with water only. The blank value is obtained in this way. Such a check was usually repeated after each measurement.

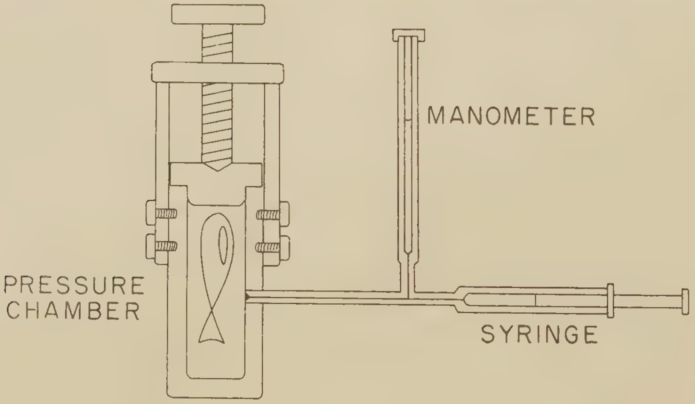

Fig. 1.

RESULTS

Swim-bladders of surface pelagic species contained 27 to 33 per cent oxygen, only slightly above that of air. This is the same as inshore marine fish taken at the surface. The fishes dip-netted at night, which are believed to have migrated up from depth, had 74 to 91 per cent oxygen. These agree well with the species taken at depth by trawling which also had 53 to 93 per cent oxygen in their swim-bladders.

Below is a list of species divided into these arbitrary categories. A range of oxygen values indicates that more than one individual of the species was measured. The amount of gas is indicated by the per cent of the total volume of the inflated fish made up by the swim-bladder gases at 1 atmosphere at the surface. The compressed gas at depth would be in a much smaller volume.

Table 1.

	Per cent O_2	Per cent volume of gas
I. *Surface pelagic species*		
Exocoetidae		
Exocoetus monocirrhus	33	3·5
Cypselurus xenopterus	23–25	
Hirundichthys sp.	33	3·1
Hemiramphidae		
Hemiramphus sp.	29	
II. *Bathypelagic fishes taken at the surface*		
Myctophidae		
Myctophum evermanni	74–91	3·2–5·0
Myctophum spinosum	77–91	4·0–5·5
Myctophum affine	90	
III. *Bathypelagic fishes taken at depth (all below* 100 *metres)*		
Sternoptychidae		
Argyropelecus lychnus	72–92	32–65
Argyropelecus affinis	67–93	42–55
Sternoptyx obscura	71–88	
Vinciguerria lucetia	78–90	32–52
Ichthyococcus sp.	77–83	
Melamphaidae		
Melamphaes macrocephalus	73–87	37–65
Melamphaes nigrofulvus	67–77	56
Melamphaes opisthopterus ?	71	
Melamphaes nycterinus	54–93	48–54
Melamphaes cristiceps ?	61–81	
Myctophidea		
Lampanyctus omostigma	89	53
Lampadena bathyphila	85	

Several factors tend to produce errors in the compositions and amounts of gas in the deep fishes. When a fish enters the net it is forced back into the cod end where it probably does not live very long. Since some of the tows lasted several hours, a fish may have been dead nearly this long before being sampled. In such a fish, diffusion will have begun to bring the bladder gases into equilibrium with the rest of the fish and the outside sea water. This will lower the oxygen and raise the nitrogen percentage. Experiments at the surface showed that the oxygen percentage could decrease as much as 10 to 20 per cent in a few hours. Several members of the genus *Melamphaes* were particularly sensitive to this.

The swim-bladders in some of these relatively fragile mid-water fish may have ruptured into the body cavity. Diffusion would then work more quickly to vary the gas composition. Gas would also likely be lost in such a fish. Thus the oxygen content and the amount of gas shown above for the deep fishes can only be considered minimal values. There is little point in computing the size of the swim-bladder at depth from these figures. All that can be said is that the deep fishes had much more gas than those taken on the surface. This is to be expected since a greater absolute amount of gas is necessary to maintain a constant swim-bladder volume at depth due to the pressure.

Oxygen increases with the depth of the fish and at about 200 metres can constitute more than 90 per cent of the gas mixture in the bladder. All deep fish tended toward 80 to 90 per cent. The lower values are probably due to the errors mentioned above.

DISCUSSION

The scattering of sound by horizontally layered marine organisms has been observed over most of the oceans of the world. The identity of the animals that make up these scattering layers had been discussed in several articles (RAITT, 1948; MOORE, 1950). MARSHALL (1951) has shown that fish with functional swim-bladders are widely distributed and may be a principal cause. This is an attractive hypothesis since a gas-filled bladder is a much more efficient scatterer of sound that invertebrates or fishes without enclosed gases.

Since the tissue of fishes is denser than sea water, a gas-filled swim-bladder is necessary if a fish is to adjust itself to neutral buoyancy. An amount of gas equal to about 4 per cent of the body volume of the fish is needed. If these fish migrate vertically, the gas will expand or contract with the changes in hydrostatic pressure. To keep the swim-bladder at the same relative volume, gas must be either secreted or absorbed. PARR (1937) recognized that this places limitations on the amount and speed with which such fishes can change their depth. The secretion of a gas under pressure represents work that must be done by the fish. It is interesting to compute the rate and amount of work represented by some observed migrations in the scattering layer.

A fish must keep its swim-bladder a constant size if its buoyancy is not to change during migration. On this assumption, the work performed in migrating between pressures p_1 and p_2 will vary as :

$$W = 2{\cdot}3 \, \mathrm{v} \, p_2 \log \frac{p_2}{p_1}$$

where v is the volume of the swim-bladder.

Fig. 2 shows the accumulated work necessary to migrate from the surface to various depths if the swim-bladder is kept constant at 4 per cent of the volume of the fish. The figures are for a 10 g fish with a 0·4 ml swim-bladder. Another atmosphere of gas must be supplied for every 10 metres increase in depth. Since this has to be secreted at continually higher pressure, the rate of doing work increases with depth. This is shown by the increasing slope of the curve with depth. This is only true if the fish keeps in step with the pressure and maintains neutral buoyancy at all depths. MARSHALL (1951, 1954) has discussed the amount of work necessary to migrate vertically. He apparently believes the amount of gas is not increased by secretion in going down, so that the fish gets heavier at great depths.

One can compute the amount of work represented by gas secretion and relate this to what fishes are capable of metabolically. Since many assumptions are necessary the accuracy of such a calculation is open to question. From data of SCHOLANDER *et al.* (1953), a 10 g fish would use about 0·4 ml oxygen per hour. This is equal to 2 g calories under conditions of aerobic oxidation of food stuffs. Anatomically it seems likely that not more than one third of a fish's circulation would go to the swim-bladder. Let us assume that the secretion process is 25 per cent efficient, and that one third of a fish's metabolic work is available for the task. This would allow the fish to secrete an amount of gas equivalent to about 0·15 g calories of work per hour. A scale is included in Fig. 2 representing the number of hours necessary at this rate to attain neutral buoyancy at a given depth. Thus 33 hr would be needed to go to a depth of 400 metres. Such a figure is unrealistic since the scattering layer migration must be made daily. If fishes with swim-bladders make up part of such a layer, their specific gravity probably differs appreciably from sea water at either the top or bottom of their migration. This cannot be too severe a handicap since many species have no swim-bladder. They are successful in spite of having to swim all the time to keep from sinking.

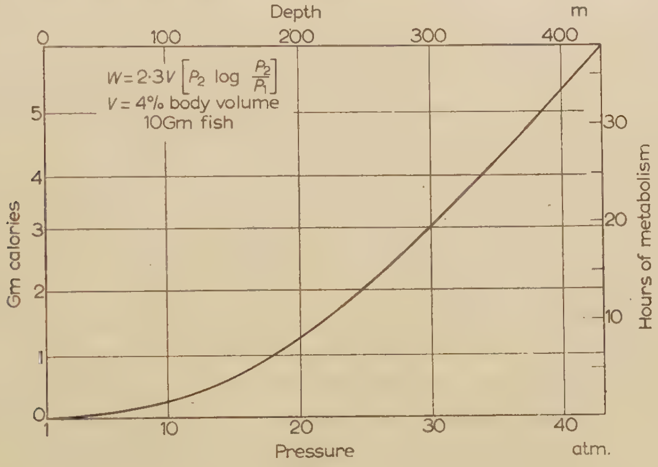

Fig. 2.

LANTERN FISHES

The various lantern fishes taken with a dip net at the surface at night all had swim-bladders with high percentages of oxygen. SCHOLANDER and co-workers (1951, 1953) only found such a gas composition in fishes taken at a considerable depth. Considering this, the high oxygen values in the present fishes strongly infer that the gas was secreted at depth before they migrated to the surface. The amount of gas was 3 to 5·5 percent of total body volume. This is just the quantity necessary to make the fish neutrally buoyant at the surface. None of these species were caught at depth during daytime tows. This is not surprising since they showed great speed on the surface when chased by squid. If they are part of the most persistent scattering layer, they spend the daytime between 300 and 400 metres. From the metabolic considerations in Fig. 2, it seems unlikely that they could also secrete enough gas to be weightless at depth. Yet one wonders how the fish would determine the proper amount of gas to secrete at depth to give it the correct-sized swim-bladder, 4 per cent of body volume, at the surface. Whether daily secretion occurs during vertical migration one cannot say without the necessary daytime data. However, the lantern fish do seem to be migrating vertically with a swim-bladder containing gas. Since they are so common they may well be an important sound scatterer.

OXYGEN MINIMUM

The eastern tropical Pacific form which these collections were made has a highly developed oxygen minimum. The dissolved oxygen in the sea water is generally below 0·25 ml per litre from the thermocline at about 100 metres down to 600 or 800 metres. Below this it gradually increases. Winkler oxygen determinations of less than 0·1 ml per litre are common. In spite of these low values very rich collections were made in this water. In addition, scattering layers were always seen at these depths during both the day and night. One component of the layer appeared to migrate wholly within this region. Marshall (1954) has noted that a variety of animals seem to thrive in the oxygen-poor waters of the ocean. It is not clear whether they are the cause or effect of the oxygen minimum.

The hatchet fishes in particular were taken in large numbers in the oxygen minimum, as many as several hundred being caught in one haul. All of them were bloated with large amounts of gas, which was mostly oxygen. Harden Jones and Marshall (1953) state that the proportion of oxygen in the swim-bladder decreases when fish are kept in low-oxygen water. This is apparently not so for these species.

At depth the partial pressure of oxygen in the swim-bladders of these fishes may amount to 25 or 50 atmospheres, while the oxygen tension in the surrounding sea water is only 1/250 of an atmosphere. The fish maintains its swim-bladder oxygen against a diffusion gradient of 10,000 to 1. Marshall (1954) noted that the swim-bladders of deep living fishes have much more developed *retia mirabilia* and gas gland than those of shallow fishes. Scholander (1954) has shown that the *rete* can function as a counter current diffusion system capable of maintaining a large tension gradient across the bladder wall. Some such special system must be present for blood to flow in and out of the bladder without the gases being lost. It is not known whether the gas is initially secreted at these depths and at these low oxygen concentrations in the sea water.

PARTIAL MIGRATIONS

Since the hatchet fish seemed abundant enough to account for sound scattering, an attempt was made to see if they made a diurnal migration. A series of tows before and after the evening ascent indicated that they were associated with a layer which in the daytime was at 380 to 450 metres. At night it rose to 300 to 350 metres. Since this does not represent a large percentage change in pressure, the fish could probably let the swim-bladder change in volume without having to secrete or absorb during such a migration.

At the same time diffuse scattering at grater depths during the daytime moved up at night and concentrated at about 400 metres. *Melamphaes* with swim-bladders and other black fish characteristic of greater depths were caught here at night.

There are not enough daytime hauls to be certain such species are at greater depths. However, collection records of past Scripps Institute of Oceanography expeditions indicate that these species are caught at shallower depths at night than during the day.

Many mid-water fish with swim-bladders seem to perform partial vertical migrations that do not carry them all the way to the surface. These movements may be limited by the amount of distension the swim-bladder can withstand. For a given fractional change in pressure, a deep fish has much more vertical range than a shallow one. HARDEN JONES (1952) has shown that some fresh water fishes can stand a 20 per cent change in pressure without compensating. This may also be the case for these marine fishes.

CONCLUSIONS

(1) Measurements were made of the composition and amount of swim-bladder gases in some pelagic fishes of the eastern Pacific. In deep fishes the oxygen content approached 80 to 90 per cent of the gas. In strictly surface fish the gas contained slightly more oxygen than air. Some fishes taken at the surface at night had high oxygen. The gas was thought to have been secreted at depth since it was from species that are known to migrate vertically.

(2) Net tows indicated that some gas-containing fishes are associated with scattering layers which rise but do not come all the way to the surface at night.

(3) Energy considerations make it unlikely that neutral buoyancy can be maintained by gas secretion during very extensive diurnal vertical migrations.

Acknowledgements—We are indebted to Mr. MARK CLAFF for his expert craftsmanship in constructing the chamber used to determine gas volumes. The work would also have been impossible without the net tows made by the members of the crew of the R/V *Horizon*.

Contribution No. 888 *from the Woods Hole Oceanographic Institution and from Scripps Institution of Oceanography, new series, No.* 908

REFERENCES

BEEBE W. (1935) *Half mile down* John Lane, London.

HARDEN JONES F. R. (1951) The swim bladder and the vertical movements of teleostean fishes, I. Physical factors. *J. Exp. Biol.* **28**, 553-566.

HARDEN JONES F. R. (1952) The swim bladder and the vertical movements of teleostean fishes, II. The restriction to rapid and slow movements. *J. Exp. Biol.* **29**, 94-109.

HARDEN JONES F. R. and MARSHALL N. B. (1953) The structure and functions of the teleostean swim bladder. *Biol. Rev.* **28** (1), 16-83.

ISAAC J. D. and KIDD L. W. (1953) Isaacs-Kidd midwater trawl. *Scripps Institution of Oceanography*, Ref. 53-3 (unpublished manuscript).

MARSHALL N. B. (1951) Bathypelagic fishes as sound scatterers in the ocean. *J. Mar. Res.* **10** (1), 1-17.

MARSHALL N. B. (1954) *Aspects of deep sea biology* Philosophical library, New York.

MOORE H. B. (1950) The relation between the scattering layer and the Euphausiacea. *Biol. Bull.* **99** (2), 181-212.

PARR A. E. (1937) Concluding report on fishes. *Bull. Bingham Oceanog. Coll.* **3** (7), 1-79.

RAITT R. W. (1948) Sound scatterers in the sea. *J. Mar. Res.* **7**, 393-000.

SCHOLANDER P. F. CLAFF C. L. TENG C. T. and WALTERS V. (1951) Nitrogen tension in the swim bladder of marine fishes in relation to depth. *Biol. Bull.* **101** (2), 178-193.

SCHOLANDER P. F. and VAN DAM L. (1953) Composition of the swim bladder gas in deep sea fishes. *Biol. Bull.* **104** (1), 75-86.

SCHOLANDER P. F. (1954) Secretion of gas against high pressures in the swim bladder of deep sea fishes. *Biol. Bull.* **107** (2), 260-277.

Printed in Great Britain by The Salisbury Press Ltd., Publicity House, Wilton Road, Salisbury, Wilts. (5030)

Contribution No. 889

AN AIRBORNE FLAME PHOTOMETER AND ITS USE IN THE SCANNING OF MARINE ATMOSPHERES FOR SEA-SALT PARTICLES

By A. H. Woodcock and A. T. Spencer

Woods Hole Oceanographic Institution[1]

(Original manuscript received 25 January 1957; revised manuscript received 22 March 1957)

ABSTRACT

An airborne flame photometer for the identification of large sodium-bearing aerosols from aircraft is briefly described. This instrument is a modified form of a laboratory device which has been used to count sodium particles. A rough calibration of the flame photometer, in terms of the total amounts of sea-salt in marine air, is discussed. Preliminary observations in trade-wind areas are given and an interesting concentration of sodium in cumulus clouds is indicated.

1. Introduction

Evidence of the association of bubbles in the sea with sea-salt nuclei in the air and of the connection between these nuclei and salts in solution in rain waters [see references 1, 3, 16, 18 and 20] has directed our attention to problems requiring more knowledge of the quantities of these nuclei in the atmosphere. In some of these problems an instrument was required which would make possible a rapid scanning from aircraft of the distribution of salt of certain particle-size ranges in the lower layers of marine atmospheres. In these air layers and in the clouds which are often found in them, the difference in the horizontal and vertical distribution of the weight of sea-salt per unit volume of air commonly amounts to several orders of magnitude [17]. Hence, no great instrumental accuracy was initially needed to obtain a useful exploratory tool.

Methods presently available for obtaining the weight of salt per unit volume or weight of air[2] are very slow and laborious. A further objection to most of these methods is that the quantities measured often represent average values along extended air paths due to the necessarily prolonged time required to obtain an adequate sample. Hence these methods are not useful where rapid and rough mapping of the distribution of sodium-bearing particles in the lower layers of marine atmosphere is required.

Soudian [12] and Vonnegut [15] have developed a useful instrument which applies the principles of flame-photometry to the problem of detection of sodium-bearing aerosols. Their instruments are laboratory models, capable of giving relatively instantaneous indications of these aerosols. However, neither author calibrated his instrument in terms of the weight of sodium per unit volume of air nor adapted it for use in aircraft.

The purpose of this article is to describe briefly a flame photometer designed for use in an airplane (see figs. 1 and 2) to discuss its use in conjunction with a different method of measuring airborne salt, and to give some of the first data obtained. This instrument amplifies and records the average voltage developed across the photocell load resistor, which is proportional to the photocell current produced by sodium flashes in a flame. This voltage has been related to the quantity of sea-salt particles in the air, by comparison with direct simultaneous sampling of these salt particles, so that it provides a rapid indication of the weight of sea-salt present. The justification for this comparison of sodium-flash intensity, as represented by the photocell current, to the mass of sea-salt particles in the atmosphere, is to be found in the work of Junge [7, p. 130]. He showed that the ratio of the sodium to the chloride in the giant nuclei in marine air is about the same as this ratio in sea-salts. Hence it was expected that the sodium-flash intensity would be a nearly constant function of the quantity of sea-salt in the air, since the ratio of sodium to total salts in sea-salt is a constant.

2. A brief description of the instrument

The instrument, shown in section in fig. 1, consists of an enclosed gas burner, or torch, into which a mixture of air and propane gas is introduced. The mixture is ignited in flight by a spark which crosses the gap between the center electrode of the spark plug and the outer edge of the burner. Fig. 2 shows the mounting of the flame photometer under the wing of an aircraft.

The flame is viewed by a 1P21 photomultiplier tube through a lens and a multilayer interference filter. This filter has its transmission peak at 5892A, and in-

---

[1] Contribution number 889 from the Woods Hole Oceanographic Institution. This paper represents the results of research carried out by the WHOI under contract with the Office of Naval Research. Reproduction in whole or in part is permitted for any purpose of the United States Government.

[2] For filtration methods see references [5 and 9], and for impingement methods see references [6, 10, 11 and 19].

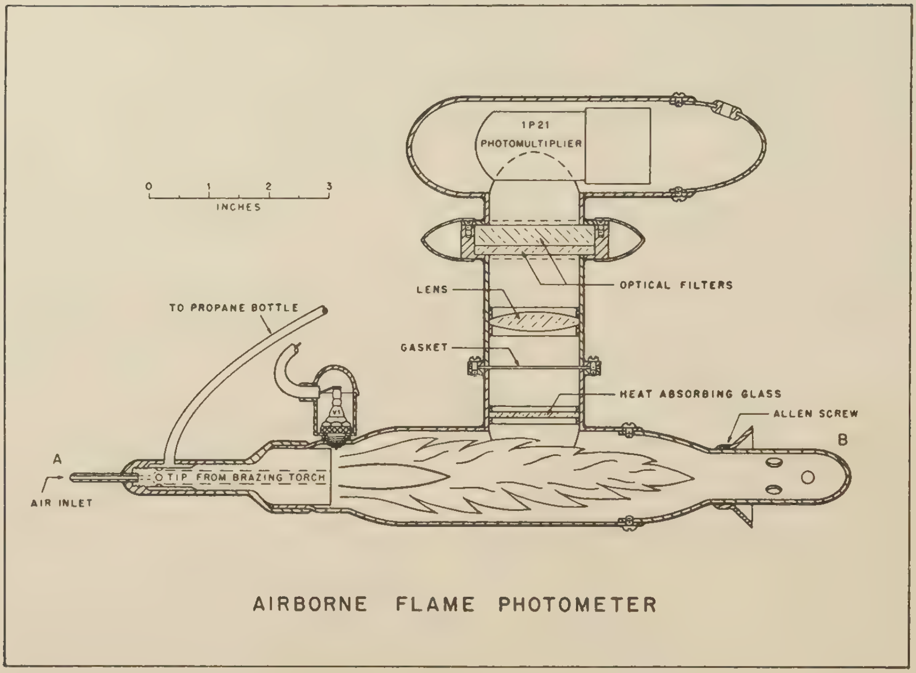

FIG. 1. Schematic drawing of airborne flame photometer.

cludes an additional colored-glass filter for the elimination of side bands.

The output current of the photomultiplier tube is a function of the light from the sodium flashes which occur in the flame as the salt aerosols are heated. This signal from the phototube, after suitable amplification, integration and recording, is related to the airborne salt through comparison with salt-aerosol samples taken and measured by an entirely different technique. This comparison is discussed later in this paper.

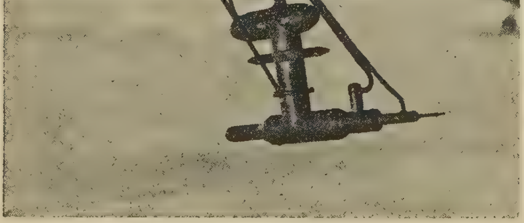

FIG. 2. Photograph of flame-photometer housing mounted under the wing of a small aircraft.

The flow of propane gas to the flame is controlled by a pressure-regulating valve and a floating-ball flow meter. The air enters the burner at A (see fig. 1) at a speed which is controlled by the selected speed of flight. The diameter of the air-intake orifice and the propane-intake pressure required for efficient flame production by the burner were determined by trial in flight at speeds of 70 to 105 mph. It was found that the best flame characteristics for this instrument were obtained with an air speed of about 90 mph, an air-intake orifice diameter of 2.36 mm and a propane flow rate of about 57 gms per hour.

3. Calibration

The sea-salt-particle sampling technique, which was used to indicate the range of usefulness of the output current of the photomultiplier tube as a measure of airborne salt, is one which has been described by Woodcock [16 and 19] and further tested by Twomey [14] and Crozier [4]. This technique involves the exposure to the air of small glass slides and the subsequent measurement with a microscope, under constant relative humidity conditions, of the salt aerosols impinged upon them. When these aerosols are crystalline particles they range in size from about one to ten μ radius and they are known to contain over 90 per cent of the total mass of sea-salts usually present in marine air (Junge, [7] p. 135). The amplifier used with the flame photometer, as presently designed, is sensitive to only the larger of these particles.

In comparing techniques in flight, the small glass slides were exposed simultaneously with the operation of the photometer. Over seventy comparative tests have been made in the lower atmosphere (Altitude 200 to 7000 feet) over the sea in the Florida and West Indian regions. During these tests, many factors such as air speed, airplane flight attitude, propane gas flow, phototube supply voltage, etc., which were found to effect the photocell output current, were held reasonably constant.

Fig. 3 shows the results of these comparative tests. Graph (A) in this figure gives the earlier observa-

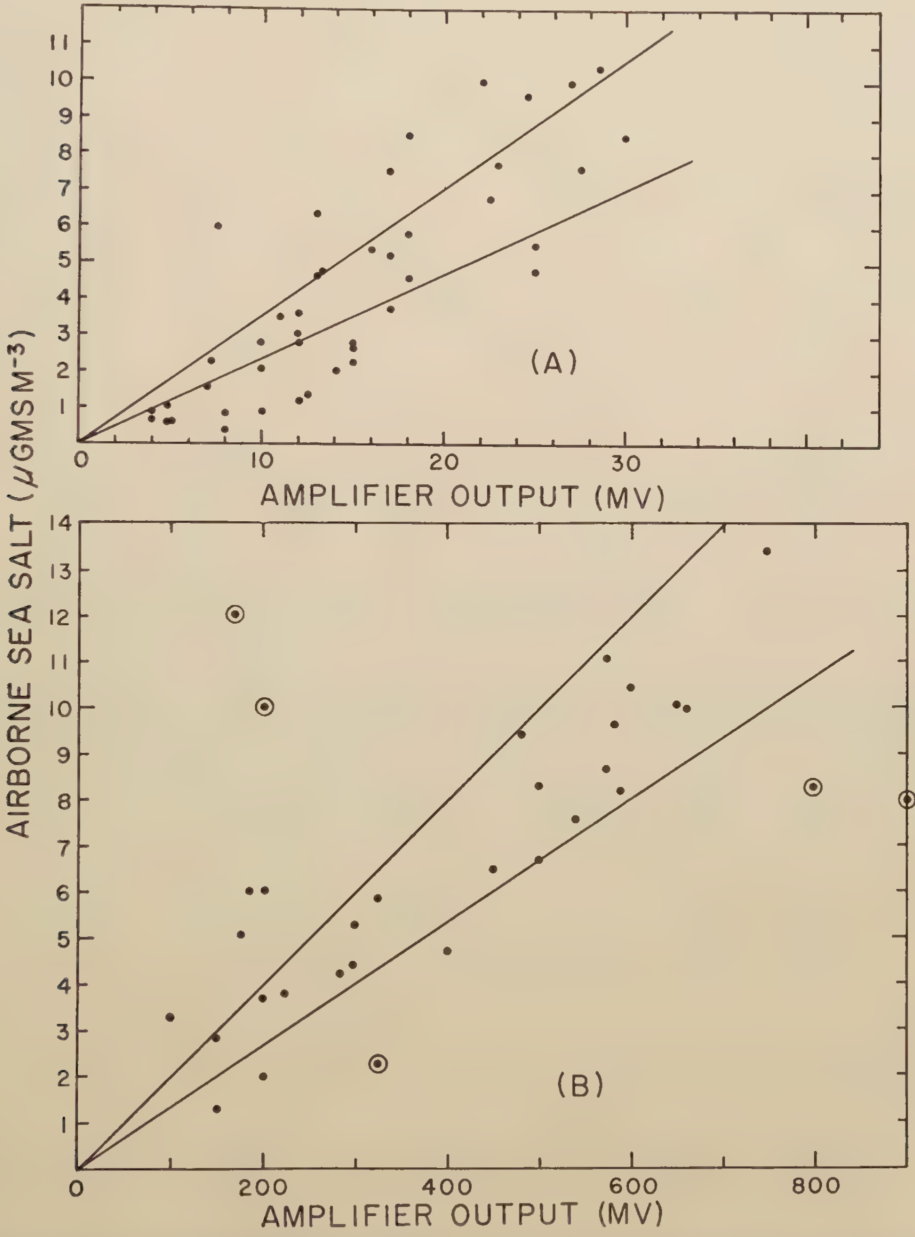

Fig. 3. A comparison of the average photocell output signal, during the periods (30 to 100 seconds) required to obtain the sea-salt particle samples, to the total quantity of sea-salt. The quantities of sea-salt represented by the circled points were derived by extrapolation from a partial sampling with the glass slides of the total range of particle size. These values are therefore subject to the uncertainties of partial sampling. See text for further explanation.

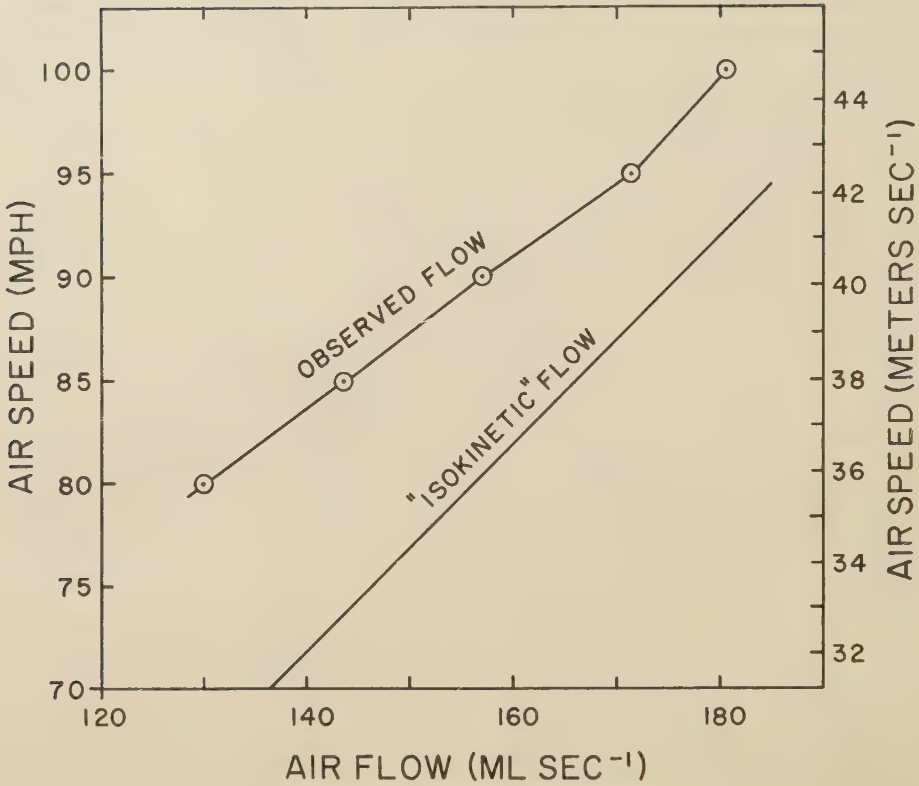

FIG. 4. Measured air flow into photometer intake orifice, compared to ideal (isokinetic) flow. Orifice inside diameter 2.36 mm.

tions made over the ocean east of Pompano Beach, Florida, and graph (B) gives the latest data from the Virgin Island area. The large apparent increase in the voltage on graph (B), as compared to graph (A), is due to increased amplification of the signal in a later model of the instrument. This later model also had an increased sensitivity to the larger sodium flashes. The two diverging lines are introduced among the observed points in order to show the maximum error of the isopiestic method (*i.e.*, ± 20 per cent; see reference [19] p. 181), as applied to the problem of determining the weight of sea-salt particles on the glass slides. These sodium data will be discussed later in this paper.

4. Collection efficiency

May [10] and many other workers have emphasized the importance of "isokinetic" conditions in the intake orifices of aerosol samplers in order to insure that a representative number of particles enter. In other words, with the intake orifice facing directly into the wind, the air speed within the orifice should equal that in the main airstream on the outside. Lower or higher air speeds within the orifice will alter the number of particles which can enter, and hence will alter the apparent concentration of particles in the free air.

In the first exploratory studies of atmospheric sodium particles, no suction was applied to the tail pipe (see B, fig. 1), in order to speed the flow of air through the flame chamber. Hence, internal friction caused the rate of flow of air inside the intake orifice tube (A) to be somewhat less than the air speed of the aircraft. This was demonstrated by placing the instrument in an air stream of a known velocity and measuring the quantity of air passing out of the vent pipe. These quantities were determined by measuring the time required to trap certain volumes of air in a thin-walled rubber balloon. Fig. 4 shows the observed inflow amounts at various air speeds compared to the ideal isokinetic inflow. Note that the measured air inflow at 80 mph was about 17 per cent less than ideal, and at 90 mph about 11 per cent less. These data were obtained with the flame turned off. However, operation of the flame was found to have no measurable effect upon the air-inflow rate at these speeds.

It was sufficient for our present purposes to demonstrate that the amounts of particulate sodium which do enter the orifice and flame, produce a varying sodium-flash signal which in the average is quantitatively related to the varying averaged amounts of sea-salt sampled on the glass slides. It is thought that the

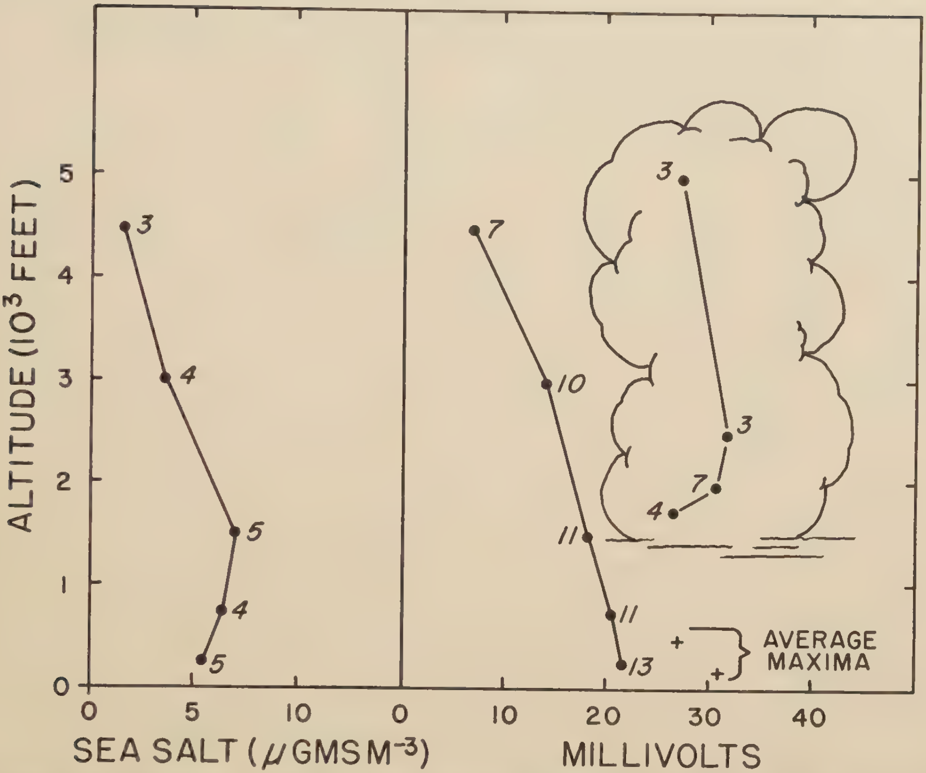

Fig. 5. Average vertical distribution of weight of sea-salt in the clear air compared to the average airborne sodium in the clear air and in cumulus clouds. The sodium is represented by the millivolts output of the amplifier, which is proportional to the photocell current. These measurements were made over the sea, from one-half to two miles east of Pompano Beach, Florida, and during July 22, 23, 24, 25, 27 and 28, 1955. Average local surface winds force 3, ESE. See text for further discussion.

above near-isokinetic-flow values assure a collection efficiency which is quite high enough for the initial exploration discussed here, especially since the outside diameter of intake pipe is so small (2.4 mm) that it would have a high collection efficiency for the particles concerned, from consideration of orifice size alone.

Figs. 5 and 6 show a comparison of the average sodium-flash signal intensity, as indicated by the amplifier-voltage output, to the average quantity of sea-salt found among particles collected on the glass slides. The number of observations averaged in each case is shown near each point. It is apparent on these figures that the differences which occur in the airborne sea-salt and sodium, with increasing altitude, are very similar in trend. This result was expected, since the constancy of the relationship of the sea-salt, among the giant salt nuclei, to the chloride [14 and 19] and to the sodium [6] has been shown.

In figs. 5 and 6 the voltage values are also given for periods when the flame photometer was operated within relatively small nonprecipitating cumulus clouds. Due to the increased mass of the salt particles in the clouds (they become large cloud droplets), the collection efficiency of the photometer intake orifice for these particles would be more nearly unity than for the same particles in the clear air. Thus, these photometer currents obtained within the clouds probably more nearly represent the total sodium present than do the values measured in the clear air.

It will be noted that the average photocell currents in the clouds are similar to, but somewhat greater than, the average in the subcloud layer of air. Until further measurements become available, this similarity is tentatively interpreted as showing that the clouds are largely composed of air which has come from the subcloud layer. The higher values obtained in the clouds as compared to the values in the subcloud layer, are thought to result from (1), the tendency for the clouds to be made up of the subcloud air containing the highest amounts of salt (compare cloud voltages on figs. 5 and 6 to the average voltage maxima as shown by the plus signs); (2), a somewhat higher instrumental sampling efficiency in the clouds; and (3), an increase in the concentration (no. per unit volume of air) of the larger salt particles during their growth to large cloud droplets. This third factor is one utilized by Bowen [2] to explain the concentrations of rain-

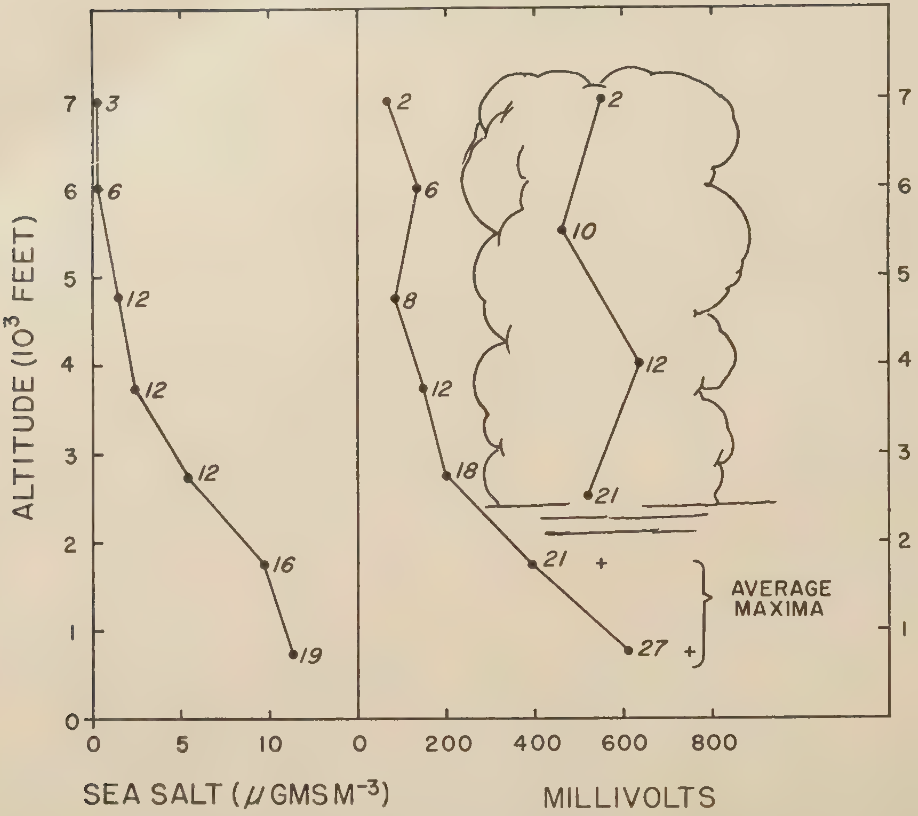

FIG. 6. Average vertical distribution of weight of sea-salt in the clear air, compared to the average airborne sodium in the clear air and in small cumulus clouds. The sodium is represented by the millivolts output of the amplifier, which is proportional to the photocell current. These measurements were made over the sea about five miles southeast of the island of St. Thomas, V. I., and during thirteen days between the dates May 25, 1956 and June 10, 1956. Surface winds force 3 to 5 E to ESE.

drops in clouds, and its application to salt particles is being investigated. It is very unlikely that correction for "sampling efficiency" will significantly alter the cloud sodium values given here. However, until this error is eliminated, these values should be regarded as tentative.

5. Discussion

There is a considerable scatter of the observed points on fig. 3 beyond the ± 20 per cent maximum error of the glass slide method. This is thought to be due in large part to the difficulties of properly integrating the highly variable signal from the phototube, and to variations in the relative mass of salt (or sodium) present in the salt-particle size range sampled by the flame photometer. The variability of the photometer signal during "calibration sampling runs" indicated that the slide samples were averaging a greatly varying quantity. The second of the above factors will be discussed in some detail later. The justification for using the photometer data at this time, despite the above rather large scatter in the calibration values, lies in the close similarity of the changes in the average photometer results, at different altitudes and positions, to changes in the average amounts of sea-salt present (see figs. 5 and 6).

At this stage of its development, the airborne flame photometer is regarded as an exploratory probe in areas where the differences in salt amount are great, and as a device for rapidly "roughing-in" the distributional picture of the sodium-bearing particles in these areas. There is a great difference in the time required to obtain the results by the slide method as compared to the photometer method. For example, the salt data from the glass slides which are shown on fig. 6, required forty hours to produce, while the flame photometer data on this figure are the result of two hours work.

The photometer is especially useful in areas of marked change in aerosol population, such as those which occur while ascending from the subcloud to the cloud and above-cloud layers and while flying through and near cumulus clouds. Where particle size distribution and greater accuracy are required, other methods

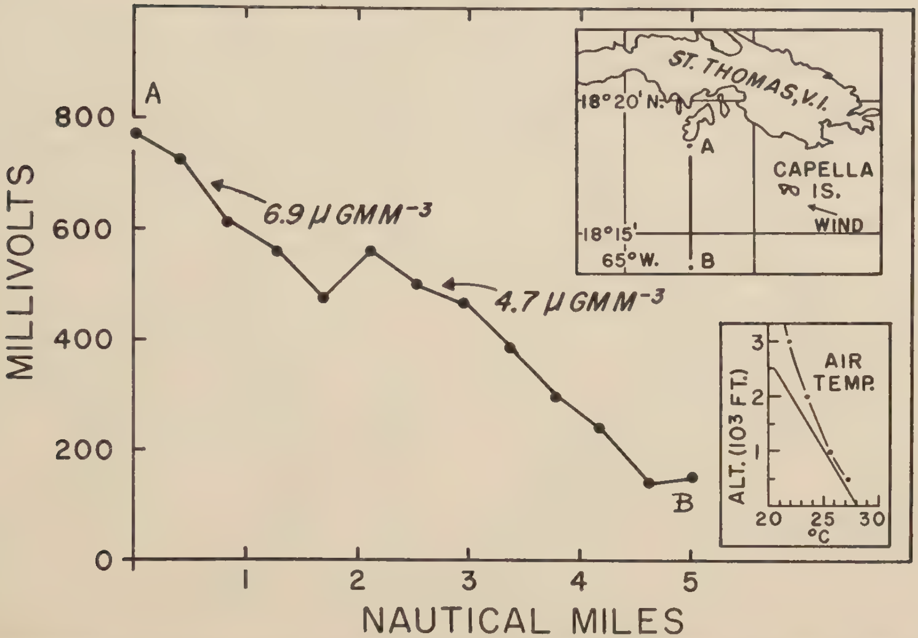

Fig. 7. An example of horizontal differences which occurred in the photocell output signal along the flight line A B (see insert map). The weight values shown represent sea-salt sampled on glass slides a short time later and in the approximate position shown by the arrow marks. Date: June 7, 1956, alt. 500 ft.

may be used. In these cases the photometer is sometimes a valuable supplemental tool. For instance, in some of our problems it is useful to know the maximum quantities of salt present, among certain particle size ranges, along a given flight line. Previous methods required that glass sampling slides be exposed as rapidly as possible and at numerous intervals along this line. The "reading" of these many slides was very time consuming and laborious. The continuous record of the photometer makes it possible, however, to scan a flight path and then, upon reversal of course, to use this record as a guide in relocating the areas of maximum salt. Salt samples may then be taken in these areas of interest only, thus saving much time and work.

Fig. 7 shows an example of an interesting horizontal difference in sodium or salt content in the air at constant altitude near an island. This difference, which is not unusual at other levels, is probably due in large part to the convergence of surface air towards the island (caused by island heating) and the consequent subsidence of the relatively salt-free air from higher levels at the off-shore location about five miles south of the island. It may also be due in part to increased wind force near the island causing a greater local production of salt particles by the sea surface (see references [1] and [17] about role of wind in nuclei production).

Though we have used this instrument at low air speeds on a small aircraft, our experience has indicated that it could be readily adapted for use at the higher speeds of larger airplanes.

In using the flame photometer within clouds, it is reasonable to question the possible effects of cloud water on the flame and on the sodium-flash intensity. It might be supposed that the heat required to vaporize the water on the cloud droplets passing through the flame might, in some cases, so lower the flame temperature that an inadequate amount of heat would remain to heat all of the sodium in each salt particle to incandescence. However, this seems unlikely since the propane burning rate of 67 grams per hour releases from 300 to 1000 times as much heat as that required to vaporize the water found in the average cloud (*i.e.*, from 0.1 to 1 gm m^{-3}). This excess of heat is derived assuming isokinetic flow in the orifice. With this flow, the air passes air through the flame at a rate of about 0.157 liters per second at the airplane speed of 35.8 meters per second (80 mph). The heat of combustion of the propane gas is about 1380 cal per gram.

On several occasions the airplane was directed through "cloud ghosts," or areas in which clouds had recently evaporated leaving an invisible residue of vapor, aerosols and turbulence. These areas also showed the characteristic large increase in sodium-signal intensity which we had found in the visible clouds. Thus it appeared that the increased signal associated with the clouds (see figs. 5 and 6) was not due to some unknown effect arising from the high state of dilution of the salt particles as cloud droplets.

The effects of changing pressure (altitude) on the gas delivery rate of the commercial "constant-flow valve" used was also measured. The maximum increase in this flow rate due to decreasing pressure with altitude was only seven per cent at 10,000 feet. This increase produces no noticeable effect upon the flame or its sodium-flash signal.

As previously suggested, it is thought that one source of the errors in relating photocell current to individual sea-salt samples taken with the glass slides, (see fig. 3) lies in the changing relative distribution of mass of salt among particles of different sizes. The

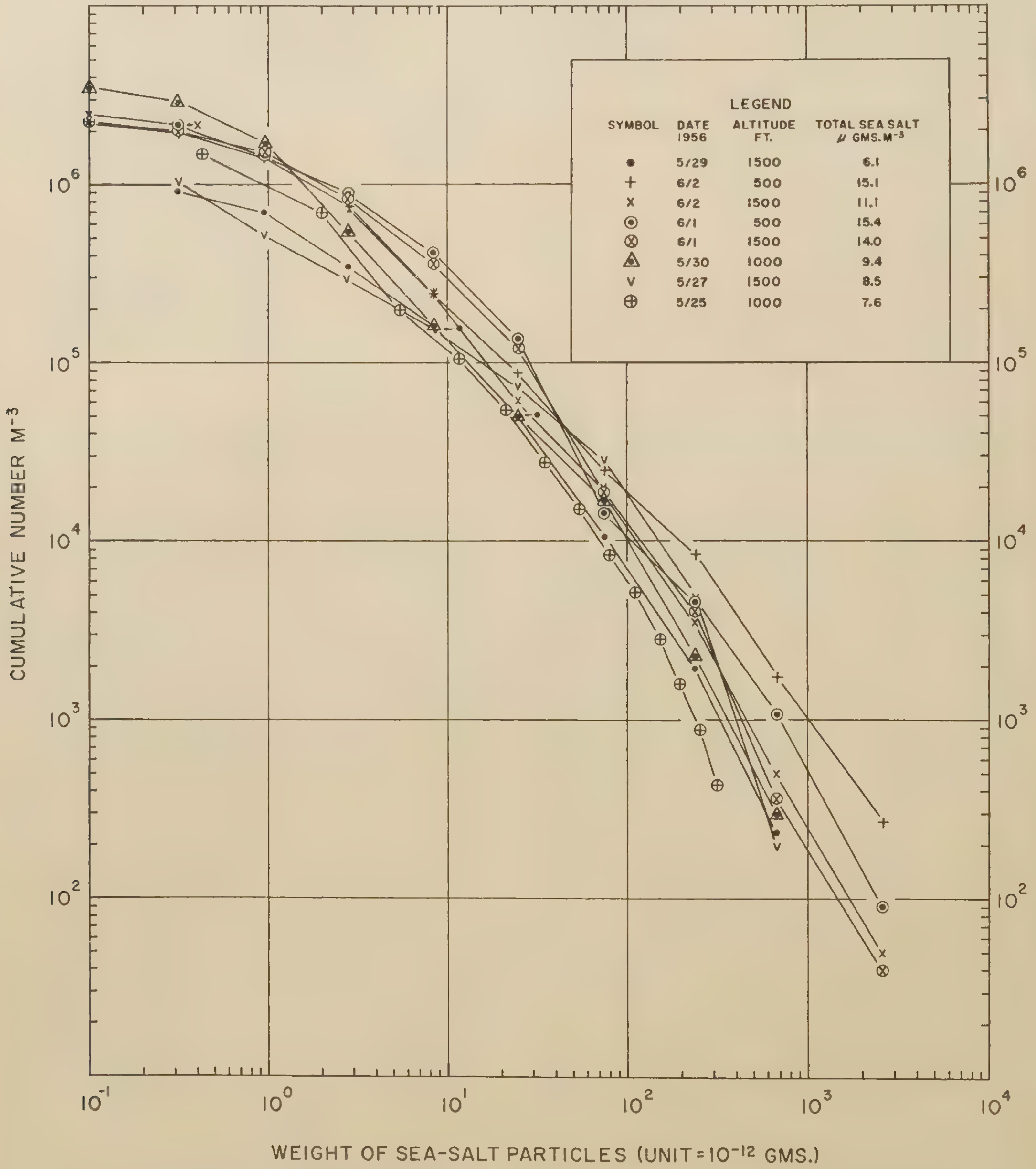

FIG. 8. Cumulative number distribution curves for the samples represented on fig. 9. On this figure and on fig. 9, the symbols represent the lower limiting weight in each weight-range category.

photometer amplifier, as presently constituted, is sensitive to an alternating sodium-flash signal from the larger particles and not to signals from relatively steady sodium light. From a study of the photocell output records from the St. Thomas data, it is known that the major portion of the sodium signal comes from flashes which occur at frequencies of about one per second or less. (There was too little amplification to detect the more numerous weaker flashes.) If we assume that the air entered the intake orifice at a speed of 35.8 m $\sec^{-1}$, the rate at which air passed through the flame is simply the product of the cross-sectional area of the orifice (.04375 cm^2) and the air speed (3.58×10^3 cm $\sec^{-1}$). From this product, which is 0.157 liters per second, and from the spatial distribution of the salt particles, we can determine the particle weight range which produces the flashes of one or less per second. This is done, using the salt-particle distributions derived by the glass-slide technique.

Fig. 8 shows graphically the cumulative number distribution of particles of various weights sampled by the glass slides over the ocean in the Virgin Island area. On this figure one can readily see that the lower limit of the weight range of particles present in numbers sufficient to cause one flash or less per second in 0.157 liters of air (*i.e.*, about 7×10^3 particles or less m^{-3}), is not a constant value. In fact, the "lower limit weight" varies during the several days represented, from about 1×10^{-10} grams to 2.7×10^{-10} gram.[3] Fig. 9, which shows cumulative mass distribution of the salt particles, may be used to determine the relative proportion of the total airborne salt present in nuclei larger than the limiting weight.

As a result of the variable distribution of mass in the weight range sampled by the flame photometer, the instrument probably "sees" a variable proportion of the total salt present. For example, table 1, column 7, shows this varying proportion, expressed as the ratio of the total airborne salt to the salt present in the particles larger than the above-mentioned "lower limit" particle weight. These ratios are derived from the data on figs. 8 and 9 in the following manner. On fig. 8 note that the June 2 salt-particle distribution curve, for the 500-foot level, crosses the limiting number of 7×10^3 particles per cubic meter at a nucleus weight of 270×10^{-12} gram. On fig. 9 the cumulative per cent mass distribution curve for the same day and altitude shows that 34 per cent of the mass of salt was present in particles larger than 270×10^{-12} gram. Table 1, column 7, shows this and other figures for the relative mass of salt present in particles larger than the "lower limit" weight. Correction of the data for this source of error proved inconclusive. This is thought to be due to the small amount of data showing a significantly large difference, and to the obscuring effects of other variables such as the error of the glass-slide method.

Table 1. Showing differences in the ratio of the computed weight of salt which produces the sodium-flash signal, to the total weight of salt in all of the particles sampled by the glass slides. The symbols refer to the data of the six days when the most complete salt-particle samples were taken with the slides (see figs. 8 and 9).

Symbol	Date	Altitude	Airborne sea salt	Particle* weight	Total sea salt in particles equal to or larger than (W)	M2/M1
	1956	ft	M1 μ gms m^{-3}	(W) 10^{-12} g	M2 μ gms m^{-3}	
⊕	5/25	1000	7.6	90	1.22	0.16
v	5/27	1500	8.5	190	2.55	0.30
●	5/29	1500	6.1	100	1.58	0.26
△	5/30	1000	9.4	120	1.88	0.20
⊙	6/1	500	15.4	160	3.24	0.21
⊗	6/1	1500	14.0	155	2.24	0.16
+	6/2	500	15.1	270	5.13	0.34
×	6/2	1500	11.1	150	2.55	0.23

* Weight of the smallest particle among the salt nuclei numerous enough to produce one sodium flash a second (*i.e.*, a cumulative number of 7×10^3 particles m^{-3}—see text).

From the above analysis it is seen that an instrument sensitive to only a portion of the range of salt particles entering the orifice should record a signal variability from changing relative mass distribution among these particles. It is clear that a variable signal does not, therefore, necessarily indicate differences in the total mass of salt in the particle size range sampled by the glass slides. Also, there is little doubt that much larger differences in the ratios M2/M1 (see table 1) often occur. Consequently, the present circuit which amplifies the photoelectric cell signal is now being altered to broaden its sensitivity to a greater range of sodium-flash signal frequency. This is expected to remove much of the above source of error.

Alterations are being made in the form of the tail pipe in order to produce a pressure reduction there which will cause the flow rate on the inside of the intake orifice to be equal to that in the free-air stream. The efficiency of the optical system is also being improved. A more detailed description of the airborne flame photometer and of the above improvements is in preparation by the second author.

In the meantime, the present instrument is a useful exploratory tool in those areas of the lower atmosphere where large differences in sodium content are the major features to be studied. We hope to apply the instrument in various field studies. For instance, we would like to know the differences in the salt-aerosol load of the marine air masses moving into "disturbed areas" in the North Atlantic trade-wind system. It is already known that differences in the salt load of the subcloud air of the order of ten to a thousand times are directly related to the speed at which this air has been moving [17]. It has also been shown that these aerosols are

---

[3] The fact that the air entered the orifice at a speed somewhat less than that of the aircraft will alter these values somewhat, but will not alter the basic argument concerning this source of error.

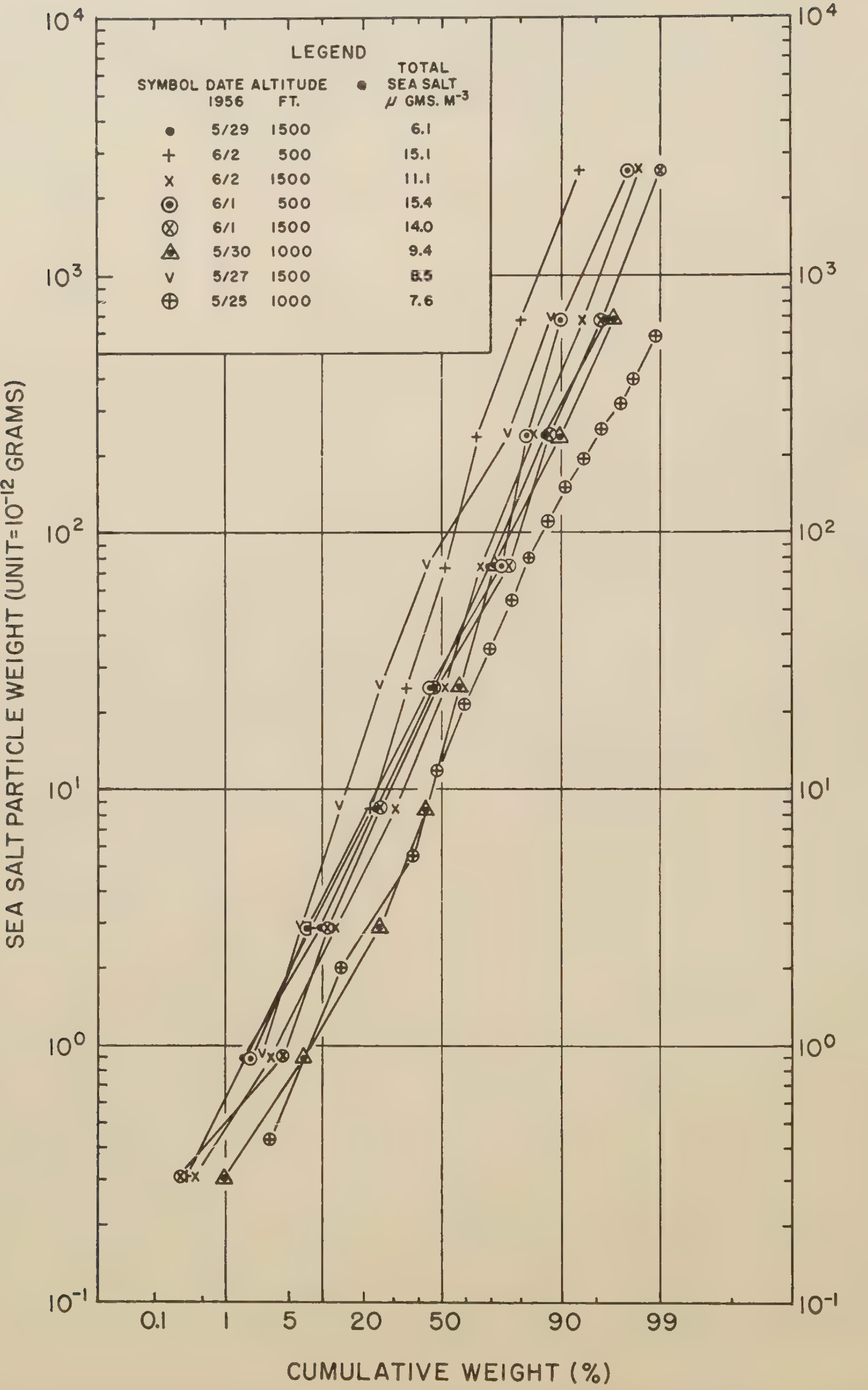

Fig. 9. Cumulative per cent weight-distribution curves, representing atmospheric salt-particle samples taken at the altitudes where, due to more complete sampling, the widest range of particle size was obtained. The sampling location was over the sea in the Virgin Islands region.

probably connected in some way with the rain-forming process [16, 18, and 20]. Large differences in their distribution in air which is moving into a "disturbed area" may be directly connected with the rate and position of release of heat (precipitation) in these areas.

The instrument may also be useful in testing the idea of tradewind cloud growth by the "entrainment" of environmental air. If subsequent measurements continue to show a high relative sodium content in the clouds, it will become necessary to reconsider this idea of cumulus growth. This reasoning follows from the fact that the clear air between the clouds contains relatively small quantities of salt (see figs. 5 and 6 and reference [17]). Hence the extensive mixing of this environmental clear air with cloud air, as pictured in the entrainment hypothesis, should produce a diminishing sodium amount at increasing altitudes in the clouds. This decrease is not revealed by the photometer data thus far. At the present time it seems most likely that the high sodium values in clouds are due to an increase in the number of the salt particles during their growth to large droplets. As previously mentioned, this is one of the questions now being studied with the airborne flame photometer and the glass slide methods.

Acknowledgments.—The authors are indebted to Dr. W. S. Richardson for his valuable suggestions about various aspects of instrument design and to Mr. D. D. Ketchum and Mr. R. G. Walden for their very considerable thought and work in designing and building the amplifying circuits.

REFERENCES

1. Blanchard, D. C., and A. H. Woodcock, 1957: Bubble formation and modification in the sea and its meteorological significance. *Tellus*, **9**, 145–158.
2. Bowen, E. G., 1950: The formation of rain by coalescence. *Australian J. sci. Res.*, **A**, **3**, 193–213.
3. Boyce, S. G., 1954: The salt spray community. *Ecological Monographs*, **24**, 29–67.
4. Crozier, W. D., 1954: Errors in the "isopiestic" method for measuring masses of salt particles. *Science*, **120**, 840–841.
5. Jacobs, W. C., 1939: Apparatus for determining the salt content of the air. *Bull. Amer. met. Soc.*, **20**, 38–42.
6. Junge, C. E., 1954: The chemical composition of atmospheric aerosols, I: measurements at Round Hill field station, June–July, 1953. *J. Meteor.*, **11**, 323–333.
7. Junge, C. E., 1956: Recent investigations in air chemistry. *Tellus*, **8**, 127–139.
8. Langmuir, Irving, and K. B. Blodget, 1945: A mathematical investigation of water droplet trajectories. *Gen. Elect. Res. Lab. rpt.*, ATSC Contract W–33-038–AC–9151, pp. 1–47.
9. Lodge, J. P., 1954: Analysis of micron-sized particles. *Anal. Chem.*, **26**, 1829–1831.
10. May, K. R., 1945: The cascade impactor; an instrument for sampling coarse aerosols. *J. sci. Insti.* **22**, 187–195.
11. Seeley, B. K., 1955: Detection of certain ions in 10^{-10} to 10^{-15} gram quantities. *Anal. Chem.*, **27**, 93–95.
12. Soudain, G., 1951: Realisation d'un compter automatique de noyaux de chlorune de sodium. *Journal Scientifieque de la Meteorologie*, **3**, 137–142.
13. Turner, J. S., 1955: The salinity of rainfall as a function of drop size. *Quart. J. r. meteor. Soc.*, **81**, 418–429.
14. Twomey, S., 1954: The composition of hygroscopic particles in the atmosphere. *J. Meteor.*, **11**, 334–338.
15. Vonnegut, B., 1952: Counting sodium-containing particles in the atmosphere by their spectral emission in a hydrogen flame. *Occasional report, Project Cirrus, General Electric Co.*, No. 38, 1–18.
16. Woodcock, A. H., 1952: Atmospheric salt particles and rain drops. *J. Meteor.*, **9**, 200–212.
17. Woodcock, A. H., 1953: Salt nuclei in marine air as a function of altitude and wind force. *J. Meteor.*, **10**, 362–371.
18. Woodcock, A. H., and D. C. Blanchard, 1955: Tests of the salt-nuclei hypothesis of rain formation. *Tellus*, **7**, 437–448.
19. Woodcock, A. H., and Mary M. Gifford, 1949: Sampling atmospheric sea-salt nuclei over the ocean. *J. marine Res.*, **8**, 177–197.
20. Woodcock, A. H., and W. A. Mordy, 1955: Salt nuclei, wind and daily rainfall in Hawaii. *Tellus*, **7**, 291–300.

Contribution No. 891

Reprinted from the JOURNAL OF CELLULAR AND COMPARATIVE PHYSIOLOGY
Vol. 49, No. 1, February 1957

SUPERCOOLING AND OSMOREGULATION IN ARCTIC FISH[1]

P. F. SCHOLANDER, L. VAN DAM, J. W. KANWISHER, H. T. HAMMEL AND M. S. GORDON
Woods Hole Oceanographic Institution and Cornell University, Department of Zoology

FIVE FIGURES

It is generally recognized that the freezing point of the blood of most teleost fishes is around — 0.5 and — 0.8°C. (cp. Black, '51). It is also known that Eskimos in many places catch fish through the sea ice, sometimes in the middle of the winter when the water temperature is — 1.7° or colder. Hydrographic work during the summer by Iselin ('32) and Nutt ('53) established that the water at the bottom of several fjords in northern Labrador maintains a temperature of — 1.7° to — 1.8°C.; i.e., right at the freezing point of the fjord water. By dredging the bottom with a trawl, R. H. Backus brought to light a considerable fish fauna living at these extreme temperatures ('51, '53).

The present investigation originated with a simple question directed to the senior author by Dr. R. H. Backus: "When arctic fishes swim about in ice water at — 1.7° to — 1.8°, why don't they freeze? Do they have twice as high an osmotic concentration as ordinary fishes, or what is the story?" Since the problem appeared attractively simple, it was decided to make a quick dash to Nain in northern Labrador in April 1953, and return with the answer, which was easy to guess anyway. A wait of three weeks, while rain rotted the ice along the Labrador coast and made airplane landings impossible, diverted the expedition from Nain to the U. S. Air Force Base at Frobisher Bay in Baffinland. With the aid of Eskimos and dogteams two of the authors (Scholander and Hammel) managed to catch three tiny sculpins in the course of two weeks and at the cost of chopping a dozen holes through four foot ice. The largest fish (about 20 gm) yielded half a cubic centimeter of blood, the medium-sized fish was eaten by a dog, and the little one (about 5 gm) yielded a tiny drop of eye chamber fluid. Freezing point determinations made in a tent 20 miles from the base showed that these fish avoid freezing simply by becoming isotonic with the sea water.

---

[1] Contribution no. 891 from the Woods Hole Oceanographic Institution. This work was carried out, in part on the Blue Dolphin Labrador Expedition, 1954, under the auspices of the Arctic Institute of North America, with funds provided by the Office of Naval Research.

These very clear but scant data could not go unchecked, so it was decided to obtain further data from the bottom of Hebron Fjord in northern Labrador, where the temperature stays near — 1.7° all year round. This led to a summer expedition in 1954 on the Blue Dolphin, under command of D. C. Nutt. To our bewilderment it was found that all the bottom fishes had a plasma freezing point of only — 0.9° to — 1.0°, and hence were permanently supercooled by almost one degree. Fishes caught in the warm surface water had very nearly the same values, and froze instantly in a vat of freezing sea water at —1.7°. When they were lowered in a net to exactly the same temperature at the bottom of the fjord they did not freeze. Conversely, when the bottom fishes, who lived all their lives at —1.7°, were put in freezing sea water of this temperature on the surface they froze. After all the thermometers had been rechecked, these conflicting facts had to be reconciled.

A chance observation on supercooled *Fundulus* at the laboratory in Woods Hole offered a solution to the mystery of the arctic fishes, and prompted a third expedition to check on the Frobisher Bay data. This took two of the authors (Scholander and Kanwisher) back to Hebron Fjord in March 1955 where fishes were readily obtained through the ice. At last, then, with two winter expeditions and one summer expedition behind us, we were able to answer this simple question of why the arctic fishes don't freeze while swimming in water of —1.7° to —1.8°.

Field facilities

The work in Baffinland (April 23–May 5, 1953) was conducted from the U. S. Air Force Base at Frobisher Bay. The field work was greatly assisted by the cooperation of the Royal Canadian Mounted Police stationed at the base. For the summer work in Hebron Fjord (July 8 to August 15, 1954), a small prefabricated and prefurnished plywood laboratory (8 × 12 feet) was set up on the shore near an area of cold deep water. The location was 17 miles inland from the Moravian Mission at Hebron. Ice for making cold mixtures and for other laboratory and camping needs was taken from a large snow field next to the camp and later from drifting ice in the fjord. Stirring motors and all other electrical equipment were run with 6 volt Hot Shot batteries. The winter work at Hebron (March 13–24, 1955) was made possible through the cooperation of the Reverend F. C. P. Grubb of the Moravian Mission, who generously provided us with native help, working space, and quarters.

In the summer the shallow water fishes were caught by gill net or hand line at the camp site, and the deep fjord material was obtained by dredging the bottom with a 16 foot regular shrimp try net (Marinovich Trawl Company, Biloxi, Mississippi). The trawl was operated with a U. S. Navy Bureau of Aeronautics light metal target-towing winch powered by a 2½ horse gasoline engine, and mounted in a 30 foot Newfoundland motorboat, run by Mr. Peter Hay, of Nain, Labrador. In the winter, fishes were obtained by jigging and baited traps.

Freezing point determinations

Determination of the freezing point, i.e., the temperature at which a small ice crystal is in equilibrium with a large amount of unfrozen solution, was made with the method of Pounder and Masson ('34), modified to fit field conditions. In this method freezing and melting are directly observed under magnification.

Apparatus (fig. 1). A 4–5 liter white enameled tin can, set into the lid of an insulated paraffin-coated plywood box, served as a cold bath. Mounted on the lid of the box was a low power binocular scope. The thermometer and sample tube were held next to each other by means of a friction clip, hinged to permit adjustment. A Magnatorque 6 volt miniature motor, mounted on the box, drove a propeller shaft directly from the armature to provide vigorous stirring. A flashlight bulb provided light. A plastic sheet painted black and white, when properly adjusted under the sample tube, made a good contrasting background against which the crystals could be observed. It was mounted on a wire stuck into a movable block on the lid of the box. The thermometer, graded in tenths of a degree, was calibrated for zero in a slush of clean snow and distilled water, kept in a Thermos bottle. The sample tube was made from a thin-walled 1.5–2 mm glass tubing pulled out to a long taper point. The open wide end was

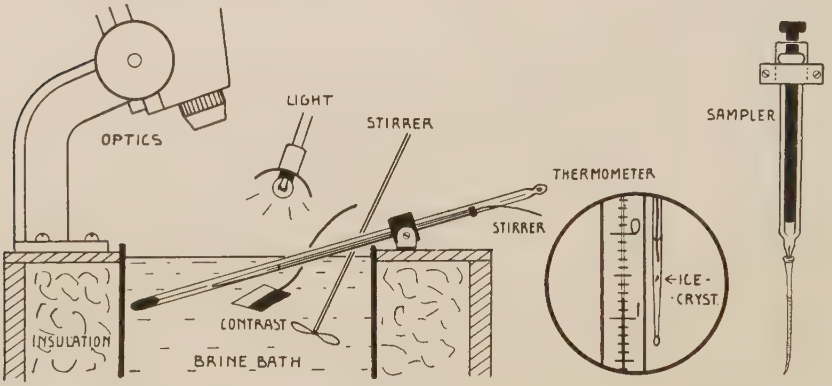

Fig. 1 Method for freezing point determinations modified for field work from the method of Pounder and Masson ('34). In circle: Thermometer and freezing tube. To the right: Syringe burette used as sampler.

closed by a vaccine stopper through which a Saran filament fitted loosely to act as a stirrer.

The temperature of the brine bath would rise 0.1° in three minutes, depending upon the room or tent temperature. It could be lowered or raised at any time by adding pieces of ice or snow, or by introducing hot water either directly or enclosed in a tube.

Procedure. The sample, 10 mm^3 or less, was drawn into a fine polyethylene tubing attached to a tuberculin syringe with a pulled out tip (fig. 1), and transferred to the sample tube, avoiding evaporation loss through exposure to the open air. It was shaken down into the tip of the sample tube, which was closed with the stopper and provided with the Saran filament for stirring. The sample was frozen in a Thermos bottle containing a snow and salt mixture at about — 10°. The sample tube was then placed in the friction clip and introduced into the brine bath, which was set at a few tenths of a degree lower than the freezing point of the sample. A test tube with warm water, or a finger, was held next to the stirred sample for a moment until all but a few crystals were melted. Stirring is necessary to abolish the concentration gradients produced by the freezing or thawing. As the temperature rose slowly in the brine bath, the ice crystals were watched. In melting, the edges of the crystals dull, and very small crystals disappear. This is the melting temperature. Before the last crystal was gone, the temperature was lowered slowly by adding snow to the brine. In freezing, the crystal edges sharpen up and new spicules may begin to form. This is the incipient freezing temperature. The average of these two readings is the freezing point.

Accuracy. In simple salt or sugar solutions melting and freezing temperatures were found to differ by some 0.05°, although theoretically they are, of course, the same. The average of these two readings gave the freezing point of NaCl, NH_4Cl and sucrose to within 0.05° of the Handbook values for $\frac{1}{2}$ and $\frac{1}{4}$ molar solutions, which covered the relevant range.

In fish plasma, especially that of the winter fishes, the melting and freezing temperatures were less sharp, and often as far apart as 0.1°.

Chloride determinations in blood plasma

Blood obtained by heart puncture was drawn into a syringe which had been rinsed with 0.2 M saline, and transferred to a dry vial containing a trace of powdered heparin. The plasma was separated in a hand centrifuge and stored for analysis. A sample of 0.1 ml of the plasma was digested on waterbath with a mixture of $AgNO_3$, H_2O_2 and nitric acid. It was titrated under ether according to the method of Rehberg as modified by Schnohr ('34). A 1 ml tuberculin syringe with plastic tip and friction clip (fig. 1) served as an excellent field micro burette. The titration and stirring were either performed free hand (Scholander, '47), or by screw activation and air bubbling (van Dam, '35). The plunger setting was read with a handlens and in either case duplicate analyses agreed within 0.01 M.

TABLE 1

Plasma freezing point of shore fishes in Hebron Fjord. Summer. Water temperature + 4° to + 7°. Depth 2–6 m

Gadus ogac, Fjord cod	— 0.77	— 0.77	— 0.78	— 0.81	— 0.83	— 0.85	(av. — 0.80)
Myoxocephalus scorpius, Sculpin	— 0.78	— 0.78	— 0.79	— 0.79	— 0.81	— 0.87	(av. — 0.80)
Salvelinus alpinus, Arctic char	— 0.80	— 0.80	— 0.81	— 0.82			(av. — 0.81)

Freezing point of plasma in summer fishes

Shallow water fishes. The freezing point depression of the plasma in fishes taken along the shore in shallow and relatively warm water will be seen in table 1. In all three species (fjord cod, sculpin, and arctic char) the freezing point usually lies between —0.75° and —0.85°, which is well within the limits of common southern marine teleosts (Black, '51).

Deep water fishes. The plasma freezing point of five species of fishes caught in the cold bottom water of the fjord at —1.73° is slightly lower (table 2), with specific averages running from —0.90° in *Liparis* to —1.0° in *Boreogadus.* The blood data were confirmed by freezing point determinations in the eye fluids and lenses of several of the same species of bottom fishes (table 3).

TABLE 2

Plasma freezing point of deep water fishes in Hebron Fjord
Water temperature — 1.73°

SPECIES	100 m			200 m	
Boreogadus saida	— 0.97			— 1.07	
Lycodes turneri	— 0.88	— 0.98		— 1.03	— 0.97
Liparis koefoedi	— 0.91	— 0.91		— 0.90	
Gymnacanthus tricuspis	— 0.94	— 0.95	— 0.89		
Icelus spatula	— 0.96				

TABLE 3

Freezing point of eye constituents in deep water fishes

SPECIES	100 m			200 m
Myoxocephalus scorpius	— 0.75[1]			
Lycodes turneri	— 0.91[1]	— 0.95[2]	— 0.96[2]	
Liparis koefoedi				— 0.93[2]
Gymnacanthus tricuspis	— 0.84[1]	— 0.85[1]		
Icelus spatula	— 0.84[1]			— 0.90[2]

[1] Chamber fluid.

[2] Lens.

The remarkable thing is that these fishes are living in water which is 0.75° to 0.85° below the freezing point of their blood. In other words, the whole fish fauna is supercooled by almost one degree. Inasmuch as the water temperature at the bottom stays constant all year at — 1.73° to — 1.75°, there is no reason to believe that these fishes change in the winter. Consequently they appear to live in a supercooled state all year round. It was repeatedly established that even large specimens of cod and sculpin had a body temperature within 0.1° of the sea water.

Stability of supercooled fishes

If the whole fish fauna at the bottom of Hebron Fjord is supercooled, the question arises as to how stable are such fishes against freezing. Several experiments to clarify this situation were performed both at the shore laboratory on Hebron Fjord and at the laboratory in Woods Hole.

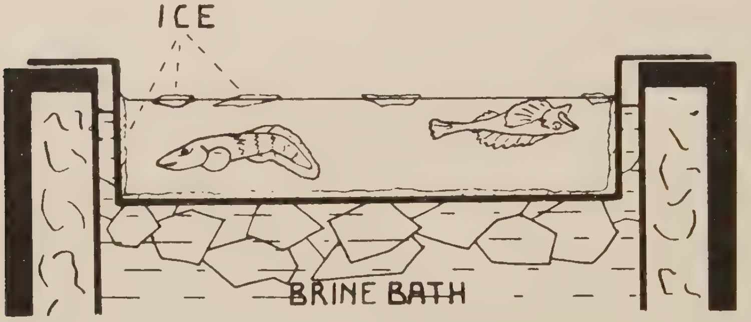

Fig. 2 Bottom fishes *(Lycodes* and *Gymnacanthus)* freezing in ice trough at — 1.7°.

(a) Freezing of bottom fishes at the surface. Many of the specimens caught in the trawl at a depth of 100 meters were lively and in good condition when brought up. They were put in a metal trough suspended in a cold mixture (fig. 2). By freezing out ice from the relatively brackish surface water, the temperature could be lowered to —1.7°, or further. When the bottom fishes were put into this water it was found that most of them became severely damaged. *Lycodes* froze partially, developing white patches and kinks in the tail. *Liparis* went into convulsions and got a kink in the tail. *Icelus* was stiff in rigor with gill covers expanded. Only some tomcods *(Boreogadus)* seemed to be unhurt at —1.73°, but they died with ice spicules visible in the eyes at —2.5°. *Lycodes* was killed at —1.9°.

(b) Freezing of shore fishes. In another series nine little sculpins (*Myoxocephalus*), of 10–15 gm weight, were caught by hand in the shallow water along the shore. These were put in the freezing trough. At —1° they were motionless on their backs, and ice masses filled their eyes. This could easily be seen under the binocular. With a touch of the fingers the eyes cleared. A medium sized sculpin, of 25–40 gm, froze stiff and white at —1.5° in 20 minutes, and died.

Four little sculpins were put in the ice trough at —1.7°. The eyes froze in a few minutes. One fish survived after 10 minutes in the bath. None survived after 20 minutes. Hence it was established that these little sculpins would regularly die of freezing when subjected to —1.7° in the trough for 20 minutes.

(c) Survival of fishes at —1.7° on the bottom. In two experiments sixteen small sculpins were put in a net and lowered to a temperature of —1.73° at 100 meters' depth. They were left there for one to three hours. When hauled up, fourteen were still lively. When some of these were put into the freezing trough at —1° their eyes froze in an hour.

Finally, in two experiments, two fjord cod and two sculpins were kept for four and eight days in the cold bottom water, without freezing or other signs of damage. They did, however, markedly lower the freezing point of their blood (see below).

(d) Hydrostatic effect on freezing point of plasma. Why then did the fishes not freeze at all on the bottom when they froze to death at the same temperature on the surface? One rather remote possibility was that the ten atmospheres' hydrostatic pressure would significantly lower the freezing point and protect the deep sea fish. This was tested by sealing a thin-walled freezing tube to a screw-activated piston pump. The air pressure was increased to ten atmospheres, and the freezing and melting were observed as usual. In plasma and eye fluid of sculpin and in isotonic saline solution the freezing points at 10 atmospheres were found to be 0.04°, 0.06°, and

0.08° lower than at 1 atmosphere, which checks the Handbook data for distilled water within the limits of our method. The pressure effect is therefore normal and nowhere near large enough to account for the non-freezing at the bottom.

(e) Stability of plasma supercooled to —2°. Plasma from *Myoxocephalus, Gadus ogac, Icelus,* and *Liparis* was transferred to the thin-walled freezing tubes. These were put into a brine solution in a Thermos flask, and placed in an icebox. Throughout most of a week's time the temperature was kept at —2°C. In a week most of the samples had become infected, but none froze. Dorsey ('48) kept vials of supercooled water for 10 months at —8° to —10° without the occurrence of freezing, so the results of our experiment were not surprising.

Ice seeding of supercooled fishes

Sea water can readily be supercooled to —3° in a beaker suspended in a thermoregulated bath. It may be stirred gently by air bubbling. Several species of fish taken in cold water at Woods Hole in the winter (*Fundulus,* cunner, eel, toadfish, tautog) were found to survive for some time in such water. Cunner and *Fundulus* were kept in —3° water for 12 hours. They were torpid, but breathed slowly, and survived apparently without any harmful effects.

If the water containing the fish is supercooled to —2° or —3°, while gently stirred by air bubbling, and is then seeded with a few ice crystals, the water fills up with a whole flurry of ice crystals immediately. The practically motionless fish goes into a few violent convulsions, whitens in patches, and freezes stiff (fig. 3A). In other words, direct ice contact seeds the supercooled fish right through the integument. This happened in all of the five species enumerated above, and also in frogs.

If a fish frozen in this manner is plunged into sea water of room temperature, it will initially float due to the ice in its body, but will soon settle to the bottom when the ice thaws.

If such a partly thawed fish, which has ice only in its core (fig. 3C), is placed in a beaker of supercooled water, the water will shortly thereafter freeze, showing that the ice formation will also be propagated across the integument from inside outward.

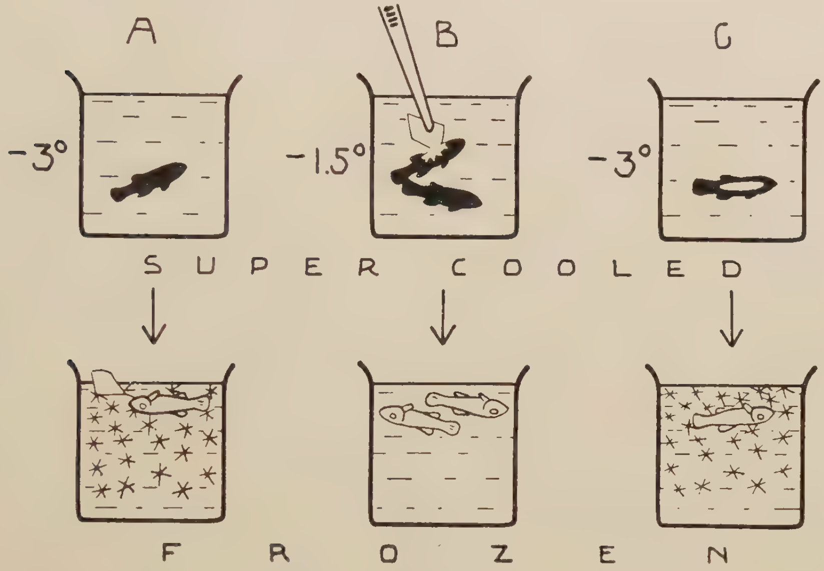

Fig. 3 Seeding experiments on *Fundulus.* A. Fish freezes when supercooled water is seeded. B. Supercooled fish freezes when touched with ice in water above freezing point. One fish may by contact seed another. C. Thawed fish with ice core freezes, and seeds supercooled water.

Fundulus, toadfish, and eel were supercooled in water of —1.5° to —1.7°; i.e.; in sea water warmer than its freezing point. If these fishes were touched with an ice cube (fig. 3B), they would go into convulsions, stiffen, and gradually whiten in freezing. Indeed, if only one fish were seeded and frozen, soon the other would freeze also by contact with the first, although the water could not freeze.

From the ice seeding experiments in live fishes it was clear that ice formation would pass right through the integument. This was studied further on pieces of skin of the eel, tautog, toadfish, and frog. The skin was stretched across one orifice of a piece of tubing, which was then filled with isotonic saline, and the whole assembly was placed in supercooled sea water. Seeding on either side of the skin would propagate through and seed the other side.

It was found that ice would propagate through a Corning glass filter, UF with 1–2 μ pores, but not through dialyzing cellophane at a supercooling temperature of —3°. In respect to ice propagation, therefore, fish and frog integuments seem to be relatively open structures. Considering that they maintain considerable osmotic gradients, it appears that the ice actually spears its way through the tissue. This is suggested by the following observation. If a fish is placed in freezing sea water with its gills exposed these will freeze white rapidly. If the fish is thawed and then put back in the cold water, the gills will not freeze again, probably because the ice crystals have pierced and damaged the osmotic barriers.

Freezing point of arctic fishes in the winter

From Dorsey's experiment with supercooled water samples, kept at —8° to —10° for months, it is clear that supercooled water possesses a certain degree of stability, and evidently more the less it is supercooled. Therefore, if ice seeding is absent, freezing may never occur at a slight degree of supercooling. This is undoubtedly what saves the supercooled bottom fishes in Hebron Fjord from freezing. Their supercooling is slight, and they live so deep that ice can never reach them.

But what about the shallow water fishes living all winter long near or amongst the floating ice? The answer was already indicated by our two little sculpins caught through the ice in Baffinland in the winter of 1953. Their plasma freezing point was —1.5° to —1.6°, i.e., very nearly the same as the sea water, and hence they could not be seeded by ice. This called for further study, and in March, 1955, we (Scholander and Kanwisher) returned to Hebron Fjord. Our Eskimo friends patiently jigged fjord cod and sculpins through holes cut in four foot ice along the shore in from 2 to 8 meters' depth of water. The fish were immediately taken into a heated tent next to the fishing hole, so that blood could be taken by heart puncture. Outside, the blood froze in the needle immediately.

The results will be seen in table 4. The sea water was at its freezing point of —1.73°, and the plasma freezing point in the cod averaged —1.47°, in the sculpin —1.50°, as against the summer value of —0.80° for both species (fig. 4).

The shallow water winter fishes had therefore almost doubled their osmolarity, but some were nevertheless as much as 0.2–0.4° supercooled. Several specimens were therefore transferred directly into a large freezing trough which contained floating pieces of ice in sea water. In this, most of the fishes died, undoubtedly by contact freezing. Two codfish were placed in a flour sack together with a piece of clear ice, and were suspended in the fjord. After a day one fish died, very probably from freezing. The other stayed alive, and was taken out of the bag, still living, after three days. It had then a freezing point of — 1.52° and a markedly elevated chloride concentration (cp. fig. 5).

We see, therefore, that considerable adjustments take place in those fishes which risk seeding by contact with ice. From the experiments where sculpins and cod were transferred in the summer to the deep water of — 1.73°, it seems clear that the adjustments are conditioned by the change in temperature, rather than by the presence of ice. Whether or not seasonal changes take place in the fishes at the bottom, which live under perfectly constant temperature conditions is not known, but it seems improbable.

Freezing point of invertebrates

A series of freezing point determinations was made in the blood obtained from various marine invertebrates. The summer data are given in table 5. It will be seen that they

TABLE 4

Plasma freezing point of shore fishes in Hebron Fjord. Winter. Water temperature —1.73°. Depth 2–8 m

Gadus ogac	—1.36	—1.36	—1.41	—1.49	—1.51	—1.52	—1.56	—1.57
Myoxocephalus scorpius	(—1.16)	—1.36	—1.43	—1.55	(—1.60	—1.54 Baffinland)		

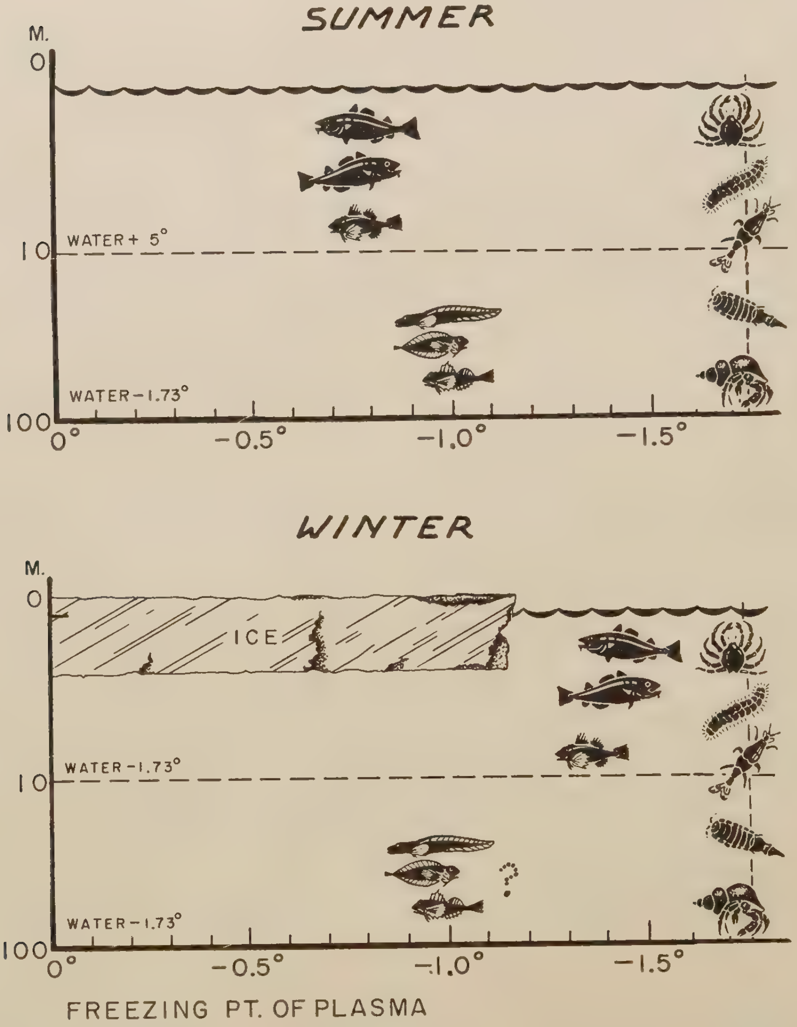

Fig. 4 Freezing point of plasma in shallow water fishes (fjord cod and sculpin) and in deep water fishes *(Lycodes, Liparis, Gymnacanthus)*. Position of fishes on abscissa indicates the freezing point of their plasma.

cluster closely around the osmoconcentration of the sea water. Two observations were made in the winter on spider crabs (*Hyas araneus*) taken at a depth of 1 meter under the ice. The freezing points were again close to that of sea water, namely, — 1.68° and — 1.73°, as would be expected. Thanks to the isosmosity of arctic as well as non-arctic marine invertebrates they face no danger of freezing except when trapped and frozen into the fjord ice, or when frozen entirely out of water. Even so, many tidal forms have been shown to stand a large amount of internal freezing (Kanwisher, '55).

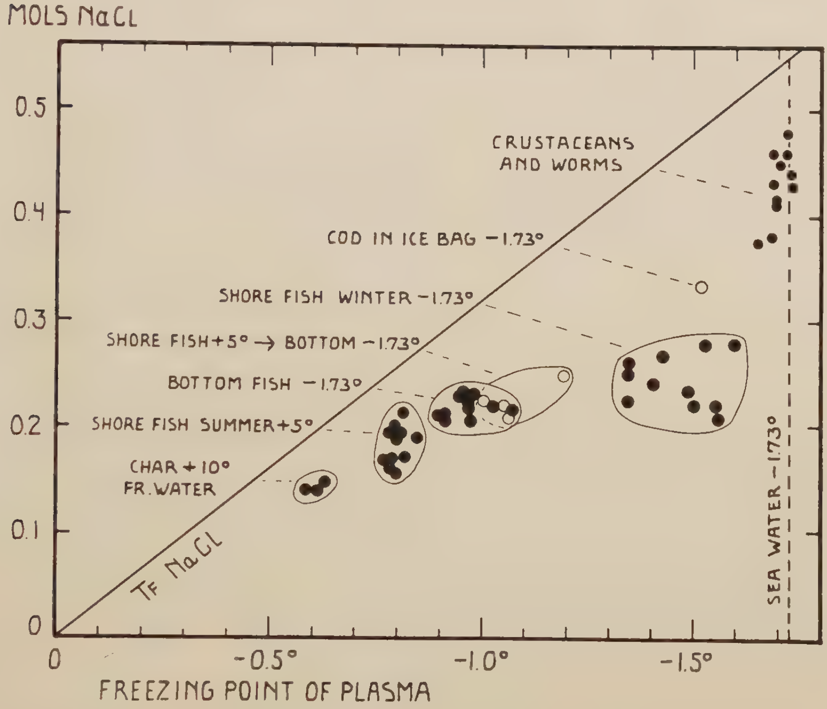

Fig. 5 Freezing point versus chlorides in fishes and invertebrates from Hebron Fjord. Shallow water fishes are here called shore fishes.

Osmoregulation by chlorides

Most of the plasma samples taken for freezing point determinations were also analyzed for chlorides (fig. 5). It will be seen that the chlorides (halides) make up for about 80% of the osmotic pressure in both deep and shallow water summer fishes; i.e., those which have what might be called a normal osmoconcentration.

In the fishes which were transferred from the warm surface water to the bottom at —1.73°, the total osmoconcentration increased, but the chlorides rose relatively less, and in the great elevation in osmoconcentration which takes place in shallow water fishes in the winter the chlorides contribute only half of the freezing point depression.

A single plasma determination on the Baffinland sculpin (T_f = —1.6°) showed a high non-protein nitrogen (90 mg %), which in a compound of one nitrogen atom per molecule (such as in trimethylamine oxide) could have accounted for another 0.1° depression. Added to 0.8° for the chlorides this would give a total freezing point depression of 0.9°, leaving 0.7° still unaccounted for.

TABLE 5

Blood freezing point of invertebrates in Hebron Fjord. Summer. Water temperature — 1.73°

SPECIES	100 m			200 m	
Shrimp *(Argis dentata)*	—1.68	—1.72	—1.70	—1.42	—1.65
Hermit crab *(Pagurus kröyeri)*	—1.70			—1.74	—1.60
Spider crab *(Hyas araneus)*				—1.61	
Isopod *(Saduria sabini)*	—1.68	—1.71		—1.70	—1.75
Polychaete (scale worm)	—1.67	—1.65			

It is interesting to note that the codfish which was supercooled by 0.2° and did not freeze after three days spent with a piece of ice in a flour bag at —1.73°, elevated its chlorides very markedly (fig. 5).

As in the summer fishes, the chlorides in the invertebrates are responsible for some 80% of the freezing point depression. What the other components are we do not know.

Conclusions

In the bottom waters of Hebron Fjord lives a population of fishes that are permanently supercooled by almost 1°C. If experimentally seeded with ice at their normal habitat temperature, most of them freeze and die. Ice can, of course, never reach them at the bottom, and in the absence of seeding their state of slight supercooling is stable enough to permit them to maintain their ancestral hypotonicity. Evidently spontaneous freezing takes place too rarely to be of any consequence for their survival.

Shallow water fishes, swimming about under the ice in the winter, would very likely be seeded and frozen unless they were somehow protected. They run little risk, however, because their osmoconcentration is twice as high as in the summer, which is enough to render them almost isosmotic with the sea water and hence freeze proof.

Our supercooled bottom fishes represent, we believe, the second instance known in nature where evolution has pushed life into a region of permanent physical metastability. The other case is in plants. It is generally believed that the sap in tall trees is under tension, with pressures sometimes as low as —20 atmospheres or less. The sap is therefore in a metastable and potentially almost explosive state. A return to the stable physical state would in either of these cases be fatal, but it does not occur because of the absence of proper nuclei to trigger the catastrophe.

The large rise in osmoconcentration in the winter which takes place in the arctic shallow water fishes represents a unique osmoadaptation induced by temperature, which protects the animal from freezing.

SUMMARY

A study has been made of the osmoregulation of fishes and invertebrates living at or near the freezing point of sea water. The bottom of Hebron Fjord in northern Labrador has a water temperature of —1.7° to —1.8°C. all year round. Here

lives a large population of fishes with a plasma freezing point of —0.9° to —1.0°. They are hence supercooled by —0.7° to —0.8°. When brought to the surface and put in an ice bath at —1.7° most of these fishes freeze and die. In an ice bath of this temperature surface fishes in the summer also freeze and die. Neither deep nor shallow water fishes freeze, however, when kept at the same temperature at the bottom. In supercooled sea water of —3° several species of southern fishes survive without freezing. If the water is seeded they freeze and die almost instantly. Even in water of —1.5° they freeze and die if touched with ice. It was found that seeding would propagate through pieces of fish skin in either direction. Ice will penetrate a UF glass filter with 1–2 μ pores, but not cellophane. Absence of ice seeding is therefore the condition that makes it possible for the bottom fishes to preserve their hypotonic ancestral blood, at the cost, however, of being supercooled. The shallow water fish moving about in the ice in the winter double their osmoconcentration at that time, i.e., until it almost matches the sea water, and are thereby protected against freezing. This adaptation takes place with only a slight increase in chlorides. Marine invertebrates in the summer and winter are nearly isosmotic with the sea water, and therefore, cannot freeze as long as they remain in the water.

ACKNOWLEDGMENTS

We are very much indebted to Dr. A. C. Redfield and to Dr. R. H. Backus, of the Woods Hole Oceanographic Institution, for initiating the present study and for contributing to it their advice and support. In making preparations for our expedition we wish to acknowledge the help of Admiral Edward H. Smith, Director of the Woods Hole Oceanographic Institution, who has given us the benefit of his rich arctic experience. Success in our fishing was largely due to the knowledge of Dr. Backus and of Commander David C. Nutt, Arctic Specialist at the Dartmouth College Museum and

Master of the Blue Dolphin. Commander Nutt and the crew of the Blue Dolphin rendered us invaluable help throughout the course of our summer expedition to Hebron, in transporting personnel, provisions, and equipment, in locating and setting up the land laboratory and camp, and in providing temperature data from the fjord waters. The portable plywood laboratory was designed by Mr. K. Morrison of the Woods Hole Oceanographic Institution. It was easy to erect and served its purpose admirably. We are indebted to the U. S. Navy Bureau of Aeronautics for placing at our disposal a target-towing winch. This was skillfully adapted to a trawl winch by Mr. Warren O. Bowman and Mr. Leonard S. Perry of the Woods Hole Oceanographic Institution. Mr. Peter Hay of Nain, Labrador, ably assisted us in all phases of our summer work at Hebron. We wish to thank for their fine cooperation Major Willie Knutsen, U.S.A.F., of the Survival School at the U. S. Air Force Base, Goose Bay, Labrador, Lt. W. G. Swart, U.S.A.F., commanding officer of the U. S. Air Force Detachment at Frobisher Bay, Baffinland, and Constable R. D. Van Norman, of the Royal Canadian Mounted Police, at the same base. We are likewise much indebted to the Reverend F. C. P. Grubb, of Hebron, Labrador, for giving us every possible facility and help on our last winter expedition. For identification of the crustaceans and the isopod we wish to thank Dr. Fenner A. Chace, Jr., and Dr. Thomas E. Bowman of the Smithsonian Institution.

LITERATURE CITED

BACKUS, R. H. 1951 New and rare records of fishes from Labrador. Copeia, no. 4, 288–294.

———— 1953 The marine and fresh water fishes of Labrador. Unpublished Ph.D. thesis, Cornell University. 238 pp.

BLACK, V. S. 1951 Osmotic regulations in teleost fishes. *In* W. S. Hoar, V. S. Black, and E. C. Black. Some aspects of the physiology of fish. Univ. Toronto Biol. Ser. No. 59, Publ. Ontario Fish. Research Lab., No. 71, II, 53–89.

DAM, L. VAN 1935 A method for determining the amount of oxygen dissolved in 1 c.c. of water. J. Exp. Biol., *12:* 80–85.

DORSEY, N. E. 1948 The freezing of supercooled water. Trans. Am. Phil. Soc., new ser., *38:* 247–328.

ISELIN, C. O'D. 1932 A report on the coastal waters of Labrador, based on explorations of the ''Chance'' during the summer of 1926. Proc. Am. Acad. Arts Sci., *66:* 1–37.

KANWISHER, J. W. 1955 Freezing in intertidal animals. Biol. Bull., *109:* 56–63.

NUTT, D. C. 1953 Certain aspects of oceanography in the coastal waters of Labrador. J. Fish. Res. Bd. Canada, *10:* 177–186.

POUNDER, F. E., AND I. MASSON 1934 Thermal analysis and its application to the dinitrobenzenes. J. Chem. Soc., 1357–1360.

SCHNOHR, E. 1934 A study on the cause of death in high intestinal obstruction. Coll. Papers XII, No. 185, Univ. Zoofysiol Lab. Kjøbenhavn.

SCHOLANDER, P. F. 1947 Simple syringe burette. Science, *105:* 581.

Contribution No. 892

Reprinted from the JOURNAL OF CELLULAR AND COMPARATIVE PHYSIOLOGY
Vol. 49, No. 1, February 1957

THE CONCENTRATION OF HEMOGLOBIN IN SOME COLD WATER ARCTIC FISHES[1]

P. F. SCHOLANDER AND L. VAN DAM
Woods Hole Oceanographic Institution

The demonstration by Ruud in 1954 that several species of cold water antarctic fishes lack hemoglobin inspired us to check on the iron content in the blood of some arctic fishes, which live all year round at extremely low temperatures. As Ruud has pointed out, a low temperature would favor a low metabolic rate and would enable plasma and water to hold more oxygen, both factors probably essential for the evolution of a fish without hemoglobin. One may point out that, although the metabolic rate in the few cold water arctic fishes that have been investigated clearly indicates an adaptive elevation, it still falls far behind the rate of a tropical fish at its habitat temperature (Scholander, Flagg, Walters and Irving, '53).

Our fishes were taken in Hebron Fjord, northern Labrador, in August. At depths of 100 meters and lower the temperature stays around —1.73°C. all year round. At depths of 5–10 meters in the summer it may rise to some 4–6°C. In the summer the oxygen content of the water at 100 meters' depth was found to vary between 6.7 and 6.9 ml/l, corresponding to 80% saturation. Nearer the surface it was 100% or more. There are hydrographic reasons to expect that these waters are well aerated throughout the year (Nutt and Coachman, '56). Blood was taken from the fishes by heart puncture, and iron analyses were performed according to the method by Wong ('28).

---

[1] Contribution No. 892 from the Woods Hole Oceanographic Institution. This work was carried out on the Blue Dolphin Labrador Expedition, 1954, under the auspices of the Arctic Institute of North America, with funds provided by the Office of Naval Research.

Table 1 shows the iron content of the blood of 4 species of arctic fishes caught in Hebron Fjord. The values range from 8.5 mg % to 21 mg %, which would normally correspond to an oxygen capacity of 3.4 vol. % to 8.4 vol. %.

Hall and Gray ('29) give iron values from 15 species of shallow water marine teleosts. They run from 45.5 mg % in the bonito to 11.5 mg % in the sand-dab. Excluding the Scombridae and the menhaden, with their exceptionally high iron content, the remaining 10 species average 19.9 mg%. Compared to these shallow water fishes, a series of 12 deep sea species have a range from 24.9 mg % in *Sebastes* to 11.9 mg % in *Cottunculus,* with an average of 19.6 mg % (van Dam and Scholander, '53). In table 2 we have listed the fishes in these two series which have the lowest iron contents in the blood.

TABLE 1

Iron content in the blood of Arctic fishes

(Blood pooled from several specimens)

	DEPTH OF CATCH	IRON
	m	*mg %*
Liparis koefoedi	100	8.5
Gymnacanthus tricuspis	100	11.3
Gadus ogac	2–5	17.2
Myoxocephalus scorpius	2–5	21.0

TABLE 2

Iron content in the blood of some southern fishes with low hemoglobin content[1]

(averages)

	DEPTH RANGE	IRON
	m	*mg %*
Cottunculus thompsonii[2]	750–915	11.9
Coryphaenoides rupestris[2]	390–865	11.9
Lophius piscatorius[3]	10–720	14.7
Opsanus tau[3]	1–50	13.5
Lophopsetta maculata[3]	1–70	11.5

[1] Depth ranges kindly furnished by Mr. W. C. Schroeder, Woods Hole Oceanographic Institution.

[2] van Dam and Scholander ('53).

[3] Hall and Gray ('29).

A glance at tables 1 and 2 will show that low hemoglobin content may be found among cold water arctic fishes as well as among cold water deep sea fishes of more southern latitudes, and shallow, relatively warm water forms, such as the sand-dab *(Lophopsetta)* are also represented. Hall and Gray ('29) pointed out that the more active species in their series, especially the Scombridae, had the highest iron values, whereas the sluggish, sedentary forms tended to be the lowest on the scale. There are, of course, many exceptions to this over-all rule. In our material *Gymnacanthus, Myoxocephalus,* and *Cottunculus* are all sculpins and presumably very similar in habits, yet *Myoxocephalus* has nearly twice as much blood pigment as the others, and while *Liparis* may be somewhat sedentary, as indicated by the suction cups on its pelvic fins, *Coryphaenoides* is certainly not.

The oxygen capacity of the blood of *Liparis* and *Gymnacanthus* at 15°–20° was found to average 3.7 and 4.1 volume per cent. Their plasma at — 1.7° could carry one more volume per cent dissolved oxygen. Even this small amount of hemoglobin represents, therefore, no less than a fivefold increase of the oxygen transport capacity over plasma alone. Whereas a 20° rise in temperature would almost halve the oxygen carrying capacity in a fish without hemoglobin, the *Liparis* or sand-dab would suffer only 10% reduction. Consequently, compared to our northern low-pigment fishes, the antarctic pigment-free fishes are much more severely restricted by temperature. One would suspect that pigment-free fishes, even in ice water, would have developed some compensatory means to offset the handicap of the low oxygen carrying capacity of their blood.

LITERATURE CITED

HALL, F. G., AND I. E. GRAY 1929 The hemoglobin concentration of the blood of marine fishes. J. Biol. Chem., *81:* 589–594.

NUTT, D. C., AND L. K. COACHMAN 1956 The oceanography of Hebron Fjord, Labrador. J. Fish. Res. Bd. Canada, *13*(5): 709–758.

RUUD, J. T. 1954 Vertebrates without erythrocytes and blood pigment. Nature, *173:* 848–850.

SCHOLANDER, P. F., W. FLAGG, V. WALTERS AND L. IRVING 1953 Climatic adaptation in arctic and tropical poikilotherms. Physiol. Zool., *26:* 67–92.

VAN DAM, L., AND P. F. SCHOLANDER 1953 Concentration of hemoglobin in the blood of deep sea fishes. J. Cell. and Comp. Physiol., *41:* 522–524.

WONG, S. Y. 1928 Colorimetric determination of iron and hemoglobin in blood. II. J. Biol. Chem., *77:* 409–412.

Contribution No. 893

Reprinted from LIMNOLOGY AND OCEANOGRAPHY
Vol. II, No. 2, April, 1957
Printed in U.S.A.

Short-Term Variations in Phytoplankton Chlorophyll and Their Significance[1]

C. S. YENTSCH AND J. H. RYTHER

Woods Hole Oceanographic Institution

ABSTRACT

Diurnal fluctuations were observed in the chlorophyll *a* content of natural phytoplankton populations, with the highest concentrations during the morning and afternoon, low values at midday and at night. This periodicity is similar to the daily rhythm of photosynthesis with which it appears closely related. The rate of synthesis of chlorophyll at optimal light intensity is dependent upon its previous rate of synthesis and concentration in the organisms. All of these factors strongly influence the capacity for photosynthesis at optimal light intensity and are probably the basis for the photosynthetic daily periodicity reported elsewhere.

INTRODUCTION

Recent experiments by Doty and Oguri (1957) have indicated a daily periodicity in the photosynthetic capacity of planktonic algae under constant illumination. Samples taken from the same population showed a seven-fold difference in their ability to assimilate C^{14} in an illuminated incubator, between the minimum at midnight and the maximum at 1000 hrs.

Marked diurnal variations in the chlorophyll content of surface populations of phytoplankton have been noted on numerous occasions by the senior author in Woods Hole (Mass.), East Sound, (Wash.) and elsewhere (Yentsch, in preparation). It is the purpose of this paper to investigate the possible relationship between the diurnal *in situ* fluctuations in the chlorophyll *a* content of phytoplankton and their photosynthetic capacity when exposed to a constant illumination.

METHODS AND RESULTS

Surface water from Woods Hole Harbor was enclosed in two carboys which were suspended at the water surface for a period of 24 hours. At four-hour intervals two one-liter samples were withdrawn, the first of which was used for the immediate determination of chlorophyll, while the second was placed in a glass container and exposed to 2000 foot candles of artificial illumination in a water-cooled incubator for four hours after which its chlorophyll content was measured. The samples were millipore filtered, their pigments extracted according to Creitz and Richards (1955), and chlorophyll *a* determined quantitatively by the spectrophotometric method of Richards with Thompson (1952).

At the same time the chlorophyll samples were taken, an additional 150 ml sample was withdrawn, enclosed in a glass-stoppered bottle, inoculated with approximately 5 μ curies of $C^{14}O_3^{=}$, and placed in the incubator for 15 minutes. After this exposure, the samples were millipore filtered, the filters dried, and their radioactivity, in counts per minute, taken as an index of relative photosynthesis. The experiment ran from 1200 on July 18 to 1200 on July 19, 1956, under completely clear skies. Solar radiation, measured with an Epply pyrheliometer, reached a maximum of approximately 1.5 g-cal/cm^2/min. at noon of each day (Fig. 1A).

A diurnal variation was observed in the photosynthesis at 2000 foot candles of samples taken from the *in situ* carboys (Fig. 1B). This was similar in its periodicity to that reported by Doty and Oguri, with a maximum at 0800 and a minimum at 2400, but the magnitude of the variation was less, with only a two-fold range.

Chlorophyll *a* samples taken directly

---

[1] Contribution No. 893 from the Woods Hole Oceanographic Institution, Woods Hole, Massachusetts. This work was supported by research grants from the National Science Foundation.

from the carboy showed a similar diurnal variation. Highest values were observed at 0800 while the lowest were at 1600. Chlorophyll *a* values increased in all samples after a four-hour exposure to 2000 f.c. The maximum rate of increase was at 0800 when the chlorophyll content was at a maximum, while the lowest rate occurred at 0400, again duplicating the daily photosynthetic pattern. *In situ* rates of pigment increase were highest during the hours of low or no illumination. Low rates of increase at 2000 f.c. and high rates of *in situ* decrease occurred during the hours of intense illumination.

In situ fluctuations in the amounts of chlorophyll are in excess of what could be expected by cell division or death alone. A decline of the chlorophyll within the cell may result from photo-oxidation of the pigmented substrates when photosynthesis is inhibited, (see Rabinowitch, Vol. 1, pp. 355–571). When light conditions are optimal for photosynthesis pigment formation usually proceeds rapidly. Thus, the alternation of low and high light intensities throughout the day results in a diurnal fluctuation in the amount of chlorophyll in surface plankton algae.

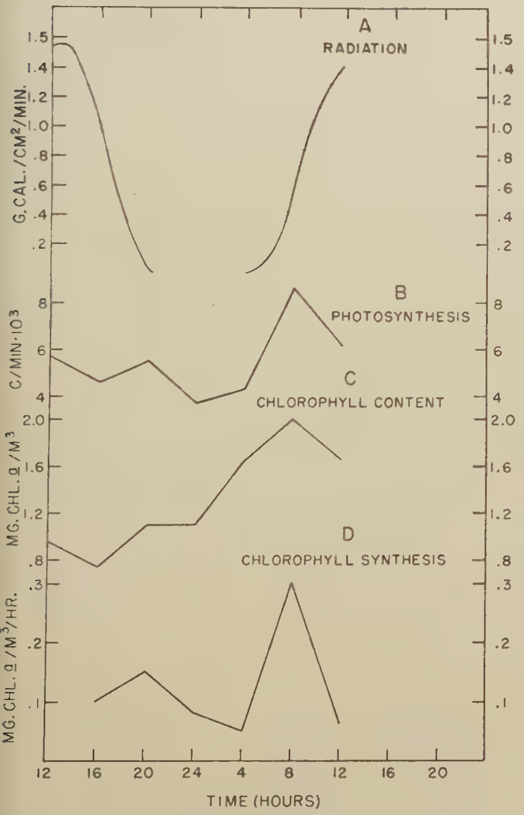

FIG. 1. (A) *In situ* solar radiation, (B) photosynthesis at 2000 foot candles as measured by 15-minute C^{14} experiments, (C) *in situ* chlorophyll *a* content, (D) chlorophyll *a* synthesis at 2000 foot candles (each point represents synthesis during previous four hours).

TABLE 1. *Rates of pigment change throughout twenty-four hours under different conditions of illumination*

Sampling time	Chlorophyll *a* change during the following four hrs in mg/m³/hr.	
	In situ	At 2000 f.c.
1200	−.21	+.10
1600	+.32	+.15
2000	+.02	+.08
2400	+.54	+.05
0400	+.35	+.30
0800	−.40	+.06

During the experiment the rate of chlorophyll synthesis under constant illumination varied considerably (Table 1). From these data it would appear as though the synthesis of the chlorophyll-protein complex was dependent upon the level of the respiratory carbon in the cell prior to the four-hour exposure to 2000 f.c. In any event, the data illustrate the difficulty encountered in comparing an instantaneous measurement of chlorophyll with a long-term measurement of photosynthesis.

These experiments illustrate the interrelationship between chlorophyll content, chlorophyll synthesis, and photosynthesis of plankton algae exposed to constant illumination. In this relationship it is difficult to distinguish between cause and effect. But it seems clear that the daily periodicity in the photosynthetic capacity of the phytoplankton, as reported by Doty and Oguri and confirmed here, may be at least partially explained on the basis of the previous history of the organisms in terms of their chlorophyll content, which in turn is light dependent and varies diurnally with the intensity of solar radiation.

REFERENCES

Creitz, G. I. and F. A. Richards. 1955. The estimation and characterization of plankton populations by pigment analysis. III. A note on the use of "Millipore" membrane filters in the estimation of plankton pigments. J. Mar. Res., **14**(3): 211–216.

Doty, M. S. and M. Oguri. 1957. Evidence for a photosynthetic daily periodicity. Limnol. & Oceanogr., **2**: 37–40.

Rabinowitch, E. I. 1945. Photosynthesis and related processes. Vol. I, Chap. **15**: 355–571. Inter-science, New York.

Richards, F. A. with T. G. Thompson. 1952. The estimation and characterization of plankton populations by pigment analysis. II. A spectrophotometric method for the estimation of plankton pigments. J. Mar. Res., **11**(2): 156–172.

Contribution No. 894

Deep-Sea Research, 1957, Vol. 4, pp. 116 to 119. Pergamon Press Ltd., London

Television-echo sounder observations of midwater sound scatterers

RICHARD H. BACKUS and HAROLD BARNES*

(*Received* 30 *January* 1957)

Abstract—Simultaneous observations with echo sounders and underwater television have been made both in and out of deep scattering layers. All the evidence indicates that, with the type of sonic gear used, micro plankton was not responsible for either the observed deep scattering layer or for detectable echo sequences on the short range equipment. It was possible to " see " for the first time the sound scatterers responsible for the typical echo sequences from single animals and to confirm the deductions of JOHNSON *et al.* (1956) that individual small fishes give rise to the sort of echo sequences that have been seen in deep scattering layers. The type of echo record and its relation to the number of fish scattering the sound was observed.

INTRODUCTION

INDIVIDUAL animals both in and out of deep scattering layers have recently been resolved by the use of short range suspended echo sounders (JOHNSON *et al.*, 1956). Furthermore, using a camera mounted alongside the echo sounder, photographs were taken when strong echo sequences were being recorded in an attempt to identify the origin of the sound scattering. In these experiments images of fishes on the photographs were always accompained by strong echo sequences ; on the other hand strong echo sequences were not invariably accompanied by images of fishes and correlations with other types of organisms could not be established. Some of these uncertainties are without doubt due to the fact that the fields of view of the camera and echo sounder may not be identical ; this problem may be largely overcome if the approximate acoustic field is viewed directly and continuously. Such viewing is obtained if the camera is replaced by an underwater television unit. It has already been shown that plankton and fishes may be viewed and sometimes counted and identified by underwater television and some success has been reported in identifying the origin of traces on conventional echo sounder records (BARNES, 1955).

APPARATUS AND PROCEDURE

The television equipment has been described (BARNES, 1953). In some of the experiments a loose fitting canvas cover was fastened to the framework. A body of water at any level is therefore to some extent trapped so that movement of water past the window is reduced and the plankters are more easily recognized. The echo soundings were made with either an Edo UQN-1B (12 kc) transducer operating at the surface or a suspended echo sounder consisting of transmitting and receiving UQN-1B transducers operating at 34 kc. The Woods Hole Oceangraphic Institution precision graphic recorder (KNOTT and HERSEY, 1956) was used with both systems. The suspended echo sounder transducers were mounted on the gantry of the television camera and aimed at a point about seven feet away on the camera's optical axis.

---

*I wish to acknowledge both the receipt of a Research Fellowship from the Woods Hole Oceanographic Institution and leave of absence granted by the Council of the Scottish Marine Biological Association.

The usual brass target ball (Johnson *et al.*, 1956) was hung below the camera also on the optical axis but at a distance of about nine feet. The depth of the equipment was determined either by echo-sounding from the surface or by a wire measuring device on the supporting cable.

EXPERIMENTS USING THE SURFACE ECHO SOUNDER

A strongly developed deep scattering layer as well as a zone of weaker scattering near the surface was observed on November 8th, 1956 at 39° 46′N, 70° 53′W in water of 920 fathoms (Fig. 1). The dominant layer was between 90-190 feet with its axis (level of strongest scattering) at 140 feet. Beginning at 00·10 hr the television camera with the canvas cover and two lights near the window was lowered by stages into the layer ; so rigged the observations relate primarily to plankton. At each depth notes were made from the screen picture and a series of counts taken by the method already described (Barnes, 1955). Between 40 and 230 feet many small copepods were seen (about the size of adult *Calanus finmarchicus*) and subjective estimates indicated little change in population density with depth. A number of euphausids were present at 120 feet. It was evident from the echo sounder record that with the lights continuously in use the intensity of sound scattering was reduced in the immediate vicinity of the camera. The lowering was therefore repeated (by which time the layer extended from 115 to 200 feet, axis 170 feet) but turning the lights on at each successive depth only for sufficient time to make a count. Each set of counts (70-100) took about five minutes during which time there was no evidence of any change in population density. The results are given in Table 1.

Table 1. *Mean number of plankters per count*, 8 *November*, 1956

04·20–05·00 hr		13·50–14·40 hr	
Depth (ft)	*No.*	*Depth (ft)*	*No.*
40	1·2	40	—
75	0·96	80	1·50
115	0·79	120	1·16
150	0·58	160	1·03
190	0·58	195	0·77
230	0·59	230	0·52

The results show that of the animals counted the greatest population density was at 40 feet ; there is no evidence that they were concentrated at the level of the scattering layer (115-200 ft) seen on the echo sounder unless the lights are considered to invalidate the results (see below for discussion).

The experiment was repeated during daylight on the same day at a position within five miles of the original observations ; by this time the deep scattering layer had migrated downwards and now lay between 960 and 1,680 ft with axes at 1,140 and 1,440 ft. The pictures appeared similar to those of the earlier experiment. The counts are shown in Table 1.

It is evident from this table that the population density and its relative distribution with depth was substantially the same for these small plankters during the night when the camera was within the deep scattering layer as during the day when the latter was well below the camera. This indicates that these small organisms were not

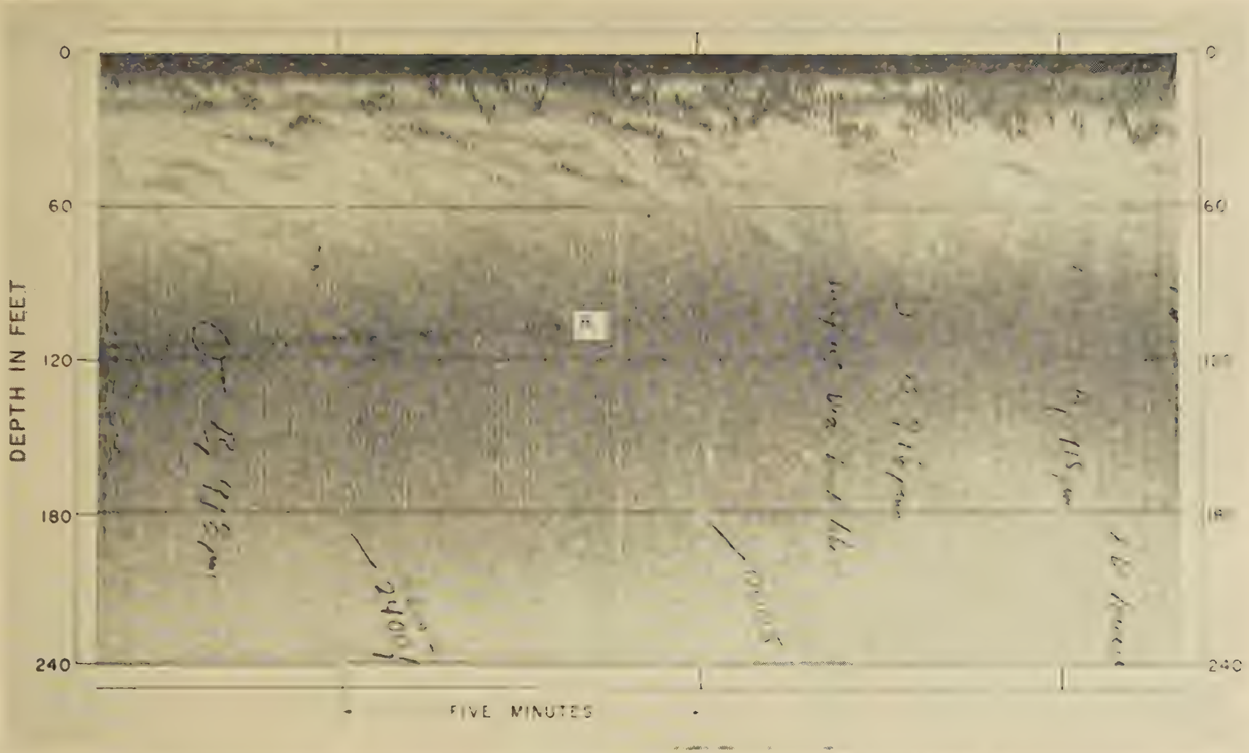

Fig. 1. Deep scattering layer near surface in 39° 46′N, 70° 53′W at about 00·05 hr. on November 8, 1956 before lowering television equipment. The bottom echo (B_1) is in a later interval and shows a depth of about 5,500 feet. A 16-foot correction (depth to transducer) should be added to indications of depth.

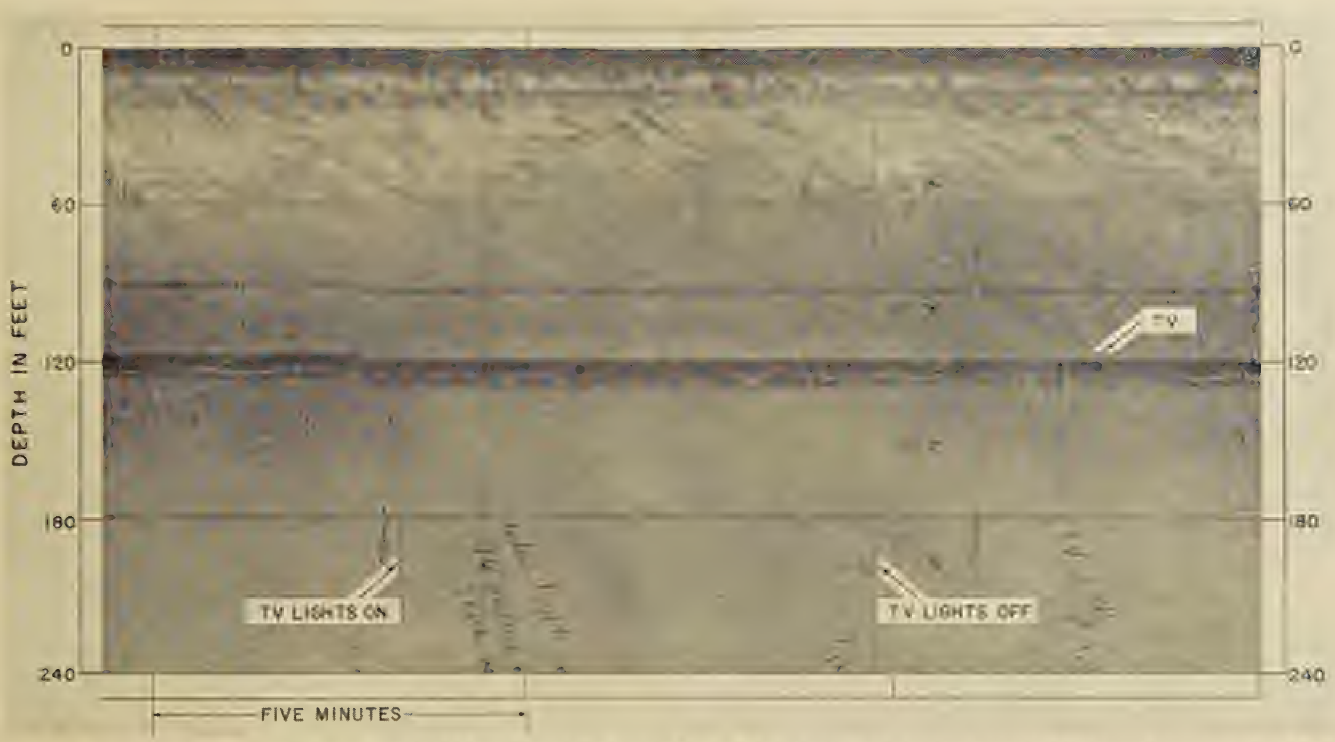

Fig. 2. Same layer as in Fig. 1 at about 01·30 hr. The disturbing effect of the television lights on many of the sound scatterers is shown. A 16-foot correction (depth to transducer) should be added to indications of depth.

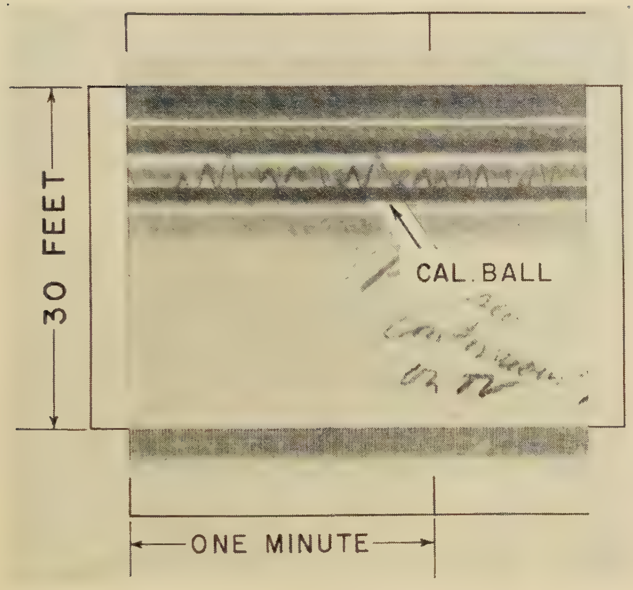

Fig. 3. Suspended echo sounder record made when a single fish was in view on television picture screen.

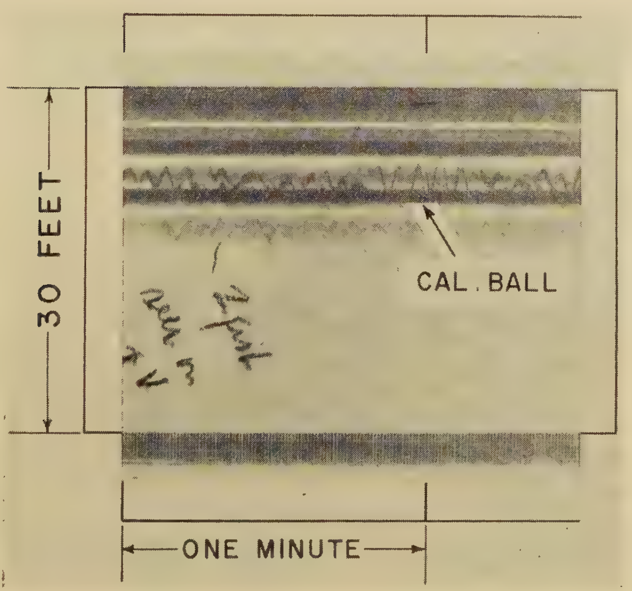

Fig. 4. As Fig. 3 but with fish in view on screen. Two echo sequences are discernible although much of one is obscured by the echo sequence from the target ball. A third echo sequence is discernible in the early part of the record at a range beyond that of the television camera.

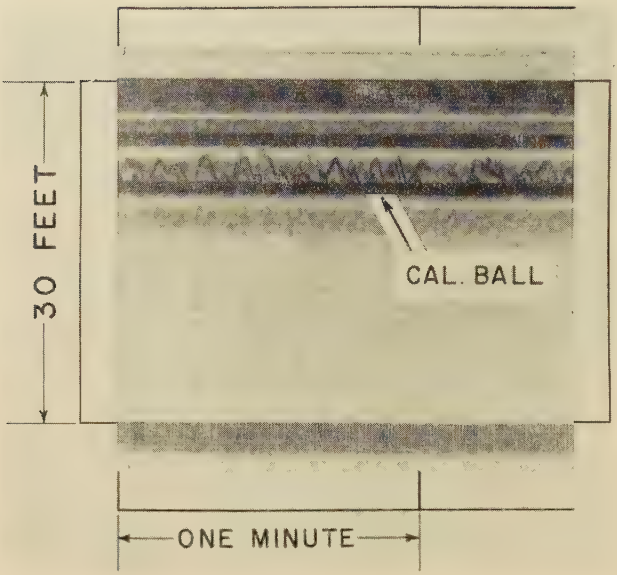

Fig. 5. As Figs. 3 and 4. 3 fish were viewed by the television and 3 echo sequences are discernible except when two or all fish are at same range.

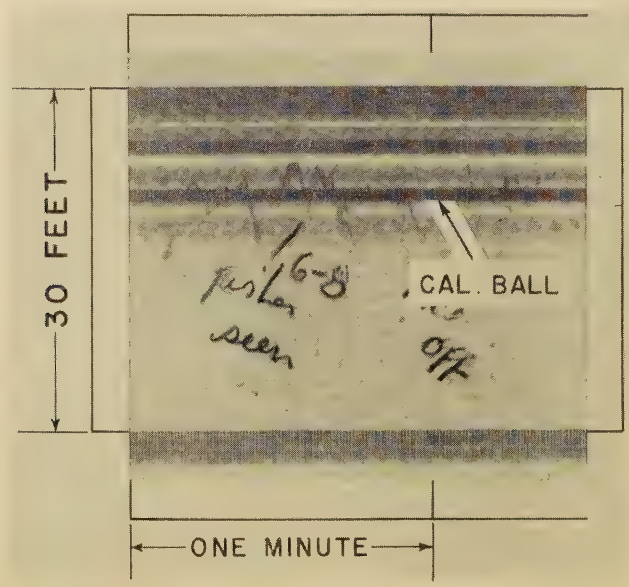

Fig. 6. As Figs. 3, 4 and 5 with 6-8 fishes present in a compact group. Individual fish are not resolved and a more complex echo sequence was produced.

responsible for the migrating deep scattering layer observed on the echo sounder.

Although it was difficult to ascertain whether or not the lights affected the near surface scatterers it was evident from the echo sounder record that, as already pointed out, the intensity of scattered sound was reduced – presumably by repulsion or dispersion of the scatterers – as the lights entered the deep scattering layer. When the camera was well within the layer, switching the lights on and off gave a rapid and marked change in the echo sounder record (Fig. 2). That the small plankters counted on the screen remained constant under such conditions indicates even more strongly that they were not responsible for the observed scattering layer. Furthermore the speed at which the sound scatterers moved away when the lights were turned on suggests that larger, strong-swimming animals were responsible. This behaviour resembles closely that of certain fishes, (RICHARDSON, 1952).

EXPERIMENTS WITH THE SUSPENDED ECHO SOUNDER

These observations were made some 25 miles to the south of those described above, at 39° 22′N, 70° 52′W on November 8th, 1956 in water of 1,350 fathoms; a less well developed scattering layer was present between surface and 250 ft with its axis at 120 ft. The surface echo sounder was used only to check the position of the suspended echo sounder-television equipment with respect to the scattering layer, the echo sounder records being taken from the suspended unit. The television camera was rigged for full forward viewing with the whole complement of lights (2 kW) and without a canvas cover. Notes from observations of the television picture screen were entered on the echo sounder record and for part of the time a remote marker switch was operated by the television viewer to locate precisely the screen observations on the echo sounder record.

The observations extended from 20·30 to 24·00 hr during which time fishes and small plankters (mainly copepods) were seen. The last were present throughout the whole period and they never gave rise to detectable echo sequences. In contrast there was a high correlation between the presence of fish in the picture and a strong echo sequence on the echo sounder record. Although the correlation was high it was not complete. Occasionally fish were seen on the screen when either no echo or very faint echoes were recorded. As indicated by subsequent experience this was probably the result of imperfect alignment between transducers and television camera. On the other hand, the fishes were not specifically identified and therefore it is possible that some had no swimbladder and consequently low target strength. In contrast, echo sequences were occasionally obtained when fish were not recorded as present on the picture. This too may have been the result of misalignment but in this case the possibility that fish or other animals may have passed unobserved on the screen must be taken into account.

Most of the individual observations were of short duration, the fish image on the screen and the accompanying echo sequence usually lasting a few seconds. Of particular significance and interest was a set of observations in which a number of fish 3in.–7in. in length), probably in this case attracted by the light, swam in and out of the field of view for about forty minutes.

The echo sounder used can resolve individual targets only when their ranges differ by more than its ping length of about 0·2 milliseconds (about 1 ft). In these experiments one, two and three fish were individually resolved (Figs. 3–5). When a compact group of 6–8 fish were present a single complex echo sequence was registered (Fig. 6) with continuous echo series whose length was greater than that of the ping. In such a case ; i.e., with several scatterers at the same or nearly the same range interference patterns (alternating maxima and minima in echo intensity resulting from phase differences) such as were seen by JOHNSON *et al.* (1956) might be expected. The absence of such interference patterns is probably to be explained by the fact that our recordings are overloaded.

The observations directly demonstrate that fishes give the type of echo sequence obtained by JOHNSON *et al.* (1956) using the short range suspended echo sounder in deep scattering layers ; small plankters at the population density present on these occasions produced no detectable echo sequences. We have no results as yet on other animals, e.g. squid, which have been proposed as the source of sound scattering in deep scattering layers.

DISCUSSION

These preliminary experiments indicate that television is useful in identifying the types and sizes of animals which produce strong echo sequences. Correlations between animal and echo sequence may be made. The establishment of such correlations is independent of any reaction of the animals to light so long as they are not completely repelled from the field of view. Observations may be made at any depth with either natural or artificial light and a picture built up of an organism-echo sequence correlation.

In spite of the reactions of the animals comprising deep scattering layers to light it is believed that further work on these lines would be valuable. The lights may be switched on only when observations are made when it is unlikely that all the scatterers will be completely repelled.

Acknowledgements—We are indebted to the officers and crew of *R/V Bear*, members of the underwater sound group at The Woods Hole Oceanographic Institution, particularly Mr. CHARLES S. INNIS, and Mr. A. G. RANDALL of The Marine Station, Millport, Scotland for their assistance. This work was done in part under contract NObsr–72521 with the Bureau of Ships, U.S. Department of the Navy.

Woods Hole Oceanographic Institution. Contribution No. 894 *from the Woods Hole Oceanographic Institution*

REFERENCES

BARNES H. (1953) Underwater television and research in marine biology, bottom topography and geology. Pt. 1, A description of the equipment and its use on board. *Dtsch. Hydro. Zeit.* **6**, 123-133.

BARNES H. (1955) Underwater television and research in marine biology, bottom topography and geology. Pt. 2, Experience with the equipment. *Dtsch. Hydro. Zeit.* **8**, 213-236.

JOHNSON H. R., BACKUS R. H., HERSEY J. B., and OWEN D. M. (1956) Suspended echo-sounder and camera studies of midwater sound scatterers. *Deep-Sea Res.* **3**, 266-272.

KNOTT S. T. and HERSEY J. B. (1956) Interpretation of high-resolution echo-sounding techniques and their use in bathymetry, marine geophysics and biology. *Deep-Sea Res.* **4**, 36-44.

RICHARDSON I. D. (1952) Some reactions of pelagic fish to light as recorded by echo-sounding. *Min. Agric.* and *Fish. Fish. Invest. Ser.* **2**, 18 (1), 1-20.

Printed in Great Britain by The Salisbury Press Ltd., Publicity House Wilton Road, Salisbury, Wilts. (3203)

Contribution No. 895

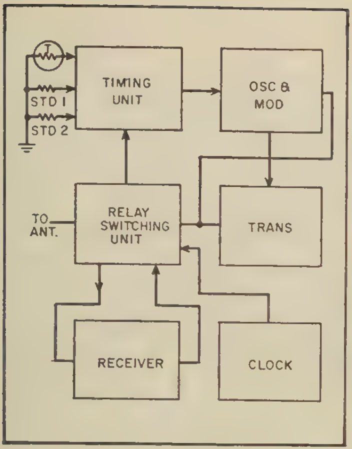

FIG. 1—All sections of telemetering buoy are controlled by relay switching unit

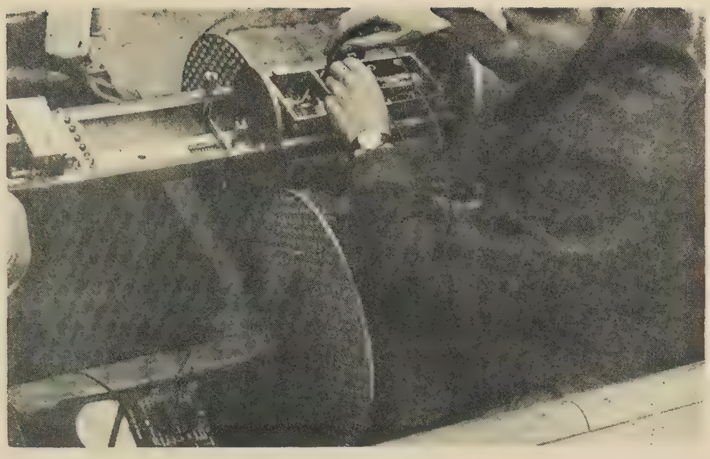

Transistor receiver is given final check before buoy is sealed for launching. Receiver is used to turn on transmitter when propagation conditions are favorable

Buoy Telemeters Ocean Temperature Data

SUMMARY —— Temperature measuring telemetering system in buoy is triggered by audio modulated r-f signal received by transistor receiver. Cycle of transmission includes two standard tones and thermistor temperature data together with identifying code signal. Data can be obtained at distances up to 600 miles by triggering at favorable propagation times

By ROBERT G. WALDEN, DAVID D. KETCHUM and DAVID N. FRANTZ, JR.
Woods Hole Oceanographic Institution
Woods Hole, Massachusetts

Contribution No. 895

INCREASING cost of operating oceanographic vessels emphasizes the need for a method of making semicontinuous measurements at many different locations independently of the ship. Telemetering anchored buoys can provide measurement of surface or deep temperatures, or when allowed to drift can provide ocean current and circulation data.

The buoy shown in the photographs can be triggered remotely by a radio signal modulated with a distinctive tone or may be triggered by an internal clock at regular intervals. A signal from the buoy, modulated by a thermistor-controlled R-C oscillator, transmits water temperature data in terms of the modulation frequency.

The buoy has been reliably triggered and read at ranges up to 300 miles at frequencies between 2 and 3 mc. This range has been increased to as much as 600 miles by triggering at times of optimum propagation.

Operation

In operation, a number of buoys are anchored at locations determined by the physical problem to be investigated. The buoys transmit and receive on the same frequency, but each buoy responds to an interrogating signal only if the signal is modulated with a tone of particular frequency.

Vibrating-reed relays are used in the output of the buoy receivers to obtain a narrow audio-frequency response that almost entirely eliminates accidental transmissions caused by noise and interference. The interrogating transmitter is modulated by tones derived from a resonant reed-controlled oscillator with a separate resonant reed for each tone.

The reception of the proper tone by the buoy receiver actuates a time-delay relay which allows quick-heating transmitter filaments five seconds warmup time. The transmitter is then keyed with the call sign followed by three consecu-

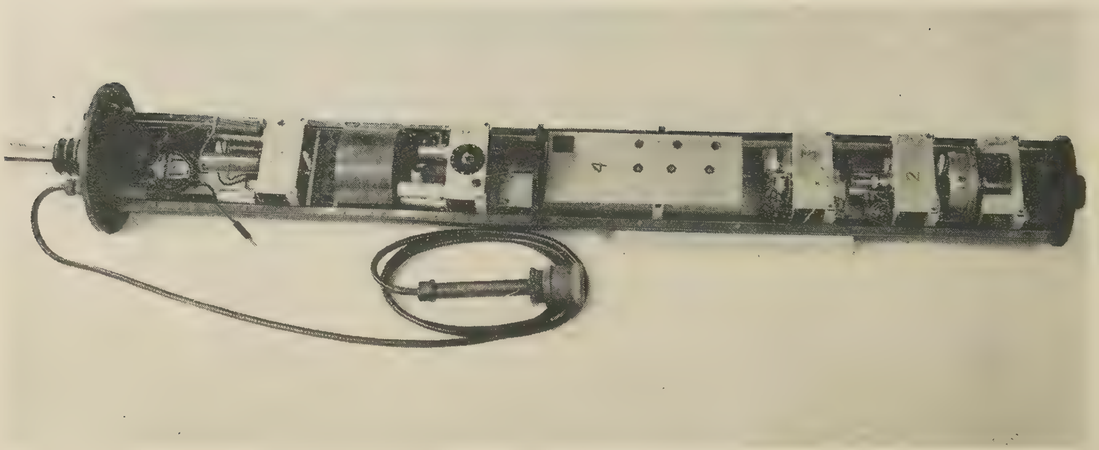

Electronic components for buoy removed from housing. Six chassis from left to right are transmitter, modulator, receiver, timing unit, relay switching unit and clock. All units are powered by battery pack

tive tones. The frequencies of the three tones are controlled by: a standard resistor representing a point at the low end of the temperature — audio-frequency curve, a standard resistor representing a point at the high end of this curve and the thermistor, which measures the water temperature.

The total transmission lasts 15 seconds. At two transmissions per day the estimated battery life is about two months. This f-m/a-m signal is received on a standard communications receiver and recorded on magnetic tape. The tone frequencies are then measured with an eput meter. In the event of garbled reception the buoy may be triggered again at a more favorable time.

The electronic equipment is contained in six aluminum chassis which plug into a cylindrical aluminum and bakelite rack. A two-inch aluminum channel, which forms the backbone of the rack, carries the receptacles and interconnecting wiring. The entire rack fits snugly into the tubing that forms the buoy. A glass fiber center-loaded marine antenna, supported by the end cap, effectively withstands the salt atmosphere and the force of moderate seas that occasionally break over the buoy. The cylindrical battery stack consists of 18 45-volt B batteries and 17 No. 6 1.5-volt cells.

Timing

Figure 1 shows a block diagram of the electronic circuits. The electrically wound clock and a transistor receiver operate continuously with relatively low battery drain. The clock may be set to operate a switch once or twice daily at any desired time. The clock switch actuates a sequential circuit in the relay switching unit that applies filament power to the modulator and transmitter, allows about five seconds warm-up time and then operates the antenna relay and timing unit. The timing unit then keys the modulator to transmit call signal and temperature data.

At the end of the thermistor tone, power is removed from the transmitter and modulator, the antenna is switched back to the receiver, and the device is ready for another cycle. The same sequence of events may also be initiated through the receiver by reception of the proper signal from a remote ship or shore station.

Since the receiver must run continuously during the life of the buoy, the most important design consideration is low battery drain. The receiver, shown in Fig. 2, employs nine transistors in a conventional superheterodyne circuit. To achieve the high sensitivity required for long-range operation, a stage of r-f preselection and two i-f amplifiers are included.

All stages through the second detector are surface-barrier transistors, chosen for their high-frequency response and low power consumption. The local oscillator is crystal controlled. Stable operation of the r-f and i-f stages is effected by not bypassing a portion of the emitter resistor in each stage.

The push-pull, class-B output stage drives a resonant-reed relay. No forward emitter bias is used in this amplifier, since distortion of the output signal does not materially affect operation of the relay. Power consumption of the output stage is thus negligible in the absence of an input signal. The resonant-reed relay contacts are in series with a sensitive d-c relay shunted by a capacitor.

The discharge time constant of

Complete assembly consists of (l to r) battery pack, electronic unit and buoy case

the combination is long enough to hold the contacts closed during the intervals when the vibrating contacts of the relay are open. An input signal with a duration of about one second is sufficient to set the relay switching unit in operation.

Receiver sensitivity is defined as the minimum value of r-f voltage appearing across the antenna terminals required to hold the d-c relay contacts closed. An r-f generator, 100-percent modulated with the appropriate audio-frequency signal, provides the test voltage. The measured generator impedance and the calculated receiver input impedance are used to arrive at the sensitivity figure. A typical value is 2 to 5 microvolts.

Overall bandwidth of the r-f and i-f sections was found to be about five kilocycles between half-power points. The actual bandwidth of the receiver, however, is determined by the resonant-reed relay, whose bandwidth increases somewhat with the amplitude of the driving current.

Relay Response

The usable response of the relay is at most only a few cycles wide. The result is an excellent overall s/n ratio and almost complete elimination of response to unwanted signals.

Total receiver power consumption with no signal present is 40 milliwatts. With full audio output the batteries must supply about 150 milliwatts.

Because an efficient avc system is not easy to achieve in a transistor receiver, this feature, for simplicity, was omitted. This defect, particularly in the high-gain circuit described, results in overloading with a moderately strong input signal. If the signal is not 100-percent modulated, the entire modulation envelope may be clipped off in the i-f stages, causing loss of audio output. This disadvantage is easily overcome by reducing the power of the interrogating transmitter when the buoy is nearby.

The operation of the relay switching unit shown in Fig. 3 is as follows: When the switch S_1 is operated capacitor C_1 discharges through the coil of the high-resistance relay RE_1, closing the contacts and holding them long enough to actuate RE_3. Relay RE_3 turns on the transmitter and modulator filaments and locks up RE_1 through RE_4. At this time capacitors C_1 and C_2 charge to the voltage across the coil of RE_1.

After five seconds, the time-delay relay RE_2 operates starting the timing motor, which closes S_2 and operates RE_4 and RE_5. As the contacts of RE_4 break, RE_1 holds due to the charge on C_1 and C_2, holding in RE_2 and RE_3. Then RE_4 and RE_5 close, holding in RE_2 and RE_3, switching the antenna, and energizing the voltage-regulator tube for the multivibrator power supply. After one revolution of the timing motor S_2 opens, and the circuit returns to its original state. Closure of the receiver relay contacts initiates the same train of events, except that RE_3 operates first, causing RE_1 to close and lock.

Timing Unit

The 4-rpm timing motor is directly coupled to a commutator. A code wheel is also coupled to the motor through a 1-to-3 gear train. The teeth on the code wheel correspond to the buoy's call sign in International Morse code and oper-

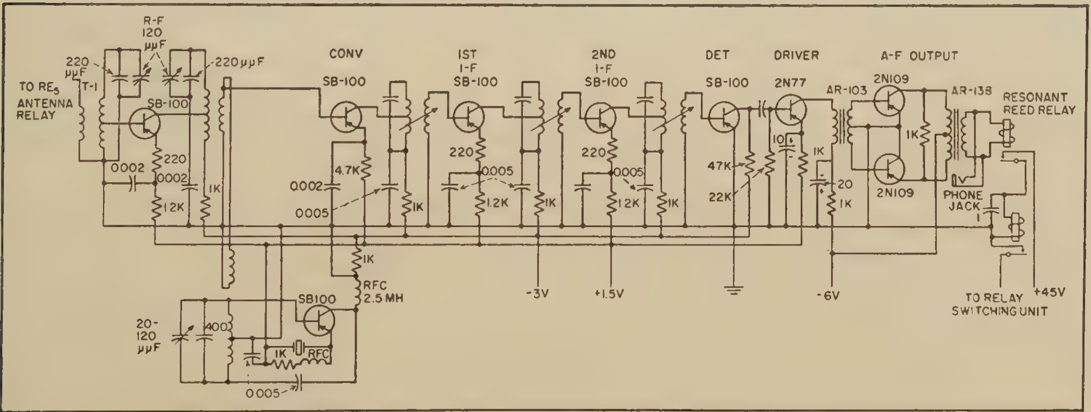

FIG. 2—Transistor superheterodyne receiver turns on transmitter when interrogated with signal modulated with proper audio tone

ate a keying switch.

The commutator is shown as it would appear at the start of a cycle. For the first 120 degrees of rotation RE_6 is energized through the keying switch contacts, thus keying the multivibrator by completing its grid return circuits through the precision 50,000-ohm resistors. During 120 degrees of commutator rotation the code wheel makes one revolution.

At the end of the first 120 degrees the commutator operates RE_7, which inserts the 150,000-ohm precision resistors in the multivibrator grid circuits to generate the first standard tone. After 60 degrees of travel RE_6 is again operated. The 50,000-ohm resistors are now in the multivibrator grid circuits, resulting in the generation of the second standard tone.

This tone continues for another 60 degrees of rotation, followed by the operation of RE_8, which substitutes the thermistor for the multivibrator grid resistors. The frequency of this final tone is a function of water temperature. At the end of one revolution a cam on the commutator opens S_2, the relays in the relay switching unit drop out and the timing motor stops.

Modulator Unit

The modulator unit consists of a multivibrator, driver and push-pull modulator, all of conventional design. The frequency of oscillation of the multivibrator is controlled by the grid resistors.

Precision, low temperature coefficient resistors are used to establish the two standard tones, whose frequencies correspond to the upper and lower extremes of the thermistor range. Thus a means is provided to detect frequency drift caused by decay of the battery supply voltages. Both plate voltage and filament current of the multivibrator are regulated to insure maximum frequency stability with supply voltage variation.

A plot of frequency against thermistor temperature is made while the batteries are fresh, and the frequencies of the two standard tones are noted at the same time. When the buoy is in operation, a rough correction may be applied to this curve by noting the deviation of the standard tones from their original values. A typical plot is shown in Fig. 4.

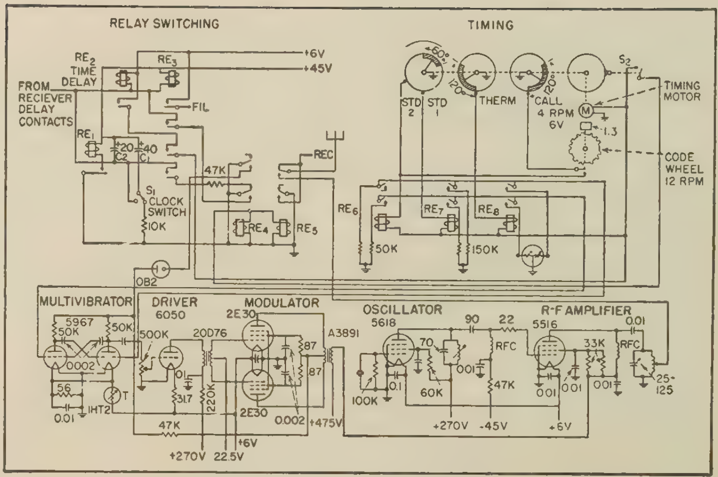

FIG. 3—Relay switching unit and timing motor control operation of telemetering transmitter to broadcast standard tones, temperature tone and identifying code signal

Transmitter Unit

A crystal oscillator designed to operate in the 2-to-3 megacycle range drives a single-ended plate-modulated power amplifier in the transmitter unit. Fast-heating filament-type tubes are used to minimize warm-up time and consequent battery drain. Input power to the final is approximately 30 watts.

The accuracy of temperature measurement is almost wholly dependent upon the frequency stability of the multivibrator. Although a resolution of 0.1 C is obtainable, the maximum error is ±0.2 C. This error was determined by comparisons with measurements taken with a precision thermometer.

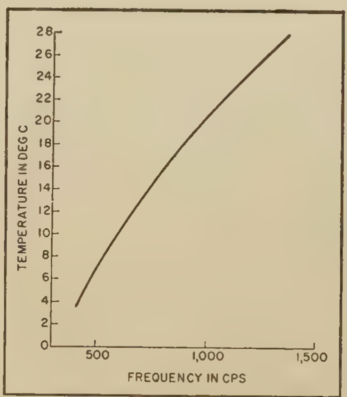

FIG. 4—Typical plot of temperature against frequency of multivibrator

The frequency of the multivibrator is sensitive to changes in both plate voltage and filament current. Regulation of these quantities and the use of precision resistors to generate standard tones reduces the error to the amount stated. Unfortunately, the simple regulators do not completely eliminate the effects of battery decay. More development is needed to produce a frequency-stable oscillator requiring minimum power.

Although a system has been described which was designed specifically for the remote measurement of ocean temperature, it is obvious that the device is easily adaptable to the measurement of other quantities by the substitution of different transducers for the thermistor. Modulation schemes other than the resistance-controlled oscillator could also be profitably investigated. Within the limitations of battery life it appears feasible that a number of quantities could be measured with the data transmitted in sequence.

The authors acknowledge the assistance of Elmer Barstow, Edward Chute and Paul Dingwell, who constructed and tested much of the original equipment. The development work was supported by the Office of Naval Research. Contribution No. 895 from the Woods Hole Oceanographic Institution.

Contribution No. 897

Reprint OIKOS 8:I 1957

THE NORTHERN LIMITS OF *BALANUS BALANOIDES* (L).

BY

H. BARNES

(The Marine Station, Millport and The Woods Hole Oceanographic Institution[1])

GURJANOVA, SACHS and USCHAKOV (1925), as a result of their work in northern Russian Seas, consider that the arctic littoral zone may be divided into three provinces: these are, high arctic, with an abiotic littoral zone, arctic with only traces of a littoral fauna and flora and sub-arctic, relatively rich in species. The validity, or at least the usefulness, of such a division has been questioned by MADSEN (1936) who prefers in the present state of knowledge to distinguish only between arctic and sub-arctic (boreo-arctic) provinces. He draws the northern boundary of the sub-arctic where littoral molluscs, in particular *Littorina saxatilis* var. *groenlandica* (most important when the limit is not very distinct) and *Mytilus edulis* together with the cirripede *Balanus balanoides* disappear; these animals do not occur in his arctic province. (We are not here concerned with the southern limits of the sub-arctic). Because the arctic, as so-defined, extends south on the east coast of Greenland to the Angmagssalik district (65°36′N) where the climate is milder than at say Upernavik (72°47′N) on the west coast, he considers that the disappearance of *Balanus balanoides* and littoral molluscs is not due to any special littoral factors associated with the arctic province and this leads him to infer that the cause must be sought in the sub-littoral; in support of this thesis he points to the fact that a similar limit to the arctic sub-littoral has been suggested by THORSON (1934) to lie between Angmagssalik and Kangerdlugssuak.

The Northern Limits of *Balanus balanoides*

The distribution of this barnacle in polar regions has been discussed by BROCH (1924, 1933), MADSEN (1936) and more recently by FEYLING-HANSSEN

---

[1] Contribution No. 897 from the Woods Hole Oceanographic Institution. The author wishes to acknowledge the receipt of a Research Fellowship from the Institution and leave of absence granted by the Council of the Scottish Marine Biological Association.

(1953a). We may briefly recapitulate the facts taking note of a number of references not quoted by the above authors. The distribution in Greenland is fairly wellknown. On the west coast it extends as far north as Prøven (72°25′N) and a single specimen has been recorded from Upernavik (72°47′N) by Vibe, (1939); an earlier reference to its more frequent occurrence at Upernavik (Madsen, 1936) appears to be erroneous or at least doubtful (Vibe, 1939; Madsen, 1940). Feyling-Hanssen (1953a) and Madsen (1940) have searched the littoral northwards from 72°N as far as Amdrup Ø (74°43′N) without finding it; northwards from here to Thule (76°23′N) the coast is very inaccessible owing to the enormous glaciers and the almost constant fog (see p. 8). The record (Stimpson, 1864) for Port Foulke, north of Thule, quoted by Steven (1938) following Stephensen (1936), is probably invalid. The barnacle is common in the littoral south of Prøven (see for example Steven, 1938). It was found by the Godthaab Expedition on the rocky shores of Egedesminde (65°40′N) but not further north. On the east coast of Greenland the cirripede only extends as far north as Angmagssalik (65°36′N) where it is fairly common in the tidal zone, dominating the epi-fauna on both rocks and stones (Bertelsen, 1937). It is absent north of this point (Madsen, 1936; Bertelsen, 1937). On the basis of this evidence we set the north limits in Greenland as approximating to 72°N on the west coast and on the eastern coast at 66°N.

On the Arctic coast of Canada it is recorded from Cumberland Sound and Arctic Island (Pilsbry, 1916) and extends southwards along the Labrador Coast (Pilsbry, 1916: Tanner, 1944; Bousfield, 1955). Further records are given by Bousfield (loc. cit., see also Dunbar, 1951) for Ungava Bay, Hudson Strait, Frobisher Bay and Cumberland Sound as well as Nottingham Island in the north eastern Hudson Bay region. Dr. D. V. Ellis has confirmed in correspondence that both *B. balanoides* and *Littorina saxatilis* have their northern limit on Baffin Island at Cumberland Sound and that both here and at Frobisher Bay the shores are free of ice longer than in the more northerly regions. Clearly it only extends as far north in the Canadian Arctic as on the east coast of Greenland — Cumberland Sound and Angmagssalik are on the same latitude. It is not recorded from the remainder of the Canadian Arctic coast nor from the northern coast of Alaska.

According to Shelford (1930) *B. balanoides* thrives on the eastern side of the Bering Strait. It is present at Unalaska and Sitka (57°N) (Henry, 1942). It would appear, therefore, that there is a discontinuous distribution around the Alaskan Peninsula and the southern coast of Alaska; further exploration might well reveal that this in fact is due to a lack of observations in the area. Indeed Mr. C. S. Yentsch has informed me that he has collected it in South West Bay, Kodiak Island and at Sandy Point and Cardova on the mainland.

It has not been recorded on the Arctic coast of Siberia between the Bering

Straits and the Kara Sea. It has been found in the Kara Sea (BAINO-RODZEVICH, 1923) and by GURJANOVA (1932). STRELNIKOV (1929) and TARASOV (1937) have found it in the Varnek Bay region on the southern side of Vaigatsh Island. HOEK (1882) reports it from the Matotchkin Strait, Novaya Zemlya, but the species thus reported is considered by BROCK (1924) to have been *B. crenatus:* however, this criticism may not be entirely valid (see FEYLING-HANSSEN, 1953a, for a discussion). Westwards from Novaya Zemlya it has been reported from Cheshskaya Bay on the eastern side of the Kanin Peninsula by GURJANOVA (1929) and by BROTSKY and ZENKEWITSH (1932); however, BROCH (1936) re-examined material from this region and came to the conclusion that the above records were incorrect and refer to *B. crenatus*. *B. balanoides* is recorded from the White Sea (WELTNER, 1898, 1900; STEPHENSEN, 1913; DERJUGIN, 1928) and the Murman Coast (STEPHENSEN, 1936; DERJUGIN, 1928) and the northern coast of Norway (BROCH, 1924). GURJANOVA, SACHS and USCHAKOV (1925, 1928, 1930) in their discussion of the Arctic littoral give the White Sea area a special sub-province, more severe than their Arctic because of its heavy ice-cover but not truly high Arctic. The barnacle is wellknown from the coasts of Iceland. The most northerly records of *B. balanoides* are those of FEYLING-HANSSEN (1953a) who found it on the west and north coasts of West Spitzbergen and in the fjords of that region, as far north as 80°4′N latitude.

The Factors Affecting the Limits of Distribution

Although the animal does sometimes occur in the sub-littoral (see particularly BOUSFIELD, 1952–53) and can certainly grow and reproduce in the boreal region when kept constantly submerged as, for example, on experimental panels (BARNES and POWELL, 1953; BARNES, 1952–53, 1955) in nature it is essentially intertidal. We have seen that Madsen considers that the relative distribution on the east and west Greenland coasts together with a comparison of the climates of the two regions indicate that the northern limit is set, not by the conditions within the littoral zone, but by factors that also affect the sub-littoral. However, climate is not the only factor that must be taken into account. The littoral conditions that limit the northern extension of *B. balanoides* may be effective through the adult especially with respect to its growth and breeding, through the planktonic larval phases or through the settling stage of the cyprid and growth of the young spat; both air and sea conditions must be taken into account. Any hypothesis that we erect to explain the limits must also be capable of explaining similar limits for the littoral molluscs although it must be stressed that the mechanism of this limitation need not be the same as for *B. balanoides;* the biology of the individual species must be taken into account.

The Ice Limits of the Arctic Seas

Conditions within the Arctic and northern Seas are greatly influenced by the effects of snow and ice cover. It is of interest therefore to examine these limits; the mean annual September limits of the ice (the maximal northerly retreat) are shown in Fig. 1, plotted from the charts of the U. S. Navy Hydrographic Office (1946). It is strikingly evident that these southern limits cut the shores (with one exception, see p. 8) at the northern limits of *B. balanoides*. Feyling-Hanssen's results would have been expected and further work should reveal the presence of the barnacle (in the absence of any exceptional local conditions) on the western coast of Novaya Zemlya. The ice-limits quoted refer of course to pack ice and while it is not inferred that this *per se* sets the northern limit of *B. balanoides*, it is suggested that a consideration of the conditions which these limits indicate should help in an interpretation of the factors determining the distribution of the barnacle. In particular the ice-limits, which are related to the warm and cold current conditions, indicate the severity of the conditions; these can be expected to be more rigorous along the shores from which the pack ice does not recede (see p. 8).

The Problem of the Ice-Foot

The ice-foot is that part of the ice cover of the Arctic Seas that is frozen to the shore during the winter months. An intertidal animal must be capable during the winter either of withstanding burying under the ice-foot or of retreating to the sub-littoral. Since *B. balanoides* is not mobile, unless the upper part of the intertidal is re-populated each year it must exist under the ice cover. The important variables that must be considered with respect to the ice-foot are the time of its formation and disappearance, the total duration and possibly the thickness.

For an ice-foot to be formed, in addition to low temperatures a considerable tidal rise and fall is necessary. Although there are many scattered references to the ice-foot in accounts of Polar exploration (BENTHAM, 1937; JOYCE, 1950; FEYLING-HANSSEN, 1953b) it has been the subject of little systematic work; most frequently zoological expeditions are only present when the shore is ice-free. Although it may not extend to the low tide level, particularly in regions where there are no heavy seas and where therefore the ice does not get broken up, there seems little doubt that in contradistinction to the suggestion of STEVEN (1938) *B. balanoides* does not in general re-populate the upper intertidal from a low level ice-free population each spring. Both Madsen and Feyling-Hanssen have found several year classes in the upper littoral zone. We must assume that in the Arctic, the barnacle can withstand winter freezing in the ice-foot. The duration of the ice-foot varies from season to season; in Spitzbergen it does not generally form until the early part of December and breaks down again about May. Similar conditions probably pertain for the southwest Greenland coasts. It is also quite evident from BOUSFIELD's account (1952–53) of conditions in the Miramichi Estuary that the barnacle can withstand ice-cover from December until mid-April. Dr. M. J. DUNBAR has confirmed that adult animals can withstand complete enclosure in ice in Ungava Bay and Frobisher Bay where he has observed quite large living animals just recently released from the ice-foot in Spring.

The scouring action of moving ice is frequently the cause of the destruction of intertidal animals even though they can live beneath ice, (AURIVILLUIS, 1895). BOUSFIELD (loc. cit) records the destruction of barnacle populations in this way, and Feyling-Hanssen has pointed out that on Spitzbergen the cirripede is often limited to cracks and fissures in the rocks. STEPHENSON (1954) refers to similar phenomena in Nova Scotia. It is probable therefore that an ice-foot may act beneficially in protecting intertidal animals that can withstand its cover from the heavy abrasion caused by moving ice. Indeed this scouring action may be particularly important along the Alaskan and Russian sectors of the Arctic coast where great masses of ice from the polar basin are driven landwards by the wind.

We may here consider the effect of low air temperatures. The contrast between the distribution of the animal on the east and west coasts of Greenland, at places where the air conditions are similar, indicates, as indeed was stressed by Madsen, that these do not determine the northern limits on the east coast. KANWISHER (1955) has recently considered the problems associated with freezing in intertidal animals and it is of interest to note that *B. balanoides*, *Mytilus edulis* and *Littorina* sp. can withstand temperatures at which he finds some 60% of their body-water is frozen. He also points out that these animals, which in summer are subject to moderately high temperatures, can withstand extremely low temperatures better than sub-littoral animals which live at -1.7°C throughout the year. I have recently observed *B. balanoides* in the Buzzards Bay region frozen into ice and burried under snow for weeks and have hatched nauplii from such animals and from held adults maintained dry for days at a temperature of –10°C.

While continuing low air temperatures and an ice-foot of long duration would clearly inhibit the survival of *B. balanoides*, (or any other intertidal animal) as presumably happens in the high Arctic province of the Russian workers, it is evident that neither of these two factors can account for the known distribution of *B. balanoides* in the arctic and northern seas. The effect of these two being eliminated as decisive, we must consider other variables.

The Distribution and Severity of Conditions

In spite of the above suggestion that, since adult barnacles can withstand winter freezing beneath the ice-foot the latter *per se* does not determine the northern limits, it is nervetheless proposed that the conditions in the littoral, as distinct from factors in the water, are responsible for the observed northern distribution. Further, it is suggested that the limiting factors are indicated by the summer boundary of the pack-ice. It is considered that although this affects the time available for feeding and therefore development of sexual products of the adult (the embryos over-winter in the mantle cavity) the important factor is the time available for the development of the planktonic larvae, the settlement of the cyprid and the growth of the young spat. All this must be completed to a stage at which the young adults are capable of withstanding the onset of winter conditions. This period is determined by time between the melting of the ice, when the diatom outburst takes place and when the ripe embryos are hatched as Stage I nauplii (BARNES, in press) and the reformation of winter ice.

There is some information of the period of planktonic existence. In Scottish waters with a Spring temperature between 6–7°C PYEFINCH (1948) estimates a total planktonic life of about three weeks. At Halifax Harbour, with a temperature below 3°C BOUSFIELD (1952–53) estimates that 5–6 weeks are spent in the planktonic phase. The quantity of food available may, however, be more important than the temperature on the rate of planktonic development (BARNES, unpublished results) in which case development even at the low Arctic temperatures may be rapid as a result of the dense diatom population. The rate of growth varies greatly with conditions (BARNES and POWELL, 1953; BARNES, 1955). In Spitzbergen a size of about 2.5 mm. is reached in one month's growth.

It would seem that conditions on Spitzbergen are as severe as will allow the continued existence of *B. balanoides;* a diatom outburst in June–July, with a barnacle spat-fall in July–August, followed by growth up to 2–3mm. basal diameter ensures that the animals are able to over-winter. Even so the spat-fall may fail completely in some years, if the available period is shortened. For example, FEYLING-HANSSEN (loc. cit) found that in 1952 there were no first year specimens at Kapp Liné, which since maturity is only obtained in the second year in these regions, he considers as indicating the failure of the 1951 spat-fall. In the most northern parts of Spitzbergen (Birgerbukta, 79°48′N) nauplii had not been shed by August 23rd and he believed that there would be no spat-fall in this district for that year: an unfavourable Spring followed by a cold autumn with an early formation of the ice-foot will then often lead to the absence of a successful spat-fall.

Now the length of time of this ice-free period is a function of the position of the summer ice-limits shown in Fig. 1. Conditions will therefore be limiting

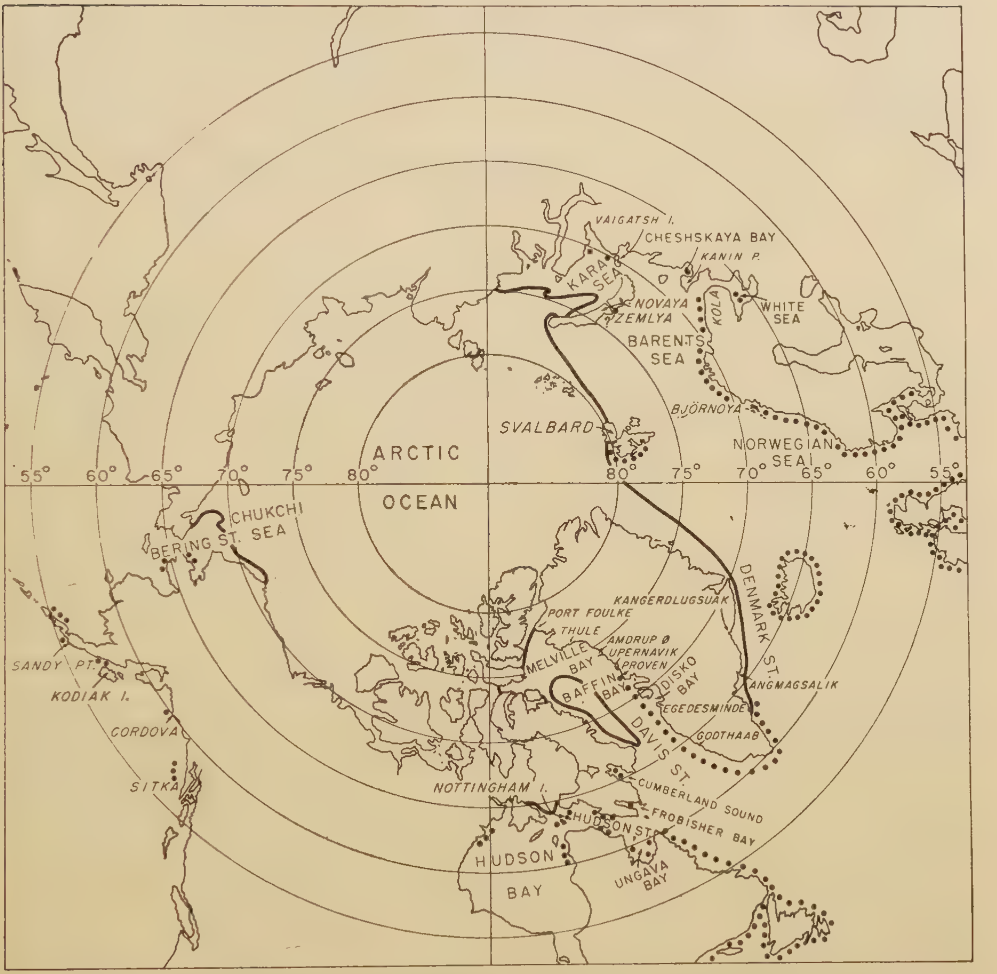
VAIGATSH I.
CHESHSKAYA BAY
KANIN P.
KARA SEA
NOVAYA ZEMLYA
KOLA
WHITE SEA
BARENTS SEA
BJÖRNOYA
SVALBARD
NORWEGIAN SEA
ARCTIC
OCEAN
55°
60°
65°
70°
75°
80°
80°
75°
70°
65°
60°
55°
CHUKCHI SEA
BERING ST.
KANGERDLUGSUAK
PORT FOULKE
THULE
AMDRUP Ø
UPERNAVIK
PROVEN
MELVILLE BAY
BAFFIN BAY
DISKO BAY
DENMARK ST.
ANGMAGSALIK
EGEDESMINDE
GODTHAAB
DAVIS ST.
CUMBERLAND SOUND
FROBISHER BAY
HUDSON ST.
NOTTINGHAM I.
HUDSON BAY
UNGAVA BAY
SANDY PT.
KODIAK I.
CORDOVA
SITKA

Fig. 1. The mean annual ice limits for September (representing average position of the pack ice at maximal retreat, U. S. Navy Hydrographic Office, 1946) and the northern limits of *Balanus balanoides*.

at points which 'correspond' to Spitzbergen on this map. South of the points where this line cuts the coasts, *B. balanoides* should, and indeed does (with one exception, see below) maintain itself.

It may be pointed out that on the basis of the above discussion it is not necessary to consider *B. balanoides* a 'less arctic' species than *B. crenatus* (Brock, 1924); a comparison between an intertidal and a sub-littoral animal is difficult to make with respect to their behaviour in arctic regions and all the evidence indicates that physiologically *B. balanoides* is just as 'arctic' as *B. crenatus*; the former has to withstand the arctic littoral conditions which set its northern limits at a lower latitude than *B. crenatus* which is only subject to the relatively milder conditions of the sub-littoral arctic conditions (see also p. 5); mobile species often retreat to the sub-littoral from the littoral zone during the arctic winter.

Conditions on the West Coast of Greenland

The one exception to the above hypothesis that the northern limits are indicated by summer limits of the pack-ice, is in the Baffin Bay region, the west coast of Greenland and the eastern shores of Baffin Island. The mean ice limit for the summer is at 78°N on the former coast and 75°N on the latter, whereas we have seen that *B. balanoides* does not extend beyond 73°N on east side of Baffin Bay and is not recorded on the west side. Relatively little shore collecting has been done on Baffin Island, (see p. 2) but the northern Limit on the west coast of Greenland can be placed with some certainty at about 73°N. It is suggested that local conditions are the limiting factor in this region.

Between Upernavik and the southern side of Melville Bugt there is a profusion of small islands, and further exploration may reveal *B. balanoides*. Along the whole stretch of the coast, however, glaciers discharge into fjords and nearly one-fifth of the ice front reaches the sea. (Sailing Directions, U. S. Hydrographic Office, 1947). Further north, the coast of Melville Bugt is almost entirely covered by enormous glaciers which front on to the sea, and in addition the north-setting current carries a great deal of shore ice into the bay. As VIBE (1939) has pointed out the bay is true arctic in character; it is ice covered during most of the year, the cover only breaking up in July and re-forming during August. The conditions are here locally equivalent to those north of the summer ice limits. The coastal conditions and topography north of Upernavik are therefore very inimical to the existence of an intertidal animal and it is considered that these prevent the northern extension of *B. balanoides* up the west Greenland coast. Relatively small unfavourable stretches of coast may often severely limit the spread of intertidal species and even small sea barriers may be difficult to pass as has been pointed out by CRISP (1953) in reference to the intertidal fauna of southwest Britain and Ireland. Unfavourable current systems and a long stretch of sandy coast may also have delayed the spread of *Elminius modestus* into the Clyde Estuary, since although this immigrant is common in the Irish Sea as far north as the Cumberland coast only a solitary specimen has so far been found in the Clyde Estuary (CONNELL, 1955). It should be pointed out that since *B. balanoides* is a strictly cross-fertilizing hermaphrodite, a relatively high population density with numbers of contiguous animals is necessary for its maintenance and spread.

That the barrier of Melville Bugt is particularly effective with respect to the intertidal fauna is indicated by VIBE's work (loc. cit) which indicates a similar sub-littoral *Macoma calcaria* community on the north and the south sides of the bay. Further, the sub-littoral *Buccinum finmarchianum* whose distribution in the arctic closely follows that of *B. balanoides* extends to the Thule District (THORSON, 1944). It may be noted that recently VIBE (1950) has found *Mytilus edulis* on the north side of the Melville Bugt, and he thinks that the general amelioration of the Greenland climate could account for this northward spread.

The Limits of *Mytilus edulis*, L.

As we pointed out in the introduction any hypothesis which explains the distribution of the sessile *B. balanoides* must also be capable of indicating the same distribution of *Mytilus edulis* since the two together with *Littorina saxatilis* (see below) mark the northern limit of Madsen's sub-arctic. Now the mussel, whilst not moving about with great frequency is certainly mobile and could therefore like some other species seek refuge in the sub-littoral and so escape the severe winter conditions. However, Madsen states that in general wherever *Mytilus* is found in Greenland it is found in the intertidal zone even if it also occurs in the sub-littoral. The animal can certainly withstand low air temperatures; the earlier evidence (BLEGVAD, 1929) for its capacity to withstand ice cover is somewhat conflicting but recent work (e. g. KANWISHER, 1955) and personal reports indicate that survival under ice does in fact occur. Now *Mytilus* has planktonic larvae: the gametes are ripened during the Spring and Summer and shed in the Autumn in northern waters (VANHÖFFEN, 1897). Clearly, with a Summer or Autumn spawning animal which has to ripen its sexual products in the same season as they are shed, the arguments put forward for *Balanus balanoides*, whose eggs are fertilised in the late Summer of the previous year, the embryos being carried in the mantle cavity through the winter, will apply with even greater force. It may be noted that THORSON (1936) has pointed out that the pelagic larval stage of *Mytilus edulis* takes about three weeks even at a temperature of 20°, and he suggests the possibility that in northeast Greenland the metabolism of the larvae may not be sufficiently rapid to complete their larval development in the short season. There will be a limit set by the time required for these processes and this is apparently of the same order as that required by *B. balanoides*. In a recent paper MADSEN (1940) has pointed out that on the West coast of Greenland *Mytilus* goes further north to Tasiusak (73°22′N) than *Balanus balanoides* but only in the sub-littoral. Further in Novaya Zemlya, the mussel is restricted to the sub-littoral zone, a fact stressed by a number of workers. (JENSEN, 1905; GRIEG, 1924; STRELNIKOV, 1929 and MESSAJATZEW, 1931).

The mussel is absent from Spitzbergen, although it was present in quantity in the warmer post-Pleistocene Period, as it was in the northern parts of Greenland.

The Limits of *Littorina saxatilis*, Olivi, var. *groenlandica*, Mencke

Once again the hypothesis has to be considered in relation to this mollusc, also a marker of the northern sub-arctic regions. This like *Mytilus* is a mobile species. There are no direct observations on its behaviour in Greenland but it appears to spend the winter in the sub-littoral at its northern limit in Europe, and they have been found in the sub-littoral of East Greenland immediately before and after the winter. The animal, like so many arctic species does not have planktonic larvae; the eggs and embryos are developed in a breeding chamber from which they escape and begin the young crawling phase. Nothing is known of their breeding season in the arctic but further south the animal breeds throughout the year. As far as can be ascertained they are in their breeding behaviour suited to the arctic region beyond their present limits; the relatively short season cannot prevent them reproducing as it can with *Balanus balanoides* and *Mytilus edulis* with their planktonic larvae. Further, as already pointed out, the adults could retreat to the sub-littoral during the winter. It is difficult without further information to know therefore why the northern limits are associated with those of the barnacle and mussel. It may perhaps be that the food of the adult, small algae, are absent north of the limiting line. An alternative possibility is that *Littorina* cannot withstand the reduced salinity of the melt period; there is a conspicuous lack of infauna molluscs in the region just below low tide level and in the true arctic and it has been ascribed to this effect. Indeed Dr. Thorson has stresssed this possible deleterious effect of the melt water on both the adults and larvae of bottom forms. The nauplii of *Balanus balanoides* can withstand considerable reductions of salinity down to 3 $^0/_{00}$ (Barnes, 1953) and so can the adults which penetrate into the Baltic; nothing is known regarding the effect of reduced salinity on the behaviour of *Littorina.*

Discussion

Dunbar (1951) has considered the limits of the arctic; he points out that if the marine areas are defined in terms of arctic water, that is, water which has originated from the upper 200 metres of the arctic basin, the general distribution of arctic and sub-arctic can be seen from the physical properties (T-S relations) of the water. The boundaries of these water masses – pure arctic and arctic mixed with Atlantic or Pacific water – cannot be so detected. On the basis of a number of biological indicators including *B. balanoides* and the littoral molluscs he arrives at a tentative set of limits for the arctic and sub-arctic. The shoreward limits are very similar to those given by Madsen and by the summer ice limits shown in Fig. 1. The suggestion of Madsen that these limits reflect a change of productivity are tentatively accepted.

The argument relating to productivity rests on the basis of two facts; first that the climate at say Upernavik is similar to that at a comparable latitude on the east coast at which the animals are not found; therefore this cannot be the limiting factor. Secondly, that the biomass of the bottom fauna is less in the northern parts of the east coast and that this results from a lower productivity, which in turn affects the littoral fauna. Apart from the fact that any change in the productivity of a district might be expected to affect the fauna gradually rather than produce sharp limits, there are many factors other than the productivity of the water which may affect the biomass of bottom living animals. This low biomass of the bottom fauna is to some extent related to the fjord complexes rather than the open coast (SPÄRCK, 1933; THORSON, 1933, 1934) and as the latter has shown the bottom fauna is very much reduced near the mouths of the fjords. One would prefer more direct information regarding relative productivity. The only detailed information is that of DIGBY (1953). In the Scoresby Sound area he found that whilst production under the ice in the winter months was very low there was some 9,000 Harvey units/m^3 of net plankton pigment at the diatom increase and even as late as August the value was some 2,500 units/m^3. The mean value for the year was 670 units/m^3 which may be compared with the mean annual standing crop equivalent to 680 units/m^3 found by HARVEY (1934) for the English Channel. (Although in the latter region there may be more net-passing plankton.) According to the estimates by FRIEDRICH (1950) there is no gross reduction in productivity immediately north of Angmagssalik. In some areas nutrient content and standing crops are a poor estimate of productivity but in the Arctic where, with a stable water column, the top 25 metres may be completely depleted and where the short period for the growth of diatoms and low temperatures probably allow little re-cycling of available nutrients, the phosphate content of water may be taken as a rough guide to the potential productivity. HAGEN's results (1931, 1936) are therefore of interest; in the upper layers complete depletion of phosphate was often found but at 25, 50 and 100 metres the mean value of the phosphate in the Baffin Bay region was higher north of Upernavik than to the south. This, of course, could mean there was less phosphate utilised and less productivity therefore to the north. However, even if the change in the productivity was the cause of the change in the bottom biomass it does not follow that this need similarly affect the littoral fauna; the distribution of the latter could be determined by a different cause or by the same factor affecting the productivity but not acting through it.

We have rather taken the view that factors other than overall productivity limit these littoral animals although quite clearly reduced productivity and increasing severe littoral conditions could and would limit eventually their distribution. We have also stressed that whilst a common factor must be important in its effect on a group of species which show a common limit, it is important to consider the biology of the individual species if one is to understand the mechanism by which the limitation takes place. The mechanism may be different for the individual species of the group with a common limit.

Acknowledgements

I have had the benefit of discussion regarding Arctic conditions and the hypothesis set out above with a number of people and would particularly thank, Dr. B. H. Ketchum and Mr. Wm. G. Metcalf of the Woods Hole Oceanographic Institution, Dr. G. Thorson, The Zoological Museum, Copenhagen and Dr. M. J. Dunbar and Dr. Ellis of McGill University, Canada.

Summary

1. The suggestion of Madsen that the northern limit of *B. balanoides* and certain littoral molluscs is determined by conditions in the sub-littoral is briefly reviewed.

2. The northern limits of the cirripedes are discussed in some detail.

3. It is pointed out that the limits are closely paralleled by the summer limits of the pack ice, i.e. its annual maximal retreat.

4. It is suggested that while the ice-limits as such do not determine the limits of these intertidal animals the conditions which they indicate are responsible. In particular they indicate the severity of conditions and the time available for nauplii to be released, for the plankton phase to develop and for settlement and some growth to ensue.

5. The apparent exception is the west coast of Greenland; here it is considered that local factors, particularly the high arctic conditions in Melville Bight, are limiting.

6. Application of these ideas is made to the littoral molluscs.

7. It is stressed that even when found associated at a common limit, the biology of the individual species should be considered in attempting to assess the determining factor in their distribution.

References

Aurivillius, C. W. S., 1895: Littorafaunans förhållenden vid tiden för havets isläggning Övers. K. V. A. S. Forhandl., *52*, pp. 133–150.

Baino-Rodzevich, M. A., 1923: Decapoda, Isopoda, Cirripedia, Copepoda-material from the Kara-expeditions. Contr. Petrograd. Inst. Leshaft., *7*.

Barnes, H., 1952–3: The effect of light on the growth rate of two barnacles *Balanus balanoides* (L.) and *B. crenatus* Brug. under conditions of total submergence. Oikos, *4*, pp. 104–111.

Barnes, H., 1953: The effect of lowered salinity on some barnacle nauplii. J. Anim. Ecol., *22*, pp. 328–330.

Barnes, H., 1955: The growth rate of *Balanus balanoides* (L.). Oikos, *6*, pp. 109–113.

Barnes, H., 1957: Processes of restoration and synchronization in marine ecology; the spring diatom increase and the 'spawning' of the common barnacle, *Balanus balanoides* (L.). In "International Colloqium on Marine Biology" ed. P. Drach. Ann. Sci. Nat. *1*.

Barnes, H. and H. T. Powell, 1953: The growth of *Balanus balanoides* (L.) and *B. crenatus* Brug. under varying conditions of submersion. J. Mar. biol. Ass. U. K., *32*, pp. 107–128.

Blegvad, H., 1929: Mortality among animals of the littoral region in ice winters. Rep. Danish Biol. Stat., *35*, pp. 51–62.

Bentham, R. 1937: The ice-foot. Appendix III in Shackleton: Arctic Journeys. The story of the Oxford University Ellesmere and Land Expedition 1934–5. London.

Bertelsen, E., 1937: Contributions to the animal ecology of the fjords of Anmagssalik and Kangerdlugssuaq in East Greenland. Medd. om Grønl. *108*, Nr. 3.

Bousfield, E. L., 1952–53: The distribution and spawning seasons of barnacles on the Atlantic coast of Canada. Ann. Rep. Nat. Mus. Canada for the fiscal year 1952–53, Bull. No. 132, pp. 112–154.

Bousfield, E. L., 1955: The Cirripede crustacea of the Hudson Strait Region, Canadian Eastern Arctic. "*Calanus*" Series No. 7. J. fish. res. Board Canada, *12*, pp. 762–767.

Broch, H., 1933: Cirripedia Thoracica von Norwegen und dem norwegischen Nordmeere. Eine systematische und biologisch-tiergeographische Studie. Videnskap Selsk. Skrifter. I. Mat.-Naturv. Klasse No. 17.

Broch, H., 1933: Einige Probleme der biogeographischen Abgrenzung der arktisch Region. Mitt. Zool. Mus. Berlin *19*.

Broch, H., 1936: Cirripedia. Norwegian North Polar Exp. Maud, 1918–1925, Sci. Res. *19*, pp. 1–5.

Brotzky, V. and L. Zenkewitch, 1932: Materials for the quantitative evaluation of the bottom fauna of the Barents, White and Kara Seas. Nr. 6. The bottom fauna of the Cheshskaya Bay. Trans. State. Oceanog. Inst. U.S.S.R. *2*, Nr. 2, pp. 41–57.

Connell, J., 1955: *Eliminius modestus* Darwin, a northward extension of the range. Nature, London., *175*, p. 954.

Crisp, D. J. and A. J. Southward, 1953: Isolation of intertidal animals by sea barriers. Nature, London, *172*, p. 208.

Derjugin, K., 1928: Die Fauna des Weissen Meeres und ihre Existenzbedingungen. Expl. Mers. d'U.S.S.R. 7–8, I–XII.

Digby, P. S. B., 1953: Plankton production in Scoresby Sound, East Greenland. J. Anim. Ecol., *22*, pp. 289–322.

Dunbar, M. J., 1951: Eastern arctic waters. Fish. Res. Bd. Canada, Bull. No. 88.

Feyling-Hanssen, R. W., 1953a: The barnacle *Balanus balanoides* (Linné, 1766) in Spitzbergen. Norsk Polarinstitutt. Skr., Nr. 98.

Feyling-Hanssen, R. W., 1953b: Brief account of the ice-foot. Norsk. Geogr. Tidsskr., *14*, pp. 45–52.

Friedrich, H., 1950: Versuch einer Darstellung der relativen Besiedlungsdichte in den Oberflächenschichten des Atlantischen Ozeans. Kiel. Meeresforsch., *7*, Heft 2, pp. 108–121.

Grieg, J. A., 1924: Molluscs, brachiopods and echinoderms from Novaya Zemlya. Rep. Sci. Res. Norw. Exp. to Novaya Zemlya 1921, No. 26.

Gurjanova, E., 1929: Contributions to the question of the distribution of the benthos in the Cheshskaya Bay. Trans. Inst. Scient. Explor. North, No. 43, pp. 98–100.

Gurjanova, E., 1932: Some contributions to the fauna of Crustacea of the Brother Laptev's Sea. Explor. des mers de l'U.S.S.R. *15*, Inst. Hydrol. Leningrad, pp. 157–187.

Gurjanova, E., J. Sachs and P. Uschakov, 1925: Comparative survey of the littoral of the northern seas. Trav. de la Murman Biol. Stat., *1*.

Gurjanova, E., J. Sachs and P. Uschakov, 1928: Das Littoral des Kola-Fjords. Trav. Soc. Nat. Leningr., *58*(*2*), pp. 89–143.

Gurjanova, E., J. Sachs and P. Uschakov, 1930: Das Littoral des Kola-Fjords. Teil III. Existenzbedingungen auf dem Littoral des Kola-Fjords und dessen Biocoenosen. Trav. Soc. Nat. Leningr., *60*(*2*), pp. 17–101.

Hagen, S. K., 1931: Die Godthaabexpedition 1928. Berichte über die Chemischen Arbeiten I. Medd. om Grønl., *78*, Nr. 2.

Hagen, S. K., 1936: Die Godthaabexpedition 1928. Berichte über die Chemischen Arbeiten II. Medd. om Grønl., *78*, Nr. 4.

Harvey, H. W., 1934: Measurement of phytoplankton population. J. Mar. biol. Ass. U. K., *19*, pp. 761–773.

Henry, D. P., 1942: Studies on the sessile cirripedia of the Pacific coast of North America. Univ. of Washington, Publ. in Oceanog., *4*, pp. 95–134.

Hoek, P. P. C., 1882: Die Crustacean gesammelt während der Fahrten des "Willem Barents" in den Jahren 1878 und 1879. Nied. Arch. für Zool. Suppl. *1*., pp. 1–75.

Jensen, A. S., 1905: On the Mollusca of East Greenland. I. Lamellibranchiata. Medd. om Grønl., *29*, Nr. 9, pp. 289–362.

Joyce, J. R. F., 1950: Notes on ice-foot development, Neny Fjord, Graham Land, Antarctica. J. Geol., *55*, pp. 646–649.

Kanwisher, J. W., 1955: Freezing in intertidal animals. Biol. Bull. *109*, pp. 56–63.

Madsen, H., 1936: Investigations on the shore fauna of East Greenland with a survey of the shores of other arctic regions. Medd. om Grønl., *100*, Nr. 8.

Madsen, H., 1940: A study of the littoral fauna of north-west Greenland. Medd. om Grønl., *124*, Nr. 3.

Messjatzew, I. I., 1931: Mollusken des Barents-Meeres. Trans. Oceanog. Inst., *1*, pp. 3–168.

Pilsbry, H., 1916: The sessile barnacles (Cirripedia) contained in the collections of the U. S. National Museum including a monograph of the American species. U. S. Nat. Mus. Bull., No. 93.

Pyefinch, K. A., 1948: Notes on the biology of cirripedes. J. Mar. biol. Ass. U. K., *27*, pp. 464–503.

Shelford, V. E., 1930: Geographic extent and succession in Pacific North American intertidal (Balanus) communities. Publ. Puget Sd. Mar. (biol.) Sta., *7*, pp. 217–224.

Spärck, R., 1933: Contributions to the animal ecology of the Franz Joseph Fjord and adjacent East Greenland Waters. I–II. Medd. om Grønl., *100*, Nr. 1.

Stephensen, K., 1913: Grønlands Krebsdyr og Pycnogonider. Conspectus Crustaceorum et Pycnogonidorum Groenlandiae. Medd. om Grønl., *22*, 479 pp.

Stephensen, K., 1936: Crustacea Varia. The Godthaab Expedition, 1928. Medd. om Grønl., *80*, Nr. 2.

Stephenson, T. A. and A. Stephenson, 1954: Life between tide marks in North America. IIIA. Nova Scotia and Prince Edward Island: Description of the region. J. Ecol., *42*, pp. 14–45.

Stephenson, T. A. and A. Stephenson, 1954: Life between tide marks in North America. IIIB. Nova Scotia and Prince Edward Island: The geographical features of the region. J. Ecol., *42*, pp. 46–70.

Steven, D., 1938: The shore fauna of Amerdlog Fjord, West Greenland. J. Anim. Ecol., *7*, pp. 53–70.

Stimpson, W. M., 1864: Synopsis of the marine invertebrata collected by the late Arctic Expedition under Dr. J. J. Hayes. Proc. Acad. Nat. Sci. Philadelphia, 1863, pp. 138–142.

STRELNIKOV, J. D., 1929: Les conditions écologiques d'existence de la faune de la mer de Kara. C. R. Acad. Sci., Paris, *188*, pp. 931–933.

TANNER, V., 1944: Outlines of the geography, life and customs of Newfoundland-Labrador (the eastern part of the Labrador Peninsula). Acta Geographica, *8*, No. 1, Helsinki.

TARASOV, N., 1937: Contribution to the fauna of Cirripedia thoracica of the Arctic Ocean. III. Trans. Arctic Inst., *50*, pp. 35–59.

THORSON, G., 1933: Investigations on shallow water animal communities in the Franz Joseph Fjord (East Greenland) and adjacent waters. Medd. om Grønl., *100*, Nr. 2.

THORSON, G., 1934: Contributions to the animal ecology of the Scoresby Sound Fjord Complex, (East Greenland). Hydrography by H. Ussing. Medd. om Grønl., *100*, Nr. 3.

THORSON, G., 1936: The larval development, growth and metabolism of Arctic marine bottom invertebrates compared with those of other seas. Medd. om Grønl., *100*, Nr. 6.

THORSON, G., 1944: Marine *Gastropoda Prosobranchiata*. In: The Zoology of East Greenland. Medd. om Grønl., *121*, Nr. 13.

U. S. NAVY DEPARTMENT, 1943: Sailing directions for East Greenland and Iceland. H. O. No. 75, Washington, 589 pp.

U. S. NAVY DEPARTMENT, 1946: Ice Atlas of the Northern Hemisphere. H. O. No. 550, Washington.

U. S. NAVY DEPARTMENT, 1947: Sailing directions for Baffin Bay and Davis Strait. H. O. No. 76, Washington, 626 pp.

VANHÖFFEN, E., 1897: Die Fauna und Flora Grønlands. Grønlands-Exp. Ges. f. Erdk. 1891–93, *2*, 1, 383 pp., Berlin.

VIBE, C., 1939: Preliminary investigations on shallow water animal communities in the Upernavik- and Thule-districts (Northwest Greenland). Medd. om Grønl., *124*, Nr. 2.

VIBE, C., 1950: The marine mammals and the marine fauna in the Thule district (Northwest Greenland) with observations on ice conditions in 1939–41. Medd. om Grønl., *150*, 6.

WELTNER, W., 1898: Verzeichnis der bisher beschreibenen recenten Cirripedienarten. Arch. f. Naturgesch. Abt. f. Syst. Jahrg. *63*, 1, pp. 227–280, 1897. Berlin.

WELTNER, W., 1900: Die Cirripedien der Arktis. Fauna Arctica. *1*, pp. 289–312, Jena.

OIKOS 8:I, Copenhagen 1957

Contribution No. 898

(*Reprinted from Nature, Vol.* 179, *pp.* 1302–1304, *June* 22, 1957)

A Non-Extractive Method for the Quantitative Estimation of Chlorophyll in Algal Cultures*

THE standard method for the quantitative estimation of chlorophyll usually involves the extraction of this fat-soluble pigment in either ether, acetone, or alcohol. When quantities of chlorophyll are large, as is frequently found in culture experiments, large errors may result from incomplete extraction.

Goldberg *et al.*[1] introduced a cell-counting method, utilizing the millipore filter, which was rendered transparent by the addition of cedar oil. In the same manner a portion of algal culture may be concentrated on a millipore filter, quickly dried, cleared with cedar oil, and pressed between two cover

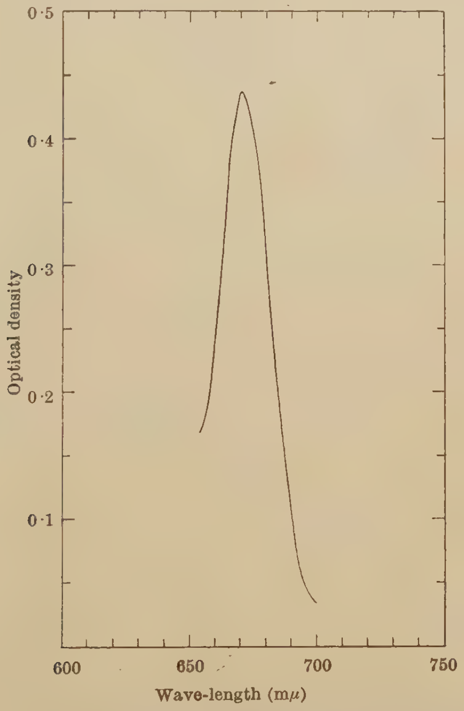

Fig. 1. Absorption of ***Phaeodactylum*** cells on a clear millipore filter, between wave-lengths 750 and 600 mμ

glasses. The slide may then be examined in a spectrophotometer and the concentration of chlorophyll determined from the optical density of the principal absorption peak.

---

* Contribution No. 898 from the Woods Hole Oceanographic Institution.

A measured portion of an algal culture is concentrated on a millipore-type '*AA*' filter (47 mm. diameter). The filter is quickly dried at 85° C. for 10 min. Preliminary examination has shown that the short exposure to heat does not damage the pigment. The dried filter is placed on a No. 2 35 mm. × 50 mm. cover glass to which several drops of cedar oil are added. A second cover glass is placed on top, and the two glasses with the filter between are firmly pressed together. The residual filter is carefully cut away and the excess cedar oil is wiped from both glasses.

The 'wafered' filter is placed in one half of the standard Beckman *D.U.* 5·0-cm. cell carriage. A backing block of brass ensures the centring of the filter directly behind the opening in the cell carrier. Air is used as the blank standard. Monochrometer slit-widths range between 0·02 and 0·06 mm.

The spectrum of *Phaeodactylum* cells on a cleared millipore filter is shown in Fig. 1. The principal peak is at 670 mμ, which agrees with other workers' findings for chlorophyll absorption within the cell. Acetone, ether and alcohol solvents shift this peak to 655–665 mμ. Optical density readings at 670 mμ are the sum of absorption and scattering. The scattering, however, arises from particles much larger than the wave-lengths of light encountered ; hence all visible wave-lengths in the red spectrum are scattered equally, not selectively, as is the case when the particle size approaches the dimensions of the wave-length. Therefore, scattering may be detected at 750 mμ where pigment absorption is negligible. Table 1 shows optical density measurements at 670 mμ and 750 mμ using air as one reference and the cleared filter as the other. About 50 c.c. of *Phaeodactylum* culture had been filtered. Using air as the reference, the optical density at 670 mμ is the sum of chlorophyll absorption and scattering resulting from the

Table 1. COMPARISON OF SCATTERING CORRECTIONS

Wave-length (mμ)	Optical density (Ref. : air)	Optical density (Ref. : cleared filter)
670	0·120	0·069
750	0·064	0·013
Corrected O.D. 670	0·056	0·056

cedar oil complex and the cellular material on the filter. True chlorophyll absorption is the difference between optical density readings at 670 and 750 mμ. When a cleared filter is used as the reference, the optical density at 750 mμ is representative of particulate material on the filter. In the example shown in Table 1, about 80 per cent of the scattering resulted from the cedar oil filter complex, thus indicating that the refractive indices of cedar oil and cell material are about the same.

To calibrate this method, comparisons with acetone extracts were made. The methods for concentrating, extracting and determination have been outlined by Richards with Thompson[2] and Creitz and Richards[3]. Table 2 shows the ratios for seven species between the corrected optical density at 670 mμ and milligrams of chlorophyll *a* in the acetone extract. For most of the cultures listed only two determinations were made at different concentrations; however, *Dunaliella* and *Phaeodactylum* cultures were calibrated from six comparisons each, covering a wide range of concentrations. Chlorophyll in milligrams per litre of filtered culture may be calculated by using these ratios in the following formula:

$$\text{Chlorophyll } a \text{ (mgm./litre)} = \frac{(\text{O.D.})\ (K)}{\text{Volume filtered in litres}}$$

where O.D. $= D_{670} - D_{750}$. It should be noted that, in the calibration procedure, the optical density at 670 mμ has been compared directly with values obtained for chlorophyll *a*. Some interference by other chlorophylls can be expected at this wavelength; however, this probably does not exceed 5 per cent of chlorophyll *a*.

Table 2. RATIO (K) BETWEEN CHLOROPHYLL *a* (mgm.) IN ACETONE EXTRACT (A) AND THE CORRECTED OPTICAL DENSITY VALUES AT 670 Mμ (B) FOR EQUIVALENT VOLUMES OF FILTERED CULTURES

		A*	B	$K = \frac{A}{B}$
Skeletonema costatum	I	$4{\cdot}00 \times 10^{-3}$	0·039	0·102
	II	$7{\cdot}50 \times 10^{-3}$	0·071	0·105
Chaetoceras sp.	I	$1{\cdot}11 \times 10^{-3}$	0·022	0·131
	II	$2{\cdot}50 \times 10^{-3}$	0·049	0·130
Lauderia sp.	I	$1{\cdot}24 \times 10^{-3}$	0·030	0·105
	II	$2{\cdot}20 \times 10^{-3}$	0·052	0·104
Phaeodactylum tricornutum	I	$1{\cdot}44 \times 10^{-3}$	0·033	0·110
	II	$7{\cdot}00 \times 10^{-3}$	0·162	0·108
Dunaliella euchlora	I	$2{\cdot}02 \times 10^{-3}$	0·045	0·114
	II	$4{\cdot}05 \times 10^{-3}$	0·092	0·111
Nannochloris sp.	I	$1{\cdot}16 \times 10^{-3}$	0·026	0·103
	II	$3{\cdot}36 \times 10^{-3}$	0·081	0·104
Olisthodiscus sp.	I	$1{\cdot}66 \times 10^{-3}$	0·032	0·130
	II	$4{\cdot}00 \times 10^{-3}$	0·077	0·131

* 5 c.c. 90 per cent acetone extract

As only a small portion of the entire filter is examined in the spectrophotometer, large errors could result from the accumulation of cells in particular sections of the disk. By rotating the filter so that the light-path passes through three different areas, the maximum deviation recorded was 15 per cent.

The non-extractive method is much more sensitive than direct estimates of pigment from cell suspensions. It is comparable in sensitivity to optical density measurements on chlorophyll–acetone solutions using a 5·0-cm. light-path. The common use of the millipore filter makes the non-extractive method highly desirable in studies involving carbon-14 uptake and chlorophyll analysis.

This work has been supported by a grant from the National Science Foundation.

CHARLES S. YENTSCH

Woods Hole Oceanographic Institution,
Massachusetts.

March 26.

[1] Goldberg, E. D., Baker, M., and Fox, D. L., *J. Mar. Res.*, 11 (2), 194 (1952).

[2] Richards, F. A., with Thompson, T. G., *J. Mar. Res.*, 11 (2), 156 (1952).

[3] Creitz, G. I., and Richards, F. A., *J. Mar. Res.*, 11 (2), 156 (1955).

Printed in Great Britain by Fisher, Knight & Co., Ltd., St. Albans.

Contribution No. 899

Särtryck ur Tellus nr 3, 1957

Steady Convective Motion in a Horizontal Layer of Fluid Heated Uniformly from Above and Cooled Non-uniformly from Below

By HENRY STOMMEL and GEORGE VERONIS, Woods Hole Oceanographic Institution[1]

(Manuscript received March 28, 1957)

Abstract

A gravitationally stable fluid layer is heated non-uniformly (sinusoidally) at the bottom (or top) and a thermal convection regime is established. Examples are worked out for cases (i) without rotation (ii) with uniform rotation, and (iii) with non-uniform rotation (beta-plane).

1. Introduction

The study described in this paper is an outgrowth of a very interesting Russian paper by Lineykin (1955) in which he attempted to determine whether geostrophic currents, produced in a stable sea by wind, extend only to a certain limiting depth. There is, of course, ample observational evidence to indicate that currents decrease with depth because of the baroclinity of the ocean. The essential features which Lineykin incorporated into his model to limit the depth of currents were stratification of the ocean (in equilibrium, a linear increase of density with depth) and the Coriolis parameter (uniform rotation). The scale length of the model was taken to be 100 km so that his results could not be applied directly to large-scale oceanic motions. Evidently Lineykin had the Caspian Sea in mind, because attempts to extend his results to systems of horizontal oceanic scale lead to essentially barotropic (vertically uniform) velocities for depths of 5 km. It appears therefore that some additional physical factor—such as the variation of the Coriolis parameter—must be added in order to limit the depth of the currents much more drastically than the mechanisms envisaged by Lineykin. We have incorporated the variation of the Coriolis parameter into a simple model (§ 5) and have shown that it does indeed limit the currents to a depth which is much more realistic.

However, the basic objection to Lineykin's model and to the one discussed in this short paper is that the mean density structure of the ocean cannot be approximated by a constant vertical potential temperature gradient. Indeed, the problem appears to be essentially non-linear with advective processes playing a fundamental role in the formation of the main thermocline. For this reason we hesitate to offer the following results as a real explanation of the observed phenomena in the ocean.

Recently we attended a series of lectures on tropical meteorology by Drs. Herbert Riehl, Eric Palmén, and Joanne S. Malkus, and we realized that in some respects the atmosphere in the vicinity of the trade-wind regions is a more suitable phenomenon to which to apply Lineykin's analysis. In particular, it is much more nearly uniformly stable, and therefore, Lineykin's linearization procedure is more justifiable. It occurred to us that Lineykin's model might be formulated in such a way as to give a crude theory of the Trades. We are not qualified to judge whether the model is truly applicable to the Trades, but we have worked out the analytical details involved and present them here for the convenience of other workers. Also, of course, the results are in themselves of some interest.

2. Basis of the Model

Consider a fluid in a horizontal layer heated uniformly at the top and cooled below. Because of the thermal expansion of the fluid the density decreases upward, and the fluid is gravitationally stable. A uniform gradient of temperature $\partial\vartheta/\partial z$ (where z is directed positively upward and ϑ indicates temperature) is established; the heat flux $\varkappa\frac{\partial\vartheta}{\partial z}$ is determined by thermometric conductivity ($\varkappa$) alone and there is no fluid motion.

---

[1] Contribution No. 899 from the Woods Hole Oceanographic Institution. This work was done under the auspices of the Office of Naval Research.

If the fluid is cooled non-uniformly below by a temperature perturbation $\vartheta_0 \cos ly$ impressed at the boundary $z=0$, then we may anticipate horizontal differences of density in the fluid. Buoyancy forces produce convective motions which must be maintained against viscous and conductive dissipation; hence the amplitude and vertical extent of the convection must be determined. The present communication endeavors to describe these convective motions in the case where the motions are very slow and the disturbances of the temperature field are very slight (as compared to the basic uniform temperature field); in other words, this is a linearized perturbation theory.

The perturbation equations which we shall use are:

$$-f\varrho_0 v = -\frac{\partial p}{\partial x} + A\varrho_0\frac{\partial^2 u}{\partial z^2} \qquad (1)$$

$$f\varrho_0 u = -\frac{\partial p}{\partial y} + A\varrho_0\frac{\partial^2 v}{\partial z^2} \qquad (2)$$

$$g\varrho = -\frac{\partial p}{\partial z} \qquad (3)$$

$$\frac{\partial u}{\partial x} + \frac{\partial v}{\partial y} + \frac{\partial w}{\partial z} = 0 \qquad (4)$$

$$w\overline{\frac{\partial\vartheta}{\partial z}} = \varkappa\frac{\partial^2\vartheta}{\partial z^2} \qquad (5)$$

$$\varrho = \varrho_0(1-\alpha\vartheta) \qquad (6)$$

Equations (1) and (2) are the linearized steady state equations of motion for a rotating system (f is the Coriolis parameter). Since the vertical scale of the perturbation fields in the examples discussed is much less than the horizontal scale, there appears to be no reason to carry the full Laplacian in the frictional term and we have kept only the vertical viscous shearing stress term. Equation (3) is the hydrostatic equation. Equation (4) is the Boussinesq approximation to the conservation of mass equation. Equation (5) is the steady state perturbation heat flow equation linearized by taking $w\overline{\frac{\partial\vartheta}{\partial z}}$ (where the bar indicates the mean unperturbed thermal gradient) as the only important heat advection term. We suppose this to be balanced by the divergence of the vertical conductive perturbed heat transport. Equation (6) is a simple linear equation of state.

We now proceed to discuss solutions of these equations for those cases (§ 3) no rotation, (§ 4) uniform rotation, and (§ 5) non-uniform rotation.

3. No rotation

Consider solutions independent of the x-direction, and in which $f=0$. Eliminate all dependent variables except ϑ, thus obtaining the equation

$$\frac{\partial^6\vartheta}{\partial z^6} = -\frac{g\varrho_0\alpha b}{A\varkappa}\frac{\partial^2\vartheta}{\partial y^2} \qquad (7)$$

where we have introduced b to represent the basic temperature gradient $\overline{\partial\vartheta/\partial z}$. Consider a simple bottom temperature perturbation of the form $\vartheta=\vartheta_0\cos ly$, and a solution of the form $\vartheta=\Theta(z)\cos ly$, in which case equation (7) reduces to an ordinary differential equation

$$\frac{d^6\vartheta}{dz^6} = F^6\vartheta \qquad (8)$$

where

$$F = \sqrt{\frac{g\varrho_0 abl^2}{A\varkappa}}$$

The quantity F^{-1} is the characteristic vertical scale of the convection field. We can call it the "frictional depth".

The solution is of the form

$$\vartheta = \vartheta_0\cos ly\sum c_i e^{p_i Fz} \qquad (9)$$

where the p_i are the sixth roots of unity. If we consider only the three terms which become negligibly small for large z, we need two boundary conditions at $z=0$ in addition to the condition $\Theta(0)=\vartheta_0$. Physically it is clear that at the bottom $w=v=0$ are these conditions; in terms of Θ these two additional conditions are

$$\frac{d^2\Theta}{dz^2} = \frac{d^3\Theta}{dz^3} = 0,$$

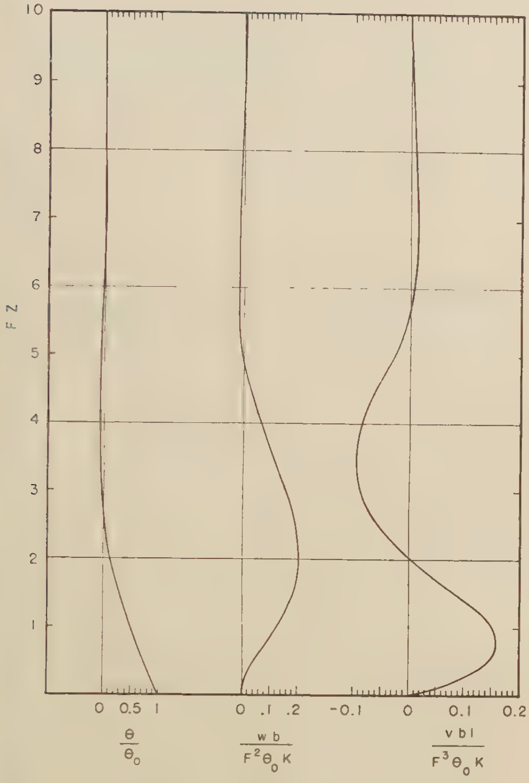

Fig. 1. Amplitude of perturbation temperature, and of the vertical and horizontal components of velocity as a function of altitude for the non-rotating case. Both coordinates are dimensionless.

from equations (5) and (4) respectively. The solutions of the problem are

$$\vartheta = \vartheta_0 \cos ly \left\{ \frac{1}{2} e^{-Fz} + \frac{1}{2} e^{-\frac{Fz}{2}} \left(\cos \frac{\sqrt{3}}{2} Fz + \right.\right.$$

$$\left.\left. + \frac{\sqrt{3}}{3} \sin \frac{\sqrt{3}}{2} Fz \right) \right\} \qquad (10)$$

$$w = \frac{F^2 \vartheta_0 \varkappa}{2b} \cos ly \left\{ e^{-\frac{Fz}{2}} + e^{-\frac{Fz}{2}} \left(- \cos \frac{\sqrt{3}}{2} Fz + \right.\right.$$

$$\left.\left. + \frac{\sqrt{3}}{3} \sin \frac{\sqrt{3}}{2} Fz \right) \right\} \qquad (11)$$

$$v = \frac{F^3 \vartheta_0 \varkappa}{2bl} \sin ly \left\{ -e^{-Fz} + e^{-\frac{Fz}{2}} \left(\cos \frac{\sqrt{3}}{2} Fz + \right.\right.$$

$$\left.\left. + \frac{\sqrt{3}}{3} \sin \frac{\sqrt{3}}{2} Fz \right) \right\} \qquad (12)$$

These relations are plotted in Fig. 1. The convective motion is in the form of long strip cells, or rolls, with axes in the x-direction. Fluid rises over warm portions of the bottom, and sinks over colder portions. The amplitude of the motion is proportional to the temperature perturbation at the bottom. The vertical extent of the motion is directly proportional to viscosity, conductivity, and horizontal scale. It varies inversely as the gravitational stability of the mean density field.

4. Uniform Rotation

In this case f is a constant and there is an x-component of velocity, u, but all variables are independent of the x-coordinate. Elimination of variables leads to an equation analogous to equation (8).

$$-\frac{1}{E^4} \frac{d^7\vartheta}{dz^7} + \frac{d^3\vartheta}{dz^3} - L^2 \frac{d\vartheta}{dz} = 0 \qquad (13)$$

where

$$E^4 = -\frac{f^2}{A^2}, \; L^2 = \frac{g\varrho_0 abl^2}{f^2} \frac{A}{\varkappa}$$

The quantity $2\pi/E$ is the well-known "Ekman depth" and the quantity L^{-1} can be called the "Lineykin depth".

In the case where the only terms admitted in the solution are those which vanish at infinity and $L \gg E$ the solutions are

$$\frac{\vartheta}{\vartheta_0 \cos ly} = 2e^{-\frac{E}{\sqrt{2}}z} \left[D_1 \cos z \frac{E}{\sqrt{2}} \right.$$

$$\left. + D_2 \sin z \frac{E}{\sqrt{2}} \right] + Ce^{-Lz} \qquad (14)$$

$$\frac{u}{\vartheta_0 \sin ly} = \frac{\sqrt{2} g\alpha l}{Ef} \left[(D_1 - D_2) \sin \frac{E}{\sqrt{2}} z - \right.$$

$$\left. - (D_1 + D_2) \cos \frac{E}{\sqrt{2}} z \right] e^{-\frac{E}{\sqrt{2}}z} -$$

$$- \frac{g\alpha l}{Lf} Ce^{-Lz} - \frac{\sqrt{2} A\varkappa E^5}{flb} \left[(D_1 - D_2) (\cos \frac{E}{\sqrt{2}} z + \right.$$

$$\left. + (D_1 + D_2) \sin \frac{E}{\sqrt{2}} z \right] e^{-\frac{E}{\sqrt{2}}z} +$$

$$+ \frac{A\varkappa}{flb} CL^5 e^{-Lz} + \text{const.} \qquad (15)$$

$$\frac{v}{\vartheta_0 \sin ly} = \frac{\sqrt{2}E^3\varkappa}{lb}\left\{(D_2 - D_1)\sin\frac{E}{\sqrt{2}}z - \right.$$
$$\left. -(D_1 + D_2)\cos\frac{E}{\sqrt{2}}z\right\}e^{-\frac{E}{\sqrt{2}}z} +$$
$$+\frac{\varkappa L^3}{lb}Ce^{-Lz} \tag{16}$$

$$\frac{w}{\vartheta_0 \cos ly} = \frac{2E^2\varkappa}{b}\left\{D_1 \sin\frac{E}{\sqrt{2}}z - \right.$$
$$\left. -D_2\cos\frac{E}{\sqrt{2}}z\right\}e^{-\frac{E}{\sqrt{2}}z} + \frac{\varkappa L^2}{b}Ce^{-Lz} \tag{17}$$

where

$$D_1 = \frac{L^2(2L^2 - E^2)}{4L^4 - 2L^2E^2 + 2\sqrt{2}LE^3 + 2E^4}$$

$$D^2 = \frac{L^2(E^2 + \sqrt{2}LE)}{4L^4 - 2L^2E^2 + 2\sqrt{2}LE^3 + 2E^4}$$

$$C = \frac{E^3}{E^3 - EL^2 + \sqrt{2}L^3}$$

These relations are plotted in Fig. 2. The Ekman layer is noticeable only in the lowest portion of the figure, the remainder of the profile being controlled essentially by the Lineykin depth. Qualitatively gravitational stability and horizontal scale have the same kind of influence on the vertical extent of the convective motion as in the non-rotating case, but their influence is stronger. On the other hand, the viscosity and conductivity enter as a ratio: if, in large-scale problems one were to suppose that they are to be interpreted as eddy-coefficients of comparable magnitude, the Lineykin depth must be largely *independent* of their amplitude. The ordinates are plotted non-dimensionally for Lz since L^{-1} is the controlling depth, but if E is changed the shape of the lower portions of the curves is modified. Thus the curves in Fig. 2 are not universal curves in the same sense as those in Fig. 1. The origin for the u-curve in Fig. 2 is arbitrary as indicated by the constant in equation (15). The constant can be determined by specifying the pressure at the level $z = 0$. If one imposes $u = 0$ at $z = 0$, u approaches a constant value with height. If u is supposed to vanish at infinity it is finite at $z = 0$. In either case, however, $\partial u/\partial z$ vanishes at $z = 0$.

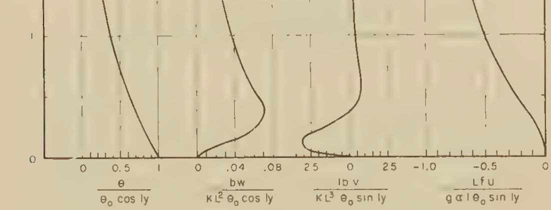

Fig. 2. Amplitude of the perturbation temperature and components of velocity as functions of altitude for the case of uniform rotation. The ordinate is the dimensionless quantity Lz expressed in terms of the Lineykin-depth. However, since there is an additional characteristic depth E^{-1}, it is not possible to present universal curves, particularly for the lowest values of Lz. The abscissae are dimensionless.

5. Non-uniform Rotation

Let us now consider the case where the Coriolis parameter varies with latitude, i.e., $\beta = \partial f/\partial y \neq 0$. For reasons that will become evident, the geometry of the problem is also changed; the perturbed boundary condition is taken as a function of x instead of y; at $z = 0$, $\vartheta = \vartheta_0 \cos lx$; and also, in order to correspond to the ocean, the top instead of the bottom is taken at $z = 0$. We are thus concerned with the solution in the region $z \leq 0$. It can be shown that for a certain choice of parameters (in particular large horizontal scale of oceanic dimensions) the main features of the temperature field come from the following approximate equation for ϑ:

$$\frac{\partial^4\vartheta}{\partial z^4} = \frac{\beta g\alpha b}{f^2\varkappa}\frac{\partial\vartheta}{\partial x} \tag{18}$$

and if we let $\vartheta = \Theta e^{ilz}$ we obtain

$$\frac{d^4\Theta}{dz^4} = iG^4\Theta$$

where $G = \sqrt[4]{\frac{\beta g\alpha b l}{f^2\varkappa}}$

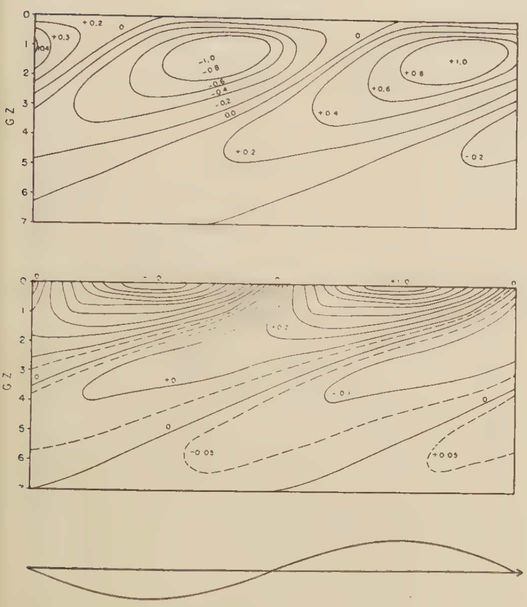

Fig. 3. (a) Contours of equal perturbation temperature (Ocean example with the non-dimensional depth Gz measured positive downward) in the case of non-uniform rotation. The horizontal coordinate is directed eastward toward the right of the figure. The perturbation temperature at the surface ($z=0$) is a sine function. The origin of the x-coordinate is in the center of the figure. The numbers on the contours represent the fraction of the amplitude of the surface perturbation.

$$2\sqrt{2}\,\frac{wf^2r^2}{\beta g\alpha lT_0}$$

(b) Contours of the vertical velocity component in dimensionless form

The vertical scale in both (a) and (b) is exaggerated.

These equations can be obtained directly from equations (1)—(6) if the viscous terms in (1) and (2) are omitted. (It can be shown that for large-scale disturbances the effect of A is negligible below the Ekman layer.) The quantity defines a new characteristic depth which depends upon a different combination of parameters. There is a phase shift toward the west with depth, so that regions (or cells) whose perturbation temperature has the same sign tilt toward the west. Figures similar to Figs. 1 and 2 are not so easily interpretable. Therefore the full non-dimensional field of ϑ and w in the x—z plane is shown in Fig. 3, according to the solutions of equation (18):

$$\vartheta=\frac{\vartheta_0}{2}\Big\{\cos lx\Big[e^{-Gz\cos\frac{\pi}{8}}\cos\Big(Gz\sin\frac{\pi}{8}\Big)+ +e^{-Gz\cos\frac{3\pi}{8}}\cos\Big(Gz\sin\frac{3\pi}{8}\Big)\Big]+ +\sin lx\Big[e^{-Gz\cos\frac{\pi}{8}}\sin\Big(Gz\sin\frac{\pi}{8}\Big)- -e^{-Gz\cos\frac{3\pi}{8}}\sin\Big(Gz\sin\frac{3\pi}{8}\Big)\Big]\Big\}. \tag{19}$$

$$w=\frac{\sqrt{2}}{4}\frac{G^2\varkappa\vartheta_0}{b}\Big\{\cos lx\Big[e^{-Gz\cos\frac{\pi}{8}}\Big(\cos\Big(Gz\sin\frac{\pi}{8}\Big)+\sin\Big(Gz\sin\frac{\pi}{8}\Big)\Big)-e^{-Gz\cos\frac{\pi}{8}}\Big(\cos\Big(Gz\sin\frac{3\pi}{8}\Big)-\sin\Big(Gz\sin\frac{3\pi}{8}\Big)\Big)\Big] +\sin lx\Big[-e^{-Gz\cos\frac{\pi}{8}}\Big(\cos\Big(Gz\sin\frac{\pi}{8}\Big) -\sin\Big(Gz\sin\frac{\pi}{8}\Big)\Big)+e^{-Gz\cos\frac{3\pi}{8}} \Big(\cos\Big(Gz\sin\frac{3\pi}{8}\Big)+\sin\Big(Gz\sin\frac{3\pi}{8}\Big)\Big]\Big)\Big\} \tag{20}$$

Table 1.

Parameters	Experimental Water Model	Atmosphere	Ocean	Units
A	10^{-2}	$5 \cdot 10^{5}$	5	cm²/sec
K	10^{-3}	$5 \cdot 10^{5}$	5	»
$\overline{\frac{1}{\varrho}\frac{\partial\varrho}{\partial z}}$	$2.5 \cdot 10^{-4}$	$2.5 \cdot 10^{-7}$	$5 \cdot 10^{-9}$	cm^{-1}
l	10^{-1}	10^{-8}	10^{-8}	cm^{-1}
f	1	10^{-4}	10^{-4}	sec^{-1}
α	$2.5 \cdot 10^{\ 4}$	$2.5 \cdot 10^{-3}$	$2.5 \cdot 10^{-4}$	°C^{-1}
β		$2 \cdot 10^{-13}$	$2 \cdot 10^{-13}$	cm^{-1} sec^{-1}
F^{-1}	0.4	$1.5 \cdot 10^{5}$	$9 \cdot 10^{3}$	cm
E^{-1}	0.1	$0.7 \cdot 10^{5}$	$2.2 \cdot 10^{2}$	cm
L^{-1}	7.0	$6.3 \cdot 10^{5}$	$45.0 \cdot 10^{5}$	cm
G^{-1}		$3.2 \cdot 10^{5}$	$0.46 \cdot 10^{5}$	cm

$$F^{-1} = \left[\frac{A\varkappa}{g\frac{1}{\varrho}\frac{\partial\varrho}{\partial z}l^2}\right]^{1/6}$$

$$E^{-1} = \left[\frac{A}{f}\right]^{1/2}$$

$$L^{-1} = \left[\frac{f^2}{g\frac{1}{\varrho}\frac{\partial\varrho}{\partial z}l^2}\cdot\frac{\varkappa}{A}\right]^{1/2}$$

$$G^{-1} = \left[\frac{f^2\varkappa}{g\frac{1}{\varrho}\frac{\partial\varrho}{\partial z}l\beta}\right]^{1/4}$$

6. Discussion of Results

In order to exhibit the contrast in temperature and velocity structure in the different cases, parameters appropriate to three different physical situations are inserted into the expressions for the various characteristic lengths and the results tabulated in Table I.

The water experimental model is envisaged as being about 10 cm deep, with a basic vertical temperature gradient of 1°/cm. The bottom temperature is perturbed with a wave length of 60 cm, and an amplitude of not much more than 0.1° C (otherwise the perturbation approximation breaks down). The viscosity and conductivity coefficients are molecular. Under these conditions a very thin ($F^{-1} = 0.4$ cm) convective cellular motion arises with rising over the warm areas of the bottom and sinking over the cool areas, and compensating horizontal flows. As can be seen from Fig. 1, the top of the cells is effectively at $Fz = 6$, or about 2.4 cm. If this whole system is uniformly rotated at about one revolution every twelve seconds, the height of the cellular pattern increases about seventeen times, a thin Ekman layer appears close to the bottom, and a large component of geostrophic flow transverse to the horizontal temperature gradients appears. As it is not easy to picture how a non-uniformly-rotating experimental model could be constructed this case is not discussed.

The parameters in the atmospheric case are chosen to coincide as nearly as possible to

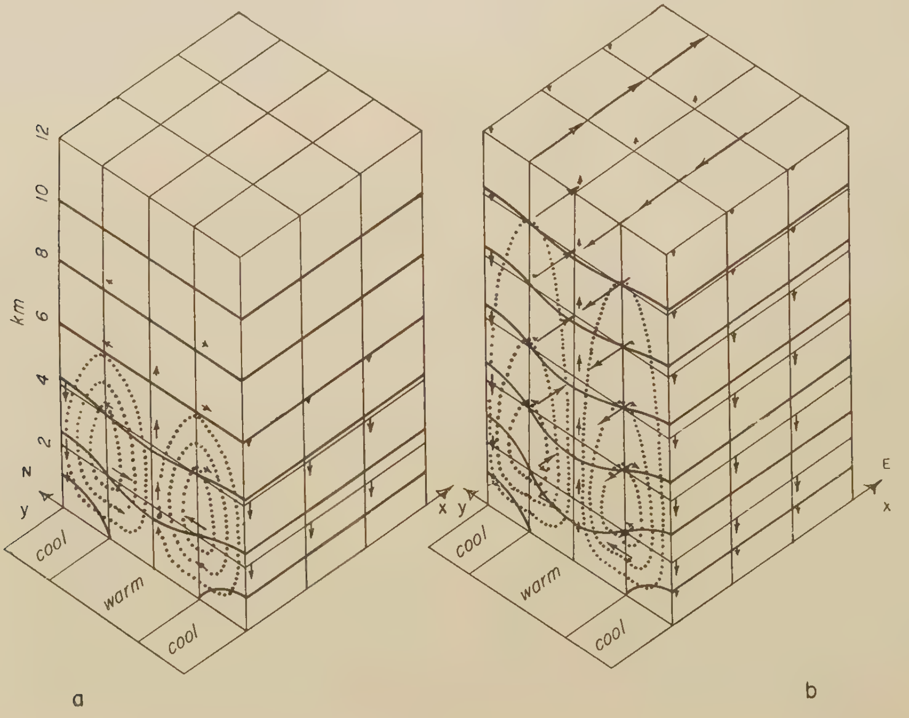

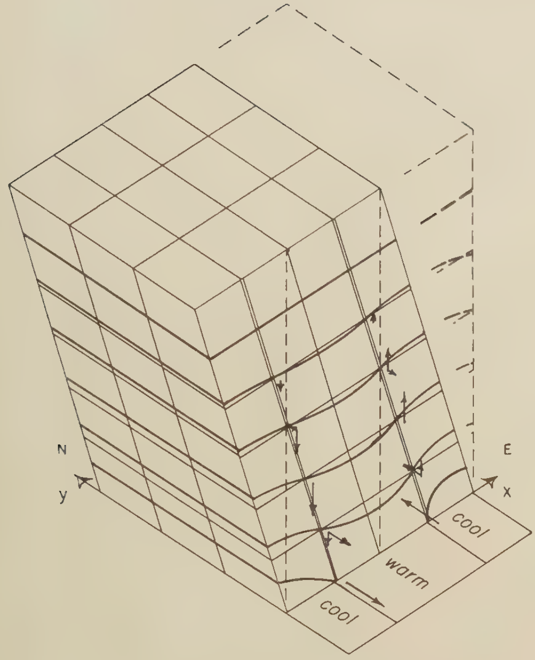

C

Fig. 4. Three cases using parameters for the atmosphere as given in Table I, with the vertical scale greatly exaggerated. The velocity components at selected points are shown by arrows. The heavy lines delineate iso-thermal surfaces. The dotted curves are the two-dimensional streamfunction in the y—z plane. Case (a) is non-rotating, there is no x-component of velocity as there is in case (b) of uniform rotation. In the case of non-uniform rotation (c) the applied boundary temperature is a function of x (instead of y as in (a) and (b)). The dashed lines represent the vertical, and the regions of perturbation temperature of same sign are enclosed by the tilted lines. Thus in (c) each warm and cold cell is tilted toward the west. On the other hand there is no x-component of velocity: all motion is confined to planes x-constant.

those used by Malkus and Riehl in a discussion of the Trades. The extremely large eddy coefficients are meant to include effects of cumulus convection as turbulent eddies. The mean stability corresponds to a vertical potential temperature lapse rate of 1°/100 m. The perturbation wave length is 6,000 km. The characteristic lengths are computed in Table I, and a three-dimensional sketch of the three atmospheric cases is shown in Fig. 4. Uniform rotation (b) produces a much higher cell than no rotation (a), and introduces zonal winds. The model for non-uniform rotation, in which the perturbed bottom temperature is a function of longitude (4c) instead of latitude, has a marked westward tilt with height. There is no horizontal component of cross-isobar flow because in the simplified case treated in Section 5 there is no friction. All flow patterns are geostrophic and in vertical meridional planes. The vertical velocity components are associated with the planetary divergence of the meridional winds.

The oceanic model in Table I is very unrealistic on account of the absence of meridional barriers. It is interesting to note that lack of the rotation gives a very shallow depth of penetration of the perturbation temperature (or broadly speaking, depth of the main thermocline) (90 meters); in the uniform rotation case the Lineykin depth of the current is 45 km; non-uniform rotation (c) leads to a thermocline depth of 470 meters.

REFERENCES

LINEYKIN, P. S., 1955: On the determination of the thickness of the baroclinic layer in the sea. *Doklady SSSR Akad. Nauk*, Tom 101, p. 461.

PRINTED IN SWEDEN
ESSELTE, STHLM 57

Contribution No. 901

Reprinted from COPEIA, 1957, No. 3, pp. 242–244, August 26
Printed in U.S.A.

DISTRIBUTIONAL RECORDS OF FISHES FROM WATERS OFF NEW ENGLAND AND THE MIDDLE ATLANTIC STATES.—The data recorded here concern either species which are new to or have seldom been recorded from certain areas, or distributional information which has bearing upon the life histories of species. In addition to our personal observations, sources of records, for which we are greatly appreciative, include Captain Norman Benson, Mr. L. R. Day, of the Fisheries Research Board of Canada, and members of the crews and scientific parties of the research vessels ATLANTIS, BEAR, BLUE DOLPHIN, and CARYN of the Woods Hole Oceanographic Institution.

Hypoprion signatus. Night Shark. Taken, probably at the surface, from the R/V ATLANTIS, October 16, 1953, at 38°22′N, 69°35′W. Bigelow and Schroeder (1948, Fishes of the Western North Atlantic I: 316–319) record this species from off South Carolina (33°37′N, 77°36′30″W), previously the northernmost record.

Elops saurus. Ten Pounder. Four specimens, 29.3–31.8 cm. fork length, were taken in Benson's trap net at Quisset, Massachusetts (Buzzards Bay) on October 18, 1955. While this species is occasional near Long Island and southern Cape Cod, most are seen before October.

Sphyraena borealis. Northern Barracuda. A specimen, 21 cm. fork length, was taken by Norman Benson in James Pond, Martha's Vineyard, on October 30, 1955. This is in keeping with previous accounts (cf. Nichols and Breder, 1934, Zoologica 9: 1–92) that the species is most often seen after October 1. Since young are more frequently taken than adults, in northern waters, the present specimen is noteworthy.

Katsuwonus pelamis. Oceanic Bonito. L. R. Day reports one specimen 43.5 cm. fork length, taken in a drift gill net at 41°06′N, 64°12′W, on July 19 or 20, 1955, and another was caught from the R/V BEAR on September 18, 1956 at 40°40′N, 68°28′W. Nichols and Breder (1934, *loc. cit.*) state that this species is irregular in the New York-New England area, but numerous offshore. There are few published records for the western Atlantic off northern North America, but it is frequently taken in the summer by sport fishermen in Middle Atlantic and southern New England waters. It is more common in tropical waters. Another record of this species from a fish trap near Provincetown, Massachusetts, in the summer of 1954 is the second Gulf of Maine specimen (the first since 1880; cf. Bigelow and Schroeder, 1953, Fishes of the Gulf of Maine).

Thunnus albacares. Yellowfin Tuna. Two specimens taken on trolled lines from the R/V ATLANTIS: one, 66.1 cm. fork length, on August 19, 1953 at 37°22′N, 71°05′W, the other 113.4 cm. fork length on September 29, 1954 at 37°02′N, 67°34′W; and one, 58.0 cm. fork length, from the R/V CARYN on August 9, 1949 at 38°21′N, 71°37′W. These records, together with those of Mather, 1954 (Copeia (4): 292), seem to indicate a fairly regular occurrence of yellowfins during the fall (August to November) not far off the continental shelf south of New England. Perhaps long-line fishing would establish the presence of a relatively regular seasonal population at greater depths than are normally fished.

Thunnus alalunga. Albacore. A specimen 81 cm. in fork length was caught by trolling from the R/V BEAR, September 12, 1956 at 39°45′N, 73°00′W and preserved by R. H. Backus. While this species may not be uncommon in the western North Atlantic, most reports of it have not been substantiated by specimens. Bullis and Mather (1956, Amer. Mus. Novitates 1765: 1–12) give data on Caribbean specimens, and Mowbray (1956, Proc. Gulf and Carib. Fish. Inst. 8th Ann. Sess. 1955: 138) reports the capture of specimens by means of a long-line near Bermuda. The specimen reported here is the northernmost substantiated record in the western North Atlantic.

Auxis thazard. Frigate Mackerel. Cape Cod has commonly been considered the northern limit for this species. A specimen about 33 cm. fork length from a fish trap at Barnstable, Massachusetts on August 1, 1954 may represent a most northerly record, and is the first record for the Gulf of Maine. Several offshore records from near the supposed northern limit include the following: six specimens from 40°58′N, 64°06′W, and 15 specimens from 41°06′N, 64°12′W, sizes ranging from 29.5–32.5 cm. fork length, taken with drift gill nets from July 12–20, 1955, reported by L. R. Day; one, 34.6 cm. from the M/V BLUE DOLPHIN, June 29, 1953, at 40°05′N, 70°05′W. Mather has caught four specimens near No Man's Land off Martha's Vineyard in late July and early August 1954 and 1955, although he had never taken one in extensive fishing in this area in the years 1947–1953.

Sarda sarda. Common Bonito. Mr. J. Israel Pothier of the Wedgeport Tuna Guides Association showed us a specimen of this species, taken in a herring net off Shag Harbour (Lobster Bay), Nova Scotia on September 10, 1956, and brought to him by Captain John Jacquard. Bigelow and Schroeder (1953, *op. cit.*) report the species as uncommon in the northern Gulf of Maine, but note that young have been taken at Halifax. The present specimen was an adult, approximately 13 inches long.

Scomberomorus cavalla. King Mackerel. Nine specimens were noted in 1955 from Benson's trap in Buzzards Bay, Massachusetts, two on September 14, four on October 3 and three on October 18. These were all about the same size, two measured fish being 23½ inches and 27½ inches fork length. There is a record of this species from North Truro, Massachusetts, in the Gulf of Maine (Bigelow and Schroeder, 1953. *Op. cit.*: 349). Generally speaking, however, the northern limit of its range appears to be the south side of Cape Cod, from which it has been reported in the past (cf. Sumner, *et al.*, 1913, Bull. U. S. Bur. Fish. 21: 750), but where it has been rare in recent years.

Caranx crysos. Blue Runner. This species continues to be the most abundant Carangid in the Woods Hole area, having been noted from September 10 to October 20, 1955 in Benson's trap in Buzzards Bay, and in large schools in Woods Hole Harbor. Most of these were in the size range of 13–20 cm. fork length (about 6–8 inches) with a modal length of about 16 cm. This is somewhat larger than the modal length of the specimens reported by Mather (1954, *loc. cit.*) from offshore areas south of Martha's Vineyard on August 26 and September 10, 1953. There is thus some indication that many of the juveniles spawned offshore (Nichols, 1939, Bull. Bingham Ocean. Coll. 7: 1–19) or drifted northward in the Gulf Stream come inshore to the southern New England coast enroute to the southern habitat of the larger individuals.

Caranx hippos. Jack Crevalle. Although reported as common about Woods Hole, Mather (1954, *loc. cit.*) found it not so in 1953. In 1955, more than 100 were caught in Benson's trap in Buzzards Bay, September 9. Those were all about the same size; two measured were 27.5 cm. fork length. Later, from October 3–19, several specimens were taken in the same trap, but these ranged from about 13–20 cm., half the size of the September specimens. These latter are apparently rather large for northern specimens.

Three small specimens were taken by the ATLANTIS at a night light at 40°02′N, 70°42′W, July 7, 1954. They ranged from 2.4–3.1 cm. fork length.

Rachycentron canadus. Cobia. A specimen about 4 feet long was taken in Benson's Buzzard's Bay trap in early September 1951. There are only a few previous Woods Hole records for this stray, from July and September.

Decapterus punctatus. Round Robin. Eight small specimens, 2.7–4.9 cm. fork length, were taken at a night light from the ATLANTIS at 40°02′N, 70°42′W, on July 7, 1954.

Selar crumenophthalmus. Goggle-eye Scad. Twelve specimens from the Buzzard's Bay trap and from Woods Hole, on October 18 and 19, 1955 were 11–15 cm. fork length. These are all smaller than the series from Quisset, September 26–October 9, 1953 reported by Mather (1954, *loc. cit.*).

Alectis crinitus. Threadfish. One specimen of this rare species (in northern waters) measuring 110 mm. fork length, was taken off the dock of the Woods Hole Oceanographic Institution, September 29, 1954.

Lutianus analis. Muttonfish. Captain Charles A. Mayo, Jr., reported seeing a specimen about 30 inches long among the landings at Provincetown, Massachusetts on October 1, 1955. Captain Mayo, an experienced Florida fisherman, is well acquainted with the species. This specimen is the first Gulf of Maine record and probably the northernmost record.

Mullus auratus. Northern Goatfish. One specimen, 3.75 cm. fork length, was taken at a night light from the ATLANTIS on July 7, 1954 at 40°02′N, 70°42′W.

Otophidium welshi. Welsh's Cusk Eel. A specimen, 161 mm. standard length, brought to us by Norman Benson, was taken in Tisbury Pond, Martha's Vineyard, October 1, 1954. It is now in the Museum of Comparative Zoology as number 39690. Previously this species had been reported only from the coast of the Gulf of Mexico (Allen, 1931, Copeia (1): 28; Woods, 1942, Copeia (3): 192), and from off New Jersey (Fowler, 1952, Proc. Acad. Nat. Sci. Phila. 104: 134).—FRANK J. MATHER III, AND ROBERT H. GIBBS, JR., *Woods Hole Oceanographic Institution, Woods Hole, Massachusetts. Contribution No. 901.*

Contribution No. 902

Reprinted from LIMNOLOGY AND OCEANOGRAPHY
Vol. II, No. 3, July, 1957
Printed in U.S.A.

The Estimation of Phytoplankton Production in the Ocean from Chlorophyll and Light Data[1]

J. H. RYTHER AND C. S. YENTSCH

Woods Hole Oceanographic Institution, Woods Hole, Massachusetts

ABSTRACT

The relationship was determined between photosynthetic rate at light saturation and chlorophyll content in natural populations and cultures of marine phytoplankton. A mean value of 3.7 g C assimilated/hour/g chlorophyll was obtained from the experimental results and from data present in the literature.

A method is described by means of which organic production beneath a unit of sea surface may be estimated from the chlorophyll content of the water, the total daily solar radiation reaching the sea surface, and the extinction coefficient of visible light in the water column. Production values calculated by this method are compared with values obtained by *in situ* productivity measurements.

INTRODUCTION

In an earlier paper (Ryther 1956a) a relationship was described between the photosynthesis of phytoplankton populations and the amount of solar radiation falling on the surface of the ocean throughout a day. A graph was constructed, reproduced here as the broken line in Figure 1, showing relative photosynthesis beneath a square meter of sea surface for different values of total daily radiation incident to the sea surface. The value for photosynthesis (the right-hand ordinate in Figure 1), when divided by the extinction coefficient of visible light in the water column in meters (k), gives photosynthesis beneath a square meter of sea surface per day relative to the rate of photosynthesis per cubic meter per hour at light saturation.

For situations in which phytoplankton populations are distributed homogeneously with depth, an absolute value of daily photosynthesis by the entire phytoplankton population may be obtained from the expression

$$P = \frac{R}{k} \times p(\text{sat.}) \qquad (1)$$

where

P = photosynthesis of the phytoplankton population in g carbon/m^2/day,
R = relative photosynthesis from Figure 1 (broken line) for the appropriate value of surface radiation,
k = extinction coefficient, per meter, as measured,
p (sat.) = photosynthesis of a sample of the population at 2000 foot-candles, as measured, in g carbon/m^3/hour.

If the phytoplankton are not distributed evenly with depth, photosynthesis must be calculated separately for several depths considering both the standing crop and the light at each depth. The solid lines in Figure 1 show daily photosynthesis per cubic meter (the left-hand ordinate) relative to photosynthesis per cubic meter per hour at light saturation at the sea surface (I_0) and at the depths where the surface light intensity is reduced to 50%, 25%, 10%, and 1% respectively. An absolute value for daily photosynthesis at each of these depths may be obtained from the expression:

$$P_d = R_d \times p_d\,(\text{sat.}) \qquad (2)$$

where

P_d = daily photosynthesis (g carbon/m^3) at depth (d),

---

[1] Contribution No. 902 from the Woods Hole Oceanographic Institution. This work was carried out with the assistance of research grants from the National Science Foundation.

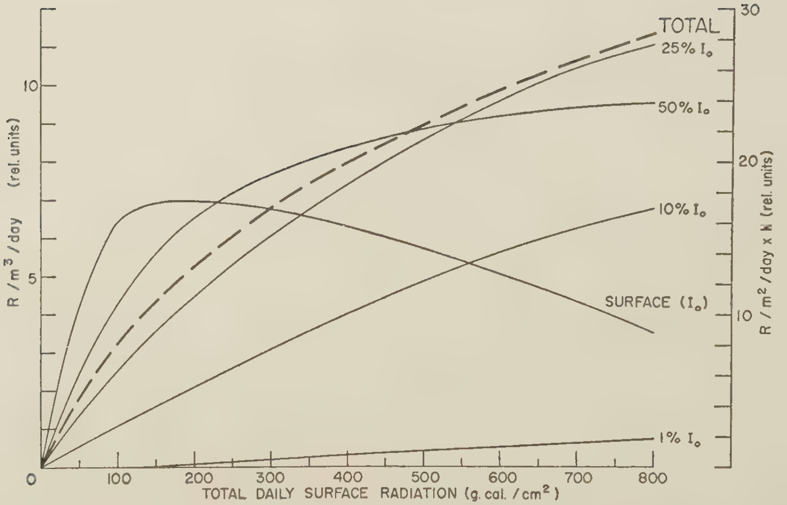

FIG. 1. The relation between total daily surface radiation and daily relative photosynthesis (R) beneath a unit of sea surface (broken line) and at the depths where the surface light intensity is reduced by specified amounts (solid lines).

R_d = relative photosynthesis at depth (d) from Figure 1 for the appropriate value for surface radiation,

p_d (sat.) = photosynthesis of a water sample from depth (d) at 2000 foot-candles, as measured, in g carbon/m^3/hour.

Daily photosynthesis beneath a square meter of sea surface may then be calculated by graphic integration of the values so obtained for each depth.

The method described above, in either of its variations, represents a decided improvement over the alternative of collecting water samples from a series of depths and resuspending them at these depths for whatever period of time is necessary to detect measurable photosynthesis. However, even the practice of carrying out measurements on shipboard under constant illumination leaves much to be desired. Temperature control becomes a problem, particularly if samples from several depths of a thermally stratified water column are being measured at once. But the principle difficulty arises from the fact that no satisfactory experimental technique exists for measuring photosynthesis in the oligotrophic waters of the open ocean, even under controlled illumination. The uptake of C^{14} (Steemann Nielsen 1952), cannot be interpreted in terms of total photosynthetic rates without accompanying measurements of respiration (see Ryther 1956b). The measurement of oxygen production by means of the "light and dark bottle" technique cannot be detected in experiments of less than several days, and the interpretation of values so obtained is equally questionable. Consequently the authors have turned to chlorophyll *a* as an index of photosynthesis, and have attempted to relate photosynthesis at light saturation to the chlorophyll content of the phytoplankton.

THE RELATIONSHIP BETWEEN CHLOROPHYLL AND PHOTOSYNTHESIS AT LIGHT SATURATION

A rather constant relationship between chlorophyll and photosynthesis at any given light intensity has been described by several authors who have worked both in the field (Manning and Juday 1941, Gessner 1949, Edmondson 1955) and in the laboratory (Fleischer 1935, Emerson *et al.* 1940, Blaauw-Jansen *et al.* 1950, Ryther 1956b). In these studies, the relationship appears to hold constant for different species (Edmondson, Ryther) and within a wide range of chlorophyll content of the organisms resulting from their state of nutrition (Fleischer) or the duration or intensity of light to which they had been previously exposed (Blaauw-Jansen *et al.*, Ryther).

A series of measurements were made by the present authors of chlorophyll *a* content and rate of photosynthesis at light saturation of natural phytoplankton populations occurring in the coastal waters around Woods Hole, Massachusetts.

Chlorophyll *a* was determined by filtering 1–3 liters of sea water through a millipore filter and extracting the pigments with acetone (Creitz & Richards 1955). Light absorption of the acetone extract was measured at selected wavelengths in a Beckman Model DU Spectrophotometer according to the methods of Richards with Thompson (1952), and chlorophyll *a* calculated from the nomographs of Duxbury and Yentsch (1956).

Photosynthesis measurements were made under 2000 foot-candles of fluorescent illumination in an incubator cooled by running sea water which kept the experimental vessels within 1°C of the water from which the samples had been taken. Photosynthesis was determined from the difference in dissolved oxygen concentration (Winkler method) in triplicate series of transparent and darkened 30-ml glass-stoppered bottles after 24 hours. The photosynthesis: chlorophyll ratio is expressed as grams carbon assimilated per hour per gram chlorophyll *a*. Carbon assimilation was calculated from evolved oxygen assuming a photosynthetic quotient $\frac{(+O_2)}{(-CO_2)}$ of 1.25 (see Ryther 1956b).

Measurements were made during the period March–July, 1956, at times when the water temperature was 10°, 15° and 20°C, respectively. The mean ratio (photosynthesis: chlorophyll) and standard deviation of approximately 10 measurements at each temperature is given in Table 1. Also included in this table is the mean ratio of 45 measurements made throughout the year between March, 1956, and February, 1957. Although winter values tended to be lower, indicating a temperature effect, the trend was not clear enough to permit a temperature correction. A series of anomalous results, giving ratios 10–20 times those reported in Table 1 was obtained with natural populations from two salt ponds, Eel Pond in Woods Hole and Great Pond in Falmouth, Massachusetts. The phytoplankton in these ponds was characterized by an abundance of small, green algae. It is believed that the high values resulted at least in part from the inability to extract completely the pigments from these cells. These atypical results have not been included here.

TABLE 1. *The ratio of photosynthesis at light saturation to chlorophyll (g carbon assimilated/hour/g chlorophyll) in phytoplankton populations and cultures*

Source	Reference	No. measurements	Temp. (°C.)	*R*	
				Mean	Std. dev.
Coastal water (Woods Hole)	Ryther & Yentsch				
March–April		15	10	3.4	2.8
May		7	15	5.2	0.9
June–July		9	20	5.2	2.5
Annual average		45		5.7	2.8
Cultures—marine phytoplankton	Ryther & Yentsch	18	10	2.8	2.1
		7	15	4.8	0.8
Georges Bank	Riley (1941)	Annual mean		3.0	
Wesslingsee, Bavaria	Gessner (1949)	Annual mean		3.0	
Wisconsin lakes	Manning & Juday (1941)	19		2.1	1.8
Mean				3.7	

Similar measurements were made with cultures of marine phytoplankton including the diatoms *Skeletonema costatum*, *Amphora perpusilla*, *Navicula* sp., *Nitzschia palea*, and *Nitzschia closterium* (*Phaeodactylum tricornutum*); the green flagellates *Dunaliella euchlora* and *Chlamydomonas* sp.; the dinoflagellate *Prorocentrum micans*; and the chrysophyte *Olisthodiscus* sp.

The cultures were routinely grown at 15°C under approximately 1000 foot-candles of fluorescent illumination. Prior to the experiments the cultures were diluted with enriched sea water so that the cell suspensions did not appreciably reduce the light intensity. Mean values and standard deviations for all species at 10° and 15° are given in Table 1. The low ratio at 10° may have resulted in part from the fact that the organisms were not previously conditioned

TABLE 2. *A comparison of some* in situ *productivity measurements with values estimated from chlorophyll, radiation, and extinction coefficient*

Place	Reference	Surface radiation (g cal./cm²/day)	k	Chlorophyll (mg/m³)	Calculated production	Measured production
					(g C/m²/day)	
N. W. Atlantic	Riley (1939)					
4 northern stations		460[1]	0.10	2.1	1.67	0.70
14 tropical stations		460[1]	0.05	1.0	1.57	1.18
Long Island Sound	Riley (1956) Conover (1956)					
March–May, '52		400	0.46	7.2	1.17	1.06
Feb.–March, '53		252	0.73	11.8	0.90	1.32
Aug.–Nov., '53		347	0.63	5.6	0.61	0.95
Friday Harbor, Washington	Yentsch (unpubl.)	300	0.13	1.0	0.48	0.34
East Sound, Washington	Yentsch (unpubl.)	700	0.30	15.0	4.80	5.10
Gulf of Alaska	Yentsch (unpubl.)	229[1]	0.10	2.5	1.34	1.50
Woods Hole Harbor	Ryther & Yentsch	550	0.27	3.35	1.05	1.63
		480	0.27	1.69	0.51	0.79
		610	0.24	2.80	1.04	1.10

[1] Estimated from Kimball (1928).

to that temperature before the start of the experiments.

Also included in Table 1 are photosynthesis:chlorophyll ratios from a series of Wisconsin lakes (Manning and Juday 1941), the Wesslingsee (Gessner 1949) and George's Bank (Riley 1941). The ratios compiled in the table are in such close agreement that the mean from all sources has been taken as a working value, which is 3.7 g carbon/hour/g chlorophyll.[2]

THE ESTIMATION OF PRODUCTION FROM RADIATION, TRANSPARENCY, AND CHLOROPHYLL

Assuming now that 3.7 g carbon are assimilated per hour at light saturation for each gram of phytoplankton chlorophyll, Equation (1) may be written

$$P = \frac{R}{k} \times C \times 3.7 \tag{3}$$

where

C = g chlorophyll/m³ in a sample of a homogeneously distributed population.

Similarly Equation (2) may be written

$$P_d = R_d \times C_d \times 3.7 \tag{4}$$

where

C_d = g chlorophyll/m³ at depth (d).

In Table 2 are given some production values obtained from *in situ* "light and dark bottle" oxygen experiments (Yentsch, Ryther and Yentsch), and from *in situ* changes in dissolved oxygen in the water column or a combination of the two methods (Riley). For each value are also given data for chlorophyll, daily surface radiation, and extinction coefficient, measured or estimated as indicated in the table. Except in the case of Woods Hole Harbor, where the phytoplankton are known to have been evenly distributed with depth, the vertical distribution of chlorophyll is not known. Consequently production has been calculated from Equation (3), assuming even vertical distribution, though this was probably not true in every case. The calculated values are given in Table 2 beside those obtained from *in situ* measurements.

DISCUSSION

There is, on the whole, close agreement between production values calculated by the method outlined above and those obtained from *in situ* rate measurements. This agreement, which is consistent for situations in which production varies by an order of magnitude, represents the best approximation of a critical test of the method. However, it should be pointed out that production values calculated from long term *in situ* bottle experiments are, themselves, subject to severe criticism, and, as a consequence, disagreement between values obtained by the new method and the earlier estimates does not necessarily represent the inadequacy of the former.

---

[2] This is equivalent to an assimilation number (g/CO_2 assimilated/hour/g chlorophyll) of 13.6.

Probably the weakest point in the foregoing treatment is the photosynthesis-chlorophyll factor. There is little reason to assume that this must be constant under all conditions. The presence of inactive chlorophyll in plants, as reported by Smith (1954) and others, and the findings by Gillbricht (1951) and Krey (1952) of relatively large quantities of chlorophyll associated with non-living detrital material indicate that the pigment is not an infallible indicator of photosynthetic capacity. However, much of the error from these sources may be circumvented by using precise, narrow band spectrophotometric analyses, as referred to above, since neither the precursors nor the degradation products of chlorophyll have exactly the same absorption characteristics as the active pigment. The fact that the chlorophyll concentration of phytoplankton varies diurnally in nature (Yentsch and Ryther 1957) further complicates the picture. There is undoubtedly some temperature effect. Finally, the relationship between chlorophyll and photosynthesis undoubtedly shows some variability between the major groups and perhaps even between species of plankton algae. The need is apparent for a more detailed study of this relationship which would perhaps allow the investigator to take into account such factors as temperature, light, season, time of day, or species composition in refining the value suggested above. However, much of the variability in the photosynthesis: chlorophyll ratio indicated in Table 1 is undoubtedly due to errors in the measurement of both of these variables by standard field methods, particularly at their lower limits of detectability—errors which are compounded by taking their quotient.

Despite these errors and any true variability in the photosynthesis: chlorophyll ratio, it seems unlikely in view of the existing evidence that a correct ratio under most conditions differs from that suggested above by more than a factor of two. When one considers that both radiation and chlorophyll concentration fluctuate in nature by more than an order of magnitude it is obvious that any departure from the mean photosynthesis: chlorophyll ratio employed above will be of relatively minor significance in affecting the calculated value for production.

The obvious advantage of this method is that it completely eliminates the necessity for making time studies of photosynthesis or other related changes which are awkward, time consuming, and, in the case of oligotrophic ocean waters, unreliable. For routine survey work, average radiation data for any date and latitude may be obtained from the tables of Kimball (1928). If a submarine photometer is not available, the extinction coefficient may be estimated from Secchi disc readings (see Poole and Atkins 1929). Filtered chlorophyll samples may be stored for a period of months if properly treated (Creitz and Richards 1955) and the determinations carried out ashore. As a consequence, productivity measurements may now be made a routine phase of oceanographic investigation requiring a minimum of time, expense, and interference with other activities.

Algal cultures used in the experiments described above were originally obtained from Dr. B. M. Sweeney (*Prorocentrum micans*), Dr. L. Provasoli (*Amphora perpusilla, Nitzschia palea, Olisthodiscus* sp.), and Dr. R. Lewin (*Skeletonema costatum*). The other species were isolated in this laboratory. The authors gratefully acknowledge the technical assistance of Mrs. R. W. Kahler.

REFERENCES

Blaauw-Jansen, G., J. G. Komen, and J. B. Thomas. 1950. On the relation between the formation of assimilatory pigments and the rate of photosynthesis in etiolated oat seedlings. Biochim. et Biophys. Acta., **5**: 179–185.

Conover, S. A. M. 1956. Oceanography of Long Island Sound, 1952–1954. IV. Phytoplankton. Bull. Bingham Oceanogr. Coll., **15:** 62–112.

Creitz, G. I., and F. A. Richards. 1955. The estimation and characterization of plankton populations by pigment analyses. III. A note on the use of "millipore" membrane filters in the estimation of plankton pigments. J. Mar. Res., **14:** 211–216.

Duxbury, A. C., and C. S. Yentsch. 1956. Plankton pigment nomographs. J. Mar. Res., **15:** 92–101.

Edmonson, W. T. 1955. Factors affecting productivity in fertilized salt water. Pap. Marine Biol. & Oceanogr. Supp. to Vol. 3, Deep-Sea Res., 451–464.

Emerson, R., L. Green, and J. L. Webb. 1940. Relation between quantity of chlorophyll and capacity for photosynthesis. Plant Physiol., **15:** 311–317.

Fleischer, W. E. 1935. The relation between chlorophyll content and rate of photosynthesis. J. Gen. Physiol., **18:** 573–597.

Gessner, F. 1949. Der Chlorophyllgehalt im See und seine photosynthetische Valenz als geophysikalische Problem. Schweiz. Zeit. Hydrol., **11:** 378–410.

Gillbricht, M. 1951. Untersuchungen zur Productions biologie des Planktons in der Kieler Bucht. I. Kieler Meeresf., **8:** 173–191.

Kimball, H. H. 1928. Amount of solar radiation that reaches the surface of the earth on the land and on the sea, and the methods by which it is measured. Mon. Weath. Rev., **56:** 393–398.

Krey, J. 1952. Untersuchungen zum Sestongehalt des Meerwassers 1: Der Sestongehalt in der westlichen Ostsee und unter Helgoland. Ber. Deutsch. Komm. Meeresf., **12:** 431–456.

Manning, W. M., and R. E. Juday. 1941. The chlorophyll content and productivity of some lakes in northeastern Wisconsin. Trans. Wis. Acad. Sci., Arts Lett., **33:** 363–393.

Poole, H. H., and W. R. G. Atkins. 1929. Photo-electric measurements of submarine illumination throughout the year. J. Mar. Biol. Assoc., U. K., **16:** 297–324.

Richards, F. A., with. T. G. Thompson. 1952. The estimation and characterization of plankton populations by pigment analyses. II. A spectrophotometric method for the estimation of plankton pigments. J. Mar. Res., **11:** 156–172.

Riley, G. A. 1939. Plankton studies II. The western North Atlantic, May–June, 1939. J. Mar. Res., **2:** 145–162.

——— 1941. Plankton studies IV. Georges Bank. Bull. Bingham Oceanogr. Coll., **7**(4): 1–73.

——— 1956. Oceanography of Long Island Sound, 1952–1954. IX. Production and utilization of organic matter. Bull. Bing. Oceanogr. Coll., **15:** 324–334.

Ryther, J. H. 1956a. Photosynthesis in the ocean as a function of light intensity. Limnol. & Oceanogr., **1:** 61–70.

——— 1956b. The measurement of primary production. Limnol. & Oceanogr., **1:** 72–84.

Smith, J. H. C. 1954. The development of chlorophyll and oxygen evolving power in etiolated barley leaves when illuminated. Plant Physiol., **29:** 143–148.

Steemann Nielsen, E. 1952. The use of radioactive carbon (C^{14}) for measuring organic production in the sea. J. Cons. Int. Explor. Mer., **18:** 117–140.

Yentsch, C. S., and J. H. Ryther. 1957. Short term variations in phytoplankton chlorophyll and their significance. Limnol. & Oceanogr., **2:** 140–142.

Contribution No. 903

Reprinted from LIMNOLOGY AND OCEANOGRAPHY
Vol. II, No. 3, July, 1957
Printed in U.S.A.

An Improved Method for the Determination of Preserved Plankton Volumes[1]

With the increasing use of plankton volumes as a parameter in marine biology it seemed desirable to eliminate certain difficulties in the usual method of volume determination by filtration (see Yentsch and Hebard 1957). The objections to this method are: (1) getting rid of interstitial water during filtration and, (2) loss and mangling of delicate specimens making later identification difficult if not impossible. It is thought that the method presented here will eliminate these objections with no increase in time or labor.

The principle is based on the colorimetric method of volume determination of blood plasma utilizing a coloring material which is not taken up by the blood cells or, in this case, the preserved plankton organisms. The procedure consisted of making up the plankton sample with sea water and formalin to a known volume in a volumetric flask, preferably as small as convenience would allow for later sampling. The sample was shaken and allowed to settle for five minutes (more for very small organisms), leaving a supernatant fluid only slightly cloudy with animal fragments and various debris. A small sample was withdrawn from the supernatant, measured as a blank in a Klett-Summerson colorimeter, and returned to the flask together with 1 ml of a stock color solution (diluted india ink). The flask was then shaken again and allowed to settle for five minutes after which a second measurement was made with the Klett. A simple computation gave the volume of contained plankton:

$$\text{plankton volume} = (V_F + 1) - \frac{(V_S + 1)K_S}{(K_T - K_B)}$$

where:

V_F = volume of flask containing plankton
V_S = any convenient but known volume of water in which 1 ml of stock coloring has been diluted for measurement, in this case 100 ml
K_S = Klett units, measurement of V_S
K_B = Klett units, for blank supernatant from plankton sample made up to V_F
K_T = Klett units for supernatant from plankton sample plus 1 ml stock color.

Some comparisons of the filtration and colorimetric technique are given in Table 1. It will be noted that volumes determined colorimetrically are less than those by filtration, which is attributed to the interstitial fluid remaining after filtration. The differences between filtration and colorimetric determinations are generally comparable to those obtained by Yentsch and Hebard (1957) who compared filtration volumes with those of plankton air-dried for 24 hours. Filtration volumes in this report were obtained by measuring the total sample volume, vacuum filtering through fine bolting silk, and then subtracting the volume of the filtrate from that of the original sample.

TABLE 1. *Comparison of plankton volumes (in ml) by two methods*

Filtration	Colorimetric
85	80
12	10
77	69
82	79

Greater accuracy in the colorimetric method is obtained by keeping the volume to which the plankton sample is made up small and by using a more concentrated color stock. A convenient concentration was found to be approximately 2 ml of Higgins American India Ink diluted to about 200 ml with water. The addition of 1 ml of this stock produced no objectionable color in the plankton sample and, indeed, could hardly be distinguished from some samples whose contents had been leached by standing several months in preservative. All samples used were preserved with formalin neutralized with borax.

---

[1] Contribution No. 230 from the Bermuda Biological Station. Contribution No. 903 from the Woods Hole Oceanographic Institution.

REFERENCES

Yentsch, C. S., and J. F. Hebard. 1957. A gauge for determining plankton volume by the mercury immersion method. Journ. du Cons., **22**: 184–190.

W. H. Sutcliffe, Jr.
Bermuda Biological Station
St. George's, Bermuda

Contribution No. 905

COMPARISON OF CLAY FROM THE CONTINENTAL SHELF OFF LONG ISLAND WITH THE GARDINERS CLAY

WILLIAM D. ATHEARN

Reprinted for private circulation from
THE JOURNAL OF GEOLOGY
Vol. 65, No. 4, July 1957
PRINTED IN U.S.A.

COMPARISON OF CLAY FROM THE CONTINENTAL SHELF OFF LONG ISLAND WITH THE GARDINERS CLAY[1]

WILLIAM D. ATHEARN
Woods Hole Oceanographic Institution

Late in 1955 the Woods Hole Oceanographic Institution received from Moran, Proctor, Mueser, and Rutledge, consulting engineers of New York City, a few samples taken from a boring made at the proposed site of an Air Force Texas Tower (TT-4), located about 60 miles south of Moriches Bay, Long Island. Among these samples was an undisturbed clay sample, suggestive of the Pleistocene Gardiners clay of Long Island. For purposes of comparison, the same company later made available a group of ten core samples collected from a formation thought to be Gardiners clay on western Long Island. Standard mechanical analysis procedures were carried out on certain of these samples prior to their being examined for microfossils.

The sample from the TT-4 site was located 70 feet below the ocean bottom under a water depth of 185 feet. The overlying sediments were coarse sand and fine gravel. The moist color of this sample was olive-gray as determined from the "Rock Color Chart" published by the Geological Society of America in 1951. The sediment is a silty clay with a sand content of about 6 per cent. The sand is mostly quartz with a number of reddish-brown silt-stone particles presumably reworked from an older formation. Occasional Foraminifera are found in this coarser fraction.

The more common species are *Elphidium clavatum* Cushman, *E. incertum* (Williamson), and *Quinqueloculina* cf. *lata* Terquem or *seminulum* (Linné). There were also a few reworked fossil species of the genera *Gyroidina*, *Elphidium*, and *Cassidulina*(?). These probably came from late Cretaceous or Tertiary coastal-plain deposits to the northwest. The unreworked assemblage corresponds fairly closely to those found by L. Weiss (1954) in certain samples of the Gardiners clay on eastern Long Island, even to the absence of arenaceous forms. Except for this absence, he states that the Gardiners clay assemblages are very similar to those found at present in Great South Bay, Long Island (p. 156–157). He suggests that the lack of arenaceous forms may possibly indicate warmer climatic conditions during the Gardiners time than at present.

Of the ten samples from western Long Island, four were selected for mechanical analysis and microfossil examination. The boring was located near an old arm of Jamaica Bay (now filled in) about 1½ miles north of Idlewild Airport in the Burrough of Queens. The samples used were collected from levels 90 feet (1-U), 107 feet (4-U), 148½ feet (7-U), and 179 feet (10-U) below the surface. Ground elevation here is 16.6 feet above present sea level.

In color, samples 1-U and 7-U were olive-gray, 4-U was dark greenish-gray, and 10-U was olive-black. It is to be noted that Weiss reports a considerable variation in color within the various levels of the Gardiners clay throughout Long Island.

The coarse-grained fraction of each sample here composed less than 1 per cent of the total, except in sample 10-U, where it was about 2.5 per cent. This fraction was composed entirely of fine sand sizes with a considerable amount of mica. Sample 4-U also contained a noticeable amount of fibrous plant material.

Silt sizes comprised 58–64 per cent and clay sizes 30–40 per cent of the total sample

---

[1] Manuscript received March 4, 1957. Contribution No. 905 from the Woods Hole Oceanographic Institution.

weights. No attempt was made to determine the mineralogy of the fine sizes either of these samples or of that from the TT-4 site. Considering the analyses, these sediments are actually clayey silts. Possibly this is true of much of the Gardiners clay.

Inspection of the samples for microfossils was not very rewarding. There were no Foraminifera found in any of the four samples studied. Sample 1-U, however, did contain a considerable population of diatoms of circular shape. The genera *Coscinodiscus* and *Actinoptychus* are probably represented here. Sample 4-U also contained a few diatoms of the same type, along with the previously mentioned fibrous plant material.

Weiss noted similar assemblages of diatoms with no other microfossils in some layers of green-gray and black micaceous Gardiners clay from the Brookhaven area in eastern Long Island.

There is little doubt that the samples from the Idlewild Airport vicinity belong to the Gardiners clay group. The variability reported in thickness, color, lithology, and faunal content is indicative of a shallow-water, lagoonal environment of deposition similar to that of the present bays along the south shore of Long Island. Weiss states that the deposition apparently occurred during the last interglacial (Sangamon) stage and seems to be the only marine fossiliferous clay in the Pleistocene deposits of Long Island (p. 148).

The general similarity in lithology and faunal content between the TT-4 sample and some of the Gardiners clay deposits suggests that this sediment may also be Gardiners clay. The overlying coarser sediments may well be deposits from the Hudson River accompanying the general postglacial rise in sea level.

REFERENCES CITED

WEISS, L., 1954, Foraminifera and origin of the Gardiners clay (Pleistocene), eastern Long Island, New York: U.S. Geol. Survey, Prof. Paper 254-G, p. 143–163.

Contribution No. 907

Reprinted from the Proceedings of the National Academy of Sciences,
Vol. 43, No. 7, pp. 576–580. July, 1957.

*STRONTIUM 90 IN NORTH ATLANTIC SURFACE WATER**

By Vaughan T. Bowen and T. T. Sugihara

WOODS HOLE OCEANOGRAPHIC INSTITUTION AND CLARK UNIVERSITY

Communicated by C. O'D. Iselin, April 26, 1957

The various test nuclear fission explosions carried out since 1945 have resulted in the world-wide dissemination of detectable amounts of long-lived radioactive strontium 90.[1] This isotope must have been delivered to the Atlantic Ocean essentially completely as fallout, and consequently to the surface layers only. Since the half-life of the radioactivity is long (28 years) compared with the time span over which it has been delivered, measurements of the concentration of radioactivity in sea-water strontium may be used to test various hypotheses both of the marine geochemistry of strontium and of the circulatory mechanism of the upper layers of the oceans.

Theorizing about the marine geochemistry of strontium radioisotopes is made simple by the high concentration of the element in sea water (about 8.2 mg/l at chlorinity 19.38 per mill).[2] The strontium is present preponderantly as ions in solution and at so high a concentration that biological and chemical processes rarely produce a detectable change in the Sr:Cl ratio. This same high concentration, coupled with the higher concentration of calcium, makes the chemical preparation of small amounts of strontium radioactivity a difficult task. Fortunately strontium 90 decays to produce daughter radioactive yttrium 90 (half-life, 64 hours), and in this form there can be prepared for counting nearly weightless samples, which represent the radioactivity of very large amounts of elemental strontium. It was our initial hope that the yttrium 90 radioactivity of sea water could be extracted directly, but several attempts with thenoyltrifluoroacetone in benzene as extractant yielded products too heavily contaminated with natural radioactivities.

The procedure which we have finally adopted, and which has yielded the data presented below, is based on the initial precipitation of strontium and calcium together as carbonates, their reprecipitation as carbonates in the presence of enough tetrasodium ethylenediamine tetraacetate (EDTA) to hold most of the calcium in solution, and separation of strontium as nitrate in 78 per cent HNO_3. This last step is repeated once after ferric hydroxide and barium chromate scavenging to remove natural radioactivities, and the strontium is collected and weighed as $SrCO_3$. This precipitate, redissolved, can be milked, at intervals of two weeks or more, of the yttrium 90, which is then counted in a small volume GM counter[3] with anticoincidence shielding, substantially as described by Martell.[4] Our milking procedure for yttrium 90 consists of coprecipitation as hydroxide with 5 mg. of specially purified ferric ion and filtration on commercial Millipore HA filters.

These filters contribute no radioactivity and conform easily to the Bakelite hemicylindrical sample holder of the counter.

Initially, considerable difficulty was experienced in obtaining good yields from the 50 to 200-liter samples of sea water required. In fact, the yields on the samples reported here (Table 1) varied from low to very low. Modification of the detailed procedure in the direction of higher carbonate concentrations at precipitation, and of reduction of the HNO_3 concentration in the nitrate precipitations, has led to recoveries in the neighborhood of 70 per cent on several samples.

TABLE 1

STRONTIUM 90 IN NORTH ATLANTIC SHELF WATER

	STATION				
	Woods Hole	Bear 91	Bear 94	Bear 98	Bear 104
Position	41°31′ N., 70°40′ W.	40°18′ N., 71° W.	40° N., 71° W.	39°42′ N., 71°W.	39°10′ N., 71° W.
Date (1956)	6/4	2/9	2/10	2/10	2/11
Sr^{90} d/min/100 liters	12.7 ± 3.4	15.0 ± 3.0	30.0 ± 1.6	10.3 ± 1.6	6.3 ± 1.6
Salinity (per mill)	31–32	32.74	33.20	34.23	34.42
Depth (meters)	5	110	275	2,000	2,750
Depth of mixed layer (from O_2 curve)	. . .	90	40	100	160
Sr^{90} d/min/100 cm² (calculated for mixed layer)	6.3	135	120	100	100

Although satisfactory blank determinations are difficult to devise, we have carried out two: one on distilled water and the other on 400 gm. of reagent-grade calcium chloride. Since neither yielded any radioactivity assignable to strontium 90, we are satisfied that no reagent blank ought to be subtracted from the results obtained.

Counting Corrections and Calculations.—The observed activity is resolved by half-life into 64-hour (Y^{90}) and other components (if any). In no case has there been more than 0.2 counts per minute (cpm) of a contamination activity of half-life longer than that of Y^{90}. The activity of Y^{90} is extrapolated to the time of separation of Y from Sr. The observed counting rate is converted to an absolute disintegration rate by applying the appropriate counting corrections[3, 5] (1) for absorption of radiation by the Mylar cover, by the air path to the counter, and by the wall (2.70 mg/cm²); (2) for self-absorption of radiation by the sample itself; (3) for backscattering of radiation by the Bakelite cylinder; and (4) for the geometrical solid angle subtended by the counter. The method of Libby and co-workers is intended for "thick" samples, more than one absorption half-thickness thick. It is equally applicable for thinner samples as long as the third correction is indicated. The backscattering factor has been determined experimentally. The fourth factor has been determined with natural K^{40} as described by Martell.

In magnitude, the correction factors are (1) +2 per cent; (2) +1 per cent; (3) −13 per cent; and (4) 0.33—that is, the counter on purely geometrical grounds can see 33 per cent of the radiation emitted by the sample.

Since at the time of separation Y^{90} was in secular equilibrium with Sr^{90}, the calculated Y^{90} disintegration rate is also that of Sr^{90}.

Except for one series of measurements in which temperature control was poor, at no time did the background counting rate (average 0.43 cpm) fluctuate more than 0.04 cpm from the average. Background measurements were made at least once a day.

Results and Discussion.—The Sr^{90} concentrations and other pertinent data for five surface sea-water samples are presented in Table 1. The four offshore samples (Bear numbers) were taken during a cruise studying the physical oceanography of shelf waters.[6] Our colleagues supplied data on the distribution, to depths of 250 meters, of temperature, salinity, dissolved oxygen, and total phosphorus. As shown in Figure 1, the curves of density (σ_T) versus depth for these stations indicate no density gradient sufficient to prevent mixing down to considerable depths. However, the oxygen concentration is uniform generally to lesser depths. At this season in the North Atlantic, dissolved oxygen is supplied principally by solution at the surface, low light intensity keeping photosynthesis minimal. We have, then, taken the nearly straight portion of the curve of dissolved oxygen versus depth as an indicator of the minimum depth to which mixing was actually taking place. By extending the concentration of Sr^{90} found at the surface (Table 1, third line) over these minimum depths (Table 1, sixth line), the minimum amount of Sr^{90} delivered per unit area of sea surface has been calculated (Table 1, seventh line). The 5-meter depth, which was used in the calculation for Woods Hole Harbor, is certainly not applicable, since this is a mixture of recently introduced water from Buzzards Bay and from Vineyard and Nantucket sounds. A proper figure for depth here does not seem to be assessable, but, as we shall see, some conclusions can be drawn from the very absurdity of the value calculated.

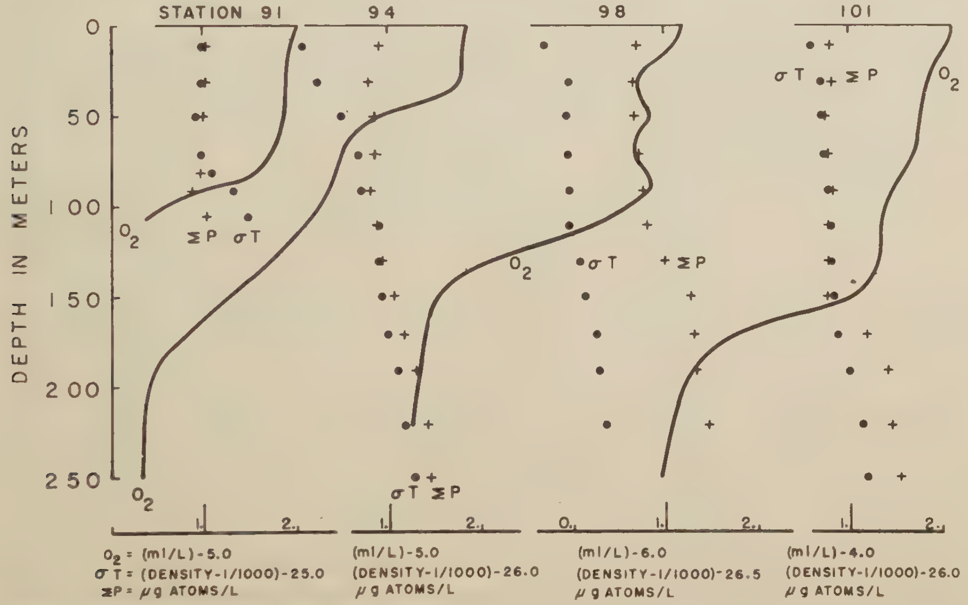

FIG. 1.—Variation with depth of dissolved oxygen (O_2), total phosphorus (ΣP), and density (σ_T) at the four offshore stations.

Libby[1] has estimated from the fallout measurements by the Atomic Energy Commission that at the end of 1955 the mean total delivery of Sr^{90} from all nuclear tests amounted to 112 disintegrations per minute per 100 cm^2 in the continental United States, or to 23.2 d/min/100 cm^2 for the rest of the Northern Hemisphere between 0° and 50° N. Since the figure for the continental United States is heavily weighted by close-in fallout from the Nevada tests, it seems unlikely that the coastal-shelf area we are considering can be estimated to have received as much as 80 d/min/100 cm^2. Furthermore, this must be thought to have been delivered over a period of years, though relatively little before 1953. In northern waters, where winter cooling annually permits mixing to considerable depths, this slow rate of delivery must have permitted a considerable transport of Sr^{90} vertically beyond the present minimum mixed depth indicated by the dissolved oxygen curves. In fact, however, our analyses are incompatible with mixing even within the layer of uniform oxygen content. A supply of Sr^{90} of 80 d/min/100 cm^2 could be mixed to a depth of only 25 meters to permit the high concentration of 30 d/min/100 liters found at Station Bear 94.

We should not try to explain these discrepancies only in terms of local variations in the depth to which the water column has been thoroughly mixed. In addition to the inherent improbability of such an explanation, from the oceanographic point of view, it seems unlikely to be simple coincidence that the two samples overlying deep water are lower in Sr^{90} than are the three overlying shallow water. It seems most probable that slow mixing in the horizontal plane has permitted long-term retention of individuality by the water masses. The other properties which are measured either are active, in that salinity and temperature cannot vary without modifying the density and consequently the position of a water mass, or, if inert, are rapidly modified by the position of the water, oxygen being supplied at the surface by solution, and both oxygen and phosphorus being affected by biological processes in the illuminated zone. Thus it is not inherently improbable that a mass of water should appear uniform by the usual oceanographic criteria and still exhibit considerable inhomogeneity with respect to the radioisotope like Sr^{90}, which, we believe, once added to the water, can have its concentration altered only by mixing with water of lower concentration. Until we have obtained some series annually from the same ocean areas and some series of vertically spaced samples as well, it will not be possible to estimate how much of the isotope distribution discrepancy is to be assigned to a given plane.

Some tritium analyses on Labrador Sea samples collected by Soule in 1954 and reported by Begemann and Libby[7] are pertinent. In this area, although in March the uniform density layer extended to considerable depths, variations in tritium concentration by a factor of five were found within tens of miles at the surface and within tens of meters in depth. Unfortunately the depth sampling did not extend beyond 180 meters, but within this range the tritium variation appeared to be random. It would evidently be most instructive to have both Sr^{90} and tritium analyzed on the same samples. Should low isotope concentrations coincide with any regularity, it would be difficult to avoid conceiving of convective mixing in northern waters as occurring by the transport of large boluses of water of equal density, coming quickly to equilibrium with respect to components supplied at the surface or controlled by biological activity, but retaining their identity with respect to some components for which there is no source of rapid supply. It appears that mixing in this way might provide much greater mass transport to depth at the seasonal breakdown of thermal stratification than would conventional turbulent mixing.

Our present program includes a series of vertical sampling stations in both North and South Atlantic waters to be analyzed for a series of radioisotopes, as well as being part of extensive physical oceanographic analyses. We are at present in the process of analyzing a series of surface samples along the line 60° W. longitude from 17° N. to 28° N., where the thermal structure is very different.

It appears to us that the relatively high Sr^{90} concentration of Woods Hole Harbor water, which represents large areas of shallow basins where interaction between water and bottom ought to be maximal, may be taken as indicating that transfer of the radioisotope to sediments must be very slow. It has been estimated from other considerations by Odum[8] that the half-time of strontium in the oceans is about a million years, and, because of the high strontium concentration of sea water, we do not expect isotope exchange to favor Sr^{90} transfer to the sediments. With Professor E. H. Moore, we are now in the process of examining the Sr^{90} content of a number of Buzzards Bay surface sediments whose biological activity and physical properties are being separately studied.

It is a pleasure to acknowledge the assistance of Miss Sybil A. Campbell with the chemistry and of Messrs. P. J. Drevinsky and S. Klainer with counting measurements.

---

* Contribution No. 907 from the Woods Hole Oceanographic Institution. Work supported by the Office of Naval Research under Contract Nonr-1238(00). Low-level counting equipment largely supported by National Science Foundation Grant 984 to T. T. Sugihara.

[1] W. F. Libby, "Radioactive Strontium Fallout," these PROCEEDINGS, **42,** 365–390, 1956.

[2] T. J. Chow, and T. G. Thompson, "Flame Photometric Determination of Strontium in Sea Water," *Anal. Chem.*, **27,** 18–21, 1955; H. T. Odum, "Notes on the Strontium Content of Sea Water, Celestite Radiolaria and Strontianite Snail Shells," *Science*, **114,** 211–213, 1951.

[3] T. T. Sugihara, R. L. Wolfgang, and W. F. Libby, "Large Thin-Wall Geiger Counter," *Rev. Sci. Instr.*, **24,** 511–512, 1953.

[4] E. A. Martell, *Absolute Assay of Strontium 90 in Biological Materials, Soil, Waters and Air Filters* (U. S. Atomic Energy Comm. Rept. AECU 3262, 1956).

[5] W. F. Libby, "Relationship between Energy and Half-Thickness for Absorption of Beta Radiation," *Phys. Rev.*, **103,** 1900–1901, 1956; A. D. Suttle, Jr., and W. F. Libby, "Absolute Assay of Beta Radioactivity in Thick Solids," *Anal. Chem.*, **27,** 921–927, 1955.

[6] This cruise was supported by the United States Fish and Wildlife Service under Contract 14-19-008-2377.

[7] F. Begemann and W. F. Libby, *Continental Water Balance and Storage Times, Surface Ocean Mixing Rates and World-wide Water Circulation Patterns from Cosmic Ray and Bomb Tritium* (AD-110 381, 1956).

[8] H. T. Odum, "The Stability of the World Strontium Cycle," *Science*, **114,** 407–411, 1951.

Contribution No. 908

(*Reprinted from Nature, Vol.* 180, *p.* 291 *only, Aug.* 10, 1957)

Underwater Sounds heard from Sperm Whales*

While the sperm whale (*Physeter catodon*) is one of the more conspicuous cetaceans, it has not figured among the relatively few that have been demonstrated to make underwater sounds, although they have occasionally been suspected of doing so. We have now obtained reliable evidence that they, too, are soniferous.

On March 28, 1957, off the North Carolina coast, our vessel *Atlantis* encountered five sperm whales which permitted the ship to approach as close as 15 metres. During the hour spent with the whales, the engines were frequently shut off to permit listening by means of the echo-sounding receiver. Unfortunately phonographic equipment was not available.

Three types of sound were distinguished. The first, heard before the whales were sighted, was a muffled, smashing noise, with impulses about half a second apart, increasing in intensity to the end of the series. At first it was supposed to be hammering somewhere in the ship, but it was determined that the sound was not made on board. Later, when the whales were in plain sight most of the time, this sound was less conspicuous. A second sound was a grating sort of groan, very low in pitch, which reminded some of a rusty hinge creaking. This lasted as long as five seconds at a time. By far the most common sounds were series of sharp clicks, which were loud enough to blacken the sounding recorder paper, and which usually occurred at intervals of about half a second, but occasionally as rapidly as about five clicks per second. As many as 73 successive clicks were counted. They usually came in groups of 20 or so. Different individuals chimed in from time to time, and there was no period of more than a few seconds without clicks.

The echo-sounding receiver was used for listening on at least thirty different occasions before and after this encounter, and no similar noises were heard.

These observations on *Atlantis* were made by Worthington. It is to be hoped that they will be repeated by others fortunate enough to meet sperm whales, and that they will be supported by phonographic recordings. Although relatively few ships carry broad-band listening and recording gear, many nowadays have echo-sounding equipment. Ordinarily, this can be used for listening, with the transmitter silenced. It is true that most such devices will convey an imperfect version of the sounds heard, since they are designed for a very narrow frequency band centred on the transmitting frequency, and are then often heterodyned well down the spectrum. This, for example, applies to the sounds reported by Worthington, whose equipment selected and emphasized frequencies between 10–17 kc./s. and delivered them to him near 4 kc./s. Nevertheless, at this early stage in our study of marine sounds, such a phonograph record may still be of value, especially if the characteristics of the listening and recording system are known.

---

* Contribution No. 908 from the Woods Hole Oceanographic Institution

While the absence of adequate records makes the matter speculative, it seems likely that the clicks heard by *Atlantis* may correspond to the familiar clicks employed in echo-location by the smaller odontocetes[1]; the 'groan' reported by Worthington may turn out to be a rapid succession of clicks.

Occasionally, in the accounts of the nineteenth-century open-boat sperm whalers, there are allusions to comparable sounds made by the quarry. Thus Bennett's creaking[2] reminds one of Worthington's groan. One of the last of the New Bedford whalers, the late Mr. Henry Mandly, jun., has told Schevill of hearing, in calm weather, impulsive noises from below while waiting in the boats for sperm whales to reappear; these he said were believed to be the whale "snapping his spouters". In spite of the allusions of Davis[3], which describe this act as occurring in air at the surface, it seems improbable that the blowhole as such is involved. Possibly this 'snapping' and Worthington's loud clicks are the same. It is quite likely that the whalers, undisturbed by engine noises, could at times have heard these abrupt under-water sounds.

Note added in proof. On June 4 and 27, R. H. Backus, in our vessel *Bear*, succeeded in making phonographic recordings of sperm whales some 200 miles south of Cape Cod. These recordings closely resemble Worthington's description.

L. V. Worthington
William E. Schevill
Woods Hole Oceanographic Institution,
Woods Hole, Massachusetts. April 24.

---

[1] Schevill, W. E., and Lawrence, B., Breviora, Mus. Comp. Zool. Harvard, No. 53, 5 (1956).

[2] Bennett, F. D., "Narrative of a Whaling Voyage round the Globe", 2, 206 (London, 1840).

[3] Davis, W. M., "Nimrod of the Sea", pp. 236, 355 (New York, 1874).

Printed in Great Britain by Fisher, Knight & Co., Ltd., St. Albans.

Contribution No. 909

Oceanus goes to the bottom of the Sea

Jan Hahn

Reprinted from ***Oceanus,*** Vol. V, nos. 1 and 2, pp. 20 - 31.
Contribution No. 909 from the Woods Hole Oceanographic Institution.

A sea mount in the western Caribbean Sea rises 5,400 feet above the ocean bottom. A remarkable feature are the foothills to one side of the mount and the level plain on the other side. Steepness of the mount is greatly exaggerated. The distance between the times 0740 and 0840 represents about ten miles.

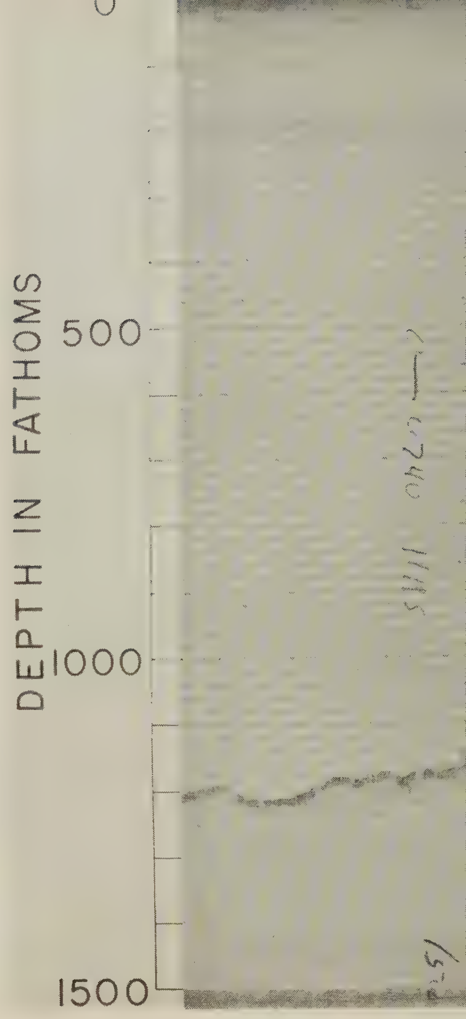

Oceanus goes to the bott

THE ocean bottom has a peculiar fascination; what does it look like? what is its topography? how does it form? are but a few questions arising as we think of that surface lying miles below a ship. To watch the profile of the ocean bottom unrolling on the paper of a recording echo sounder is as fascinating as observing the heavens through a powerful telescope. Moving the ship or moving the field of view of the telescope may, at any moment, reveal a hitherto unknown feature. More so in the case

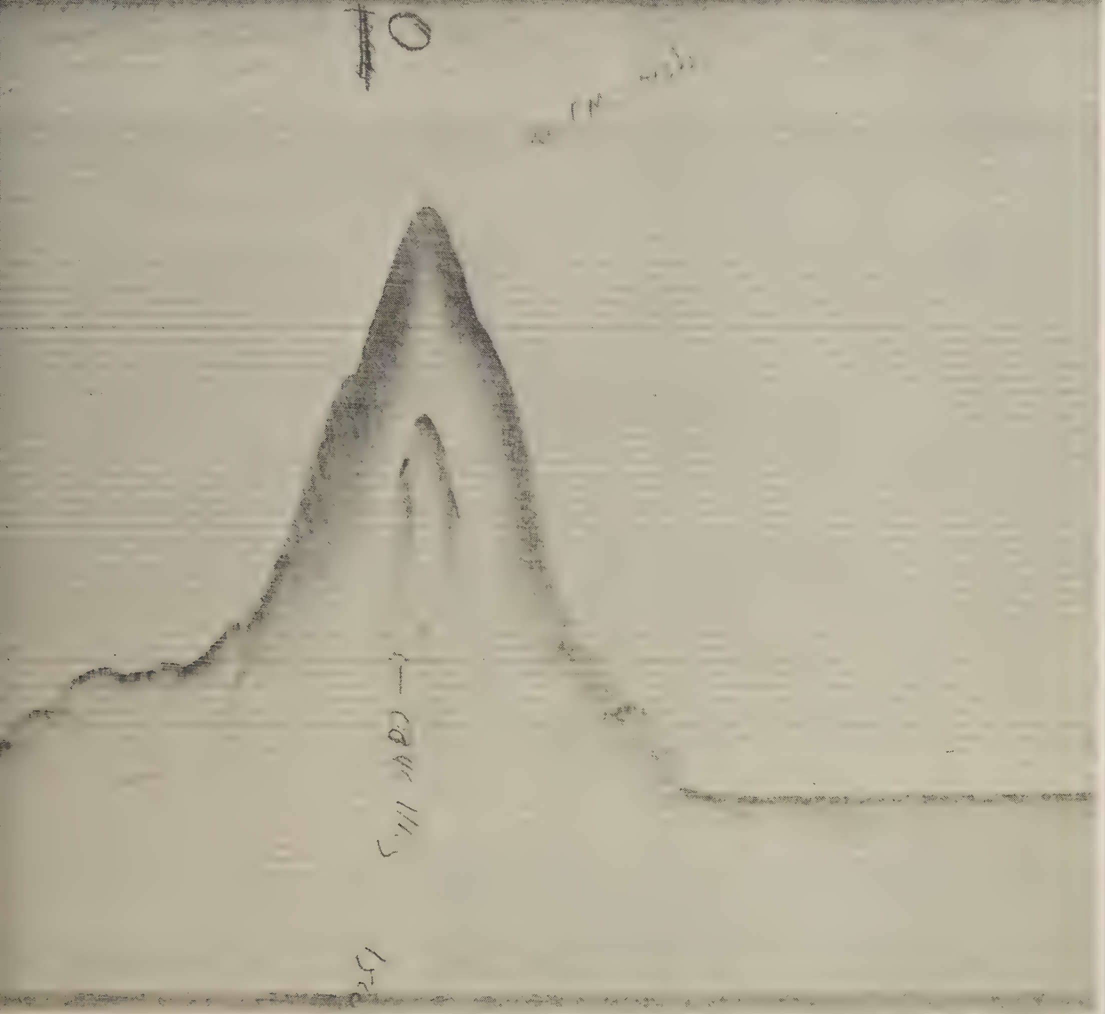

the sea.

of echo sounding, as the ocean bed still is inadequately charted.

Two years ago we described the precision echo sounder recording system developed at the Institution by S. T. Knott and others of Dr. J. B. Hersey's geophysics group*. Able to measure the sound pulse's travel time with great accuracy, this versatile system has been used extensively on many cruises of our ships and now has been developed to the

---

* See: New Instruments, Oceanus, Vol. III, No. 2

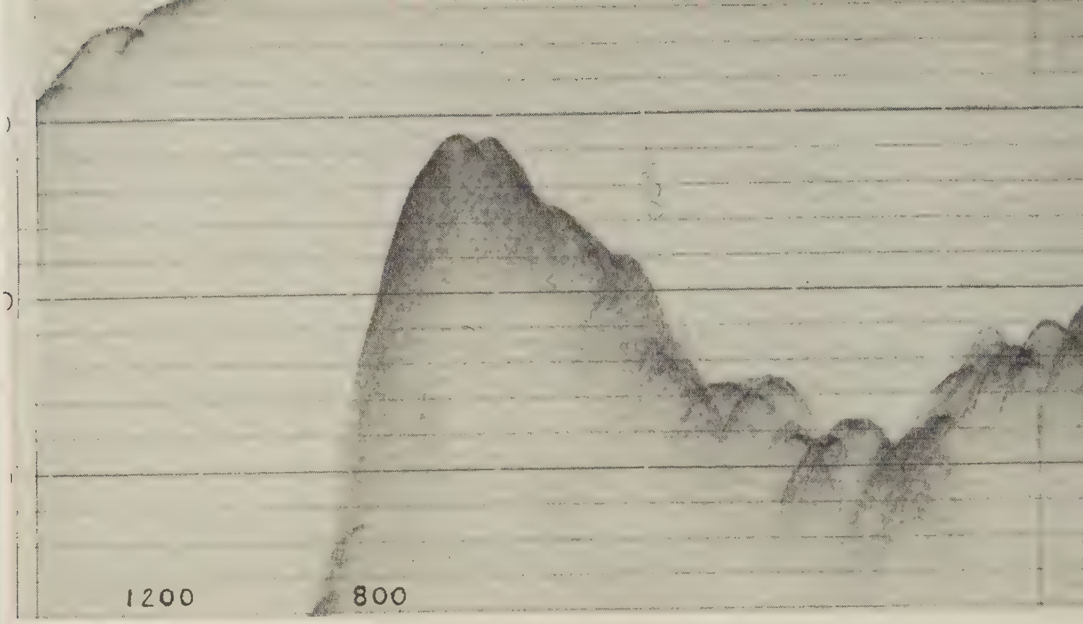

Four hundred fathom interval recording shows how correct depth has to be marked on the paper.
The precision echo-sounder recording system has some 16 speeds available, ranging through a wide selection of depth intervals from a 20-fathom sweep to a 4,000-fathom sweep.

extent that the rather alarming appearing apparatus can be operated by someone who is not an electronic wizard. Spewing out reams of paper, the apparatus cannot be left alone very long. Times and positions must be marked, as well as ship's heading, cruise number, date, etc. No amount of trouble, however, can take away from the utter enchantment of watching an unknown moutain arise before one's eyes. Although the echo sounding trace does not show us the actual contours, the colors and the full view, this is what the pathfinders of the West must have felt as they encountered new mountains. Oceanographers are lucky in that they do not have to scale theirs.

A paper on the Woods Hole recording system has just been published, see: S. T. Knott and J. B. Hersey, 1956, "High-resolution echo-sounding techniques and their uses in bathymetry, marine geophysics, and biology", Deep-Sea Research, Vol. 4, No. 1, pp. 36 to 44.

Up, down or level, the sea bottom is recorded.

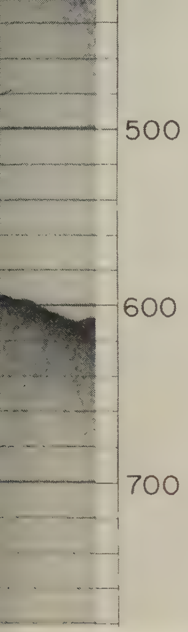

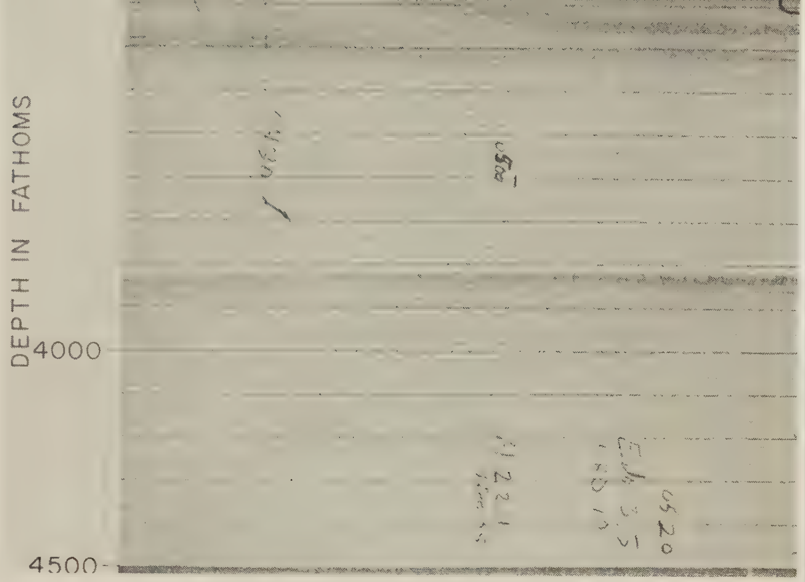

Vast areas of the sea bottom form smooth, level plains, generally at depths from 2,800 to 3,200 fathoms (16,800 to 19,200 feet). For instance five million square miles of the Pacific Basin, equivalent to the areas of China and India, is smooth. Geophysicists, first enthusiastic about the newly discovered roughness of the ocean bottom, now have become intensely interested in these great level areas.

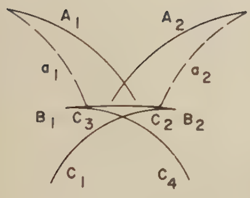

Dashed lines may represent canyon walls.

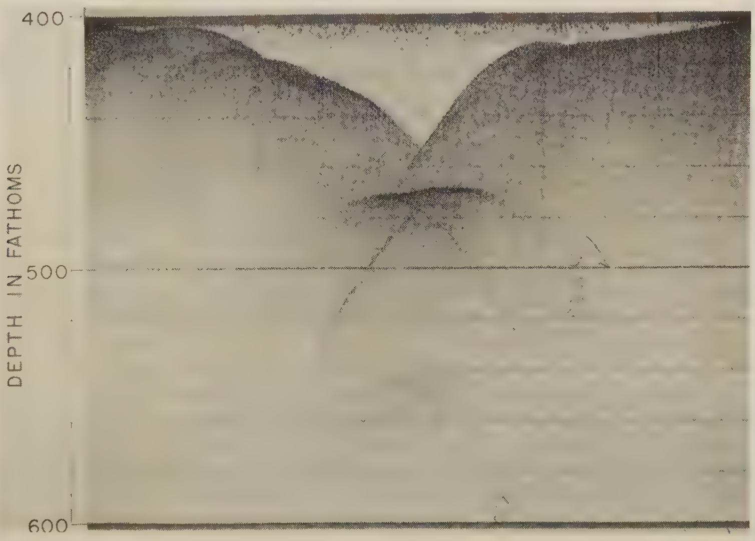

This recording of a submarine canyon, at a depth of 470 fathoms, shows clearly how the broad sound cone may be reflected from some distance up or down the slope or from the sides. The heavy line in the middle represents the flat bottom of the canyon, hence the shape of the canyon is more like a wide-bottomed V. The inverted Λ under the flat bottom is caused by highlights from the corners of the canyon bottom as the ship approached and passed.

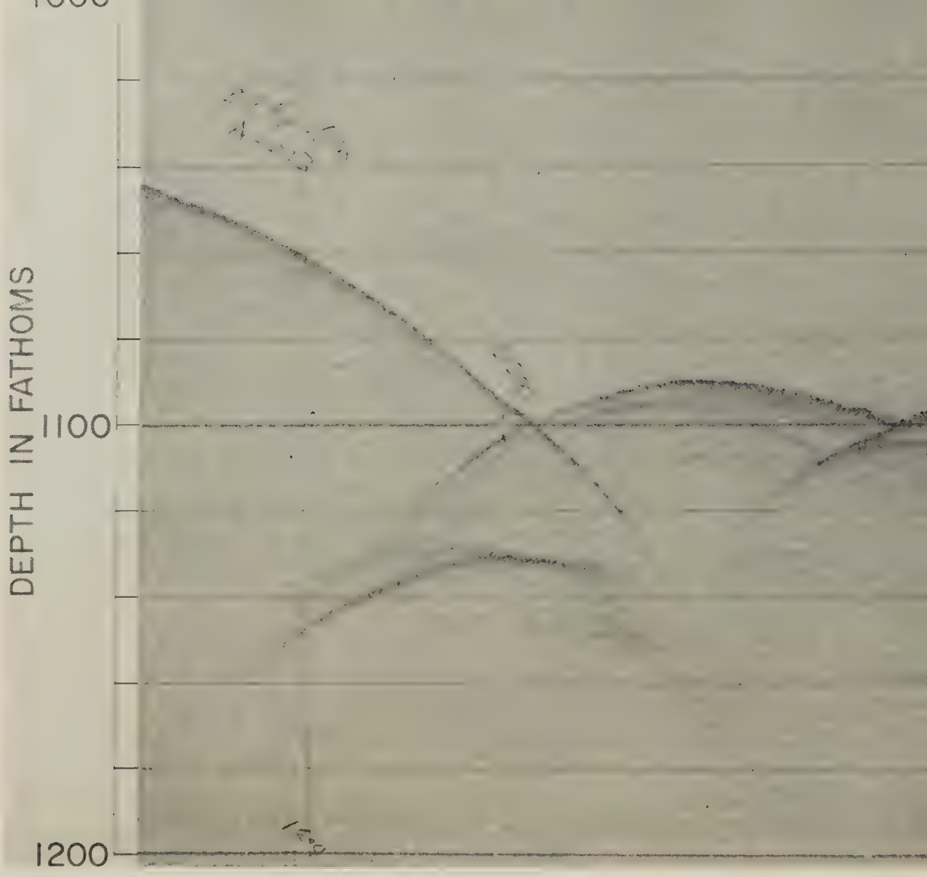

These crescent shapes do not represent the true shape of the bottom. Beca
of the wide angle of the sound beam, sound is reflected from points on the si
of rugged terrain. These reflections may arrive at the echo sounder before

Flat bottom of the Oriente Deep south of Cuba, at a depth of 3,535 fathoms (21,150 feet). Many of the deeps and trenches which have been charted by modern methods show a flat bottom surrounded by extremely rugged topography.
The diagonal lines are timing lines made by a chronometer attached to the precision echo-sounding recorder.

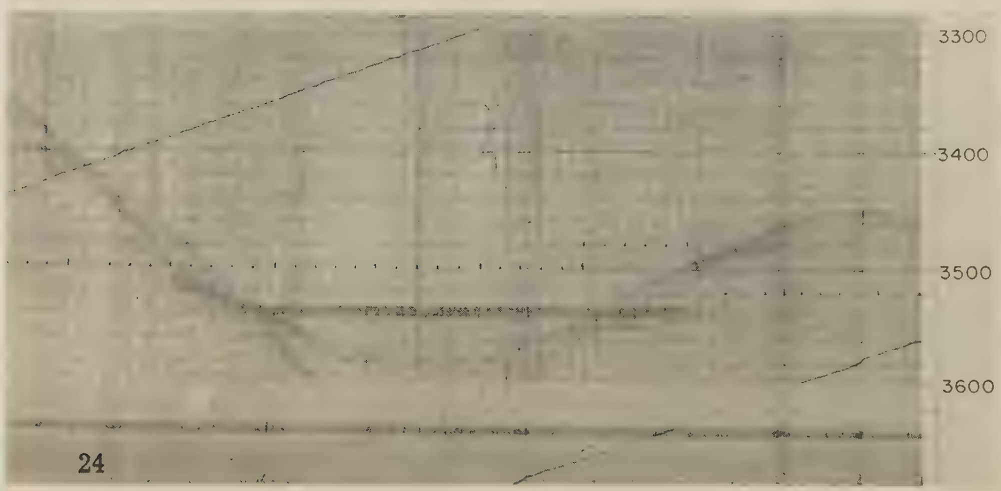

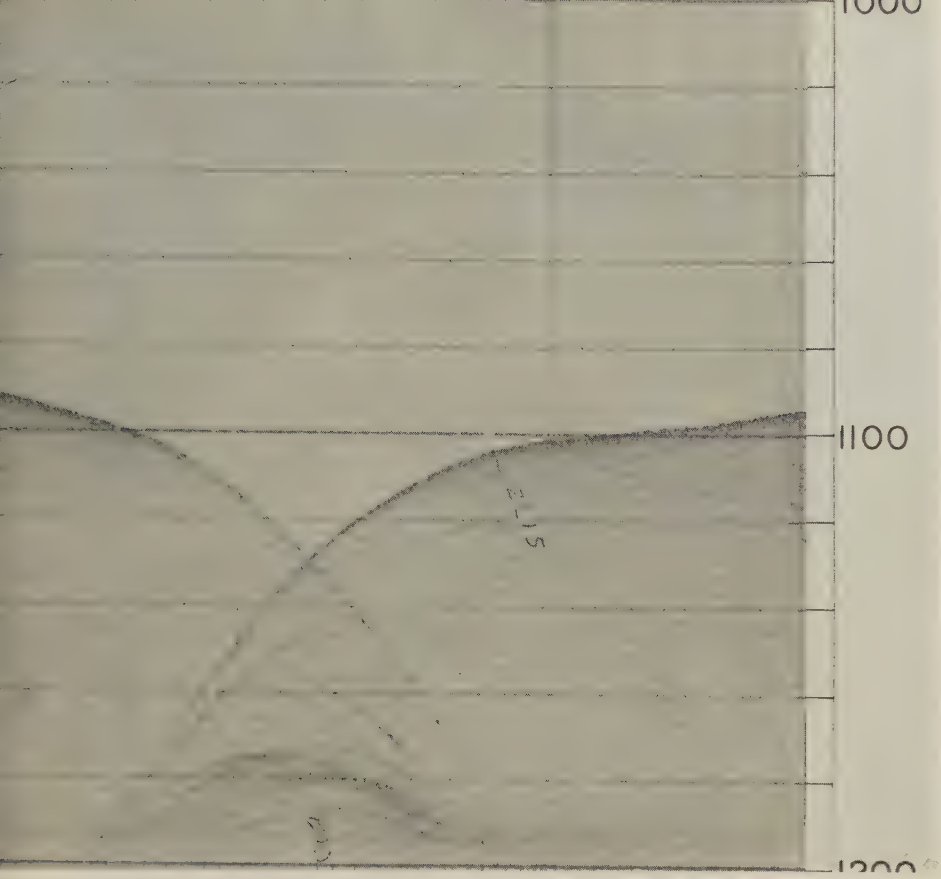

hoes from the bottom directly below the ship. The multiple echoes received
om the bottom sometimes make interpretation of the records difficult.

Small bumps about six to fifty feet high on the bottom of the Florida Straits have been found under the Florida Current on various cross sections. It is not yet known what they are and what they signify. The second bottom reflection is shown at about 100 fathoms on this trace. Horizontal lines represent 20-fathom intervals. A timing device breaks the lines every five minutes.

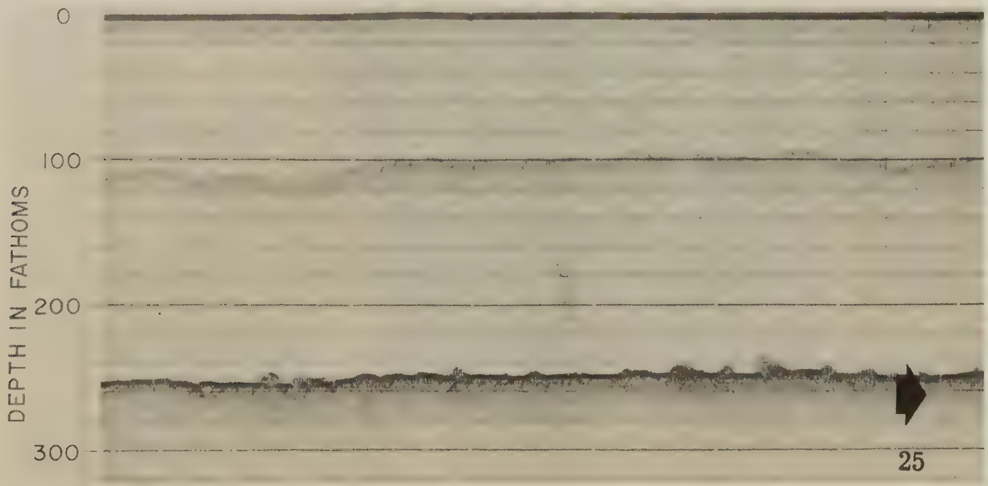

Echo sounding has been used for more than twenty-five years as an aid to navigation in shallow water. As the commercial echo sounders were developed it became possible to obtain deeper and deeper soundings while the old system of depth indication by light flashes on a graduated scale evolved into continuous recording on paper. Some notable investigations were made in the early 1930's by the U. S. Coast and Geodetic Survey while charting the New England canyons, but it was not until after World War II that our ships and other oceanographic vessels were fitted with continuously recording sounders, able to record the bottom at thousands of fathoms below the sea surface. This resulted in changing the concept of the ocean bottom as a generally level plain broken only by occasional mountain ridges, deeps and trenches. New sea mounts, canyons, deeps, faults, even mountain chains in the Pacific Ocean, were discovered, while inadequately known features were charted in detail. Geophysicists soon found that the recording of commercial echo sounders was not sufficiently precise for their scientific requirements. Both at Columbia University's Lamont Geological Observatory and at the Woods Hole Oceanographic Institution precision recording equipment was developed to obtain a better knowledge of the hidden sea floor. Echo sounding together with seismic refraction and reflection "shooting" now have evolved to the point where the presence of the water column makes certain observations easier to obtain than similar ones on land.

Deep underwater photography developed also into a practical art and soon will be more and more useful to marine geophysics and marine biology. On the following pages we have included some examples of the use of self-contained undersea cameras.

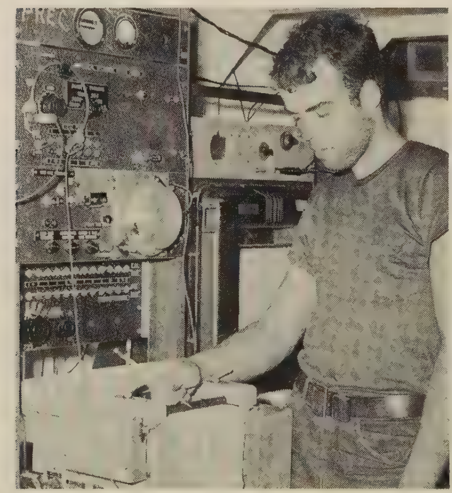

The Woods Hole precision recording system uses Alden facsimile recorders and can be connected to Edo, Raytheon, or other echo sounders.
The array of switches, buttons, and dials are viewed with equanimity by summer student Conrad Malicoat on board the R. V. "Crawford".

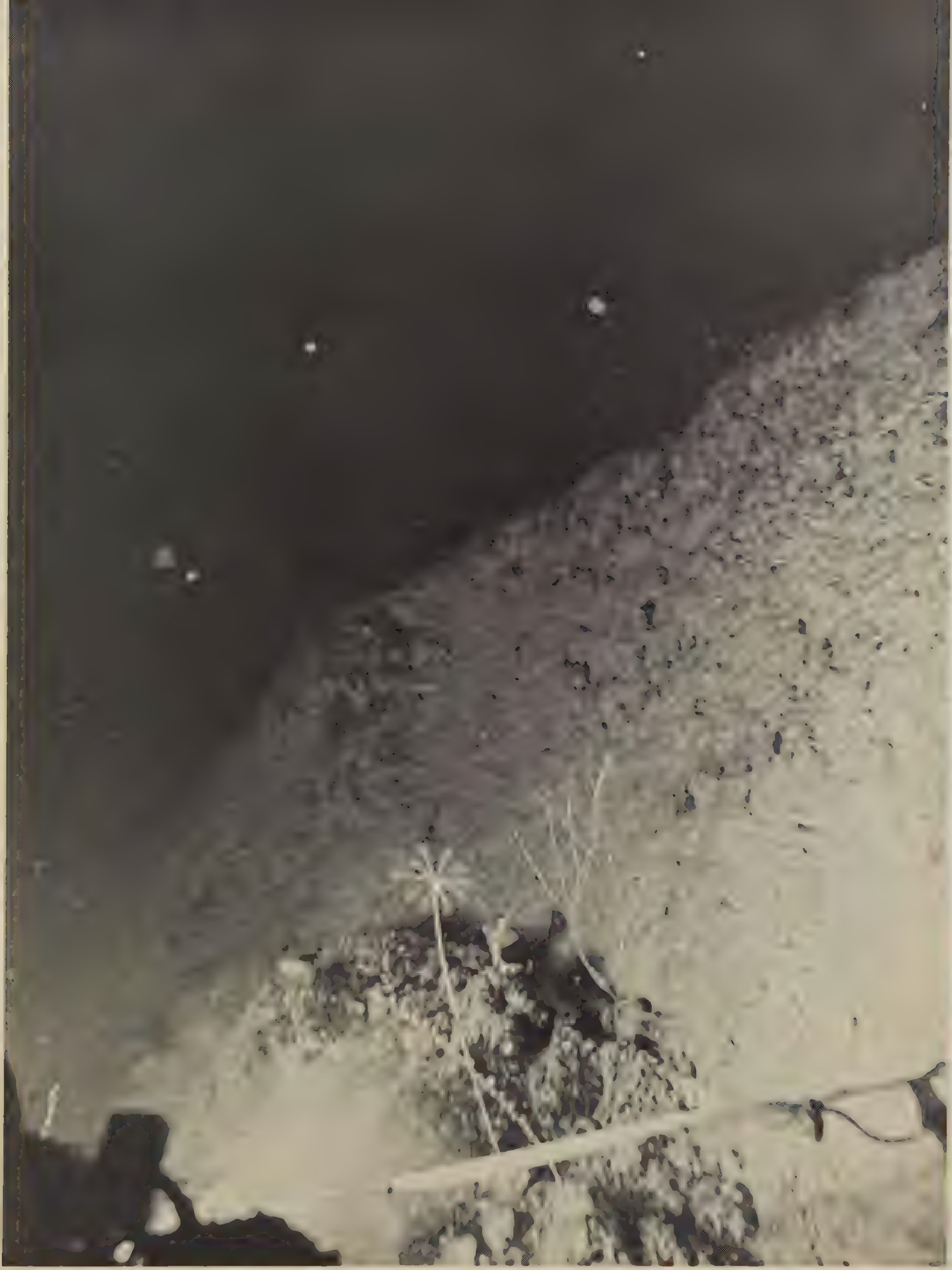

D. M. Owen

A deep-sea camera lowered from the "Atlantis" provided this view of a steep cliff rising 7,200 feet from the sea bottom off the west coast of Florida.

Taken at a depth of 6,600 feet, the photograph shows in the foreground a crinoid or sea lily. Several gorgonians are also shown (crinoids and gorgonians are animals, not plants).

➧

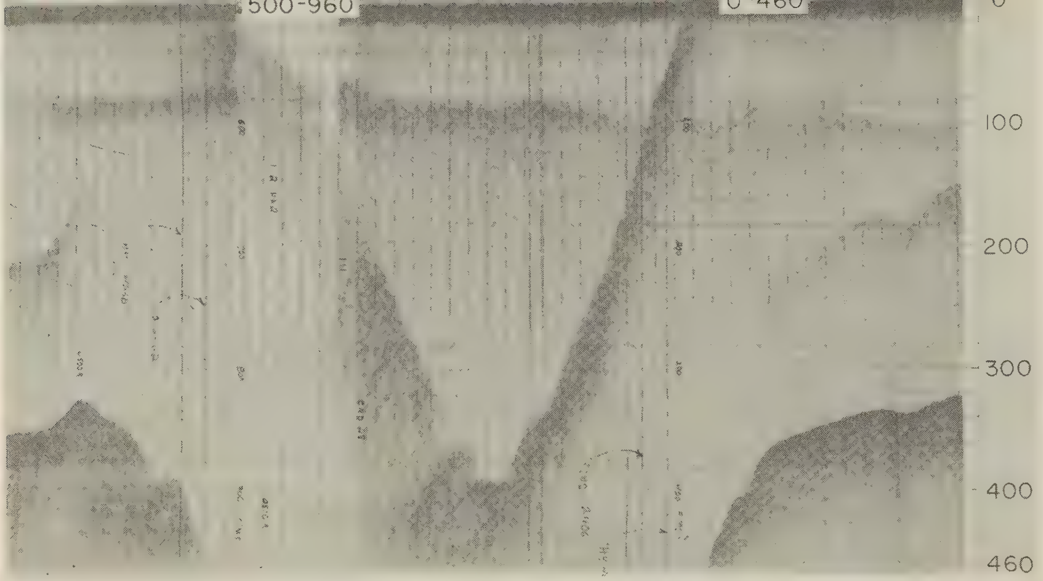

A **"view"** of Hudson Canyon illustrates continuous operation on the 500-fathom sweep. As the canyon deepens the bottom is recorded on the next sweep and the correct depth interval has to be assigned by the operator on watch; however, note that a scattering layer occurs at about 100 fathoms and remains in the 0 to 500 fathom interval.
Arrows on vertical time-marking lines indicate exact moments in which Loran positions were obtained for accurate plotting of the data on a bathymetric chart.

Scattering Layers*

During underwater sound experiments made off California during World War II it was discovered that echoes were received from unidentifiable targets at mid-depths. Named the scattering layer it was soon determined that such a layer could be recorded on echo sounders. This can be seen on many of the records reproduced here. Many investigators at many laboratories since have studied this phenomenon which is not yet satisfactorily explained. Early in the investigation it was found that the layer moved down at sunrise and toward the surface at sunset. Other layers at various depths were discovered, some of which remained at one level or went down instead of up at sunset.

What are they? Numerous hypotheses were formed; the movement of the layers pointed to a biological origin, apart from the fact that no evidence of physical or chemical anomalies, which also might scatter sound, was found. Euphausiids — tiny shrimplike animals — squid, larval fishes, and deep-sea fishes were all considered as likely causes for the scattering. Many studies have been made, both by using underwater sound of varying frequencies and by mid-water trawls, whose content do not necessarily show which animals were scatterers. By combining an underwater camera with acoustical apparatus our scientists have been able to nab some of the culprits.

---

* See: Sound in Marine Research, Oceanus, Vol. III, No. 1.

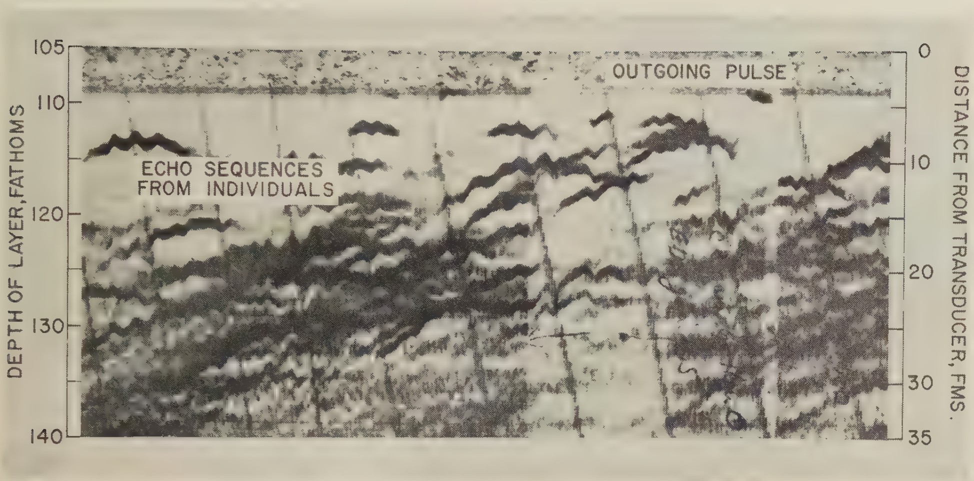

Sound scatterers in the sea appear as a mass of individual crescents when an echo sounder is close to the scatterers. The crescent shape is due to the relative movement between the ship and the scatterers.

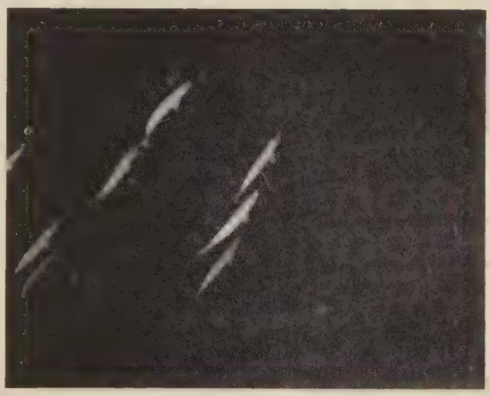

Photograph and simultaneous acoustic record of eight unidentified fishes at a depth of 100 feet in 6,000 feet of water (After: Johnson, Backus, Hersey, and Owen).

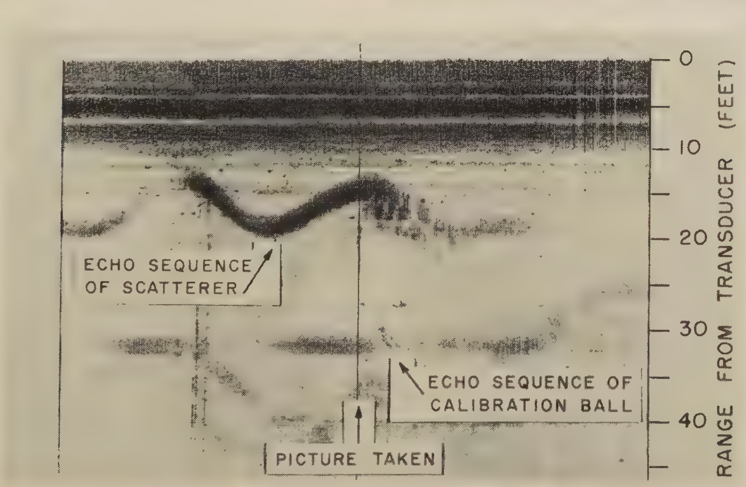

Working up the data takes time.

After many cruises to help collect the data, Charles S. Innis and William M. Dunkle are plotting ship's tracks and soundings on an overlay prior to the drawing of a bathymetric chart.

What happens to the hundreds of feet of recording paper representing thousands of miles of ocean bottom? Some of the records, depicting new features or detailed surveys, are published directly in scientific papers. For the making of bathymetric charts many steps are necessary since the records do not represent the true depth. The velocity of underwater sound, about 4,900 feet per second, is influenced by temperature, salinity, and pressure changes. Hence, tables have been developed to make the necessary corrections, depending on locality and availability of hydrographic observations.

To obtain true depths in areas of rugged topography, such as the Peru-Chile Trench where echoes are received from a wide area thereby confusing the record, slope correction techniques may be applied. The vertical exaggeration of the original sounding records is indicated by the illustrations on the next page prepared by H. Small of our staff for a paper on the work done by the "Atlantis" on the South Pacific cruise made in 1955-56.

Accurate plots are being made on chart overlays with the aid of Loran or celestial observations and, finally, after much plotting of many overlapping tracks, a bathymetric chart may be produced.

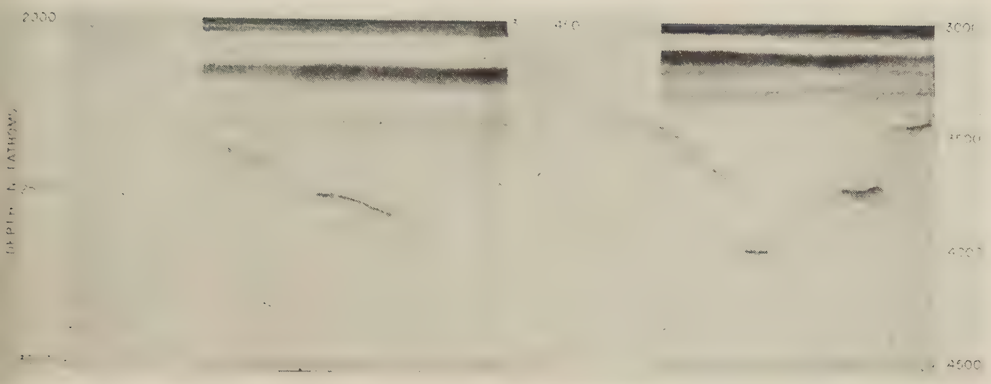

Actual soundings. Note multiple echo surfaces.

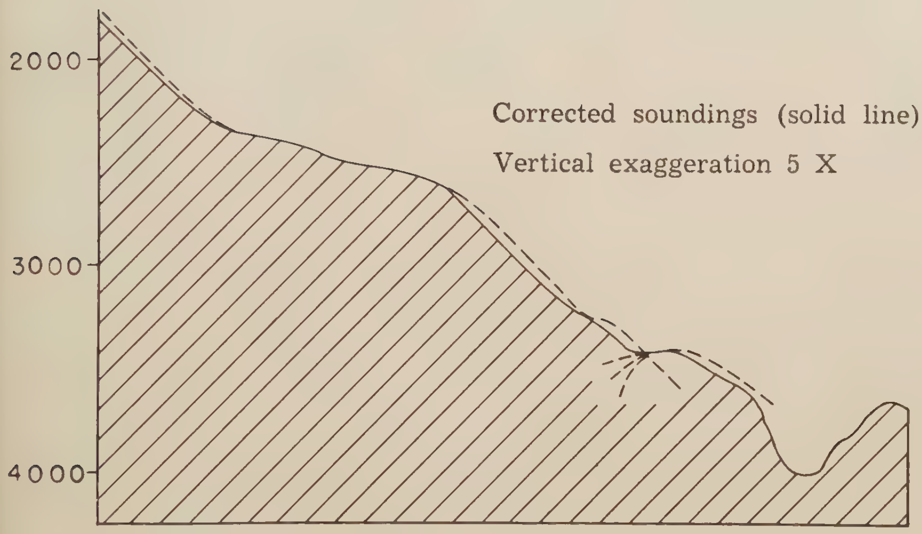

Corrected soundings (solid line)
Vertical exaggeration 5 X

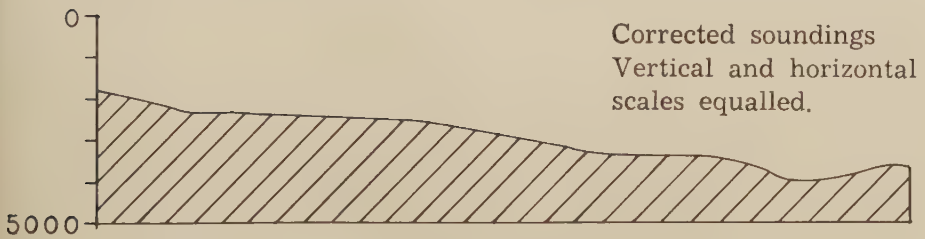

Corrected soundings
Vertical and horizontal
scales equalled.

Contribution No. 910

(*Reprinted from Nature, Vol.* 179, *pp.* 1183–1184, *June* 8, 1957)

Measurements of Deep Currents in the Western North Atlantic*

THE depth of the level of no motion has been a controversial matter among oceanographers for many years. In calculating currents from observed pressure distributions, it has often been assumed that the motion of the deep water must be so slow as to be negligible[1,2]. On the other hand, Defant[3] and Wüst[4] have arrived at consistent pictures of the circulation in the Atlantic using a surface of no motion at intermediate depths. More recently, Stommel[5] has suggested that there should be a deep current along the western boundary of the Atlantic, associated with an internal thermohaline mode of circulation, in the opposite direction to the Gulf Stream.

Some measurements of deep water movements were made during March and early April of this year, using neutrally buoyant floats[6], in an attempt to throw some light on this question of the position of the level of no motion.

In choosing the most suitable part of the Gulf Stream system in which to work, various factors were considered. The surface velocities in the stream off the American continent usually exceed 200 cm./sec., and it was felt that such strong currents would make it difficult to keep track of the deep floats. At Stommel's suggestion, an area off Cape Romain, South Carolina, was chosen. Here the shallow (less than 800 m.) Florida Current flows over the Blake Plateau, while strong pressure gradients are found in the deep water farther offshore. Farther north, towards Cape Hatteras, the violent shallow gradients are superimposed on the deep ones. To the south the deep gradients dwindle away in a manner not yet understood. On these counts it was decided to place the floats as close as was practicable to the junction of the surface Stream with the deep water.

The bulk of the work was carried out in about lat. 33° N., and between long. 75° 30′ W. and 76° W. Excellent Loran coverage exists in this area. Two ships took part in this work, which was a joint venture of the National Institute of Oceanography and the Woods Hole Oceanographic Institution. The current measurements were made by the R.R.S. *Discovery II*, while the R.V. *Atlantis* occupied hydrographic stations, in which serial observations of temperature and salinity were made in order to provide a nearly synoptic picture of the deep pressure conditions.

---

* Contribution No. 910 from the Woods Hole Oceanographic Institution.

Nine floats were followed, of which seven were in deep south-going water. The measurements lasted for periods of 1–4 days, with some overlaps when more than one float was being followed. Three floats at 2,500 metres moved in directions between south and south-west with mean velocities between 2·6 and 9·5 cm./sec., and four floats at 2,800 metres depth moved almost due south with velocities of 9·7–17·4 cm./sec. Additional evidence for a south-going deep current was obtained by A. S. Laughton, who took underwater photographs[7] of the deflexion of a ball suspended on a string, only 50 cm. above the sea floor, in a depth of 3,200 metres. A southward movement of about 5 cm./sec. was found at that depth.

The *Atlantis* hydrographic stations were made at right angles to the drift of each float. The spacing of the stations, eighty-eight in number, did not exceed ten miles in the vicinity of the floats. In one case a rectangular pattern of eight stations not more than three miles apart was laid. There are some irregularities in the slopes of the deep isobars; but the average conditions suggest that the level of no motion in this area most probably lies between 1,500 and 2,000 metres, if the southerly movement of the deep water is to be accounted for by the geostrophic equation.

J. C. SWALLOW
National Institute of Oceanography,
Wormley, Godalming,
Surrey.

L. V. WORTHINGTON
Woods Hole Oceanographic Institution,
Woods Hole, Mass.

May 13.

[1] Sverdrup, H. U., Johnson, M. W., and Fleming, R. H., "The Oceans", 456 (Prentice-Hall, Inc., New York, 1942).

[2] Sverdrup, H. U., "The Earth as a Planet", edit. G. P. Kuiper, chapter 5, "Oceanography", 243 (University of Chicago Press, 1954).

[3] Defant, A., *Wiss. Erg. deutsch. Atlant. Exp. "Meteor"* 1925–27, **6**, (2), 5, 191 (1941).

[4] Wüst, G., *Pap. Mar. Biol. and Oceanogr., Deep-Sea Res.* Supp. to vol. 3, 373 (1955).

[5] Stommel, H., *J. Geophys. Res.*, **61**, 2 320 (1956).

[6] Swallow, J. C., *Deep-Sea Res.*, **3**, 74 (1955).

[7] Laughton, A. S., *Deep-Sea Res.*, **4**, 120 (1957).

Printed in Great Britain by Fisher, Knight & Co., Ltd., St. Albans.

Contribution No. 911

Reprinted from LIMNOLOGY AND OCEANOGRAPHY
Vol. II, No. 4, October, 1957
Printed in U.S.A.

The Effect of Circularly Polarized Light on the Photosynthesis and Chlorophyll *a* Synthesis of Certain Marine Algae[1]

G. C. McLEOD

Woods Hole Oceanographic Institution, Woods Hole, Mass.

ABSTRACT

The net photosynthesis and chlorophyll *a* synthesis of certain marine algae show a gradation in response to various types of polarized light. Right circularly polarized light increases the net photosynthesis and chlorophyll *a* synthesis as compared with light through neutral density filters, whereas the effect is reversed with left circularly polarized light. This suggests that the receptor pigments are anisotropic and exhibit circular dichroism.

There are contradictory views in the literature on the part played by polarized light in certain photochemical reactions and in photosynthesis. Zurzycki (1955) in a recent paper, reviewed the literature, and disclaimed any significant effects of linearly or circularly polarized light on the photosynthesis of *Lemna trisulca* L. leaves. Rabinowitch (1951), however, has pointed out that chloroplasts may exhibit circular dichroism (*i.e.*, differential absorption of right- and left-handed circularly polarized light), particularly in weak light and when the chloroplast is in the profile position. Measurements of circular dichroism are important aids in the study of the optical properties of compounds.

In the following report some experiments will be described concerning the effects of various types of polarized light on carbon-14 uptake and chlorophyll *a* synthesis in the unicellular marine flagellate, *Dunaliella euchlora*.

One and one-half liters of enriched sea water medium were inoculated with a bacteria-free culture of *Dunaliella euchlora* giving an initial cell concentration of 10^5 cells/ml.

The culture was kept in the dark for two days, and then exposed to approximately 1000 foot-candles of non-polarized fluorescent light at 20°C. After 12 hours the culture contained 2×10^5 cells/ml. Exponential growth continued for four days, and the growth stopped after the fifth day.

During the exponential growth aliquots of the culture were suspended in enriched sea water, and the cell density was adjusted to 1×10^5 to 1.5×10^5 cells/ml. The cell suspension was tagged with carbon-14, after the method of Steemann Nielsen (1952), and siphoned into 35-ml glass-stoppered bottles which were placed in finger bowls blackened so that light could enter only through a three-inch square at the top. Neutral-density or polaroid filters were taped to the top of the finger bowls.

The samples were placed at 20°C under 1000 foot-candles of fluorescent light. With filters this intensity was reduced to 300 to 500 foot-candles, which was above the light saturation of the organisms used (Ryther 1956). After varying lengths of exposure, the samples were filtered on millipore filters, the filters dried, and the radioactivity and chlorophyll *a* content (Yentsch 1957) were determined on samples from each experiment. In a series of similar experiments the rate of oxygen production was measured under polaroid and neutral-density filters. Oxygen production was measured by the Winkler method and corrected for respiration by means of a third sample in a darkened bottle.

A bank of daylight fluorescent lamps, used as a light source, showed no polarization when tested with a polaroid analyzer. Light polarization was obtained by Polaroid HN plastic filters, which circularly polarize light throughout the visible spectrum.

---

[1] Contribution No. 911 from the Woods Hole Oceanographic Institution. Done under contract with the National Science Foundation, Grant G-2510.

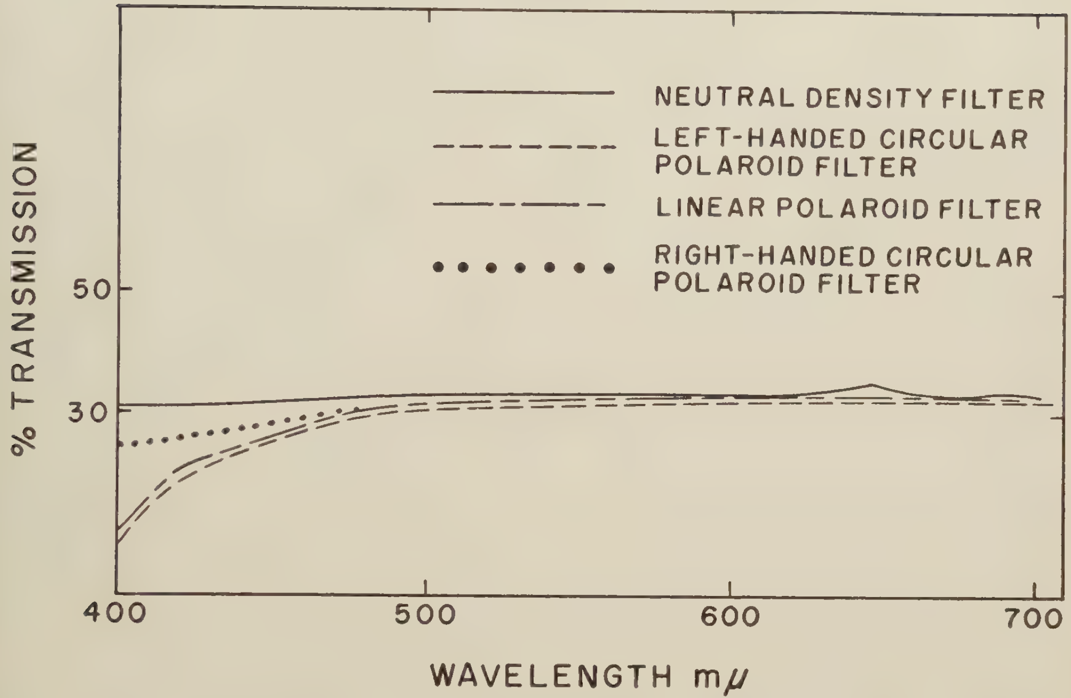

FIG. 1. Transmission curves for polaroid and neutral density filters.

TABLE 1. *Per cent transmission of polaroid and neutral-density filter*

Filter	% transmission
Left-circular polaroid	33.0
Linear polaroid	34.2
Right-circular polaroid	35.8
Neutral-density	37.0

TABLE 2. *Mean percentage increase in carbon-14 uptake, chlorophyll* a *content and oxygen production in* Dunaliella euchlora *under right-circular polaroid filter as compared with neutral-density filter*
Light intensity 300–500 foot candles.

Exposure (hours)	Number of experiments	Carbon-14 uptake (cpm)	Chlorophyll *a* content (mg chl *a*/L)	Oxygen production (ml/L)
2	3	29	24	
3	2	24	28	
4	3	29	20	5
5	3	23	33	
9	3	35		
10	3	32	17	
15	3	22		
16	3	27	17	14
24	3	26	15	5

TABLE 3. *Effect of neutral-density, linear polaroid, and right-circular polaroid filters on the photosynthesis of four unicellular marine organisms*
Light intensity 300–500 foot-candles. Exposure 10 hours.

Organisms	Carbon-14 uptake Per cent increase over neutral-density	
	Linear	Right-circular
Dunaliella euchlora	4	25
Porphyridium cruentum	2	29
Skeletonema costatum	0	29
Olisthodiscus sp.	−2	25

TABLE 4. *Mean of four experiments showing chlorophyll* a *content of* Dunaliella euchlora *after ten hours exposure to polarized light*

	Filters			
	Neutral-density	Linear polaroid	Right-circular polaroid	Left-circular polaroid
mg chlorophyll *a*/liter	.22	.24	.30	.17
Percent increase over neutral-density	—	9	36	−23

Three types of polarization were tested: linear, left-handed circular, and right-handed circular polarization. For control measurements, neutral-density filters made from photographic film were mounted on glass plates.

Transmission curves for the polaroid and neutral density filters were plotted from measurements made in a Beckman DU spectrophotometer (Fig. 1). These curves show that the transmission within the visible radiation range is very similar for all filters.

To compare total intensities of the light transmitted by each of the filters, measurements were made with a General Electric Exposure Meter, Type DW—68. The readings indicated that the polaroid filters transmitted less light than the neutral density filters as shown in Table 1.

Table 2 shows the effects of right-handed circularly polarized light on the photosynthesis of *Dunaliella euchlora*. In every case, this type of polarized light significantly increased the carbon-14 uptake and chlorophyll *a* content over that shown by the neutral-density filter.

The differences between values obtained by measuring oxygen production are less than those obtained by measuring carbon-14 uptake. The oxygen values were corrected for respiration and represent total photosynthesis, whereas the carbon-14 uptake is a measure only of photosynthesis above respiration (Ryther 1954). Since respiration was probably rather high compared to photosynthesis at the relatively low light intensities used in these experiments, the percentage differences between net photosynthesis (*i.e.*, total photosynthesis minus respiration) would appear larger than the differences between total photosynthesis.

A series of 10-hour experiments with four different unicellular marine organisms show that in all cases right-handed circularly polarized light increased the photosynthesis (Table 3), whereas there was no significant difference in photosynthesis between the organisms under the neutral-density and the linear polaroid filters.

According to physical theory (Glasstone 1940) there should be a gradation in response to various types of polarization. The absorption characteristics of linearly polarized light should not differ from those of unpolarized light, but right- and left-handed circularly polarized light should be absorbed to a different extent by the dextro and laevo molecules of an optically active substance.

Table 4 shows the effects of three different polaroid filters on the chlorophyll *a* synthesis of *Dunaliella euchlora*, over a period of ten hours. Again, right-handed circularly polarized light is most effective in chlorophyll *a* synthesis, whereas linearly polarized light is not significantly different from the control. The chlorophyll *a* synthesis with left-handed circularly polarized light, however, is below that of the control. This is in accord with an explanation based on simple circular dichroism of the receptor pigments.

These experiments indicate that chlorophyll *a* production and photosynthesis in certain unicellular marine algae are affected by polarized light, and suggest that the photosynthetic pigments may be anisotropic and exhibit circular dichroism. Waterman (1955) has shown that linearly polarized light penetrates to considerable depths in natural waters. If the same is true of circularly polarized light, it might have ecological significance in photosynthesis under natural conditions.

REFERENCES

Glasstone, S. 1940. Textbook of physical chemistry. Van Nostrand & Co., New York, pp. 594–597.

Rabinowitch, E. 1951. Photosynthesis. Interscience Publishers, Inc., New York. Vol. I, pp. 362 and 366.

Ryther, J. H. 1954. The ratio of photosynthesis to respiration in marine plankton algae and its effect upon the measurement of productivity. Deep-Sea Res., **2:** 134–139.

———. 1956. The measurement of primary production. Limnol. & Oceanog., **1:** 72–85.

Steemann Nielsen, E. 1952. The use of radioactive carbon (C^{14}) for measuring organic production in the sea. J. Cons. Int. Explor. Mer, **43:** 117–140.

Waterman, T. H. 1955. Polarization of sunlight in deep water. Deep-Sea Res., **3:** 426-434.

Yentsch, C. S. 1957. A non-extractive method for the estimation of chlorophyll. Nature, (in press).

Zurzycki, J. 1955. Photosynthesis in polarized light. Acta Soc. Bot. Polon., **24**(3): 539–547.

Contribution No. 912

Deep-Sea Research, 1957, Vol. 4, pp. 230 to 237. Pergamon Press Ltd., London

A taxonomic analysis of *Myctophum affine* and *M. nitidulum*, two lantern-fishes previously synonymized, in the western North Atlantic

ROBERT H. GIBBS, JR.

(*Received* 4 *June* 1957)

Abstract—The lantern-fishes currently known as *Myctophum affine* constitute two distinct species. *M. affine* has ctenoid scales, a rounded upper opercle, PLO photophore about midway between pectoral fin insertion and lateral line, and more gill rakers. *M. nitidulum* has cycloid scales, an angulated upper opercle, PLO nearer pectoral insertion, and fewer gill rakers. *M. affine* is a smaller fish and develops caudal-peduncle luminous scales at a smaller size than *M. nitidulum.* No significant meristic differences were found between samples from the western North Atlantic, the Gulf of Mexico, and the Caribbean Sea.

INTRODUCTION

THE widespread and common lantern-fish known as *Myctophum affine* has, for many years, been in a state of systematic confusion. This has been recognized by recent workers (PARR, 1928 ; BOLIN, 1939, 1946 ; FRASER-BRUNNER, 1949), who have partially investigated the problems, but who have been able to solve only a few. Recent collections made by means of a dip-net at a surface light at night have provided material from several areas of the western North Atlantic. These collections have revealed the existence in this region of two species which fit current descriptions of *Myctophum affine.* These are analysed herein.

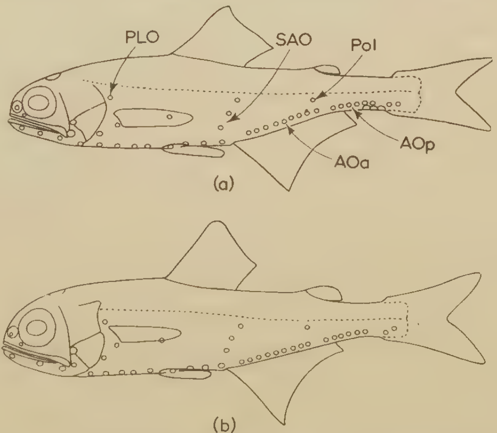

Fig. 1. Body form and photophore arrangement in (A) *Myctophum affine* and (B) *M. nitidulum.* From specimens 49·2 mm and 48·2 mm, respectively, collected at 39° 28′N, 69° 30′W on October 30, 1957. The specimen of *M. nitidulum* lacked caudal-peduncle luminous scales.

METHODS

Counts and measurements have been made in accordance with HUBBS and LAGLER (1947). Designation of photophore groups follows the system used by most current authors and exemplified by FRASER-BRUNNER (1949). Many previous workers have counted all the elements in the dorsal and anal fins of Myctophids. My counts were *principal* ray counts, which do not include three spinous elements in the dorsal fin and two in the anal. For comparison with others, these can be added at the appropriate places in the frequency distributions.

NOMENCLATURE

In the most recent key to the genus *Myctophum* (FRASER-BRUNNER, 1949), any member of this genus with the three SAO photophores (see Fig. 1) in a straight line and with Pol below the adipose fin comes out to *M. affine*. In the collections reported herein, variants were noted which did not correspond to other points in FRASER-BRUNNER's synopsis, and which upheld the suspicion voiced by BOLIN (1939) that certain *M. affine* have ctenoid or crenulated scales. Further investigation has shown that the cycloid and ctenoid forms do, indeed, represent two species, which are distinctly, if subtly, characterized. These species have also been recognized by BOLIN, who will report on them and their nomenclature in a forthcoming publication. He has informed me that the ctenoid-scaled species is the true *M. affine*. The earliest available name for the cycloid-scaled species is *M. nitidulum* (GARMAN, 1899). These names will be used in the remainder of this paper.

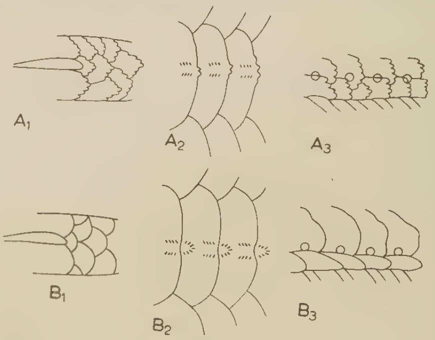

Fig. 2. Configuration of scales of (A) *Myctophum affine* and (B) *M. nitidulum.* (1) Dorsal region behind dorsal fin. (2) Lateral line. (3) Region above anal fin.

TAXONOMIC CHARACTERS

The two species may be easily recognized without reference to counts or measurements. In *M. affine*, except in some specimens smaller than about 25 mm, the scales are ctenoid, strongly so in the mid-dorsal region and the lower part of the sides posterior to the pelvic insertion, but even the large lateral-line scales are at least weakly toothed near the median notch ; in

Table 1. *Frequency distribution of meristic characters of* Myctophum affine *and* M. nitidulum

	Dorsal rays				*Anal rays*					*Pectoral rays*					
	9	10	11	$\bar{x}$	16	17	18	19	$\bar{x}$	11	12	13	14	15	$\bar{x}$
affine	4	84	7	10·0	14	67	14	—	17·0	—	16	113	57	—	13·2
nitidulum	1	63	6	10·1	1	26	37	6	17·7	1	13	60	56	6	13·4

	AOa					*AOp*				*Total AO*					
	7	8	9	10	$\bar{x}$	4	5	6	$\bar{x}$	12	13	14	15	16	$\bar{x}$
affine	—	47	48	—	8·5	9	64	22	5·1	2	38	47	8	—	13·6
nitidulum	1	16	47	6	8·8	8	47	15	5·1	1	16	41	11	1	13·9

	Lateral-line scales							*Upper rakers*					
	36	37	38	39	40	41	$\bar{x}$	4	5	6	7	8	$\bar{x}$
affine	1	5	23	41	23	2	38·9	—	8	73	13	1	6·1
nitidulum	1	4	29	22	12	1	38·6	1	55	12	1	—	5·2

	Lower rakers						*Total rakers*							
	13	14	15	16	17	$\bar{x}$	18	19	20	21	22	23	24	$\bar{x}$
affine	2	16	53	21	3	15·5	—	7	12	43	27	5	1	21·0
nitidulum	19	34	16	—	—	13·9	181	31	12	8	—	—	—	19·1

M. nitidulum, the scales are uniformly cycloid (Fig. 2). The opercular margin of *M. affine* is rounded in its dorsal half, curving in a regular arc ; in *M. nitidulum*, the margin forms a decided angle in its dorsal half (Fig. 1). The PLO photophore in *M. affine* is approximately mid-way between the pectoral insertion and the lateral line, whereas in *M. nitidulum* it is decidedly nearer the pectoral insertion (Fig. 1).

Frequency distributions of certain meristic characters are shown in Table 1. The most significant of these with respect to identification is the number of gill rakers. In *M. affine* the total number is seldom less than twenty-one, in *M. nitidulum*, seldom more than twenty. Other characters show slight mean differences which are, however, not useful in identification. One of these, it should be noted, is the number of AO photophores, upon which much taxonomic weight is placed in other species.

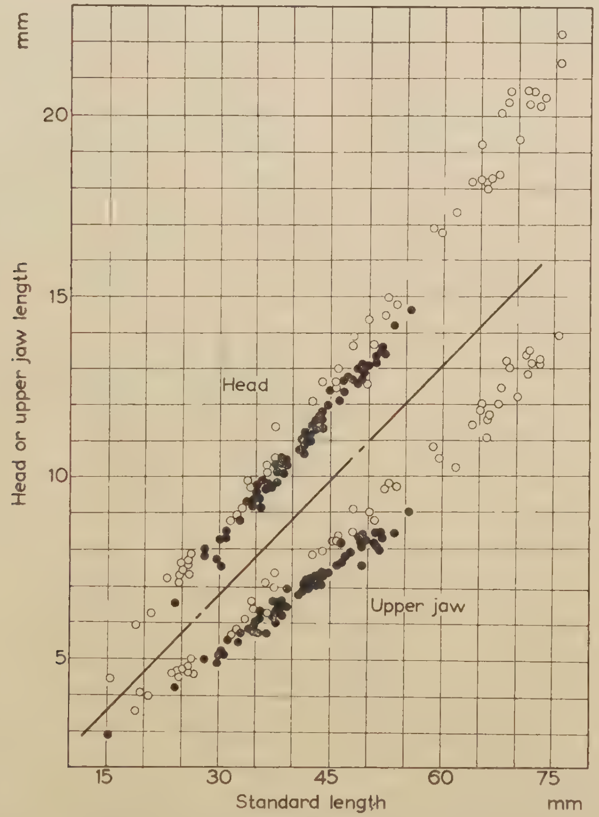

Fig. 3. Head length and upper jaw length plotted against standard length in *Myctophum affine* (black dots) and *M. nitidulum* (open circles).

Eleven measurements of body parts were taken and plotted against standard length. Of these, the two which showed differences worthy of consideration are shown in Fig. 3. The lengths of both head and upper jaw are greater in *M. nitidulum* than in *M. affine*, and the points for each species are rather well-separated.

SIZE AND MATURITY

Table 2 lists the largest specimen of *M. affine* and *M. nitidulum* in each collection used in this study, which contained specimens at least 40 mm long. This shows a

Table 2. Sizes of largest specimens of Myctophum nitidulum *and* M. affine *in each containing individuals* 40 mm *long or longer*

nitidulum				*affine*	
45·8	63·3	68·0	73·1	42·0	52·1
45·9	65·2	71·4	74·6	42·3	52·2
46·0	65·2	71·5	75·1	43·5	53·2
52·2	65·4	71·5	75·4	46·0	55·6
52·3	66·0	71·8	75·7	49·2	57·6
62·0	66·2	72·1	79·4	49·4	58·0
62·3	66·4	72·2		49·4	58·9
63·2	67·8	72·5		51·3	60·3
average : 65·95				average : 51·31	

14·6 mm difference in the average size of these specimens, *M. nitidulum* being the larger. The largest specimen of *M. nitidulum* is 19·1 mm larger than the largest *M. affine*. Fig. 3 also indicates a lack of *M. affine* in the larger size range.

That this is not due to insufficient material is shown by the relative size at which the luminous scales of the caudal peduncle are developed. These scales are believed to indicate maturity in at least certain species of Myctophidae. Although I have not checked sex internally, I presume, as others have previously, that those specimens possessing dorsal luminous scales on the caudal peduncle are males, those having ventral ones, females. In the species under consideration, males of *M. affine* usually have seven or eight such scales, males of *M. nitidulum* six or seven, seven being the mode in each. Female *M. affine* usually have three luminous ventral scales, *M. nitidulum* three or four. (One large specimen of *M. nitidulum* from the Gulf of Mexico had both dorsal and ventral luminous scales).

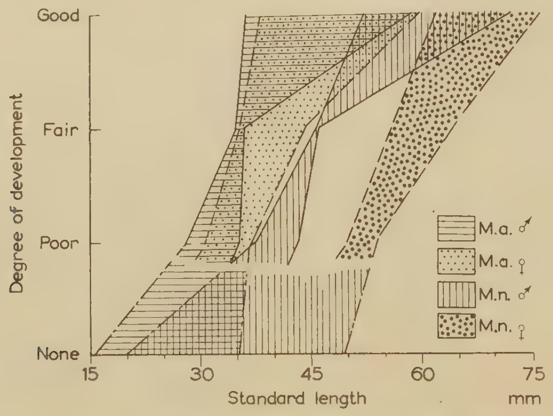

Fig. 4. Diagram showing relative development of caudal-peduncle luminous scales in *Myctophum affine* and *M. nitidulum*. There is very little overlap either between the species or between males or females. The region of undeveloped scales is indicated by the male symbol for each species, although the sex of these specimens was undetermined.

The relative size at which these luminous scales are developed is shown in Fig. 4. The degrees of development used are arbitrary, but are believed to represent the observations satisfactorily.

In both species, the luminous scales of the male develop at a smaller size than those of the female. Between males, there is little overlap in size at any given degree of development of these scales. The smallest male *M. affine* to show luminous scale development is 9·3 mm smaller than the similar *M. nitidulum*. The largest *M. affine* with well-developed luminous scales is 59·0 mm, the smallest *M. nitidulum* 52·2 mm.

The difference between females is even more striking. The smallest female *M. affine* to show luminous-scale development is 30·4 mm, the smallest *M. nitidulum* 48·2 mm. There is no overlap between *M. nitidulum* and *M. affine* females with well-developed luminous scales.

The difference in the size at which the luminous scales are developed, therefore, supports the conclusion that *Myctophum affine* is a smaller fish than *M. nitidulum*. Even considering species regardless of sex, Fig. 4 indicates very little overlap in size at all between specimens of each degree of development.

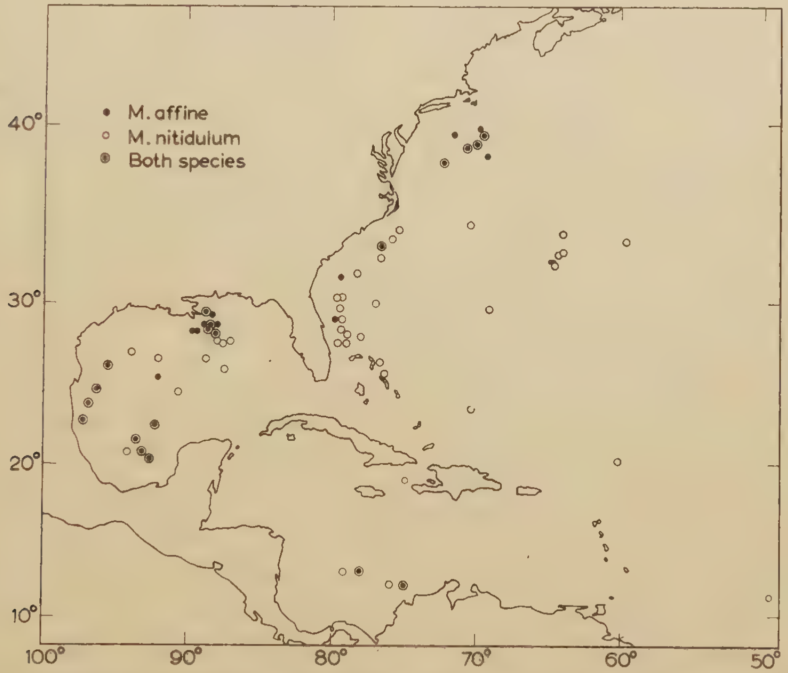

Fig. 5. Distribution of collections of *Myctophum affine* and *M. nitidulum* used in this study.

GEOGRAPHIC VARIATION AND DISTRIBUTION IN THE WESTERN NORTH ATLANTIC

From the collections at hand, there is no convincing evidence of any difference in distribution of the two species. They have both been taken in the western Atlantic proper, the Gulf of Mexico, and the Caribbean Sea, and they have often been taken together in each of these regions (Fig. 5). At twenty-three out of seventy-six collecting stations, the two were both present.

Breakdown of the meristic data for each species into the three regions is shown in Tables 3 and 4. Too few specimens are available from the Caribbean to justify any conclusions. In the Atlantic and Gulf samples of *M. affine*, there is a slight modal difference in number of AO photophores, which is the only character suggesting distinctiveness of the two populations. In *M. nitidulum* there is a notable difference in number of lateral-line scales, and less-trenchant modal differences in numbers of pectoral rays and gill rakers. This data seems to indicate that Gulf and Atlantic populations of *M. nitidulum* are more effectively isolated than those of *M. affine*, but that gene flow is not greatly restricted in either species between the two areas.

Table 3. Frequency distributions of meristic characters of Myctophum affine *from different geographical areas*

	Dorsal rays				*Anal rays*				*Pectoral rays*			
	9	10	11	$\bar{x}$	16	17	18	$\bar{x}$	12	13	14	$\bar{x}$
Atlantic	3	35	2	10·0	5	31	4	17·0	6	37	37	13·4
Gulf	1	46	5	10·1	8	34	10	17·0	10	74	15	13·1
Caribbean	—	3	—	10·0	1	2	—	16·7	—	2	4	13·7

	AOa			*AOp*				*Total AO*				
	8	9	$\bar{x}$	4	5	6	$\bar{x}$	12	13	14	15	$\bar{x}$
Atlantic	21	19	8·5	7	27	6	5·0	2	21	14	3	13·5
Gulf	24	28	8·5	2	37	13	5·2	—	17	31	4	13·8
Caribbean	2	1	8.3	—	—	3	6·0	—	—	2	1	14·3

	Lateral-line scales							*Upper rakers*			
	36	37	38	39	40	41	$\bar{x}$	5	6	7	$\bar{x}$
Atlantic	1	1	8	21	8	1	38·9	3	28	9	6.2
Gulf	—	4	12	20	14	1	38·7	5	43	4	6·0
Caribbean	—	—	3	—	—	—	38·0	1	2	—	5·7

	Lower rakers						*Total rakers*						
	13	14	15	16	17	$\bar{x}$	19	20	21	22	23	24	$\bar{x}$
Atlantic	—	6	23	10	1	15·2	2	4	16	13	5	—	21·4
Gulf	1	9	30	10	2	15·5	3	8	27	—	—	1	21·0
Caribbean	1	1	—	1	—	14·3	2	—	—	1	—	—	20·0

It is interesting to speculate about the mechanisms for reproductive isolation in these two species. The photophore and luminous scale patterns would seem to be the logical species-specific recognition characters, but these are almost identical in *M. affine* and *M. nitidulum*. Since all the collections used in this study were made at the surface, there is no suggestion of a possible difference in depth at which spawning might take place ; nor do published references help, as they do not distinguish between the two species. It may be that lack of interbreeding is due to physiological mechanisms, which must have developed during a former isolation. The similarity of the present ranges of these species gives no hint of such a past separation. It is possible, though improbable, that the similarities of these two forms are due to convergence, and that they are members of different phylogenetic groups. The present state of Myctophid systematics does not permit an answer to this.

Table 4. Frequency distributions of meristic characters of Myctophum nitidulum *from different geographical areas*

	Dorsal rays				*Anal rays*					*Pectoral rays*					
	9	10	11	$\bar{x}$	16	17	18	19	$\bar{x}$	11	12	13	14	15	$\bar{x}$
Atlantic	—	29	2	10·1	—	11	15	5	17·8	—	3	22	31	4	13·6
Gulf	—	27	4	10·1	1	9	20	1	17·7	—	8	33	19	2	13·3
Caribbean	1	7	—	9·8	—	6	2	—	17·3						

	AOa					*AOp*				*Total AO*					
	7	8	9	10	$\bar{x}$	4	5	6	$\bar{x}$	12	13	14	15	16	$\bar{x}$
Atlantic	1	4	22	4	8·9	5	21	5	5·0	1	6	19	4	1	13·9
Gulf	—	8	22	1	8·8	3	20	8	5·1	—	8	17	6	—	13·9
Caribbean	—	4	3	1	8·6	—	6	2	5·3	—	2	5	1	—	13·9

	Lateral-line scales							*Upper rakers*				
	36	37	38	39	40	41	$\bar{x}$	4	5	6	7	$\bar{x}$
Atlantic	1	4	18	7	1	—	38·1	—	26	4	1	5·2
Gulf	—	—	7	13	11	—	39·1	1	23	7	—	5·2
Caribbean	—	—	4	2	—	1	38·7	—	6	1	—	5·1

	Lower rakers				*Total raker:*				
	13	14	15	$\bar{x}$	18	19	20	21	$\bar{x}$
Atlantic	15	14	2	13·6	12	14	4	1	18·8
Gulf	5	15	11	14·2	6	13	6	6	19·4
Caribbean	—	4	3	14·4	—	4	2	1	19·6

Acknowledgements—For material obtained by others than myself, I am grateful to the crew of the Fish and Wildlife Service vessel *Delaware*, and to WILLIAM MURPHY in particular ; to HARVEY R. BULLIS and the crew of the *M/V Oregon* ; to members of the scientific parties of the *R/V Crawford*, JAN HAHN in particular ; to Captain W. SCOTT BRAY of the *R/V Atlantis*, and to RICHARD H. BACKUS, who collected from the later vessel. For the privilege of examining materials in their collections, thanks are due to ROYAL D. SUTTKUS of Tulane University ; GILES W. MEAD of the U.S. Fish and Wildlife Service in Washington, D.C., WILLIAM W. ANDERSON of the Fish and Wildlife Service at Brunswick, Ga.; and the curatorial staffs of the U.S. National Museum and the Museum of Comparative Zoology.

The work was done under a grant from the National Science Foundation.

Contribution No. 912 *from the Woods Hole Oceanographic Institution*

Woods Hole Oceanographic Institute
Woods Hole, Mass., U.S.A.

REFERENCES

BOLIN R. L. (1939) A review of the Myctophid fishes of the Pacific Coast and of lower California. *Stanford Ichthyol. Bull.* **1**, 89–156.

Bolin R. L. (1946) Lantern fishes from " Investigator " station 670, Indian Ocean. *Stanford Ichthyol. Bull.* **3**, 137–152.

Fraser-Brunner A. (1949) A classification of the fishes of the family Myctophidae. *Proc. Zool. Soc., Lond.* **118**, 1019–1106.

Garman S. (1899) Reports on an exploration off the west coasts of Mexico, Central and South America, and off the Galapagos Islands, etc. XXVI. The fishes. *Mem. Mus. Comp. Zool.* **24**, 1–431.

Hubbs C. L. and Lagler K. L. (1947) Fishes of the Great Lakes region. *Cranbrook Inst. Sci. Bull.* **26**, i-xi + 1–186.

Parr A. E. (1928) Deep-sea fishes of the order Iniomi from the waters around the Bahama and Bermuda Islands with annotated keys to the Sudidae, Myctophidae, Scopelarchidae, Evermannellidae, Omosudidae, Cetomimidae and Rondeletiidae of the world. *Bull. Bingham Oceanogr. Coll.* **3**, Art. 3, 1–193.

Printed in Great Britain by The Salisbury Press Ltd., Publicity House, Wilton Road, Salisbury, Wilts. (6898)

Contribution No. 913

THE AMERICAN MINERALOGIST, VOL. 42, NOVEMBER-DECEMBER 1957

PRELIMINARY REPORT ON THE MINERALOGY AND PETROLOGY OF SOME MARINE BOTTOM SAMPLES OFF THE COAST OF PERU AND CHILE[1]

E-AN ZEN, *Woods Hole Oceanographic Institution, Woods Hole, Massachusetts.*

ABSTRACT

Marine bottom core samples from the coast of Peru and Chile were studied by x-ray and optical methods. For the fourteen cores included in this report, the following minerals are definitely identified: quartz, plagioclase, illite, chlorite, kaolinite, montmorillonite, calcite, aragonite, pyroxene, amphibole (both exclusively detrital), and an oxide of iron. The distribution of the minerals in a given core, as well as their textural relations, tends to remain constant, although considerable differences exist among the cores.

Volcanic glass is a common phase in many samples. Much of the glass is partially or completely devitrified; the products of devitrification include the clay minerals and calcite and demonstrate the exchange of material between the glass and the surroundings. Detailed study of such mineral assemblages should shed light on the equilibrium relations among these minerals in sediments.

INTRODUCTION

During the last months of 1955, the research vessel *Atlantis* of the Woods Hole Oceanographic Institution, under the leadership of B. Kummel and the late H. C. Stetson, undertook a cruise (no. 221) off the Pacific coast of Peru and northern Chile, to collect hydrographic data and bottom sediment samples from this part of the continental margin of South America. A free-running, Stetson-type coring tube was used, and eighty-four cores were recovered. The mineralogy and petrology of these cores have been studied since the autumn of 1956; this paper is a preliminary report of the investigations to date.

The west central coast of South America had been chosen for the investigation for various reasons. Study of the modern sediments from this area have been confined to reconnaissances (Revelle, 1944). The area, however, possesses a combination of both shallow and deep bottoms close to land, strong subaerial relief, and extensive Tertiary and modern volcanism. Sedimentological studies here thus might yield information useful in the interpretation of ancient sediments. Bottom profiles along the coring traverses are being prepared by J. M. Zeigler of the Woods Hole Oceanographic Institution. In addition, broad surveys of the coastal geology may be found in the works of Jenks (1946; 1956), Cristi (*in* Jenks, 1956), and Rüegg (1957); of the bottom topography by Schweigger (1947); and of the surface hydrography by Gunther (1936).

---

[1] Contribution No. 384 from the Department of Mineralogy and Petrography, Harvard University; No. 913 from the Woods Hole Oceanographic Institution.

LABORATORY PROCEDURE

Identification of the minerals in the core samples was principally by means of the Norelco recording Geiger-counter diffractometer, aided by the petrographic microscope with oil-immersion lens. As results using the diffractometer are highly sensitive to experimental methods, a description of the procedure follows.

Samples were taken from a given core at intervals of about 10 centimeters, or wherever visible variations of lithology occur such as color, grain size, and reactivity with HCl. The sample was dried, ground fine, and divided into several portions. One part was saved for heat-treatment and another part used directly for *x*-ray study. Copper radiation with nickel filter was used at 45 KV and 20 ma. A typical instrumental setting was as follows: goniometer speed, 1° 2θ per minute; chart speed, $\frac{1}{2}''$ per minute; scale factor, 4; multiplier, 1; time constant, 4 or 8 seconds; and divergent, scatter, and receiving slits, 1°, 1°, and 0.003″, respectively.

The diffraction patterns were compared with standards for identification. For samples suspected of kaolinite and/or chlorite, a second portion was heated in a muffle furnace to between 550 and 600° C. for $\frac{1}{2}$ hour and *x*-rayed under identical conditions (Brindley and Robinson, *in* Brindley, 1951, p. 188); for samples suspected of montmorillonite, an additional portion was saturated with glycerin and *x*-rayed (MacEwan, *in* Brindley, 1951, p. 115).

Samples were mounted for *x*-ray work using a small hand press. Although this method of sample preparation is liable to uncontrolled orientation effects for some minerals, for routine identification work this effect is an advantage, since commonly the platy minerals occur only in small amounts and without preferred orientation their presence in a crude sample might be undetected.

IDENTIFICATION OF MINERALS

To avoid any possible confusion, the nomenclature used for the various platy minerals is set out below. It should be emphasized that the names do not necessarily correspond to distinct mineral phases, many of which cannot be differentiated by the adopted techniques.

Illite

This name is used in the sense of Grim (1953, p. 35), and applies to all platy minerals in the samples with a strong reflection at about 10 Å. Although much of this is probably related to muscovite, phases such as glauconite and biotite, with 10 Å basal spacings, are possibly present and not distinguished. Nagelschmidt (1937, p. 519) suggests the use of the

(060) line to distinguish the dioctahedral from the trioctahedral micas, a criterion which Grim, Bradley, and Brown (*in* Brindley, 1951, p. 159) point out does not apply to glauconite. Moreover, the criterion is unsuitable for samples with minerals such as kaolinite and quartz with interfering diffraction lines (see, e.g., Brindley and MacEwan, *in* Brindley, 1951, Table XIV, 1, II). Nagelschmidt also suggests (1937, p. 519) that the relative weakness or absence of the 5 Å basal reflection is suggestive of trioctahedral micas. Most of the 10 Å micas from the cores show this relationship. However, this does not seem to be a reliable criterion, as prolonged grinding of natural, coarsely crystalline muscovite has resulted in the complete obliteration of the 5 Å line while the 10 Å line remains strong.

The possibility exists that the 10 Å "illite" in some samples represents intergrowth of muscovite and montmorillonite. Such interlayering may be detected by the angular displacement of the basal reflection spacings of the untreated samples (Brown and MacEwan, *in* Brindley, 1951, p. 277), and by additional displacements upon thermal and organic complexation treatments (MacEwan, *op. cit.*, pp. 118–121; Yoder and Eugster, 1955, p. 249). Detailed studies on a few cores (cores nos. 70 and 74) so far have failed to show the existence of such interlayering.

Kaolinite

This is applied to platy minerals with a ca. 7 Å line, that becomes destroyed by heating to 550–600° C. for ½ hour (Brindley and Robinson, *op. cit.*, p. 188).[2] Although probably predominantly kaolinite, other phases with the same structure cannot be distinguished.

Chlorite

This name applies to a non-swelling platy mineral with a 14 Å line, or, in those cases where this is too weak to be resolved, a 7 Å line which is not destroyed by heating. This criterion is subject to the reservations already discussed in the previous paragraph.

Montmorillonite

This is defined by the presence of a diffraction line between 10 and 14 Å, which swells to ca. 17 Å upon saturation with glycerin (MacEwan, *op. cit.*, p. 115), and collapses to 10 Å upon heating to 550–600° C. Montmorillonite is found in several cores as an important clay-mineral phase; however, as remarked earlier, there is no conclusive evidence for the existence of its intergrowth with muscovite-type layers.

---

[2] Johns, Grim, and Bradley (1954, p. 243) suggest that the loss of diffraction lines after heating to 450° C. is attributable to chlorite, whereas their retention is due to kaolinite. Bradley's suggestion (1954, p. 328) of partial replacement of brucite-layers by "hydrous layers" in some sedimentary chlorites may eventually explain the apparently contradictory observations. The applicability of Brindley and Robinson's criterion to the Peruvian samples is being studied.

Many of the samples have been examined microscopically. Such optical studies yield information on the textural relations in the samples, as well as the presence of fossils and material amorphous to the *x*-ray, such as certain siliceous microfossils and volcanic glass. They also conveniently check the *x*-ray results on mineral identification.

Description of the Cores

The course of cruise 221 of the *Atlantis* was so arranged that seven coring traverses were made roughly normal to the shore line, and one long traverse parallel thereto. The traverses span the region between the coastline and the Peru-Chile trench, a submarine deep running roughly parallel to the west coast of South America (Schweigger, 1947). Not all the cores are yet studied; instead two or three cores from each transverse cruise, one from each end and one from the middle, were taken for the reconnaissance work. The locations of the fourteen cores reported here are given in Fig. 1; in Table 1 the results are summarized in terms of the megascopic lithology (somewhat generalized) and *x*-ray and microscopic mineralogy of the corresponding intervals.

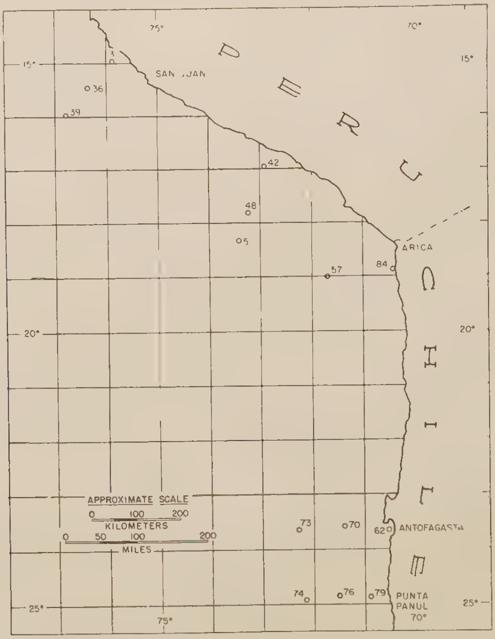

Fig. 1. Map showing locations of the fourteen cores.

TABLE 1. DATA ON THE CORES

Depth interval from top of core, cm.	Megascopic description	Mineralogy
Core no. 31–3. Depth of water: 225 meters		
0–12	Empty	
12–17	Dark olive-brown, homogeneous clayey mud. Weak HCl reaction	Quartz: present but subsidiary Plagioclase: local, subsidiary Illite: trace to absent Kaolinite: rare trace Samples are largely microfossils showing no *x*-ray pattern and optically isotropic
17–23	Grades down from above through light brown silt to white, friable, sandy layer (2 cm.). No HCl reaction	Same as above
23–42	Sharp contact above; fine brown clayey mud. No HCl reaction	Same as above
42–48	Grading down into yellowish white sandy layer (2 cm.) with irregular bodies of brown mud. No HCl reaction	Same as above
48–62	Sharp upper contact; brown mud with light-coloured sandy layers 1 mm. thick, locally crossbedded. No HCl reaction	Same as above
62–77	Brown clayey mud. No HCl reaction	Same as above
77–90	Alternation of 1 mm. layers of brown clayey and pale sandy layers, with planar beddings. No HCl reaction	Same as above
90–107	Brown clayey mud with occasional shell remains. Weak HCl reaction	Abundant quartz at 97 cm., otherwise same as above
107–115	Like 77–90, but strongly crossbedded. Weak HCl reaction	Same as above
115–174	Brown mud, with thin white layers at irregular intervals. The latter type becoming rarer towards the bottom. No HCl reaction except locally	Same as top of core, with rare calcite. (124–162 cm. levels: abundant quartz, variable amount of plagioclase)
174–183	Like 77–90. Weak to no HCl reaction	Same as top of core
Core no. 36–3. Depth of water: 4,435 meters		
0–199	Deep olive brown, clayey mud. Uniform textured, without visible grains. Occasional irregular patches varying in colour from pale brown to dark brown. Rare white ovoids scattered throughout the core. No reaction with HCl except in depth intervals between 45 and 120 cms	Quartz and plagioclase: predominant Kaolinite Illite Pyroxene and amphibole: detrital Calcite: an added phase between 45 and 120 cm. levels Glass: fairly common, mostly devitrified Fossils: abundant throughout the core

TABLE 1. *(continued)*

Depth interval from top of core, cm.	Megascopic description	Mineralogy
Core no. 39–3. Depth of water: 2,600 meters		
0–30	Brown, friable silt with scattered white and black spots. Vigorous HCl reaction	Calcite: predominant, mostly organic remains Quartz and plagioclase: subsidiary; partly detrital Illite Kaolinite or chlorite Glass: abundant
30–36	Grades down to white silty loam, with sharp contact at the bottom. Moderate to weak HCl reaction	Plagioclase: predominant Quartz: trace Illite (possibly biotite) Glass: abundant No calcite
36–63	Brown silt with interspersed layers of white chalky silt in the upper part; otherwise same as 0–30 cm. Sharp contact at the bottom, changing to	Calcite: predominant, organic remains Quartz and plagioclase: abundant Illite Kaolinite: local Pyroxene and amphibole: rare, detrital Glass: abundant
63–90	Pale, chalky silt, with vigorous HCl reaction, grading down to	Calcite: predominant, organic remains Quartz and plagioclase: trace Illite: trace Glass: abundant
90–185	Pure white chalk, without stratification. Vigorous HCl reaction	Calcite: nearly pure sample; organic remains Quartz: very rare
Core no. 42–4. Depth of water: 1,152 meters		
0–40	Unconsolidated, medium sand. Massive and homogeneous, dark olive-green in colour. Rare 1 mm. laminae of white sand. Vigorous HCl reaction except for the top 10 cm.	Quartz and plagioclase: predominant. Mostly as angular (detrital?) grains but partly probably as devitrification product Illite Kaolinite: above 30 cm. level Chlorite: below 30 cm. level Calcite: present except in the top 10 cm; as large rhombs and as devitrification product Pyroxene and amphibole: angular, detrital Glass: abundant, in various stages of devitrification
40–80	Gradationally changes from above downward into olive-yellow colour with local brown stain; otherwise no change in lithology. Vigorous HCl reaction	Same as above, with chlorite Aragonite: between 40 and 60 cm. levels; probably shell fragments
80–86	Gradationally changes from above into light gray, fine silt with dark green partings. Vigorous HCl reaction	Same as 0–40 cm., with chlorite

TABLE 1. *(continued)*

Depth interval from top of core, cm.	Megascopic description	Mineralogy
	Core no. 48–4. Depth of water: 6,146 meters	
0–14	Sticky, fine clayey mud, mostly olive to brown, with local black layers. No HCl reaction	Quartz and plagioclase: predominant; at least partly detrital Illite Kaolinite Pyroxene and amphibole: detrital Biotite: rare, detrital (?) Iron oxide (hydrous?) Glass: abundant Microfossils
14–16	Light brown, friable layer with oölitic texture. No HCl reaction	Quartz and plagioclase: predominant Illite and kaolinite: subsidiary Glass Microfossils
16–80	Same as 0–14 cm.; below 32 cm. level largely olive brown with faint, irregular layering due to colour variation. No HCl reaction	Quartz and plagioclase Illite Chlorite down to 56 cm. Kaolinite below 56 cm. Pyroxene and amphibole: detrital Glass Microfossils: very abundant
80–82	Yellowish-olive, silty clay. No HCl reaction	Same as above, with kaolinite
82–151	Same as 16–80 cm. No HCl reaction	Same as above
	Core no. 51–4. Depth of water: 4,456 meters	
0–18	Empty	
18–80	Deep brown, plastic clayey mud, uniform and homogeneous, nonstratified, with rare white, tiny ovoids. Gradually becomes brownish-gray towards the bottom. No HCl reaction	Quartz: very abundant Plagioclase: abundant Illite Kaolinite Montmorillonite (?) Pyroxene and amphibole: detrital Glass: rare Microfossils: present, but not abundant
80–91	Same as above, except that the mud is hard and non-plastic	Same as above
91–254	Brown plastic mud as above, gradually becoming olive-brown below 200 cm. level. Very local HCl reaction	Same as above
	Core no. 57–5. Depth of water: 4,106 meters	
0–60	Dull whitish green-gray mud, fine, compact, hard, with irregular, thin films of a green colour criss-crossing the sample at intervals of a few mms. No HCl reaction	Quartz: predominant Plagioclase: important Illite and kaolinite: in appreciable amounts Pyroxene and amphibole: scattered Glass: abundant, partly devitrified Microfossils: abundant

TABLE 1. *(continued)*

Depth interval from top of core, cm.	Megascopic description	Mineralogy
60–62	Angular fragments of fine white silty matter in green argillaceous matrix. No HCl reaction	Same as above
62–118	Same as 0–60 cm. levels	Same as above
118–138	Olive brown, unconsolidated, well sorted sand with pale, argillaceous cement; sharp contacts. No HCl reaction	Plagioclase: predominant Quartz: important Illite and kaolinite: absent to barely detectable Glass: abundant Microfossils: abundant
138–175	Same as 62–118 cm. levels	Same as above 118 cm. level
Core no. 62–6. Depth of water: 79 meters		
0–30	Massive, olive coloured, well sorted, unconsolidated sand, grains about 0.5 mm. across. Scattered shells of complete or fragmentary gastropods and pelecypods; locally concentrating into layers. Vigorous HCl reaction	Calcite: predominant Plagioclase: important Quartz: variable in amount, generally subsidiary Illite: only between 60 and 90 cm. levels Kaolinite and/or chlorite: in small amounts, not differentiated Aragonite: probably shell fragments, locally important Amphibole and pyroxene Glass: present in small amounts Fossils: very abundant, including considerable foraminifera
30–90	Same as above but with dark brown argillaceous layers interspersed, up to 2 cm. thick, at irregular intervals	Same as above
90–122	Same as above, but the sand becomes finer-grained approaching silt; core well stratified by colour variation (coarser, olive-colour vs. finer, brown colour)	Same as above
Core no. 70–6. Depth of water: 6,999 meters		
0–70	Fine, sticky, dark brown, homogeneous clayey mud with only occasional colour variations to suggest layering. No HCl reaction	Quartz and plagioclase: predominant. Most of these are large, angular, probably detrital grains Chlorite and illite Kaolinite: local Montmorillonite: local only. With illite, chlorite, and possibly kaolinite Pyroxene and amphibole: detrital, subsidiary Biotite: rare, may be detrital Iron oxide (hydrous?) Glass: moderate in amount, in various stages of devitrification Microfossils: rare

TABLE 1. *(continued)*

Depth interval from top of core, cm.	Megascopic description	Mineralogy
70–131	Gradual change from above; slowly becomes a clay-mud of steel gray colour but with the same texture. No HCl reaction	Same as above; no evidence for montmorillonite
131–134	Gray, friable, fine silt with gradational upper and sharp lower contacts. No HCl reaction	Same as above; grains well sorted Glass: abundant
134–138	Steel gray fine clayey mud as before. No HCl reaction	Same as 0–131 cm. levels
138–141	Same as 131–134 cm., with gradational upper and sharp lower contacts. No HCl reaction	Same as above; much volcanic glass. Grains well sorted
141–145	Olive gray-green clayey mud. No HCl reaction	Same as 0–131 cm. levels
	Core no. 73–6. Depth of water: 4,279 meters	
0–31	Empty	
31–107	Deep chocolate brown, sticky, clayey mud. Uniform and homogeneous, without stratification. Locally (67–72 cm.) vaguely layered due to slight colour differences, or motley-coloured (78–88 cm.). Colour grades downwards into pale choc. brown. No HCl reaction	Quartz: moderately abundant Plagioclase: present, locally abundant Illite Kaolinite Chlorite: locally present Pyroxene and amphibole: detrital Glass Microfossils: present
107–110	Yellowish brown silty mud, with sharp contacts. No HCl reaction	Same as above, with abundant fresh colourless glass
110–279	Same as above 107 cm. level, except that a 2 mm. silty layer exists at 111 cm. level. Colour is predominantly chocolate brown near the top, grading downwards through yellow-brown to gray brown. No HCl reaction	Same as above 107 cm. level; kaolinite more common than chlorite Much glass, mostly devitrified
	Core no. 74–7. Depth of water: 3,968 meters	
0–98	Deep brown, fine, hard mud, with thin, faint layerings at 1–5 mm. intervals due to colour variations. HCl reaction: above 36 cm., none; 36–70 cm., moderate; 70–98 cm., none	Quartz and plagioclase: abundant Illite: abundant Kaolinite: in small amounts Montmorillonite: present Chlorite: in small amounts Calcite: in moderate amounts between 36 and 70 cm. levels Glass: abundant, in various stages of devitrification Microfossils: abundant
98–108	Same as above, with faint, irregular layers of buff mud. HCl reaction: moderate	Same as above, with abundant calcite

TABLE 1. *(continued)*

Depth interval from top of core, cm.	Megascopic description	Mineralogy
108–121	Same as 0–98 cm. levels. HCl reaction: moderate	Same as 0–98 cm. levels
121–141	Same as 98–108 cm. levels. HCl reaction: moderate	Same as 98–108 cm. levels, with abundant glass
141–149	Same as 108–121 cm. levels. HCl reaction: weak to none	Same as 0–98 cm. levels, with chlorite and montmorillonite
149–160	Same as 121–141 cm. levels. HCl reaction: moderate to good	Same as above, with abundant calcite
160–173	Deep brown clayey mud with numerous fine, even layers of light buff mud. HCl reaction: vigorous	Calcite: predominant Plagioclase: abundant Quartz: subsidiary Kaolinite and chlorite: subsidiary, undifferentiated Glass: abundant Microfossils
	Core no. 76–7. Depth of water: 5,669 meters	
0–6	Empty	
6–8	Dark brown mud, uniform and homogeneous. No HCl reaction. (type "A")	Plagioclase: predominant Quartz: in moderate amounts Microcline: possibly present locally Illite Kaolinite Pyroxene and amphibole: detrital Calcite: very rare Glass: abundant Microfossils
8–18	Same, with about equal amounts of irregular patches of fine, buff mud (type "B"); the two types in sharp contact. No HCl reaction	Same as above
18–30	Like type A, but with HCl reaction	Calcite: predominant (organic remains) Quartz and plagioclase: subsidiary Kaolinite Illite: in small amounts Pyroxene and amphibole: rare Glass: rare but present
30–35	Type B, with HCl reaction	Same as above
35–40	Type A, with HCl reaction	Same as above
40–61	A and B in about equal amounts, forming layers or with B in irregular patches. HCl reaction	Same as above
61–70	A, with HCl reaction	Same as above

TABLE 1. (*continued*)

Depth interval from top of core, cm.	Megascopic description	Mineralogy
70–78	A and B in about equal amounts, with B in irregular patches. HCl reaction	Same as above
78–103	A, with HCl reaction	Same as above
	Core no. 79–7. Depth of water: 1,856 meters	
0–2	Empty	
2–26	Olive green, medium-fine, massive sand, with mud matrix. Local shell fragments. Vigorous HCl reaction	Quartz, plagioclase, and calcite: predominant Kaolinite Illite Chlorite Pyroxene and amphibole: detrital Glass: abundant, some very fresh Microfossils: abundant
26–30	Same as above, with 3–5 mm. white sand layers at 3–5 mm. distance apart	Same as above
30–82	Same as 2–26 cm. levels	Same as above
82–85	Gray unconsolidated, well-sorted sand, medium-coarse, without matrix material. Gradational upper, and sharp lower contacts	Quartz, plagioclase, and calcite: predominant Platy minerals: accessory only Pyroxene and amphibole No glass Microfossils: abundant, mostly foraminifera Note: all the microscopically resolved mineral grains are angular and apparently detrital
85–118	Fine brown clayey silt, uniform but for one pale, sandier layer between 94 and 96 cm. levels. Visible quartz and mica grains rarely present	Same as between 2–26 cm. levels
118–131	Intimate interlayering of brown, muddy and white, sandy silt, grading down to uniform fine muddy silt	Same as above
131–138	Slightly coarser silt, same as above 118 cm. level	Same as above
138–140	Same as between 82–85 cm. levels; gradational upper and sharp lower contacts	Same as between 82–85 cm. levels Montmorillonite (?)
140–150	Same as above 138 cm. level, with two thin sandy layers near the upper contact	Same as between 131–138 cm. levels
150–152	Same as between 138–140 cm. levels; gradational upper and sharp lower contacts	Same as between 138–140 cm. levels
152–156	Same as above 150 cm. level	Same as between 140–150 cm. levels

TABLE 1. (*continued*)

Depth interval from top of core, cm.	Megascopic description	Mineralogy
156–158	Same as between 150–152 cm. levels; gradational upper contact	Same as between 150–152 cm. levels
	Core no. 84–5. Depth of water: 933 meters	
0–76	Deep olive-brown, unconsolidated, nonclayey sand. Uniform, nonstratified. Scattered calcareous shell remains throughout. HCl reaction: moderate to weak	Quartz and plagioclase: predominant, mostly detrital Illite: trace Kaolinite: subsidiary Chlorite: found at 40 cm. level only Pyroxene and amphibole: detrital Calcite: small amounts, as product of devitrification Glass: abundant Microfossils: abundant
76–156	Much like above, but with numerous small (about 2 mm. × 4 mm.) irregular light-coloured patches scattered in the core, locally concentrated to suggest layering. Moderate HCl reaction	Same as above

DISCUSSION AND INTERPRETATION

The detrital portions of the cores studied are generally well-sorted. The detrital grains consist largely of volcanic glass in various stages of devitrification, angular grains of quartz, feldspar (plagioclase), pyroxene, amphibole, and also grains comprised of exceedingly fine mineral aggregates, possibly representing fragments of pre-existing rocks. Nevertheless, for a given core at a given depth level, the grains show good sorting, suggesting current action, even though a sample may be largely volcanic glass. This point is supported by observed graded bedding, cross-bedding, and fine-scale interlamination of different lithologies in many of the cores, even one (no. 31) composed nearly exclusively of tests of microfossils.

The gross lithology as well as mineralogy of any given core tends to be constant. Although the contrast amongst cores may be great, samples from a given core, with a few exceptions, tend to have the same minerals in comparable proportions, including the micaceous portions. There seems to be little difference in the *x*-ray patterns between the top of a core, presumably fresh sediment, and the lower, better indurated parts, such as reported by Murray and Harrison (1956, p. 36). True enough, the cores are extremely superficial samples of the sedimentary columns, nonetheless the relative constancy remains striking.

Volcanic glass is commonly encountered. As noted previously, these glass fragments are fairly well-sorted and at places finely interlaminated with other lithologic types—for instance calcitic layers. Quite possibly, these represent ash beds which, as far as microscopic determinations permit, are remarkably free of other types of material, except microfossils, although in this grain-size range it is admittedly difficult to detect rock fragments with any degree of certainty. The fragments of glass in a given sample show very different degrees of devitrification. Some fragments are fresh, the only crystalline phases being occasional unaltered phenocrysts, chiefly plagioclase (usually labradorite to andesine) and pyroxene or amphibole; but other fragments are partly or completely devitrified. Indices of refraction of the unaltered glass commonly yield values near or slightly greater than 1.56 and suggest basaltic composition, although rarely the index may be down to 1.51 and suggests a highly siliceous glass (Williams, Turner, and Gilbert, 1955, p. 28).

The difference in the extent of devitrification may be due to differences in the ages of the fragments, brought together through fluviatile agents. On the other hand, it may also be due to variations in the rates of devitrification, reflecting differences in the thermal history of the fragments, such as the degree of annealing and rate of chilling. Such a phenomenon is known to occur in rhyolitic flows (Boyd, 1957, p. 52); however, few laboratory data exist on this problem.

The most common, and nearly ubiquitous product of devitrification is a non-swelling mica which gives a well-defined reflection at about 10 Å. This is probably closely related to muscovite. A second common product is a 7 Å micaceous mineral, presumably kaolinite. Chlorite is relatively rare, montmorillonite is scarce; but calcite is fairly common. Quartz and an oxide of iron complete the list; whether any other phase results from devitrification is not established.

The formation of calcite and kaolinite, through hydration and carbonation of volcanic glass, is interesting in that it demonstrates the existence of interaction between the glass and its surroundings. Through the intimate association of these two minerals in a matrix of volcanic glass, as determined optically, they are probably stable together, and exclude, under the specific conditions, anorthite as a stable phase. Many samples, on the other hand, have only kaolinite and no recognizable calcite or any other diagenetic essential calcium phase; calcium may have been leached out of these samples.

Another point of interest is the role of iron and magnesium in the devitrification process. At least part of the iron goes to an "oxide" as noted. Apart from this, however, the only recognized essentially ferromagnesian phase is occasional chlorite. While it is possible that part of the magnesium goes into a 10 Å mica, a good proportion of the iron and magnesium may have become dissolved in the surrounding water and lost to the sediment. In general, the more devitrified a volcanic glass is, the lighter its color tends to be.

SUMMARY

Preliminary mineralogical examination of cores collected from the coast of Peru and Chile has revealed some features of mineralogical interest. Chief among these is the presence of abundant volcanic glass in many of the cores. Devitrification of the glass, in contact with sea water, results in minerals whose intimate association suggests approach towards chemical equilibrium; study of the detailed nature of these mineral associations therefore should yield data on the phase relations at the lowest end of the spectrum of diagenetic-metamorphic conditions. On the other hand, it should be emphasized that the very presence of volcanic glass indicates that the samples, as a whole, are not equilibrium systems although portions of them may locally be so.

The principal limitations in a mineralogical-petrological study of sediments lie in the fine grain size and the identification of clay minerals. While the use of modern x-ray diffractometers considerably reduces the size problem, it appears that for many sediments even x-rays are too coarse a probe, which must be supplemented by techniques such as electron microscopy and differential thermal analysis. On the other hand, conventional optical methods can also yield information valuable in the interpretation of the sediment samples.

The principles and methods of clay-mineral identification have been summarized elsewhere (Brindley, 1951; Grim, 1953; Weaver, 1956). Work is currently in progress on the detailed and specific identification of the clay-fraction of the core samples. Results to date, however, do indicate that the clay mineral phases listed in this report are essentially correct.

The geological interpretation of the mineralogical results cannot be made without a comprehensive study of the regional geology, as well as an understanding of the oceanography around the depositional site. Such an interpretation will be deferred to a later date.

ACKNOWLEDGMENTS

I wish to thank Drs. E. H. Smith and C. O. Iselin, past and present Directors, respectively, of the Woods Hole Oceanographic Institution, for their administrative support of the study. The Faculty of the Division of Geological Sciences at Harvard University has generously made available to me all the laboratory facilities. Discussions with Professors B. Kummel and J. B. Thompson, Jr., have been stimulating; their encouragement is gratefully acknowledged. The manuscript was critically reviewed by Professors C. Frondel, B. Kummel, R. Siever, and J. B. Thompson, Jr., all of Harvard University.

REFERENCES

BOYD, F. R. (1957), Geology of the Yellowstone rhyolite plateau. Harvard University Ph.D. Thesis. 134 pp.

BRADLEY, W. F. (1954), X-ray diffraction criteria for the characterization of chloritic material in sediments. *In* Clays and clay minerals, Publ. no. 327, Nat. Acad. Sci. and Nat. Res. Council. pp. 324–334.

BRINDLEY, G. W., ed. (1951), *X*-ray identification and crystal structures of clay minerals. London: The Mineralogical society. 345 pp.

GRIM, R. E. (1953), Clay mineralogy. New York: McGraw-Hill Book Co., 384 pp.

GUNTHER, E. R. (1936), A report on oceanographical investigations in the Peru coastal current. *Discovery* Reports, **13**, pp. 107–276.

JENKS, W. F. (1946), Preliminary note on geologic studies of the Pacific slope on southern Peru. *Amer. Jour. Sci.*, **244**, 367–372.

JENKS, W. F., ed. (1956), Handbook of South American geology. *Geol. Soc. Amer., Mem.* **65**, 378 pp.

JOHNS, W. D., GRIM, R. E., AND BRADLEY, W. F. (1954), Quantitative estimations of clay minerals by diffraction methods. *Jour. Sed. Pet.*, **24**, 242–251.

MURRAY, H. H., AND HARRISON, J. L. (1956), Clay mineral composition of recent sediments from Sigsbee Deep. *Jour. Sed. Pet.*, **26**, 363–368.

NAGELSCHMIDT, G. (1937), X-ray investigation on clays, Pt. III. *Zeit. Krist.*, **97**, 514–521.

REVELLE, R. R. (1944), Marine bottom samples collected in the Pacific Ocean by the Carnegie on its seventh cruise. *Carnegie Inst. Wash. Publ.* **556**, Pt. I. pp. 1–180.

RÜEGG, W. (1957), Geologie zwischen Cañete-San Juan 13°00′–15°24′ Südperu. *Geol. Rundschau*, **45**, 775–858.

SCHWEIGGER, E. (1947), La fosa de Lima. *Bol. Soc. Geol. del Peru*, **20**, 35–50.

WEAVER, C. E. (1956), The distribution and identification of mixed-layer clays in sedimentary rocks. *Am. Mineral.*, **41**, 202–221.

WILLIAMS, H., TURNER, F. J., AND GILBERT, C. M. (1955), Petrography. San Francisco: W. H. Freeman and Co., 406 pp.

YODER, H. S., AND EUGSTER, H. P. (1955), Synthetic and natural muscovites. *Geoch. et Cosmoch. Acta*, **8**, 225–280.

Contribution No. 914

Reprinted from Biological Bulletin, Vol. 113, No. 2, 286–295, October, 1957
Printed in U. S. A.

SOUND PRODUCTION IN THE SPINY LOBSTER PANULIRUS ARGUS (LATREILLE)

JAMES M. MOULTON
Bowdoin College, Brunswick, Maine

SOUND PRODUCTION IN THE SPINY LOBSTER PANULIRUS ARGUS (LATREILLE)[1, 2]

JAMES M. MOULTON
Bowdoin College, Brunswick, Maine

That crustaceans contribute significantly to marine sound is well-known. A list of marine sound producers prepared by the United States National Museum as early as 1942 included members of 17 crustacean families (Fish, 1954). The significance of crustacean sounds to crustacean behavior and to the behavior of other marine animals is, however, largely unknown. There is some evidence that spiny lobsters can detect the vibrations of the sounds they produce (Lindberg, 1955; Dijkgraaf, 1955). Cohen (1955) rejects the statocysts of the lobster, *Homarus americanus,* as auditory organs in the sense of responding to pressure waves in the water, but suggests that statocyst vibration receptors may detect substrate vibrations accompanying sounds.

During June, July and August of 1956, while a guest of the Lerner Marine Laboratory of the American Museum of Natural History, I studied the acoustical behavior of the West Indian spiny lobster, *Panulirus argus.* A study was made of the anatomy of its sound-producing mechanism, and recordings were taken of the sounds produced by this species under various conditions. Through direct observation and motion pictures, data were obtained on the behavior of this spiny lobster in relation to sound production. The study was performed on North Bimini Island, the site of the Lerner Marine Laboratory.

Listening and recording equipment used in the investigation consisted of two Rochelle salt hydrophones, one an AX–58–C, the other undesignated, a Woods Hole Suitcase amplifier or a modified Heathkit amplifier Model A–7C, and an Ekotape tape recorder Model 205. Recordings were made at speeds of 3¾ and 7½ in./sec., and were analyzed on a Vibralyzer vibration frequency analyzer at the Woods Hole Oceanographic Institution. Sound-generating equipment employed in the experiments consisted of a Hewlett-Packard audio oscillator Model LAJ or the Ekotape tape recorder, a Craftsman C550 amplifier, and a QBG transducer.

THE MECHANISM OF SOUND PRODUCTION

Stridulation by spiny lobsters (*Palinuridae*) has been described by a number of authors (Mobius, 1867; Kent, 1877; Goode, 1878; Parker, 1878; Heldt, 1929; Parker and Haswell, 1940, p. 455; MacGinitie and MacGinitie, 1949, p. 282; Dijkgraaf, 1955; Lindberg, 1955) and reference to it is found in classical literature (Yonge, 1854, p. 537). The characteristic rasp of palinurids is produced by an

---

[1] Contribution No. 914 from the Woods Hole Oceanographic Institution.

[2] The work was performed at the Lerner Marine Laboratory of the American Museum of Natural History and at the Woods Hole Oceanographic Institution, under grants of the Institution and of the Bowdoin College Faculty Research Fund established by the Class of 1928.

intricate stridulatory mechanism which has been partially described by Parker (1878) and Dijkgraaf (1955) in a Mediterranean species (*Palinurus vulgaris*). The following description is based on the mechanism as it exists in both males and females of *Panulirus argus,* and adds detail to descriptions previously published of other species.

The acoustic mechanism of *P. argus* consists in part of a toothed ridge, orange-colored in life, rising from the surface of the carapace medial to each antennal base and extending anteriorly from beneath each stalked eye (Fig. 1a). A medial process of the basal segment of each antenna fits over the corresponding ridge; as an antenna is raised, a chitinous longitudinally-ridged membrane, the stridulatory membrane (Fig. 2c), forming part of the undersurface of the medial process, moves proximally over the toothed ridge, in the manner described by Dijkgraaf (1955) for *P. vulgaris,* so that a sound may be produced; the sound varies with the rate and force of raising of the antenna.

That a sound is produced only when the stridulatory membrane moves proximally over the toothed ridge—that is, when the antennae are raised—is due to a combination of factors. The medial process of the antenna is itself jointed, the process being divided into a basal flange (Figs. 1c, 2a) firmly united with the basal antennal segment, and a terminal portion (Figs. 1b, 2d) joined to the posterior edge of the flange. This terminal portion, which Dijkgraaf describes as being a freely-projecting skin-fold in *P. vulgaris,* is covered on its upper surface in *P. argus* with typical exoskeleton. Most of its under surface is formed by a soft chitinous membrane covered with a dense mat of minute setae, the setae becoming sparse along the leading edge of the stridulatory membrane. The under surface of the joint between the basal flange and the terminal portion is the site of the stridulatory membrane.

As a result of the arrangement described, when an antenna is suddenly swept back, the jointed edge of the basal flange bears down on the stridulatory membrane so that the latter is forced to rub proximally over the toothed, orange ridge and a sound is created. Lowering of the antenna relieves pressure on the membrane.

The second factor which determines the effective direction of antennal movement in producing sound is the presence on the portion of the orange ridge over which the stridulatory membrane moves of anteriorly projecting microscopic teeth (Fig. 5) against which the stridulatory membrane is forced when the antennae are swept back. These minute teeth are arranged in shingle-like fashion, teeth of adjacent rows alternating with each other, and the teeth of one row appearing to project from beneath those of the row behind. Anteriorly on the toothed ridge, the leading edges of the teeth form an angle of approximately 60 degrees with the surface of the ridge; in the posterior third of the stridulatory portion of the ridge, the edges are more nearly vertical. Anteriorly the edges of the teeth are slightly serrated; posteriorly they are smooth. In a narrow transition zone (transverse groove between a and b in Fig. 4) between the stridulatory (Fig. 4b) and non-stridulatory (Fig. 4a) parts of the ridge, the teeth give way to blunter microscopic projections, irregularly distributed, which are characteristic of the general carapace.

The presence of the teeth lends to the stridulatory portion of the orange ridge a dull appearance when the ridge is dry; the posterior portion of the ridge, from which the teeth are lacking, possesses a shiny surface when dry. The presence of the teeth can be detected by drawing the tip of the finger posteriorly along the

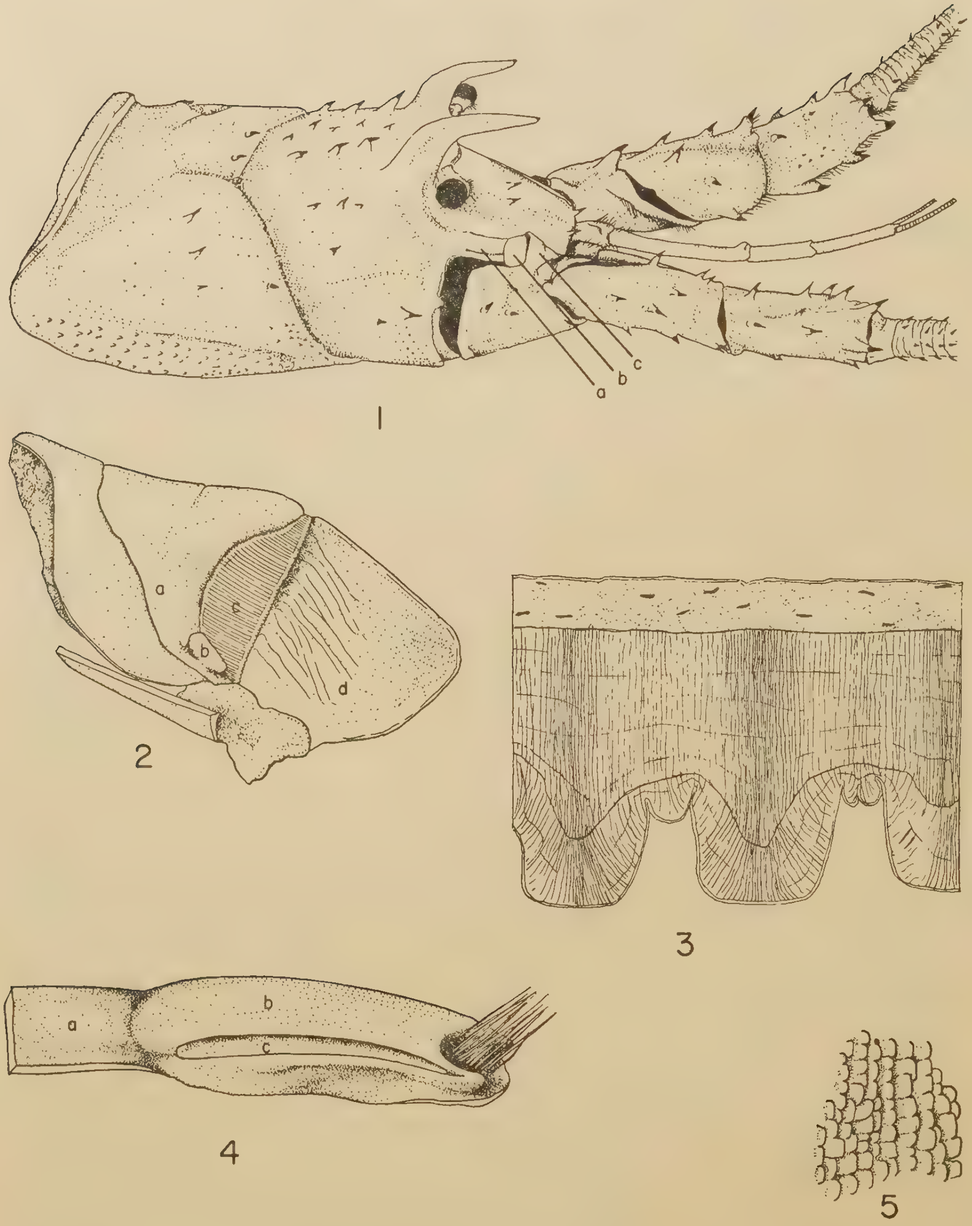

Stridulatory mechanism of *Panulirus argus.*

FIGURE 1: dorso-lateral view of head region; a) toothed portion of orange ridge, b) terminal portion of medial antennal process, c) basal flange. × 1.3.

FIGURE 2: under surface of medial process of right antenna; a) basal flange, b) guiding knob, c) stridulatory membrane, d) terminal portion. × 11.

FIGURE 3: cross-section of stridulatory membrane. × 650.

FIGURE 4: lateral view of right orange ridge; a) smooth portion, b) toothed portion, c) groove receiving guiding knob. × 7.

FIGURE 5: shingle-like teeth of dorsal surface of right orange ridge (anterior to the right). × 500.

toothed portion of the orange ridge. No difference to the touch between tooth-bearing and toothless portions of the orange ridge can be detected when the finger tip is drawn anteriorly.

The region of transition between the toothed and toothless regions of the ridge is marked by a shallow transverse groove (Fig. 4) which is the posterior limit reached by the stridulatory membrane when an antenna is raised. The action of the stridulatory membrane is guided by the presence of a small knob (Fig. 2b) projecting from the ventrolateral surface of the basal flange adjacent to the lateral end of the stridulatory membrane; the knob during raising and lowering of the antenna runs in a well-defined groove (Fig. 4c) on the lateral surface of the orange ridge. This groove extends as far posteriorly as the transverse groove already described. Behind the transverse groove, the orange ridge gradually flattens to the contour of the general carapace.

That the mat of short setae covering most of the under surface of the terminal portion of the medial antennal process becomes very sparse adjacent to the proximal edge of the stridulatory membrane allows one to observe that the surface from which the setae arise bears a polygonal, usually hexagonal, configuration. In this area individual setae spring from individual polygons; elsewhere, two to several setae arise from each polygon, and the dense mat of setae resulting obscures the underlying membrane.

Parker (1878) has figured a cross-section of the ridges of the stridulatory membrane in *P. vulgaris*. In *P. argus*, this membrane is constructed as follows (Fig. 3): there is a basal stratified layer of squamous epithelial cells. From this layer outward, the membrane is vertically striated to the level of the grooves between ridges, in a pattern which suggests that the major portion of the membrane is comprised of many fused setal processes. The ridges themselves comprise approximately ⅖ of the thickness of the membrane, and within the ridges, the striations radiate outward to the surface of each ridge. The whole surface of the stridulatory membrane is covered with a thin cuticular layer following the contour of the membrane. In surface view, the ridges are sculptured in a finely polygonal, usually hexagonal, pattern, the size of the polygons decreasing in the direction of the basal flange. Within the grooves between ridges the cuticular border is somewhat folded and the appearance of surface granulation of the ridges is absent. The stridulatory membrane is somewhat flexible, the relatively stiff ridges yielding a rasping sound when the tip of a dissecting needle is drawn across them.

The stridulatory membrane, as seen in cross-section, is also striated horizontally, in a pattern reminiscent of growth lines in skeletal parts of other animals (*e.g.*, tooth enamel, fish scales and otoliths). These horizontal lines continue into the ridges where they are curved in the contour of the ridges.

If the stridulatory membrane and the terminal portion of the medial antennal process are removed, raising of the antenna by hand produces only a slight squeaking sound as the joint edge of the basal flange bears directly on the toothed part of the orange ridge. The spiny lobster itself produces no sound on raising of an antenna so treated, as Parker (1878) also observed.

A specimen of *P. argus* which shed in one of the cement pools of the Lerner Marine Laboratory during the night of August 11–12, 1956, stridulated as usual in the morning, although the general exoskeleton was still soft. No animal from which the stridulatory mechanism had been removed shed during the summer, so that regeneration of the mechanism cannot be stated as fact.

The Sounds of Panulirus argus

The observation of Kent (1877), questioned by Goode (1878), that a shrill squeaking sound is produced by the spiny lobster (*Palinurus quadricornis*) by rubbing together of abdominal segments was probably accurate. During abdominal contractions, after *P. argus* is taken from the water, the abdomen is at times held tightly for a few moments under the cephalothorax, and a rather intense vibration is felt throughout the hand-held animal. At such times a squeaking sound, higher pitched than any antennal noise, may occasionally be heard. The body vibration accompanying this action is similar to that sometimes produced by the lobster, *Homarus americanus,* freshly removed from a trap or tank; while the latter does not produce an audible sound, vibration is at times so intense that an inexperienced person may drop the animal. This matter requires further study.

The antennal sounds of *P. argus* most frequently heard are either a rasp or a slow rattle of longer duration. The slow rattle, recorded during my study only when several animals were confined together in a live car, is seen after vibration analysis to consist of 5 or 6 pulses of sound spanning approximately .5 to 3.3 kc., the rattle lasting about ¼ second. The pulses are produced at an average rate of 27/second, varying in several cases from 24 to 31/second. The greatest intensity of each of these pulses lies at approximately .6 kc.

The antennal rasp, which usually accompanies abdominal contractions when a specimen is held in the hand in air or water, is a single burst of sound in which the individual pulses of sound cannot be distinguished. The sound lasts slightly over .1 second, and spans frequencies from below .04 kc. to approximately 9 kc. The zones of greatest intensity lie at .8 kc. and in a rather broad band between approximately 2.5 and 4.7 kc.

As a hand-held animal slows or ceases its abdominal contractions, the antennae may be swept back alternately rather than together. In sounds created by this action, individual pulses can be distinguished on vibration analysis. They are produced at rates varying between 56 and 133/second, with intensity peaks at the levels of the antennal rasp.

The rasp of *P. argus* can be roughly duplicated through moving the antennae upward by hand. The vibration analyses of sounds thus produced are like those of the rasp, except that instead of a single burst of sound there are from four to several bursts at somewhat irregular intervals; the upper peak intensity is more diffuse than in the normally produced rasp, and the lower peak (.8 kc.) of the normally produced sound is lacking. It has not been possible by this method to duplicate the slow rattle recorded from confined animals undisturbed by the observer.

Sound Production and the Behavior of Panulirus argus

That the production of sound by the spiny lobster is a response to definite stimuli is indicated by the observations of Lindberg (1955) and Dijkgraaf (1955). The antennae of *P. argus* are frequently moved without the production of sound, even when the basal segment of the antenna is involved. Aquarium-confined spiny lobsters trained to accept food offered by hand from above during the summer of 1956 characteristically raised themselves on their anterior legs, reaching their antennae up toward the proffered food. At such times, no sound was produced. Similarly, observations on live-car confined animals disclosed no antennal sounds produced during listening by hydrophone at times when the majority of animals were moving their antennae.

Although conditions surrounding production of the slow rattle are obscure, the sound bursts characteristic of the rasp frequently accompany strong, rapid abdominal contractions which are characteristic of the hand-held or net-captured animal. During these contractions, whether the restrained *P. argus* is struggling in the water or in air, the antennae are held back over the body and each forward thrust of the rapidly and forcefully contracting abdomen is accompanied by a brief rasp as the stridulatory membrane rubs over the orange ridge. Sounds intermediate between the slow rattle and the rasp are produced by antennal movements in the absence of abdominal contractions; although these intermediate sounds are difficult to distinguish by ear from the rasp, vibration analysis distinguishes them.

It is evident that the sounds produced by *P. argus* and the behavior which they accompany differ with circumstances. Dijkgraaf describes production of the rasp during struggling between two individuals of *P. vulgaris.* Circumstances under which the rasp is produced in *P. argus* (grasping in the hand, capturing in a net, injury) suggest that this sound is related to defensive behavior. This relationship is further emphasized by the fact that during production of the rasp, the spiny antennae are held over the back, tightly depressed against the carapace or against the grasping hand. During abdominal contractions, the forward-directed spines of the carapace are driven against the hand, and the hand is driven against the backward-directed spines of the antennae; blood is frequently drawn. At the same time, the abdominal contractions provide an efficient scissor-like action through the sharp edges of the abdominal exoskeleton, and the fingers caught within the scissors may be cut. Presumably the action described would also be performed against natural captors in the sea.

Gradual subsidence of abdominal contractions and of antennal sound by the hand-held animal will take place. A sudden movement of the hand will, however, re-initiate the whole process, and again a gradual subsidence, usually through a period of alternate antennal stridulations, will occur. The response gradually diminishes.

At the Lerner Marine Laboratory, up to several dozen spiny lobsters are confined at a time in a live car of screen and boards adjacent to the Laboratory dock in Bimini Harbor. When a hydrophone was lowered into this live car and left hanging in it during the daytime, the slow rattle already described was frequently heard. The individual pulses of the slow rattle, probably produced as the stridulatory membrane skips along the orange ridge, can be detected. The sound does not necessarily accompany marked activity of the animals to judge from visual observations, and is not recorded from a highly active animal. This slow rattle seems to be more in the nature of a conversational sound, as compared with implications of argument suggested by circumstances under which the rasp is produced.

The slow rattle could not be heard with the equipment employed 30 feet from the live car, although the rasp was clear over this distance underwater.

That the slow rattle is not produced by accidental movements of the antennae is suggested by the following observations: if the spiny lobsters in the live car were stirred up with an oar neither the slow rattle nor the rasp was heard, and after this procedure it was some time before the slow rattle was heard again; nearly constant antennal movements by isolated animals moving about in glass aquaria did not result in production of any sound, nor was the slow rattle recorded from any isolated animal; the slow rattle was recorded only during daylight, not at night when the spiny lobsters were moving about the live car; if an animal were suddenly clamped to the bottom with the edge of a dip net, only the rasp was heard to accompany the animal's activity, never the slow rattle which might have been anticipated if it were an accidental sound.

During the daytime, undisturbed *P. argus* tended to remain heaped in the corners of the live car; at night the animals were more obviously active, moving about the screen forming the sides of the car. Yet the slow rattle was heard only during the daytime. Thus, during 1½ hours of listening between 0900 and 1100 the morning of 21 June, the slow rattle was heard 76 times, whereas it was not heard at all during comparable time between 1950 and 2130 the evening of 20 June under an approximately ⅚ full moon. These observations were made when the live car contained between two and three dozen animals.

The stridulatory mechanism is best rendered inoperative by bilateral removal of the medial process of the antenna, at the junction of the basal flange and basal segment of the antenna. It is difficult effectively to remove the stridulatory membrane without removing the whole medial process, since even a remnant of the ridges will produce considerable sound.

A male spiny lobster with the stridulatory mechanism bilaterally removed was confined in an aquarium with a normal male of similar size during July of 1956. The normal animal was the dominant individual, frequently approaching the operated animal head-on with extended anterior walking legs and slightly raised antennae, walking forward as the operated animal retreated to a corner. At such times, no sounds were heard.

Numerous attempts to influence the behavior of spiny lobsters by playing recordings of the rasp and of the slow rattle into the live car and into aquaria containing individual specimens were unsuccessful, nor did recorded sounds of spiny lobsters played underwater noticeably alter the distribution of various fishes confined with them. The same was true if pulsating signals generated with the audio oscillator set at 17 to 40 cps. (Moulton, 1956) were played into the water.

Discussion

The production of two characteristic sounds by *Panulirus argus* and the behavior which the sounds accompany, parallel a situation occurring among fishes in sea robins (*Prionotus* spp.) which when free during the breeding season produce a staccato call, but which when disturbed in various ways produce a vibrant grunt of other frequency characteristics (Moulton, 1956). Like the staccato call of the sea robins, the slow rattle of the crayfish has not been recorded from hand-held or otherwise disturbed specimens. As the grunt and the staccato call of the sea robins relate to two different patterns of behavior, thus the rasp and the slow rattle of the spiny lobster, *P. argus,* do also.

The significance of their sound production to the survival of spiny lobsters is unknown. Lindberg (1955, pp. 178–179) observed that *P. interruptus* did not stridulate unless it and an attacking fish touched each other. Since the sounds produced by *P. argus* span the frequency sensitivity of various fishes which have been tested (Kleerekoper and Chagnon, 1954), it is not impossible that a combination of sound production and injurious strokes of the abdomen may combine as a deterrent to predators. Unfortunately, information is lacking on this point. My own observations concur with those of Lindberg in denying an obvious effect of the rasp on fish behavior. A mutilated specimen of *P. argus* passing, while vigorously rasping, through approximately 25 feet of clear water at Bimini on the west side of Turtle Rocks, did not immediately nor during several minutes of observation through glass panels at the surface attract any of the numerous reef fishes feeding within the zone of observation, nor did visible fishes which might be anticipated to feed on injured spiny lobster noticeably alter their behavior.

Dijkgraaf's (1955) observation that stridulation could be induced in a highly excited *P. vulgaris* by imitating the rasp adjacent to the aquarium is compatible with Lindberg's observation that *P. interruptus* moved away from other animals forced to stridulate nearby but out of sight. Lindberg observed that stridulation occurred only upon impending conflict and thus considers the sound "a threat rather than an alarm." Several *P. argus* contained in aquaria at Bimini moved rapidly away from a net or grasping hand, but did not stridulate until grasped or captured in the net—that is, the rasp was not necessarily produced during rather violent escape maneuvers.

The failure of fishes to respond to the sounds of *P. argus* is consistent with previous observations on the responses of free fishes to sound generally (Moulton and Backus, 1955; Moore and Newman, 1956). Since, however, several kinds of fishes will respond initially by quickened swimming movements—startle reactions—to sounds which later will fail to affect their behavior, it is possible that a sudden rasp by a mouth-held palinurid might cause a preying fish to release its hold and thus its prey, particularly if the sound were accompanied by strong abdominal contractions. This is to suggest that the rasp may act as a double assurance mechanism.

Vibration analyses of various fish sounds recorded from identified species at Woods Hole and Bimini indicate that sounds produced by several kinds of fishes under duress of various types are more like the rasp of the spiny lobster than like the slow rattle of undisturbed *P. argus* or than like the staccato call of free sea robins during the breeding season. The burst of sound characterizing the spiny lobster rasp also characterizes the sounds produced, during handling, by sea robins (*Prionotus* spp.), grouper and hind (*Epinephalus* spp.), angelfish (*Pomacanthus* spp. and *Angelichthyes ciliaris*), squirrelfish (*Holocentrus ascensionis*), triggerfish (*Balistes vetula* and *Melichthyes piceus*), swellfish (*Spheroides* spp.), porcupinefish (*Diodon hystrix*), a jack (*Caranx hippos*), and grunts (*Haemulon* spp.)—defensive behavior of all of these includes production of sounds lacking sharply defined individual pulses within the limits of the analyses. Thus sounds produced in a variety of ways—by stridulation of skeletal parts, by muscle contraction against an air bladder or adjacent tissue, by pounding of pectoral fins against the body—

but under similar circumstances, present similar, although not identical, vibration analyses. These observations, combined with observations on the slow rattle of *P. argus* and the staccato call of sea robins, suggest that while sounds produced by undisturbed marine fishes and crustaceans are likely to be sounds comprised of individual pulses of brief duration, sounds of marine fishes and crustaceans under duress are more likely to be bursts of sound of longer duration in which individual pulses are obscured or absent.

Another category of marine sound, comparable in its vibration analyses to sounds produced under duress by fishes and to the rasp of the spiny lobster, is the feeding noise of such fishes as wrasses (*Labridae*), porcupinefish, swellfish, triggerfish, and angelfish. If sound bursts comprise threats or alarms, as conditions of their production would suggest, noisy eating by these organisms may serve to repel rather than to attract predators.

Exceptional in producing sounds of sharp individual pulses during defensive behavior are representatives of two crustacean groups in the Bimini area, the stomatopod (*Gonodactylus oerstedi*) and several kinds of snapping shrimp (*Alpheidae*), especially *Alpheus armatus* and *Synalpheus* spp. (Pearse, 1950). Although produced in a different way, the sound of the mantis shrimp is like that of the snapping shrimp (Goode, 1878; Johnson, Everest and Young, 1947; Fish, 1954), and their vibration analyses are indistiguishable. Both are either burrowers or symbionts of organisms providing highly protected situations (Pearse, 1950; Townsley, 1953; Banner, 1953; Clarke, 1955). Further, the sounds produced are the by-products of accompanying movements which have a distinctly protective value—the decisive closure of the snapping shrimp large chela with its accompanying squirt of water (Schmitt, 1931, p. 192; Johnson *et al.,* 1947) and the stinging extension of the raptorial appendage of the mantis shrimp.

That some sounds of marine arthropods are other than accidental is, however, clearly indicated by the intricate stridulatory mechanism found among the spiny lobsters (Palinuridae). The usefulness of the sounds produced, as of the sounds produced by many kinds of fishes, is yet to be determined.

I am indebted for constructive criticism to Mr. William Schevill who read the manuscript of this paper, and for careful execution of the drawings to Mr. Ernest R. Powell, an undergraduate of Bowdoin College.

Summary

1. The intricate stridulatory mechanism of the West Indian spiny lobster, *Panulirus argus,* and the sounds it produces are described. The sounds are related to various patterns of behavior.

2. On the basis of behavioral evidence it is suggested that a slow rattle is characteristic of spiny lobsters when contained in groups, and that a rasp is a usual component of defensive behavior.

3. The characteristics of the sounds of *P. argus* are compared to those of other marine sounds of biological origin. On the basis of this comparison, an attempt is made to generalize (a) the type of sound which accompanies defensive behavior of marine fishes and crustaceans, and (b) the type of sound stemming from marine fishes and crustaceans when undisturbed.

4. It is concluded that the intricacy of the sound-producing mechanism of *P. argus,* and of other palinurids, justifies a conclusion of a significance of sound to the biology of spiny lobsters. While certain suggestions of a possible value of the rasp to survival of spiny lobsters are presented, a consistent effect of the rasp on the behavior of other spiny lobsters and on predator organisms has yet to be demonstrated.

LITERATURE CITED

BANNER, A. H., 1953. The Crangonidae, or snapping shrimp, of Hawaii. *Pacific Science,* **7**: 3–144.

CLARKE, W. D., 1955. A new species of the genus Heteromysis (Crustacea, Mysidacea) from the Bahama Islands, commensal with a sea-anemone. Amer. Museum Nov., No. 1716: 1–13.

COHEN, M. J., 1955. The function of the receptors in the statocyst of the lobster *Homarus americanus. J. Physiol.,* **130**: 9–34.

DIJKGRAAF, S., 1955. Lauterzeugung und Schallwahrnehmung bei der Languste (*Palinurus vulgaris*). *Experientia,* **11**: 330–331.

FISH, M. P., 1954. The sonic marine animal problem. Research Reviews, Dec.: 13–18.

GOODE, G. B., 1878. The voices of crustaceans. *Proc. U. S. Nat. Mus.,* **1**: 7–8.

HELDT, H., 1929. Rapport sur la langouste vulgaire (*Panulirus vulgaris* Latreille). *Rapports et Procès-Verbaux des Réunions, Commission Internationale pour l'Exploration Scientifique de la Mer Méditérranée,* **4**: 113–126.

JOHNSON, M. W., F. A. EVEREST AND R. W. YOUNG, 1947. The role of snapping shrimp (*Crangon* and *Synalpheus*) in the production of underwater noise in the sea. *Biol. Bull.,* **93**: 122–138.

KENT, W. S., 1877. Sound-producing arthropods. *Nature,* **17**: 11.

KLEEREKOPER, H., AND E. C. CHAGNON, 1954. Hearing in fish, with special reference to *Semotilus atromaculatus atromaculatus* (Mitchill). *J. Fish. Res. Bd. Can.,* **11**: 130–152.

LINDBERG, R. G., 1955. Growth, population dynamics, and field behavior in the spiny lobster, *Panulirus interruptus* (Randall). *Univ. Calif. Publ. Zool.,* **59**: 157–247.

MACGINITIE, G. E., AND N. MACGINITIE, 1949. Natural history of marine animals. McGraw-Hill Book Co., Inc., New York.

MOBIUS, K., 1867. Ueber die Entstehung der Töne, welche *Palinurus vulgaris* mit den äusseren Fühlern hervorbringt. *Arch. f. Naturgeschift.,* **33**: 73–75.

MOORE, H. L., AND H. W. NEWMAN, 1956. Effects of sound waves on young salmon. Spec. Sci. Report, Fisheries No. 172, U. S. Fish and Wildlife Service.

MOULTON, J. M., 1956. Influencing the calling of sea robins (*Prionotus* spp.) with sound. *Biol. Bull.,* **111**: 393–398.

MOULTON, J. M., AND R. H. BACKUS, 1955. Annotated references concerning the effects of man-made sounds on the movements of fishes. Fisheries Circ. No. 17, Dep't of Sea and Shore Fisheries, Augusta, Maine.

PARKER, T. J., 1878. Note on the stridulating organ of *Palinurus vulgaris. Proc. Zool. Soc. London,* 1878: 442–444.

PARKER, T. J., AND W. A. HASWELL, 1940. A text-book of zoology, 6th ed., rev. by O. Lowenstein. Macmillan and Co., Ltd., London.

PEARSE, A. S., 1950. Notes on the inhabitants of certain sponges at Bimini. *Ecology,* **31**: 149–151.

SCHMITT, W., 1931. Crustaceans. *Smithsonian Scientific Series,* **10**, Part 2: 192–199.

TOWNSLEY, S. J., 1953. Adult and larval stomatopod crustaceans occurring in Hawaiian waters. *Pacific Science,* **7**: 399–437.

YONGE, C. D., 1854. Translation of *The Deipnosophists* or *Banquet of the Learned* of Athenaeus, Vol. 2. Henry G. Bohn, London.

Contribution No. 916

EXTRAIT DU JOURNAL DU CONSEIL INTERNATIONAL
POUR L'EXPLORATION DE LA MER
VOL. XXII. No. 2. 1957

Contribution No.916 from the Woods Hole Oceanographic Institution

Factors Affecting the Accuracy of Thermometric Depth Determinations

By

G. G. Whitney, Jr.

A point in oceanography upon which a considerable difference of opinion appears to exist is the accuracy of depth measurements made by the use of deep-sea reversing thermometers. The perhaps over-optimistic view taken by some observers is that such thermometers are absolutely reliable, and that depth determinations made in this manner are accurate to the last metre. At the other extreme are those who prefer to trust their meter wheel, trigonometry, and strain calculations to give them depths based on wire-angle and length, and are suspicious of all thermometers.

In order to attempt to clarify the issue and resolve these differences of opinion, it is proposed herein to examine the problem in some detail, and to set forth the various factors which may affect the potential accuracy of thermometric depth determinations, exclusive of mathematical errors. It is hoped that this discussion will be of benefit to those who have occasion to use one of the oceanographer's most basic tools, the reversing thermometer.

In the following paragraphs dealing with the possible sources of error, protected thermometers graduated in 0·05°C. (20 scale divisions per degree) and unprotected thermometers graduated in 0·1°C. (10 scale divisions per degree) will be used as examples. In general, if the number of scale divisions per degree is halved, the possible error will be doubled.

In common practice, the technique used in thermometric determination of depth is to pair an unprotected reversing thermometer (bulb exposed to pressure of the water) with a protected one (bulb shielded from water pressure) in the same frame on the hydrographic cable so that they are reversed simultaneously at the same depth and temperature. The actual temperature in situ (T_w) can be determined, after certain corrections, from the reading of the protected thermometer, while the actual temperature plus the effect of the water pressure at that depth (T_u) is indicated, after certain corrections, by the reading of the unprotected thermometer. The difference between these two readings (T_u–T_w) is the result of pressure exerted on the bulb of the unprotected thermometer by the depth of the water. From laboratory tests (pressure factor determinations) prior to use at sea, the amount of increase in reading of each unprotected thermometer due to a given amount of pressure on the bulb (given depth) has been established; this being known, T_u–T_w can be translated into depth.

This pressure factor, or Q, is generally expressed in degrees Centigrade per kilogramme per square centimetre. Its magnitude will usually be between 0·0750°/Kg./cm^2. and 0·1250°/Kg./cm^2. In referring to Q, the unnecessary parts of the expression are normally omitted, so that the two noted above would be written simply ·0750 and ·1250.

When Q is large, the potential accuracy of the depth indication is also large, but the useful range of the instrument is small. If the Q of a shallow-water unprotected thermometer (range −2 to 30°C.) were as high as 0·2000 the reading increase due to pressure at 1000 metres would be of the order of 20·5°C. or 0·02° per metre. Since an instrument of this range can easily be read to the nearest 0·01°, one could theoretically detect a change of half a metre in depth, but the instrument would not be usable much below 1000 metres, as T_u would then be apt to be above the upper limit of the scale.

General practice in the manufacture of shallow-water unprotected thermometers is to attempt to achieve the largest pressure factor (for accuracy) consistent with the ability to use the instrument to depths somewhat below 2000 m. Deep-water unprotected thermometers (range −2 to 60°C.) of necessity have somewhat smaller pressure factors, of the order of 0·0800. The bulbs must have somewhat stronger walls to withstand pressure at depths down to around 6000 m., and hence respond less to a given pressure load. While these can be used at any depth down to the limit of the scale, because of their small Q and large graduation interval (0·2°), precise results are difficult to obtain. For special purposes, thermometers have been designed and built, for the Woods Hole Oceanographic Institution, which have a scale running from 35° to 60°C. (with zero point) graduated in 0·1°, and having a very small Q. These are usable only at depths below 4000 m., but are capable of a high degree of accuracy from that level down to the very deepest parts of the Atlantic Ocean, about 8000 m.

Since the Q of each unprotected thermometer depends upon the shape, size, wall thickness, and glass characteristics of the main bulb, there is no way of controlling its exact value in manufacture; Q may well vary ±0·0050 or more from the nominal value desired. For this reason, the Q for each unprotected thermometer must be determined by laboratory test.

In such tests, the unprotected thermometer is reversed at a known temperature and pressure, and the Q determined according to the formula $Q = \frac{T_u - T_w}{P}$, where T_u is the unprotected reading after application of scale correction, T_w is the actual temperature at the time of reversal, and P is the pressure expressed in Kg./cm^2. T_w may be determined either by immersing the pressure vessel in melting ice (0·00°C.) or by placing a protected thermometer in the pressure vessel with one or more unprotected thermometers, in which case T_w is taken as the corrected reading of the protected thermometer. This latter method is employed at this laboratory, although ice is used in the water bath surrounding the pressure vessel to keep the temperature essentially level near 0°C. (Whitney, 1955).

Since no thermometer can be expected to show exactly the actual temperature at all points on the thermometer scale, all reversing thermometers must be calibrated to establish the required scale corrections prior to the pressure factor tests and issue for use at sea.

It is obvious, therefore, that a large number of tests and readings are necessary to certify a reversing thermometer before the oceanographer sits down to make his final temperature and depth calculations. There are discussed below the factors which may affect the ultimate accuracy of thermometric depth determinations. It will be noted that each point covered involves a possible error.

Probable Accuracy of Standard Thermometer

In order to establish the necessary scale corrections for thermometers, a temperature standard is required. At the Woods Hole Oceanographic Institution, a set of specially designed mercury-in-glass thermometers, covering several temperature ranges, are used for this purpose. These themselves require scale corrections, which have been determined by the National Bureau of Standards. Frequent checks in melting ice are made of these standard thermometers to note any shift in the reading at 0·000°C. (which would cause an equal shift in the scale corrections at all other points on the scale). It is considered that these standards, as corrected, give temperature values within ±0·003°C. of the actual temperature.

Since these standard thermometers are used to determine scale corrections for both the protected and unprotected thermometers, this possible source of error must be taken into consideration twice, once for each type of reversing thermometer.

Possible Error in Thermometer Scale Corrections after Calibration

Necessary scale corrections for both protected and unprotected thermometers are determined in a controlled temperature tank. Readings of the reversing thermometers for three to five reversals at the same nominal temperature are compared with readings of the standard thermometer at those same temperatures. The arithmetical average of the indicated corrections for all tests at each nominal temperature is used as the final stated correction for the instrument at that temperature. For example, if the indicated corrections for five reversals at a given temperature were —0·045, —0·040, —0·043, —0·045, and —0·038, the final stated correction at that temperature would be —0·042°. It is considered that this final correction value will be accurate to within ±0·002° if the scale is graduated in 0·05° increments (protected thermometer) or within ±0·004° if the scale is graduated in 0·1° (unprotected thermometer).

Possible Interpolation Error

Reversing thermometers are usually calibrated every fifty scale divisions (every five degrees if the scale is graduated in 0·1° increments). Exceptions are those of range −2 to 8°C., which are calibrated every forty scale divisions (two degrees), and sometimes those of range −2 to 15°C., which may be calibrated every sixty scale divisions (three degrees). If the scale corrections vary greatly from one calibration point to the next, the interpolation necessary to arrive at the correction for a reading lying between two such calibration points can lead to a very substantial error, as there is no way of knowing that the correction change is linear between the two points. If the rate of change of corrections is less than 0·1 scale division per degree (as usually specified), the interpolation error in applying scale corrections to readings of the unprotected thermometers during pressure factor tests should not be more than ±0·004°. Since these Q tests are made at temperatures approximating to 0°C., the known 0° correction of the protected thermometer used as a standard is applied, and no interpolation is necessary, so no error should exist from this source.

Possible Reading Error during Q Tests

Even the eye of an experienced technician may, on occasion, make minor errors in reading the thermometers during Q tests. Fogging and parallax are frequently encountered. While errors of this nature will generally average out, they may not, and this possible error must be taken into consideration. Such reading error might be ±0·002° for the protected thermometer (pressure standard), and ±0·004° for the unprotected thermometers.

If the total amount of the possible errors noted so far are added, the sum is ±0·022°, the probable accuracy of the thermometer as ready for use at sea.

Inherent Accuracy of Thermometer

The heart of any reversing thermometer is its break-off point, the junction of the main capillary bore with the so-called appendix, or "dead arm", at which point the mercury column is supposed to separate when the instrument is reversed. The precision and care with which this break-off point is made determines the inherent accuracy or reproducibility of the thermometer. A good instrument should be able consistently to reproduce readings at the same temperature to within ±0·1 scale division (within ±0·005° for a protected thermometer graduated in 0·05°; within ±0·01° for an unprotected thermometer graduated in 0·1°). Some of the very best instruments will reproduce to within less than half these limits, but the larger figures should be used in considering possible errors.

Possible Reading Error at Sea

When the thermometer is used at sea, some of the same sources of error are again present, so that additional errors may be introduced at each

Sources of Error in Thermometric Depth Determinations

	Affecting protected thermometres		Affecting unprotected thermometres	
	0·05° graduations	0·1° graduations	0·1° graduations	0·2° graduations
Probable accuracy of standard thermometer, as corrected	±0·003°C.	±0·003°C.	±0·003°C.	±0·003°C.
Possible error in thermometer scale corrections after calibration......	0·002	0·004	0·004	0·008
Possible interpolation error in correcting thermometers during *Q* tests (may be much greater if rate of change of scale corrections is large)	None	–	0·004	0·008
Possible reading error during *Q* tests	0·002	–	0·004	0·008
Probable inherent accuracy of thermometers	0·005	0·010	0·010	0·020
Possible reading error at sea	0·005	0·010	0·010	0·020
Possible interpolation error in correcting thermometers (may be much greater if rate of change of scale corrections is large)	0·002	0·004	0·004	0·008
Possible errors in rounding scale corrections to nearest 0·01°	0·005	0·005	0·005	0·005
Total possible error...............	±0·024°C.	±0·036°C.	±0·044°C.	±0·080°C.

Total possible error of column 1 paired with column 3.......	±0·068
Total possible error of column 2 paired with column 3.......	±0·080
Total possible error of column 1 paired with column 4.......	±0·104

hydrographic station. Conditions for reading the thermometers at sea are frequently far from ideal, and it may be expected that reading errors of ±0·005° for the protected, and ±0·01° for the unprotected thermometers may commonly occur.

Possible Interpolation Errors in Correcting Thermometers

Since readings at sea seldom come at points of known correction on the scale (calibration points), interpolation of the scale corrections must usually be made. If the rate of change of scale corrections is small, as mentioned above, the possible interpolation error might be ±0·002° for the protected thermometer and ±0·004° for the unprotected thermometer. As stated previously, if the rate of change of scale corrections is large, these interpolation errors may be very much greater.

Possible Error in Rounding-off Scale Corrections

To simplify the final calculation of temperature and depth, scale corrections which are stated to the nearest 0·001° are commonly rounded to the nearest 0·01° (−0·034 becomes −0·03; −0·035 becomes −0·04). In this way, additional error in each thermometer may be introduced up to ±0·005°.

Summation of Possible Errors

If all of these possible errors are added together, the result is a total of ±0·068 (see table). If Q is large (i. e., 0·1250) this would result in a possible error in depth of ±5·4 m. per 1000 m., or 0·54%. If Q were small, (i. e., 0·0750) the error might be ±0·91%. It is most unlikely that all errors would be in the same direction in any given case, so the accuracy should generally be much better than this.

If an unprotected thermometer graduated in 0·2° is used, the total possible error might be increased by ±0·036°, or about 53% more error than shown in the table. If a protected thermometer graduated in 0·1° were used to determine T_w at sea, the total error might be increased by ±0·012°, or 18% more than shown in the table.

Exception for Depth less than 1000 Metres

This reasoning does not, however, hold for depths between 1000 m. and the surface. The nature of the depth calculation is such that at these shallower depths, errors in reading and in the apparent accuracy of the thermometers become increasingly more significant at a rapid rate as one approaches the surface. In addition, tests tend to indicate that the pressure factor of many unprotected thermometers becomes unreliable, and may change 0·0003 or more at depths less than 500 m.; in other words, it becomes inconstant at low pressure.

WÜST (1932) made an extensive examination of this matter in connexion with the thermometers used by the "Meteor" Atlantic Expedition, for which he assumed a general average value of the pressure factor of 0·0900. He concluded that the maximum probable error of depth determination might be ±1·0% at 5000 m., ±1·4% at 1000 m., and ±6·0% at 100 m. He also postulated that the mean accuracy might be expected to be ±0·4% at 5000, ±0·6% at 1000, and ±3·0% at 100 m.

If the same relation of probable maximum to probable mean accuracy used by WÜST is applied to the estimated maximum probable errors stated above and shown in the table, the resulting probable mean errors would be ±0·23% if Q were large, or ±0·38% if Q were small, at depths of about 1000 m. These percentages would decrease slightly at greater depths, and increase considerably toward the surface.

It may be noted that WÜST attributed a rather large error, ±0·0006, to the pressure factor. Recent investigation tends to indicate that, at depths of around 1000 m. and greater, the pressure factor can generally be expected to be accurate to within ±0·0001. On the other hand, considering the many possible sources of very minor errors arising in the calibration of the reversing thermometers and their reading and correction at sea, as shown in the table, WÜST's estimate of errors attributable to reading and correction (ΔT) of ±0·04°–0·05° maximum, or ±0·02° mean, was perhaps on the conservative side. Although WÜST considered the possible error of ϱ m. in his calculations, this is so small, except at the very shallowest depths, that for all practical purposes it may be disregarded.

Conclusion

It is perhaps interesting to note the relative similarity of the ultimate conclusions reached by Wüst and in the present work with different lines of reasoning.

All of the foregoing assumes that instruments of good quality, which have been carefully calibrated, are used by competent observers, and that functioning of the thermometers is normal. Major malfunctions, in which the thermometer reads incorrectly by upwards of a degree or more, are relatively easy to detect. Minor malfunctions, in which the reading is wrong by a few hundredths or tenths of a degree frequently are not apparent, and result in false temperatures and/or depths. Malfunctions of this sort may be considered responsible for much of the criticism of the accuracy of reversing thermometers. From the same standpoint, unreliable thermometers are a serious handicap to oceanographers, so the very best instruments obtainable should be well worth the investment.

On the basis of the present work, it is therefore concluded that thermometric depth determinations are usually accurate to within 5 m. per 1000 m., and if the best instruments are used under good conditions, it would not be unreasonable to expect an accuracy to within 2 m. per 1000 m.

Summary

The technique of thermometric depth determination is briefly described, with comments on design factors affecting the magnitude of the pressure factor Q. The technique of laboratory tests of pressure factor determination is briefly described.

A detailed analysis of the nature and magnitude of the various possible sources of error involved in the calibration, pressure factor determination, reading, and correction of protected and unprotected deep-sea reversing thermometers leads to the conclusion that the accuracy of thermometric depth determinations is usually within 0·5%, and is frequently within 0·2%.

Bibliography

Whitney, G. G., Jr. "A note on non-linear behavior of unprotected reversing thermometers". W.H.O.I. Tech. Rep., 55–62 (unpublished MS). November, 1955.

Wüst, G. "Thermometrische Tiefenmessung". Deutsch. Atlant. Exped. "Meteor", **4**, 1, p. 60. 1932.

Wüst, G. "Thermometric measurement of depth". Hydrogr. Rev., **10**, pp. 28–39. November, 1933.

Contribution No. 917

Deep-Sea Research, 1957, Vol. 4, pp. 149 to 184. Pergamon Press Ltd., London

A survey of ocean current theory

HENRY STOMMEL

(*Received* 25 *January* 1957)

INTRODUCTION

DURING the past half century there have been several independent lines of development of theory of ocean currents. The interconnections among them have not been generally recognized in the literature; but these are so interesting and instructive, especially from a physical point of view, that it seems worthwhile to attempt to describe and compare them in a brief survey article. Moreover it seemed desirable to try to isolate the basic physical ideas in each of the theoretical studies and to present them in pictorial diagrammatic form, without mathematics. The construction of the various models and of the illustrations is based, of course, on the full mathematical development.

HOUGH (1897) devoted a minor portion of his famous theoretical study of tides on a rotating globe to a discussion of the currents produced by a zonal distribution of precipitation and evaporation, ignoring friction. He found that a uniformly accelerated system of purely east-west geostrophic currents would exist, but because of the uncertainty of how to treat friction he was unable to obtain steady state solutions and thus to conclude whether precipitation and evaporation are capable of being a significant cause of real ocean currents. A more important limitation of HOUGH's ocean current model is the absence of meridional boundaries in the ocean. GOLDSBROUGH (1933) discussed a model with such boundaries and found that he could construct steady stationary current fields provided only that the integral of the precipitation-evaporation function, taken along each parallel of latitude between the two boundaries, vanishes. The steadiness of the GOLDSBROUGH solutions does not depend upon friction. However, Nature affords no guarantee that the above integral of the applied precipitation-evaporation distribution shall vanish, nor are the causes of oceanic circulation limited to precipitation and evaporation (HOUGH and GOLDSBROUGH did not imply they were so limited, but employed them for simplicity's sake).

Considered from the vantage point of the present, it is astonishing to recognize that the theories of HOUGH and GOLDSBROUGH, although as originally proposed, considered only evaporation-precipitation as a cause of currents, are actually more general than at first appears, and in fact contain the main dynamical features of our present view of oceanic circulation. Indeed, one needs merely to introduce two additional physical ideas:

(1) EKMAN's (1905) notion that the direct frictional stress of the wind is confined to a thin surface " boundary layer," and that viscous shearing stresses are unimportant dynamically in the deeper body of the ocean, excepting, perhaps, at the bottom.

(2) The concept of a narrow western boundary current of a highly frictional (MUNK and CARRIER, 1950; HIDAKA, 1950) and/or inertial (CHARNEY, 1955; MORGAN, 1956) character.

These physical ideas are applied to the HOUGH-GOLDSBROUGH models in the following way. EKMAN's frictional boundary layer provides a way of converting the field of applied wind stress into a field of vertical velocity just beneath the surface and just above the bottom. Hence the main body of ocean water can be treated as frictionless and in geostrophic motion. The analysis proceeds the same as for the model driven by precipitation-evaporation, the water being supplied or abstracted by convergent or divergent boundary layers at the top and bottom.

The second physical idea, that of the western boundary current, frees the forcing function from the above-mentioned unnatural integral constraint. Thus in GOLDSBROUGH's original model, if precipitation exceeded evaporation over a latitude circle between two meridional coasts, there would be a net transport toward the equator, and mass conservation would be violated in the steady state. It now appears physically that in fact a narrow return flow would develop along the western coast sufficient to preserve mass conservation. Today it is believed that the Gulf Stream itself is an example of such a higher-order-dynamics western boundary current. MUNK (1950), CHARNEY (1955), and MORGAN (1956) have discussed the conditions in such currents in some detail, but from the point of view of the general oceanic circulation the main interest is not in the detail, but the mere fact of their existence because they provide a means of satisfying mass conservation in oceans bounded by meridians for quite arbitrary forms of the forcing functions. From a physical point of view it seems that such meridional boundaries and their associated western boundary currents are perhaps the essential difference between the regimes of circulation in the ocean and the atmosphere.

The work of the tidal theorists was confined to homogeneous oceans. SVERDRUP (1947) showed that in the steady state vertical variations of density do not need to be taken into account explicitly providing vertically integrated velocities are employed rather than the velocities themselves. Moreover, MORGAN (1956) has shown that density stratification does not prevent the formation of western boundary currents. Thus the form of the vertically integrated velocity field in central oceanic regions (or, simply, the net transport field) is independent of the details of the density structure. This powerful simplification enables us to construct net transport fields of steady ocean current circulations caused by wind or by precipitation-evaporation quite easily. Within the same framework the thermohaline circulation appears as an internal mode, and completely vanishes when integrated vertically. There is one reservation about the method of vertical integration which should be stated explicitly: the method is strictly limited to cases where appreciable velocity does not extend to large-scale irregularities of the bottom. In the case of a homogeneous ocean this is patently not the case, but the tidal theorists have written their theories to accommodate non-uniformity of the depth. For example, LAMB (1932, p. 326) finds that non-uniformity of depth in models with uniform rotation introduces second class waves of much the same character as non-uniformity of rotation introduces on the betaplane, or spherical ocean of uniform depth. Also EKMAN (1932) recognized the analogous effects of non-uniform depth and non-uniform rotation in large-scale circulations. He called them topographic and planetary effects, but he did not construct a complete ocean current theory, evidently because of the want of the western boundary current.

Another example of the close connection of the work of the tidal theorists with more recent studies in oceanography and meteorology is the topic of large-scale transient motions. Oceanographers and meteorologists distinguish between long inertio-gravitational waves on one hand, and quasi-geostrophic waves (e.g. planetary waves in the westerlies) on the other ; but this distinction is already implicit in the tidal theorists' classification of waves of the first and second class (LAMB, 1932, p. 350). The recent study of free and forced motions of a two-density layered ocean on the beta-plane by VERONIS and STOMMEL (1956) is really a study of these same waves of both external and internal modes. It is found that the transient response of the ocean to time-variable forces depends essentially upon the vertical density structure.

The current systems of HOUGH *and* GOLDSBROUGH

In order to compare more closely the solutions obtained by HOUGH and GOLDSBROUGH we take a particularly simple pattern of distribution of precipitation and evaporation: precipitation over one hemisphere, evaporation over the other. The two cases are distinguished by choosing these hemispheres as the northern and southern respectively in the HOUGH case, and as the western and eastern in the GOLDSBROUGH case. The only difference between the two cases is that the distribution of precipitation-evaporation has been rotated 90°. The motion in both cases is regarded as very slow so that inertial effects are negligible ; also friction is neglected. The rain does not impart momentum to the ocean; the ocean is homogeneous in density, uniform in undisturbed depth, and covers the entire globe.

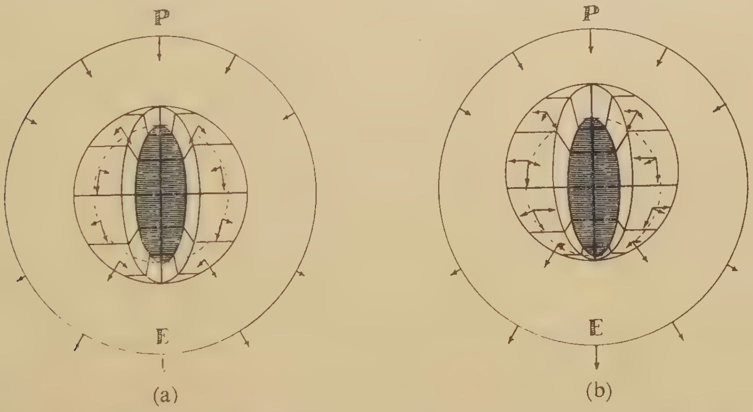

(a) (b)

Fig. 1 (a and b). Two successive stages of the HOUGH-type circulation pattern, driven by precipitation distributed over the northern hemisphere (P) and evaporation distributed over the southern hemisphere. The hovering arrows indicate the distribution of precipitation-evaporation. The arrows drawn on the surface of the spheres are velocity components. The zonal currents grow with time. The central solid portion of the earth is shown as shaded in the cut-away mid-section.

First consider the HOUGH case, illustrated in Figs. 1 (a) and 1 (b), with precipitation in the northern hemisphere, and evaporation in the southern hemisphere. The solid lines are contours of equal precipitation-evaporation rate. The circulation is not steady, hence Figs. 1 (a) and 1 (b) represent two successive stages in the development of the field of flow. The elevation of the free surface and the zonal velocity component vary linearly with time as shown by comparing the two figures, but the meridional component of velocity and the vertical component of velocity are independent of time. The horizontal components of velocity are independent of depth ; the vertical component of velocity varies linearly from the surface to zero at the bottom. At the surface the vertical component of velocity (measured positive from the centre of the globe) is the sum of the rate of increase of the elevation of the free surface and of the evaporation. Pressure is determined hydrostatically. As can been seen from the cut-away portions of Figs. 1 (a) and 1 (b), as time progresses not all of the water which is precipitated upon the northern hemisphere crosses the equator to the evaporation hemisphere, but some is used to build up an ever-increasing high-pressure region centred at the North Pole, and an ever-depressed low-pressure region grows around the South Pole. Thus meridional pressure gradients increase with time; and associated with them are two geostrophic zonal currents that also grow linearly with time. The zonal current is zero at the poles and at the equator. The meridional component of velocity is directed southward everywhere, and reaches its maximum where it crosses the equator. Although it flows from a region of high to a region of low pressure this meridional component is not driven by the pressure gradient, but is related through the Coriolis force only to the acceleration of the zonal current (remember there is no friction). Of course, a uniformly accelerated system of this kind persisting throughout all time is wholly unphysical – at some stage the velocities would no longer be small, our premise of slow motion would be violated, and at some stage the regime should become unstable or the effects of friction should intrude. Although instability of the flow pattern may be more plausible physically as a means of braking the motion, and indeed does seem to occur in the atmosphere, there is reason to believe, as we will see below, that in low latitude at least, the ocean circulation is stable. A simple braking of the currents in the HOUGH case can also be introduced by putting in a large virtual turbulent eddy viscosity, which leads to a steady state circulation pattern qualitatively similar to the pattern shown in Fig. 1 (b), as though the HOUGH solution were suddenly arrested. Introduction of large horizontal eddy viscosities is convenient mathematically, but the physical justification is doubtful.

The chief interest of the HOUGH case lies in the remarkable contrast which is produced by simply rotating the distribution of the precipitation-evaporation distribution 90°, so that the precipitation-evaporation maxima lie on the equator instead of at the poles. This is a special case of the GOLDSBROUGH type solution, shown in different views in Fig. 2. Here, even without friction, the field of pressure and flow is steady. Both horizontal velocity components are completely geostrophic – the flow is along isobars. The vertical component of velocity is zero at the bottom and varies linearly with depth up to the surface where it equals the precipitation-evaporation rate. The pressure field (obtained hydrostatically from the elevation of the free surface) is a rather complicated one. On the eastern edge of the hemisphere of precipitation there are two low-pressure cells; on the western edge, two high-pressure cells. The general pattern of flow is therefore a flow across both polar regions from the region of evaporation into the region of precipitation, and a flow in tropical and sub-tropical latitudes in the opposite direction. The difference of these two transports is, of course, equal to the precipitation in the western hemisphere.

The fact that there can be a net transfer of mass from one hemisphere to another by geostrophic flow in a closed system of isobars is simply a result of the fact that the

Coriolis parameter varies along the meridian between the hemispheres. The lower the latitude the greater the transport between two isobars.

Geostrophic flow with a meridional component, in a homogeneous ocean of uniform depth, must exhibit a horizontal divergence – positive if directed toward the equator, negative if directed poleward. This is readily seen from Fig. 3 (a) in which a portion of a homogeneous, uniform depth ocean, bounded by two isobars *ab* (high pressure) and *cd* (low pressure) is envisaged as flowing toward the equator. The pressure difference across section *ac* is thus the same as that across *bd*, independent of how wide these sections may be, but the Coriolis parameter is less at the latter, hence the geostrophic transport across *ac* is less than across *bd*. Inasmuch as no geostrophic flow can occur across *ab* and *cd* the excess of water must be supplied from somewhere – and in the steady system envisaged by GOLDSBROUGH this excess is provided by precipitation. In Fig. 2 the reader will note that the flow is entirely equatorward in the precipitation hemisphere. Similar remarks apply to poleward flows in the evaporation hemisphere. From a physical point of view the GOLDSBROUGH type circulation is constructed simply by choosing the particular system of geostrophic flow whose distribution of divergence (or convergence) is everywhere sufficient to absorb (or give up) the water locally precipitated (or evaporated). For certain types of precipitation-evaporation distribution there are no geostrophic flow patterns that can operate in this fashion, and it is under these circumstances that HOUGH-type solutions occur. Similar considerations apply to a plane ocean of variable depth (Fig. 3b), the geostrophic transport across *ac* being less than that across *bd* on account of lesser depth rather than larger Coriolis parameter.

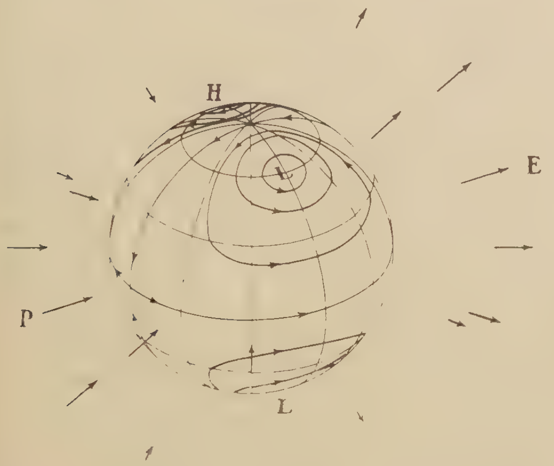

Fig. 2. The GOLDSBROUGH-type steady solution driven by precipitation over the western hemisphere, and evaporation over the eastern. The curve lines with arrows on them are isobars. The centers of high- and low-pressure cells are indicated by H and L.

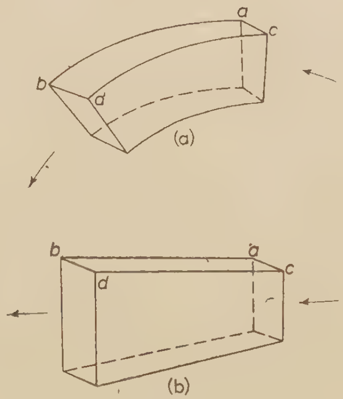

Fig. 3. (a) Divergence of geostrophic flow associated with change of latitude. (b) Divergence of geostrophic flow associated with non-uniform depth.

Several further features of the GOLDSBROUGH solution should be mentioned here. First, in Fig. 2, it is clear that a coastal barrier could be placed along any complete isobar without affecting the solution, for example, along the meridional circle passing through the centres of the precipitation and evaporation hemispheres, or as another example the equator itself could be replaced by a coastal barrier.

There is an important restriction upon the kinds of precipitation-evaporation distribution that allow of GOLDSBROUGH-type solutions. Since there can be no net steady geostrophic transport across a latitude circle it is necessary that the integral of the imposed distribution of precipitation or evaporation along a latitude circle shall vanish. This is a very severe restriction which no natural distribution of precipitation-evaporation necessarily fulfills.

Extension to the wind as a causal agent and to more general ocean-basin shapes

For the sake of simplicity we retain at this stage of the discussion the homogeneity of the ocean and its uniformity of depth, and inquire into more general causes of oceanic circulation and the influence of the introduction of various forms of coastal boundary.

EKMAN (1905) (or LAMB, 1932, p. 593) has shown that the currents directly produced by the stress of the wind are confined to a thin surface layer of less than 100 m thickness. Non-uniformity of the wind stress over the ocean causes a convergence or divergence within the EKMAN layer, and this integrated over the depth of the layer is independent of the details of the turbulent eddy structure of the layer. In the steady state, by conservation of mass, these distributions of net horizontal divergence produce an impressed vertical velocity on the top of the body of water immediately below the EKMAN layer. A particular example is illustrated in Fig. 4. The applied wind stress is purely zonal. The total transport of the wind-driven layer to the right (in the northern hemisphere) of the wind stress is indicated by the horizontal arrows labelled T_e. It is worth stating that the vertical scale in the diagrams is generally greatly exaggerated. Since these EKMAN transports are opposed, and since we can rule out an escape of water across the top surface, the water must escape the EKMAN layer from the bottom with a vertical component labelled w_e. Moreover, within the linearized dynamical framework under consideration, it does so without carrying any horizontal momentum with it. Thus it is immediately evident that so far as the deep frictionless layer is concerned it might just as well be operated upon by a precipi-

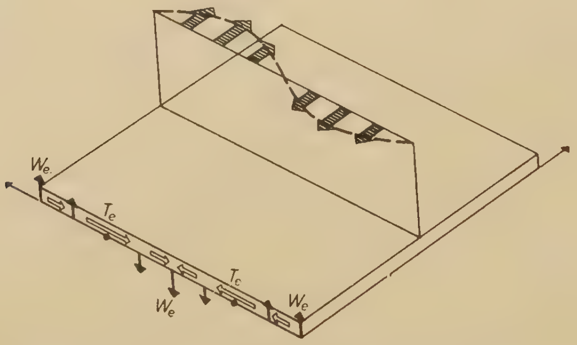

Fig. 4. The surface EKMAN layer, produced by a wind-field with sinusoidal pattern (the shaded arrows hovering above the surface). The EKMAN layer transports to the right of the wind are indicated by the open arrows labelled T_e. The vertical velocities produced by convergence and divergence of the EKMAN transports, and thus impressed upon lower layers, are indicated by solid arrows labelled w_e.

tation-evaporation distribution equivalent to w_e. We are thus permitted to investigate the transports of the deep layer within the framework of the HOUGH-GOLDSBROUGH-type solutions*.

The magnitude of w_e depends upon the magnitude of the curl of the quotient of the wind-stress and the Coriolis parameter. The mean pattern of wind-stress over the real oceans is predominantly a zonal one, and were the real ocean unbounded by coasts, would produce a HOUGH-type circulation, which, as we have seen, in the absence of friction or instability, does not admit a steady solution. However, if a meridional boundary is introduced it is possible to construct a steady solution starting at this boundary and working toward the west. SVERDRUP (1947) has shown that this is possible even in a density-layered ocean, but he does not explain why the development cannot be made eastward from a coast, nor does he indicate how the other side of the ocean is to be treated. Before attempting to explain these points, it is perhaps best to first describe a very simple SVERDRUP-type system: a homogeneous ocean, bounded by an eastern coast, and acted upon by a zonal wind stress. Fig. 5 shows the type of solution which applies in this case. At the surface there is a zonal wind stress similar to the distribution of the Northern Hemisphere westerlies and Trades over the real ocean. The mathematical solution from which the figure is drawn was obtained on the so-called beta-plane – a plane system of co-ordinates in which the Coriolis parameter is treated as a constant except where differentiated in the meridional direction. The transport of the EKMAN layer is indicated by the open arrows everywhere proportional to and to the right of, the wind. There is a vertically downward velocity imposed in central regions of the diagram: between the maximum

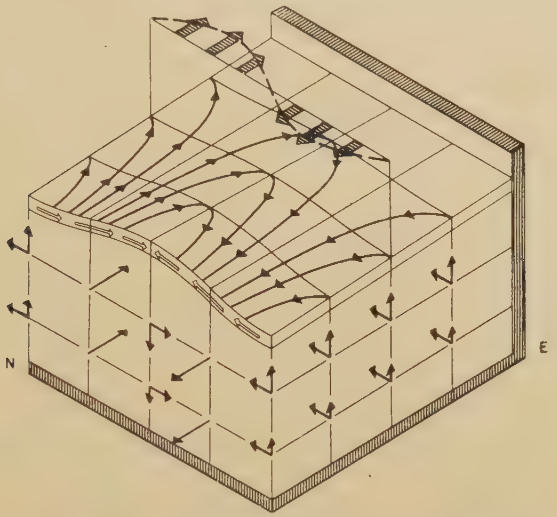

Fig. 5. SVERDRUP-type solution in homogeneous ocean of uniform depth, bounded by meridional coastal wall on the east. The wind system and EKMAN layer are the same as in Fig. 4. The curved lines with arrows on them are isobars ; the arrowheads indicate direction of the geostrophic horizontal flow (independent of depth). The components of velocity at a number of subsurface depths are shown by the solid arrows.

---

*Dr. K. YOSHIDA has pointed out to me that he and Dr. HAN-LEE MAO used these ideas in an unpublished (1954) paper on coastal upwelling off California.

westerlies and maximum easterlies. Outside this zonal belt the impressed vertical velocity is upward. From the bottom of the EKMAN layer to the bottom of the ocean this vertical velocity component diminishes linearly to zero. This water is absorbed, so to speak, by the divergence of the meridional component of the geostrophic velocity. Thus at midlatitudes where the vertical velocity is downward, the meridional component of geostrophic velocity is southward. The zonal components of the geostrophic transport are introduced to preserve mass continuity. At the latitude of maximum westerlies, for example, where there is no impressed vertical velocity the geostrophic flow is entirely zonal, diminishing linearly toward the coast. The contours of surface height, which determine the pressure field associated with the geostrophic flow field, are also shown in Fig. 5. The reader will remember that we are here dealing with a specially simplified case of the SVERDRUP-type model. We have constructed a geostrophic current system, consistent with the eastern coastal boundary condition which matches by its field of divergence and convergence (due to the meridional variation of the Coriolis parameter) the impressed field of convergence and divergence of the thin surface EKMAN wind-driven layer. We have obtained a steady-state solution. But it is also evident that we cannot satisfy conditions at the western coast unless some additional physical feature is introduced. But before looking further into this question, let us first consider what is involved if the eastern coast is removed. The there will be no possibility of an east-west pressure gradient, no meridional component of geostrophic flow, and the solution would accelerate. EKMAN has already discussed this case. He suggests that one may introduce a bottom frictional layer, with transports just opposite to those in the surface wind-driven layer. The final current system consists of three layers: the surface EKMAN layer, the intermediate layer of geostrophic flow, and a bottom EKMAN layer. The vertical velocity is constant with depth within the geostrophic layer (which being purely

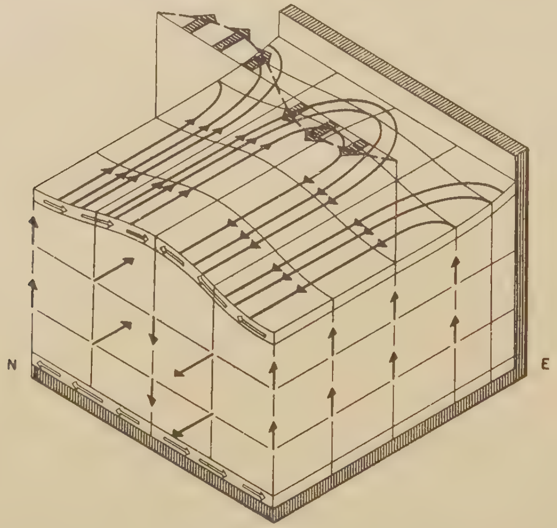

Fig. 6. EKMAN-type solution for the same wind field and shape ocean as shown in Fig. 5. In this case, with no divergence associated with geostrophic meridional currents, the compensating divergence occurs in a bottom frictional layer.

zonal has no horizontal divergence). The amplitude of the geostrophic current at mid-depths depends entirely upon the size of the frictional coefficients of the bottom layer. If there were no variation of the Coriolis parameter with latitude a meridional wall would cause the zonal current to turn around within a region more or less as wide as the width of the zonal current (Fig. 6), and the amplitudes of the motion would not be affected markedly. Far from the coast the flow is the same as in the absence of the coastal barrier. In Fig. 5, which has both the wall and variation of Coriolis parameter with latitude the situation is quite different: the flow never becomes purely zonal no matter how far removed from the coast one may be. A number of further comparisons between the regimes indicated in Fig. 5 and 6 can be seen by studying the illustrations: note for example the different dependence of the vertical velocity component upon depth in the two cases, the different form the surface elevation, etc. There are also marked quantitative differences in the transports in the two models: for example if the depth is increased in Fig. 5 the geostrophic transport remains constant, but the velocity decreases, but in Fig. 6 the geostrophic transport increases and the geostrophic velocity remains constant.

Further complications of the simple homogeneous model are, of course, possible. Non-uniform rotation and bottom friction may be both introduced simultaneously, also lateral friction, and even bottom topography of various simple forms. MUNK (1950) has given an indication of the possible role of lateral friction near the eastern coast. Quantitative comparison of the transports in simple models and as inferred from hydrographic data suggests that in the middle regions of sub-tropical and equatorial oceans, at least, topographic and frictional influences play a negligible role, and that the dynamical framework shown in Fig. 5 is more akin to that of the real ocean than that of Fig. 6. Lack of friction places an upper limit on the realizable transport in ocean currents, and this seems to be realized (e.g. SVERDRUP, 1947 ; REID, 1948, etc).

The fact that higher order physical processes might be important only at the western boundary of the oceans was first suggested by MUNK's (1950) grouping of the terms in his solution for a wind-driven, laterally viscous ocean. CARRIER (MUNK and CARRIER 1950) was apparently the first to recognize that this was tantamount to treating the intense western current by the mathematical technique of the boundary layer; that is to say, for certain values of the physical parameters determining ocean circulation the higher order effects of friction and inertia can be neglected everywhere in the ocean except in the theory of the narrow high velocity current along the western coast of the ocean. For further details about the theories and observational material on the viscous western boundary current, and the more recent inertial theory, I refer the reader to my book on the Gulf Stream (STOMMEL, 1957).

The main point that ought to be made here is that we can always fit a narrow western boundary current to a SVERDRUP- or GOLDSBROUGH-type solution. And we can do it symbolically – there is little to gain, from the point of view of the large-scale mid-ocean general circulation, by attempting to discuss the detailed structure of the western boundary current. We regard the western boundary current as a device for satisfying mass conservation and applying a physically realistic western boundary condition. In a word, it frees us from the crippling restriction upon the distribution of the driving agency already indicated by GOLDSBROUGH (above).

It would be misleading to give the impression that the theory of the western boundary current is complete. There is a complete theory of the purely lateral-viscous western boundary current (Munk 1950; Munk and Carrier, 1950), but the theory, so far developed, of the inertial boundary current applies only to the growth region, or region of formation of the western current – where the transport of the stream increases in the down stream direction. The remainder of the inertial boundary current, where it must gradually leave the boundary and broaden out to join the sluggish interior solution, has not been studied. Evidently in nature, there is a rather complicated " decay region," meanders and breakdown of the western current, and a tendency of the boundary current to pull away from the coast bodily and thus to penetrate quite far into the interior without at once diminishing its narrow intense character (Fofonoff's (1954) free solutions are enlightening in this respect).

The chief ingredients of the ocean current as outlined here are as follows :

(1) The simple precipitation-evaporation distribution may be replaced by an Ekman-type wind-driven surface layer.

(2) A meridional boundary converts an otherwise accelerated Hough-type solution to a steady Goldsbrough-type one, developed westward from the boundary.

(3) A western boundary current preserves mass conservation and satisfies the boundary conditions at the western boundary of the ocean.

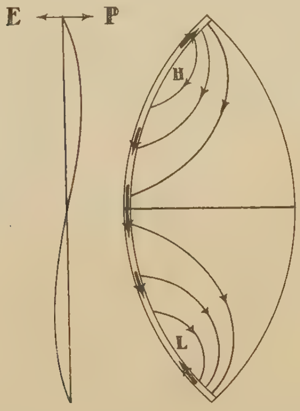

Fig. 7. The steady circulation produced in a uniform depth ocean bounded by meridional coasts 60° apart under the influence of precipitation in the northern hemisphere and evaporation of the southern hemisphere. The curve lines with arrowheads are isobars. The western boundary current is drawn schematically within the double line on the western coast.

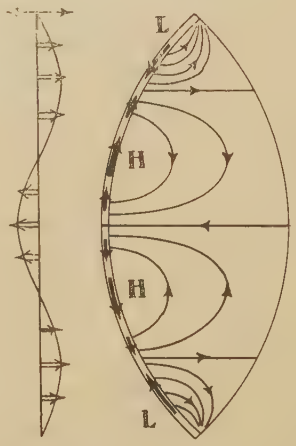

Fig. 8. The steady circulation produced in an ocean of same shape as that in Fig. 7, but acted upon by a particular distribution of zonal winds, shown at the left. The western boundary current is shown schematically by the double line at the western coast, and its transport is indicated by heavy arrows.

Further, as Sverdrup (1947) has shown in the steady-state vertical density stratification does not materially affect the conclusion. Sverdrup's well-known curl-equation merely states that the meridional component of the vertically integrated geostrophic transport at each point in the ocean is precisely that required to counterbalance the divergence impressed by the Ekman layer. The zonal component of the vertically integrated transport is obtained from the continuity equation, and the boundary condition of no normal transport through the eastern coast. The discussion of internal modes of circulation, whose vertically integrated transport vanishes, is reserved until later.

In order to demonstrate these ideas implemented in two special cases, Figs. 7 and 8 have been prepared. In each case the ocean is bounded by meridians 60° apart. In Fig. 7 the northern hemisphere is one of precipitation, the southern of evaporation. The distribution of precipitation-evaporation is somewhat similar to that shown in Fig. 1, except near the poles where it has been altered to avoid infinities, but otherwise it would be expected, in the absence of the meridional barriers, to lead to an accelerated HOUGH-type system. The presence of the meridional barriers permits pressure gradients along the latitude circles, and a steady geostrophic flow field with meridional components. The impressed precipitation or evaporation is absorbed or given up by the meridional geostrophic flow at each point in the ocean. The isobars, or lines of equal elevation of the sea-surface are shown. The flow is along these lines, but they are not transport lines, of course. The eastern coast and equator are isobaric. At the equator, where there is no evaporation or precipitation in Fig. 7, there is no meridional component of geostrophic flow; hence all of the water precipitated in the northern hemisphere must cross the equator at the western coast as a western boundary current. Slightly north and south of the equator there are meridional components of flow in the central portions of the ocean, but these are not sufficient to carry all the flow across the latitude circle that is required by mass conservation, so that much of this flow likewise occurs in the western boundary current. At sufficiently high latitudes the meridional geostrophic transport is just sufficient to carry away the mass added further northward: there is no western boundary current at these latitudes. Poleward of these points the mid-ocean geostrophic transports exceed the available supply of water added by precipitation to the northward, and hence the western boundary currents reverse, and actually flow toward the north.

In Fig. 8 a similar model is portrayed, except that here the causal agent is a zonal wind-stress distribution (indicated to the left) blowing upon an ocean, also with meridional boundaries 60° a part. Between 30° latitude and the poles prevailing westerlies are depicted; the trades extend across the equator from 30°S to 30°N latitude. This is, of course, only a very crude representation of the real wind system over the globe. The lines are isobars parallelling the geostrophic flow. In this case there is a certain amount of EKMAN wind-drift transport in the surface layers which ought to be added to the geostrophic transport field to give an accurate picture of the total transport field, but this is omitted in the figure to preserve simplicity of presentation. Here we obtain, by a series of arguments similar to those used in justifying Fig. 7, a system of gyres and western currents resembling that obtained in the complete theory of MUNK (1950) and HIDAKA (1950). The boundaries between the gyres correspond to latitudes of no EKMAN layer convergence. The regions of maximum geostrophic meridional flows in each gyre correspond to the latitudes of maximum convergence (equatorward flow) or divergence (poleward meridional flow) of the EKMAN wind-driven layer. The zonal geostrophic transports are constructed by continuity from the eastern coast, and western boundary currents are fitted where needed to conserve mass.

Some of the features of the oceanic circulations described in this section have been qualitatively reproduced by von Arx (1954) in a circular rotating basin using a density-homogeneous water layer of non-uniform depth. von Arx's model is driven by applied wind-stress. In experimental work it is not possible to avoid bottom friction altogether, but evidently, with sufficiently deep layers the divergence of meridional geostrophic flows dominates over that of the bottom frictional layer. To date, quantitative experimental studies have not been made.

Some integral relations pertaining to thermohaline and internal mode circulations and application to interpretation of the atlantic ocean circulation

Before proceeding to the topic of the next section, where an effort is made to visualize the physical factors governing the vertical density distribution in the ocean, it is perhaps worthwhile to indicate here that formally, the simple ideas described above, and applied to a homogeneous or vertically integrated ocean, can also be employed to elucidate certain features of internal modes of circulation in the ocean by simply dividing the ocean into two layers by a *level surface* at mid-depth, say 1500 or 2000 m and specifying the vertical mass transport across this level surface as a function of geographical position. What is taken from one layer is added to the other. A pattern of geostrophic flow can be constructed in each layer to absorb (or give up) the water required for the vertical transport across the level surface, and a western boundary current fitted where needed in each layer. The vertically integrated transport over both layers taken together vanishes: the circulation is a

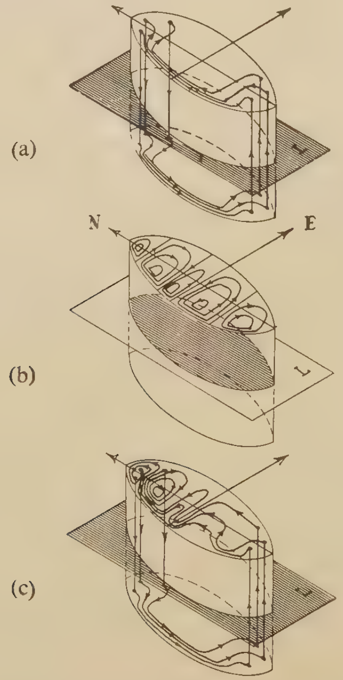

Fig. 9. A schematic interpretation of the circulation in the Atlantic Ocean constructed by superposition of an internal mode associated with flow across a level surface L at mid-depth (a) and a purely wind-driven circulation in the surface layers (b). The sub of these two is shown in figure (c).

pure internal mode, except perhaps where topographic effects dominate. These considerations, and the pictures derivable from them, are not *theories*. They merely provide an interpretative tool, and indicate what flow patterns must be associated with various distributions of vertical transport across level surfaces. As an illustration of the use of this tool, a rudimentary interpretation of the Atlantic Ocean circulation is presented here.

Consider the schematic ocean drawn in Fig. 9 (a), extending from pole to pole across the equator and bounded by meridional boundaries roughly 60° apart. A level surface L which divides the ocean into an upper and a lower layer is also shown. Now suppose that some thermohaline process, into the nature of which we do not here inquire, causes a sinking of water across the level surface in subarctic latitudes, and a rising of water across the level surface in subantarctic latitudes, as indicated by the vertical transport lines drawn in Fig. 9 (a) across the level surface. Our argument is that having specified the quantity and location of the vertical transport across level L, the rest of the transport picture in each layer is completely determined, in fact looks very much like that shown in Fig. 7 for a different physical situation.

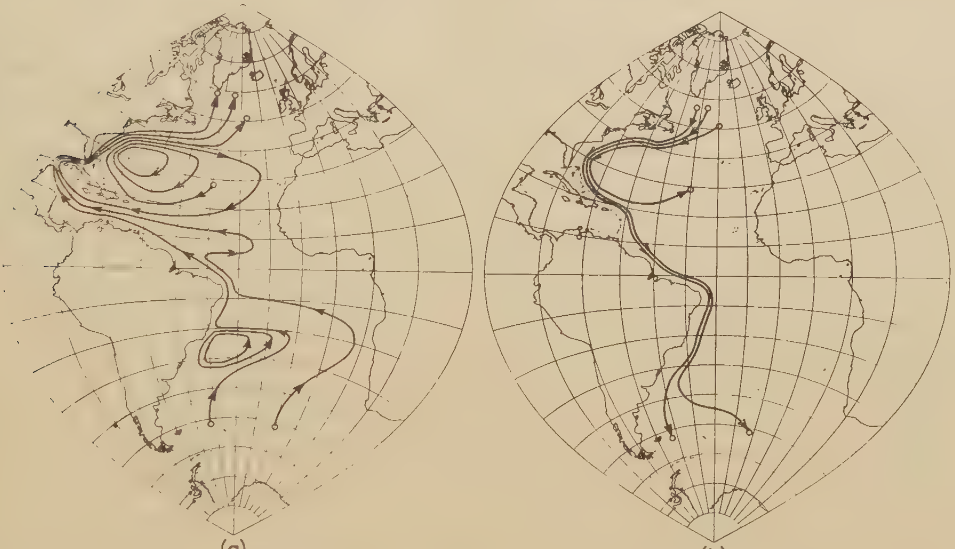
(a) (b)

Fig. 10. A similar interpretation of the total transports in the surface layer (a) and bottom layer (b) but drawn on a chart of the Atlantic Ocean. Points of sinking and upwelling across the level surface are indicated by the little circles.

Thus for example, in the subarctic regions of the mid-oceanic portions of the upper layer the horizontal flow field is convergent, hence it must have a northward directed meridional component. The zonal component is determined by continuity, starting at the eastern boundary. Similar reasoning is applied to the lower layer and then to both layers in the subantarctic region. In subtropical and tropical latitudes we have specified no vertical transport across the level surface, and there is no geostrophic in the mid-oceanic regions of either layer. The transport of water between hemispheres which is required for conservation of upper layer and lower layer water separately must be accomplished by a narrow western boundary current. The field of motion is entirely internal; its vertically integrated transport vanishes everywhere. Fig. 10 (a) portrays the resulting circulation pattern.

Now consider separately a wind-driven circulation in the upper layer maintained by the impressed vertical velocity field due to an EKMAN layer as shown in Fig. 9 (b). It looks much like that shown in Fig. 8, except that there is an additional gyre just north of the equator (after MUNK, 1950) which is presumably caused by the existence of a doldrum area in the winds just north of the equator. Within the simple framework of the linear mechanics of the models under consideration these two circulations (Figs. 10 a and 10 b) are additive. The sum is shown in Fig. 9 c. Note the absence of the Brazil Current, the very intense Gulf Stream. The picture looks much more realistic than the simple gyre system (Fig. 9 b) alone. A slightly different interpretation is drawn in Fig. 10 upon two charts of the Atlantic Ocean, the right figure representing the lower layer, the left the upper layer, and I have placed the diving reference level at 1500 metres. It seems probable that over subtropical and tropical latitudes there must be certain small upward flux of mass across the level surface to maintain the observed vertical increase of density with depth against eddy diffusion, so I have drawn the figure showing one transport line ascending through the reference level in midlatitudes. Each transport line corresponds to about 10 million m^3/sec. There are a number of features in this diagram which should be noted. For example, the vertically integrated transports of the Brazil Current and the Gulf Stream are the same, but according to the interpretation suggested here the current in the deep layer opposes the Gulf Stream, whereas it has the same direction as the Brazil Current. The opposite is true in the upper layer: the Gulf Stream is re-enforced by the thermohaline component, the Brazil Current so weakened that it almost disappears. The number of solenoids (intersections of surfaces of equal pressure and specific volume) in the Gulf Stream is very much greater than in the Brazil Current, thus by ordinary oceanographic reasoning the Gulf Stream would look like a current of very much greater transport than the Brazil Current. We identify the deep current with North Atlantic Deep Water. The reader will find it interesting to examine in some detail such features as the vanishing of the western current in the region of latitude of the Equatorial Counter-current, the curious spiral in the subarctic region of Fig. 9 (c), etc. This picture of the circulation of the Atlantic is certainly not to be dignified by calling it a theory. It is simply offered as an interesting example of how far reaching the consequences of specifying the vertical velocity at the surface and some mid-depth level can be.

There is a further reason for focussing attention on the vital role played by the vertical velocity distribution, and hence the field of horizontal divergence in the ocean: namely, to emphasize the danger of making the assumption that because the vertical velocity is small it may be neglected – or even arbitrarily set equal to zero. For example, HIDAKA (1955) has recently worked out an elaborate numerical theory of the general circulation of the Pacific Ocean, interpreting it as a purely wind-driven phenomenon and assuming that the vertical velocity vanishes exactly everywhere. As HIDAKA himself has commented there is no clear physical explanation or interpretation of his numerical results ; indeed, from the point of view of this survey, it could hardly be otherwise. As I see it, the chief way that the Ekman layer affects deeper portions of the ocean is by imposing a vertical velocity upon them at the top, and chief agent of the thermohaline circulation is the slow vertical advection of density which balances the vertical diffusive loss of density to the surface.

Another example is NEUMANN's attempt (1955) to identify DEFANT's intuitive choice of reference level (DEFANT, 1941) in the Atlantic Ocean with a rigid impenetrable surface through which no water can pass. As I have indicated elsewhere (STOMMEL, 1956) the DEFANT level may actually be the level of no horizontal divergence in the ocean, in other words the level of maximum vertical velocity. This review is no place to attempt a detailed critique of the above studies of HIDAKA and NEUMANN. One can only point out that, on physical grounds, the field of vertical velocity is so intimately connected with the large scale circulation patterns that arbitrary assumptions about the vertical velocity structure in the ocean are attended by the most far-reaching implications concerning the form of the horizontal current patterns; and that unless this is fully recognized in setting up theoretical models, the results may be disastrous.

Extension to density-layered models in the steady state

The fact that SVERDRUP's theory gives the field of vertically integrated transport makes it possible to construct certain elementary models in which the density layering is specifically taken into account. The most elementary model is one in which the density is essentially inactive – that is to say, the amount of water of each density is specified to begin with; no particle of water can change its density. One thus con-

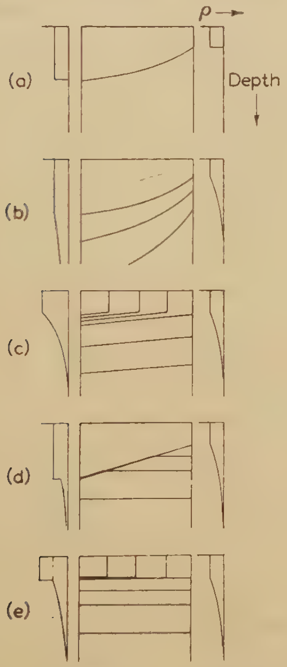

Fig. 11. These five vertical profiles (a, b, c, d, e) show the density structure which different models obtain in the plane *AA'B* of Fig. 12. See text for explanation.

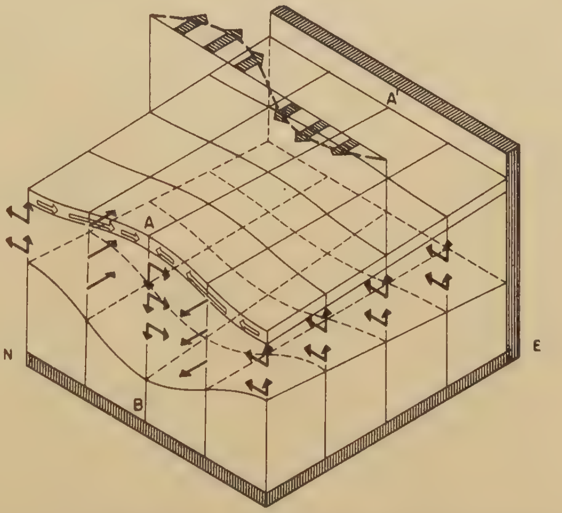

Fig. 12. The circulation in a SVERDRUP-type model such as shown in Fig. 5, but with two immiscible layers of slightly different density. The interface is shown by dashed lines.

siders density as an immiscible property – various portions of the ocean remain unmixed, like layers of oil and water. This is, of course, a considerable oversimplification of the state of affairs in nature.

For example one might consider an ocean consisting of two separate layers each of uniform density, the top layer being slightly less dense than the lower layer. A vertical sounding (of density against depth) in such an ocean would look like one of the curves in Fig. 11 (a). If there is no friction across the interface, and the ocean bottom is of uniform depth, the deep layer cannot move, and the slope of the interface must entirely counterbalance the horizontal pressure gradient associated with the geostrophic flow in the upper layer. If the distribution of wind is the same as that shown in the homogeneous model depicted in Fig. 5, the state of the two-layer system is as depicted in Fig. 12. The vertical section of the density field along the latitude of maximum wind-stress curl (the $AA'B$ plane) is shown in Fig. 11 (a). The densities of the two layers are taken as constants in the model. The depth of the interface at the eastern coast is also an arbitrary constant. The functional dependence of the depth of the interface on position, subject to the constraint of the SVERDRUP theory, is then completely determined. Since there must be the same geostrophic transport to the south across each unit width of the section, and the depth of the interface increases by a marked fraction of its mean value, the geostrophic velocities and slope of the interface must diminish somewhat with distance from the wall.

REID (1948) has given another model which exhibits much similarity with reality, based upon an arbitrary vertical distribution of density sketched in Fig. 11 (b). Here the ocean is covered everywhere by a thin homogeneous layer of uniform density, but of variable depth, and is underlain by a region in which the density increases to a fixed bottom density by an exponential law – the coefficient of depth in the exponential function being inversely proportional to the depth of the homogeneous upper layer. This is, of course, a very special form of density law, but it must be said that it closely resembles the form of density distribution in the Eastern Equatorial Pacific quite well. As in two-layer model it contains only one dependent variable. Again the functional form of this variable is completely specified subject to SVERDRUP's constraint on the distribution of vertically integrated transport. The analog of the vertical density profile along the latitude of maximum curl of the wind stress for REID's density model is shown in Fig. 11 (b).

STOCKMANN (1953) has worked with a different type of density field. Suppose that a density anomaly is defined by subtracting from actual densities the bottom density, and at the eastern wall a density anomaly vs depth curve is drawn of any arbitrary or observed shape (Fig. 11 c). The density structure at other stations is now assumed to be formed by multiplying the given curve by a constant factor (constant with depth at any one station, but variable from station to station). This again is an attempt to describe the density field in terms of a single dependent variable. The density field along $AA'B$ according to STOCKMANN's model is sketched in Fig. 11 (c).

It is important to note, at this point, that in the models of REID and STOCKMANN, the fluid cannot be regarded as inactive or immiscible. There is in both models an unstated but implicit assumption about transfer of mass across isopycnic surfaces. The deeper layers are supposed, in the section $AA'B$ to be moving geostrophically in a meridional direction, and this can only occur with divergence. In the top layer this horizontal divergence is balanced by the impressed vertical velocity from the

Ekman surface layer ; in deeper layers by a flow across isopycnic surfaces. Thus strictly speaking an explicit assumption of immiscibility would lead to profiles of the form shown in Figs. 11 (d) and 11 (e), instead of those of 11 (b) and 11 (c). Indeed it ought to be possible to compute the amount of mixing in nature from these considerations (Stommel, 1956).

The models mentioned above suffer being highly artificial, highly specified in form of the density field, and even more disconcerting, they involve implicit assumptions about the nature of the mixing processes. It would be very interesting to invert the problem: to make explicit assumptions about the nature of the mixing processes and, subject to integral constraints of the Sverdrup kind, to find the resulting density fields. One might even hope to find a partial explanation of the main thermocline.

The pioneer effort in this direction is reported in an important Russian paper by Lineykin (1955). The model, and its implications, are best described in terms of the illustration in Fig. 13. One begins by considering a basic state in which there is no motion – and no wind blowing over the ocean. There is, however, a uniform vertical stability maintained by vertical eddy conduction. We might suppose for example that the ocean is heated from above, and cooled from below, thus maintaining a constant and uniform heat flux downward, and a stable stratification of density. This is, it must be admitted, a rather artificial way to begin – the only excuse for it is that this conductive stable state is used as a basic state upon which to build a linearized perturbation theory when the surface is subjected to an infinitesimal wind-stress distribution of the form indicated by the large arrows hovering over the diagram. In the surface there is an Ekman transport to the right of the wind, and an impressed vertical velocity field just beneath it. Lineykin found that if the Coriolis parameter is taken as a constant, and for such choice of the parameters as make the scale of the phenomenon truly oceanic, this vertical velocity perturbs the density field by vertical advection of heavy in such a way as to produce a perturbed field as portrayed by the lines in Fig. 13. Isopycnals are depressed in regions of downward flow, and vice versa.

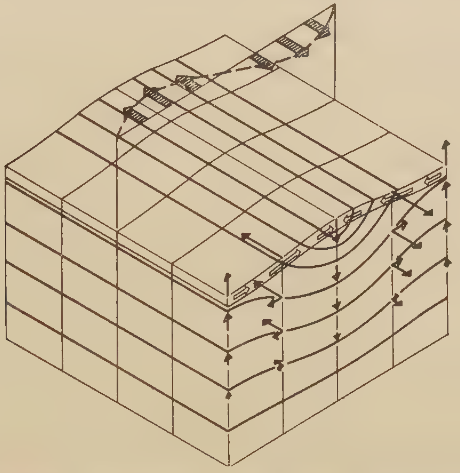

Fig. 13. Lineykin's explanation of the depth to which the baroclinic geostrophic currents produced by the wind extend in a stable ocean. The isopycnal surfaces are shown by the wavy nearly horizontal solid lines. The velocity components are shown by solid arrows.

Where the isopycnals slope most strongly the geostrophic subsurface currents are strongest. As is shown by the velocity arrows, this subsurface geostrophic current is generally in the direction of the surface wind, and there is a small non-geostrophic component (below the EKMAN layer but associated with friction) across the isopycnals directed from the region of downwelling toward the region of upwelling. This non-geostrophic flow at mid-depth compensates for the divergence of the EKMAN surface layer

The most interesting feature of LINEYKIN's model is the fact that the geostrophic currents decrease exponentially with depth at a rate completely determined by the physical parameters of the problem (and not by arbitrary assumption). LINEYKIN has treated the problem rather generally, retaining non-isotropic viscosity and diffusivity, etc. But for the purposes of this exposition we ignore large-scale lateral turbulent exchanges, and hence, on account of the small vertical scale of the phenomenon (remember the vertical scale in the diagrams is greatly exaggerated) only vertical viscous and diffusive transports need be considered. It may be shown that if the turbulent coefficients of viscosity and diffusivity are roughly of the same magnitude – which there is generally reason to suppose is the case and, as in fact LINEYKIN does – the depth to which the geostrophic currents extend is independent of the eddy coefficients. This LINEYKIN-depth depends only upon the geometry of the system, the unperturbed vertical stability, and the Coriolis parameter. If the LINEYKIN-depth be defined as that depth at which the amplitude of the density perturbation is reduced to exp $(-\pi)$ of its service amplitude, the ratio of the LINEYKIN-depth to the half-wavelength of the wind system is equal to the ratio of the Coriolis frequency f to the VAISALA or BRUNT frequency, $\sqrt{gs}$, where s is the mean stability of the model. In midlatitudes this ratio must be taken somewhere between 0·1 and 0·01, but in the neighbourhood of the equator it is certainly much less. One can see, therefore that although the LINEYKIN depth may be a fair representation of, and model for, the depth of the baroclinic layer in a small basin such as the Caspian Sea. it is several orders of magnitude too great to provide a reasonable explanation of the depth of the main thermocline in the oceans in midlatitudes. This, of course, does not detract the fact that LINEYKIN's paper has been a most stimulating and interesting one.

It seems likely that it is necessary to construct a somewhat different version of the LINEYKIN model to account for the density field in the ocean. In particular one would like to introduce the variation of the Coriolis parameter with latitude, since this has already been demonstrated to produce a marked tendency toward limiting currents to the upper layers (VERONIS and STOMMEL, 1956).

VERONIS and I have shown (VERONIS and STOMMEL, 1957) in a short contribution to the theory of thermally driven circulations based upon the LINEYKIN stable model, how the introduction of the variable Coriolis parameter modifies the depth obtained in uniform rotation (the LINEYKIN depth). I will give here a slight modification of these published results to make the physics as clear as possible. Consider (Fig. 14) a horizontal layer of fluid conducting heat downward by eddy conduction from a fixed hot surface temperature, to a fixed cold bottom temperature. Now suppose we can add water to the top, or take it away, without altering the fixed surface temperature. We can effect this, for example, by imposing a distribution of bands of precipitation and evaporation parallel to meridians (indicated in Fig. 14 by the hovering arrows), or probably equally well by putting a thin wind-driven EKMAN layer on top. Thus in Fig. 14 the vertical velocity imposed at the top surface is a function of longitude only, downward in the mid portions of the diagram, and upward along the outer east and west edges. At some distance below the surface the temperature field is perturbed by the vertical advection of heat, which in turn is held steady by conductive reaction of the perturbed temperature field. The model shown in Fig. 14 is computed in a beta-plane, so that vertical gradients of the vertical velocity are intimately related to the horizontal meridional components of the geostrophic sub-surface currents, and in addition the vertical gradient of the horizontal component of velocity is related to the horizontal gradients of the temperature field through the well-known thermal wind relation. These necessary relations are sufficient to define the entire temperature and velocity fields as shown in Fig. 14. It is interesting to note the asymmetrical distortion of the isothermal surfaces; the maximum perturbation of temperature moves toward the west with increasing depth. If the east-west dimensions of the bands of precipitation-evaporation, or of wind stress, have a wavelength of 6000 km, the vertical eddy diffusivity is 5 cm^2 sec and the mean vertical temperature gradient is 5°C/km, the depth of the maximum amplitude of perturbed temperature lies at about 1000 metres in midlatitudes, and decreases markedly toward the equator. Comparison of different latitudes on the beta-plane is possible by treating the Coriolis parameter parametrically. There is an indication of a rudimentary thermocline in Fig. 14, at about this depth (the thermocline tilts downward toward the west, and one also gets the impression of a tongue-like protrusion of warm water downward and westward, between cold tongues moving upward and eastward. However this is only an illusion, and not at all like a true tongue or

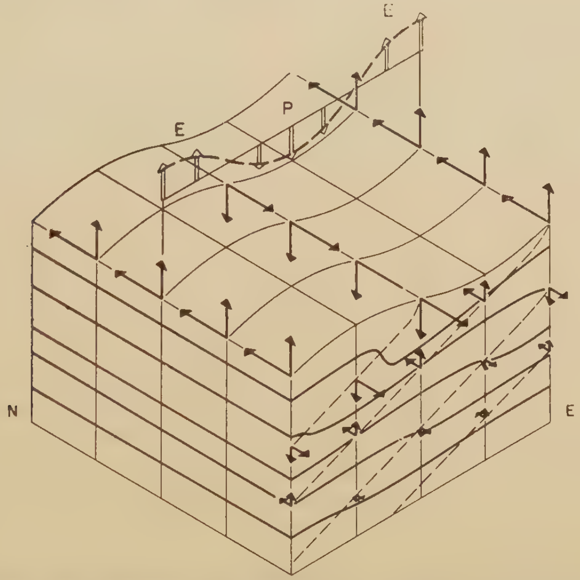

Fig. 14. Modification of the LINEYKIN model caused by introduction of a variable Coriolis parameter. The sloping dashed lines indicate the limits of the regions of positive and negative perturbation temperature (hot and cold cells) ; the rest of the diagram is labelled in the same manner as Fig. 13, but for convenience the model is driven by meridional bands of precipitation and evaporation (the hovering open arrows).

" Kernschicht " because there is no east-west component of velocity anywhere in the model. All motion is confined to vertical meridional planes. Although this model contains eddy diffusivity, it does not contain eddy viscosity.

The physical setup of this model is contrived to make the mathematics easy, consequently the regime does not look much like naturally occurring ones. The distribution of causal agent in parallel meridional bands is clearly an artifice. Over real oceans winds and heating and cooling are much more nearly functions of latitude than of longitude. The LINEYKIN model (Fig. 13) is completely indifferent to a shift of axes of the causal agent, but the model on the beta-plane (Fig. 14) is very sensitive to a shift of axes. If in the latter case the perturbing forces are made functions of latitude rather than of longitude, the meridional components of geostrophic flow vanish, and the flow pattern deepends and is transformed to the LINEYKIN one. In such a case the variation of Coriolis parameter with latitude would enter only parametrically. However, the introduction of a meridional barrier into the model would force strong meridional components of geostrophic flow by making the zonal turn around, and we can anticipate that this would permit the variation of Coriolis parameter to play an important role over a large distance from the coast, a distance possibly as great as the entire width of terrestrial oceans. Thus it seems possible that the vertical distribution of density and currents in a more realistically setup theoretical model (with zonal winds, the beta-plane, and a meridional boundary) might resemble that in the extremely artificial model of Fig. 14. To date it has not been possible to work out the mathematics of such a happier model.

There are more serious drawbacks to these models, however, than superficial similarity to nature. First, the strong vertical stability, uniform with depth, is merely a contrivance that permits a linear perturbation analysis ; it has no counterpart in the ocean. Actually all the heat advective terms in the heat transfer equation must be significant. Secondly, the parametric treatment of the eddy coefficients is exceedingly primitive and misleading. Even if oceanic turbulence at mid-depths is not directly related to the mean flow, it is desirable to have some physical understanding as to what causes this turbulence. At present we simply regard these coefficients as given arbitarily, at best we infer them from water-mass analysis. Our models are, so to speak, externally stirred. And perhaps they actually are, through short internal waves generated by storms. But this is all sheer speculation.

Time variable systems : *Free Waves on a Homogeneous Ocean of Uniform Depth*

The purpose of this section is to give a general description – in physical terms – of the types of free wave motion which are possible on a rotating globe. In order to avoid the almost endless variety of small-scale waves that are discussed in the general hydrodynamic literature, and have no special significance for phenomena of the oceanographic scale, only waves in which hydrostatic equilibrium exists at all times are considered. Thus we confine our attention to dynamical systems akin to those discussed in LAMB's chapter on tidal waves. The reader will note that the term " waves " is used in a somewhat general way, to embrace not only those transient phenomena which are customarily considered examples of hydrostatic wave motion (tides, seiches, long-period internal waves, surges, etc.) but also to include certain transient ocean current systems which propagate themselves in a wave-like manner. Thus the term is used more in the meteorologists' sense – it can include quasi-geostrophic disturbances of large-scale circulation systems – or in certain contexts, the largest scale systems themselves, there being no implicit upper limit to the length of the period admitted. On the other hand, certain familiar types of waves, such as ocean surface waves, being of too high a frequency, too small a scale, and not at all hydrostatic, are not considered at all.

First let us consider some of the results of the tidal theorists (HOUGH, as summarized by LAMB, 1932, pp. 349-350) in particular the case of free waves on a homogeneous ocean of uniform depth on a rotating globe. In order to limit discussion only the case of uniform depth of 14,520 feet is considered here, a particular depth being chosen so that numerical values for periods of various waves can be given. In Figs. 15 (a, b, c, d) the deformation of the elevation of the free surface are independent of longitude. In Fig. 15 (a) there is only one nodal circle at the equator, the elevation of the surface seesaws from north to south across the equator in a huge standing oscillation. For the actually rotating earth with depth 14,520 feet the free period of this standing wave across the equator is 25 hr 28 m, but if the earth did not rotate the period would be 41 hr 55 m – it is striking how much the rotation of the earth alters the free period of this large-scale oceanic standing wave, or seiche.

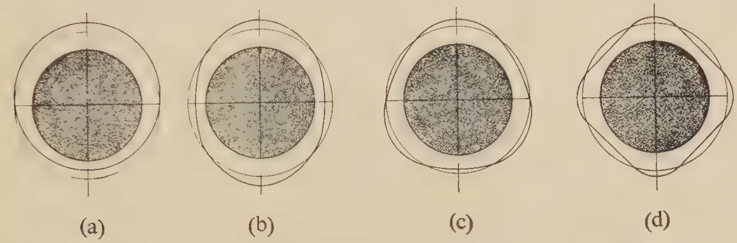

Fig. 15. Four different symmetrical modes of oscillation of the free surface (heavy line) about the undisturbed sea level (light line) on a globe. The figure represents a section through the globe's axis of rotation.

The second case shown, in Fig. 15 (b), has two nodal latitude circles at about 30°N and 30°S. The elevation of the free surface alternates between polar regions and tropical regions. The free period, as might be expected is shorter than for the case with one nodal circle, namely 15 hr 11 m (23 hr 12 m without rotation). Similarly higher numbers of nodal circles lead to shorter periods : thus in Fig. 15 (c), with three nodal circles the period is 11 hr 54 m (16 hr 08 m without rotation) ; or in Fig. 15 (d) with four nodal circles the period is 10 hr 01 m (12 hr 23 m without rotation). As the number of latitudinal nodal circles is increased the effect of the rotation on the period becomes negligible. For example, the case with twelve latitudinal nodal circles has a period of 4 hr 12 m (4 hr 21 m without rotation). This is an illustration of the more general fact that the earth's rotation does not apparently affect wave motions with a frequency much higher than the rotational frequency of the earth (2π radians a day).

Now it is an important thing to note at this point that any one of the configurations of the free surface associated with the axisymmetrical waves drawn in Fig. 15 can also be maintained, within the framework of this simple frictionless dynamical system, with infinite period by an appropriate system of steady zonal geostrophic currents. For example, in Fig. 15 (b) westward flowing geostrophic zonal currents in both hemispheres would balance the particular deformation of the free surface there depicted.

We will now proceed to describe wave forms which are not axisymmetrical and will find similar geostrophic current systems, which are functions of longitude as well as of latitude, and whose periods are not infinite, but are quite long relative to the period of inertio-gravitational waves with the same shape of the free surface. They are more like wavy current systems such as one encounters in the atmosphere.

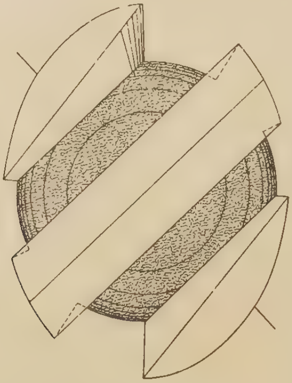

Fig. 16. Antisymmetrical mode of oscillation.

In Fig. 16 a wave is illustrated in which one complete meridian and the equator are nodes. The ocean is 14,520 feet deep. Consider waves moving east or west : waves in which the equatorial node remains fixed, but the meridional node moves around the earth. The wave toward the east has a period of 19 hr 16 m ; the wave toward the west, 12 hr 51 m (without rotation both waves have the period 23 hr 12 m). Waves of this kind – whose period approaches a finite value as the rotation is decreased toward zero – are called waves of the First Class and correspond physically to what one usually has in mind when he thinks of long tidal waves (this is also true of the finite period waves in Fig. 15).

In addition to the high-frequency First Class waves, there is a nearly geostrophic wave of much the same form (the actual form shown in Fig. 16 is computed from HOUGH's expansion, 1897, II, p. 167) which travels only toward the west) there is no eastward counterpart) and has a period of 11 days. These waves are called Second Class waves by the tidal theorists and are distinguished by the fact that they become stationary (their period becomes infinite) if the rotation of the globe is reduced to zero. As we have seen, in the special case of axisymmetric waves (Fig. 15) the period of of the Second Class motions is always infinite. From a physical point of view these waves of the Second Class are moving current systems. In the presence of a basic zonal current waves of the Second Class may be identified with ROSSBY's planetary waves (ROSSBY, 1939). The Second Class waves are essentially the building blocks from which the general forced wave motions characterizing the transient ocean current theory are constructed. One more example of free wave motions on the sphere may be of interest to mention. GOLDSBROUGH (1933) has obtained the free periods of waves in a homogeneous ocean of uniform depth (12,880 ft) bounded by meridional coasts 60° apart. In addition to two First Class waves (rotary tidal waves with periods

12 hr 25 m and 10 hr 18 m) he has also found a Second Class wave with a period of 7·2 days. This wave might be spoken of as a free quasi-geostrophic seiche. One supposes that the Atlantic Ocean must be somewhat resonant to weekly periods of atmospheric disturbance. The successive elevations of the free surface characterizing this Second Class standing oscillation of GOLDSBROUGH are sketched in Fig. 17 : only the first quarter period is illustrated.

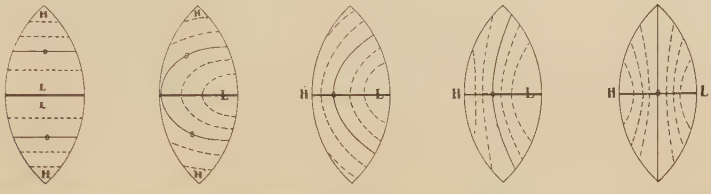

Fig. 17. Sketch of successive contours of surface level in GOLDSBROUGH's 7·2 day geostrophic standing wave (Second Class) in an ocean bounded by meridians 60° apart ; only the first quarter period is depicted.

It is much more convenient, in trying to obtain a clear physical understanding of the differences between the First and Second Class waves, and in working out simple mathematical examples, to abandon the co-ordinate system of the sphere, and to make use of a plane system of co-ordinates, introduced by ROSSBY (1939) in which the variation of the Coriolis parameter is taken as a constant over the plane, and the Coriolis parameter itself is also taken as a constant wherever it occurs in undifferentiated form. This so-called beta-plane has been widely adopted in dynamical meteorology on account of analytical advantages and the simplicity of physical interpretation of the phenomena which it exhibits. On the other hand, one should keep in mind the fact that the beta-plane is not a perfect analogue of this sphere.

Consider now free harmonic waves propagated along the east-west direction with horizontal crests and troughs parallel to the north-south axis, as sketched in Fig. 18 (a-f). The undisturbed depth is uniform and the water homogeneous. Hydrostatic equilibrium prevails; the pressure gradients are independent of depth and depend only upon the instantaneous slope of the disturbed surface (remember the vertical scale in the diagrams is much exaggerated). Thus the horizontal components of velocity are independent of the vertical co-ordinate. The vertical component of velocity varies linearly with depth in such a manner as to vanish at the bottom and to equal to time rate of change of surface elevation at the top of water layer. For any wavelength there are three possible such waves on the beta-plane. Two are First Class; one, Second Class. A so-called frequency diagram is sketched in Fig. 19. The ordinate is frequency, the abscissa wave number or reciprocal wave length. THOMPSON (1952) has given a very clear review of the theory of these different waves. We will content ourselves here with a simple physical description. The curve marked I in Fig. 19 corresponds to First Class Waves which can move either towards the east or the west. They have relatively high frequency, and are simply the familiar long gravitational-inertial waves. For short wavelengths (region 1 in Fig. 19) the First Class waves are unaffected by the earth's rotation, are ordinary long gravitational or tidal waves, and are non-dispersive. The particle orbits are indicated in Figs. 18 (a) and 18 (b). Particles move in straight-line segments (neglecting the very small vertical displacements) alternately toward the west and east, the maximum horizontal velocity being toward the direction of wave propagation under a crest, and in the opposite direction under a trough. For longer wave lengths (region 2, Fig. 19) the First Class waves are dispersive, and the period approaches half a pendulum day. These waves were first discussed in detail by SVERDRUP (1927), in connection with tides on the North Siberian Shelf. In addition to the back-and-forth particle motion in the direction of wave propagation, there are also components of horizontal motion transverse to the direction of wave propagation, so that the particles execute elliptical orbits, (Fig. 18c, d) which, as the frequency approaches half a pendulum day, tend to become circular – the limit particle motion in pure inertial circles. Density stratification introduces free internal modes, which, for a given wavelength are much more affected by the earth's rotation (VERONIS and STOMMEL, 1956), but it would be too much of a

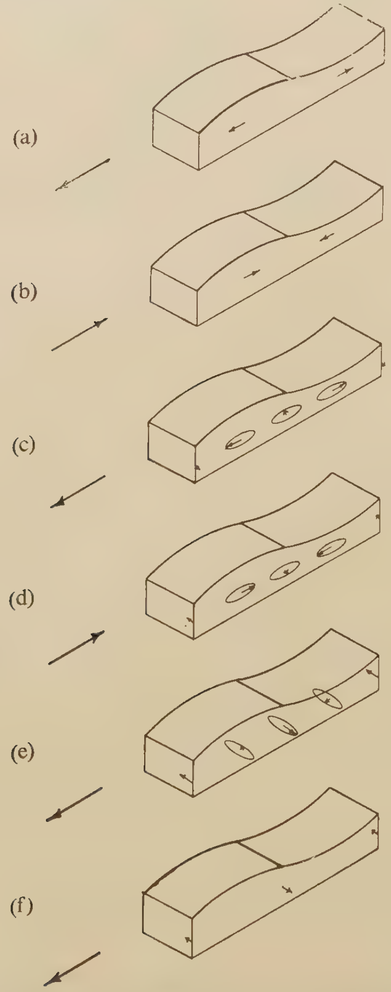

Fig. 18. Sketch of surface perturbation, instantaneous particle velocity (arrows), hodograph (ellipses) for different kinds of free long waves. The arrows on the left show the direction of propagation. By convention we take left ward as westward.

digression from the main theme of this review to consider First Class waves much further here.

The second curve in Fig. 19, marked II, gives the frequency vs. wave length relation for Second Class waves in the homogeneous ocean on the beta-plane (Rossby 1939). There are two distinct regions to the curve : a long wave length region (region 3 in Fig. 19) with long periods, the waves being non-dispersive, and another region (region 4 in Fig. 19) of shorter wavelengths, also of long period. These short waves are highly dispersive, and interesting enough are of such a nature as to have very little horizontal divergence. The two regions 3 and 4 are connected by a shorter period transition region. The minimum period of Second Class waves appears in this transition region. The free waves of Second Class move only to the west. The orbits are essentially horizontal ellipses with major axes parallel to the crests, as shown in Fig. 18 (e). The particle orbits become more and more eccentric as the period increases, for both long and short wavelengths (Fig. 18f). It is clear that the Second Class waves are essentially geostrophic current systems which because of the planetary geostrophic divergence inherent in the beta-plane cannot remain stationary. Consider the Second Class wave shown in Fig. 18 (f). The current is toward the south and the Coriolis force is balanced by the eastward horizontal pressure gradient due to the slope of the free surface. The divergence of this geostrophic current can be balanced in two ways : (1) first, the free surface can drop over southward currents and rise over northward ones (northern hemisphere) – which leads to the non-dispersive westward propagation of the wave form indicated by region 3 in Fig. 19; (2) the southward current is subject to an increase in relative vorticity, the elevation of the free surface producing negligible divergence, and northward current suffer a decrease in relative vorticity, thus shifting the vorticity pattern toward the west as indicated by the region 4 in Fig. 19. The transition region in Fig. 19 combines both these effects.

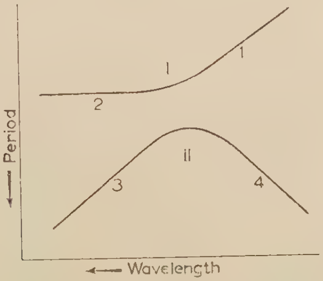

Fig. 19. Period-wave length relation for First Class (I) and Second Class (II) waves in a homogeneous layer on the beta-plane.

Two free progressive Second Class waves of the same frequency can also be combined to permit reflection from a meridional barrier (Arons and Stommel, 1956). Both the waves move in the same direction of course, but the group velocity is opposite for the incident and reflected wave, and there is no net energy flux. If the homogeneous water layer is bounded on both the east and west by meridional walls there are only certain discrete free frequencies allowed – an eigenvalue problem which gives the free Second Class periods of closed basins.

Free Second Class waves in a density-stratified system

The introduction of vertical density stratification in the model permits internal or baroclinic modes of both First and Second Class. The periods for a given wavelength are much longer than for the external or barotropic mode. Since the frequency

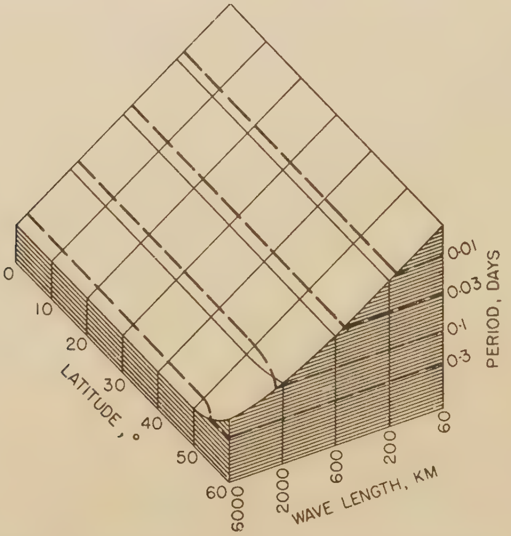

Fig. 20. Periods of First Class barotropic ocean waves.

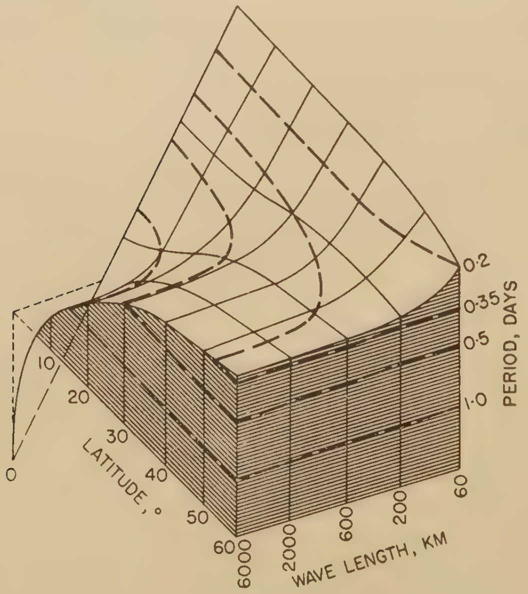

Fig. 21. Periods of First Class baroclinic ocean waves.

diagram of these different classes and modes is partly a function of latitude, and of density structure, a single curve will not be very helpful. Therefore I have prepared four block diagrams that give periods of free waves as a function of latitude and wave length for the cases : First Class barotropic, Fig. 20 ; First Class baroclinic, Fig. 21 ; Second Class barotropic, Fig. 22 ; and Second Class baroclinic, Fig. 23. The baroclinic diagrams are prepared by using a two density layer model (VERONIS and STOMMEL, 1956) with thickness of the layers and density difference chosen to match as nearly as possible that of the North Atlantic for each latitude. The barotropic diagrams are prepared using representative depths of the North Atlantic. Hence the diagrams are not quite as smooth looking as they would be if computed entirely from a single geometry and density difference.

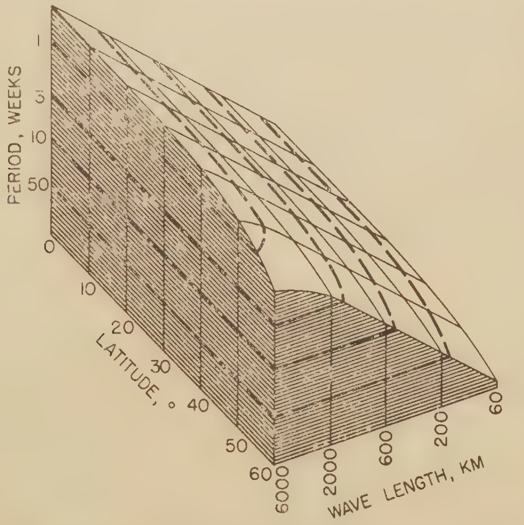

Fig. 22. Periods of Second Class barotropic ocean waves.

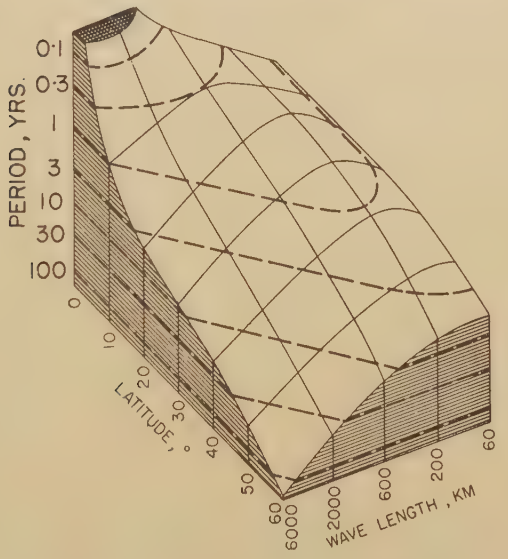

Fig. 23. Periods of Second Class baroclinic ocean waves.

The Second Class barotropic waves have periods, for wavelengths corresponding to oceanic dimensions, of about a week. Second Class baroclinic waves of oceanic dimension have very long periods ; only near the equator is there a period as short as a year, however it should be remembered that the approximations in the beta-plane are bad at the equator, so that the results there must be received with caution.

Transient response of the ocean to a variable driving force

The properties of free waves in a two-layer stratified fluid on the beta-plane are helpful in understanding physically the response of a stratified system to changes in the driving system. Quantitative theoretical studies of the response to changing forces are rather involved, and it seems fruitless to try to explain them verbally. A set of references to work in this field is given in another place (VERONIS and STOMMEL, 1956). In this brief review article we must be satisfied by a brief statement of the main results of the theories.

First of all, very short period or abrupt changes in the driving forces such as earthquakes, or sudden storms over shallow seas excite mainly the First Class barotropic mode. VERONIS (1956) has shown that when the interval during which an applied wind stress is changed from one value to another exceeds a half pendulum day most of the work done by the wind stress upon the sea goes into Second Class waves, that is, into currents. If this interval during which the wind changes is smaller, energy goes into First Class wave motions. Within the Second Class motions themselves the distribution of energy between barotropic and baroclinic modes depends very much upon whether the period of the forcing function is closer to the barotropic free period corresponding to the wave length of the forcing function. Thus in midlatitudes a large-scale storm of dimensions 600-2000 km and duration of three to five days will excite the barotropic mode of the Second Class. The Second Class baroclinic mode is also excited, but its amplitude is much smaller than would be expected were the storm to become stationary and to blow constantly for a long time. This can be seen by comparing Figs. 22 and 23. The currents produced will be largely independent of depth (beneath the surface friction layer of course) and the thermal structure of the ocean will not be much influenced. On the other hand in low latitudes a large scale fluctuation of the winds with a period of a year (for example, the Indian Ocean Monsoon) will nearly be in resonance with the Second Class baroclinic mode, as can be seen from Fig. 23. Hence in this case the currents responded chiefly in the upper layer, and the density structure changes markedly to accommodated them. In high latitudes seasonal changes in the winds are not so near to resonance with the Second Class baroclinic mode ; for example one might expect the Antarctic Circumpolar Current to show little seasonal change of deep thermal structure due to seasonal wind changes.

In a simple two-density layered ocean in a closed basin the steady state vertically integrated transport is given by the SVERDRUP solution. If there is no mass transport or mixing across the interface, all the steady motion is in the upper layer. If the wind-stress distribution is now changed, from one pattern to another, on an oceanic scale, the vertically integrated transport distribution adjusts itself to that corresponding to a new steady state distribution within a few weeks ; but the vertical distribution of velocities is very different from that of the final steady state. The simple two-layer theory indicates that several years or decades (in midlatitudes) are necessary before the vertical distribution of velocities approaches that of the steady state solution with all the velocity in the upper layer. Thus we see that the total vertically integrated transport responds rapidly to changes in applied wind stress, but the internal density field responds quite slowly. The response of the internal density field is not governed by the period of inertial-gravitational (First Class) waves, as is sometimes thought by hydrographers, but by the much longer period Second Class internal waves.

As another illustration, this time a hypothetical one, imagine a two-layer ocean completely at rest. The surface and the interface are horizontal. Now suppose that a constant convergent EKMAN wind-driven layer with maximum convergence at the midlatitude of the diagram (Fig. 24 a, b, c) is superposed at the surface in such a manner that the response of the ocean is mostly in the Second Class baroclinic mode – in particular, the large wavelength non-dispersive portion of the frequency diagram.

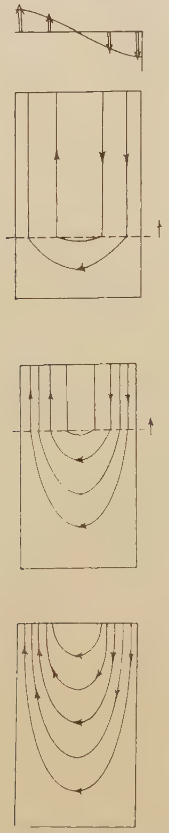

Fig. 24. Three successive stages of the slow development of the steady deformation of the thermocline from rest by a wind stress distribution as shown at the left. The dashed line is a " front " moving slowly (a mile a day) from the eastern coast to the western coast. On the left of the front the thermocline steadily deepends; on the right it is stationary in the SVERDRUP manner (Fig. 12).

Under these circumstances the first response of the interior of the ocean is a simple deepening of the interface at a constant rate equal to the supply of water at the surface from the EKMAN layer. Near the coast there is a sharp transition from this simple response of the interior to a configuration of the interface characteristic of the steady state solution which would exist had the wind blown forever (Fig. 12). The region of transition from one type of solution to the other slowly moves westward until the entire ocean is covered by the steady state solution. Two successive stages of this development and motion of the discontinuity between types of solution are drawn in Fig. 24 (a, b, c). One assumes that the whole process is so slow that at every stage of development there is a western current equilibrium at the western boundary that is able to cope with the need for a western boundary condition.

The stability of the solutions and the dilemma of the Antarctic circumpolar current

One of the most unsatisfactory aspects of the theoretical solutions so far developed in oceanography is the fact that they have not been exmined for stability. Dynamical meteorologists are convinced that a steady state model does not apply to the atmosphere except possibly in the Trade Wind regions. Elsewhere large quasigeostrophic wave disturbances appear and disappear spontaneously in the zonal wind systems and play a very important dynamical role in the general circulation of the atmosphere. Some investigators even believe that disturbances maintain the zonal flows. Should this be the case, it is obvious that steady state models incorporating large arbitrary lateral eddy coefficients would scarcely be very enlightening. By analogy with developments in the study of meteorology, oceanographers are warned to employ steady-state theories of the ocean with caution – especially models which employ large-scale eddy coefficients. In the tropics and subtropics the SVERDRUP theory seems to apply quantitatively to the ocean circulation, although there is not sufficient observational material for a completely convincing demonstration one way or the other. This suggests that the SVERDRUP model is essentially stable in the tropics, but we are far from a mathematical demonstration of its stability. In general it seems to me that we might expect theoretical models of oceanic circulation to be much more stable than those of the atmosphere on account of the presence of the meridional barriers because the high velocity zonal currents characteristic of instability in the atmosphere are suppressed by the coasts. This is, of course, sheer speculation.

A numbers of authors (e.g. MUNK and PALMEN, 1951) have pointed to the Antarctic Ocean as an example of an ocean without meridional barriers, and as such one in which a SVERDRUP type solution cannot be constructed. In an ocean without meridional barriers there can be no net meridional component of geostrophic flow, and we are forced back to circulations like the HOUGH regimes. A very crude model of the Antarctic Circumpolar Current can be constructed by employing lateral viscosity. Several Japanese authors (HIDAKA and TSUCHIYA, 1953, and others) have constructed models of the Antarctic Circumpolar Current as essentially a laterally viscous zonal stream driven by the southern hemisphere westerlies. In order to limit the total transport of the Circumpolar Current to about 100×10^6 m^3/sec a lateral eddy viscosity of more than 10^{10} cm^3/sec is required – several orders of magnitude greater than that generally envisaged in other oceanic currents. If vertical viscosity is employed very large coefficients are also required. On the other hand, the fact that the deep warm water in the Circumpolar Current preserves its Atlantic characteristics even into the Pacific Ocean suggests that the lateral diffusivity can hardly exceed 10^7 cm^2/sec, nor the vertical diffusivity be much greater than 10 cm^2/sec. Thus the implications of water-mass analysis are not compatible with the large turbulent coefficients required in the purely zonal and frictional theory.

There have been several other mechanisms suggested for the Antarctic Circumpolar Current (Munk and Palmen, 1951; Fofonoff, 1955) all of which regard it as a purely zonal phenomenon. The cross section of the channel between the Cape of Good Hope and Antarctica is quite broad and deep (Fig. 25a), and a section straight from Cape Horn and Graham Land is also quite adequate (Fig. 25b) to permit the Circumpolar Current to pass through. However, if one plots the minimum depth for each complete latitude circle, it is found that the latitude circles that pass through Drake Passage are blocked by the island arc somewhat to the east. The minimum depths are plotted in Fig. 25 (c). It is seen that nowhere in the Antarctic Water-Ring is there a latitude with a deeper threshold than 1000 m. The Antarctic Circumpolar Current therefore cannot be purely zonal. In fact (Deacon, 1937) there seems to be a general southward component of the current over the entire southern ocean except just after passing through Drake Passage, where it is deflected sharply north by about 10° of latitude in a very limited narrow region, and possibly also to some extent just after passing New Zealand. Now if there is anything to this picture it suggests that the Antarctic Circumpolar Current is essentially amenable to treatment by the Sverdrup theory; that the current is essentially frictionless except in a narrow region just after it passes through Drake Passage. In this one limited region we anticipate that all the dissipation of energy, any instability, and higher order processes occur. The remarks which follow cannot be considered to be a theory; they are merely suggestive of one, and they do illustrate some of the physical ideas described in this survey.

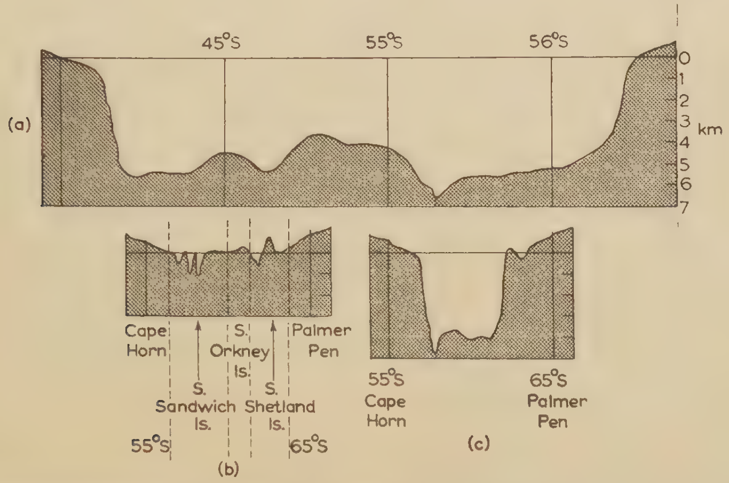

Fig. 25. Depth profiles across the Southern Ocean : (a) From Cape of Good Hope to Antarctica ; (b) From Cape Horn to Palmer Peninsula ; (c) Minimum depth of each latitude circle.

Before attempting to interpret the internal modes of circulation, we first consider only the vertically integrated flow – it is only necessary to consider a simple homogeneous ocean of uniform depth. In order to proceed simply we first consider that Drake Passage is closed (Fig. 26a). This barrier is indicated by the heavy radial line in the figures, joining the schematic Antarctic continent. The assumed zonal wind system is shown in Fig. 26 (a). Trades from the Equator to 30°S, westerlies from 30°

to a little over 60°S, and further to the south a small zone of Easterlies. The EKMAN drift is northward in the westerlies, southward in the easterlies. South of about 50°–55°S the EKMAN drift is divergent, in more northerly latitudes it is convergent. According to our simple physical notions we expect this divergence to be compensated by the planetary divergence of meridional components of geostrophic flow. There is no difficulty in obtaining such a flow in the ocean of Fig. 26 (a) because there is a complete meridional barrier. The necessary meridional components are shown by heavy arrows in Fig. 26 (a). The full transport field is developed by continuity from the eastern side of the ocean (western coast of South America) and fitted with an intense western boundary current at the western coast of the ocean. There are two immense gyres in Fig. 26 (b). wrapped around the world parallel to latitude circles. A simple calculation shows that the transport in the southern gyre amounts to somewhat more than 100 × 10^6 m^3/sec, the northern gyre somewhat less. Thus

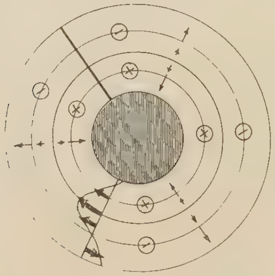

Fig. 26 (a). The schematic Southern Ocean. Antarctica is the solid black circle. The meridional barrier extending northward from Antarctica is represented by the solid heavy black vertical line. The schematic wind system (purely zonal) is depicted by the heavy arrows on the lower left. The concentric circles are latitude circles. Latitudes of EKMAN convergence and sinking at the surface are indicated by minus signs, latitudes of EKMAN divergence and upwelling are indicated by plus signs. The direction of the required meridional geostrophic flow is indicated by light radial arrows.

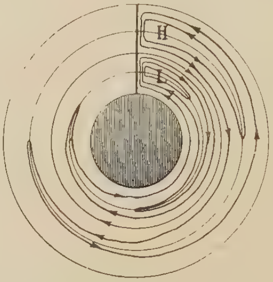

Fig. 26 (b). Transport lines of the solution for the model depicted in Fig. 26 (a). The western boundary currents are to be interpreted schematically.

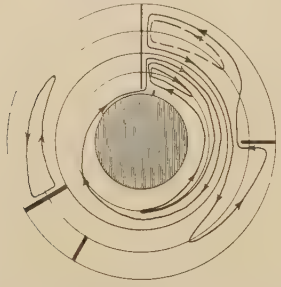

Fig. 26 (c). Modification of the transport field produced by introduction of other meridional barriers corresponding to Africa, Australia, and New Zealand, and by breaking the American-Antarctic barrier so as to admit a very constricted Davis Straits.

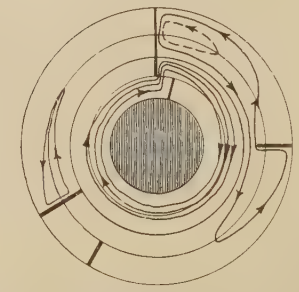

Fig. 26 (d). Hypothetical form of the solution that results from rupturing the American-Antarctic barrier in such a way as to permit water to flow through, but to obstruct all latitude circles.

each line in Fig. 26 (b) is roughly 30 × 10^6 m^3/sec. Actually the northern gyre is broken up by the African and Australia-New Zealand continents so that it must be modified in some such way as indicated in Fig. 26 (c). In this figure a small breach has been made in the South America to Antarctica barrier, enough to permit one transport line to pass through, otherwise the general shape of the southern gyre is not much altered. If the barrier is broken in a manner indicated in Fig. 26 (d), so that there is no unbounded latitude circle, but there is a pass for water to flow through to the north, it seems to me that the pattern of flow must then look something like drawn. This picture is obtained by keeping all mid-ocean transport lines north of the latitude of the passage just the same as in Fig. 26 (b), but south of this latitude by developing the transport function from the western coast of the ocean (the east coast of the Palmer Peninsula) toward the east. The flow through the passage itself is something of a mystery, but doubtless models can be devised to describe it. Due to the extreme elongation of the flow pattern illustrated in Fig. 26 (d) the current looks like a purely zonal one at first glance. The over-all agreement of this picture with the lines of equal dynamic height in DEACON's study (1937) is fairly striking. Thus we see that there is some reason to suppose that the Antarctic Circumpolar Current is not such a dynamical misfit as originally it was thought to be. One need merely recognize that it is not a zonal current after all. Fig. 27 shows the homogeneous model in perspective. The transport lines are parallel to the surface height contours everywhere except in the narrow passage where they cross isobars in a downhill direction. A water particle does not drop the full dynamic height difference across the Antarctic Circumpolar Current each time it makes a circuit around the world, but requires from three to five circuits on the average it drops the full dynamic height and rises to the surface, and is carried away to the north across the latitude of maximum westerlies in the surface EKMAN layer. The EKMAN northward transport is non-geostrophic, and distributed all around the southern ocean ; it is indicated by the radial arrows in Fig. 28. For entire 55°S latitude circle it must amount to at least 20 × 10^6 m^3/sec. This is the latitude of maximum westerlies, and there is no mid-ocean meridional flow where the EKMAN layer is non-divergent. There is a western current on the western coast of the ocean (eastern South America) setting southward, and just to the north of Drake Passage. Thus it is that the water which replenishes that lost to all the oceans north of 55°S by the EKMAN layer, is drawn mostly from the South Atlantic western trough. There is reason to suppose that this supply is largely Atlantic Deep Water.

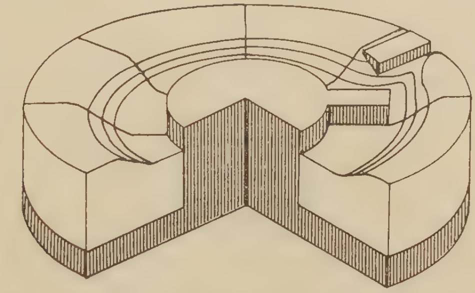

Fig. 27. Surface contours (or isobars) of the hypothetical Circumpolar Current shown in Fig. 26 (d).

The actual Antarctic circulation is partly baroclinic. We now proceed to make a crude interpretation of the internal structure of the flow. In Fig. 28a schematic diagram of the southern ocean is presented, showing the Antarctic continent as the central cylinder, and the American Barrier with Drake Passage indicated to the right. Two level surfaces intersect the body of the ocean: L_1 at a depth of approximately 600 and L_2 at a depth of about 3500 to 4000 meters. Let us now specify the vertical transfer across these levels. Across level L_1 there is a general upward flux of mass from the warm deep layer, apparently almost enough to compensate for the water lost by the upper layer to the divergent EKMAN layer on the very top. Across level L_2 there is very little vertical transfer, except near the Weddell Sea where some Antarctic Bottom Water sometimes sinks across it. The Bottom Water cannot flow anywhere to speak of except up the western coast of the ocean in a narrow western boundary current beneath L_2, because the rest of the layer is non-divergent. The whole of the large body of warm saline water between level L_2 and L_1 is apparently convergent on account of the flux upwards across L_1. As we have seen, a system of this sort can develop a strong geostrophic component of flow everywhere in mid-ocean by spiralling in towards the Antarctic Continent except for the abrupt northward displacement that occurs in Drake Passage. The supply of water for this main body of the Circumpolar Current comes from a narrow stream of Atlantic Deep Water flowing, as western boundary current, down the west side of the South Atlantic Ocean. In the layer between 600 m and the bottom of the EKMAN layer it is not clear just how to interpret the state of affairs. If this layer is slightly convergent it should move more or less along with the deep water ; if it is non-divergent – that is, loses as much to the EKMAN layer as it gains from the warm deep layer, it may move more nearly

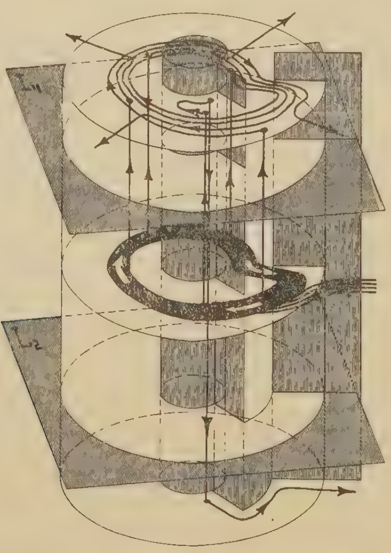

Fig. 28. Schematic three-dimensional diagram illustrating the hypothetical schematic internal structure of the Circumpolar Current (see text for detailed explanation). Two reference levels, L_1 and L_2, intersect the body of the ocean. The central shaded cylinder is the Antarctic Continent. The vertical plane attached to it at the forward right is Palmer Pensula, and the detached vertical plane at the extreme right is South America. The curved lines with arrow heads are transport lines. In order to avoid complicating the diagram, the more realistic spiralling motion is not shown.

zonally than the deep water, because it is not so completely blocked by the island arc from attaining zonal flow, or if it is divergent it may drift northward everywhere with the surface EKMAN drift. The simple picture shown in Fig. 28 does not extend north of the Antarctic Convergence, so no attempt is made to interpret the formation of Antarctic Intermediate water, etc.

Finally I should like to make an apology for ending this survey article with such a sketchy and incomplete interpretation of the Antarctic Circumpolar Current as I have just given above. I should have hesitated to do so were it not for the fact that it so clearly illustrates both the usefulness and weakness of the physical ideas reviewed above.

Acknowledgements—I am particularly indebted to Mr. GALE PASLEY for drafting some of the intricate diagrams in this article, to Dr. G. VERONIS and Dr. G. MORGAN for many discussions during the past year, and to the Office of Naval Research for underwriting my studies.

Woods Hole Oceanographic Institution. Contribution No. 917 *from the Woods Hole Oceanographic Institution*

REFERENCES

ARONS A. B. and STOMMEL H. (1956) A β-plane analysis of free periods of the Second Class in meridional and zonal oceans. *Deep-Sea Res.* **4** (1), 23-31.

CHARNEY J. G. (1955) The Gulf Stream as an Inertial Boundary Layer. *Proc. Nat. Acad. Sci.* (*U.S.A.*) **41** (10), 731-740.

DEACON G. E. R. (1937) The hydrology of the Southern Ocean. *'Discovery' Rep.* **15**, 1-124.

DEFANT A. (1941) Die absolute Topographie des physikalischen Meeresniveaus und der Druckflächen, sowie die Wasserbewegungen im Atlantischen Ozean. *Deutsche Atlantische Exped. " Meteor "* 1925-27, *Wiss. Ergeb.* **6**, 191-260.

EKMAN V. W. (1905) On the influence of the earth's rotation on ocean currents. *Arkiv f. Matematik, Astronomi, och Fysik* **2** (11), 1-52.

EKMAN V. W. (1923) Uber horizontal Zirkulation bei winderzeupten Meeresströmungen. *Ibid.* **17** (26), 1-74.

FOFONOFF N. (1954) A steady flow in a frictionless homogeneous ocean. *J. Marine Res.* **13**, 254-262.

FOFONOFF N. (1955) A theoretical study of zonally uniform oceanic flow. Doctoral Dissert., Department of Oceanography Brown Univ., 36. (Unpublished).

GOLDSBROUGH G. R. (1933) The tides in oceans on a rotating globe IV. *Proc. Roy. Soc.* **A140**, 241-253.

GOLDSBROUGH G. R. (1933) Ocean currents produced by evaporation and precipitation. *Proc. Roy. Soc.* **A141**, 512-517.

HIDAKA K. (1950) Drift currents in an enclosed ocean. *Tokyo Univ., Geophys. Notes* **3** (23), 1-23.

HIDAKA K. (1955) A theoretical study of the general circulation of the Pacific Ocean. *Pacific Science* **9** (2), 183-220.

HIDAKA K. and TSUCHIYA M. (1953) On the Antarctic Circumpolar Current. *J. Marine Res.* **12**, 214-222.

HOUGH S. S. (1897) On the application of harmonic analysis to the dynamical theory of the tides. Part I : On Laplace's " Oscillations of the first species," and on the dynamics of ocean currents. *Phil. Trans.* (A) **189** (IX), 201-258.

HOUGH S. S. (1898) On the application harmonic analysis to the dynamical theory of tides. Part II : On the general integration of Laplace's dynamical equations. *Phil. Trans.* (A) **191** (V), 139-186.

LAMB H. (1932) *Hydrodynamics* (Sixth Edition) Cambridge Univ. Press, 738 pp.

LINEYKIN, P. C. (1955) On the determination of the thickness of the baroclinic layer in the sea. *Dokl. Akad. Nauk SSSR* **101**, 461-464.

MORGAN G. W. (1956) On the wind-driven circulation. *Tellus* **8** (3), 301-320.

MUNK W. H. (1950) On the wind-driven ocean circulation. *J. Met.* **7**, 79-93.

MUNK W. H. and CARRIER G. F. (1950) On the wind-driven circulation in ocean basins of various shapes. *Tellus* **2**, 158-167.

MUNK W. H. and PALMÉN E. (1951) Notes on the dynamics of the Antarctic Circumpolar Current. *Tellus* **3** 53-55.

NEUMANN G. (1956) Notes on the horizontal circulation of ocean currents. *Bull. Amer. Met. Soc.* **37**, 96-100.

REID R. O. (1948) A model of the vertical structure of mass in the equatorial wind-driven currents of a baroclinic ocean. *J. Marine Res.* **7**, 304-312.

ROSSBY C. -G. (1939) Relation between variations in the intensity of the zonal circulation of the atmosphere and the displacements of the semi-permanent centres of action. *J. Marine Res.* **2**, 38-55.

STOCKMANN V. B. (1953) Several questions on the dynamics of ocean currents. *Izv. Akad. Nauk SSSR* Seriya Geofizicheskaya, (1), 69-77.

STOMMEL H. (1956) On the determination of the depth of no meridional motion. *Deep-Sea Res.* **3**, 273-278.

STOMMEL H. (1957) *The Gulf Stream* Univ. of California Press (in press).

STOMMEL H. and VERONIS G. (1957) Steady convective motion in a horizontal layer of fluid heated uniformly from above and cooled non-uniformly from below. *Tellus* (in press).

SVERDRUP H. U. (1927) Dynamics of tides on the North Siberian Shelf. *Geofys. Publ.* **4**, (5), 75.

SVERDRUP H. U. (1947) Wind-driven currents in a baroclinic ocean ; with application to the Equatorial Currents in the eastern Pacific. *Proc. Nat. Acad. Sci.* (*U.S.A.*) 33, 318-326.

THOMPSON P. D. (1952) Notes on the theory of large-scale disturbances in atmospheric flow with applications to numerical weather prediction. *Geophys. Res. Pap.* (U.S. Air Force Cambridge Research Center) No. 16, 107 pp.

VERONIS G. (1956) Partition of energy between geostrophic and non-geostrophic oceanic motions. *Deep-Sea Res.* **3**, 157-177.

VERONIS G. and STOMMEL H. (1956) The action of variable wind stresses on a stratified ocean. *J. Marine Res.* **15** (1), 43-75.

VON ARX W. S. (1952) A laboratory study of the wind-driven ocean circulation. *Tellus* **4**, 311-318.

Printed in Great Britain by The Salisbury Press Ltd., Publicity House, Wilton Road, Salisbury, Wilts. (5027)

Contribution No. 919

Deep-Sea Research, 1957, Vol. 4, pp. 238 to 249. Pergamon Press Ltd., London

Profiles across the Peru–Chile Trench

J. M. Zeigler, W. D. Athearn and H. Small

(*Received* 1 *July* 1957)

Abstract—Three general types of profile across the Peru–Chile Trench are shown : trench with gently basined topography, trench with smooth flattish floor, and trench with abrupt topography. Differences in trench shape are ascribed to differences in agents and rates of sedimentation.

Production of plankton whose skeletons might accumulate as bottom sediment is reasonably uniform along the length of the area examined, therefore differences in sedimentation must be associated with available supply from the South American continent. Presumably the supply would be greater north of the Chilean desert because more streams reach the sea and in some places, such as near Talara, Peru, the coastal sediments are less resistant than the volcanics along much of the Chilean coast.

If the trench is not the same age throughout its length, then the arguments for different sedimentary environments do not necessarily explain differences in bottom topography, nor from profiles alone is it possible to say which end of the trench is younger ; however a progressively growing earth flexture must then be assumed.

Topographic features such as subsidiary trenches to the side of the main trench, grabens and horsts, and submarine canyons are described.

INTRODUCTION

The deep, narrow trench whose trend closely parallels the western coast of South America from Ecuador to Chile is a submarine feature of great interest. This trench in its entirety will be referred to as the Peru-Chile Trench (see Fisher and Revelle, 1955). The Woods Hole Oceanographic Institution's research vessel *Atlantis*, under the leadership of the late H. C. Stetson and P. D. Trask, occupied 100 coring stations off the coasts of Peru and northern Chile during November and December, 1955 for the purpose of investigating sediments of this trench. The track of the vessel and positions of coring stations are shown in Fig. 1.

PREVIOUS WORK

Insofar as we can ascertain, first knowledge of these deep areas dates back 80 or 90 years. Submarine telegraph cables were laid as early as 1875 along parts of the west coast of South America (Milne, 1897, pp. 266–267) ; and it is likely that cable ships first discovered the deeps. The cable ship *Relay* of the Central and South American Cable Company reported a wire sounding of 4175 fathoms (7635 m) in the Richards Deep off Taltal, Chile, in 1890 (Bencker, 1930). Deep soundings given in the same report for the Haeckel Deep (approximately 32°S) and for the Krümmel Deep (approximately 18°S) probably were taken by cable ships also. The deepest sounding reported prior to the " Shellback " expedition for the Milne-Edwards Deep off Callao (approximately 12°S) was taken by the U.S.S. *Alaska* in 1881.

The " Shellback " expedition of 1952 carried out by the research vessel *Horizon* made several crossings of the trench between the latitudes of Guayaquil, Ecuador, and Callao, Peru, and the *Atlantis* cruise of 1955 made several crossings between the latitudes of Talara, Peru, and 25°S (about 75 miles south of Antofagasta, Chile). These are the only two scientific expeditions ever to undertake anything like a systematic exploration of the trench. Other research ships which made occasional crossings and some soundings did so principally to reach ports in the area. These include the Italian *Vettor Pisani* in 1884, the U.S. Fish Commission Steamer *Albatross* in 1904, and the non-magnetic ship *Carnegie* in 1929.

The first charts to show deep areas along the west coast of South America were published by Sir JOHN MURRAY in 1895 along with his summary of the scientific results of the *Challenger* expedition (THOMPSON and MURRAY, 1895). These charts were the result of plotting and contouring of all available soundings deeper than 1000 fathoms (1830 m). Areas deeper than 3000 fathoms (5500 m) were called deeps and were given distinctive names (MURRAY, 1899). Thus it appears that MURRAY not only first charted the deeps of the Peru–Chile Trench but also named them. From north to south these were (1) Milne-Edwards Deep, a nearly circular area north-west of Callao; (2) Krümmel Deep, a circular area off Arica, Peru; (3) Richards Deep, an elongated area extending from 19·5°S to 28°S off northern Chile ; and (4) Haeckel Deep, a small elongated area north-west of Valparaiso. Four years later a slightly revised chart was published along with a review of existing knowledge of ocean bottom conditions (MURRAY, 1899). Contours of Milne–Edwards Deep, Krümmel Deep, and Haeckel Deep remained about the same, but Richards Deep of the 1895 chart was divided into two deeps with a shallower " saddle " between. The name Richards Deep was retained for the more southerly area between 23°S and 26°S while the more northerly area between 19°S and 21°S was named Bartholomew Deep. Thirteen years later, in their book *The Depths of the Ocean* MURRAY and HJORT (1912) reproduced this 1899 chart in essentially its original form.

Available bathymetric charts of the area produced since the advent of echo sounding portray the trench and its deeps in about the same form and position as given by MURRAY's charts. Most notable of these is the *General Bathymetric Chart of the Oceans*, published by the INTERNATIONAL HYDROGRAPHIC BUREAU of Monaco. The most recent edition of the sheet covering the southern Atlantic and south-eastern Pacific Oceans (Sheet A'_1) was published in 1936. The Geologic Map of South America, published in 1950 by the Geological Society of America, also includes contours of the Peru–Chile Trench, but does not show soundings upon which the contours were based. Another recent set of charts showing the trench and its deep areas was published in a paper dealing principally with the submarine configuration off Callao and Lima by SCHWEIGGER (1947). It is interesting to note that SCHWEIGGER, who based his contours on soundings from charts of the U.S. Hydrographic Office and of the Peruvian Hydrographic Service, neglected earlier names for the deeps and applied new names to two, leaving the others unnamed. Those renamed are Fosa de Lima (Milne–Edwards Deep) and Fosa de Arica (Krümmel Deep).

It is clear from a perusal of data presented on the more recent charts that a great deal more surveying needs to be done before the exact shape of the Peru–Chile Trench can be determined. Profiles resulting from the " Shellback " and *Atlantis* expeditions are steps in accomplishing this work.

INSTRUMENTS AND NAVIGATION

Echo sounding data, obtained in conjunction with the coring programme, are

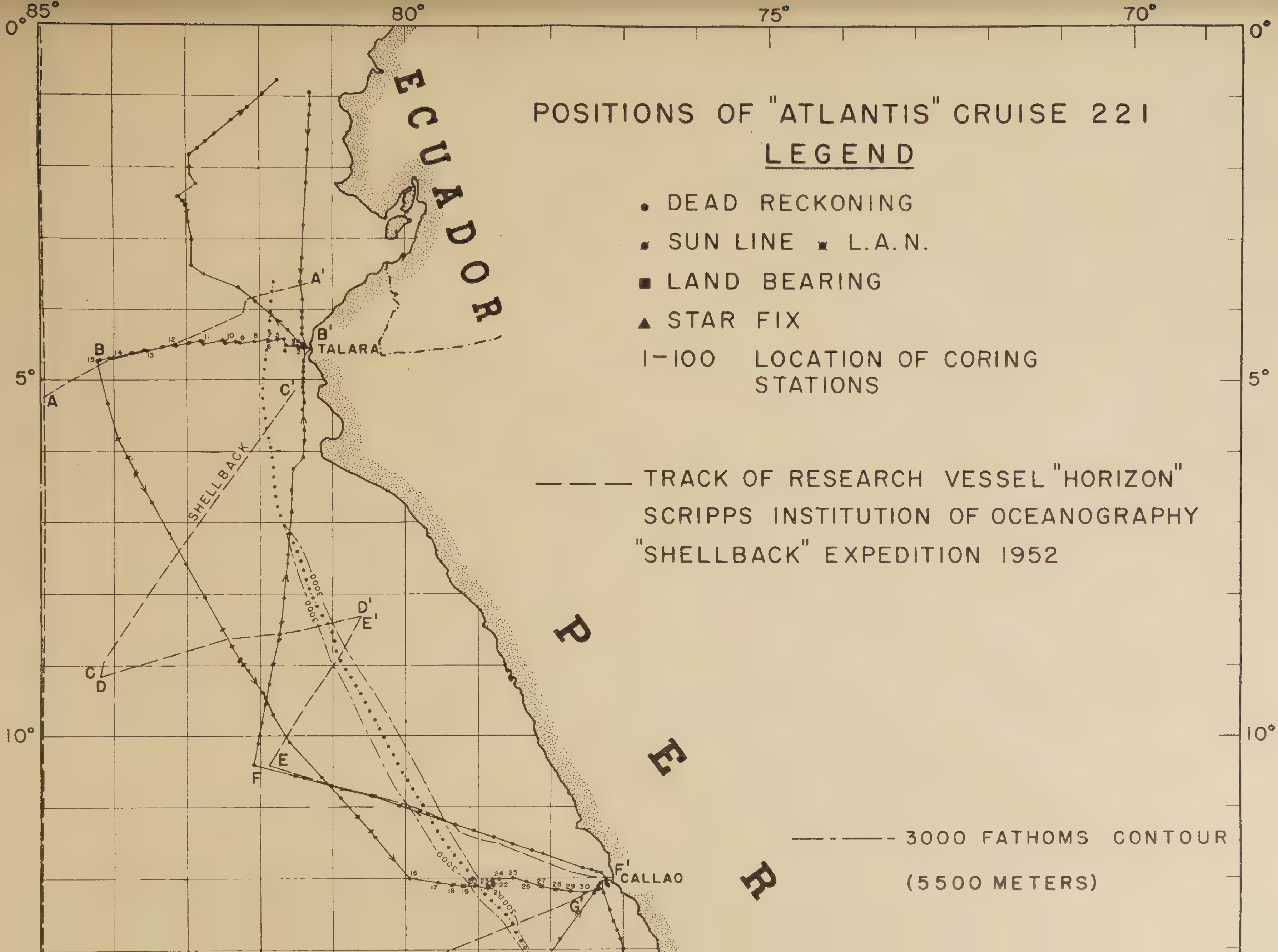
POSITIONS OF "ATLANTIS" CRUISE 221
LEGEND
• DEAD RECKONING
• SUN LINE ✱ L.A.N.
■ LAND BEARING
▲ STAR FIX
1–100 LOCATION OF CORING STATIONS
TRACK OF RESEARCH VESSEL "HORIZON"
SCRIPPS INSTITUTION OF OCEANOGRAPHY
"SHELLBACK" EXPEDITION 1952
3000 FATHOMS CONTOUR
(5500 METERS)
ECUADOR
PERU
TALARA
CALLAO
SHELLBACK
3000
A
A'
B
B'
C
C'
D
D'
E
E'
F
F'
G'
85°
80°
75°
70°
0°
5°
10°

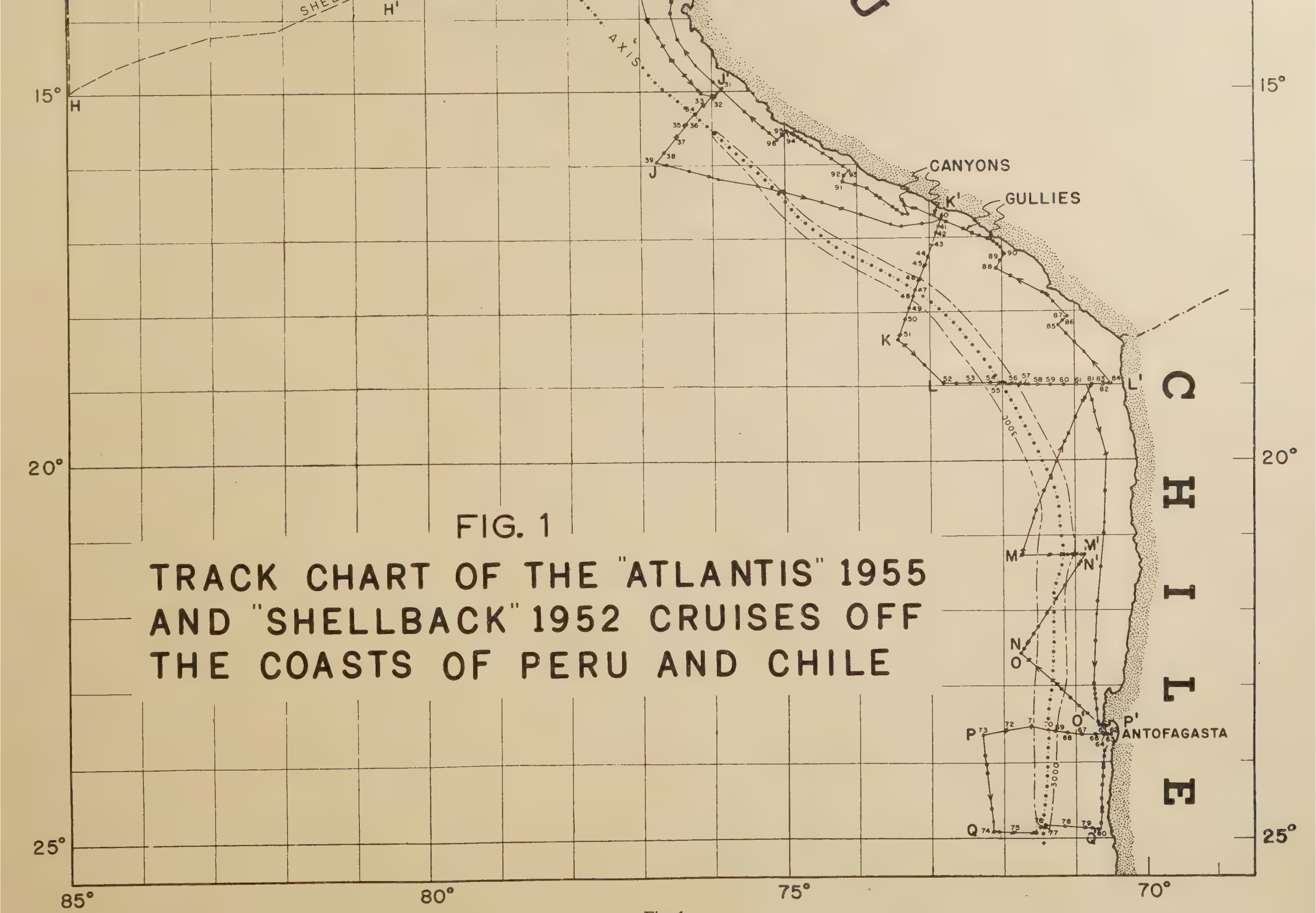

FIG. 1

TRACK CHART OF THE "ATLANTIS" 1955 AND "SHELLBACK" 1952 CRUISES OFF THE COASTS OF PERU AND CHILE

CHILE
ANTOFAGASTA
CANYONS
GULLIES
AXIS
SHEL
H
H'
J
J'
K
K'
L
L'
M
M'
N
N'
O
O'
P
P'
Q
Q'
3000
15°
20°
25°
85°
80°
75°
70°

Fig. 1.

presented as a series of profiles across the trench. The sounding equipment used consists of an EDO echo sounder and transducer and a variable-speed, precision-powered, correlation recorder developed at the Woods Hole Oceanographic Institution. The records are produced on Alfax type A, 19 in. wide, damp chemical paper. Instrumentation is described in detail by KNOTT and HERSEY (1956).

Because no modern navigational aids such as Loran or other radio-time location systems are available off the western coast of South America, navigational controls used by the *Atlantis* depended upon various types of astronomic fixes, occasional land bearings, and dead reckoning. Almost continuously overcast weather made star fixes rare, and strong surface currents occasionally caused the ship to be set in unpredictable ways. The ship's pitometer log, designed to register distance travelled through water and the continuous course recorder which is coupled with the gyrocompass and plots changes in the ship's heading against time, were especially useful in navigation.

Particular care was taken to plot the ship's track as accurately as possible, especially where bottom profiles were to be constructed. Inaccuracies in plotting distance could cause distortion of slopes shown in profiles, particularly in areas of much relief. It was found after a number of comparisons that distance travelled between known positions (such as those determined by land bearings when the ship was near the coast) was consistently about 1·1 times that registered by the pitometer log. This factor was used generally between dead-reckoning positions. Each track has also been adjusted as well as possible for current set.

Inasmuch as some profiles can be constructed more accurately than others, the type of positional control is indicated along each leg of cruise track. Five types of fixes are differentiated on the cruise plot (Fig. 1) and on each of the *Atlantis* profiles. In decreasing order of reliability these are : (1) Land-bearing fixes ; (2) Star fixes ; (3) Local apparent noon sun lines, abbreviated L.A.N. ; (4) Sun lines ; and (5) Dead-reckoning positions.

Because some navigational uncertainty could not be eliminated, particularly at deep coring stations, profiles as drawn show breaks of an arbitrary but consistent width at the station. Breaks near the westerly end of profile NN′ (Fig. 5) result, however, from obscurities in the echogram which could not be resolved and not from stops at stations. It will be noted that sometimes the ship appeared to drift back on its track. At other times the ship drifted ahead (see Station 76, Profile QQ′, Fig. 5). Usually this backward or forward drift at stations had a sidewise component. Therefore, those profiles along which there are coring stations should properly be considered as a series of short, broken profiles lying not entirely in a straight line.

All depths given in the text and figures are based on a velocity of sound in water of 4800 ft/sec. To obtain a closer approximation of true depths at specific locations, corrections based on the average sound velocity in the water from surface to bottom must be applied. MATTHEWS (1939) has published tables of such corrections for all ocean areas. These corrections cannot be assumed to be absolutely accurate, but will generally give more nearly true soundings than uncorrected values, particularly in very deep water where the positive correction becomes in the order of 4 per cent. For example, using MATTHEWS' tables to correct the deepest *Atlantis* sounding which was 4180 fathoms (7645 m), a corrected value of 4360 fathoms (7975 m) is obtained. Corrections based on MATTHEWS' tables have been applied to Profile

MM′ (Fig. 5). Here the exaggerated profile consists of two lines ; the upper is the profile interpreted from the echogram, while the lower is the corrected profile. In deeper parts of the trench corrections are considerable.

Unfortunately echo sounders record the closest bottom first, whether that bottom is in front of, behind, or to the side of the vessel. In some areas of rough bottom several echoes are recorded at different depths for the same position of the ship. The problem of deciding what the true depth is and how to correct bottom slope can be somewhat resolved either analytically or graphically. An excellent treatment of analytical slope corrections and the distortion of topographic shapes produced by the echo sounder was given by DE VANSSAY DE BLAVOUS (1930 ; 1933). His work is the more remarkable in that it was written in the early days of echo sounding with equipment in mind that would give only spot soundings rather than a continuous record of soundings and would time only the first echo arrival rather than resolve multiple echo surfaces. However, his analyses can well be extended to apply to records from modern high-resolution echo sounders. The usual method for graphical slope corrections, swinging arcs with the apparent soundings as radii and fitting a curve tangent to these to represent the true bottom surface, has been described by MURRAY (1941). Slope corrections were made by the graphical method to part of profile MM′ landward of the trench bottom and the comparison between apparent bottom type and corrected bottom shape may be seen in Fig. 2. When topography is rough, as was usual on the western or seaward side of the trench, slope corrections are too time-consuming and about all one can do is to plot the highest and lowest points of the features shown on echograms and estimate slopes in between. For

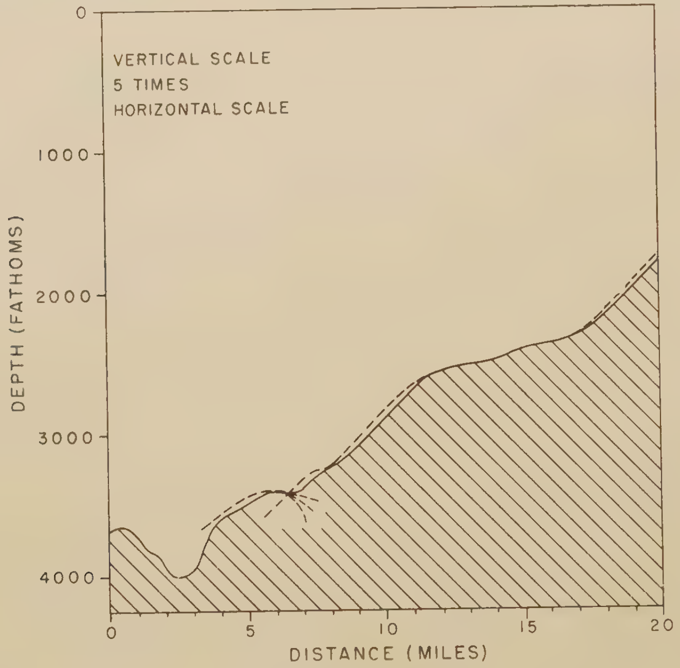

Fig. 2. Comparison between recorded depth (dotted line) and adjusted depth (solid line) for part of Profile MM′.

rigorous application of slope corrections, the sounding profile must be normal to the contour lines and it must be assumed that the echo path from ship to bottom is normal to the tangent of the bottom surface at the point of reflection. Except for the example cited, slope corrections were omitted or only estimated in preparing these profiles.

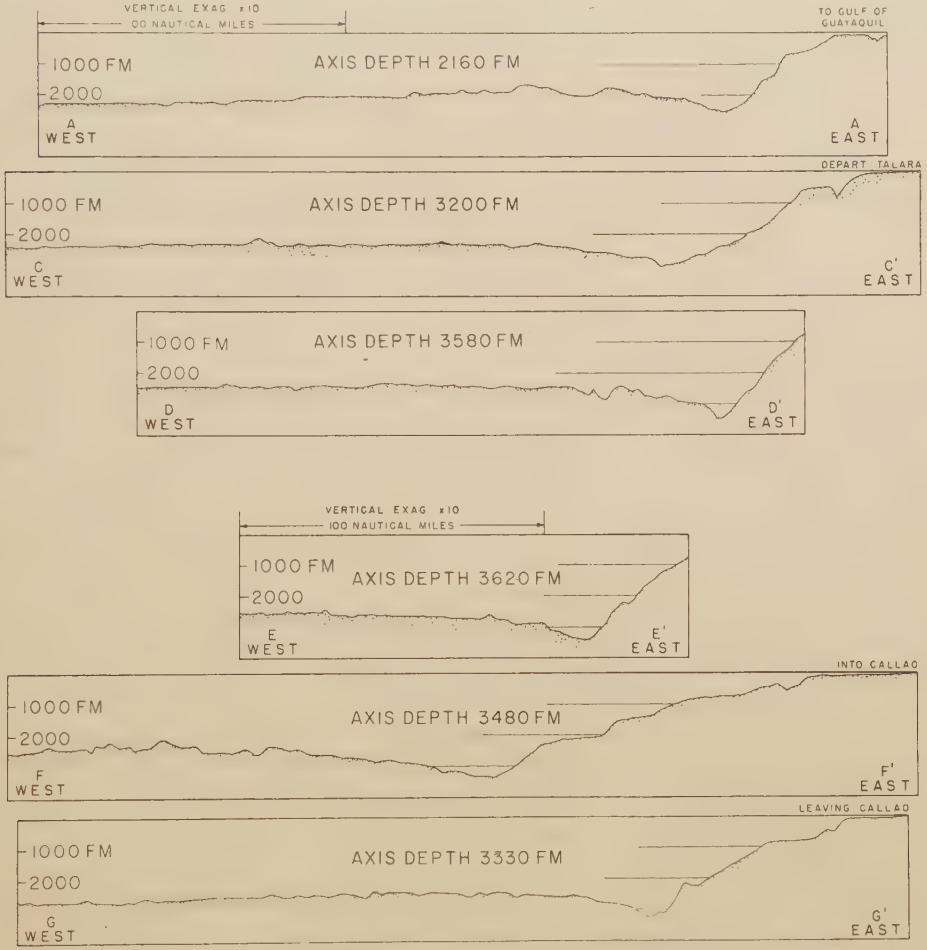

Fig. 3. "Shellback" profiles between Talara and Callao, Peru (AA′ to GG′).

DESCRIPTION

Each *Atlantis* traverse more or less normal to the coast, crossed a trench and although there were gaps up to 120 miles wide between some traverses, it is probable that the Peru–Chile Trench is continuous between northern Peru and north central Chile. Shumway (1957) reports the trench as far north as Ecuador, between Carnegie Ridge and the South American continent, and this trench is contoured on the Geologic Map of South America (Stose, 1950) to 36°S lat. almost to Conception, Chile.

The deepest uncorrected echo sounding obtained by the *Atlantis* (4180 fathoms [7645 m]) was located about 40 miles west of Antofagasta, Chile, on Profile PP′

(Fig. 5). The trench becomes shallower to the north and is only 2000 fathoms (4750 m) deep off Talara, Peru (Profile AA′, Fig. 3). The 3000 fathom contour (5500 m) is not continuous for the full length of the trench, but encloses two narrow strips with a somewhat shallower " saddle " between them. The *Atlantis* crossed this " saddle " at 15·4°S, 76·3°W (Profile JJ′, Fig. 4) obtaining a depth of approximately 2600 fathoms (4750 m), which even here is almost 900 fathoms (1645 m) deeper than the sea floor on the seaward side of the trench.

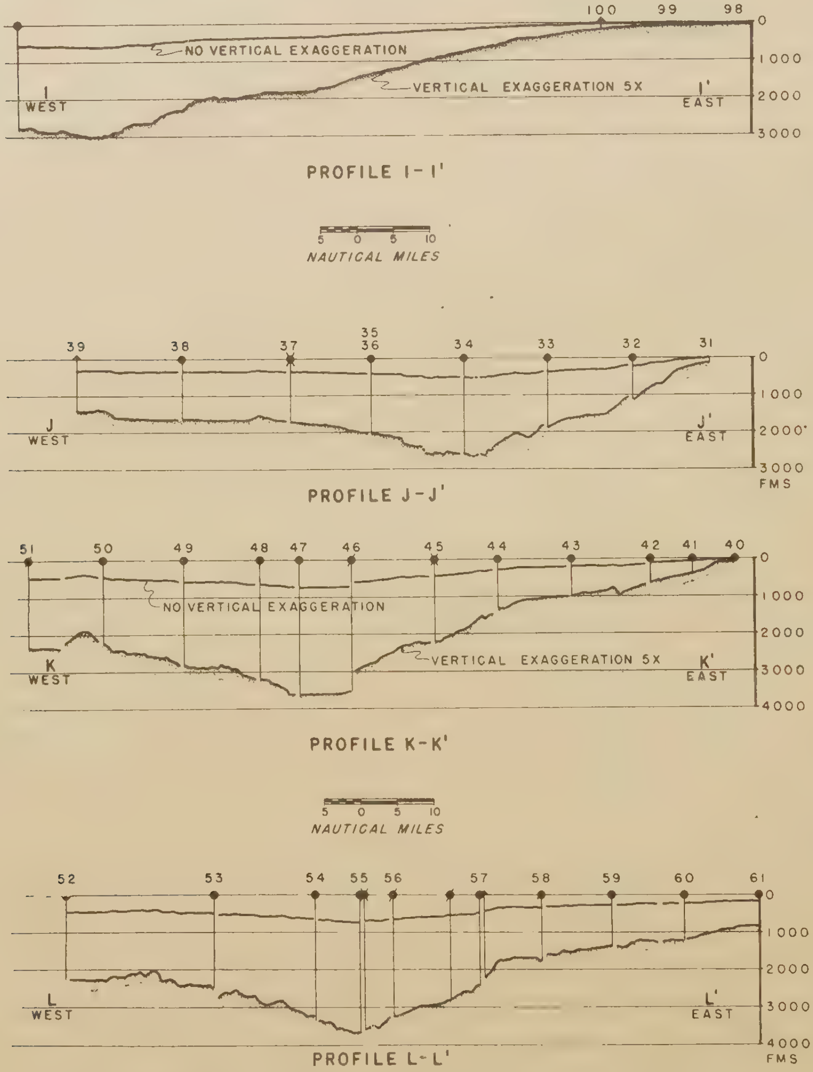

Fig. 4. *Atlantis* profiles between Chincha Islands, Peru and Punta Madrid, Chile (II′ to LL′).

Cross-sections of bottom topography across the Peru–Chile Trench may be classed as three general types. In the first, along the north and central Peruvian coast from Talara to the Chincha Islands (Profiles AA′ through II′), the relief is not great and the trench appears broad and only gently basined. It should be noted that the northern sections shown in Fig. 3 (Profiles AA′ through GG′) are “ Shellback ” profiles and have a vertical exaggeration of ten times the horizontal scale and therefore the cross-sections of the trench appear somewhat sharper than they do at five to one exaggeration used in Figs. 4 and 5. In the second category are cross-sections with smooth, flattish bottoms (Fig. 6) located in the bend of the South American coast off southern Peru and northern Chile (Profiles KK′ and LL′). Unfortunately the profiles are so reduced in scale that many of these smooth bottoms do not show, but they are strikingly apparent on the echograms. In the third category are cross-sections with narrower, sharper axes and pronounced bottom roughness. They are the southernmost profiles MM′, PP′, QQ′ and JJ′.

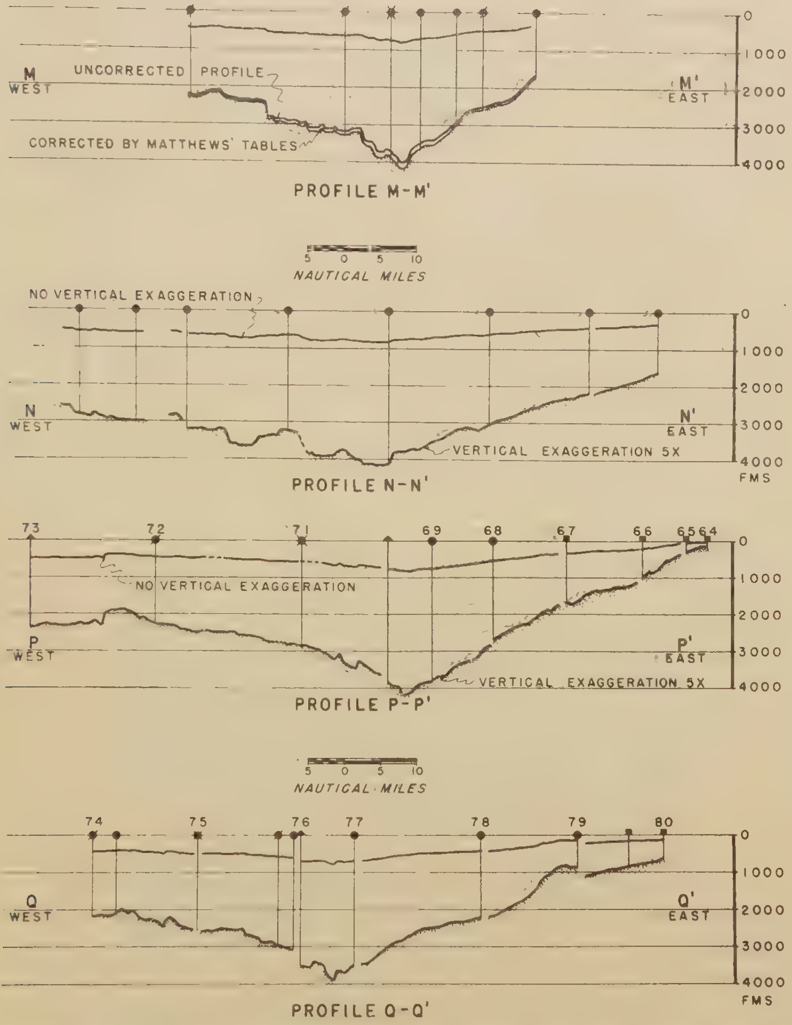

Fig. 5. *Atlantis* profiles between Punta Guanillo and Punta Posallaves, Chile (MM′ to QQ′).

Generally the roughest terrain is found immediately seaward of the trench axis. This is particularly noticeable in profiles off southern Peru and northern Chile.

More intense tectonic activity seaward of the axis may have produced this effect, but it seems more likely that heavier sedimentation on the landward side has subdued equally rough topography. Indeed, occasional strong features do appear to protrude through the sediment blanket, or at least interrupt the smoother profile attributed to the sedimentary blanket (see Profiles GG′, JJ′ and LL′). Notches near the landward ends of Profiles CC′ and KK′ are interpreted as more or less oblique sections of small canyons crossing the continental terrace. Occasional scarps such as those found in Profile MM′ (Fig. 5) seaward of the trench axis have up to 2400 feet (730 m) of relief and attain a slope angle approaching 45°.

CANYONS

There are two general areas of canyons and gullies along the Peruvian coast. Ones lies between the Peru-Chile boundary on the south (about 18° 20′S lat.) and Paracas Peninsula at about 14°S on the north (see canyon and gully notation in Fig. 1). The second area lies along the coast of northern Peru between Cabo Illesca (6°S lat.) on the south and the Gulf of Guayaquil on the north.

The *Atlantis* crossed what appears to be the most significant canyon in the southerly area at 16° 49′S lat., 73° 32′W long. (about 30 miles south south-westward of Pescadores Point, Peru) on her southward voyage (Fig. 7) and attempted to locate the shoreward end of this canyon on the homeward leg of the cruise. A canyon was crossed 20 miles northeast of that position at 16° 35′S, 73° 20′W. Although it cannot be stated definitely that this was the same canyon, an axial line drawn between both positions does run perpendicular to the trend of the continental slope.

If these two profiles do represent different sections of one single canyon, its size is comparable to those on the continental slope of the eastern United States (e.g. Oceanographer or Lydonia Canyon off Georges Bank). Echograms of the seaward traverse made on the southward leg show 2100–2400 ft (640–730 m) of relief, with a rim-to-rim width of 3¼ miles and a bottom width of 1½ miles (Fig. 7). Echograms of the landward crossing made on the homeward leg of the cruise show a maximum relief of 2750 ft (840 m), with a rim-to-rim width of 4 miles and a bottom width of ½ mile.

Other small canyons and gullies occur along this part of the Peruvian coast. A shallower canyon (Fig. 8) was crossed 9 miles offshore from Pejehun Point, or about 20 miles south-eastward from the larger canyon discussed above. Here maximum relief is about 1100 ft (335 m) with a rim-to-rim distance of about 3¼ miles. Further investigation might show this to develop seaward into a somewhat larger canyon than is indicated from the single profile obtained by the *Atlantis*. About 10 miles seaward of Cape Picata, 60 miles north-westward from the Peru-Chile border, is a series of gullies (Fig. 9) whose profiles have a vertical depth range of approximately 600 ft (180 m). Some of these gullies seem to be a seaward extension of sub-aerial drainage lines. In several other locations along the coast between Cape Picata and Paracas Peninsula such gullies were observed, but their seaward development is not known.

Although a little attention has been given to the canyons and gullies of this area by submarine geologists (Hess and MacClintock, 1936 ; Shepard and Beard, 1938 ; Shepard, 1948), submarine cable companies have been well aware of their existence since the 1870s. Sediment movements of one sort or another in these

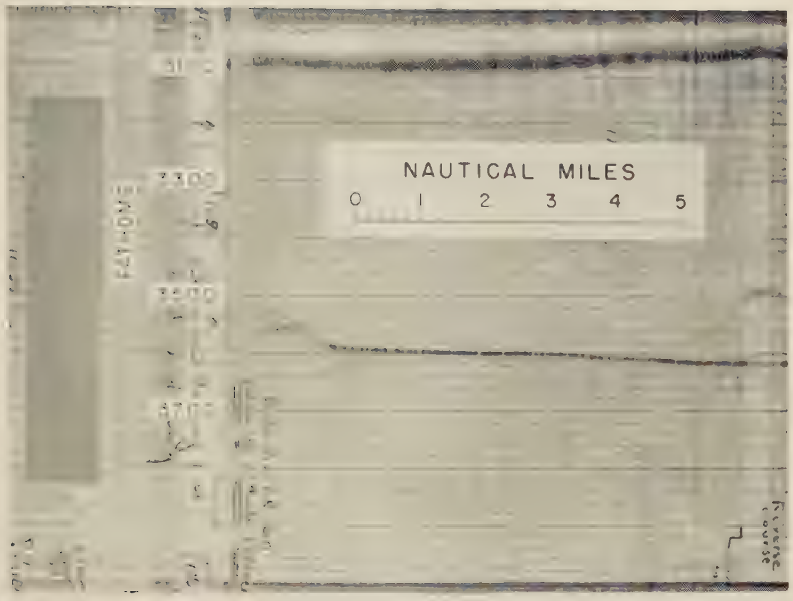

Fig. 6. Smooth bottom characteristics of some portions of Peru–Chile Trench.

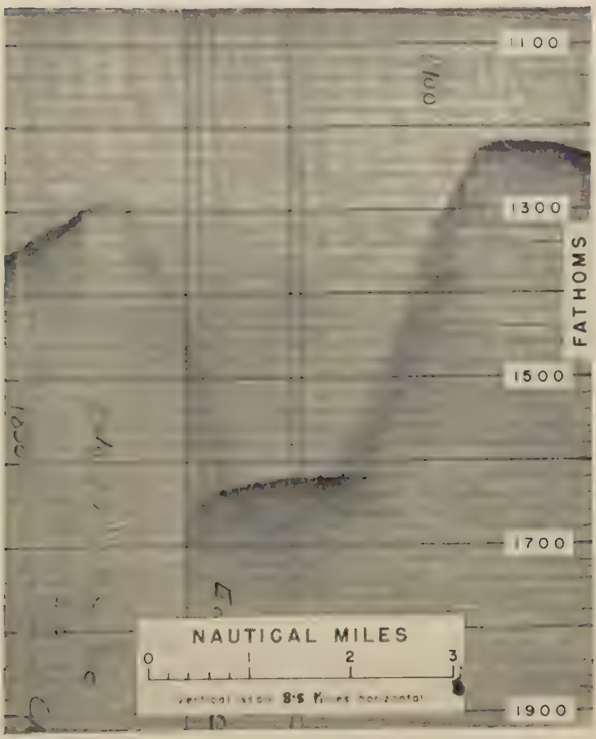

Fig. 7. Echogram of canyon 30 miles south south-west of Pescadores Point, Peru.

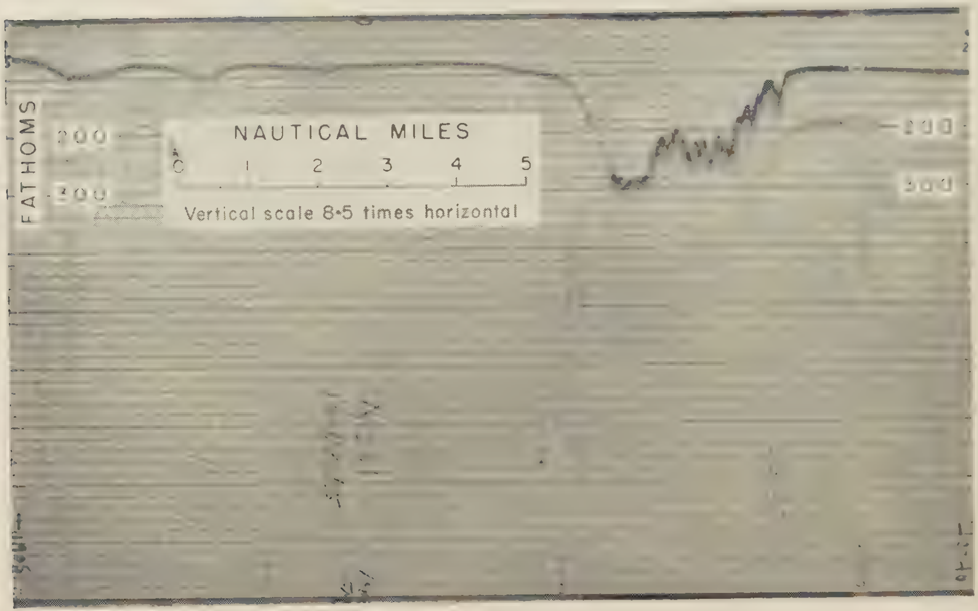

Fig. 8. Echogram of canyon located 9 miles south-west of Pejehun Point, Peru.

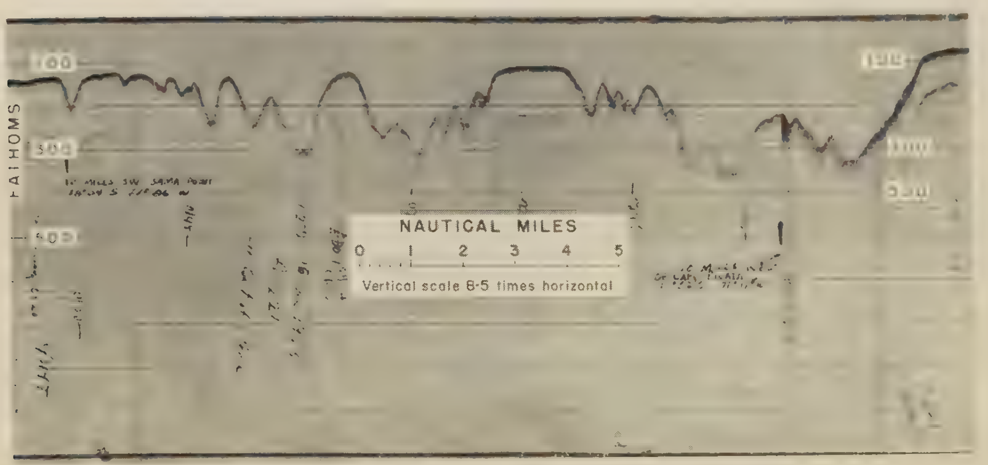

Fig. 9. Echogram of gullied area off Cape Picata, Peru.

gullies were responsible for frequent dislocation and rupture of the coastal cables, particularly off Mollendo (17°S, 72°W) and off Pescadores Point, until the early 1890s when the cables were moved shoreward of the gullyheads. This was the necessary remedy and the companies were no longer plagued by the frequent breaks (Benest, 1899).

There is little doubt that the larger canyon discussed above was well known to cable companies and probably much information concerning it remains in company files, but the present writers know of no detailed discussion of it in the literature.

Canyons and gullies in the northerly area were not investigated by *Atlantis* geologists but their existence was recorded by the echo sounder as the ship approached Talara, Peru, from the south. The whole section of echogram running due north from a point 15 miles off Punta Negra to the continental shelf just south of Punta Parinas is interrupted by gullies. These were of about the same dimensions as those found in the Cape Picata and Pejehun Point area (cf. Figs. 8 and 9). One of the largest, as might be expected, was just seaward of the mouth of the Rio Chira, north of Paita. Gullies and cable breaks in this general area are also discussed briefly by Benest.

DISCUSSION

The three general types of cross-sections across the trench, each restricted to its own particular area, may reflect variations in the sedimentary environment or possibly a difference in age between separate areas. Sharp, V-shaped profiles located off northern and north-central Chile suggest a young trench in which relatively little sedimentation has yet occurred. It does not follow, however, that the broader, shallower sections off northern Peru are older features partly filled by large accumulations of sediment. The broader sections may indicate the early stages of a trench which is evolving a greater relief. Consequently our data cannot properly support assumptions concerning the relative age of portions of the trench. It is possible that the trench is the same age throughout its length but that rates of sedimentation are different along different portions of the South American coast under study. There are many more rivers reaching the sea between Arica in northern Chile and Talara, Peru, than between Arica and Caldera on the desert coast which is crossed only by the Loa River. Summer rain falls at progressively lower altitudes on the mountain slopes from Chile to northern Peru until in northernmost Peru at Tumbez some rain falls on the coast (Murphy, 1936, p. 98). Where greater volumes of water reach the sea, more sediment may reach the Peruvian trench. Thus the more gently basined parts of the trench may reflect a greater supply of sediment from the continent than the sharp, V-shaped profiles.

Variations in resistance of rocks to coastal erosion might also influence sedimentation rates. Some of the volcanics are much more resistant to erosion than sedimentary strata. The volcanics near Antofagasta, Chile, and much of the adjacent coast offer more resistance to wear than do the softer sediments near Talara, Peru.

No differences in productivity of plants and animals in the waters off the coast are established which might explain lack of topography in one portion of the trench and not in another. As a matter of fact, Murphy (1936, pp. 263, 267) stresses the uniformity of the biota and the physical characteristics which control it along the coast between Antofagasta, Chile, and Paita, Peru.

The writers believe turbidity currents to be the principal agents of sedimentation in the smooth-bottomed portions of the Peru-Chile Trench. Canyons and gullies cutting the continental slope in this area offer numerous channels for localized turbidity flows which may have originated at the gully heads as a result of spring floods or seismic activity. BENEST (1899) observed that submarine cable breaks off Pescadores Point and Mollendo, mentioned previously, occurred during the season of heavy rains in the Arequipa district directly inland. He cites instances when the ends of broken cables were recovered entangled with boles and branches of olive trees found growing not closer than 80 miles from the coast. Intermittent streams carried flood debris to lagoons behind the beach, but as no debris was found on the seaward side of the beach BENEST suggested that underground rivers head under the lagoons and discharge large quantities of debris underwater at the gully heads. MILNE (1897) discussed seismic activity as a possible cause of " landslides " in the gullies. ERICSON, EWING and HEEZEN (1952) and NORTHRUP (1954) consider that the flat bottom of the Puerto Rico Trough resulted from deposition of large quantities of shallow-water sediments by turbidity currents. Graded bedding and high calcium carbonate content found in cores from the deep, flat floor of the trough support their view. MENARD (1955), BRUUN and KIILERICH (1955) and RAITT, FISHER and MASON (1955) suggest rapid deposition by turbidity currents to have been operative in Pacific trenches. There are many small gullies between Punta Negra and Talara, Peru, and yet the trench opposite those places is not flat bottom in the sense under discussion. The presence of canyons and gullies on slopes adjacent to trenches does not in itself mean that sufficient material will move down the canyons to form flat bottoms in the trenches. Why one area should have flattish bottoms and another not, is still not clear to us.

Smooth-bottom depressions in conjunction with side topography (Profile NN′) present an interesting puzzle. The flattish areas in question are on the seaward side of the main trench axis. Either they form the floor of side trenches subsidiary to the main trench or perhaps they form floor of submarine canyons entering the main trench from the seaward side. These two smooth-floored depressions are successively shoaler than the main trench axis, the first by approximately 150 fathoms and the second by 500 fathoms. A smooth-topped divide separates the two depressions. The profile shape of this portion of the trench is most suggestive of graben and horst topography.

The smooth top of the divide suggests that heavy deposition is not necessary for the formation of smooth bottoms and, indeed, when we devise mechanisms for depositing sediment in these basins we are faced with difficulty. If the sediment source is the South American continent, then the material must have been transported across the deeper, main trench. If the depressions are canyons and turbidity currents originating on the continental slope, the transporting agents, the currents had to flow up hill as much as 500 fathoms before depositing its load in the upper canyon. We are not accustomed to thinking that turbidity currents originate seaward from sites of deposition.

In conclusion the writers recognize that the bathymetric data from the *Atlantis* cruise have presented more problems than answers regarding the interpretation of the features of the Peru–Chile Trench. It is hoped that this paper may serve as a guide to further investigations in the area.

Acknowledgements—The writers wish to acknowledge the active cooperation of the governments of Chile and Peru. Lieut. José Carvajal Pareja of the Peruvian Navy shared in the work as long as he was on board. Mr. José Stuardo of the Chilean Biological Station assisted greatly by standing regular watches and working on all phases of the coring operation. The writers owe much to their colleagues and to the officers and crew of the *Atlantis.*

The cruise would not have been possible without the liberal support from the Socony-Vacuum Laboratories, the Woods Hole Oceanographic Institution, and the Office of Naval Research.

Five profiles off northern Peru (Fig. 3), constructed from data taken on the " Shellback " expedition of the Scripps Institution of Oceanography in 1952, were kindly put at the disposal of the writers by Mr. George Shumway of the Naval Electronics Laboratory at San Diego, California.

Woods Hole Oceanographic Institution, Woods Hole Massachusetts

Contribution No. 919 *from the Woods Hole Oceanographic Institution*

REFERENCES

Bencker H. (1930) The bathymetric soundings of the oceans. *Hydrogr. Rev.* 7, No. 2 ,64-97.

Benest H. (1899) Submarine gullies, river outlets, and fresh-water escapes beneath the sea level. *Geogr. J.* **14**, No. 4, 394–413.

Bruun A. Fr. and Kiilerich A. (1955) Characteristics of the water-masses of the Philippine, Kermadec and Tonga Trenches. *Papers in Marine Biology and Oceanography, Deep-Sea Res.* **3** (Suppl.), 418–425.

Ericson D. B., Ewing M. and Heezen B. C. (1952) Turbidity currents and sediments in the North Atlantic. *Bull. Amer. Ass. Pet. Geol.* **36**, No. 3, 489–511.

Fisher R. L. and Revelle R. (1955) The trenches of the Pacific. *Sci. Amer.* **193, No. 5,** 36–41.

Hess H. H. and MacClintock P. (1936) Submerged valleys on continental slopes and changes of sea level. *Science* **83** No. 2153, 332–334.

International Hydrographic Bureau (1936) *General Bathymetric Chart of the Oceans.* Information concerning the preparation of the Third Edition of Sheet A'_1 *Southern Part of the South Atlantic Ocean.* Special Publication No. 30, Part A'_1, Monaco.

Knott S. T. and Hersey J. B. (1956) Interpretation of high-resolution echo-sounding techniques and their use in bathymetry, marine geophysics, and biology. *Deep-Sea Res.* **4**, No. 1, 36–44.

Matthews D. J. (1939) Tables of the velocity of sound in pure water and sea water for use in echo-sounding and sound-ranging. *Brit. Admiralty Hydrogr. Dept.* Publ. H. D. 282.

Menard H. W. (1955) Deformation of the northeastern Pacific basin and the west coast of North America. *Bull. Geol. Soc. Amer.* **66**, No. 9, 1149–1198.

Milne J. (1897) Sub-oceanic changes. *Geogr. J.* **10**, No. 2, 129–146 ; **10**, No. 3, 259-289.

Murphy R. C. (1936) *Oceanic Birds of South America* Vol. I. The Macmillan Co., American Museum of Natural History, New York.

Murray H. W. (1941) Submarine mountains in the Gulf of Alaska. *Bull. Geol. Soc. Amer.* **52**, 333–362.

Murray Sir J. (1899) Oceanography. *Geogr. J.* **14**, No. 4, 426–441.

Murray Sir J. and Hjort J. (1912) *The Depths of the Ocean.* Macmillian, London.

Northrup J. (1954) Bathymetry of the Puerto Rico Trench. *Trans. Amer. Geophys. Union.* **35**, No. 2, 221–225.

Raitt R. W., Fisher R. L. and Mason R. G. (1955) Tonga Trench. *Spec. Publ. Geol. Soc. Amer.* **62** (Crust of the Earth) 237–254.

Shepard F. P. (1948) *Submarine Geology.* Harper and Brothers, New York.

Shepard F. P. and Beard C. N. (1938) Submarine canyons : distribution and longitudinal profiles. *Geogr. Rev.* **28**, No. 3, 439–451.

SCHWEIGGER E. (1947), La fosa de Lima. *Bol. Soc. Geol. Perú* **20**, 35–50.
SHUMWAY G. (1957) Carnegie Ridge bathymetry. *Deep-Sea Res.* **4**, 250–253.
STOSE G. W. (1950) Geologic map of South America. *Geol. Soc. Amer.* in co-operation with *Amer. Geogr. Soc.* and *U.S. Geol. Surv.*
THOMPSON Sir C. W. and MURRAY Sir J. (1895) Report on the scientific results of the voyage of *H.M.S. Challenger* during the years 1872–76: A summary of the scientific results, first part. London.
DE VANSSAY DE BLAVOUS P. (1930, 1933) Slope corrections for echo soundings. *Hydrogr. Rev.* **7**, No. 2, 50–63 ; **10**, No. 1, 41–45.

Printed in Great Britain by The Salisbury Press Ltd., Publicity House, Wilton Road, Salisbury, Wilts. (6899)

Contribution No. 921

EXCERPTUM

Acta Physiologica Scandinavica 1957. Vol. 41. Fasc. 4.

From the Woods Hole Oceanographic Institution and the Institute of
Zoophysiology, University of Oslo.

Oxygen Dissociation Curves in Fish Blood.[1]

By

P. F. SCHOLANDER.

Received 24 August 1957.

---

[1] Contribution No. 921 from the Woods Hole Oceanographic Institution. This investigation was supported by a grant from the National Science Foundation.

Fish blood shows certain peculiarities in the binding of oxygen which have not so far been described for mammalian blood. When CO_2 or acid is added to the blood, part of the hemoglobin may become completely unable to combine with oxygen, even at very high pressure, and in some species one obtains dissociation curves which are undulatory. We shall describe below the blood of a fish which displays both of these features, and we shall discuss briefly the binding of oxygen by hemoglobin in the light of some recently published high pressure dissociation curves.

It was discovered by ROOT (1931) that when the blood of tautog or toadfish was acidified with CO_2 or lactic acid it produced not simply a Bohr effect, *i. e.*, a lowering of the oxygen affinity, with full oxygenation still obtainable at high enough pressure but it apparently suffered a loss of oxygen capacity. The highest oxygen pressure used by ROOT was only that of air, but it was shown by GREEN and ROOT (1933) and by ROOT and IRVING (1941) that part of the hemoglobin remained unoxygenated even at near one atmosphere's p_{O_2}. It has long been believed that this "Root effect" is the direct chemical cause of the oxygen secretion in the swimbladder of fishes. This could be true, however, only if the dissociation pressure of oxygen produced by adding CO_2 or acid were greater than the oxygen pressure known to exist in the swimbladder of the fish. This prompted an investigation of the oxygen dissociation in the blood of a dozen deep sea fishes at various acidities and at p_{O_2} ranging from 0.2 to 140 atmospheres (SCHOLANDER and VAN DAM 1954). The result was that in some species the Root effect persisted at very high pressures, but in others full saturation was reached at a pressure much lower than that against which the fishes are known to secrete, which casts serious doubt on the Root effect as the cause of high pressure oxygen secretion.

Another interesting feature found in the whole blood of some fishes is that the oxygen dissociation curve at slight acidity or CO_2 tension is undulatory, with two portions concave to the abscissa. Such curves have been described for the toadfish (GREEN and ROOT 1933) and for tautog (ROOT and IRVING 1941). Undulating curves are striking in the blood of certain mollusks and crustaceans containing hemocyanin (REDFIELD and INGALLS 1933).

In our studies on deep sea marine fishes we came across one single species, the common silver hake (*Merluccius bilineatus*) which at pH 6 showed, like so many other species, a pronounced Root effect, *i. e.*, the dissociation curve remained horizontal from 20 to 140 atmospheres' p_{O_2} at a saturation of 40 %. At a pH of about 7, however, the curve was conspicuously diphasic, with a plateau at 55—60 % saturation when the p_{O_2} was between 20 and 40 atmospheres. Full saturation was reached at near 100 atmospheres. With less acidity the plateau gradually vanished (Fig. 1).

It is of interest that among 30—40 high pressure curves which showed a Root effect there is no apparent tendency for the inactivation plateaus to cluster around even quarters, *i. e.*, at 25, 50 and 75 % saturation. The curves may level off at any saturation from 30 % and up to 100 %. This situation cannot readily be derived from either the intermediate compound theory of ADAIR (1925), or from the heme-heme interaction theory of PAULING (1935), if we assume that our fish blood has four hemes per molecule of hemoglobin, such as indicated by the work of SVEDBERG and HEDENIUS (1934).

The multiple component theory was evolved by REDFIELD and INGALLS (1933), who showed that it applies very accurately to the oxygen combination with hemocyanin. The theory postulates a heterogeneous population of oxygen-combining molecules in the same blood, each component obeying the Hill equation. If each hemoglobin molecule contains four hemes, n may be taken

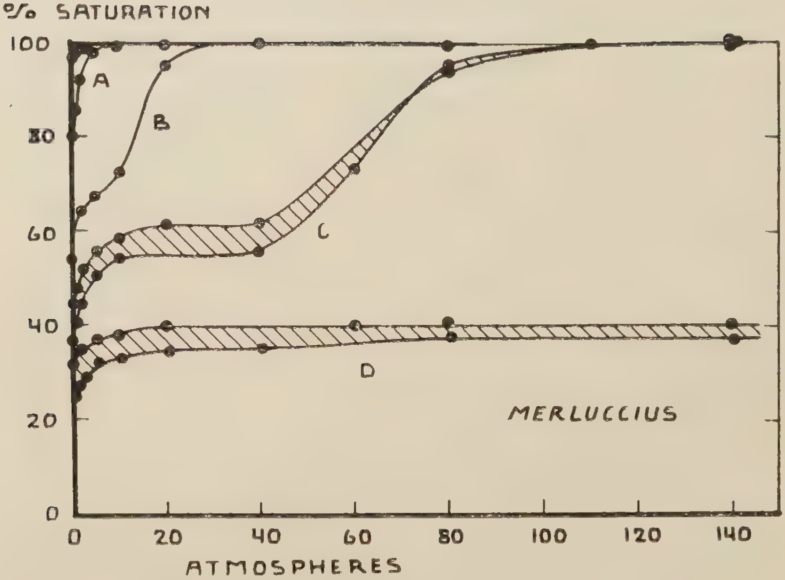

Fig. 1. Oxygen dissociation curves for the blood of silver hake (*Merluccius bilineatus*). Blood acidified with lactic acid. A corresponds to pH 7.7 C to 7.0, and D to 5.9.

as 1, 2, 3 or 4, K may be any number, and the fraction of each component (a) may be any number from 0 to 1. This of course represents a very considerable freedom in the choice of constants, and various authors have been able to construct curves which fit blood data from fish very closely, whether they are simple hyperbolic curves, sigmoid curves, curves with a Root effect, or undulating curves. Usually one need only postulate a mixture of two different components in order to produce a good fit to any given curve.

According to this theory each component would also produce plateaus determined by the number of inactivated hemes in the molecule, and in order to get a plateau in a four heme compound between even quarters at least two components would have to be present, each with a plateau at a different quarter, *e. g.*, one at 25 %, the other at 50 % saturation. This, again, means that any curve with a plateau between even quarters must be treated as the sum of two curves and cannot physically be regarded as a simple hyperbolic or exponential curve asymptotic to this plateau.

Our high pressure curves demonstrate clearly that one cannot estimate the fraction of hemoglobin inactivation from a pressure range of only 0—1 atmosphere. When dealing with a Root effect there is always (in our material) a substantial rise beyond a p_{O_2} of 1 atmosphere. The p_{O_2} must usually be at least 10—20 atmospheres before the final plateau is reached (cp. Fig. 1 and SCHOLANDER and VAN DAM 1954, Figs. 3—4). The consequence of this may be seen from the following example. Root and IRVING (1941) published a series of careful analytical data on the effect of CO_2 on the oxygen dissociation curve of tautog. At 90 mm CO_2 pressure there was seemingly a clear Root effect with a plateau estimated at 55 % saturation, *i. e.*, 45 % of the hemoglobin was inactivated. The highest oxygen tension used was a little less than 1 atmosphere. The data could be closely fitted to a hyperbola with an asymptote at 55 % saturation. Our tautog data (l. c., 1954, Fig. 3) show, however, that there is no such oxygen asymptote at this CO_2 pressure, but that the curve continues to rise and reaches some 90 % saturation at 40 atmospheres' oxygen pressure. For reasons stated above, a single hyperbola with an asymptote at 55 % saturation cannot be derived from the multiple component theory when dealing with 4 hemes. The found hyperbola must therefore be regarded as the sum of two curves, and one must postulate further that one or two more curves must be added onto these in order to account for the slow rise above 40 atmospheres. By suitable choice of constants this can probably be done, but such mathematical transactions can hardly disclose much of the underlying physical reality.

The slope from 0 to 1 atmosphere's p_{O_2}, both for this curve and for many other carefully determined curves showing a Root effect, is already as steep as possible, namely, corresponding to an n of one, and it is therefore impossible to describe in one equation the full extent of such a curve. It could possibly be approximated by choosing n as a small fraction of one, but this again would hardly have any physical meaning. In fact, when n is determined from our curves by plotting log HbO_2/Hb versus log p_{O_2} it starts as a small fraction of one and increases to 2 or more as saturation is approached.

The data in Fig. 1, as well as our other high pressure observations, were obtained spectrophotometrically on whole blood and often under field conditions, and we cannot claim for them the high standard of accuracy applicable to much previous data obtained in the low pressure range by gasometric methods, but we believe the accuracy is good enough to illustrate the main points we have made. In all events, it seems justified to say that present theories of oxygen dissociation do not apply well to fish blood. BLACK and IRVING (1938) and ROOT, IRVING and BLACK (1939) showed the rather disturbing fact that both the Bohr and the Root effects in the blood of some fishes are greatly diminished or abolished when the blood is hemolyzed, *i. e.*, one cannot from the behavior of a solution of fish hemoglobin predict the dissociation curve of whole blood. The difficulty arises that one does not know to what extent conditions in the plasma, such as acidity and other factors, reflect the conditions within the cells.

It may be concluded that the current theories, designed to explain the oxygen combination with hemoglobin in the relatively simple system of mammalian blood, present considerable difficulties when applied to fish blood, especially when the pressure range is extended beyond that of 1 atmosphere's p_{O_2}. These theories also seem unable to account for the action of acid and CO_2 on fish blood.

Summary.

The oxygen dissociation curve of the common silver hake (*Merluccius bilineatus*) is described at pH 5.9—7.7 and p_{O_2} 0.2—140 atmospheres. At pH 7 the curve has a conspicuous plateau before it reaches full saturation at about 100 atmospheres. It is pointed out that high pressure curves from fish in general cannot readily be described or interpreted in terms of current theories evolved for mammalian blood.

Acknowledgment.

The present data were obtained on a deep sea cruise conducted by Mr. W. C. SCHROEDER from the Woods Hole Oceanographic Institution. I am indebted to Dr. L. VAN DAM for help in securing the data, which I have had the privilege of discussing with Dr. A. C. REDFIELD and Dr. F. J. W. ROUGHTON.

References.

ADAIR, G. S., J. biol. Chem. 1925. *63*. 529.
BLACK, E. C. and L. IRVING, J. cell. comp. Physiol. 1938. *12*. 255.
GREEN, A. A. and R. W. ROOT, Biol. Bull. 1933. *64*. 383.
PAULING, L., Proc. nat. Acad. Sci. (Wash.) 1935. *21*. 186.
REDFIELD, A. C. and E. N. INGALLS, J. cell. comp. Physiol. 1933. *3*. 169.
ROOT, R. W., Biol. Bull. 1931. *61*. 427.
— and L. IRVING, Biol. Bull. 1941. *81*. 307.
— — and E. C. BLACK, J. cell. comp. Physiol. 1939. *13*. 303.
SCHOLANDER, P. F. and L. VAN DAM, Biol. Bull. 1954. *107*. 247.
SVEDBERG, T. and A. HEDENIUS, Biol. Bull. 1934. *66*. 191.

Stockholm 1958. Kungl. Boktr. P. A. Norstedt & Söner

Contribution No. 922

Reprinted from
BULLETIN OF MARINE SCIENCE
OF THE GULF AND CARIBBEAN
Vol. 7, No. 4, pp. 360-369
DECEMBER, 1957

PRELIMINARY ANALYSIS OF THE DISTRIBUTION OF WHITE MARLIN, *MAKAIRA ALBIDA* (POEY), IN THE GULF OF MEXICO[1]

ROBERT H. GIBBS, JR.
Woods Hole Oceanographic Institution, Woods Hole, Massachusetts

ABSTRACT

Records of white marlin, *Makaira albida* (Poey), from long-line stations of the Fish and Wildlife Service M/V OREGON indicate a concentration of this species in the Mississippi delta region in midsummer, followed by a gradual dispersal to other parts of the Gulf of Mexico. In April and May the marlin again move northward. The northward distribution and migration appears limited by the 75° surface isotherm. There is no evidence of correlation of either presence or abundance with depth of water. Some distributional similarities between white marlin and yellowfin tuna are noted, and a few pertinent literature references mentioned. The need for further study is emphasized.

INTRODUCTION

The white marlin, *Makaira albida,* is a valued game fish in the western North Atlantic, yet in spite of the avidity of sport fishermen for catching this fish, little is known of its distribution or habits. It is well known that this species apparently congregates in large numbers in the summer off the middle Atlantic states, and that Ocean City, Maryland, has been the principal area from which anglers sought the marlin in this region. Certain areas off southeast Florida, the Bahamas and Cuba appear to harbor white marlin at certain times, but not in the concentration boasted by Ocean City. The fish is sold on the market in Cuba and other West Indian Islands. In the Gulf of Mexico, almost nothing is known.

Beginning in 1954, the U. S. Fish and Wildlife Service vessel OREGON has made a series of cruises, using Japanese long-line gear, to explore the potential production of pelagic fishes, particularly tunas, in the Gulf of Mexico and adjacent waters (Bullis, 1955). Careful records were kept at each station of the entire catch. These records have been kindly made available to me by Harvey R. Bullis. The present analysis is based entirely on these records from the M/V OREGON.

The conclusions or deductions presented here are highly tentative. The study of pelagic fishes is in its infancy; data are difficult to come by and are not usually as complete as would be desired. The major impediment in this study has been the lack of adequate coverage, either in time or in area. This is inherent when the accumulation of data is dependent upon an organization, in this case the Fisheries Exploration and Gear Research Section of the U. S. Fish and Wildlife Service, which must be primarily motivated by immediate commercial interests rather than the quest for more abstract scientific information, the value of which is not always readily apparent. Other organizations are presently actively engaged in the study of marlin distribution, particularly the Marine Laboratory of the University of Miami, the American Museum of Natural History, and the Woods Hole Oceanographic Institution. It is hoped that the analysis here will stimulate others to gather similar data in order to fill in gaps and present a more satisfactory picture. Meanwhile, the conclusions which follow may serve as a guide, to stand or fall on the basis of future evidence.

---

[1] Contribution No. 922 from the Woods Hole Oceanographic Institution. Work done under a grant from the National Science Foundation.

Distribution and Movements

The stations at which white marlin were caught by the OREGON are plotted by months in Figure 1. While lack of coverage in vital areas obscures the over-all picture, some conjecture is possible. For all practical purposes, the collections in February and October are too few to contribute anything. Of the others, April and September do not sample the region of the Mississippi Delta (off Louisiana), and July and August do not sample any region except the Delta. In the following discussion, the "Delta region" will refer to the rectangle between about 26°30′ N lat. and the northern Gulf coast, and between 87° and 90° W long.

The weights of the marlin caught were predominantly between 30 and 60 pounds, the range being from 19 to 110 pounds. Using average weights per station, 73 stations fall between 30 and 60 pounds, 2 less than 30, 8 more than 60. The following discussion is therefore based on a rather uniform size group.

Bullis (1955) has noted that yellowfin tuna (*Thunnus albacares*) are apparently absent from the Delta region in March. This seems to be true also for white marlin, as none of four stations produced these fish in that month, which would be most unusual for any other time. In March, however, marlin have been taken in the southwest Gulf and the Bay of Campeche. Beginning in April there is indicated a gradual movement out of the southwest Gulf and toward the Delta region. Despite fairly active collecting in May, no white marlin were taken in the Gulf of Campeche, but each of two stations in the Delta produced them. June stations, despite inadequate coverage, show a

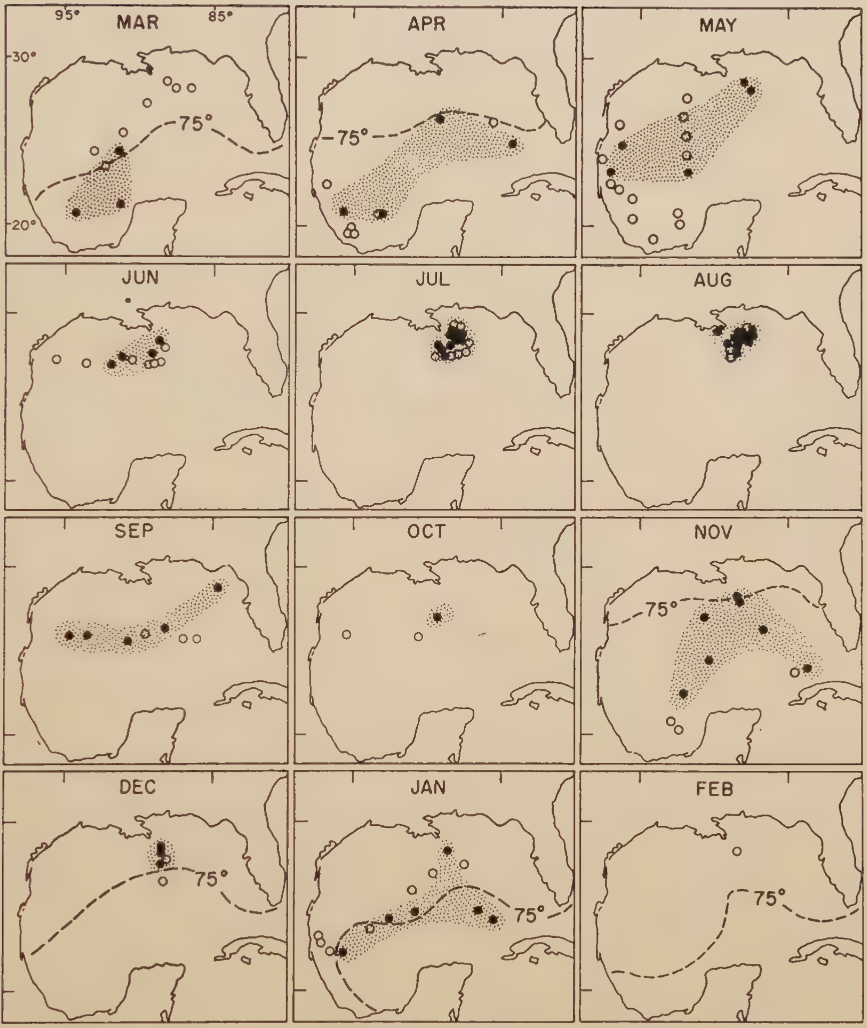
95°
MAR
85°
30°
20°
75°
APR
75°
MAY
JUN
JUL
AUG
SEP
OCT
NOV
75°
DEC
75°
JAN
75°
FEB
75°

FIGURE 1. Distribution of white marlin in the Gulf of Mexico by months. Black dots = successful stations. Open circles = unsuccessful stations. General range, as indicated by the data, shown by cross-hatched area. 75-degree isotherm from Fuglister, 1947.

decided grouping of marlin at the Delta, with some still slightly westward from it. In July and August, the concentration in the Delta is extremely heavy. As will be shown later, success is the rule in these two months both in number of stations taking marlin and in number of marlin taken per set. Thus the lack of coverage in other regions does not completely offset the fact that the fish do concentrate in the Delta at this time. This compares to the rather similar concentration off Ocean City, Maryland, also in July and August. Beginning in September, the fish again become dispersed more or less throughout the Gulf.

RELATION TO TEMPERATURE

Some of the above observations may be roughly correlated with temperature distribution. Surface temperatures were recorded at almost all stations. Although the long-line gear usually was fished at 10-20 fathoms, the temperature at the lower depth is probably little different than that at the surface. Even so, the surface temperature may be construed as an index.

On the maps (Figure 1), the approximate contour line for 75° surface temperature is indicated (from Fuglister, 1947). From May through October, the average is nowhere less than 75° in the Gulf, but beginning in November, the 75° contour gradually recedes southward and in March again advances northward. It is noteworthy that almost none of the successful marlin stations have been in water far north of this average 75° contour. The only seemingly anomalous record is one in January in the Delta. Apparently the Delta region has some sort of attraction, generally speaking. Had this anomaly occurred anywhere else, there would have been need for extensive explanation. In the Delta, it is not surprising.

Figure 2 tends to uphold the presumed correlation with the 75° contour. From June through November, all stations were made in water at least 75° at the surface. In the other months, when stations were made in colder water, the lack of success below 74° or 75° is notable. The catch in December at 71° is the anomaly discussed above.

RELATION TO SEASON

In this section, the catch, as judged by number of stations at which at least one marlin was caught and by average number of marlin caught at each station, is analyzed (Table 1).

From April to August in the Delta region, with one exception, half or more of the stations produced marlin. Because of the paucity of stations in April and May, little can be said of these months except that marlin are present. The poor success in June indicates that the concentration is just beginning. In July and particularly in August,

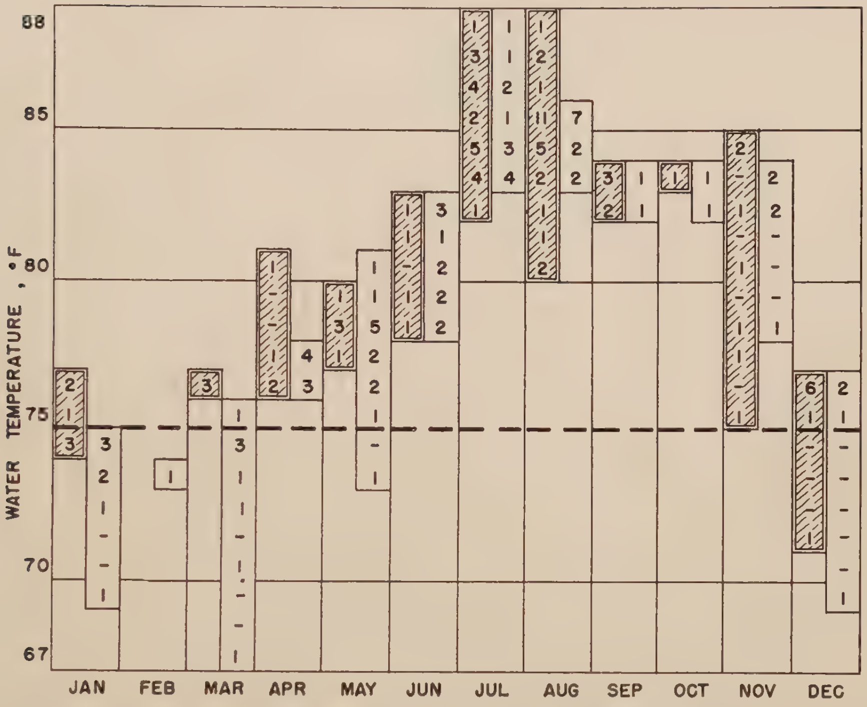

FIGURE 2. Surface temperatures of stations where white marlin were caught (cross-hatched bars) and of unsuccessful stations. Numbers in the bars indicate number of sets at each temperature.

success in both number of stations and average number of fish per station is high. This supports the contention that this is an actual concentration of fish, and is not due merely to the lack of fishing in other areas at the same time. From September through January, the few samples indicate the presence of marlin, but little else. The notable lack of success in February and, especially, March, has already been interpreted as indicating a lack of marlin for a short period, perhaps due to low water temperatures, perhaps to spawning elsewhere.

In areas outside the Delta, few conclusions can be drawn. The average number of fish per successful station is never great. The large number of successful stations in September, all in the northern Gulf, may be sampling fish which are moving away from the Delta, but have not yet dispersed completely. To some extent, success seems dependent upon water temperature, as noted previously. The drop in success in April and May is possibly due to the postulated movement toward the

TABLE 1

Successful and unsuccessful white marlin stations by months. S= successful. U = unsuccessful. Avg. fish = average number of marlin taken per successful set.

	Non-Delta					Delta				
	S	U	%S	No. Fish	Avg. Fish	S	U	%S	No. Fish	Fish Avg.
Jan.	5	5	50	6	1.2		2	33	2	2
Feb.	0	0	—	—	—	0	1	0	—	—
Mar.	3	4	43	7	2.3	0	4	0	—	—
Apr.	3	8	27	4	1.3	1	1	50	2	2
May	3	14	18	4	1.3	2	1	67	2	1
June	2	3	40	3	1.5	2	7	22	2	1
July	0	0	—	—	—	20	12	63	35	1.75
Aug.	0	0	—	—	—	24	11	69	102	4.3
Sept.	5	2	71	8	1.6	0	1	0	—	—
Oct.	0	2	0	—	—	1	0	100	3	3
Nov.	6	5	55	14	2.3	1	0	100	3	3
Dec.	0	1	0	—	—	1	2	33	1	1

Delta and away from the southwest Gulf, where quite a few stations were fished, but where success was poor.

RELATION TO DEPTH OF WATER

Table 2 shows the number of successful stations and the numbers of fish caught in relation to water depths. In the Delta, there are no stations over a bottom deeper than 1,700 fathoms. Here, above bottoms from 500 to 1,200 fathoms, successful stations are the majority. The greatest number of fish per set is over 1,000 fathoms of water. This extremely high average is principally due to three sets made at almost the same point (28° 47-50′ N, 87° 48-50′ W) on three consecutive days in August, on which a total of 32 fish were caught. If these are subtracted from the rest, an average catch of 1.8 results, which is actually slightly less than that for the adjacent months.

In the rest of the Gulf, no pattern is shown. Successful stations are scattered over depths of from 600 to 2,100 fathoms. Average catch is consistently somewhat less than at most stations in the Delta. Noteworthy are the catches over depths of more than 1,800 fathoms.

Since white marlin are probably independent of the bottom, these data are useful mainly in further pointing out the wide distribution of the species in the pelagic habitat. The summer congregation, which is over the continental slope, is believed to be a feeding congregation, not

TABLE 2

Successful and unsuccessful white marlin stations according to depth of water. See Table 1 for explanations. Asterisks indicate a station for which number of fish was not recorded.

Depth of Water	Non-Delta					Delta				
	S	U	% S	No. Fish	Avg. Fish	S	U	% S	No. Fish	Avg. Fish
< 100 fm	0	1	0	—	—	0	0	—	—	—
100	0	0	—	—	—	*1	0	100	?	?
200	0	0	—	—	—	0	0	—	—	—
300	0	0	—	—	—	0	1	0	—	—
400	0	1	0	—	—	0	2	0	—	—
500	0	1	0	—	—	3	2	60	10	3.3
600	3	3	50	4	1.3	5	3	63	6	1.2
700	1	2	33	2	2	8	5	62	18	2.25
800	0	2	0	—	—	4	0	100	10	2.25
900	1	1	50	5	5	11	3	79	31	2.8
1000	0	4	0	—	—	8	8	50	41	5.125
1100	2	3	40	3	1.5	4	2	67	9	2.25
1200	3	6	50	7	2.3	2	1	67	8	4
1300	1	3	33	1	1	*3	4	43	5	2.5
1400	0	0	—	—	—	2	4	50	3	1.3
1500	0	2	0	—	—	0	2	0	—	—
1600	1	2	33	1	1	0	2	0	—	—
1700	0	3	0	—	—	0	0	—	—	—
1800	3	2	60	6	2	0	0	—	—	—
1900	3	2	60	5	1.67	0	0	—	—	—
2000	4	3	57	5	1.25	0	0	—	—	—
2100	1	0	100	1	1	0	0	—	—	—
2200	0	1	0	—	—	0	0	—	—	—

a spawning one. Because of nutrients contributed by the Mississippi affluence, this is undoubtedly an area rich in small fish and squids, on which the marlin can feast.

The data also tend to support the reality of this presumed summer congregation in the absence of stations outside the Delta in that season. The number of successful stations is higher, and the average number of fish per station is also high.

Breaking the depth data into months (Table 3) shows no particular correlation of depth with season in regions outside the Delta, and only during the summer in the Delta area.

COMPARISON WITH YELLOWFIN TUNA

Since the primary purpose of the OREGON's long-lining activities was to catch yellowfin tuna, it is of interest to make some rough comparisons between that species and the white marlin. This information has been gleaned from the unpublished cruise reports distributed from

TABLE 3

Successful and unsuccessful white marlin stations by months and by depths. Figures without parentheses = number of marlin. Figures in parentheses = average number of marlin per set. The superscript ^{x} indicates that there were unsuccessful stations.

	Non-Delta				Delta			
	Depth Range				Depth Range			
	<600	600-1099	1100-1599	>1600	<600	600-1099	1100-1599	>1600
Jan.	—x	—	1	6(1.5)^x	—	—	2(2)^x	—
Feb.	—	—	—	—	—	—x	—	—
Mar.	—	—	3(3)	1(1)^x	—	—	—x	—
Apr.	—	1(1)^x	3(1.5)^x	—x	—	—	2(2)	—
May	—x	1(1)^x	—x	2(2)^x	—	1(1)	1(1)	—
June	—	3(3)^x	—	—	—	1(1)^x	—x	—
July	—	—	—	—	1(1)^x	26(1.6)^x	3(2.7)^x	—
Aug.	—	—	—	—	14(4.7)^x	72(4)^x	8(4)	—
Sept.	—	—	3(1.5)^x	5(1.7)	—	—	—	—
Oct.	—x	—	—	—	—	—	3(3)	—
Nov.	—	7(3.5)^x	2(2)^x	4(1.3)	—	3(3)	—x	—
Dec.	—	—	—	—	—	—	1(1)^x	—

Pascagoula, Mississippi. The writer has not gathered complete data on the distribution of yellowfin, but since the stations are the same ones that are plotted on the maps in Figure 1, some deductions may be made.

Table 4 lists the approximate average number of hooks set out for each fish caught by monthly periods. This, roughly, indicates the abundance of the tuna at these times; the smaller the number of hooks,

TABLE 4

Average number of hooks set for each yellowfin tuna caught by month and year. Where open blanks occur, the figure above is a combination for the two months.

	1954	1955	1956	Avg.	Total Sets
Jan.	—	75	258.6	166.8	13
Feb.	—	?	—	?	1
Mar.	—	?	?	?	11
Apr.	?	?		?	12
May	126.5	117.2	—	121.9	18
June			—		14
July	19.0	—	35.7	22.4	34
Aug.	56.2	19.8	—	33.0	35
Sept.	46.2	—	—	46.2	8
Oct.		—	—		3
Nov.	143	—	22.1	33.2	12
Dec.	34.4	—			13

presumably the more the tuna present. The greatest abundance occurs in July and August, both of which include only the Delta region. In September, there is a slight decline, followed by a strong decline in November. December is anomalously high, but January is again low. No figures are available for February through April, but Bullis' statement (1955) that yellowfins are apparently absent from the Delta in March is significant.

Thus, to a certain extent, the yellowfin show a distributional similarity to white marlin. The catch is rather uniformly low through most of the year, but indicates that they are scattered throughout much of the Gulf. The March disappearance from the Delta suggests that yellowfin, too, may be following a receding isotherm. And again, like the marlin, they apparently concentrate in the Delta during July and August. This concentration, in contrast to presumptions concerning white marlin, is believed to be a spawning phenomenon (Bullis, *in litt.*).

PREVIOUS KNOWLEDGE OF GULF WHITE MARLIN

While white marlin have been well-known from the Atlantic and the West Indies, their presence in the Gulf of Mexico west of the Indies has not been widely noticed. Baughman (1941, 1950) reports sight records from Port Isabel and Port Aransas, Texas, but these appear to be the only references for the area.

The large concentration in the Delta region in July and August, and the similar congregation off Ocean City, Maryland, at the same time, have both been tentatively considered post-spawning feeding congregations. Evidence for this has not been published, but this seems to be the case. Little is known of the spawning habits in the Gulf (or anywhere else for that matter). Few notable concentrations other than the midsummer ones have been noted. Erdman (1956), however, records April as the peak month off Puerto Rico and states that enlarged ovaries have been reported during that month. The best-developed ovary that he had seen was from a fish caught on June 9, 1956. In the sporting literature, Hemingway (in Vesey-Fitzgerald and LaMonte, 1949:156) reports the heaviest run of white marlin north of Cuba in the last two weeks in May. Farrington (Ibid. 1:155) notes a "terrific run," the "largest in the Atlantic" in April off Miami Beach, Florida. It is possible that these are spawning runs of some nature, and they do precede the observed summer concentrations. The precise nature of these runs, however, needs to be examined, as does that of the summer aggregations.

LITERATURE CITED

BAUGHMAN, J. L.
1941. Scombriformes, new, rare, or little known in Texas waters with notes on their natural history or distribution. Trans. Tex. Acad. Sci., *24:* 14-26.
1950. Random notes on Texas fishes, Part II. Tex. J. Sci., *2* (2): 242-263.

BULLIS, HARVEY R., JR.
1955. Preliminary report on exploratory long-line fishing for tuna in the Gulf of Mexico and the Caribbean Sea. Part I. Comm. Fish. Rev., *17* (10): 1-15.

ERDMAN, DONALD S.
1956. Recent fish records from Puerto Rico. Bull. Mar. Sci. Gulf and Caribbean, *6* (4): 315-340.

FUGLISTER, FREDERICK C.
1947. Average monthly sea surface temperatures of the western North Atlantic Ocean. Pap. Phys. Ocean. Meteor., *10* (2): 1-25.

VESEY-FITZGERALD, BRIAN AND FRANCESCA LAMONTE
1949. Game fish of the world. N. Y. Harper & Bros., pp. xx + 446.

Contribution No. 924

Deep-Sea Research, 1957, Vol. 5, pp. 259 to 262. Pergamon Press Ltd., London

The qualitative determination of some organic compounds in marine sediments

MARY A. PLUNKETT

(*Received* 1 *July* 1957)

Abstract—Four sediment samples from the Caribbean Sea were analysed qualitatively for free sugars, amino acids and simple organic acids. Two of the samples were from an anaerobic basin; two were from aerobic areas. The sediments were extracted with hot water and 70 per cent ethanol and the residues from these extractions were hydrolysed with 6 N hydrochloric acid. The organic materials in the extracts were separated and studied qualitatively on paper chromatograms. Six free sugars, eight amino acids and seven acids were detected in one or more of the sediments analysed.

INTRODUCTION

LITTLE is known about specific organic compounds present in marine sediments in general and particularly in those laid down under anaerobic conditions. ERDMAN, MARLETT and HANSON (1956) have reported the presence of amino acids in marine sediment hydrolysates. The work of VALLENTYNE (1954) on amino acids in lake sediments and WHITTAKER and VALLENTYNE (1957) on free sugars in lake sediment extracts together with that of ABELSON (1954, 1955), WAKSMAN and IGER (1933) and PINCK, DYAL and ALLISON (1954) demonstrates that both amino acids and sugars in certain environments are comparatively stable.

During the recent investigation of the Cariaco trench, an anaerobic basin in the Caribbean Sea (RICHARDS and VACCARO, 1956), cores were collected inside the basin and in adjacent aerobic areas. This paper reports and compares results of analyses of four of these cores for free sugars, amino acids and organic acids or their salts.

EXPERIMENTAL

Sampling. Sediments used in this study were collected at four different stations in the Caribbean Sea. The positions at which the cores were taken are given in Table 1.

Table 1. *Location of sediment samples*

Core No.	*Position*	*Length* (cm)
5	10° 37·5′N 65° 24′W	43
9	10° 46·5′N 64° 52′W	35
12	12° 36′N 58° 32′W	27
15	11° 27′N 61° 32′W	22

Cores 5 and 9 are from the Cariaco trench; cores 12 and 15 are from outside the Cariaco trench. The cores were collected in February, 1955 with the Phleger sampler and were immediately frozen. The portions studied were cut from the centres of the frozen cores with a circular saw and were dried at a temperature of below 45°C. After drying the samples were ground to a fine powder.

Extraction. Samples (15–20 g) of each core were extracted successively with ethyl ether, hot water and 70 per cent ethanol and the residues from the extractions were finally hydrolysed by boiling with 6 N hydrochloric acid. The ethanol and acid solutions were deionized by passage through Dowex 50 cation-exchange resin. The salt free solutions were evaporated to dryness in a Rinco rotating vacuum evaporator and the residues were taken up in distilled water. The ethanol extracts were analysed for sugars and the acid hydrolysates were analysed for amino acids. The water extracts were evaporated to dryness in the same manner as the other extracts and were taken up in distilled water. The water solutions were made alkaline with NH_3 (Kennedy and Barker, 1951) and were analysed for organic acids. The ether extracts were saved for later study.

Qualitative paper chromatography. The one-dimensional ascending technique on Whatman No. 1 filter paper was used to resolve the organic materials present in the extracts. Positive identifications of individual compounds were obtained by comparison of R_f values using pure materials for reference and by means of specific colour reagents.

Table 2. Sugar determinations on sediment samples

Sugar	*Inside basin*		*Outside basin*	
	Core 5	*Core 9*	*Core 12*	*Core 15*
Sucrose	+	+	+	+
Glucose	+	+	+	+
Fructose	+	+	+	+
Galactose	—	+	—	+
Arabinose	+	+	—	—
Xylose	+	—	—	—

+ = detected
— = not detected

Table 3. Amino acid determinations on sediment samples

Amino acid	*Inside basin*		*Outside basin*	
	Core 5	*Core 9*	*Core 12*	*Core 15*
Leucine	+	+	+	+
Isoleucine	+	+	—	—
Glycine	+	+	+	+
Phenylalanine	+	+	+	+
Valine	+	+	+	—
Aspartic acid	+	+	+	+
Arginine	—	+	—	—
Tyrosine	—	—	—	—
Glutamic acid	—	+	—	+

+ = detected
— = not detected

Analysis of ethanol extract. An equilibrated mixture of butanol-1, acetic acid and water in the proportions of 4 : 1 : 5 v/v/v (Bersin and Müller, 1952) was used as solvent. The chromatograms were developed for varying periods up to 72 hr. Triphenyltetrazolium chloride (Wallenfels, 1950) and benzidine (Horrocks, 1949) for reducing sugars and orcinol (Forsyth, 1948) and naphthoresorcinol (Partridge, 1948) for ketoses were used as colour reagents. Results of these tests are reported in Table 2.

Analysis of acid hydrolysates. Butanol-1, acetic acid and water in the proportions 250 : 60 : 250 v/v/v (Woiwood, 1949) and phenol and water in the proportions 100 : 20 v/v, Mallinckrodt liquid phenol in the presence of 1 : 1 acetic acid (Consden, Gordon and Martin, 1944), were used as solvents. Ninhydrin was used as a colour reagent to locate the amino acids. Results of these tests are reported in Table 3.

Analysis of water extract. Several organic acids or their salts were tentatively identified in the water extract. Propanol, ammonia, in the proportions of 7 : 3 v/v (Isherwood and Hanes, 1953) and ethanol, ammonia and water, in the proportions of 8 : 1 : 1 v/v/v (Jones, 1953) were used as solvents. Bromcresol green (Lugg and Overell, 1947, 1948) was used to locate the acids. Papers were also treated with ninhydrin to reveal the positions of any amino acids which might have vitiated the identification of the acids. Acids detected are listed in Table 4.

Table 4. Organic acid determinations on sediment samples

	Inside basin		*Outside basin*	
Acid	*Core 5*	*Core 9*	*Core 12*	*Core 15*
Propionic	+	+	—	—
Fumaric	+	+	—	+
Lactic	+	+	—	+
Tartaric	+	+	+	+
Citric	+	+	+	+
Oxalic	+	+	+	—
Glutaric	+	+	+	+

+ = detected
— = not detected

DISCUSSION

The information presented here indicates that the number and variety of organic materials in sediments from anaerobic basins may be greater than in sediments laid down in aerobic areas. In the cores studied the number of free sugars detected in those from the anaerobic basin was 5 for each as compared to 3 and 4 for those from the aerobic area. All of the sediments contained sucrose, glucose and fructose ; some of them contained galactose, arabinose and xylose.

The number of amino acids detected in the anaerobic basin cores was 6 and 8 as compared to 5 for each of the aerobic area cores. Leucine, glycine, phenylalanine, valine and aspartic acid were found in acid hydrolysates of each of the cores ; isoleucine, arginine and glutamic acid were detected in one or more of the hydrolysates.

Seven organic acids or their salts were found in each of the anaerobic basin cores ; 4 and 5 were found in the cores from the aerobic area. Acids detected include propionic, fumaric, lactic, tartaric, citric, oxalic and glutaric.

This data suggests a slower decomposition rate of organic matter in the sediments from the anaerobic basin or at least a greater stability of certain compounds under the conditions existing there. At the same time they support the earlier work cited (Whittaker and Vallentyne, 1957 and Erdman, Marlett and Hanson, 1956) on the stability of sugars and amino acids in sediments.

This work will be continued and extended in order to show whether or not the differences noted are significant and perhaps to offer some explanation for the presence of the materials detected.

*Woods Hole Oceanographic Institution, Woods Hole, Massachusetts**
Contribution No. 924 *from Woods Hole Oceanographic Institution*

**Present address: Vassar College, Poughkupsie, New York*

REFERENCES

ABELSON P. H. (1954) Organic constituents of fossils. *Science* **119**, 576 ; also *Carnegie Inst. Wash. Year Book* No. 53, 97–101.

ABELSON P. H. (1955) Organic constituents of fossils. *Carnegie Inst. Wash. Year Book* No. 54, 107–109.

BERSIN T. and MÜLLER A. (1952) Die Ring-papierchromatographie von Zuckern. *Helv. Chim. Acta* **35**, 475–478.

CONSDEN R., GORDON A. H. and MARTIN A. J. P. (1944) Qualitative analysis of proteins : A partition chromatographic method using paper. *Biochem. J.* **38**, 224–232.

ERDMAN J. G., MARLETT E. M. and HANSON W. E. (1956) Survival of amino acids in marine sediments. *Science* **124**, 1026.

FORSYTH W. C. (1948) Colour reagents for paper chromatography of sugars. *Nature, Lond.* **161**, 239–240.

HORROCKS R. H. (1949) Paper partition chromatography of reducing sugars with benzidine as a spraying reagent. *Nature, Lond.* **164**, 444.

ISHERWOOD F. A. and HANES C. S. (1953) Separation and estimation of organic acids on paper chromatograms. *Biochem. J.* **55**, 824–830.

JONES A. R. (1953) Identification of some organic acids by paper chromatography. *Anal. Chem.* **25**, 394–396.

KENNEDY E. P. and BARKER H. A. (1951) Paper chromatography of volatile acids. *Anal. Chem.* **23**, 1033–1034.

LUGG J. W. H. and OVERELL B. T. (1947) Partition chromatography of organic acids on a paper sheet support. *Nature, Lond.* **160**, 87–88.

LUGG J. W. H. and OVERELL B. T. (1948) One- and two-dimensional partition chromatographic separation of organic acids on an inert support. *Aust. J. Sci. Res.* **A1**, 98–111.

PARTRIDGE S. M. (1948) Filter-paper chromatography of sugars. *Biochem. J.* **42**, 238–249.

PINCK L. A., DYAL R. S. and ALLISON F. E. (1954) Protein-mont-morillonite complexes, their preparation and the effects of soil microorganisms on their decomposition. *Soil Sci.* **78**, 109.

RICHARDS F. A. and VACCARO R. F. (1956) The Cariaco Trench, an anaerobic basin in the Caribbean Sea. *Deep-Sea Res.* **3**, 214–228.

VALLENTYNE J. R. (1954) Biochemical liminology. *Science* **119**, 605.

WAKSMAN S. A. and IGER K. R. N. (1933) Fixation of proteins by lignins and formation of complexes resistant to microbial decomposition. *Soil. Sci.* **36**, 69.

WALLENFELS K.(1950) Über einen neuen Nachweis reduzierender Zucker in Papierchromatogramm und dessen quantitative Auswertung. *Naturwissenschaften* **37** (21), 491–492.

WHITTAKER J. R. and VALLENTYNE J. R. (1957) On the occurrence of free sugars in lake sediments. *Limnol. Oceanogr.* **2**, No. 2, 98–110.

WOIWOOD A. J. (1949) A method for the estimation of micro amounts of amino nitrogen and its application to paper partition chromatography. *Biochem. J.* **45**, 412–417.

Printed in Great Britain by The Salisbury Press Ltd., Publicity House, Wilton Road, Salisbury, Wilts. (6902)

Contribution No. 926

A New Technique for Studying Non-tidal Drift with Results of Experiments off Gay Head, Mass., and in the Bay of Fundy[1]

BY DEAN F. BUMPUS, JOSEPH CHASE, C. GODFREY DAY,
DAVID H. FRANTZ JR., DAVID D. KETCHUM AND ROBERT G. WALDEN

Woods Hole Oceanographic Institution[2]
Woods Hole, Massachusetts, U.S.A.

ABSTRACT

A transponding drift buoy has been developed to aid in the study of the horizontal motions of surface waters. Experiments to study the non-tidal drift off Martha's Vineyard, Mass., in June 1956, off Yarmouth, N.S., in October and November 1956, in Grand Manan Channel in October 1956, and off Saint John, N.B., in December 1956, are described and discussed.

INTRODUCTION

THE DRIFT of a body of water and/or the planktonic forms contained therein has been the concern of the fishery biologist for a long time. The need for knowledge of the direction and speed of drift from the spawning ground, together with the eventual location of fish larvae when they cease their planktonic existence, has prompted many attempts to deduce the non-tidal drift in many parts of the sea.

One of the commonest techniques has been to broadcast drift bottles over the area of interest with the hope of recovering a sufficient number of them within a limited elapsed time to allow the construction of a map of the probable drift of these bottles with respect to both routes and speeds. The chief criticisms of this method have been that:

(a) The bottles may be subject to considerably more wind influence than the upper 5 or 10 m. of water in which the planktonic elements reside.

(b) Knowledge of only the point and time of release and the point and time of recovery leaves the assumed intervening route of each bottle entirely up to the deductions of the investigator.

(c) The elapsed time between stranding and discovery of the drift bottle or the possible temporary stranding at some other location prior to the final stranding and discovery, adds to the uncertainty of the rates of drift.

We have succeeded, we believe, in building and using a better drift bottle which we have called a "Transponding Drift Buoy". This buoy is not as elaborate as Stommel's (1954) nor as simple as that of Volkmann, Knauss and Vine (1956). It could readily be adapted for use with a parachute drogue for studying subsurface ocean currents after the method of Volkmann *et al.*

---

[1] Received for publication February 26, 1957.

[2] Contribution No. 926 from the Woods Hole Oceanographic Institution.

J. FISH. RES. BD. CANADA, 14(6), pp. 931–944, 1957.
Printed in Canada.

Brief Description of Transponding Drift Buoy

Each buoy is 20 feet long, 6 inches in diameter, constructed of aluminum, loaded with a radio transmitter and receiver and a battery stack (Walden, Ketchum and Frantz, 1957) and ballasted with lead. The buoy floats vertically with 2 feet of freeboard surmounted with a 13-foot whip antenna. Total weight in air is 230 lb. A 4-foot-diameter disc of plywood, painted orange and bearing an identifying letter, is tethered to each buoy to improve visual identification from the air.

When the receiver is energized by a short, 1- to 2-sec. tone-modulated signal on 2398 kc., the transmitter responds with CW signals on 2398 kc. of 15 sec. duration. This signal may be DF'd by ship or aircraft. Repetitions of this procedure and suitable manoeuvring of the ship or aircraft will bring the target buoy within visual range where a fix may be made either by loran, cross bearings on objects of known positions, or whatever other method is suitable.

The expected life of the power supply in each buoy under normal tracking conditions, i.e., located once per day, is 2 to 3 weeks.

In the experiments described below, two cases of buoy failure can be definitely attributed to the antenna breaking in rough weather. It is reasonable to attribute the loss of the three still missing buoys to similar troubles. Steps currently being taken to remedy this fault and other minor ones which we have been able to isolate should add greatly to buoy efficiency.

Since the buoys used in these experiments are intended to follow the movement of the upper 5 m. of water, they are ballasted to make the normal freeboard as little as possible consistent with reliable radio transmission in a seaway, thus mimimizing the direct effect of windage. A rough calculation, based on only the relative areas exposed to air and water, shows the buoy to move in still water at approximately one-sixtieth the wind velocity, a motion which is negligible relative to the other inaccuracies of these experiments. In the presence of steep waves, the motion is surely somewhat greater than this, because of the frictional motion of the surface layers and because of the actual transport due to the wave motion. But until we have more knowledge of actual velocity profiles near the surface under various conditions of wind, sea and temperature, we feel justified in assuming that the motion of these buoys indeed represents the data sought, the average horizontal velocity of the upper 5 m. of water.

EXPERIMENTS

Five sets of experiments have been performed with these buoys:

A. A trial test of the development model southwest of Gay Head, Martha's Vineyard, Mass., in June 1956.

B. An experiment in the Lurcher Shoals–Trinity Ledge area off Yarmouth, N.S., in October 1956 with one buoy.

C. An experiment in Grand Manan Channel in October 1956 with three buoys.

D. An experiment in the Lurcher Shoals–Trinity Ledge area off Yarmouth in November 1956 with six buoys.

E. An experiment off Saint John, N.B., in December 1956 with four buoys.

The experiments in Fundian waters were conducted at the invitation of the Fisheries Research Board of Canada Biological Station, St. Andrews, N.B., as a part of their joint Fisheries Research Board of Canada–U.S. Fish and Wildlife Service herring investigations. These drift buoy experiments were sandwiched in between a series of cruises by two vessels, *Harengus* and *Silver Bay*, to discover where young herring are produced and where they drift during the first few months after hatching. These distribution and dispersal cruises traversed the Bay of Fundy, the Gulf of Maine and Georges Bank. Regular drift bottles were set out at frequent intervals along the ships' tracks on these cruises. The over-all picture, as deduced from their pattern of returns, will be the subject of another paper. Drift bottles were also set out with each of the transponding drift buoys.

EXPERIMENT A

On 11 June, one transponding drift buoy was set adrift 30 miles WSW. off Gay Head, Martha's Vineyard. During the following 2 weeks the position of the buoy was determined as often as weather conditions and other commitments of our aircraft permitted. The buoy was located six times (Fig. 1). It was last located within 7 (nautical) miles of its initial position, but in the course of 2 weeks had drifted throughout at least one clockwise orbit, having been 18 miles to the ESE. and 21 miles to the WSW. of the initial position. The buoy responded at 1345 on 26 June while our boat *Asterias* was en route to recover it but failed to respond at 1430 and at frequent triggerings thereafter. We eventually learned that a tug with a tow had wiped off the antenna at 1420 on the same date. The buoy was picked up by a U.S. Navy destroyer escort and returned to us otherwise undamaged.

The indicated rates of drift of this buoy are of interest. Following a relatively slow northward drift on the first day the buoy moved southeasterly at a rate of 15 miles per day, then westerly and southwesterly at decreasing rates. During the last week, with fixes on 18 and 25 June, the drift was NNE. at only 2 miles per day. It is possible that had fixes been made more often during the last week the rates of drift would have been larger, for we have no reason to believe, on the basis of its drift during the previous week, that it went directly to its last observed position.

Conventional drift bottles set out by the U.S. Fish and Wildlife Service vessel *Albatross III* (Cruise 76) on 11 and 23 June in this area moved northward into coastal waters in about a month, or with an average non-tidal drift of 1+ miles per day.

This first experiment with the transponding drift buoy suggests that prior to the eventual northward set these waters underwent an anticyclonic irrotational motion, one erratic in its rates of movement and direction, suddenly speeding up and gradually slowing down. It may have been repeated several times as these waters drifted shoreward.

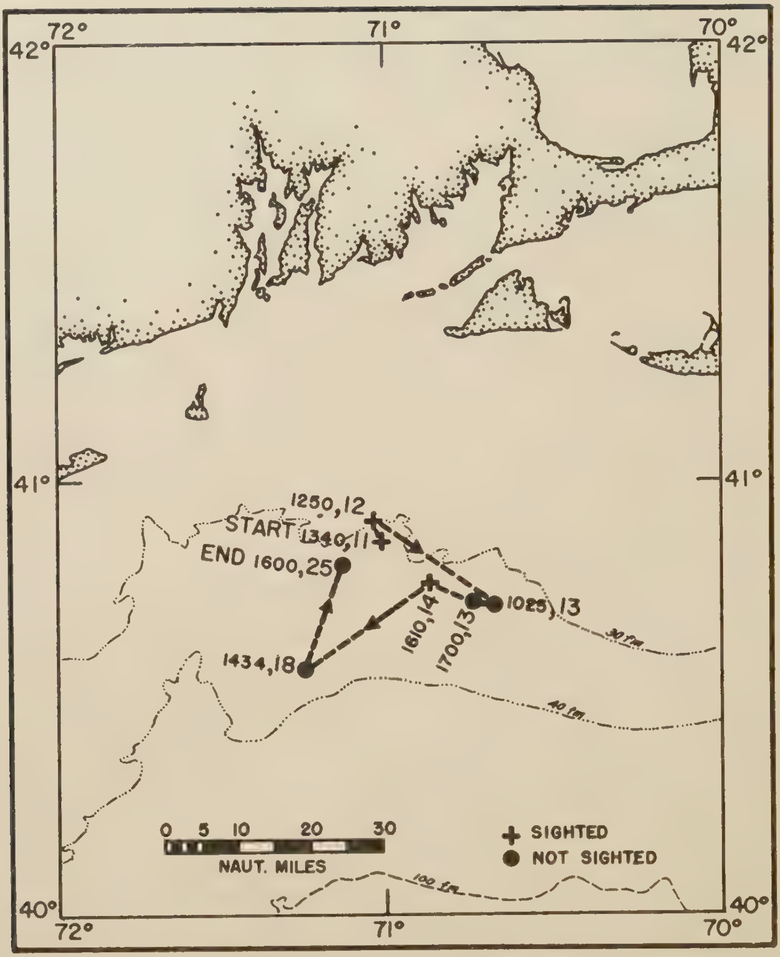
72°
71°
70°
42°
42°
41°
41°
40°
40°
72°
71°
70°
1250,12
START
1340,11
END 1600,25
1025,13
1610,14
1700,13
1434,18
30 fm
40 fm
100 fm
0 5 10 20 30
NAUT. MILES
SIGHTED
NOT SIGHTED

Fig. 1. Experiment A, June 1956, SW. of Gay Head, Mass. Numbers indicate time (EDST) and date of buoy location.

Experiment B

It was our intent for the first experiment in the Bay of Fundy to set out several buoys in the Lurcher Shoals–Trinity Ledge region (an area considered to be one of the major herring spawning grounds) and to allow them to drift for the first 2 weeks of October. As is commonly the case with newly developed electronic equipment, we were troubled with failures. We did succeed, however, in tracking one buoy for a period of 6 days, 4–10 October 1956 (Fig. 2).

This buoy was launched at position "Y" halfway between Lurcher Shoals and Trinity Ledge. At the end of 5 days the buoy was in the mouth of Saint Mary Bay and on the afternoon of the sixth day it was off Digby Neck in the Bay of Fundy, about 43 miles from position "Y". One would presume that it went through Petite Passage, though it may have gone through Grand Passage

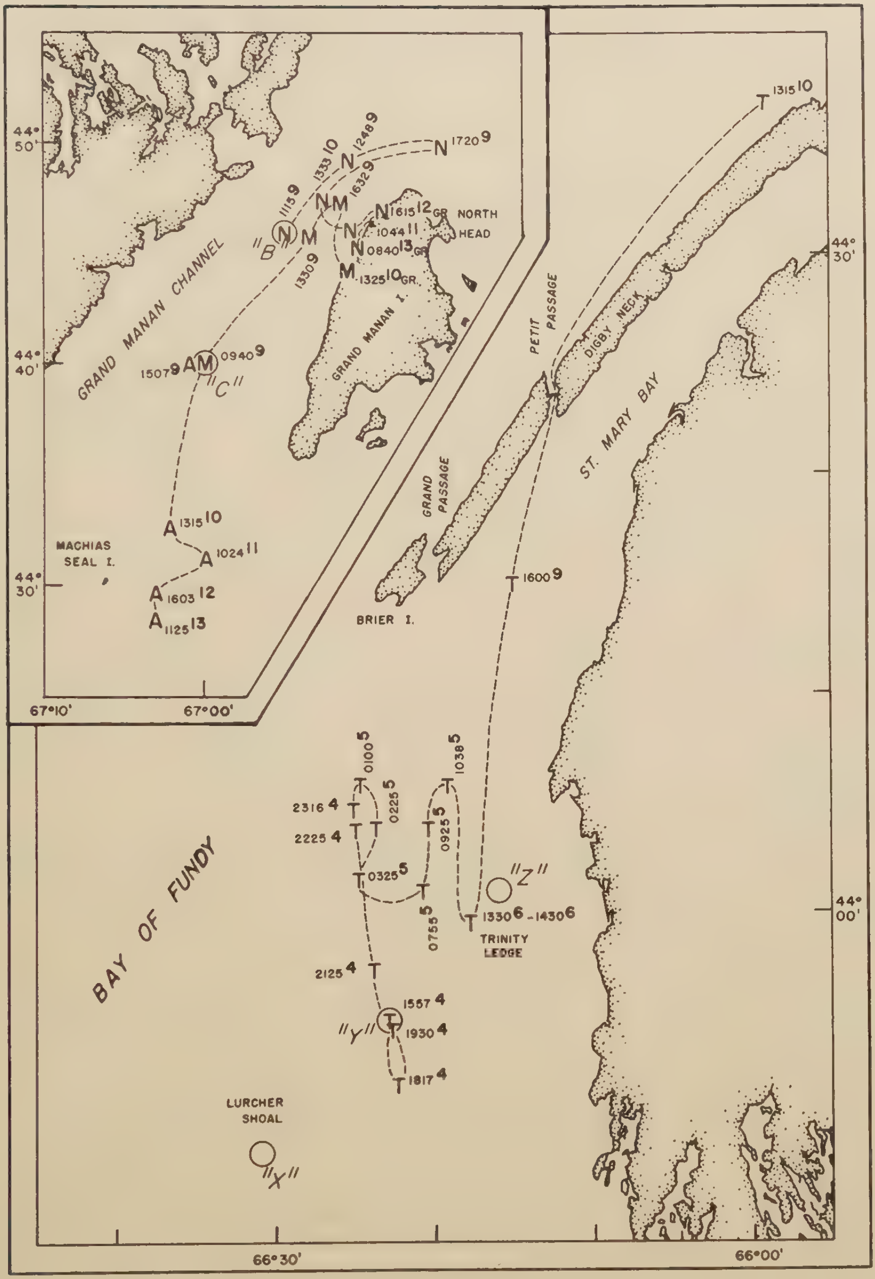
44° 50'
44° 40'
44° 30'
67°10'
67°00'
GRAND MANAN CHANNEL
N 1720 9
1248 9
1333 10
N
1632 9
1115 9
N M
"B"
N
M
1330 9
N 1615 12 GR
NORTH HEAD
N 1044 11
N 0840 13 GR
M 1325 10 GR.
GRAND MANAN I.
1507 9 AM 0940 9
"C"
A 1315 10
A 1024 11
MACHIAS SEAL I.
A 1603 12
A 1125 13
BRIER I.
GRAND PASSAGE
PETIT PASSAGE
DIGBY NECK
ST. MARY BAY
T 1315 10
44° 30'
T 1600 9
44° 00'
BAY OF FUNDY
0100 5
2316 4
0225 5
2225 4
T 0325 5
1038 5
0925 5
0755 5
"Z"
T 1330 6 - 1430 6
TRINITY LEDGE
2125 4
1557 4
"Y"
1930 4
T 1817 4
LURCHER SHOAL
"X"
66°30'
66°00'

FIG. 2. *Lower*—Experiment B, October 1956, Lurcher Shoal—Trinity Ledge area.
Upper—Experiment C, October 1956, Grand Manan Channel.
Numbers indicate time (AST) and date of buoy location.

or even around Brier Island. Suffice it to say that the resultant non-tidal drift on that occasion was northerly at slightly greater than 7 miles per day. Except for a half a day of strong SE. wind the winds were light throughout the period of drift.

EXPERIMENT C

In order to facilitate repairs and experimenting, the field team shifted its scene of operation to the Grand Manan Channel, just a few hours steaming time from the Biological Station at St. Andrews. Here three buoys were set adrift and tracked for a period of 4 days, 9–13 October 1956 (Fig. 2, inset). The buoys were set out at Station "*C*" near the beginning of the flood, at Station "*B*" 1½ hours later, and at Station "*C*" at the beginning of the ebb.

The results of this experiment suggested that there is a tendency toward a non-tidal set onto the western shore of Grand Manan Island, superimposed on the large (8- to 9-mile) tidal excursion. The buoy at position "*C*" moved well up the channel on the flood and was found stranded on the western shore of Grand Manan the following afternoon. The buoy set out at "*B*" also moved northerly on the flood to a position NNE. of North Head, returned into Grand Manan Channel by the following afternoon, and stranded on the western shore of Grand Manan 2 days later.

On the other hand, the buoy launched at "*C*" at the beginning of the ebb moved southerly out of the area a distance of about 7 miles the first day, then more slowly on successive days to the vicinity of Machias Seal Island. The resultant drift after the buoy left the effect of the strong tidal excursions of the Grand Manan Channel was about a mile per day, southerly.

EXPERIMENT D

Owing to the large tidal excursions common in the Fundian region, we planned for this November experiment to set out the buoys at position "*X*", "*Y*" and "*Z*" (Fig. 3) at the beginning of the flood and at the beginning of the ebb, one-half tidal cycle apart.

The first string of buoys was set out near the beginning of the flood as planned, but due to electrical failures only two buoys were set out in the second string, at Stations "*Y*" and "*Z*", one and one-half tides later. A third setting was made several days later irrespective of the tidal phase (Fig. 3).

Buoy *Tango* (T), set out at "*X*" on 2 November, moved northwesterly for 1¼ days at a rate of about 17 miles per day and then failed to respond and remained lost.

Buoy *India* (I), set out on 2 November at "*Y*", also failed to respond, was sighted by the vessel *Silver Bay* at Northwest Ledge off Brier Island on the 7th, and henceforth remained lost. It had moved to its last seen position at better than 4 miles per day. The orange disc for this buoy was sighted a month later about 60 miles to the northeastward, 8 miles northeast of Parker Cove.

Buoy *Mike* (M), set out the same day at "*Z*", moved southwesterly, northwesterly, southerly, then northerly into the Bay of Fundy, the final resultant being about 4 miles per day.

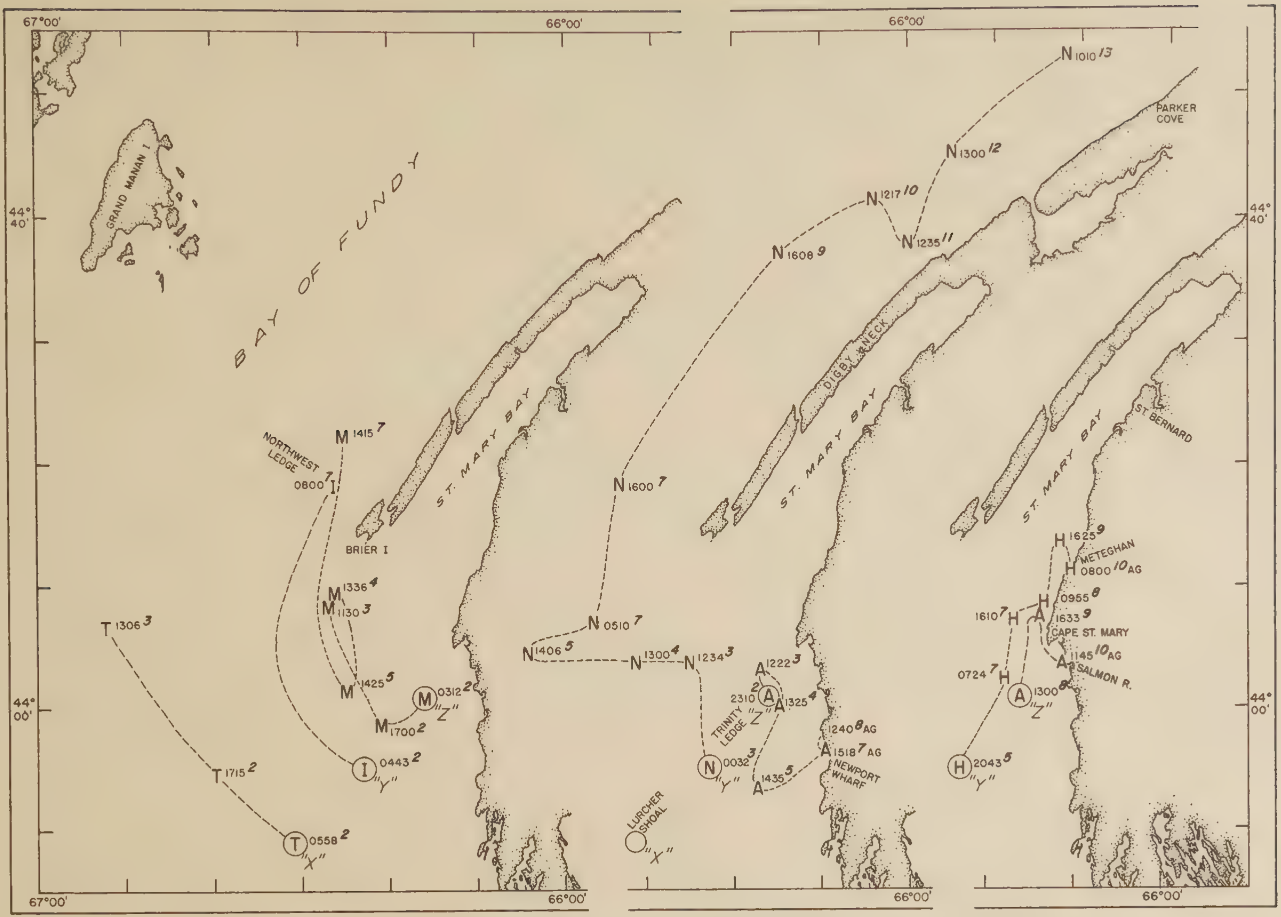
67°00'
66°00'
44° 40'
44° 00'
GRAND MANAN I
BAY OF FUNDY
ST. MARY BAY
BRIER I
NORTHWEST LEDGE
DIGBY NECK
PARKER COVE
ST BERNARD
METEGHAN
CAPE ST. MARY
SALMON R.
TRINITY LEDGE
NEWPORT WHARF
LURCHER SHOAL
M 1415 7
0800 7 I
M 1336 4
M 1130 3
M 1425 5
M 0312 2 "Z"
M 1700 2
I 0443 2 "Y"
T 1306 3
T 1715 2
T 0558 2 "X"
N 1010 13
N 1300 12
N 1217 10
N 1235 11
N 1608 9
N 1600 7
N 0510 7
N 1406 5
N 1300 4
N 1234 3
N 0032 3 "Y"
A 1222 3
2310 2 A "Z"
A 1325 4
1240 8 AG
A 1518 7 AG
A 1435 5
"X"
H 1625 9
H 0800 10 AG
H 0955 8
1610 7 H
A 1633 9
A 1145 10 AG
0724 7 H
A 1300 8 "Z"
H 2043 5 "Y"

FIG. 3. Experiment D. November 1956, Lurcher Shoal–Trinity Ledge Area. Part I–left, Part II–centre, Part III–right. Numbers indicate time (AST) and date of buoy location.

The second string of buoys was set out near midnight of 2–3 November. Buoy *November* (N) at "Y" moved northerly, westerly and then northeasterly at 4 to 16 miles per day with a resultant when picked up 10 days later off Parker Cove of 7.5 miles per day. On the other hand, Buoy *Alpha* (A), set out at "Z", moved northerly, then southerly and easterly at much slower rates, 3 to 7 miles per day, and stranded off Newport Wharf on 7 November only 7 miles from Trinity Ledge.

The third part of this experiment was begun by setting out Buoy *Hotel* (H) at "Y" on the evening of 5 November and by resetting *Alpha* at "Z" near noon on the 8th. *Hotel* moved northerly past Cape St. Mary into the mouth of St. Mary Bay at about 5 miles per day, then southerly during the latter part of the 9th to strand at Meteghan. *Alpha* moved northerly past Cape St. Mary on the 8th and 9th at about the same rate as *Hotel*, then southerly as did *Hotel*, to strand near the mouth of Salmon River.

It is apparent that there is no set pattern of drift away from the Lurcher Shoals–Trinity Ledge area which is repetitive day after day. The first string of buoys set out in November exhibited a decided offshore drift during the first day, followed by a northwesterly drift, possibly a reversal on 4 and 5 November as indicated by *Mike*, and then a northerly drift out of the area into the Bay of Fundy proper. This suggests very strongly a wind influence superimposed on the non-tidal drift. The winds were fresh northeasterly on the 2nd and 3rd, fresh northerly on the 4th and 5th, followed by westerlies and southwesterlies (see accompanying Table). This is further indicated by the drift of Buoys *November* and *Alpha* in Part II and *Hotel* and *Alpha* in Part III of the experiment. For instance, the tendency following the early morning of 2 November was offshore, westerly and then northerly out of the area. Following midnight on the 2nd, the tendency was northerly and westerly out of the middle of area "Y" but ultimately toward shore from Trinity Ledge ("Z"). After the 5th the tendency was northeasterly towards St. Mary Bay with a southeasterly reversal onshore on the 9th and 10th. One of the drift bottles set out with Buoy *Hotel* on the 5th at position "Y" was found 9 days later on the eastern shore of St. Mary Bay at St. Bernard, having continued its northeasterly drift into St. Mary Bay at a speed of 3.5 miles per day. A second bottle was found on the 28th near where *Hotel* came ashore.

These experiments suggest that while the general tendency for the non-tidal drift is northerly across this area at a relatively high speed, 5 to 10 miles per day, there can be broad dispersion of fish eggs and larvae deposited in the water in the area due to the tendency of drift offshore, northerly, southerly or onshore, as modified by the wind pattern, in addition to the dispersion created by the regular tidal fluctuations.

It does seem, however, that the waters which drift across the Lurcher Shoal–Trinity Ledge area find their way into the Bay of Fundy in a relatively short time, 7 to 10 days, to off Digby with perhaps a small quantity of water being deflected into St. Mary Bay from time to time.

Surface winds in study areas as determined from U.S. Weather Bureau surface maps.

Date, 1956	Average wind	
	Direction	Force
	Lurcher Shoals area	
Oct.		
4	W.	3
5	NW.	3
6	E.	3
7	SW.	3
8	WSW.	4
9	WNW.	4
10	WNW.	3
	Grand Manan Channel	
Oct.		
9	WNW.	3
10	WNW.	3
11	WNW.	3
12	W.	2
13	W.	1
	Lurcher Shoals area	
Nov.		
2	NNE.	4
3	N.	3
4	N.	4
5	N.	4
6	NNW.	3
7	SW.	3
8	SW.	2
9	NW.	4
10	NNW.	5
11	SW.	3
12	SSW.	5
13	NW.	4
	Bay of Fundy	
Dec.		
4	NW.	5
5	NE.	1
6	SSE.	3
7	W.	3
8	N.	3
9	NNE.	4
10	Variable	
11	SSW.	4
12	W.	5
13	ENE.	3
14	ENE.	4

EXPERIMENT E

The experiment in December was shifted to the area off Saint John, N.B., in order to avoid fouling the myriad lobster pot buoys and lines attendant to the opening of the lobster fishing season which commenced on 1 December. Only four buoys were available for this experiment (Fig. 4) inasmuch as *Tango* and *India* remained unreported. The experiment commenced on the 4th. Minor troubles were experienced and corrected until the night of 11–12 December when

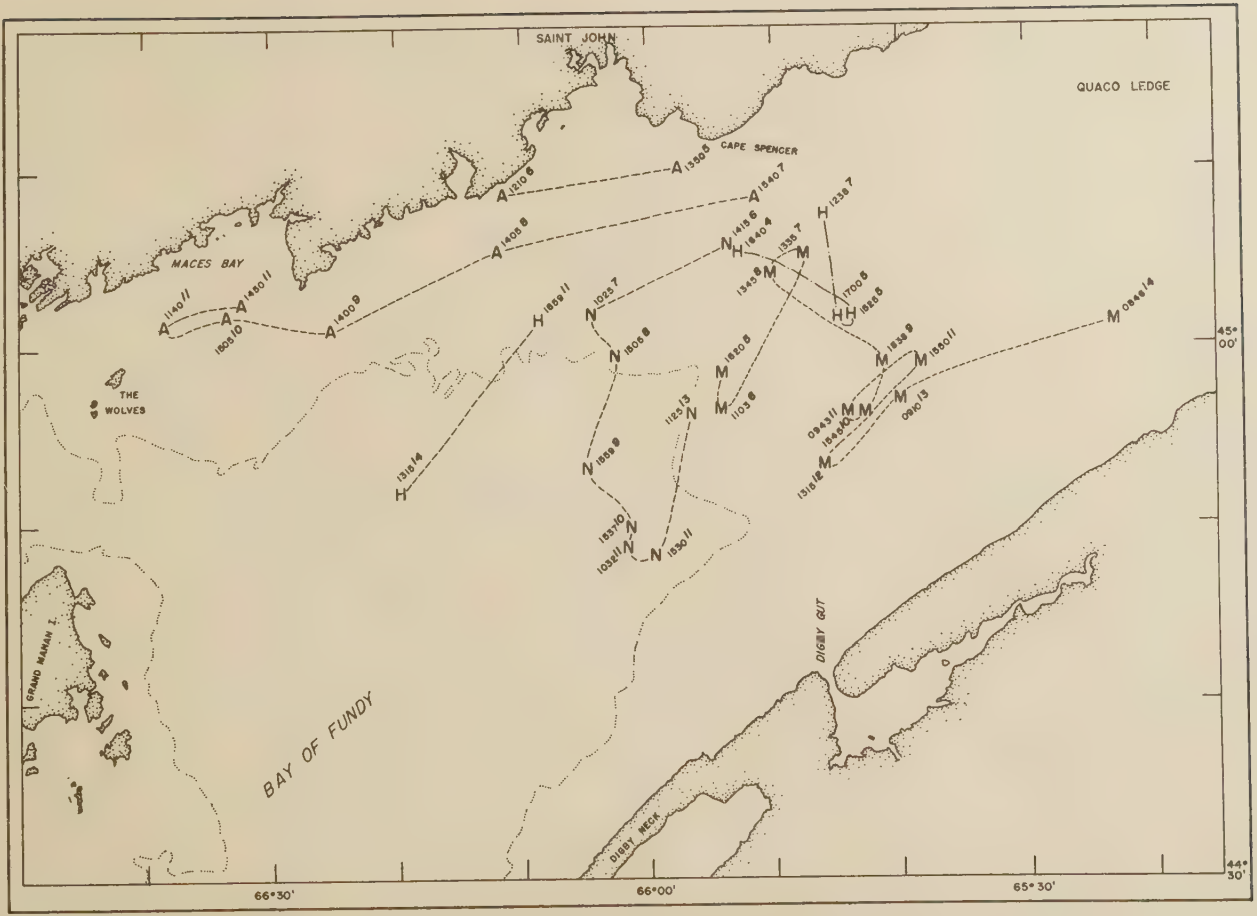
SAINT JOHN
QUACO LEDGE
CAPE SPENCER
MACES BAY
THE WOLVES
GRAND MANAN I.
BAY OF FUNDY
DIGBY GUT
DIGBY NECK
A 1140 11
A 1450 11
A 1805 10
A 1400 9
A 1405 8
A 1210 6
A 1350 5
A 1540 7
H 1859 11
H 1318 14
H 1238 7
H 1640 4
H 1700 5
H 1826 5
N 1025 7
N 1806 8
N 1559 9
N 1537 10
N 1032 11
N 1530 11
N 1125 13
N 1415 6
M 1335 7
M 1345 8
M 1620 5
M 1103 6
M 1839 9
M 1550 11
M 0943 11
M 1546 10
M 0910 13
M 1318 12
M 0846 14
66°30'
66°00'
65°30'
45° 00'
44° 30'

FIG. 4. Experiment E. December 1956, Central Bay of Fundy. Numbers indicate time (AST) and date of buoy location.

three of the buoys (*Alpha*, *Hotel* and *November*) lost their antennae in a storm. Two of these three (*Hotel* and *November*) were recovered, the vessel *Harengus* being conned to their location by the aircraft which was able to trigger the buoys from a distance of about 2 miles in spite of the absence of the antennae. The third buoy (*Alpha*) had not been recovered by the end of the experiment.

Buoy *Alpha* had been set out 2 miles southwest of Cape Spencer on 5 December and drifted westerly to less than a mile offshore at a speed of 10 miles per day. This buoy was picked up and relocated farther offshore on the 7th. It again drifted westerly at high speeds to the offing of Maces Bay where it stagnated. *Alpha* was not located again following the afternoon of the 11th until late in December when it was sighted by a lobsterman on Muir Ledges south of Grand Manan. The presumption is that its antenna was broken off in the storm referred to above.

Buoy *Hotel*, set out 7 miles south of Cape Spencer on 4 December, drifted 7.5 miles southeasterly, then northerly where it was picked up for repairs on the 7th.

Buoy *November*, set out 6 miles south of Cape Spencer on 6 December near *Hotel*, moved westerly at a fairly high speed until the 7th, then veered southerly at speeds averaging 3+ miles per day, then northeasterly.

Buoy *Hotel*, set out on 11 December just west of where *November* veered southerly, was found 3 days later 12 miles to the southwest.

Buoy *Mike*, set out farther offshore 13 miles south of Cape Spencer on 5 December, underwent a series of irregular courses until at the end of 7 days it was oscillating forth and back just outside the easterly flowing current on the southeast side of the bay. On the 12th, *Mike* became entrained in the easterly current and had drifted 18 miles to the eastward by the morning of the 14th.

Buoy *Hotel* was also allowed to drift for a period of two days (9–11 December) in the area about 12 miles south of Cape Spencer (not figured) in which it described an arc to the south and east, moving at about 3 miles per day.

This experiment has revealed several things of interest, namely:

(a) The width of the westerly flowing non-tidal drift on the northwest side of the bay; the width of the easterly flowing non-tidal drift on the southeast side of the bay; and the irregular cyclonic eddying motion in the central portion of the Bay of Fundy between the coastal drifts.

(b) It is apparent that the westerly drift along the New Brunswick coast extends to a distance of about 6 miles south of Cape Spencer. Note that *Hotel*, launched at this distance from the Cape on the 4th, drifted southeasterly out of this flow but that *November*, launched on the 6th, remained in it until the following morning when it veered southerly out of the drift. This drift appears to have a speed of the order of 10 to 15 miles per day.

(c) The easterly coastal drift on the southwest side of the bay appears to be about 10 miles wide, opposite Cape Spencer. Note that Buoy *November* had been carried by this drift one month before to a position just south of where *Mike* performed the hesitation waltz on the 9th to 12th prior to being entrained in the coastal drift.

(d) The apparent irregular wanderings of Buoys *Hotel, November*, and *Mike* are suggestive of cyclonic motions in the central part of the bay lying between and contiguous to the west-moving and east-moving coastal currents.

(e) The non-tidal drifts did not appear to be as much affected by wind in this area as they had been in the Lurcher Shoal–Trinity ledge area. In several instances adjacent buoys in the centre of the bay moved in opposite directions during periods of high wind force.

Obviously it would have been desirable in these experiments to have established each buoy position at the same state of the tide, in order to minimize the periodic excursions due to tidal currents alone. It soon became apparent that this was impossible because of the generally poor flying weather and the shortness of the daylight hours at this time of year. However, an attempt was made to correct the positions of Buoys *Mike* and *November* in this last experiment to the nearest time of high water at St. John on the basis of published data (Canada, 1928). These buoys drifted in an area fairly close to Station *A*, 44° 58.5′ N., 65° 57.0′ W., of the survey made in 1907 of the tidal currents in the Bay of Fundy by the Canadian Hydrographic Service. These corrections were made by integrating the published hourly current vectors at the station and correcting the resultant displacements for the difference of the actual range of tide at Saint John and the 21-foot range of the tables. The results were somewhat inconclusive. There was, perhaps, a tendency to smooth out the trajectory of Buoy *November*, and the apparently random initial excursions of Buoy *Mike* assumed a more definitely counterclockwise appearance; but application of the correction would not warrant a change in interpretation of the data. Since these tidal data were available in only one location in the area of this experiment, and since our justification for using them even a few miles from the original current stations is questionable, we have not attempted to apply tidal corrections to the observed positions.

CONCLUSION

These experiments have added some detail to the general description of the circulation in the Bay of Fundy as summarized by Ketchum and Keen (1953, pp. 98–99) and have confirmed the existence of the same general pattern for the late autumn period, there being no previous drift experiments at this time of year in this region. The inflowing drift, restricted to the southeasterly side of the bay, averages about 10 miles per day, and the outflowing drift is restricted to the northwest side at comparable speeds. The inflowing drift is about 10 miles wide off Digby and the outflowing drift is about 6 miles wide off Cape Spencer. While some trajectories from the Lurcher Shoal–Trinity Ledge region may penetrate well up the bay, perhaps even to its head, the cyclonic rotations with speeds of 2 to 4 miles per day between the two drifts may shorten the route and provide for the distribution of herring larvae all along the New Brunswick coast, beginning about 15 to 20 days after hatching. Because of the streakiness of the drift, these planktonic elements may become considerably dispersed and take much longer to arrive.

The above time agrees with that of Fish and Johnson (1937, p. 200) but we postulate higher speeds along the periphery and slower ones in the central eddying motions, and possible deeper penetration into the bay along the southeast side prior to crossing over to the other shore. Mavor (1922), Fish and Johnson (1937) and Hachey and Bailey (1953) have tended to restrict the routes of drift bottles reaching the New Brunswick shore to the vicinity of the 50-fathom contour. However, many drift bottles have penetrated to the eastern end of the bay at all seasons of the year (Bigelow, 1927; Hachey and Bailey, 1952; Day, 1957). We believe that the transfer from the inflowing to the outflowing drift can take place all along the centre portion well up into the bay. Further experiments comparable to those we have reported above will be required to demonstrate this.

We have not added much to an understanding of the circulation around Grand Manan. We must agree with the conclusion of MacGregor and McLellan (1951) that the residual current in Grand Manan Channel may be variable depending upon tidal range and meteorological conditions.

ACKNOWLEDGMENTS

The transponding drift buoy was designed and developed under Contract Nonr-769(00) with the U.S. Office of Naval Research by Messrs. Walden, Ketchum and Frantz. The aircraft was made available through the same contract. The six buoys were constructed and the field work was carried out under Contract No. 14-19-008-2377 with U.S. Fish and Wildlife Service. The assistance of the Fisheries Research Board of Canada Biological Station at St. Andrews, in particular through Mr. S. N. Tibbo, is gratefully acknowledged as are the services of the Canadian Department of Fisheries vessel *Harengus,* Capt. L. J. Lewis, Master. We are also indebted to the crew of the PBY aircraft, Capt. Norman Gingrass, together with the scientific observers who assisted in the field work. Thanks are due to Messrs. Dingwell, Chute, Barstow and Wing for their efforts in construction and repair of the instruments, and to Mr. G. Pasley for preparing the Figures.

The Canadian Department of Transport kindly permitted the experiment to be carried out in waters under its jurisdiction. The U.S. Coast Guard, through its Local Notice to Mariners, and the Canadian Broadcasting Corporation, through its 5 p.m. "Fisherman's Broadcast", kept mariners informed of the project and indirectly helped to recover some of the "lost" buoys. Mr. E. G. Sollows of the Fisheries Research Board, at Yarmouth, N.S., also rendered assistance through his contacts with the fishermen along the Nova Scotia coast.

We are also indebted to the Commanding Officer, Dow Air Force Base, Bangor, Me., and the Commanding Officer, Greenwood RCAF Base, N.S., for use of base facilities by the PBY aircraft and personnel.

REFERENCES

Bigelow, H. B. 1927. Physical oceanography of the Gulf of Maine. *Bull. U.S. Bur. Fish.*, **40**(2): 511–1027.

Canada, Tidal and Current Survey Division of the Hydrographic Service, Department of Marine and Fisheries (1928). Tables of hourly direction and velocity of the currents and time of slack water in the Bay of Fundy and its approaches as far as Cape Sable.

Day, C. G. 1957. Drift bottle studies over the Gulf of Maine and Georges Bank. WHOI Ref. No. 57–1 (unpublished).

Fish, C. J., and M. W. Johnson. 1937. The biology of the zooplankton population in the Bay of Fundy and Gulf of Maine with special reference to production and distribution. *J. Biol. Bd. Canada,* **3**(3): 189–322.

Hachey, H. B., and W. B. Bailey. 1952. The general hydrography of the waters of the Bay of Fundy. *Fish. Res. Bd. Canada, MS Report* No. 455 (unpublished).

Ketchum, B. H., and D. J. Keen. 1953. The exchanges of fresh and salt waters in the Bay of Fundy and in Passamaquoddy Bay. *J. Fish Res. Bd. Canada,* **10**(3): 97–124.

MacGregor, D. G., and H. J. McLellan. 1952. Current measurements in the Grand Manan Channel. *J. Fish. Res. Bd. Canada,* **9**(5): 213–222.

Mavor, J. W. 1922. The circulation of the water in the Bay of Fundy. Pt. I. Introduction and drift bottle experiments. *Contr. Canadian Biol., N.S.,* **1**(8): 101–124.

Stommel, H. 1954. Serial observations of drift currents in the central North Atlantic Ocean. *Tellus,* **6**(3): 204–214.

Volkmann, G., J. Knauss and A. Vine. 1956. The use of parachute drogues in the measurement of subsurface ocean currents. *Trans. Am. Geophys. Union,* **37**(5): 573–577.

Walden, R. G., D. D. Ketchum and D. H. Frantz, Jr. 1957. Buoy telemeters ocean temperature data. *Electronics,* **30**(6): 164–167.

Contribution No. 929

Reprinted from
THE EFFECTS OF ATOMIC RADIATION ON OCEANOGRAPHY AND FISHERIES
PUBLICATION NO. 551, NATIONAL ACADEMY OF SCIENCES—NATIONAL RESEARCH COUNCIL, 1957

CHAPTER 12

ON THE TAGGING OF WATER MASSES FOR THE STUDY OF PHYSICAL PROCESSES IN THE OCEANS[1]

THEODORE R. FOLSOM, *Scripps Institution of Oceanography,* La Jolla, California

and

ALLYN C. VINE, *Woods Hole Oceanographic Institution,* Woods Hole, Massachusetts

FINDING, identifying, and plotting the courses of characteristic masses of water in the oceans are major activities of the physical oceanographer. Assistance from the new techniques that have come with the use of radioactive materials has been welcomed by him; some of these techniques have already been put into service for tracing the water. It is not generally realized how much experience has been gained, beginning with the 1946 tests in Bikini Lagoon, in tracing water masses contaminated with radioactive materials from weapons' tests. And many thoughts are now turning toward the radioactive tagging of ocean water by other means in regions where knowledge of underlying physical processes are meager, especially in the very deep waters. Proposals for the disposal in the sea of atomic energy wastes cannot be properly evaluated until estimates can be improved concerning the motion of this deep water.

Many of the advantages (familiar in the laboratory) of using radioactive identifying tags can be realized at sea, even though rendered difficult by the very large physical dimensions of the oceans. What appeals most to the oceanographer is his new ability, under certain circumstances, to make very rapid identifications of water lying on the surface or deep below his ship; thus allowing large volumes to be surveyed in three dimensions and in more detail than ever before possible.

Three layers in the ocean are distinguished clearly by structure and behavior: the mixed layer near the surface; the intermediate layer lying just below wherein the temperature changes rapidly with depth (this thermal stratification bringing about great stability) ; and finally, the large, nearly uniform bottom water mass extending to the sea floor with so little variation in density that very stable stratification is not possible. Each water mass reacts differently when disturbed, and therefore, mixing occurs differently in response to currents and mass intrusions. Experiments conducted in any one of these domains must take into consideration the special features that exist, and must call upon equipment most suited to these sections. Equipment specialized for radiological survey work in any of these oceanographic domains is still primitive. However, it can be said that equipment for detecting and measuring radiation is not a bit less highly developed than are the equipment and techniques needed for navigating a ship, and for maneuvering detectors at sea, especially at great depth. So much information now can be reported by radiological means in a short time that a ship now has more reason than heretofore for precise navigation. In some cases, the depth and position of the detector relative to the ship must be known instantly, and almost always must be controlled far better than has been accepted by traditional hydrography. It is difficult to record data in full detail in many cases, and in others it is difficult to evaluate features rapidly enough to alter maneuvers to best advantage; an oceanographer can now expect to be aware of a strongly active layer in less than one second after his electronic probe makes contact, and he even may make use of a fast moving airplane to outline radioactive areas on the surface.

---

[1] Contribution from the Scripps Institution of Oceanography, New Series, No. 905.

Contribution No. 929 from Woods Hole Oceanographic Institution. Part of Table 2 was computed with the collaboration of John Harley of AEC, New York City Operations Office, who gave much other counsel for which the authors are grateful.

Instrument Sensitivity and Natural Backgrounds

Many promising measuring schemes have been proposed. However, it is profitable to compare the equipment and techniques which have been used already at sea. At the top of Table 2 is presented the background radiations coming from cosmic rays and from the natural potassium in the sea, and the activity level now believed tolerable for drinking water also is given for comparison.

At the bottom of Table 2 are listed, in the brief numerical form in which they are commonly stated, the sensitivities of three measuring techniques which actually have been used for radiological exploration at sea. Many aspects of the measurement problem are oversimplified by a comparison of this sort, but the table does indicate that present shipboard beta analysis is capable of measuring beta tracer activity below the background beta activity due to the potassium in the sea water, whereas gamma detectors so far have been limited at levels above the gamma backgrounds of the sea. On surveys covering large distances, such as on Operation TROLL (U. S. Atomic Energy Commission 1956), and on the SHUNKOTU MARU Expedition (Mujoke, Sugiura, and Kameda 1954), there is ample time for water analyses, and advantage can be made of beta techniques. Nevertheless, there are many circumstances where direct measurements by gamma devices are necessary for rapidly locating small contaminated water masses, and it is likely that gamma techniques will be perfected so as to allow use at levels far below their present capability.

There are occasions at sea in which a gamma detector must indicate the presence of tracer activity within a few seconds after making contact. The limitations imposed by this sort of time restriction in the presence of statistical fluctuations in the signals are discussed in Appendix A, and are summarized in Table 3.

Other important details concerning the radioactive background in the sea have not been thoroughly explored. It may be too late to estimate the background level that existed a decade ago for some isotopes, and this should not be forgotten in planning future surveys. Of particular interest are background conditions near the sea floor where radium and thorium activity are known to accumulate in sediments; but little is known in detail about the lateral distribution of bottom activity.

More complete utilization of weapons' tests for the marine sciences

It appears likely that large weapons will continue to be tested in oceanic areas and that radioactive materials will be strewn from time to time over the surface of the sea. Valuable oceanographic data already has come from such sources; for example, direct measurements have been made of the rate of mixing downward from the surface to the thermocline, and also, direct information has been obtained regarding mass motion and lateral mixing. One special feature of benefit in studying weapons tests is the unique initial boundary condition provided by the arrival of fallout activity almost simultaneously over an area having dimensions very large compared with the depth of water involved; downward mixing appears as a relatively simple phenomena following this initial condition, and can be studied under almost ideal circumstances.

Two expeditions mentioned above have proven that further information concerning lateral mixing and flow can be gained for many months after a weapons' test, and obviously this fact should be exploited fully by marine scientists of all nations. Ancillary benefits might come from more or less fixed monitoring stations; if, for example, following the 1954 test, repeated sampling had been done off Guam it would have furnished data of value for interpolating observations made in the two follow-up cruises mentioned.

Bottom exploration following weapons' tests has not been given deserved attention, and insufficient attention has been paid to getting even purely oceanographic information from these sources into the form needed by those people who are charged with making decisions regarding the ominous waste disposal problem.

Hazards involved in the deliberate tagging of ocean waters

Safety of the research staff is always a consideration; at sea because of special circumstances the handling of extremely large amounts of activity is not too difficult or hazardous. Protection can be secured very cheaply by towing the larger sources of radioactivity aft of the ship, preferably slightly submerged on a suitable barge or special vessel. Bringing large quantities of activity to the waterfront promises to be more expensive, but practical experience in this should be valuable for later planning of large-scale disposals.

The more controversial question of how much radioactivity can safely be introduced into the sea is not without reasonable solutions; but the recommendations depend upon the circumstances, especially, upon the particular part of the oceans to be studied. At the outset, barren areas of ocean rather than those productive of things leading to human food must be selected since the former can yield equally good information regarding purely physical phenomena.

Deliberate tagging of surface waters (Operation PORK CHOP)

Surface waters mix in a turbulent manner due to forces not yet fully understood. Better knowledge of this layer is badly needed justifying the consideration of water tracing experiments involving introduction of fairly large amounts of activity. Greatest care must be exercised here because these waters are those most close to humans, in several senses.

Rate of mixing to the bottom of the mixed layer, and rate and character of lateral motion as functions of the usual parameters of the sea are of most immediate interest, and observations lasting even a few days or few weeks would be of great value at the outset, especially if repeated frequently. A simple surface water experiment now will be proposed in briefest possible outline.

Figure 1 presents schematically some of the procedure which might be used and some of the phenomena to be expected. Guided by suitable navigational aids, here represented by deep-anchored buoys No. 1 and No. 2, the ship A proceeds on a straight course while dropping two quantities of radioactive materials (a and a′) mixed with enough surface water to leave near the surface a small contaminated patch having nearly neutral buoyance. These are essentially point-source initial conditions in this scale of dimensions; although, they are not as convenient as the plane-source initial conditions

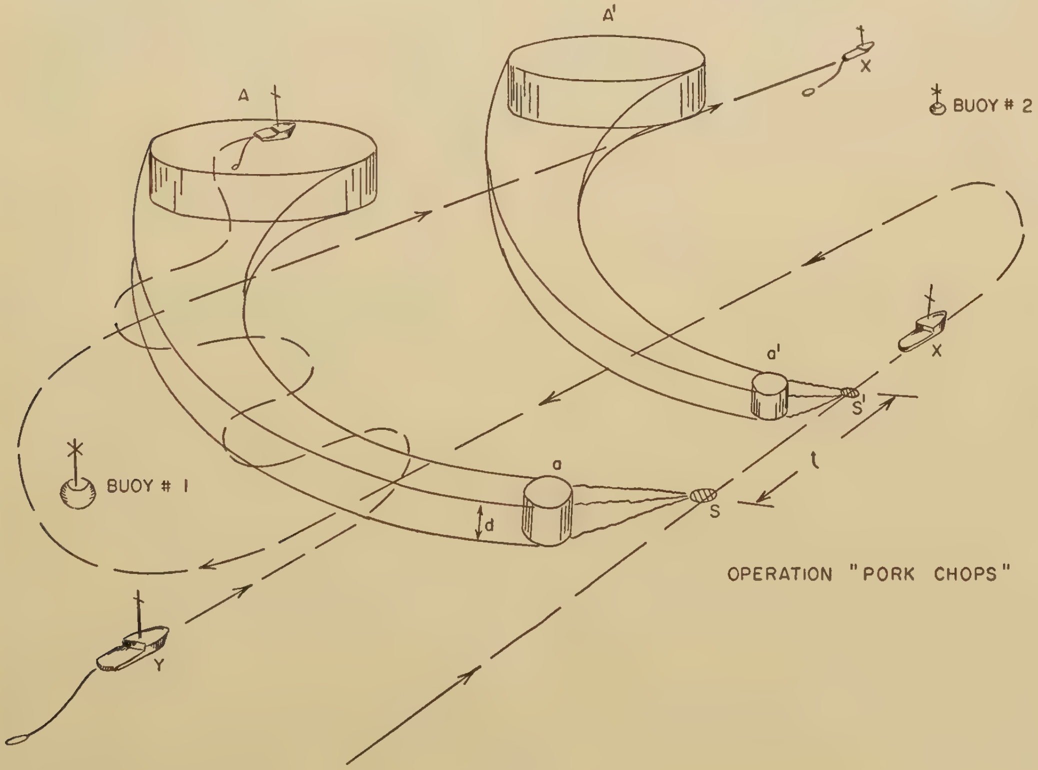

FIGURE 1

provided by fallout, they have some mathematical simplicity. It would appear economical and informative to drop two sources almost simultaneously, some distance apart — say one to ten kilometers; this would permit large-scale advection also to be studied at little extra ship cost.

From the sources s and s′ will grow a larger more dilute patch of water finally ceasing to penetrate rapidly downward at depth d. The rate and lateral spread prior to this time as functions of wind velocity are of special interest. After further downward penetration is retarded, the areas a and a′ move and expand to the larger areas A and A′ conserving most of the original radioactive material, and the product of activity and area should be almost constant after correction is made for the known rates of decay of radioactive constituents.

Dual ship operations

Experience has shown that operations on the scale of this sort can scarcely hope to be successful unless more than one ship is used; even with the best facilities one ship may lose contact with the invisible patch and waste valuable time locating it. One ship, X, must stay in or near the tagged mass while the other one, Y, may survey the area in detail, inspecting sections across the mass, studying the bottom for reference features, and chasing missing buoys if necessary.

Ultimate disposal of hazard in surface waters

Reduction of activity to a level below that of the natural activity of sea water is one criterion which has been used for planning disposals (Glueckoff 1955), and this is fairly reassuring provided the specifically dangerous and the long-lived activities are eliminated, for example, after radiostrontium and radiocesium are removed from raw fission wastes. Present evidence permits the conclusion that in the open ocean, when winds are above the critical white-cap level and under circumstances where mixing ceases at a depth of about 30 to 50 meters, as much as 1,000 curies would mix to a safe dilution in less than 40 days. An example of the dispersal rate in the open sea will now be given.

Brief outcome of an experimental tagging of surface waters in the open sea

Surface water made active by introducing fission products concentrated within a few square kilometers was intercepted by a ship 36 days after inoculation and traversed for 10 days. After corrections were made for the drift of the water during the survey, and for radioactive decay, a synoptic picture could be drawn roughly locating the contours of activity. This estimate of radioactive distribution was referred to the time of 40 days after the start of dispersal.

The contamination had mixed significantly only to about 30 to 60 meters, although the thermocline lay nearer to 100 meters depth. The following tabular description of this synoptic sketch can be made.

TABLE 1 APPROXIMATE DISTRIBUTION OF RADIOACTIVITY FOUND IN THE SURFACE WATERS OF THE OPEN SEAS 40 DAYS AFTER BEING INTRODUCED SUDDENLY AS A "POINT SOURCE." (A SYNOPTIC PICTURE COMPUTED FROM MEASUREMENTS MADE ON SEVERAL DIFFERENT DAYS.)

Areas inside contours of equal concentration in square kilometers.	Areas inside the contours as percentages of the area of the maximum contour.	Concentration of radioactivity (as per cent of the maximum concentration measured).
40,000 (km^2)	100%	10%
24,000	65	20
14,000	38	30
8,000	22	40
800	2	60
490	1	80
35	0.1	100

At the end of 40 days, the center of gravity of this distribution was about 120 miles from the point of inoculation and the pattern was about four times longer than broad. The wind was 3 and 4 of Beaufort's scale for the first 20 days, but was much calmer for the last 20 days.

If the average mixing depths are taken as 50 meters, then, 1,000 curies distributed over 40,000 square kilometers would result in an average concentration of $1.5 \times 10^{-10}/\mu c/ml$. This would certainly be safe sea water in most senses; and even in the smaller areas where much less than the average dispersal took place the water should also be safe. In fact, the experiment indicated that it is likely that after 40 days, following the introduction of 1,000 curies of activity into the surface waters of the open sea, only about 0.1 per cent of the total area should retain contamination above the tolerance concentration permitted for potable water, and even in this small region the residual artificial activity would amount to less than the normal natural activity of sea water.

It is evident from Table 2 and Table 3 that shipboard beta measurements would suffice to detect the more radioactive spots if there were initially 1,000 curies of slowly decaying beta activity; it is apparent, however, that direct measurements by gamma detectors might be sufficient for several days or even weeks. Surface experiments are by far the easiest to conduct and implement — they are limited largely by considerations of hazard to humans. Two more difficult experiments will now be described.

Investigations in the thermocline layer by use of radioactivity

The thermocline lying between perhaps 100 meters depth on an average, and 800 meters or more, can be thought of as being a lid which restrains deeper water from reaching the surface. Experiments in this stable region must take into consideration the fact that any liquid introduced here will seek the level of its own density and will then spread out in a very thin layer. An experiment in this layer has been

TABLE 2 Approximate Sensitivities of Three Detecting and Measuring Techniques Presently Available for Use At Sea Compared With the Activity of Sea Water and With That of Fresh Water.

A *Common background radiation levels:*				
d/m/l	curies/l	microcuries/ml	rad/hr[2]	mrad/yr[3]
Activity in normal sea water due to potassium:[1]				
Gamma rays 70..........	3×10^{-11}	3×10^{-8}	1×10^{-7}	0.9
Beta rays 660............	3.0×10^{-10}	3.0×10^{-7}	—	—
Maximum permissible[4] *concentration of unknown mixed beta activities in drinking water:*				
Beta rays 220............	11×10^{-10}	1×10^{-7}	—	—
Cosmic ray background at sea surface:[5]				
At equator 61............	—	—	—	33
At 55°N (mag)..........	—	—	—	37
B *Sea water activities at which present measurements are significant.*				
Shipboard water analysis[6] *for mixed beta emitters, 60 minutes count after removal of potassium:*				
50 ± 15	2×10^{-11}	2×10^{-8}	—	—
Uderwater gamma detector,[7] *1956 scintillation rate-meter of AEC-NYOO:*				
220 (approx) .... (0.6 MEV gammas assumed)	—	—	1.4×10^{-7}	1.2
Underwater gamma detector,[8] *1955 geiger instruments of SIO. (counting pulses):* (See also table 3 for other cases)				
Case A: Used in deep water where net background is 15 CPM, assume photons of 0.6 Mev; assume short measurements required, $t = 5$ sec.				
6600	3×10^{-9}	3×10^{-6}	3.8×10^{-6}	30
Case B: Towed on surface, assume constant background 60 CPM, assume photons of 0.6 Mev; assume long measurements permitted, $t = 5$ min.				
520	2×10^{-10}	2×10^{-7}	0.3×10^{-6}	3

[1] Assuming normal sea water has 3.8×10^{-4} gk/g sea water, that beta activity is 29 d/s/gk and that gamma activity is 3 d/s/gk.

[2] The rad unit is somewhat larger than the more familiar roentgen unit; 1 rad = 1.1 roentgen approximately for gamma rays. Values in this column were computed upon the assumption that the activity was uniformly distributed in the water and that the detector was a meter or more from any boundary.

[3] Referring to beta ray activity in rad units in roentgen units is a dangerous practice—much further specification depending upon the individual experiment is required.

[4] Handbook 52 of the National Bureau of Standards. The values given refer to the case where the nature of the activity is unknown; certain radioisotopes can be tolerated at much higher levels.

[5] See Table 1 in the accompanying paper "Comparisons of Some Natural Radiations Received by Selected Organisms" by T. R. Folsom, and John H. Harley for variation of cosmic rays with depth and altitude.

[6] Cosmic rays are counted by most geiger counters at the average rate of approximately one count/min/sq cm of counter area.

[7] This information was supplied by J. H. Harley from personal communication with H. D. LeVine of the New York City Operations Office of the Atomic Energy Commission who designed this equipment.

[8] This detector was not intended previously for use at low intensities, but rather for measuring a wide range of intensities of gamma rays. Additional geiger tubes might easily be added to increase the sensitivity by at least five fold. Still more sensitive gamma devices are now used in oil well logging.

TABLE 3 COMPARISON OF MINIMUM DETECTABLE CONCENTRATIONS USING SEVERAL MEASURING TIMES AND ASSUMING SEVERAL BACKGROUNDS

(a) Minimum detectable anomolous activity if potassium of the sea produced the only background, i.e., $B = 1.2 \times 10^{-3}$ gammas/sec/ml.

Counting time in secs. t	Minimum detectable concentration γ/sec/ml C_a	$= \gamma$/min/l	Net signal counts/min $C_aVe = 30C_a$	Total net counts $30C_at$	Rads/hour	
					Photons .6 mev	Photons 1.5 mev
3	.19	11,000	5.7	17	6.5×10^{-6}	16×10^{-6}
5	.11	6,600	3.3	17	3.8	9.5
60	.010	600	0.3	18	.3	.8
180	.0039	230	.12	22	.13	.33
300	.0026	160	.078	23	.09	.22
600	.0016	99	.048	30	.06	.14
Very large	$0.025/\sqrt{t}$					

(b) Minimum concentration detectable if backround were 15 CPM, i.e., an actual background signal experienced in deep water.

	C_b					
3	.19	11,000	5.7	17	6.5×10^{-6}	16×10^{-6}
5	.11	6,600	3.3	17	3.8	9.5
60	.010	590	.29	17	.33	.84
180	.0058	350	.17	32	.20	.50
300	.0049	290	.15	45	.17	.42
600	.0032	190	.096	58	.11	.28
Very large	$0.067/\sqrt{t}$					

(c) Minimum detectable concentration if total background were 60 CPM, i.e., an actual background signal experienced at the sea surface.

	C_c					
3	.205	12,000	6.1	18	7.1×10^{-6}	18×10^{-6}
5	.133	8,000	4.0	20	4.6	12
60	.0222	1,330	.67	40	1.9	7.5
180	.0116	700	.35	63	.4	1.0
300	.0087	520	.26	78	.3	.74
600	.0059	354	.17	102	.2	.51
Very large	$0.13/\sqrt{t}$					

described in some detail by Revelle, Folsom, Goldberg, and Isaacs (1955), and discussed in several of the accompanying papers. It will be discussed here only in the matter of difficulty of survey. Although mixing is known to be very slow in the thermocline, it is not certain how direct is the path from this *fringe* biosphere to human food supply, so that the hazard of a long remaining concentration of activity is not easily evaluated. Revelle et al., prefer to suggest the experimental use of the conservative amounts of 10 to 100 curies, and they then show that such small sources of radioactivity might be practical none the less.

Actual field experience has shown that layers as thin as one or two meters thick are extremely difficult to sample for water analyses even after being located by gamma ray detectors. Folsom (1956) has emphasized that future deep surveys with radioactive tags must rely heavily upon discovery of radioactive water by means of gamma detectors, and has urged that specialized forms of these be brought to perfection.

In this particular layer, geometric factors are not adverse for maneuvering a detector into the water mass to be studied; a probe is dropped rapidly and more or less vertically so as to intersect and pierce a rather broad horizontal lamina, sharply confirming the activity. Some difficulty would be encountered in holding the probe in the thin layer long enough to permit accurate measurements after the activity falls to such a low level that statistical fluctuation becomes the predominant source of error; however, the major difficulty even at these depths is holding the ship in the general area of active pools of small size. Any area of less than a square mile below the surface is a tiny detail in the open sea, and oceanographers never before have realized how hard it is to navigate and maneuver to study areas so small. Multi-ship operation, the use of the best position-locating gear, and careful crew training and teamwork are necessary for subsurface radiological surveys even at these moderate depths.

Outline of tagging experiment in the thermocline layer

Figure 2 illustrates certain features which must be considered in this region. The ship, A, may lower a gamma sonde through an activated pool and detect its presence by the receiving of a signal like that shown on the right side of the figure; the hydrographer may obtain a water sample by triggering electrically a water sampler at the moment the detector indicates that the sampler is within the active layer. The data in Table 3 make it clear that rapid response is important during this sort of measurement; a statistically significant signal must be accumulated in the short period during which the probe is passing through the active layer.

Attention is called to the need for navigational and maneuvering aids here by including schematically the parachute-drogue C. It is difficult to maneuver a weighted detector horizontally in order to study the lateral distribution in detail. The use is suggested of towed gamma detectors depressed to the desired level by hydrofoils controllable from the surface, more or less as illustrated schematically at the left of Figure 2. By means of a swivel-clamp, SC, a pennant several meters long containing a row of Geiger tubes or other gamma detectors, might be suspended above the depressor so as to present a vertical, linear array, thus giving a high probability of intersecting wide lateral distributions of activity. This sort of gear should not be too awkward nor fragile for deck handling at sea. Signals might be recorded partially, or entirely inside the depressor, or reported to the ship electronically or sonically.

Ship A or a sister ship with similar gear might stay in the pool during the whole experiment, however, if the pool were lost after its depth was established, then Ship B would likely be the first to find it again with its towed detector.

Difficulties in sounding and exploring very deep waters

Bottom exploration so far has been confined largely to sonic plotting and sounding by solid cable; very deep wire casts are very time consuming and difficult; the ship generally is moved laterally by surface currents before the

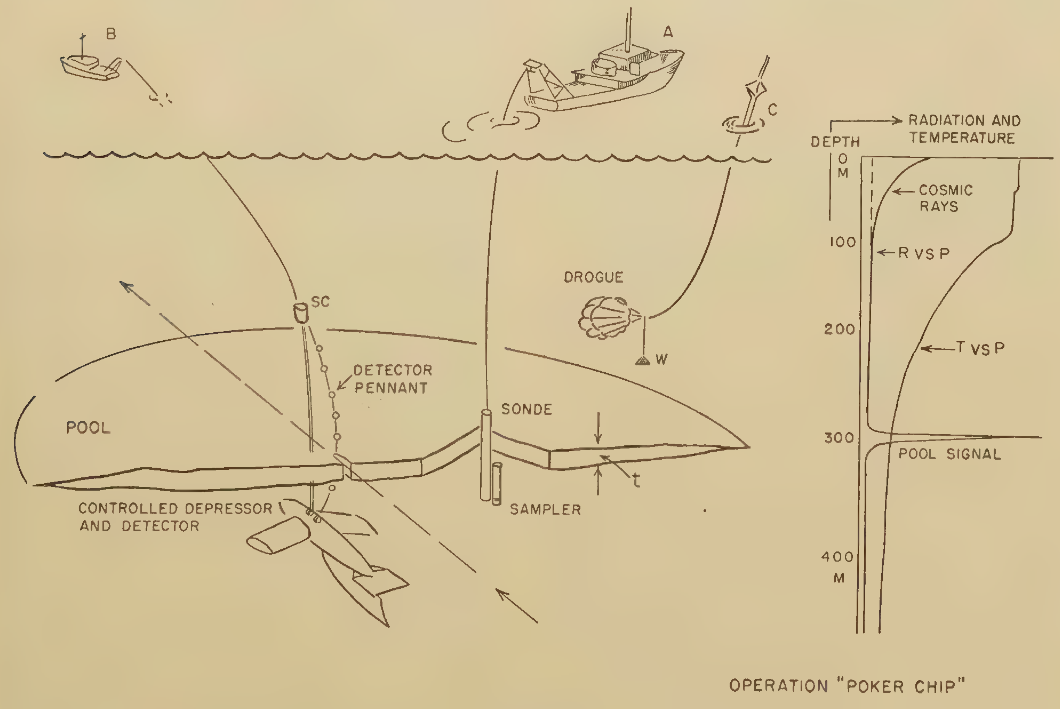

OPERATION "POKER CHIP"

FIGURE 2

wire touches bottom. Oceanographers seldom hope to place their sondes and coring tools upon any pre-selected topographic detail of small area. However, it is quite likely that a technique can be perfected for dragging a detecting instrument along the bottom in many areas of the oceans' floor, and with a dragged detector a large region might be traversed rapidly, and tagged water masses near the sea floor might be located and surveyed. A proposal for tagging bottom waters now will be outlined.

Difficulties in tagging bottom waters

Fortunately, little hazard to human populations would result from putting into the deep bottom waters in certain latitudes almost any amount of activity which might be readily available in the near future, or which would be easy to handle safely ashore and on ordinary surface vessels. After all, these amounts would be only the feeble forerunners of what may have to follow.

The problem is that of displaying even a relatively large radioactive source economically in face of the immensity of the abyssal reaches. One can think of many things which must not be done; heavy, radioactive liquid cannot be merely poured overboard, for example. Matching density at intermediate layers or attempting to insert a strata at a selected depth also would appear experimentally difficult in view of the limited knowledge presently available; an unequilibrated liquid mass might wander about like a sinking dinnerplate — and soon become lost. In the absence of the restraining forces found in more stable waters, the pouring of streams of dense solution downward from a height above the bottom, or alternately the releasing of lighter material upward from the bottom would surely cause mass motion which might not cease until the streams had moved long distances and perhaps had curled into configurations quite unsuited as initial boundary conditions for water tracing experiments. Furthermore, activity spread initially in more or less vertical lines would make very poor targets for detectors trailing on the end of wires three miles long, and would be wasteful in terms of radioactive material and of expedition time.

One might, of course, carefully select a perfect basin, and might gently introduce into it a dense radioactive solution. This certainly should be considered since only a small amount of activity might suffice for tagging the waters in a small basin and valuable information regarding motion and dispersion in basins might result, but results would not lead to a realistic picture of the large scale flow over bottom which may have to disperse the wastes dumped in the future. The results of an experiment set up in this way would be inadequate, and, in fact, might be misleading in a dangerous direction.

Production and use of horizontal line-sources near the bottom

"Operation HARE and HOUND"

It is evident that distribution of activity in a horizontal line near the bottom would be most easy to intercept by a detector dragged along the bottom, and it appears also to be something which would be relatively easy to produce, and economical. It should be possible to hold tagged water near the bottom by mixing it with a very dense solution; and there are two ways immediately evident for effectively spreading streaks of dense solution for long distances over the bottom terrain.

Figure 3 illustrates the two methods proposed for tagging bottom water, and the method proposed for locating the tagged masses later. The Ship B' is shown dragging a "Hare" D, across the bottom leaving behind a streak of contaminated water. Alternately, Ship B is shown just after it has dropped to the sea floor a specialized water blending device which might well be called a "quern" [1], C, which generates for a few minutes or hours, a stream of dense, radioactive solution on the slope of a carefully selected large topographical ridge b — d; this stream flows away very much like one of the submarine currents which are now called "turbidity currents" by geologists. Violence of this sort of free current might theoretically be controlled through wide limits by adjusting the densities of the solution. The essential features of a water-tagging quern are shown in the upper right of Figure 3. Radioactive material, AS, is combined in predetermined proportions with a heavy salt solution by metering pump, P, and the two are then fed to a fan-type mixer, and are there blended with a large volume of

---

[1] Old English name for a mill for grinding all sorts of things. (Ruggoff, 1949.)

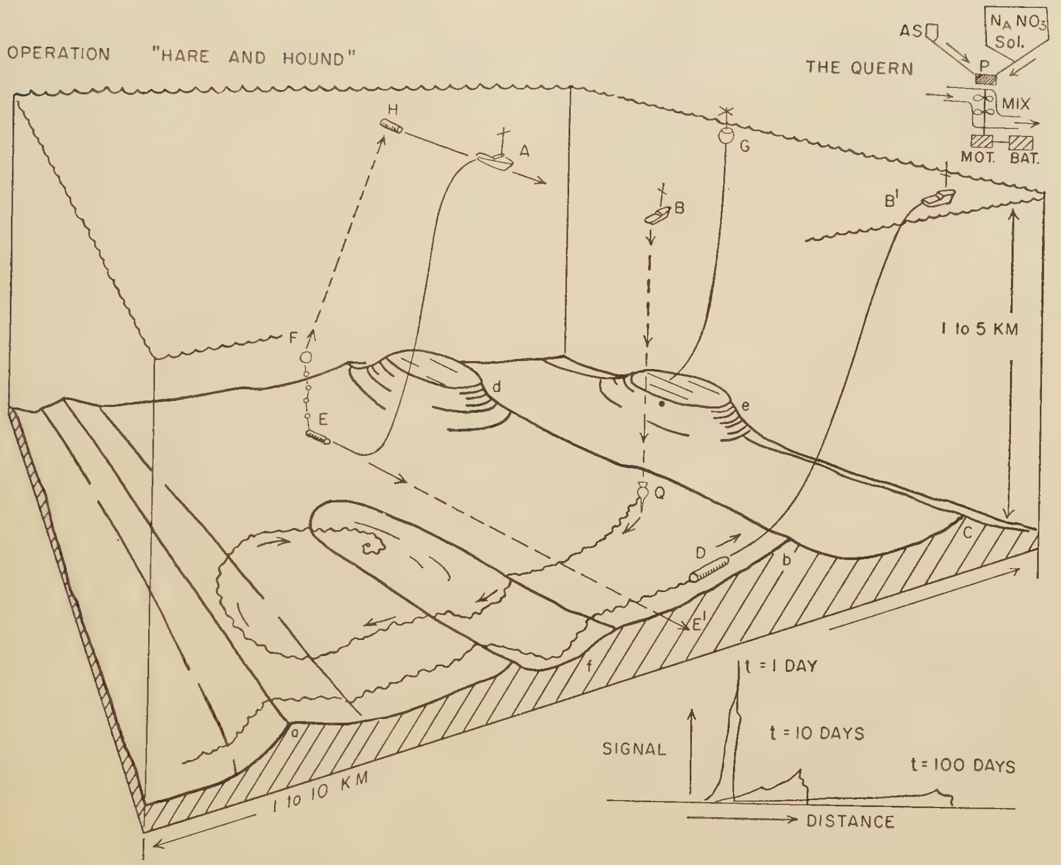

FIGURE 3

local water. There are several reasons for preferring a design leading to inexpensive construction and single use; the cost of decontamination of apparatus of this type would outweigh any benefit from repeated use. Suggestion is made of the use of a salt such as sodium nitrate which has both high solubility, and an endothermic heat of solution which would serve to overcome the adiabatic heat set free during lowering. It would appear that one or more tons of a nitrate salt, mixed into bottom water by use of a few kilowatt hours of energy, stored in oil-sealed accumulators, could produce a compact body of very heavy water which would rush like a freight train across the terrain dropping a streak of traceable radioactive eddies as it traveled.

A fixed, water-mixing quern, of the sort described, might produce a tagged water mass behaving in a manner appearing realistic to both the disposal planner and the submarine geologist; however, its use is not likely to lead directly to the extremely simple results needed for the very first experiments. The employment of a dragged hare might be preferable at the outset — and its metering machinery might be somewhat less elaborate than that of the quern just described.

One might contemplate using 1,000 or more curies for making streaks several kilometers long so that location would not be difficult with a simple gamma device dragged by a ship. In Figure 3, Ship A is shown dragging such a detector which might be called a "hound" for obvious reasons. For very great depths, no electrical wire is presently available with the durability equal to that of an ordinary dredging cable. It would, therefore, be wise to first consider the use of a compact multichannel chart recorder inside the dragged pressure shell E so as to make permanent records of signals picked up by a set of gamma detectors suspended by an oil-filled float F. Numerous accessories might profitably ornament this sort of gear, but the one which might prove most rewarding would be a sound producer capable of reporting the moment of contact with the tagged water mass; even a crude sonic signal sent from a transducer on the float, F to the ship, A, via the towed hydrophone, H, would suffice. Details of the gamma signals need only be recorded so that they might be inspected later on the recorder chart, however, it would be important for the navigator to recognize instantly when contact was made so that he could maneuver the ship economically.

The operations proposed above are not unlike those used successfully by cable ships when retrieving submarine wires. Careful preliminary surveys of the whole area, the selection of identifying landmarks, and the laying of the marking buoys also appear essential for success in work of this type.

The final results might have the general character of the hypothetical signals shown graphically at lower right in Figure 3. Change in amplitude and displacement, and skewness of the signal records should lead to estimates of both velocity and rate of mixing. If each survey included ten or more intersectings, and if each contact brought separate gamma signals from several detectors distributed along the hound's vertical "tail," then the data of the sort needed would accumulate quickly.

Rough estimate of effectiveness of 1,000 curies for tagging bottom waters

It appears possible to distribute radioactivity uniformly along the course of a device dragged over the sea bottom, and it would appear possible also to deposit the material so gently that it would come to rest within a few meters of the precise course. If, for a rough evaluation, we assume that local diffusion sooner or later produced a uniform distribution within a radius of 10 meters, and that the total activity, M, was 1,000 curies, then the length of the water mass which might be tagged can be stated

$$l = \frac{M}{C\pi r^2}. \qquad (1)$$

where C is the average concentration of activity within the tagged mass.

If now we assume that only 10 seconds can be allotted for traversing 20 meters (that is the ship's speed is about 4 knots), then the equation (9) of Appendix A indicates that a single detector like the 1955 SIO Geiger instrument could detect, in the presence of a realistic deep-water background of 15 cps, a limiting gamma source concentration of 0.061 disintegrations/sec/ml, or $C=0.061/3.7\times10^{-10}$ curies/ml, and the length of traverse which could be tagged with 1,000 curies would be, under these assumptions,

$$l = \frac{1000}{1.65\times10^{-12}\pi(1000)^2} = 1900 \text{ Km} \qquad (2)$$

It would appear feasible to locate and allocate by ordinary navigational means a geographical line in the deep sea floor of less than two kilometer's length, so that the hypothetical example just given suggests that 1,000 curies could equally well be used to produce a very concentrated streak of activity having a length of two or three kilometers which might still be detected with ease after it had diffused, mixed, or decayed to less than one percent of its initial concentration. Thus it can be concluded that 1,000 curies, or even less activity, put into bottom water would be quite adequate for tracing movements on a scale large enough to contribute information useful in disposal planning.

SUMMARY AND CONCLUSIONS

1. Consideration has been given some of the problems involved in tagging water masses in the open ocean.
2. The problems are different in the three major strata; the surface layers, the thermocline, and the deep water layer.
3. It appears that under certain circumstances water tagged with even moderate quantities of activity can be followed for at least several weeks; surface waters contaminated by large activities such as result from fallout can certainly be followed for a year or more.
4. Much field experience in radiological oceanography has been gained already. A fairly clear direction for development of instruments has been indicated.
5. The need is seen for attention to the perfection of navigational aids, for use of specialized vessels and gear, and for the use of several vessels simultaneously in oceanic surveys of this sort.

APPENDIX A

In practice, many factors tend to limit the effectiveness of an under sea gamma detector, but the random fluctuation of a feeble radiation may alone prevent its recognition in the presence of a background of similar magnitude. The lowest detectable concentration, limited only by statistical considerations, may be expressed in terms of the strength of the background, the time permitted for measurement, and the measuring efficiency of the instrument.

Let the sea water be contaminated with a concentration of radioactivity N curies/ml, and let this activity cause m counts/sec to be indicated by the instrument, and let the average background be b counts/sec. The relative accuracy, n, of a single measurement made during t seconds will depend upon signal strength and background strength; if the fluctuations are purely random, the error, 95 per cent of the time will be equal to, or less than,

$$n=\frac{2\sigma}{mt}=\frac{2\sqrt{\sigma_M^2 \div \sigma_B^2}}{mt}=\frac{2\sqrt{mt \div bt}}{mt} \qquad \text{A.1}$$

and solving for the net signal gives,

$$mt=\frac{2+2\sqrt{1 \div n^2bt}}{n^2}. \qquad \text{A.2}$$

Now, the counting efficiency of the instrument logically should be derived from the ratio of counts recorded to the photons striking the instrument. This ratio would be impossible to evaluate, but it is approximated when the instrument is small, and easily penetrated by,

$$e=\frac{mt}{3.7\times 10^{10}Nvt} \qquad \text{A.3}$$

that is by the ratio of the net counts recorded to the photons emitted in a volume of liquid, v, equal to that displaced by the detector. Solving this equation for concentration,

$$N=\frac{mt}{3.7\times 10^{10}vet} \qquad \text{A.4}$$

curies/ml, and substituting here the value for net count, mt, obtained in equation (2) when the background rate is b, and accuracy is, n, the limiting concentration can be expressed,

$$N=\frac{2+2\sqrt{1+n^2bt}}{3.7\times 10^{10}n^2vet} \qquad \text{A.5}$$

curies/ml, wherein b expresses the background rate actually indicated when the instrument is surrounded by clean sea water. If no other background exists except that coming from a surrounding solution having specific activity B, and if the instrument counts this activity with the same efficiency, e, than the limiting detectable concentration becomes, in curies/ml,

$$N=\frac{2+2\sqrt{1+Bn^2vet}}{3.7\times 10^{10}n^2vet}. \qquad \text{A.6}$$

Numerical examples applying to an actual undersea instrument

The sensitive portion of the 1955 model of the Scripps Institution of Oceanography's Geiger instrument has a volume of about 1,000 ml. The ratio e, applying to hard gamma rays, was measured directly by submerging the instrument in a tank containing potassium solution of known concentration, and was found to be approximately 0.03.

If by "detection" is meant the measurement of the concentration with an error of not more than 50 per cent, then, n=0.5.

Formulas (5) and (6) may now be applied to three characteristic background circumstances:

Case 1: Here no other background is evident except that caused by a solution having specific activity $B=1.2\times 10^{-3}$ gammas/sec/ml such as comes from the natural potassium in normal sea water. From (6), the limiting detectable concentration,

$$C_1=\frac{2+2\sqrt{1+0.009t}}{7.5t} \qquad \text{A.7}$$

gammas/sec/ml, and when t becomes very large this approaches,

$$C_1=\frac{0.035}{\sqrt{t}} \qquad \text{A.8}$$

Case 2: In deep water cosmic rays may be neglected, and the S. I. O. probe is likely to indicate a total background of about 15 CPM, or b=0.25 counts/sec, therefore, the concentration just delectable is,

$$C_2=\frac{2+2\sqrt{1+0.063t}}{\sqrt{t}} \qquad \text{A.9}$$

gammas/sec/ml, which approaches as t increases to a large value,

$$C_2=\frac{0.067}{\sqrt{t}} \qquad \text{A.10}$$

Case 3: In shallow water where cosmic rays are unattenuated, the background on the S. I. O. probe amounts to about 60 CPM, or b=1.0

counts/sec, therefore the minimum detectable concentration becomes,

$$C_3 = \frac{2+2\sqrt{1+0.25t}}{7.5t} \qquad \text{A.11}$$

gammas/sec/ml which approaches for very large values of t,

$$C_3 = \frac{0.13}{\sqrt{t}}. \qquad \text{A.12}$$

Tabulations

Table 3 compares the effect of increasing the period of measurement with the effect of diminishing the background. It is evident that a substantial change in background has relatively small practical effect on any measurement made so rapidly that only a very poor sample is taken out of the fluctuating signal; however, when sufficient time can be alloted for good sampling, the background level becomes the limiting factor. It should not be overlooked that in practical field work, instrument imperfections may contribute to the overall error more or less proportionally with time of measurement, and that measurement time must be spent economically on almost all oceanographic expeditions. It is apparent therefore that efforts should be made towards increasing the counting rate, ve, while reducing the relative value of the background count by all possible means. Technique for cleanliness and for discrimination of background by electronic means have not yet been fully developed for this purpose.

REFERENCES

FOLSOM, THEODORE R. 1956. Problems peculiar to direct radiological measurements at sea. Paper presented at Nat. Acad. of Science Meeting, 29 Feb.-1 Mar. 1956. Washington, D. C. Proceedings (in press).

GLUECKOFF. 1955. Long term aspects of fission product disposal. United Nations Conference on the Peaceful Uses of Atomic Energy, Geneva. Paper No. 398: 11 pp.

MIYAKE, Y., Y. SUGIURA, and K. KAMEDA. 1954. On the distribution of radioactivity in the sea around Bikini Atoll in June 1954. Paper in meteor and geophys., Meteorol. Research Institute, Tokyo, 5:253–262.

REVELLE, R. R., T. R. FOLSOM, E. D. GOLDBERG, and J. D. ISAACS. 1955. Nuclear science and oceanography. United Nations International Conference on the Peaceful Uses of Atomic Energy, Geneva. Paper No. 277:22 pp.

RUGGOFF, MILTON D. (Editor) Why the sea is salt (an abstract from a translation from the Norse by Sir George Weble) pp 672–676 in Harvest of World Folk Tales. XViii+734 pages, Viking Press.

U. S. ATOMIC ENERGY COMMISSION and OFFICE OF NAVAL RESEARCH. 1956. Operation TROLL. Health and Safety Laboratory, U.S.A.E.C., New York Operations Office, NYO-4656, Ed. by J. H. Harley: 37 pp.

U. S. DEPARTMENT OF COMMERCE. 1953. Maximum permissible amounts of radioisotopes in the human body, and maximum permissible concentrations in air and water. National Bureau of Standard Handbook 52:445 pp.

Report for the year 1957

THE
WOODS HOLE OCEANOGRAPHIC INSTITUTION

REPORT FOR THE YEAR
1957

1958

TABLE OF CONTENTS

PAGE

I. Trustees, as of December 31, 1957 3

II. Members of the Corporation, as of December 31, 1957 . . . 4

III. Research Staff 6

IV. Director's Report 10

V. Treasurer's Report 36

I. TRUSTEES

(As of December 31, 1957)

Honorary Trustees

Henry B. Bigelow, Museum of Comparative Zoology, Cambridge 38, Mass.
L. O. Colbert, 4408 29th Street, N. W., Washington, D. C.
Marion Eppley, 510 Park Avenue, New York, N. Y.
Alexander Forbes, 610 Harland Street, Milton, Mass.
Arnaud C. Marts, 521 Fifth Avenue, New York, N. Y.
Lawrason Riggs, Riggs, Ferris and Geer, Room 1201, 74 Trinity Place, New York 6, N. Y.
Henry L. Shattuck, 10 Milk Street, Boston, Mass.

To serve until 1961

Frank A. Howard, 30 Rockefeller Plaza, New York, N. Y.
Robert R. Shrock, Department of Geology and Geophysics, Massachusetts Institute of Technology, Cambridge 39, Mass.
Edward H. Smith, Woods Hole, Mass.
Raymond Stevens, c/o Arthur D. Little, Inc., 30 Memorial Drive, Cambridge 42, Mass.
E. Bright Wilson, Jr., Department of Chemistry, Harvard University, Cambridge 38, Mass.

To serve until 1960

Detlev W. Bronk, The Rockefeller Institute of Medical Research, 66th Street and York Avenue, New York 21, N. Y.
Noel B. McLean, Edo Corporation, College Point 56, New York
Daniel Merriman, Bingham Oceanographic Laboratory, Yale University, New Haven, Conn.
Emanuel R. Piore, International Business Machines Corporation, 590 Madison Avenue, New York 22, N. Y.
Alfred C. Redfield, Maury Lane, Woods Hole, Mass.
Gerard Swope, Jr., c/o International General Electric Co., 570 Lexington Avenue, New York, N. Y.

To serve until 1959

J. S. Coles, Bowdoin College, Brunswick, Maine
Carl H. Eckart, Scripps Institution of Oceanography, La Jolla, Calif.
Ross G. Harrison, Osborn Zoological Laboratory, Yale University, New Haven, Conn.
Milford R. Lawrence, Siders Pond Road, Falmouth, Mass.
Harlow Shapley, Sharon Cross Road, Peterborough, N. H.
Francis C. Welch, 73 Tremont Street, Boston, Mass.

To serve until 1958

Charles F. Adams, Raytheon Manufacturing Company, 138 River Street, Waltham 54, Mass.
Horace S. Ford, 77 Massachusetts Avenue, Cambridge 39, Mass.
Albert E. Parr, American Museum of Natural History, Central Park West at 79th Street, New York, N. Y.
Athelstan F. Spilhaus, Institute of Technology, University of Minnesota, Minneapolis 14, Minn.
Selman A. Waksman, Institute of Microbiology, Rutgers University, New Brunswick, N. J.

Ex Officio

Edwin D. Brooks, Jr., P. O. Box 1135, Boston 3, Mass.
Mary Sears, Woods Hole Oceanographic Institution, Woods Hole, Mass.
Columbus O'D. Iselin, Woods Hole Oceanographic Institution, Woods Hole, Mass.

Officers

Raymond Stevens, President of the Corporation, c/o Arthur D. Little, Inc., 30 Memorial Drive, Cambridge 42, Mass.
Henry B. Bigelow, Chairman of the Board of Trustees, Museum of Comparative Zoölogy, Cambridge 38, Mass.
Edwin D. Brooks, Jr., Treasurer, P. O. Box 1135, Boston 3, Mass.
Mary Sears, Clerk of the Corporation, Woods Hole Oceanographic Institution, Woods Hole, Mass.

II. MEMBERS OF THE CORPORATION

Charles F. Adams, Raytheon Manufacturing Company, 138 River Street, Waltham 54, Mass.
Oliver Ames, III, North Easton, Mass.
Philip Armstrong, Medical Center of Syracuse, State University of New York, Syracuse, N. Y.
Eric G. Ball, Harvard Medical School, Shattuck Street, Boston, Mass.
Henry B. Bigelow, Museum of Comparative Zoology, Cambridge 38, Mass.
Lindsay Bradford, 215 East 72nd Street, New York, N. Y.
Detlev W. Bronk, The Rockefeller Institute of Medical Research, 66th Street and York Avenue, New York 21, N. Y.
Edwin D. Brooks, Jr., P. O. Box 1135, Boston 3, Mass.
C. Lloyd Claff, Single Cell Research Foundation, Inc., 5 Van Beal Road, Randolph, Mass.
E. L. Cochrane, Office of Vice President for Industrial and Governmental Relations, Massachusetts Institute of Technology, Cambridge 39, Mass.
L. O. Colbert, 4408 29th Street, N. W., Washington, D. C.
Kenneth S. Cole, National Institute of Health, Bethesda 14, Md.
J. S. Coles, Bowdoin College, Brunswick, Maine
Henry B. DuPont, Wilmington, Del.
Ferdinand Eberstadt, 39 Broadway, New York 6, N. Y.
Carl H. Eckart, Scripps Institution of Oceanography, La Jolla, Cal.
Harrison P. Eddy, c/o Metcalf & Eddy, 1300 Statler Building, Boston, Mass.
Marion Eppley, 510 Park Avenue, New York, N. Y.
Alexander Forbes, 610 Harland Street, Milton, Mass.
Horace S. Ford, 77 Massachusetts Avenue, Cambridge, Mass.
John A. Gifford, 14 Wall Street, New York 5, N. Y.
Ross G. Harrison, Osborn Zoological Laboratory, Yale University, New Haven, Conn.
Hudson Hoagland, Worcester Foundation for Experimental Biology, 222 Maple Avenue, Shrewsbury, Mass.
Frank A. Howard, 30 Rockefeller Plaza, New York, N. Y.
Columbus O'D. Iselin, Woods Hole Oceanographic Institution, Woods Hole, Mass.
Augustus B. Kinzel, Union Carbide Corporation, 30 East 42nd Street, New York 17, N. Y.
Milford R. Lawrence, Siders Pond Road, Falmouth, Mass.
Lamar R. Leahy, 910 Park Avenue, New York, N. Y.
Alfred L. Loomis, Room 2420, 14 Wall Street, New York, N. Y.
Arnaud C. Marts, 521 Fifth Avenue, New York, N. Y.
Robert E. McConnell, Hobe Sound, Fla.
Noel B. McLean, Edo Corporation, College Point 56, N. Y.
Daniel Merriman, Bingham Oceanographic Laboratory, Yale University, New Haven, Conn.
Henry S. Morgan, 2 Wall Street, New York, N. Y.
Frank A. Pace, General Dynamics Corporation, 445 Park Avenue, New York 22, N. Y.
Albert E. Parr, American Museum of Natural History, Central Park West at 79th Street, New York, N. Y.
Emanuel R. Piore, International Business Machines Corporation, 590 Madison Avenue, New York 22, N. Y.
Alfred C. Redfield, Maury Lane, Woods Hole, Mass.

Lawrason Riggs, Riggs, Ferris and Geer, Room 1201, 74 Trinity Place, New York 6, N. Y.
George H. Richards, 68 Williams Street, New York, N. Y.
Francis C. Ryder, 37 Larchwood Drive, Cambridge 38, Mass.
Mary Sears, Woods Hole Oceanographic Institution, Woods Hole, Mass.
Harlow Shapley, Sharon Cross Road, Peterborough, N. H.
Henry L. Shattuck, 10 Milk Street, Boston, Mass.
Robert R. Shrock, Department of Geology and Geophysics, Massachusetts Institute of Technology, Cambridge 39, Mass.
Edward H. Smith, Woods Hole Oceanographic Institution, Woods Hole, Mass.
Athelstan F. Spilhaus, Institute of Technology, University of Minnesota, Minneapolis 14, Minn.
Lyman Spitzer, Jr., Princeton University Observatory, 14 Prospect Ave., Princeton, N. J.
Raymond Stevens, c/o Arthur D. Little Inc., 30 Memorial Drive, Cambridge 42, Mass.
Julius A. Stratton, Office of the Vice President and Provost, Massachusetts Institute of Technology, Cambridge 39, Mass.
Gerard Swope, Jr., c/o International General Electric Co., 570 Lexington Avenue, New York, N. Y.
J. H. Van Vleck, Lyman 332, Harvard University, Cambridge 38, Mass.
Selman A. Waksman, Institute of Microbiology, New Brunswick, N. J.
Thomas J. Watson, Jr., International Business Machines Corporation, 590 Madison Avenue, New York 22, N. Y.
Franics C. Welch, 73 Tremont Street, Boston, Mass.
E. Bright Wilson, Jr., Department of Chemistry, Harvard University, Cambridge 38, Mass.

III. RESEARCH STAFF

(As of December 31, 1957)

Arnold B. Arons, Professor of Physics, Amherst College; Associate in Physical Oceanography.

William D. Athearn, Research Associate in Geology.

John C. Ayers, Associate Professor, Great Lakes Research Institute, and Associate Professor of Zoology, Department of Zoology, University of Michigan; Associate in Marine Biology.

Richard H. Backus, Research Associate in Marine Biology.

John P. Barlow, Assistant Professor of Oceanography, Cornell University; Associate in Marine Biology.

Lincoln Baxter II, Research Associate in Physics.

David L. Belding, Professor of Bacteriology and Experimental Pathology (Emeritus), Boston University; Consultant, U. S. Fish and Wildlife Service; Associate in Marine Biology.

Bruce B. Benson, Associate Professor of Physics, Amherst College; Associate in Physics.

Henry B. Bigelow, Professor of Zoology (Emeritus), Harvard University; Research Oceanographer, Museum of Comparative Zoology; Associate in Oceanography.

Duncan C. Blanchard, Research Associate in Meteorology.

Vaughan T. Bowen, Lecturer in Zoology, Yale University; Geochemist.

Bobert R. Brockhurst, Research Associate in Physics.

John G. Bruce, Jr., Research Associate in Physics.

Dean F. Bumpus, Oceanographer.

Elizabeth T. Bunce, Research Associate in Physics.

Andrew F. Bunker, Meteorologist.

Cornelia L. Carey, Associate Professor in Botany (retired), Barnard College; Associate in Marine Bacteriology.

Charles E. Carver, Jr., Research Associate in Hydraulics.

Joseph Chase, Research Associate in Meteorology.

George L. Clarke, Associate Professor of Zoology, Harvard University; Marine Biologist.

Nathaniel Corwin, Research Associate in Chemistry.

Herbert Curl, Jr., Research Associate in Marine Biology.

L. A. Earlston Doe, Associate in Physical Oceanography.

Willard Dow, Electronics Engineer.

Richard S. Edwards, Research Associate in Geophysics.

Maurice Ewing, Professor of Geology, Columbia University; Director, Lamont Geological Observatory; Associate in Geophysics.

Alan J. Faller, Research Associate in Meteorology.

Harlow G. Farmer, Jr., Research Associate in Hydraulics.

Charles J. Fish, Professor of Marine Biology, University of Rhode Island; Director, Narragansett Marine Laboratory; Associate in Marine Biology.

David H. Frantz, Jr., Research Associate in Engineering.

Frederick C. Fuglister, Physical Oceanographer.

Michael Garstang, Research Associate in Meteorology.

Robert H. Gibbs, Jr., Research Associate in Marine Biology.

Donald R. Griffin, Professor of Zoology, Harvard University; Associate in Physiology.

Bernhard Haurwitz, Professor of Meteorology and Chairman of the Department of Meteorology and Oceanography, New York University; Associate in Meteorology.

Earl E. Hays, Physicist.

J. B. Hersey, Geophysicist.

Edward M. Hulburt, Research Associate in Marine Biology.

Laurence Irving, Biologist, Arctic Health Research Center; Associate in Physiology.

Columbus O'D. Iselin, Associate Professor of Physical Oceanography, Harvard University; Research Oceanographer, Museum of Comparative Zoology; Senior Oceanographer.

Henry R. Johnson, Research Associate in Underwater Acoustics.

John W. Kanwisher, Research Associate in Biophysics.

Bostwick H. Ketchum, Senior Oceanographer.

Sydney T. Knott, Jr., Research Associate in Engineering.

Bernhard Kummel, Associate Professor of Geology, Harvard University; Associate in Submarine Geology.

Benjamin B. Leavitt, Associate Professor of Biological Sciences, University of Florida; Associate in Marine Biology.

Joyce C. Lewin, Research Associate in Marine Biology.

Robert A. Lufburrow, Research Associate in Physics.

Joanne S. Malkus, Meteorologist.

Willem V. R. Malkus, Physical Oceanographer.

Wilbur Marks, David Taylor Model Basin; Research Associate in Physical Oceanography.

Frank J. Mather III, Research Associate in Oceanography.

William G. Metcalf, Research Associate in Physical Oceanography.

Arthur R. Miller, Research Associate in Physical Oceanography.

Robert L. Miller, Associate Professor in Qualitative Sedimentology, University of Chicago; Associate in Submarine Geology.

Raymond B. Montgomery, Associate Professor of Oceanography, Chesapeake Bay Institute, Johns Hopkins University; Associate in Physical Oceanography.

Hilary B. Moore, Professor in Marine Biology and Assistant Director, Marine Laboratory, University of Miami; Associate in Marine Biology.

James M. Moulton, Assistant Professor in Biology, Bowdoin College; Associate in Marine Biology.

Jerome Namias, Chief, Extended Forecast Section, U. S. Weather Bureau; Associate in Meteorology.

Daniel R. Norton, Research Chemist, Sprague Electric Company, North Adams, Mass.; Associate in Chemical Oceanography.

Charles B. Officer, Jr., Associate Professor of Geology, Rice Institute; Geophysicist.

David M. Owen, Research Associate in Underwater Photography.

Mary Alys Plunkett, Associate Professor of Chemistry, Vassar College; Associate in Chemistry.

Roy L. Rather, Jr., Associate in Underwater Acoustics.

Alfred C. Redfield, Professor of Physiology (Emeritus), Harvard University; Senior Oceanographer.

Charles E. Renn, Professor of Sanitary Engineering, School of Engineering, Johns Hopkins University; Associate in Engineering.

Francis A. Richards, Chemical Oceanographer.

William S. Richardson, Physical Chemist.

Gordon A. Riley, Associate Director, Bingham Oceanographic Laboratory, Yale University; Associate in Marine Biology.

Nathan W. Riser, Professor of Zoology, Northeastern University; Associate in Marine Biology.

Helen M. Roberts, Assistant Professor of Mathematics, University of Connecticut; Associate in Mathematics.

F. Claude Rönne, Research Associate in Photography.

John H. Ryther, Marine Biologist.

Howard L. Sanders, Research Associate in Marine Biology.

Harold E. Sawyer, Research Engineer.

Marshall Schalk, Associate Professor of Geology and Geography, Smith College; Associate in Geology.

Irving I. Schell, Research Associate, Department of Geology, Tufts University; Associate in Meteorology.

William E. Schevill, Research Associate in Zoology, Museum of Comparative Zoology, Harvard University; Associate in Oceanography.

Karl E. Schleicher, Research Associate in Physics.

Per F. Scholander, Professor of Physiology, University of Oslo; Director, Institute of Zoophysiology; Associate in Physiology.

William C. Schroeder, Associate Curator of Fishes, Museum of Comparative Zoology, Harvard University; Ichthyologist.

George T. Scott, Professor of Zoology, Oberlin College; Associate in Physiology.

Mary Sears, Planktonologist.

Raymond Siever, Assistant Professor of Geology, Harvard University; Associate in Geology.

Edward H. Smith, Research Associate in Oceanography.

Paul Ferris Smith, Electronics Engineer, Rockefeller Institute for Medical Research; Associate in Physical Oceanography.

Floyd M. Soule, Oceanographer, U. S. Coast Guard; Associate in Physical Oceanography

Allard T. Spencer, Research Associate in Engineering.

Athelstan F. Spilhaus, Dean, Institute of Technology, University of Minnesota; Associate in Physical Oceanography.

Henry M. Stommel, Physical Oceanographer.

Thomas T. Sugihara, Assistant Professor of Chemistry, Clark University; Associate in Geochemistry.

William H. Sutcliffe, Jr., Director, Bermuda Biological Station for Research, Inc.; Associate in Marine Biology.

Parker D. Trask, Professor of Geological Engineering, University of California; Associate in Submarine Geology.

Harry J. Turner, Jr., Lecturer in Zoology, University of New Hampshire; Marine Biologist.

Ralph F. Vaccaro, Research Associate in Microbiology.

George Veronis, Research Associate in Mathematics.

Allyn C. Vine, Physical Oceanographer.

William S. von Arx, Physical Oceanographer.

Arthur D. Voorhis, Research Associate in Physics.

Robert G. Walden, Research Associate in Electronics.

Edmond E. Watson, Professor of Physics, Queen's University, Kingston, Ontario; Associate in Physical Oceanography.

Stanley W. Watson, Research Associate in Bacteriology.

Raymond Wexler, Meteorologist.

Geoffrey G. Whitney, Jr., Research Associate in Physical Oceanography.

Alfred H. Woodcock, Oceanographer.

George P. Woollard, Professor of Engineering Geology and Geophysics, University of Wisconsin; Associate in Geophysics.

L. Valentine Worthington, Research Associate in Physical Oceanography.

John M. Zeigler, Research Associate in Marine Geology.

ADMINISTRATIVE STAFF

Columbus O'D. Iselin	Director
Richard G. Leahy	Assistant to the Director
Ronald A. Veeder	Assistant to the Director
John McGilvray	Business Manager
Jan Hahn	Public Information
Norman T. Allen	Administrator
Harvey MacKillop	Controller
John F. Pike	Port Captain
Delmar R. Jenkins	Purchasing Agent
Otis E. Hunt	Laboratory Services

IV. DIRECTOR'S REPORT

Introduction

During the past year we have had some notable scientific successes, as I will try to explain below, but we have also been going through some very rough weather financially. As the year progressed funds available through the military services for the support of basic research steadily declined. Were it not for the extra appropriations for the International Geophysical Year we would have had to curtail drastically much of our field work. As it turned out we just managed to finish out the year with a small deficit, but I do not remember a year when the budget involved so much worry and uncertainty. Inflation in the costs of carrying on oceanography has, of course, been increasingly severe.

The future would look most uncertain indeed were it not for the establishment of a new Committee on Oceanography by the National Academy of Sciences-National Research Council. This group, under the chairmanship of Professor Harrison Brown, is charged with studying the national needs in oceanography and with making recommendations as to how these can best be met. Financial support of these studies has been made available by the Office of Naval Research, by the U. S. Fish and Wildlife Service and by the Atomic Energy Commission. It has become more generally realized in Washington, D. C., that research cannot be carried on effectively under a system that results in widely fluctuating annual budgets.

The other important development of the past year is the enthusiasm which has continued to mount for the oceanographic program of the International Geophysical Year. In fact, we have already carried out a good deal more than the originally agreed program of deep observations and even more ambitious plans are in the making.

Studies of Oceanic Circulation both on a Large Scale and on a Small Scale

Nearly half the work going on at the laboratory and at sea falls under this general heading and excellent progress has been made during recent months. The basic material which we work with consists of measurements of temperature, salinity, and dissolved oxygen. A good deal of skill is required to obtain such observations from depths greater than about 3,000 meters, yet more than half the water in the ocean lies at depths greater than this.

In February, as part of our contribution to the International Geophysical Year, Mr. Frederick C. Fuglister set out on the Crawford with a relatively green crew of observers to obtain four complete east-west trans-Atlantic profiles. The expedition was away from Woods Hole for four months and steamed about 18,500 miles. They occupied a total of 114 stations, nearly all of which extended down to within a few meters of the bottom. When you consider that he was using a vessel displacing less than 300 tons when fully loaded it was a remarkable job indeed.

The primary objective was to re-occupy two of the METEOR profiles across the tropical South Atlantic that were made about 30 years ago. Until very recent years these were the best data for large-scale circulation problems that had ever been obtained. Using a ship only a fifth the size, Mr. Fuglister and his assistants obtained about twice as many points of observation as the METEOR on each crossing, including a great many close to the bottom. When these data are combined with the additional sections expected to be obtained during the remainder of I.G.Y., the basic information for Atlantic large-scale circulation problems will have been improved by a whole order of magnitude. Especially this is true for salinity, thanks to the new conductivity bridges developed by Mr. Alvin L. Bradshaw and Mr. Karl E. Schleicher.

Meanwhile, the ATLANTIS and the British research vessel DISCOVERY II had also "jumped the gun" for I.G.Y. They met at Bermuda in March and proceeded to make a very critical and successful series of observations in the waters over the outer limits of the Blake Plateau off Charleston.

Of recent years, as our ability to measure temperature close to the bottom improved, we have found that very deep crosscurrent density gradients exist under the Gulf Stream System. If one assumes that the Gulf Stream extends down to only 1,500 or 2,000 meters, theoretical considerations demand that the waters below this level are flowing in the opposite direction. Thus the problem was to locate the layer of minimum motion below the Gulf Stream System and to learn whether or not a countercurrent exists below this level.

Off Charleston, because of the presence of the Blake Plateau, the situation was particularly favorable for the success of such measurements, for the deep flow (whatever its direction) is not under the swift Florida Current, but lies well east of it. Thus at this point in the system the ships would not be handicapped by strong near-surface currents.

In spite of some bad weather the results were clear-cut. At about 2,000 meters there is, indeed, a layer of minimum motion and at 2,800 meters the water is moving toward the south at a rate of about 8 miles per day.

This is the first time we have traded scientific parties and techniques with our British friends and the exchange was highly successful for both groups. We gained first-hand experience in handling Dr. John C. Swallow's new neutrally buoyant floats and the British profited by observing our techniques of measuring the very deep density gradients. Now that the ice has been broken it should be easier to arrange for continuing international cooperation in oceanography.

On the voyage back to England, Mr. L. Valentine Worthington and Mr. William G. Metcalf aboard the DISCOVERY had the opportunity of securing a very complete profile from the eastern edge of the Grand Banks to the approaches to the English Channel. None of our vessels could have worked this section successfully except in summer.

In short, between the DISCOVERY and the CRAWFORD five complete trans-Atlantic profiles were secured last winter. During October and November each vessel secured two more, and it is planned that in February the ATLANTIS will make a crossing at about Latitude 35°S.

It will be very exciting indeed to put all these new data together within a consistent framework. This will be the first time that it has been possible to treat the North and the South Atlantic Oceans as a single unit in a more or less synoptic manner.

There are many by-products of the long east-west profiles. In the first place, the improvements in the recording echo sounders, for which Mr. Sidney T. Knott is chiefly responsible, are producing much useful detail about the bottom topography. In addition, we have by no means neglected to collect samples of water for chemical analysis.

In September at Toronto an ambitious international symposium was held on problems of deep circulation. Our new data were presented there and it is hoped that what we have been accomplishing in the Atlantic during recent years will stimulate others to obtain similar data from other areas.

Dr. Richard G. Leahy, who joined our staff last winter, has been organizing and coordinating our I.G.Y. effort. In addition to the field work already mentioned which the CRAWFORD and the ATLANTIS are carrying out, he has supplied the Arctic ice flow camps with two oceanographic observers who have been studying the currents under the ice and he has stimulated several of Professor Birch's graduate students at Harvard to build equipment to measure the heat flow through the bottom sediments in the Arctic basin. This is a particularly favorable situation for such measurements because the probe can probably be left in the bottom for considerable periods of time, so slow are the ice movements. Dr. Leahy has also been testing our new CO_2 analyzer and developing, with the help of others, suitable plumbing so that it can be operated in our new airplane. While the major effort during I.G.Y. will be to gain a census of the CO_2 in the atmosphere, several of our staff have designs on this very exact instrument for studying the CO_2 cycle in the sea.

While improvement in the quality of the observations at sea has seemed to me the outstanding development of recent months, other groups have not been idle. We now have a particularly strong team attacking circulation problems by means of mathematical models. These are becoming increasingly elaborate and at the same time more convincing.

All during the winter our people met every two weeks with the corresponding team at the Massachusetts Institute of Technology. Not only were many formal papers given, but in the evenings at dinner and afterwards there was much stimulating discussion. The theoretical approach, both in meteorology and in oceanography, is now in very competent hands and it would be surprising indeed if some major break-throughs did not occur before long. I will mention only one of the lines of reasoning that seems profitable. Last winter Mr. Fuglister called attention to a peculiarity of the North Atlantic. Both because of geographical reasons and because of the wind system there is a net northward movement of the near-surface waters. Sea level must be higher in the northern North Atlantic than in any other ocean area. Estimates of the northward transport of surface water range as high as $20 \text{ x } 10^{6}/\text{m}^{3}\text{sec}^{-1}$. The theoreticians then began to think about the character of the return flow in view of the rotation of the earth. As usual Mr. Henry Stommel came up with a very intriguing mathematical model which seems to explain not only the countercurrent under the Gulf Stream but also the relative weakness of the Brazil Current which is its counterpart in the South Atlantic.

It has recently been possible for Mr. Alan J. Faller to check experimentally some of the basic new ideas concerning such forced circulations. Incidentally, Mr. Faller has been invited to join the experimental group at the University of Chicago during the winter of 1957–58 and I am certain this added experience will be of great help to his future work here.

For the time being, at least, Dr. William S. von Arx has lost some of his enthusiasm for hydraulic models and has turned his main attention to other matters, notably the new navigating systems which are coming into being. In most of these the ocean enters into the picture in rather subtle ways and by studying the disagreement of the various systems it is possible to find out some things about the ocean. The U.S.S. Compass Island, which is the ship being used for research by the Navy in precise navigation, is in effect a powerful tool for oceanography and Dr. von Arx has stimulated the very able officers on this ship to take the ocean into account in the course of using a huge array of very precise and complicated navigational instruments.

This is but one sample of his many activities. During the first half of last winter Dr. von Arx gave a successful course in oceanography at Massachusetts Institute of Technology and has recently been appointed an Associate

Professor there. The other half of the course was given jointly by Dr. Joanne S. Malkus and Dr. J. Bracket Hersey.

As far as coastal currents are concerned, Mr. Dean F. Bumpus, assisted by Mr. C. Godfrey Day and Mr. Joseph Chase, has continued to compile temperature and salinity data along the whole coast so as to study seasonal and longer term fluctuations from the fisheries standpoint. Our contract with the U. S. Fish and Wildlife Service has been continued for two more years, but on a somewhat reduced basis.

Mr. Day has made a rather thorough study of the modern drift bottle results and this has served as background for the setting out of a number of our new radio telemetering buoys, both in the Bay of Fundy and on Georges Bank. As experience with these free-floating buoys accumulates it is evident that they could be useful for many different sorts of problems, both physical and biological. Last year they survived November and December weather in the Bay of Fundy. In March four buoys were set adrift on Georges Bank in the area where haddock spawn. The movements of the water due to the local wind were studied intensively during about a six-week period, using the ALBATROSS III rather than our plane for locating the buoys at frequent intervals. After a storm two buoys failed to answer and were given up for lost. More than two months later one of these buoys suddenly began to be heard again and was located off New York. Its southwesterly progress has been at the rate of about four miles per day.

Mr. David H. Frantz and Mr. Robert G. Walden are engaged in improving the amount of information the buoys are able to report. In other words, the early ones when interrogated gave only a signal that could be homed-on or located by triangulation. Now this signal is being coded to transmit additional data that have been stored in the buoy since the last transmission.

Two more aspects of the buoy development work seem to deserve mention. The testing of the various components of Mr. Frantz' submerged buoy, known as the "pop-up," has just about been completed. This has turned out to be a long, slow job because the buoy and its sensing elements were designed to have a useful life of nearly a year. While the original buoy made here functioned as it was supposed to, there were a number of defects in the ten supposedly improved copies that were made commercially in the hope of making this type of device available to the other laboratories.

Mr. Gordon H. Volkmann, after spending nearly three years at Scripps, has recently returned to Woods Hole and is devoting full time to the development of our version of the Swallow-type, submerged, free-floating buoy.

Dr. William S. Richardson, Mr. Allyn C. Vine and Dr. J. B. Hersey have continued their program of employing vertically spaced arrays of thermistors to study shallow temperature distributions. The earlier tests made from our own ships ATLANTIS and BEAR in the Cayman Sea in 1956 clearly indicated that the thermistor array could be much more effectively towed from a larger ship and with more fully designed towing gear. Accordingly Mr. Roy L. Rather, an associate of the Institution, through his company, The Commercial Engineering Company, Inc., designed and constructed a chain, in which the thermistors and connecting wires could be mounted, and a diesel-powered winch for towing and handling the chain. In the spring of 1957 this winch assembly was mounted on the stern of the Coast Guard Ship YAMACRAW, which was made available to the Institution for this purpose through the Office of Naval Research. An enormous quantity of new type temperature data was recorded in the following months in the Sargasso Sea and along the east coast from Nova Scotia to Charleston, S. C.

The chain was 600 feet long and had 23 thermistors mounted on it at 25-foot intervals. Each thermistor was connected to a self-balancing bridge and digitizer, which in turn fed into an electric typewriter. The whole instrument was calibrated and programmed so that the temperature in degrees centigrade at each thermistor is typed on a long strip of paper in a pattern corresponding to the vertical arrangement of thermistors in the water. Thus water temperatures at 23 different depths could be measured repeatedly at two-minute intervals while the ship is underway, providing a much more detailed temperature section than has hitherto been possible. Individual temperatures are accurate to ±0.01°C, a considerable increase in accuracy over the bathythermograph. Obviously the depth pattern of the measurements varies with the towing speed, to almost the full 600 feet at slow speeds and to about 400 feet at full speed (12 knots). Two depth meters mounted on the chain provide repeated depth checks. Thus far water structures between the east coast and Bermuda have been studied revealing in great detail the complicated surface structures between the coast and the Gulf Stream, those at the edge of the Stream, and the more constant structures in the western part of the Sargasso Sea. As I reported last year from the earlier observations in the Cayman Sea, this more sensitive instrument reveals considerable complexity even in the wind-mixed surface layers. Our acousticians are studying the significance of these findings to sound transmission, and it is quite obvious that these data will be very useful to students of mixing processes and energy exchange between the atmosphere and the ocean.

The YAMACRAW has provided many of our staff with an opportunity to work with a larger ship, and to be able to work and transit in rougher weather than we can in our smaller ships. All members of the Institution staff who have had the pleasure of working with the Coast Guard crew of YAMACRAW have been impressed with the fine spirit of cooperation with which they have undertaken their assignment throughout.

Geophysics and Underwater Acoustics

For several years Dr. Hersey, Mr. Knott and others of the staff have been developing a high-definition seismic reflection apparatus for exploring shallow sediment structures in water-covered areas. It operates somewhat as an echo sounder, but differs by employing a broad spectrum sound pulse so that sound reflected from the bottom and rock layers below the bottom can be filtered to develop and emphasize subbottom reflections. Thus, it can be used to measure the thickness and sound velocity of sediments up to several hundreds of feet thick. In the late winter of 1957 the apparatus was used in Narragansett Bay to determine the depth to bedrock so as to aid the Navy in estimating the cost of deepening a channel there, and we are at this writing about to send ASTERIAS back to Narragansett Bay for a similar investigation for the Corps of Engineers in connection with their study of hurricane protection construction for that area. Mr. Don R. Fink and Miss Elizabeth T. Bunce are conducting the survey.

These engineering studies have the considerable advantage that bottom corings have been made which can be compared directly with reflection observations accurately placed at the core locations.

In addition, Dr. Earl E. Hays and Mr. J. Rietzel have used the reflection apparatus in a preliminary study of shifting sand bars in Vineyard Sound and Mr. Fink has started a detailed study of Buzzards Bay. We have also shared our instrument design with the Lamont Geological Observatory. Lamont staff members have employed the apparatus with considerable success in Long Island Sound and Chesapeake Bay.

Dr. Hersey and Miss Bunce have completed an intensive study of seismic data taken over the ocean area comprising the continental shelf, the Blake Plateau and adjacent deep water between the latitudes of Cape Henry, Va., and Jacksonville, Fla. The observations at sea were made on various cruises in 1954, 1955, and 1956, as I reported in 1956. These permit reasonable speculation about the geologic history and structure of the area which suggests that the Blake Plateau was formerly much shoaler, with an aspect similar to the modern Bahamas, and that a string of reefs or volcanic islands once stood along a southeasterly trend from Cape Fear about four hundred miles out to sea.

Dr. Charles B. Officer, Jr. (of the Rice Institute) and Mr. John Ewing (of Lamont Geological Observatory) have completed the analysis of seismic data from their two expeditions on our vessels to the Caribbean and have published two of a projected series of papers. Their results are a fundamental contribution to understanding the tectonics of this region and other island arc structures.

The Yamacraw was the means of getting many people to sea during the summer months. Among the observational programs carried out were a series of tests in three photographic projects in which different members of our staff have collaborated with Professor Harold E. Edgerton of the Massachusetts Institute of Technology. Professor Edgerton has developed a series of underwater cameras using his high-intensity electronic flash. Mr. Lloyd D. Hoadley of the Institution staff has worked with Professor Edgerton in the camera design, and Mr. David M. Owen has used the cameras at sea for a variety of observations during the past several years. Dr. Richard H. Backus, Mr. Henry R. Johnson, and others have used Edgerton cameras in conjunction with a suspended echo sounder for photographing individual sound scatterers in the deep scattering layers.

In addition Dr. Charles J. Hubbard carried out a program of measurements of the spectral distribution of sunlight under water. He used a deck recording spectrophotometer which scanned the optical spectrum from 400 to 650 μ at depths to 1500 feet. This type of data is basic to the problem of proper design of underwater television and other underwater optical equipment.

Professor Edgerton had also constructed a camera especially designed to take repeated photographs of the bottom when suspended on a long wire cable or line from a drifting ship. He uses no electrical leads in the suspending cable. The camera is coupled with a repeating electronic flash and a sound projector which sends out a series of short, intense pulses of sound. The research ship receives and measures the time interval between these pulses and their reflections from the bottom as an indication of the distance of the camera from the bottom. The distance can be adjusted by changing the wire out. This camera system was tested by Professor Edgerton, Dr. Backus and Dr. Hersey at three locations from the Yamacraw. They obtained several hundred photographs on each lowering of the camera, indicating that such an approach to bottom photography can be used for detailed exploration in deep water.

For the past several years Dr. Backus, Mr. Johnson and others have been developing a technique for photographing individual sound scatterers in deep scattering layers. This technique has been emphasized because it appears to be the most promising means of identifying the organisms which scatter the sound received as "scattering layers" on ship-mounted echo sounders. This method consists of lowering an echo sounding system mounted with a camera into the scattering layer under study. The echo sounder and camera are electrically connected to the research ship so that an observer watching the sound recording can determine exactly when to actuate the camera to photograph an object scattering sound.

Dr. Harold Barnes of the Marine Station, Millport, U. K., collaborated with Dr. Backus and others in various investigations with the British underwater television apparatus which was so kindly loaned to the Institution upon his recommendation by the Scottish Home Department. The television equipment was combined with the suspended echo sounder for studying open ocean sound scatterers in the fall of 1956. These studies served to confirm previous observations made with the echo sounder and underwater camera discussed above, but unfortunately the cruises were plagued by bad weather, so that their studies did not progress further. In shallow water they made a number of interesting observations of the bottom which were combined with detailed, short pulse echo sounder recordings. This work has encouraged them to regard this combination of techniques as promising for study of acoustical properties of the bottom.

Geology

Arrangements have been made recently for Professor Raymond Siever, who came to Harvard University in the autumn on a permanent basis, to take over general supervision of our sedimentary research. In effect he will be taking over Mr. Henry C. Stetson's duties. His interests, however, run along somewhat more chemical lines. This is also the area in which Dr. Leahy has specialized so it is expected that in the future the chemistry of marine sediments will receive rather more attention here than has been the case in the past.

Meanwhile Dr. Parker D. Trask, Professor Bernhard Kummel, and Dr. E-an Zen are hard at work analyzing the sediment cores which Mr. Stetson secured during his last expedition to the waters off the coast of Peru.

Dr. John M. Zeigler and his several assistants have continued to study beach dynamics vigorously. He and Mr. William D. Athearn have also become interested in the long cores supplied by the Raymond Concrete Pile Company from the radar tower sites. The borings off New York are especially provocative, for they reached down to some well-dated Long Island clay. These very long cores indicate that the rate of deposition of sand across the continental shelf has been remarkably rapid (about 90 feet) since glacial times. It is planned to follow up this clue and to renew studies of the transportation of the offshore sands.

Marine Meteorology

Field work in meteorology has been more or less at a standstill during recent months due to the fact that we have been in the process of changing over from the PBY-type plane to a DC3. Since over the years the PBY had become a well-calibrated meteorological instrument, much effort has been required to bring the new plane up to these standards. The first flights gathering meteorological data took place during July, but for other purposes the plane has been flying since early spring. The chief advantages of the DC3 are more working space in the cabin, which also has acoustical insulation; the top speed is considerably greater than the PBY, but it can also fly slowly; and it can fly safely on one engine which the older plane could not do for any considerable distance.

Meanwhile, good use of the time has been made in the laboratory to improve the instrumentation and to complete papers based on the accumulated data.

A recent visit of Dr. Joanne S. Malkus to Stockholm was particularly fruitful. Dr. C.-G. Rossby had arranged before he died for her to use the Swedish computer to work out the events following the arrival of a bubble of warm air at cloud base.

Dr. Raymond Wexler, Mr. Alfred H. Woodcock, and Dr. Malkus each have produced a paper on hurricanes during recent months. Although financial support on the part of the Weather Bureau for hurricane research has been shrinking steadily, there is no lack of interest on the part of the people here. Mr. Michael Garstang, a keen student of tropical meteorology, has joined our staff recently and spent much of August and September at sea on the CRAWFORD in order to test some of the ideas which he formed about the early stages of a hurricane when he was stationed at Trinidad.

We have yet to solve the problem of observing wind direction and velocity aloft from a small vessel in fairly rough seas, but our electronics people have by no means run out of ideas and it is hoped by next season we will have a reliable system for measuring the vertical wind profile. Such observations are critical to the various models which have been devised in an effort to explain the early stages of a hurricane.

Wave Studies

The David Taylor Model Basin allowed Mr. Wilbur Marks to return to Woods Hole for two months last summer in order to finish up the analysis of the motions of the launch RISK which were made several years ago. This should become a classical paper in the literature of naval architecture for it is one of the first to apply modern theory to the response of a model ship to an irregular, natural sea. Mr. Richard G. Barakat and Mr. Charles E. Carver are planning to extend such studies to the CRAWFORD and to a self-propelled model of the CRAWFORD. The newly-constructed wave tower, which will be planted soon in Buzzards Bay, is the first step in this new attack on wave-measuring techniques.

Last winter a long visit by the German wave expert, Dr. Hans Walden, did much to stimulate the various members of our staff interested in wave problems.

The very considerable labor of deriving the power spectrum from wave records has been a serious bottleneck in wave research. A new and very versatile electronics computer has recently been developed for wave investigations at the Sperry Gyroscope Company and this should greatly accelerate not only the program here but also the studies of other interested groups.

Biology and Chemistry

The following section of this report was prepared by Dr. Bostwick H. Ketchum and consequently fails to indicate the important part he is playing in leading and organizing our expanding program in marine biology.

We have initiated an intensive study of the plankton populations in the waters over the continental shelf. This program is supported jointly by Institution funds and by a grant from the Atomic Energy Commission under the supervision of Dr. Ketchum and Dr. Vaughan T. Bowen. Dr. Mary Sears and Dr. John H. Ryther are cooperating in the investigation. The program has also increased the opportunities for observations at sea for Mr. Ralph F. Vaccaro and Mr. Charles S. Yentsch, both of whom are supported by research grants from the National Science Foundation.

Periodic observations of the plankton populations and of the chemistry of the water are being made and the plan is to continue such observations for a period of at least three years in an effort to understand more completely the ecological conditions which determine the size, productivity, and succession of plankton populations in a coastal area.

The cruises have been planned to provide two cross sections of the continental shelf with stations in water ranging in depth from 30 meters to 2,000 meters. Thus a comparison between the ecology of inshore coastal populations and of offshore populations is provided. Six replicate cruises to the area were completed in 1957. A preliminary survey of the results of the program was presented at the meeting of the American Society of Limnology and Oceanography held in Woods Hole in September. Dr.

Ketchum and Dr. Ryther participated in a Symposium on Oceanic Productivity held in Bergen, Norway, at the end of September.

A relatively cold, low salinity body of water was found from about 30 meters to the bottom in the section south of Montauk Point in September. This water was isolated from surface water by an intense temperature gradient and from the offshore waters by an intense salinity gradient. No water of these characteristics was present in the section running seaward from Barnegat Lightship off the coast of New Jersey, though water of intermediate characteristics was found in the area of the Hudson Canyon. This suggests that the Hudson Canyon has a profound influence on the mixing of waters in this area. In July of this year this cold water was again present in the same locality, and an effort was made to track it eastward and northward into the Gulf of Maine, where similar water is found in the summertime. No continuity between the cold water on the continental shelf south of Cape Cod and the cold water in the Gulf of Maine was found. It, therefore, appears that this body of water is formed during the wintertime on the continental shelf and remains isolated from adjacent bodies of water throughout the summer. This isolated body of water may make it possible to follow biological changes in the water more easily than would be the case where mixing and circulation is more vigorous. It also seems clear that sea disposal of wastes or radioactive materials should be planned to avoid this body of water, where considerable accumulations could develop.

On these cruises Dr. Ryther and Mr. Yentsch have continued their studies of productivity in relationship to chlorophyll and light intensity. Quantitatively, the rates of photosynthesis observed in this area are comparable to those which have been observed in other coastal regions. It is, however, becoming increasingly apparent that the respiration of phytoplankton populations fluctuates widely. At some times virtually all of the new organic material produced by photosynthesis is utilized directly by the phytoplankton in their respiration; at other times large amounts of organic material in excess of respiratory needs are produced and this excess is available for the zooplankton and other members of the aquatic community. This empirical observation emphasizes the necessity of understanding the physiological state of the phytoplankton population in order to evaluate measurements of photosynthesis or of productivity.

Dr. Ryther and Mr. Yentsch have developed a method of calculating the rate of organic production in the ocean from measurements of the chlorophyll content of the plankton, of the daily radiation incident to the sea surface, and of the transparency of the water. By using this method, productivity values may be obtained quickly and easily at sea with a minimum of interference with other activities, and without the services of a specialist in the field. This method has proved satisfactory in comparison with other more complex methods such as the measurement of the rate of assimilation of carbon-14 in bottles suspended at various depths for one half to one day periods.

Measurements of primary production were made on all IGY cruises during 1957 using this new method. They have been made on eight sections at a total of approximately 160 stations, representing about a tenfold increase in the existing productivity data for the open Atlantic.

A study of the plankton ecology and related chemistry and hydrography of the Sargasso Sea was initiated in cooperation with the Bermuda Biological Station under contract with the AEC by Dr. Ryther and Dr. David Menzel. This study is being conducted with the Station's Research Vessel PANULIRUS. Observations are made in conjunction with the regular hydrographic station which has been occupied at regular intervals throughout the past several years under the direction of Mr. Stommel, and include biweekly measurements of primary production, phytoplankton, zooplankton, and plant nutrients.

A survey was conducted in June of Great South Bay and Moriches Bay, Long Island at the request of the Townships of Islip and Brookhaven by Dr. Ryther, Dr. Edward M. Hulburt, Mr. Vaccaro and Mr. Yentsch. Similar studies of this area have been made annually since 1950 and provide a continuing record of the ecology of these embayments in relation to their pollution and unique hydrographic features. A supplementary study of the dynamics of a diatom bloom was made at the same time in a tributary of Moriches Bay and has since been submitted for publication.

Doctors Ryther and Clarke were Institution delegates to the 9th Pacific Science Congress held in Bangkok, November 1–17, 1957. Both read papers at the Oceanography Section. En route to Bangkok they visited laboratories and gave lectures at Hawaii, Japan, and Hong Kong, and following the Bangkok meetings they made a brief lecture tour of India under the sponsorship of UNESCO.

Mr. Guy C. McLeod, working with Dr. Ryther under a grant from the National Science Foundation, has constructed an ultra-violet submarine filter photometer with which he has studied the penetration of ultra-violet radiation in coastal and offshore waters. He has also made laboratory studies of the effects of ultra-violet on photosynthesis by marine phytoplankton, and visited the Oak Ridge National Laboratories where, with Dr. W. J. Arnold, he measured the action spectrum of photosynthesis throughout the visible and ultra-violet spectrum in several species of marine algae.

The cycle of nutrients in the coastal area have been followed by Mr. Vaccaro and Mr. Nathaniel Corwin. In the inshore waters inorganic phosphate is always present even when inorganic nitrogen compounds are exhausted, indicating that available nitrogen probably limits the growth of the phytoplankton. Further analysis of these data should give an independent estimate of the productivity of this region, and it is hoped that it will also help to explain the variations in the physiological conditions of the plankton which lead to the variations in respiration and in the net production of organic matter mentioned above.

The regeneration of plant nutrients in the sea has been studied particularly in relation to microbial nitrification (i.e., oxidation of ammonia to nitrite and nitrate) by Dr. Stanley W. Watson and Mr. Vaccaro. While in a preliminary phase, these investigations permit some definite conclusions concerning the role of these organisms in the sediments of the continental shelf. Nitrifiers are present in the shallow sediments but absent from the sediments underlying water deeper than 100 meters. It appears that much of the process of nitrification in shallow waters occurs in the sediments but at deeper offshore locations most of the nitrification must occur in the water column. Attempts to isolate nitrifying bacteria from the water have been unsuccessful, but are being continued.

The species composition of the phytoplankton populations is being studied by Dr. Hulburt. Dramatic changes in the character of the population are commonly observed over the edge of the continental shelf where abrupt changes from characteristically coastal water to characteristically oceanic water are also observed. So far the biologists can give no definite answer to the question "What ecological property of the water determines the type of organism which is able to thrive in it?" It is hoped that our observations of both the population and various aspects of the water character and chemistry will help to solve this problem. However, it seems probable that no definite answer will be possible until we learn to culture some of these oceanic species in the laboratory and are able to evaluate their response to changes in environmental conditions.

The zooplankton populations are being studied by Dr. Sears and Miss Constance Chadwick. Nearly twenty years have passed since Dr. Bigelow and Dr. Sears completed their previous study of the zooplankton of the continental shelf. Unfortunately none of the Institution vessels can be run at a slow and uniform speed as could be done when ATLANTIS had the variable pitch propeller. The variation in speed during the two makes it difficult to obtain quantitative samples from known depths. Nevertheless, it is hoped that these samples will provide a better understanding of the ecological relationships of the zooplankton which will supplement the productivity estimates made at the same time.

Studies of zooplankton populations were also conducted during the past winter by Mrs. Angeles Alvariño de Leira, Instituto Español de Oceanografia, Madrid. During her visit she analyzed the zooplankton obtained in the Gulf of Maine by the U. S. Fish and Wildlife Service in 1956. The distribution of arrow worms in this area afforded contrasts and comparisons with similar distributions she had observed at Plymouth, England, and off the coast of Spain.

Dr. T. S. Satyanarayana Rao of Andhra University, India, has studied the seasonal variation of the zooplankton population in the Woods Hole area. Dr. William H. Sutcliffe, Jr., Director of the Bermuda Biological Laboratory, spent two months in Woods Hole analyzing the copepods in the plankton tows obtained during the "Trade Wind" cruise by the ATLANTIS in 1952.

Studies of the silica metabolism of diatoms have been conducted by Dr. Joyce C. Lewin. The silicate skeletons of marine diatoms are resistant to solution in sea water, and Dr. Lewin has shown that this depends upon the formation of an insoluble linkage with a trivalent cation. Iron and aluminum have been shown to be effective, and studies of other cations are planned.

Dr. Vaughan T. Bowen and Dr. Thomas T. Sugihara have continued their studies of the concentration of long-lived radioisotopes contributed by fall-out to the sea. The concentration of strontium-90 in surface water samples was higher than would be estimated from the published terrestrial measurements in this latitude. Although these analyses were performed on surface water, which could be assumed to reach horizontal homogeneity during the several years that strontium-90 has been accumulating, the analyses reveal a five-fold variation in concentration. This result indicates that mixing cannot have reached, in either the vertical or horizontal directions, the uniformity which is indicated by the analysis of other chemical properties of the water. Methods for the determination of other long-lived fission products in sea water have been devised and the analyses will include determinations of cerium-144, cesium-137, promethium-147 and antimony-125 in the studies of the fission-product distribution and concentration in the sea.

The cruises planned for the International Geophysical Year have afforded an opportunity to obtain samples of water at various depths for studies of the distribution of natural radioisotopes. Samples for this purpose were obtained at six stations during CRAWFORD Cruise 10 to the South Atlantic and at four stations on CRAWFORD Cruise 16. The CO_2 was extracted from these samples on shipboard and the isotope ratios of C^{12}, C^{13}, and C^{14} will be determined on these samples. After the extraction of CO_2, thirty gallons of the water were returned to Woods Hole in plastic drums. These samples will be analyzed for the fission-product radioactivities, for tritium, and for the rare-earth elements.

Dr. Bowen and Dr. Leahy, as a part of the Institution's IGY program, have been investigating the CO_2 content of the atmosphere. An infra-red absorption CO_2-analyzer has been obtained and modified both physically and electronically to permit its use on the Institution's airplane. Dr. Leahy has made several flights in conjunction with studies being carried out by Mr. Andrew Bunker. Although the program for production of standard $CO_2.N_2$ mixtures has not developed on the anticipated national cooperative basis, some comparative data has been obtained. Whereas some, but not all, vertical soundings over warm water have shown more CO_2 at 500 feet than at 1000 to 10,000 feet, none of these made over cold water have shown this pattern. In the Trade Winds area, even above the inversion layer, considerable fluctuation of CO_2 content was found, appearing to coincide with the passage of different air masses. This program is being continued and, with the help of Dr. John W. Kanwisher, being expanded.

Professor Edward W. Moore, from the Department of Sanitary Engineering at Harvard University, has been working during the past year in collaboration with Dr. Bowen developing methods for the determination of strontium-90 in marine sediments. Samples of various muds in the neighborhood of Woods Hole have been processed and the analyses will be completed in the near future.

Dr. Francis A. Richards has received a Guggenheim Fellowship and spent the winter at the University of Oslo, Norway. This has given him an opportunity to continue his studies of the chemistry of anaerobic waters in the fjords in Norway, and he also worked on the development of new methods for the determination of ammonia in sea water. After his return from Norway in September, he re-visited the Cariaco Trench on the ATLANTIS with the scientific party headed by Dr. Zeigler. A more accurate description of the sulfide distribution in the anaerobic water was obtained using plastic lined sampling bottles which do not react with the sulfide in the water as the all-metal Nansen bottles did. Other chemical variables were observed, in an attempt to relate the unique chemistry of the water column to that of the sediments.

Mr. Harry J. Turner has continued his studies of shellfish and other marine bottom populations for the Department of Conservation of the Commonwealth of Massachusetts. In collaboration with Dr. Nathan W. Riser he has been rearing larvae and young juvenile quahogs in the laboratory and has completed a study of the processes of fertilization and maturation of the quahog egg. A paper describing the chromosome number and the early development stages of this organism has been prepared for publication.

This work may be a milestone in shellfish culture since it lays the groundwork for possible genetic and breeding studies of this organism. It is hoped to extend the studies of the spawning and development of larvae of shellfish to other forms, and an investigation of the spawning behavior of the bay scallop has already been initiated. Mr. Turner has also undertaken a study of the hydrography and circulation of Nantucket Sound to determine if the extensive bed of large quahogs now under exploitation are likely to be the parent stocks of inshore populations along Cape Cod and the Island.

Mr. James E. Hanks has undertaken an investigation of the early life history of the clam drill, *Polinices.* He has demonstrated that egg-laying is stimulated by warm temperatures and an adequate food supply with little or no seasonal influence. The larvae of this species have been maintained as long as a month on a diet of phytoplankton.

A similar study of the larval development of the common mud snail, *Nassarius*, was conducted by Mr. Rudolf Sheltema on a summer fellowship, Mr. Sheltema demonstrated conclusively that metamorphosis of the larvae of this species is stimulated by the presence of certain kinds of substrata containing a heat labile substance.

Dr. Howard L. Sanders has continued his studies of both the bottom populations in Buzzards Bay and the significance to crustacean evolution of *Hutchinsoniella macracantha* which he discovered in Long Island Sound and has found in Buzzards Bay. This unusual crustacean has many characteristics which are intermediate between the long extinct Trilobites and various modern crustacea, and the study of these characteristics may give important clues to the ways in which crustacean evolution has taken place. His studies of the bottom populations have correlated the species present and the density of the population with the physical characteristics of the bottom and with the circulation of the water which determines the type of sediment found in various locations. Dr. Wolfgang Wieser, Universität Wien, Vienna, is extending these investigations this summer by studying smaller members of these communities.

Dr. Harold Barnes of the Marine Station, Millport, Scotland, received a fellowship as a visiting investigator at the Institution. During his visit he continued his studies of the biology of barnacle populations and conducted investigations of the usefulness of underwater television in studies of the scattering layer and of bottom populations.

Dr. George L. Clarke has continued his investigations of light conditions in the sea and of the control by light and other factors of the vertical distribution of pelagic organisms. These relations are of interest not only in the fundamental ecology of the deep sea but also in relation to the transport of radioactive materials, which may be concentrated in the bodies of animals, from one level in the ocean to another. Improvement of the bathyphotometer made possible the measurement of total light at all levels to a depth of one mile. In addition an underwater spectroscope and a scattering meter have been built. In clear ocean water, during the middle of the day, light from the surface was measured to about 2,000 feet. From about 1,500 feet to 6,000 feet flashes of luminescent animals were detected in great profusion. Quantitative records of the frequency, duration, and intensity of these flashes revealed the presence of very different populations at various depths. A camera which will be activated by light flashes is now being coupled with the photometer in order to show photographically which types of luminescent animals are present at various levels at different times of day.

Direct studies of the migrations and reactions of animals are difficult but it is expected that further knowledge of the mechanisms involved may be obtained by the closer studies of the vertical movements of zooplankton possible in fresh-water ponds and of the behavior of animals brought into the laboratory. For this purpose an investigation of diurnal migration was undertaken in Flax Pond and in Duck Pond on Cape Cod. The latter is of particular interest because its transparency was found to be comparable to clear ocean water and far clearer than most ponds or lakes. Investigation has also been begun of improved methods for culturing oceanic zooplankton —a technique which has never been adequately developed. When healthy animals are maintained in the laboratory, not only may their reactions to light and other factors be studied but opportunity will be presented for testing directly their ability to concentrate radioactive materials.

Dr. John Kanwisher has continued his studies of shore plants and animals that were previously found to be frozen for long periods during the winter. Microscopic examination of the frozen specimens shows considerable internal disruption from the ice formation but gives no clue to survival. An automatic recording oxygen system has been developed and is being used to determine photosynthesis and respiration of macroscopic algae as a function of temperature and illumination. From such data and the size of the standing crop productivity can be estimated. Measurements were also made on live porpoises at Marineland to compare their body temperature regulating mechanisms with those of large whales previously studied. The smaller but structually similar animal must conserve heat more efficiently because of its much larger surface to volume ratio.

A report by Dr. H. B. Bigelow and Mr. William C. Schroeder on the relationship of the shark genera of the suborder Squaloidea was published in August 1957. A paper describing several new skates from the Gulf of Mexico and off the Bahamas together with further notes on recently described species is in press. Dr. Bigelow and Mr. Schroeder are now working on the family Osmeridae, the capelin and smelts, to be included in Part 3 of Fishes of the Western North Atlantic. Mr. Schroeder is also preparing a report on the offshore lobster fishery which is becoming increasingly important commercially, and a section comprising the elasmobranchs of the western North Atlantic that will form part of a monograph on aquatic biology, sponsored by the National Research Council.

The research program dealing with the biology of the larger pelagic fishes, supported by a grant from the National Science Foundation, has made good progress under the direct supervision of Dr. Robert H. Gibbs, Jr. About 100 bluefin tuna, 100 yellowfin tuna and over 400 white marlin were tagged in an effort to learn more about their migratory habits and various data have been collected bearing on the biology of these and other species. Near the end of the year Mr. Frank J. Mather III returned from his leave of absence in the Virgin Islands and is continuing the program on pelagic fishes.

Dr. Backus has continued his studies of pelagic sharks. The crews of the Institution's research ships have contributed greatly to this end by keeping logs of their shark captures. These studies have been concerned chiefly with the great blue and white-tip sharks. Both of these animals are abundant and widespread on the high seas. The great blue shark is a known man-eater and the white-tip is probably such, and so these animals constitute to some extent a hazard to "survivors" at sea. In this connection Dr. Backus has been working with a Navy-and Air Force-supported group which is exploring the means by which a better shark repellent may be developed.

Dr. Backus has completed a paper on the fishes of Labrador which culminates three summers of observation made on BLUE DOLPHIN Labrador Expeditions. These expeditions were in part Institution-sponsored.

Mr. William E. Schevill has continued his studies of the natural history of whales and porpoises, particularly in connection with their sound production and its significance to the animal. The underwater sounds of the sperm and right whales have recently been recorded for the first time. After years of only occasional sightings, Institution vessels encountered sperm whales half a dozen times during the summer of 1957 in waters between Nova Scotia and Bermuda. Migrating right whales have called in Vineyard Sound during March and April of 1956 and 1957.

Mr. Schevill is also studying the systematics, distribution and natural history of the widely-distributed whale genus *Globicephala* (the pothead whales or blackfish). This study should lead to conclusions as to what factors constitute the boundaries on the high seas between the ranges of closely-allied species of larger marine animals.

This rather complete account of the work in progress during 1957 has been prepared partly for the assistance of Dr. Paul M. Fye, who will take over from me as Director in June 1958, and also to indicate to other interested persons the very wide range of activity that is now in progress. Oceanography has indeed grown both in quantity and in quality during the life of this Institution, and it has been a great privilege to the present Director to witness the whole of this development and to know intimately the many people who have contributed to the total effort. We all look forward, and the present writer probably most of all, to the return to Woods Hole next spring of Dr. Fye. There is every expectation that under his leadership we can increasingly help the science of oceanography to mature.

Research Vessels

Major repairs to our vessels during 1957 include a thorough inspection and repair of the mainmast of ATLANTIS. A large area of dry rot about half way up the mast had been discovered last autumn and patched in a temporary manner. The BEAR also was found to be suffering from dry rot and was fitted with a new bow at considerable expense.

When the CRAWFORD returned from the South Atlantic in June it was found that both engines required excessive maintenance. A study of the situation revealed that because of her increased displacement the screws had been overloading the engines and to correct the situation their pitch has been decreased. The engines now can turn up to their designed top speed and are able to operate easily at about 85% of full power, whereas before, especially after some fouling had occurred, they were laboring hard at cruising speed.

Since spring the CARYN has again been advertised as being for sale. We have removed all the Navy-owned equipment and have replaced the skylight over the main cabin, but as yet we have had no serious offer.

Publications

During 1957, 71 papers bearing contribution numbers were published:

	Contr. No.
RICHARDS, F. A., 1957. Oxygen in the ocean. Ch. 9 in: Treatise on Marine Ecology and Paleoecology, Vol. 1. *Mem., Geol. Soc. Amer.*, 67: 185–238	714
HULBURT, E. M., 1957. Distribution of phosphorus in Great Pond, Massachusetts. *J. Mar. Res.*, 15(3): 181–192	748
BARLOW, J. P., 1957. Effect of wind on salinity distribution in an estuary. *J. Mar. Res.*, 15(3): 193–204	752

	Contr No.
Marks, Wilbur, and Joseph Chase, 1957. Observation of the growth and decay of a wave spectrum. Interaction of sea and atmosphere, a group of contributions. *Meteorol. Monogr.*, 2(10) : 67–75	769
Gordon, M. S., and R. H. Backus, 1957. New records of Labrador fishes with special reference to those of Hebron Fjord. *Copeia*, 1957(1) : 17–20	800
Blanchard, D. C., 1957. The supercooling, freezing and melting of giant raindrops at terminal velocity in air. Conference on the Physics of Cloud Precipitation Particles, Woods Hole, Sept. 1955. In: Artificial Stimulation of Rainfall, Pergamon Press, Ltd., 233–249	809
Blanchard, D. C., 1957. Discussion of raindrop distributions made during Project SHOWER, Hawaii, 1954. Conference on the Physics of Cloud Precipitation Particles, Woods Hole, Mass., Sept. 1955. In: Artificial Stimulation of Rainfall, Pergamon Press, Ltd., 213–223	812
von Arx, W. S., 1957. An experimental approach to problems in physical oceanography. In: Progress in Physics and Chemistry of the Earth, Pergamon Press, Ltd. 2: 1–29	820
Redfield, A. C., and A. R. Miller, 1957. Water levels accompanying Atlantic coast hurricanes. Interaction of sea and atmosphere, a group of contributions. *Meteorol. Monogr.*, 2(10) : 1–23	828
Miller, A. R., 1957. The effects of steady winds on sea level at Atlantic City. Interaction of sea and atmosphere, a group of contributions. *Meteorol. Monogr.*, 2(10) : 24–31	829
Bunker, A. F., 1957. Turbulence measurements in a young cyclone over the ocean. *Bull., Amer. Meteorol. Soc.*, 38(1–1) : 13–16	833
Hulburt, E. M., 1957. The taxonomy of unarmored Dinophyceae of shallow embayments of Cape Cod, Massachusetts. *Biol. Bull.*, 112(2) : 196–219	838
Officer, C. B., J. I. Ewing, R. S. Edwards and H. R. Johnson, 1957. Geophysical investigations in the eastern Caribbean, Antilles Island Arc and Puerto Rico Trench. *Bull., Geol. Soc., Amer.*, 68(3) : 359–378	839
Malkus, J. S., 1957. Trade cumulus cloud groups: some observations suggesting a mechanism of their origin. *Tellus*, 9(1) : 33–44	843
Richards, F. A., 1957. Some current aspects of chemical oceanography. In: Progress in Physics and Chemistry of the Earth, Pergamon Press, Ltd., 2: 77–128	844
Stommel, Henry, 1957. Florida Straits transports, 1952–1956. *Bull. Mar. Sci., Gulf & Caribbean*, 7(3) 252–254	845
Bigelow, H. B., and W. C. Schroeder, 1957. A study of the sharks of the suborder Squaloidea. *Bull. Mus. Comp. Zool.*, Harvard Coll., 117(1) : 1–150	848
Walden, H., and H. G. Farmer, 1957. Auswertung von Seegangsregistrierungen des Forschungsschiffes Atlantis mit dem "ship-borne wave recorder" sowie Vergleich mit entsprechenden Seegangsberechnungen aus den Windverhältnissen (hindcasting). *Deutsche Hydrogr. Zeits.*, 10(4) 121–134	850
Vine, A. C., 1957. Some trends in oceanographic instrumentation. *Proc. UNESCO Symp., Phys. Ocean., Tokyo*, 1955 : 49–52	851

	Contr. No.
Backus, R. H., 1957. Northern record of the snake eel, *Ophichthus gomesi* (Castelnau). *Copeia* 1957(1): 61	854
Backus, R. H., 1957. Notes on western north Atlantic sharks. *Copeia*, 1957(3): 246–248	857
Friedman, I., and A. H. Woodcock, 1957. Determination of deuterium-hydrogen ratios in Hawaiian waters. *Tellus*, 9(1): 553–556	860
Ewing, J. I., C. B. Officer, H. R. Johnson and R. S. Edwards, 1957. Geophysical investigations in the eastern Caribbean; Trinidad Shelf, Tobago Trench, Barbados Ridge, Atlantic Ocean. *Bull., Geol. Soc., Amer.*, 68(7): 897–912	861
Rutstein, M. S., 1957. Flooded quarries for experimental work. *Trans. Amer. Geophys. Union*, 38(5): 688–690	866
Gordon, M. S., 1957. Observations on osmoregulation in the Arctic char (*Salvelinus alpinus* L.). *Biol. Bull.*, 112(1): 28–33	868
Wooster, W. S., and B. H. Ketchum, 1957. Transport and dispersal of radio active elements in the sea. In: The effects of atomic radiation on oceanography and fisheries. *Nat. Acad. Sci.-Nat. Res. Counc., Publ.* 551: 43–51	870
Ketchum, B. H., 1957. The effects of the ecological system on the transport of elements in the sea. In: The effects of atomic radiation on oceanography and fisheries. *Nat. Acad. Sci.-Nat. Res. Counc., Publ.*, 551: 52–59	871
Blanchard, D. C., and A. H. Woodcock, 1957. Bubble formation and modification in the sea and its meteorological significance. *Tellus*, 9(2): 145–158	875
Soule, F. M., and J. E. Murray, 1957. Physical oceanography of the Grand Banks and Labrador Sea in 1956. *U.S.C.G. Bull.*, No. 42: 35–100	877
Kanwisher, J. W., and H. Leivestad, 1957. Thermal regulation in whales. *Norsk Hvålfangst-Tid.*, 46(1): 1–5	878
Sanders, H. L., 1957. Cephalocarida and crustacean phylogeny. *Syst. Zool.*, 6(3): 112–128, 148	882
Ayers, J. C., and Roger Bachman, 1957. Simplified computations for the dynamic height method of current determination in lakes. *Limnol. & Oceanogr.*, 2(2): 155–157	883
Zeigler, J. M., and F. C. Ronne, 1957. Time-lapse photography — an aid to studies of the shoreline. *Research Reviews*, (Apr. 1957): 1–6	884
Torphy, S. R., and J. M. Zeigler, 1957. Submarine topography of the Eastern Channel, Gulf of Maine, *J. Geol.*, 65(4): 433–441	885
Turner, H. J., Jr., and D. L. Belding, 1957. The tidal migrations of *Donax variabilis* Say. *Limnol. & Oceanogr.*, 2(2): 120–124	886
Kanwisher, J. W., 1957. Freezing and drying in intertidal algae. *Biol. Bull.*, 113(2): 279–285	887
Kanwisher, J. W., and A. Ebeling, 1957. Composition of the swim-bladder gas in bathypelagic fishes. *Deep-Sea Res.*, 4(3): 211–217	888
Woodcock, A. H., and A. T. Spencer, 1957. An airborne flame photometer and its use in the scanning of marine atmospheres for sea salt particles. *J. Meteorol.*, 14(5): 437–447	889

	Contr. No.
van Bergeijk, W. A., and Emil Witschi, 1957. The basilar papilla of the anuran ear. *Acta Anatomica*, 30 : 81 -91	890
Scholander, P. F., L. van Dam, J. W. Kanwisher, H. T. Hammel and M. S. Gordon, 1957. Supercooling and osmoregulation in Arctic fish. *J. Cell. Comp. Physiol.*, 49(1) : 5–24	891
Scholander, P. F., and L. van Dam, 1957. The concentration of hemoglobin in some cold water Arctic fishes. *J. Cell. Comp. Physiol.*, 49(1) : 1–4	892
Yentsch, C. S., and J. H. Ryther, 1957. Short-term variations in phytoplankton chlorophyll and their significance. *Limnol. & Oceanogr.*, 2(2) : 140–142	893
Backus, R. H., and H. Barnes, 1957. Television echo sounder observations of midwater sound scatterers. *Deep-Sea Res.*, 4(2) : 116–119	894
Walden, R. G., D. D. Ketchum and D. H. Frantz, Jr., 1957. Buoy telemeters ocean temperature data. *Electronics*, 30(6) : 164–167	895
Backus, R. H., 1957. The fishes of Labrador. *Bull., Amer. Mus. Nat. Hist.*, 113(4) : 277–337	896
Barnes, H., 1957. The northern limits of *Balanus balanoides* (L.). *Oikos*, 8(1) : 1–15	897
Yentsch, C. S., 1957. A non-extractive method for the quantitative estimation of chlorophyll in algal cultures. *Nature*, 179 : 1302–1304	898
Stommel, Henry, and George Veronis, 1957. Steady convective motion in a horizontal layer of fluid heated uniformly from above and cooled non-uniformly from below. *Tellus*, 9(3) : 401–407	899
Mather, F. J., III, and R. H. Gibbs, Jr., 1957. Distribution records of fishes from waters off New England and the middle Atlantic states. *Copeia* 1957(3) : 242–244	901
Ryther, J. H., and C. S. Yentsch, 1957. The estimation of phytoplankton production in the ocean from chlorophyll and light data. *Limnol. & Oceanogr.*, 2(3) : 281–286	902
Sutcliffe, W. H., Jr., 1957. An improved method for the determination of preserved plankton volumes. *Limnol. & Oceanogr.*, 2(3) : 295–296	903
Bumpus, D. F., 1957. Surface water temperatures along Atlantic and Gulf coasts of the United States. *U.S.F.W.S., Spec. Sci. Rept., Fish.*, No. 214 : 153 pp.	904
Athearn, W. D., 1957. Comparison of clay from the continental shelf off Long Island with Gardiners clay. *J. Geol.*, 65(4) : 448–449	905
Bowen, V. T., and T. T. Sugihara, 1957. Strontium 90 in North Atlantic surface water. *Proc. Nat. Acad. Sci.*, 43(7) : 576–580	907
Worthington, L. V., and W. E. Schevill, 1957. Underwater sounds heard from sperm whales. *Nature* 180 (4580) : 291	908
Hahn, Jan, 1957. Oceanus goes to the bottom of the sea. *Oceanus* 5(1–2) : 20–31	909
Swallow, J. C., and L. V. Worthington, 1957. Measurement of deep currents in the western North Atlantic. *Nature* 179 : 1183–1184	910
McLeod, G. C., 1957. The effect of circularly polarized light on the photosynthesis and chlorophyll *a* synthesis of certain marine algae. *Limnol. & Oceanogr.*, 2(4) 360–362	911

	Contr. No.
Gibbs, R. H., Jr., 1957. A taxonomic study of *Myctophum affine* and *M. nitidulum*, two lantern-fishes previously synonymized, in the western North Atlantic. *Deep-Sea Res.*, 4(4): 230–237	912
Zen, E-an, 1957. Preliminary report on the mineralogy and petrology of some marine bottom samples off the coast of Peru and Chile. *Amer. Mineralog.* 42: 889–903	913
Moulton, J. R., 1957. Sound production in the spiny lobster, *Panulirus argus* (Latreille). *Biol. Bull.*, 113(2): 286–295	914
Whitney, G. G., Jr., 1957. Factors affecting the accuracy of thermometric depth determinations. *J. du Cons.*, 22(2): 167–173	916
Stommel, Henry, 1957. A survey of ocean current theory. *Deep-Sea Res.*, 4(3): 149–184	917
Bumpus, D. F., 1957. Oceanographic observations, 1956, east coast of the United States. *U.S.F.W.S. Spec. Sci. Rept., Fish.*, No. 233: 132 pp.	918
Zeigler, J. M., W. D. Athearn and Herbert Small, 1957. Profiles across the Peru-Chile Trench. *Deep-Sea Res.*, 4(4): 238–249	919
Scholander, P. F., 1957. Oxygen dissociation curves in fish blood. *Acta Physiol. Scandinavica* 41(4): 340–344	921
Gibbs, R. H., Jr., 1957. Preliminary analysis of the distribution of white marlin, *Makaira albida* (Poey) in the Gulf of Mexico. *Bull. Mar. Sci., Gulf & Caribbean*, 7(4): 360–369	922
Plunkett, M. A., 1957. The quantitative determination of some organic compounds in marine sediments. *Deep-Sea Res.*, 4(4): 259–262	924
Bumpus, D. F., Joseph Chase, C. G. Day, D. H. Frantz, Jr., D. D. Ketchum, and R. G. Walden, 1957. A new technique for studying non-tidal drift with results of experiments off Gay Head, Mass., and in the Bay of Fundy. *J. Fish. Res. Bd, Canada*, 16(6): 931–944	926
Folsom, T. R., and A. C. Vine, 1957. On the tagging of water masses for the study of physical processes in the oceans. In: The effects of atomic radiation on oceanography and fisheries. *Nat. Acad. Sci.-Nat. Res. Counc., Publ.*, 551: 121–132	929
Bumpus, D. F., and C. G. Day, 1957. Drift bottle records for the Gulf of Maine and Georges Bank, 1931–1956. *U.S.F.W.S. Spec. Sci. Rept., Fish.*, No. 242: 61 pp.	941

Personnel

Two members of our staff who had a long association with this laboratory died during the year. Dr. Carl-Gustaf Rossby had visited Woods Hole many times since the first year of the Institution's existence. He was a member of the Board of Trustees and one of the most distinguished members of the staff. As Director of the Institute of Meteorology in Stockholm he was the universally acknowledged leader of the theoretical approach in both meteorology and oceanography. Several of our staff have recently worked there. Dr. Arnold B. Arons is at present enjoying a sabbatical leave at Dr.

Rossby's institute. Dr. Louis W. Hutchins also died suddenly. He had worked at Woods Hole during the war years on the ecology of fouling organisms and then went on to be the Director of the Bermuda Biological station. He was studying our collection of fouling organisms in Washington at the time of his death.

There were a very large number of visitors at Woods Hole during the past summer. Several committees, both national and international, held meetings at the laboratory. In addition, more than one hundred people worked here temporarily during the summer.

Among the visiting investigators who worked at the laboratory for considerable periods of time during the past year were the following:

Angeles Alvariño de Leira	Spanish Institute of Oceanography (Navy Ministry), Spain
Harold Barnes	Marine Station, Millport, Scotland
Thanom Charernlarb	Royal Thai Navy, Thailand
Robert Conover	University of Rhode Island
Richard Fay	United States Weather Bureau
Takashi Ichiye	Central Meteorological Office, Tokyo University, Japan
Jack McLachlan	Oregon State College
Allen Milne	Pacific Naval Laboratory, British Columbia
E. G. Pringsheim	Pflanzenphysiologisches Institut, Germany
T. S. Satyanarayana Rao	Andhra University, India
Carl-G. Rossby	Institute of Meteorology, University of Stockholm, Sweden
William H. Sutcliffe, Jr.	Bermuda Biological Station, Bermuda
John B. Tait	Marine Laboratory, Scottish Home Department, Aberdeen, Scotland
Hans Walden	Deutscher Wetterdienst, Germany
Georg Wüst	Institut für Meereskunde der Universität, Germany

The following persons were awarded grants, honoraria or fellowships during 1957:

Angeles Alvariño de Leira	Spanish Institute of Oceanography (Navy Ministry), Spain
Thomas S. Austin	Pacific Oceanic Fisheries Investigations, Hawaii
Harold Barnes	Marine Station, Millport, Scotland
Duncan C. Blanchard	Massachusetts Institute of Technology
K. F. Bowden	University of Liverpool, England
Norman A. Chamberlain	Johns Hopkins University
Leon S. Ciereszko	University of Oklahoma
Waller MacN. Conard	Putney School

Gunther Dietrich	Deutsches Hydrographisches Institut, Germany
El Sayed Mohamed Hassan	New York University
Alan Haught	Amherst College
Bernhard Haurwitz	New York University
Louis W. Hutchins	Washington, D. C.
James M. Moulton	Bowdoin College
Roderic B. Park	California Institute of Technology
Mary A. Plunkett	Vassar College
C. H. B. Priestly	Commonwealth Scientific & Industrial Research Organization, Australia
Carol Reichert	Antioch College
Gordon A. Riley	Yale University
Allan R. Robinson	Harvard University
Rudolf S. Scheltema	University of North Carolina
Theodore J. Smayda	University of Oslo, Norway
Edith L. Stetson	Smith College
Raymond G. Stross	University of Wisconsin
Edward D. Stroup	Johns Hopkins University
William H. Sutcliffe, Jr.	Bermuda Biological Station
John B. Tait	Marine Laboratory, Scottish Home Department, Aberdeen, Scotland
Olive Tattersall	London University, England
John E. Tyler	Scripps Institution of Oceanography
B. Volcani	Biochemical Laboratories, Massachusetts General Hospital
Hans Walden	Deutscher Wetterdienst, Germany
Wolfgang Wieser	Zoological Institute, University of Vienna, Austria
E-an Zen	Harvard University

V. TREASURER'S REPORT

The accounts for the year 1957 have been audited by Lybrand, Ross Bros. & Montgomery.

The book value of endowment funds at December 31, 1957 was $3,268,095, of which $836,574 represented accumulated net gains from sales of investments. The market value of endowment assets on the same date, including real estate at book amount, was $4,346,208. Endowment fund investments and income received therefrom are summarized in Schedule D.

Income received on endowment assets, including interest charged on the advance to current funds, was $180,593 for the year ended December 31, 1957, compared with $167,380 the previous year. This income represented a return on endowment fund assets of 4.2% at year-end market quotation, 5.5% on the book amount and 7.4% on the contributed amount of the endowment fund.

Endowment income was allocated for 1957 operating expenses at the rate of 5.3% of the book amount of original endowment funds, or $128,328; the rate was the same as that of the previous year. The balance of endowment income, $52,265, was transferred to the income and salary stabilization reserve. Advances were made from endowment funds to current funds during portions of the year, but all such advances were paid off prior to the end of the year.

Deferred charges amounting to $248,320 (see balance sheet for breakdown) represented expenditures for the benefit of future years. A proportionate part of these charges will be added to current costs, or other appropriate accounts, as the benefits accrue.

The details of unexpended balances of gifts and receipts for research, other than government, are shown in Schedule C. The income from Woods Hole Oceanographic Associates for the year amounted to $76,907. Expenditures and allocations to specific projects of $77,841, plus $11,000 of life memberships transferred to endowment assets reduced the balance on hand of $71,549 at December 31, 1956 to $59,615 on December 31, 1957.

The Institution's 1957 contribution to the Woods Hole Oceanographic Institution's Employees Retirement Trust amounted to $68,898. The trust is administered by three trustees. The balance of the old Retirement Fund, administered by the Treasurer, amounted to $65,973 as at December 31, 1957. This balance consisted of amounts on deposit in sixteen savings bank accounts held in trust for ten members of the plan. No contributions to the old plan were made in 1957. Interest totalling $2,079 was credited to the savings accounts during the year.

In the financial statements that follow it is interesting to note that for each dollar spent 79 cents was spent for direct costs of research activity, 15.5 cents for general and administration expenses and 5.5 cents for plant operation and miscellaneous. Administrative salaries amounted to only 6 cents of each dollar of total expense. Included in the 15.5 cents for general and administration expenses was 3.8 cents for staff benefits (group insurance, social security taxes, and contributions to retirement plan.)

BALANCE SHEET

As at December 31, 1957

ASSETS

ENDOWMENT FUND ASSETS:		
Investments (Schedule D):		
Bonds (market quotations $1,770,412)		$1,869,682
Stocks (market quotations $2,414,953)		1,237,570
Real estate		98,417
		3,205,669
Cash		62,426
		3,268,095
PLANT ASSETS (note):		
Laboratory plant and equipment		578,401
Vessels and equipment		364,983
Other property		161,541
		1,104,925
CURRENT FUND ASSETS:		
Cash		16,402
Accounts receivable:		
U. S. Government	$298,452	
Other	5,935	304,387
Unbilled costs on research contracts:		
U. S. Government	188,682	
Other	6,216	194,898
Supply inventories		31,687
Deferred charges:		
Reconditioning boat Crawford	200,881	
Electronic equipment	31,055	
Other	16,384	248,320
		795,694
		$5,168,714

LIABILITIES

ENDOWMENT FUNDS:		
Unrestricted		$2,012,101
For upkeep of plant		419,420
Accumulated net gain on sale of investments		836,574
		3,268,095
FUNDS INVESTED IN PLANT		1,104,925
CURRENT LIABILITIES AND FUNDS:		
Accounts payable and accrued expenses		157,687
Contribution payable to employees' retirement plan and trust		68,898
Unexpended balances of gifts and grants:		
For research:		
Government	$109,228	
Other (Schedule C)	9,942	119,170
Oceanographic Associates		59,615
General fund:		
General plant and equipment reserve	211,888	
Income and salary stabilization reserve	166,589	
Unappropriated	11,847	390,324
		795,694
		$5,168,714

Note — Since 1945 the Institution has provided for depreciation of plant assets other than vessels at annual rates of 2% on buildings and 5% to 33⅓% on equipment, carrying the amounts to general plant and equipment reserve.

STATEMENT OF INCOME, OPERATING EXPENSES AND UNAPPROPRIATED GENERAL FUND

For the Year Ended December 31, 1957

INCOME:		
Receipts for sponsored research:		
For direct costs		$1,857,053
For indirect costs		472,888
Fees for use of facilities		76,548
		2,406,489
Endowment income after amortization of bond premiums (Schedule D)	$180,593	
Less amount added to income and salary stabilization reserve	52,265	128,328
Miscellaneous		421
Total income availed of		2,535,238
OPERATING EXPENSES:		
Direct costs of research activity (Schedule A):		
Salaries and wages		938,678
Vessel operations		564,337
Materials and services		394,399
Travel		91,356
		1,988,770
Indirect costs:		
General and administration (Schedule B)	392,220	
Plant operation (Schedule B)	136,325	
Miscellaneous	3,795	532,340
Total operating expenses		2,521,110
EXCESS OF INCOME		14,128
Additions to plant from current funds — books and equipment purchased		28,541
		(14,413)
UNAPPROPRIATED GENERAL FUND, JANUARY 1, 1957		26,260
UNAPPROPRIATED GENERAL FUND, DECEMBER 31, 1957		$ 11,847

SCHEDULE A

DIRECT COSTS OF RESEARCH ACTIVITY

For the Year Ended December 31, 1957

	Salaries and Wages	Vessel Operations	Materials and Services	Travel	Total
U.S. GOVERNMENT CONTRACTS	$814,514	$504,840	$321,098	$79,849	$1,720,301
OTHER SPONSORED RESEARCH	38,698	40,104	55,884	2,066	136,752
Total direct costs of sponsored research	853,212	544,944	376,982	81,915	1,857,053
INSTITUTION RESEARCH	85,466	19,393	17,417	9,441	131,717
Total direct costs of research	$938,678	$564,337	$394,399*	$91,356	$1,988,770

* Includes grants and fellowships:

Other sponsored research	$21,491
Institution research	450
	$21,941

SCHEDULE B

GENERAL AND ADMINISTRATION EXPENSES AND EXPENSES FOR PLANT OPERATION

For the Year Ended December 31, 1957

GENERAL AND ADMINISTRATION

GENERAL EXPENSES:		
Staff benefits:		
Contributions to retirement plan		$68,898
Social security taxes		25,656
Group insurance		2,324
		96,878
Shop services		83,824
Housing, net		2,303
ADMINISTRATION EXPENSES:		
Salaries and wages	$152,662	
Insurance, travel, supplies and other	56,553	209,215
		$392,220

PLANT OPERATION

SALARIES AND WAGES		48,417
PROVISION FOR DEPRECIATION (credited to general plant and equipment reserve)		27,566
OTHER REPAIR COSTS	10,018	
HEAT, LIGHT AND POWER	21,111	
CARYN LAY-UP COSTS	18,243	
OTHER	10,970	60,342
		$136,325

SCHEDULE C

SUMMARY OF GIFTS AND RECEIPTS FOR RESEARCH

Year Ended December 31, 1957

	Unexpended Balance January 1, 1957	Received	Expended		Other Charges or (Credits)	Unexpended Balance December 31, 1957
			Direct Costs	Indirect Costs		
American Society of Limnology and Oceanography		$ 856	$ 598	$ 258		
Arctic Institute of North America — freezing of living tissue		3,500	2,510	990		
Bermuda Biological Station for Research		253	244	9		
Commonwealth of Massachusetts — shellfish propagation	$ 5,100	20,000	14,435	8,882		$1,783
Esso Research and Engineering Company:						
Foraminifera cataloging		108	108			
Peruvian samples analysis	2,000		2,000			
Gordon project		85	72	8	$ 5 (a)	
Manufacture, sale, and calibration of instruments		2,173	20,372	5,060	(15,029) (b) (8,230) (c)	
Lou Marron science fund — pelagic fish studies		1,000	2,405		(1,659) (d)	254
Munitalp Foundation — meteorological research		6,500	4,500	300		1,700
National Academy of Sciences — project Nobska		41	41			
National Lead Company		2,532	2,303	229		
Oceanographic Associates:						
Deuterium studies		1,000	245	58		697
Peruvian core analysis	10,482		7,156	220		3,106
Crawford Meteorological expedition		38,247	38,247			
Other (including fellowships, lectureships, and portion of research costs)		37,245	34,904	682	1,659 (d)	
Research Corporation — instrument fund	2,558		364	181	(389) (e)	2,402
Socony-Mobil Laboratories — Peruvian samples analysis	1,000		1,000			
Sundry work done for others		5,056	4,161	895		
Town of Islip, New York — Great South Bay survey	567	1,000	1,087	480		
	$21,707	$119,596	$136,752	$18,252	($23,643)	$9,942

(a) Credited to income. (b) Transferred to laboratory equipment. (c) Charged to other projects. (d) Transfers. (e) Sales.

Schedule D

SUMMARY OF INVESTMENTS

As at December 31, 1957

	Book Amount	% of Total	Market Quotation	% of Total	Income
Bonds:					
U. S. Government........	$ 326,070	10.17	$ 317,281	7.41	$ 11,691
Railroad.................	525,855	16.40	464,558	10.84	21,694
Public utility............	397,039	12.39	389,970	9.10	11,373
Industrial...............	365,494	11.40	340,390	7.95	11,884
Financial and investment..	255,224	7.96	258,213	6.03	10,181
Total bonds.........	1,869,682	58.32	1,770,412	41.33	66,823
Stocks:					
Preferred...............	295,309	9.21	283,663	6.62	15,100
Common:					
Public utility..........	314,988	9.83	525,382	12.26	22,460
Industrial............	449,257	14.02	1,316,525	30.73	57,018
Miscellaneous.........	178,016	5.55	289,383	6.76	13,472
Total common stocks	942,261	29.40	2,131,290	49.75	92,950
Total stocks.........	1,237,570	38.61	2,414,953	56.37	108,050
Real Estate...............	98,417	3.07	98,417*	2.30	5,092
Total investments....	$3,205,669	100.00	$4,283,782	100.00	179,965
Interest on Advance to Current Funds Charged to Miscellaneous Operating Expense..........					628
Total Endowment Fund Income..........					$180,593

* At book amount.

Woods Hole Oceanographic Institution
Woods Hole, Massachusetts

We have examined the balance sheet of Woods Hole Oceanographic Institution as at December 31, 1957 and the related statement of income, operating expenses and unappropriated general fund for the year then ended. Our examination was made in accordance with generally accepted auditing standards, and accordingly included such tests of the accounting records and such other auditing procedures as we considered necessary in the circumstances; however, it was not practicable to confirm receivables from United States Government departments, as to which we have satisfied ourselves by means of other auditing procedures.

In our opinion, the accompanying financial statements present fairly the position of Woods Hole Oceanographic Institution at December 31, 1957 and the results of its operations for the year then ended, on a basis consistent with that of the preceding year.

Boston, Massachusetts
May 12, 1958

Lybrand, Ross Bros. & Montgomery

List of Contributions

LIST OF CONTRIBUTIONS

FROM THE WOODS HOLE OCEANOGRAPHIC INSTITUTION

See Author, Subject-Locality, Taxonomic Index, pubilshed in 1957, for a complete list up to 1956.

No. 601. Floyd M. Soule, P. S. Branson and R. P. Dinsmore. Physical Oceanography of the Grand Banks Region and the Labrador Sea in 1951. *U. S. Coast Guard Bull.*, No. 37, pp. 17–85. 1952.

No. 602. Mary Sears. Notes on Siphonophores. 2. A Revision of the Abylinae. *Bull. Mus. Comp. Zool.*, Vol. 109, No. 1, pp. 1–119. 1953. (Not included in *Collected Reprints*).

No. 603. I. I. Schell. On the Role of the Ice off Iceland in the Decadal Air Temperatures of Iceland, and some other Areas. *Jour. du Conseil*, Vol. 18, No. 1, pp. 11–36. 1952.

No. 604. D. B. Ericson, Maurice Ewing and Bruce C. Heezen. Turbidity Currents and Sediments in the North Atlantic. *Bull. Amer. Assoc. Petrol. Geol.*, Vol. 36, No. 3, pp. 489–511. 1952.

No. 605. Andrew F. Bunker. On the Determination of Moisture Gradients from Radiosonde Records. *Bull. Amer. Meteorol. Soc.*, Vol. 34, No. 9, pp. 406–409. 1953.

No. 606. Frank J. Mather, III and Howard A. Schuck. Additional Notes on the Distribution of the Blackfin Tuna (*Parathunnus atlanticus*). *Copeia*, No. 4, p. 267. 1952.

No. 607. Mary Sears. Notes on Siphonophores. 3. *Nectopyramis spinosa* n. sp. *Breviora*, No. 3, pp. 1–4. 1952.

No. 608. W. V. R. Malkus and M. E. Stern. Determination of Ocean Transports and Velocities by Electromagnetic Effects. *Sears Found., Jour. Mar. Res.*, Vol. 11, No. 2, pp. 97–105. 1952.

No. 609. Joanne Starr Malkus. The Slopes of Cumulus Clouds in Relation to External Wind Shear. *Quart. Jour. Roy. Meteor. Soc.*, Vol. 78, No. 338, pp. 530–542. 1952.

No. 610. Henry B. Bigelow and William C. Schroeder. A New Species of the Cyclostome Genus *Paramyxine* from the Gulf of Mexico. *Breviora*, No. 8, pp. 1–10. 1952.

No. 611. Frank J. Mather, III. Sport Fishes of the Vicinity of the Gulf of Honduras, certain Caribbean Islands, and Carmen, Mexico. *Proc. Gulf and Caribbean Fish. Inst.*, pp. 118–129. 1952.

No. 612. C. O'D. Iselin. The Gulf Stream System. *Proc. Amer. Philos. Soc.*, Vol. 96, No. 6, pp. 660–662. 1952.

No. 613. Frederick B. Laidlaw. The History of the Prevention of Fouling. *U. S. Naval Inst. Proc.*, Vol. 78, No. 7, Whole No. 593, pp. 768–779. 1952.

No. 614. Gary Felsenfeld. The Binding of Copper by Hemocyanin. *Jour. Cell. and Comp. Physiol.*, Vol. 43, No. 1, pp. 23–38. 1954

No. 615. Harry J. Turner, Jr. Fourth Report on Investigations of the Shellfisheries of Massachusetts. *Com. Mass., Dept. Cons., Div. Mar. Fish.*, pp. 1–21. 1951.

No. 616. Henry Stommel and Harlow G. Farmer. Abrupt Change in Width in Two-Layer Open Channel Flow. *Sears Found., Jour. Mar. Res.*, Vol. 11, No. 2, pp. 205–214. 1952.

No. 617. Joanne Starr Malkus and Andrew F. Bunker. Observational Studies of the Air Flow over Nantucket Island during the Summer of 1950. *Papers in Physical Oceanography and Meteorology*, Vol. 12, No. 2, pp. 1–50. 1952.

No. 618. Andrew F. Bunker. Measurements of the Vertical Water Vapor Transport and Distribution within Unstable Atmospheric Ground Layers and the Turbulent Mass Exchange Coefficient. *Papers in Physical Oceanography and Meteorology*, Vol. 12, No. 3, pp. 1–42. 1952.

No. 619. William L. Ford and A. R. Miller. The Surface Layer of the Gulf Stream and Adjacent Waters. *Sears Found., Jour. Mar. Res.*, Vol. 11, No. 3, pp. 267–280. 1952.

No. 620. Willem V. R. Malkus. The Heat Transport and Spectrum of Thermal Turbulence. *Proc. Roy. Soc.*, A, Vol. 225, pp. 196–212. 1954. (Not included in *Collected Reprints*).

No. 621. William S. von Arx. Notes on the Surface Velocity Profile and Horizontal Shear across the Width of the Gulf Stream. *Tellus*, Vol. 4, No. 3, pp. 211–214. 1952.

No. 622. William S. von Arx. A Laboratory Study of the Wind-driven Ocean Circulation. *Tellus*, Vol. 4, No. 4, pp. 311–318. 1952.

No. 623. Helen S. Vishniac and S. W. Watson. The Steroid Requirements of *Labyrinthula vitellina* var. *pacifica*. *Jour. Gen. Microbiol.*, Vol. 8, No. 2, pp. 248–255. 1953.

No. 624. Joanne Starr Malkus and Melvin E. Stern. The Flow of a Stable Atmosphere over a Heated Island, Part I. *Jour. Meteorology*, Vol. 10, No. 1, pp. 30–41. 1953.

No. 625. Melvin E. Stern and Joanne Starr Malkus. The Flow of a Stable Atmosphere over a Heated Island, Part II. *Jour. Meteorology*, Vol. 10, No. 2, pp. 105–120. 1953.

No. 626. William E. Schevill. On the Nomenclature of the Pacific Gray Whale. *Breviora*, No. 7, pp. 1–3. 1952.

No. 627. Alfred C. Redfield. The Flushing of Harbors and other Hydrodynamic Problems in Coastal Waters. In: *Hydrodynamics in Modern Technology*, Mass. Inst. Tech., pp. 127–135, December 1951.

No. 628. L. V. Worthington. Oceanographic Results of Project Skijump I and Skijump II in the Polar Sea, 1951–1952. *Trans. Amer. Geophys. Union*, Vol. 34, No. 4, pp. 543–551. 1953.

No. 629. Charles B. Officer, Jr. The Refraction Arrival in Water Covered Areas. *Geophysics*, Vol. 18, No. 4, pp. 805–819. 1953.

No. 630. Harry J. Turner, Jr. The Drilling Mechanism of the Naticidae. *Ecology*, Vol. 34, No. 1, pp. 222–223. 1953.

No. 631. Andrew F. Bunker. Diffusion, Entrainment and Frictional Drag Associated with Non-Saturated, Buoyant Air Parcels rising through a Turbulent Air Mass. *Jour. Meteorology*, Vol. 10, No. 3, pp. 212–218. 1953.

No. 632. P. F. Scholander and L. van Dam. Composition of the Swimbladder Gas in Deep Sea Fishes. *Biol. Bull.*, Vol 104, No. 1, pp. 75–86. 1953.

No. 633. L. van Dam and P. F. Scholander. Concentration of Hemoglobin in the Blood of Deep Sea Fishes. *Jour. Cell. and Comp. Physiol.*, Vol. 41, No. 3, pp. 522–524. 1953.

No. 634. Willem V. R. Malkus. A Recording Bathypitotmeter. *Sears Found., Jour. Mar. Res.*, Vol. 12, No. 1, pp. 51–59. 1953.

No. 635. A. B. Arons and C. F. Kientzler. Vapor Pressure of Sea Salt Solutions. *Trans. Amer. Geophys. Union*, Vol. 35, No. 5, pp. 722–728. 1954.

No. 636. Alfred C. Redfield. Interference Phenomena in the Tides of the Woods Hole Region. *Sears Found., Jour. Mar. Res.*, Vol. 12, No. 1, pp. 121–140. 1953.

No. 637. Floyd M. Soule. Physical Oceanography of the Grand Banks Region and the Labrador Sea in 1952. *U. S. Coast Guard Bull.*, No. 38, pp. 31–100. 1953.

No. 638. Harlow G. Farmer and George W. Morgan. The Salt Wedge. *Proc. Third Conf. on Coastal Engineering*, Cambridge, Mass., October 1952, pp. 54–64. 1953.

No. 639. J. R. D. Francis. A Note on the Velocity Distribution and Bottom Stress in a Wind-Driven Water Current System. *Sears Found., Jour. Mar. Res.*, Vol. 12, No. 1, pp. 93–98. 1953.

No. 640. Henry Stommel. Computation of Pollution in a Vertically Mixed Estuary *Se.wage and Industrial Wastes*, Vol. 25, No. 9, pp. 1065–1071. 1953.

No. 641. Jack L. Hough. Pleistocene Climatic Record in a Pacific Ocean Core Sample. *Jour. Geology*, Vol. 61, No. 3, pp. 252–262. 1953.

No. 642. Bostwick H. Ketchum. Circulation in Estuaries. *Proc. Third Conf. on Coastal Engineering*, Cambridge, Mass., October 1952, pp. 65–76. 1953.

No. 643. A. H. Woodcock. Salt Nuclei in Marine Air as a Function of Altitude and Wind Force. *Jour. Meteorology*, Vol. 10, No. 5, pp. 362–371. 1953.

No. 644. Henry Stommel, W. S. von Arx, D. Parson and W. S. Richardson. Rapid Aerial Survey of Gulf Stream with Camera and Radiation Thermometer. *Science*, Vol. 117, No. 3049, pp. 639–640. 1953.

No. 645. Henry Stommel. Examples of the Possible Role of Inertia and Stratification in the Dynamics of the Gulf Stream System. *Sears Found., Jour. Mar. Res.*, Vol. 12, No. 2, pp. 184–195. 1953.

No. 646. Henry C. Stetson. The Sediments of the Western Gulf of Mexico. Part I. The Continental Terrace of the Western Gulf of Mexico: its Surface Sediments, Origin and Development. *Papers in Physical Oceanography and Meteorology*, Vol. 12, No. 4, pp. 1–45. 1953.

No. 647. Parker D. Trask. The Sediments of the Western Gulf of Mexico. Part II. Chemical Studies of Sediments of the Western Gulf of Mexico. *Papers in Physical Oceanography and Meteorology*, Vol. 12, No. 4, pp. 47–120. 1953.

No. 648. William E. Schevill and Barbara Lawrence. Auditory Response of a Bottlenosed Porpoise, *Tursiops truncatus*, to Frequencies above 100 kc. *Jour. Exper. Zool.*, Vol. 124, No. 1, pp. 147–165. 1953.

No. 649. William S. von Arx. Cartographic Principles Applied to Wide-Field Photography. *Photogr. Engineering*, Vol. 4, No. 2, pp. 60–73. 1953.

No. 650. Betty Lee Gealy. Topography of the Continental Slope in Northwest Gulf of Mexico. *Bull. Geol. Soc. Amer.*, Vol. 66, No. 2, pp. 203–227. 1955.

No. 651. Frank J. Mather III and C. Godfrey Day. Observations of Pelagic Fishes of the Tropical Atlantic. *Copeia*, No. 3, pp. 179–188. 1954.

No. 652. Joseph Chase. A Comparison of Certain North Atlantic Wind, Tide Gauge and Current Data. *Sears Found., Jour. Mar. Res.*, Vol. 13, No. 1, pp. 22–31. 1954.

No. 653. Barbara Lawrence and William E. Schevill. *Tursiops* as an Experimental Subject. *Jour. Mammalogy*, Vol. 35, No. 2, pp. 225–232. 1954.

No. 654. William E. Schevill. Sight Records of the Gray Grampus, *Grampus griseus* (Cuvier). *Jour. Mammalogy*, Vol. 35, No. 1, pp. 123–124. 1954.

No. 655. Henry Stommel. The Role of Density Currents in Estuaries. *Proc. Minnesota Int. Hydraulics Conv.*, Sept. 1–4, 1953, pp. 305–312. 1953.

No. 656. Harry J. Turner, Jr. Fifth Report on Investigations of the Shellfisheries of Massachusetts. *Com. Mass., Dept. Cons., Div. Mar. Fish.*, pp. 1–37. 1952.

No. 657. Henry B. Bigelow and William C. Schroeder. A New Family, a New Genus, and Two New Species of Batoid Fishes from the Gulf of Mexico. *Breviora*, No. 24, 16 pp. 1954.

No. 658. Duncan C. Blanchard. Raindrop Size-Distribution in Hawaiian Rains. *Jour. Meteorology*, Vol. 10, No. 6, pp. 457–473. 1953.

No. 659. Duncan C. Blanchard. A Simple Recording Technique for Determining Raindrop Size and Time of Occurrence of Rain Showers. *Trans. Amer. Geophys. Union*, Vol. 34, No. 4, pp. 534–538. 1953.

No. 660. A. H. Woodcock. Hawaii as a Cloud Physics Laboratory. *Pacific Science*, Vol. 7, No. 4, pp. 522–524. 1953.

No. 661. Daniel R. Norton, Mary A. Plunkett and Francis A. Richards. Spectrophotometric Determination of Uric Acid and Some Redeterminations of its Solubility, *Analytical Chemistry*, Vol. 26, No. 3, pp. 454–457. 1954.

No. 662. C. B. Officer, Jr. and Maurice Ewing. Geophysical Investigations in the Emerged and Submerged Atlantic Coastal Plain. *Bull. Geol. Soc. Amer.*, Vol. 65, pp. 653–670. 1954.

No. 663. William E. Schevill and Barbara Lawrence. High-Frequency Auditory Response of a Bottlenosed Porpoise, *Tursiops truncatus* (Montagu). *Jour. Acoust. Soc. Amer.*, Vol. 25, No. 5, pp. 1016–1017. 1953.

No. 664. R. B. Montgomery. Analysis of a Hugh M. Smith Oceanographic Section from Honolulu Southward across the Equator. *Sears Found., Journ. Mar. Res.*, Vol. 13, No. 1, pp. 67–75. 1954.

No. 665. C. H. Keith and A. B. Arons. The Growth of Sea-Salt Particles by Condensation of Atmospheric Water Vapor. *Jour. Meteorology*, Vol. 11, No. 3, pp. 173–184. 1954.

No. 666. L. V. Worthington. The Temperature Increase in Caribbean Deep Water since 1933. *Deep-Sea Research*, Vol. 3, pp. 234–235. 1956.

No. 667. Joanne Starr Malkus. Some Results of a Trade-Cumulus Cloud Investigation. *Jour. Meteorology*, Vol. 11, No. 3, pp. 220–237. 1954.

No. 668. F. C. Fuglister. Average Temperature and Salinity at a Depth of 200 Meters in the North Atlantic. *Tellus*, Vol. 6, No. 1, pp. 46–58. 1954.

No. 669. Hilary B. Moore, Harding Owre, Everett C. Jones and T. Dow. Plankton of the Florida Current. III. The Control of the Vertical Distribution of Zooplankton in the Daytime by Light and Temperature. *Bull. Mar. Sci. Gulf and Caribbean*, Vol. 3, No. 2, pp. 83–95. 1953.

No. 670. Willem V. R. Malkus. Discrete Transitions in Turbulent Convection. *Proc. Roy. Soc.*, A, Vol. 225, pp. 185–195. 1954. (Not included in *Collected Reprints*).

No. 671. Mary Sears. Notes on the Peruvian Coastal Current. 1. An Introduction to the Ecology of Pisco Bay. *Deep-Sea Research*, Vol. 1, pp. 141–169. (Also published as: Notas sobre la Corriente Costanera del Peru. 1. Introduccion a la Ecologia de la Bahia de Pisco. *Bol. Cient. Cia. Admora. Guano*, Lima, Peru, Vol. 1, No. 2, pp. 133–179). 1954.

No. 672. Ralph F. Wyrick. Observations on the Movements of the Pacific Gray Whale *Eschrichtius glaucus* (Cope). *Journ. Mammalogy*, Vol. 35, No. 4, pp. 596–598. 1954.

No. 673. A. H. Woodcock, C. F. Kientzler, A. B. Arons and D. C. Blanchard. Giant Condensation Nuclei from Bursting Bubbles. *Nature*, Vol. 172, No. 4390, pp. 1144–1145. 1953.

No. 674. Harry J. Turner, Jr. An Improved Method of Staining the External Organelles of Hypotrichs. *Jour. Protozoology*, Vol. 1, No. 1, pp. 18–19. 1954.

No. 675. Floyd M. Soule, A. J. Bush and J. E. Murray. Physical Oceanography of the Grand Banks Region and the Laborador Sea in 1953. *U. S. Coast Guard Bull.*, No. 39, pp. 45–138. 1955.

No. 676. J. B. Hersey and R. H. Backus. New Evidence that Migrating Gas Bubbles, Probably the Swimbladders of Fish, are Largely Responsible for Scattering Layers on the Continental Rise South of New England. *Deep-Sea Research*, Vol. 1, pp. 190–191. 1954.

No. 677. Ilmo Hela, Hilary B. Moore and Harding Owre. Seasonal Changes in the Surface Water Masses and in their Plankton in the Bermuda Area. *Bull. Mar. Sci. Gulf and Caribbean*, Vol. 3, No. 3, pp. 157–167. 1953.

No. 678. B. Haurwitz. The Occurrence of Internal Tides in the Ocean. *Arch. Meteorol. Geoph. u. Bioklim.*, Ser. A, Meteorol. und Geoph., Band 7, pp. 406–424. 1954.

No. 679. Gunther K. Wertheim. Studies of the Electric Potential between Key West, Florida, and Havana, Cuba. *Trans. Amer. Geophys. Union*, Vol. 35, No. 6, pp. 872–882. 1954.

No. 680. John C. Ayers. A Method for Rendering Wood Resistant to Marine Borers. *Bull. Mar. Sci. Gulf and Caribbean*, Vol. 3, No. 4, pp. 297–304. 1954.

No. 681. William S. von Arx. Some Techniques for Laboratory Study of the Primary Ocean Circulation. Fluid Models in Geophysics. In: Proc. First Symp., Models in Geophysical Fluid Dynamics, The Johns Hopkins University, Sept. 1–4, 1953, pp. 89–99. 1956.

No. 682. A. F. Bunker. Measurements of Counter-Gradient Heat Flows in the Atmosphere. *Australian Jour. Physics*, Vol. 9, No. 1, pp. 133–143. 1956.

No. 683. R. F. Vaccaro and J. H. Ryther. The Bactericidal Effects of Sunlight in Relation to "Light" and "Dark" Bottle Photosynthesis Experiments. *Jour. du Conseil*, Vol. 20, No. 1, pp. 18–24. 1954.

No. 684. J. H. Ryther and R. F. Vaccaro. A Comparison of the Oxygen and 14C Methods of Measuring Marine Photosynthesis. *Jour. du Conseil*, Vol. 20, No. 1, pp. 25–34. 1954.

No. 685. John H. Ryther. The Ecology of Phytoplankton Blooms in Moriches Bay and Great South Bay, Long Island, New York. *Biol. Bull.*, Vol. 106, No. 2, pp. 198–209. 1954.

No. 686. E. E. Watson. An Experiment to Determine the Hydrodynamic Forces on a Cable Inclined to the Direction of Flow. *Sears Found.*, *Jour. Mar. Res.*, Vol. 12, No. 3, pp. 245–248. 1953.

No. 687. Bostwick H. Ketchum. Mineral Nutrition of Phytoplankton. *Ann. Rev. Plant Physiol.*, Vol. 5, pp. 55–74. 1954.

No. 688. Francis A. Richards and Alfred C. Redfield. Oxygen-Density Relationships in the Western North Atlantic. *Deep-Sea Research*, Vol. 2, pp. 182–199. 1955.

No. 689. William S. von Arx. Measurements of the Oceanic Circulation in Temperate and Tropical Latitudes. In: Oceanographic Instrumentation. *National Research Council Publ.*, No. 309, pp. 13–35. 1954.

No. 690. M. S. Longuet-Higgins, M. E. Stern and Henry Stommel. The Electrical Field Induced by Ocean Currents and Waves, with Applications to the Method of Towed Electrodes. *Papers in Physical Oceanography and Meteorology*, Vol. 13, No. 1, pp. 1–37. 1954.

No. 691. C. F. Kientzler, A. B. Arons, D. C. Blanchard and A. H. Woodcock. Photographic Investigation of the Projection of Droplets by Bubbles Bursting at a Water Surface. *Tellus*, Vol. 6, No. 1, pp. 1–7. 1954.

No. 692. Henry B. Bigelow and William C. Schroeder. Deep Water Elasmobranchs and Chimaeroids from the Northwestern Atlantic Slope. *Bull. Mus. Comp. Zool.*, Vol. 112, No. 2, pp. 37–87. 1954.

No. 693. Henry Stommel. Exploratory Measurements of Electrical Potential Differences between Widely Spaced Points in the North Atlantic Ocean. *Arch. Meteorol.*, *Geoph. u. Bioklim.*, Ser. A, Meteorol. und Geoph., Band 7, pp. 292–304. 1954.

No. 694. L. V. Worthington. Three Detailed Cross-Sections of the Gulf Stream. *Tellus*, Vol. 6, No. 2, pp. 116–123. 1954.

No. 695. Francis A. Richards and Alfred C. Redfield. A Correlation between the Oxygen Content of Sea Water and the Organic Content of Marine Sediments. *Deep-Sea Research*, Vol. 1, pp. 279–281. 1954.

No. 696. Allyn C. Vine. Oceanographic Instruments for Measuring Temperature. In: Oceanographic Instrumentation. *National Research Council Publ.*, No. 309, pp. 55–69. 1954.

No. 697. J. B. Hersey. Acoustic Instrumentation as a Tool in Oceanography. In: Oceanographic Instrumentation. *National Research Council Publ.*, No. 309, pp. 101–122. 1954.

No. 698. A. B. Arons. Underwater Explosion Shock Wave Parameters at Large Distances from the Charge. *Jour. Acoust. Soc. Amer.*, Vol. 26, No. 3, pp. 343–346. 1954.

No. 699. P. F. Scholander and L. van Dam. Secretion of Gases against High Pressures in the Swimbladder of Deep Sea Fishes. I. Oxygen Dissociation in Blood. *Biol. Bull.*, Vol. 107, No. 2, pp. 247–259. 1954.

No. 700. P. F. Scholander. Secretion of Gases against High Pressures in the Swimbladder of Deep Sea Fishes. II. The Rete Mirabile. *Biol. Bull.*, Vol. 107, No. 2, pp. 260–277. 1954.

No. 701. R. B. Montgomery. Convection of Heat. *Arch. Meteorol., Geoph. u. Bioklim.*, Ser. A, Meteorol. und Geoph., Band 7, pp. 125–132. 1954.

No. 702. Frank J. Mather III. Northerly Occurrences of Warm Water Fishes in the Western Atlantic. *Copeia*, No. 4, pp. 292–293. 1954.

No. 703. C. W. Newton. Analysis and Data Problems in Relation to Numerical Prediction. *Bull. Amer. Meteorol. Soc.*, Vol. 35, No. 7, pp. 287–294. 1954.

No. 704. George L. Clarke. Elements of Ecology. John Wiley & Sons, Inc., New York. 534 pp. 1954. (Not included in *Collected Reprints*).

No. 705. L. van Dam. On the Respiration in Scallops (Lamellibranchiata). *Biol. Bull.*, Vol. 107, No. 2, pp. 192–202. 1954.

No. 706. Joanne Starr Malkus and R. S. Scorer. The Erosion of Cumulus Towers. *Jour. Meteorol.*, Vol. 12, No. 1, pp. 43–57. 1955.

No. 707. Athelstan F. Spilhaus. Sea and Air Resources. *Geogr. Rev.*, Vol. 44, No. 3, pp. 346–351. 1954.

No. 708. Charles J. Fish and Mary Curtis Cobb. Noxious Marine Animals of the Central and Western Pacific Ocean. Fish and Wildlife Service, *Research Report* 36, 45 pp., 1954.

No. 709. P. F. Scholander, Warner E. Love and John W. Kanwisher. The Rise of Sap in Tall Grapevines. *Plant Physiol.*, Vol. 30, No. 2, pp. 93–104. 1955. (Not included in *Collected Reprints*).

No. 710. P. F. Scholander, L. van Dam and Susan I. Scholander. Gas Exchange in the Roots of Mangroves. *Amer. Jour. Bot.*, Vol. 42, No. 1, pp. 92–98. 1955.

No. 711. Duncan C. Blanchard. A Simple Method for the Production of Homogenouse Water Drops down to 1 Micron Radius. *Jour. Colloid Sci.*, Vol. 9, No. 4, pp. 321–328. 1954.

No. 712. John H. Ryther. Ecology of Autotrophic Marine Dinoflagellates with Refence to Red Water Conditions. In: The Luminescence of Biological Systems, F. H. Johnson, Edit., Publ. by Amer. Assoc. Adv. Sci., Washington, pp. 387–414. 1955.

No. 713. Henry Stommel. Serial Observations of Drift Currents in the Central North Atlantic Ocean. *Tellus*, Vol. 6, No. 3, pp. 203–214. 1954.

No. 714. Francis A. Richards. Oxygen in the Ocean. *Geol. Soc. Amer.*, Mem. 67, Vol. 1, Ch. 9, pp. 185–238. 1957.

No. 715. Harry J. Turner, Jr. and J. Arthur Posgay. Sixth Report on Investigations of the Shellfisheries of Massachusetts. *Com. Mass., Dept. Nat. Res., Div. Mar. Fish.*, pp. 1–74. 1953.

No. 716. Joanne Starr Malkus and Claude Ronne. On the Structure of Some Cumulonimbus Clouds which Penetrated the High Tropical Troposphere. *Tellus*, Vol. 6, No. 4, pp. 351–366. 1954.

No. 717. L. V. Worthington. A Preliminary Note on the Time Scale in North Atlantic Circulation. *Deep-Sea Research*. Vol. 1, pp. 244–251. 1954.

No. 718. Arthur R. Miller. Some Suggestions for more precise Loran Navigation. *Navigation*, Vol. 3, Nos. 1 and 2, pp. 23–29. 1951. (Included in *Collected Reprints* for 1953).

No. 719. Henry B. Bigelow and Isabel Pérez Farfante. Fishes of the Western North Atlantic. Lancelets. *Mem. Sears Found. Mar. Res.*, No. 1, Pt. 1, Ch. 1, pp. 1–28. 1948. (Not included in *Collected Reprints*).

No. 720. Henry B. Bigelow and William C. Schroeder. Fishes of the Western North Atlantic. Cyclostomes. *Mem. Sears Found. Mar. Res.*, No. 1, Pt. 1, Ch. 2, pp. 29–58. 1948. (Not included in *Collected Reprints*).

No. 721. Henry B. Bigelow and William C. Schroeder. Fishes of the Western North Atlantic. Sharks. *Mem. Sears Found. Mar. Res.*, No. 1, Pt. 1, Ch. 3, pp. 59–576. 1948. (Not included in *Collected Reprints*).

No. 722. Arthur H. Clarke, Jr. Some Mollusks from the Continental Slope of Northeastern North America. *Breviora*, No. 40, 11 pp. 1954.

No. 723. C. W. Newton. Frontogenesis and Frontolysis as a Three-Dimensional Process. *Jour. Meteorology*, Vol. 11, No. 6, pp. 449–461. 1954.

No. 724. Charles B. Officer. Southwest Pacific Crustal Structure. *Trans. Amer. Geophys. Union*, Vol. 36, No. 3, pp. 449–459. 1955.

No. 725. K. G. Wilson and A. B. Arons. Osmotic Pressures of Sea Water Solutions Computed from Experimental Vapor Pressure Lowering. *Sears Found., Jour. Mar. Res.*, Vol.14, No. 2, pp. 195–198. 1955.

No. 726. Joanne Starr Malkus. On the Formation and Structure of Downdrafts in Cumulus Clouds. *Jour. Meteorol.*, Vol. 12, No. 4, pp. 350–354. 1955.

No. 727. Joanne Starr Malkus. The Effects of a Large Island upon the Trade-Wind Air Stream. *Quart. Jour. Roy. Meteor. Soc.*, Vol. 81, No. 350, pp. 538–550. 1955.

No. 728. Paul Ferris Smith. Further Measurements of the Sound Scattering Properties of Several Marine Organisms. *Deep-Sea Research*, Vol. 2, pp. 71–79. 1954.

No. 729. Willard Dow. Underwater Telemetering. *Deep-Sea Research*, Vol. 2, pp. 145–151 (erroneously dated 1954). 1955.

No. 730. John H. Ryther. Inhibitory Effects of Phytoplankton upon the Feeding of *Daphnia magna* with Reference to Growth, Reproduction, and Survival. *Ecology*, Vol. 35, No. 4, pp. 522–533. 1954.

No. 731. Charles B. Officer. A Deep-Sea Seismic Reflection Profile. *Geophysics*, Vol. 20, No. 2, pp. 270–282. 1955.

No. 732. Henry B. Bigelow and William C. Schroeder. Occurrence off the Middle and North Atlantic United States of the Offshore Hake *Merluccius albidus* (Mitchill) 1818, and of the Blue Whiting *Gadus (Micromesistius) poutassou* (Risso) 1826. *Bull. Mus. Comp. Zool.*, Vol. 113, No. 2, pp. 205–226. 1955.

No. 733. John H. Ryther. The Ratio of Photosynthesis to Respiration in Marine Plankton Algae and its Effect upon the Measurement of Productivity. *Deep-Sea Research*, Vol. 2, pp. 134–139 (erroneously dated 1954). 1955.

No. 734. Duncan C. Blanchard. Bursting of Bubbles at an Air-Water Interface. *Nature*, Vol. 173, p. 1048. 1954.

No. 735. Joseph Chase. Winds and Temperatures in Relation to the Brood-Strength of Georges Bank Haddock. *Jour. du Conseil*, Vol 21, No. 1, pp. 17–24. 1955.

No. 736. Grace I. Creitz and Francis A. Richards. The Estimation and Characterization of Plankton Populations by Pigment Analysis. III. A Note on the use of "Millipore" Membrane Filters in the Estimation of Plankton Pigments. *Sears Found., Jour. Mar. Res.*, Vol. 14, No. 3, pp. 211–216. 1955.

No. 737. Charles J. Fish. Preliminary Observations on the Biology of Boreo-Arctic and Subtropical Oceanic Zooplankton Populations. In: Symposium on Marine and Fresh-Water Plankton in the Indo-Pacific, Bangkok, Jan. 25–26, 1954, FAO-UNESCO, Sect. 1, No. 1, pp. 1–7, 1955. (Not included in *Collected Reprints*).

No. 739. William G. Metcalf. On the Formation of Bottom Water in the Norwegian Basin. *Trans. Amer. Geophys. Union*, Vol. 36, No. 4, pp. 596–600. 1955.

No. 740. Andrew F. Bunker. Turbulence and Shearing Stresses Measured over the North Atlantic Ocean by an Airplane-Acceleration Technique. *Jour. Meteorol.*, Vol 12, No. 5, pp. 445–455. 1955.

No. 741. Wilbur Marks and F. Claude Ronne. Aerial Stereo-Photography and Ocean Waves. *Photogr. Engineering*, March 1955, pp. 107–110. 1955.

No. 742. Malcolm S. Gordon. Summer Ecology of Oceanic Birds off Southern New England. *The Auk*, Vol 72, pp. 138–147. 1955.

No. 743. Charles B. Officer. Geologic Interpretation of a Series of Seismic Reflection Profiles from Bermuda to the Continental Margins. *Deep-Sea Research*, Vol. 2, pp. 253–260. 1955.

No. 744. J. W. Kanwisher and Gordon Volkmann. A Scattering Layer Observation. *Science*, Vol. 121, No. 3134, pp. 108–109. 1955.

No. 745. Irving I. Schell. Interrelations of Arctic Ice with the Atmosphere and the Ocean in the North Atlantic — Arctic and Adjacent Areas. *Jour. Meteorol.*, Vol. 13, No. 1, pp. 46–58. 1956.

No. 746. H. G. Farmer, W. Marks, R. G. Walden and G. G. Whitney, Jr. A Technique for Ocean Wave Measurements. In: Proc. First Conf., Ships and Waves, Oct. 1954, Counc. Wave Res. and Soc. Naval Arch. and Mar. Eng., pp. 11–32. 1955.

No. 747. Duncan C. Blanchard. Electrified Droplets from the Bursting of Bubbles at an Air-Sea Water Interface. *Nature*, Vol. 175, No. 4451, pp. 334–336. 1955.

No. 748. E. M. Hulburt. Distribution of Phosphorus in Great Pond, Massachusetts. *Sears Found., Jour. Mar. Res.*, Vol. 15, No. 3, pp. 181–192. 1956.

No. 749. F. C. Fuglister. Alternative Analyses of Current Surveys. *Deep-Sea Research*, Vol. 2, pp. 213–229. 1955.

No. 750. Gilbert L. Voss. The Cephalopoda Obtained by the Harvard-Havana Expedition off the Coast of Cuba in 1938–39. *Bull, Mar. Sci., Gulf and Caribbean*, Vol. 5, No. 2, pp. 81–115. 1955.

No. 751. Frank S. Essapian. Speed-Induced Skin Folds in the Bottle-Nosed Porpoise, *Tursiops truncatus*. *Breviora*, No. 43, 4 pp., 9 Pls. 1955.

No. 752. John P. Barlow. Effect of Wind on Salinity Distribution in an Estuary. *Sears Found., Jour. Mar. Res.*, Vol. 15, No. 3, pp. 193–203. 1956.

No. 753. John P. Barlow. Physical and Biological Processes Determining the Distribution of Zooplankton in a Tidal Estuary. *Biol. Bull.*, Vol. 109, No. 2, pp. 211–225. 1955.

No. 754. Alan J. Faller. A Demonstration of Fronts and Frontal Waves in Atmospheric Models. *Jour. Meteorol.*, Vol. 13, No. 1, pp. 1–4. 1956.

No. 755. P. F. Scholander. Evolution of Climatic Adaptation in Homeotherms. *Evolution*, Vol. 9, No. 1, pp. 15–26. 1955.

No. 756. Hilary B. Moore. Variations in Temperature and Light Response within a Plankton Population. *Biol. Bull.*, Vol. 108, No. 2, pp. 175–181. 1955.

No. 757. A. H. Woodcock and W. A. Mordy. Salt Nuclei, Wind and Daily Rainfall in Hawaii. *Tellus*, Vol. 7, No. 3, pp. 291–300. 1955.

No. 758. Floyd M. Soule and J. E. Murray. Physical Oceanography of the Grand Banks Region and the Laborador Sea in 1954. *U. S. Coast Guard Bull.*, No. 40, pp. 79–168. 1955.

No. 759. Bostwick H. Ketchum, Nathaniel Corwin and D. Jean Keen. The Significance of Organic Phosphorus Determinations in Ocean Waters. *Deep-Sea Research*, Vol. 2, pp. 172–181. 1955.

No. 760. Dean F. Bumpus and E. Lowe Pierce. The Hydrography and the Distribution of Chaetognaths over the Continental Shelf off North Carolina. Pap. Mar. Biol. and Oceanogr., *Deep-Sea Research*, Suppl. to Vol. 3, pp. 92–109. 1955. (Included in *Collected Reprints* for 1955, Part II).

No. 761. A. H. Woodcock. Bursting Bubbles and Air Pollution. *Sewage and Industrial Wastes*, Vol. 27, No. 10, pp. 1189–1192. 1955.

No. 762. Gordon A. Riley. Review of the Oceanography of Long Island Sound. Pap. Mar. Biol. and Oceanogr., *Deep-Sea Research*, Suppl. to Vol. 3, pp. 224–238. 1955. (Included in *Collected Reprints* for 1955, Part II).

No. 763. Talbot H. Waterman. Polarization of Scattered Sunlight in Deep Water. Pap. Mar. Biol. and Oceanogr., *Deep-Sea Research*, Suppl. to Vol. 3, pp. 426–434. 1955. (Included in *Collected Reprints* for 1955, Part II).

No. 764. E. M. Hulburt. The Phytoplankton of Great Pond, Massachusetts. *Biol. Bull.*, Vol. 110, No. 2, pp. 157–168. 1956.

No. 765. C. O'D. Iselin. Recent Advances in our Understanding of the Circulation Problem and their Implications. *Sears Found., Jour. Mar. Res.*, Vol. 14, No. 4, pp. 315–322. 1955.

No. 766. John C. Ayers. Population Dynamics of the Marine Clam, *Mya arenaria*. *Limnol. and Oceanogr.*, Vol. 1, No. 1, pp. 26–34. 1956.

No. 767. Edward M. Thorndike. Hydroscopes. *Trans. Amer. Geophys. Union*, Vol. 36, No. 3, pp. 470–472. 1955.

No. 768. A. H. Woodcock and D. C. Blanchard. Tests of the Salt-Nuclei Hypothesis of Rain Formation. *Tellus*, Vol. 7, No. 4, pp. 437–448. 1955.

No. 769. Wilbur Marks and Joseph Chase. Observation of the Growth and Decay of a Wave Spectrum. In: Interaction of Sea and Atmosphere. *Meteorol. Monogr.*, Vol. 2, No. 10, pp. 67–74. 1957.

No. 770. C.-G. Rossby and H. Egnér. On the Chemical Climate and its Variation with Atmospheric Circulation Pattern. *Tellus*, Vol. 7, No. 1, pp. 118–133. 1955.

No. 771. Stefan Machlup and J. B. Hersey. Analysis of Sound-Scattering Observations from Non-Uniform Distributions of Scatterers in the Ocean. *Deep-Sea Research*, Vol. 3, pp. 1–22. 1955.

No. 772. Bostwick H. Ketchum. Distribution of Coliform Bacteria and other Pollutants in Tidal Estuaries. *Sewage and Industrial Wastes*, Vol. 27, No. 11, pp. 1288–1296. 1955.

No. 773. Susan I. Scholander. Land Birds over the Western North Atlantic. *The Auk*, Vol. 72, pp. 225–239. 1955.

No. 774. Harvey R. Bullis, Jr. and F. J. Mather, III. Tunas of the Genus *Thunnus* of the Northern Caribbean. *Novitates*, No. 1765, 12 pp. 1956.

No. 775. Bostwick H. Ketchum and D. Jean Keen. The Accumulation of River Water over the Continental Shelf between Cape Cod and Chesapeake Bay. Pap. Mar. Biol. and Oceanogr., *Deep-Sea Research*, Suppl. to Vol. 3, pp. 346–357. 1955. (Included in *Collected Reprints* for 1955, Part II).

No. 776. Alfred C. Redfield. The Hydrography of the Gulf of Venezuela. Pap. Mar. Biol. and Oceanogr., *Deep-Sea Research*, Suppl. to Vol. 3, pp. 115–133. 1955. (Included in *Collected Reprints* for 1955, Part II).

No. 777. Harry J. Turner, Jr. How Clam Drills Capture Razor Clams. *The Nautilus*, Vol. 69, No. 1, pp. 20–22. 1955.

No. 778. J. W. Kanwisher. Freezing in Intertidal Animals. *Biol. Bull.*, Vol. 109, No. 1, pp. 56–63. 1955.

No. 779. Ruth D. Turner. Scaphopods of the *Atlantis* Dredgings in the Western Atlantic with a Catalogue of the Scaphopod Types in the Museum of Comparative Zoology. Pap. Mar. Biol. and Oceanogr., *Deep-Sea Research*, Suppl. to Vol. 3, pp. 309–320. 1955. (Included in *Collected Reprints* for 1955, Part II).

No. 780. E. Steemann Nielsen. The Production of Antibiotics by Plankton Algae and its Effect upon Bacterial Activities in the Sea. Pap. Mar. Biol. and Oceanogr., *Deep-Sea Research*, Suppl. to Vol. 3, pp. 281–286. 1955. (Included in *Collected Reprints* for 1955, Part II).

No. 781. W. T. Edmondson. Factors Affecting Productivity in Fertilized Water. Pap. Mar. Biol. and Oceanogr., *Deep-Sea Research*, Suppl. to Vol. 3, pp. 451–464. 1955. (Included in *Collected Reprints* for 1955, Part II).

No. 782. Henry C. Stetson. Patterns of Deposition at the Continental Margin. Pap. Mar. Biol. and Oceanogr., *Deep-Sea Research*, Suppl. to Vol. 3, pp. 298–308. 1955. (Included in *Collected Reprints* for 1955, Part II).

No. 783. Harry J. Turner, Jr. and Stanley Scher. Seventh Report on Investigations of the Shellfisheries of Massachusetts. *Com. Mass., Dept. Nat. Res., Div. Mar. Fish.*, 35 pp. 1954.

No. 785. Earl Barrett and Gunnar Brodin. The Acidity of Scandinavian Precipitation. *Tellus*, Vol. 7, No. 2, pp. 251–257. 1955.

No. 786. T. F. Goreau and V. T. Bowen. Calcium Uptake by a Coral. *Science*, Vol. 122, No. 3181, pp. 1188–1189. 1955.

No. 787. Henry B. Bigelow, William C. Schroeder and Stewart Springer. Three New Shark Records from the Gulf of Mexico. *Breviora*, No. 49, 12 pp. 1955.

No. 788. Dean F. Bumpus. The Circulation over the Continental Shelf South of Cape Hatteras. *Trans. Amer. Geophys. Union*, Vol. 36, No. 4, pp. 601–611. 1955.

No. 789. Donald R. Griffin. Hearing and Acoustic Orientation in Marine Animals. Pap. Mar. Biol. and Oceanogr., *Deep-Sea Research*, Suppl. to Vol. 3, pp. 406–417. 1955. (Included in *Collected Reprints* for 1955, Part II).

No. 790. William C. Schroeder. Report on the Results of Exploratory Otter-Trawling along the Continental Shelf and Slope between Nova Scotia and Virginia during the Summers of 1952 and 1953. Pap. Mar. Biol. and Oceanogr., *Deep-Sea Research*, Suppl. to Vol. 3, pp. 358–372. 1955. (Included in *Collected Reprints* for 1955, Part II).

No. 791. L. V. Worthington. A New Theory of Caribbean Bottom-Water Formation. *Deep-Sea Research*, Vol. 3, pp. 82-87. 1955.

No. 792. C. O'D. Iselin. Coastal Currents and the Fisheries. Pap. Mar. Biol. and Oceanogr., *Deep-Sea Research*, Suppl. to Vol. 3, pp. 474–478. 1955. (Included in *Collected Reprints* for 1955, Part II).

No. 793. Barbara Lawrence and William E. Schevill. The Functional Anatomy of the Delphinid Nose. *Bull. Mus. Comp. Zool.*, Vol. 114, No. 4, pp. 103–151. 1956. (Not included in *Collected Reprints*).

No. 794. William S. Von Arx and W. S. Richardson. On the Fine-Structure of the Gulf Stream Front. *Deep-Sea Research*, Vol. 3, pp. 46–65. 1955.

No. 795. P. F. Scholander, L. van Dam, C. Lloyd Claff and J. W. Kanwisher. Micro Gasometric Determination of Dissolved Oxygen and Nitrogen. *Biol. Bull.*, Vol. 109, No. 2, pp. 328–334. 1955.

No. 796. Henry Stommel. Lateral Eddy Viscosity in the Gulf Stream System. *Deep-Sea Research*, Vol. 3, pp. 88–90. 1955.

No. 797. Irving I. Schell. Further Evidence of Dynamic Persistence and of its Application to Foreshadowing. *Jour. Meteorol.*, Vol. 13, No. 5, pp. 471–481. 1956.

No. 798. Nora Gladwin Fairbank. Methods and Preliminary Results in a Study of Minerals from the Eastern Gulf of Mexico. *Jour. Sed. Petrol.*, Vol. 26, No. 3, pp. 268–275. 1956.

No. 799. Henry Stommel, Arnold B. Arons and Duncan Blanchard. An Oceanographical Curiosity: the Perpetual Salt Fountain. *Deep-Sea Research*, Vol. 3, pp. 152–153. 1956.

No. 800. M. S. Gordon and Richard H. Backus. New Records of Labrador Fishes with Special Reference to those of Hebron Fjord. *Copeia*, No. 1, pp. 17–20. 1957.

No. 801. Floyd M. Soule and J. E. Murray. Physical Oceanography of the Grand Banks and the Labrador Sea in 1955. *U. S. Coast Guard Bull.*, No. 41, pp. 59–114. 1956.

No. 802. James M. Moulton and Richard H. Backus. Annotated References Concerning the Effects of Man-Made Sounds on the Movements of Fishes. *Dept. Sea and Shore Fish.*, Augusta, Maine, Fish. Circ. No. 17, 8 pp. 1955.

No. 804. W. V. R. Malkus. Outline of a Theory of Turbulent Shear Flow. *Jour. Fluid Mech.*, Vol. 1, Pt. 5, pp. 521–539. 1956.

No. 805. John Mackiewicz and Richard H. Backus. Oceanic Records of *Lasionycteris noctivagans* and *Lasiurus borealis*. *Jour. Mammalogy*, Vol. 37, No. 3, pp. 442–443. 1956.

No. 806. Allyn C. Vine. Oceanographic Instrumentation. *Science*, Vol. 122, No. 3173, pp. 748–751. 1955.

No. 807. P. F. Scholander and William E. Schevill. Counter-Current Vascular Heat Exchange in the Fins of Whales. *Jour. Appl. Physiol.*, Vol. 8, No. 3, pp. 279–282. 1955.

No. 808. E. Steemann Nielsen. The Interaction of Photosynthesis and Respiration and its Importance for the Determination of ^{14}C-Discrimination in Photosynthesis. *Physiologia Plantarum*, Vol. 8, pp. 945–953. 1955.

No. 809. Duncan C. Blanchard. The Supercooling, Freezing and Melting of Giant Waterdrops at Terminal Velocity in Air. Proceedings of the First Conference on the Physics of Cloud Precipitation Particles, Woods Hole, September 7–10, 1955. In: Artificial Stimulation of Rain, pp. 233–249. Pergamon Press, New York, London, Paris. 1957.

No. 810. Karl E. Schleicher and Alvin Bradshaw. A Conductivity Bridge for Measurement of the Salinity of Sea Water. *Jour. du Conseil*, Vol. 22, No. 1, pp. 9–20. 1956.

No. 811. G. W. Morgan. On the Wind-Driven Ocean Circulation. *Tellus*, Vol. 8, No. 3, pp. 301–320. 1956.

No. 812. Duncan C. Blanchard. Discussion of Raindrop Distributions made during Project Shower, Hawaii, 1954. Proceedings of the First Conference on the Physics of Cloud Precipitation Particles, Woods Hole, September 7–10, 1955. In: Artificial Stimulation of Rain, pp. 213–223. Pergamon Press, New York, London, Paris. 1957.

No. 813. R. W. Holmes. The Annual Cycle of Phytoplankton in the Labrador Sea, 1950–51. *Bull. Bingham Oceanogr. Coll.*, Vol. 16, Art. 1, 74 pp. 1956. (Not included in Collected Reprints).

No. 814. Richard H. Backus, Stewart Springer and Edgar L. Arnold, Jr. A Contribution to the Natural History of the White-Tip Shark, *Pterolamiops longimanus* (Poey). *Deep-Sea Research*, Vol. 3, pp. 178–188. 1956.

No. 815. William E. Schevill. *Lagenorhynchus acutus* off Cape Cod. *Jour. Mammalogy*, Vol. 37, No. 1, pp. 128–129. 1956.

No. 816. P. F. Scholander, L. van Dam and Theodore Enns. Nitrogen Secretion in the Swimbladder of Whitefish. *Science*, Vol. 123, No. 3185, pp. 59–60. 1956.

No. 817. Harold E. Edgerton and Lloyd D. Hoadley. Cameras and Lights for Underwater Use. *Jour. Soc. Motion Pic. and Tel. Eng.*, Vol. 64, pp. 345–350. 1955.

No. 818. P. F. Scholander, John W. Kanwisher and D. C. Nutt. Gases in Icebergs. *Science*, Vol. 123, No. 3186, pp. 104–105. 1956.

No. 819. John H. Ryther. Photosynthesis in the Ocean as a Function of Light Intensity. *Limnol. and Oceanogr.*, Vol. 1, No. 1, pp. 61–70. 1956.

No. 820. William S. von Arx. An Experimental Approach to Problems in Physical Oceanography. In: Progress in Physics and Chemistry of the Earth, Vol. 2, pp. 1–29. Pergamon Press, London, New York, Paris. 1957.

No. 821. George L. Clarke and Gunther K. Wertheim. Measurements of Illumination at Great Depths and at Night in the Atlantic Ocean by Means of a New Bathyphotometer. *Deep-Sea Research*, Vol. 3, pp. 189–205. 1956.

No. 822. P. F. Scholander. Hydrostatic Pressure in Coconuts. *Plant Physiol.*, Vol. 30, No. 6, pp. 560–561. 1955.

No. 823. John C. Ayers. A Dynamic Height Method for the Determination of Currents in Deep Lakes. *Limnol. and Oceanogr.*, Vol. 1, No. 3, pp. 150–161. 1956.

No. 824. Parker D. Trask. The *Atlantis* Marine Geological Expedition to Peru and Chile. *Nature*, Vol. 177, pp. 454–455. 1956.

No. 825. John H. Ryther. The Measurement of Primary Production. *Limnol. and Oceanogr.*, Vol. 1, No. 2, pp. 72–84. 1956.

No. 826. Robert L. Miller. Trend Surfaces: Their Application to Analysis and Description of Environments of Sedimentation. 1. The Relation of Sediment-Size Parameters to Current-Wave Systems and Physiography. *Jour. Geology*, Vol. 64, No. 5, pp. 425–446. 1956.

No. 827. Joanne Starr Malkus. On the Maintenance of the Trade Winds. *Tellus*, Vol. 8, No. 3, pp. 335–350. 1956.

No. 828. Alfred C. Redfield and Arthur R. Miller. Water Levels Accompanying Atlantic Coast Hurricanes. In: Interaction of Sea and Atmosphere. *Meteorol. Monogr.*, Vol. 2, No. 10, pp. 1–23. 1957.

No. 829. Arthur R. Miller. The Effect of Steady Winds on Sea Level at Atlantic City. In: Interaction of Sea and Atmosphere. *Meteorol. Monogr.*, Vol. 2, No. 10, pp. 24–31. 1957.

No. 830. Francis A. Richards and Ralph F. Vaccaro. The Cariaco Trench, an Anaerobic Basin in the Caribbean Sea. *Deep-Sea Research*, Vol. 3, pp. 214–228. 1956.

No. 831. David C. Nutt and Lawrence K. Coachman. The Oceanography of Hebron Fjord, Labrador. *Jour. Fish. Res. Bd. Canada*, Vol. 13, No. 5, pp. 709–758. 1956.

No. 832. William E. Schevill and Barbara Lawrence. Food-Finding by a Captive Porpoise (*Tursiops truncatus*). *Breviora*, No. 53, 15 pp. 1956.

No. 833. A. F. Bunker. Turbulence Measurements in a Young Cyclone over the Ocean. *Bull. Amer. Meteorol. Soc.*, Vol. 38, No. 1, pp. 13–16. 1957.

No. 834. Richard H. Backus and J. B. Hersey. Echo-Sounder Observations of Midwater Nets and their Towing Cables. *Deep-Sea Research*, Vol. 3, pp. 237–241. 1956.

No. 835. Joseph Chase. The Bermuda-Azores High Pressure Cell. Its Surface Wind Circulation. *Miscelânea Geofísica*, pp. 29–54. Luanda, Angola. 1956.

No. 837. A. H. Woodcock. Dimorphism in the Portuguese Man-of-War. *Nature*, Vol. 178, No. 4527, pp. 253–255. 1956.

No. 838. E. M. Hulburt. The Taxonomy of Unarmored Dinophyceae of Shallow Embayments on Cape Cod, Massachusetts. *Biol. Bull.*, Vol. 112, No. 2, pp 196–219. 1957.

No. 839. C. B. Officer, J. I. Ewing, R. S. Edwards and H. R. Johnson. Geophysical Investigations in the Eastern Caribbean: Venezuelan Basin, Antilles Island Arc, and Puerto Rico Trench. *Bull. Geol. Soc. Amer.*, Vol. 68, pp. 359–378. 1957.

No. 840. Francis A. Richards. On the State of our Knowledge of Trace Elements in the Ocean. *Geochimica et Cosmochimica Acta*, Vol. 10, No. 4, pp. 241–243. 1956.

No. 841. Henry R. Johnson, Richard H. Backus, J. B. Hersey and D. M. Owen. Suspended Echo-Sounder and Camera Studies of Midwater Sound Scatterers. *Deep-Sea Research*, Vol. 3, pp. 266–272. 1956.

No. 842. John H. Ryther. Interrelation between Photosynthesis and Respiration in the Marine Flagellate, *Dunaliella euchlora*. *Nature*, Vol. 178, pp. 861–862. 1956.

No. 843. Joanne Starr Malkus. Trade Cumulus Cloud Groups: Some Observations Suggesting a Mechanism of Their Origin. *Tellus*, Vol. 9, No. 1, pp. 33–44. 1957.

No. 844. Francis A. Richards. Some Current Aspects of Chemical Oceanography. In: Progress in Physics and Chemistry of the Earth, Vol. 2, pp. 77–128. 1957.

No. 845. Henry Stommel. Florida Straits Transports, 1952–1956. *Bull. Mar. Sci., Gulf and Caribbean*, Vol. 7, No. 3, pp. 252–254. 1957.

No. 846. Henry Stommel. On the Determination of the Depth of No Meridional Motion. *Deep-Sea Research*, Vol. 3, pp. 273–278. 1956.

No. 847. Athelstan Spilhaus. Control of the World Environment. *Geogr. Rev.*, Vol. 46, No. 4, pp. 451–459. 1956.

No. 848. Henry B. Bigelow and William C. Schroeder. A Study of the Sharks of the Suborder Squaloidea. *Bull. Mus. Comp. Zool.*, Vol. 117, No. 1, pp. 1–150. 1957. (Not included in *Collected Reprints*).

No. 850. von H. Walden and H. G. Farmer. Auswertung von Seegangsregistrierungen des Forschungsschiffes "Atlantis" mit dem "Ship-Borne Wave Recorder" sowie Vergleich mit entsprechenden Seegangsberechnungen aus den Windverhaltnissen (Hindcasting). *Deutsche Hydrogr. Zeitschrift*, Bd. 10, Heft 4, pp. 121–134. 1957.

No. 851. Allyn C. Vine, Some Trends in Oceanographic Instrumentation. *Proc. UNESCO Symp. Phys. Oceanogr.*, Tokyo, 1955: 49–52. 1597. (Not included in *Collected Reprints*).

No. 852. Francis A. Richards and Nathaniel Corwin. Some Oceanographic Applications of Recent Determinations of the Solubility of Oxygen in Sea Water. *Limnol. and Oceanogr.*, Vol. 1, No. 4, pp. 263–267. 1956.

No. 853. Irving I. Schell. On the Nature and Origin of the Southern Oscillation. *Jour. Meteorol.*, Vol. 13, No. 6, pp. 592–598. 1956.

No. 854. Richard H. Backus. Northern Record of the Snake Eel *Ophichthus gomesi* (Castelnau). *Copeia*, No. 1, p. 61. 1957.

No. 855. A. B. Arons and Henry Stommel. A β-Plane Analysis of Free Periods of the Second Class in Meridional and Zonal Oceans. *Deep-Sea Research*, Vol. 4, pp. 23–31. 1956.

No. 856. Gordon Volkmann, John Knauss and Allyn Vine. The Use of Parachute Drogues in the Measurement of Subsurface Ocean Currents. *Trans. Amer. Geophys. Union*, Vol. 37, No. 5, pp. 573–577. 1956.

No. 857. Richard H. Backus. Notes on Western North Atlantic Sharks. *Copeia*, No. 3, pp. 246–248. 1957.

No. 858. George L. Clarke and Richard H. Backus. Measurements of Light Penetration in Relation to Vertical Migration and Records of Luminescence of Deep-Sea Animals. *Deep-Sea Research*, Vol. 4, pp. 1–14. 1956.

No. 859. G. Veronis and Henry Stommel. The Action of Variable Wind Stresses on a Stratified Ocean. *Sears Found., Jour. Mar. Res.*, Vol. 15, No. 1, pp. 43–75. 1956.

No. 860. I. Friedman and A. H. Woodcock. Determination of Deuterium-Hydrogen Ratios in Hawaiian Waters. *Tellus*, Vol. 9, No. 4, pp. 553–556. 1957.

No. 861. J. I. Ewing, C. B. Officer, H. R. Johnson, and R. S. Edwards. Geophysical Investigations in the Eastern Caribbean: Trinidad Shelf, Tobago Trough, Barbados Ridge, Atlantic Ocean. *Bull. Geol. Soc. Amer.*, Vol. 68, pp. 897–912. 1957.

No. 862. James M. Moulton. Influencing the Calling of Sea Robins (*Prionotus* spp.) with Sound. *Biol .Bull.*, Vol. 111, No. 3, pp. 393–398. 1956.

No. 863. S. T. Knott and J. B. Hersey. Interpretation of High-Resolution Echo-Sounding Techniques and their Use in Bathymetry, Marine Geophysics, and Biology. *Deep-Sea Research*, Vol. 4, pp. 36–44. 1956.

No. 864. H. B. Moore and E. G. Corwin. The Effects of Temperature, Illumination, and Pressure on the Vertical Distribution of Zooplankton. *Bull. Mar. Sci., Gulf and Caribbean*, Vol. 6, No. 4, pp. 273–287. 1956.

No. 865. Richard S. Edwards and Francis A. Richards. A Bottom-Water Sampler. *Deep-Sea Research*, Vol. 4, pp. 65–66. 1956.

No. 866. M. S. Rutstein. Flooded Quarries for Experimental Work. *Trans. Amer. Geophys. Union*, Vol. 35, No. 5, pp. 688–690. 1957.

No. 867. Irving Friedman, Daniel R. Norton, Douglas B. Carter and Alfred C. Redfield. The Deuterium Balance of Lake Maracaibo. *Limnol. and Oceanogr.*, Vol. 1, No. 4, pp. 239–246. 1956.

No. 868. M. S. Gordon. Observations on Osmoregulation in the arctic char (*Salvelinus alpinus* L.). *Biol. Bull.*, Vol. 112, No. 1, pp. 28–33. 1957.

No. 869. Helen S. Vishniac. On the Ecology of the Lower Marine Fungi. *Biol. Bull.*, Vol. 111, No. 3, pp. 410–414. 1956.

No. 870. W. S. Wooster and Bostwick H. Ketchum. Transport and Dispersal of Radioactive Elements in the Sea. In: The Effects of Atomic Radiation on Oceanography and Fisheries. Publ. No. 551, Nat. Acad. Sci.-Nat. Res. Council, Chapt. 4, pp. 43–51. 1957.

No. 871. Bostwick H. Ketchum. The Effects of the Ecological System on the Transport of Elements in the Sea. In: The Effects of Atomic Radiation on Oceanography and Fisheries. Publ. No. 551, Nat. Acad. Sci.-Nat. Res. Council, Chapt. 5, pp. 52–59. 1957.

No. 873. Lawrence K. Coachman, E. Hemmingsen and P. F. Scholander. Gas Enclosures in a Temperate Glacier. *Tellus*, Vol. 8, No. 4, pp. 415–423. 1956. (Not included in *Collected Reprints*).

No. 875. Duncan C. Blanchard and A. H. Woodcock. Bubble Formation and Modification in the Sea and its Meteorological Significance. *Tellus*, Vol. 9, No. 2, pp. 145–158. 1957.

No. 876. Harry J. Turner, Carl J. George and Joseph H. Connell. Eighth Report on Investigations of the Shellfisheries of Massachusetts. *Com. Mass., Dept. Nat. Res., Div. Mar. Fish.*, 25 pp. 1955.

No. 878. J. W. Kanwisher and H. Leivestad. Thermal Regulation in Whales. *Norwegian Whaling Gazette*, No. 1, pp. 1–5. 1957.

No. 879. P. F. Scholander and L. van Dam. Micro Gasometric Determination of Oxygen in Fish Blood. *Jour. Cell. and Comp. Physiol.*, Vol. 48, No. 3, pp. 529–532. 1956.

No. 880. P. F. Scholander. Observations on the Gas Gland in Living Fish. *Jour. Cell. and Comp. Physiol.*, Vol. 48, No. 3, pp. 523–528. 1956.

No. 881. P. F. Scholander, L. van Dam and Theodore Enns. The Source of Oxygen Secreted into the Swimbladder of Cod. *Jour. Cell. and Comp. Physiol.*, Vol. 48, No. 3, pp. 517–522. 1956.

No. 882. H. L. Sanders. The Cephalocarida and Crustacean Phylogeny. *Syst. Zool.*, Vol. 6, No. 3, pp. 112–129. 1957.

No. 883. John C. Ayers and Roger Bachmann. Simplified Computations for the Dynamic Height Method of Current Determination in Lakes. *Limnol. and Oceanogr.*, Vol. 2, No. 2, pp. 155–157. 1957.

No. 884. John M. Zeigler and F. C. Ronne. Time-Lapse Photography - - an Aid to Studies of the Shoreline. *Research Reviews*, Office of Naval Research, Washington, April, pp. 1–6. 1957.

No. 885. Shannon R. Torphy and John M. Zeigler. Submarine Topography of Eastern Channel, Gulf of Maine. *Jour. Geology*, Vol. 65, No. 4, pp. 433–441. 1957.

No. 886. Harry J. Turner and David L. Belding. The Tidal Migrations of *Donax variabilis* Say. *Limnol. and Oceanogr.*, Vol. 2, No. 2, pp. 120–124. 1957.

No. 887. J. W. Kanwisher. Freezing and Drying in Intertidal Algae. *Biol. Bull.*, Vol. 113, No. 2, pp. 275–285. 1957.

No. 888. J. W. Kanwisher and Alfred Ebeling. Composition of the Swim-Bladder Gas in Bathypelagic Fishes. *Deep-Sea Research*, Vol. 4, pp. 211–217. 1957.

No. 889. A. H. Woodcock and A. T. Spencer. An Airborne Flame Photometer and its Use in the Scanning of Marine Atmospheres for Sea-Salt Particles. *Jour. Meteorol.*, Vol. 14, No. 5, pp. 437–447. 1957.

No. 890. Willem A. van Bergeijk and Emil Witschi. The Basilar Papilla of the Anuran Ear. *Acta Anatomica*, Vol. 30, pp. 81–91. 1957. (Not included in *Collected Reprints*).

No. 891. P. F. Scholander, L. van Dam, J. W. Kanwisher, H. T. Hammel and M. S. Gordon. Supercooling and Osmoregulation in Arctic Fish. *Jour. Cell. and Comp. Physiol.*, Vol. 49, No. 1, pp. 5–24. 1957.

No. 892. P. F. Scholander and L. van Dam. The Concentration of Hemoglobin in Some Cold Water Arctic Fishes. *Jour. Cell. and Comp. Physiol.*, Vol. 49, No. 1, pp. 1–4. 1957.

No. 893. Charles S. Yentsch and John H. Ryther. Short-term Variations in Phytoplankton Chlorophyll and Their Significance. *Limnol. and Oceanogr.*, Vol. 2, No. 2, pp. 140–142. 1957.

No. 894. Richard H. Backus and Harold Barnes. Television-Echo-Sounder Observations by Midwater Sound Scatterers. *Deep-Sea Research*, Vol. 4, pp. 116–119. 1957.

No. 895. Robert G. Walden, David D. Ketchum and David H. Frantz, Jr. Buoy Telemeters Ocean Temperature Data. *Electronics*, Vol. 30, No. 6, pp. 164–167. McGraw Hill Co., New York. 1957.

No. 896. Richard H. Backus. The Fishes of Labrador. *Bull. Amer. Mus. Nat. Hist.*, Vol. 113, Art. 4, pp. 273–337. 1957. (Not included in *Collected Reprints*).

No. 897. Harold Barnes. The Northern Limit of *Balanus balanoides* (L). *Oikos*, Vol. 8, No. 1, pp. 1–15. 1957.

No. 898. Charles S. Yentsch. A Non-Extractive Method for the Quantitative Estimation of Chlorophyll in Algal Cultures. *Nature*, Vol. 179, pp. 1302–1304. 1957.

No. 899. Henry Stommel and George Veronis. Steady Convective Motion in a Horizontal Layer of Fluid Heated Uniformly from Above and Cooled Non-Uniformly from Below. *Tellus*, Vol. 9, No. 3, pp. 401–407. 1957.

No. 901. Frank J. Mather III and Robert H. Gibbs. Distributional Records of Fishes from Waters off New England and the Middle Atlantic States. *Copeia*, No. 3, pp. 242–244. 1957.

No. 902. John H. Ryther and Charles S. Yentsch. The Estimation of Phytoplankton Production in the Ocean from Chlorophyll and Light Data. *Limnol. and Oceanogr.*, Vol. 2, No. 3, pp. 281–286. 1957.

No. 903. W. H. Sutcliffe, Jr. An Improved Method for the Determination of Preserved Plankton Volumes. *Limnol. and Oceanogr.*, Vol. 2, No. 3, pp. 295–296. 1957.

No. 904. Dean F. Bumpus. Surface Water Temperature along Atlantic and Gulf Coasts of the United States. U. S. Fish and Wildlife Service, Spec. Sci. Rept. — Fisheries No. 214, 153 pp. 1957. (Not included in *Collected Reprints*).

No. 905. William D. Athearn. Comparisons of Clay from the Continental Shelf off Long Island with the Gardiners Clay. *Jour. Geology*, Vol. 65, No. 4, pp. 448–449. 1957.

No. 907. Vaughan T. Bowen and T. T. Sugihara. Strontium 90 in North Atlantic Surface Water. *Proc. Nat. Acad. Sci.*, Vol. 43, No. 7, pp. 576–580. 1957.

No. 908. L. V. Worthington and William E. Schevill. Underwater Sounds Heard from Sperm Whales. *Nature*, Vol. 180, p. 291. 1957.

No. 909. Jan Hahn. Oceanus Goes to the Bottom of the Sea. Reprinted from *Oceanus*, Vol. 5, Nos. 1 and 2, pp. 20–31. 1957.

No. 910. J. C. Swallow and L. V. Worthington. Measurements of Deep Currents in the Western North Atlantic. *Nature*, Vol. 179, pp. 1183–1184. 1957.

No. 911. G. C. McLeod. The Effect of Circularly Polarized Light on the Photosynthesis and Chlorophyll *a* Synthesis of Certain Marine Algae. *Limnol. and Oceanogr.*, Vol. 2, No. 4, pp. 360–362. 1957.

No. 912. Robert H. Gibbs, Jr. A Taxonomic Analysis of *Myctophum affine* and *M. nitidulum*, two Lantern-Fishes Previously Synonymized, in the Western North Atlantic. *Deep-Sea Research*, Vol. 4, pp. 230–237. 1957.

No. 913. E-an Zen. Preliminary Report on the Mineralogy and Petrology of Some Marine Bottom Samples off the Coast of Peru and Chile. *Amer. Mineralogist*, Vol. 42, pp. 889–903. 1957.

No. 914. James M. Moulton. Sound Production in the Spiny Lobster *Panulirus argus* (Latreille). *Biol. Bull.*, Vol. 113, No. 2, pp. 286–295. 1957.

No. 916. G. G. Whitney, Jr. Factors Affecting the Accuracy of Thermometric Depth Determinations. *Jour. du Conseil*, Vol. 22, No. 2, pp. 167–173. 1957.

No. 917. Henry Stommel. A Survey of Ocean Current Theory. *Deep-Sea Research*, Vol. 4, pp. 149–184. 1957.

No. 918. Dean F. Bumpus. Oceanographic Observations 1956, East Coast of the United States. U. S. Fish and Wildlife Service, Spec. Sci. Rept. — Fisheries No. 233, 132 pp. 1957. (Not included in *Collected Reprints*).

No. 919. John M. Zeigler, W. D. Athearn and H. Small. Profiles across the Peru-Chile Trench. *Deep-Sea Research*, Vol. 4, pp. 238–249. 1957.

No. 921. P. F. Scholander. Oxygen Dissociation Curves in Fish Blood. *Acta Physiol Scand.*, Vol. 41, No. 4, pp. 340–344. 1957.

No. 922. Robert H. Gibbs, Jr. Preliminary Analysis of the Distribution of White Marlin, *Makaira albida* (Poey), in the Gulf of Mexico. *Bull. Mar. Sci., Gulf and Caribbean*, Vol. 7, No. 4, pp. 360–369. 1957.

No. 924. MARY A. PLUNKETT. The Qualitative Determination of Some Organic Compounds in Marine Sediments. *Deep-Sea Research*, Vol. 4, pp. 259-262. 1957.

No. 926. DEAN F. BUMPUS, JOSEPH CHASE, C. GODFREY DAY, DAVID H. FRANTZ, JR., DAVID D. KETCHUM and ROBERT G. WALDEN. A new Technique for Studying Non-Tidal Drift with Results of Experiments off Gay Head, Mass., and in the Bay of Fundy. *Jour. Fish. Bd. Canada*, Vol. 14, No. 6, pp. 931–944. 1957.

No. 929. THEODORE R. FOLSOM and ALLYN C. VINE. On the Tagging of Water Masses for the Study of Physical Processes in the Oceans. In: The Effects of Atomic Radiation on Oceanography and Fisheries. Publ. No. 551. Nat. Acad. Sci.-Nat. Res. Council, Chapt. 12, pp. 121-132. 1957.

No. 941. DEAN F. BUMPUS and C. GODFREY DAY. Drift Bottle Records for the Gulf of Maine and Georges Bank, 1931–56. U.S. Fish and Wildlife Service, Spec. Sci. Rept. — Fisheries No. 242, 61 pp. 1957.